Prestressed Concrete

Sixth Edition

IS: 1343-2012
BS EN: 1992-1-1-2004
ACI: 318M-2011

About the Author

N. Krishna Raju, Emeritus Professor of Civil Engineering, M S Ramaiah Institute of Technology, Bangalore, earned his PhD degree from the University of Leeds, UK. He has taught at the College of Engineering, Guindy, Chennai; Regional Engineering College, Calicut; Lanchester College of Technology, Coventry, UK; Indian Institute of Science, Bangalore; and the Karnataka Regional Engineering College, Surathkal. He was also a visiting professor at the University of Basrah, Iraq, during 1979–82.

Dr Raju is the recipient of several awards, prominent among them being The Sir Bowen Memorial Prize, Garudacharya and Krishna Iyengar Gold Medals, UP Government National Award, Birla Super Endowment Award, Eminent Civil Engineers Award, George Oomen Memorial Prize, Institution of Engineers Prize, Naghadi Award and the ICI Silver Jubilee Award.

Dr Raju has published over 60 research papers in reputed journals and is the author of several engineering monographs like *Design of Concrete Mixes, Prestressed Concrete, Design of Reinforced Concrete Structures, Advanced Reinforced Concrete Design, Design of Bridges, Design and Drawing of Reinforced Concrete and Steel Structures, Numerical Methods for Engineering Problems, Structural Design and Drawing, Prestressed Concrete (Problems & Solutions), Reinforced Concrete Structural Elements, Advanced Mechanics of Solids and Structures,* and *Prestressed Concrete Bridges*.

Dr Raju's textbooks have also been published in Indonesian and Arabic languages. He is also a member of the Institution of Structural Engineers, London, UK, the Institution of Engineers, India, and the Indian Concrete Institute. He is socially active serving as the President of the Vijayanagar Senior Citizen's Forum and as an active anchor of Jai Maruthi Laughter Yoga Club at Vijayanagar, Bangalore.

Prestressed Concrete

Sixth Edition

IS: 1343-2012
BS EN: 1992-1-1-2004
ACI: 318M-2011

N. Krishna Raju

B.E., M.Sc (Engg), Ph.D., M.I.E., M.I. Struct.E

Emeritus Professor of Civil Engineering
M S Ramaiah Institute of Technology, Bangalore

McGraw Hill Education (India) Private Limited

CHENNAI

McGraw Hill Education Offices

Chennai New York St Louis San Francisco Auckland Bogotá Caracas
Kuala Lumpur Lisbon London Madrid Mexico City Milan Montreal
San Juan Santiago Singapore Sydney Tokyo Toronto

McGraw Hill Education (India) Private Limited

Published by McGraw Hill Education (India) Private Limited,
444/1, Sri Ekambara Naicker Industrial Estate, Alapakkam, Porur, Chennai-600116.

Prestressed Concrete, 6e

1 2 3 4 5 6 7 8 9 D101417 22 21 20 19 18

Printed and bound in India

Print Edition:
ISBN-13: 978-93-87886-20-9
ISBN-10: 93-87886-20-4

e-Book Edition:
ISBN-13: 978-93-87886-25-4
ISBN-10: 93-87886-25-5

Director—Science & Engineering Portfolio: *Vibha Mahajan*
Senior Portfolio Manager—Science & Engineering: *Hemant K Jha*
Associate Portfolio Manager—Science & Engineering: *Tushar Mishra*

Content Development Lead: *Shalini Jha*
Content Developer: *Amit Chatterjee*

Production Head: *Satinder S Baveja*
Copy Editor: *Taranpreet Kaur*
Assistant Manager—Production: *Atul Gupta*

General Manager—Production: *Rajender P Ghansela*
Manager—Production: *Reji Kumar*

Typeset at The Composers, 260, C.A. Apt., Paschim Vihar, New Delhi 110 063 and printed at

Cover Printer:

Visit us at: www.mheducation.co.in

Write to us at: info.india@mheducation.com

CIN: U22200TN1970PTC111531

Toll Free Number: 1800 103 5875

Eugene Freyssinet
(Father of Prestressing)

The book is dedicated to the pioneers and research workers

Eugene Freyssinet, Yves Guyon, Gustav Magnel,
Paul W. Abeles, M. Birkenmaier, F. Dischinger, Finister Walder,
T.Y. Lin, Fritz Leonhardt, Ben C. Gerwick Jr, R.H. Evans, E.W. Bennett,
P.E. Regan, J.J. Mc Namee, Y. Guyon, D.J. Dowrick, T.N. Subba Rao,
V.V. Mikhailov, V.K. Raina, Brandestini, Ros, Vogt, J.R. Libby, J. Muller,
R.E. Rowe, O.C. Zienkienwicz, W. Rockenhouser, P.B. Morice, A.R. Anderson,
W. Podolony, J.M. Crom, A.H. Mattock, Lee McCall, Shu-Tien-Li, G.S. Rama Swamy

and a host of others who toiled incessantly for the development and widespread use of Prestressed Concrete

Contents

Preface to the Sixth Edition

About the Book

The universal use of **prestressed concrete** as a versatile construction material is well established due to its suitability in multifarious types of structural applications. During the last six years, the fifth edition of this book has witnessed seventeen reprints, establishing the popularity of this book among the civil, structural and highway engineering students, teachers, practising engineers, design consultants and as a valuable reference guide for research workers. The contents of the book reflect the rapid changes witnessed in the technology of materials, types of construction techniques, codified procedures of the country and ever increasing structural applications. The fifth edition has served its purpose by establishing itself as the leading monograph on the subject of Prestressed Concrete among the various books published and marketed in the country.

Periodical revisions of the countries' codes and the new worldwide applications in the use of prestressed concrete have necessitated the revision of this book. This edition incorporates the changes made in the latest Indian Standard Code on prestressed concrete (IS: 1343-2012) and the unified Indian Roads Congress Codes, (IRC: 6-2014) and (IRC: 112-2011) replacing the older codes. The basic concepts of the philosophy of limit state design adopted universally in structural design is incorporated in the design examples. Most of the chapters are updated with appropriate changes required in the design computations involving the limit states of strength and serviceability. Two new chapters dealing with the precast prestressed concrete structural elements in the construction industry and a brief survey of prominent outstanding structures of prestressed concrete around the world are included. The last chapter presents the prospective progress in prestressed concrete in the light of innovations in nano concrete and nano engineered steels.

Highlights of the Book

- Comprehensive coverage of important topics of prestressed concrete
- Latest Indian (IS: 1343-2012), (IRC: 6-2014), (IRC: 112-2011), British (BS EN: 1992-1-1-2004) and American (ACI: 318M-2011) codes are used throughout the book
- Limit state philosophy of design is followed for all examples

- Emphasis has been given on limit states of strength and serviceability in structural design examples
- Comprehensive coverage on prestressed concrete bridges
- Applications of prestressed concrete in precast concrete industry are covered in the text
- Prominent prestressed concrete structures around the world are compiled
- A critical survey of prospective progress in prestressed concrete is presented
- The present edition is enriched with rich pedagogy, which includes:
  - Solved Examples: 178
  - Review Questions: 280
  - Objective Questions: 280
  - Exercise Questions: 132
  - Selective Illustrations: 405
  - Exhaustive References: 616

Web Supplements

Instructors can access teaching supplements at http://www.mhhe.com/kr/psc6

Structure of the Book

The monograph covers the theory and design of prestressed concrete prescribed for the senior undergraduate and postgraduate students of civil, structural and transportation engineering streams of various technical institutions across India. The structural design aspects are useful for the design consultants and practising structural engineers. The book presents a concise exposition of the integrated limit state design principles illustrated by worked out examples relevant to design practise. The book incorporates the specifications of various national and international codes such as IS: 1343-2012, IS: 456-2000, IRC: 112-2011, BS EN: 1992-1-1-2011 and ACI: 318M-2011.

The introductory **Chapter 1** traces the historical development of prestressed concrete from its inception including the development of high strength materials, terminology, advantages and applications of prestressed concrete. The salient properties of high strength concrete and steel specified in the revised codes are examined in **Chapter 2**. Prestressing systems and the analysis of stresses, losses of prestress and deflection characteristics of prestressed members under serviceability limit states are covered in **Chapters 3 to 6**. The flexural, shear and torsional resistance of prestressed concrete members together with the design of anchorage zone reinforcements are examined in the light of various codified procedures in **Chapters 7 to 10**.

The development and application of limit state design concepts for the design of prestressed concrete members followed by the design of prestressed concrete sections, pretensioned and post-tensioned flexural members, composite construction, continuous beams and portal frames are covered in **Chapters 11 to 15**. The design of sanitary structures like pipes, tanks and flat structural elements like floor and roofing systems comprising slabs, grids, shells and folded plates and miscellaneous structures like poles, piles, pressure vessels and pavements are covered in **Chapters 16 to 19**. A brief introduction to the optimum design of prestressed members is presented in **Chapter 20**.

The designs of bridge decks comprising the slab, tee beam, cellular box and rigid frame types conforming to the revised IRC codes are covered in **Chapter 21**. The design of prestressed concrete roofing systems is outlined in **Chapter 22**. The planning and economical aspects together with the construction management of prestressed concrete structures are covered in **Chapters 23 and 24**. Maintenance and rehabilitation along with case histories of restoration of damaged prestressed concrete structures are presented in **Chapter 25**. The application of high performance and nano concrete technology in prestressed concrete structures is presented in **Chapters 26 and 27**.

New to the Edition

The new **Chapter 28** compiles the application of prestressed concrete in precsat concrete industry with illustrative examples. **Chapter 29** deals with a concise compilation of the prominent and outstanding prestressed concrete structures like the longest span bridges of different types, largest domes, tanks, shell roofs, pipes and silos and longest beams, trussed girders, folded plates and poles spread in different countries around the world. **Chapter 30** presents a critical analysis of the prospective progress in prestressed concrete in the light of developments in nano concrete and nano engineered steels and their applications in construction technology.

Most of the chapters are fortified with numerical examples followed by exhaustive references which will be immensely useful to students, teachers and practising engineers. The exercise examples will help the students preparing for the university and competitive examinations. The review and objective questions are intended for a critical understanding of the subject matter presented in the chapter. In keeping with the spirit of '**drawing is the language of the engineer'**, numerous figures in the various chapters will help in a clearer understanding of the subject matter.

Acknowledgements

I gratefully acknowledge the following institutions, associations, societies and journals for the reproduction of certain design data, tables, figures and reference material mentioned throughout the text: American Concrete Institute, Prestressed Concrete Institute, British Standards Institution, Bureau of Indian Standards, Australian Standards Association and German Standards Institution, Federation International Precontrainte, European Concrete Committee, American Water Works Association, Cement and Concrete Association, Institution of Civil Engineers, American Society of Civil Engineers, Institution of Engineers (India), International Association for Bridge and Structural Engineering, Structural Engineering Research Centre, Roorkee, Concrete Development Company, Iver (Bucks), Magazine of Concrete Research, Building Science, Indian Concrete Journal and Structural Engineer. The complete details of the sources are presented in the form of references at the end of each chapter.

I am deeply indebted to Dr E W Bennett, Prof Fritz Leonhardt and Prof. Ben C Gerwick Jr., whose innumerable works served as a source material and inspired me in the preparation of this book. During the course of writing, I have had the advantage of the generous help of many, but in particular, I would wish to acknowledge with thanks the help rendered by Shri B P Mallikarjuna, Prof P Surya Prakasha Rao and the encouragement provided by Prof B S Basavarajaiah and other colleagues of the civil engineering faculty of the Karnataka Regional Engineering College, Srinivasnagar.

I herewith express my gratitude to my former colleagues at M S Ramaiah Institute of Technology, Bangalore, for their constant encouragement and kind cooperation.

I would also like to thank the following reviewers for their valuable suggestions and comments:

Pradeep Kumar Mehta	*MNNIT Allahabad*
S B Singh	*BITS Pilani*
Nazrul Islam	*Jamia Millia Islamia, New Delhi*
Amlan Das	*National Institute of Technolgy, Durgapur*
S S Mishra	*National Institute of Technolgy, Patna*
G Bhaskar	*Institute of Road and Transport Technology, Erode, Tamil Nadu*
Nagamani K	*College of Engineering, Anna University, Chennai*
G Rajesh Kumar	*National Institute of Technology, Warangal*
Ravi Sinha	*IIT, Mumbai*
R Prabhakara	*University of Bengaluru*
N M Janakiram	*University of Bengaluru*
K U Muthu	*Visvesvaraya Technological University, Belgaum*

I would like to express my gratitude to many of my colleagues in my profession and practising engineers for providing useful data on the latest developments in the field of prestressed nano and high performance concretes. I am grateful to my wife, Pramila Raju, for assisting in the preparation of the text matter on computer. Sincere thanks are also due to Tushar Mishra and Amit Chatterjee of McGraw-Hill Education (India) for their continued encouragement and effective cooperation in bringing out this edition in a record time.

Feedback

Constructive feedbacks/opinions from the readers will be of great help and the author welcomes any constructive criticism(s) and suggestion(s) which will be immensely helpful in updating the text in future reprints and editions. Readers can send their feedback to *nkrishna1935@gmail.com*

N. Krishna Raju

Preface to the First Edition

The prophetic words of Yves Guyon, “there is probably no structural problem to which prestressed concrete cannot provide a solution and often a revolutionary one” have been amply justified if one scans through the tremendous progress achieved in the field of analysis, design and construction of prestressed concrete structures, during the last three decades. Prestressed concrete is often preferred, and not without valid reason, in the construction of building, sanitary, hydraulic, highway, nuclear and marine structures. As such it is a powerful tool for a structural engineer.

The subject of prestressed concrete is compulsorily included in the undergraduate curriculum of civil engineering and postgraduate courses in structural engineering of various universities in India and abroad. With the introduction of limit state concepts, the traditional method of elastic and ultimate load designs are unified to form the basis of limit state design, the impact of which can be seen in the revised versions of the various national and international codes on structural concrete.

The book covers the subject of theory and design of prestressed concrete to the extent required by senior undergraduate and postgraduate students and partially fulfils the requirements of practising structural design engineers. The book presents a concise exposition of the integrated design principles, illustrated by worked out examples relevant to design practice. The book is based on the various national codes, such as the Indian (IS: 1343–1980), British (CP: 110: 1972) and American (ACI: 318–71) codes, and the recommendations of the European Concrete Committee. The International system (SI) of units has been used throughout and the notation generally conforms to the prescribed norms set by the European Concrete Committee in 1971 and since adopted as standard by the American, British and Indian standard codes of practice.

The basic concepts of prestressing and the salient properties of high strength concrete and steel which form the main constituents of prestressed concrete are covered in the first two chapters. The various prestressing systems are examined in Chapter 3, while the analysis of stresses, losses of prestress and deflection characteristics of prestressed members under serviceability limit states are covered in Chapters 5 and 6. The flexural, shear and torsional resistance of prestressed concrete members and the design of anchorage zone reinforcement are examined in the light of several codified procedures in Chapters 7 to 10.

The subsequent Chapters 11 to 15 deal with the development and application of limit state design concepts for the design of prestressed concrete members followed by the design of prestressed sections, pretensioned and post-tensioned flexural members composite construction continuous beams and portal frames.

The design of sanitary structures, such as pipes and tanks, floor and roof systems comprising slabs, grids, shells and folded plates, and miscellaneous structures like poles, piles, pressure vessels and pavements are covered in Chapters 16 to 19. The book concludes with a brief introduction to the optimum design of prestressed concrete structures. The numerical examples worked out in the “various chapters and the additional examples presented at the end of each chapter are intended for students preparing for university examinations while the exhaustive reference material quoted will be useful to research students and practising engineers.

In keeping with the spirit of ‘drawing is the language of the engineer’, numerous figures have been included which it is hoped will help in a clearer understanding of the subject matter. Finally, the author welcomes constructive criticisms and suggestions which will be immensely helpful in updating the text.

N. Krishna Raju

List of Symbols

1. Latin upper case letters

A	Cross-sectional area of member
A_{br}	Bearing area
A_c	Area of concrete section
A_{ct}	Area of concrete in tension zone
A_i	Area of the *in situ* concrete section
A_{pf}	Area of prestressing steel for flange
A_{pw}	Area of prestressing steel for web
A_{ps}	Area of prestressing tendons
A_{pun}	Punching area
A_s	Area of non prestressed tension reinforcement
A_s'	Area of compression reinforcement
A_{sl}	Area of longitudinal reinforcement for torsion
A_{st}	Area of transverse reinforcement for torsion
A_{sv}	Area of transverse reinforcement for shear
A_{tot}	Area of total reinforcement
C	Torsional moment of inertia
C_{min}	Minimum cover to tensile steel
C_x	Torsional rigidity in the x-direction
C_y	Torsional rigidity in the y-direction
D_c	Density of concrete
D_f	Thickness of flange
D_x	Flexural rigidity in the x-direction
D_y	Flexural rigidity in the y-direction
E_c	Modulus of elasticity of concrete
E_{ce}, $E_{c,eff}$	Effective (long-term) modulus of elasticity of concrete
EI	Flexural rigidity
E_s	Modulus of elasticity of steel
F_{bst}	Bursting tension
F_d	Design load
F_k	Characteristic load
G_k	Characteristic dead load
I	Second moment of area of section
I_c	Second moment of area of uncracked concrete section
$I_{e,}$	Effective second moment of area for computation of deflection

I_r	Second moment of area of cracked concrete section
K	Friction coefficient for wave effect
K_1, K_2, K_3	Constants
L	Effective span
L_t	Transmission length
M	Bending moment
M_{cr}	Cracking moment
M_d	Design moment (serviceability state)
M_g	Bending moment due to dead loads
M_o	Moment necessary to produce zero stress in concrete at depth 'd'
M_q	Bending moment due to live loads
M_u	Ultimate moment
N	Force normal to a section
N_{adm}	Safe allowable axial load on column
N_{cr}	Cracking load
N_d	Design tensile load
N_{min}	Minimum tensile load
N_u	Ultimate load capacity of axially loaded short column
N_{ub}	Ultimate load capacity of a short column subjected to axial load and bending moment
P	Prestressing force
P_k	Characteristic load in tendon
P_o	Prestressing force in the tendon at the jacking end
P_i	Initial prestresing force
P_t	Prestressing force after time 't'
P_x	Prestressing force at a distance 'x' from the jack
Q_k	Characteristic variable load
R	Radius of the shell structure
RH	Relative humidity of the ambient environment in percent
S	Statical moment or first moment of area of concrete section
T	Torsional moment due to ultimate loads
T_{tp}	Torsional resistance moment of the prestressed concrete section
T_{ts}	Torsional resistance due to non prestressed reinforcement
T_t	Ultimate torsional resistance
V	Shear force at a section
V_c	Ultimate shear resistance of concrete
V_{cw}	Ultimate shear resistance of concrete section uncracked in flexure (web cracks)
V_{cf}	Ultimate shear resistance of concrete section cracked in flexure
V_u	Ultimate shear force
W_k	Characteristic concentrated wind load
Z	Section modulus
Z_t	Section modulus of top fiber of beam section
Z_b	Section modulus of bottom fiber of beam section

2. Latin lower case letters

a	Deflection
a_1	Spacing's of ribs in X-direction
b	Breadth of section or compression face
b_1	Spacings of ribs in Y-direction
b_w	Breadth of web
c	Cover to steel reinforcement
d	Effective depth of tension reinforcement
d'	Cover to compression reinforcement
d_{ps}	Depth from compression face to tensioned steel
d_{us}	Depth from compression face to untensioned steel
e	Eccentricity of prestressing force with respect to the centroid of section
f_c	Compressive stress in concrete
f_c', f_{cy}	Characteristic cylinder compressive strength of concrete
f_{ck}, f_{cu}	Characteristic cube strength of concrete
f_{ci}	Compressive strength of concrete at initial transfer of prestress
f_{cp}	Compressive stress at centroidal axis due to prestress
f_{cr}', f_{cr}	Flexural tensile strength of concrete
f_{ct}	Allowable compressive stress in concrete at initial transfer of prestress
$f_{ct,eff}$	Tensile strength of concrete at the time of cracking
f_{cw}	Allowable compressive stress in concrete under service loads
f_{ctd}	Design value of concrete tensile strength (f_{ct}/γ_m)
f_{ctm}	Mean value of axial tensile strength of concrete
$f_{ctm,\,fl}$	Mean flexural tensile strength of reinforced concrete
f_d	Design strength of material
f_h	Direct stress
f_{inf}	Prestress in concrete at bottom of section (inferior)
f_k	Characteristic strength of material
f_{max}, f_{min}	Maximum and minimum principal stresses
f_p	Characteristic strength of prestressing steel
f_{pb}	Tensile stress in tendons at failure
f_{pe}	Effective stress in tendons after losses
f_{pi}	Initial stress in tendons
f_{pu}, f_p	Characteristic strength of prestressing tendons
f_s	Stress in reinforcement
f_{sc}	Compressive stress in reinforcement
f_{st}	Tensile stress in reinforcement
f_{sup}	Prestress in concrete at top of section (superior)
f_t	Characteristic tensile strength of concrete
f_{tt}	Allowable tensile stress in concrete at initial transfer of prestress
f_{tw}	Allowable tensile stress in concrete under service loads
f_v	Transverse tensile stress
f_y, f_{yk}	Characteristic tensile strength of reinforcement

f_{yl} Characteristic strength of stirrups for torsion
f_{yv} Characteristic strength of stirrups for shear
g Distributed dead load or acceleration due to gravity
h Overall depth of the member
h_f Thickness of compression flange
h_{max} The larger dimension of the section
h_{min} The smaller dimension of the section
i Radius of gyration
k Constant
m Modular ratio
n Neutral axis depth factor
q Distributed load
s Spacing of stirrups or links
t Time
u Perimeter
w_c Density of concrete
w_{cr} Design surface crack width
w_k Characteristic crack width
w_{min} Minimum uniformly distributed load
w_{ud} Ultimate design load
w Crack width
x Linear coordinate of depth of neutral axis
x_1 Smaller dimension of transverse reinforcement
x_u Neutral axis depth
y Vertical distance of a point from centroid of concrete section
y_b Distance of lower point (inferior) from centroid of concrete section
y_1 Larger dimension of transverse reinforcement
y_o Half depth of bearing area anchorage zone
y_{po} Half depth of punching area of anchorage zone
y_t Distance of highest (superior) point from centroid of cross section
z Lever arm between the compressive force in concrete and the tensile force in steel

3. Greek lower case letters

α Angle, ratio or dimensionless coefficient
α_e Modular ratio
β Dimensionless coefficient
γ_f Partial safety factor for loads
γ_m Partial safety factor for material strength
ε Strain
ε_c Strain in concrete
ε_{ce} Ultimate creep strain in concrete
ε_{cs} Total shrinkage strain
ε_{cd} Drying shrinkage strain
ε_{ca} Autogeneous shrinkage strain

$\varepsilon_{\mathrm{cm}}$	Mean strain in concrete between cracks
$\varepsilon_{\mathrm{cu}}$	Ultimate compressive strain in concrete
ε_{m}	Average strain at the level where the cracking is considered
ε_{s}	Strain in steel
$\varepsilon_{\mathrm{se}}$	Effective strain in tendons after all losses
$\varepsilon_{\mathrm{sm}}$	Mean strain in the reinforcement
P	Reinforcement ratio
$\rho_{\rho,\,\mathrm{eff}}$	Effective reinforcement ratio based on an effective concrete tension area
η	Reduction factor for loss of prestress or loss ratio
θ	Rotation of the beam at supports
μ	Coefficient of friction
τ	Shear stress
τ_{b}	Bond stress, generally
τ_{c}	Shear stress in concrete
τ_{bp}	Bond stress between concrete and prestressing steel
τ_{t}	Shear stress due to torsion, ϕ
τ_{u}	Ultimate shear stress
τ_{v}	Shear stress due to transverse shear
ϕ	Creep coefficient or capacity reduction factor
ϕ_{I}	Initial curvature
ϕ_{mt}	Change of curvature caused by transverse loads
ϕ_{pt}	Change of curvature caused by prestress
ν_{c}	Poisson's ratio for concrete
ν_{s}	Poisson's ratio for steel
Δ	Difference in increment
ψ	Dimensionless coefficient
ϕ	Diameter of the reinforcing bar
β_1	Factor depending upon the compressive strength of concrete
λ	Factor depending upon the density of concrete
ξ_c	Design shear strength of concrete
Σ	Sum

1 Introduction

1.1 Basic Concepts of Prestressing

Prestressed concrete is basically concrete in which internal stresses of a suitable magnitude and distribution are introduced so that the stresses resulting from external loads are counteracted to a desired degree. In reinforced concrete members, the prestress is commonly introduced by tensioning the steel reinforcement.

The earliest examples of wooden barrel construction by force-fitting of metal bands and shrink-fitting of metal tyres on wooden wheels indicate that the art of prestressing has been practised from ancient times. The tensile strength of plain concrete is only a fraction of its compressive strength and the problem of it being deficient in tensile strength appears to have been the driving factor in the development of the composite material known as "reinforced concrete".

The development of early cracks in reinforced concrete due to incompatibility in the strains of steel and concrete was perhaps the starting point in the development of a new material like "**prestressed concrete**". The application of permanent compressive stress to a material like concrete, which is strong in compression but weak in tension, increases the apparent tensile strength of that material, because the subsequent application of tensile stress must first nullify the compressive prestress. In 1904, Freyssinet[1] attempted to introduce permanently acting forces in concrete to resist the elastic forces developed under loads and this idea was later developed under the name of "**prestressing**".

1.2 Historical Development

The present state of development in the field of prestressed concrete is due to the continuous research done by engineers and scientists in this field during the last 90 years.

In 1886, Jackson of San Francisco applied for a patent for "construction of artificial stone and concrete pavements", in which prestress was introduced by tensioning the reinforcing rods set in sleeves. Dohring of Germany manufactured slabs and small beams in 1888, using embedded tensioned wires in concrete to avoid cracks.

The idea of prestressing to counteract the stresses due to loads was first put forward by the Austrian engineer, Mandl, in 1896. M Koenen, of Germany, further developed the subject by reporting, in 1907, on the losses of prestress due to elastic shortening of concrete. The importance of losses in prestressing due to shrinkage of concrete was first recognised by Steiner in the United States around 1908. In 1923, Emperger[2] of Vienna developed a method for making wire-bound reinforced concrete pipes by binding high-tensile steel wires on pipes at stresses ranging from 160 to 800 N/mm^2.

The use of unbonded tendons was first demonstrated by Dischinger, in 1928, in the construction of a major bridge of the deep-girder type, in which prestressing wires were placed inside the girder without any bond. Losses of prestress were compensated by the subsequent retensioning of the wires. Based on the exhaustive studies of properties of concrete and steel, Freyssinet demonstrated, in 1928, the advantages of using high-strength steel and concrete to account for the various losses of prestress due to creep and shrinkage of concrete.

The development of vibration techniques for the production of high-strength concrete and the invention of the double-acting jack for stressing high-tensile steel wires are considered to be the most significant contributions made by Freyssinet between 1928 and 1933.

The use of prestressed concrete spread rapidly from 1935 onwards and many long-span bridges were constructed between 1945 and 1950 in Europe and the United States. During the last 60 years, prestressed concrete has been widely used for the construction of long-span bridges, industrial shell roofs, marine structures, nuclear pressure vessels, water-retaining structures, transmission poles, railway sleepers and a host of other structures. In the words of Guyon[3]: "**There is probably no structural problem to which prestress cannot provide a solution, and often a revolutionary one. Prestress is more than a technique; it is a general principle**".

1.3 Need for High-Strength Steel and Concrete

The significant observations which resulted from the pioneering research on prestressed concrete were:

1. Necessity of using high-strength steel and concrete.
2. Recognition of losses of prestress due to various causes.

The early attempts to use mild steel in prestressed concrete were not successful, as a working stress of 120 N/mm^2 in mild steel is more or 1ess completely lost due to elastic deformation, creep and shrinkage of concrete.

The normal loss of stress in steel is generally about 100 to 240 N/mm^2 and it is apparent that if this loss of stress is to be a small portion of the initial stress, the stress in steel in the initial stages must be very high, about 1200 to 2000 N/mm^2. These high stress ranges are possible only with the use of high-strength steel.

High-strength concrete is necessary in prestressed concrete, as the material offers high resistance in tension, shear, bond and bearing. In the zone of anchorages, the bearing stresses being higher, high-strength concrete is invariably preferred to minimise costs. High-strength concrete is less liable to shrinkage cracks, and has a higher modulus of elasticity and smaller ultimate creep strain, resulting in a smaller loss of prestress in steel. The use of high-strength concrete results in a reduction in the cross-sectional dimensions of prestressed concrete structural elements. With a reduced deadweight of the material, longer spans become technically and economically practicable.

1.4 Terminology

Various terms commonly used in the study of prestressed concrete are outlined in this section. The definitions detailed in this section largely comply with those recommended in the relevant Indian standard code of practise[4].

Tendon A stretched element used in a concrete member of structure to impart prestress to the concrete. Generally, high-tensile steel wires, bars cables or strands are used as tendons.

Anchorage A device generally used to enable the tendon to impart and maintain prestress in the concrete. The commonly used anchorages are the Freyssinet, Magnel Blaton, Gifford-Udall, Leonhardt-Baur, LeeMcCall, Dywidag, Roebling and BBRV systems.

Pretensioning A method of prestressing concrete in which the tendons are tensioned before the concrete is placed. In this method, the prestress is imparted to concrete by bond between steel and concrete.

Post-tensioning A method of prestressing concrete by tensioning the tendons against hardened concrete. In this method, the prestress is imparted to concrete by bearing.

Bonded prestressed concrete Concrete in which prestress is imparted to concrete through bond between the tendons and surrounding concrete. Pretensioned members belong to this group.

Non-bonded prestressed concrete A method of construction in which the tendons are not bonded to the surrounding concrete. The tendons may be placed in ducts formed in the concrete members or they may be placed outside the concrete section.

Full prestressing Prestressed concrete in which tensile stresses in the concrete are entirely obviated at working loads by having sufficiently high prestress in the members.

Limited or partial prestressing The degree of prestress applied to concrete in which tensile stresses to a limited degree are permitted in concrete under working loads. In this case, in addition to tensioned steel, a considerable proportion of untensioned reinforcement is generally used to limit the width of cracks developed under service loads.

Moderate prestressing In this type, no limit is imposed upon the magnitude of the tensile stresses at working loads. According to Leonhardt[5], this form of construction is not really prestressed concrete but is to be regarded as reinforced concrete with reduced cracking and the sections should be analysed according to the rules of reinforced concrete, as a case of bending combined with axial force.

Axial prestressing Members in which the entire cross-section of concrete has a uniform compressive prestress. In this type of prestressing, the centroid of the tendons coincides with that of the concrete section.

Eccentric prestressing A section at which the tendons are eccentric to the centroid, resulting in a triangular or trapezoidal compressive stress distribution.

Concordant prestressing Prestressing of members in which the cables follow a concordant profile. In the case of statically indeterminate structures, concordant prestressing does not cause any change in the support reactions.

Non-distortional prestressing In this type, the combined effect of the degree of prestress and the deadweight stresses is such that the deflection of the axis of the member is prevented. In such cases, the moments due to prestress and deadweight exactly balance resulting only in an axial force in the member.

Uniaxial, biaxial and triaxial prestressing These terms refer to the cases where concrete is prestressed (i) in only one direction, (ii) in two mutually perpendicular directions, and (iii) in three mutually perpendicular directions.

Circular prestressing The term refers to prestressing in round members, such as tanks and pipes.

Transfer The stage corresponding to the transfer of prestress to concrete. For pretensioned members, transfer takes place at the release of prestress from the bulkheads; for post-tensioned members, it takes place after the completion of the tensioning process.

Supplementary or untensioned reinforcement Reinforcement in prestressed members not tensioned with respect to the surrounding concrete before the application of loads. These are generally used in partially prestressed members.

Transmission length The length of the bond anchorage of the prestressing wire from the end of a pretensioned member to the point of full steel stress.

Cracking load The load on the structural element corresponding to the first visible crack.

Creep in concrete Progressive increase in the inelastic deformation of concrete under sustained stress component.

Shrinkage of concrete Contraction of concrete on drying.

Relaxation in steel Decrease of stress in steel at constant strain.

Proof stress The tensile stress in steel which produces a residual strain of 0.2 per cent of the original gauge length on unloading.

Creep-coefficient The ratio of the total creep strain to elastic strain in concrete.

Cap cable A short curved tendon arranged at the interior supports of a continuous beam. The anchors are in the compression zone, while the curved portion is in the tensile zone.

Degree of prestressing A measure of the magnitude of the prestressing force related to the resultant stress occurring in the structural member at working load.

Debonding Prevention of bond between the steel wire and the surrounding concrete.

1.5 Advantages of Prestressed Concrete

Prestressed concrete offers great technical advantages in comparison with other forms of construction, such as reinforced concrete and steel. In the case of fully prestressed members, which are free from tensile stresses under working loads, the cross-section is more efficiently utilised when compared with a reinforced concrete section which is cracked under working loads. Within certain limits, a permanent dead load may be counteracted by increasing the eccentricity of the prestressing force in a prestressed structural element, thus effecting savings in the use of materials.

Prestressed concrete members possess improved resistance to shearing forces, due to the effect of compressive prestress, which reduces the principal tensile stress. The use of curved cables, particularly in long-span members, helps to reduce the shear forces developed at the support sections.

A prestressed concrete flexural member is stiffer under working loads than a reinforced concrete member of the same depth. However, after the onset of cracking, the flexural behaviour of a prestressed member is similar to that of a reinforced concrete member.

The use of high-strength concrete and steel in prestressed members results in lighter and slender members than is possible with reinforced concrete. The two structural features of prestressed concrete, namely high-strength concrete and freedom from cracks, contributes to the improved durability of the structure under aggressive environmental conditions. Prestressing of concrete improves the ability of the material for energy absorption under impact loads. The ability to resist repeated working loads has been proved to be as good in prestressed as in reinforced concrete.

The economy of prestressed concrete is well established for long-span structures. According to Dean[6], standardised precast bridge beams between 10 and 30 m long and precast prestressed piles have proved to be more economical than steel and reinforced concrete in the United States. According to Abeles[7], precast prestressed concrete is economical for floors, roofs, and bridges of spans up to 30 m, and for cast *in situ* work, up to 100 m. In the long-span range, prestressed concrete is generally more economical than reinforced concrete and steel.

Prestressed concrete has considerable resilience due to its capacity for completely recovering from substantial effects of overloading without undergoing any serious damage. Leonhardt[8] points out that in prestressed concrete elements, cracks which temporarily develop under occasional overloading close up completely when the loads are removed. Since the fatigue strength of prestressed concrete is comparatively better than that of other materials, chiefly due to the small stress variations in prestressing steel, it is recommended for dynamically loaded structures, such as railway bridges and machine foundations. Due to the utilisation of concrete in the tension zone, an extra saving of 15 to 30 per cent in concrete is possible in comparison with reinforced concrete. The savings in steel are even higher, 60 to 80 per cent, mainly due to the high permissible stresses allowed in the high-tensile wires. Although there is considerable saving on the quantity of materials used in prestressed concrete members in comparison with reinforced concrete members, it is not much significant due to the additional costs incurred for the high-strength concrete, high-tensile steel, anchorages, and other hardware required for the production of prestressed members. However, there is an overall economy in using prestressed concrete, as the decrease in dead weight reduces the design loads and the cost of foundations.

1.6 Applications of Prestressed Concrete

It is a well-established fact that the basic economy of prestressed concrete lies in its high strength to weight and strength to cost ratios, its resistance to fire and cracking, and its versatility and adaptability.

The use of prestressed concrete has revolutionised the entire building industry in the erstwhile USSR, USA, UK, Japan and the Continent. Prestressed concrete building components comprising hollow cored and ribbed slabs are widely used in the erstwhile Russia. Single- and double-tee units and channel sections are popular in the USA for the construction of floors in buildings. Figure 1.1 shows the use of precast prestressed double-T beams[9] for floor construction. Typical prestressed concrete *flat slab floor* construction using the lift slab technique[10] is shown in Fig. 1.2.

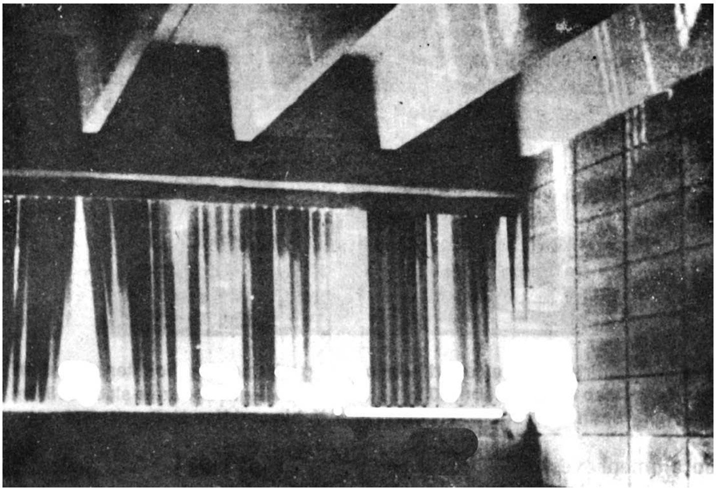

Fig. 1.1 *Precast prestressed double-T floor beams (Courtesy: Arthur H Nilson, Ref. 9)*

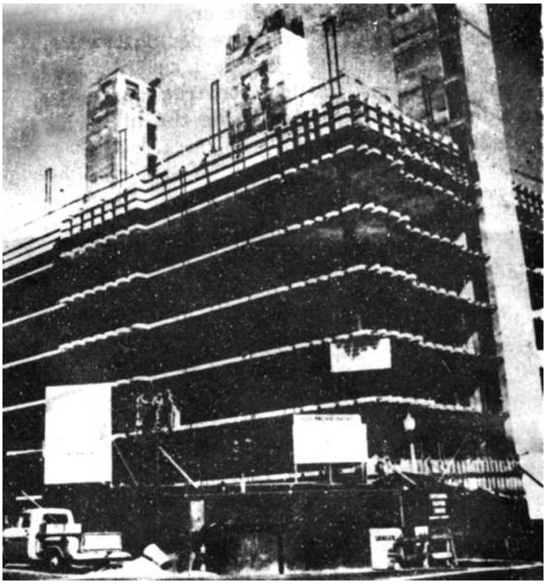

Fig. 1.2 *Thirteen storey apartment building with precast post-tensioned in slab construction, 203 mm thick light weight concrete slabs of 8.6 m span San Francisco (Courtesy: TV Lin and Ned H Burns, Ref. 10)*

Prestressed concrete is ideally suited for long-span bridge construction. A typical twin-box girder bridge under construction, using the segmentally cast cantilever method, is shown in Fig. 1.3. The present trend is to adopt prestressed concrete for long-span cable-stayed bridges which are aesthetically superior and economical in comparison with steel bridges. A typical cable-stayed bridge[11] of 365 m main span, constructed at Tampa Bay, Florida, USA, is shown in Fig. 1.4. The longest precast prestressed concrete cable-stayed box girder, the Chaco-Corrientes bridge constructed in Argentina, South America, is shown in Fig. 1.5.

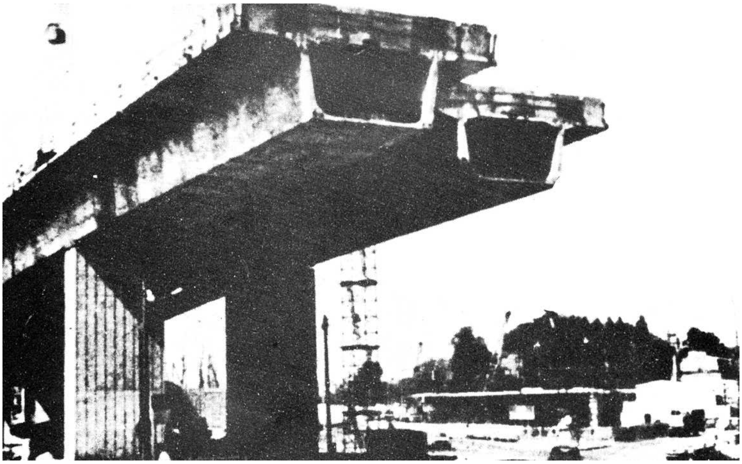

Fig. 1.3 *Post-tensioned prestressed concrete twin box girder bridge under construction using the segmentally cast cantilever method (Courtesy: Arthur H Nilson, Ref. 9)*

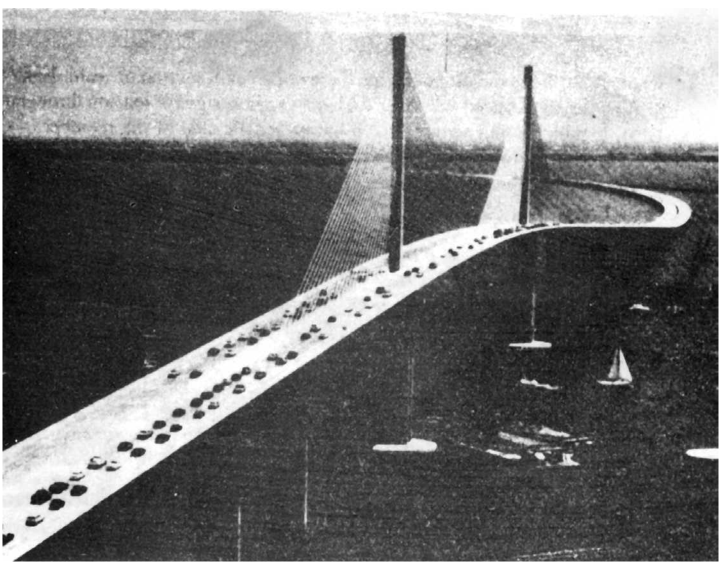

Fig. 1.4 *Sunshine Sky Bridge, Tampa Bay, Florida, 365 m main span cable-stayed bridge (Courtesy: Edward G Nawy, Ref. 11)*

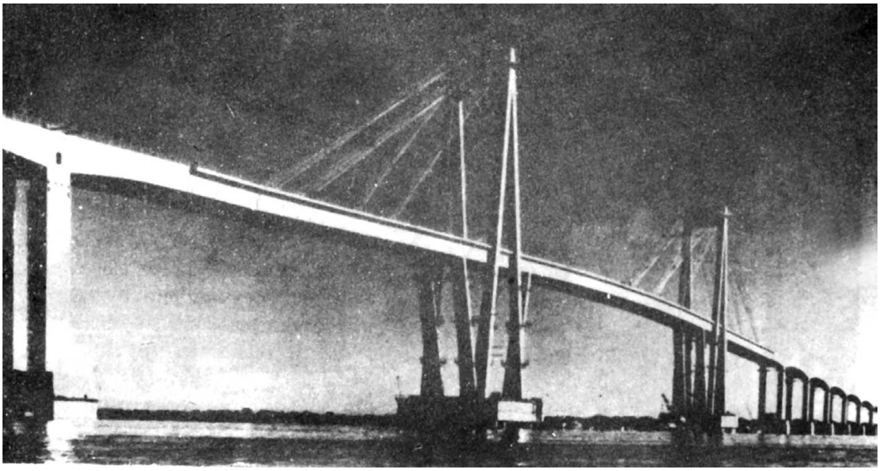

Fig. 1.5 *Chaco-Corrientes Bridge, Argentina, the longest precast prestressed concrete cable-stayed box girder bridge in South America (Courtesy: Edward G Nawy, Ref. 11)*

Typical use of prestressed concrete simple-span box girders for the Bay area rapid-transit system in San Francisco, California, is shown in Fig. 1.6. Prestressed concrete has found extensive applications in the construction of long-span folded plate roofs[12], aircraft hangers[13], nuclear containment vessels[14], pavements[15,16], rail-road sleepers[17], poles[18,19], piles[20], television towers and masts[21].

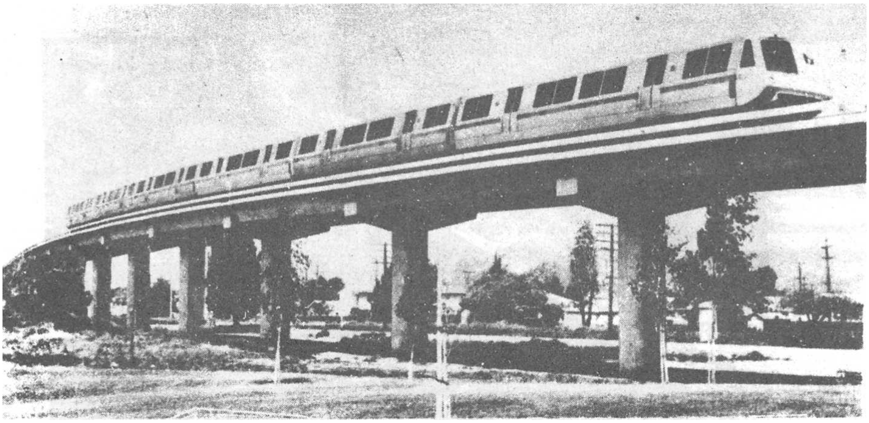

Fig. 1.6 *Precast prestressed box girders of 21 m span and 3.35 m wide, California Guide Ways (Courtesy: Eward G Nawy, Ref. 11)*

Figure 1.7 shows a typical long-span folded plate roof with draped tendons in the plates. A prestressed concrete space-frame used for an aircraft service depot at Gatwick, England, is shown in Fig. 1.8.

Fig. 1.7 *Prestressed concrete folded plate roof structure (Courtesy: Arthur H Nilson, Ref. 9)*

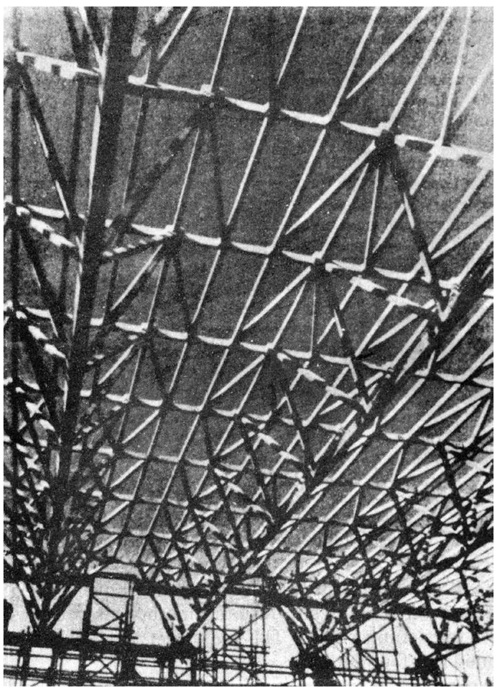

Fig. 1.8 *Prestressed concrete space frames for Aircrafts Service Depot at Gatwick, England*

In recent years, prestressed concrete has found novel applications in the construction of a variety of marine structures,[22] such as floating docks, off-shore oil-drilling platforms, giant floating liquefied gas and oil-storing vessels[23]. Typical examples of these various types of structures are shown in

Figs. 1.9 to 1.12. Prestressed concrete has found extensive application in the construction of large-capacity liquid-retaining structures. Figure 1.13 shows the circumferential wire-winding operation for a prestressed concrete tank wall.

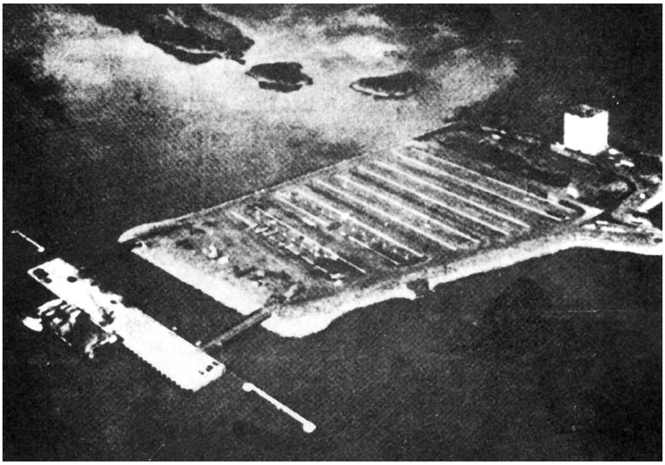

Fig. 1.9 *Prestressed concrete Valdez Floating Dock, built in two pieces in Tacoma, Washington and towed to Alaska by deployment (Courtesy: Edward G Nawy, Ref. 11)*

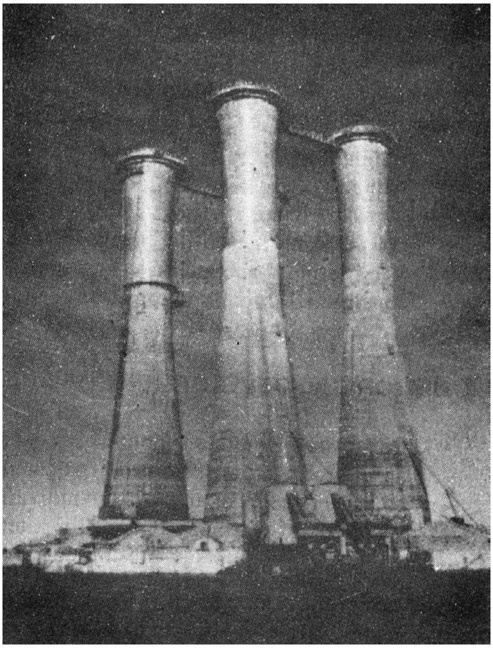

Fig. 1.10 *Stratfjord "B" condeep off shore oil drilling platform, Norway (Courtesy: Ben C Gerwick, Ref. 22)*

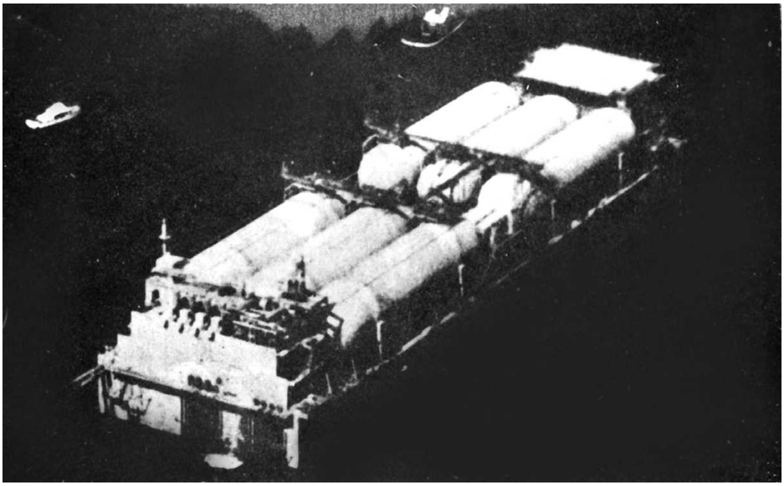

Fig. 1.11 *Arco Floating LPG. Barge: ABAM-designed largest floating prestressed hull in the world (Courtesy: Edward G Nawy, Ref. 11)*

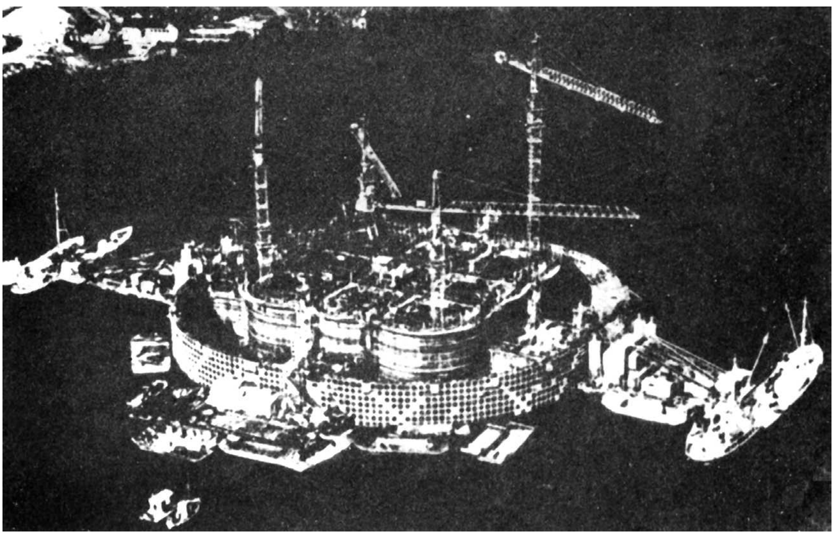

Fig. 1.12 *Ekofisk off shore reservoir in the North Sea with combined precast and cast in place concrete post-tensioned to form completed structure (Courtesy: TY Lin and Ned. H Burns, Ref. 10)*

The application of prestressed concrete in tall towers to support restaurants, observation decks, radio and television facilities originated in 1953 with the famous Stuttgart Tower, which is 211 m tall and designed by Prof. Fritz Leonhardt. The CNN Tower, shown in Fig. 1.14, is 553 m tall located in Toronto. The Burj Khalifa building (Dubai, UAE) is the world's tallest building soaring up to a height of 828 m.

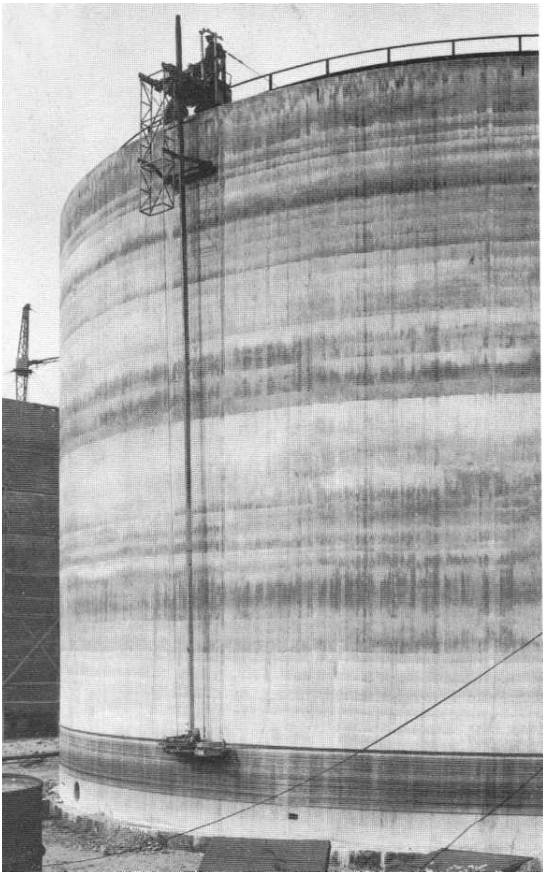

Fig. 1.13 *Prestressing preload circular tank wall with wire winder, Preload Technology, New York*

Notable examples of prestressed concrete structures in India include:

1. The Lubha bridge[24], the nation's longest single-span 172 m long prestressed concrete box-girder-type continuous bridge built across a 30 m deep gorge of the Lubha river in Assam. (Fig. 1.15)
2. Gomti aqueduct, which is the longest and the biggest aqueduct in India comprising 9.9 m deep prestressed concrete girders each weighing as much as 5500 kN over a span of 31.8 m, located in Uttar Pradesh.
3. Ball tank, Trombay, Maharashtra, consisting of a prestressed concrete tank of four million litre capacity for the department of atomic energy.
4. The Boeing hanger at Santa Cruz airport with a roof consisting of barrel shells supported on prestressed concrete edge beams spanning over 45.73 m.
5. Ganga bridge in Patna, the longest prestressed concrete bridge in the world has a total length of 5575 m consisting of continuous spans of 121.65 m long prestressed concrete girders of variable depth.

6. Silo in Nangal, 312 m long, built with precast concrete segments and *in situ* joints which are prestressed for the storage of fertilisers.

Fig. 1.14 *The world's tallest prestressed concrete CN Tower, Toronto, 553 m overall height (Courtesy: Arthur H Nilson, Ref. 9)*

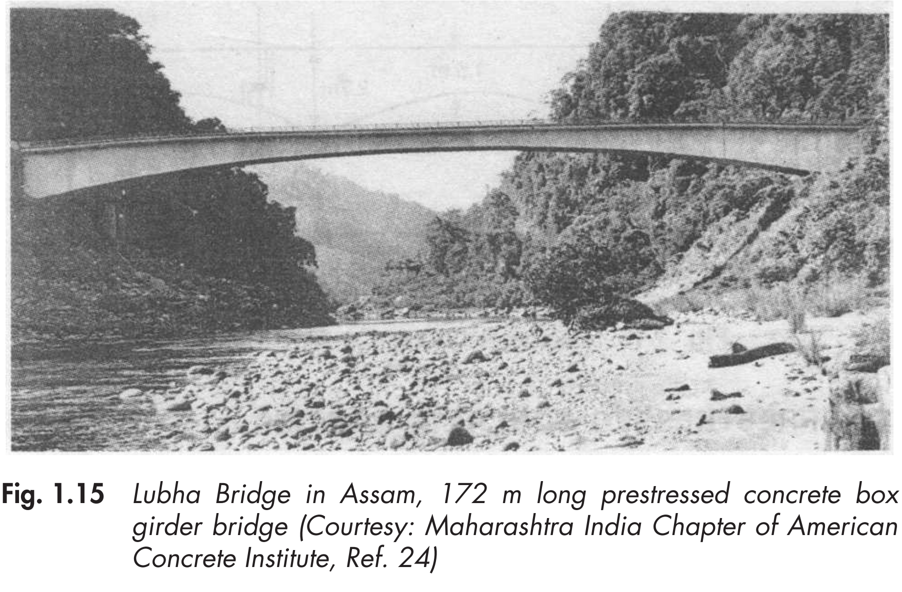

Fig. 1.15 *Lubha Bridge in Assam, 172 m long prestressed concrete box girder bridge (Courtesy: Maharashtra India Chapter of American Concrete Institute, Ref. 24)*

7. Zuari bridge in Goa, 807 m long, comprising prestressed concrete cantilever box girders with four main spans of 122 m, two end spans of 69.5 m and a via duct with five spans of 36 m. The precast segments 3 m long, varying in depth from 2.07 m to 8.05 m were assembled and prestressed using Freyssinet system (Fig. 1.16).

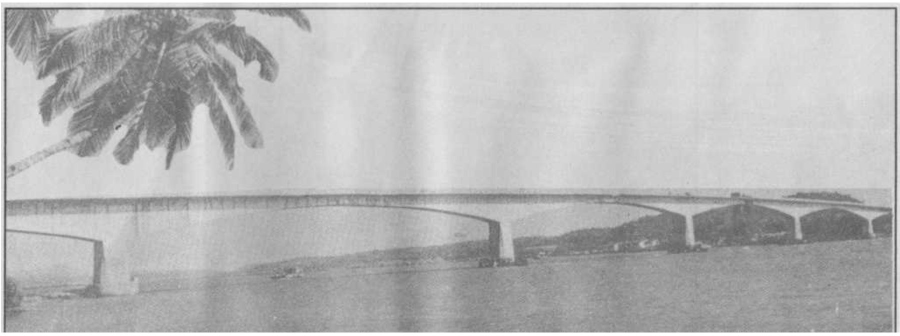

Fig. 1.16 *Zuari Bridge, Goa, 807 m long, four span double cantilever prestressed concrete box girder bridge (Courtesy: Maharashtra India Chapter of American Concrete Institute, Ref. 24)*

8. Cable-stayed prestressed concrete bridge across the Brahmaputra in Jogighopa, Assam, with a span of 286 m between the two towers and two side spans of 114 m, comprising single-cell prestressed concrete box-girders.
9. The Vidyasagar Sethu, cable-stayed bridge in Kolkata, shown in Fig. 1.17, with a central span of 457 m, is the longest cable-stayed bridge in India. At present, Russia holds the record for the longest span cable-stayed bridge "Russky" located in Vladivostok with a span of 1104 m and completed in 2012. The record for longest span prestressed concrete bridge is currently held by China with the bridge Shibanpo, constructed in 2006 at Chongqing with a span of 330 m. At present, China is credited to have more than 50 per cent of the world's ten longest cable-stayed bridges located in its various provinces.

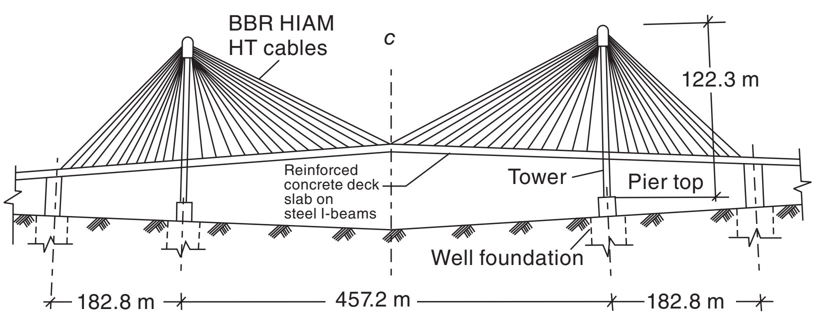

Fig. 1.17 *Vidyasagar Sethu cable-stayed bridge in Kolkata*

10. The tallest cable-stayed bridge is located outside Millau in France. The bridge extending over a length of 2.46 km is considered as an engineering feat since some of its pillars rise gracefully to a height more than 300 m. The bridge designed by the famous British architect, Sir Norman Foster, is currently the world's tallest cable-stayed bridge and is shown in Fig. 1.18.

Fig. 1.18 *World's tallest and longest cable-stayed bridge in France*

11. The Ministry of Surface Transport, Government of India, has launched the Golden Quadrilateral Scheme connecting the capital cities of various states with modern highways. Bridges being the basic components of highway systems, have witnessed rapid progress and innovations during the last decade. Unprecedented increase in traffic in the capital cities of various states has necessitated the use of urban flyovers adopting prestressed concrete girder decks to support the metro rail and roadways.
12. Rapid developments in the field of concrete technology has resulted in concretes of characteristic strength reaching that of mild steel. New materials like silica fume and nano cements have significantly increased the compressive strength of concrete resulting in longer span lengths of prestressed concrete girders in highway systems throughout the world.

It is a fact that prestressing was a big break for the art of reinforcing. The brilliant idea of prestressing, conceived and put to practise by Freyssinet in the twentieth century, is considered to be the most significant event in the history of the art and technology of construction.

Freyssinet took patents in 1928 and was well set to sell the most exciting building material. Unfortunately, there were no buyers at that time. He had a bitter struggle for seven long years for the cause of prestressed concrete. The big boom in prestressed concrete was heralded only after the Second World

War when prestressed concrete was extensively used for over 300 bridges built in Germany during 1949–53. Prestressed concrete was introduced in the USA in 1949 for Magnel's Walnut bridge and around the same time for Coleroon bridge in South India using the Freyssinet system.

During the last sixty years, prestressed concrete has been used in the construction of buildings, and in transportation, marine, nuclear, environmental, power transmission and oil exploration structures. However, the idea of prestressing arose out of bridges and, according to Raina[25], bridges have the most impressive engineering applications of prestressed concrete.

The twenty-first century is all set to witness challenging and innovative applications of prestressed concrete in structural engineering practise.

References

1. Freyssinet, E, "The birth of prestressing," *Cement and Concrete Association Translation, No. CJ.* 59, London, 1956, p. 44.
2. Emperger, F, "Concrete tubes for internal pressure," *Concrete and Constructional Engineering,* Vol. 18, 1923, pp 701–708.
3. Guyon, Y, *Prestressed Concrete (Preface),* Vol. I, C.R. Books Ltd., London, 4th edn, 1960.
4. IS: 1343 *Indian Standard Code of Practice for Prestressed Concrete* (Second revision), Bureau of Indian Standards, New Delhi, (To be published).
5. Leonhardt, F, *Prestressed Concrete Design and Construction,* Wilhelm Ernst and Sohn, Berlin, 1964, p. 7.
6. Dean, WE, "Prestressed concrete difficulties overcome in Florida bridge practice," *Civil Engineering,* Vol. 27, June 1957, pp 404–408.
7. Abeles, PW, *An Introduction to Prestressed Concrete,* Vol. II, Concrete Publications Ltd., London 1965, p. 555.
8. Leonhardt, F, *Prestressed Concrete Design and Construction,* Wilhelm Ernst and Sohn, Berlin, 1964, pp 13-14.
9. Nilson Arthur, H, *Design of Prestressed Concrete,* 2nd edn, John Wiley and Sons, New York, 1987, pp 3–541.
10. Lin, TY and H Burns Ned, *Design of Prestressed Concrete Structures,* (3rd edn) (SI - Version), John Wiley and Sons, New York, 1982, pp 8–40.
11. Nawy Edward, G, *Prestressed Concrete, A Fundamental Approach,* Prentice-Hall, Englewood Cliffs, New Jersey 1989, pp 3–700.
12. Firnkas, S, "Prestressed folded plate hanger for Allegheny Airlines–Design and construction," *Journal of Prestressed Concrete Institute,* Vol. 16, No. 2, March-April 1971, pp 43–62.
13. Haines, WJM and AJ Harris, "Structure of aircraft service depot at Gatwick for Transair Limited," *Journal of Prestressed Concrete Institute*, Vol. 4, No. 3, December 1959, pp 46–60.
14. Hannah, IW, "Structural engineering of prestressed concrete reactor pressure vessels," *Nuclear Engineering and Design,* Vol. 50, No. 3, Nov. 1978, pp 443–462.

15. Sargious, M and SK Wang, "Economical design of prestressed concrete pavements," *Journal of Prestressed Concrete Institute,* Vol. 16, No. 4, July–August 1971, pp 64–79.
16. "Prestressed concrete pavement: Status Report," *Civil Engineering,* Vol. 54, No. 12, December 1984, pp 53–55.
17. Hanna, AN, "Prestressed concrete ties for North American rail roads," *Journal of the Prestressed concrete Institute,* Vol. 24, No. 5, September–October 1979, pp 32–61.
18. Zacharia George, KV Swaminathan, KG Salvi, and P Dayaratnam, "Prestressed Concrete Poles: State of the Art", *International Symposium on Prestressed Concrete Pipes Poles, Pressure Vessels and Sleepers, Proceedings* Vol. 1, Madras, India, 1974 PL/o pp 1–35.
19. Rodgers, TE, "Prestressed concrete poles: State of the art", *Journal of the Prestressed Concrete Institute,* Vol. 29, No. 5, September–October 1984. pp 52–103.
20. Abeles, PW and BK Bardhan-Roy, *Prestressed Concrete Designer's Handbook,* (3rd edn), A View-Point Publications, Cement and Concrete Association, Wexhamsprings, Slough, UK 1981, pp 425–436.
21. "Slip-formed tower post-tensioned to record height of 1805 ft," *Engineering News Record,* May 23, 1974, pp 18–20.
22. Gerwick, Jr, BC, "Concrete structures: key to development of the oceans," *Journal of the American Concrete Institute,* Vol. 71, No. 12, December 1974, pp 611–616.
23. Anderson, AR, "World's largest prestressed LPG floating vessel," *Journal of Prestressed Concrete Institute,* Vol. 22, No. 1, January–February 1977, pp 12–31.
24. Outstanding Concrete Structures of India, Compiled by *Maharashtra India Chapter of the American Concrete Institute,* Bombay, 1984, p. 120.
25. Raina, VK, *Concrete Bridge Practice, Analysis, Design and Economics,* Tata McGraw-Hill Publishing Co, New Delhi, 1991, pp 587–603.

Review Questions

1.1 What is the basic principle of prestressed concrete?
1.2 Why did the early attempts in prestressing using ordinary mild steel fail?
1.3 What is the necessity of using high-strength concrete and high tensile steel in prestressed concrete?
1.4 Distinguish between the terms (a) uniaxial (b) biaxial and (c) triaxial pre-stressing?
1.5 Where do you adopt circular prestressing?
1.6 Bring out the difference between concentric and eccentric prestressing.
1.7 Differentiate between full prestressing and partial prestressing.
1.8 What is non-distortional prestressing?
1.9 What is the necessity of using supplementary or untensioned reinforcement in prestressed concrete members?
1.10 What is debonding?

Objective-type Questions

1.1 In prestressed concrete members, the steel is under
(a) compression (b) tension (c) torsion

1.2 In axially prestressed members, the concrete is under
(a) tension (b) compression (c) torsion

1.3 Prestressing is possible by using
(a) mild steel
(b) high-strength deformed bars
(c) high-tensile steel

1.4 Prestressing steel has an ultimate tensile strength nearly
(a) twice that of HYSD bars
(b) thrice that of mild steel reinforcements
(c) four times that of HYSD bars

1.5 Prestressing is economical for members of
(a) long span (b) medium span (c) short span

1.6 Linear prestressing is adopted in
(a) circular tanks (b) pipes (c) beams

1.7 Circular prestressing is advantageous in
(a) beams (b) columns (c) pipes and tanks

1.8 Prestressing wires in electric poles are
(a) concentric (b) eccentric (c) parabolic

1.9 In the construction of large circular water tanks, it is economical to adopt
(a) reinforced concrete
(b) prestressed concrete
(c) steel

1.10 In cable-stayed bridges, the cables supporting the deck of the bridge are under
(a) compression (b) torsion (c) tension

Answers to Objective-type Questions

1.1 (b)	1.2 (b)	1.3 (c)	1.4 (c)	1.5 (a)
1.6 (c)	1.7 (c)	1.8 (a)	1.9 (b)	1.10 (c)

2 Materials for Prestressed Concrete

2.1 High-Strength Concrete

2.1.1 High-Strength Concrete Mixes

Prestressed concrete requires concrete which has a high compressive strength at a reasonably early age, with comparatively higher tensile strength than ordinary concrete. Low shrinkage, minimum creep characteristics and a high value of Young's modulus are generally deemed necessary for concrete used for prestressed members. Many desirable properties, such as durability, impermeability and abrasion resistance, are highly influenced by the strength of concrete. With the development of vibration techniques in 1930, it became possible to produce, without much difficulty, high-strength concrete having 28-day cube compressive strength in the range of 30–70 N/mm^2. Recent developments in the field of concrete-mix design have indicated that it is now possible to produce even ultra high-strength concrete, of any desired 28-day cube compressive strength ranging from 70–100 N/mm^2, without taking recourse to unusual materials or processing and without facing any significant technical difficulties.

Experimental investigations by Erntroy and Shacklock[1] have indicated that in high-strength concrete mixes, workability, type and maximum size of aggregate, and the strength requirement influence the selection of the water/cement ratio. Crushed rock aggregates, being angular, generally produce stronger concretes at the same age in comparison with gravel aggregates.

High-strength concrete mixes can be designed by using any of the following established methods:

1. Erntroy and Shacklock's empirical method[1]
2. American Concrete Institute's mix-design procedure for no slump concrete[2]
3. British D.O.E. method based on the work of Teychenne, Franklin and Erntroy[3] which has replaced the traditional Road Note No. 4 mix-design procedure[4]
4. Indian Standard Code method[5]

The author has demonstrated, through a number of examples in a separate monograph[6], the use of these methods for designing high-strength concrete-mixes. The Indian standard code IS: 1343[7] stipulates that only controlled concrete should be used for prestressed concrete construction. The exact specifications with regard to the acceptance criteria for concrete generally vary from one code to another. The British code BS EN: 1992[8] stipulates that not more than five per cent of the test results should fall below the 28-day characteristic compressive strength, while the Indian standard codes IS: 456–2000[9] and IS: 1343 prescribe a similar stipulation of five per cent.

2.1.2 Strength Requirements

(a) Compressive Strength

High strength concrete is generally used in prestressed concrete structures and the strength designations and classifications followed in the Indian and Euro Code-2 (British: BS EN: 1992-1-1-2004) are compiled in Table 2.1(a) given as follows:

Table 2.1(a) *Grade or class of concrete*

S.No.	*Indian Code (IS: 1343-2012)*	*Euro Code-2 (British BS EN: 1992)*
1	M-30	C30/37
2	M-35	C35/45
3	M-40	C40/50
4	M-45	C45/55
5	M-50	C50/60
6	M-55	C55/67
7	M-60	C60/75
8	M-65	—
9	M-70	C70/85
10	M-75	—
11	M-80	C80/95
12	—	C90/105

In the British/Euro code classification, a class 35/45 concrete has a characteristic cylinder compressive strength of 35 N/mm^2 and cube strength of 45 N/mm^2. The ratio of cylinder to cube strength varies from a value of 0.8 for lower grades of M-30 and increases to 0.85 for higher grades of M-90 concrete.

(b) Flexural Strength

The flexural strength is also referred to as modulus of rupture and considered as the stress at which flexural cracks develop in concrete beams. According to the Indian Standard Code (IS: 1343-2012), the flexural strength is expressed by the empirical relation given by:

$$f_{cr} = 0.7\sqrt{f_{ck}}$$

where

f_{ck} = Characteristic cube compressive strength (N/mm^2)

f_{cr} = Flexural strength (N/mm^2)

The American Code ACI 318M-2011 specifies the relation as follows:

$$f_r = 0.62\,\lambda\sqrt{f_c'}$$

where

f_c' = Cylinder compressive strength

f_r = Flexural strength

λ = 1.0 for normal weight concrete

= 0.85 for sand light weight concrete

= 0.75 for all other light weight concrete

(c) Tensile Strength

The Indian Standard Code does not recommend any specific value for the tensile strength of concrete. However, the British Code (EC-2) provides mean values of the axial tensile strength of concrete as shown in Table 2.1(b).

Table 2.1(b) *Mean 28-day tensile strength (f_{ctm}) of concrete (BS EN 1992-1-1-2004)*

	Strength Class (f_{cy}/f_{ck})						
	C30/37	*C40/50*	*C50/60*	*C60/75*	*C70/85*	*C80/95*	*C90/105*
f_{ctm}(N/mm^2)	2.9	3.5	4.1	4.4	4.6	4.8	5.0

The mean flexural tensile strength of reinforced concrete members depends upon the mean tensile strength and the depth of the cross-section expressed as,

$$f_{ctm,fl} = \left[1.6 - \left(\frac{h}{1000}\right) f_{ctm}\right]$$

where, h = Total depth of the member (mm)

f_{ctm} = Mean axial tensile strength as given in Table 2.1(b).

A comparative analysis indicates that the tensile strength values recommended by the British code are significantly less (as much as 30 per cent) than that specified by the Indian Standard Code but somewhat nearer to the values resulting from the empirical relation of the American code.

The split tensile strength represents the direct tensile strength of concrete akin to the axial tensile strength. Standard tests are not prescribed in any code to determine the axial or direct tensile strength of concrete due to the difficulties in testing of concrete in pure tension. However, the split tension test specified in codes using standard concrete cylindrical specimens yields a fairly good estimate of the axial tensile strength. The split tensile strength is about 2/3 of the flexural strength of concrete determined using beam specimens.

The split tensile strength of concrete is useful in the design of structural concrete members subjected to direct tension such as the walls of a cylindrical water tank and the tension members of prestressed concrete trusses used to cover larger spans in industrial structures specially located in coastal regions where steel trusses are not recommended due to high maintenance costs.

The minimum 28-day cube compressive strength prescribed in the Indian Standard Code IS: 1343 is 40 N/mm^2 for pretensioned members and 30 N/mm^2 for post-tensioned members. The ratio of standard cylinder to cube strength may be assumed to be 0.8 in the absence of any relevant test data. A minimum cement content of 300 to 360 kg/m^3 is prescribed mainly to cater to the durability requirements. In high-strength concrete mixes, the water content should be as low as possible with due regard to adequate workability, and the concrete should be suitable for compaction by the means available at the site. It is a general practice to adopt vibration to achieve thorough compaction of concrete used for prestressed members. To safegaurd against excessive shrinkage, the code prescribes that the cement content in the mix should preferably not exceed 530 kg/m^3. The specified work cube strength of 40 N/mm^2 required for prestressed members can easily be achieved even at the age of seven days using rapid hardening Portland cement.

2.1.3 Permissible Stresses in Concrete

The permissible compressive and tensile stress in concrete at the stage of transfer and service loads are defined in terms of the corresponding compressive strength of concrete at each stage. The provisions made in the Indian[7], British[8], American[10] and FIP[11] recommendations regarding the maximum allowable stresses are compiled in Table 2.2.

In the Indian Standard Code, the reduction coefficient applied to compute the design maximum permissible compressive stress in flexure varies from a value of 0.41 for M-30 grade concrete to a value of 0.35 for M-60 grade concrete. In comparison, the British and American codes provide for uniform reduction coefficients for compressive strength at transfer and design loads. However, to account for the severity of stresses in the axial loading case, the reduction coefficients are further reduced in the case of the British code for members under direct compression. The permissible tensile stresses at the stage of transfer and working loads are related to the compressive strength of concrete in the British and American codes. On the other hand, the IS code provides for tensile stresses in Class 2 and 3 type members at serviceability limit states.

2.1.4 Shrinkage of Concrete

The shrinkage of concrete in prestressed members is due to the gradual loss of moisture which results in changes in volume. The drying shrinkage depends

Table 2.2 *Maximum permissible stresses in concrete (N/mm^2)*

Stage of stress	*Type of stress*	*IS 1343-2012*	*ACI 318M-2011*	*BS EN 1992-1-1-2004*	*FIP 1984*
At transfer	Compressive stress	Varies linearly from 0.54 to 0.37 f_{ci} for post-tensioned work and 0.51 to 0.44 f_{ci} for pretensioned work depending upon f_{ck}	$\leq 0.60\, f'_{ci}$	$\leq 0.5\, f_{ci}$ for bending and 0.4 f_{ci} for axial loads	—
	Tensile stress	—	When $f_t > 0.50\sqrt{f'_{ci}}$ at ends of simply supported members or $0.25\sqrt{f'_{ci}}$ at other locations, additional bonded reinforcement designed to resist the tensile force	$\leq 0.5\, f_{ctm}$ for uncracked sections	—
At service loads	Compressive stress	Varies linearly from 0.41 to 0.35 f_{ck} In Zone-I and from 0.34 to 0.27 f_{ck} In Zone-II	Not to exceed 0.60 f'_{ci} For Class U and T type members	$\leq 0.60\, f_{ck}$	$\leq 0.50\, f_{ck}$
	Tensile stress	Type-1 - No tensile stress Type-2 - Not to exceed 3 N/mm^2 Type-3 - 3.2 to 7.3 N/mm^2 based on limiting crack width	Class U (uncracked) $\leq 0.62\sqrt{f'_c}$ Class T (transition from uncracked to cracked) $0.62\sqrt{f'_c} \leq f_t \leq \sqrt{f'_c}$ Class-3 (Cracked) No requirement	Class-1 Type - 0 For other types hypothetical tensile stresses up to 0.25 f_{ck} depending upon the crack widths	Class-1 - 0 Class-2 up to 0.75 f_t Class-3 no limit but degree of prestress controlled by limiting deflection and crack width

on the aggregate type and quantity, relative humidity, water/cement ratio in the mix, and the time of exposure. Rich mixes exhibit a relatively greater shrinkage than lean mixes since the contraction of the cement gel increases with the cement content. The shrinkage also depends upon the degree of hardening of the concrete at the commencement of drying.

The rate and amount of shrinkage of the structural members under ambient conditions will depend very much upon the ratio of surface area to volume of the member, as the exchange of moisture between the concrete and the atmosphere must take place through the surface. Aggregates of rock types having high moduli of elasticity and low values of deferred strain are more effective in restraining the contraction of the cement paste and their use reduces the shrinkage of concrete. The commonly used aggregates, in increasing order of effectiveness in restraining shrinkage, are sandstone, basalt, gravel, granite, quartz and limestone.

Shrinkage in structural concrete members is due to the reduction in the volume of the member as it hardens with time. The shrinkage is liable to cause cracking, but it also has the beneficial effect of strengthening the bond between the concrete and steel reinforcement. The total shrinkage of concrete is influenced by its ingredients, size of the member and environmental conditions. The total shrinkage depends upon the total amount of water present in the concrete at the time of mixing and it can be reduced by using minimum cement content and lower water/cement ratios. When the tensile stresses caused by shrinkage or thermal movement exceed the strength of concrete, cracks develop normally on the surface of the members. To control the width of cracks, steel reinforcement must be provided close to the concrete surface. The codes of practise specify minimum quantities of reinforcement for this purpose.

The total shrinkage strain (ε_{cs}) comprises of two components, the drying shrinkage strain (ε_{cd}) and the autogenous shrinkage strain (ε_{ca}) expressed as,

$$\varepsilon_{cs} = (\varepsilon_{cd} + \varepsilon_{ca})$$

The autogeneous shrinkage strain develops during the hardening of concrete and the significant part develops in the early days after casting. This type of strain is considered as a linear function of the concrete strength. In the absence of accurate field or laboratory data, the revised Indian Standard Codes IS: 456 and IS: 1343-2012 recommend the values as given in Table 2.3.

Table 2.3 *Autogenous shrinkage (IS: 1343-2012)*

Grade of Concrete	*Autogenous Shrinkage* ($\varepsilon_{ca} \times 10^{-6}$)
M-30	35
M-35	45
M-45	65
M-50	75
M-60	95

The IS: 1343-2012 code provides formulae to evaluate the components of autogenous and drying shrinkage strains at various ages of the concrete.

The development of autogenous shrinkage strain with time is expressed as follows:

$$\varepsilon_{ca}(t) = \beta_{as}(t)\ \varepsilon_{ca}$$

where, $\beta_{as}(t) = [1 - e^{-0.2\sqrt{t}}]$ and t in days

The drying shrinkage strain depends upon the environmental conditions and it is a function of the migration of water through the hardened concrete. The final value of shrinkage strain $\varepsilon_{cd,}$ may be taken equal to $k_h\ \varepsilon_{cd}$ and the recommended mean values with a coefficient of variation of about 30 per cent are compiled in Table 2.4(a) for relative humidities of 50 and 80 per cent.

Table 2.4(a) *Unrestrained drying shrinkage values ($\varepsilon_{cd} \times 10^6$) for concrete with Portland cement (IS: 1343-2012)*

Characteristic Cube strength (f_{ck}) N/mm²	*Unrestrained Drying Shrinkage Strain values ($\varepsilon_{cd} \times 10^{-6}$) for Concrete with Portland Cement for Relative Humidity*	
	50 per cent	*80 per cent*
25	535	300
50	420	249
75	330	190

The British code (BS EN: 1992-1-1-2004) lists the values of unrestrained drying shrinkage for different grades of concrete varying from M-25 to M-105 for various relative humidities varying from 20 to 100 per cent as shown in Table 2.4 (b).

Table 2.4(b) *Nominal unrestrained drying shrinkage strain (BS EN: 1992-1-1-2004)*

Grade of Concrete f_{ck} (N/mm²)	*Relative Humidity (per cent)*					
	20	*40*	*60*	*80*	*90*	*100*
25	0.62	0.58	0.49	0.30	0.17	0.00
50	0.48	0.46	0.38	0.24	1.13	0.00
75	0.38	0.36	0.30	0.14	0.10	0.00
95	0.30	0.28	0.24	0.15	0.08	0.00
105	0.27	0.25	0.21	0.13	0.07	0.00

The development of drying shrinkage strain with time is expressed by the function,

$$\varepsilon_{cd}(t) = \beta_{ds}(t, t_s)\, k_h \cdot \varepsilon_{cd}$$

$$\beta_{ds}(t, t_s) = \left[\frac{(t - t_s)}{(t - t_s) + 0.04\sqrt{h_0^3}}\right]$$

where, t = Age of the concrete at the moment considered in days

t_s = Age of the concrete at the beginning of drying shrinkage in days, normally taken from the end of curing stage

h_o = Notional size of the cross-section in mm, computed as $(2A_c/u)$, where A_c is the concrete cross-sectional area and u is the perimeter of that part of the cross-section which is exposed to drying

The values of coefficient k_h depending upon the notional size h_o are listed in Table 2.5.

Table 2.5 *Values of coefficient (k_h) (IS: 1343-2012)*

h_o (mm)	k_h
100	1.00
200	0.85
300	0.75
≥ 500	0.70

2.1.5 Creep of Concrete

The progressive inelastic strains due to creep in a concrete member are likely to occur under the smallest sustained stresses at ambient temperatures. Shrinkage and creep of concrete are basically similar in origin, being largely the result of the migration of water in the capillaries of the cement paste. For design purposes, it is convenient to differentiate between the deformation due to externally applied stress, generally referred to as creep, and the deformation which occurs without externally applied stresses, referred to as shrinkage. As the increase in strain under a sustained stress is several times larger than the strain on loading, it is of considerable importance in prestressed structural members.

The failure of early efforts at prestressing was largely attributed to a lack of knowledge concerning the creep of concrete, which can be considered as the main source of loss if the precompression in concrete is high. The various factors influencing creep of concrete are relative humidity, stress level, strength of the concrete, age of the concrete at loading, duration of stress, water/cement ratio and the type of cement and aggregate in the concrete. For stresses up to about half the crushing strength of concrete, the creep is directly proportional to the stress, but above this value it increases more rapidly. Creep of concrete continues for a very long time, tending towards a limiting value after an infinite time under load, though the rate of creep decreases with time. It has been estimated that nearly 55 per cent of a 20-year creep occurs in three months, while 76 per cent occurs in one year.[12] If creep after one year under load is taken as unity, the average values of creep at later ages are 1.26 after 10 years and 1.36 after 30 years.[13]

The Indian Standard Code for prestressed concrete (IS: 1343-2012) specifies the method of computing the creep coefficient by considering the various influencing parameters like age of concrete at loading, duration of loading and relative humidity. As long as the stress in concrete does not exceed one-third of the characteristic compressive strength, creep may be assumed as proportional to the stress.

The creep coefficient is expressed as $\phi(t, t_o) = \left(\dfrac{\varepsilon_{cc}(t)}{\varepsilon_{ci}(t_o)}\right)$

where, $\varepsilon_{cc}(t)$ = Creep strain at time $t > t_o$
$\varepsilon_{ci}(t_o)$ = Initial strain at loading
t_o = Initial time of loading

The creep coefficient $\phi(t, t_o)$ is given by the relation,

$$\phi(t, t_o) = \phi_o \cdot \beta(t, t_o)$$

where, ϕ_o = Notional creep coefficient to which the creep coefficient reaches asymptotically with time (this can be taken as the value reached in 70 years)
$\beta(t, t_o)$ = Coefficient describing development of creep with time as follows:

$$\phi(t, t_o) = \beta(t, t_o)\phi_o$$

$$\beta(t, t_o)\phi_o = \left[\frac{t - t_o}{\beta_H + (t - t_o)}\right]^{0.3}$$

where, t = Age of concrete in days at the moment considered
t_o = Age of concrete at loading in days
$(t - t_o)$ = Duration of loading in days
β_H = A coefficient depending upon the relative humidity (RH in per cent) and the notional member size (h_o in mm)

$$\beta_H = 1.5\left[1 + \left(1, 2\left\{\frac{RH}{RH_o}\right\}\right)^{18}\right]h_o + 250 \leq 1500 \qquad \text{for } f_{ck} \leq 45 \text{ MPa}$$

$$= 1.5\left[1 + \left(1, 2\left\{\frac{RH}{RH_o}\right\}\right)^{18}\right]h_o + 250\,\alpha_3 \leq 1500\,\alpha_1 \quad \text{for } f_{ck} \leq 45 \text{ MPa}$$

RH = Relative humidity expressed as per cent
RH_o = 100 (Hundred per cent relative humidity)
$\alpha_1, \alpha_2, \alpha_3$ = Coefficients based on the strength of concrete

$$\alpha_1 = \left[\frac{45}{f_{ck} + 8}\right]^{0.7}, \quad \alpha_2 = \left[\frac{45}{f_{ck} + 8}\right]^{0.2}, \quad \alpha_3 = \left[\frac{45}{f_{ck} + 8}\right]^{0.5}$$

The notional creep coefficient ϕ_o is expressed as:

$$\phi_o = \phi_{RH}\,\beta(f_{cm}) \cdot \beta(t_o)$$

where, ϕ_{RH} = A factor to allow for the effect of relative humidity on the notional creep coefficient

$$= 1 + \left[\frac{1-\left(\frac{\mathrm{RH}}{100}\right)}{0.1\sqrt[3]{h_o}}\right] \quad \text{for } f_{ck} \le 45 \text{ MPa}$$

$$= 1 + \left[\frac{1-\left(\frac{\mathrm{RH}}{100}\right)}{0.1\sqrt[3]{h_o}} \cdot \alpha_1\right] \cdot \alpha_3 \quad \text{for } f_{ck} \ge 45 \text{ MPa}$$

RH = Relative humidity of the ambient environment in per cent

h_o = Notional size of the member expressed in mm = $(2A_c/u)$

A_c = Cross-sectional area

u = Perimeter of the member in contact with the atmosphere

$\beta(f_{cm})$ = A factor to allow for the effect of concrete strength on the notional creep coefficient

$$= \left[\frac{16.8}{\sqrt{f_{ck}+8}}\right]$$

$\beta(t_o)$ = A factor to allow for the effect of concrete age at loading on the notional creep coefficient

$$= \left[\frac{1}{0.1+t_o^{0.20}}\right]$$

The IS: 1343-2012 code specifies the values of final creep coefficient for design of normal weight concrete of grades between M-30 and M-60 subject to the condition that the compressive stress does not exceed 0.36 f_{ck} at the age of loading. The ultimate creep coefficient values are compiled in Table 2.6.

Table 2.6 *Final values of creep coefficient (IS: 1343-2012)*

Age at Loading (t_o) (days)	*Creep Coefficient ϕ_0 (70 yr, t_0) of an Ordinary Structural Concrete After 70 years of Loading*					
	Under Dry Atmospheric Conditions (RH 50%) Notional Size ($2A_c/u$)(mm)			*Under Humid Atmospheric Conditions (Outdoor) (RH 80%) Notional Size ($2A_c/u$)(mm)*		
	50	*150*	*600*	*50*	*150*	*600*
1	5.8	4.8	3.9	3.8	3.4	3.0
7	4.1	3.3	2.7	2.7	2.4	2.1
28	3.1	2.6	2.1	2.0	1.8	1.6
90	2.5	2.1	1.7	1.6	1.5	1.3
365	1.9	1.6	1.3	1.2	1.1	1.0

The British, Indian, American and European[11] practises are to use the creep coefficient for computing the loss of prestress due to creep of concrete. The magnitude of creep coefficient varies from 2 to 4.5 depending upon the type of aggregate used, water/cement ratio of the mix, degree of hardening, relative humidity and other parameters.

The effect of creep is to increase deflections with time and hence should be computed to check the limit state of serviceability in structural concrete elements. The Indian and British codes use the concept of effective modulus, $E_{ce} = [E_c/(1+ \phi)]$, where ϕ is the creep coefficient equal to the ratio of creep strain to initial elastic strain for computing the long-term effects of creep on deflections of flexural members.

The ACI 318-11 code provides for the effects of creep in computing long-term deflections of flexural members. Multiplying factors expressed as a function of the time dependent factor varying from 1 to 2.0 for sustained loads over periods from 3 months to 5 years, respectively, are recommended to compute the enhanced deflections due to the effects of creep.

The FIP[11] recommendations include mean values for the final shrinkage and creep coefficient for a concrete subjected to a stress not exceeding $0.4 f_{cj}$ at age j from loading as compiled in Table 2.7. These limiting values are applicable only for a concrete of medium consistency and made with rapid hardening Portland cement and for constant thermo-hygrometric conditions (the mean temperature of the concrete being 20°C and the relative humidity (RH) as indicated). In special cases, such as free cantilever construction or structures where concretes of different ages are combined, more detailed information, in the CEB manual on structural effects of time-dependent behaviour of concrete[14] and in the CEB manual on cracking and deformation[15], is useful.

Table 2.7 *Final values of shrinkage and creep coefficient (FIP)*

Equivalent Thickness $(2\,A_c/u)^{\#}$		*Atmospheric Conditions*			
		Humid (RH = 75%)		*Dry (RH = 55%)*	
		Small 200 mm	*Large 600 mm*	*Small 200 mm*	*Large 600 mm*
Shrinkage* $\varepsilon_{cs}(t_\infty, t_0) \times 10^3$	Fresh (3–7 days)	0.26	0.21	0.43	0.31
	Medium (7–60 days)	0.23	0.21	0.32	0.30
	Mature (> 60 days)	0.16	0.20	0.19	0.28
Creep$^+$ $\phi(t_\infty, t_0)$	Fresh (3–7 days)	2.7	2.1	3.8	2.9
	Medium (7–60 days)	2.2	1.9	3.0	2.5
	Mature (> 60 days)	1.4	1.7	1.7	2.0

\# A_c denotes the area of the concrete section
u is the perimeter in contact with atmosphere (which includes the interior perimeter of a hollow section only, if there is a connection between the interior and the free atmosphere)

* t_0: Age of concrete at the instant from which the shrinkage effect is being considered

\+ t_0: Age at the commencement of loading

2.1.6 Deformation Characteristics of Concrete

The complete stress-strain characteristics of concrete in compression are not linear, but for loads not exceeding 30 per cent of the crushing strength, the load deformation behaviour may be assumed to be linear. The deformation characteristics of concrete under short-term and sustained loads are necessary for determining the flexural strength of beams and for evaluating the modulus of elasticity of concrete, which is required for the computation of deflections of prestressed members.

The short-term modulus of elasticity, which is specified in most of the codes, corresponds to the secant modulus determined from an experimental stress-strain relation exhibited by standard specimens under loads of one-third of the cube compressive strength of concrete. The modulus of elasticity of concrete increases with the average compressive strength of concrete, but at a decreasing rate. Several empirical formulae have been recommended in various national codes for the computation of secant modulus of elasticity of concrete, which is invariably expressed as a function of the compressive strength of concrete.

1. According to the Indian Standard Code (IS: 1343-2012),

$$E_c = 5000\sqrt{f_{ck}}\ \text{N/mm}^2$$

2. The American Concrete Institute (ACI: 318M-2011) recommends an empirical formula of the type,

$$E_c = w_c^{1.5}\, 0.043\sqrt{f_c'}\ \text{N/mm}^2$$

where,

w_c = Density of concrete in the range of 1440 to 2560 kg/m^3

f_c' = Cylinder compressive strength of concrete

However, for normal density concrete, the following relation may be used.

$$E_c = 4700\sqrt{f_c'}\ \text{N/mm}^2$$

3. The International Federation for Prestressed Concrete (FIP) recommends values of the secant modulus for short-term loading, as shown in Fig. 2.1, covering the range of compressive strength of concrete from 12 to 80 N/mm^2.
4. The British code BS EN: 1992–1–1: 2004 for the structural use of concrete specifies the mean values of the modulus of elasticity of concrete, which is related to the characteristic cube strength of normal weight gravel concrete as detailed in Table 2.8(a). For lime stone aggregate, these values should be reduced by a factor of 0.9 and for harder stone aggregates like basalt and granite, the values are increased by a factor of 1.2. It is recommended that under conditions of sustained loading, appropriate allowances for shrinkage and creep are to be made.

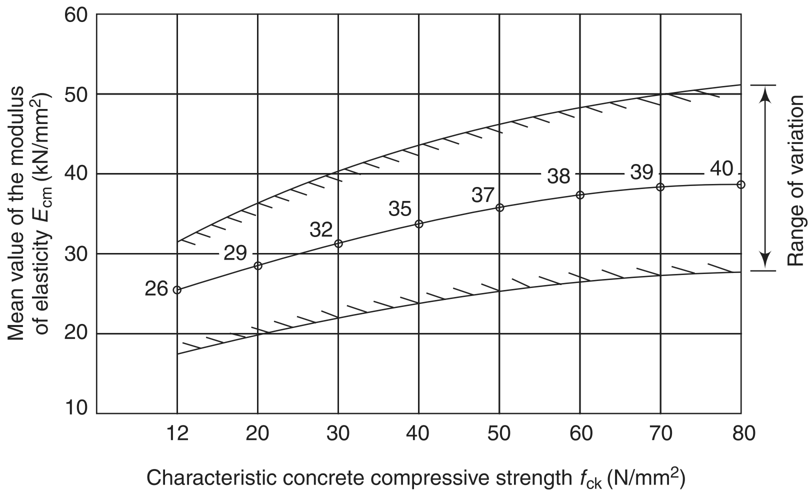

Fig. 2.1 *Variation of e-modulus with compressive strength*

Table 2.8(a) *Short-term modulus of elasticity of normal weight gravel concrete (BS EN: 1992-1-1-2004)*

Characteristic Compressive Strength (f_{cy}/f_{ck}) [Cylinder/Cube] (N/mm²)	*Static (Secant) Modulus (E_c) (kN/mm²)*
20/25	30
25/30	31
30/35	33
35/40	34
40/50	35
50/60	37
60/70	39
70/80	41
80/90	42
90/105	44

5. The average values for the modulus of elasticity and Poisson's ratio of concrete, as specified by the German specification, DIN–4227[16], are given in Table 2.8(b).

Table 2.8(b) *Modulus of elasticity and Poisson's ratio of concrete (DIN-4227)*

Concrete Quality	*M-25*	*M-30*	*M-45*	*M-60*	*N/mm²*
Modulus of elasticity (E_c)	24	30	35	40	kN/mm²
Poisson's ratio (μ)	0.15-0.18	0.17-0.20	0.20-0.25	0.25-0.30	

Experimental investigations[17] have indicated that the present Indian Standard Code provisions generally underestimate the modulus of elasticity of concrete for grades from M-30 to M-60 and overestimate for the higher grades exceeding M-60 in comparison with the British code.

2.1.7 Design of High-Strength Concrete Mixes

The properties of high strength concrete mix with a compressive strength in the range of 40 to 100 N/mm^2 is greatly influenced by the type of cement, water/cement ratio and properties of aggregates. To achieve high strength, it is necessary to use lower water/cement ratio which invariably affects the workability of the concrete mix and necessitates the use of special vibration techniques for proper compaction. In the present state of the art, a concrete with a desired characteristic compressive strength in the range of 40 to 100 N/mm^2 can be made by suitably designing the mix proportions and using vibration for compaction. The various methods of designing concrete mixes were identified in Section 2.1.1.

The reader may refer to a separate monograph by the author[6] for detailed concrete mix design procedures with examples. However, the design of a high strength concrete mix according to the specifications of the Indian Standard Code (IS: 10262-1982)[5] is outlined as follows:

Indian Standard Code Method of Design

The Indian Standard Code procedure is outlined in the following steps:

1. The target mean strength is determined by the relation,

$$f_{ck} = f_{ck} + t \cdot s$$

where, f_{ck} = Target mean strength
f_{ck} = Characteristic compressive strength at 28 days
s = Standard deviation
t = A statistical value depending upon the accepted proportion of low results related to the number of tests as shown in Table 2.9

The suggested values of standard deviation (s) as recommended in IS: 10262-1982 for different degrees of control are compiled in Table 2.10.

Table 2.9 *Values of - t*

Percentage of results below the characteristic strength	*Values of - t*
50	0
16	1.00
10	1.28
5	1.65
2.5	1.96
1.0	2.33
0.5	2.80

Table 2.10 *Suggested values of standard deviation (s)*

Concrete Grade	*Standard Deviation for Different Degrees of Control (N/mm^2)*		
	Very Good	*Good*	*Fair*
M-15	2.5	3.5	4.5
M-20	3.6	4.6	5.6
M-25	4.3	5.3	6.3
M-30	5.0	6.0	7.0
M-35	5.3	6.3	7.3
M-40	5.6	6.6	7.6
M-45	6.0	7.0	8.0
M-50	6.4	7.4	8.4
M-55	6.7	7.7	8.7
M-60	6.8	7.8	8.8

2. The water/cement ratio for the target mean strength is selected from Fig. 2.2.

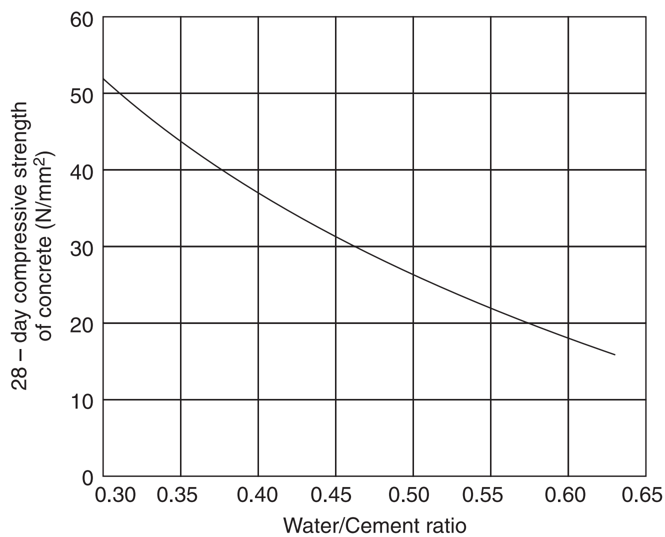

Fig. 2.2 *Generalised relationship between water/cement ratio and compressive strength of concretes*

The water/cement ratio selected is checked against the limiting W/C ratio prescribed for the requirement of durability using Tables 2.11 and 2.12 and the lower of the two values adopted. A more precise estimate of the preliminary water/cement ratio corresponding to the target mean strength and type of cement used is made from the relationship shown in Fig. 2.3.

Table 2.11 *Minimum cement content and maximum water/cement ratio and minimum grade of concrete for different exposures with normal weight aggregates of 20 mm nominal maximum size*

S.No.	*Exposure*	*Prestressed Concrete*		
		Minimum Cement Content (kg/m³)	*Maximum Free W/C Ratio*	*Minimum Grade of Concrete*
1	Mild	300	0.55	M-30
2	Moderate	300	0.50	M-30
3	Severe	320	0.45	M-30
4	Very Severe	340	0.45	M-35
5	Extreme	360	0.40	M-40

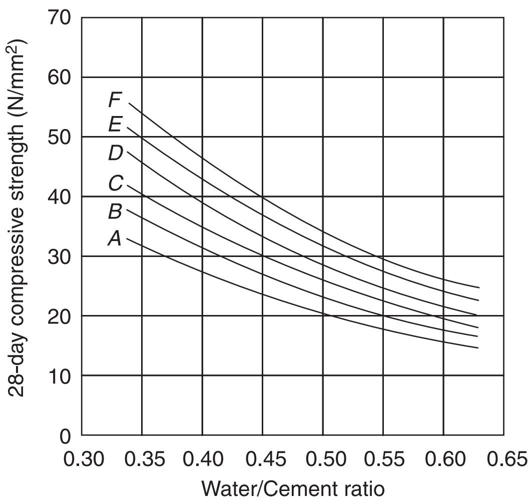

28-day strength of cement tested according to IS: 4031–1968
A = 31.9–36.8 N/mm^2 (325–375 kg/cm^2)
B = 36.8–41.7 N/mm^2 (375–425 kg/cm^2)
C = 41.7–46.6 N/mm^2 (425–475 kg/cm^2)
D = 46.6–51.5 N/mm^2 (475–525 kg/cm^2)
E = 51.5–56.4 N/mm^2 (525–575 kg/cm^2)
F = 56.4–61.3 N/mm^2 (575–625 kg/cm^2)

Fig. 2.3 *Relation between free water/cement ratio and concrete strength for different cement strength*

3. The entrapped air content is estimated from Table 2.13 for the maximum size of aggregate used.

Table 2.12 *Requirements for prestressed concrete exposed to sulphate attack (IS:1343–2012)*

S.No.	*Class*	*Concentration of Sulphates, Expressed as SO_3*			*Type of Cement*	*Dense, Fully Compacted Concrete, Made with 20 mm Nominal Maximum Size Aggregates Complying with IS 383*	
		In Soil		*In Ground Water*			
		Total SO_3	*SO_3 in 2:1 Water: Soil Extract*			*Minimum Cement Content kg/m^3*	*Maximum Free Water-Cement Ratio*
		Per cent	*g/l*	*g/l*			
(1)	*(2)*	*(3)*	*(4)*	*(5)*	*(6)*	*(7)*	*(8)*
(i)	1	Traces (<0.2)	Less than 1.0	Less than 0.3	Ordinary Portland cement or Portland slag cement or Portland pozzolana cement	280	0.55
(ii)	2	0.2–0.5	1.0–1.9	0.3–1.2	Ordinary Portland cement or Portland slag cement or Portland pozzolana cement	330	0.50
					Super sulphated cement or Sulphate resisting Portland cement	310	0.50
(iii)	3	0.5–1.0	1.9–3.1	1.2–2.5	Super sulphated cement or Sulphate resisting Portland cement	330	0.50
					Portland pozzolana cement or Portland slag cement	350	0.45

(*Contd.*)

Table 2.12 *(Contd.)*

(iv)	4	1.0–2.0	3.1–5.0	2.5–5.0	Super sulphated or sulphate resisting Portland cement	370	0.45
(v)	5	More than 2.0	More than 5.0	More than 5.0	Sulphate resisting Portland cement or supersulphated cement with protective coatings	400	0.40

Notes:

1. Cement content given in this table is irrespective of grades of cement. Suitable adjustment may be made in the minimum cement content specified in case of use of aggregate other than 20 mm nominal maximum size.

2. Use of supersulphated cement is generally restricted where the prevailing temperature is above 40°C.

3. Supersulphated cement gives an acceptable life provided that the concrete is dense and prepared with a water-cement ratio of 0.4 or less, in mineral acids, down to pH 3.5.

4. The cement contents given in col 6 of this table are the minimum recommended. For SO_3 contents near the upper limit of any class, cement contents above these minimum are advised.

5. For severe conditions, such as thin sections under hydrostatic pressure on one side only and sections partly immersed, considerations should be given to a further reduction of water-cement ratio.

6. Where chloride is encountered along with sulphates in soil or ground water, ordinary Portland cement with C_3A content from 5 to 8 per cent shall be desirable to be used in concrete, instead of sulphate resisting cement.

Table 2.13 *Approximate entrapped air content*

Nominal Maximum Size of Aggregate (mm)	*Entrapped Air as Percentage of Volume of Concrete*
10	3.0
20	2.0
40	1.0

4. The water content and percentage of sand in the total aggregate by absolute volume are next selected from Tables 2.14 and 2.15 for concrete of grades up to and beyond M-35 for the following standard reference conditions:
   (a) Crushed (angular) coarse aggregate
   (b) Fine aggregate consisting of natural sand conforming to the grading zone-II of IS: 383-1970[18] in standard surface dry condition
   (c) Water/cement ratio of 0.60 and 0.35 for medium and high strength concrete respectively
   (d) Workability corresponding to compaction factor value of 0.80

Table 2.14 *Approximate sand and water contents per cubic metre of concrete for grades up to M-35*

Nominal Maximum Size of Aggregate (mm)	*Water Content* per cubic meter of Concrete (kg)*	*Sand as percentage of Total Aggregates by Absolute Volume*
10	208	40
20	186	35
40	165	30
* Water content corresponding to saturated surface dry aggregate Water/cement ratio = 0.60 and Workability = 0.80 (C.F)		

Table 2.15 *Approximate sand and water contents per cubic metre of concrete for grades above M-35*

Nominal Maximum Size of Aggregate (mm)	*Water Content* per cubic meter of Concrete (kg)*	*Sand as percentage of Total Aggregates by Absolute Volume*
10	200	28
20	180	25
* Water content corresponding to saturated surface dry aggregate Water/cement ratio = 0.35 and Workability = 0.80 (C.F)		

5. For other conditions of workability, W/C ratio, grading of fine aggregate and for rounded aggregates (gravel), adjustments in the water content and percentage of sand in total aggregate are made as shown in Table 2.16.

Table 2.16 *Adjustments of values in water content and sand percentage for other conditions*

Change in Condition Stipulated for Tables 2.14 and 2.15	*Adjustment required in*	
	Water Content	*Percentage of Sand in Total percentage*
For sand conforming to grading Zones - 1, III or IV of Table-4 of IS: 383-1970*	0	+ 1.5% for Zone-1 – 1.5% for Zone III – 0.3% for Zone IV
Increase or decrease in the value of compacting factor by 0.1	± 3 per cent	0
Each 0.05 increase or decrease in free water/cement ratio	0	± 1 per cent
For rounded aggregates	–15 kg/m^3	– 7 per cent

* Specification for coarse and fine aggregates from natural sources for concrete (second revision)

6. The cement content is calculated from the W/C ratio and the final water content is computed after adjustment. The cement content so calculated is checked against the minimum cement content from other requirements of durability (Tables 2.11 and 2.12) and the greater of the two values adopted.
7. With the quantities of water and cement per unit volume of concrete and the percentage of sand in the total aggregate already determined, the coarse and fine aggregate content per unit volume of concrete is calculated by the absolute volume method.

Example 2.1 Design a concrete mix for casting the precast pretensioned girder to suit the following requirements:

Characteristic cube strength: M-45

Type of cement: Ordinary Portland corresponding to type F (57.5 – 62.5 N/mm^2)

Fine aggregate: Natural river sand conforming to grading zone II or IS: 383

Coarse aggregate: Crushed granite (angular) of 20 mm maximum size conforming to IS: 383 code requirement

Specific gravities of cement, sand and coarse aggregates are 3.14, 2.63 and 2.61, respectively

Type of exposure: Mild

Degree of quality control: Very good

Degree of workability: CF = 0.75

Mix Design Procedure

1. ***Target mean strength***

$$\bar{f}_{ck} = (f_{ck} + t.s) = (45 + 1.65 \times 6) = 55 \text{ N/mm}^2$$

2. ***Selection of water/cement ratio*** The preliminary free W/C ratio by weight corresponding to the target mean strength at 28 days for different mixes is selected from Fig. 2.3. Corresponding to a target mean strength of 55 N/mm^2, (using F-grade cement) the W/C ratio is interpolated as 0.35. From Table 2.11, for durability requirements, the maximum water/cement ratio for mild exposure condition is 0.55. Hence, the lower water/cement ratio of 0.35 from strength considerations is selected.

3. ***Air content*** From Table 2.13, for a nominal maximum size of 20 mm aggregate, the entrapped air is two per cent of the volume of concrete.

4. ***Water content and fine to total aggregate ratio*** For a nominal maximum size of 20 mm aggregate, from Table 2.15, for concrete of grade above M-35, the water and sand content are obtained as 180 kg/m^3 and 25 per cent, respectively.

5. ***Adjustment of values in water content and sand percentage*** Referring to Table 2.16, the following adjustments are required:

Change in Condition (Refer to Table 2.16)	*Adjustments required in*	
	Water Content (per cent)	*Percentage of Sand in total aggregate*
M-45 grade concrete		
(a) For decrease in the compacting factor of (0.80 – 0.75) = 0.05	–1.5%	0
(b) For decrease in free water cement ratio by (0.35 – 0.35) = 0	0	0

6. ***Final water and sand contents***

$$\text{Water content} = 180 - \left(\frac{1.5 \times 180}{100}\right) = 177.3 \text{ kg/m}^3$$

$$\text{Sand content} = 25 \text{ per cent}$$

7. ***Determination of cement content***

$$\text{W/C ratio} = 0.35$$

$$\text{Water content} = 177.3 \text{ kg/m}^3$$

$$\therefore \quad \text{Cement content} = \left(\frac{177.3}{0.35}\right) = 507 \text{ kg/m}^3$$

8. ***Check for minimum cement content:*** The calculated cement content of 507 kg/m^3 is greater than the minimum cement content of 300 kg/m^3 prescribed in Table 4 and clause 8.2.4.1 of IS: 1343.

9. ***Determination of coarse and fine aggregate content*** The amount of entrapped air for 20 mm maximum-size aggregate from Table 2.20 is two per cent. The fine aggregate required is calculated as,

$$0.98\ \text{m}^3 = \left[177.3 + \frac{507}{3.14} + \frac{1 \times f_a}{0.25 \times 2.63}\right] \times \frac{1}{1000}$$

$$\therefore \qquad f_a = 421.6\ \text{kg}$$

Coarse aggregate required is calculated as,

$$0.98\ \text{m}^3 = \left[177.3 + \frac{507}{3.14} + \frac{1 \times C_a}{(1 - 0.25)2.61}\right] \times \frac{1}{1000}$$

$$C_a = 1255.3\ \text{kg}$$

10. ***Total quantities of ingredients and mix proportions***

Cement	:	FA	:	CA	:	Water
507	:	421.6	:	1255.3	:	177.3 kg
1	:	0.83	:	2.47	:	0.35

2.1.8 Lightweight Aggregate Prestressed Concrete

The use of lightweight aggregate concrete for prestressed concrete construction is well established since 1955. The main advantage of lightweight concrete is that it reduces the self-weight of the structure, thus minimising the amount of concrete and steel required for carrying the load. The lightweight criterion becomes important especially in long-span structures where dead load forms the major portion of the total design load on the structure, or when the self-weight of the member is a factor to be considered in transportation and erection, as in the case of precast concrete construction.

In the present state of the art, it is possible to produce high-strength concrete of 28-day cube compressive strength in the range of 30–50 N/mm^2, by proper selection of lightweight aggregates in the coarser and finer fractions along with good quality cement and water. In UK, the lightweight aggregates, generally used for prestressed concrete, are foamed slag, lytag and aglite. Teychenne[19] has developed empirical graphs that relate the important parameters in a lightweight concrete mix. These graphs are convenient for estimating the trial mix-proportions of structural lightweight concrete. The ACI standard[20] provides a generally applicable method for selecting and adjusting mix proportions for structural lightweight concrete, using different types of lightweight aggregates.

The modulus of elasticity of lightweight concrete is about 50–55 per cent of the modulus of elasticity of normal-weight concrete and hence the loss of prestress due to elastic deformation is higher and deflections of flexural members are comparatively higher due to the lower values of modulus of elasticity. The unit weight of lightweight concrete varies considerably between 1450 and 1750 kg/m^3. The shrinkage and creep of lightweight concrete is comparable, with marginal variations, to that of sand and gravel concrete, as reported by various investigations of Shideler[21] and Best[22]. An excellent survey of the effective utilisation of lightweight concrete in prestressed concrete structures is reported by Gerwick[23] .

2.2 High-Tensile Steel

2.2.1 Types of High-Tensile Steel

For prestressed concrete members, the high-tensile steel used generally consists of wires, bars, or strands. The higher tensile strength is generally achieved by marginally increasing the carbon content in steel in comparison with mild steel. High-tensile steel usually contains 0.6–0.85 per cent carbon, 0.7–1 per cent manganese, 0.05 per cent of sulphur and phosphorus with traces of silicon. The high-carbon steel ingots are hot-rolled into rods and cold-drawn through a series of dies to reduce the diameter and increase the tensile strength. The specification of hard-drawn steel wire for prestressed concrete (as drawn wire) are covered in the Indian Standard Code IS: 1785 (part II)–1983[24].

The process of cold-drawing through dies decreases the durability of the wires. The cold-drawn wires are subsequently tempered to improve their properties. Tempering or ageing or stress relieving by heat treatment of the wires at 150–420°C enhances the tensile strength. The cold-drawn stress relieved wires are generally available in nominal sizes of 2.5, 3, 4, 5, 7 and 8 mm diameter and they should conform to the Indian Standard Code IS: 1785(part I)–1983[25].

The hard-drawn steel wires which are indented or crimped are preferred for pretensioned elements because of their superior bond characteristics. The specifications for indented wires are covered in IS: 6003–1983[26]. The small diameter wires of 2 to 5 mm are mostly used in the form of strands comprising two, three or seven wires. The helical form of twisted wires in the strand substantially improves the bond strength. Two- and three-ply strands are made up of 2 mm and 3 mm diameter individual wires, respectively, while the 7-ply strands are twisted using wires of 2 to 5 mm diameter. The nominal diameter of 7-ply strands vary from 6.3 mm to 15.2 mm. The properties of strands are covered in IS: 6006-1983[27]

The high-tensile steel bars commonly employed in prestressing are manufactured in nominal sizes of 10, 12, 16, 20 22, 25, 28 and 32 mm diameter and are covered in 1S: 2090–1983[28]. The ultimate tensile strength of the bars does not vary appreciably with the diameter, since the high strength of the bars is due to alloying rather than to cold working as in the case of wires[29]. The British Standard Codes BS: 2691, BS: 4486 and BS: 3671[30] present specifications for the use of high-tensile wires, bars and strands, respectively. Provision has been made for the use of 19 wire strands in addition to the earlier 7-wire strands.

2.2.2 Strength Requirements

The ultimate tensile strength of a plain hard-drawn steel wire varies with its diameter. The tensile strength decreases with increase in the diameter of the wires. The ultimate tensile strength of different sizes of wires, bars and strands, as specified in the relevant Indian Standard Codes, are compiled in Tables 2.17 to 2.20.

Table 2.17 *Tensile strength and elongation characteristics of cold-drawn stress-relieved wires (IS: 1785 – part I – 1983)*

Nominal Diameter (mm)	*Tensile Strength (minimum)* (N/mm^2)	*Elongation* (per cent)
2.50	2010	2.5
3.00	1865	2.5
4.00	1715	3.0
5.00	1570	4.0
7.00	1470	4.0
8.00	1375	4.0

Table 2.18 *Mechanical properties of high-tensile steel bars (IS: 2090–1983)*

(a)	Characteristic tensile strength (minimum)	980 N/mm^2
(b)	Proof stress	Not less that 80 per cent of the minimum specified tensile strength
(c)	Elongation at rupture on a gauge length of 5.65A (minimum)	10 per cent

where A = area of cross-section

Table 2.19 *Mechanical properties of high-tensile indented wires (IS: 6003–1983)*

Nominal Diameter (mm)	*Tensile Strength (minimum)* (N/mm^2)	*Elongation* (per cent)
5.00	1570	4.00
4.00	1715	3.00
3.00	1865	2.50

Table 2.20 *Mechanical properties of uncoated stress-relieved strand (IS: 6006–1983)*

Class	*Designation*	*Nominal Diameter of Strand* (mm)	*Tolerances on the Nominal Diameter of Strand*	*Nominal Cross-sectional Area of Strand* (mm^2)	*Breaking Load Minimum (N)*	*0.2 per cent Proof Load Minimum (N)*
	2–ply 2 mm	—	—	6.28	12,750	10.840
—	2–ply 3 mm	—	—	14.14	25,500	21,670
	3–ply 3 mm	—	—	21.21	38,250	32,460
1	6.3 mm 7–ply	6.3	±0.4	23.20	40,000	34,000
	7.9 mm 7–ply	7.9	±0.4	37.40	64,500	54,700
	9.5 mm 7–ply	9.5	±0.4	51.60	89,000	75,600
	11.1 mm 7–ply	11.1	±0.4	69.70	1,20,100	1,02,300
	12.7 mm 7–ply	12.7	±0.4	92.90	1,60,100	1,36,200
	15.2 mm 7–ply	15.2	±0.4	139.40	2,40,200	2,04,200
2	9.5 mm 7–ply	9.5	+0.66 –0.15	54.80	1,02,300	87,000
	11.1 mm 7-ply	11.1	+0.66 –0.15	74.20	1,37,900	1,17,200
	12.7 mm 7-ply	12.7	+0.66 –0.15	98.70	1,83,700	1,56,100
	15.2 mm 7-ply	15.2	+0.66 –0.15	140.00	2,60,700	2,21,500

The typical stress-strain characteristics of a high-tensile steel wire is shown in Fig. 2.4. Unlike ordinary mild steel, high-tensile wires have no well-defined yield point and it is necessary to refer to the proof stresses, which correspond to specified permanent strains.

The 0.2 per cent proof stress for high-tensile steel wires and bars should not be less than 85 and 80 per cent, respectively, of the minimum specified tensile strength. An important requirement of the steel used in a prestressed member is the plasticity of the steel at stresses near the ultimate stress. This is essential to achieve progressive failure of the prestressed concrete members with sufficient warning before final failure. To avoid the possibility of brittle fracture, the normal practise is to specify that the high-tensile steel will have a minimum elongation at rupture. The Indian Standard Code prescribes a minimum percentage elongation varying from 2.5 per cent for wires to 10 per cent for bars, as specified in Tables 2.17, 2.18 and 2.19. However, for strands, the percentage elongation measured on a gauge length of not less than 600 mm should not be less than 3.5 per cent immediately prior to the fracture of any of the component wire.

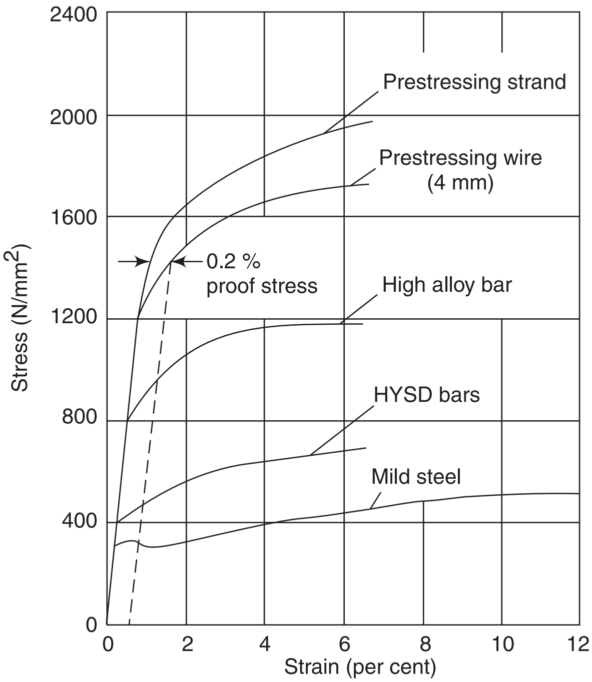

Fig. 2.4 *Stress-strain curves for reinforcing and prestressing steels*

The Indian Standard Code IS: 1343 specifies the values of the modulus of elasticity of high-tensile wires, bars and strands as 210, 200 and 195 kN/mm^2, respectively.

2.2.3 Permissible Stresses in Steel

Tensile stresses in steel at the time of tensioning behind the anchorages and after allowing for all possible losses are generally expressed as a fraction of the ultimate tensile strength or proof stress. The recommendations of the various national codes vary marginally with regard to the allowable stresses in prestressed members at different stages. The permissible stress values specified in the Indian, American and British codes and FIP[31] are compared in Table 2.21.

The British code, however, permits jacking forces up to 80 per cent of the characteristic strength of steel provided additional consideration is given to safety and to the load extension characteristics of the tendon.

2.2.4 Relaxation of Stress in Steel

When a high-tensile steel wire is stretched and maintained at a constant strain, the initial force in the wire does not remain constant but decreases with time. The decrease of stress in steel at constant strain is termed as *relaxation.* In a

Table 2.21 *Permissible stresses in high-tensile steel*

	IS: 1343	*ACI: 318M–2011*	*BS EN: 1992–1–1: 2004*	*FIP–2002*
At the time of initial tensioning	Initial prestress not to exceed 80 per cent of the characteristic tensile strength of tendons	Initial prestress due to tendon jacking force not to exceed 94 per cent of the specified yield strength but not greater than 80 per cent of the specified tensile strength of tendons.	Initial prestress should not normally exceed 70 per cent of the characteristic tensile strength and in no case should it exceed 75 per cent.	Initial prestress not to exceed 80 per cent of the characteristic tensile strength or 90 per cent of the 0.1 per cent proof stress of tendons.
Immediately after prestress transfer	—	For post-tensioning tendons at anchorages and couplers immediately after anchorages, the stress should not exceed 70 per cent of the tensile strength of tendons.		The tensile stress not to exceed 75 per cent of the characteristic tensile strength or 85 per cent of the 0.1 per cent proof-stress of tendons.
Final stress after allowing for all losses of prestress	Not less than 45 per cent of the characteristic tensile strength of tendons	—	Not greater than 60 per cent of the characteristic tensile strength of tendons.	

prestressed member, the high-tensile wires between the anchorages are more or less in a state of constant strain. However, the actual state of relaxation will be less than that indicated by a test of a wire at constant length, as there will be a shortening of the member due to other causes. In high-tensile strength steels, at elevated stresses in excess of 0.01 per cent proof stress, the relaxation of stress increases with the magnitude of initial stress. If the stress is kept constant, the material exhibits a plastic strain over and above the initial elastic strain, generally referred to as *creep*.

The cold-drawn steels creep more than heat-treated or tempered steels due to their lower magnitude of 0.01 per cent proof stress. The phenomenon of creep is influenced by the chemical composition, micro structure, grain size and variables in the manufacturing process, which results in changes in the internal crystal structure. Several hypotheses have been put forward to explain the mechanism of creep in stee1.[32,33]

The high-tensile steel tendon in a prestressed concrete member does not remain strictly under a constant condition of either stress or strain. The most severe condition occurs generally at the stage of initial stressing; subsequently, the strain in the steel reduces as the concrete deforms under the prestressing force.

The various code provisions for the relaxation of stress in steel are based on the results of a 1000-hour relaxation test on the wires. There is also provision for acceptance based on a 100-hour relaxation test. It has been observed that the loss recorded over a period of about 1000 hours from an initial stress of 70 per cent of the tensile strength is about the same as that over a period of four years from an initial stress of 60 per cent of the tensile strength. According to Stussi,[34] the relaxation curves obtained over 1000 hours can be extrapolated by a logarithmic plot.

The Indian Standard Codes for wires and bars prescribe the 1000-hour relaxation test with no relaxation exceeding five per cent of the initial stress. Alternatively, one can resort to the 100-hour relaxation test with no relaxation exceeding 3.5 per cent of the initial stress. Similar provisions have also been made in the British and American codes.

Experiments[35] have shown that a reduction in relaxation stress is possible by preliminary overstressing. A preliminary overstress of 5–10 per cent maintained for 2-3 minutes considerably reduces the magnitude of relaxation. Some codes permit temporary overstressing with corresponding lower magnitudes of relaxation stress.

2.2.5 Stress Corrosion

The phenomenon of stress corrosion in steel is particularly dangerous, as it results in sudden brittle fractures. Stress-corrosion cracking results from the combined action of corrosion and static tensile stress, which may be either residual or externally applied. This type of attack in alloys is due to the internal metallurgical structure, which is influenced by composition, heat treatment and mechanical processing. The causes of the susceptibility of high-tensile steels to stress corrosion are manifold[36]. Schwier[37] reported that heat-treated wires are specially prone to stress-corrosion fractures when compared to drawn wires. If the ducts of post-tensioned members are not grouted, there is a possibility of stress corrosion leading to a catastrophic/failure of the structure.

Other common types of corrosion frequently encountered in prestressed concrete constructions are pitting corrosion and chloride corrosion. A critical review of the different types of corrosion of high-tensile steel in structural concrete is reported elsewhere[38]. Some of the important protective measures against stress corrosion include protection from chemical contamination, protective coatings for high-tensile steel and grouting of ducts immediately after prestressing operations.

2.2.6 Hydrogen Embrittlement

Atomic hydrogen is liberated as a result of the action of acids on high-tensile steels. This penetrates into the steel surface, making it brittle and fracture-prone on being subjected to tensile stress. Even small amounts of hydrogen can cause considerable damage to the tensile strength of high-tensile steel wires.

Use of high-alumina cement and blast-furnace-slag cement, which are rich in sulphides, for making prestressed concrete can cause hydrogen embrittlement. Use of dissimilar metals such as aluminium and zinc for sheath to house high tensile steel wires will also result in hydrogen embrittlement. Similarly, minute traces of sulphur, which come in contact with high-tensile steel wires in the presence of moisture, can drastically reduce their strength.

In order to prevent hydrogen embrittlement, it is essential that the steel is properly protected from the action of acids. Protective coverings like bituminous crepe-paper covering during transport, reduces the chances of contamination. The wires should be protected from rain water and excessive humidity by storing them in dry conditions.

2.2.7 Durability, Fire Resistance and Cover Requirements for PSC Members

The alkaline environment of Portland cement concrete generally protects embedded tendons and other supplementary reinforcements against corrosion from various environmental agencies. However, the carbonation of hydrated cement gradually progresses from the surface to the interior of concrete, thus reducing the effective protection provided by the concrete against rusting of steel tendons. Many codes have provided for minimum cover requirements in this regard. It is pertinent to note that not only the thickness of cover but also the density of concrete in the cover is important to provide effective protection to steel.

The Indian Standard Code (IS: 1343) provides for a minimum clear cover of 20 mm for protected pretensioned members, while it is 30 mm or the size of the cable (whichever is bigger) in the case of protected post-tensioned members. If the prestressed members are exposed to an aggressive environment, these cover requirements are increased by 10 mm. The IS code also prescribes minimum cement content and maximum water/cement ratio in concrete to ensure durability under specified conditions of exposure as compiled in Table 2.11.

The cover requirements according to the British code BS EN: 1992–1–1: 2004 are governed by considerations of durability or fire resistance. Fire resistance is a measure of the ability of the structural member to withstand the effect of fire without reaching any of the limit states. It is expressed in terms of time by standard fire tests outlined in BS: 476 (Part 8) 1972 and ASTME 119–1979. Fire resistance of structural concrete elements is influenced by the following parameters:

1. Size and shape of the element
2. Detailing, type and quality of reinforcement or prestressing tendons
3. The level of load supported and pattern of loading
4. Type of concrete and aggregate
5. Conditions at end bearing
6. Protective cover to reinforcement

The minimum nominal covers prescribed in the British code BS EN: 1992–1–1: 2004 for protection against corrosion and fire are compiled in Tables 2.22 and 2.23, respectively. The nominal covers specified for fire-resistance relate specifically to the minimum member dimensions with beam widths in the range of 200–280 mm, rib widths varying from 125–175 mm, column widths varying from 150–450 mm, and floor thickness in the range of 75–170 mm. Guidance for increased covers, if smaller members are used, is also provided in the British code.

Table 2.22 *Nominal cover to all steel (including links) to most durability requirements (BS EN: 1992–1–1: 2004)*

Conditions of Exposure	*Nominal Cover* (mm)			
Mild	20	20*	20*	20*
Moderate	—	30	25	20
Severe	—	40	30	25
Very Severe	—	50+	40+	30
Extreme	—	—	60+	50
Maximum free water/cement ratio	0.60	0.55	0.50	0.45
Minimum cement content (kg/m^3)	300	325	350	400
Lowest grade of concrete	C35	C40	C45	C50

* These covers may be reduced to 15 mm provided that the nominal maximum size of aggregate does not exceed 15 mm.

+ Where concrete is subject to freezing whilst wet, air entrainment is used.

Note: This Table relates to the nominal-weight aggregate of 20 mm nominal maximum size.

Table 2.23 *Nominal cover to all steel to meet specified periods of fire resistance (BS EN: 1992–1–1: 2004)*

	Nominal Cover (mm)					
Fire Resistance (hours)	*Beams*		*Floors*		*Ribs*	
	Simply Supported	*Continuous*	*Simply Supported*	*Continuous*	*Simply Supported*	*Continuous*
0.5	20	20	20	20	20	20
1.0	20	20	25	20	35	20
1.5	35	20	30	25	45	35
2.0	60	35	40	35	55	45
3.0	70	60	55	45	65	55
4.0	80	70	65	55	75	65

2.2.8 Protection of Prestressing Steel, Sheathing and Anchorages

To prevent deterioration due to corrosion, unbonded tendons should be coated by non-reactive materials like epoxy or zinc or zinc aluminium. Non-corroding sheathing material like high density polyethylene (HDPE) is beneficial. The space between sheathing and duct can be filled with corrosion inhibiting materials like grease, wax or petroleum jelly. External parts of anchorages and projecting cables should be covered by suitable casing. The prestressing steel stored at site should also be protected by proper packaging films to guard against corrosion.

References

1. Erntroy, HC and BW Shacklock, "Design of high strength concrete mixes", *Proceedings of a Symposium on Mix Design and Quality Control of Concrete;* Cement and Concrete Association, London, May 1954, pp 55-65.
2. ACI Committee- 211, Guide for selecting proportions for No-Slump concrete, ACI-211.3R-97, American Concrete Institute, Farmington Hills, Michigan, USA, 1997.
3. Teychenne, DC, RE Franklin and HC Erntroy, *Design of Normal Concrete Mixes,* Department of Environment, London, HMSO, 1975, p. 31.
4. Road Research Laboratory, *Design of Concrete Mixes,* DSIR Road Note No.4, London, HMSO, 1950, pp 1-14.
5. IS: 10262-1982, *Indian Standard Guide Lines for Concrete Mix design,* Bureau of Indian Standards, New Delhi, 1983, pp 1-21.
6. Krishna Raju, N, Design of Concrete Mixes (Fifth Edition), CBS Publishers and Distributors, New Delhi, 2012, pp 102 -122.
7. IS: 1343–2012, *Indian Standard Code of Practice for Prestressed Concrete* (Second Revision), Bureau of Indian Standards, New Delhi, 2012, pp 1–56.
8. BS EN: 1992-1-1:2004, Euro Code-2, *Design of Concrete Structures - General Rules and Rules for Buildings,* British Standards Institution, 2004.

9. IS: 456-2000, *Indian Standard Code of Practice for Plain and Reinforced Concrete,* (Fourth Revision), Bureau of Indian Standards, New Delhi, 2000, pp 100.
10. ACI: 318M-2011, *Building Code Requirements for Structural Concrete,* American Concrete Institute, Farmington Hills, Michigan, USA, 2011.
11. FIP - 1984, *Recommendations on Practical Design of reinforced and Prestressed Concrete Structures,* Thomas Telford Limited, London, 1984, pp 10-22.
12. Troxel, GE, JM Raphael, and RE Davis, "Long time creep and shrinkage tests of plain and reinforced concrete," *Proceedings of the American Society of Testing Materials,* Vol. 58, 1958, pp 1101–1120.
13. Kordina, KM, "Experiments on the influence of the minerological character of aggregates on the creep of concrete," *RILEM Symposium,* Munchen, Nov. 1958.
14. *CEB Manual on Structural Effects of Time-Dependent Behaviour of Concrete,* Georgia Publishing Company, Saint-Saphorin (CH), 1984.
15. *CEB Manual on Cracking and Deformations,* Georgia Publishing Company, Saint-Saphorin (CH), 1983.
16. Leonhardt, F, *Prestressed Concrete, Design and Construction,* IInd edn, Wilhelm Ernst and Sohn, Berlin, Munich, 1964.
17. Krishna Raju, N, "Compressibility and modulus of rupture of high-strength concrete," *Journal of the Institution of Engineers* (India) Vol. 52, No.3, CI. 2, Nov. 1971, pp 98–101.
18. BS: 882–1954, *British Standard Specification for Coarse Aggregates from Natural Sources for Concrete,* British Standards Institution, London, 1954.
19. Teychenne, DC, "Structural concrete made with lightweight aggregates," *Concrete,* Vol. 1, No. 4, April 1967, pp 111–112.
20. "*ACI Standard Recommended Practice for selecting proportions for structural light weight concrete,*" ACI: 211.2 – 98. ACI Manual of Concrete Practice, American Concrete Institute, Farmington Hills, Michigan, USA, 1998;
21. Shideler, JJ, "Lightweight aggregate concrete for structural use," *Journal of the American Concrete Institute, Proceedings,* Vol. 54, No. 4, Oct. 1957, pp 299–328.
22. Best, CH and M Polivka, "Creep of lightweight concrete," *Magazine of Concrete Research,* London, Nov. 1959, pp 129–134.
23. Gerwick, BC, *Construction of Prestressed Concrete Structures,* Wiley Inter Science, New York, 1971.
24. IS : 1785 (Part II) – 1983, *Indian Standard Specification for Plain Hard-Drawn Steel Wire for Prestressed Concrete,* Part II as drawn wire, (2nd revision), Indian Standards Institution, New Delhi, 1983.
25. IS : 1785 (Part I) – 1983, *Indian Standard Specification for Plain Hard-drawn Steel Wire for Prestressed Concrete,* Part I cold-drawn stress relieved wire, (2nd revision), Indian Standards Institution, 1983.
26. IS : 6003–1983, *Indian Standard Specification for Indented Stress-Relieved Wire for Prestressed Concrete,* (Ist revision), Indian Standards Institution, New Delhi, (Ist reprint), April 1990.
27. IS : 6006–1983, *Indian Standard Specification for Uncoated Stress Relieved Strand for Prestressed Concrete* (Ist revision), Indian Standards Institution, New Delhi, first reprint, October 1989.
28. IS : 2090–1983, *Indian Standard Specification for High-Tensile Steel Bars Used*

in Prestressed Concrete, (Ist revision), Indian Standards Institution, New Delhi, Ist reprint, October 1988.
29. Libby, J R, *Prestressed Concrete—Design and Construction,* The Ronald Press Company, New York, 1961, pp 9–11.
30. Bate, SCC and EW Bennett, *Design of Prestressed Concrete,* Surrey University Press, International Text Book Company Limited, London, 1976, pp 13–16.
31. *FIP Recommendations for Practical Design of Reinforced and Prestressed Concrete Structures,* Thomas Telford Limited, London, 1984, pp 9–12.
32. Zener, C and J H Hollomon, "Plastic flow and rupture of metals," *Transactions of the American Society of Metals*, Vol. 33, 1944, p. 163.
33. Wilms, G R and W A Wood, "Mechanism of creep in metals," *Journal of the Institute of Metals*, Vol. 82,1951–52, p. 521.
34. Stussi, F, "Zur relaxation von stahl—drahten," *IV BH Abh. 19 (1959).* S. 273–286. DISC speck F in 20 (1960) S. 391. bis 398.
35. Magnel, G, Lebeton Precontraint, Editions Fecheyr, Ghent 1948.
36. Althof, FC, Inter cristalline Korrosion and Spannungs Korrosion S. 38 ff. Katz.. W: Elsen S. 113 ff. *In Korrosion und Korrosion-sschitz watter de Gruyter U. Co.* Berlin, 1955.
37. Schwier, F, "Stress corrosion and relaxation in high-carbon steel wires for prestressed concrete," *Wire and Wire Products* 1955, pp 1473–1479.
38. Krishna Raju, N., "Corrosion of high-tensile steel in structural concrete," Proceedings of the Journal of Electro-Chemical Society of India, 22(2), 1973, pp 100–105.

Review Questions

2.1 Distinguish between low, medium and high-strength concrete.
2.2 What are the main factors influencing the design of high-strength concrete mixes?
2.3 List the various methods generally used for the design of high-strength concrete mixes.
2.4 What type of aggregates are recommended for the production of high-strength concrete?
2.5 What is the minimum concrete strength requirements prescribed for prestressed concrete members in IS: 1343 code?
2.6 Distinguish between creep and shrinkage of concrete.
2.7 What are the factors influencing the creep and shrinkage of concrete?
2.8 Mention the basic difference between mild steel, high yield strength deformed steel and high-tensile steel.
2.9 Distinguish between, proof stress and ultimate tensile stress of high-tensile steel. What is the practical significance of proof stress?
2.10 Distinguish between the terms, stress relaxation, stress corrosion and hydrogen embrittlement with reference to high-tensile steel.

Objective-type Questions

2.1 The grade of concrete for prestressed members should be in the range of
(a) M-20 to M-30 (b) M-80 to M-100 (c) M-30 to M-60
2.2 High-strength mixes should have a water/cement ratio of
(a) 0.6 to 0.8 (b) 0.3 to 0.4 (c) 0.2 to 0.3
2.3 Creep of concrete in a structural member is due to
(a) elastic strain
(b) elasto-plastic strain
(c) inelastic strain
2.4 Shrinkage of concrete in a structural member is due to
(a) dead load on the member
(b) live load
(c) loss of moisture and drying of concrete
2.5 Modulus of elasticity of concrete is generally expressed in terms of
(a) shear strength
(b) compressive strength
(c) tensile strength
2.6 Target mean strength of concrete depends upon
(a) water/cement ratio
(b) type of aggregate
(c) characteristic strength of concrete
2.7 Workability of concrete is influenced significantly by
(a) target mean strength
(b) water/cement ratio
(c) type of cement
2.8 High-tensile steel is basically
(a) low carbon steel
(b) high manganese steel
(c) high carbon steel
2.9 The creep coefficient depends upon the
(a) span of the structural member
(b) notional size of the member
(c) depth of the member
2.10 In the case of prestressing steels, the highest stress is reached in
(a) high-tensile steel wires
(b) high-tensile steel bars
(c) high-tensile strands

Answers to Objective-type Questions

2.1 (c)	2.2 (b)	2.3 (c)	2.4 (c)	2.5 (b)
2.6 (c)	2.7 (b)	2.8 (c)	2.9 (b)	2.10 (c)

3 Prestressing Systems

3.1 Introduction

The various methods by which precompression is imparted to concrete are classified[1] as follows:

1. Generation of compressive force between the structural element and its abutments using flat jacks.
2. Development of hoop compression in cylindrically shaped structures by circumferential wire winding.
3. Use of longitudinally tensioned steel embedded in concrete or housed in ducts.
4. Use of the principle of distortion of a statically indeterminate structure either by displacement or by rotation of one part relative to the remainder.
5. Use of deflected structural steel sections embedded in concrete until the hardening of the latter.
6. Development of limited tension in steel and compression in concrete by using expanding cements.

The most widely used method for prestressing of structural concrete elements is longitudinal tensioning of steel by different tensioning devices. Prestressing by the application of direct forces between abutments is generally used for arches and pavements, while flat jacks are invariably used to impart the desired forces. For circular structures, such as tanks and pipes, it is a common practise to impart precompression in concrete by circular prestressing. With the development of expansive cements, prestress in concrete can be developed by chemical prestressing.

3.2 Tensioning Devices

The various types of devices used for tensioning steel are grouped under four principal categories, namely:

1. Mechanical
2. Hydraulic
3. Electrical (thermal)
4. Chemical

The mechanical devices generally used include weights with or without lever transmission, geared transmission in conjunction with pulley blocks, screw jacks with or without gear drives and wire-winding machines. These devices are employed mainly for prestressing structural concrete components produced on a mass scale in factories.

Hydraulic jacks, being the simplest means of producing large prestressing forces, are extensively used as tensioning devices. Several commonly used patented jacks are due to Freyssinet, Magnel, Gifford Udall and Baur-Leonhardt for the range of 5–100 tonnes. Large hydraulic jacks for forces in the range of 200–600 tonnes have also been developed by Baur–Leonhardt. It is important that during the tensioning operation, the force applied should be accurately measured. In most of the jacks, calibrated pressure gauges directly indicate the magnitude of force developed during the tensioning of the wires.

Electrical devices have been successfully used in erstwhile USSR since 1958 for tensioning of steel wires and deformed bars. The steel wires are electrically heated and anchored before placing concrete in the moulds. This method is often referred to as 'thermo-electric prestressing'.

In the chemical method, expanding cements are used and the degree of expansion is controlled by varying the curing conditions. Since the expansive action of cement while setting is restrained, it induces tensile forces in tendons and compressive stresses in concrete.

3.3 Pretensioning Systems

In the pretensioning system, the tendons are first tensioned between rigid anchor-blocks cast on the ground or in a column or unit-mould-type pretensioning bed, prior to the casting of concrete in the moulds. A typical column-type pretensioning bed is shown in Fig. 3.1. The tendons comprising

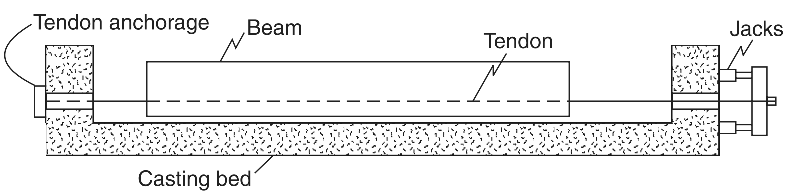

(a) Beam with straight tendon

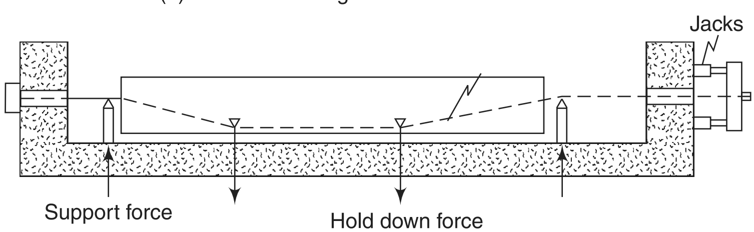

(b) Beam with variable tendon eccentricity

Fig. 3.1 *Methods of pretensioning*

individual wires or strands are stretched with constant eccentricity as shown in Fig. 3.1(a) or variable eccentricity as shown in Fig. 3.1(b) with tendon anchorage at one end and jacks at the other. With the forms in place, the concrete is cast around the stressed tendon.

High early strength concrete is often used in a factory to facilitate early stripping and reuse of moulds. When the concrete attains sufficient strength, the jacking pressure is released. The high-tensile wires tend to shorten but are checked by the bond between concrete and steel. In this way, the prestress is transferred to the concrete by bond, mostly near the ends of the beam, and no special anchorages are required in pretensioned members.

For mass production of pretensioned elements, the long-line process developed by Hoyer is generally used in a factory. In this method, the tendons are stretched between two bulk heads several hundred metres apart so that a number of similar units may be cast along the same group of tensioned wires as shown in Fig. 3.2. The tension is applied by hydraulic jacks or by a movable stressing machine. The wires or strands when tensioned singly or in groups are generally anchored to the abutments by steel wedges.

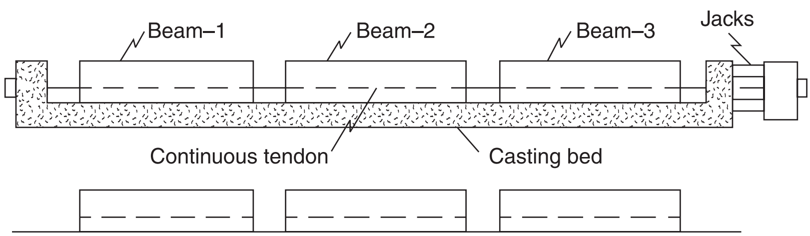

Fig. 3.2 *Hoyer's long line system of pretensioning*

The transfer of prestress to concrete is usually achieved by large hydraulic or screw jacks by which all the wires are simultaneously released after the concrete attains the requisite compressive strength. Generally, strands of up to 18 mm diameter and high-tensile wires of up to 7 mm diameter anchor themselves satisfactorily with the help of the surface bond and the interlocking of the surrounding matrix in the micro indentations on the wires. The bond of prestressing wires may be considerably improved by forming surface indentations and by helical crimping of the wires. Strands have considerably better bond characteristics than plain wires of equal cross-sectional area. Supplementary anchoring devices are required when single wires of larger diameter (exceeding 7 mm) are used in the pretensioned units. The most commonly used devices are the 'Weinberg clip' developed in France[2] and the 'Dorland clip' developed in the United States (Fig. 3.3). These clips are clamped on to the tensioned wires close to the end diaphragms of the units before concreting operations.

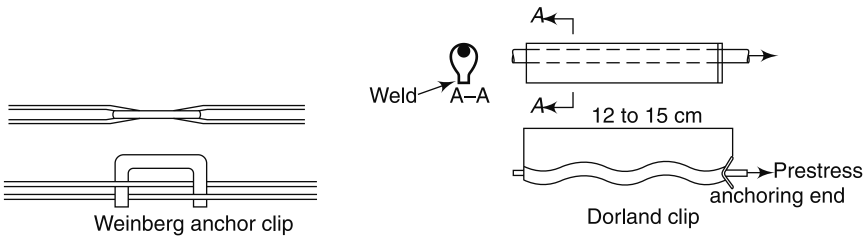

Fig. 3.3 *Supplementary anchoring devices*

3.4 Post-Tensioning Systems

3.4.1 Principles of Post-tensioning

In post-tensioning, the concrete units are first cast by incorporating ducts or grooves to house the tendons. When the concrete attains sufficient strength, the high-tensile wires are tensioned by means of jack bearing on the end face of the member and anchored by wedges or nuts. The forces are transmitted to the concrete by means of the end anchorages and, when the cable is curved, through the radial pressure between the cable and the duct. The space between the tendons and the duct is generally grouted after the tensioning operation.

Most of the commercially patented prestressing systems are based on the following principles of anchoring the tendons:

1. Wedge action producing a frictional grip on the wires.
2. Direct bearing from rivet or bolt heads formed at the end of the wires.
3. Looping the wires around the concrete.

3.4.2 Post-tensioning Anchorages

The Freyssinet system of post-tensioning anchorages which was developed in 1939, gave impetus to the various new systems devised over the years. At present, according to Abeles[4], there are over 64 patented post-tensioning systems used worldwide. Some of the more prominent systems are compiled in Table 3.1, based on the work of Abeles[4] and Bennett[5].

The post-tensioning systems based on wedge-action include the Freyssinet, Gifford–Udall, Anderson and Magnel–Blaton anchorages.

The Freyssinet anchorage system, which is widely used in Europe and India, consists of a cylinder with a conical interior through which the high-tensile wires pass and against the walls of which the wires are wedged by a conical plug lined longitudinally with grooves to house the wires as shown in Fig. 3.4(a). The main advantage of the Freyssinet system is that a large number of wires or strands can be simultaneously tensioned using the double-acting hydraulic jack as shown in Fig. 3.4(b). The Freyssinet range of anchorages available for wires and strands is compiled in Tables 1, 2 and 3 of Appendix-3.

Table 3.1 *Post-tensioning systems*

S. No.	*Post-tensioning System (Country of Origin)*	*Type of Tendon*	*Range of Force**	*Cable Duct*	*Arrangement of Tendons in Duct*	*Method of Tensioning*	*Type of Anchorage*
	(1)	*(2)*	*(3)*	*(4)*	*(5)*	*(6)*	*(7)*
1.	Anderson (USA)	Strands	Medium and large	Circular, formed by pneumatic tube or flexible corrugated metal tube	Annular, spaced by helical wire core	Hydraulic jack simultaneous tensioning of all wires	Steel socket with grooves and metal plug driven into the socket
2.	Baur-Leonhard (Germany)	Wires and strands	Very large	Wires external	Continuously wound around sides and semicircular end blocks	Hydraulic jack formed in concrete between beam and end blocks tensioning all wires together	Space between beam and end blocks concreted
3.	Billner (USA)	Wires	Medium	Formed by coating wires with bitumen	As required, wires doubled and looped at ends	Jack inserted in joint at the centre of beam	Wires looped at ends; rapid hardening grout inserted in joint at centre
4.	BBRV (Switzerland)	Wires and strands	Medium, large and very large	Circular, formed by flexible corrugated metal tube	Annular spaced with button heads	Hydraulic jack tensioning, barrel screwed on to the anchor element	Annular nut bearing against a circular anchor plate at the end of beam element

(Contd.)

Table 3.1 *(Contd.)*

5.	Dywidag (Germany)	Bars	Medium, large and very large	Circular, formed by metal sheath	Single bars	Hydraulic jack tensioning the bar	Nut tightened on pressed high-strength thread on bar, bearing on steel plate on end of beam
6.	Freyssinet (France)	Wires and strands	Medium and large	Circular, formed by pneumatic tube or metal or plastic sheath around cable	Annular, spaced by helical wire core	Hydraulic jack tensioning all wires at a time	Conical serrated concrete wedge drive by jack into female cone embedded at the end of the beam
7.	Gifford–Udall-CCL (Great Britain)	Wires	Small and medium	Circular, formed by pneumatic tube or steel rod	Evenly spaced by perforated spacers at intervals	Hydraulic jack tensioning wires singly	Split conical wedge and bush to each wire, bearing on anchor thrust plate and ring cast into end of beam
8.	Leoba (Germany)	Wires	Medium and large	Rectangular, formed by corrugated metal sheath	Two horizontal rows of six wires with spacers at intervals; wires looped at ends	Hydraulic jack pulling looped ends of wires by rod and cast-steel cross head	At fixed-end, wires hooked and concreted in. At jacking end, temporarily anchored by nut, then permanently by grouting cable
9.	Lee–McCall (Great Britain)	Bars threaded at ends	Small, medium and large	Circular, formed by pneumatic tube or flexible corrugated metal tube	Single bars	Hydraulic jack screwed to threaded end of bar	High-strength nut and spacing washers bearing on steel plate on end of beam

(Contd.)

Table 3.1 *(Contd.)*

10.	Magnel–Blaton (Belgium)	Wires	Small, medium and large	Rectangular, formed by solid rubber core or by metal sheath around cable	Horizontal rows of four wires spaced by metal grilles at intervals	Hydraulic jack tensioning two wires at a time	Pairs of wires held by flat steel wedges in sandwich plates bearing on distribution plates
11.	Prescon (USA)	Wires	Medium	Circular, formed by flexible metal tube	Annular spaced with button heads	Hydraulic jack tensioning barrel screwed on to anchor-element	Shims inserted between the anchor element and distribution plate
12.	PSC (Monowire) (Great Britain)	Wires	Small and medium	Rectangular formed by metal sheath	Evenly spaced by perforated spacers at intervals	Hydraulic jack tensioning wires singly	Individual wires fixed by split sleeves in tapered holes in bush or cast block bearing on end
13.	Losinger VSL (Switzerland)	Strands	Large to very large	Circular formed by flexible metal tube	Evenly spaced by metallic spacers	Multistrand hydraulic jack	Anchor head with VSL grippers, bearing plate and sleeve
14.	Freyssinet (International)	Strands	Large to very large	Circular formed by flexible metal tube	Evenly spaced by perforated spacers	Hydraulic jack tensioning all strands at a time	Split conical wedge and bush to each strand bearing on anchor thrust plate

*Range of forces: Small—Up to 130 kN, Medium—130–500 kN
Large—Over 500 kN, Very large—over 4500 kN

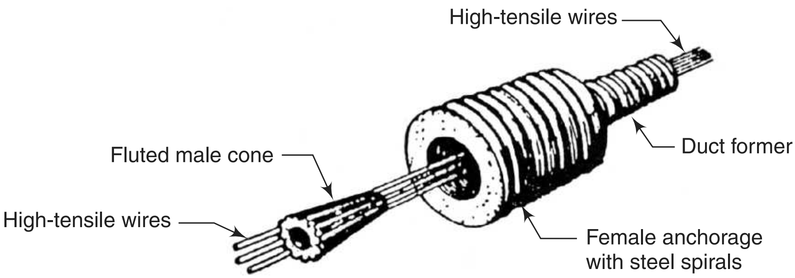

Fig. 3.4(a) *Freyssinet anchorage*

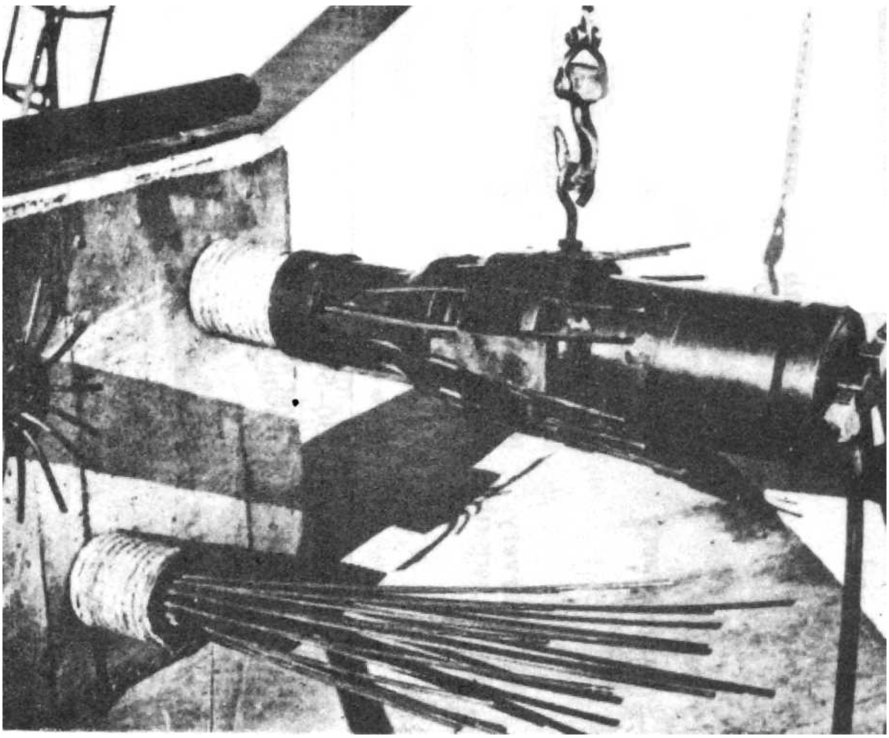

Fig. 3.4(b) *Freyssinet hydraulic jack tensioning wires*

The Gifford-Udall (CCL) system developed in UK, consists of steel split-cone and cylindrical female-cone anchorages to house the high-tensile wires bearing against steel plates as shown in Fig. 3.5. Each wire is tensioned separately and anchored by forcing a sleeve wedge into a cylindrical grip resting against a bearing plate. The ducts are generally formed by metal sheaths cast into the concrete member. The data regarding the CCL system of anchorages is compiled in Table 4 of Appendix-3.

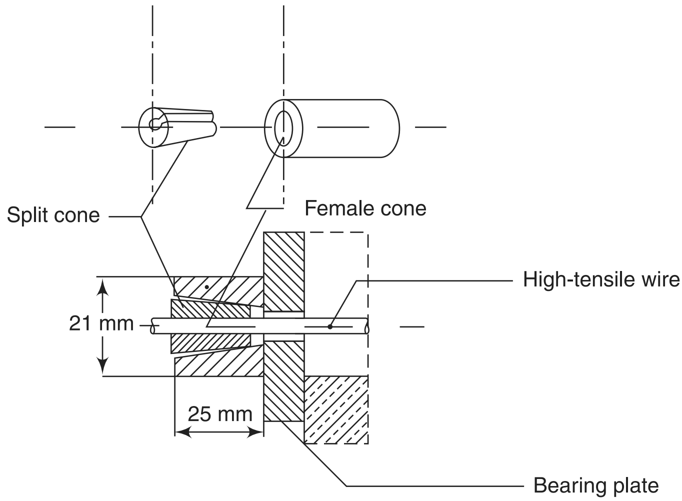

Fig. 3.5 *Gifford Udall system*

In the Lee–McCall system, the tendons comprise high-tensile bars of diameter varying from 12–40 mm which are threaded at the ends. After tensioning, each bar is anchored by screwing a nut and washer tightly against the end plates. In this system, the forces are transmitted by the bearing at the end blocks. While the system eliminates the loss of stress due to anchorage slip, it has a disadvantage that the curved tendons cannot be used. Figure 3.6 shows the typical Lee–McCall anchorage system.

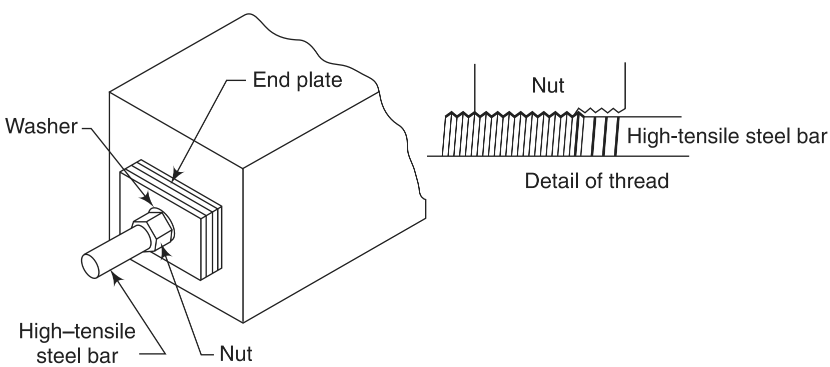

Fig. 3.6 *Lee–McCall system*

The Magnel–Blaton post-tensioning system adopts metallic sandwich plates, flat wedges, and a distribution plate for anchoring the wires. Each sandwich plate can house up to four pairs of wires. The distribution plate may be cast into the member at the desired location. The number of wires in the Magnel cable varies from 2 to 64. The Magnel–Blaton anchorage is shown in Fig. 3.7.

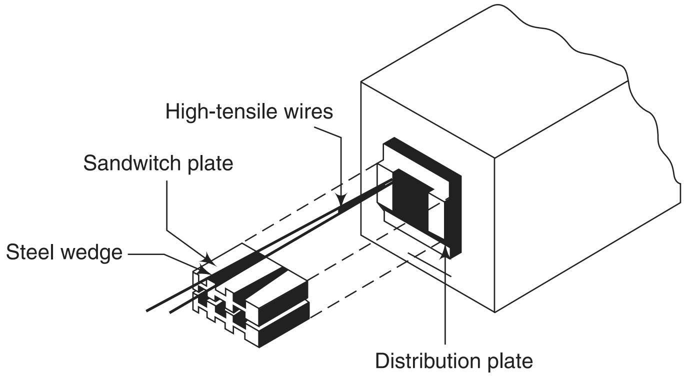

Fig. 3.7 *Magnel–Blaton system*

The BBRV post-tensioning system was developed in 1949 by four Swiss engineers—Birkenmeier, Brandestini, Ros and Vogt. This system is well suited for transmitting large forces. A BBRV tendon consists of several parallel lengths of high-tensile wires, with each end terminating in a cold-formed button head with a machined anchorage fixture as shown in Fig. 3.8(a). In the case of tendons formed by strands, they are anchored to the machined fixture by split-cone sleeves as shown in Fig. 3.8(b). At present, tendons capable of developing forces up to 12000 kN are available under this system. For heavy constructions, such as long-span bridges and nuclear containment vessels, tendons comprising 90–170 wires are commonly used. The BBRV system provides for the simultaneous stressing of all the wires in a tendon as shown in Fig. 3.8(c). After the desired extension of the tendon is reached, a threaded nut is screwed to the anchor head, which transmits the forces by bearing against the end-plate as shown in Fig. 3.8(d). The dimensions of the bearing plates, anchor head and tendons used in the BBRV system are compiled in Table 5 of Appendix-3.

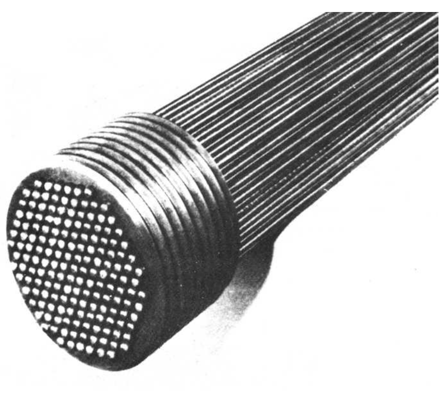

(a) BBRV wire tendon with button heads

Fig. 3.8 *(Contd.)*

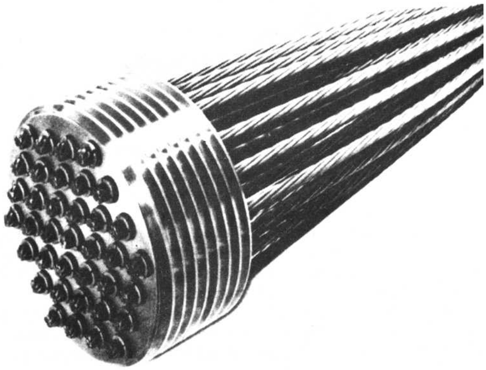

(b) BBRV strand tendon

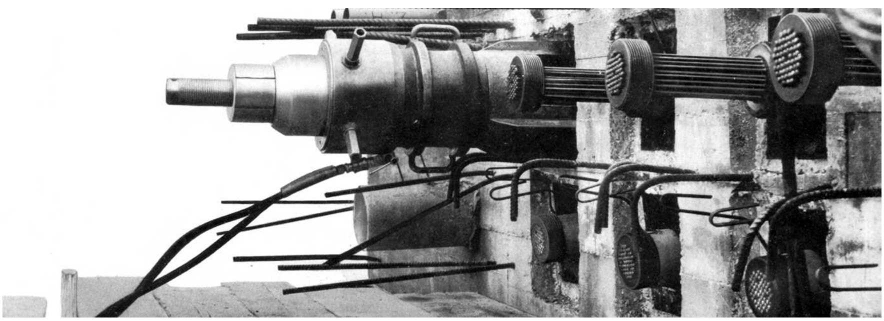

(c) Tensioning of BBRV tendons

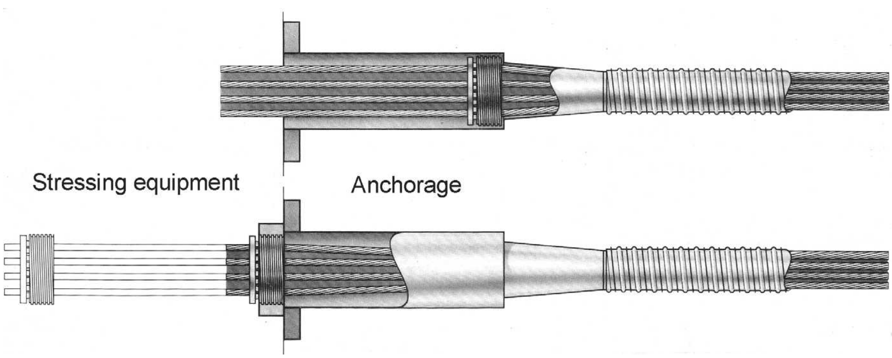

(d) Anchoring of BBRV tendons

Fig. 3.8 *BBRV post-tensioning system*

The Prescon system uses tendons consisting of 2–130 wires, which are arranged parallel in a sheath. The wires are threaded through a stressing washer at each end before the button heads at the ends are formed. After stressing, steel shims are inserted, which bear against the end-bearing plate, as shown in Fig. 3.9. The Prescon system is similar to the BBRV system with respect to the button heads formed at the ends to tendons.

The Baur–Leonhardt system, developed in Germany, belongs to the group of loop anchorages. In this system, double tendons are wrapped around the end-block, which is D-shaped at the end of the structure and is detached from the main beams. These end blocks are forced to move away by large hydraulic jacks as shown in Fig. 3.10. The gap between the end block and the main structure is filled with concrete. This system has been used in Germany for the construction of long-span bridges. The Leoba system also belongs to the group of loop anchorages.

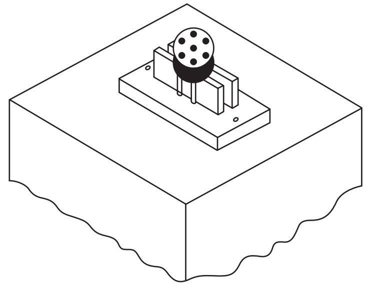

Fig. 3.9 *Prescon system*

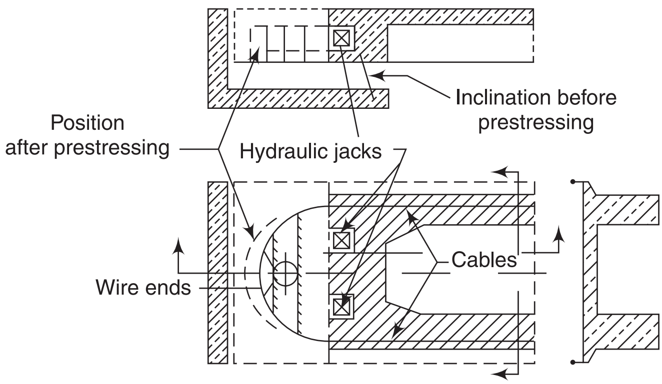

Fig. 3.10 *Baur–Leonhardt system*

The Dywidag single-bar anchorage system, developed in Germany, is extensively used in the USA and other countries where cast-in-place segments are prestressed by post-tensioning, and for many other applications. The threads formed by bar deformations make it easy to couple bars of any required length. Bond properties are also improved by the surface deformations. The Dywidag bar used in conjunction with a nut bearing on an end plate is available in sizes from 15.87–34.92 mm in diameter. The tendon characteristics and coupler details are given in Table 6 of Appendix-3.

3.4.3 Applications of Post-tensioning

Post-tensioning is ideally suited for medium to long-span *in situ* work where the tensioning cost is only a small proportion of the cost of the whole job. Hence, it is more economical to use a few cables or bars with large forces in each than a large number of small ones. Post-tensioning may be used with advantage to fabricate large members, such as long-span bridge decks of the box-girder type by prestressing together a number of smaller precast units.

Apart from this advantage, the chief merit of post-tensioning is that it allows the use of curved and stopped-off cables which helps the designer to vary the prestress distribution at will from section to section so as to counter the external loads more efficiently.

Post-tensioning is invariably used for strengthening concrete dams, circular prestressing of large concrete tanks and biological shields of nuclear reactors. Post-tensioning is ideally suited in concrete construction work involving stage prestressing[6]. Most of the long-span bridge structures are constructed using post-tensioning systems.[7]

3.4.4 Tendon Splices

In the case of continuous prestressed concrete members involving long tendons, it is necessary to splice the tendons to achieve continuity. Several types of splices have been developed over the years to suit the different types of wires and strands used as tendons. Some of the important and widely used types of splicing arrangements are grouped in Fig. 3.11.

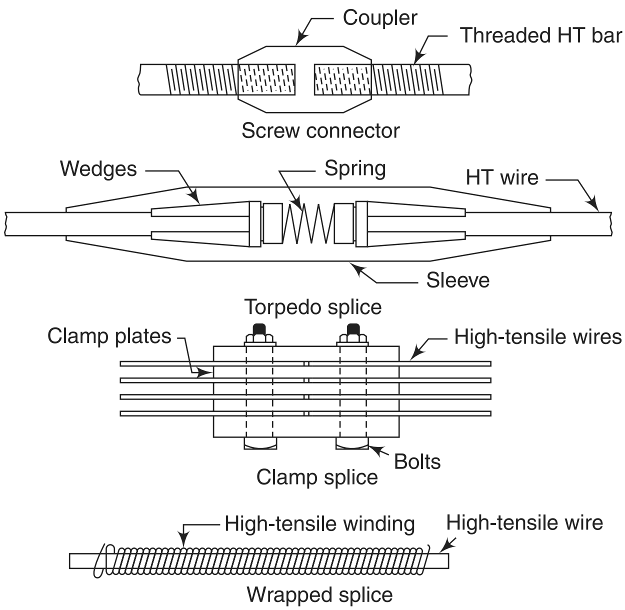

Fig. 3.11 *Tendon splices*

Screw connectors are normally employed to splice large diameter high-tensile bars which can be threaded at ends. A sheet-metal sheath of enlarged diameter and sufficient length is generally used to cover the splice. Screw-threaded connectors are not recommended for splicing heat-treated prestressing steels, which are highly susceptible to stress corrosion.

The torpedo-splice consists of triple wedges for securing the wires and the entire unit is covered and protected by a sleeve. This type of splice is largely used for splicing cold-drawn wires, which are adopted for the circular prestressing of tanks. The advantage of this splice is that there is no reduction in the strength of the wire.

Clamp splices are equipped with bolts and nuts, with a series of clamp plates to house the tendons between them. Since there will be a considerable reduction in the tensile strength of up to 50 per cent, this type of splice can be used only in locations where the prestressing force has been sufficiently reduced by the curvature of the tendon due to friction. For splicing of small diameter wires of 3–6 mm, high-tensile wire is wrapped under high tension using a wire-serving machine developed by the inventors of the BBRV system. The wrapping wire of 1 mm diameter is generally used to splice wires of up to 6 mm diameter. The length of splice may vary from 20–30 cm. The splice formed in this manner has a strength almost equal to that of the normal wire. This type of splice is generally used for the wires of circular concrete tanks and anchorage loops.

3.5 Thermo-Electric Prestressing

The method of prestressing by heated tendons, achieved by passing an electric current in the high-tensile wires, is generally referred to as 'thermo-electric prestressing'. In the erstwhile USSR, the electrothermic method[8] has been widely used since 1958 for pretensioning bar reinforcements of precast units.

The process consists of electrically heating the bars to a temperature of 300–400°C within 3–5 min. The bars undergo an elongation of about 0.4–0.5 per cent. The bars, after cooling, try to shorten but are checked by the fixed anchors at the two ends as shown in Fig. 3.12. The cooling period is reckoned to be 12–15 min.

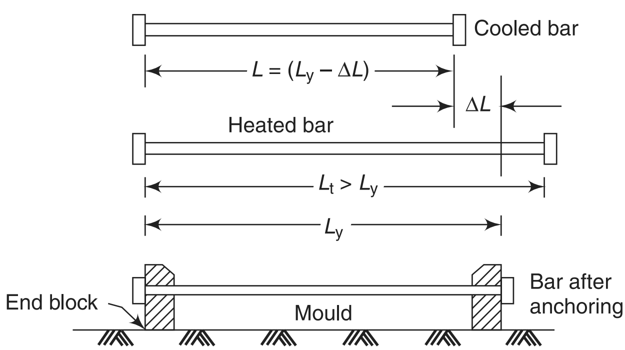

Fig. 3.12 *Electro-thermal prestressing*

By this process, it is possible to induce initial stresses of 500–600 N/mm^2 in the tendons. The concrete is placed in moulds only after the temperature of the wires falls below 90°C. In the erstwhile USSR[9], this method has been found to be more economical than conventional mechanical devices.

Thermo-electric prestressing has also been adopted in Germany[10] for the tensioning of oval-section-ribbed wires with an ultimate tensile strength of 1600 N/mm^2. A temperature of about 460°C was necessary to induce an initial stress of 55 per cent of the ultimate tensile strength; the heating time being 40–90 s at 30 V and 300–1100 A. Empirical relations for the estimation of the current, voltage and power requirements of the transformer are reported by Graduck[11].

3.6 Chemical Prestressing

Self-stressing or chemical prestressing of concrete was made possible by the development of expanding cements by Lossier[12] of France in 1944. Generally, expanding cements consist of 75 per cent Portland cement, 15 per cent high alumina cement and 10 per cent gypsum, which result in the formation of calcium sulphoaluminate. The linear expansion of the cement is about 3–4 per cent. Mikhailov[13] reported that expansive cements have been used for prestressing purposes in the erstwhile USSR since 1949. The degree of expansion can be controlled by varying the curing conditions.

Since the expansion of the concrete is restrained by high-tensile steel wires, the compressive stresses that develop in concrete and steel wires are subjected to tensile stresses. Investigations by Lin and Klein[14] have established that it is possible to obtain initial compressive stresses in concrete of 4–6.5 N/mm^2, which may be reduced to 3–6 N/mm^2 after shrinkage and creep. Tensile stresses of up to 850 N/mm^2 were developed in steel by the expansion of concrete. Results of laboratory investigations of several types of chemically prestressed elements, such as beams, slabs, frames, columns, pipes and hyperbolic paraboloid shells, have demonstrated the feasibility of chemical prestressing.

It has been found that structural elements ideally suited for chemical prestressing include pipes, thin walls and slabs, shells[15], folded plates and composite columns[16], as well as precast beams and columns[17].

In the present state of art, chemical prestressing can be applied to structural elements and systems in which the optimum amount of prestress is relatively low. The method is not suited for high degrees of prestress and high percentages of steel where mechanical prestressing can be conveniently used.

References

1. Leonhardt, F, *Prestressed Concrete Design and Construction,* 2nd edn, Wilhelm Ernst and Sohn, Berlin, Munich, 1964, p. 143.
2. Weinberg, V, *Manual du Beton Precontraint* (Handbook of prestressed concrete), Dunod, Paris, 1955, p. 308.
3. Peck, R L, *Concrete Industries Year Book,* Chicago, 1958.
4. Abeles, P W, *An Introduction to Prestressed Concrete,* Vol. 1, Concrete Publications Ltd., London, 1964, pp 30–63.

5. Evans, R H and E W Bennett, *Prestressed Concrete Theory and Design,* Chapman and Hall, London, 1958, pp 3–6.
6. Slater, W M, "Stage Post-tensioning—A Versatile and Economic Construction Technique," *Journal of the Prestressed Concrete Institute,* Vol. 20, No. 1, Jan.-Feb. 1975, pp 14–27.
7. Leonhardt, F, *Prestressed Concrete, Design and Construction,* 2nd edn, Wilhelm Ernst and Sohn, Berlin, Munich, 1964, pp 129–136.
8. Engineering developments in the USSR, *Civil Engineering and Public Works Review,* 1959 (Review from Betoni Shelesobeton), Nov. 1958, p. 311.
9. Skramtaev, B G, Electro-thermic method of pretensioning bar reinforcement of precast reinforced concrete, *Journal of the Prestressed Concrete Institute,* Vol. 6, No. 3, 1961, pp 57–71.
10. Mellentin, Ch: Der Stand des elektrischen spannens Von Spann stahl in der Dentschen Demokratischen Republic. Bau planung-Bautechnik 15, 1961, pp 13–16.
11. Graduck, II, *Prestressed Concrete,* Oxford and IBH, New Delhi, 1968, pp 135–139.
12. Lossier, H, "Cements with controlled expansion and their application to prestressed concrete," *The Structural Engineer,* Vol. 24, No. 10, Oct. 1946, pp 505–534.
13. Mikhailov, V V, Self-stressed concrete, Moscow 1955, and New developments in self-stressed concrete, *Proceedings of the World Conference on Prestressed Concrete,* San Francisco, 1957, pp 25.1–25.12.
14. Lin, T Y and A Klein, "Chemical prestressing of concrete elements using expanding cements," *ACI Journal Proceedings,* Vol. 60, No. 9, Sept. 1963, 1187–1218.
15. Bertero, V V, and J Choi, "Chemically prestressed concrete hyperbolic paraboloid shell model," *Proceedings, World Conference on Shell Structures,* San Francisco, California. Oct. 1962, pp 145–148.
16. Aroni, S, V V Bertero, and M Polvka, "Chemically prestressed concrete," *Journal of the Prestressed Concrete Institute,* Vol. 13, No. 5, Oct. 1968, pp 22–35.
17. Bertero, V V and GJ, Irragory-Montero, "Precast chemically prestressed concrete frame," *II Stmposio Panamericana de Estructuras,* Institute de Estructuras dela Universidad Nacional de Ingonieria, Lima, Peru, Vol. 1, Paper No. 12, Jan, 1964, p 53.

Review Questions

3.1 List the various types of tensioning devices used in prestressed concrete.
3.2 Distinguish between pretensioned and post-tensioned members.
3.3 Explain with sketches 'Hoyer's long line system of pretensioning'.
3.4 What are supplementary anchoring devices?
3.5 Explain the principle of post-tensioning.
3.6 What are post-tensioning anchorages?

3.7 Explain the various post-tensioning systems based on wedge action with sketches.
3.8 What are loop anchorages? Explain with sketches Baur–Leonhardt system of post-tensioning.
3.9 For what types of structures do you recommend post-tensioning?
3.10 What are tendon splices? Sketch some common types of tendon splices.

Objective-type Questions

3.1 In pretensioning system
(a) the member is cast first followed by tensioning of high-tensile wires
(b) the member is prestressed by external anchors
(c) the high-tensile wires are tensioned before placing concrete in forms

3.2 Curved cables can be used in
(a) pretensioned members
(b) externally pretressed member
(c) post-tensioned member

3.3 In long line method or pretensioning,
(a) only one member can be cast
(b) two members can be cast
(c) several members can be cast

3.4 In post-tensioning system
(a) wires are first tensioned followed by concreting
(b) tensioning of wires and concreting is simultaneously done
(c) the wires are tensioned against hardened concrete

3.5 Freyssinet system is based on the principle of
(a) direct bearing on concrete from bolt heads at the end of wires
(b) looping of the wires around concrete
(c) wedge action producing frictional grip between steel and concrete

3.6 High-tensile bars threaded at ends are used in
(a) Freyssinet system
(b) Gifford–Udall system
(c) Lee–McCall system

3.7 Looping of high-tensile tendons around the concrete is used in
(a) BBRV system
(b) Magnel–Blaton system
(c) Baur–Leonhardt system

3.8 Tendon splices are required in
(a) Hoyer's long line method of pretensioning
(b) Short span prestressed members
(c) Long span continuous members

3.9 In prestressed members requiring very large forces, the tendons preferred are
(a) wires (b) bars (c) strands

3.10 The tendon splice preferred in the case of long span continuous prestressed members is
(a) wrapped splice (b) clamp splice (c) torpedo splice

Answers to Objective-type Questions

3.1 (c)	3.2 (c)	3.3 (c)	3.4 (c)	3.5 (c)
3.6 (c)	3.7 (c)	3.8 (c)	3.9 (c)	3.10 (c)

4 Analysis of Prestress and Bending Stresses

4.1 Basic Assumptions

The analysis of stresses developed in a prestressed concrete structural element is based on the following assumptions: (i) concrete is a homogeneous elastic material, (ii) within the range of working stresses, both concrete and steel behave elastically, notwithstanding the small amount of creep which occurs in both the materials under sustained loading, and (iii) a plane section before bending is assumed to remain plane even after bending, which implies a linear strain distribution across the depth of the member.

As long as tensile stresses do not exceed the limit of modulus of rupture of concrete (corresponding to the stage of visible cracking of concrete), any change in the loading of the member results in a change of stress in the concrete only, the sole function of the prestressing tendon being to impart and maintain the prestress in the concrete. Up to the stage of visible cracking on concrete, the changes in the stress of steel, the loading being negligibly small, are generally not considered in the computations.

4.2 Analysis of Prestress

The stresses due to prestressing alone are generally combined stresses due to the action of direct load and bending resulting from an eccentrically applied load. The stresses in concrete are evaluated by using the well-known relationship for combined stresses used in the case of columns.

The following notations and sign conventions are used for the analysis of prestress:

P = Prestressing force (positive when producing direct compression)

e = Eccentricity of prestressing force

$M = P \cdot e$ = Moment

A = Cross-sectional area of the concrete member

I = Second moment of area of section about its centroid

Z_t and Z_b = Section modulus of the top and bottom fibres

f_{sup} and f_{inf} = Prestress in concrete developed at the top and bottom fibres (positive when compressive and negative when tensile in nature)

y_t and y_b = Distance of the top and bottom fibres from the centroid of the section

i = Radius of gyration

4.2.1 Concentric Tendon

Consider a concrete beam with a concentric tendon as shown in Fig. 4.1.

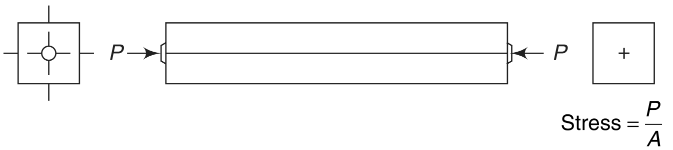

Fig. 4.1 *Concentric prestressing*

Uniform prestress in concrete = P/A, which is compressive across the depth of the beam. Generally, the applied loads and the dead load of the beam induce tensile stress towards the soffit and are counterbalanced more effectively by eccentric tendons.

4.2.2 Eccentric Tendon

Figure 4.2 shows a concrete beam subjected to an eccentric prestressing force of magnitude P located at an eccentricity e. The stresses developed at the top and bottom fibres of the beam are obtained by the following relations:

$$f_{\text{inf}} = \left(\frac{P}{A} + \frac{Pe}{Z_b}\right) = \frac{P}{A}\left(1 + \frac{ey_b}{i^2}\right)$$

$$f_{\text{sup}} = \left(\frac{P}{A} - \frac{Pe}{Z_t}\right) = \frac{P}{A}\left(1 - \frac{ey_t}{i^2}\right)$$

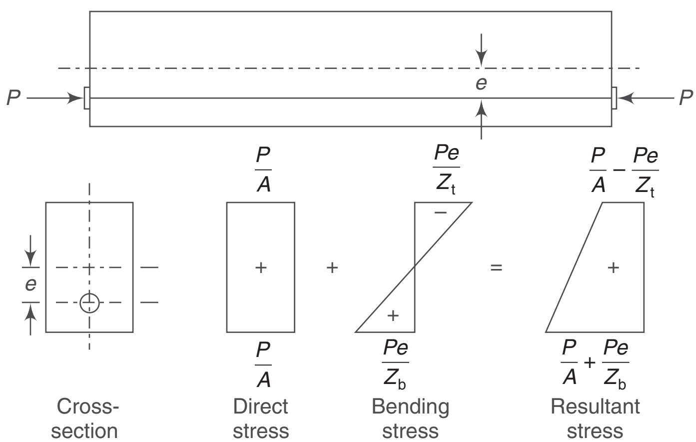

Fig. 4.2 *Eccentric prestressing*

4.3 Resultant Stresses at a Section

The concrete beam shown in Fig. 4.3, supports uniformly distributed live and dead loads of intensity q and g. The beam is prestressed by a straight tendon carrying a prestressing force P at an eccentricity e. The resultant stresses in concrete at any section are obtained by superposing the effect of prestress and the flexural stresses developed due to the loads. If M_q and M_g are the live-load and dead-load moments at the central span section, then

$$M_q = \left(\frac{qL^2}{8}\right) \quad M_g = \left(\frac{gL^2}{8}\right)$$

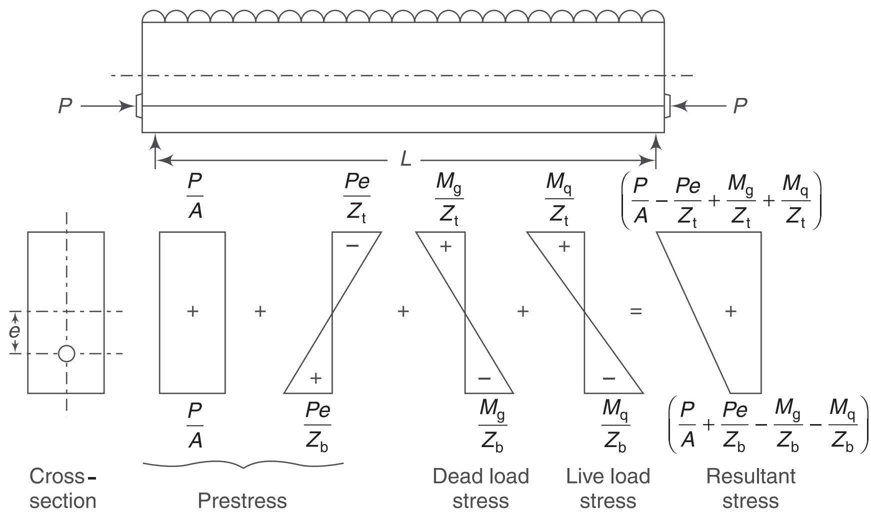

Fig. 4.3 *Stress distribution due to eccentric prestressing, dead and live loads*

The resultant stresses at the top and bottom fibres of concrete at any given section are obtained as,

$$f_{\text{sup}} = \left(\frac{P}{A} - \frac{Pe}{Z_t}\right) + \left(\frac{M_g}{Z_t}\right) + \left(\frac{M_q}{Z_t}\right)$$

$$f_{\text{inf}} = \left(\frac{P}{A} + \frac{Pe}{Z_b}\right) - \left(\frac{M_g}{Z_b}\right) - \left(\frac{M_q}{Z_b}\right)$$

In the case of prestressed members, the cross-sectional area of high-tensile steel being a very small percentage of the total concrete area, the stress computations are generally based on the nominal concrete cross-sectional properties. The use of equivalent concrete section, although important in interpreting test results of experimental investigations, generally does not significantly influence the stresses resulting from the use of nominal concrete section. This is illustrated by Example 4.1.

Example 4.1 A rectangular concrete beam 100 mm wide by 250 mm deep spanning over 8 m is prestressed by a straight cable carrying an effective prestressing force of 250 kN located at an eccentricity of 40 mm. The beam supports a live load of 1.2 kN/m.

(a) Calculate the resultant stress distribution for the centre-of-span cross-section of the beam assuming the density of concrete as 24 kN/m^3.

(b) Find the magnitude of the prestressing force with an eccentricity of 40 mm which can balance the stresses due to dead and live loads at the soffit of the centre span section.

Solution.

Prestressing force = P = 250 kN

Cross-sectional area = $A = (100 \times 250) = (25 \times 10^3)$ mm^2

Eccentricity = e = 40 mm

Self-weight of beam = $g = (0.1 \times 0.25 \times 24) = 0.6$ kN/m

Live load on the beam = q = 1.2 kN/m

b = 100 mm, d = 250 mm, Span = L = 8 m

$\therefore$ Total load on the beam = $w = (g + q) = (0.6 + 1.2) = 1.8$ kN/m

Section Modulus:

$$Z = \left(\frac{bd^2}{6}\right) = \left(\frac{100 \times 250^2}{6}\right) = (1.04 \times 10^6)\ \text{mm}^3$$

Bending moment at the centre-of-span section:

$$M = \left(\frac{wL^2}{8}\right) = \left(\frac{1.8 \times 8^2}{8}\right) = 14.4\ \text{kN m}$$

Stress due to loads:

$$\left(\frac{M}{Z}\right) = \left(\frac{14.4 \times 10^6}{1.04 \times 10^6}\right) = \pm 13.8\ \text{N/mm}^2$$

Prestress at top and bottom fibres:

$$\left[\frac{P}{A} \pm \frac{Pe}{Z}\right] = \left[\frac{250 \times 10^3}{25 \times 10^3} \pm \frac{250 \times 10^3 \times 40}{1.04 \times 10^6}\right] = [10 \pm 9.6]\ \text{N/mm}^2$$

(a) Resultant stresses:

At top fibre = $(10 - 9.6 + 13.8) = 14.2$ N/mm^2 (Compression)

At bottom fibre = $(10 + 9.6 - 13.8) = 5.8$ N/mm^2 (Compression)

(b) If P = Prestressing force required to balance the stresses at soffit, then

$$\left[\frac{P}{A} + \frac{Pe}{Z}\right] = \left[\frac{M}{Z}\right]$$

Hence, we have

$$P\left[\frac{1}{25 \times 10^3} + \frac{40}{1.04 \times 10^6}\right] = \left[\frac{14.4 \times 10^6}{1.04 \times 10^6}\right]$$

Solving, $P = (176 \times 10^3)\ N = 176$ kN.

Example 4.2 A rectangular concrete beam of cross-section 30 cm deep and 20 cm wide is prestressed by means of 15 wires of 5 mm diameter located 6.5 cm from the bottom of the beam and 3 wires of diameter of 5 mm, 2.5 cm from the top. Assuming the prestress in the steel as 840 N/mm^2, calculate the stresses at the extreme fibres of the mid-span section when the beam is supporting its own weight over a span of 6 m. If a uniformly distributed live load of 6 kN/m is imposed, evaluate the maximum working stress in concrete. The density of concrete is 24 kN/m^3.

Solution. From Fig. 4.4,

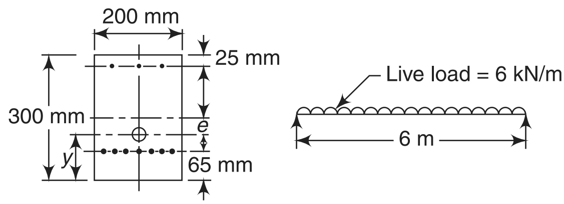

Fig. 4.4 *Prestressed beam with rectangular section supporting live loads*

Distance of the centroid of the prestressing force from the base,

$$y = \left[\frac{(15\times 65)+(3\times 275)}{18}\right] = 100 \text{ mm}$$

Eccentricity $e = (150 - 100) = 50$ mm
Prestressing force $P = (840 \times 18 \times 19.7) = 3 \times 10^5$ N
Area of cross-section $A = (300 \times 200) = 6 \times 10^4$ mm^2

Second moment of area: $$I = \left(\frac{200\times 300^3}{12}\right) = 45\times 10^7 \text{ mm}^4$$

Section modulus: $$(Z_t \text{ and } Z_b) = \left(\frac{45\times 10^7}{150}\right) = 3\times 10^6 \text{ mm}^3$$

Self-weight of beam: $$= (0.3\times 0.2\times 24) = 1.44 \text{ kN/m}$$

Self-weight moment: $$M_g = \left(\frac{1.44\times 6^2}{8}\right) = 6.48 \text{ kN m}$$

Live-load moment: $$M_q = \left(\frac{6\times 6^2}{8}\right) = 27 \text{ kN m}$$

Direct stress due to prestress: $$\left(\frac{P}{A}\right) = \left(\frac{3\times 10^5}{6\times 10^6}\right) = 5 \text{ N/mm}^2$$

Bending stress due to prestress: $$\left(\frac{Pe}{Z}\right) = \left(\frac{3\times 10^5\times 50}{3\times 10^6}\right) = 5 \text{ N/mm}^2$$

Self-weight stress: $$M_g/Z = \left(\frac{6.48\times 10^6}{3\times 10^6}\right) = 2.16 \text{ N/mm}^2$$

$$\text{Live-load stress: } M_q/Z = \left(\frac{27 \times 10^6}{3 \times 10^6}\right) = 9 \text{ N/mm}^2$$

The resultant stresses due to (self-weight + prestress + live load) are shown in Fig. 4.5. Maximum working stress in concrete = 11.16 N/mm^2 (compression).

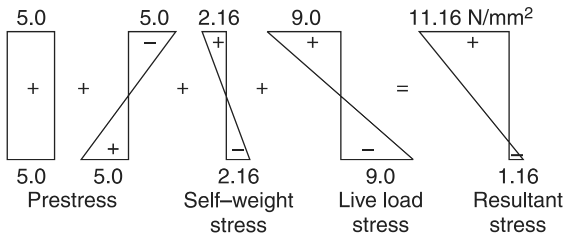

Fig. 4.5 *Analysis of stresses at mid-span*

Example 4.3 An unsymmetrical I-section beam is used to support an imposed load of 2 kN/m over a span of 8 m. The sectional details are top flange, 300 mm wide and 60 mm thick; bottom flang, 100 mm wide and 60 mm thick; thickness of the web = 80 mm; overall depth of the beam = 400 mm. At the centre of the span, the effective prestressing force of 100 kN is located at 50 mm from the soffit of the beam. Estimate the stresses at the centre-of-span section of the beam for the following load conditions:

(a) Prestress + self-weight
(b) Prestress + self-weight + live load

Solution. From Fig. 4.6,

Prestressing force $P = 100$ kN

Area of concrete $A = 46400$ mm^2

Distance of centroid from top $y = 156$ mm

$\therefore\ e = 194$ mm

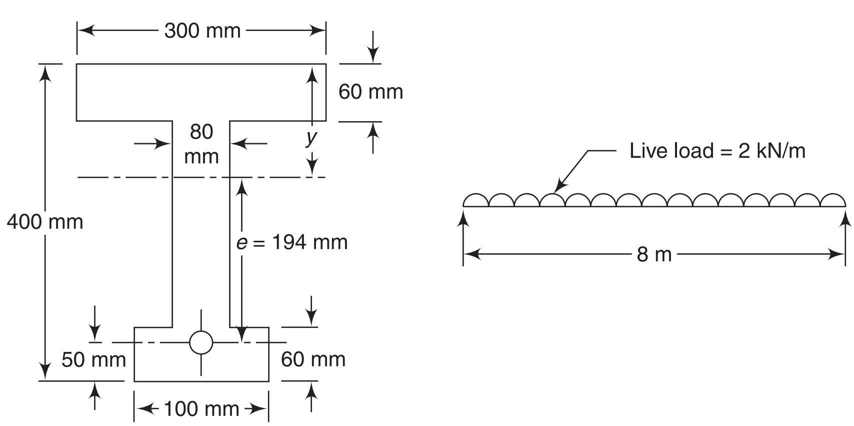

Fig. 4.6 *Prestressed beam with unsymmetrical I-section supporting live loads*

Second moment of area $I = 75.8 \times 10^7$ mm^4

$$Z_t = \left(\frac{75.8 \times 10^7}{156}\right) = 485 \times 10^4 \text{ mm}^3$$

$$Z_b = \left(\frac{75.8 \times 10^7}{244}\right) = 310 \times 10^4 \text{ mm}^3$$

$$g = (0.0464 \times 1 \times 24) = 1.12 \text{ kN m}$$

$$M_g = (0.125 \times 1.12 \times 8^2) = 8.96 \text{ kN m}$$

$$M_q = (0.125 \times 2 \times 8^2) = 16 \text{ kN m}$$

Stresses at the centre of span,

Type of Stress	*At top Fibre (N/mm^2)*	*At bottom Fibre (N/mm^2)*
Prestress	$P/A = +2.15$	$P/A = +2.15$
	$Pe/Z_t = -4.0$	$Pe/Z_b = +6.25$
Self-weight stress	$M_g/Z_t = +1.85$	$M_g/Z_b = -2.9$
Live-load stress	$M_q/Z_t = +3.3$	$M_q/Z_b = -5.15$

+ Compression, – Tension

Resultant stresses:

(a) (Prestress + Self-weight stress) = 0, and +5.5 N/mm^2

(b) Prestress + Self-weight stress
+ live-load stress) = +3.3 N/mm^2, and +0.35 N/mm^2.

Example 4.4 A rectangular concrete beam, 250 mm wide and 600 mm deep, is prestressed by means of four 14 mm diameter high-tensile bars located 200 mm from the soffit of the beam. If the effective stress in the wires is 700 N/mm^2, what is the maximum bending moment that can be applied to the section without causing tension at the soffit of the beam?

Solution.

$$A = (250 \times 600) = 15 \times 10^4 \text{ mm}^2$$

$$Z = \left(\frac{250 \times 600^2}{6}\right) = 15 \times 10^6 \text{ mm}^3$$

$$A_s = \left(\frac{\pi \times 4 \times 14^2}{4}\right) = 616 \text{ mm}^2$$

$$e = 100 \text{ mm}$$

$$P = (616 \times 700) = 431200 \text{ N}$$

$$\left(\frac{P}{A}\right) = 2.87 \text{ N/mm}^2, \left(\frac{Pe}{Z}\right) = 2.87 \text{ N/mm}^2$$

Prestress at the soffit of the beam = (2.87 + 2.87) = 5.74 N/mm^2

If M = maximum moment on the section for zero tension at the bottom face,

$$\left(\frac{M}{Z}\right) = 5.74$$

$$\therefore \quad M = (5.74 \times 15 \times 10^6) = 86.1 \times 10^6 \text{ N mm} = 86.1 \text{ kN m}$$

Example 4.5 A prestressed concrete beam of section 200 mm wide and 300 mm deep is used over an effective span of 6 m to support an imposed load of 4 kN/m. The density of concrete is 24 kN/m^3.

At the centre-of-span section of the beam, find the magnitude of

(a) the concentric prestressing force necessary for zero fibre stress at the soffit when the beam is fully loaded, and

(b) the eccentric prestressing force located 100 mm from the bottom of the beam which would nullify the bottom fibre stresses due to loading.

Solution.

$$A = (200 \times 300) = 6 \times 10^4 \text{ mm}^2$$

$$Z_b = Z_t = \left(\frac{200 \times 300^2}{6}\right) = 3 \times 10^6 \text{ mm}^3$$

$$g = (0.2 \times 0.3 \times 24) = 1.44 \text{ kN/m}$$

$$M_g = (0.125 \times 1.44 \times 6^2) = 6.48 \text{ kN m}$$

$$M_q = (0.125 \times 4 \times 6^2) = 18 \text{ kN m}$$

Tensile stress at the bottom fibre due to dead and live loads

$$= \left[\frac{(6.48 + 18)10^6}{3 \times 10^6}\right] = 8.16 \text{ N/mm}^2$$

(a) If P = concentric prestressing force, for zero stress at the soffit of the beam under loads

$$(P/A) = 8.16$$

$$\therefore \quad P = (8.16 \times 6 \times 10^4) = 489.6 \text{ kN}$$

(b) If P = eccentric prestressing force (e = 50 mm), for zero stress at the soffit of the beam under loads

$$(P/A) + (Pe/Z_b) = 8.16$$

$$\therefore \quad P\left(\frac{1}{6 \times 10^4} + \frac{50}{3 \times 10^6}\right) = 8.16$$

$$\therefore \quad P = 244.8 \text{ kN}$$

The magnitudes of the computed prestressing forces clearly indicate the advantages of eccentric prestressing in flexural members subjected to transverse loads.

4.4 Pressure Line or Thrust Line and Internal Resisting Couple

At any given section of a prestressed concrete beam, the combined effect of the prestressing force and the externally applied load will result in a distribution of concrete stresses that can be resolved into a single force. The locus of the points of application of this resultant force in any structure is termed as the 'pressure or thrust line' The concept of pressure line is very useful in understanding the load-carrying mechanism of a prestressed concrete section.

In the case of prestressed concrete members, the location of the pressure line depends upon the magnitude and direction of the moments applied at the cross-section and the magnitude and distribution of stress due to the prestressing force. Consider a concrete beam shown in Fig. 4.7, which is prestressed by force P acting at eccentricity e. The beam supports a uniformly distributed load (including self-weight) of intensity q per unit length.

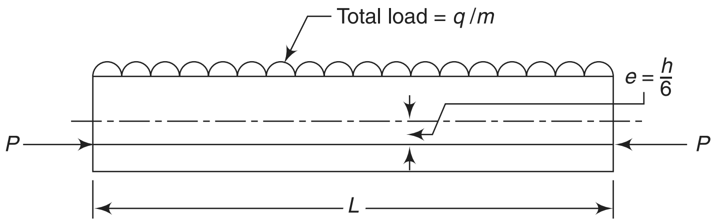

Fig. 4.7 *Beam with eccentric tendons*

The load is of such magnitude that the bottom-fibre stress at the central span section of the beam is zero. Figure 4.8 shows the resultant stress distribution at the support, centre and quarter span sections of the beam.

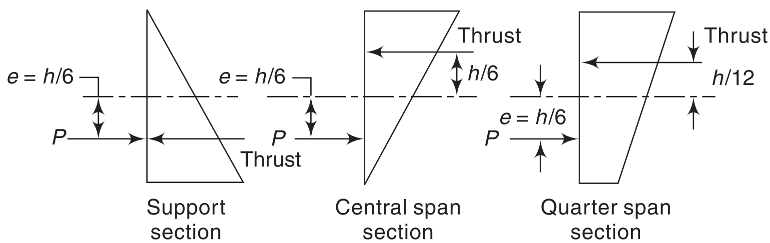

Fig. 4.8 *Distribution of stresses at various sections along the span*

At the support section, since there are no flexural stresses resulting from the external loads, the pressure line coincides with that of the centroid of steel, located at an eccentricity of $h/6$. At the centre of the span section, the external loading is such that the resultant stress developed is maximum at the top fibre and zero at the bottom fibre. It can easily be seen that for this section, the pressure line has shifted towards the top fibre by an amount equal to $h/3$ from its initial position.

The external moment at the quarter span section being smaller in magnitude, the shift in the pressure line also is correspondingly smaller, being equal to $h/4$ from the initial position. In a similar manner, it can be shown that a larger uniformly distributed load on the beam would result in the pressure line being shifted even higher at the centre and quarter span sections. The pressure line location in the beam is shown in Fig. 4.9. These observations lead to the following important principle:

"A change in the external moments in the elastic range of a prestressed concrete beam results in a shift of the pressure line rather than in an increase in the resultant force in the beam."

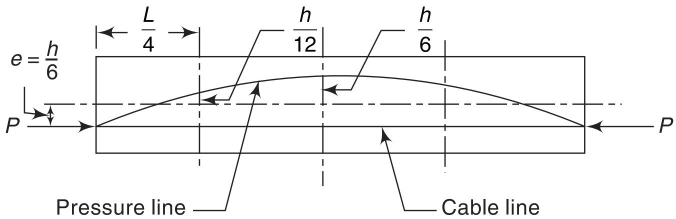

Fig. 4.9 *Location of pressure line in the prestressed beam*

This is in contrast to a reinforced concrete beam section where an increase in the external moment results in a corresponding increase in the tensile force and the compressive force. The increase in the resultant forces is due to a more or less constant lever arm between the forces, characterised by the properties of the composite section. Basically, the load-carrying mechanism is comprised of a constant force with a changing lever arm, as in the case of prestressed concrete sections, and a changing force with a constant lever arm prevailing in reinforced concrete sections as shown in Fig. 4.10. However, if a prestressed concrete member is cracked, it behaves in a manner similar to that of a reinforced concrete section.

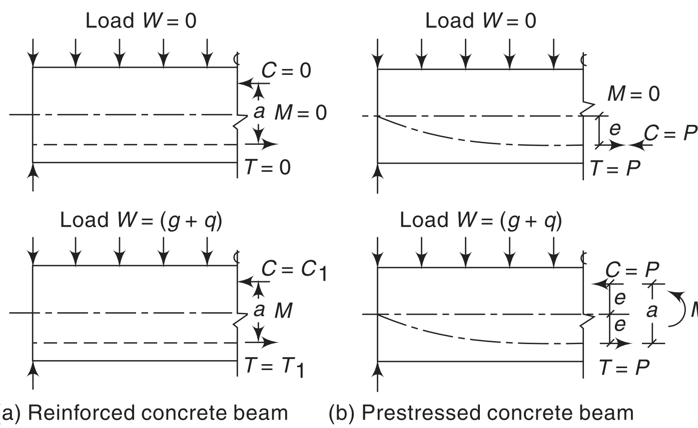

Fig. 4.10 *Load-carrying mechanism of reinforced concrete and prestressed concrete beam sections*

In contrast to the direct method of analysis of resultant stresses at a section of a prestressed concrete beam outlined in Section 4.3, the pressure or thrust line concept can also be used to evaluate the stresses. In this method, generally referred to as the internal resisting couple method or the C-line method, the prestressed beam is analysed as a plain concrete elastic beam using the basic principles of statics. The prestressing force is considered as an external compressive force with a constant tensile force T in the tendon throughout the span. Consequently, at any section of a loaded prestressed beam, equilibrium is maintained satisfying the equations, $H = 0$ and $M = 0$.

Figures 4.11(a) and (b) shows the free-body diagram of a segment of a beam without and with transverse loads, respectively. When the gravity loads are zero, the C and T lines coincide since there is no moment at the section. Under transverse loads, the C-line, or the centre of pressure or thrust line, is at a varying distance a from the T-line.

If M = Bending moment at the section due to dead and live loads

e = Eccentricity of the tendon

$T = P$ = Prestressing force in the tendon

moment equilibrium yields the relation,

$$M = Ca = Ta = Pa \quad \text{and} \quad a = \left(\frac{M}{P}\right)$$

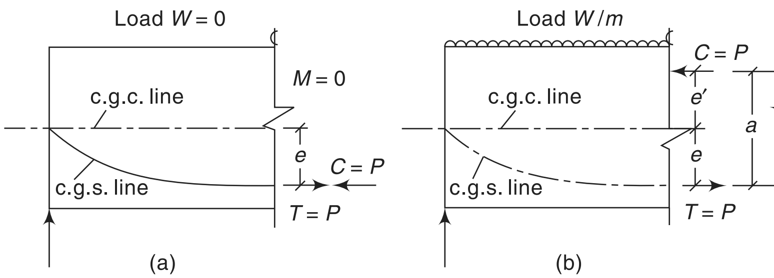

Fig. 4.11 *Free-body diagram of forces and moments at a section of prestressed concrete beam*

The shift of pressure line e' measured from the centroidal axis is obtained as,

$$e' = (a - e) = \left(\frac{M}{P}\right) - e$$

The resultant stresses at the top and bottom fibres of the section are expressed as,

$$f_{\text{sup}} = \left(\frac{P}{A}\right) + \left(\frac{Pe'}{Z_t}\right)$$

$$f_{\text{inf}} = \left(\frac{P}{A}\right) - \left(\frac{Pe'}{Z_b}\right)$$

where Z_t and Z_b are the section moduli of the top and bottom fibres, respectively.

The concepts of the pressure line and the internal resisting couple method of analysing the stresses in prestressed concrete members are outlined by the following examples.

Example 4.6 A prestressed concrete beam with a rectangular section 120 mm wide by 300 mm deep supports a uniformly distributed load of 4 kN/m, which includes the self-weight of the beam. The effective span of the beam is 6 m. The beam is concentrically prestressed by a cable carrying a force of 180 kN. Locate the position of the pressure line in the beam.

Solution.

Prestressing force, $P = 180$ kN

Eccentricity, $e = 0$

$A = 36 \times 10^3$ mm^2, $Z_t = Z_b = 18 \times 10^5$ mm^3

Bending moment at the centre of the span = $(0.125 \times 4 \times 6^2) = 18$ kN m

Direct stress: $\dfrac{P}{A} = \left(\dfrac{180 \times 10^3}{36 \times 10^3}\right) = 5$ N/mm^2

Bending stress: $\dfrac{M}{Z} = \left(\dfrac{18 \times 10^6}{18 \times 10^5}\right) = 10$ N/mm^2

Resultant stresses at the centre of the span section:
At top = (5 + 10) = 15 N/mm^2 (Compression)
At bottom = (5 – 10) = –5 N/mm^2 (Tension)

If N = resultant thrust in the section and e = corresponding eccentricity (shift of pressure line), then,

$$N/A + Ne/Z = 15$$

But $N = 180 \times 10^3$ N

$A = 36 \times 10^3$ mm^2

(solving, $e = 100$ mm)

$Z = 18 \times 10^5$ mm^3

The resultant stress distribution diagram and the pressure-line location is shown in Fig. 4.12.

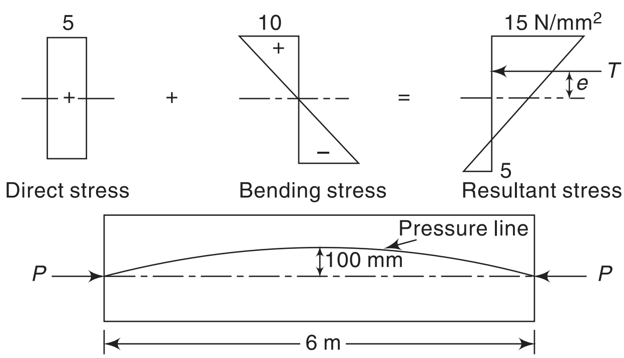

Fig. 4.12 *Distribution of stresses and location of pressure line in prestressed beam*

Example 4.7 A prestressed concrete beam of section 120 mm wide by 300 mm deep is used over an effective span of 6 m to support a uniformly distributed load of 4 kN/m, which includes the self-weight of the beam. The beam is prestressed by a straight cable carrying a force of 180 kN and located at an eccentricity of 50 mm. Determine the location of the thrust-line in the beam and plot its position at quarter and central span sections.

Solution.

$$P = 180 \text{ kN}$$
$$E = 50 \text{ mm}$$
$$A = 36 \times 10^3 \text{ mm}^2$$
$$Z = 18 \times 10^5 \text{ mm}^3$$

Stresses due to prestressing force:

$$P/A = \left(\frac{180 \times 10^3}{36 \times 10^3}\right) = +5 \text{ N/mm}^2$$

$$Pe/Z = \left(\frac{180 \times 10^3 \times 50}{18 \times 10^3}\right) = +5 \text{ N/mm}^2$$

Bending moment at the centre of the span = $(0.125 \times 4 \times 6^2) = 18$ kN m

Bending stresses at top and bottom = $\left(\frac{18 \times 10^6}{18 \times 10^5}\right) = \pm 10 \text{ N/mm}^2$

Resultant stresses at the central section:

$$\text{At top} = (5 - 5 + 10) = 10 \text{ N/mm}^2$$
$$\text{At bottom} = (5 + 5 - 10) = 0 \text{ N/mm}^2$$

Shift of pressure line from cable line = $M/P = \left(\frac{18 \times 10^6}{18 \times 10^4}\right) = 100$ mm

Bending moment at quarter span section = $(3/32)\, qL^2 = (3/32) \times 4 \times 6^2$

$$= 13.5 \text{ kN m}$$

Bending stress at top and bottom = $\left(\frac{13.5 \times 10^6}{18 \times 10^5}\right) = 7.5 \text{ N/mm}^2$

Resultant stresses at the quarter span section:

$$\text{At top} = (5 - 5 + 7.5) = 7.5 \text{ N/mm}^2$$
$$\text{At bottom} = (5 + 5 - 7.5) = 2.5 \text{ N/mm}^2$$

Shift of pressure-line from cable line $M/P = \left(\frac{13.5 \times 10^6}{18 \times 10^4}\right) = 75$ mm

The location of pressure line is shown in Fig. 4.13.

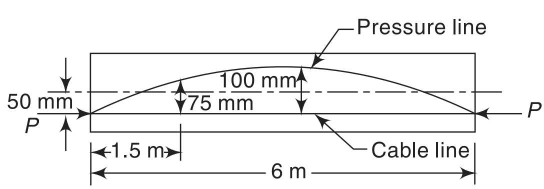

Fig. 4.13 *Location of pressure line in the prestressed beam*

Example 4.8 A rectangular concrete beam 250 mm wide and 300 mm deep is prestressed by a force of 540 kN at a constant eccentricity of 60 mm. The beam supports a concentrated load of 68 kN at the centre of a span of 3 m. Determine the location of the pressure line at the centre, quarter span and support sections of the beam. Neglect the self-weight of the beam.

Solution.

$$P = 540 \text{ kN}, \quad A = (250 \times 300) = 75 \times 10^3 \text{ mm}^2$$

$$e = 60 \text{ mm}, \quad Z = \left(\frac{250 \times 300^2}{6}\right) = 375 \times 10^4 \text{ mm}^3$$

At the centre of the span, $M_q = (0.25 \times 68 \times 3) = 51$ kN m

At the quarter span, $M_q = (0.125 \times 68 \times 3) = 25.5$ kN m

Stresses due to prestressing force:

$$\left(\frac{P}{A}\right) = \left(\frac{54 \times 10^4}{75 \times 10^3}\right) = 7.2 \text{ N/mm}^2$$

$$\left(\frac{Pe}{Z}\right) = \left(\frac{54 \times 10^4 \times 60}{357 \times 10^4}\right) = 8.6 \text{ N/mm}^2$$

Stresses due to external loads:

At the centre of span, $\left(\frac{M_q}{Z}\right) = \left(\frac{51 \times 10^6}{375 \times 10^4}\right) = 13.6 \text{ N/mm}^2$

At the quarter of span, $\left(\frac{M_q}{Z}\right) = \left(\frac{25.5 \times 10^6}{375 \times 10^4}\right) = 6.8 \text{ N/mm}^2$

The position of the resultant thrust from the top fibre of the beam is obtained from Fig. 4.14.

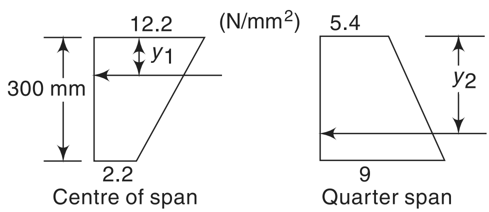

Fig. 4.14 *Distribution of stresses at centre and quarter span sections*

$$y_1 = \left[\frac{(300 \times 2.2)\,150 + \left(\frac{1}{2} \times 300 \times 10\right)100}{660 + 1500}\right] = 115 \text{ mm}$$

$$y_2 = \left[\frac{(5.4 \times 300)150 + \left(\frac{1}{2} \times 300 \times 3.6\right)200}{1620 + 540}\right] = 162 \text{ mm}$$

The locations of the pressure line and the cable line are shown in Fig. 4.15.

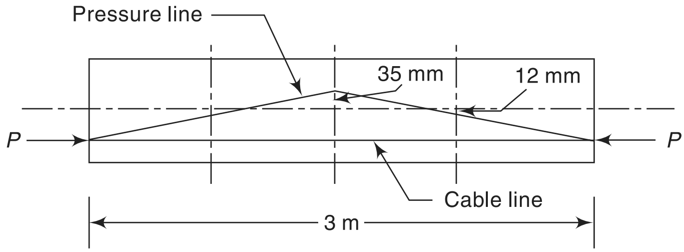

Fig. 4.15 *Location of pressure line in the prestressed beam*

Example 4.9 A box girder of prestressed concrete bridge of span 40 m has overall dimensions of 1200 mm by 1800 mm. The uniform thickness of the walls is 200 mm. The live-load analysis indicates a maximum live-load moment of 2000 kN m at the centre of the span. The beam is prestressed by parabolic cables with an effective force of 7000 kN. The cables which are concentric at supports have an eccentricity of 800 mm at the centre-of-span section. Compute the resultant stresses at the centre-of-span section using the internal resisting couple method.

Solution. The longitudinal elevation and cross-section of the girder is shown in Fig. 4.16.

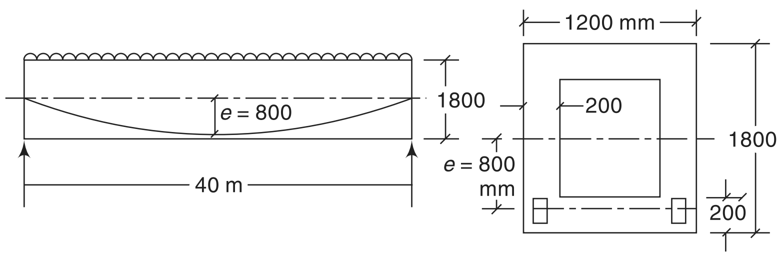

Fig. 4.16 *Prestressed concrete box section bridge girder*

$$A = (1.2 \times 1.8) - (0.8 \times 1.4) = 1.04 \text{ m}^2$$
$$g = (1.04 \times 24) = 25 \text{ kN/m}$$
$$P = 7000 \text{ kN}$$
$$e = 800 \text{ mm and } L = 40 \text{ m}$$
$$I = \frac{1}{12}[(1200 \times 1800^3) - (800 \times 1400^3)] = 40 \times 10^{10} \text{ mm}^4$$
$$Z_b = Z_t = Z = (40 \times 10^{10})/900 = 444 \times 10^6 \text{ mm}^3$$
$$M_g = (0.125 \times 25 \times 40^2) = 5000 \text{ kN m}$$
$$M_q = 2000 \text{ kN m}$$
$$M = (M_g + M_q) = (5000 + 2000) = 7000 \text{ kN m}$$

Lever arm, $a = \left(\dfrac{M}{P}\right) = \dfrac{(7000 \times 10^3)}{7000} = 1000$ mm

Shift of pressure line, $e' = (a - e) = (1000 - 800) = 200$ mm

The resultant stresses are obtained as,

$$f_{sup} = \left[\frac{P}{A} + \frac{Pe'}{Z_t}\right]$$

$$= \left(\frac{7000 \times 10^3}{1.04 \times 10^6}\right) + \left(\frac{7000 \times 10^3 \times 200}{444 \times 10^6}\right) = 9.88 \text{ N/mm}^2$$

$$f_{inf} = \left[\frac{P}{A} - \frac{Pe'}{Z_b}\right]$$

$$= \left(\frac{7000 \times 10^3}{1.04 \times 10^6}\right) - \left(\frac{7000 \times 10^3 \times 200}{444 \times 10^6}\right) = 3.58 \text{ N/mm}^2$$

Example 4.10 A prestressed concrete bridge deck comprises unsymmetrical I-section beams spanning over 20 m. The cross-section of a typical beam is shown in Fig. 4.17(a). The beam is prestressed by seven Freyssinet cables, each carrying an effective force of 600 kN located 200 mm from the soffit at the centre-of-span section. If the total maximum bending moment at the centre of span of the girder is 3600 kN m, estimate the resultant stress developed at the section using the internal resisting couple method.

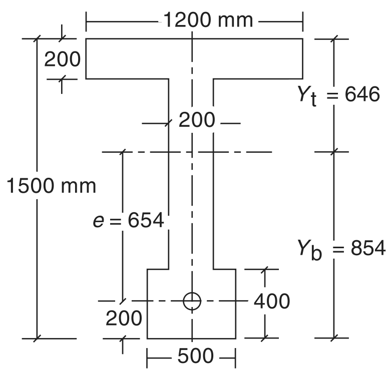

Fig. 4.17(a) *Unsymmetrical I-section bridge girder*

Solution. The sectional properties are computed as,

$$A = 62 \times 10^4 \text{ mm}^2$$

$$y_t = 646 \text{ mm} \quad \text{and} \quad y_b = 854 \text{ mm}$$

$$I = 1727 \times 10^8 \text{ mm}^4$$

$$Z_t = 2.67 \times 10^8 \text{ mm}^3 \quad \text{and} \quad Z_b = 2.02 \times 10^8 \text{ mm}^3$$

$$P = (7 \times 660) = 4620 \text{ kN}$$
$$e = 654 \text{ mm}$$
$$M = 3600 \text{ kN m}$$

Lever arm, $$a = \left(\frac{M}{P}\right) = \frac{(3600 \times 10^3)}{4620} = 779 \text{ mm}$$

Shift of pressure line above the centroidal axis is

$$e' = (a - e) = (779 - 654) = 125 \text{ mm}$$

The resultant stresses at the centre-of-span section are computed as,

$$f_{\text{sup}} = \left[\frac{P}{A} + \frac{Pe'}{Z_t}\right] = \left(\frac{4620 \times 10^3}{62 \times 10^4}\right) + \left(\frac{4620\, k \times 10^3 \times 125}{2.67 \times 10^8}\right)$$

$$= 9.61 \text{ N/mm}^2 \text{ (compression)}$$

$$f_{\text{inf}} = \left[\frac{P}{A} - \frac{Pe'}{Z_b}\right]$$

$$= \left(\frac{4620 \times 10^3}{62 \times 10^4}\right) - \left(\frac{4620 \times 10^3 \times 125}{2.02 \times 10^8}\right)$$

$$= 4.60 \text{ N/mm}^2 \text{ (compression)}$$

The resultant stress distribution across the section is shown in Fig. 4.17(b).

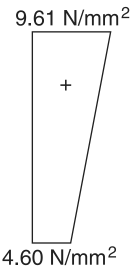

(b) Stress distribution

Fig. 4.17(b)

4.5 Concept of Load Balancing

It is possible to select suitable cable profiles in a prestressed concrete member such that the transverse component of the cable force balances the given type of external loads. This can be readily illustrated by considering the free body of concrete, with the tendon replaced by forces acting on the concrete beam as shown in Fig. 4.18 and Table 4.1.

The various types of reactions of a cable upon a concrete member depend upon the shape of the cable profile. Straight portions of the cable do not induce any reactions except at the ends, while curved cables result in uniformly distributed loads. Sharp angles in a cable induce concentrated loads. The concept of loading-balancing[1] is useful in selecting the tendon profile, which can supply the most desirable system of forces in concrete.

In general, this requirement will be satisfied if the cable profile in a prestressed member corresponds to the shape of the bending moment diagram resulting from the external loads. Thus, if the beam supports two concentrated loads, the cable should follow a trapezoidal profile. If the beam supports uniformly distributed loads, the corresponding tendon should follow a parabolic profile. The principle of load balancing is further amplified with the following examples.

Table 4.1 *Tendon profiles and equivalent loads in prestressed concrete beams*

Tendon Profile	*Equivalent Moment or Load*	*Equivalent Loading*	*Camber*
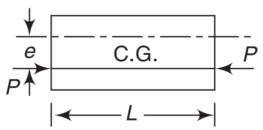	$M = Pe$	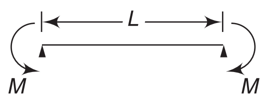	$\dfrac{ML^2}{8EI}$
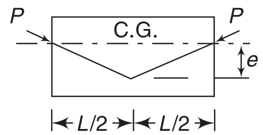	$W = \dfrac{4Pe}{L}$	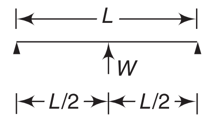	$\dfrac{WL^3}{48EI}$
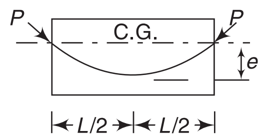	$W = \dfrac{8Pe}{L^2}$	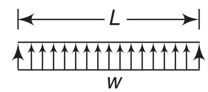	$\dfrac{5WL^4}{384EI}$
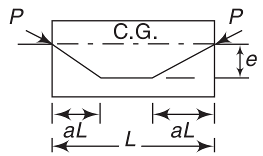	$W = \dfrac{Pe}{aL}$	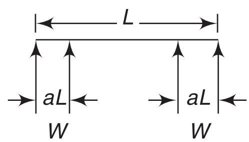	$\dfrac{a(3-4a^2)WL^3}{24EI}$

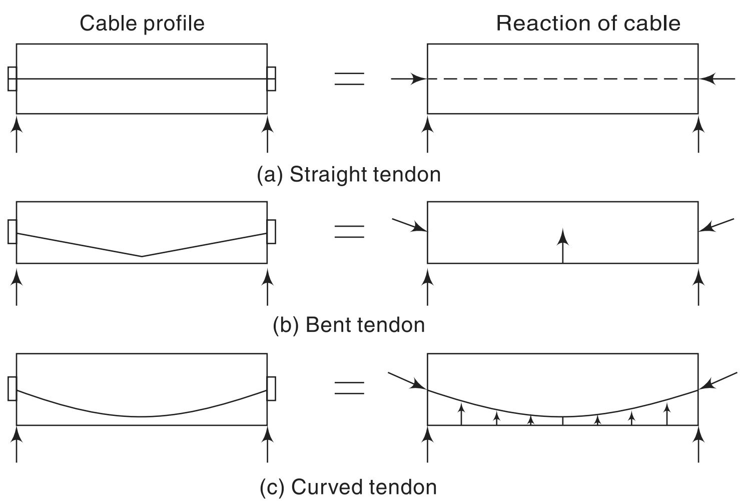

Fig. 4.18 *Reactions of cable on beam*

Example 4.11 A rectangular prestressed beam 150 mm wide and 300 mm deep is used over an effective span of 10 m. The cable with zero eccentricity at the supports and linearly varying to 50 mm at the centre, carries an effective prestressing force of 500 kN. Find the magnitude of the concentrated load Q located at the centre of the span for the following conditions at the centre-of-span section:

(a) If the load counteracts the bending effect of the prestressing force (neglecting self-weight of beam), and
(b) If the pressure line passes through the upper kern of the section under the action of the external load, self-weight and prestress.

Solution.

$$A = (150 \times 300) = 45 \times 10^3 \text{ mm}^2$$

$$Z = \left(\frac{150 \times 300^2}{6}\right) = 225 \times 10^4 \text{ mm}^3$$

Self-weight of beam, $g = (0.15 \times 0.3 \times 24) = 1.08$ kN/m

$$P = 500 \text{ kN} \quad e = 50 \text{ mm}$$

If the inclination of the cable to the horizontal is θ and Q = concentrated load at the centre of the span, for load balancing,

(a) $Q = 2P \sin\theta = 2P \tan\theta = \left(\dfrac{2 \times 500 \times 50}{5 \times 1000}\right) = 10$ kN

(b) Moment due to self-weight $= (0.125 \times 1.08 \times 10^2) = 13.5$ kN m

$$\text{Stress due to self-weight} = \left(\frac{13.5 \times 10^6}{225 \times 10^4}\right) = +6 \text{ N/mm}^2$$

$$\text{Stresses due to prestressing} = \left(\frac{P}{A} + \frac{Pe}{Z}\right)$$

$$= \left[\frac{500 \times 10^3}{45 \times 10^3}\right] + \left[\frac{500 \times 10^3 \times 50}{225 \times 10^4}\right]$$

Stress at the bottom fibre $= 22.22$ N/mm^2

If Q = concentrated load at the centre of the span,

Moment at the centre of span $= (Q \times 10)/4 = 2.5\,Q$

$$\text{Bending stress} = \left[\frac{(2.5Q) \times 10^6}{225 \times 10^4}\right]$$

If the pressure line passes through the upper kern at the section, stress at the bottom fibre = 0. Thus,

$$\left[\frac{2.5Q \times 10^6}{225 \times 10^4}\right] + 6 = 22.22 \quad \text{or} \quad Q = 14.60 \text{ kN}$$

Example 4.12 A rectangular concrete beam 300 mm wide and 800 mm deep supports two concentrated loads of 20 kN each at the third point of a span of 9 m.

(a) Suggest a suitable cable profile. If the eccentricity of the cable profile is 100 mm for the middle third portion of the beam, calculate the prestressing force required to balance the bending effect of the concentrated loads (neglect the self-weight of the beam).

(b) For the same cable profile, find the effective force in the cable if the resultant stress due to self-weight, imposed loads and prestressing force is zero at the bottom fibre of the mid-span section.
(Assume $D_c = 24\ kN/m^3$)

Solution.

(a) A trapezoidal cable profile is selected since the bending moment diagram due to the two concentrated loads is trapezoidal in shape.

Given $Q = 20$ kN, $e = 100$ mm, $L = 9$ m, $Z = 32 \times 10^6\ mm^3$

P = Prestressing force

$$Pe = \left(\frac{QL}{3}\right) \quad \therefore\ P = \left(\frac{QL}{3e}\right) = \left(\frac{20 \times 9000}{3 \times 100}\right) = 600 \text{ kN}$$

(b) Self-weight of the beam, $g = (0.3 \times 9.8 \times 24) = 5.76$ kN/m

Self-weight moment, $M_g = (0.125 \times 5.76 \times 9^2) = 58.32$ kN m

$$\text{Bending stress} = \left(\frac{58.32 \times 10^6}{32 \times 10^6}\right) = 1.82 \text{ N/mm}^2$$

$$\text{Moment at the centre due to loads} = \left(\frac{QL}{3}\right) = \frac{(20 \times 9)}{3} = 60 \text{ kN m}$$

$$\text{Stresses due to loads} = \left(\frac{60 \times 10^6}{32 \times 10^6}\right) = 1.875 \text{ N/mm}^2$$

Total tensile stress at the bottom fibre = (1.82 + 1.875) = 3.695 N/mm^2

If P = required prestressing force in the cable,

$$e = 100 \text{ mm}$$
$$A = (300 \times 800) = 24 \times 10^4 \text{ mm}^2$$

$$\left(\frac{P}{A} + \frac{Pe}{Z}\right) = 3.695$$

$$P\left(\frac{1}{24 \times 10^4} + \frac{100}{32 \times 10^6}\right) = 3.695$$

$$\therefore \quad P = 507 \times 10^3 \text{ N} = 507 \text{ kN}$$

Example 4.13 A prestressed concrete beam of rectangular cross-section 200 mm wide and 600 mm deep supports a live load of 8 kN/m spanning over 8 m. Find the effective prestressing force in the parabolic cable having an eccentricity of 80 mm at the centre of span and concentric at the supports for the following loading conditions:

(a) If the bending effect of the prestressing force is nullified by the imposed load for the mid-span section (neglecting the self-weight of the beam), and

(b) If the resultant stress due to self-weight, live load and prestressing force is zero at the soffit of the beam at centre-of-span section (assume $D_c = 24$ kN/m^3).

$A = (200 \times 600) = 12 \times 104$ mm^2, $e = 80$ mm

$Z = [(200 \times 6002)/6] = 12 \times 10^6$ mm^3, $q = 8$ kN/m

Self-weight of beam = $g = (0.2 \times 0.6 \times 24) = 2.88$ kN/m and span $L = 8$ m

Solution.

(a) If P = prestressing force, then $Pe = (qL^2/8)$

$$\therefore \quad P = \left(\frac{qL^2}{8e}\right) = \left(\frac{8 \times 8^2}{8 \times 0.08}\right) = 800 \text{ kN}$$

(b) Total load on the beam = (2.88 + 8.00) = 10.88 kN/m

Bending moment at the centre of span = $M = (0.125 \times 10.88 \times 82)$
$= 87.04$ kN m

For the bottom fibre stress to be zero, the condition is given by

$$\left(\frac{P}{A} + \frac{Pe}{Z}\right) = \frac{M}{Z}$$

Hence, we have

$$\left[\left(\frac{P}{12 \times 10^4}\right) + \left(\frac{P \times 80}{12 \times 10^6}\right)\right] = \frac{(87.04 \times 10^6)}{(12 \times 10^6)}$$

Solving for the prestressing force, $P = 483.5$ kN

Example 4.14 A concrete beam with a single overhang is simply supported at A and B over a span of 8 m and the overhang BC is 2 m. The beam is of rectangular section 300 mm wide and 900 mm deep and supports a uniformly distributed live load of 3.52 kN/m over the entire length in addition to its self-weight. Determine the profile of the prestressing cable with an effective force of 500 kN which can balance the dead and live loads on the beam. Sketch the profile of the cable along the length of the beam.

Solution. The single overhang beam ABC supporting uniformly distributed load is shown in Fig. 4.19.

Prestressing force in the cable, $P = 500$ kN

Self-weight of the beam = $(0.3 \times 0.9 \times 24) = 6.48$ kN/m

Live load on the beam = 3.52 kN/m

Total load = 10.00 kN/m

The reactions at A and B are obtained as,

$$R_A = 37.5 \text{ kN} \quad \text{and} \quad R_B = 62.5 \text{ kN}$$
$$M_B = (0.5 \times 10 \times 2^2) = 20 \text{ kN m}$$

The bending moment at a distance x from A is

$$M_x = 37.5x - 0.5 \times 10 \times x^2$$

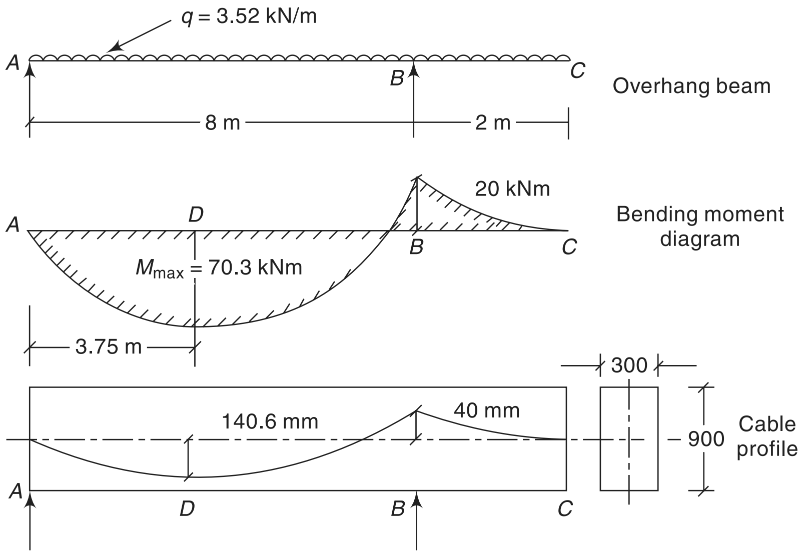

Fig. 4.19 *Prestressed concrete single overhang beam*

For maximum bending moment, $(dM_x/dx) = 0$

$\therefore$ $37.5 - 10x = 0$

Hence, $x = 3.75$ m

$$M_{max} = (37.5 \times 3.75 - 0.5 \times 10 \times 3.75^2) = 70.3 \text{ kN m}$$

$$M_x = 0 \text{ when } 5x^2 = 37.5x \quad \therefore x = 7.5 \text{ m}$$

Hence, the eccentricity of the cable at the position of maximum bending moment is computed as,

$$e = (M_{max}/P) = (70.3 \times 10^6)/(500 \times 10^3) = 140.6 \text{ mm}$$

Eccentricity of the cable at B is calculated as,

$$e = (M_B/P) = (20 \times 10^6)/(500 \times 10^3) = 40 \text{ mm}$$

Since the bending moment at A is zero, the cable is concentric at this point.

The cable profile is parabolic with eccentricities of 140.6 mm below the centroidal axis at D and 40 mm above the centroidal axis at the support section B and with zero eccentricities at A and C as shown in Fig. 4.19.

Example 4.15 A beam of symmetrical I-section spanning 8 m has a flange width of 250 mm and a flange thickness of 80 mm, respectively. The overall depth of the beam is 450 mm. Thickness of the web is 80 mm. The beam is prestressed by a parabolic cable with an eccentricity of 150 mm at the centre of span and zero at supports. The live load on the beam is 2.5 kN/m.

(a) Determine the effective force in the cable for balancing the dead and live loads on the beam.
(b) Sketch the distribution of resultant stress at the centre-of-span section for this case.
(c) Calculate the shift of the pressure line from the tendon-centre-line.

Solution. The properties of the symmetrical I-section shown in Fig. 4.20 are computed as,

$$A = 0.063 \text{ m}^2 \qquad g = 1.57 \text{ kN/m}$$
$$I = 1.553 \times 10^9 \text{ mm}^4 \qquad q = 2.50 \text{ kN/m}$$
$$Z = 6.9 \times 10^6 \text{ mm}^3 \qquad L = 8 \text{ m}$$
$$e = 150 \text{ mm}$$

The bending moments at the centre of the span are calculated as,

$$M_g = (0.125 \times 1.57 \times 8^2) = 12.56 \text{ kN m}$$
$$M_q = (0.125 \times 2.50 \times 8^2) = 20.00 \text{ kN m}$$

Total moment, $M = (M_g + M_q) = 32.56$ kN m

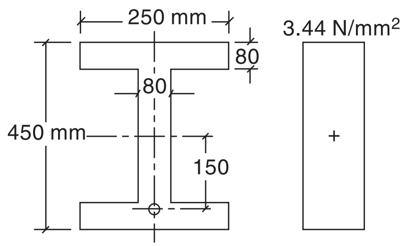

Fig. 4.20 *Prestressed concrete beam of symmetrical I-section*

If P = tendon force, for load balancing we have

$$P = (M/e) = (32.56 \times 10^3)/150 = 217 \text{ kN}$$

The centre-of-span section is subjected to a direct stress of intensity $(P/A) = (217 \times 10^3) / (0.063 \times 10^6) = 3.44 \text{ N/mm}^2$

Shift of pressure line $= (M/P) = (32.56 \times 10^6) / (217 \times 10^3) = 150$ mm

The pressure line coincides with the centroidal axis of the beam.

4.6 Stresses in Tendons

4.6.1 Effect of Loading on the Tensile Stresses in Tendons

A prestressed member undergoes deformation due to the action of the prestressing force and transverse loads acting on the member. Consequently, the curvature of the cable changes, which results in a slight variation of stresses in the tendons. Considering Fig. 4.21, in which a concrete beam of span L is prestressed by a cable carrying an effective force P at an eccentricity, e, the rotation θ_p at the supports due to hogging of the beam is obtained by applying Mohr's theorem as,

$$\theta_p = \left(\frac{\text{Area of bending moment diagram}}{\text{Flexural rigidity}}\right) = \left(\frac{PeL}{2EI}\right)$$

where, EI = flexural rigidity of the beam.

If the beam supports a total uniformly distributed load of w_d per unit length, the rotation θ_1 at supports due to sagging of the beam is evaluated from Fig. 4.22.

$$\theta_1 = \left(\frac{\frac{1}{2} \times \frac{2}{3} \times L\, w_d L^2/8}{EI} \right) = \left(\frac{w_d L^3}{24EI} \right)$$

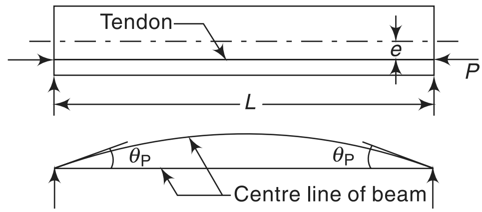

Fig. 4.21 *Effect of prestressing force on rotation of concrete beam*

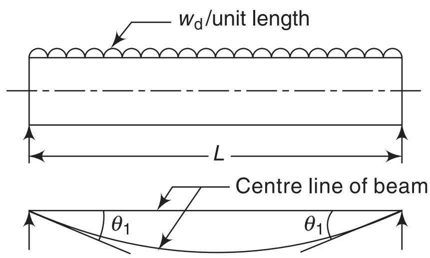

Fig. 4.22 *Effect of transverse loads on rotation of concrete beam*

If the rotation due to loads is greater than that due to the prestressing force, the net rotation θ is given by,

$$\theta = (\theta_1 - \theta_p)$$

Considering Fig. 4.23,

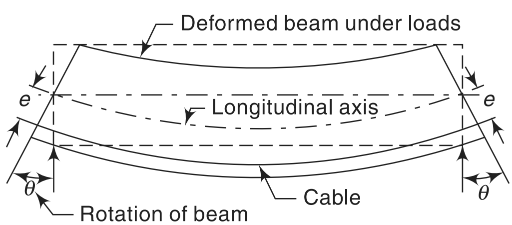

Fig. 4.23 *Rotation of beam under the action of loads*

Total elongation of the cable $= 2e\theta$

Strain in the cable $= (2e\theta/L)$

Increase in stress due to loading $= \dfrac{(E_s 2e\theta)}{L}$

Generally, in the elastic range, any increase of loading on a prestressed member does not result in any significant change in the steel stress. In other words, the stress in steel is more or less constant in the elastic range of a prestressed member. This important observation is illustrated by the following example.

Example 4.16 The cross-section of a prestressed concrete beam used over a span of 6 m is 100 mm wide and 300 mm deep. The initial stress in the tendons located at a constant eccentricity of 50 mm is 1000 N/mm^2. The sectional area of the tendons is 100 mm^2. Find the percentage increase in stress in the wires when the beam supports a live load of 4 kN/m. The density of concrete is 24 kN/m^3.

Solution. Modulus of elasticity of concrete = 36 kN/mm^2

Modulus of elasticity of steel = 210 kN/mm^2

$$\text{Second moment of area } I = \left(\frac{100 \times 300^3}{12}\right) = 225 \times 10^6 \text{ mm}^4$$

Prestressing force $P = (1000 \times 100) = 10^5$ N = 100 kN

$$\text{Rotation due to prestress } \theta_p = \left(\frac{PeL}{2EI}\right) = \left(\frac{100 \times 50 \times 6 \times 10^3}{2 \times 36 \times 225 \times 10^6}\right)$$

(hogging) = 0.00185 radians

Self-weight of the beam, $g = (0.1 \times 0.3 \times 24) = 0.72$ kN/m

Live load $q = 4$ kN/m

Total load = 4.72 kN/m

$w_d = 0.00472$ kN/mm

$$\text{Rotation due to loads } \theta_1 = \left(\frac{w_d L^3}{24EI}\right) = \left(\frac{0.00472 \times 6000^3}{24 \times 36 \times 225 \times 10^6}\right)$$

(sagging) = 0.00525 radians

Net rotation = (0.00525 – 0.00185) = 0.0034 radians

Elongation of cable = $2 \times 50 \times 0.0034 = 0.34$ mm

$$\text{Increase in stress due to loading} = \left[\frac{0.34 \times 210 \times 10^3}{6000}\right] = 12 \text{ N/mm}^2$$

Initial stress in cable = 1000 N/mm^2

$$\text{Percentage increase in stress} = \left(\frac{12 \times 100}{1000}\right) = 1.2\%$$

4.6.2 Variation of Steel Stress in Bonded and Unbonded Members

The rate of increase of stress in the tendons of a prestressed concrete member under loads depends upon the degree of bond between the high-tensile steel wires and the surrounding concrete. In the case of bonded members, such as pretensioned elements or post-tensioned grouted members, the composite action between steel and concrete prevails and the stresses in steel are computed using the theory of composite sections up to the stage of cracking. In the case of unbonded beams, the tendons are free to elongate independently throughout their length under the action of transverse loads on the beam. The increase of stress in steel depends on the average strain in concrete at the level of steel. The methods of computing the increase in stress are herewith outlined for bonded and unbonded members.

Bonded Beams

If M = moment at the section due to loads
E_s and E_c = modulus of elasticity of steel and concrete, respectively
α_e = modular ratio
y = position of steel from the centroidal axis
f = stress in concrete at level y from the centroidal axis
I = second moment of area of the concrete section

$$\text{Stress in steel} = (\text{modular ratio}) \times (\text{stress in concrete})$$

$$= \alpha_e f = \alpha_e \left(\frac{My}{I}\right)$$

Unbonded Beams

If δL = total elongation of the cable at a distance y from the centroidal axis

L = total length of the cable

M = bending moment at the cross-section

Strain in concrete at the level of steel = $(My/E_c I)$

Total elongation of fibre of concrete at the level of steel

$$= \delta L = \int_0^L \left(\frac{My}{E_c I}\right) dx$$

$$\text{Average strain} = \left(\frac{\delta L}{L}\right) = \frac{y}{E_c IL}\int_0^L M dx$$

$$\text{Stress in steel} = \left(\frac{E_s}{E_c}\right)\left(\frac{y}{IL}\right)\int_0^L M dx = \left(\frac{\alpha_e y}{IL}\right)\int_0^L M dx$$

If A = area of the bending moment diagram under a given system of loads,

$$A = \int_0^L M dx$$

Hence, stress in steel = $\left(\dfrac{\alpha_e y A}{IL}\right)$

If the beam supports only a uniformly distributed load of w_d per unit length,

Then $$A = \int_0^L M dx = \left[\left(\frac{2}{3}\right) L w_d \frac{L^2}{8}\right] = \left[w_d \frac{L^3}{12}\right]$$

Increase of stress in steel = $\left[\dfrac{\alpha_e y w_d L^2}{12 I}\right]$

The variation of stress in steel in bonded and unbonded beams is illustrated in Fig. 4.24 for different stages of loading[2]. The rate of increase of stress is larger in the case of bonded beams than in unbonded beams both in the precracking and post-cracking stages. However, after the onset of cracking, the stress in steel increases at a faster rate in both types of beams. Since the steel does not reach its ultimate strength in the case of unbonded beams, the ultimate load supported by the beam is smaller than that of a bonded beam in which the steel attains its ultimate strength at the failure stage of the member.

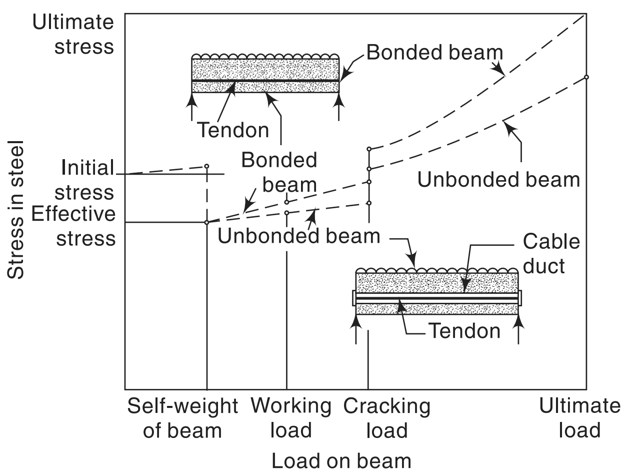

Fig. 4.24 *Variation of stress in steel in bonded and unbonded beams*

In the post-cracking stage, while the bonded beams are characterised by small cracks, which are well distributed in the zone of the larger moments, unbonded beams develop only a few cracks, which are localised at weaker sections and the crack widths are correspondingly larger in comparison with the bonded beams. The crack patterns[3] of bonded and unbonded beams are illustrated in Fig. 4.25. In general, bonded beams are preferable due to their higher flexural strength and predictable deformation characteristics.

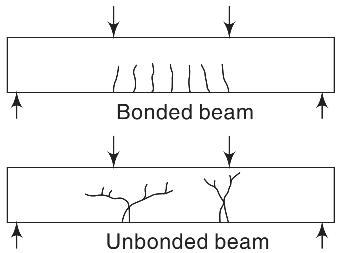

Fig. 4.25 *Typical crack patterns of bonded and unbonded beams*

Example 4.17 A post-tensioned concrete slab spanning in one direction over 8 m is 300 mm deep with tendons housed in ducts spaced at 200 mm centres and are located at an eccentricity of 100 mm. The slab supports a live load of 2.56 kN/m over a width of 200 mm. Calculate the increase in steel stress due to the following conditions:

(a) The ducts are grouted so that the strain in steel and adjacent concrete is equal.

(b) The ducts are ungrouted so that the tendons can move without friction assuming the modular ratio as six and density of concrete as 24 kN/m^3.

Solution.

Self-weight of the slab for a width of 200 mm

$$= g = [0.2 \times 0.3 \times 24] = 1.44 \text{ kN/m}$$

Live load on the slab = q = 2.56 kN/m and span of slab = L = 8 m

Total load on the slab = w_d = [1.44 + 2.56] = 4 kN/m = 4 N/mm

Second moment of area of slab section = $I = [200 \times 300^3]/12 = (45 \times 10^7)$ mm^4

Modular ratio = α_e = 6 and distance of tendons from centroid = y = 100 mm

Bending moment at the centre of span = $M = [0.125 \times 4 \times 8^2] = 32$ kN m

(a) *Bonded tendons*

$$\text{Stress in concrete at level steel} = \left(\frac{My}{I}\right) = \left(\frac{(32 \times 10^6) \times 100}{(45 \times 10^7)}\right) = 7.11 \text{ N/mm}^2$$

Stress in steel = (α_e) (Stress in concrete) = (6×7.11) = 42.66 N/mm^2

(b) *Unbonded tendons*

$$\text{Stress in steel} = \left(\frac{\alpha_e y w_d L^2}{12I}\right) = \left[\frac{6 \times 100 \times 4 \times 8000^2}{12 \times 45 \times 10^7}\right] = 28.4 \text{ N/mm}^2$$

4.7 Cracking Moment

The bending moment at which visible cracks develop in prestressed concrete members is generally referred to as the 'cracking moment'. After the transfer of prestress to concrete, the soffit of the beam will be under compression. Gradually, these compressive stresses are balanced by the tensile stresses developed due to the transverse loads on the beam, so that the resultant stress at the bottom fibre is zero. A further increase in loading results in the development of tensile stresses at the soffit of the beam. As concrete is weak in tension, microcracks develop as soon as the tensile strain in concrete exceeds about $80 - 100 \times 10^{-6}$ units[4], and if the loads are further increased, visible cracks appear in the tension zone. At this stage, it is estimated that the crack widths are of the order of 0.01 – 0.02 mm[5].

The tensile stresses developed when cracks become visible at the soffit of beams depend upon the type and distribution of steel reinforcement and the quality of concrete in the beam. However, it is generally considered that visible cracks appear when the tensile stresses at the soffit are approximately equal to the modulus of rupture of the material. The widths of the cracks are highly influenced by the degree of bond developed between concrete and steel. The following example illustrates the method of evaluating the cracking moment and load factor against cracking:

Example 4.18 A rectangular concrete beam of cross-section 120 mm wide and 300 mm deep is prestressed by a straight cable carrying an effective force of 180 kN at an eccentricity of 50 mm. The beam supports an imposed load of 3.14 kN/m over a span of 6 m. If the modulus of rupture of concrete is 5 N/mm^2, evaluate the load factor against cracking assuming the self-weight of concrete as 24 kN/m^3.

Solution.

$P = 180$ kN $I = 27 \times 10^7$ mm^4

$e = 50$ mm $Z = 18 \times 10^5$ mm^3

$A = 36 \times 10^3$ mm^2 $g = (0.12 \times 0.3 \times 24) = 0.86$ kN/m

$\therefore$ Total load $w = (g + q) = (0.86 + 3.14) = 4$ kN/m

Stresses due to prestress:

$(P/A) = 5$ N/mm^2 $(Pe/Z) = 5$ N/mm^2

Stresses due to loads:

Maximum working moment $= (0.125 \times 4 \times 6^2) = 18$ kN m

$$\left(\frac{M}{Z}\right) = \left[\frac{(18 \times 10^6)}{(18 \times 10^5)}\right] = 10 \text{ N/mm}^2$$

Stress at the bottom fibre at working load $= (5 + 5 - 10) = 0$ N/mm^2

Stress corresponding to cracking at the bottom fibre $= 5$ N/mm^2

Extra moment required to create this stress $= (5 \times 18 \times 10^5)$

$= (9 \times 10^6)$ N mm $= 9$ kN m

$\therefore$ Cracking moment $= (18 + 9) = 27$ kN m

$$\text{Load factor against cracking} = \left(\frac{\text{Cracking moment}}{\text{Working moment}}\right) = \left(\frac{27}{18}\right) = 1.5$$

References

1. Lin, TY, "Load balancing for design and analysis of prestressed concrete structures," *Journal of the American Concrete Institute*, Vol. 60, No. 6, June 1963, pp 719–742.
2. Lin, TY and H Burns Ned, *Design of Prestressed Concrete Structures*, 3rd, edn, John Wiley & Sons, New York, 1982, pp 12–24.
3. Abeles, PW, *An Introduction to Prestressed Concrete*, Vol. I, Concrete Publications Ltd., London, 1964, 293.
4. Evans, RH, "Extensibility and modulus of rupture of concrete," *The Structural Engineer*, Vol. 24, No. 12, Dec. 1946; pp 636–659.
5. Abeles, PW, "Cracks in prestressed concrete beams," *IABSE Congress*, Preliminary Report, Lisbon, 1956, pp 707–721.

Review Questions

4.1 Distinguish between concentric and eccentric tendons, indicating their practical applications.

4.2 Explain the terms—prestress, dead-load stress, live-load stress and resultant stress.

4.3 What is 'pressure or thrust line'? Explain its significance with sketches.

4.4 Explain the concept of internal resisting couple in a prestressed concrete beam supporting dead and live loads.

4.5 Distinguish between cable line and pressure line with sketches in a typical prestressed concrete beam.

4.6 Explain the difference between the load carrying mechanisms of reinforced and prestressed concrete beam sections with sketches.

4.7 Explain the concept of load balancing in prestressed concrete members.

4.8 Briefly explain the relation between tendon profiles and equivalent loads in prestressed concrete beams with sketches.

4.9 A concrete beam supports three concentrated loads equally spaced on the simply supported span. Suggest a suitable cable profile to counteract the effect of these live loads.

4.10 Explain the terms: Working moment, Cracking moment, Load factor against cracking, with respect to prestressed concrete beams.

Exercises

4.1 A rectangular concrete beam, 100 mm wide and 250 mm deep, spanning over 8 m is prestressed by a straight cable carrying an effective prestressing force of 250 kN located at an eccentricity of 40 mm. The beam supports a live load of 1.2 kN/m.

(a) Calculate the resultant stress distribution for the central cross-section of the beam. The density of concrete is 24 kN/m^3.

(b) Find the magnitude of the prestressing force with an eccentricity of 40 mm which can balance the stresses due to dead and live loads at the bottom fibre of the central section of the beam.

[Ans: (a) Stress at top = 14.2 N/mm^2 (compression), stress at the bottom = 5.8 N/mm^2 (compression); (b) Prestressing force = 170 kN]

4.2 A prestressed concrete beam supports a live load of 4 kN/m over a simply supported span of 8 m. The beam has an I-section with an overall depth of 400 mm. The thicknesses of the flange and web are 60 and 80 mm, respectively. The width of the flange is 200 mm. The beam is to be prestressed by an effective prestressing force of 235 kN at a suitable eccentricity such that the resultant stress at the soffit of the beam at the centre of the span is zero.

(a) Find the eccentricity required for the force.

(b) If the tendon is concentric, what should be the magnitude of the prestressing force for the resultant stress to be zero at the bottom fibre of the central span section.

[Ans: (a) *e* = 84 mm; (b) 450 kN]

4.3 A prestressed concrete beam, 200 mm wide and 300 mm deep, is used over an effective span of 6 m to support an imposed load of 4 kN/m. The density of concrete is 24 kN/m^3. At the quarter-span section of the beam, find the magnitude of

(a) the concentric prestressing force necessary for zero fibre stress at the soffit when the beam is fully loaded, and

(b) the eccentric prestressing force located 100 mm from the bottom of the beam which would nullify the bottom fibre stress due to loading.

[Ans: (a) 367.2 kN; (b) 183.6 kN]

4.4 A concrete beam of symmetrical I-section spanning 8 m has flange width and thickness of 200 and 60 mm, respectively. The overall depth of the beam is 400 mm. The thickness of the web is 80 mm. The beam is prestressed by a parabolic cable with an eccentricity of 15 mm at the centre and zero at the supports with an effective force of 100 kN. The live load on the beam is 2 kN/m. Draw the stress distribution diagram at the central section for

(a) Prestress + self-weight (density of concrete = 24 kN/m^3), and

(b) Prestress + self-weight + live load.

[Ans: (a) 0.7 N/mm^2 at top and 3.6 N/mm^2 at bottom (compression); (b) 7.4 N/mm^2 (compression) at top and –0.2 N/mm^2 (tension at bottom)]

4.5 A concrete beam with a double overhang has the middle span equal to 10 m and the equal overhang on either side is 2.5 m. Determine the profile of the prestressing cable with an effective force of 250 kN which can balance a uniformly distributed load of 8 kN/m on the beam, which includes the self-weight of the beam. Sketch the cable profile marking the eccentricity of cable at the support and mid span.

[Ans: *e* (support) = 100 mm; *e* (centre of span) = 300 mm]

4.6 A prestressed concrete beam, 120 mm wide and 300 mm deep, is prestressed by a cable which has an eccentricity of 100 mm at the centre-of-span section. The span of the beam is 6 m. If the beam supports two concentrated loads of 10 kN each at one-third span points, determine the magnitude of the prestressing force in the cable for load balancing for the following cases:

(a) Considering live loads but neglecting self-weight of the beam, and

(b) Considering both self-weight of the beam and live loads. ($D_c = 24$ kN/m^3)

[Ans: (a) 200 kN; (b) 238.7 kN]

4.7 A post-tensioned slab, spanning in one direction over 9 m, is 300 mm deep with straight bars at depth of 250 mm. The slab is subjected to two line loads of 15 kN spread over a width of 300 mm applied along the third-points of the span parallel to the supports. Neglecting the reduction in concrete area due to ducts, calculate the increase in steel stress due to applied loads,

(a) when the bars are efficiently grouted so that the strain in the steel and adjacent concrete is equal, and

(b) when the bars are ungrouted and can move in ducts without friction. Modulus of elasticity of steel and concrete is 210 and 35 kN/mm^2, respectively.

[Ans: (a) 40 N/mm^2; (b) 26.7 N/mm^2]

4.8 A concrete beam, 120 mm wide and 300 mm deep, is prestressed by a straight cable carrying an effective force of 180 kN at an eccentricity of 50 mm. The beam spanning over 6 m supports a total uniformly distributed load of 4 kN/m, which includes the self-weight of the beam. The initial stress in the tendons is 1000 N/mm^2. Determine the percentage increase of stress in the tendons due to the loading on the beam.

$$E_s = 210 \text{ kN/mm}^2, \qquad E_c = 35 \text{ kN/mm}^2$$

[Ans: 0.34 per cent]

4.9 A rectangular concrete beam of cross-section 300 mm deep and 200 mm wide is prestressed by fifteen 5 mm-diameter wires located 65 mm from the bottom of the beam and three 5 mm wires, 25 mm from the top. Assuming the effective stress in the steel as 840 N/mm^2. (a) Calculate the stresses at the extreme fibres of the mid-span section when the beam is carrying its own weight over a span of 6 m, and (b) If a uniformly distributed working load of 6 kN/m is imposed and the modulus of rupture of concrete is 6.5 N/mm^2, obtain the maximum working stress in concrete and estimate the load factor against cracking. The density of concrete is 24 kN/m^3.

[Ans: (a) 2.16 and 7.84 N/mm^2 (compression);
(b) 11.16 N/mm^2, load factor = 1.49]

4.10 A simply supported prestressed concrete beam spanning over 10 m is of rectangular section 500 mm wide and 750 mm deep. The beam is prestressed by a parabolic cable having an eccentricity of 200 mm at the centre of the span and zero at the end supports. The effective force in the cable is 1600 kN. If the beam supports a total uniformly distributed load, of 40 kN/m, which includes the self-weight,

(a) evaluate the extreme fibre stresses at the mid-span section using the internal resisting couple method, and

(b) calculate the force required in the cable having the same eccentricity to balance a total load of 50 kN/m on the beam.

[Ans: (a) 8.10 and 0.42 N/mm^2 (b) 3125 kN]

4.11 A concrete beam of rectangular section having a width of 300 mm and depth 500 mm, is prestressed by a cable carrying a force of 750 kN at an eccentricity of 100 mm. If the beam supports a live load of 20 kN/m over a effective span of 7 m, estimate the resultant stress at the top and bottom fibres at mid-span section due to the effect of prestress, dead and live loads. Assume unit weight of concrete as 24 kN/m^3.

[Ans: Stress at top = 10.56 N/mm^2 (compression), Stress at bottom = 2.94 N/mm^2 (compression)]

4.12 A prestressed concrete beam of rectangular cross-section 300 mm and 600 mm is 12 m long supports a live load 12 kN/m in addition to its own self-weight. The beam is prestressed by a cable having high-tensile wires of 2000 mm^2 area stressed to 800 N/mm^2. The cable is straight and located at a distance of 175 mm from the soffit of the beam. Determine the shift in the pressure line at one quarter span and centre of span, when the beam supports the service load.

[Ans: At one quarter span, shift of pressure line = 162 mm, At centre of span, shift of pressure line = 216 mm]

4.13 A concrete beam of rectangular cross-section 350 mm wide and 700 mm deep supports an uniformly distributed load of 20 kN/m in addition to its self-weight. Suggest a suitable cable profile and the prestressing force having an eccentricity of 200 mm at centre of span to support the dead and the live loads.

[Ans: Parabolic cable concentric at supports and having an eccentricity of 200 mm at centre of span. Prestressing force = 1617 kN]

Objective-type Questions

4.1 Concentric tendons in a concrete beam section induces
(a) tensile stress
(b) variable stress
(c) uniform compressive stress

4.2 Eccentric tendons in a concrete beam section induce
(a) only direct stress
(b) only bending stress
(c) direct and bending stress

4.3 Resultant stress in the cross-section of a prestressed beam comprises of
(a) prestress + dead-load stress + live-load stress
(b) prestress + dead-load stress
(c) prestress + live-load stress

4.4 In a prestressed concrete beam subjected to prestress only
(a) pressure line shifts from the cable line towards the top of beam
(b) pressure line coincides with the cable line
(c) pressure line shifts from cable line towards the soffit of beam

4.5 In a concrete beam subjected to prestress, dead and live loads the
(a) pressure line coincides with the cable line
(b) pressure line shifts uniformly towards the top of beam as load increases
(c) pressure line shifts more at centre of span and zero at supports

4.6 In a prestressed concrete beam, the applied loads are resisted by
(a) an increase in the stress in tendons

(b) a shift in the pressure line from cable line depending upon the moment
(c) an increase in the tensile stress in concrete

4.7 A concentrated live load at centre of span of a prestressed concrete beam can be counter balanced by selecting
(a) straight cable profile
(b) parabolic cable profile
(c) linearly varying profile with zero eccentricity at centre of span.

4.8 Uniformly distributed load on a concrete beam can be effectively counter balanced by selecting
(a) a concentric cable (b) an eccentric cable (c) a parabolic cable

4.9 Hoop tension developed in circular water tanks is best resisted by using
(a) parabolic tendons
(b) circular or hoop tendons
(c) straight tendons

4.10 For resisting concentrated live loads at quarter span points in a prestressed concrete beam, the ideal shape of tendon profile to be used is
(a) parabolic (b) linear (c) trapezoidal

Answers to Objective-type Questions

4.1 (c)	4.2 (c)	4.3 (a)	4.4 (b)	4.5 (b)
4.6 (b)	4.7 (c)	4.8 (c)	4.9 (b)	4.10 (c)

5 Losses of Prestress

5.1 Nature of Losses of Prestress

The initial prestress in concrete undergoes a gradual reduction with time from the stage of transfer due to various causes. This is generally referred to as 'loss of prestress'. A reasonably good estimate of the magnitude of loss of prestress is necessary from the point of view of design. The different types of losses encountered in the pretensioning and post-tensioning systems are compiled in Table 5.1.

Table 5.1 *Types of losses of prestress*

S. No.	*Pretensioning*	*S. No.*	*Post-tensioning*
1.	Elastic deformation of concrete	1.	No loss due to elastic deformation if all the wires are simultaneously tensioned. If the wires are successively tensioned, there will be loss of prestress due to elastic deformation of concrete
2.	Relaxation of stress in steel	2.	Relaxation of stress in steel
3.	Shrinkage of concrete	3.	Shrinkage of concrete
4.	Creep of concrete	4.	Creep of concrete
		5.	Friction
		6.	Anchorage slip

In addition to these, there may be losses of prestress due to sudden changes in temperature, especially in steam curing of pretensioned units. The rise in temperature causes a partial transfer of prestress (due to the elongation of the tendons between adjacent units in the long line process) which may cause a large amount of creep if the concrete is not properly cured. If there is a possibility of a change of temperature between the times of tensioning and transfer, the corresponding loss should be allowed for in the design.

5.2 Loss due to Elastic Deformation of Concrete

The loss of prestress due to elastic deformation of concrete depends on the modular ratio and the average stress in concrete at the level of steel.

If f_c = prestress in concrete at the level of steel

E_s = modulus of elasticity of steel

E_c = modulus of elasticity of concrete

$\alpha_e = \dfrac{E_s}{E_c}$ = modular ratio

Strain in concrete at the level of steel $= \left(\dfrac{f_c}{E_c}\right)$

Stress in steel corresponding to this strain $= \left(\dfrac{f_c}{E_c}\right)E_s$

$\therefore$ Loss of stress in steel $= \alpha_e f_c$

If the initial stress in steel is known, the percentage loss of stress in steel due to the elastic deformation of concrete can be computed.

Example 5.1 A pretensioned concrete beam of rectangular cross-section, 150 mm wide and 300 mm deep, is prestressed by eight high tensile wires of 7 mm diameter located at 100 mm from the soffit of the beam. If the wires are tensioned to a stress of 1100 N/mm^2, calculate the percentage loss of stress due to elastic deformation assuming the modulus of elasticity of concrete and steel as 31.5 and 210 kN/mm^2.

Solution.

Area of eight steel wires $= A_p = (8 \times 38.48) = 308$ mm^2

Prestressing force $= P = [(1100 \times 308)/1000] = 45000$ mm^2

Area of concrete section $= A = (150 \times 300) = 45000$ mm^2

Second moment of area $= I = [(150 \times 330^3)/12] = [33.75 \times 10^7]$ mm^4

Modular ratio $= \alpha_e = [E_s/E_c] = [210/31.5] = 6.66$

Eccentricity = 50 mm

Stress in concrete at the level of steel =

$$f_c = \left[\frac{338.8 \times 10^3}{45000}\right] + \left[\frac{338.8 \times 10^3 \times 50 \times 50}{33.75 \times 10^7}\right] = 10.02 \text{ N/mm}^2$$

Loss of stress due to elastic deformation $= (\alpha_e \times f_c) = (6.66 \times 10.2) = 66.73$ N/mm^2

Percentage loss of stress in steel $= [(66.73 \times 100)/1100] = 6.06\%$

Example 5.2 A rectangular concrete beam, 360 mm deep and 200 mm wide, is prestressed by means of 15 5 mm-diameter wires located 65 mm from the bottom of the beam and three 5 mm wires, located 25 mm from the top of the beam. If the wires are initially tensioned to a stress of 840 N/mm^2, calculate the percentage loss of stress in steel immediately after transfer, allowing for the loss of stress due to elastic deformation of concrete only.

Solution.

$$E_s = 210 \text{ kN/mm}^2$$
$$E_c = 31.5 \text{ kN/mm}^2$$

Position of the centroid of the wires from the soffit of the beam,

$$y = \left[\frac{(15 \times 65) + (3 \times 275)}{(15 + 3)}\right] = 100 \text{ mm}$$

$\therefore$ Eccentricity, $e = (150 - 100) = 50$ mm

Area of concrete, $A = (200 \times 300) = 6 \times 10^4 \text{ mm}^2$

Second moment of area, $I = \left(\dfrac{(200 \times 300^3)}{12}\right) = 45 \times 10^7 \text{ mm}^4$

Prestressing force, $P = (840)(18 \times 19.7) = (3 \times 10^5) \text{ N} = 300$ kN

Stresses in concrete:

$$\text{At the level of top wires} = \left(\frac{300 \times 10^3}{6 \times 10^4}\right) - \left(\frac{300 \times 10^3 \times 50 \times 125}{45 \times 10^7}\right)$$
$$= 0.83 \text{ N/mm}^2$$

$$\text{At the level of bottom wires} = \left(\frac{300 \times 10^3}{6 \times 10^4}\right) + \left(\frac{300 \times 10^3 \times 50 \times 85}{45 \times 10^7}\right)$$
$$= 7.85 \text{ N/mm}^2$$

$$\text{Modular ratio } (\alpha_e) = \left(\frac{210}{31.5}\right) = 6.68$$

Loss of stress in wires at the top $= (6.68 \times 0.83) = 5.55 \text{ N/mm}^2$

Loss of stress in wires at the bottom $= (6.68 \times 7.85) = 52.5 \text{ N/mm}^2$

Percentage loss of stress:

$$\text{For wires at top} = \left(\frac{5.55}{840} \times 100\right) = 0.66\%$$

$$\text{For wires at bottom} = \left(\frac{52.5}{840} \times 100\right) = 6.25\%$$

Example 5.3 A post-tensioned concrete beam, 100 mm wide and 300 mm deep, is prestressed by three cables, each with a cross-sectional area of 50 mm^2 and with an initial stress of 1200 N/mm^2. All the three cables are straight and located 100 mm from the soffit of the beam. If the modular ratio is 6, calculate the loss of stress in the three cables due to elastic deformation of concrete for only the following cases:

(a) Simultaneous tensioning and anchoring of all the three cables, and

(b) Successive tensioning of the three cables, one at a time.

Solution.

Force in each cable, $P = (50 \times 1200) = (60 \times 10^3) \text{ N} = 60$ kN

$$A = (3 \times 10^4)\ \text{mm}^2 \qquad I = (225 \times 10^6)\ \text{mm}^4$$
$$e = 50\ \text{mm} \qquad y = 50\ \text{mm}$$

Stress in concrete at the level of steel,

$$f_c = \left(\frac{60 \times 10^3}{3 \times 10^4}\right) + \left(\frac{60 \times 10^3 \times 50 \times 50}{225 \times 10^6}\right) = 2.7\ \text{N/mm}^2$$

Case (a)

Under simultaneous tensioning and anchoring of all the three cables, there will be no loss due to the elastic deformation of concrete.

Case (b)

When the cables are successively tensioned:
Cable 1 is tensioned and anchored—no loss due to elastic deformation
Cable 2 is tensioned and anchored—loss of stress in Cable 1 given by,
Loss of stress in Cable 1 = $\alpha_e f_c = (6 \times 2.7) = 16.2\ \text{N/mm}^2$
Cable 3 is tensioned and anchored—loss of stress in both Cables 1 and 2 given by,
Loss of stress in Cable 1 = $(6 \times 2.7) = 16.2\ \text{N/mm}^2$ (when Cable 3 is tensioned)
Loss of stress in Cable 2 = $(6 \times 2.7) = 16.2\ \text{N/mm}^2$ (when Cable 3 is tensioned)
$\therefore$ Total loss stress due to elastic deformation of concrete in

Cable 1 = $(16.2 + 16.2) = 32\ \text{N/mm}^2$
Cable 2 = $16.2 = 16.2\ \text{N/mm}^2$
Cable 3 = 0

Average loss of stress considering all the three cables = $16.2\ \text{N/mm}^2$

It can be shown that if the number of wires, bars or strands are large, the loss due to elastic shortening approaches (but does not exceed) one-half of the corresponding loss with pretensioning, i.e., loss of stress = $\left(\frac{1}{2}\alpha_e f_c\right)$, where f_c = stress in concrete at the level of steel due to the effect of all the cables simultaneously tensioned.

Applying this principle to the problem,

$$\text{Loss of stress} = \left[\frac{1}{2} \times 6 \times (3 \times 2.7)\right] = 24.3\ \text{N/mm}^2$$

5.2.1 Loss of Stress due to Successive Tensioning of Curved Cables

In most bridge girders[1], the cables are curved with maximum eccentricity at the centre of the span. In such cases, the loss of stress due to the elastic deformation of concrete is estimated by considering the average stress in concrete at the level of steel. Consider a beam shown in Fig. 5.1, which is post-tensioned by three parabolic cables. The stress distribution in concrete at the level of Cable 1 is also shown in the figure when Cable 2 is tensioned. For computing the loss of stress, the average stress (shown in figure) is considered. When Cable 3 is tensioned, there will be losses of stress in both Cables 1 and 2. This is illustrated in the following example:

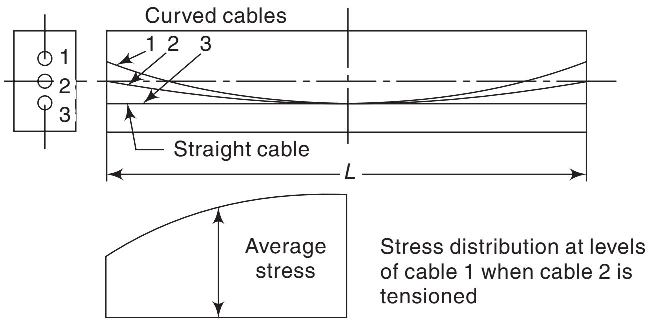

Fig. 5.1 *Successive tensioning of curved cables*

Example 5.4 A post-tensioned concrete beam, 100 mm wide and 300 mm deep, spanning over 10 m is stressed by successive tensioning and anchoring of three Cables 1, 2 and 3, respectively. The cross-sectional area of each cable is 200 mm^2 and the initial stress in the cable is 1200 N/mm^2, $\alpha_e = 6$. The first cable is parabolic with an eccentricity of 50 mm below the centroidal axis at the centre of span and 50 mm above the centroidal axis at the support sections. The second cable is parabolic with zero eccentricity at the supports and an eccentricity of 50 mm at the centre of the span. The third cable is straight with a uniform eccentricity of 50 mm below the centroidal axis. Estimate the percentage loss of stress in each of the cables, if they are successive1y tensioned and anchored.

Solution.

Force in each cable, $P = 240$ kN

$$A = (3 \times 10^4)\ \text{mm}^2 \quad \alpha_e = 6$$

$$I = (225 \times 10^6)\ \text{mm}^4$$

When Cable 1 is tensioned and anchored, there is no loss of stress due to elastic deformation of concrete. When Cable 2 is tensioned and anchored, stress at the level of Cable 1 is given by,

$$\text{Stress at support section} = \left(\frac{240 \times 10^3}{3 \times 10^4}\right) = 8\ \text{N/mm}^2$$

$$\text{Stress at the centre of span} = \left(\frac{240 \times 10^3}{3 \times 10^4}\right) + \left[\frac{(240 \times 10^3) \times 50 \times 50}{225 \times 10^6}\right]$$

$$= 10.7\ \text{N/mm}^2$$

$\therefore$ Average stress in concrete = $(8 + (2/3) \times 2.7) = 9.8$ N/mm^2

Loss of stress in Cable 1 = $(6 \times 9.8) = 58.8$ N/mm^2

When Cable 3 is tensioned and anchored, stress distribution at the levels of Cable 1 and Cable 2 and the average stress and the loss of stress is obtained as follows.

	Cable 1	*Cable 2*
Stress at support	$\left(\frac{240\times10^3}{3\times10^4}\right)-\left(\frac{240\times10^3\times50\times50}{225\times10^6}\right)$ $= 5.3$ N/mm^2	$\left(\frac{240\times10^3}{3\times10^4}\right)$ $= 8$ N/mm^2
Stress at the centre of span	$\left(\frac{240\times10^3}{3\times10^4}\right)+\left(\frac{240\times10^3\times50\times50}{225\times10^6}\right)$ $= 10.7$ N/mm^2	$\left(\frac{240\times10^3}{3\times10^4}\right)+$ $\left(\frac{240\times10^3\times50\times50}{225\times10^6}\right)$ $= 10.7$ N/mm^2
Average stress in concrete	$[5.3 + (2/3)\times5.4] = 8.9$ N/mm^2	$[8 + (2/3)\times2.7]$ $= 9.8$ N/mm^2
Loss of stress in cable	$(6\times8.9) = 53.4$ N/mm^2	$(6\times9.8) = 58.8$ N/mm^2
Total losses		*Percentage loss of stress (%)*
Cable 1, $(58.8 + 53.4) = 112.2$ N/mm^2		9.4
Cable 2, 58.8 N/mm^2		4.9
Cable 3, no loss of stress		0

Example 5.5 A simply supported concrete beam of uniform section is post-tensioned by means of two cables, both of which have an eccentricity of 100 mm below the centroid of the section at mid-span. The first cable is parabolic and is anchored at an eccentricity of 100 mm above the centroid at each end. The second cable is straight and parallel to the line joining the supports. If the cross-sectional area of each cable is 100 mm^2, the concrete beam has a sectional area of 2×10^4 mm^2 and a radius of gyration of 120 mm, calculate the loss of stress in the first cable when the second is tensioned to a stress of 1200 N/mm^2. Take the modular ratio as 6 and neglect friction.

Solution.

Area of concrete section $A = 2\times10^4$ mm^2

Radius of gyration $i = 120$ mm

Second moment of area $I = (2\times10^4\times120^2) = 288\times10^6$ mm^4

Prestressing force $P = (1200\times100) = 12\times10^4$ N

When Cable 2 is tensioned and anchored, stress at the level of Cable 1 is given by,

$$\text{Stress in concrete} = \left(\frac{12 \times 10^4}{2 \times 10^4}\right) \pm \left(\frac{12 \times 10^4 \times 100 \times 100}{288 \times 10^6}\right) = (6 \pm 4.2)$$

$= 10.2$ N/mm^2 at central section and 1.8 N/mm^2 at end section
Average stress in concrete = $[1.8 + (2/3) \times 8.4] = 7.4$ N/mm^2
Loss of stress in Cable 1 = $(6 \times 7.4) = 44.4$ N/mm^2.

5.3 Loss of Prestress due to Shrinkage of Concrete

The shrinkage of concrete in prestressed members results in a shortening of tensioned wires and hence contributes to the loss of stress. The shrinkage of concrete is influenced by the type of cement and aggregates and the method of curing used. Use of high-strength concrete with low water-cement ratios results in a reduction in shrinkage and consequent loss of prestress. The primary cause of drying shrinkage is the progressive loss of water from concrete. The rate of shrinkage is higher at the surface of the members. The differential shrinkage between the interior and surface of large members may result in strain gradients leading to surface cracking. Hence, proper curing is essential to prevent shrinkage cracks in prestressed members.

In the case of pretensioned members, generally moist curing is resorted to in order to prevent shrinkage until the time of transfer. Consequently, the total residual shrinkage strain will be larger in pretensioned members after transfer of prestress in comparison with post-tensioned members, where a portion of shrinkage will have already taken place by the time of transfer of stress. This aspect has been considered in the recommendations made by the Indian standard code (IS: 1343) for the loss of prestress due to the shrinkage of concrete and is detailed below.

As outlined in Section 2.1.4, the total shrinkage strain (ε_{cs}) comprises of two components, the drying shrinkage strain (ε_{cd}) and the autogenous shrinkage strain (ε_{ca}), expressed as,

$$\varepsilon_{cs} = (\varepsilon_{cd} + \varepsilon_{ca})$$

The loss of stress in steel due to the shrinkage of concrete is estimated by the relation,

Loss of stress = $(\varepsilon_{cs} \times E_s)$, where E_s = modulus of elasticity of steel

The value of the total shrinkage strain can be evaluated with the available data of the drying and autogenous shrinkage strain using Tables 2.3, 2.4 and 2.5. In contrast to the Indian Standard Code IS: 1343-2012, the British code lists the drying shrinkage values for humidity's varying from 20 to 100 per cent.

Example 5.6 A concrete beam is prestressed by a cable with an initial stress of 1000 N/mm^2 in the wires. The grade of concrete in the beam is M-50. The beam is located in an area having a relative humidity of 50 per cent. The beam is exposed to the environment on three sides having a depth of 400 m and a width of 300 mm. The beam was cured for seven days before it was prestressed. Using the Indian Standard Code method, estimate the loss of stress in steel due to shrinkage of concrete at the age of (a) 28 days and (b) 70 years.

Assume modulus of elasticity of steel as 210 kN/mm^2.

Solution.

Initial stress in steel wires = 1000 N/mm^2

Total shrinkage strain = $\varepsilon_{cs} = (\varepsilon_{cd} + \varepsilon_{ca})$

(a) Loss of stress in steel due to shrinkage at 28 days

At 28 days, the autogenous shrinkage strain = $\varepsilon_{ca}\,(28) = \beta_{as}(t)\,\varepsilon_{ca}$

where $\beta_{as}(t) = [1 - e^{-0.2\sqrt{t}}]$ where t = 28 days

$$= [1 - e^{-0.2\sqrt{28}}]$$
$$= 0.6321$$

From Table 2.3, corresponding to M-50 grade concrete, read the value of

$\varepsilon_{ca} = (75 \times 10^{-6})$

Autogenous shrinkage strain at 28 days is computed as,

$\varepsilon_{ca} = \beta_{as}(t)\,\varepsilon_{ca} = (0.6321)(75 \times 10^{-6}) = (42 \times 10^{-6})$

The drying shrinkage strain at the age of 28 days is computed using the expression

$\varepsilon_{cd}(t) = \beta_{ds}(t, t_s)k_h \cdot \varepsilon_{cd}$

$$\text{where, } \beta_{ds}(t, t_s) = \left[\frac{(t - t_s)}{(t - t_s) + 0.04\sqrt{h_0^3}}\right]$$

In this expression, t = 28 days and t_s = 7 days, hence $(t - t_s) = 21$

$$h_o = \left(\frac{2A_c}{u}\right) = \left(\frac{2 \times 300 \times 400}{(2 \times 400\ ) + 300}\right) = 218$$

$$\beta_{ds}(t, t_s) = \left[\frac{(28 - 7)}{21 + 0.04\sqrt{218^3}}\right] 0.14$$

From Table 2.5, read the value of k_h corresponding to a value of $h_o = 218$ as $k_h = 0.83$.

For M-50 grade concrete at a relative humidity of 50 per cent, read the value of unrestrained drying shrinkage from Table 2.4 (a) as $\varepsilon_{cd} = (420 \times 10^{-6})$

Hence, $\varepsilon_{cd}(t) = \beta_{ds}(t, t_s)k_h \cdot \varepsilon_{cd}$

$$= (0.14 \times 0.83 \times 420 \times 10^{-6})$$
$$= (49 \times 10^{-6})$$

Total shrinkage strain is computed as $= (\varepsilon_{cd} + \varepsilon_{ca})$

$$= (49 + 75) \times 10^{-6}$$
$$= (124 \times 10^{-6})$$

Loss of stress in steel due to shrinkage of concrete

$= [\varepsilon_{cs} E_s]$

$= [(124 \times 10^{-6}) \times (210 \times 10^3)]$

$= 26 \text{ N/mm}^2$

$$\text{Percentage loss of stress} = \left\{\frac{26}{1000} \times 100\right\} = 2.6\%$$

(b) Loss of stress in steel due to shrinkage at 70 years

The long-term (70 years) shrinkage strain comprises of both the autogenous and drying shrinkage strains.

For M-50 grade concrete, read the value of autogenous shrinkage strain from Table 2.3 as $\varepsilon_{ca} = -(75 \times 10^{-6})$

ε_{ca} (70 years) $= \beta_{as}(t)\, \varepsilon_{ca}$

where $\beta_{as}(t) = [1 - e^{-0.2\sqrt{t}}]$ where $t = (70 \times 365) = 25550$ days

$= [1 - e^{-0.2\sqrt{25550}}]$

$= 1$

Hence, ε_{ca} (70 years) $= (75 \times 10^{-6})$

The drying shrinkage strain at 70 years is computed as

$\varepsilon_{cd}(t) = \beta_{ds}(t, t_s)k_h \cdot \varepsilon_{cd}$

$$\text{where, } \beta_{ds}(t, t_s) = \left[\frac{(t - t_s)}{(t - t_s) + 0.04\sqrt{h_0^3}}\right]$$

In this expression, t = 25550 days and t_s = 7 days, hence $(t - t_s) = 25543$, $h_o = 218$ mm and $k_h = 0.83$.

$$\beta_{ds}(t, t_s) = \left[\frac{25543}{(25543) + 0.04\sqrt{218^3}}\right] = 1$$

Hence, $\varepsilon_{cd}(t) = \beta_{ds}(t, t_s)k_h \cdot \varepsilon_{cd}$

$= (1.0 \times 0.83 \times 420 \times 10^{-6})$

$= (348.6 \times 10^{-6})$

Total shrinkage strain $= (\varepsilon_{cd} + \varepsilon_{ca}) = (348.6 + 75)\, 10^{-6}$

$= (423.6 \times 10^{-6})$

Loss of stress in steel due to shrinkage of concrete

$= [\varepsilon_{cs} E_s]$

$= [(423.6 \times 10^{-6}) \times (210 \times 10^3)]$

$= 88.95 \text{ N/mm}^2$

$$\text{Percentage loss of stress} = \left\{\frac{88.95}{1000} \times 100\right\} = 8.895\%$$

5.4 Loss of Prestress due to Creep of Concrete

The initial stress in the tendons gradually reduces due to the creep of concrete. The factors influencing the creep of concrete are presented in detail in Section 2.1.5. In designing prestressed concrete members, a knowledge of the magnitude of loss of prestress due to creep is necessary. Various national codes recommend the creep coefficient method for estimating the loss of prestress.

Creep Coefficient Method

If ϕ_o = creep coefficient
ε_c = creep strain
ε_e = elastic strain
m = modular ratio
E_s = modulus of elasticity of steel
E_c = modulus of elasticity of concrete
f_c = stress in concrete

$$\text{Creep coefficient} = c\left(\frac{\text{creep strain}}{\text{elastic strain}}\right) = \left(\frac{\varepsilon_c}{\varepsilon_e}\right)$$

$$\therefore \qquad \varepsilon_c = \phi_o\,\varepsilon_e = \phi_o(f_c/E_c)$$

Hence, loss of stress = $(\varepsilon_c \cdot E_s) = \phi_o(f_c/E_c)\,E_s = (\phi_o \cdot f_c \cdot m)$.

The Indian and British codes recommend the values of 70 year creep coefficient for varying humidity, age at loading and the notional size of the member. The value of the creep coefficient varies from a minimum of 1.0 to a maximum of 5.8. For grades of concrete from M-30 to M-60 generally used in prestressed members, the values of creep coefficient listed in Table 2.7 are useful in computing the loss of stress due to creep of concrete.

Example 5.7 A concrete beam of rectangular section 100 mm wide and 300 mm deep is prestressed by five wires of 7 mm diameter located at an eccentricity of 50 mm, the initial stress in the wires being 1200 N/mm^2. Estimate the final loss of stress in steel due to creep of concrete according to the Indian Standard Code method (IS: 1343-2012).

Solution.

$$E_s = 210 \text{ kN/mm}^2$$
$$f_{ck} = 60 \text{ N/mm}^2$$
$$A = (3 \times 10^4) \text{ mm}^2$$
$$I = (225 \times 10^6) \text{ mm}^4$$
$$E_c = 5000\sqrt{f_{ck}} = 5000\sqrt{60} = 38729 \text{ N/mm}^2 = 38.7 \text{ kN/mm}^2$$
$$m = (E_s/E_c) = (210/38.7) = 5.4$$
$$P = (5 \times 38.5 \times 1200) = (23 \times 10^4) \text{ N}$$
$$e = 50 \text{ mm}$$

Relative humidity = 50 per cent

Age at loading = 28 days

Stress in concrete at the level of steel is given by

$$f_c = \left[\left(\frac{23\times10^4}{3\times10^4}\right) + \frac{(23\times10^4\times50)50}{(225\times10^6)}\right] = 10.2\ \text{N/mm}^2$$

Loss of stress = $(\varepsilon_c \cdot E_s) = (\phi_o \cdot f_c \cdot m)$

Assuming that the sides and bottom width of the beam is exposed to the environment

$$\text{Notional size} = h_o = \left(\frac{2A_c}{u}\right) = \left(\frac{2\times300\times100}{(2\times300)+100}\right) = 85.7\ \text{mm}$$

Referring to Table 2.7, read out the value of creep coefficient corresponding to the values of relative humidity 50 per cent, age at loading as 28 days and notional size of 85.7,

$\phi_o = 2.8$

Hence, the loss of stress due to creep = $(\phi_o \cdot f_c \cdot m) = (2.8\times10.2\times5.4) =$ 154.22 N/mm^2.

Example 5.8 A concrete beam having a width of 100 mm and depth 300 mm is post tensioned by a parabolic cable with an eccentricity of 50 mm at the centre of span and concentric at the supports. Assuming an ultimate creep coefficient of 3.0, estimate the loss of stress in the cable due to creep of concrete.

Solution.

Force in the cable = P = 240 kN

Area of cross-section = $A = (3\times10^4)$ mm^2

Second moment of area = $I = (225\times10^6)$ mm^4

Eccentricity of cable = e = 50 mm

Modular ratio = m = 6

Modulus of elasticity of steel = 210 kN/mm^2

Creep coefficient = ϕ_o = 3.0

Stress in concrete at the level of cable at support and centre of span sections are computed as,

$$\text{At support section} = \left(\frac{P}{A}\right) = \left(\frac{240000}{3\times10^4}\right) = 8\ \text{N/mm}^2$$

$$\text{At centre of span section} = \left[\frac{P}{A} + \frac{Pey}{I}\right] = \left[\frac{240000}{3\times10^4} + \frac{24\times10^4\times50\times50}{(225\times10^6)}\right]$$

$$= 10.7\ \text{N/mm}^2$$

Average stress at the level of cable = $f_c = [8 + (2/3)\times2.7] = 9.8$ N/mm^2

$\therefore$ Loss of stress in cable due to creep of concrete $= (\phi_o \cdot f_c \cdot m)$

$= (3.0\times9.8\times6)$

$= 176.4$ N/mm^2

5.5 Loss of Prestress due to Relaxation of Stress in Steel

The various factors which influence the phenomenon of creep in steel have been discussed in Section 2.2.4. Most of the codes provide for the loss of stress due to relaxation of steel as a percentage of the initial stress in steel. The Indian Standard Code recommends a value varying from 0 to 90 N/mm^2 for stress in wires varying from $0.5f_{pu}$ to $0.8f_{pu}$. The loss of prestress due to relaxation of steel recommended in British and Indian codes is compiled in Table 5.2. Temporary over-stressing by 5–10 per cent for a period of 2 min. is sometimes used to reduce this loss as in the case of drawn wires.

However, over-stressing does not appear to be beneficial for stabilised wires[2] which, as a result of heat treatment, have 0.1 per cent proof stress in excess of 85 per cent of the tensile strength, since such wires suffer very little permanent deformation when over-stressed.

Table 5.2 *Loss of prestress due to relaxation of steel*

(a) Recommendations of British codes

Type of Tendon	*Range of Characteristic Strength,* (N/mm^2)	*Modulus of Elasticity* (kN/mm^2)	*Percentage Loss of Prestress for*	
			$0.7 f_{pi}$	$0.8 f_{pu}$
Cold-drawn steel wire to BS: 2691				
1. Prestraightened (normal relax-ation)	1570–1720	200	5	8.5
2. Prestraightened (low relaxation)	1570–1720	200	2	3.0
Seven-wire strand to BS: 3617				
1. normal relaxation	1640–1820	200	7	12
2. low relaxation	1640–1820	200	2	3
Nineteen-wire strand to BS: 4757				
1. as spun	1480–1540	175	9	14
2. normal relaxation	1760	175	7	12
3. low relaxation	1760	175	2.5	3.5
Cold-worked high tensile alloy steel bars to BS: 4486	995–1030	175	4	—

(b) Relaxation losses for prestressing steel at 1000 h at 20 ± 2°C (IS: 1343)–2012

S. No.	*Initial Stress*	*Relaxation Loss* (per cent)	
		Normal	*Low*
1.	$0.5\, f_p$	0	0
2.	$0.6\, f_p$	3.0	1.0
3.	$0.7\, f_p$	5.0	2.5
4.	$0.8\, f_p$	8.0	4.5

5.6 Loss of Prestress due to Friction

In the case of post-tensioned members, the tendons are housed in ducts preformed in concrete. The ducts are either straight or follow a curved profile depending upon the design requirements. Consequently, on tensioning the curved tendons, loss of stress occurs in the post-tensioned members due to friction between the tendons and the surrounding concrete ducts. The magnitude of this loss is of the following types:

1. Loss of stress due to the curvature effect[3], which depends upon the tendon form or alignment which generally follows a curved profile along the length of the beam.
2. Loss of stress due to the wobble effect[4], which depends upon the local deviations in the alignment of the cable. The wobble or wave effect is the result of accidental or unavoidable misalignment, since ducts or sheath cannot be perfectly located to follow a predetermined profile throughout the length of the beam.

Referring to Fig. 5.2, the magnitude of the prestressing force, P_x, at a distance x from the tensioning end follows an exponential function of the type,

$$P_x = P_o e^{-(\mu\alpha + kx)}$$

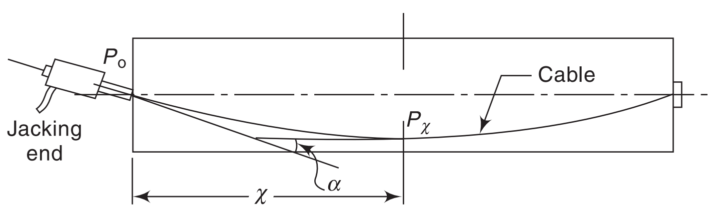

Fig. 5.2 *Loss of stress due to friction*

where P_o = prestressing force at the jacking end

μ = coefficient of friction between cable and duct

α = the cumulative angle in radians through which the tangent to the cable profile has turned between any two points under consideration

k = friction coefficient for 'wave' effect

e = 2.7183

The Indian Standard code recommendations for the values of μ and k are compiled in Table 5.3.

Table 5.3 *Recommended values of μ and k (IS: 1343-2012)*

Type of High Tensile Steel	*Type of Duct or Sheath*	*Value Recommended to be used in Design*	
		k/m	μ
Wire Cables	Bright metals	0.0091	0.25
	Galvanized	0.0046	0.20
	Lead coated	0.0046	0.18
Uncoated stress relieved strand	Bright metals	0.0046	0.25
	Galvanized	0.0030	0.20
	Lead coated	0.0030	0.18
	Corrugated HDPE	0.0020	0.17

The coefficient may be reduced to zero where the clearance between the duct and cable is sufficiently large to eliminate the 'wave' effect. The sheath is made of a heavy-gauge steel tube with water-tight joints, where a deformation of the duct profile is prevented during the vibration of concrete.

The coefficient of friction can be considerably reduced by using a variety of lubricants, particularly greases, oils, oil and graphite mixtures and paraffin. Investigations by Leonhardt[5], Foppl[6] and Morsch[7] indicate that the use of paraffin gives by far the lowest coefficient of friction, especially with high contact-pressures. It was also observed that paraffin coatings remain effective even when subjected to repeated movement at a contact pressure of 60 N/mm^2. At these pressures, the magnitude of coefficient of friction diminished to a low value of 0.004. At pressures between 20 and 5 N/mm^2, the coefficient ranged from 0.03 to 0.02. Apart from this, paraffin has been found to be harmless to concrete and grout. Another lubricant–teflon, a Dupont product, has been found to give more favourable results.

Experimental values of the coefficient of friction have been reported by Morice and Cooley[8] for different types of ducts and post-tensioning systems.

Based on experimental work, the Prestressed Concrete Institute[9] has recommended some values for the curvature and wobble coefficients in the commentary of the American Concrete Institute code[10] and these are compiled in Table 5.4 for general use. However, specific values for the friction developed with any particular type of tendon and duct should generally be obtained from the manufacturers of the tendons.

Table 5.4 *Friction coefficients for post-tensioning tendons*

Type of Tendon	*Curvature Coefficient* (μ)	*Wobble Coefficient* (k/m)
Tendons in flexible metal sheathing:		
1. Wire tendons	0.15–0.25	0.0033–0.0049
2. Seven-wire strand	0.15–0.25	0.0016–0.0066
3. High-strength bars	0.08–0.30	0.0003–0.0020
Tendons in rigid metal duct		
1. Seven-wire strand	0.15–0.25	0.0007
2. Mastic coated tendons, Wire tendons and Seven-wire strand	0.05–0.15	0.0033–0.0066
3. Pregreased tendons Wire tendons and Seven-wire strand	0.05–0.15	0.001–0.0066

Frictional losses can be reduced by several methods, such as

1. Overtensioning the tendons by an amount equal to the maximum frictional loss.
2. Jacking the tendons from both ends of the beam, generally adopted when the tendons are long or when the angles of bending are large.

Example 5.9 A concrete beam of 10 m span, 100 mm wide and 300 mm deep, is prestressed by three cables. The area of each cable is 200 mm^2 and the initial stress in the cable is 1200 N/mm^2. Cable 1 is parabolic with an eccentricity of 50 mm above the centroid at the supports and 50 mm below at the centre of span. Cable 2 is also parabolic with zero eccentricity at supports and 50 mm below the centroid at the centre of span. Cable 3 is straight with uniform eccentricity of 50 mm below the centroid. If the cables are tensioned from one end only, estimate the percentage loss of stress in each cable due to friction. Assume $\mu = 0.35$ and $k = 0.0015$ per m.

Solution.

Equation of a parabola is given by:

$$y = (4e/L^2)x(L - x)$$

$$\text{Slope at ends (at } x = 0) = dy/dx = (4e/L^2)(L - 2x) = (4e/L)$$

For Cable 1

$$\text{Slope at end} = \left(\frac{4 \times 10}{10 \times 100}\right) = 0.04$$

$\therefore$ Cumulative angle between tangents, $\alpha = (2 \times 0.04) = 0.08$ radians

For Cable 2

$$\text{Slope at end } = \left(\frac{4 \times 5}{10 \times 100}\right) = 0.02$$

$\therefore$ Cumulative angle between tangents, $\alpha = (2 \times 0.02) = 0.04$ radians
Initial prestressing force in each cable, $P_0 = (200 \times 1200) = 24{,}0000$ N
If P_x = prestressing force (stress) in the cable at the farther end,

$$P_x = P_o e^{-(\mu\alpha + kx)}$$

For small values of $(\mu\alpha + Kx)$, we can write

$$P_x = P_o[1 - (\mu\alpha + kx)]$$

$$\text{Loss of stress} = P_o(\mu\alpha + kx)$$

$$\text{Cable 1} = P_o(0.35 \times 0.08 + 0.0015 \times 10) = 0.043\ P_o$$

$$\text{Cable 2} = P_o(0.35 \times 0.04 + 0.0015 \times 10) = 0.029\ P_o$$

$$\text{Cable 3} = P_o(0 + 0.0015 \times 10) = 0.015\ P_o$$

If $\quad P_o$ = Initial stress = 1200 N/mm^2

Cable No.	*Loss of Stress* (N/mm^2)	*Percentage Loss*
1	51.6	4.3
2	34.8	2.9
3	18.0	1.5

Example 5.10 A post-tensioned concrete beam, 200 mm wide and 450 mm deep, is prestressed by a circular cable (total area = 800 mm^2) with zero eccentricity at the ends and 150 mm at the centre. The span of the beam is 10 m. The cable is to be stressed from one end such that an initial stress of 840 N/mm^2 is available in the unjacked end immediately after anchoring. Determine the stress in the wires at the jacking end and the percentage loss of stress due to friction.

Solution.

Coefficient of friction for 'curvature' effect = 0.6
Friction coefficient for 'wave' effect = 0.003/m
If R = radius of the circular cable, then $(R - 0.15)^2 + 5^2 = R^2$, which gives

$$R = 84 \text{ m}$$

If α = angle between the horizontal and the tangent drawn to the cable at support, then

$$\sin \alpha = (5/84) = 0.06 \text{ radians}$$

$\therefore$ Cumulative angle between tangents to the cable at supports

$$= (2 \times 0.06) = 0.12 \text{ radians}$$

Given, $\quad P_x$ = stress at the unjacked end = 840 N/mm^2

$\quad P_o$ = initial stress at the jacking end

$$P_x = P_o[1 - (0.6 \times 0.12 + 0.003 \times 10)] = 0.898\, P_o$$

$$\therefore \qquad P_o = \left(\frac{P_x}{0.898}\right) = \left(\frac{840}{0.898}\right) = 940 \text{ N/mm}^2$$

$$\text{Loss of stress in cable} = (940 - 840) = 100 \text{ N/mm}^2$$

$$\text{Percentage loss of stress} = \left(\frac{100}{940} \times 100\right) = 10.6\%$$

Example 5.11 A cylindrical concrete tank, 40 m external diameter, is to be prestressed circumferentially by means of a high-strength steel wire (E_s = 210 kN/mm^2) jacked at four points, 90 degrees apart. If the minimum stress in the wires immediately after tensioning is to be 600 N/mm^2 and the coefficient of friction is 0.5, calculate

(a) the maximum stress to be applied to the wires at the jack, and
(b) the expected extension at the jack.

The prestressing force at the farther end, P_x is related to the force at the jacking end, P_o, by the expression.

Solution.

$$P_x = P_o e^{-\mu\alpha}$$

$$600 = P_o e^{-(0.5 \times \pi/2)} \text{ where } e = 2.7183$$

$$\therefore \qquad P_o = (600)(2.7183^{0.79}) = 1320 \text{ N/mm}^2$$

$$\text{Average stress in wire} = \left(\frac{1320 + 600}{2}\right) = 960 \text{ N/mm}^2$$

$$\text{Length of wires} = \left(\frac{\pi \times 40 \times 1000}{4}\right) = 10^4\, \pi \text{ mm}$$

$$\text{Extension at the jack} = \left(\frac{960}{210 \times 10^3} \times 10^4 \pi\right) = 144 \text{ mm.}$$

5.7 Loss due to Anchorage Slip

In most post-tensioning systems, when the cable is tensioned and the jack is released to transfer prestress to concrete, the friction wedges, employed to grip the wires, slip over a small distance before the wires are firmly housed between the wedges. The magnitude of slip depends upon the type of wedge and the stress in the wires. In systems where the tendons are looped around concrete anchorage blocks, as in the case of Leonhardt–Baur system, loss of stress may take place due to the wires biting into the anchorage. When anchor plates are employed, it may be necessary to allow for the small settlement of the plate into the end of the concrete member.

The loss during anchoring, which occurs with wedge-type grips, is normally allowed for on the site by over-extending the tendon in the prestressing operation by the amount of the draw-in before anchoring. However, this method is satisfactory, provided the momentary over-stress does not exceed the prescribed limits of 80–85 per cent of the ultimate tensile strength of the wire.

The magnitude of the loss of stress due to the slip in anchorage is computed as follows:

If Δ = slip of anchorage, mm
L = length of the cable, mm
A = cross-sectional area of the cable, mm^2
E_s = modulus of elasticity of steel, N/mm^2
P = prestressing force in the cable, N

then,

$$\left(\frac{PL}{AE_s}\right) = \Delta$$

$$\text{Loss of stress due to anchorage slip} = \left(\frac{P}{A}\right) = \left(\frac{E_s\Delta}{L}\right)$$

Since the loss of stress is caused by a definite total amount of shortening, the percentage loss is higher for short members than for long ones. With the long-line pretensioning system, the slip at the anchorage is normally very small in comparison with the length of the tensioned wire and hence is generally ignored. While prestressing a short member, due care should be taken to allow for the loss of stress due to anchorage slip, which forms a major portion of the total loss.

Example 5.12 A concrete beam is post-tensioned by a cable carrying an initial stress of 1000 N/mm^2. The slip at the jacking end was observed to be 5 mm. The modulus of elasticity of steel is 210 kN/mm^2. Estimate the percentage loss of stress due to anchorage slip if the length of the beam is (a) 30 m; and (b) 3 m.

Solution.

$$\text{Loss of stress due to anchorage slip} = \left(\frac{E_s\Delta}{L}\right)$$

(a) For a 30 m long beam, loss of stress $= \left[\frac{(210\times 10^3)(5)}{30\times 1000}\right] = 35\ N/mm^2$

$$\therefore \quad \text{Percentage loss stress} = \left[\frac{35}{1000}\times 100\right] = 3.5\%$$

(b) For a 3 m long beam, loss of stress = $\left[\dfrac{(210\times10^3)(5)}{3\times1000}\right]$ = 350 N/mm^2

$\therefore$ Percentage loss of stress = $\left[\dfrac{350}{1000}\times100\right]$ = 35%

Example 5.13 A post-tensioned cable of beam 10 m long is initially tensioned to a stress of 1000 N/mm^2 at one end. If the tendons are curved so that the slope is 1 in 24 at each end, with an area of 600 mm^2, calculate the loss of prestress due to friction given the following data:

Coefficient of friction between duct and cable = 0.55; friction coefficient for 'wave' effect = 0.0015 per m. During anchoring, if there is a slip of 3 mm at the jacking end, calculate the final force in the cable and the percentage loss of prestress due to friction and slip. E_s = 210 kN/mm^2.

Solution.

Total change of slope from end to end, $\alpha = \left(\dfrac{2\times1}{24}\right) = \left(\dfrac{1}{12}\right)$

$$\mu\alpha = (0.55\times1/12) = 0.046$$

$$Kx = (0.0015\times10) = 0.015$$

If P_o = prestress at the tensioning or jacking end,

loss of prestress due to friction $= P_o(\mu\alpha + Kx)$

$= 1000(0.046 + 0.015) = 61$ N/mm^2

Slip at the jacking end = 3 $= \left(\dfrac{PL}{AE}\right)$

where P = force in the cable corresponding to the slip

$$\therefore \qquad P = \left(\frac{3\times210\times10^3\times600}{10\times1000}\right) = 37800 \text{ N} = 37.8 \text{ kN}$$

Loss of force due to friction = (600 × 61) = 36600 N = 36.6 kN

Total loss of force due to friction and slip = (36.6 + 37.8) = 74.4 kN

Final force in the cable = (600 – 74.4) = 525.6 kN

Percentage loss of prestress = $\dfrac{74.4}{600}\times100$ = 12.4%

5.8 Total Losses Allowed for in Design

It is normal practise in the design of prestressed concrete members to assume the total loss of stress as a percentage of the initial stress and provide for this in the design computations. Since the loss of prestress depends on several factors, such as the properties of concrete and steel, method of curing, degrees of prestress and the method of prestressing, it is difficult to generalise the exact amount of the total loss of prestress. However, typical values of the total losses of stress that could be encountered under normal conditions of work as recommended by Lin[11] are outlined as follows:

Type of Loss	*Percentage Loss of Stress*	
	Pretensioning	*Post-tensioning*
1. Elastic shortening and bending of concrete	4	1
2. Creep of concrete	6	5
3. Shrinkage of concrete	7	6
4. Creep in steel	8	8
Total	25	20

In these recommendations, it is assumed that temporary overstressing is done to reduce relaxation, and to compensate for friction and anchorage losses.

If f_{pe} = effective stress in tendons after losses

f_{pi} = stress in tendons at transfer

η = reduction factor for loss of prestress

$$\eta = \left(\frac{f_{pe}}{f_{pi}}\right)$$

The value of η is generally taken as 0.75 for pretensioning and 0.80 for post-tensioned members.

An exhaustive treatment of the losses in prestress due to creep, shrinkage and relaxation is presented by Neville[12] by considering the various influencing parameters, such as the modular ratio, creep coefficient at infinite time, ultimate shrinkage, relaxation coefficient, initial stress in concrete at the level of tendons and the intrinsic relaxation stress. Long-term field studies on the loss of prestress in post-tensioned concrete bridge girders have been carried out by Marks and Keifer[13] in which the measured creep and shrinkage losses in the girders were found to be maximum at the level of tendons.

Example 5.14 A pretensioned beam, 200 mm wide and 300 mm deep, is prestressed by 10 wires of 7 mm diameter initially stressed to 1200 N/mm^2, with their centroids located 100 mm from the soffit. Find the maximum stress in concrete immediately after transfer, allowing only for elastic shortening of concrete.

If the concrete undergoes a further shortening due to creep and shrinkage while there is a relaxation of five per cent of steel stress, estimate the final percentage loss of stress in the wires using the Indian Standard Code IS: 1343 regulations, and the following data:

$$E_s = 210 \text{ kN/mm}^2$$
$$E_c = 5700\,(f_{cu})^{1/2}$$
$$f_{cu} = 42 \text{ N/mm}^2$$

Creep coefficient $(\phi) = 1.6$

Total residual shrinkage strain $= (3 \times 10^4)$

Solution.

$$A_c = (6 \times 10^4) \text{ mm}^2$$
$$E_c = 5700(42)^{1/2} = 36900 \text{ N/mm}^2$$
$$I = 45 \times 10^7 \text{ mm}^4$$
$$\alpha_e = (E_s/E_c) = 5.7$$
$$P = (1200)(10 \times 38.5) = (462 \times 10^3) \text{ N} = 462 \text{ kN}$$

Stress in concrete at the level of steel is given by

$$f_c = \left[\frac{462 \times 10^3}{6 \times 10^4} + \frac{(462 \times 10^3 \times 50)50}{45 \times 10^7}\right] = 10.3 \text{ N/mm}^2$$

Loss of stress due to elastic deformation of concrete

$$= (5.7 \times 10.3) = 58.8 \text{ N/mm}^2$$

Force in wires immediately after transfer $= (1200 - 58.8)\ 38.5$

$$= 440\,000 \text{ N} = 440 \text{ kN}$$

Stress in concrete at the level of steel is given by

$$f_c = \left[\frac{440 \times 10^3}{6 \times 10^4} + \frac{(440 \times 10^3 \times 50)50}{45 \times 10^7}\right] = 978 \text{ N/mm}^2$$

Type of losses of prestress

1. Elastic deformation $= 58.8 \text{ N/mm}^2$
2. Creep of concrete $= (1.6 \times 9.78 \times 5.7)$ $= 89.2 \text{ N/mm}^2$
3. Shrinkage of concrete $= (3 \times 10^{-4})\ (210 \times 10^3)$ $= 63.0 \text{ N/mm}^2$
4. Relaxation of steel stress $= (5/100)\ 1200$ $= 60.0 \text{ N/mm}^2$

Total loss $= 271.0 \text{ N/mm}^2$

Final stress in wires $= (1200 - 271.0)$ $= 929.0 \text{ N/mm}^2$

Percentage loss $= \left(\dfrac{271.0}{1200} \times 100\right)$ $= 22.58\%$

Example 5.15 A prestressed concrete pile, 250 mm square, contains 60 pretensioned wires, each of 2 mm diameter, uniformly distributed over the section. The wires are initially tensioned on the prestressing bed with a total force of 300 kN. Calculate the final stress in concrete and the percentage loss of stress is steel after all losses, given the following data:

Solution.

$$E_s = 210 \text{ kN/mm}^2$$
$$E_c = 32 \text{ kN/mm}^2$$

Shortening due to creep = 30×10^{-6} mm/mm per N/mm^2 of stress
Total shrinkage = 200×10^{-6} per unit length
Relaxation of steel stress = 5 per cent of initial stress
Prestressing force, P = 300 kN, Area of steel wires = A_s = 188.4 mm^2

$$\text{Average initial stress in concrete} = \left(\frac{300 \times 10^3}{250 \times 250}\right) = 4.8 \text{ N/mm}^2$$

$$\text{Modular ratio, } \alpha = \left(\frac{E_s}{E_c}\right) = 6.58$$

$$\text{Initial stress in steel wires} = \left(\frac{300 \times 10^3}{188.4}\right) = 1590 \text{ N/mm}^2$$

Losses of stress

1.	Elastic deformation = (6.58×4.8)	= 31.5 N/mm^2
2.	Creep of concrete = $(30 \times 10^{-6})\ 4.8 \times 210 \times 10^3$	= 30 N/mm^2
3.	Shrinkage of concrete = $(200 \times 10^{-6})\ 210 \times 10^3$	= 42 N/mm^2
4.	Relaxation of steel stress = $(5/100 \times 1590)$	= 79.5 N/mm^2
	Total loss	= 183 N/mm^2

Effective prestress = (1590 – 183) = 1407 N/mm^2

$$\text{Final stress in concrete} = \left[\frac{(1407)(1884)}{250 \times 250}\right] = 4.26 \text{ N/mm}^2$$

$$\text{Percentage loss of stress in steel} = \left(\frac{183}{1590} \times 100\right) = 11.6\%$$

Example 5.16 A prestressed concrete beam, 200 mm wide and 300 mm deep, is prestressed with wires (area = 320 mm^2) located at a constant eccentricity of 50 mm and carrying an initial stress of 1000 N/mm^2. The span of the beam is 10 m. Calculate the percentage loss of stress in wires if (a) the beam is pretensioned, and (b) the beam is post-tensioned, using the following data:

Solution.

E_s = 210 kN/mm^2 and E_c = 35 kN/mm^2
Relaxation of steel stress = 5 per cent of the initial stress
Shrinkage of concrete = 300×10^{-6} for pretensioning and 200×10^{-6} for post-tensioning.
Creep coefficient = 1.6
Slip at anchorage = 1 mm

Frictional coefficient for wave effect = 0.0015 per m

$$\text{Prestressing force} = \left[\frac{(320 \times 1000)}{1000}\right] = 320 \text{ kN}$$

$$\text{Cross-sectional area, } A = (6 \times 10^4) \text{ mm}^2$$

$$\text{Modular ratio} = \alpha_e = \left(\frac{210}{35}\right) = 6$$

$$I = \left[\frac{(200 \times 300^3)}{12}\right] = (45 \times 10^7) \text{ mm}^4$$

Stress in concrete at the level of steel

$$= \left[\frac{(320 \times 10^3)}{(6 \times 10^4)} + \frac{(320 \times 10^3 \times 50 \times 50)}{(45 \times 10^7)}\right] = 7 \text{ N/mm}^2$$

The various losses are compiled in the tabular statement as follows:

Losses of Stress

Type of Loss	*Pretensioned Beam* (N/mm^2)	*Post-tensioned Beam* (N/mm^2)
1. Elastic deformation of concrete	$(6 \times 7) = 42.00$	—
2. Relaxation of stress in steel	5% of 1000 = 50.00	5% of 1000 = 50.00
3. Creep of concrete	$(1.6 \times 7 \times 6) = 67.20$	$(1.6 \times 7 \times 6) = 67.20$
4. Shrinkage of concrete	$(300 \times 10^{-6} \times 210 \times 10^3)$ $= 63.00$	$(200 \times 10^{-6} \times 210 \times 10^3)$ $= 21.00$
5. Slip at anchorage	—	$(1 \times 210 \times 10^3) / (10 \times 1000)$ $= 21.00$
6. Friction effect	—	$(1000 \times 0.0015 \times 10)$ 15.00
7. Total loss of stress	222.20	195.20
8. Percentage loss of stress	22.2%	19.52%

Example 5.17 A concrete beam *AB* of span 12 m is post-tensioned by a cable which is concentric at supports *A* and *B* and has an eccentricity of 200 mm in the mid-third span with a linear variation towards the supports. If the cable is tensioned at the jacking-end *A*, what should be the jacking stress in the wires if the stress at *B* is to be 1000 N/mm^2. Assume the coefficient of friction between the cable duct and concrete as 0.55 and the friction coefficient for the wave effect as 0.0015/m.

Solution.

$$\text{Slope of cable at } A = \left(\frac{200}{4000}\right) = 0.05$$

Total change of slope of cable from A to $B = \alpha = (2 \times 0.05)$

$$= 0.10$$

If P_o is the stress in the wires at jacking at end A, the loss of stress in the wires from A to B is

$$= P_o(\mu\alpha + Kx)$$

$$= P_o(0.55 \times 0.10 + 0.0015 \times 12)$$

$$= 0.073\ P_o$$

If P_x is the stress in wires at support B, then we have

$$P_x = P_o[1 - (\mu\alpha + Kx)]$$

$$\therefore \quad 1000 = P_o(1 - 0.073) = 0.927\ P_o$$

Hence, the jacking stress at $A = P_o = \left(\dfrac{1000}{0.927}\right) = 1078.7\ \text{N/mm}^2$.

Example 5.18 A concrete beam AB of 20 m span is post-tensioned by a cable carrying a stress of 1000 N/mm^2 at the jacking end A. The cable is parabolic between the supports A and B and is concentric at the supports with an eccentricity of 400 mm at the centre of span. The coefficient of friction between duct and cable as 0.35 and friction coefficient for wave effect is 0.15 for 100 m. Calculate the stress allowing for losses due to friction and wave effect at the following points:

(a) Assuming the jacking end as A, compute the effective stress at B
(b) If the cable is tensioned from both ends A and B, calculate the minimum stress after losses in the cable and its location.

Solution.

Span of the beam $AB = L = 20$ m
Eccentricity at centre of span $= e = 400$ mm
Coefficient of friction $= \mu = 0.35$
Friction coefficient for wave effect $= K = 0.15$ for 100 m or 0.0015/m
The cable is parabolic between the supports A and B with an eccentricity of 40 mm at the centre of span C.

Slope of cable at end support $A = \left[\dfrac{4e}{L}\right] = \left[\dfrac{4 \times 400}{20 \times 1000}\right] = 0.08$

Cumulative angle between tangents at A and $B = \alpha = (2 \times 0.08) = 0.16$ radians
Loss of stress due to friction $= P_o[\mu\alpha + Kx]$
where x = distance from the jacking end to the point under consideration.

(a) Loss of stress between A and B ($x = L = 20$ m) $= 1000\ [(0.35 \times 0.16) + (0.015 \times 20)] = 59\ \text{N/mm}^2$

Effective stress at $B = [1000 - 59] = 941\ \text{N/mm}^2$

(b) If the cable is tensioned simultaneously from both ends A and B, the minimum stress will occur at the centre of span C.

Cumulative angle between A and $C = \alpha = (2 \times 0.04) = 0.08$ radians

Loss of stress between A and $C(x = 0.5\ L = 10\ \text{m})$

$$= 1000[(0.35 \times 0.08) + (0.0015 \times 10)] = 43\ \text{N/mm}^2$$

Effective stress at the centre of span $C = [1000 - 43] = 953\ \text{N/mm}^2$

References

1. Leonhardt, F, *Prestressed Concrete, Design and Construction*, Wilhelm Ernst and Sohn, Berlin, 2nd edn., 1964, p 59.
2. Walley, F and SCC, Bate, *A Guide to the BS Code of Practice for Prestressed Concrete*, Concrete Publications, London, 1966, p 29.
3. Guyon, Y, *Prestressed Concrete*, C.R. Books Ltd., London, 1953, p 86.
4. Cooley, E H, “Friction in post-tensioned prestressing systems,” *Research Report No.1*, Cement and Concrete Association, London, 1953.
5. Leonhardt, F, *Prestressed Concrete*, *Design and Construction*, Wilhelm Ernst and Sohn, Berlin, 2nd edn., 1964, p 223.
6. Foppl, A, *Reiburg in Bruckengelenken*, Zentralblatt der Bauverwaltung, 1901, p. 197.
7. Morsch, E, “Uber die Berchungder Gelenkquader,” *Beton u. Eisen* 23, Heft-12, 1924, pp 56–161.
8. Morice, P B and E H Cooley, *Prestressed Concrete*, *Theory and Practice*, Pitman, London, 1958, pp 257–281.
9. Prestressed Concrete Institute, PCI Design Handbook, Chicago, 1985.
10. Nawy Edward, G, *Prestressed Concrete*, *A Fundamental Approach*, Prentice-Hall International, Englewood Cliffs, New Jersey, 1989, pp 65–95.
11. Lin, T Y and H Burns Ned, *Design of Prestressed Concrete Structures*, 3rd edn, John Wiley and Sons, New York, 1982, pp 115–121.
12. Neville, A M, *Creep of Concrete, Plain, Reinforced and Prestressed*, North Holland Publications, Amsterdam, 1970, pp 533–557.
13. Marks, J D and O Keifer, “Long term field study of stresses in a post-tensioned concrete girder bridge,” *First Internationally Symposium on Concrete Bridge Design*, ACI. Publication SP–23, 1969 pp 631–654.

Review Questions

5.1 List the various types of loss of prestress in pretensioned and post-tensioned members.

5.2 How do you compute the loss of stress due to elastic deformation of concrete?

5.3 “Post-tensioned members do not suffer the loss of prestress due to elastic deformation”. Why?

5.4 How do you compute the loss of stress due to elastic deformation of concrete in post-tensioned members with several cables which are successively tensioned?

5.5 How do you compute the loss of stress due to shrinkage of concrete as per IS:1343 code recommendations?

5.6 "The Indian Standard Code IS: 1343 specifies different strains for pretensioned and post-tensioned members". Explain with reasons.

5.7 What are the factors influencing the loss of stress due to creep of concrete?

5.8 What is relaxation of stress in steel? How do you account for it in prestressed members? Explain the provisions made in IS: 1343 for relaxation loss.

5.9 How do you compute the loss of stress in steel due to curvature and wobble effect?

5.10 What is anchorage slip? How do you compute the loss of stress due to anchorage slip?

Exercises

5.1 A pretensioned beam of rectangular cross-section, 150 mm wide and 300 mm deep, is prestressed by eight, 7 mm wires located 100 mm from the soffit of the beam. If the wires are initially tensioned to a stress of 1100 N/mm^2, calculate their stress at transfer and the effective stress after all losses, given the following data:

	Up to time of transfer	*Total*
Relaxation of steel	35 N/mm^2	70 N/mm^2
Shrinkage of concrete	100×10^{-6}	300×10^{-6}
Creep coefficient	—	1.6
E_s = 210 kN/mm^2,	E_c = 31.5 kN/mm^2	

[Ans: 977.5 N/mm^2, 793.6 N/mm^2]

5.2 A prestressed concrete pile of cross-section, 250 mm by 250 mm, contains 60 pretensioned wires, each of 2 mm diameter, distributed uniformly over the section. The wires are initially tensioned on the prestressing bed with a total force of 300 kN. If E_s = 210 kN/mm^2 and E_c = 32 kN/mm^2, calculate the respective stresses in steel and concrete immediately after the transfer of prestress, assuming that up to this point the only loss of stress is that due to elastic shortening.

If the concrete undergoes a further shortening due to shrinkage of 200×10^{-6} per unit length, while there is a relaxation of five per cent of steel stress due to creep of steel, find the greatest tensile stress which can occur in a pile 20 m long when lifted at two points 4 m from each end. Assume creep coefficient as 1.6.

[Ans: 1389.3 N/mm^2, 4.7 N/mm^2, –0.42 N/mm^2]

5.3 A post-tensioned cable of a beam 10 m long is initially tensioned to a stress of 1000 N/mm^2 at one end. If the tendons are curved so that the slope is 1 in 15 at each end with an area of 600 mm^2, calculate the loss of prestress due to friction, given the following data:

Coefficient of friction between duct and cable = 0.55

Friction coefficient for wave effect = 0.0015/m

During anchoring, if there is a slip of 3 mm at the jacking end, calculate the final force in the cable and the percentage loss of prestress due to friction and slip.

[Ans: 526.6 kN; 12.3 per cent]

5.4 A post-tensioned concrete beam with a cable of 24 parallel wires (total area = 800 mm^2) is tensioned with two wires at a time. The cable with zero eccentricity at the ends and 150 mm at the centre is on a circular curve. The span of the beam is 10 m. The cross-section is 200 mm wide and 450 mm deep. The wires are to be stressed from one end to a value of f_1 to overcome frictional loss and then released to a value of f_2 so that immediately after anchoring, an initial prestress of 840 N/mm^2 would be obtained. Compute f_1 and f_2 and the final design stress in steel after all losses, given the following data:

Coefficient of friction for curvature effect = 0.6

Friction coefficient for 'wave' effect = 0.003/m

Deformation and slip of anchorage = 1.25 mm

E_s = 210 kN/mm^2 E_c = 28 kN/mm^2

Shrinkage of concrete = 0.0002

Relaxation of steel stress = 3 per cent of the initial stress

[Ans: f_1 = 954 N/mm^2; f_2 = 866.2 N/mm^2; 668.4 N/mm^2]

5.5 A pretensioned beam 250 mm wide and 300 mm deep is prestressed by 12 wires each of 7 mm diameter initially stressed to 1200 N/mm^2 with their centroids located 100 mm from the soffit. Estimate the final percentage loss of stress due to elastic deformation, creep, shrinkage and relaxation using IS: 1343–80 code and the following data:

Relaxation of steel stress = 90 N/mm^2

E_s = 210 kN/mm^2 E_c = 35 kN/mm^2

Creep coefficient (ϕ) = 1.6

Residual shrinkage strain = 3×10^{-4}

[Ans: 22%]

5.6 In a post-tensioned beam of length 12 m, a cable is laid symmetrically, with its central 6 m length horizontal and the two straight end-portions sloping up at an angle with the horizontal whose tangent is equal to 0.075. The cable is tensioned by jacking at one end and is anchored at the remote end of the beam. At the jacking end the measured stress is 1040 N/mm^2. The 'wobble' coefficient K may be assumed as 0.004/m. Calculate the stress in the cable at the remote end and at the two points where the alignment of the cable changes. Assume the coefficient of friction between cable and duct as 0.40. What is the percentage loss of prestress between the jacking end and the anchored end?

[Ans: Stress at first kink = 996 N/mm^2
Stress at second kink = 972 N/mm^2
Stress at anchored end = 928 N/mm^2
Percentage loss = 10.8%]

5.7 A post-tensioned prestressed beam of span-length of 10 m has a rectangular section 300 mm wide 800 mm deep. The beam is prestressed by a parabolic cable concentric at the supports and with an eccentricity of 250 mm at the centre of span. The cross-sectional area of high-tensile wires in the cable is 500 mm^2. The wires are stressed by using a jack at the left end so that the initial force in the cable at the right end is 250 kN. Using the following data, calculate (a) the total loss of stress in the wires, (b) The jacking force required at the left end:

Coefficient of friction for curvature effect = 0.55

Friction coefficient for wave effect = 0.003/m

Anchorage slip at the jacking end = 3 mm
Relaxation of steel stress = four per cent
Shrinkage of concrete = 0.0002
Creep coefficient = 2.2
Modulus of elasticity of steel = 210 kN/mm^2

[Ans: (a) 212 N/mm^2, (b) 285 kN]

5.8 A pretensioned prestressed concrete sleeper 300 mm wide by 250 mm deep is prestressed using nine wires of 7 mm diameter. Four wires are located at top and five wires near the soffit. The effective cover being 40 mm. The initial stress in the wires is 1256 N/mm^2. Assuming the modular ratio as 6, estimate the percentage loss of stress in the top and bottom wires due to elastic deformation of concrete.

[Ans: Top wires: 2.34 per cent, Bottom wires: 3.19 per cent]

5.9 A prestressed concrete girder is post-tensioned using a cable concentric at supports and having an eccentricity of 400 mm at the centre of span. The effective span of the girder is 25 m. The initial force in the cable is 400 kN at the jacking end A. Determine the loss of force in the cable due to friction and wave effect and the effective force in the cable at the farther end B. Assume coefficient of friction $\mu = 0.30$ and coefficient for Wave effect $K = 0.0043$/m.

[Ans: Loss of prestressing force = 28 kN:
Prestressing force at B = 372 kN]

5.10 A cylindrical water tank having an external diameter of 50 m is to be prestressed circumferentially by means of high tensile wire cables jacked at four points, 90 degrees apart. If the minimum stress in the cable wires immediately after tensioning is 500 N/mm^2 and the coefficient of friction is 0.5, estimate (a) the maximum stress to be applied to the wires at the jacking end, (b) the expected extension at the jack.

Assume the modulus of elasticity of steel as 210 kN/mm^2.

[Ans: Stress in wires at jacking end = 1102 N/mm^2;
Extension at the jacking end = 149.7 mm]

Objective-type Questions

5.1 In a pretensioned beam, there will be loss of stress due to
(a) friction
(b) anchorage slip
(c) elastic deformation of concrete

5.2 In a post-tensioned beam there will be loss of stress due to
(a) elastic deformation of concrete
(b) shrinkage of concrete
(c) friction

5.3 Loss of stress due to elastic deformation of concrete depends upon
(a) relaxation of steel
(b) friction and anchorage slip
(c) modular ratio

5.4 Loss of prestress due to shrinkage of concrete depends upon
  (a) modulus of elasticity of concrete
  (b) stress in concrete at level of steel
  (c) shrinkage strain

5.5 Loss of stress due to creep of concrete is influenced by
  (a) friction (b) creep coefficient (c) anchorage slip

5.6 Loss of stress in steel due to creep of concrete is proportional to
  (a) the elastic deformation of concrete
  (b) anchorage slip
  (c) modulus of elasticity of steel

5.7 Loss of stress due to relaxation of steel is influenced by
  (a) shrinkage of concrete
  (b) friction between steel and concrete
  (c) initial stress in steel

5.8 Loss of stress due to friction depends upon
  (a) modulus of elasticity of concrete
  (b) coefficient of friction
  (c) relaxation of steel

5.9 The loss of stress due to creep in a prestressed concrete beam is influenced by
  (a) span of the member
  (b) notional size of the member
  (c) ultimate tensile strength of tendons

5.10 The loss of stress due to friction is maximum in the case of
  (a) linear members
  (b) circular members
  (c) inclined members

Answers to Objective-type Questions

5.1 (c)	5.2 (b)	5.3 (c)	5.4 (c)	5.5 (b)
5.6 (c)	5.7 (c)	5.8 (b)	5.9 (b)	5.10 (b)

6 Deflections of Prestressed Concrete Members

6.1 Importance of Control of Deflections

The philosophy of design, termed "limit state approach," adopted by the Russian code in 1954 and the American and British codes in 1971, requires a proper knowledge of the behaviour of structural concrete members at the multiple limit states, of which deflection forms an important criterion for the safety of the structure. It is the general practise, according to various national codes, that structural concrete members should be designed to have adequate stiffness to limit deflections, which may adversely affect the strength or serviceability of the structure at working loads.

Suitable control on deflectional[1] is very essential for the following reasons:

1. Excessive sagging of principal structural members is not only unsightly, but at times, also renders the floor unsuitable for the intended use.
2. Large deflections under dynamic effects and under the influence of variable loads may cause discomfort to the users.
3. Excessive deflections are likely to cause damage to finishes, partitions and associated structures.

In recent years, damage to partitions and finishes has been the most important consequence of excessive deflections. A field survey conducted by Mayer[2] in Germany, revealed over 80 examples of damage to partition walls, of which 21 had estimated deflections within the prescribed code-limits. The survey also indicated that a maximum limit on deflection should be specified in addition to a limiting deflection–span ratio, since it was recognised that as the span increases, the former limitation is likely to control. For a reasonably accurate assessment of deflections, it is very essential to consider the various factors which influence them.

6.2 Factors Influencing Deflections

The deflections of prestressed concrete members are influenced by the following salient factors:

1. Imposed load and self-weight
2. Magnitude of the prestressing force

3. Cable profile
4. Second moment of area of cross-section
5. Modulus of elasticity of concrete
6. Shrinkage, creep and relaxation of steel stress
7. Span of the member
8. Fixity conditions

In the precracking stage, the whole cross-section is effective and the deflections in this stage are computed by using the second moment of area of the gross concrete section. The computation of short-term or instantaneous deflections, which occur immediately after transfer of prestress and on application of loads, is conveniently done by using Mohr's theorems.

In the post-cracking stage, a prestressed concrete beam behaves in a manner similar to that of a reinforced concrete beam and the computation of deflections at this stage is made by considering moment–curvature relationships which involve the section properties of the cracked beam.

In both cases, the effect of creep and shrinkage of concrete is to increase the long-term deflections under sustained loads, which is estimated by using empirical methods that involve the use of effective (long-term) modulus of elasticity or by multiplying short-term deflections by suitable factors.

6.3 Short-term Deflections of Uncracked Members

6.3.1 Mohr's Theorems

Short-term or instantaneous deflections of prestressed members are governed by the bending moment distribution along the span and the flexural rigidity of the members. Mohr's moment area theorems[3] are readily applicable for the estimation of deflections due to the prestressing force, self-weight and imposed loads. Consider Fig. 6.1 in which the beam *AB* is subjected to a bending moment distribution due to the prestressing force or self-weight or imposed loads. *ACB* is the centre line of the deformed structure under the system of given loads.

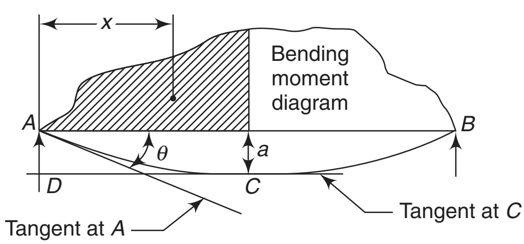

Fig. 6.1 *Slope and deflection of beam*

If θ = slope of the elastic curve at A

AD = intercept between the tangent at C and the vertical at A

a = deflection at the centre for symmetrically loaded, simply supported beam (since the tangent is horizontal for such cases)

A = area of the BMD between A and C

x = distance of the centroid of the BMD between A and C from the left support

EI = flexural rigidity of the beam

then, according to Mohr's first theorem,

$$\text{Slope} = \frac{\text{area of BMD}}{\text{flexural rigidity}}$$

$$\theta = \frac{A}{EI}$$

Mohr's second theorem states that

$$\text{Intercept, } a = \left(\frac{\text{moment of the area of B.M.D}}{\text{flexural rigidity}}\right)$$

$$= \left(\frac{Ax}{EI}\right)$$

The deflection of symmetrically loaded and simply supported beams at the mid-span point are directly obtained from the second moment area theorem since the tangent is horizontal at this point. More complicated problems involving unsymmetrical loading may be solved by combining both the moment area theorems.

6.3.2 Effect of Tendon Profile on Deflections

In most of the cases of prestressed beams, tendons are located with eccentricities towards the soffit of beams to counteract the sagging bending moments due to transverse loads. Consequently, the concrete beams deflect upwards (camber) on the application or transfer of prestress. Since the bending moment at every section is the product of the prestressing force and eccentricity, the tendon profile itself will represent the shape of the BMD. The method of computing deflections of beams with different cable profiles is outlined as follows:

Straight Tendons Figure 6.2 shows a beam with a straight tendon at a uniform eccentricity below the centroidal axis.

If upward deflections are considered as negative and

P = effective prestressing force

e = eccentricity

L = length of the beam

$$a = -\frac{(PeL)(L/4)}{EI} = -\frac{PeL^2}{8EI}$$

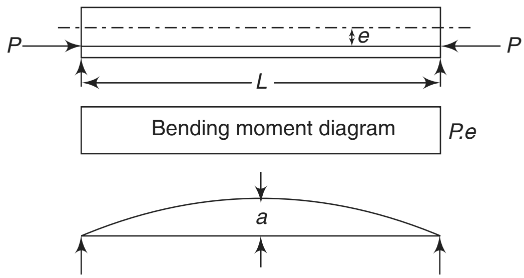

Fig. 6.2 *Camber of beam with straight tendons*

Trapezoidal Tendons A draped tendon with a trapezoidal profile is shown in Fig. 6.3. Considering the BMD, the deflection at the centre of the beam is obtained by taking the moment of area of the BMD over one-half of the span. Thus,

$$a = -\frac{Pe}{EI}[l_2(l_1 + l_2/2) + (l_1/2)(2/3l_1)] = -\frac{Pe}{6EI}[2l_1^2 + 6l_1l_2 + 3l_2^2]$$

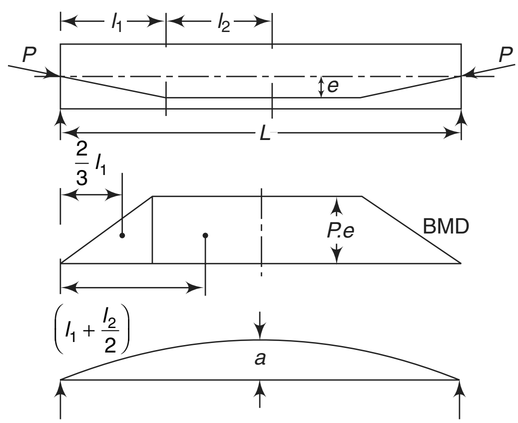

Fig. 6.3 *Trapezoidal or draped tendons*

Parabolic Tendons (Central Anchors) The deflection of a beam with parabolic tendons (Fig. 6.4) having an eccentricity e at the centre and zero at the supports is given by,

$$a = -\frac{Pe}{EI}\left[\frac{2}{3},\frac{L}{2},\frac{5}{8},\frac{L}{2}\right] = -\left(\frac{5\,PeL^2}{48\,EI}\right)$$

Parabolic Tendons (Eccentric Anchors) Figure 6.5 shows a beam with a parabolic tendon having an eccentricity e_1 at the centre of span and e_2 at the support sections. The resultant deflection at the centre is obtained as the sum of the upward deflection of a beam with a parabolic tendon of eccentricity $(e_1 + e_2)$ at the centre and zero at the supports and the downward deflection of a beam subjected to a uniform sagging bending moment of intensity Pe_2 throughout the length. Consequently, the resultant deflection becomes,

$$a = \left[\frac{-5}{48}\frac{PL^2}{EI}(e_1 + e_2)\right] + \left[\frac{Pe_2 L^2}{8EI}\right]$$

$$a = \frac{PL^2}{48\,EI}(-5e_1 + e_2)$$

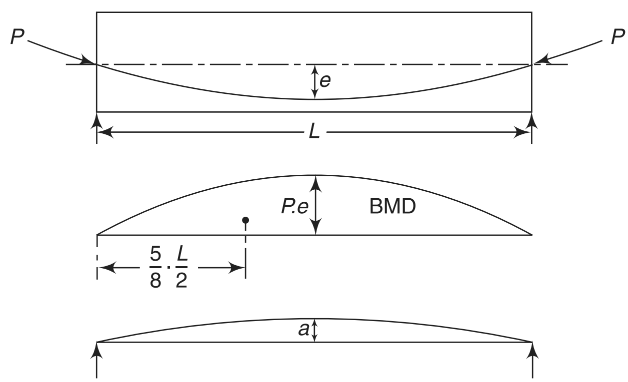

Fig. 6.4 *Parabolic tendons (Central anchors)*

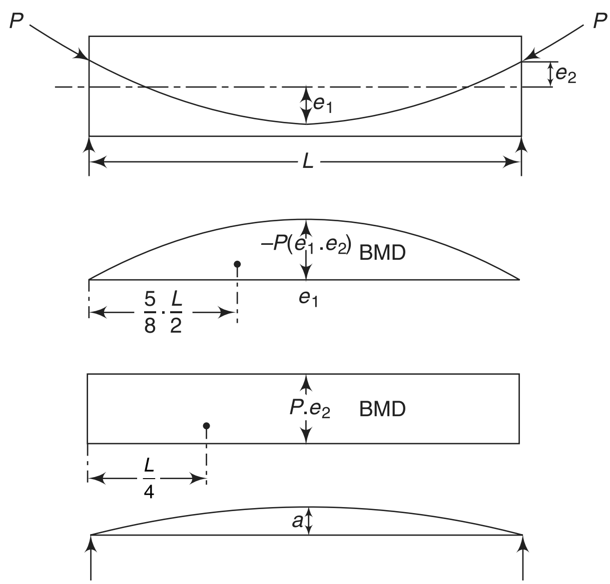

Fig. 6.5 *Parabolic tendons (Eccentric anchors)*

Sloping Tendons (Eccentric Anchors) From Fig. 6.6, the deflection is computed in a way similar to method 4 described earlier. Thus,

$$a = \left[-\frac{PL^2}{12\,EI}(e_1 + e_2)\right] + \left[\frac{Pe_2L^2}{8\,EI}\right] = \frac{PL^2}{24\,EI}(-2e_1 + e_2)$$

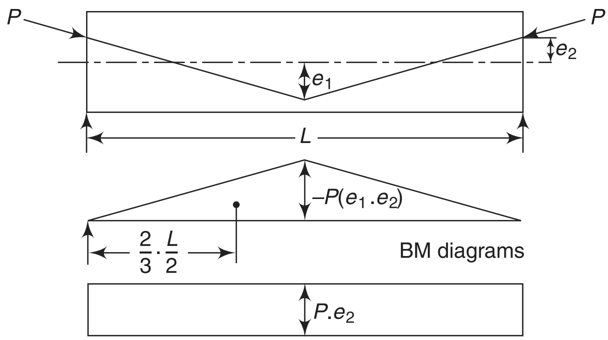

Fig. 6.6 *Sloping tendons*

Parabolic and Straight Tendons Referring to Fig. 6.7, the deflection at the centre of the beam is obtained as,

$$a = -\frac{Pe}{EI}\ [(2/3)l_1\ (5/8)l_1 + l_2(l_1 + l_2/2)]$$

$$a = -\frac{Pe}{EI}[(5l_1^2 + 12l_1l_2 + 6l_2^2)]$$

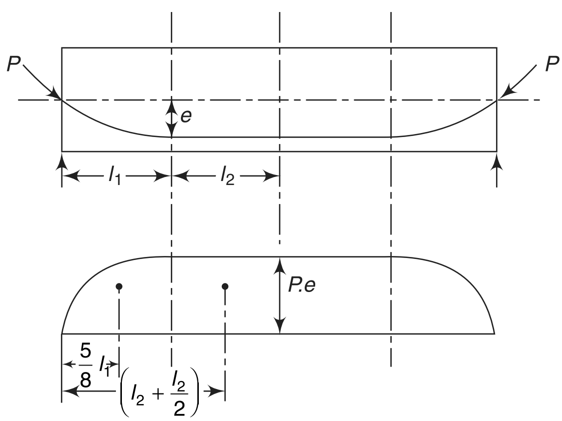

Fig. 6.7 *Parabolic and straight tendons*

Parabolic and Straight Tendons (Eccentric Anchors) The maximum central deflection is obtained by superposition as in method 4. From Fig. 6.8, it is seen that,

$$a = -\frac{P(e_1+e_2)}{12EI}[5l_1^2 + 12l_1l_2 + 6l_2^2] + \left[\frac{Pe_2L^2}{8EI}\right]$$

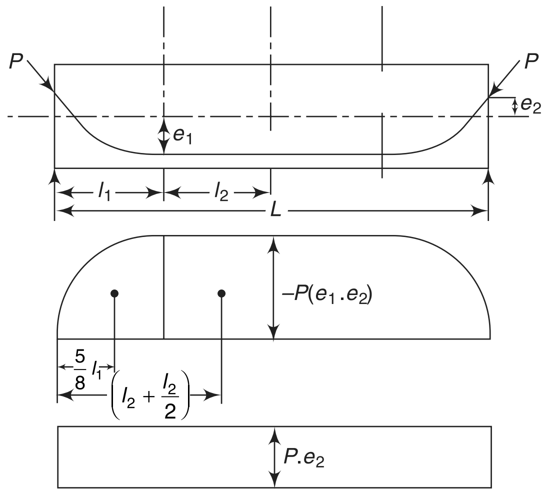

Fig. 6.8 *Parabolic and straight tendons (Eccentric anchors)*

6.3.3 Deflections due to Self-Weight and Imposed Loads

At the time of transfer of prestress, the beam hogs up due to the effect of prestressing. At this stage, the self-weight of the beam induces downward deflections, which further increase due to the effect of imposed loads on the beam.

If g = self-weight of the beam/m

q = imposed load/m (uniformly distributed),

the downward deflection is computed as,

$$a = \frac{5(g+q)L^4}{384EI}$$

Deflections due to concentrated live loads can be directly computed by using Mohr's theorems.

Example 6.1 The deck of a prestressed concrete culvert is made up of a slab 500 mm thick. The slab is spanning over 10.4 m and supports a total uniformly distributed load comprising the dead and live loads of 23.5 kN/m^2. The modulus of elasticity of concrete is 38 kN/mm^2. The concrete slab is prestressed by straight cables each containing 12 high-tensile wires of 7 mm diameter stressed to 1200 N/mm^2 at a constant eccentricity of 195 mm. The cables are spaced at 328 mm intervals in the transverse direction. Estimate the instantaneous deflection of the slab at centre of span under prestress and the imposed loads.

Solution.

Considering 1 m width of cable, the properties of the cross-section are computed.

Thickness of slab = d = 500 mm   Width of slab = b = 1000 mm

Span of the slab = L = 10.4 m

Second moment of area = $I = \left[\dfrac{bd^3}{12}\right] = \left[\dfrac{1000 \times 500^3}{12}\right] = (1041 \times 10^7)\text{mm}^4$

Force in each cable = $\left[\dfrac{12 \times 38.5 \times 1200}{1000}\right] = 554$ kN

Spacing of cables in the transverse direction = 328 mm

Hence, the prestressing force per metre width of slab is computed as,

$$P = \left[\frac{1000 \times 554}{328}\right] = 1689 \text{ kN} \qquad \text{Eccentricity} = e = 195 \text{ mm}$$

Total uniformly distributed load on the beam

$$= w = 33.5 \text{ kN/m} = 0.0335 \text{ kN/mm}$$

Deflection due to prestressing force = $a_p = \left[\dfrac{-PeL^2}{8EI}\right]$

$$= -\left[\frac{1689 \times 195 \times (10.4 \times 1000)^2}{8 \times 38 \times 1041 \times 10^7}\right]$$

$$= -11.25 \text{ mm (Upwards)}$$

Deflection due to loads = $a_w = \left[\dfrac{5wL^4}{384EI}\right] = \left[\dfrac{5 \times 0.0335 \times (10.4 \times 1000)^4}{384 \times 38 \times 1041 \times 10^7}\right]$

$$= 12.90 \text{ mm (downwards)}$$

Resultant deflection = (12.90 – 11.25) = 1.65 mm (downwards).

Example 6.2 A prestressed concrete beam of rectangular section 120 mm wide and 300 mm deep, spans over 6 m. The beam is prestressed by a straight cable carrying an effective force of 200 kN at an eccentricity of 50 mm. The modulus of elasticity of concrete is 38 kN/m^2. Compute the deflection at centre of span for the following cases:

(a) Deflection under (prestress + self-weight)

(b) Find the magnitude of the uniformly distributed live load which will nullify the deflection due to prestress and self-weight.

Solution.

$P = 200$ kN $I = (27 \times 10^7)$ mm^4

$g = 0.86$ N/mm $e = 50$ mm

$L = 6000$ mm $E = 38$ kN/mm^2

Deflection due to the prestressing force is computed as,

$$a_p = \left[\frac{-PeL^2}{8EI}\right] = -\left[\frac{200\times 50\times 6000^2}{8\times 38\times 27\times 10^7}\right] = -4.38 \text{ mm (upwards)}$$

Deflection due to self-weight of the beam is

$$a_g = \left[\frac{5gL^4}{384\,EI}\right] = -\left[\frac{5\times 0.86\times 6000^4}{384\times 38\times 10^3\times 27\times 10^7}\right] = 1.40 \text{ mm (downwards)}$$

(a) Deflection due to (prestress + self-weight) = [1.40 – 4.38] = –2.98 mm (upwards)

(b) If q = uniformly distributed live load on the beam which neutralises the deflection due to prestress and self-weight, its magnitude is calculated as,

$$a_v = \left[\frac{a\times 384\,EI}{5\times L^4}\right] = \left[\frac{2.98\times 384\times 38\times 10^3\times 27\times 10^7}{5\times 6000^4}\right] = 1.81\,\text{N/mm} = 1.81\,\text{kN/m.}$$

Example 6.3 A rectangular concrete beam of cross-section 150 mm wide and 300 mm deep, is simply supported over a span of 8 m and is prestressed by means of a symmetric parabolic cable, at a distance of 75 mm from the bottom of the beam at mid span and 125 mm from the top of the beam at support sections. If the force in the cable is 350 kN and the modulus of elasticity of concrete is 38 kN/mm^2, calculate

(a) The deflection at mid-span when the beam is supporting its own weight.

(b) The concentrated load which must be applied at mid-span to restore it to the level of supports.

Solution.

$P = 350$ kN, $E_c = 38$ kN/mm^2,

$I = 3375\times 10^5$ mm^4 $e_1 = 75$ mm, $e_2 = 25$ mm

Net deflection due to the prestressing force

$$= \frac{PL^2}{48EI}(-5e_1 + e_2) = \left(\frac{350\times 8000^2}{48\times 38\times 3375\times 10^5}\right)(-5\times 75 + 25)$$

$$= 12.7 \text{ mm (upwards)}$$

Self-weight of the beam, $g = (0.15\times 0.30\times 24) = 1.08$ kN/m

$= 0.00108$ kN/mm

$$\text{Downward deflection due to self-weight} = \left(\frac{5\times 0.00108\times 8000^4}{384\times 38\times 3375\times 10^5}\right) = 4.5 \text{ mm}$$

(a) Deflection due to (prestress + self-weight) = (–12.7 + 4.5) = –8.2 mm (upwards)

(b) If Q = concentrated load required at the centre of span,

Then, $$\left(\frac{QL^3}{48EI}\right) = 8.2$$

$$\therefore \qquad Q = \left(\frac{8.2 \times 48 \times 38 \times 3375 \times 10^5}{8000^3}\right) = 9.9 \text{ kN}$$

6.4 Prediction of Long-time Deflections

The deformations of prestressed members change with time as a result of creep and shrinkage of concrete and relaxation of stress in steel. The deflection of prestressed members can be computed relative to a given datum, if the magnitude and longitudinal distribution of curvatures for the beam span are known for that instant based on the load history, which includes the prestressing forces and the live loads.

The prestressed concrete member develops deformations under the influence of two usually opposing effects, which are the prestress and transverse loads. The net curvature ϕ_t at a section at any given stage is obtained.

$$\phi_t = \phi_{mt} + \phi_{pt}$$

where ϕ_{mt} = change of curvature caused by transverse loads

ϕ_{pt} = change of curvature caused by prestress

Under the section of sustained transverse loads, the compressive stress distribution in the concrete changes with time.

However, in practical cases, the change of stress being small, it may be assumed that the concrete creeps under constant stress. The creep strain due to transverse loads is directly computed as a function of the creep coefficient so that the change of curvature can be estimated by the expression,

$$\phi_{mt} = (1 + \phi)\phi_i$$

where ϕ = creep coefficient

ϕ_i = initial curvature immediately after the application of transverse loads

The change of curvature due to the sustained prestress (ϕ_{pt}) depends upon the cumulative effects of creep and shrinkage of concrete and relaxation of stress in steel. Several methods have been proposed to evaluate the curvature under simplified assumptions. The important ones are attributed to Busemann[4] McHenry, Douglas[5] and Corley, Sozen and Siess[6].

According to Neville[7] and the ACI committee report[8], the creep curvature due to prestress is obtained on the simplified assumption that creep is induced by the average prestress acting over the given time. Using this approach, if

P_i = initial prestress

P_t = prestress after a time, t

Loss of prestressing force due to relaxation, shrinkage and creep, $L_p = (P_i - P_t)$

e = eccentricity of the prestressing force at the section

EI = flexural rigidity

The curvature due to prestress after time t can be expressed as

$$\phi_{pt} = -\frac{P_i e}{EI}\left[1 - \frac{L_p}{P_i} + \left(1 - \frac{L_p}{2P_i}\right)\phi\right]$$

If a_{i1} = initial deflection due to transverse loads

a_{ip} = initial deflection due to prestress

then, the total long-time deflection after time t is obtained from the expression,

$$a_f = a_{i1}\,(1 + \phi) - a_{ip}\left[\left(1 - \frac{L_p}{P_i}\right) + \left(1 - \frac{L_p}{2P_i}\right)\phi\right]$$

In this expression, the negative sign refers to deflections in the upward direction (camber).

A much simplified but an approximate procedure is suggested by Lin[9] for computing long-time deflections. In this method, the initial deflection due to prestress and transverse loads is modified to account for the loss of prestress which tends to decrease the deflection, and the creep effect which tends to increase the deflection. The principle of reduced modulus involving the creep coefficient is used to amplify the initial deflections. According to this method, the final long-time deflection is expressed as,

$$a_f = \left[a_{il} - a_{ip} \times \frac{P_t}{P_i}\right](1 + \phi)$$

The use of the various methods discussed above is illustrated by the following examples.

Example 6.4 A post-tensioned roof girder spanning over 30 m has an unsymmetrical I-section with a second moment of area of section of (72490×10^6) mm^4 and an overall depth of 1300 mm. The effective eccentricity of the group of parabolic cables at the centre of span is 580 mm towards the soffit and 170 mm towards the top of beam at supports. The cables carry an initial prestressing force of 3200 kN.

The self-weight of the girder is 10.8 kN/m and the live load on the girder is 9 kN/m. The modulus of elasticity of concrete is 34 kN/mm^2. If the creep coefficient is 1.6, and the total loss of prestress is 15 per cent, estimate the deflections at the following stages and compare them with the permissible values according to the Indian Standard Code (IS: 1343) limits:

(a) Instantaneous deflection due to (prestress + self-weight).

(b) Resultant maximum long-term deflection allowing for loss of prestress and creep of concrete.

Solution.

$P = 3200$ kN $\quad I = (72490 \times 10^6)$ mm^4

$e_1 = 580$ mm $\quad e_2 = 170$ mm $\quad L = 30$ m

$E = 34$ kN/mm^2 $\quad$ Creep coefficient $= \varphi = 1.6$

$g = 10.8$ kN/m $= 0.0108$ kN/mm $\quad q = 9$ kN/m $= 0.009$ kN/mm

Loss ratio $= \eta = 0.85$

Deflection due to initial prestress $= a_p = \left[\dfrac{PL^2}{48\,EI}\right](-5e_1 + e_2)$

$$a_p = \left[\frac{3200 \times 10^3 \times 30000^2}{48 \times 38 \times 72490 \times 10^6}\right](-5 \times 580 + 170) = -74.7 \text{ mm (upwards)}$$

Deflection due to self-weight $= \left[\dfrac{5gL^4}{384\,EI}\right] = \left[\dfrac{5 \times 0.0108 \times 30000^4}{384 \times 34 \times 72490 \times 10^6}\right]$

$$= 46.2 \text{ mm (downwards)}$$

(a) Instantaneous deflection due to (prestress + self-weight) = (–74.7 + 46)

$$= -28.7 \text{ mm (upwards)}$$

Permissible upward deflection according to IS: 1343 $= \left[\dfrac{\text{span}}{300}\right] = \left[\dfrac{30000}{300}\right]$

$$= 100 \text{ mm}$$

Deflection due to live load $= \left[\dfrac{5qL^4}{384\,EI}\right] = \left[\dfrac{5 \times 0.009 \times 30000^4}{384 \times 38 \times 72490 \times 10^6}\right]$

$$= 38.5 \text{ mm (downwards)}$$

If creep coefficient $= \varphi = 1.6$,

(a) Long-term modulus of elasticity of concrete is given by

$$E = \left[\frac{E}{1+\varphi}\right] = \left[\frac{E}{1+1.6}\right] = \left[\frac{E}{2.6}\right]$$

∴ Resultant maximum long-term deflection

$$= [(2.6 \times 46) + 38.5 - (0.85 \times 74.7)] = 95 \text{ mm}$$

which is less than the IS: 1343 code limit of $\left[\dfrac{\text{span}}{250}\right] = \left[\dfrac{30000}{250}\right] = 120$ mm

Example 6.5 A simply supported beam with a uniform section spanning over 6 m is post-tensioned by two cables, both of which have an eccentricity of 100 mm below the centroid of the section at mid-span. The first cable is parabolic and is anchored at an eccentricity of 100 mm above the centroid at each end, the second cable is straight and parallel to the line joining the supports. The cross-sectional area of each cable is 100 mm^2 and they carry an initial stress of 1200 N/mm^2. The concrete has a cross-section of 2×10^4 mm^2 and a radius of gyration of 120 mm.

The beam supports two concentrated loads of 20 kN each at the third points of the span, $E_c = 38$ kN/mm^2. Calculate using Lin's simplified method

(a) The instantaneous deflection at the centre of span.

(b) The deflection at the centre of span after two years, assuming 20 per cent loss in prestress and the effective modulus of elasticity to be one-third of the short-term modulus of elasticity.

Solution.

$$A = 2 \times 10^4 \text{ mm}^2 \qquad i = 120 \text{ mm}$$

$$I = Ai^2 = (2 \times 10^4 \times 120^2) = 288 \times 10^6 \text{ mm}^4$$

$$P = 120 \text{ kN} \qquad e_1 = e_2 = 100 \text{ mm}$$

$$L = 6000 \text{ mm}$$

Self-weight, $g = 0.00048$ kN/mm

Concentrated loads at third point of span, $Q = 20$ kN

(a) Downward deflection due to self-weight of the beam

$$= \left[\frac{5 \times 0.00048 \times 6000^4}{384 \times 38 \times 288 \times 10^6}\right] = 0.74 \text{ mm}$$

Downward deflection due to concentrated loads $= \left(\dfrac{23QL^3}{648EI}\right)$

$$= \left[\frac{23 \times 20 \times 6000^3}{648 \times 38 \times 288 \times 10^6}\right] = 14.10 \text{ mm}$$

Deflection due to prestressing force

Deflection due to the parabolic cable $= \left(\dfrac{PL^2}{48EI}\right)(-5e_1 + e_2)$

$$= \left(\frac{120 \times 6000^2}{48 \times 38 \times 288 \times 10^6}\right)(-5 \times 100 + 100) = -3.27 \text{ mm (upward)}$$

Deflection due to the straight cable $= \left(\dfrac{-PeL^2}{8EI}\right) = -\left(\dfrac{120 \times 100 \times 6000^2}{8 \times 38 \times 288 \times 10^6}\right)$

$$= -4.92 \text{ mm (upward)}$$

Instantaneous deflection due to (prestress + self-weight + live loads)

$$= (-3.27 - 4.92) + 0.74 + 14.10 = 6.65 \text{ mm (downward)}$$

(b) At the end of two years,

$$E_{ce} = \frac{E}{3} \text{ and loss of prestress} = 20\%$$

∴ Upward deflection = 3 [0.8 (3.27 + 4.92)] = 19.65 mm

Downward deflection = 3 (0.74 + 14.10) = 44.52 mm

Net downward deflection = (44.52 – 19.65) = 24.87 mm

6.5 Deflections of Cracked Members

6.5.1 Short-time Deflections of Cracked Members

In the design of limited or partially prestressed (Class 3 type) structures, cracks of limited width are acceptable under occasional over-loads or even under working loads according to the CEB-FIP recommendations[10]. Hence, a knowledge of the load deformation characteristics of cracked members is essential to comply with the limit state of deflection.

The load-deflection characteristics of a typical prestressed concrete structural element under flexure is shown in Fig. 6.9. If the beam is sufficiently loaded, tensile stresses develop in the soffit and when this exceeds the tensile strength of concrete, cracks are likely to develop in the member.

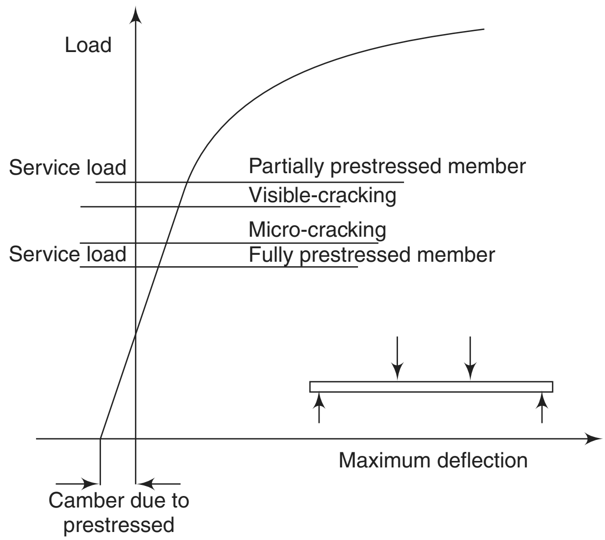

Fig. 6.9 *Load-deflection characteristics of prestressed members*

Experimental investigations[11] have shown that micro-cracks develop at a tensile stress of about 3 N/mm^2 which are invisible to the naked eye. On further loading, cracks are first visible at flexural tensile stresses between 3.5 and 7 N/mm^2, the higher values generally correspond to beams with well-bonded steel distributed close to the tensile face, as in the case of pretensioned members.

The load-deflection curve is approximately linear up to the stage of visible cracking, but beyond this stage the deflections increase at a faster rate due to the reduced stiffness of the beam. In the post-cracking stage, the behaviour of the beam is similar to that of reinforced concrete members.

The deflection of cracked structural concrete members may be estimated by the unilinear or bilinear method recommended by the European concrete committee[12]. In the unilinear method, the deflections are computed by a simple equation of the form,

$$a = \left(\frac{\beta L^2 M}{E_c I_r}\right)$$

where a = maximum deflection
L = effective span

M = maximum moment in the beam
E_c = modulus of elasticity of concrete
I_r = second moment of area of equivalent or transformed cracked section
β = a constant depending upon the end conditions, position of the given section and load distribution

Values of β are shown in Fig. 6.10 for different types of loading and support conditions. However, the unilinear method results in gross overestimation of deflections, particularly in the working load range, and underestimates for higher load ranges.

Support conditions and load	Values of β
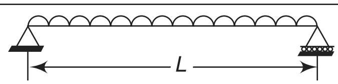	$\frac{5}{48}$
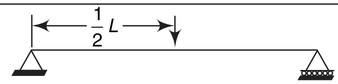	$\frac{1}{12}$
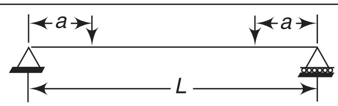	$\frac{1}{24}\left[3-4\left(\frac{a}{L}\right)^2\right]$
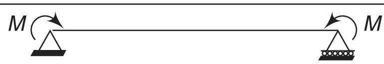	$\frac{1}{8}$
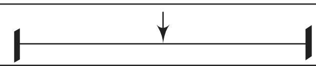	$\frac{1}{24}$
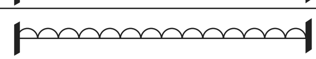	$\frac{1}{16}$
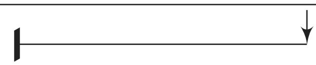	$\frac{1}{3}$
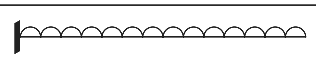	$\frac{1}{4}$
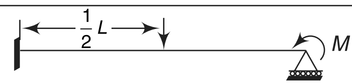	$\frac{1}{20}$
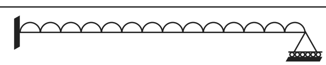	$\frac{1}{23}$

Fig. 6.10 *Values of constant β for different types of loading and support*

In the bilinear method recommended by the 1963 European Concrete Committee, the moment curvature is approximated by two straight lines, as shown in Fig. 6.11. Experimental investigations[13] have shown that a closer approximation to the actual load-deflection behaviour is possible by assuming bilinear moment–curvature relationships: the slope of the first line corresponding to the stiffness of the uncracked section and the slope of the second line to that of the cracked section. The instantaneous deflection in the post-cracking stage is obtained as the sum of the deflection up to the cracking load based on gross section and beyond the cracking load considering the cracked section. Hence, the deflections are estimated by an expression of the following type:

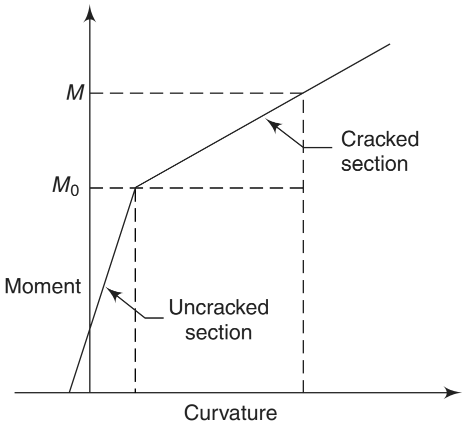

Fig. 6.11 *Bilinear moment curvature relationships*

$$a = \beta L^2 \left[\frac{M_{cr}}{E_c I_c} + \left(\frac{M - M_{cr}}{0.85 E_c I_r} \right) \right]$$

where M_{cr} = cracking moment

M = moment at which the deflection is required

I_c = second moment of area of the uncracked equivalent concrete section

I_r = second moment of area of the cracked equivalent concrete section

β = constant shown in Fig. 6.10

In computing I_c, it is satisfactory to ignore the effect of reinforcement in the section. However, some advantage may be gained by taking account of it, particularly in sections with large percentages of steel. The revised American code (ACI 318M–2011) considers the bilinear character of the load-deflection characteristics by incorporating a suitable effective value of the flexural rigidity in the unilinear formula. The modulus of elasticity is expressed as a function of the cylinder compressive strength of the form,

$$E_c = W_c^{1.5}\, 0.043 \sqrt{f_c'}\ (\text{N/mm}^2)$$

for values of density of concrete W_c, between 1500 and 2500 kg/m^3. For normal-density concrete, the modulus of elasticity is expressed as,

$$E_c = 4700 \sqrt{f_c'}$$

where f_c' = cylinder compressive strength in N/mm^2.
The effective moment of inertia is expressed as,

$$I_e = \left(\frac{M_{cr}}{M_a}\right)^3 I_g + \left[1 - \left(\frac{M_{cr}}{M_a}\right)^3\right] I_{cr}$$

where M_{cr} = cracking moment = $(f_{cr}\, I_g)/(y_t)$
M_a = moment at which deflection is required
I_g = moment of inertia of the gross concrete section about the centroidal axis, neglecting reinforcement
I_{cr} = moment of inertia of the cracked transformed section
I_e = effective moment of inertia for computation of deflection
f_{cr} = modulus of rupture of concrete
y_t = distance from the centroidal axis to the extreme fibre in tension

This method has been reported to predict deflections which are in general agreement with the experimental results of tests on class 3-type beams[14].

The British code (BS EN 1992–1–1) approach is to compute deflections using the curvature diagrams. The curvature for cracked and uncracked sections is computed with the assumptions of stress distribution as shown in Fig. 6.12. The reinforcement, whether in tension or in compression, is assumed to be elastic with a modulus of elasticity of 200 kN/mm^2. The short-term modulus of the elasticity of concrete, obtained from Table 2.8(a), appropriate to the characteristic strength of the concrete. Under long-term loading, an effective modulus with an effective value of $1/(1 + \phi)$ times the short-term modulus may be adopted; where ϕ is the appropriate creep coefficient.

For the uncracked section, the curvature is computed from the equation,

$$\left(\frac{1}{r_b}\right) = \left(\frac{M}{E_I T}\right)$$

where M = moment at the section considered
I = second moment of area
$\frac{1}{r_b}$ = curvature at mid-span or for cantilevers at the support section
E_c = short-term modulus of concrete

For cracked sections the curvature is expressed as,

$$\left(\frac{1}{r_b}\right) = \left(\frac{f_c}{xE_c}\right) = \left\{\frac{f_s}{(d-x)E_s}\right\}$$

where f_c = design service stress in concrete
f_a = estimated design service stress in tension reinforcement
d = effective depth of the section
x = depth of neutral axis
E_s = modulus of elasticity of reinforcement
E_c = modulus of elasticity of concrete

The assumptions made in calculating the curvatures of cracked and uncracked sections are outlined in Fig. 6.12.

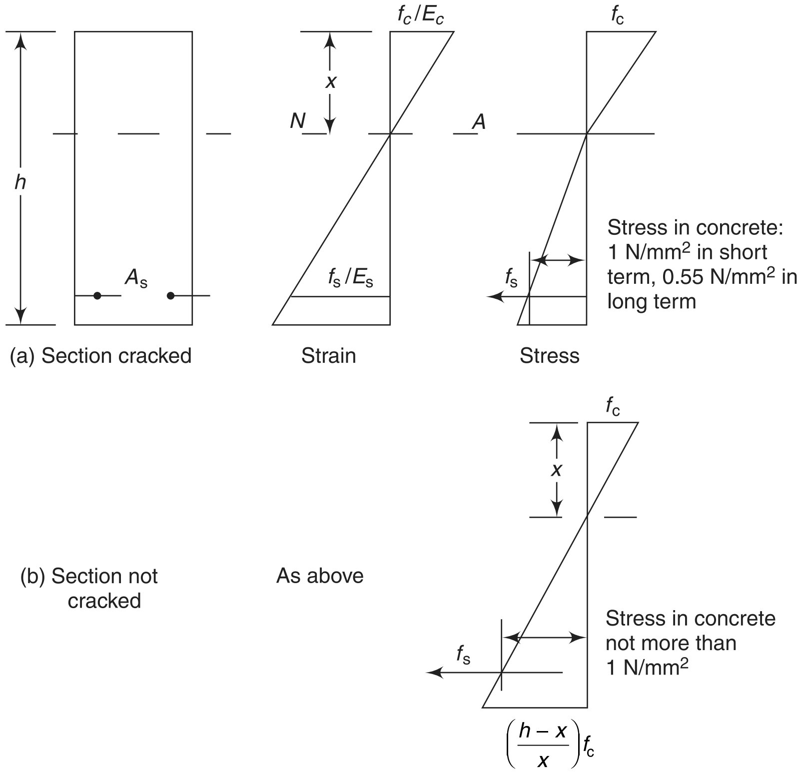

Fig. 6.12 *Assumption made in calculating curvatures (BS EN: 1992–1–1)*

The British code recommends that the tensile stress (f_{ct}) in concrete at the level of steel may be assumed as

1. 1 N/mm^2 for short-term loading, and
2. 0.55 N/mm^2 for long-term loading.

These assumptions are found to result in a realistic evaluation of deflections of cracked prestressed members.

In a partially cracked section, the realistic neutral-axis depth should be computed by equating the tensile and compressive forces. For practical applications, the simplifying assumption is made that the neutral axis depth is independent of the moment and forces on the section and is computed by equating the first moment of the areas above and below the neutral axis. Evans and Kong[15] have presented graphical aids, shown in Fig. 6.13, for the computation of the neutral-axis depth and the second moment of area of cracked section transformed to concrete.

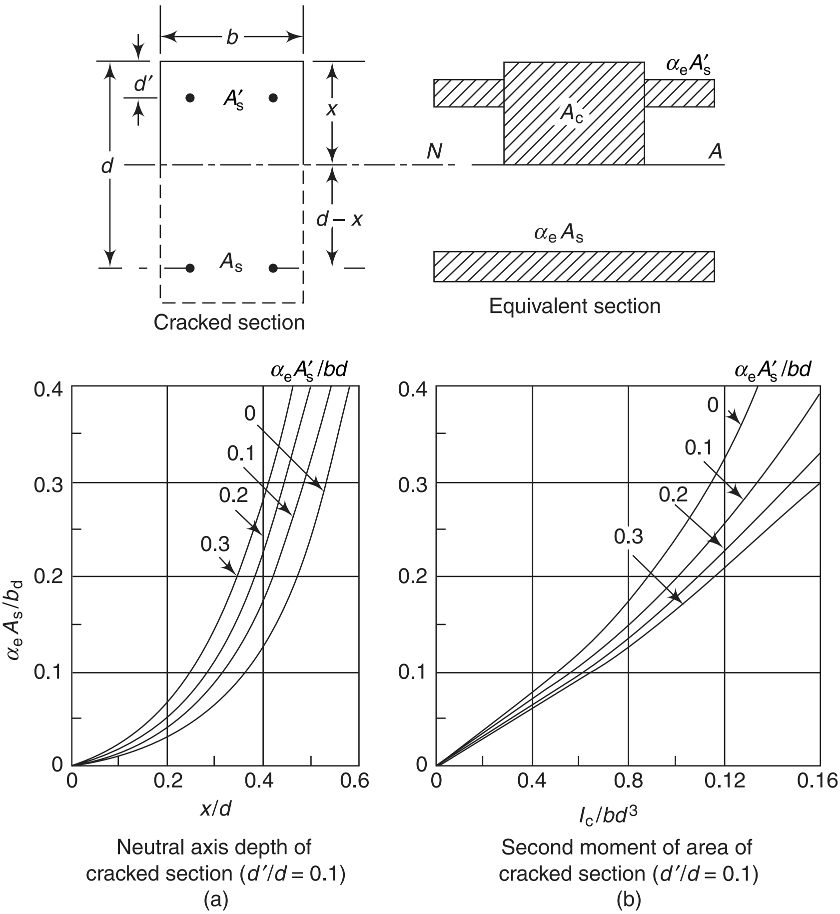

Fig. 6.13 *Neutral axis and second moment of area of cracked RC sections*

A rigorous evaluation of the curvature of a partially cracked section involves the computation of the moment resisted due to concrete section. Considering Fig. 6.14, the average tensile areas in concrete is expressed as

$$\frac{1}{2}\left\{\frac{(h-x)}{(d-x)}\right\} f_{ct}$$

$\therefore$ Tensile force in concrete $= \dfrac{1}{2} b\left\{\dfrac{(h-x)^2}{(d-x)}\right\} f_{ct}$

Lever arm of this force about the neutral axis = (2/3) $(h - x)$

$\therefore$ Moment due to concrete tension

$$\frac{1}{3} b\left\{\frac{(h-x)^3}{(d-x)}\right\} f_{ct}$$

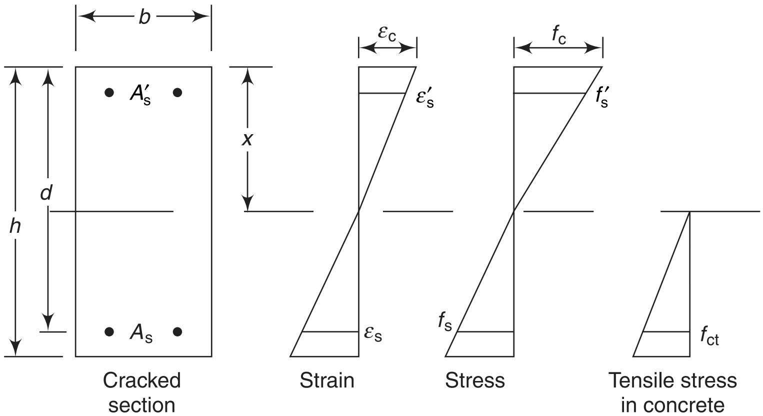

Fig. 6.14 *Stress distribution in cracked RC section*

Hence, when a moment M is applied to the partially cracked section, a part of it is resisted by the concrete tension: the net moment to be resisted by the concrete compression and by the forces in the reinforcement is given by,

$$M_{net} = M - \frac{1}{3} b \left\{ \frac{(h-x)^3}{(d-x)} \right\} f_{ct}$$

The curvature produced by the moment M_{net} is expressed as,

$$\left(\frac{1}{r}\right) = \left(\frac{M_{net}}{E_c I_{cr}}\right)$$

For assessing the long-term deflection, the procedure outlined in BS : 8110–1985 (Part-2) may be conveniently summarised in the following sequential steps:

1. Calculate the instantaneous curvature $(1/r_{it})$ under the total load and the instantaneous curvature $(1/r_{ip})$ due to the permanent load. Compute the difference $(1/r_{it} - 1/r_{ip})$.
2. Calculate the long-term curvature $(1/r_{1p})$ due to the permanent load.
3. Add to the long-term curvature $(1/r_{1p})$ the difference $(1/r_{it} - 1/r_{ip})$.
4. Calculate the shrinkage curvature $(1/r_{cs})$ given by the relation,

$$\left(\frac{1}{r_{cs}}\right) = \left(\frac{\varepsilon_{cs}\alpha_e S_s}{I}\right)$$

where α_e = modular ratio = (E_s/E_{eff})

ε_{cs} = free shrinkage strain (refer to Sec. 2.1.4)

E_{eff} = effective modulus of elasticity of concrete which can be taken to be equal to $E_c/(1 + \phi)$

ϕ = creep coefficient

I = second moment of area of either the cracked or the gross section, whichever is appropriate

S_s = first moment of area of the reinforcement about the centroid of the cracked or gross section, whichever is appropriate

5. The total curvature is expressed as,

$$\left(\frac{1}{r_b}\right) = \frac{1}{r_{1p}} + \left(\frac{1}{r_{it}} - \frac{1}{r_{ip}}\right) + \frac{1}{r_{cs}}$$

6. From the total curvature so determined, the long-term deflections are computed using the equation,

$$a = \beta L^2 \left(\frac{1}{r_b}\right)$$

where a = maximum deflection

$\frac{1}{r_b}$ = total curvature at mid-span for beams and at support section for cantilevers

L = effective span of the member

β = a constant that depends upon the shape of the bending moment diagram compiled in Fig. 6.10

6.5.2 Long-time Deflection of Cracked Members

The prediction of time-dependent deflections is complicated in the case of cracked members due to the redistribution of flexural stresses. According to Neville[16], an exact solution results in non-linear integral equations, for which no closed solution is available. The numerical solutions developed[17] ignore the influence of the tensile concrete zone on the strain distribution in the section, which considerably effects deflections.

The British code BS EN: 1992–1–1[18] recommendations are comprehensive in this regard, as they incorporate the use of curvature of cracked sections, including the effect of shrinkage and creep in computing long-term deflections. In contrast, the American Concrete Institute code ACI: 318M–2011[19] uses a simpler approach, whereby the additional long-term deflection resulting from creep and shrinkage of flexural members is determined by multiplying the immediate deflection caused by the sustained load considered by the factor

$$\lambda = \left(\frac{\xi}{1 + 50\rho'}\right)$$

where ρ' = (A'_s/bd) at mid-span for simple and continuous beam and at support for cantilevers

A'_s = area of compression reinforcement

b = width of the section

d = effective depth

ξ = time-dependent factor having the following values for different age

5 years or more	2.0
12 months	1.4
6 months	1.2
3 months	1.0

The following examples illustrate the use of various codified methods for the computation of long-term deflections.

Example 6.6 A prestressed concrete beam having a cross-sectional area (A) of 5×10^4 mm^2 is simply supported over a span of 10 m. It supports a uniformly distributed imposed load of 3 kN/m, half of which is non-permanent. The tendon follows a trapezoidal profile with an eccentricity of 100 mm within the middle-third of the span and varies linearly from the third-span points to zero at the supports. The area of tendons, A_p = 350 mm^2, have effective prestress of 1290 N/mm^2 immediately after transfer. Using the following data, calculate

(a) The short-term deflections.

(b) The long-term deflections.

Solution.

Assume $I_g = 4.5 \times 10^8$ mm^4	Density of concrete = 23.6 kN/m^3
$E_c = 34$ kN/mm^2	Creep coefficient = 2
$A = 5 \times 10^4$ mm^2	Concrete shrinkage, $\varepsilon_{cs} = 450 \times 10^{-6}$
$E_s = 200$ kN/mm^2	Relaxation of steel stress = 10%

(a) Short-term deflection

Initial prestressing force, $P = (350 \times 1290) = 4{,}51{,}500$ N

$$\text{Self-weight of the beam} = \left(\frac{5 \times 10^4}{10^6} \times 23.6\right) = 1.18 \text{ kN/m}$$

Non-permanent load = 1.5 kN/m

Permanent load = dead load + sustained live load

$$= (1.18 + 1.5) = 2.68 \text{ kN/m}$$

(i) Deflection due to the prestressing force Referring to Fig. 6.3 and substituting the value of L_1 and L_2 in the equation for deflection, we have

$$a_p = -\frac{Pe}{6EI}[2L_1^2 + 6L_1L_2 + 3L_2^2]$$

$L_1 = 3.333$ m and $L_2 = 1.666$ m and $e = 100$ mm. Thus,

$$a_p = \left(\frac{4{,}51{,}500 \times 100}{6 \times 34 \times 10^3 \times 4.5 \times 10^8}\right)[2 \times 3333^2 + 6(3333 \times 1666) + 3 \times 1666^2]$$

$$= -31 \text{ mm (upwards)}$$

(ii) Deflection due to non-permanent load (live load)

$$q = 1.5 \text{ kN/m}$$

$$a_q = \left(\frac{5qL^4}{384\,EI}\right) = \left(\frac{5 \times 1.5 \times (10 \times 10^3)^4}{384 \times 34 \times 10^3 \times 4.5 \times 10^8}\right) = 12.8 \text{ mm (downwards)}$$

(iii) Deflection due to permanent load (sustained load)

$$g = 2.68 \text{ kN/m}$$

$$a_g = \left(\frac{5gL^4}{384EI}\right) = \left[\frac{5 \times 2.68 \times (10 \times 10^3)^4}{384 \times 34 \times 10^3 \times 4.5 \times 10^8}\right] = 22.8 \text{ mm (downwards)}$$

(iv) Short-term deflections

- When the non-permanent load is acting, the short-term deflection is given by

$$a_s = (-31 + 12.8 + 22.8) = 4.6 \text{ mm (downwards)}$$

- When the non-permanent load is not acting, the short-term deflection is given by

$$a_s = (-31 + 22.8) = -8.2 \text{ mm (upwards)}$$

(b) Long-term deflection Stress in concrete at the level of steel

$$f_c = \left(\frac{4,51,500}{5 \times 10^4}\right) + \left(\frac{4,51,500 \times 100 \times 100}{4.5 \times 10^8}\right) = 19 \text{ N/mm}^2$$

$$\alpha_e = \left(\frac{E_s}{E_c}\right) = \left(\frac{200}{34}\right)$$

$$= 5.88$$

(i) Loss due to relaxation = 10% = 129 N/mm^2
(ii) Loss due to shrinkage = $(450 \times 10^{-6} \times 200 \times 10^3) = 90$ N/mm^2
(iii) Loss due to creep = $(2 \times 5.88 \times 19) = 223$ N/mm^2
Total loss = 442 N/mm^2

P = Initial prestressing force = 4,51,500 N
δP = Loss of prestressing force = (442×350) = 1,54,700 N
$(P - \delta P)$ = Final prestressing force = (4,51,500 – 1,54,700) = 2,96,800 N

$$\text{Average prestressing force} = \left[\frac{(4,51,500 + 2,96,800)}{2}\right] = 3,74,150 \text{ N}$$

(i) Long-term deflection due to prestress

a_p = [Deflection due to the initial prestressing force (P)] – [Deflection due to loss of prestressing force (δP)]
+(Deflection due to the average prestressing force due to creep with $\phi = 2$)

$$= 31 - \left(\frac{1,54,700 \times 31}{4,51,500}\right) + \left(\frac{3,74,150 \times 31}{4,51,500}\right)2$$

$$= (31 - 10.6 + 51.4) = 72 \text{ mm (upwards)}$$

(ii) Long-term deflection due to permanent load

$$a_g = (1 + \phi) \text{ (short-term deflection)}$$

$$= (1 + 2)(22.8) = 68.4 \text{ mm (downwards)}$$

(iii) Long-term deflection due to non-permanent load

$$a_q = 12.8 \text{ mm (downwards)}$$

The total long-term deflection is computed as,

- When the non-permanent load is acting:
  Mid-span deflection = (–72 + 68.4 + 12.8) = 9.2 mm (downwards)
- When the non-permanent load is not acting:
  Mid-span deflection = (–72 + 68.4) = –3.6 mm (upwards)

Example 6.7 A post-tensioned prestressed concrete beam of rectangular section 200 mm wide and 400 mm deep, is simply supported over a span of 5 m. The beam is prestressed by a parabolic cable containing 16 wires of 7 mm diameter with an eccentricity of 140 mm at the centre of span and concentric at supports. The initial stress in the wires is 1000 N/mm^2. Loss ratio is 0.8. The permanent load on the beam (inclusive of self weight) is 40 kN/m, whereas the total load (inclusive of non-permanent load) is 50 kN/m.

Calculate the long-term deflection of the beam using the British code BS EN: 1992–1–1, specifications and the following data for the following cases:
(a) Neglecting tensile resistance of concrete.
(b) Considering tensile resistance of concrete.

Modulus of elasticity of steel = 200 kN/mm^2

Modulus of elasticity of concrete = 33 kN/mm^2

Modulus of rupture of concrete = 4 N/mm^2

Creep coefficient, $\phi = 2$: Concrete shrinkage strain, $\varepsilon_{cs} = 300 \times 10^{-6}$

Solution.

(a) Neglecting tensile resistance of concrete

(i) *Properties of section*

$$A = (200 \times 400) = 8 \times 10^4 \text{ mm}^2$$

$$I_g = \left(\frac{200 \times 400^3}{12}\right) = 10.67 \times 10^8 \text{ mm}^4$$

$$Z = \left(\frac{200 \times 400^2}{6}\right) = 5.33 \times 10^6 \text{ mm}^3$$

$$L = 5000 \text{ mm}$$

$$e = 140 \text{ mm}$$

$$E_s = 200 \text{ kN/mm}^2$$

$E_c = 33$ kN/mm^2 $\qquad f_{ct} = 1$ N/mm^2 (short-term loading)

$\alpha_c = (E_s/E_c) = 6.06$ $\qquad = 0.55$ N/mm^2 (long-term loading)

$$f_{cr} = 4 \text{ N/mm}^2$$

$$A_p = (16 \times 38.4) = 615 \text{ mm}^2$$

Initial prestressing force, $P = \left(\dfrac{615 \times 1000}{1000}\right) = 615$ kN

Final prestressing force = $\eta P = (0.8 \times 615) = 492$ kN
Loss of prestressing force = $(615 - 492) = 123$ kN
Average prestressing force = $0.5\,(615 + 492) = 553.5$ kN

(ii) *Deflection due to prestressing force*

Deflection due to the initial prestressing force,

$$a_p = \left(\frac{5\,PeL^2}{48 E_c\, I_g}\right) = \left(\frac{5 \times 615 \times 10^3 \times 140 \times 5000^2}{48 \times 33 \times 10^3 \times 10.67 \times 10^8}\right) = 6.37 \text{ mm (upwards)}$$

Deflection due to loss of prestressing force

$$= \left(\frac{6.37}{615} \times 123\right) = 1.27 \text{ mm (downwards)}$$

Deflection due to the average prestressing force due to creep with $\phi = 2$,

$$= \left(\frac{6.37}{615} \times 553.5\right) 2 = 11.47 \text{ mm (upwards)}$$

∴ Long-term deflection due to prestressing force

α_p = (deflection due to the initial prestressing force)
– (deflection due to loss of prestressing force)
+ (deflection due to the average prestressing force due to creep with $\phi = 2$)

$\alpha_p = (6.37 - 1.27 + 11.47) = 16.57$ mm (upwards)

(iii) *Cracking load*

Effective prestressing force = 492 kN
Stress at the bottom of the beam

$$f_c = \left(\frac{492 \times 10^3}{8 \times 10^4}\right) + \left(\frac{492 \times 10^3 \times 140}{5.33 \times 10^6}\right) = 19.07 \text{ N/mm}^2$$

Moment required to cause a tensile stress equal to the modulus of rupture ($f_{er} = 4$ N/mm^2) at the soffit of the beam is given by

$$M_{cr} = (19.07 + 4)\,(5.33 \times 10^6)$$
$$= (123 \times 10^6) \text{ N mm} = 123 \text{ kN m}$$

Cracking load $= \left(\dfrac{8 \times 123}{5^2}\right) = 39.9$ kN/m

Hence, under total and permanent loads of 50 and 40 kN/m, the beam is cracked.

(iv) *Instantaneous curvature under total and permanent loads*

$$M_p = \text{Moment under permanent loads} = \left(\frac{40 \times 5^2}{8}\right) = 125 \text{ kN m}$$

$$M_t = \text{Moment under total loads} = \left(\frac{50 \times 5^2}{8}\right) = 156.25 \text{ kN m}$$

$$\left(\frac{1}{r_{it}}\right) = \text{Instantaneous curvature under total loads}$$

$$\left(\frac{1}{r_{ip}}\right) = \text{Instantaneous curvature under permanent loads}$$

$$\alpha_e = \left(\frac{E_s}{E_c}\right) = \left(\frac{200}{33}\right) = 6.06$$

Let x = depth of the neutral axis

b = width of the section

d = effective depth

A_p = area of steel reinforcement

$$\left(\frac{bx^2}{2}\right) = \alpha_e A_p(d - x)$$

$$\left(\frac{200x^2}{2}\right) = 6.06 \times 615(340 - x)$$

On solving, $x = 95$ mm

The second moment of area of the cracked section transformed to concrete is computed as,

$$I_{cr} = \left[\left(\frac{bx^3}{3}\right) + \alpha_e A_s r^2\right]$$

$$= \left[\left(\frac{200 \times 95^3}{3}\right) + 6.06 \times 615 \times 245^2\right] = (2.8 \times 10^8) \text{ mm}^4$$

Neglecting the contribution of tensile resistance of concrete, the difference in curvatures,

$$\left(\frac{1}{r_{it}} - \frac{1}{r_{pi}}\right) = \left(\frac{M_t - M_p}{E_c I_{cr}}\right)$$

$$= \left[\frac{156.25 - 125}{(33 \times 10^3)(2.8 \times 10^8)}\right] 10^6 = (3.38 \times 10^{-6}) \text{ mm}^{-1}$$

(v) *Long-term curvature under permanent loads*

$$E_c(\text{long-term}) = \left(\frac{E_c}{1+\phi}\right) = \left(\frac{33}{1+2}\right) = 11 \text{ kN/mm}^2$$

$$\alpha_e = \left(\frac{200}{11}\right) = 18.18$$

If x = depth of the neutral axis under long-term permanent loads, then

$$\left(\frac{bx^2}{2}\right) = \alpha_e A_p(d-x)$$

$$\left(\frac{200x^2}{2}\right) = (18.18 \times 615)(340-x)$$

On solving, $x = 145$ mm

$$I_{cr} = \left(\frac{200 \times 145^3}{3}\right) + (18.18 \times 615 \times 195^2)$$

$$= (6.28 \times 10^8) \text{ mm}^4$$

$$\left(\frac{1}{r_1 p}\right) = \left(\frac{M_p}{E_c I_{cr}}\right) = \left(\frac{125 \times 10^6}{11 \times 10^3 \times 6.28 \times 10^8}\right) = (18 \times 10^{-6}) \text{ mm}^{-1}$$

(vi) *Shrinkage curvature*

$$\left(\frac{1}{r_{cs}}\right) = \left(\frac{\varepsilon_{cs}\alpha_e S_s}{I_{cr}}\right)$$

where $\varepsilon_{cs} = (300 \times 10^{-6})$

$$\alpha_e = \left(\frac{E_s}{E_{eff}}\right)$$

$$E_{eff} = \left(\frac{E_c}{1+\phi}\right) = \left(\frac{33}{1+2}\right) = 11 \text{ kN/mm}^2$$

$$\alpha_e = \left(\frac{200}{11}\right) = 18.18$$

$$I_{cr} = (6.28 \times 108) \text{ mm}^4$$

$$S_s = A_p r_p$$

$$= (615 \times 267.5)$$

$$= (0.164 \times 10^6)$$

$$\therefore \quad \left(\frac{1}{r_{cs}}\right) = \left(\frac{300 \times 10^{-6} \times 18.18 \times 0.164 \times 10^6}{6.28 \times 10^8}\right)$$

$$= (1.42 \times 10^{-6}) \text{ mm}^{-1}$$

(vii) *Total long-term curvature*

$$\frac{1}{r_b} = \frac{1}{r_{1p}} + \left(\frac{1}{r_{it}} - \frac{1}{r_{ip}}\right) + \frac{1}{r_{cs}}$$

$$= (18 \times 10^{-6}) + (3.38 \times 10^{-6}) + (1.42 \times 10^{-6})$$

$$= (22.8 \times 10^{-6})\ \text{mm}^{-1}$$

(viii) *Long-term deflection due to loads*

$$a_w = \left(\beta L^2 \frac{1}{r_b}\right)$$

From Fig. 6.10, $\beta = \left(\frac{5}{48}\right) = 0.104$

$$\therefore \quad a_w = (0.104 \times 5000^2 \times 22.8 \times 10^{-6}) = 59.28\ \text{mm}$$

(ix) *Final deflection due to prestressing force and loads*

The final long-term deflection,

$$a = (a_w + a_p)$$

$$= (59.28 - 16.57) = 42.71\ \text{mm (downwards)}$$

(b) Considering tensile resistance of concrete

$$(M_t)_{net} = M_t - \frac{1}{3}\left\{\frac{b(h-x)^3}{d-x}\right\} f_{ct}$$

$$= (156.25 \times 10^6) - \frac{1}{3}\left\{\frac{200(400-95)^3}{340-95}\right\} 1$$

$$= (148.53 \times 10^6)\ \text{N mm}$$

$$(M_p)_{net} = M_p - \frac{1}{3}\left\{\frac{b(h-x)^3}{d-x}\right\} f_{ct}$$

$$= (125 \times 10^6) - \frac{1}{3}\left\{\frac{200(400-95)^3}{340-95}\right\} 1$$

$$= (117.28 \times 10^6)\ \text{N mm}$$

$$\left(\frac{1}{r_{it}} - \frac{1}{r_{ip}}\right) = \left(\frac{(M_t)_{net} - (M_p)_{net}}{E_c I_{cr}}\right)$$

$$= \left[\frac{(148.53 - 117.28)10^6}{(33 \times 10^3)(2.8 \times 10^8)}\right]$$

$$= (3.38 \times 10^{-6})\ \text{mm}^{-1}$$

It is important to note that

$$(M_t - M_p) = (M_t)_{net} - (M_p)_{net}$$

since the terms involving f_{ct} cancel out.

$$(M_p)_{net} = M_p - \frac{1}{3}\left\{\frac{b(h-x)^3}{d-x}\right\} f_{ct}$$

$$= (125 \times 10^6) - \frac{1}{3}\left\{\frac{200(400-145)^3}{340-145}\right\} 0.55$$

$$= (121.89 \times 10^6)\ \text{N mm}$$

$$\therefore \qquad \left(\frac{1}{r_{1p}}\right) = \left[\frac{(M_p)_{net}}{E_c I_{cr}}\right]$$

$$= \left[\frac{121.89 \times 10^6}{(11 \times 10^3)(6.28 \times 10^8)}\right] = (17.6 \times 10^{-6})\ \text{mm}^{-1}$$

$$\frac{1}{r_b} = \frac{1}{r_{1p}} + \left(\frac{1}{r_{it}} - \frac{1}{r_{ip}}\right) + \frac{1}{r_{cs}}$$

$$= (17.6 \times 10^{-6}) + (3.38 \times 10^{-6}) + (1.42 \times 10^{-6})$$

$$= (22.4 \times 10^{-6})\ \text{mm}^{-1}$$

$$\therefore \qquad a_w = \left(\beta L^2 \frac{1}{r_b}\right) = (0.104 \times 5000^2 \times 22.4 \times 10^{-6}) = 58.24\ \text{mm}$$

$\therefore$ The resultant long-term deflection, considering the tensile resistance of concrete, is

$$a = (a_w + a_p) = (58.24 - 16.57) = 41.67\ \text{mm}$$

The percentage difference in deflection when the tensile resistance of concrete is also considered as

$$\left(\frac{42.71 - 37.15}{38.19}\right) \times 100$$

which is only 2.43 per cent.

6.6 Requirements of Various Codes of Practise

It is the general practise in most of the codes to safeguard against excessive deflections under serviceability limit states, either indirectly by prescribing a minimum span to depth ratio for the member, or directly by specifying a maximum permissible deflection expressed as a fraction of the span.

The recommendations of the Indian Standard Code (IS: 1343)[20] with regard to the limit state of deflection are as follows:

1. The final deflection, due to all loads including the effects of temperature, creep and shrinkage should normally not exceed span/250.

2. The deflection, including the effects of temperature, creep and shrinkage occurring after the erection of partitions and the application of finishes, should not normally exceed span/350 or 20 mm, whichever is less.
3. If finishes are to be applied to the prestressed concrete members, the total upward deflection should not exceed span/300, unless uniformity of camber between adjacent units can be ensured.
4. The British code (BS EN: 1992–1–1) specifies a maximum deflection limit of span/250, beyond which the sag in a member will usually become noticeable. To prevent damage to non-structural elements, the code recommends that the deflection after the installation of finishes and partitions should not exceed the following values:
   (a) Span/500 or 20 mm, whichever is less, for brittle materials.
   (b) Span/350 or 20 mm, whichever is less, for non-brittle partitions or finishes.

According to the American code (ACI: 318M–2011), the permissible deflections depend upon the type of member as outlined in Table 6.1. The FIP–1984[21] recommends the following suitable deflection limits for floors, roofs and other horizontal members in buildings as follows:
(a) Total deflection below the level of supports: (span/200)to (span/300)
(b) Deflection that occurs after addition of partitions (span/500) to (span/1000)

Table 6.1 *Maximum permissible deflections (ACI: 318M–2011)*

	Type of Member	*Deflection to be Considered*	*Deflection Limitation*
1.	Flat roofs not supporting and not attached to non-structural element likely to be damaged by large deflections	Immediate deflection	$\left(\frac{\text{span}}{180}\right)$
2.	Floors not supporting and not attached to non-structural elements likely to be damaged by large deflections	Immediate deflection due to the live load	$\left(\frac{\text{span}}{360}\right)$
3.	Roof or floor construction supporting or attached to non-structural elements likely to be damaged by large deflections	That part of the total deflection which occurs after attachment of the non-structural elements (sum of the long time deflection due to all sustained loads and the immediate deflection due to any additional live load)	$\left(\frac{\text{span}}{480}\right)$
4.	Roof or floor construction supporting or attached to non-structural elements not likely to be damaged by large deflections		$\left(\frac{\text{span}}{240}\right)$

More detailed guidance regarding limiting deflections is presented in ISO standard[22].

The French code limits the deflection of members carrying masonry and partition walls to span/500, which is the total increase in deflection (due to short-term and sustained loads) over the instantaneous deflection due to self-weight. The German code prescribes limits to the depth/span ratio depending upon the support conditions.

Example 6.8 A concrete beam with a symmetrical I-section has flange width and depth of 200 mm and 60 mm, respectively. The thickness of the web is 80 mm and the overall depth is 400 mm. The beam is prestressed by a cable carrying a force of 1000 kN. The span of the beam is 8 m. The centre line of the cable is 150 mm from the soffit of the beam at the centre of span, linearly varying to 250 mm at the supports. Compute the initial deflection at mid-span due to prestress and the self-weight of the beam, assuming $E_c = 38\ \text{kN/mm}^2$. Compare the deflection with the limiting deflection permitted in IS: 1343 ($D_c = 24\ \text{kN/m}^3$).

Solution.

Self-weight of the beam, $g = 1.12$ kN/m $= 0.00112$ kN/mm

Prestressing force $P = 1000$ kN, $I = (847 \times 10^6)\ \text{mm}^4$

$e_1 = 50$ mm, $e_2 = 50$ mm, $L = 8000$ mm

Deflection due to self-weight

$$= \left(\frac{5 \times 0.00112 \times 8000^4}{384 \times 38 \times 847 \times 10^6}\right) = 1.86 \text{ mm (downward)}$$

Deflection due to the prestressing force

$$= \left[\frac{Pe_2 L^2}{8EI} - \frac{P(e_1 + e_2)L^2}{12EI}\right]$$

$$= \left(\frac{1000 \times 8000^2}{38 \times 847 \times 10^6}\right)\left[\frac{50}{8} - \frac{(50+50)}{12}\right]$$

$$= -4.1 \text{ mm (upward)}$$

$\therefore$ Deflection due to (prestress + self-weight)

$$= (-4.1 + 1.86) = -2.24 \text{ mm (upward)}$$

Maximum permissible deflection according to IS: 1343

$$= \left(\frac{\text{span}}{300}\right) = \left(\frac{8000}{300}\right) = 26.6 \text{ mm (upward)}$$

Hence, the actual deflection is within permissible limits.

Example 6.9 A prestressed concrete beam of rectangular section 120 mm wide and 300 mm deep, spans over 6 m. The beam is prestressed by a straight cable carrying an effective force of 180 kN at an eccentricity of 50 mm. If it supports an imposed load of 4 kN/m and the modulus of elasticity of concrete is 38 kN/mm^2, compute the deflection at the following stages and check whether they comply with the IS code specifications:

(a) Upward deflection under (prestress + self-weight).

(b) Final downward deflection under (prestress + self-weight + imposed load) including the effects of creep and shrinkage. Assume the creep coefficient to be 1.80.

Solution.

$P = 180$ kN	Self-weight, $g = 0.86$ N/mm
$e = 50$ mm	Imposed load, $q = 4$ N/mm
$I = (27 \times 10^7)$ mm^4	$E_c = 38$ kN/mm^2
$L = 6000$ mm	

Deflection due to the prestressing force

$$= \left(\frac{PeL^2}{8EI}\right) = \left(\frac{180 \times 50 \times 6000^2}{8 \times 38 \times 27 \times 10^7}\right) = 4.0 \text{ mm (upward)}$$

Deflection due to the self-weight of the beam

$$= \left(\frac{5gL^4}{384EI}\right) = \left(\frac{5 \times 0.86 \times 6000^4}{384 \times 38 \times 10^3 \times 27 \times 10^7}\right) = 1.4 \text{ mm}$$

Deflection due to self-weight and live load

$$= \left[\frac{5(g+q)L^4}{384EI}\right] = \left[\frac{5 \times 4.86 \times 6000^4}{384 \times 38 \times 10^3 \times 27 \times 10^7}\right] = 8.0 \text{ mm}$$

(a) Deflection due to (prestress + self-weight) = $(-4.0 + 1.4) = -2.6$ mm

Permissible upward deflection as per draft IS: 1343

$$= \left(\frac{\text{span}}{300}\right) = \left(\frac{6000}{300}\right) = 20 \text{ mm}$$

Hence, the upward deflection is within permissible limits.

(b) Deflection due to (prestress + self-weight + live load) including effects of creep and shrinkage

$$= (-4.0 + 8.0)\,(1 + \phi) = (4.0)\,(1 + 1.8) = 11.2 \text{ mm}$$

Permissible downward deflection as per IS: 1343

$$= \left(\frac{\text{span}}{250}\right) = \left(\frac{6000}{250}\right) = 24 \text{ mm}$$

Hence, the final downward deflection is within permissible limits.

Example 6.10 A prestressed concrete beam having a rectangular section 100 mm wide and 200 mm deep spans over 2.76 m. The beam is prestressed by a straight cable containing five wires of 5 mm diameter stressed to 1200 N/mm^2 at an eccentricity of 37 mm. Assume the modular ratio $\alpha_e = 6.2$. If the modulus of elasticity of concrete is

34 kN/mm^2 and modulus of rupture is 4 N/mm^2, calculate the maximum deflection of the beam at the following stages:

(a) prestress + self-weight of the beam
(b) prestress + self-weight + imposed load of 8.4 kN/m
(c) cracking load
(d) 1.46 times the working load
(e) 1.8 times the working load

Solution. Properties of the section

$A = 2 \times 10^4$ mm^2 $\qquad e = 37$ mm

$I_g = 666 \times 10^5$ mm^4 $\qquad P = (5 \times 19.6 \times 1200)/10^3 = 120$ kN

$Z = 666 \times 10^3$ mm^3 $\qquad E_c = 34$ kN/mm^2

$L = 2760$ mm $\qquad \alpha_e = 6.2$

Modulus of rupture, $f_{cr} = 4$ N/mm^2
Self-weight of the beam, $g = 0.48$ N/mm

$$\text{Deflection due to prestress} = \left(\frac{PeL^2}{8E_cI_g}\right) = \left(\frac{12 \times 10^4 \times 37 \times 2760^2}{8 \times 34 \times 10^3 \times 666 \times 10^5}\right)$$

$$= 1.88 \text{ mm (upward)}$$

$$\text{Deflection due to self-weight} = \left(\frac{5gL^4}{384E_cI_g}\right) = \left(\frac{5 \times 0.48 \times 2760^4}{384 \times 34 \times 10^3 \times 666 \times 10^5}\right)$$

$$= 0.16 \text{ mm}$$

Working load on the beam = (0.48 + 8.4) = 8.88 kN/m = 8.88 N/mm

$$\text{Deflection due to the working load} = \left(\frac{5 \times 8.88 \times 2760^4}{384 \times 34 \times 10^3 \times 666 \times 10^5}\right)$$

$$= 2.96 \text{ mm}$$

Working moment = $(0.125 \times 8.88 \times 2.76^2) = 8.447$ kN m
Stress at the bottom fibre due to (prestress + working load)

$$= \left[\left(\frac{12 \times 10^4}{2 \times 10^4}\right) + \left(\frac{12 \times 10^4 \times 37}{666 \times 10^3}\right) - \left(\frac{8.447 \times 10^6}{666 \times 10^3}\right)\right] = -0.017 \text{ N/mm}^2$$

The cracking load on the beam corresponds to the load which causes a stress which is equivalent to the modulus of rupture at the soffit of the beam. The extra moment (over and above the working moment) required to cause a tensile stress of 4 N/mm^2 at the soffit is given by

$$\frac{(4 \times 666 \times 10^3)}{10^6} = 2.664 \text{ kN m}$$

$\therefore$ Cracking moment = (8.447 + 2.664) = 11.111 kN/m

$$\text{Cracking load} = \frac{(8 \times 11.111)}{2.76^2} = 11.7 \text{ kN/m} = 11.7 \text{ N/mm}$$

Deflection due to the cracking load = $\left(\dfrac{5\times 11.7\times 2760^4}{384\times 34\times 10^3\times 666\times 10^5}\right)$

$= 3.90$ mm

Properties of the cracked transformed section

If x = depth of the neutral axis from the top fibre

b = width of the cross-section

d = effective depth

$$(b\,x^2/2) = \alpha_e A_s(d-x)$$

$$(100\times x^2/2) = 6.2\times 100(137-x)$$

Solving, $x = 35.5$ mm

If I_r = second moment of area of the cracked transformed section then,

$$I_r = \left(b\frac{x^3}{3}\right) + \alpha_e\, A_s r^2$$

$$= \frac{(100\times 35.5^3)}{3} + (6.2\times 100\times 101.5^2) = (79\times 10^5)\text{ mm}^4$$

Deflection due to 1.46 times the working load

Load at this stage $= (1.46\times 8.88) = 13$ kN/m

Corresponding moment $= \dfrac{(13\times 2.76^2)}{8} = 12.4$ kN m

Corresponding deflection $= \dfrac{5L^2}{48}\left[\dfrac{M_{cr}}{E_c I_g} + \dfrac{M - M_{cr}}{0.85 E_c I_r}\right]$

$$= \frac{5\times 2760^2}{48}\left[\left(\frac{11.111\times 10^3}{34\times 666\times 10^5}\right) + \left(\frac{12.4\times 10^3 - 11.111\times 10^3}{0.85\times 34\times 79\times 10^5}\right)\right] = 8.3\text{ mm}$$

Deflection due to 1.8 times the working load

Load corresponding to this stage $= (1.8\times 8.88) = 16$ kN/m

Corresponding moment $= [(16\times 2.76^2)/8] = 15.1$ kN m

Corresponding deflection is

$$= \frac{5\times 2760^2}{48}\left[\left(\frac{11.111\times 10^3}{34\times 666\times 10^5}\right) + \left(\frac{15.1\times 10^3 - 11.111\times 10^3}{0.85\times 34\times 79\times 10^5}\right)\right] = 17\text{ mm}$$

Final deflections at various stages of loading

(i) Prestress + self-weight $= (-1.88 + 0.16) = -1.72$ mm (upward)

(ii) Prestress + working load $= (-1.88 + 2.96) = 1.08$ mm (downward)

(iii) Cracking load $= (-1.88 + 3.90) = 2.02$ mm

(iv) 1.46 times the working load $= (-1.88 + 8.3) = 6.42$ mm
(v) 1.8 times the working load $= (-1.88 + 17.0) = 15.12$ mm

Example 6.11 In Example 6.10, estimate the long-term deflection of the beam under a sustained load of 1.8 times the working load. Assume the value of creep coefficient ϕ to be 2.00.

Solution. Short-term deflection corresponding to 1.8 times the working load is

$$a_i = 15.12 \text{ mm}$$

Long-term deflection, $a_f = (a_i)(1 + \phi)$

$$= (15.12)(1 + 2) = 45.36 \text{ mm}$$

Example 6.12 A prestressed concrete slab bridge deck designed for IRC loads has the following parameters. Estimate the long-term deflection of the slab using the following data:

Effective span of slab = L = 10.4 m
Total dead load = g = 14 kN/m = 0.014 kN/mm
Live load due to IRC loads at centre of span = Q = 93.2 kN
Effective prestressing force after losses = P = 1350 kN per metre width of slab
Modulus of elasticity of concrete = E_c = 33 kN/mm^2
Second moment of area of cross-section of slab = $I = (10.4 \times 10^9)$ mm^4
Eccentricity of parabolic cable at centre of span = e = 195 mm

Solution.

Upward deflection due to prestressing force

$$a_p = \left(\frac{5PeL^2}{48E_cI}\right) = \left(\frac{5 \times 1350 \times 195 \times 10400^2}{48 \times 33 \times (10.4 \times 10^9)}\right) = 8.69 \text{ mm (upwards)}$$

Downward deflection due to dead load

$$a_g = \left(\frac{5gL^4}{384E_cI}\right) = \left(\frac{5 \times 0.014 \times 10400^4}{384 \times 33 \times (10.4 \times 10^9)}\right) = 6.2 \text{ mm (downwards)}$$

Downward deflection due to live load

$$a_Q = \left(\frac{QL^3}{48E_cI}\right) = \left(\frac{93.2 \times 10400^3}{48 \times 33 \times (10.4 \times 10^9)}\right) = 6.36 \text{ mm (downwards)}$$

Maximum deflection due to prestress + self-weight + live load

$$a_r = (a_p + a_g + a_Q) = (-8.69 + 6.2 + 6.36) = 5.67 \text{ mm}$$

Long-term deflection considering the effect of creep is limited to (span/250).

Notional size of cross-section $= (2A_c/u) = [(2 \times 1000 \times 500)/2000] = 500$ mm. From Table 2.7, interpolate the final creep coefficient for the given notional size of 500 mm at relative humidity of 50 per cent and age at loading of 28 days as $\phi = 2.50$.

Effective modulus of elasticity of concrete

$$= E_{c,eff} = \left[\frac{E_c}{1+\phi}\right] = \left[\frac{E_c}{1+2.5}\right] = \left[\frac{E_c}{3.5}\right]$$

Maximum long-term deflection = (3.5 × 5.67)

= 19.84 mm < (10400/250) = 41.6 mm

References

1. Beeby, AW and JR Miles, "Proposals for the control of deflection in the new unified concrete code", *Journal of the Concrete Society,* London, Vol. 3, March 1969, pp 101–110.
2. Mayer, H, Bauschaden als folge der durchbiegung von stahlbeton bauterilen, Report, No. 68, *Material Prufungsamt fur das Bauwesen der Technischen Hochschule,* Munchen, 1966.
3. Warnock, FM, *Strength of Materials*, Pitman Publications, London.
4. Busemann, R, Kriechberechnung von verbundtragern unter Bentzung von zwei Kriechfasern, Der *Bauingenieur*, 25, Hesft 11, 1950, pp 418–420.
5. McHenry, D, "A new aspect of creep in concrete and its applications to design", *Proceedings of the American Society for Testing Materials*, Vol. 43, 1943, pp 1969–1984.
6. Corley, WG, MA Sozen, and CP Siess, "Time dependent deflections of prestressed concrete beams", Bulletin No. 307, *Highway Research Board,* 1961, pp 1–25.
7. Neville, AM, *Creep of Concrete-Plain, Reinforced and Prestressed,* North Holland Publications, Amsterdam, 1970, pp 554–557.
8. ACI Committee Report-435, Deflections of prestressed concrete members, ACI *Manual of Concrete Practice, Part-II,* pp 435–439.
9. Lin, TY, *Design of Prestressed Concrete Structures,* Asia Publishing House, 1962, p. 230.
10. *International Recommendations for the Design and Contruction of Concrete Structures*, *Principles and Recommendations,* June 1970, FIP Sixth Congress, Prague, Cement and Concrete Association, London, 1970.
11. Abeles, PW, *An Introduction to Prestressed Concrete,* Vol. II, Concrete Publications Ltd., London, 1966, pp 542–554.
12. Recommendations for an International Code of Practice for Reinforced Concrete, American Concrete Institute and Cement and Concrete Association, London, 1964.
13. Bebby, AW, "Short-term deformations of reinforced concrete members," *Technical Report* TRA-408, Cement and Concrete Association, London, March 1968.
14. Parameswaran, VS, and G, Annamalai, "Flexural behaviour of Class 3 beams", *Indian Concrete Journal,* Vol. 49, No.7, July 1975, pp 206–212.
15. Kong, FK and RH, Evans, *Reinforced and Prestressed Concrete,* (3rd edn), English Language Book Society, Van Nostrand Reinhold (International), London, 1987, pp 156–173.

16. Neville, A M, *Creep of Concrete-Plain, Reinforced and Prestressed,* North Holland Publications, Amsterdam, 1970, p. 501.
17. Elias, E., “Einfluss des Kriechens auf einen gebogenen Stahl beton. Rechteckbalken im Stadium II,” *Der Bauingenieur*, Vol. 36, No. 3, 1961, pp 93–99.
18. BSEN: 1992–1–1 Euro Code 2–Design of Concrete structures, General Rules and Rules for buildings, British Standards Institution, London 2004.
19. ACI: 318M–2011, *Building Code Requirements for Structural Concrete*, American Concrete Institute, Farmington Hills, Michigan, 2011.
20. IS: 1343-2012, Indian Standard Code of Practice for Prestressed Concrete, Second Revision, Bureau of Indian Standards, New Delhi, 2012, pp. 1– 54.
21. *FIP, Recommendations for Practical Design of Reinforced and Prestressed Concrete Structures,* Thomas Telford, Limited, London, 1984, pp 21–23.
22. International Standard ISO: 4356, *Basis for the Design of Structures, Deformations of Buildings at the Serviceability Limit States.* International Standards Organization, Geneva, 1977.

Review Questions

6.1 List the various factors influencing the deflections of prestressed concrete members.

6.2 Distinguish clearly between short-term and long-term deflections of prestressed concrete beams.

6.3 Explain with examples the effect of tendon profile on deflections of prestressed concrete members.

6.4 A concrete beam is prestressed by a parabolic cable having an eccentricity of e_1 towards the soffit at centre of span and an eccentricity of e_2 towards the top near support sections. Find the ratio of these eccentricities for zero deflection at the centre of span due to prestress only.

6.5 Briefly explain the importance of creep of concrete in long-term deflections of prestressed members.

6.6 Discuss the various methods of predicting long-term deflections of uncracked prestressed concrete members.

6.7 How do you use bilinear moment-curvature relationships for computation of deflections of cracked prestressed members?

6.8 Outline the various factors influencing the effective moment of inertia of cracked concrete sections.

6.9 How do you compute long-term deflections of cracked prestressed concrete beams?

6.10 Discuss briefly the recommendations of the Indian, British and American codes regarding the limit state of deflection of prestressed concrete flexural members.

Exercises

6.1 A simply supported concrete beam of span 8 m and rectangular cross-section 125 mm wide and 250 mm deep, is prestressed by a single cable in which the total tensile force is 220 kN. The centre line of the cable is parallel to the axis of the beam and 75 mm above the soffit over the middle-third of the span and is curved upward in a parabola over the outer-thirds of the span to a distance of 175 mm above the soffit at the supports. If the modulus of elasticity of concrete is 35 kN/mm^2 and the density of concrete is 24 kN/m^3, calculate

(a) The upward deflection at mid-span due to prestress only.
(b) The deflection when the beam is supporting its own weight.
(c) The magnitude of concentrated loads Q placed at the third points of the span, which would result in a limiting short-term deflection of span/500.

[Ans: (a) 30.3 mm (upward); (b) 23.3 mm (upward); (c) Q = 12.3 kN]

6.2 A concrete beam with a rectangular section 100 mm wide and 300 mm deep, is stressed by three cables, each carrying an effective force of 240 kN. The span of the beam is 10 m. The first cable is parabolic with an eccentricity of 50 mm below the centroidal axis at the centre of span and 50 mm above the centroidal axis at the supports. The second cable is parabolic with zero eccentricity at the supports and an eccentricity of 50 mm at the centre of span. The third cable is straight with a uniform eccentricity of 50 mm below the centroidal axis.

If the beam supports a uniformly distributed live load of 5 kN/m and $E_c = 38$ kN/mm^2, estimate the instantaneous deflection at the following stages:

(a) Prestress + self-weight of beam.
(b) Prestress + self-weight + live load.

[Ans: (a) 32.9 mm (upward); (b) 43.6 mm (downward)]

6.3 A prestress concrete beam spanning over 8 m is of rectangular section 150 mm wide and 300 mm deep. The beam is prestressed by a parabolic cable having an eccentricity of 75 mm below the centroidal axis at the centre of span and an eccentricity of 25 mm above the centroidal axis at the support sections. The initial force in the cable is 350 kN. The beam supports three concentrated loads of 10 kN each at intervals of 2 m. $E_c = 38$ kN/mm^2.

(a) Neglecting losses of prestress, estimate the short-term deflection due to (prestress + self-weight).
(b) Allowing for 20 per cent loss in prestress, estimate the long-term deflection under (prestress + self-weight + live load), assuming creep coefficient as 1.80.

[Ans: (a) 8.2 mm (upward); (b) 36.7 mm (downward)]

6.4 A prestressed beam of rectangular section 100 mm wide and 200 mm deep, has a straight duct 25 mm by 40 mm with its centre located at 50 mm from the soffit of the beam which is prestressed by 12 wires of 7 mm diameter stressed to 600 N/mm^2. The beam supports an imposed load of 4 kN/m over a span of 6 m. The modulus of elasticity of concrete is 38 kN/mm^2. Estimate the central deflection of the beam under the action of prestress, self-weight and live load

(a) Based on net section (beam ungrouted).
(b) Based on transformed section (beam grouted).

[Ans: (a) 4.5 mm (downward); (b) 1.3 mm (downward)]

6.5 A prestressed concrete beam with a cross-section 120 mm wide and 300 mm deep, is used to support a uniformly distributed live load of 3 kN/m over an effective span of 6 m. The beam is prestressed by a straight cable carrying an effective prestressing force of 180 kN at a constant eccentricity of 50 mm. Given $E_c = 38$ kN/mm^2, the modulus of rupture = 5 N/mm^2, area of the cable = 200 mm^2 and modular ratio = 6, estimate the deflection of the beam at the following stages:

(a) Working load (b) cracking load

(c) 1.5 times the cracking load

[Ans: (a) 2.3 mm; (b) 5.6 mm; (c) 54.8 mm]

6.6 A concrete beam with a section 90 mm wide and 180 mm deep, is prestressed by two wires of 7 mm diameter initially stressed to 920 N/mm^2. The wires are located in a parabolic profile with an eccentricity of 36.8 mm at the centre span (3 m) and concentric at the supports: The beam supports two concentrated Live loads of 7 kN each spaced 1 m apart. The modulus of elasticity of concrete is 30.9 kN/mm^2. Compute the initial deflection of the beam at the centre of span under (prestress + self-weight) and the final deflection, including live loads, assuming 15 per cent loss in prestress due to various causes. Compare these deflections with the limits prescribed in the IS: 1343. Assume creep coefficient as 1.6.

[Ans: Initial deflection = 3.33 mm (upward) within permissible
Final deflection = 9.074 mm (downward) limits specified in IS: 1343]

6.7 A post-tensioned prestressed concrete beam of span 8 m with a rectangular section 300 mm wide by 400 mm deep, is prestressed by a cable containing high-tensile wires of cross-sectional area 2000 mm^2. If the beam supports a live load of 20 kN/m excluding its self-weight, compute the initial deflection due to prestress, self-weight and live loads for the following cases:

(a) The cable profile is straight with a constant eccentricity of 100 mm.

(b) The cable profile is parabolic with a dip of 100 mm at mid-span and concentric at supports. Assume the modulus of elasticity of concrete as 36 kN/mm^2.

[Ans: Case (a): 0.33 mm downwards, Case (b): 3.80 mm downwards]

Objective-type Questions

6.1 Maximum permissible final deflection of a beam should not exceed

(a) span/350 (b) span/250 (c) span/480

6.2 Suitable control on deflections is essential to

(a) prevent failure of the member
(b) avoid damage to partitions and finishes
(c) prevent failure due to shear

6.3 Deflection of prestressed concrete beam is excessive in the

(a) precracking stage (b) elastic stage (c) post-cracking stage

6.4 The magnitude of deflection of a prestressed beam is directly proportional to

(a) modulus of elasticity of concrete
(b) prestressing force in the cable
(c) second moment of area of the cross-section

6.5 The deflection of a pretensioned beam is influenced by
(a) tendon profile (b) anchorage slip (c) imposed load

6.6 Short-term deflection of a prestressed beam can be computed using
(a) elastic theory (b) Mohr's theorem (c) Shear force diagram

6.7 A parabolic cable profile with maximum eccentricity at mid-span and concentric at supports when stressed results in
(a) zero deflection
(b) downward deflection
(c) upward deflection

6.8 The deflection of a cracked prestressed concrete beam can be computed by
(a) stress-strain diagram
(b) bending moment diagram
(c) bilinear moment-curvature relationships

6.9 Creep coefficient used for estimating the long-term deflection of a prestressed concrete member is influenced by the parameter
(a) modulus of elasticity
(b) notional size of member
(c) span length

6.10 Long-term deflection of a prestressed member depends upon
(a) type of tendons
(b) modulus of rigidity
(c) relative humidity

Answers to Objective-type Questions

6.1 (a)	6.2 (b)	6.3 (c)	6.4 (b)	6.5 (c)
6.6 (b)	6.7 (c)	6.8 (c)	6.9 (b)	6.10 (c)

7 Flexural Strength of Prestressed Concrete Sections

7.1 Types of Flexural Failure

When prestressed concrete members are subjected to bending loads, different types of flexural failures are possible at critical sections, depending upon the principal controlling parameters, such as the percentage of reinforcement in the section, degree of bond between tendons and concrete, compressive strength of concrete and the ultimate tensile strength of the tendons. In the post-cracking stage, the behaviour of a prestressed concrete member is more akin to that of a reinforced concrete member and the theories used for estimating the flexural strength of reinforced concrete section may as well be used for prestressed concrete sections.

The various types of flexural failures encountered in prestressed concrete members are examined in the light of recommendations of various codes of practise.

Fracture of steel in tension The sudden failure of a prestressed member without any warning is generally due to the fracture of steel in the tension zone. This type of failure is imminent when the percentage of steel provided in the section is so low that when the concrete in the tension zone cracks, the steel is not in a position to bear up the additional tensile stress transferred to it by the cracked concrete. This type of failure can be prevented by providing a certain minimum percentage of steel in the cross-section.

The Indian Standard Code IS: 1343 prescribes a minimum longitudinal reinforcement of 0.2 per cent of the cross-sectional area in all cases except in the case of pretensioned units of small sections. When a high-yield strength deformed reinforcement is used, the minimum steel percentage is reduced to 0.15 per cent. The percentage of steel provided, both tensioned and untensioned taken together, should be sufficient so that when the concrete in the precompressed tensile zone cracks, the steel is in a position to bear the additional tensile stress transferred to it by the cracking of the adjacent fibres of the concrete, thereby preventing a sudden failure of the beam due to fracture of steel in tension.

In contrast, the British code BSEN: 1992–1–1 prescribes that the number of prestressing tendons should be such that cracking of the concrete precedes the failure of the beam. This requirement will be satisfied if the ultimate moment of resistance of the section exceeds the moment necessary to produce a flexural tensile stress in the concrete at the extreme tension fibres of magnitude equal to $0.6\sqrt{f_{cu}}$. In these computations, the effective prestress in concrete should be considered after allowing for the various losses.

The American Concrete Institute code ACI: 318M–2011 specifies that the minimum area of bonded reinforcement should be not less than 0.004 times the area of that part of cross-section which is between flexural tension face and the centre of gravity of the gross concrete section.

Failure of under-reinforced sections If the cross-section is provided with an amount of steel greater than the minimum prescribed in case 1, the failure is characterised by an excessive elongation of steel followed by the crushing of concrete. As bending loads are increased, excessive elongation of the steel raises the neutral axis closer to the compression face at the critical section.

The member approaches failure due to the gradual reduction of the compression zone, exhibiting large deflections and cracks, which develop at the soffit and progress towards the compression face. When the area of concrete in the compression zone is insufficient to resist the resultant internal compressive force, the ultimate flexural failure of the member takes place through the crushing of concrete. Large deflections and wide cracks are the characteristic features of under-reinforced sections at failure (Fig. 7.1). This type of behaviour is generally desirable since there is considerable warning before the impending failure. As such, it is a common practise to design under-reinforced sections which become more important in the case of statically indeterminate structures. An upper limit on the maximum area of steel is generally prescribed in various codes for under-reinforced sections.

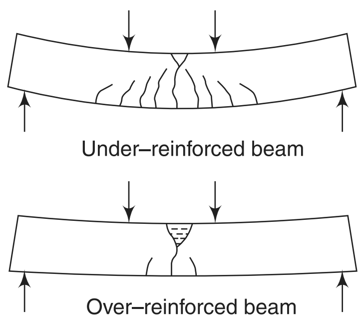

Fig. 7.1 *Flexural failure modes of prestressed beams*

Failure of over-reinforced sections When the effective reinforcement index, which is expressed in terms of the percentage of reinforcement, the compressive strength of concrete and the tensile strength of steel exceed a certain range of values, the section is said to be over-reinforced. Generally, over-reinforced members fail by the sudden crushing of concrete, the failure being characterised by small deflections and narrow cracks (Fig. 7.1). The area of steel being comparatively large, the stresses developed in steel at failure of the member may not reach the tensile strength and in many cases it may well be within the proof, stress of the tendons.

In structural concrete members, it is undesirable to have sudden failures without any warning in the form of excessive deflections and widespread cracks, and consequently the use of over-reinforced sections is discouraged. The amount of reinforcement used in practise should, preferably, not exceed that required for a balanced section. In this connection, most of the codes follow a conservative approach in formulating the evaluation procedures for flexural strength calculations of over-reinforced sections.

The redistribution of moments in an indeterminate structure depends upon the rotation capacities of the critical sections of the member under a given system of loads. The use of over-reinforced sections in such structures curtails the rotation capacity of the sections, consequently affecting the ultimate load on the structure.

Other modes of failure Prestressed concrete members subjected to transverse loads may fail in shear before their full flexural strength is attained, if they are not adequately designed for shear. Web shear cracks may develop if the principal stresses are excessive, and if thin webs are used, the failure may occur due to web crushing. In the case of pretensioned members, the failure of the bond between the steel and the surrounding concrete is likely due to the inadequate transmission lengths at the ends of members. In post-tensioned members, anchorage failures may take place if the end block is not properly designed to resist the transverse tensile forces.

7.2 Strain Compatibility Method

The rigorous method of estimating the flexural strength of prestressed concrete section is based on the compatibility of strains and equilibrium of forces acting on the section at the stage of failure[1]. The basic theory is applicable to all structural concrete sections, whether reinforced or prestressed, and generally the following assumptions are made:

1. The stress distribution in the compression zone of concrete can be defined by means of coefficients applied to the characteristic compressive strength and the average compressive stress and the position of the centre of compression can be assessed.
2. The distribution of concrete strain is linear (plane sections normal to axis remain plane after bending).
3. The resistance of concrete in tension is neglected.
4. The maximum compressive strain in concrete at failure reaches a particular value.

The flexural compressive stress in the compressive zone closely follows the stress-strain curve of concrete. The properties of the concrete stress block can be expressed in terms of the characteristic ratios k_1 and k_2. Much research has been carried out to study the characteristics of the stress block[2,3,4]. In particular the tests by Hognestad *et. al*[5,6] had considerable influence on the American and, indirectly, on the British and Indian Standard Codes. Figure 7.2 shows the stress and strain distribution at the limit state of collapse for a rectangular section with steel in the tension zone. The parameters $k_1$and k_2 are not constant but depend upon the compressive strength of concrete. Investigations by Hognestad *et. al* have shown that k_1 varies between 0.5 and 0.7 and k_2

between 0.42 and 0.47 for the concrete compressive strength varying from 60 to 20 N/mm^2.

The characteristics of Hognestad *et. al's* stress block are summarised in Fig. 7.3, in which the concrete cube strengths f_{ck} have been obtained from the cylinder strength f'_c using conversion factor of 0.8, as reported by Kong and Evans[7]. The figure shows that the ultimate strain ε_{cu} varies with the concrete strength.

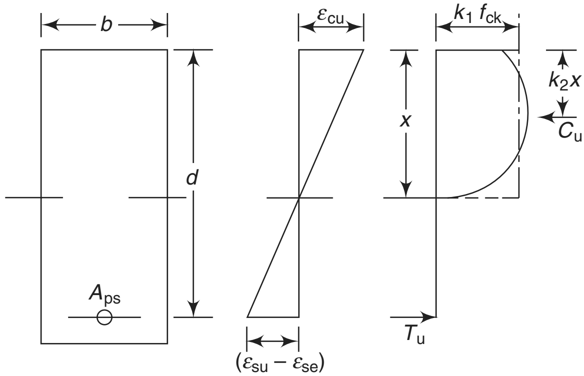

Fig. 7.2 *Stress-Strain distribution at failure*

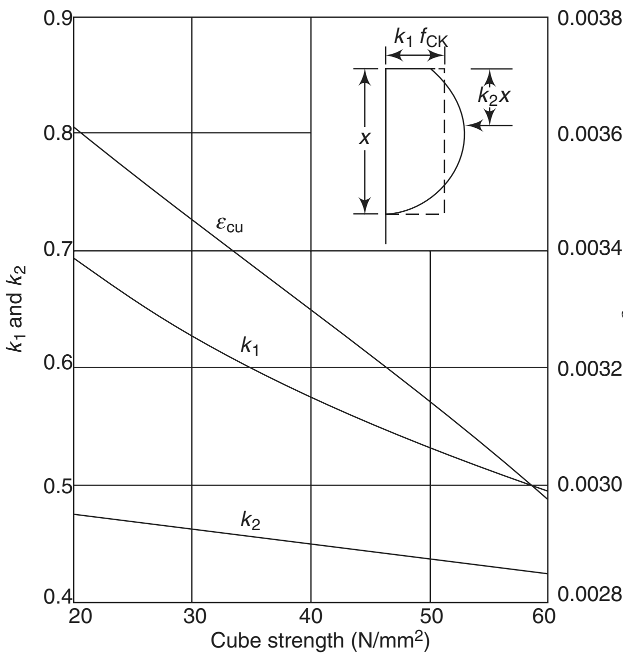

Fig. 7.3 *Characteristics of Hognestad et. al's stress block*

However, the current British[8], American[9] and Indian[10] Standard Codes assume, for the sake of simplicity, a constant value for ultimate compressive strain in concrete irrespective of the strength of concrete.

Referring to Fig. 7.2,

Total compressive force $C_u = k_1 f_{ck}\, bx$

Total tensile force $T_u = A_{ps} f_{pb}$

The ultimate flexural strength of the section is expressed as

$$M_u = A_{ps} f_{pb}\,(d - k_2 x) = k_1 f_{ck}\, bx(d - k_2 x)$$

A knowledge of the stress-strain characteristics of steel that is used as prestressing tendons is necessary for flexural strength computations by the strain compatibility method. A typical short-term design stress–strain curve for concrete recommended in the British and Indian Standard Codes is shown in Fig. 7.4. The typical stress–strain characteristics of different types of tendons used in prestressed concrete as recommended in the British and Indian standard codes are illustrated in Figs 7.5 (a), (b) and (c).

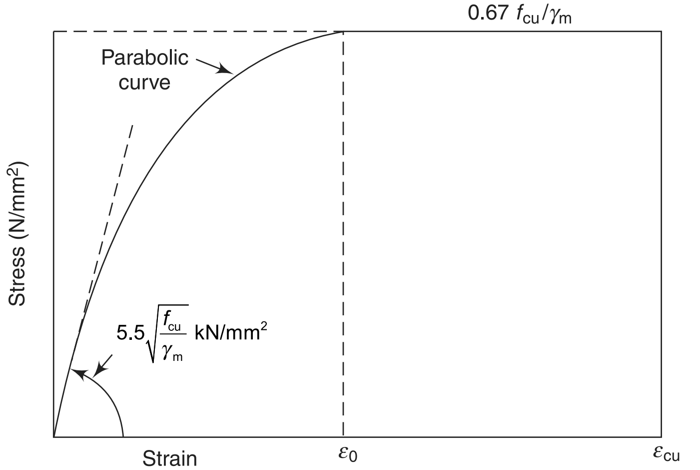

	ε_0	ε_{cu}
BS EN: 1992–1–1	$2.4 \times 10^{-4}\sqrt{\frac{f_{cu}}{\gamma_m}}$	0.0035
IS: 1343	0.002	0.0035

Fig. 7.4 *Short-term design stress-strain curve for normal weight concrete (BS and IS codes)*

The idealised curves refer to the design strength of the materials, which is obtained by dividing the characteristic strength by the partial safety factor for materials (refer Chapter 11).

The major steps to be followed in the strain compatibility method are summarised as follows:

1. Compute the effective strain ε_{sc} in steel due to prestress after allowing for an losses from the stress-strain curve for steel.

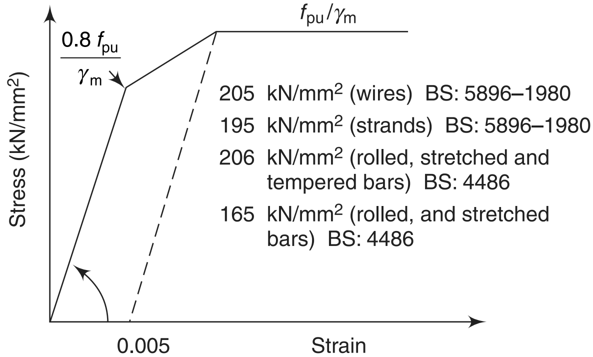

(a) Short-term design stress-strain curve for prestressing tendons (BS EN: 1992–1–1)

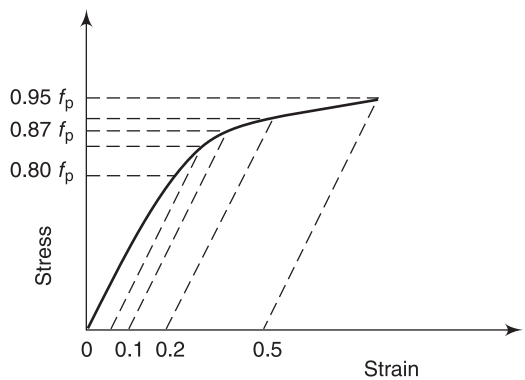

(b) Stress-Strain curve for stress-relieved strands and bars (IS: 1343)

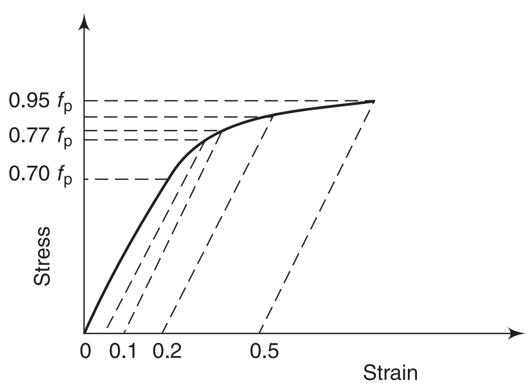

(c) Stress-Strain curve for as drawn wires (IS: 1343)

Fig. 7.5

2. Assume a trial value for the neutral axis depth x and evaluate $(\varepsilon_{su} - \varepsilon_{sc})$ from the strain diagram (assuming $\varepsilon_{cu} = 0.0035$, compute the value of ε_{sc}).
3. Using the stress-strain curve for steel, determine the value of stress in steel at failure f_{pb} corresponding to ε_{su}.
4. Compute the total compression C_u and tension T_u.
5. If the compressive and tensile forces are equal, then the assumed value of x is correct. If the tension is less than compression, decrease the value of x and if tension exceeds compression, increase x and repeat steps 2 to 4 until a reasonable agreement is achieved.
6. Evaluate the ultimate moment M_u using the expression,

$$M_u = A_{ps} f_{pb}(d - k_2 x)$$

Generally, it is possible to achieve force equilibrium within two or three trials. The strain compatibility method is very useful for estimating the ultimate flexural strength of over-reinforced sections in which the stresses in steel at failure do not reach the ultimate strength values.

Morsch[11] has suggested a graphical version of the strain compatibility method in which the failure of the compressive zone is assumed when the extreme compressive fibre reaches a strain limit of 0.2 per cent. Correspondingly for under-reinforced sections, the failure of the prestressing steel is assumed to take place at a maximum tensile strain of 0.5 per cent. However, the method can be considerably simplified for under-reinforced sections, in which the stress in tensile steel at the collapse stage is more or less equal to the characteristic tensile strength of the tendons. Considering this aspect, many codes have recommended simplified procedures for calculating the flexural strength of concrete sections which are reinforced with high-tensile steel in the tension zone.

The use of the strain compatibility method, generally applicable for both under- and over-reinforced sections, is illustrated by the following examples:

Example 7.1 A pretensioned concrete beam with a rectangular section 100 mm wide and 160 mm deep, is prestressed by 10 high-tensile wires of 2.5 mm-diameter located at an eccentricity of 40 mm. The initial force in each wire is 6.8 kN. The strain loss in wires due to elastic shortening, creep and shrinkage of concrete is estimated to be 0.0012 units. The characteristic cube strength of concrete is 40 N/mm^2. Given the load-strain curve of 2.5 mm-diameter steel wire (Fig. 7.6), estimate the ultimate flexural strength of the section using the strain compatibility method.

Solution. For $f_{ck} = 40$ N/mm^2, read out $\varepsilon_{cu} = 0.0033$, $k_1 = 0.57$ and $k_2 = 0.45$ from Fig. 7.3. Strain due to load of 6.8 kN in wire is 0.0073. Effective strain in steel after all losses is given by

$$\varepsilon_{se} = (0.0073 - 0.0012) = 0.0061$$

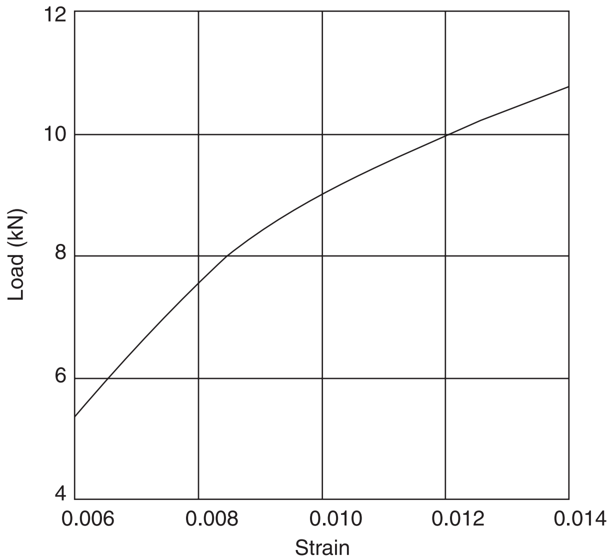

Fig. 7.6 *Load-Strain curve for 2.5 mm wire*

First trial

Assume $x = 60$ mm

From the strain diagram (Fig. 7.2), $(\varepsilon_{su} - \varepsilon_{se}) = 0.0033$.

$$\therefore \quad \varepsilon_{su} = (0.0033 + 0.0061) = 0.0094$$

Corresponding force in the wire = 8.4 kN

Total tensile force = (10 × 8.4) = 84 kN

Total compressive force $= (k_1 \cdot f_{ck} \cdot b \cdot x)$

$$= \left[\frac{(0.57 \times 40 \times 100 \times 60)}{1000}\right] = 136.8 \text{ kN}$$

Since tension is less than compression, decrease x for the second trial.

Second trial

Assume $x = 43$ mm

$$(\varepsilon_{su} - \varepsilon_{se}) = 0.0059$$

$$\therefore \quad \varepsilon_{su} = (0.059 + 0.0061) = 0.012$$

Corresponding force in the wire = 9.9 kN

Total tensile force = (10 × 9.9) = 99 kN

$$\text{Total compressive force} = \left[\frac{(0.57 \times 40 \times 100 \times 43)}{1000}\right] = 98 \text{ kN}$$

Since tension is nearly equal to compression, strain compatibility is established.

$$M_u = A_{ps} f_{pb} (d - k_2 x)$$
$$= (99 \times 10^3) \times (120 - 0.45 \times 43)$$
$$= (9.96 \times 10^6) \text{ N mm} = 9.96 \text{ kN m}$$

Example 7.2 If the number of wires in Example 7.1 is increased to 16, estimate the flexural strength of the section.

Solution.

First trial

Assume $x = 60$ mm

$$(\varepsilon_{su} - \varepsilon_{se}) = 0.0033$$

$$\therefore \quad \varepsilon_{su} = (0.0033 + 0.0061) = 0.0094$$

Corresponding force in the wire = 8.4 kN

Total tensile force = $(16 \times 8.4) = 134.4$ kN

$$\text{Total compressive force} = \left[\frac{(0.57 \times 40 \times 100 \times 60)}{1000}\right] = 136.8 \text{ kN}$$

Since tension is nearly equal to compression, strain compatibility is established.

$$M_u = A_{ps} f_{pb}(d - k_2 x) = 134.4\left[\frac{(120 - 0.45 \times 60)}{1000}\right] = 12.5 \text{ kN m}$$

7.3 Simplified Code Procedures

7.3.1 Indian Code Provisions

The Indian Standard Code method (IS: 1343-2012) for computing the flexural strength of rectangular and T-sections in which neutral axis lies within the flange is based on the parabolic stress block as shown in Fig. 7.7.

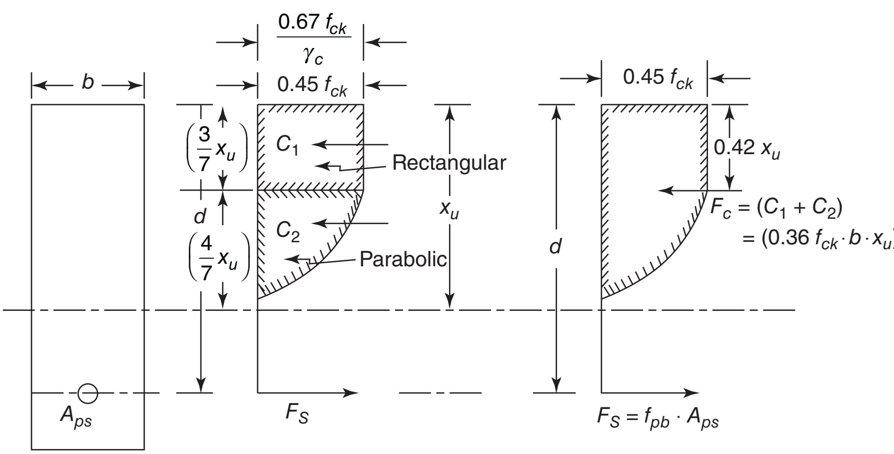

Fig. 7.7 *Concrete stress block parameters (IS: 1343-2012)*

The moment of resistance is obtained from the equation,

$$M_u = f_{pb} A_{ps} (d - 0.42 x_u)$$

Where M_u = ultimate moment of resistance of the section
f_{pb} = tensile stress in tendons at failure
f_{pu} = characteristic tensile strength of prestressing tendons
A_{ps} = area of tendons in the tension zone
d = effective depth to the centroid of tendons
x_u = neutral axis depth

The value of f_{pb} and (x_u/d) depends upon the effective reinforcement ratio $\left(\dfrac{A_{ps}.f_{pu}}{b.d.f_{ck}}\right)$.

For pretensioned and post-tensioned members with effective bond between concrete and tendons, the value of f_{pb} and x_u are given in Table 7.1.

Table 7.1 *Conditions at the ultimate limit state for rectangular beams with pretensioned tendons or with post-tensioned tendons with effective bond (Table 11 of IS: 1343-2012)*

Ratio $\left(\dfrac{A_{ps}.f_{pu}}{b.d.f_{ck}}\right)$	*Stress in Tendon as Proportion of the Design Strength* $\left(\dfrac{f_{pb}}{0.87f_{pu}}\right)$		*Ratio of the Depth of Neutral Axis to that of the Centroid of Tendon in tension zone* $\left(\dfrac{x_u}{d}\right)$	
	Pretensioning	*Post-tensioning with Effective Bond*	*Pretensioning*	*Post-tensioning with Effective Bond*
0.025	1.0	1.0	0.054	0.054
0.05	1.0	1.0	0.109	0.109
0.10	1.0	1.0	0.217	0.217
0.15	1.0	1.0	0.326	0.326
0.20	1.0	0.95	0.435	0.414
0.25	1.0	0.90	0.542	0.488
0.30	1.0	0.85	0.655	0.558
0.40	0.9	0.75	0.783	0.653

The ultimate moment of resistance of flanged sections in which neutral axis falls outside the flange is computed by combining the moment of resistance of the web and flange portions and considering the stress blocks shown in Fig. 7.8.

If A_{pw} = area of prestressing steel for web
A_{pf} = area of prestressing steel for flange
D_f = thickness of flange

Then, $$A_p = (A_{pw} + A_{pf})$$

But, $$A_{pf} = 0.45f_{ck}(b - b_w)\left(\frac{D_f}{f_p}\right)$$

After evaluating A_{pf}, the value of A_{pw} is obtained as,

$$A_{pw} = (A_p - A_{pf})$$

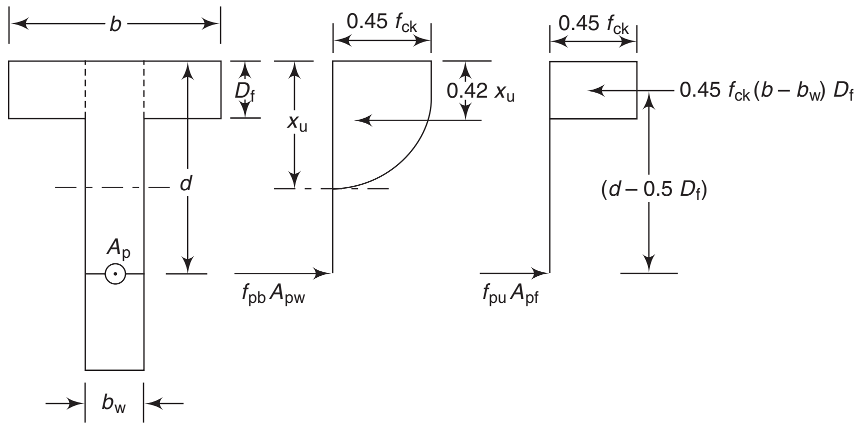

Fig. 7.8 *Moment of resistance of flanged sections ($x_u > D_f$) (IS: 1343)*

For the effective reinforcement ratio $\left(\dfrac{A_{ps}.f_{pu}}{b.d.f_{ck}}\right)$, the corresponding values of $\left(\dfrac{f_{pb}}{0.87 f_{pu}}\right)$ and (x_u/d) are interpolated from Table 7.1. The ultimate moment of resistance of the flanged section is expressed as,

$$M_u = A_{fb} A_{pw}\,(d - 0.42x_u) + 0.45 f_{ck}(b - b_w) D_f (d - 0.5 D_f)$$

The following examples illustrate the application of the IS Code provisions regarding the ultimate flexural strength of bonded prestressed concrete sections.

Example 7.3 A pretensioned prestressed concrete beam having a rectangular section with a width of 150 mm and overall depth of 350 mm is prestressed by tendons of effective area 461 mm^2 at an effective depth of 300 mm. Assuming the characteristic strength of concrete and steel as 40 and 1600 N/mm^2, estimate the ultimate flexural strength of the section using the provisions of the Indian Standard Code.

Solution.

Given data: $f_{ck} = 40$ N/mm^2 $\quad b = 150$ mm

$f_{pu} = 1600$ N/mm^2 $\quad d = 300$ mm

$A_p = 461$ mm^2

The effective reinforcement ratio is given by

$$\left(\frac{A_{ps} \cdot f_{pu}}{b.d.f_{ck}}\right) = \left(\frac{461 \times 1600}{150 \times 300 \times 40}\right) = 0.40$$

From Table 7.1, the corresponding values are interpolated as,

$$\left(\frac{f_{pb}}{0.87 f_{pu}}\right) = 0.9 \text{ and } \left(\frac{x_u}{d}\right) = 0.783$$

$$\therefore \quad f_{pb} = (0.87 \times 0.9 \times 1600) = 1253 \text{ N/mm}^2$$

$$x_u = (0.783 \times 300) = 234.9 \text{ mm}$$

$$\begin{aligned} M_u &= f_{pb} A_{ps}(d - 0.42 x_u) \\ &= (1253 \times 461)(300 - 0.42 \times 234.9) \\ &= (116 \times 106) \text{ N mm} \\ &= 116 \text{ kN m} \end{aligned}$$

Example 7.4 A pretensioned T-beam has a flange width of 300 mm and thickness of 200 mm. The rib is 150 mm wide by 350 mm deep. The beam is prestressed by tendons of cross-sectional area 200 mm^2 at an effective depth of 500 mm. If $f_{ck} = 50$ N/mm^2 and $f_{pu} = 1600$ N/mm^2, estimate the flexural strength of the section using the Indian Standard specifications.

Solution.

Given data: $f_{ck} = 50$ N/mm^2 $\quad b = 300$ mm

$f_{pu} = 1600$ N/mm^2 $\quad d = 500$ mm

$A_p = 200$ mm^2

The effective reinforcement ratio is given by

$$\left(\frac{A_{ps} . f_{pu}}{b.d.f_{ck}}\right) = \left(\frac{200 \times 1600}{300 \times 500 \times 50}\right) = 0.04$$

From Table 7.1, the corresponding values are interpolated as,

$$\left(\frac{f_{pb}}{0.87 f_{pu}}\right) = 1.0 \text{ and } \left(\frac{x_u}{d}\right) = 0.09$$

$$\therefore \quad f_{pb} = (0.87 \times 1.0 \times 1600) = 1392 \text{ N/mm}^2$$

$$x_u = (0.09 \times 500) = 45 \text{ mm}$$

The assumption that neutral axis falls within the flange is correct. Hence, the ultimate flexural strength of the T-section is computed as,

$$\begin{aligned} M_u &= f_{pb} A_{ps}(d - 0.42 x_u) \\ &= (1392 \times 200)(500 - 0.42 \times 45) \\ &= (134 \times 10^6) \text{ N mm} \\ &= 134 \text{ kN m} \end{aligned}$$

Example 7.5 A precast pretensioned T-beam has a flange width of 1200 mm and thickness of 150 mm. The width and depth of the rib are 300 and 1500 mm, respectively. The high tensile steel tendons of cross-sectional area 4700 mm^2 are located at an effective depth of 1600 mm. If the characteristic strength of concrete and steel are 40 and 1600 N/mm^2, respectively, calculate the flexural strength of the T-section using Indian Standard Code provisions.

Solution.

Given data: $f_{ck} = 40$ N/mm^2 $\quad b = 1200$ mm

$f_{pu} = 1600$ N/mm^2 $\quad d = 1600$ mm

$A_p = 4700$ mm^2 $\quad D_f = 150$ mm

$b_w = 300$ mm

The area of steel being large, the neutral axis depth is likely to exceed the thickness of the flange.

$$A_p = (A_{pw} + A_{pf})$$

and

$$A_{pf} = 0.45\, f_{ck}\,(b - b_w)\,(D_f / f_{pu})$$

$$= (0.45 \times 40)(1200 - 300)\left(\frac{150}{1600}\right)$$

$$= 1518 \text{ mm}^2$$

$$\therefore \quad A_{pw} = (4700 - 1518) = 3182 \text{ mm}^2$$

Hence, the ratio $\left(\dfrac{A_{pw} \cdot f_{pu}}{b_w \cdot d \cdot f_{ck}}\right) = \left(\dfrac{3182 \times 1600}{300 \times 1600 \times 40}\right) = 0.265$

From Table 7.1, the corresponding values are interpolated as,

$$\left(\frac{f_{pb}}{0.87 f_{pu}}\right) = 1.0 \text{ and } \left(\frac{x_u}{d}\right) = 0.56$$

$$\therefore \quad f_{pb} = (0.87 \times 1600) = 1392 \text{ N/mm}^2 \text{ and } x_u = (0.56 \times 1600) = 896 \text{ mm}$$

$$M_u = f_{pb} A_{pw}(d - 0.42x_u) + 0.45 f_{ck}(b - b_w)D_f(d - 0.5D_f)$$

$$= (1392 \times 3182)(1600 - 0.42 \times 896) + (0.45 \times 40(1200 - 300)150(1600 - 0.5 \times 150)$$

$$= [(5420 \times 10^6) + (3705 \times 10^6)]$$

$$= (9125 \times 10^6) \text{ N mm}$$

$$= 9125 \text{ kN m}$$

Example 7.6 A post-tensioned prestressed concrete bridge deck slab has the following design parameters. Estimate the ultimate flexural strength of the slab according to the Indian Standard Code specifications.

Solution.

$b = 1000$ mm $\quad f_{ck} = 40$ N/mm^2 $\quad A_{ps} = 1408$ mm^2

$d = 445$ mm $\quad f_{pu} = 1500$ N/mm^2

Compute the ratio $\left(\dfrac{A_{ps} f_{pu}}{b.d.f_{ck}}\right) = \left(\dfrac{1408 \times 1500}{1000 \times 445 \times 40}\right) = 0.118$

Refer Table 7.1 and interpolate the values of the ratios $\left(\dfrac{f_{pb}}{0.87 f_{pu}}\right)$ and (x_u/d) as,

$$\left(\frac{f_{pb}}{0.87 f_{pu}}\right) = 1.0 \text{ and } (x_u/d) = 0.267$$

Hence, $\quad f_{pb} = (1.0 \times 0.87 \times 1500) = 1305$ N/mm^2

and $\quad x_u = (0.267 \times 445) = 118.8$ mm

$\therefore$
$$\begin{aligned} M_u &= f_{pb} A_{ps} (d - 0.42\, x_u) \\ &= [(1305 \times 1408)(445 - 0.42 \times 118.8)] \\ &= (727.8 \times 10^6)\text{N mm} = 727.8 \text{ kN m} \end{aligned}$$

Example 7.7 A post-tensioned bridge girder with bonded tendons is of box section having overall dimensions 1200 mm wide and 1800 mm deep, with wall thickness of 150 mm. The high tensile steel located at an effective depth of 1600 mm has a cross-sectional area of 4000 mm^2. If the characteristic strength of concrete and steel are 40 and 1600 N/mm^2, respectively, estimate the flexural strength of the box girder using Indian Standard Code specifications.

Solution.

Given data: $\quad A_{ps} = 4000$ mm^2 $\quad f_{ck} = 40$ N/mm^2

$b_w = 300$ mm $\quad f_{pu} = 1600$ N/mm^2

$d = 1600$ mm $\quad D_f = 150$ mm

$b = 1200$ mm

$$\begin{aligned} A_{ps} &= (A_{pw} + A_{pf}) \\ A_{pf} &= 0.45\, f_{ck}\, (b - b_w)\, (D_f/f_{pu}) \\ &= (0.45 \times 40)\,(1200 - 300)\,(150/1600) \\ &= 1518 \text{ mm}^2 \\ A_{pw} &= (4000 - 1518) = 2482 \text{ mm}^2 \end{aligned}$$

$$\text{Ratio } \left(\frac{A_{pw} f_{pu}}{b_w d f_{ck}}\right) = \left(\frac{2482 \times 1600}{300 \times 1600 \times 40}\right) = 0.206$$

Refer Table 7.1 and interpolate the following values

$$\left(\frac{f_{pb}}{0.87 f_{pu}}\right) = 0.95 \text{ and } \left(\frac{x_u}{d}\right) = 0.414$$

$$f_{pb} = (0.95 \times 0.87 \times 1600) \text{ and } x_u = (0.414 \times 1600) = 662.4 \text{ mm}$$
$$= 1322 \text{ N/mm}^2$$
$$M_u = f_{pb}A_{pw}(d - 0.42x_u) + 0.45f_{ck}(b - b_w)D_f(d - 0.5D_f)$$
$$= (1322 \times 2482)(1600 - 0.42 \times 662.4) + (0.45 \times 40)(1200 - 300)150(1600 - 0.5 \times 150)$$
$$= (4338 + 3705) \times 10^6 \text{ N mm}$$
$$= 8043 \text{ kN m}$$

7.3.2 British Code Provisions

The British Code BS EN: 1992-1-1-2004 provides that for structural concrete members, the stress distribution in concrete at the limit state of collapse may be assumed to be rectangular with an average stress having values expressed as a function of the characteristic compressive strength of concrete. The depth of the rectangular stress block is also expressed as a function of neutral axis depth. For computations of the ultimate moment of resistance of the concrete section, the stress and strain distribution at the collapse state is assumed with values as shown in Fig. 7.9(a).

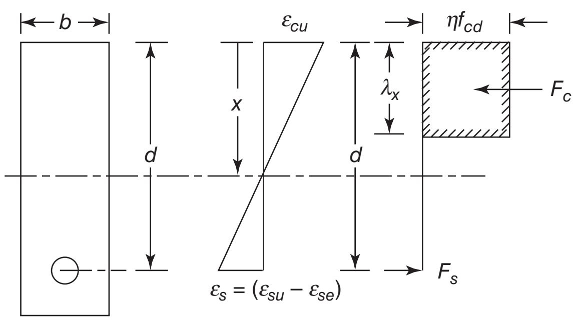

Fig. 7.9 (a) *Rectangular stress distribution (BS EN: 1992-1-1-2004)*

Where

b = effective width of concrete section or flange in the compressive zone

d = effective depth

A_{ps} = area of prestressing tendons in tension zone

x = depth of neutral axis

ε_{cu} = ultimate strain in concrete

ε_s = ultimate strain in steel

f_{cd} = design value of concrete compressive strength
$= (\alpha_{cc}f_{ck}/\gamma_c)$

f_{ck} = characteristic compressive strength of concrete

α_{cc} = coefficient influencing the long-term effects on the compressive strength and of unfavourable effects resulting from the way the load is applied.

The recommended value for use in a country should lie between 0.8 and 1.0.

The value recommended in national Annexure for UK is 1.0.

γ_c = partial safety factor for concrete (1.5)

λ = factor depending upon the strength of concrete and defining the depth of stress block having values given as,

= 0.8 for $f_{ck} \le 50$ N/mm^2

= $[0.8 - (f_{ck} - 50)/400]$ N/mm^2 for $50 \le f_{ck} \le 90$ N/mm^2

η = factor depending upon the strength of concrete and defining the width of stress block having values given as,

= 1.0 for $f_{ck} \le 50$ N/mm^2

= $[1.0 - (f_{ck} - 50)/200]$N/mm^2 for $50 \le f_{ck} \le 90$ N/mm^2

The idealised and design stress-strain diagrams for prestressing steel are shown in Fig 7.9 (b).

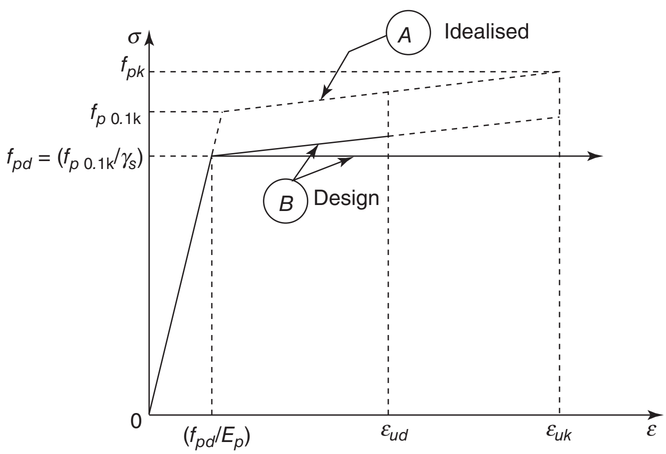

Fig. 7.9 (b) *Idealised design stress-strain diagrams for prestressing steel (BS EN: 1992-1-1-2004)*

The following assumptions are made for the values shown in the diagrams.

f_{pk} = characteristic tensile strength of prestressing steel

$f_{p0.1k}$ = characteristic 0.1 per cent proof stress of prestressing steel = 0.9 f_{pk}

γ_s = partial safety factor for steel (1.15)

E_p = design value of modulus of elasticity of prestressing steel which may be assumed equal to 205 GPa for wires and bars. The actual value can range from 195 to 210 GPa, depending on the manufacturing process. The design value for strands may be assumed as 195 GPa.

f_{pd} = design value of the stress in prestressing steel is taken to be $(f_{p0.1k}/\gamma_s)$

ε_{uk} = characteristic strain of prestressing steel at maximum load
ε_{ud} = design ultimate strain with the recommended value = 0.9 ε_{uk} = 0.02

When determining the ultimate moment of resistance of prestressed concrete sections, the code stipulates that the compressive strain in concrete should be limited to 0.26 to 0.31 per cent depending upon the characteristic strength of concrete and the stress-strain curve of the tendon.

Also, the initial strain in the prestressing tendons is taken into account when assessing the stresses in the tendons. The strains in the tendons should be limited ε_{ud} as shown in Fig. 7.9 (b).

The British code prescribes that the design of prestressed concrete structural elements should be based on the actual stress/strain relationship, if this is known, with the stress above the elastic limit reduced analogously as shown in Fig. 7.9 (b). The code also permits the use of external non-bonded tendons with the use of proper anchorages. The code also specifies detailed cover requirements based on the environmental factors and the classification of the structure. The minimum cover requirements vary from 10 mm to 65 mm.

Example 7.8 A pretensioned beam of rectangular section 400 mm wide by 600 mm deep, is stressed by high tensile steel of area 1700 mm^2 located at 100 mm from the soffit of the section. If the characteristic strength of concrete and steel are 50 and 1600 N/mm^2, respectively, estimate the ultimate moment of resistance of the section assuming the effective stress and strain in steel after all losses as 960 N/mm^2 and 0.0047, respectively, using the British and Indian Standard Code specifications.

Solution.

$$A_{ps} = 1700 \text{ mm}^2 \qquad f_{ck} = 50 \text{ N/mm}^2$$
$$b = 400 \text{ mm} \qquad f_{pu} = 1600 \text{ N/mm}^2$$
$$d = 500 \text{ mm} \qquad f_{pe} = 960 \text{ N/mm}^2$$
$$\lambda = 0.8 \qquad \eta = 1.0$$

Interpolate the value of compressive strain in concrete at failure from Fig. 7.3. Corresponding to $f_{ck} = 50$ N/mm^2, $\varepsilon_{cu} = 0.00315$ and from stress-strain curve of the prestressing steel, the value of strain corresponding to 960 N/mm^2 is interpolated as $\varepsilon_{se} = 0.0047$.

(a) British Code Method

First trial

Assume the value of neutral axis depth = $x = 200$ mm

$$\lambda x = (0.8 \times 200) = 160 \text{ mm}$$
$$\eta = 1.0$$

Design compressive strength of concrete = $F_{cd} = (\alpha_{cc} f_{ck}/\gamma_c) = [(1.0 \times 50)/1.5]$
$= 33.3$ N/mm^2

The forces in concrete and steel are computed from the stress/strain relations shown in Fig. 7.9(a) and (b).

Compressive force in concrete = $F_c = [(33.3 \times 400 \times 160)/1000] = 2133$ kN

From the strain diagram, Fig. 7.9 (a), corresponding to $\varepsilon_{cu} = 0.00315$ and $x = 200$ mm,

the value of $(\varepsilon_{su} - \varepsilon_{se}) = [(300 \times 0.00315)/200] = 0.0047$

$$\therefore \quad \varepsilon_{su} = (0.0047 + 0.0047) = 0.0094$$

From stress-strain diagram of steel, read out the stress in steel corresponding to this value of strain as $f_s = 1370$ N/mm^2

Total tensile force = $F_s = [(1370 \times 1700)/1000] = 2329$ kN

Since $F_c < F_s$, increase the value of neutral axis depth x.

Second trial

Assume the value of neutral axis depth = $x = 220$ mm

$$\lambda x = (0.8 \times 220) = 176 \text{ mm and } \eta = 1.0$$

$$F_c = [(33.3 \times 400 \times 176)/1000] = 2344 \text{ kN}$$

$$(\varepsilon_{su} - \varepsilon_{se}) = [(295 \times 0.00315)/205] = 0.0045$$

$$\therefore \quad \varepsilon_{su} = (0.0045 + 0.0047) = 0.0092 \text{ and } f_s = 1370 \text{ N/mm}^2$$

$$F_s = [(1370 \times 1700)/1000] = 2329 \text{ kN}$$

Based on the two trial values, it can be estimated that the correct value of

$$F_s = F_c \cong 0.5(2344 + 2329) = 2336 \text{ kN for } x \cong 218 \text{ mm}$$

Hence, the ultimate moment of resistance is computed as,

$$M_u = [(2336)(500 - 0.5 \times 218)/1000]$$
$$= 913 \text{ kN m}$$

(b) Indian Standard Code Method

Compute the effective reinforcement ratio $= \left(\dfrac{A_{ps} f_{pu}}{b.d.f_{ck}}\right) = \left(\dfrac{1700 \times 1600}{400 \times 500 \times 50}\right)$
$= 0.272$

From Table 7.1, interpolate the values of the ratios

$$\left(\frac{f_{pb}}{0.87 f_{pu}}\right) = 1.0 \text{ and } (x_u/d) = 0.60$$

Hence, $f_{pb} = (1 \times 0.87 \times 1600) = 1392$ N/mm^2 and $x_u = (0.60 \times 500) = 300$ mm

$$M_u = f_{pb} A_{ps} (d - 0.42 x_u)$$
$$= (1392 \times 1700)(500 - 0.42 \times 300)/1000$$
$$= 885 \text{ kN m}$$

The moment of resistance computed by the Indian and British code methods are more or less similar.

Example 7.9 A concrete beam of rectangular section 400 mm wide by 1200 mm deep, is prestressed by tendons of area 3300 mm^2 at an effective depth of 870 mm with an effective stress 960 N/mm^2 of all losses. If the characteristic compressive and tensile strength of concrete and steel are, respectively, 60 and 1700 N/mm^2, estimate the ultimate flexural strength of the section using British and Indian Standard Code provisions.

Solution.

(a) British Code method

$A_{ps} = 3300$ mm^2	$f_{ck} = 60$ N/mm^2
$b = 400$ mm	$f_{pu} = 1700$ N/mm^2
$d = 870$ mm	$f_{pe} = 960$ N/mm^2
$\lambda = [0.8 - (f_{ck} - 50)/400]$	$f_{cd} = (\alpha_{cc} f_{ck}/\gamma_c)$
$= [0.8 - (60 - 50)/400]$	$= (1.0 \times 60/1.5)$
$= 0.775$	$= 40$ N/mm^2
$\eta = [1.0 - (60 - 50)/200]$N/mm^2	$\eta\, f_{cd} = (0.95 \times 40)$
$= 0.95$	$= 38$ N/mm^2

Interpolate the value of compressive strain in concrete at failure from Fig. 7.3.

Corresponding to $f_{ck} = 60$ N/mm^2, $\varepsilon_{cu} = 0.003$ and from stress-strain curve of the prestressing steel, the value of strain corresponding to 960 N/mm^2 is interpolated as $\varepsilon_{se} = 0.0047$.

First trial

Assume the neutral axis depth = x = 400 mm

$$\lambda x = (0.775 \times 400) = 310 \text{ mm}$$

Compressive force = $F_c = [(38 \times 400 \times 310)/1000] = 4712$ kN

From strain diagram with $\varepsilon_{cu} = 0.003$ and $x = 400$ mm, $(d - x) = (870 - 400) = 470$ mm

$$(\varepsilon_{su} - \varepsilon_{se}) = [(470 \times 0.003)/400] = 0.0035$$

$$\therefore \quad \varepsilon_{su} = (0.0035 + 0.0047) = 0.0082 \text{ and } f_s = 1480 \text{ N/mm}^2$$

$$F_s = [(1480 \times 3300)/1000] = 4884 \text{ kN}$$

Since $F_c < F_s$, increase the value of neutral axis depth x.

Second trial

Assume the value of neutral axis depth = x = 410 mm and $\eta x = (0.95 \times 410) = 390$ mm

$$\lambda x = (0.775 \times 410) = 318 \text{ mm}$$

$$F_c = [(38 \times 400 \times 318)/1000] = 4833 \text{ kN}$$

$$(\varepsilon_{su} - \varepsilon_{se}) = [(460 \times 0.003)/410] = 0.0033$$

$$\therefore \quad \varepsilon_{su} = (0.0033 + 0.0047) = 0.008 \text{ and } f_s = 1480 \text{ N/mm}^2$$

$$F_s = [(1480 \times 3300)/1000] = 4884 \text{ kN}$$

Based on the two trial values, it can be estimated that the correct value of

$$F_s = F_c \cong 0.5(4833 + 4884) = 4858 \text{ kN for} \cong 412 \text{ mm}$$

Hence, the ultimate moment of resistance is computed as,

$$M_u = [(4858)(870 - 0.5 \times 0.95 \times 412)/1000]$$
$$= 3279 \text{ kN m}$$

(b) Indian Code Method

Compute the effective reinforcement ratio $= \left(\dfrac{A_{ps} f_{pu}}{b.d.f_{ck}}\right) = \left(\dfrac{3300 \times 1700}{400 \times 870 \times 60}\right)$

$$= 0.27$$

From Table 7.1, interpolate the values of the ratios

$$\left(\frac{f_{pb}}{0.87 f_{pu}}\right) = 1.0 \text{ and } (x_u/d) = 0.60$$

Hence, $f_{pb} = (1 \times 0.87 \times 1700) = 1479$ N/mm^2 and $x_u = (0.60 \times 870) = 522$ mm

$$M_u = f_{pb} A_{ps} (d - 0.42\, x_u)$$
$$= (1479 \times 3300)(870 - 0.42 \times 522)/1000$$
$$= 3177 \text{ kN m}$$

The moment of resistance computed by the Indian and British code methods are more or less similar.

Example 7.10 A post-tensioned bonded prestressed concrete beam of tee section has a flange width of 1500 mm and depth of 250 mm. The thickness and depth of the web are 200 and 1400 mm, respectively. The girder is prestressed by high tensile cables of cross-sectional area 5000 mm^2 located at an effective depth of 1600 mm. If the characteristic strength of concrete and steel are 40 and 1600 N/mm^2, estimate the ultimate flexural strength of the tee section using the British and Indian Code methods.

Solution.

Given data: $A_{ps} = 5000$ mm^2 $\qquad f_{ck} = 40$ N/mm^2

$b = 1500$ mm & $b_w = 200$ $\qquad f_{pu} = 1600$ N/mm^2

$d = 1600$ mm & $h_f = 250$ mm $\qquad f_{pe} = 960$ N/mm^2

$\lambda = 0.8$ $\qquad f_{cd} = (\alpha_{cc} f_{ck}/\gamma_c)$

$\eta = 1.0$ $\qquad = (1.0 \times 40/1.5) = 26.6$ N/mm^2

$f_{pd} = (f_{pu}/\gamma_s) = (1600/1.15)$

$= 1392$ N/mm^2

(a) British Code Method

From Fig 7.3, interpolate the value of $\varepsilon_{cu} = 0.0033$ for $f_{ck} = 40$ N/mm^2.

First trial

Assume the neutral axis depth = x = 250 mm

$$\lambda x = (0.8 \times 250) = 200 \text{ mm}$$

Compressive force = F_c = [(26.6 × 1500 × 200)/1000] = 7980 kN

From strain diagram,

$$(\varepsilon_{su} - \varepsilon_{se}) = [(1350 \times 0.0033)/250] = 0.0178$$

$$\therefore \quad \varepsilon_{su} = (0.0178 + 0.0047) = 0.022 \text{ and } f_s = 1392 \text{ N/mm}^2$$

$$F_s = [(1392 \times 5000)/1000] = 6960 \text{ kN}$$

Since $F_c > F_s$, decrease the value of neutral axis depth x for the second trial.

Second trial

$$x = 220 \text{ mm}$$

$$\lambda x = (0.8 \times 220) = 176 \text{ mm}$$

$$F_c = [(26.6 \times 1500 \times 176)/1000] = 7038 \text{ kN}$$

The value of F_s will not change and is equal to 6960 kN.

The correct value of $F_s = F_c \cong 0.5(6960 + 7038) = 7000$ kN for $x \cong 220$ mm. Hence, the ultimate moment of resistance is computed as,

$$M_u = [(7000)(1600 - 0.5 \times 220)/1000]$$

$$= 10430 \text{ kN m}$$

(b) Indian Code Method

Compute the effective reinforcement ratio = $\left(\dfrac{A_{ps} f_{pu}}{b.d.f_{ck}}\right) = \left(\dfrac{5000 \times 1600}{1500 \times 16000 \times 40}\right)$ = 0.083.

From Table 7.1, interpolate the values of the ratios

$$\left(\frac{f_{pb}}{0.87 f_{pu}}\right) = 1.0 \text{ and } (x_u/d) = 0.15$$

Hence, $f_{pb} = (1 \times 0.87 \times 1600) = 1392$ N/mm^2 and $x_u = (0.15 \times 160000) = 240$ mm

$$M_u = f_{pb} A_{ps} (d - 0.42\, x_u)$$

$$= (1392 \times 5000)\,(1600 - 0.42 \times 240)/1000$$

$$= 10433 \text{ kN m}$$

The moment of resistance computed by the Indian and British code methods are more or less similar.

Example 7.11 A pretensioned beam of rectangular section 300 mm wide and 700 mm deep, is stressed by 800 mm^2 of high-tensile steel located at effective depth of 600 mm. The beam is also reinforced with supplementary reinforcements consisting of four bars of 25 mm diameter of Fe-415 grade HYSD steel, located 100 mm from the soffit. Estimate the flexural strength of the section. Assume the ultimate tensile strength of tendons as 1600 N/m^2 and the characteristic cube strength of concrete of as 40 N/mm^2.

Solution.

Given data: $b = 300$ mm $\quad d = 600$ mm

$f_{ck} = 40$ N/mm^2 $\quad f_p = 1600$ N/mm^2

$f_y = 415$ N/mm^2 $\quad A_p = 800$ mm^2

$A_s = 1964$ mm^2

The untensioned supplementary reinforcement is replaced by an equivalent area of prestressing steel given by the relation

$$\left(\frac{A_s f_y}{f_p}\right) = \left(\frac{1964 \times 415}{1600}\right) = 509 \text{ mm}^2$$

Total area of prestressing steel = $A_p = (800 + 509) = 1309$ mm^2

$$\text{Ratio} \quad \left(\frac{f_p A_p}{f_{ck} b d}\right) = \left(\frac{1600 \times 1309}{40 \times 300 \times 600}\right) = 0.29$$

From Table 7.1, the corresponding value of $\left(\dfrac{f_{pb}}{0.87 f_p}\right) = 0.86$ and $\left(\dfrac{x_u}{d}\right) = 0.63$.

Hence, we have

$$f_{pb} = (0.86 \times 0.87 \times 1600) = 1197 \text{ N/mm}^2$$

$$x_u = (0.63 \times 600) = 378 \text{ m}$$

$$\begin{aligned} M_u &= f_{pb} A_p (d - 0.42\, x_u) \\ &= (1197 \times 1309)(600 - 0.42 \times 378) \\ &= (691.36 \times 10^6) \text{ N mm} \\ &= 691.36 \text{ kN m} \end{aligned}$$

7.3.3 American Code Recommendations

The building code requirements of the American Concrete Institute ACI: 318M–2011 recommends separate expressions for estimating the ultimate moment capacity of under-reinforced and over-reinforced rectangular and flanged sections with or without compression reinforcement. The expressions are based on the assumption that the maximum strain in concrete, $\varepsilon_{cu} = 0.003$, and the average concrete compressive stress in the rectangular stress block is $0.85\, f'_c$ at the limit state of flexural failure. The following notations are applicable in the various strength equations:

A_{ps} = area of prestressing reinforcement in the tension zone (mm^2)

A_s = area of non-prestressed reinforcement in the tension zone (mm^2)

= area of non-prestressed reinforcement in the compression zone (mm^2)

b = width of compression face of a member (mm)

b_w = thickness of web in flanged sections (mm)

d = effective depth of non-prestressed reinforcement (mm)

h_f = thickness of flange

d' = cover to compression reinforcement (mm)

d_p = effective depth to prestressing tendons (mm)

f'_c = specified compressive strength of concrete (N/mm^2)

f_{ps} = stress in prestressed reinforcement at limit state of failure (N/mm^2)

f_{pu} = specified tensile strength of tendons (N/mm^2)

f_{py} = specified yield strength of tendons (N/mm^2)

f_y = specified yield strength of non-prestressed reinforcement (N/mm^2)

f_{se} = effective stress in prestressed reinforcement (after allowance for all losses) (N/mm^2)

ρ = ratio of non-prestressed tension reinforcement

$$= \left(\frac{A_s}{bd}\right)$$

ρ' = ratio of compression reinforcement

$$= \left(\frac{A'_s}{bd}\right)$$

ρ_p = ratio of prestressed reinforcement

$$= \left(\frac{A_{ps}}{bd_p}\right)$$

$$\left.\begin{aligned} \omega &= \left(\frac{\rho f_y}{f'_c}\right) \\ \omega' &= \left(\frac{\rho f_y}{f'_c}\right) \\ \omega_\rho &= \left(\frac{\rho_p f_{ps}}{f'_c}\right) \end{aligned}\right\} \text{Effective reinforcement index}$$

ω_w, ω_{pw}, ω'_w = reinforcement indices for flanged sections computed for ω and ω' except that b shall be the web width b_w and the reinforcement area shall be that required to develop the compressive strength of the web only.

β_1 = a factor depending upon the compressive strength of concrete given by

$$\beta_1 = \{0.85 - (f'_c - 30)0.008\}$$

except that β_1 shall not be taken to be less than 0.65 (corresponding to $f'_c = 56$ N/mm^2).

γ_p = a factor depending upon the type of prestressing tendons having values

= 0.55 for (f_{py}/f_{pu}) not less than 0.80

= 0.40 for (f_{py}/f_{pu}) not less than 0.85

= 0.28 for (f_{py}/f_{pu}) not less than 0.90

For bonded tendons, the ACI 318M–2011 permits the value of f_{ps} to be taken as follows provided f_{sc} is not less than 0.50 f_{pu}. Thus,

$$f_{ps} = f_{pu}\left[1 - \frac{\gamma_p}{\beta_1}\left\{\rho_p\left(\frac{f_{pu}}{f'_c}\right) + \frac{d}{d_p}(\omega - \omega')\right\}\right]$$

If compression reinforcement is included ($\omega' > 0$), the term

$$\rho_p\left(\frac{f_{pu}}{f'_c}\right) + \frac{d}{d_p}(\omega - \omega')$$

shall be taken not less than 0.17 and d' shall not be greater than 0.15 d_p.

Limitation of effective reinforcement index The reinforcements in under-reinforced sections, which fail by yielding of reinforcement, should satisfy the following conditions:

$$\omega_p \le 0.36\beta_1$$

$$\omega_p + \frac{d}{d_p}(\omega - \omega') \le 0.36\,\beta_1$$

$$\left[\omega_{pw} + \frac{d}{d_p}(\omega_w - \omega'_w)\right] \le 0.36\,\beta_1$$

For sections satisfying the above conditions, the ultimate flexural strength is computed by using the following relations:

Sections with tension reinforcement only (bonded tendons) Referring to Fig. 7.10 For rectangular or flanged sections in which the depth of the stress block (a) does not exceed the thickness of the flange (h_f), the ultimate moment M_n is computed by:

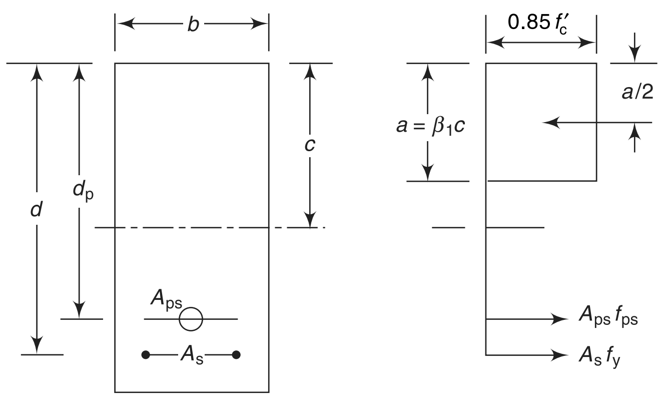

Fig. 7.10 *Moment of resistance of rectangular sections (ACI: 318M-2011)*

$$M_u = \left[A_{pw} f_{ps}\left(d_p - \frac{a}{2}\right) + A_s f_y\left(d - \frac{a}{2}\right)\right]$$

where $$a = \left[\frac{A_{ps} f_{ps} + A_s f_y}{0.85 f'_c.b}\right]$$

When the compression flange thickness (h_f) is less than the depth of the stress block (a), as shown in Fig. 7.11, the ultimate moment may be computed by:

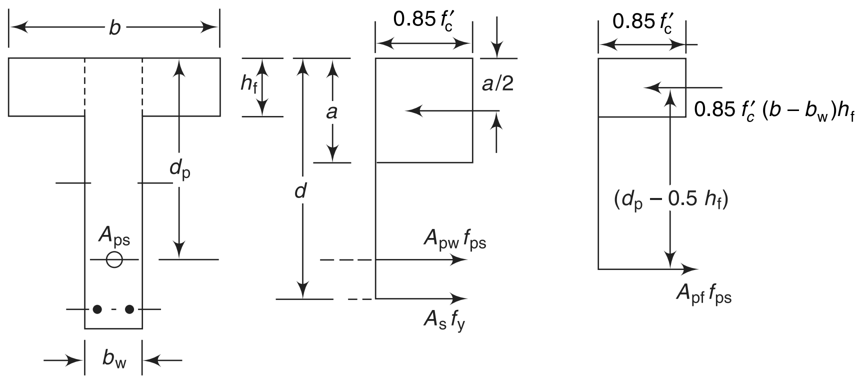

Fig. 7.11 *Moment of resistance of flanged sections (ACI: 318M-2011)*

$$M_u = \left[A_{pw} f_{ps}\left(d_p - \frac{a}{2}\right) + A_s f_y (d - d_p) + 0.85 f'_c (b - b_w) h_f (d_p - 0.5 h_f)\right]$$

where $$A_{pw} = \left[A_{ps} + A_s\left(\frac{f_y}{f_{ps}}\right) - \frac{0.85 f'_c (b - b_w) h_f}{f_{ps}}\right]$$

and $$a = \left(\frac{A_{pw} f_{ps}}{0.85 f'_c b_w}\right)$$

Rectangular sections with compression reinforcement For rectangular sections, the ultimate moment M_n is computed as follows:

If $$\left[\frac{A_{ps} f_{ps} + A_s f_y - A'_s f_y}{bd}\right] \geq 0.85 \beta_1 f'_c \left(\frac{d'}{d}\right)\left(\frac{600}{600 - f_y}\right)$$

then

$$M_u = \left[A_{ps} f_{ps}\left(d_p - \frac{a}{2}\right) + A_s f_y\left(d - \frac{a}{2}\right) + A'_s f_y\left(\frac{a}{2} - d'\right)\right]$$

where $$a = \left[\frac{A_{ps} f_{ps} + A_s f_y - A'_s f_y}{0.85 f'_c b}\right]$$

When the value of $[(A_{ps}f_{ps} + A_s f_y - A'_s f_y)/bd]$ is less than the value specified above, the stress in the compression reinforcement is less than the yield strength f_y. In such cases, the effect of compression reinforcement may be neglected and a conservative estimate of the moment capacity may be obtained by equations given for rectangular sections. However, a rigorous analysis based on stress-strain compatibility will yield an accurate estimate of the ultimate moment capacity of the section.

Sections with unbonded tendons For members with unbonded tendons and with a span/depth ratio not exceeding 35, the stress in tendons at failure is computed by the relation,

$$f_{ps} = \left[f_{se} + 70 + \frac{f'_c}{100\rho_p} \right]$$

but f_{ps} is limited to the values of f_{py} or $(f_{se} + 420)$.

For members with unbonded tendons having a span/depth ratio exceeding 35,

$$f_{ps} = \left[f_{se} + 70 + \frac{f'_c}{300\rho_p} \right]$$

but f_{ps} is limited to the values of f_{py} or $(f_{se} + 210)$.

Moment capacity of over reinforced sections Rectangular or flanged sections having the effective reinforcement index exceeding 0.36 β_1 are considered as over-reinforced, and when the neutral axis lies within the flange, the ultimate moment is computed by the relation,

$$M_u = f'_c b d^2{}_p (0.36\beta_1 - 0.08\beta_1^2)$$

For flanged sections in which the neutral axis is located outside the flange, the ultimate moment is computed by the relation,

$$M_u = [f'_c b_w d_p^2 \; (0.36\beta_1 - 0.08) + 0.85\, f'_c (b - b_w) h_f (d_p - 0.5h_f)]$$

Example 7.12 A pretensioned prestressed concrete beam of rectangular section 150 mm wide and 350 mm deep, has an effective cover of 50 mm. If $f'_c = 40$ N/mm^2, $f_{pu} = 1600$ N/mm^2, $(f_{py}/f_{pu}) = 0.90$, determine, using ACI 318M–2011 recommendations:

(a) The minimum area of prestressing steel to avoid failure of section by fracture of steel;
(b) The maximum area of prestressing steel which just ensures failure by yielding of steel;
(c) Ultimate flexural strength corresponding to case (b); and
(d) The ultimate flexural strength of the section if the area of prestressing steel in case (b) is doubled in the section.

Solution.

Case (a) Minimum area A_{ps} of prestressing steel is given by

$$A_{ps} = 0.004\,A \qquad \text{where } A = (bh/2)$$
$$= [0.004(150 \times 350)/2] = 105 \text{ mm}^2$$

Case (b) $\beta_1 = [0.85 - (f'_c - 30)\, 0.008] = [0.85 - (40 - 30)0.008] = 0.77$

The maximum effective reinforcement index which just ensures of failure of section by yielding of steel is given by

$$\omega_p = 0.36\,\beta_1$$

$$\left(\frac{A_{ps} f_{ps}}{b d_p f'_c}\right) = 0.36\beta_1$$

$$\therefore \qquad A_{ps} = \left(\frac{0.36\,\beta_1 . b . d_p \cdot f'_c}{f_{ps}}\right)$$

where
$$f_{ps} = f_{pu}\left[1 - \frac{\gamma_p}{\beta_1}\left\{\rho_p\left(\frac{f_{pu}}{f'_c}\right)\right\}\right]$$

$$= 1600\left[1 - \frac{0.28}{0.77}\left\{\left(\frac{A_{ps}}{150 \times 300}\right)\left(\frac{1600}{40}\right)\right\}\right] = (1600 - 0.52\,A_{ps})$$

$$\therefore \qquad A_{ps}(1600 - 0.52 A_{ps}) = 0.36\beta_1 \cdot b \cdot d_p \cdot f'_c$$

$$= (0.36 \times 0.77 \times 150 \times 300 \times 40) = 4{,}98{,}960$$

or
$$[A_{ps}^2 - 3077\,A_{ps} + 9{,}59{,}538] = 0$$

Solving, we get,

$$A_{ps} = 350 \text{ mm}^2$$

$$f_{ps} = (1600 - 0.52 \times 350) = 1418 \text{ N/mm}^2$$

Case (c)

$$M_u = A_{ps} f_{ps}\left(d_p - \frac{a}{2}\right)$$

where
$$a = \left(\frac{A_{ps} f_{ps}}{0.85 f'_c b}\right)$$

$$a = \left(\frac{350 \times 1418}{0.85 \times 40 \times 150}\right) = 97.31 \text{ mm}$$

$$\therefore \qquad M_u = 350 \times 1418\,(300 - 0.5 \times 97.31)$$

$$= 124.7 \times 10^6 \text{ N mm} = 124.7 \text{ kN m}$$

Case (d) If the area of prestressing steel is doubled,

$$A_{ps} = (2 \times 350) = 700 \text{ mm}^2$$

and
$$\omega_p > 0.36\,\beta_1$$

Hence, the section is over-reinforced.

$$\therefore \qquad M_u = f'_c b d_p^2 \,(0.36\beta_1 - 0.08\,\beta_1^{\,2})$$

$$= 40 \times 150 \times 300^2(0.36 \times 0.77 - 0.08 \times 0.77^2)$$

$$= 124.1 \times 10^6 \text{ N mm} = 124.1 \text{ kN m}$$

Example 7.13 An unsymmetrical I-section has a top flange-width of 300 mm. The thickness of the flange varies from 80 mm at the ends to 100 mm at the junction of the web, which is 80 mm thick. The effective depth to the tendons is 400 mm. Given $= 40$ N/mm^2, $f_{pu} = 1600$ N/mm^2, the ratio $(f_{py}/f_{pu}) = 0.90$, $f_{se} = 800$ N/mm^2, and $A_{ps} = 400$ mm^2, estimate the flexural strength of the section if it is (a) fully bonded, (b) unbonded, using ACI 318–2005 code provisions. Assume the equivalent uniform thickness of flange, h_f as 87.3 mm.

Solution.

$$A_{ps} = 400 \text{ N/mm}^2$$

$$f_{ps} = f_{pu}\left[1 - \frac{\gamma_p}{\beta_1}\left\{\frac{A_{ps} f_{pu}}{b d_p f'_c}\right\}\right]$$

$$\gamma_p = 0.28 \text{ and } \beta_1 = 0.77 \text{ for } f'_c = 40 \text{ N/mm}^2$$

$$f_{ps} = 1600\left[1 - \left(\frac{0.28}{0.77}\right)\left\{\frac{400 \times 1600}{300 \times 400 \times 40}\right\}\right]$$

$$= 1522 \text{ N/mm}^2$$

$$a = \left[\frac{A_{ps} f_{ps}}{0.85\, f'_c b}\right]$$

$$= \left[\frac{400 \times 1522}{0.85 \times 40 \times 300}\right] = 59.68 \text{ mm}$$

Hence, the depth of the stress block is less than the thickness of the flange.

(a) Bonded tendons

$$M_u = A_{ps}\, f_{ps}\left(d_p - \frac{a}{2}\right)$$

$$= [400 \times 1522(400 - 0.5 \times 59.6)]$$

$$= (225.3 \times 10^6) \text{ N mm} = 225.3 \text{ kN m}$$

(b) Unbonded tendons

$$f_{ps} = \left[f_{se} + 70 + \frac{f'_c}{100\rho_p}\right]$$

$$\rho_p = \left(\frac{A_{ps}}{b d_p}\right) = \left(\frac{400}{300 \times 400}\right) = 0.0033$$

$$\therefore \qquad f_{ps} = \left[800 + 70 + \frac{40}{100 \times 0.0033}\right]$$

$$= 991.2 \text{ N/mm}^2$$

$$M_u = A_{ps} f_{ps}\left(d_p - \frac{a}{2}\right)$$

$$= (400 \times 991.2)\left(400 - \frac{59.6}{2}\right) = (146.7 \times 10^6) \text{ N mm} = 146.7 \text{ kN m}$$

Example 7.14 A pretensioned beam of rectangular section 300 mm wide and 700 mm deep, is stressed by 800 mm^2 of high-tensile steel at an effective depth of 600 mm. The beam is reinforced with supplementary steel consisting of two bars each of 25 mm diameter located 100 mm from the soffit. Given $f'_c = 40$ N/mm^2, $f_{pu} = 1600$ N/mm^2, $f_y = 460$ N/mm^2, $(f_{py}/f_{pu}) = 0.92$, estimate the moment capacity of the section according ACI 318M–2011 code provisions.

Solution.

Given data:

$A_{ps} = 800$ mm^2 $\qquad b = 300$ mm

$A_s = 982$ mm^2 $\qquad d = d_p = 600$ mm

$f_{pu} = 1600$ N/mm^2 $\qquad \beta_1 = 0.77$

$f_y = 460$ N/mm^2 $\qquad \gamma_p = 0.28$

$f'_c = 40$ N/mm^2

Thus, $$\rho_p = \left(\frac{A_{ps}}{bd_p}\right) = \left(\frac{800}{300 \times 600}\right) = 0.0044$$

and $$\omega = \left(\frac{A_s f_y}{bdf'_c}\right) = \left(\frac{982 \times 460}{300 \times 600 \times 40}\right) = 0.0627$$

$$f_{ps} = f_{pu}\left[1 - \frac{\gamma_p}{\beta_1}\left\{\rho_p\left(\frac{f_{pu}}{f'_c}\right) + \frac{d}{d_p}(\omega - \omega')\right\}\right]$$

$$= 1600\left[1 - \left(\frac{0.28}{0.77}\right)\left\{0.0044\left(\frac{1600}{40}\right) + \left(\frac{1600}{40}\right) + \frac{600}{600}(0.0627 - 0)\right\}\right]$$

$$= 1462 \text{ N/mm}^2$$

$$\omega_p = \left(\frac{A_{ps} f_{ps}}{bd_p f'_c}\right) = \left(\frac{800 \times 1462}{300 \times 600 \times 40}\right) = 0.162$$

For the section to be under-reinforced,

$$\omega_p + \frac{d}{d_p}(\omega - \omega') \le 0.36\,\beta_1$$

or $$\left[0.162 + \frac{600}{600}(0.0627 - 0)\right] \le (0.36 \times 0.77)$$

or $$0.225 \le 0.275$$

Hence, the section is under-reinforced.

$$a = \left[\frac{A_{ps}f_{ps} + A_s f_y}{0.85 f_c' b}\right] = \left[\frac{(800 \times 1462) + (982 \times 460)}{0.85 \times 40 \times 300}\right]$$

$$= 159 \text{ mm}$$

$\therefore$ $$M_u = A_{ps}f_{ps}\left(d_p - \frac{a}{2}\right) + A_s f_y\left(d - \frac{a}{2}\right)$$

$$= (800 \times 1462)\left(600 - \frac{159}{2}\right) + (982 \times 460)\left(600 - \frac{159}{2}\right)$$

$$= (843.8 \times 10^6)\text{ N mm} = 843.8 \text{ kN m}$$

7.4 Comparative Analysis of Code Procedures

A comparative analysis of the various national code provisions for the estimation of flexural strength of prestressed concrete sections indicates that the Indian and British codes are more or less similar with regard to the computation of stress in high-tensile steel at failure of the section as a function of the effective reinforcement ratio. The American code is more comprehensive in its recommendations since it includes both under-reinforced and over-reinforced sections by clearly demarcating between the two types and limiting the effective reinforcement index in under-reinforced sections to a factor which depends upon the compressive strength of concrete. In addition, the American code provisions cover sections with tension and compression reinforcements, rectangular and flanged sections, with bonded and unbonded tendons. Separate expressions are recommended for over-reinforced sections which fail by crushing of concrete.

The ultimate flexural strength of under-reinforced sections, according to the British and American codes, is based on force compatibility relationships consistent with rectangular stress block, the depth of which is determined by the equilibrium of forces in the section. The Indian code provisions are based on a stress block comprising of a rectangle and parabola. In general, the stresses developed in bonded tendons gradually reduce to about 70 per cent of the characteristic tensile strength when the effective reinforcement ratio, according to the British code, reaches a value of 0.50. In the case of members with unbonded tendons, the stress in steel at failure is influenced by the effective prestress in tendons after all losses, the effective reinforcement ratio and the span/depth ratio of the member with an upper ceiling of 70 per cent of the characteristic tensile strength.

A critical review of the provisions of the three codes indicates that the American code recommendations are by far the most comprehensive and a large number of parameters are considered in the formulation of equations for the computation of moment capacity of rectangular and flanged sections.

Example 7.15 A post-tensioned bonded prestressed concrete beam is of rectangular section 200 mm wide and 400 mm deep. The beam is prestressed by 300 mm^2 of high-tensile steel located at an eccentricity of 100 mm. The characteristic tensile strength of prestressing steel is 1600 N/mm^2 and the characteristic cube compressive strength of concrete is 40 N/mm^2. Estimate the ultimate moment capacity of the section using (a) Indian, (b) British, and (c) American code regulations.

Solution. Given data:

$$A_p = A_{ps} = 300 \text{ mm}^2 \qquad b = 200 \text{ mm}$$
$$f_p = f_{pu} = 1600 \text{ N/mm}^2 \qquad d = d_p = 300 \text{ mm}$$
$$f_{pe} = 800 \text{ N/mm}^2 \qquad f_{ck} = f_{cu} = 40 \text{ N/mm}^2$$
$$f'_c = 0.8\, f_{ck} = 32 \text{ N/mm}^2$$
$$\gamma_p = 0.28$$

(a) IS: 1343 Code Procedure

$$\text{Ratio} \quad \left(\frac{A_p f_p}{b d f_{ck}}\right) = \left(\frac{300 \times 1600}{200 \times 300 \times 40}\right) = 0.2$$

From Table 7.1,

$$\left(\frac{f_{pb}}{0.87 f_p}\right) = 0.95 \quad \text{and} \quad \left(\frac{x_u}{d}\right) = 0.414$$

$$\therefore \quad f_{pb} = (0.95 \times 0.87 \times 1600) = 1322.4 \text{ N/mm}^2 \qquad x_u = (0.414 \times 300) = 124.2 \text{ mm}$$

$$\therefore \quad M_u = f_{pb} A_p (d - 0.42\, x_u)$$
$$= (1322.4 \times 300)(300 - 0.42 \times 124.2)$$
$$= (98.32 \times 10^6) \text{ N mm} = 98.32 \text{ kN m}$$

(b) BS EN: 1992-1-1 Code Procedure

For $f_{ck} = 40$ N/mm^2, $\lambda = 0.8$

$$\eta = 1.0$$

$$f_{cd} = (\alpha_{cc} f_{ck}/\gamma_c) = (1.0 \times 40/1.5) = 26.6 \text{ N/mm}^2$$

For $f_{pu} = 1600$ N/mm^2

$$f_{pd} = 0.87\, f_{pu} = (0.87 \times 1600) = 1392 \text{ N/mm}^2$$

From Fig 7.3, interpolate the value of $\varepsilon_{cu} = 0.0033$ for $f_{ck} = 40$ N/mm^2.

First trial

Assume the neutral axis depth = x = 120 mm

$$\lambda x = (0.8 \times 120) = 96 \text{ mm}$$

Compressive force = $F_c = [(96 \times 200 \times 26.6)/\ 1000] = 510$ kN
From strain diagram,

$$(\varepsilon_{su} - \varepsilon_{se}) = [(180 \times 0.0033)/120] = 0.00495$$

$$\therefore \quad \varepsilon_{su} = (0.00495 + 0.0047) = 0.0096 \text{ and } f_s = 1392 \text{ N/mm}^2$$

$$F_s = [(1392 \times 300)/1000] = 418 \text{ kN}$$

Since $F_c > F_s$, decrease the value of neutral axis depth x for the second trial.

Second trial

Assume the neutral axis depth = x = 100 mm

$$\lambda x = (0.8 \times 100) = 80 \text{ mm}$$

Compressive force = $F_c = [(80 \times 200 \times 26.6)/1000] = 425$ kN
From strain diagram,

$$(\varepsilon_{su} - \varepsilon_{se}) = [(200 \times 0.0033)/100] = 0.0066$$

$$\therefore \quad \varepsilon_{su} = (0.0066 + 0.0047) = 0.0113 \text{ and } f_s = 1392 \text{ N/mm}^2$$

$$F_s = [(1392 \times 300)/1000] = 418 \text{ kN}$$

Hence, the correct value of $F_s = F_c \cong 0.5(425 + 418) = 421$ kN for $x \cong 220$ mm.
Hence, the ultimate moment of resistance is computed as,

$$M_u = [(421)\ (300 - 0.5 \times 100)/1000]$$
$$= 105 \text{ kN m}$$

(c) ACI: 318M–2011 Code Procedure

$$\beta_1 = 0.85 - (f'_c - 30)0.008 = 0.85 - (32 - 30)0.008 = 0.834$$

$$\therefore \quad f_{ps} = f_{pu} = \left[1 - \frac{\gamma_p}{\beta_1}\left\{\rho_p\left(\frac{f_{pu}}{f'_c}\right)\right\}\right]$$

$$= 1600\left[1 - \left(\frac{0.28}{0.834}\right)\left(\frac{300}{200 \times 300}\right)\left(\frac{1600}{32}\right)\right]$$

$$= 1465 \text{ N/mm}^2$$

Ratio $\left(\dfrac{A_{ps} f_{ps}}{b d_p f_c'}\right) = \left(\dfrac{300 \times 1465}{200 \times 300 \times 32}\right) = 0.228$

But $0.36\beta_1 = (0.36 \times 0.834) = 0.30$

Since $\omega_p = 0.228 < 0.36\,\beta_1 = 0.30$

the section is under-reinforced.

$$a = \left(\frac{A_{ps} f_{ps}}{0.85 f_c' \cdot b}\right) = \left(\frac{300 \times 1465}{0.85 \times 32 \times 200}\right) = 80.73 \text{ mm}$$

$$\therefore \quad M_u = A_{ps} f_{ps}\left(d_p - \frac{a}{2}\right)$$

$$= [300 \times 1465\,(300 - 0.5 \times 80.73)]$$

$$= (114 \times 10^6) \text{ N mm} = 114 \text{ kN m.}$$

The Indian, British and American code methods result in more or less similar values of the ultimate moment of resistance of the prestressed sections.

7.5 Sections with Steel in Compression Zone

Structural concrete flexural members are generally provided with nominal reinforcements in the compression zone to support the web reinforcements. In the case of pretensioned purlins, some of the tensioned wires are located in the compression zone which serve the dual purpose of controlling the handling stresses and as hanger bars for vertical shear reinforcements. In such cases, an estimate of the ultimate strength of the members in flexure is desirable to compute the load factor against the limit state of collapse.

The rigorous strain compatibility method can be directly used if the sections are under- or over-reinforced. However, for sections designed to fail by excessive elongation of steel followed by crushing of concrete, a simplified version of the strain compatibility method can be used to estimate the flexural strength of such sections with nominal untensioned or tensioned steel in the compression zone.

7.5.1 Section with Untensioned Steel in the Compression Zone

Referring to Fig. 7.12,

A'_s = area of untensioned reinforcement in the compression zone

c = effective cover

d = effective depth

A_{ps} = area of prestressing steel in the tension zone

ε_{cu} = strain in concrete at compression face

E_s = modulus of elasticity of steel

x = depth of the rectangular stress block

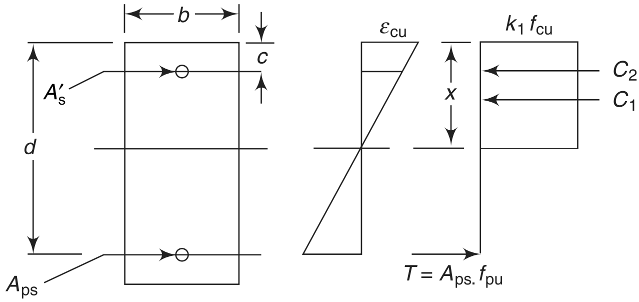

Fig. 7.12 *Moment of resistance of rectangular section with untensioned steel in the compression zone*

Strain in compression reinforcement at failure = $\varepsilon_{cu}\left(1-\dfrac{c}{x}\right)$

Stress in compression steel = $E_s\,\varepsilon_{cu}\left(1-\dfrac{c}{x}\right)$

Force in compression steel = $C_2 = A'_s E_s \varepsilon_{cu}\left(1-\dfrac{c}{x}\right)$

Force in concrete stress block = $C_1 = k_1 f_{cu}\, b\, x$

Force in tension steel = $T = A_{ps} f_{pu}$

Compatibility of forces acting on a section yield

$$A_{ps} f_{pu} = (C_1 + C_2) = k_1 f_{cu}\, b\, x + A'_s E_s\,\varepsilon_{cu}\left(1-\frac{c}{x}\right)$$

The depth of stress block is determined by trial and error from this expression and the stress in compression steel is limited to a value not exceeding the yield stress.

The ultimate moment of resistance of the section is obtained from the expression,

$$M_u = k_1 f_{cu}\, b\, x\left(d-\frac{x}{2}\right) + A'_s E_s\,\varepsilon_{cu}\left(1-\frac{c}{x}\right)(d-c)$$

7.5.2 Section with Tensioned Steel in the Compression Zone

If I_{pe} = effective prestress in wires located in the compression zone after all losses,

Stress in wires at the compressive zone = $\left[f_{pe} - E_s\varepsilon_{cu}\left(1-\dfrac{c}{x}\right)\right]$

Force in wires in the compression zone = $C_2 = A'_s \left[f_{pe} - E_s \varepsilon_{cu} \left(1 - \frac{c}{x} \right) \right]$

Force in tension steel = $A_{ps} f_{pu}$

For equilibrium of forces,

$$A_{ps} f_{pu} = (C_1 + C_2) = k_1 f_{cu}\, b\, x + A'_s \left[f_{pe} - E_s \varepsilon_{cu} \left(1 - \frac{c}{x} \right) \right]$$

The magnitude of x is estimated from this expression by trial and error and the stress in compression steel should not exceed f_{py} or 0.2 per cent of the proof stress.

The ultimate moment of resistance of the section is evaluated by the expression,

$$M_u = k_1 f_{cu}\, b\, x \left(d - \frac{x}{2} \right) + A'_s \left[f_{pe} - E_s \varepsilon_{cu} \left(1 - \frac{c}{x} \right) (d - c) \right]$$

In most cases, the effective prestress f_{pe} being not less than 50 per cent of the tensile strength of tendons, the strain of the concrete in compression zone will reduce this stress but will probably not be sufficient to cause compressive failure of the wires located in the compression zone. Consequently, these tendons have an unfavourable effect on the ultimate moment and, in cases where the failure is due to excessive elongation of steel, the effect of reinforcements in the compression zone is usually small enough to be neglected.

Example 7.16 A pretensioned prestressed concrete beam of rectangular section 100 mm wide and 250 mm overall depth, is reinforced with high-tensile steel (f_{pu} = 1600 N/mm^2) of area 150 mm^2 located at 50 mm from the soffit of the beam. Two 8 mm diameter high-yield strength deformed bars with characteristic tensile strengths of 460 N/mm^2 are provided near the compression face at an effective cover of 30 mm. If the characteristic cube strength of the concrete is 40 N/mm^2, determine the ultimate flexural strength of the section using

(a) the strain compatibility method and assuming the modulus of elasticity of steel as 210 kN/mm^2,

(b) American Concrete Institute method (ACI: 318M–2011).

Solution.

Given data:

$$f_{pu} = 1600 \text{ N/mm}^2 \qquad \left(\frac{f_{yp}}{f_{pu}} \right) = 0.90 \qquad \therefore\ \gamma_p = 0.28$$

$$f_y = 460 \text{ N/mm}^2 \qquad c = d' = 30 \text{ mm}$$

$$f_{cu} = 40 \text{ N/mm}^2 \qquad A_{ps} = 100 \text{ mm}^2$$

$$f'_c = (0.8 \times 40) = 32 \text{ N/mm}^2 \qquad A'_s = 100 \text{ mm}^2$$

$$b = 100 \text{ mm} \qquad E_s = 210 \text{ kN/mm}^2$$

$$d = 200 \text{ m}$$

(a) Strain compatibility method For $f_{cu} = 40$ N/mm^2, read out $\varepsilon_{cu} = 0.0033$, $k_1 = 0.57$ and $k_2 = 0.45$ from Fig. 7.3.

First trial

Assume x =100 mm

Force in the concrete stress block $= k_1 f_{cu}\, b\, x$

$$= (0.57 \times 40 \times 100 \times 100) = 228000 \text{ N}$$

Force in compression steel $= A'_s E_s\, \varepsilon_u \left(1 - \dfrac{c}{x}\right)$

$$= 100 \times 210 \times 10^3 \times 0.0033\ (1 - 30/100) = 48510 \text{ N}$$

Force in tensile steel $= A_{ps} f_{pu} = (150 \times 1600) = 240\,000$ N

Total compressive force = (228 000 + 48510) = 276 510 N

Since the tensile force is less than the compressive force, decrease x for the second trial.

Second trial

Assume x = 86 mm

Force in the concrete stress block = $(0.57 \times 40 \times 100 \times 86) = 196\,080$ N

Force in compression steel = $(100 \times 210 \times 10^3 \times 0.0033\ (1 - 30/86)$

$$= 45738 \text{ N}$$

Total compressive force = (196080 + 45738) = 241818 N

Total tensile force = 240 000 N

Since the compressive and tensile forces are nearly equal, force compatibility is achieved.

Stress in compression steel $= E_s\, \varepsilon_{cu} \left(1 - \dfrac{c}{x}\right)$

$$f_{sc} = 210 \times 10^3 \times 0.0033\ (1 - 30/86)$$

$$= 451.8 \text{ N/mm}^2 < f_y = 460 \text{ N/mm}^2$$

The ultimate flexural strength of the section is computed by taking moments of compressive forces. Thus,

$$M_u = k_1 f_{cu} b\, x (d - k_2 x) + A'_s f_{sc} (d - c)$$

$$= [196080(200 - 0.45 \times 86) + 100 \times 451.3\ (200 - 30)]$$

$$= (39.3 \times 10^6) \text{ N mm} = 39.3 \text{ kN m}$$

(b) American concrete institute method

$$\beta_1 = 0.85 - (f'_c - 30)\ 0.008 = 0.85 - (32 - 30)\ 0.008 = 0.834$$

$$f_{ps} = f_{pu}\left[1 - \frac{\gamma_p}{\beta_1}\left\{\rho_p\left(\frac{f_{pu}}{f'_c}\right) + \frac{d}{d_p}(\omega - \omega')\right\}\right]$$

$$\omega = 0$$

$$\omega' = \left(\frac{100 \times 460}{100 \times 200 \times 32}\right) = 0.071$$

$$\rho_p = \left(\frac{A_{ps}}{bd_p}\right) = \left(\frac{150}{100 \times 200}\right) = 0.0075$$

$\therefore$
$$f_{ps} = 1600\left[1 - \left(\frac{0.28}{0.834}\right)\left\{0.0075\left(\frac{1600}{32}\right) + 1(0 - 0.071)\right\}\right]$$

$$= 1435 \text{ N/mm}^2$$

$\therefore$
$$\omega_p = \left(\frac{A_{ps} f_{ps}}{bd_p f_c'}\right) = \left(\frac{150 \times 1435}{100 \times 200 \times 32}\right) = 0.335$$

So,
$$\omega_p + \frac{d}{d_p}(\omega - \omega') \le 0.36\,\beta_1$$

or
$$0.335 + 1(0 - 0.071) \le (0.36 \times 0.834)$$

or
$$0.264 \le 0.30$$

Hence, the section is under-reinforced.

Also, for the compression steel to reach the yield stress, the following condition has to be satisfied:

$$\left(\frac{A_{ps} f_{ps} - A_s' f_y}{bd}\right) \ge 0.85\,\beta_1\, f_c'(d'/d)\left(\frac{600}{600 - f_y}\right)$$

or
$$\left[\frac{(150 \times 1435) - (100 \times 460)}{100 \times 200}\right] < 0.85 \times 0.834 \times 32\left(\frac{30}{200}\right)\left(\frac{600}{600 - 460}\right)$$

or
$$8.66 < 14.58$$

Hence, the stress in compression steel is less than the yield strength f_y.
Therefore, the ultimate flexural strength is computed by neglecting the compression steel.
Neglecting the effect of compression steel,

$$f_{ps} = 1600\left[1 - \left(\frac{0.28}{0.834}\right)\left\{\left(\frac{150}{100 \times 200}\right)\left(\frac{1600}{32}\right)\right\}\right]$$

$$= 1399 \text{ N/mm}^2$$

$$a = \left(\frac{A_{ps} f_{ps}}{0.85 f_c' b}\right) = \left(\frac{150 \times 1399}{0.85 \times 32 \times 100}\right) = 77 \text{ mm}$$

$\therefore$
$$M_n = A_{ps} f_{ps}\left(d_p - \frac{a}{2}\right)$$

$$= [150 \times 1399(200 - 0.5 \times 77)]$$

$$= (33.89 \times 10^6)\text{ N mm} = 33.89 \text{ kN m}$$

Example 7.17 A pretensioned purlin with a rectangular section of 150 mm width and 350 mm over all depth, is stressed by high-tensile steel of area 200 mm^2 located at an effective depth of 300 mm. The section is also reinforced with two bars of 8 mm diameter, both in the tension and compression faces, at an effective cover of 50 mm.

f_{pu} = 1600 N/mm^2, f_{pe} = 800 N/mm^2, f_y = 415 N/mm^2, f_{cu} = 40 N/mm^2, E_s = 210 kN/mm^2. Estimate the moment capacity of the section using

(a) the strain compatibility method and
(b) the British code BS EN: 1992–1–1 method, neglecting the effect of compression steel.

Solution.

Given data:

$A_{ps} = 200$ mm^2	$E_s = 210$ kN/mm^2	$b = 150$ mm
$A_s = 100$ mm^2	$f_y = 415$ N/mm^2	$d = 300$ mm
$A'_s = 100$ mm^2	$f_{pu} = 1600$ N/mm^2	$c = 50$ mm
$f_{cu} = 40$ N/mm^2	$f_{pe} = 800$ N/mm^2	

(a) Strain compatibility method

For f_{cu} = 40 N/mm^2, read out ε_{cu} = 0.0033, k_1 = 0.57 and k_2 = 0.45 from Fig. 7.3.

First trial

Assume x = 100 mm

Force in the concrete stress block = $(k_1 f_{cu}\, bx)$

$$= (0.57 \times 40 \times 150 \times 100) = 342000 \text{ N}$$

Force in compression steel = $A'_s E_s \varepsilon_{cu}\left(1 - \dfrac{c}{x}\right)$

$$= 100 \times 210 \times 10^3 \times 0.0033\ (1 - 50/100) = 34650 \text{ N}$$

Force in tension steel $= (A_{ps} f_{pu} + A_s f_y)$

$$= (200 \times 1600 + 100 \times 415) = 361500 \text{ N}$$

Total compressive force = (34200 + 34650) = 376650 N

Total tensile force = 361500 N

Since the tensile force is less that the compressive force, decrease x for the second trial.

Second trial

Assume x = 96 mm

Force in the concrete stress block = (0.57 × 40 × 150 × 96) = 328320 N

Force in compression steel $= 100 \times 210 \times 10^3 \times 0.0033\left(1 - \dfrac{50}{96}\right) = 33206$ N

Total tensile force $= 361500$ N

Total compressive force $= (328320 + 33206) = 361526$ N

Since the tension is nearly equal to the compression, force compatibility is achieved.

Stress in compression steel $= E_s \varepsilon_{cu} \left(1 - \dfrac{c}{x}\right)$

$$= 210 \times 10^3 \times 0.0033 \left(1 - \frac{50}{96}\right)$$

$$= 333 \text{ N/mm}^2 < f_y = 415 \text{ N/mm}^2$$

Hence, the ultimate moment capacity of the section is expressed as,

$$M_u = k_1 f_{cu} bx(d - k_2 x) + A'_s E_s \varepsilon_{cu} \left(1 - \frac{c}{x}\right)(d - c)$$

$$= 328320\,(300 - 0.45 \times 96) + 33206\,(300 - 50)$$

$$= 92.37 \times 10^6 \text{ N mm} = 92.37 \text{ kN m}$$

(b) British Code BS EN: 1992-1-1 Method

$$A_{pse} = A_{ps} + (A_s f_y / f_{pu})$$

$$= [200 + (100 \times 415/16000]$$

$$= 226 \text{ N/mm}^2$$

For $f_{ck} = 40$ N/mm^2, $\lambda = 0.8$

$$\eta = 1.0$$

$$f_{cd} = (\alpha_{cc} f_{ck}/\gamma_c) = (1.0 \times 40/1.5) = 26.6 \text{ N/mm}^2$$

For $f_{pu} = 1600$ N/mm^2

$$f_{pd} = 0.87\, f_{pu} = (0.87 \times 1600) = 1392 \text{ N/mm}^2$$

From Fig 7.3, interpolate the value of $\varepsilon_{cu} = 0.0033$ for $f_{ck} = 40$ N/mm^2.

First trial

Assume the neutral axis depth $= x = 100$ mm

$$\lambda x = (0.8 \times 100) = 80 \text{ mm}$$

Compressive force $= F_c = [(80 \times 150 \times 26.6)/ 1000] = 319$ kN

$$(\varepsilon_{su} - \varepsilon_{se}) = [(200 \times 0.0033)/100] = 0.0066$$

$$\therefore \quad \varepsilon_{su} = (0.0066 + 0.0047) = 0.013 \text{ and } f_s = 1392 \text{ N/mm}^2$$

$$F_s = [(1392 \times 226)/1000] = 314 \text{ kN}$$

Hence, the correct value of $F_s \cong F_c = 314$ kN.

Hence, the ultimate moment of resistance is computed as,

$$M_u = [(314)\,(300 - 0.5 \times 100)/1000] = 78.5 \text{ kN m}$$

References

1. Jones, LL, *Ultimate Load Analysis of Reinforced and Prestressed Concrete Structures,* Chatto and Windus, London, 1986, pp 23–57.
2. ACI – ASCE Committee 327, Ultimate Strength Design, *Proceedings of American Concrete Institute,* Vol. 52, No. 5, Jan. 1956, pp 505–24.
3. Evans, RH, The Plastic Theories for the Ultimate Strength of Reinforced Concrete Beams, *Journal of the Institution of Civil Engineers,* London, Vol. 21, Dec. 1943, pp 98–121.
4. Rusch, H, Research towards a General Flexural Theory tor Structural Concrete, *Proceedings of American Concrete Institute,* Vol. 57, No.1, July, 1960, pp 1–28.
5. Hognestad, E, NW Hanson, and D Mc Henry, Concrete Stress Distribution in Ultimate Strength Design, *Proceedings of the American Concrete Institute,* Vol. 52, No.4, Dec. 1955, pp 455–80.
6. Mattock, AH, LB Kriz, and E Hognestad, Rectangular Concrete Stress Distribution in Ultimate Strength Design, *Proceedings of the American Concrete Institute*, Vol. 57, No. 8, Feb. 1961, pp 875–928.
7. Kong, FK and RH, Evans, *Reinforced and Prestressed Concrete,* ELBS, Van Nostrand Reinhold (International) 3rd edn, London, 1987, pp 92–100.
8. BSEN: 1992–1–1, Euro Code –2. Design of Concrete structures, General Rules and Rules for Buildings, British Standards Institution, 2004.
9. ACI 318M–2011, Building Code Requirements for Standard Concrete, American Concrete Institute Farmington Hills, Michigan, 2005.
10. IS: 1343, Indian Standard Code of Practice for Prestressed Concrete (Second Revision), Bureau of Indian Standards, New Delhi (Under Print).
11. Morsch, E, Die ermitt lung des bruch moments von spannbeton balken, *Beton u. Stahlbeton,* Vol. 45, No. 7, 1950, pp 149–157.

Review Questions

7.1 What are the different types of flexural failure modes observed in prestressed concrete beams? Explain with sketches.

7.2 What is strain compatibility method? Outline the various steps followed in computing the flexural strength of prestressed concrete sections.

7.3 Explain with sketches the IS: 1343 code method of computing the moment of resistance of rectangular sections.

7.4 What is 'effective reinforcement ratio'? In what way will it influence the stress in tendons and the neutral axis depth at the limit state of collapse of prestressed concrete sections?

7.5 Explain with sketches the method of estimating the ultimate flexural strength of flanged prestressed concrete sections according to IS: 1343 code specifications.

7.6 What is the difference in the types of stress blocks adopted in Indian and British code specifications regarding flexural strength computations?

7.7 What is the effect of using untensioned reinforcement in the compression and tension zones of prestressed concrete sections?

7.8 How do you compute the ultimate flexural strength of sections with tensioned and untensioned reinforcements in the tension zone of concrete sections?

7.9 Briefly outline the strain compatibility method of computing the flexural strength of concrete sections with tension and compression reinforcement.

7.10 Under what situations and types of structures would you recommend the use of unbonded tendons?

Exercises

7.1 The cross-section of a symmetrical I-section prestressed beam is 300 mm by 750 mm (overall), with flanges and web 100 mm thick. The beam is post-tensioned by cables containing 48 wires of 5 mm diameter high-tensile steel wires at an eccentricity of 250 mm. The 28-day strength of concrete in compression is 40 N/mm^2 and the ultimate tensile strength of wires is 1700 N/mm^2. Assuming that the grouting of the tendons is 100 per cent effective, determine the ultimate moment of the section. (Adopt IS: 1343 provisions)

[Ans: 571 kN m]

7.2 An unsymmetrical I-section has an overall depth of 2000 mm. The top flange-width and depth are equal to 1200 and 300 mm, respectively, and the bottom flange width and depth are equal to 750 and 200 mm, respectively. The thickness of the web is 300 mm. The tendons having a cross-sectional area of 7000 mm^2 are located 200 mm from the soffit. If the ultimate compressive strength of concrete and the tensile strength of steel are 42 and 1750 N/mm^2 respectively, and the tendons are effectively bonded to concrete, estimate the flexural strength of the section. (Adopt IS: 1343 provisions)

[Ans: 15366 kN m]

7.3 A double T-section having a flange 1200 mm wide and 150 mm thick is prestressed by 4700 mm^2 of high-tensile steel located at an effective depth of 1600 mm. The ribs have a thickness of 150 mm each. If the cube strength of concrete is 40 N/mm^2 and tensile strength of steel is 1600 N/mm^2, determine the flexural strength of the double T-girder using IS: 1343 provisions.

[Ans: 9069 kN m]

7.4 A post-tensioned prestressed concrete T-beam with unbonded tendons is made up of a flange 300 mm wide and 150 mm thick and the width of the rib is 150 mm. The effective depth of the section is 320 mm. The beam is prestressed by 24 wires each of 5 mm diameter having a characteristic strength of 1650 N/mm^2. The effective stress after all losses is 900 N/mm^2. If the cube strength of concrete is 56 N/mm^2, estimate the flexural strength of the section using provisions of (a) Indian (b) British and (c) American codes.
Assume (L/d) ratio = 20

[Ans: (a) 185.2 kN m (b) 185 kN m (c) 254 kN m]

7.5 An unsymmetrical I-section bridge girder has the following section properties:
Width and thickness of top flange = 1200 and 360 mm, respectively, thickness of web = 240 mm, centroid of section located at 580 mm from the top, the girder is used over a span of 40 m, and the tendons (bonded) with a

cross-section of 7000 mm^2 are parabolic with an eccentricity of 1220 mm at the centre of span and zero at the supports. Given f_{cu} = 45 N/mm^2 and f_{pu} = 1700 N/mn^2, estimate the ultimate flexural strength of the centre-of-span section using IS: 1343 provisions. **[Ans: 17416 kN m]**

7.6 A bonded prestressed concrete beam is of rectangular section of width 400 mm and overall depth 1200 mm. The tendons consisting of 3300 mm^2 of standard strands with a characteristic strength of 1700 N/mm^2, are stressed to an effective prestress of 910 N/mm^2. The strands are located 870 mm from the top face of the beam. The characteristic cube strength of concrete is 60 N/mm^2. Estimate the ultimate moment capacity of the section using British code (BS: 8110–1985) provisions. **[Ans: 2830 kN m]**

7.7 A post-tensioned bonded T-section has a flange with width 800 mm and thickness 250 mm. Thickness of the web is 200 mm. The area of high-tensile steel located at an effective depth of 1200 mm is 4000 mm^2. The characteristic strength of steel and the cube strength of concrete are 1500 N/mm^2 and 40 N/mm^2, respectively. The effective prestress after all losses is 900 N/mm^2 and the ratio of yield stress to the tensile strength of steel is 0.90. Estimate the ultimate moment capacity of the T-section using (a) IS: 1343–1980 (b) BS: 8110–1985 and (c) ACI 318–1989 code recommendations.

[Ans: (a) 5716 kN m (b) 5639 kN m (c) 6030 kN m]

7.8 A pretensioned beam of rectangular section 400 mm wide and 900 mm deep, is stressed by 1400 mm^2 of high-tensile steel at an effective depth of 800 mm. The beam is also reinforced with supplementary reinforcements consisting of 2 bars each of 25 mm diameter located 100 mm from the soffit of the beam. Given f'_c = 40 N/mm^2, f_{pu} = 1600 N/mm^2, f_y = 460 N/mm^2 and (f_{py}/f_{pu}) = 0.90, estimate the moment capacity of the section using American code provisions.

[Ans: 1769 kN m]

7.9 A post-tensioned bonded beam of rectangular section 300 mm wide and 650 mm deep, is stressed by 800 mm^2 of high-tensile steel at an effective depth of 600 mm. The beam is provided with two 25 m diameter, high-yield strength deformed bars both at the compressive and tension faces with an effective cover of 50 mm. Given f_c = 40 N/mm^2, f_{pu} = 1600 N/mm^2, f_y = 460 N/mm^2 and (f_{py}/f_{pu}) = 0.90, estimate the ultimate moment capacity of the section using American code provisions. **[Ans: 901 kN m]**

7.10. A bonded post-tensioned beam of rectangular section 400 mm wide and 1200 mm deep, is stressed by 6000 mm^2 of high-tensile steel at an effective depth of 1000 mm. Given f_{pu} = 1600 mm^2, f_{ck} = 40 N/mm^2, f'_c = 32 N/mm^2 estimate the ultimate flexural strength of the section using (a) the ACI method (b) the strain compatibility method. Assume E_s = 210 kN/mm^2.

[Ans: (a) 3690 kN m (b) 4453 kN m]

Objective-type Questions

7.1 Prestressed concrete beam fails suddenly without warning due to
(a) failure of concrete in compression zone
(b) failure of concrete in tension zone
(c) failure of steel in tension

7.2 Failure of under reinforced prestressed concrete beam is preceded by
(a) very few cracks near centre of span
(b) very little deflections
(c) large number of cracks with large deflections

7.3 Failure of over-reinforced prestressed concrete beam is characterised by
(a) large number of cracks with large deflections
(b) explosive failure due to crushing of concrete in compression zone
(c) sudden failure due to fracture of steel in tension

7.4 The moment of resistance of a rectangular section depends upon
(a) ultimate strain in concrete
(b) area of high-tensile tendons
(c) tensile stress in concrete

7.5 In a prestressed beam with bonded tendons, the value of tensile stress in steel at failure stage of beam is influenced by
(a) the compressive stress in concrete
(b) effective reinforcement ratio
(c) neutral axis depth

7.6 The maximum effective reinforcement ratio of a bonded prestressed concrete beam at failure according to IS: 1343 is limited to a value of
(a) 0.15 (b) 0.40 (c) 0.25

7.7 The ultimate flexural strength of post-tensioned beams with unbonded tendons depends upon
(a) characteristic tensile strength of prestressing steel
(b) effective stress in tendons after all losses
(c) tensile strength of concrete

7.8 The moment of resistance of a prestressed beam is generally higher if it is
(a) post-tensioned with bonded tendons
(b) post-tensioned with unbonded tendons
(c) pretensioned

7.9 The main reason for not recommending the use of unbonded tendons in prestressed concrete elements in the Indian Standard Code is to prevent
(a) excessive deflections
(b) sudden failure
(c) impairment of flexural strength

7.10 The use of bonded tendons in prestressed beams results in
(a) sudden failure
(b) large deflections
(c) progressive failure

Answers to Objective-type Questions

7.1 (c)	7.2 (c)	7.3 (b)	7.4 (b)	7.5 (b)
7.6 (b)	7.7 (b)	7.8 (c)	7.9 (b)	7.10 (c)

8 Shear and Torsional Resistance of Prestressed Concrete Members

8.1 Shear and Principal Stresses

The shear distribution in an uncracked structural concrete member for which the deformation is assumed to be linear is a function of the shear force and the properties of the cross-section of the member. The shear stress at a point is expressed as,

$$\tau_v = \left(\frac{VS}{Ib}\right)$$

where τ_v = shearing stress due to transverse loads
V = shearing force
S = statical moment (first moment of area)
I = second moment of area of section about its centroid
b = breadth of section at the given point

The effect of this shear stress is to induce principal tensile stresses on diagonal planes. The strength of concrete subjected to pure shear being nearly twice that in tension[1], local failures first appear in the form of diagonal tension cracks in regions of high shear stresses.

In a prestressed concrete member, the shear stress is generally accompanied by a direct stress in the axial direction of the member, and if transverse, vertical prestressing is adopted, compressive stresses in the direction perpendicular to the axis of the member will be present in addition to the axial prestress.

The most general case of an element subjected to a two-dimensional stress system is shown in Fig. 8.1.

The maximum and minimum principal stresses developed are given by,

$$f_{\substack{\max\\\min}} = \left[\left(\frac{f_x + f_y}{2}\right) \pm \frac{1}{2}\sqrt{(f_x - f_y)^2 + 4\tau_v^2}\right]$$

where f_x and f_y are the direct stresses and τ_v, is the shear stress acting at the point.

In prestressed concrete members, the direct stresses f_x and f_y being compressive, the magnitude of the principal tensile stress is considerably reduced, and in some cases even eliminated, so that under working loads, both major and minor principal stresses are compressive, thereby eliminating the risk of diagonal tension cracks in concrete.

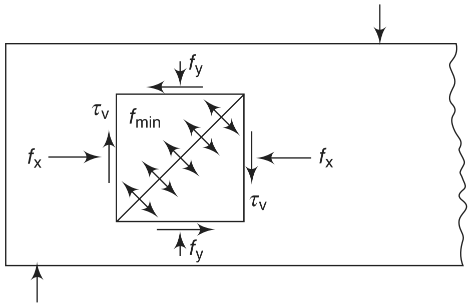

Fig. 8.1 *Principal tensile stresses in a prestressed member*

In general, there are three ways of improving the shear resistance of structural concrete members by prestressing techniques:

1. Horizontal or axial prestressing
2. Prestressing by inclined or sloping cables
3. Vertical or transverse prestressing

The effect of these different techniques of prestressing on the magnitude of principal tensile stress is illustrated by the following examples.

Example 8.1 A prestressed concrete beam (span = 10 m) of rectangular section 120 mm wide and 300 mm deep, is axially prestressed by a cable carrying an effective force of 180 kN. The beam supports a total uniformly distributed load of 5 kN/m which includes the self-weight of the member. Compare the magnitude of the principal tension developed in the beam with and without the axial prestress.

Solution.

$$A = (120 \times 300) = 36 \times 10^3 \text{ mm}^2$$
$$I = 27 \times 10^7 \text{ mm}^4$$
$$w_d = 5 \text{ kN/m}$$

Shear force at support, $V = \left(\dfrac{5 \times 10}{2}\right) = 25 \text{ kN}$

Maximum shear stress at support,

$$\tau_v = \left(\frac{3V}{2bh}\right) = \left(\frac{3}{2} \times \frac{25 \times 10^3}{120 \times 300}\right) = 1.05 \text{ N/mm}^2$$

Principal stresses $= \pm\dfrac{1}{2}\sqrt{4\tau_v^2} = \pm\tau_v = 1.05 \text{ N/mm}^2$ (compression and tension)

Axial prestress, $f_x = \left(\dfrac{180 \times 10^3}{36 \times 10^3}\right) = 5 \text{ N/mm}^2$

Maximum and minimum principal stress $= \left(\dfrac{f_x}{2}\right) \pm \dfrac{1}{2}\sqrt{f_x^2 + 4\tau_v^2}$

$$= \left(\frac{5}{2}\right) \pm \frac{1}{2}\sqrt{5^2 + 4 \times 1.05^2} = 2.5 \pm 2.73$$

$$= +5.23 \text{ N/mm}^2 \text{ (compression)} = -0.23 \text{ N/mm}^2 \text{ (tension)}$$

Hence, with axial prestress, the principal tension is reduced by,

$$\left(\frac{1.05 - 0.23}{1.05}\right) \times 100 = 78\%$$

Example 8.2 For the beam in Example 8.1, instead of axial prestressing, a curved cable having an eccentricity of 100 mm at the centre of span and reducing to zero at the supports is used, the effective force in the cable being 180 kN. Estimate the percentage reduction in the principal tension in comparison with the case of axial prestressing.

Solution.

Slope of cable at support $= \left(\frac{4e}{L}\right) = \left(\frac{4 \times 100}{10 \times 1000}\right) = 0.04$ radians

Vertical component of the prestressing force = (180 × 0.04) = 7.2 kN
Horizontal component of the prestressing force = 180 kN

∴ Net shear at support, $V = (25 - 7.2) = 17.80$ kN

$$\text{Maximum shear stress} = \left(\frac{3}{2}\frac{V}{bh}\right) = \frac{3}{2}\left(\frac{17.8 \times 10^3}{120 \times 300}\right) = 0.74 \text{ N/mm}^2$$

Axial prestress, $f_x = \left(\frac{180 \times 10^3}{120 \times 300}\right) = 5 \text{ N/mm}^2$

$$\therefore \quad f_{\substack{max \\ min}} = \frac{5}{2} \pm \frac{1}{2}\sqrt{5^2 + 4 \times 0.74^2} = (2.5 \pm 2.62)$$

$$= +5.12 \text{ N/mm}^2 \text{ (compression)} = -0.12 \text{ N/mm}^2 \text{ (tension)}$$

In comparison with axial prestressing, the percentage reduction in principal tensile stress is,

$$\left(\frac{0.23 - 0.12}{0.23}\right) \times 100 = 48\%$$

When compared with a beam without any prestress, the percentage reduction in principal tension is

$$\left(\frac{1.05 - 0.12}{1.05}\right) \times 100 = 88.5\%$$

Example 8.3 If the beam in Example 8.2 is additionally prestressed by vertical cables imparting a stress of 2.5 N/mm^2 in the direction of the depth of the beam, estimate the nature of principal stresses developed at the support section.

Solution.

Vertical prestress, $f_y = 2.5 \text{ N/mm}^2$

Horizontal prestress, $f_x = 5\ \text{N/mm}^2$
Shear stress, $\tau_v = 0.74\ \text{N/mm}^2$

$$f_{\substack{max\\min}} = \left(\frac{5+2.5}{2}\right) \pm \frac{1}{2}\sqrt{(5-2.5)^2 + 4 \times 0.74^2} = (3.75 \pm 1.45)$$

$$= 5.2\ \text{N/mm}^2\ \text{(compression)} = 2.3\ \text{N/mm}^2\ \text{(compression)}$$

By transverse prestressing, the principal tension is completely eliminated resulting in a compressive state of stress at the support.

Vertical prestressing is not generally adopted because the length of the cables being short, the loss of prestress due to anchorage slip is excessively large. However, Freyssinet[2] has used vertical tensioned stirrups in pretensioned beams and also in precast prestressed units used for the construction of Marine bridges. In this construction, the looped ends of the web stirrups were embedded in the top and bottom flanges, which were cast first, followed by the tensioning of stirrups by jacking the flanges apart and casting web concrete.

Post-tensioning is generally uneconomical for vertical prestressing due to the large number of anchorages required and the losses of prestress encountered. A viable alternative is to use pretensioned vertical wires closely spaced to achieve the desired prestress.

The concept of load balancing, discussed in Section 4.5, is useful in selecting the profile of the cable which can result in the most desirable system of forces in concrete. The following example shows that the cable profile selected on the basis of load-balancing eliminates the shear forces at the support, resulting in a uniform compressive state of stress at the support.

Example 8.4 A concrete beam having a rectangular section 150 mm wide and 300 mm deep, is prestressed by a parabolic cable having an eccentricity of 100 mm at the centre of span, reducing to zero at the supports. The span of the beam is 8 m. The beam supports a live load of 2 kN/m. Determine the effective force in the cable to balance the dead and live loads on the beam. Estimate the principal stresses at the support section.

Solution.

Self-weight of the beam = $(0.15 \times 0.30 \times 24) = 1.08$ kN/m
Total load = $(1.08 + 2.0) = 3.08$ kN/m
Eccentricity of cable at the centre of span = 100 mm
Using the concept of load balancing, if P = effective prestressing force,

$$(P \times 100) = \left(\frac{3.08 \times 8000^2}{8}\right)$$

$$\therefore \qquad P = 246400\ \text{N} = 246.4\ \text{kN}$$

Slope of cable at support, $\theta = (4e/L) = \left(\frac{4 \times 100}{8 \times 1000}\right) = \left(\frac{1}{20}\right)$

Vertical component of prestressing force = $(246.4 \times 1/20) = 12.32$ kN

Reaction at support due to dead and live loads = $\left(\frac{3.08 \times 8}{2}\right) = 12.32$ kN

Hence, net shear force V at support = 0

$$\text{Horizontal prestress at support} = \left(\frac{246400}{150 \times 300}\right) = 5.5 \text{ N/mm}^2$$

$$\text{Principal stress at support} = 5.5 \text{ N/mm}^2 \text{ (compression)}$$

Example 8.5 A concrete beam of rectangular section has a width of 250 mm and depth of 600 mm. The beam is prestressed by a parabolic cable carrying an effective force of 1000 kN. The cable is concentric at supports and has a maximum eccentricity of 100 mm at the centre of span. The beam spans over 10 m and supports a uniformly distributed live load of 20 kN/m. Assuming the density of concrete as 24 kN/m^3, estimate (a) the maximum principal stress developed in the section of the beam at a distance of 300 mm from the support, (b) the prestressing force required to nullify the shear force due to dead and live loads at the support section.

Solution.

$A = (250 \times 600) = (15 \times 10^4)\text{mm}^2$, $L = 10$ m, $e = 100$ mm

$I = \left[\dfrac{250 \times 600^3}{12}\right] = (45 \times 10^8)\text{ mm}^4$, $P = 1000$ kN

$Z = \left[\dfrac{250 \times 600^2}{6}\right] = (15 \times 10^6)\text{ mm}^3$, $b = 250$ mm and $h = 600$ mm

Self-weight of the beam = $g = (0.25 \times 0.6 \times 24) = 3.6$ kN/m
Live load on the beam = $q = 20$ kN/m
Total load on the beam = $w = (g + q) = (3.6 + 20) = 23.6$ kN/m
Shear force at support section = 0.5 (23.6 × 10) = P = 118 kN
Shear force at a section 300 mm from the support = [118 – (0.3 × 23.60)]
= 110.92 kN

$$\text{Slope of the cable at support} = \left[\frac{4e}{L}\right] = \left[\frac{4 \times 100}{10 \times 1000}\right] = 0.04$$

Slope of the cable (α) at 300 mm from support is computed by the relation

$$\alpha = \frac{4e}{L^2}[(L - 2x)] = \frac{4 \times 100}{10000^2}[(10000 - 2 \times 300)] = 0.0376$$

Vertical component of prestressing force at support = (118 × 0.04) = 4.72 kN
Vertical component of prestressing force at 300 mm from support is obtained as

$$P\,\alpha = (118 \times 0.0376) = 4.43 \text{ kN}$$

Net shear force at 300 mm from support = V = (110.92 – 4.43) = 106.49 kN

(a) The maximum shear stress at 300 mm from support at neutral axis level is given by

$$\tau_v = \frac{3}{2}\left[\frac{V}{bh}\right] = \frac{3}{2}\frac{[106.49 \times 10^3]}{(250 \times 600)} = 1.06 \text{ N/mm}^2$$

$$\text{Direct stress due to prestressing force} = \left[\frac{P}{A}\right] = \left[\frac{1000 \times 13^3}{15 \times 10^4}\right] = 6.67 \text{ N/mm}^2$$

Maximum principal stresses $= \left(\dfrac{6.67}{2}\right) \pm \dfrac{1}{2}[6.67^2 + 4 \times 1.06^2]^{0.5}$

$= 6.835$ N/mm^2 (compression)

$= -0.165$ N/mm^2 (tension)

(b) If P = prestressing force required to nullify the shear force at support due to dead and live loads

Sin $\theta = \theta$ = slope of the cable at support

We have the relation P. Sin $\theta = 118$

$$\therefore \qquad P = \left[\frac{118}{0.04}\right] = 2950 \text{ kN}$$

Example 8.6 A prestressed I-section has the following properties:

Area = (55×10^3) mm^2

Second moment of area = (189×10^7) mm^4

Statical moment about the centroid = (468×10^4) mm^3

Thickness of web = 50 mm

It is prestressed horizontally by 24 wires of 5 mm diameter and vertically by similar wires at 150 mm centres. All the wires carry a tensile stress of 900 N/mm^2. Calculate the principal stresses at the centroid when a shearing force of 80 kN acts upon this section.

Solution.

$$\text{Shear stress} = \frac{V}{Ib}(Ay') = \left(\frac{80 \times 10^3}{189 \times 10^7 \times 50}\right)(468 \times 10^4) = 3.95 \text{ N/mm}^2$$

$$\text{Horizontal prestress at centroid} = \left(\frac{(24 \times 19.7 \times 900)}{55 \times 10^3}\right) = 7.75 \text{ N/mm}^2$$

$$\text{Vertical prestress} = \left(\frac{19.7 \times 200}{150 \times 50}\right) = 2.46 \text{ N/mm}^2$$

Hence, $f_x = 7.75$ N/mm^2

$f_y = 2.46$ N/mm^2

$f_v = 3.95$ N/mm^2

Maximum and minimum principal stresses

$$= \left(\frac{f_x + f_y}{2}\right) \pm \frac{1}{2}\sqrt{(f_x - f_y)^2 + 4 \cdot \tau_v^2}$$

$$= \left(\frac{7.75 + 2.46}{2}\right) \pm \frac{1}{2}\sqrt{(7.75 - 2.46)^2 + 4 \times 3.95^2}$$

$= (5.1 \pm 4.7) = 9.8$ and 0.4 N/mm^2 (compression)

The principal tension is completely eliminated due to vertical prestressing.

Example 8.7 A cantilevered portion of a prestressed concrete bridge with a rectangular cross-section 600 mm wide and 1650 mm deep, is 8 m long and carries a reaction of 350 kN from the suspended span at the free end, together with a uniformly distributed load of 60 kN/m inclusive of its own weight. The beam is prestressed by seven cables each carrying a force of 1000 kN, of which three are located at 150 mm, three at 400 mm and one at 750 mm from the top edge.

Calculate the magnitude of the principal stresses at a point 550 mm from the top of cantilever at the support section.

Solution. Centroid of the prestressing force from the top edge,

$$y = \left[\frac{(3\times 150)+(3\times 400)+(1\times 750)}{(3+3+1)}\right] = 343 \text{ mm}$$

Eccentricity, $e = (825 - 343) = 482$ mm

Prestressing force, $P = 7000$ kN

Moment on the section due to prestressing force,

$$Pe = (7000 \times 0.482) = 3374 \text{ kN m}$$

Moment due to external loads at support section

$$= \left[(350\times 8)+\left(\frac{60\times 64}{2}\right)\right] = 4720 \text{ kN m}$$

Maximum shear at support = $(350 + 60 \times 8) = 830$ kN

Second moment of area, $I = 225 \times 10^9\ \text{mm}^4$

Resultant direct stress at 550 mm from the top edge of support section

$$= \left[\left(\frac{7000\times 10^3}{600\times 1650}\right)+\left(\frac{3374\times 10^6\times 275}{225\times 10^9}\right)-\left(\frac{4720\times 10^6\times 275}{225\times 10^6}\right)\right] = 5.43\ \text{N/mm}^2$$

Maximum shear stress at 550 mm from the top edge of support section

$$= \frac{V}{Ib}(Ay') = \left(\frac{830\times 10^3}{225\times 10^9\times 600}\right)\times(600\times 550\times 550) = 1.1\ \text{N/mm}^2$$

Maximum and minimum principal stresses are

$$= \left(\frac{5.43}{2}\right)\pm\frac{1}{2}\sqrt{5.43^2+4\times 1.1^2} = 5.65\ \text{N/mm}^2 \text{ (compression)}$$

$$= -0.21\ \text{N/mm}^2 \text{ (tension)}$$

8.2 Ultimate Shear Resistance of Prestressed Concrete Members

8.2.1 Types of Shear Cracks

Research over the years have shown that there are two major modes of shear cracking in structural concrete beams[3, 4]. These two types, generally referred to as web-shear and flexure-shear cracks, are illustrated in Fig. 8.2. Web-shear cracks generally start from an interior point, when the local principal tensile stress exceeds the tensile strength of concrete. Web-shear cracks are likely to develop in highly prestressed beams with thin webs[5], particularly when the beam is subjected to large concentrated loads near a simple support. Flexure-shear cracks are first initiated by flexural cracks in the inclined direction. Flexure-shear cracks develop when the combined shear and flexural tensile stresses produce a principal tensile stress exceeding the tensile strength of concrete. In members without shear reinforcement, the inclined shear cracks extend to the compression face resulting in sudden explosive failures. This is sometimes referred to as the diagonal tensile mode of failure.

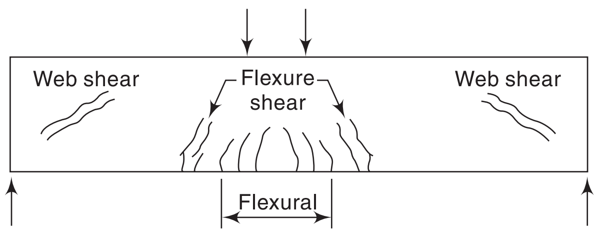

Fig. 8.2 *Types of shear cracks in structural concrete members*

The Indian, British and American standard codes distinguish between the failure of prestressed concrete members in shear due to web shear cracks and flexure shear cracks separately, and recommend empirical equations for the estimation of the ultimate shear strength by considering the various parameters influencing the shear strength of prestressed concrete beams.

8.2.2 Indian Standard Code (IS: 1343-2012) Recommendations

Computation of the Ultimate Shear Resistance

The Indian Standard Code[6] distinguishes between the section cracked due to web shear (near supports) and cracked in flexure (beyond supports), and specifies empirical equations to compute the ultimate shear resistance of the sections as follows:

(a) Sections Cracked due to Web Shear

The ultimate shear resistance of a section cracked due to web shear is computed by the expression,

$$V_c = V_{co} = 0.67\, bD \sqrt{(f_t^2 + 0.8 f_{cp} f_t)}$$

Where

b = breadth of the member for which T, I and L beams should be replaced by the breadth of the rib b_w

D = overall depth of the member

f_t = maximum principal tensile stress given by $0.24\sqrt{f_{ck}}$ taken as positive, where f_{ck} is the characteristic compressive strength of concrete

f_{cp} = compressive stress at the centroidal axis due to the prestress taken as positive

In flanged members where the centroidal axis falls in the flange, the principal tensile stress should be limited to $0.24\sqrt{f_{ck}}$ at the intersection of the flange and web. In this calculation, 0.8 times of the stress due to prestress at this intersection may be used in the calculation of V_{co}.

For sections uncracked in flexure, prestressed with inclined tendons or vertical prestress, the component of prestressing force normal to the longitudinal axis of the member may be added to the value of V_{co}.

(b) Sections Cracked in Flexure

The ultimate shear resistance of a section cracked in flexure is computed using the empirical relation given as,

$$V_c = V_{cr} = \left\{1 - 0.55\left(\frac{f_{pe}}{f_p}\right)\tau_c bd + M_0\left(\frac{V}{M}\right)\right\}$$

Where

f_{pe} = effective prestress after all losses have occurred, which shall not be taken as greater than $0.6\,f_p$

f_p = characteristic strength of prestressing steel

τ_c = ultimate shear stress capacity of concrete specified in Table 8.1

b = breadth of the member, which for flanged sections, shall be taken as the breadth of web, b_w

d = distance from the extreme compression fibre to the centroid of the tendons at the section considered

M_0 = moment necessary to produce zero stress in the concrete at the depth given by $M_0 = 0.8\,f_{pt}\,(I/y)$ where

f_{pt} = stress due to prestress only at the depth d and distance y from the centroid of the concrete section which has second moment of area I

V and M = shear force and bending moment, respectively, at the section considered due to ultimate loads

V_{cr} should be taken as not less than $0.1\,b\,d\sqrt{f_{ck}}$.

The value of V_{cr} calculated at a particular section may be assumed to be constant for a distance equal to $d/2$, measured in the direction of the increasing moment from the particular section. Also, the code specifies that for sections cracked in flexure, the contribution of the vertical component of the inclined prestressing tendons should be ignored.

The code also stipulates that in circumstances where the shear stress in a section under ultimate loads exceeds the value of the maximum shear stress listed in Table 8.2, the section should be redesigned to reduce the shear stresses within the limits shown in Table 8.1.

Table 8.1 *Design shear strength of concrete (τ_c) N/mm^2 (IS: 1343-2012)*

$100\left(\frac{A_p}{bd}\right)$	*Concrete Grade*		
	M-30	*M-35*	*M-40 and above*
≤ 0.15	0.29	0.29	0.30
0.25	0.37	0.37	0.38
0.50	0.50	0.50	0.51
0.75	0.59	0.59	0.60
1.00	0.66	0.67	0.68
1.25	0.71	0.73	0.74
1.50	0.76	0.78	0.79
1.75	0.80	0.82	0.84
2.00	0.84	0.86	0.88
2.25	0.88	0.90	0.92
2.50	0.91	0.93	0.95
2.75	0.94	0.96	0.98
3.00	0.96	0.99	1.01

Table 8.2 *Maximum shear stress (IS: 1343-2012)*

Concrete Grade	*M-30*	*M-35*	*M-40*	*M-45*	*M-50*	*M-55 and above*
Maximum Shear Stress (N/mm^2)	3.5	3.7	4.0	4.3	4.6	4.8

8.2.3 British Code (BS EN: 1-1-2004) Recommendations

The British code[7] specifies separate methods for the estimation of the ultimate shear resistance of prestressed concrete beams in two different categories, considering the maximum ultimate shear and flexure zones in a beam. In zones near the supports, the shear forces are maximum resulting in web shear cracks and suitable reinforcements have to be designed. However, in sections far away from the supports, where flexure dominates, shear reinforcements may not be required since the concrete section in conjunction with the axial prestressing force can resist the shear forces in these zones. However, minimum reinforcements have to be designed throughout the length of the beam after computations of the ultimate shear resistance of the sections.

Ultimate Shear Resistance of Prestressed Concrete Sections

The design value of the shear resistance of the member without shear reinforcement, $V_{Rd,c}$, is given by the relation,

$$V_{Rd.c} = [0.12k\,(100\,\rho_1 f_{ck})^{0.33} + 0.15\sigma_{cp}]\,b_w.d$$

Subject to a minimum of

$$V_{Rd.c} = [v_{min} + 0.15\,\sigma_{cp}]\,b_w.d$$

Where $\rho_1 = \left(\dfrac{A_{sl}}{b_w \cdot d}\right) \le 0.02$

$$k = \left[1 + \sqrt{\frac{200}{d}}\right] \le 2.0$$

A_{sl} = area of longitudinal reinforcement in the member
b_w = width of member in slabs and width of rib in beams
d = effective depth of the member in mm

$$v_{min} = 0.035\ k^{3/2}\sqrt{f_{ck}}$$

$\sigma_{cp} = (P/A_c) < 0.2\,f_{cd}$ expressed in N/mm^2
f_{cd} = design value of concrete compressive strength = (f_{ck}/γ_c)

In regions uncracked in flexure (near supports), where the flexural tensile stress is smaller, the ultimate shear resistance of the section is limited by the tensile strength of the concrete. In these regions, the shear resistance is given by the relation,

$$V_{Rd.c} = \left(\frac{Ib_w}{S}\right)\sqrt{(f_{ctd})^2 + \alpha_1 \sigma_{cp} f_{ctd}}$$

Where

I = second moment of area
b_w = width of cross-section at centroidal axis
S = first moment of the area above and about the centroidal axis
$\alpha_1 = (l_x/l_{pt2}) \le 1.0$ for pretensioned tendons
= 1.0 for other types of prestressing
l_x = distance of the section considered from the starting point of the transmission length
l_{pt2} = upper bound value of the transmission length of the prestressing element expressed as $l_{disp} = \sqrt{l_{pt}^2 + d^2}$
σ_{cp} = concrete compressive stress at the centroidal axis due to axial loading and/or prestressing
f_{ctd} = design tensile strength = (f_{ctk}/γ_c) and f_{ctk} = characteristic tensile strength
γ_c = partial safety factor for concrete

8.2.4 American Code (ACI: 318M-2011)[8] Recommendations

The shear strength of prestressed concrete members with effective prestress not less than 40 per cent of the tensile strength of flexural reinforcement is computed by the relation expressed as,

$$V_c = \left[0.05\ \lambda\sqrt{f_c'} + 4.8\left(\frac{V_u d_p}{M_u}\right)\right] b_w d$$

Where, V_c need not be taken $< 0.17\,\lambda\sqrt{f_c'}b_w d$ and not $> 0.42\,\lambda\sqrt{f_c'}\,b_w d$.

Also the value of the ratio $\left(\dfrac{V_u d_p}{M_u}\right)$ shall not be taken > 1.0, where M_u occurs simultaneously with V_u at the section. V_u and M_u are the factored shear force and bending moment at the section. λ' is a variable multiplying factor[9] depending upon the type of concrete.

In the case of members with flexure-shear cracking, the ACI-ASCE Committee[10] has suggested that the shear resistance of such members is evaluated by the expression,

$$V_{ci} = 0.05\,\lambda\sqrt{f_c'}\,b_w d_p + V_d + \left(\frac{V_i M_{cre}}{M_{max}}\right)$$

Where, d_p need not be taken less than $0.80h$ and the cracking moment M_{cre} is computed as,

$$M_{cre} = \left(\frac{I}{y_t}\right)(0.5\,\lambda\sqrt{f_c'} + f_{pe} - f_d)$$

The values of M_{max} and V_i should be computed from the load combination causing maximum factored moment to occur at the section and V_{ci} need not be taken less than $0.14\lambda\sqrt{f_c'}\,b_w d$.

In the case of members with low span/depth ratios failing due to web shear cracks[11], the shear resistance at the section is computed using the relation,

$$V_{cw} = (0.29\,\lambda\sqrt{f_c'} + 0.3 f_{pc} b_w d_p + V_p)$$

Where, d_p need not be taken less than $0.80h$ and V_p is the upward force contributed by the curved tendons near supports which reduce the shear developed by the external loads.

Example 8.8 An unsymmetrical I-section is used for a 30 m span prestressed concrete bridge girder having the top flange width and thickness of 1200 and 250 mm, respectively. The web is 1500 mm deep and 200 mm thick. The bottom flange is 500 mm wide and 400 mm deep. The girder is prestressed by cables having an initial tensile force of 6053 kN at an eccentricity of 850 mm at centre of span and 180 mm at the supports. The girder has to support an ultimate shear force of 1909 kN at the supports. The loss ratio is 0.85. Estimate the ultimate shear resistance of the support section.

Solution.

The properties of the cross-section are as follows:

$A = (73 \times 10^4)\ \text{mm}^2$

$y_t = 750\ \text{mm}$ and $y_b = 1050\ \text{mm}$

$D = 1800\ \text{mm}$

$I = (2924 \times 10^8)\ \text{mm}^4$

$Z_t = (389 \times 10^6)\ \text{mm}^3$ and $Z_b = (278 \times 10^6)\ \text{mm}^3$

$$P = 6053 \text{ kN and loss ratio} = \eta = 0.85$$
$$f_{ck} = 50 \text{ N/mm}^2$$
$$f_y = 415 \text{ N/mm}^2$$
$$f_t = 0.24\sqrt{f_{ck}} = 0.24\sqrt{50} = 1.7 \text{ N/mm}^2$$
$$f_{cp} = (\eta P/A) = (0.85 \times 6053 \times 10^3)(73 \times 10^4) = 7.04 \text{ N/mm}^2$$

The ultimate shear resistance of the support section failing due to web shear cracking is estimated by the expression,

$$V_c = V_{co} = 0.67\, bD\sqrt{(f_t^2 + 0.8 f_{cp} f_t)}$$
$$= 0.67(150 \times 1800)\sqrt{(1.7^2 + 0.8 \times 7.04 \times 1.7)}$$
$$= (1309 \times 10^3) \text{ N}$$
$$= 1309 \text{ kN}$$

Example 8.9 The cross-section of a prestressed concrete beam is an unsymmetrical T-section with an overall depth of 1300 mm. Thickness of web = 150 mm. Distances of top and bottom fibres from the centroid are 545 mm and 755 mm, respectively.

At a particular section, the beam is subjected to an ultimate moment $M = 2130$ kN m and a shear force $V = 237$ kN.
Effective depth $d = 1100$ mm
Cube strength of concrete = 45 N/mm^2
Effective prestress at the extreme tensile face of the beam $f_{ep} = 19.3$ N/mm^2
Second moment of area $I = 665 \times 10^8$ mm^4
Area of steel in the section $A_p = 2310$ mm^2
Tensile strength of tendons $f_p = 1500$ N/mm^2
Effective stress in tendons after all losses $f_{pe} = 890$ N/mm^2
Estimate the flexure-shear resistance of the section using Indian or British code regulations.

Solution.

$$M_O = \left(\frac{0.8 f_{ep} I}{y_b}\right) = \left(\frac{0.8 \times 19.3 \times 665 \times 10^8}{755}\right) = 136 \times 10^7 \text{ N mm}$$

$$\left(\frac{100 A_p}{b_w d}\right) = \left(\frac{100 \times 2310}{150 \times 1100}\right) = 1.40$$

From Table 8.1, $\tau_c = 0.77$ N/mm^2
The flexure-shear resistance of the section is

$$V_{cf} = (1 - 0.55\, f_{pe}/f_p)\, \tau_c b_w d + (M_O/M)\, V$$

or $$V_{cf} = \left[\left(1 - \frac{0.55 \times 890}{1500}\right) 0.77 \times 150 \times 1100\right] + \left[\left(\frac{136 \times 10^7}{2130 \times 10^6}\right) 237 \times 10^3\right]$$

$$= (240 \times 10^3) \text{N} = 240 \text{ kN}$$

Since the actual shear (237 kN) is less than the ultimate shear resistance of the section, only the minimum shear reinforcements are required.

8.3 Design of Shear Reinforcements

8.3.1 Indian Code Recommendations (IS: 1343-2012)

When the ultimate shear force V at any section due to ultimate loads is less than the shear resistance V_c, then minimum shear reinforcements should be provided in the form of vertical stirrups of cross-sectional area given by the relation,

$$A_{sv} = \left(\frac{0.4 b s_v}{0.87 f_y}\right)$$

Where A_{sv} = total cross-sectional area of stirrup legs effective in shear
b = breadth of the member, which for flanged sections, shall be taken as the breadth of web, b_w
s_v = spacing of stirrups along the length of the member
f_y = characteristic strength of stirrup reinforcement which shall not be taken greater than 415 N/mm^2

The code also exempts the use of shear reinforcements in the following cases:

(a) Where V is less than 0.5 V_c
(b) In members of minor importance

When the ultimate shear force at the section exceeds V_c, shear reinforcements should be designed using the relation,

$$A_{sv} = \left(\frac{s_v (V - V_c)}{0.87 f_y d_t}\right)$$

Where, d_t = depth from the extreme compression fibre either to the longitudinal bars or to the centroid of the tendons, whichever is greater.

The spacing of stirrups along the member should neither exceed 0.75 d_t nor four times the thickness of the web for flanged members.

When V exceeds 1.8 V_c, the maximum spacing should be reduced to 0.5 d_t. The lateral spacing of the individual legs of stirrups provided at a cross-section should not exceed 75 d_t.

The code also stipulates that in no circumstances the maximum shear stress at any section due to ultimate shear force V, exceeds the appropriate values compiled in Table 8.2.

8.3.2 British Code (BS EN: 1992-1-1-2004) Recommendations

At supports of prestressed beams, the ultimate shear force being higher than that resisted by the concrete, shear reinforcements are to be designed to take up the balance shear force in the form of vertical stirrups. For members with vertical shear reinforcement, the shear resistance, $V_{Rd.s}$ is expressed by the relation,

$$V_{\text{Rd.s}} = \left(\frac{A_{\text{sw}} z \cdot f_{\text{ywd}}}{s} \right)$$

Where A_{sw} = cross-sectional area of the shear reinforcement
s = spacing of the stirrups
f_{ywd} = design yield strength of the shear reinforcement
z = inner lever arm = 0.9 d

The shear reinforcement ratio is given by the expression,

$$\rho_{\text{w}} = \left(\frac{A_{\text{sw}}}{s \cdot b_{\text{w}}} \right)$$

The minimum shear reinforcement specified in the code is given by the relation,

$$\rho_{\text{w.min}} = \left(\frac{A_{\text{sw}}}{b_{\text{w.}} s} \right) = \left(\frac{0.08\sqrt{f_{\text{ck}}}}{f_{\text{yk}}} \right)$$

The code also stipulates that the maximum effective shear reinforcement should satisfy the relation given by

$$\left(\frac{A_{\text{sw,max.}}\ f_{\text{ywd}}}{b_{\text{w}}\ s} \right) \le \left(\frac{1}{2} \alpha_{\text{cw}} v_1 f_{\text{cd}} \right)$$

Where

α_{cw} = 1.25 for $0.25\, f_{cd} < \sigma_{cp} \le 0.5\, f_{cd}$

f_{cd} = design value of concrete compressive strength = $(\alpha_{cc} f_{ck} / \gamma_c)$

α_{cc} = 1.0 and $\gamma_c = 1.5$

v_1 = 0.6 for $f_{ck} \le 60$ N/mm^2

= $(0.9 - f_{ck}/200) > 0.5$ for $f_{ck} \ge 60$ N/mm^2

8.3.3 American Code (ACI: 318M-2011) Recommendations

Shear reinforcements have to be designed for the balance shear $V_s = (V_u - \phi V_c)$ using the relation,

$$\left(\frac{A_{\text{v}}}{s} \right) = \left[\frac{V_{\text{u}} - \phi V_{\text{c}}}{\phi f_{\text{yt}}\, d} \right]$$

Minimum shear reinforcements ($A_{v,min}$) should be provided in all prestressed members where V_u exceeds $0.5\phi V_c$. The minimum shear reinforcement should not be less than the smaller value obtained using the following empirical relations (a) and (b).

(a) $A_{\text{v,min}} = 0.062\sqrt{f_c'} \left(\dfrac{b_{\text{w}} s}{f_{\text{yt}}} \right)$ but not less than $(0.35 b_w s)/f_{yt}$

(b) $A_{v,\min} = \left(\dfrac{A_{ps} f_{pu} s}{80 f_{yt} d}\right)\sqrt{\dfrac{d}{b_w}}$

Example 8.10 A prestressed girder of rectangular section 150 mm wide and 300 mm deep, is to be designed to support an ultimate shear force of 130 kN. The uniform prestress across the section is 5 N/mm^2. Given the characteristic cube strength of concrete as 40 N/mm^2 and Fe-415 HYSD bars of 8 mm diameter, design suitable spacing for the stirrups conforming to the Indian standard code IS: 1343 recommendations. Assume cover to the reinforcement as 50 mm.

Solution. Given data:

$b_w = 150$ mm $\quad f_{ck} = 40$ N/mm^2
$D = 300$ mm $\quad f_{cp} = 5$ N/mm^2
$d = 250$ mm $\quad f_y = 415$ N/mm^2
$V = 130$ kN $\quad f_t = 0.24\sqrt{f_{ck}} = 0.24\sqrt{40} = 1.518$ N/mm^2

According to the recommendations of the IS: 1343–2000 code, the ultimate shear strength of the section uncracked in flexure is given by

$$V_{cw} = V_c = 0.67\, b_w\, D\sqrt{f_t^2 + 0.8 f_{cp} f_t}$$

$$= [0.67\,150 \times 300\sqrt{1.518^2 + (0.8 \times 5 \times 1.518)}]$$

$$= 87260 \text{ N} = 87.26 \text{ kN}$$

Hence, balance shear = $[V - V_c]$ = [130 – 87.26] = 42.74 kN.
Using 8 mm diameter two-legged stirrups, the spacing of the stirrups is

$$s_v = \left[\frac{A_{sv}\, 0.87 f_y d}{(V - V_c)}\right] = \left[\frac{2 \times 50.26 \times 0.87 \times 415 \times 250}{42.74 \times 10^3}\right] = 212.28 \text{ mm}$$

Maximum permissible spacing = (0.75 d) = (0.75 × 250) = 187.5 mm
Adopt 8 mm diameter two-legged stirrups at 180 mm centres.

8.4 Prestressed Concrete Members in Torsion

8.4.1 Shear and Principal Stresses due to Torsion

In the case of structural concrete members subjected to torsion, shear stresses develop depending upon the type of cross-section and magnitude of torque. The shear stresses in association with the flexural stresses may give rise to principal tensile stress, the value of which when it exceeds tensile strength of the concrete results in the development of cracks on the surface of the member.

The distribution of torsional shear stress is uniform in circular sections where the magnitude of the shear stress is proportional to the distance from the centre. In the case of non-circular sections involving warping of the cross-section, approximate formulae have been proposed based on the elastic analysis, due to St. Venant[12] and Bach[13], to estimate the maximum torsional shear stress for uncracked elements. The values suggested by Seely and Smith[14] for different cross-sections are compiled in Table 8.3. An analysis of principal stresses in prestressed concrete members should include the combined effect of shear stress due to transverse loads and torsion, together with direct stresses due to flexure and prestress.

Table 8.3 *Shear stress in members due to torsion*

S. No.	*Name of Section*	*Shape of Section*	*Maximum Shear Stress*
1.	Circle	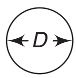	$(16\ T/pD^3)$
2.	Rectangle	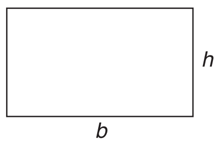	$(T/\alpha\, b\, h^2)$ where α varies from 0.208 to 0.333 as (b/h) varies from 1 to ∞ (Refer Appendix-5)
3.	Flanged sections	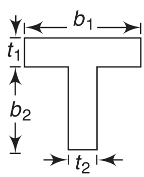	$(3\ Tt_i)/(\Sigma b_i t_i^3)$ where t_i is t_1 or t_2 and b_i is b_1 or b_2
4.	Box sections	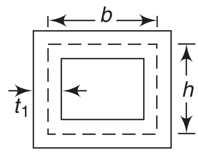	$(T/2\ A\ t_i)$ where, $A = bh$

Example 8.11 A pretensioned girder having a T-section is made up of a flange 200 mm wide and 60 mm thick. The overall depth of the girder is 660 mm. The thickness of the web is 60 mm. The horizontal prestress at a point 300 mm from the soffit is 10 N/mm^2. The shear stress due to transverse load acting at the same point is 2.5 N/mm^2. Determine the increase in the principal tensile stress at this point if the T-section is subjected to a torque of 2 kN m.

Solution.

Principal tensile stress (without torque) is given by

$$f_{\min} = \left(\frac{10}{2}\right) - \frac{1}{2}\sqrt{10^2 + 4 \times 2.5^2} = -0.6 \text{ N/mm}^2 \text{ (tension)}$$

Shear stress due to torque at the centre of the web,

$$\tau_t = \left[\frac{3Tt_i}{\Sigma b_i t_i^3}\right] = \left[\frac{3 \times 2 \times 10^6 \times 60}{(60^3 \times 200) + (60^3 \times 600)}\right] = 2.1 \text{ N/mm}^2$$

$\therefore$ Total shear stress = (2.5 + 2.1) = 4.6 N/mm^2

Principal tensile stress (with torque) is given by,

$$f_{\min} = \left(\frac{10}{2}\right) - \frac{1}{2}\sqrt{10^2 + 4 \times 4.8^2} = -1.8 \text{ N/mm}^2 \text{ (tension)}$$

Increase in principal tensile stress due to torque is = (1.8 – 0.6) = 1.2 N/mm^2.

Example 8.12 The cross-section of a prestressed concrete beam is rectangular with a width of 350 mm and an overall depth of 700 mm. The prestressing force of 180 kN acts at an eccentricity of 190 mm. If the bending and twisting moments at the section are 80 and 20 kN m, respectively, calculate the maximum principal tensile stress at the section.

In beams subjected to combined torsion and bending, the middle of the bottom face is the critical point where the principal tension is maximum.

Solution.

$$A = (350 \times 700) = 245 \times 10^3 \text{ mm}^2$$

$$I = \left[\frac{(350 \times 700^3)}{12}\right] = 10^{10} \text{ mm}^4$$

Shear stress due to torque at the soffit of the beam is given by

$$\tau_t = \left(\frac{T}{\alpha h b^2}\right) \text{ where } T = 20 \text{ kN m}, b = 700 \text{ mm}, h = 350 \text{ mm}$$

For a ratio of (700/350) = 2, from the tables of Seely and Smith[14] for $(b/h) = 2$, $a = 0.246$.

$$\therefore \quad \tau_t = \left[\frac{20 \times 10^6}{(0.246 \times 350 \times 700^2)}\right] = 0.474 \text{ N/mm}^2$$

The compressive stress due to prestressing force at the soffit of the beam, is given by

$$f_b = \left(\frac{180 \times 10^3}{245 \times 10^3}\right) + \left(\frac{180 \times 10^3 \times 190 \times 350}{10^{10}}\right) = 1.936 \text{ N/mm}^2$$

Tensile stress at the soffit due to bending moment

$$= \left(\frac{80 \times 10^6 \times 350}{10^{10}}\right) = 2.8 \text{ N/mm}^2$$

Resultant direct stress at the soffit = (1.936 – 2.8) = –0.864 N/mm^2 (tension)

Principal tensile stress at the soffit

$$f_{\min} = \left[(-0.864/2) - \frac{1}{2}\sqrt{(-0.864)^2 + (4 \times 0.474^2)}\right] = -1.072 \text{ N/mm}^2 \text{ (tension)}$$

8.4.2 Pure Torsion

The failure of a prestressed concrete member without additional untensioned reinforcement, under pure torsion, is more or less similar to that of plain concrete where sudden failure is imminent almost simultaneously with the formation of the first crack. However, research by Humphrey[15] and Zia[16] has shown that by suitably adjusting the value of the prestressing force, the torsional resistance can be increased by as much as 2.5 times that for the corresponding plain concrete member. For members subjected to pure torsion, concentric prestress is more advantageous than eccentric prestress. The use of longitudinal steel or spirals independent of each other does not increase the ultimate torsional resistance. But when both longitudinal steel and spirals are provided in prestressed members, the ultimate torsional resistance is enhanced and, according to Zia[17] can be expressed as,

$$T_t = T_{tp} + T_{ts}$$

where T_{tp} is the torsional resistance moment of the prestressed concrete section and T_{ts} is the additional torsional resistance moment of the non-prestressed reinforcement, which must consist of spirals and longitudinal steel.

The design of reinforcement for prestressed members subjected to pure torsion is illustrated by the following example:

Example 8.13 A rectangular concrete box-section has an overall depth of 1200 mm and an overall width of 900 mm. The concrete walls are 150 mm thick on both horizontal and vertical parts of the box.

(a) Determine the maximum permissible torque if the section is uniformly prestressed by a force of 450 kN. The maximum permissible diagonal tensile stress in concrete is 0.63 N/mm^2.

(b) Also, determine the amount of non-prestressed reinforcement required for the box-section if the torsional resistance moment of the section is to be increased to 345 kN m. The permissible tensile stress in steel is 230 N/mm^2. Allow for 50 mm cover.

Solution.

$$\text{Horizontal prestress} = \left[\frac{450 \times 10^3}{(1200 \times 900) - (900 \times 600)}\right] = 0.83 \text{ N/mm}^2$$

If the permissible diagonal tensile stress = 0.63 N/mm^2 and τ_t = corresponding shear stress, then

$$f_{min} = -0.63 = [(0.83/2) - 0.5\sqrt{0.83^2 + 4\tau_t^2}]$$

$$\therefore \quad \tau_t = 0.97 \text{ N/mm}^2$$

(a) Maximum permissible torque $T = 2\, A\, t_i\, \tau_t$

$$= [2 \times 150(1200 - 150)\,(900 - 150)\,0.97]/10^6 = 230 \text{ kN m}$$

(b) Allowing for 50 mm cover,

$$x_1 = (900 - 2 \times 50) = 800 \text{ mm}$$

$$y_1 = (1200 - 2 \times 50) = 1100 \text{ mm}$$

Permissible torque on the concrete section, $T_{tp} = 230$ kN m

Torque to be resisted by reinforcement (spirals and longitudinal steel) is

$$T_{ts} = [(345 \times 10^6) - (230 \times 10^6)] = 115 \times 10^6 \text{ N mm}$$

If S = spacing of the closed stirrups, using 12 mm-diameter stirrups, $A_{sv} = 226 \text{ mm}^2$

$$S = \left[\frac{0.8 f_s A_{sv} x_1 y_1}{T_{ts}}\right] = \left[\frac{0.8 \times 230 \times 226 \times 800 \times 1100}{115 \times 10^6}\right]$$

$$= 318 \text{ mm}$$

If A_{sL} = area of longitudinal steel distributed around the hoops, then

$$A_{sL} = \left[\frac{A_{sv}(x_1 + y_1)}{S}\right] = \left[\frac{226(800 + 1100)}{318}\right] = 1350 \text{ mm}^2$$

Using 12 mm-diameter bars the number of longitudinal bars required are given as (1350/113) = 12 bars. These bars are distributed at regular spacings around the perimeter of the stirrups.

8.4.3 Combined Bending Moment and Torsion

Prestressed concrete members under combined bending moment and torsion exhibit a progressive failure pattern with extensive cracking. Research by Warwaruk[17] and Rowe[18] indicates that the presence of a small bending moment increases the torsional strength of the member, while the addition of a small torque slightly decreases the moment capacity. The interaction curves of combined bending and torsion for prestressed members is somewhat similar to that of reinforced concrete members. Evans[19] has suggested a procedure for designing prestressed concrete members of additional web rectangular section under combined bending and torsion. According to this procedure, the member is first proportioned for bending moment, followed by a superposition of additional web reinforcement to resist the twisting moment.

Based on the analysis of several experimental investigations, Ananthanarayana *et al.*[20] have proposed circular interaction curves for concentric and eccentrically prestressed sections involving various parameters, such as pure torsional strength and flexural strength of the members.

8.4.4 Combined Bending Moment, Shear and Torsion

In most practical situations, prestressed members are subjected to torsion and bending together with transverse shear forces. A common example of this type are the sections in between the support and span in a curved continuous prestressed concrete spine beam deck used in flyovers. Investigations by Gausel[21] indicated a circular interaction diagram between the moment causing flexural shear and torque, both expressed in a non-dimensional form against their individual capacities. Based on experimental investigations, Bishara[22] suggested parabolic interaction curves in a non-dimensional form, relating bending and twisting moments as well as shear and torque.

The behaviour of a prestressed concrete member is affected by the relative magnitude of the internal actions, such as torque, bending moment and shear force, in critical regions. If torsion is small, it has little effect on the overall behaviour and the failures are controlled by either flexure or shear.

Members subjected to torque, bending and shear are generally reinforced with longitudinal and transverse reinforcements. In order to study the contribution of the longitudinal and transverse reinforcement in resisting flexure, torsion and shear forces, it becomes necessary to analyse the system of forces acting on the warped cross-sections of the structural element at the limit state of failure. At present, three semi-rational theories form the basis of the various codified procedures. The three main approaches are:

1. The *skew bending theory,* which is based on the plane deformation approach to plane sections subjected to bending and torsion.
2. The *space truss analogy theory*, which is a modification of the planar truss analogy for shear. According to this theory, the space truss, which is composed of longitudinal bars and diagonal concrete struts, is subjected to twist in which the stirrups and longitudinal bars are considered the tension members and the diagonal concrete struts at an angle θ between the cracks are considered the compression members. The angle θ is generally idealised to 45 degrees.
3. The *compression field theory,* which is a powerful modification of the truss analogy theory and is based on a more realistic evaluation of the inclination angle θ of the compression struts between the inclined cracks.

The skew bending theory was initially proposed by Lessig, with subsequent contributions from Collins[23], Hsu[24], Zia[25], Gesund[26], Mattock[27] and Elfgreen[28]. Of the several researchers in this field, Hsu[29] made the most significant contribution based on the experimental investigations. His work forms the basis of the American, Australian (AS 1481)[30] and Indian code (IS: 1343) provisions.

The truss theory was originally developed by Rausch[31] and later extended by Lampert and Collins[32] and improved by Hsu, Thurliman, Elfgreen and others. The British code (BS EN: 1992–1–1) and the European codes are based on the space truss model.

The compression field theory can be treated as a special case of the general truss theory. Major contributions in the compression field theory are due to Elfgreen, Collins and Mitchell[33]. Elfgreen proposed the compression fields for the various components of the plasticity truss model, currently used in the European (GEB) code with modifications by Collins and Mitchell. When prestressed concrete members are subjected to shear, torsion and bending, three different modes of failure are identified depending upon the magnitude of the various parameters. The different modes of failures are identified as follows:

(a) *Mode 1 failure:* This type of failure is applicable to most of the beams, subjected to high torsion and bending. The failure surface is warped with the oblique compressive zone and the cracks spiral around the beam joining the compressive zone.

(b) *Mode 2 failure:* If the magnitude of torsion is very large relative to flexure and if the beam section is narrow and deep, so that its resistance to lateral bending is much smaller than its resistance to vertical bending, then the mode 2 type failure may result with the compressive crushing zone parallel to one side of the beam.

(c) *Mode 3 failure:* If the bending moment is small relative to torsion and if the beam contains very little longitudinal reinforcement in the upper surface, then failure may occur due to negative bending with the skewed compressive crushing zone in the bottom face. This type is referred to as mode 3 failure.

8.5 Design of Reinforcements for Torsion Shear and Bending

8.5.1 British Code (BS EN: 1992-1-1-2004) Recommendations

The British code specifies that where the static equilibrium depends upon the torsional resistance of elements of the structure, a full torsional design, covering both ultimate and serviceability states, is necessary. The torsional resistance of a section may be calculated on the basis of a thin walled closed section, in which the equilibrium is satisfied by closed shear flow. In the case of flanged members like T-sections, the element may be divided into series of subsections, each of which is considered as an equivalent thin walled section, and the total torsional resistance is taken as the sum of the capacities of the individual elements.

According to Lin and Chow[34] , the torsional resistance of a prestressed concrete member is significantly higher than that of the corresponding reinforced concrete member due to the prestress in concrete. This fact has been recognised in formulating the design procedure for combined torsion, shear and bending by the Prestressed Concrete Institute[35] and is part of the Canadian Building Code.

The maximum resistance of a member subjected to combined torsion and shear is limited by the capacity of the concrete struts. In order not to exceed this resistance, the following condition should be satisfied.

$$\left[\frac{T_{\text{Ed}}}{T_{\text{Rd,max}}}+\frac{V_{\text{Ed}}}{V_{\text{Rd,max}}}\right]\leq 1.0$$

Where

T_{Ed} = design torsional moment

V_{Ed} = design shear force

$T_{\text{Rd, max}}$ = design torsional resistance moment, expressed as:

$T_{\text{Rd, max}} = 2\nu\, \alpha_{\text{cw}} f_{\text{cd}} A_{\text{k}}\, t_{\text{ef, i}} \sin\theta \cos\theta$

Where

v = strength reduction factor for concrete cracked in shear

$$= 0.6\left[1 - \frac{f_{ck}}{250}\right] \text{N/mm}^2$$

$\alpha_{cw} = 1.25$ for $0.25\, f_{cd} < \sigma_{cp} \leq 0.5\, f_{cd}$

And $\left[2.5\left(1 - \frac{\sigma_{cp}}{f_{cd}}\right)\right]$ for $0.5\, f_{cd} < \sigma_{cp} \leq 1.0\, f_{cd}$

f_{cd} = design value of concrete compressive strength = $(\alpha_{cc} f_{ck}/\gamma_c)$

A_k = area enclosed by the centre lines of the connecting walls in hollow sections

= $(b_1 d_1)$, where b_1 and d_1 are the effective cover to the reinforcement at the sides and top and bottom, respectively

$t_{ef,\,i}$ = effective wall thickness in hollow sections. It may be taken as (A/u), where A is the total area of the cross-section and u is the outer circumference of the cross-section

θ = angle between the concrete compression strut and the beam axis perpendicular to the shear force

For rectangular solid sections, only minimum reinforcement is required, provided the following interaction condition is satisfied.

$$\left[\frac{T_{Ed}}{T_{Rd,c}} + \frac{V_{Ed}}{V_{Rd,c}}\right] \leq 1.0$$

Where

$T_{Rd,\,c}$ = torsional cracking moment computed by setting $\tau_{ti} = f_{ctd}$

$V_{Rd.c} = [0.12k\,(100\,\rho_1 f_{ck})^{0.33} + 0.15\,\sigma_{cp}]b_w.d$

In most cases, the shear reinforcement links designed for resisting the ultimate shear will provide for the minimum torsion links required. The longitudinal spacing of the torsion links should not exceed $(u/8)$, where u is the outer perimeter of the hollow box section or the lesser of the solid beam cross-section. The minimum reinforcement is given by the relation,

$$\rho_{w.min} = \left(\frac{A_{sw}}{b_{w.}s}\right) = \left(\frac{0.08\sqrt{f_{ck}}}{f_{yk}}\right)$$

8.5.2 American Code (ACI: 318M-2011) Recommendations

The American code prescribes that for prestressed concrete members, torsion effects can be neglected if the factored torsional moment T_u is less than the value given by the relation,

$$\phi(0.083\lambda\sqrt{f_c'})\left[\frac{A_{cp}^2}{\rho_{cp}}\right]\sqrt{1+\frac{f_{pc}}{0.33\lambda\sqrt{f_c'}}}$$

Where

A_{cp} = area of concrete section in solid rectangular beam and in flanged sections. The area of slab equal to four times the thickness of the slab is also included.

ρ_{cp} = outside perimeter of concrete section

ϕ = capacity reduction factor

λ = modification factor to include the reduced mechanical properties of light weight concrete in relation to that of normal concrete

f_{pc} = compressive stress in concrete (after allowing for all losses) at centroid of cross-section

In prestressed concrete members subjected to combined torsion and shear, the design of cross-section should conform to the empirical relations given as follows:

(a) For solid sections

$$\sqrt{\left(\frac{V_u}{b_w d}\right)^2+\left(\frac{T_u p_h}{1.7A_{oh}^2}\right)^2}\le\phi\left(\frac{V_c}{b_w d}+0.66\sqrt{f_c'}\right)$$

(b) For hollow-box sections

$$\left(\frac{V_u}{b_w d}\right)+\left(\frac{T_u p_h}{1.7A_{oh}^2}\right)\le\phi\left(\frac{V_c}{b_w d}+0.66\sqrt{f_c'}\right)$$

Where

V_u = factored shear force

T_u = ultimate torsional moment

V_c = nominal shear strength provided by concrete

A_{oh} = area enclosed by centreline of the outer most closed transverse torsional reinforcement

p_h = perimeter of centerline of outer most closed transverse torsional reinforcement

ϕ = capacity reduction factor

When torsional reinforcement is required in prestressed members, the minimum area of transverse closed stirrups is computed using the relation,

$$(A_v + A_t) = 0.062\sqrt{f_c'}\left(\frac{b_w s}{f_{yt}}\right) \text{ but not less than } 0.35\left(\frac{b_w s}{f_{yt}}\right)$$

Where

A_v = area of shear reinforcement with spacing '*s*'

A_t = area of one leg of closed stirrup resisting torsion with spacing '*s*'

The minimum area of longitudinal torsional reinforcement $A_{l,\,min}$ is computed as,

$$A_{\mathrm{l,min}} = \left(\frac{0.42\sqrt{f_c'}\,A_{\mathrm{cp}}}{f_{\mathrm{y}}}\right) - \left(\frac{A_{\mathrm{t}}}{s}\right) p_{\mathrm{h}} \left(\frac{f_{\mathrm{yt}}}{f_{\mathrm{y}}}\right)$$

Where, $\left(\frac{A_{\mathrm{t}}}{s}\right)$ should be not less than $0.175\left(\frac{b_{\mathrm{w}}}{f_{\mathrm{yt}}}\right)$.

f_{yt} refers to closed transverse torsional reinforcement and f_{y} refers to longitudinal reinforcement.

The spacing of torsion reinforcement should not exceed the smaller of the values given by ($p_{\mathrm{h}}/8$) or 300 mm. Also, the torsion reinforcement should extend to a distance of ($b_{\mathrm{t}} + d$) beyond the point required by analysis, where 'b_{t}' is the width of cross-section containing closed loops resisting torsion and 'd' is the effective depth.

8.5.3 Indian Code (IS: 1343) Recommendations

The Indian Standard Code (IS: 1343) recommendations for the design of prestressed members subjected to shear, torsion and bending are more or less similar to the Australian AS: 1481[30] code provisions, which are based on the design procedures proposed by Rangan and Hall[36].

The code provisions are based on the skew bending theory, which is most useful for cases where shear is small and the standard flexural failure mode is modified by the presence of torsion. The space truss theory[37] is particularly appropriate for the analysis of failure in the presence of high shear and large torsion. The design equations developed from the two different approaches give rather similar results. The Indian Standard Code provisions for the design of structural members under combined bending, shear and torsion are applicable for beams of solid rectangular cross-section, hollow rectangular beams, *T* and *I*-beams. In all cases, the beams should have an average intensity of prestress of not less than 0.3 f_{ck}. The design of longitudinal and transverse reinforcement is as follows:

Longitudinal reinforcement The longitudinal reinforcement is designed to resist an equivalent ultimate bending moment M_{e1} given by,

$$M_{\mathrm{e1}} = M + M_{\mathrm{t}}$$

where M = applied ultimate bending moment at the cross-section, acting in combination with ultimate torque T

$M_{\mathrm{t}} = T\sqrt{1+(2D/b)}$ the sign of M_{t} being the same as that of M

D = overall depth of the beam

b = breadth of the member which for *T* and *I* beams shall be taken as the breadth of the web b_{w}

If the numerical value of M is less than that of M_{t}, the member should also be designed to withstand a moment M_{e2} given by

$$M_{\mathrm{e2}} = M_{\mathrm{t}} - M$$

the moment M_{e2} being taken as acting in the opposite sense to the moment M.

In cases where the numerical value of M is less than or equal to that of M_t, the beam is designed to withstand an equivalent transverse bending moment M_{e3} (not acting simultaneously with M_{e1}), which is given by

$$M_{e3} = M_t\left(1+\frac{x_1}{2e}\right)^2\left[\frac{1+(2b/D)}{1+(2D/b)}\right]$$

and acting about an axis at right angles to the axis of M, where x_1, is the smaller dimension of a closed hoop used as torsional shear reinforcement and $e = (T/V)$, where V is the ultimate shear force.

Transverse reinforcement In prestressed beams, the horizontal prestress is beneficial in reducing the effective torsional moment and shear. This fact is taken into account in the IS code recommendations.

The reduced torsional moment carried by the concrete T_{c1} is given by,

$$T_{c1} = T_c\left(\frac{e}{e+e_c}\right)$$

where
$$T_c = 0.15\, b^2 D\left(1-\frac{b}{3D}\right)\lambda_p\sqrt{f_{ck}}$$

$$e = (T/V)$$

$$e_c = (T_c/V_c)$$

$$\lambda_p = \sqrt{\left(1+\frac{12f_{cp}}{f_{ck}}\right)}$$

where T_c = torsional moment carried by concrete

b = breadth of the member, which for T- and I-beams shall be taken as the breadth of the web b

D = overall depth of the beam

f_{ck} = characteristic compressive strength of concrete

T = torsional moment applied to a cross-section under ultimate load conditions

V = shearing force at a cross-section calculated for the specified ultimate loads

V_c = theoretical shear strength at a cross-section, assuming the most unfavourable conditions for inclined cracking that is smaller of V_{cw} and V_{cf} given by the following equations:

$$V_{cw} = 0.67\, b\, D\sqrt{f_t^2 + 0.8 f_{cp} f_t}$$

where f_t = maximum principal tensile stress given by $0.24\sqrt{f_{ck}}$

f_{cp} = compressive stress at the centroidal axis due to prestress

$$V_{cf} = \left(1-0.55\frac{f_{pe}}{f_p}\right)\tau_c\, bd + M_o\,(V/M)$$

where f_{pe} = effective stress in steel after all losses but not greater than $0.6\, f_p$

f_p = characteristic tensile strength of prestressing steel

τ_c = ultimate shear stress capacity of concrete obtained from Table 8.1 (refer Section 8.2.3)

b = breadth of a member, which for flanged sections shall be taken as the breadth of the web b_w

d = distance from the extreme compression fibre to the centroid of the tendons at the section considered

M_o = moment necessary to produce zero stress in the concrete at the depth given by

$$M_o = 0.8 f_{pt} = \left(\frac{I}{Y}\right)$$

where f_{pt} = stress due to prestress only at depth d and distance y from the centroid of the concrete section which has a second moment of area I

V and M = shear force and bending moment due to ultimate loads, respectively, at the section considered

V_{cf} should be taken as not less than 0.1 $d\sqrt{f_{ck}}$.

The shear force V_{c1} carried by the concrete is given by,

$$V_{c1} = V_c\left(\frac{e}{e+e_c}\right)$$

where V_c is smaller of V_{cw} and V_{cf}.

The area of cross-section A_{sv} of the closed stirrup enclosing the corner longitudinal bars is taken as the larger of the following two values:

$$A_{sv} = \left(\frac{M_t S_v}{1.5 b_1 d_1 f_y}\right)$$

and $$A_{sv} = (A_v + 2A_T)$$

where $$A_v = \left[\frac{(V - V_{c1})S_v}{0.87 f_y d_1}\right]$$

$$A_t = \left[\frac{(T - T_{c1})S_v}{0.87 b_1 d_1 f_y}\right]$$

In these expressions,

S_v = spacing of stirrup reinforcement

b_1 = centre-to-centre distance between corner bars in the direction of the width

d_1 = centre-to-centre distance between corner bars in the direction of the depth

However, the minimum reinforcement should not be less than that given by

$$= \left(\frac{A_{sv}}{bs_v}\right) = \left(\frac{0.4}{0.87 f_y}\right)$$

Distribution of torsion reinforcement Members designed for torsion should be reinforced as follows:

(a) All transverse reinforcement for torsion should be in the form of closed stirrups perpendicular to the axis of the members.
(b) The spacing S_v of the stirrups shall not exceed $(x_1 + y_1)/4$ or 200 mm, whichever is smaller, where x_1 and y_1 are respectively short and long dimensions of the stirrup.
(c) Each end of the bar forming the stirrup shall be anchored in accordance with IS: 456–2000.
(d) Torsional reinforcement shall continue to a distance not less than $(D + b_w)$, beyond the point at which it is no longer than theoretically required, where D is the overall depth and b_w is the effective width of the web of a flanged member.

Example 8.14 A post-tensioned bonded prestressed concrete beam of rectangular cross-section 400 mm wide and 550 mm deep, is subjected to a service-load bending moment of 166.6 kN m, torsional moment of 46.6 kN m and shear force of 66.6 kN. The section has an effective prestressing force, determined from service load requirements, of magnitude 500 kN at an eccentricity of 150 mm, provided by five numbers of 12.5 mm stress-relieved strands of cross-sectional area 506 mm^2 with an ultimate tensile strength of 1820 N/mm^2. If the cube strength of concrete is 40 N/mm^2, design suitable longitudinal and transverse reinforcements in the beam using,
(a) IS: 1343 code recommendations based on the skew bending approach
(b) space-truss analogy

Solution. Given data:
Ultimate bending moment, $M = (1.5 \times 166.6) = 250$ kN m
Ultimate torsional moment, $T = (1.5 \times 46.6) = 70$ kN m
Ultimate shear force, $V = (1.5 \times 66.6) = 100$ kN
Area of prestressing strands, $A_p = 506$ mm^2
Ultimate tensile strength of strands, $f_p = 1820$ N/mm^2
Cube strength of concrete, $f_{ck} = 40$ N/mm^2
Yield strength of transverse reinforcement, $f_y = 250$ N/mm^2
Prestressing force, $P = 500$ kN
Eccentricity, $e = 150$ mm
Width of section, $b = 400$ mm
Overall depth, $D = 550$ mm
Area of concrete section, $A = (22 \times 10^4)$ mm^2

$$\text{Second moment of area, } I = \left(\frac{400 \times 550^3}{12}\right) = (5.54 \times 10^9) \text{ mm}^4$$

Effective stress in steel $= (500 \times 10^3/506) = 988$ N/mm^2
Effective depth, $d = 425$ mm

(a) Skew bending approach (IS: 1343)

Design of longitudinal reinforcements

$$M_{e1} = M + M_t$$

where $$M_t = T\sqrt{1+\left(\frac{2D}{b}\right)} = 70\sqrt{1+\left(\frac{2\times 550}{400}\right)} = 136 \text{ kN m}$$

$$M_{e1} = (250 + 136) = 386 \text{ kN m}$$

The longitudinal steel in the section is designed for the ultimate moment of 386 kN m.

The ultimate moment capacity of the section with prestressing steel is first determined and for the balance moment, mild steel reinforcement will be designed.

For the prestressed section, we have

$$f_p = 1820 \text{ N/mm}^2 \qquad b = 400 \text{ mm}$$
$$A_p = 506 \text{ mm}^2 \qquad d = 425 \text{ mm}$$
$$f_{ck} = 40 \text{ N/mm}^2$$

$$\text{Ratio} = \left(\frac{f_p A_p}{f_{ck} bd}\right) = \left(\frac{1820\times 506}{40\times 400\times 425}\right) = 0.135$$

From Table 7.1,

$$\left(\frac{f_{pu}}{0.87 f_p}\right) = 1.0$$

$\therefore$ $$f_{pu} = (0.87\times 1820) = 1583 \text{ N/mm}^2$$

and $$\left(\frac{x_u}{d}\right) = 0.287$$

$$x_u = (0.287\times 425)$$
$$= 122 \text{ N/mm}^2$$

$\therefore$ $$M_u = f_{pu}A_p(d - 0.42x_u) = (1583\times 506)\,(425 - 0.42\times 122)$$
$$= (299\times 10^6) \text{ N mm} = 299 \text{ kN m}$$

But the total moment to be resisted by the section is 386 kN m.

$\therefore$ Balance moment, $M_u = (386 - 299) = 87$ kN m

Providing mild steel reinforcement at an effective depth of 500 mm, we get

$$M_u = 0.87 f_y A_{st}\, d\left[1-\left(\frac{A_{st} f_y}{b\,d\,f_{ck}}\right)\right]$$

or $$(87\times 10^6) = (0.87\times 250\times A_{st}\times 500)\left[1-\left(\frac{A_{st}\times 250}{400\times 500\times 40}\right)\right]$$

solving, $A_{st} = 840 \text{ mm}^2$

Provide two bars of 25 mm diameter each at an effective depth of 500 mm ($A_{st} = 982 \text{ mm}^2$).

Design of transverse reinforcement

Average intensity of prestress at the centroid, $= f_{cp} = (P/A)$

$$= (500 \times 10^3)/(22 \times 10^4) = 2.27 \text{ N/mm}^2$$

Tensile strength of concrete, $f_t = 0.24\sqrt{f_{ck}} = 0.24\sqrt{40} = 1.51 \text{ N/mm}^2$

The reduced torsional moment T_{cl} carried by the concrete is given by,

$$T_{cl} = T_c\left(\frac{e}{e + e_c}\right)$$

where $T_c = 0.15b^2D\left[1 - \left(\dfrac{b}{3D}\right)\right]\lambda_p\sqrt{f_{ck}}$

$$\lambda_p = \sqrt{\left(1 + \frac{12 f_{cp}}{f_{ck}}\right)} = \sqrt{\left(1 + \frac{12 \times 2.27}{40}\right)} = 1.296$$

$$T_c = (0.15 \times 400^2 \times 550)\left(1 - \frac{400}{3 \times 550}\right)1.296\sqrt{40}$$

$$= (82 \times 10^6) \text{ N/mm} = 82 \text{ kN m}$$

$$e = (T/V) = (70/100) = 0.7 \text{ m} = 700 \text{ mm}$$

$e_c = (T_c/V_c)$, where V_c is smaller of V_{cw} and V_{cf}

$$V_{cw} = 0.67bD\sqrt{f_t^2 + 0.8 f_{cp} f_t}$$

$$= (0.67 \times 400 \times 550)\sqrt{1.51^2 + (0.8 \times 2.27 \times 1.51)}$$

$$= 330176 \text{ N} = 330 \text{ kN}$$

$$V_{cf} = \left(1 - 0.55\frac{f_{pe}}{f_p}\right)\tau_c b_w d + \left(\frac{M_o}{M}\right)V$$

but not less than $0.1\, b_w d\sqrt{f_{ck}}$.

Equivalent area of prestressing steel is obtained as,

$$A_p = 506 + A_{us}\,(f_y/f_p) = [506 + 982(250/1820)] = 641 \text{ mm}^2$$

$$= \left(\frac{100 A_p}{bd}\right) = \left(\frac{100 \times 635}{400 \times 425}\right) = 0.373$$

From Table 8.1, for M–40 grade concrete, the design shear strength $\tau_c = 0.44 \text{ N/mm}^2$.

$$M_o = 0.8\, f_{pt} = \left(\frac{I}{y}\right)$$

$$f_{pt} = \left[\left(\frac{P}{A}\right) + \left(\frac{Pey}{I}\right)\right]$$

$$= \left[\left(\frac{500 \times 10^3}{400 \times 550}\right) + \left(\frac{500 \times 10^3 \times 150 \times 150}{5.54 \times 10^9}\right)\right] = 4.3 \text{ N/mm}^2$$

$$M_o = (0.8 \times 4.3)\left(5.54 \times \frac{10^9}{150}\right) = (127 \times 10^6)\ \text{N mm}$$

$$V_{cf} = \left[1 - 0.55\left(\frac{988}{1820}\right)\right](0.44 \times 400 \times 425) + \left[\frac{(127 \times 10^6)}{(250 \times 10^6)}\right](100 \times 10^3)$$

$$= 103309\ \text{N} = 103.3\ \text{kN}$$

Smaller of the values of V_{cw} and V_{cf} obtained as $V_c = 103.3$ kN.

$$e = \left(\frac{T}{V}\right) = \left(\frac{70 \times 10^6}{100 \times 10^3}\right) = 700\ \text{mm and}$$

$$e_c = \left(\frac{T_c}{V_c}\right) = (82/103.3) = 0.793\ \text{m} = 793\ \text{mm}$$

$$T_{c1} = T_c\left(\frac{e}{e + e_c}\right) = 82\left(\frac{700}{700 + 793}\right) = 38.44\ \text{kN m}$$

$$V_{c1} = V_c\left(\frac{e}{e + e_c}\right) = 103.3\left(\frac{700}{700 + 793}\right) = 48.43\ \text{kN m}$$

$\therefore$ $(V - V_{c1}) = (100 - 48.43) = 51.57$ kN

$(T - T_{c1}) = (70 - 38.44) = 31.56$ kN m

The cross-section A_{sv} of closed stirrups enclosing the longitudinal bars is designed for the larger of the following two values:

$$A_{sv} = \left(\frac{M_t S_v}{1.5 b_1 d_1 f_y}\right) \quad \text{and} \quad A_{sv} = (A_v + 2A_T)$$

where $$A_v = \frac{(V - V_{c1})S_v}{0.87 f_y d_1}$$

$$A_T = \frac{(T - T_{c1})S_v}{0.87 b_1 d_1 f_y}$$

In the present problem, $b_1 = 350$ mm

$d_1 = 450$ mm

Using a pitch of 80 mm and $f_y = 250$ N/mm^2

$$A_{sv} = \left(\frac{136 \times 10^6 \times 80}{1.5 \times 350 \times 450 \times 250}\right) = 184\ \text{mm}^2$$

Also, $$A_v = \left(\frac{51.57 \times 10^3 \times 80}{0.87 \times 250 \times 450}\right) = 42\ \text{mm}^2$$

$$A_T = \left(\frac{31.56 \times 10^6 \times 80}{0.87 \times 350 \times 450 \times 250}\right) = 74\ \text{mm}^2$$

$$A_{sv} = (A_v + 2A_T) = (42 + 2 \times 74) = 190\ \text{mm}^2$$

The larger value of $A_{sv} = 190$ mm^2.

Providing 12 mm diameter two-legged stirrups at a spacing of 80 mm which provides $A_{sv} = 226\ \text{mm}^2$

Check for spacing of stirrups:

$$x_1 = 382\ \text{mm} \qquad y_1 = 482\ \text{mm}$$

$$\therefore \qquad \left[\frac{(x_1 + y_1)}{4}\right] = \left[\frac{(382 + 482)}{4}\right] = 216\ \text{mm} > 80\ \text{mm}$$

(b) Space-truss analogy

$$M = 250\ \text{kN m}$$
$$T = 70\ \text{kN m}$$
$$V = 100\ \text{kN}$$

The yield force in the prestressing steel = $(506 \times 1820) = 920 \times 10^3$ N

Providing top and bottom covers of 50 mm and side covers of 25 mm, we have, $b_1 = 350$ mm and $d_1 = 450$ mm

Distance from the top longitudinal bars to the prestressing steel = 375 mm.

Contribution of prestressing steel to the moment capacity of beam,

$$(920 \times 0.375) = 345\ \text{kN m}$$

Since this exceeds the required moment capacity of $M = 250$ kN m, only the longitudinal reinforcing bars are to be designed to resist the torque and shear only.

The shear flow due to torsion is given by,

$$q_T = \left(\frac{T}{2A_o}\right) = \left(\frac{70 \times 10^6}{2 \times 350 \times 450}\right) = 222\ \text{N/mm}$$

where A_o = area enclosed within the perimeter connecting the stringers

The shear flow due to the shear force is obtained from the relation

$$q_v = \left(\frac{V}{2d_1}\right) = \left(\frac{100 \times 10^3}{2 \times 450}\right) = 111\ \text{N/mm}$$

The maximum shear flow is

$$(222 + 111) = 333\ \text{N/mm}$$

The force in the stirrups is obtained from the expression

$$S = q\, s \tan \alpha$$

where q = total shear flow

s = spacing of vertical stirrups

a = angle of imaginary concrete strut (Assumed as 45°)

$$\therefore \qquad S = 333\ \text{s N}$$

The required stirrups reinforcement is therefore computed as,

$$= \left(\frac{A_{sv}}{S}\right) = \left(\frac{S}{f_y}\right) = \left(\frac{333}{250}\right) = 1.333\ \text{mm}^2/\text{mm}$$

Adopt 12 mm diameter two-legged stirrups at 80 mm centres.

The additional longitudinal reinforcements provided at the bottom left- and right-hand corner, required to resist the torsion and shear, are computed using following equations:

$$A_{sl} = \frac{1}{2f_y}\left[\frac{V}{2} + \frac{T}{2A_o}(b_1 + d_1)\right]$$

$$= \frac{1}{2 \times 250}\left[\frac{100 \times 10^3}{2} + 222(350 + 450)\right] = 456 \text{ mm}^2$$

$$A_{sr} = \frac{1}{2f_y}\left[\frac{T}{2A_o}(b_1 + d_1) - \frac{V}{2}\right]$$

$$= \frac{1}{2 \times 250}\left[222(350 + 450) - \left(\frac{100 \times 10^3}{2}\right)\right] = 255 \text{ mm}^2$$

For the sake of symmetry, provide $A_{sl} = A_{sr}$, hence, 25 mm-diameter bars of area 491 mm^2 are provided at the left- and right-hand bottom corners.

A comparison between the skew bending approach and the space-truss analogy indicates that both the methods result in more or less similar quantities of longitudinal and transverse reinforcements.

References

1. Murashev, V, E Sigalov, and V, Balkov, *Design of Reinforced Concrete Structures,* Mir Publishers, Moscow, 1968, pp 31–34.
2. Freyssinet, E, “Prestressed concrete principles and applications,” *Journal of the Institution of Civil Engineers,* Vol. 33, 1950, pp 331–380.
3. McGregor, JG and JM Hanson, “’Proposed changes in shear provisions for reinforced and prestressed concrete beams,” *Proceedings of the American Concrete Institute,* Vol. 66, No. 4, 1969, pp 276–288.
4. ACI: 318M–2011, Metric Building Code Requirements for Structural Concrete and Commentary, ACI Committee–318, American Concrete Institute, Farmington Hills, Michigan, 2011.
5. Bennett, EW, and BMA Balasoorya, “Shear strength of prestressed beams with thin webs failing in inclined compression,” *Journal of the American Concrete Institute,* Vol. 68, No. 3, March 1971, pp 204–212.
6. IS: 1343, *Indian Standard Code of Practice for Prestressed Concrete* (2nd revision), Bureau of Indian Standards, New Delhi, 2012, pp. 55.
7. BSEN: 1992–1–1, Euro Code–2, Design of Concrete Structures, General Rules and Rules for Buildings, British Standards Institution, 2004, pp. 225.
8. ACI: 318M–2011, Metric Building Code Requirements for Structural Concrete and Commentary, ACI Committee–318, American Concrete Institute, Farmington Hills, Michigan, 2011.
9. Nawy Edward, G, *Prestressed Concrete, A Fundamental Approach,* Prentice-Hall International, Englewood Cliffs, New Jersey, 1989, pp 200–307.
10. ACI-ASCE Committee–326, “Shear and diagonal tension,” *Proceedings of the American Concrete Institute,* Vol. 59, Jan/Feb – 1962, pp 1–30 and 277–334.
11. Mast, PE, “Shortcuts for the shear analysis of standard prestressed concrete members,” *Journal of the Prestressed Concrete Institute,* Vol. 9, No. 5, October 1964, pp 15–47.

12. Tod Hunter, I, and K Pearson, *A History of the Theory of Elasticity and of the Strength of Materials, Part 1*. Dover Publications, New York, 1960, pp 1–69.
13. Timoshenko, S, *The Strength of Materials,* Macmillan, London, 1930.
14. Seely Fred, B and O Smith James, *Advanced Mechanics of Materials,* 2nd edition, Wiley International, John Wiley, 1952, New York, pp 266–294.
15. Humphreys, R, "Torsional properties of prestressed concrete members," *Structural Engineer*, Vol. 35, No. 6, June 1957, pp 213–225.
16. Zia, P, "Torsional strength of prestressed concrete members," *Journal of the American Concrete Institute Proceedings,* Vol. 57, April 1961, pp 1337–59.
17. Mukherjee, PR and J Warwaruk, "Bending and torsion of rectangular prestressed concrete beams with mild steel reinforcements," *Proc. of the International Conference on Shear, Torsion and Bond in Reinforced and Prestressed Concrete*, Coimbatore, India, January 1969.
18. Rowe, RE, "Discussion of experiments on the torsional strength of prestressed concrete," by Cowan, HJ, *FIP Third Congress,* Session-I, paper No. 14, 1958, pp 147–157.
19. Evans, RH and MGA Khalil, "A Design method of prestressed concrete beams subjected to combined bending and torsion," *Proceedings of the International Conference on Shear Torsion and Bond in Reinforced and Prestressed Concrete,* Coimbatore, India, January 1969.
20. Ananthanarayana, Y, N Arunachalam, and V Ramakrishnan, "The use of plastic kinematic hardening law in interpreting the combined flexure and torsion of prestressed concrete structural members," *Seminar on Problems of Prestressing*, *Preliminary Publications,* Madras, 1970, IV, pp 31–39.
21. Gausel, E, "Spannbeton balken mit I-formigem querschnitt beigleichzeitiger ein wirkiung von torsion, querkraft und moment," *Die Technische Hochsohule Norwegens*, Trondheim, April 1968, pp 116.
22. Bishara, A, "Prestressed concrete beams under combined torsion, bending and shear," *Journal of the American Concrete Institute, Proceedings,* Vol. 66, No. 7, July 1969, pp 525–538.
23. Collins, MP, "The normal moment yield criterion applied to beams in flexure and torsion," *Proceedings of the International Conference on Shear, Torsion and Bond in Reinforced and Prestressed Concrete,* P.S.G. College of Technology, Coimbatore, India, January 1969.
24. Hsu, TTC, "Torsion of structural concrete" – Interaction surface for combined torsion, shear and bending in beams without stirrups," *ACI Journal*, Vol. 65, No.1, January 1968, pp 51–60.
25. Zia, P, "What do we know about torsion in concrete members," *Proceedings ASCE,* Vol. 96, ST6, June 1970, pp 1185–1199.
26. Gesund FJ, GR Scheulte, Buchanan, and GA Gray, "'Ultimate strength in combined bending and torsion of concrete beams containing both longitudinal and transverse reinforcement," *ACI Journal, Proceedings,* Vol. 61, December, 1964, pp 1509–1522.
27. Mattock, AH, "How to design for Torsion," *Torsion of Structural Concrete, Special Publication, SP-18,* American Concrete Institute, 1968, pp 469–495.
28. Elfgren, L, "Reinforced concrete beams loaded in combined torsion bending and shear – A study of the ultimate load-carrying capacity," *Publications No.* 71:3, Chalmers University of Technology, Goteborg, second edition, 1971, p. 230.

29. Hsu, TTC, "Torsion in structural concrete – uniformly prestressed members without web reinforcement," *Journal of the Prestressed Concrete Institute,* Vol. 13, 1968, pp 34–44.
30. AS: 1481–1974, Australian Prestressed Concrete Code, 1974.
31. Rausch, E, "*Berechnung des Eisenbetons gegen verdrehung and Abscheren* (Design of reinforced Concrete for Torsion and Shear)," Springer Verlag, Berlin, 1929.
32. Lampert, P and MP, Collins, "Torsion, bending and confusion – An attempt to establish the facts," *Journal of the ACI.* Vol. 69, No. 8, August 1972, pp 500–504.
33. Collins, MP and D Mitchell, "Shear and torsion design of prestressed and non-prestressed concrete beams," *Journal of the Prestressed Concrete Institute,* Vol. 25, 1980, pp 32–100.
34. Lin, TY and P Chow, *Looking into the Future – A Handbook of Structural Concrete,* edited by Kong FK, Evans, RH, Cohen, E and Roll, F Pitman, London and McGraw-Hill, New York, 1983, Chapter 1. Warner RF, Prestressed Concrete and Partially Prestressed Concrete, Chapter 19, pp 19–1 to 19–52.
35. *Prestressed Concrete Institute PCI Design Handbook, Chicago,* Prestressed Concrete Institute, 1985.
36. Rangan, BV and AS Hall, "Design of prestressed concrete to beams subjected to combined bending, shear and torsion," *ACI Journal Proceedings,* Vol. 72, No. 3, March 1975.
37. Warner, RF and KA Faulkes, *Prestressed Concrete,* Pitman, Australia, 1978, pp 175–182.

Review Questions

8.1 What are the different ways of improving the shear resistance of structural concrete members by prestressing techniques?

8.2 Distinguish between web-shear, flexural and flexure-shear cracks in concrete beams with sketches.

8.3 How do you estimate the ultimate shear strength of prestressed concrete sections with web-shear cracks?

8.4 Outline the factors influencing the ultimate shear resistance of prestressed concrete sections with flexure-shear cracks.

8.5 What is the effect of torsion on prestressed concrete sections? How do you compute the shear stress developed in different types of cross-sections due to torque?

8.6 Explain the various modes of failure encountered in prestressed concrete beams subjected to bending moment, shear and torsion.

8.7 Discuss briefly the basis of Indian standard IS: 1343 code recommendations regarding the design of reinforcements in prestressed sections subjected to moment, shear and torsion.

8.8 Briefly outline the skew bending theory and space truss analogy with respect to design of reinforcements in prestressed sections subjected to combined moment, shear and torsion.

8.9 List some practical examples of structures subjected to combined bending, shear and torsion.

8.10 Sketch a typical cross-section of a concrete beam showing various reinforcements designed for combined bending, shear and torsion.

Exercises

8.1 The horizontal prestress at the centroid of a concrete beam of rectangular cross-section 120 mm and 250 mm, is 7 N/mm^2 and the maximum shearing force on the beam is 70 kN. Calculate the maximum principal tensile stress. What is the minimum vertical prestress required to eliminate this principal tensile stress?

[Ans: 1.4 N/mm^2; 1.75 N/mm^2]

8.2 A prestressed concrete beam having an unsymmetrical I-section, has a fibre stress distribution of 13 N/mm^2 (compression) at the top edge and linearly reducing to zero at the bottom. The top flange width and thickness are 2400 and 400 mm, respectively, the bottom flange width and thickness are 1200 and 900 mm, respectively, and the depth and thickness of the web are 1000 and 600 mm, respectively. The total vertical service-load shear in the concrete at the section is 2350 kN. Compute and compare the principal tensile stress at the centroidal axis and at the junction of the web with the lower flange.

[Ans: At centroidal axis, tensile stress = 0.7 N/mm^2
At junction of web and bottom flange = 0.85 N/mm^2]

8.3 A concrete beam of rectangular section 200 mm wide and 600 mm deep, is prestressed by a parabolic cable located at an eccentricity of 100 mm at midspan and zero at the supports. If the beam has a span of 10 m and carries a uniformly distributed live load of 4 kN/m, find the effective force necessary in the cable for zero shear stress at the support section. For this condition, calculate the principal stresses. The density of concrete is 24 kN/m^3.

[Ans: 860 kN; 7.2 N/mm^2]

8.4 The shear stress due to the imposed load at the centre of the web in an I-section is 3 N/mm^2 and the horizontal prestress at this point is 8.4 N/mm^2. The details of the cross-section are:

Width of top and bottom flanges = 250 mm, average thickness of top and bottom flanges = 120 and 80 mm respectively, overall depth = 750 mm, and thickness of web = 80 mm. Find the increase in the principal tensile stress if, due to eccentricity of the load, a torque of 5 kN m is applied on the section.

[Ans: 0.9 N/mm^2]

8.5 A concrete beam of rectangular section 250 mm wide and 650 mm overall depth, is subjected to a torque of 20 kN m and a uniform prestressing force of 150 kN. Calculate the maximum principal tensile stress. Assuming 15 per cent loss of prestress, calculate the prestressing force necessary to limit the principal tensile stress to 0.4 N/mm^2 **[Ans: 1.46 N/mm^2, 1570 kN]**

8.6 A concrete beam of rectangular section 300 mm wide and 800 mm deep, is subjected to a twisting moment of 30 kN m and a prestressing force of 150 kN acting at an eccentricity of 220 mm. Calculate the maximum principal tensile stress. If the beam is subjected to a bending moment of 100 kN m in addition to the twisting moment, calculate the maximum principal tensile stress.

[Ans: 1.52 N/mm^2 (top fibre); 2.22 N/mm^2 (bottom fibre)]

8.7 A concrete box section girder has an overall depth and width of 800 and 600 mm, respectively. The concrete walls are 100 mm thick on both the horizontal and vertical parts of the box. Determine the maximum permissible torque if the section is uniformly prestressed by a force of 200 kN. Assume the maximum permissible diagonal tensile stress as 0.7 N/mm^2. **[Ans: 72.1 kN m]**

8.8 An unsymmetrical I-section bridge girder has the following sectional properties: Area of cross-section = 777×10^3, second moment of area = 22×10^{10} mm^4, width and thickness of top flange = 1200 and 360 mm, respectively, and thickness of web = 240 mm. The centroid of the section is located at 580 mm from the top. The girder is used over a span of 40 m. The tendons with a cross-section of 700 mm^2 are parabolic with an eccentricity of 1220 mm at the centre of span and zero at the supports. The effective prestress in the wires is 800 N/mm^2. If the tensile strength of concrete is 4.5 N/mm^2, estimate the ultimate shear resistance of the section, assuming failure to take place when the principal tensile stress reaches a value equal to the tensile strength of concrete.

[Ans: 2860 kN]

8.9 The support section of a prestressed concrete beam, 100 mm wide by 250 mm deep, is required to support an ultimate shear force of 80 kN. The compressive prestress at the centroidal axis is 5 N/mm^2. The characteristic cube strength of concrete is 40 N/mm^2. The cover to the tension reinforcement is 50 mm. If the characteristic tensile strength of stirrups is 415 N/mm^2, design suitable shear reinforcements in the section using IS code recommendations.

[Ans: 8 mm diameter two-legged stirrups at 150 mm centres]

8.10 A post-tensioned bonded prestressed concrete beam of rectangular section 350 mm wide by 700 mm deep, is prestressed by an effective force of 180 kN acting at an eccentricity of 190 mm. At service-load conditions, a section of the beam is subjected to a bending moment of 250 kN m, a torsional moment of 100 kN m and a transverse shear force of 100 kN. If $f_{ck} = 40$ N/mm^2, $f_y = 415$ N/mm^2, $f_p = 1600$ N/mm^2, design suitable longitudinal and transverse reinforcements in the section using IS: 1343–1980 code recommendations.

[Ans: Longitudinal reinforcement: three bars of 25 mm diameter
Transverse reinforcement: 12 mm diameter two-legged stirrups
at 100 mm centres]

8.11 A prestressed concrete tee beam has a flange 1000 mm wide and 200 mm thick. The web is 200 mm thick and 1000 mm deep. At a particular section the beam is subjected to an ultimate moment and shear force of 2000 kN.m and 250 kN, respectively. Calculate the flexure-shear resistance and design suitable shear reinforcements at the section using the following data:
Effective depth = 1100 mm, Cube strength of concrete = 40 N/mm^2
Effective prestress at the extreme tensile face of beam = 19.3 N/mm^2
Second moment of area of cross-section = 7.533×10^{10} mm^4
Area of prestressing steel = 2310 mm^2
Tensile strength of tendons = 1500 N/mm^2
Effective stress in tendons after all losses = 900 N/mm^2

[Ans: V_{cf} = 278 kN, A_{sv} = 100 mm^2, provide 8 mm diameter,
two-legged stirrups at 400 mm centres.]

8.12 A tee beam section has a flange width and thickness of 500 mm and 200 mm, respectively. The web is 200 mm thick and 600 mm deep. The beam spanning over 16 m is prestressed using a cable carrying an effective force of 2000 kN. The cable is parabolic with an eccentricity of 600 mm at centre of span and 300 mm at supports. Estimate the ultimate shear resistance at the support section. Also, evaluate the maximum permissible uniformly distributed working load on the beam assuming a load factor of 2 and characteristic compressive strength of concrete as 40 N/mm^2.

[Ans: V_{cw} = 541 kN, w_w = 33.8 kN/m]

Objective-type Questions

8.1 Horizontal or axial prestressing of concrete beams
(a) reduces the shear strength of the member
(b) has no effect on the shear strength
(c) increases the shear strength

8.2 Prestressing a concrete beam with sloping or curved cables
(a) increases the shear strength
(b) increases the flexural strength
(b) decreases the shear strength

8.3 Web-shear cracks are likely to develop in prestressed beams with
(a) rectangular section
(b) tee section
(c) I-section with thin webs

8.4 Ultimate shear resistance of concrete beams failing due to web-shear cracks depends upon
(a) width of compression face
(b) compressive strength of concrete
(c) compressive prestress in concrete

8.5 Ultimate shear strength of prestressed beams failing due to flexure-shear cracks is influenced by
(a) the width of the section
(b) effective prestress after all loses
(c) tensile strength of concrete

8.6 The spacings of stirrups in a prestressed beam should
(a) not exceed the overall depth
(b) not be greater than effective depth
(c) not exceed 0.75 times the effective depth

8.7 Torsional shear stresses developed in prestressed members is inversely proportional to the
(a) magnitude of torsion
(b) Grade of concrete
(c) depth of the member

8.8 Large magnitudes of torsion are better resisted by selecting beams of
(a) rectangular section
(b) hollow box-girder section
(c) I-section

8.9 Torsional shear stresses are likely to develop in structural concrete members like
- (a) simply supported beams
- (b) ring beams of water tanks
- (c) tee beams

8.10 The ideal cross-section recommended to resist shear and torsion in bridge girders is
- (a) rectangular
- (b) tee
- (c) hollow box

Answers to Objective-type Questions

8.1 (c)	8.2 (a)	8.3 (c)	8.4 (a)	8.5 (b)
8.6 (c)	8.7 (c)	8.8 (b)	8.9 (b)	8.10 (c)

9 Transfer of Prestress in Pretensioned Members

9.1 Transmission of Prestressing Force by Bond

In a pretensioned system, when a wire is released from its temporary anchorage on the prestressing bed, the end of the wire swells as a result of the recovery of the lateral contraction and develops a wedge effect. This is to enable the prestressing force to become zero at the end of the wire. This is generally referred to as the Hoyer Effect[1]. The swelling of the wire is only a few thousandths of a millimetre, but it nevertheless produces considerable radial pressures on the concrete, giving rise to large frictional forces.

The transmission of prestressing force from steel to concrete is generally through a bond comprising (i) adhesion, (ii) friction, and (iii) shearing resistance (dilatancy). At intermediate points along the length of a beam, the bond stress is resisted by adhesion, while in the transfer zone the tendons invariably slip and sink into the concrete, destroying most of the adhesion. Consequently, the bond stresses are due to the friction and shearing resistance. The distribution of bond stress, stress in steel and concrete in the transmission zone are shown in Fig. 9.1. The maximum bond stress is reached in the zone of transverse compression. When the bond stress is zero, the stress in steel and concrete reach their maximum values, and uniform stress distribution is prevalent from this section. The length needed for achieving this is termed as *transmission length*.

9.2 Transmission Length

The length required at the ends of a pretensioned member for the build-up of stress in concrete is of great importance, particularly in short pretensioned units, since it controls the working bending moment and the shear force allowable on the section. The transmission length depends mainly on the diameter and surface characteristics of the wire, the elastic properties of steel and concrete, and the coefficient of friction between steel and concrete.

Based on the wedge action, Hoyer developed an expression for computing the transmission length, which is given by,

$$L_t = \frac{\phi}{2\mu}(1+\nu_c)\left(\frac{\alpha_e}{\nu_s} - \frac{f_{pi}}{E_c}\right)\left(\frac{f_{pe}}{2f_{pi} - f_{pe}}\right)$$

where L_t = transmission length
ϕ = wire diameter
μ = coefficient of friction between steel and concrete
ν_c = Poisson's ratio for concrete
ν_s = Poisson's ratio for steel
α_e = modular ratio (E_s/E_c)
E_c = modulus of elasticity of concrete
f_{pi} = initial stress in steel
f_{pe} = effective stress in steel

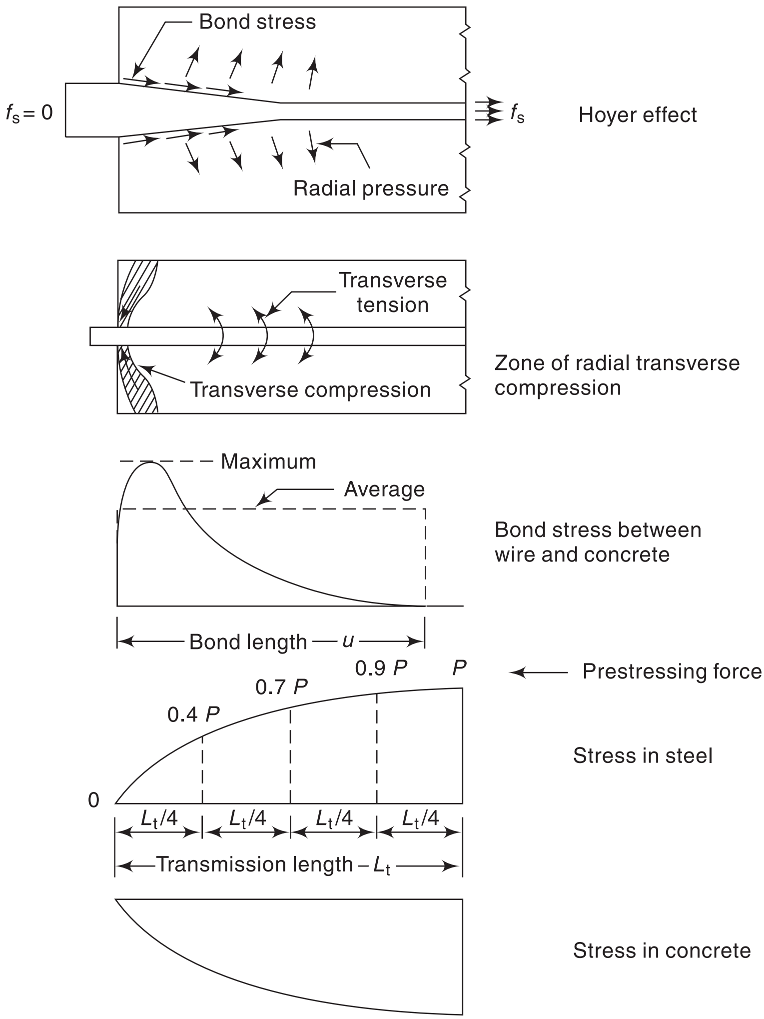

Fig. 9.1 *Distribution of bond stresses*

Under the normal range of values of these parameters, the transmission length is likely to vary from 80 to 160 ϕ.

Several tests have been carried out by many investigators to determine the transmission length. These methods can be classified into different categories depending upon the principles under which the solutions are obtained. Some of the notable investigations are:

1. Tests due to Evans and Robinson[2], Guyon[3] and Marshall and Krishna Murthy[4], in which the pull in or slip of the tendons into the concrete at the time of transfer is the influencing parameter.
2. Tests due to Rusch and Rehm[5], based on the basic law of the bond.
3. Tests due to Marshall[6], based on the theoretical investigations of Janney[7] and Guyon.

A comparative analysis of various proposals indicate that the semi-empirical relations suggested by Marshall and Krishna Murthy are applicable for both plain smooth wires and strands. The experimental results have been found to be in general agreement with the predictions for transmission lengths based on the empirical formulae,

$$L_t = \sqrt{\frac{\sqrt{f_{cu}} \times 10^3}{\beta}}$$

where f_{cu} = cube strength of concrete at transfer, expressed in N/mm^2

L_t = transmission length in mm

β = constant, depending upon the details of strand and wire

The values of constant β for some of the typical wires and strands are compiled in Table 9.1.

Table 9.1 *Values of constant β*

S.No.	*Details of Wire or Stand*	β
1	2 mm dia. wire	0.144
2	5 mm dia. wire	0.0235
3	7 mm dia. wire	0.0174
4	10 mm dia., seven-wire strand	0.144
5	12.5 mm dia., seven-wire strand	0.058
6	18 mm dia., 19-wire strand	0.0235
7	19 mm dia., seven-wire strand	0.0235
8	Twin twisted wires or 6.25 mm dia., seven-wire strand	0.077

The transmission length prevailing at the time of transfer does not remain constant, but increases at a decreasing rate with time due to the effects of creep and shrinkage of concrete. Using radiographic strain measuring techniques, Evans and Robinson[2] have conclusively shown that the influence of passage of time is to increase the transmission length and to move it bodily away from the end face of the member. This factor is significant, especially in fixing up the support points of short pretensioned members. The anchorage of smooth wires by adhesion alone is, therefore, not reliable, particularly in the case of short members and members subjected to repetitive loads.

The crimping of wires by passing them between toothed wheels results in their becoming resistant to slip by an increased amount, although it may slightly reduce the tensile strength of the wire. There are a number of methods by which a reliable shear bond can be achieved. This differs from the ordinary bond of smooth wires in that it is not dependent upon adhesion or friction alone. Several methods used for obtaining shear bond are as follows:

1. The surface of drawn round wires is roughened by pickling to produce fine irregularities which interlock with the concrete[8]
2. Twisting of round wires into strands
3. Cold rolling of elliptical or rhombic shallow indentations on the surface of wires
4. Hot rolling of oblique transverse ribs on wires which are subsequently heat treated[9]

According to Ros[10], the transmission length of smooth, round wires of 1.5–5 mm diameter varies approximately from 100–300 diameter, respectively, after allowing for the time-dependent inelastic effects like creep. With crimping or indentations, these values could be considerably reduced. Also, a sudden release of wires by flame-cutting or other means results in increased bond length in the units near the releasing end of the bed. As such, the force in the tendons at transfer should be gradually and completely released before the tendons are cut between the units.

Example 9.1 Calculate the transmission length at the end of a pretensioned beam as per Hoyer's method using the following data:

Span of the beam = 50 m
Diameter of wires used = 7 mm
Coefficient of friction between steel and concrete = 0.1
Poisson's ratio for steel = 0.30
Poisson's ratio for concrete = 0.15
$E_s = 210\ \text{kN/mm}^2$ and $E_c = 30\ \text{kN/mm}^2$
Ultimate tensile strength of steel wire, $f_{pu} = 1500\ \text{N/mm}^2$
Initial stress in steel, $f_{pi} = 0.7\, f_{pu} = 1050\ \text{N/mm}^2$
Effective stress in steel, $f_{pe} = 0.6\, f_{pu} = 900\ \text{N/mm}^2$.

Solution.

Using Hoyer's expression,

$$L_t = \frac{\phi}{2\mu}(1+\nu_c)\left(\frac{\alpha_e}{\nu_s} - \frac{f_{pi}}{E_c}\right)\left(\frac{f_{pe}}{2f_{pi} - f_{pe}}\right)$$

$$= \frac{\phi}{(2\times 0.1)}(1+0.15)\left(\frac{7}{0.30} - \frac{0.7\times 1500}{30\times 10^3}\right)\left(\frac{900}{2\times 1050 - 900}\right)$$

$$L_t = 100\phi = 100(7) = 700\ \text{mm}$$

If the beam is simply supported over a span of 50 m, there should be at least 700 mm of beam projection beyond the centre of supports at each end. Therefore, the total length of the beam required to be cast at site is given by,

Overall length = $(50 + 2 \times 0.7)$ m = 51.4 m

Example 9.2 Estimate the transmission length at the ends of a pretensioned beam prestressed by 7 mm-diameter wires. Assume the cube strength of concrete at transfer as 42 N/mm². (Adopt Krishna Murthy's empirical relation)

Solution.

$$L_t = \sqrt{\frac{\sqrt{f_{cu}} \times 10^3}{\beta}}$$

For 7 mm-diameter smooth wires, $\beta = 0.0174$ (from Table 9.1) and $f_{cu} = 42$ N/mm², thus

$$L_t = \sqrt{\frac{\sqrt{42} \times 10^3}{0.0174}} = 610 \text{ mm} = 87\phi$$

If on the other hand, 5 mm-diameter wires are used, $\beta = 0.0235$, we get

$$L_t = \sqrt{\frac{\sqrt{42} \times 10^3}{0.0235}} = 525 \text{ mm} = 105\phi$$

9.3 Bond Stresses

The magnitude of bond stresses developed between concrete and steel and its variation in the transfer zone of pretensioned beams is shown in Fig. 9.2. The bond stress is zero at the ends but builds up rapidly to a maximum over a very short length. This value decreases as the stress in the wire builds up. At a distance equal to the transmission length, the bond stress is almost zero while the stress in steel and concrete reach their maximum values.

If $(\tau_{bp})_{max}$ = maximum value of bond stress

$(\tau_{bp})_x$ = bond stress at a distance x from the free end

φ = diameter of the wire

f_s = stress in steel at distance x from the free end

f_{sc} = effective stress in steel at the end of transfer zone

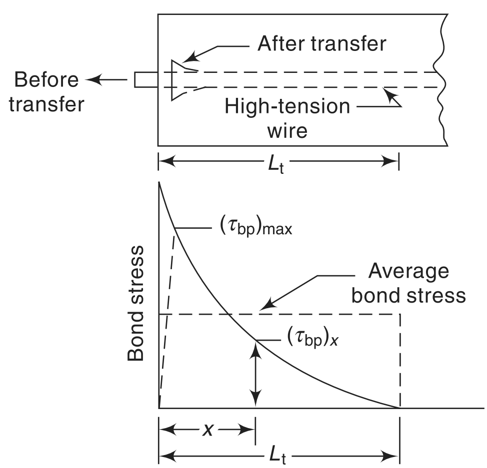

Fig. 9.2 *Bond stress in pretensioned beams*

Based on tests conducted at the University of Leeds, the following relations have been proposed by Marshall[11]:

$$(\tau_{bp})_x = (\tau_{bp})_{max}\, e^{-4\psi x/\phi}$$

$$f_s = f_{se}(1 - e^{-4\psi x/\phi})$$

where ψ = constant, expressed as the ratio of change in bond stress to steel stress

x = distance measured from the free end, expressed in mm

Based on tests using wires of 2 and 5 mm diameter stressed to 1575 and 1100 N/mm^2, respectively, in conjunction with a concrete having a cube crushing strength of 80 N/mm^2, the values of maximum bond stress $(\tau_{bp})_{max}$ and constant ψ were found to be 7.42 N/mm^2 and 0.00725, respectively. However, the magnitude of the average bond stress is considerably less than the maximum local bond stress. According to the investigations of Ros[10], the average bond stress varied from 3.25 to 1 N/mm^2 for round wires of 1.5 to 5 mm diameter in the case of wires initially tensioned to a stress of 1200 N/mm^2.

The stress in a steel wire gradually increases from zero at the end of the beam to 100 per cent of the effective stress at the end of the transmission length (Fig. 9.1). While 75 to 80 per cent of the effective prestressing force develops at about half of the transmission length, 90 to 95 per cent of the prestressing force is attained at about three-fourths of the transmission length from the end face of the beam.

Example 9.3 A pretensioned beam is prestressed using 5 mm-diameter wires with an initial stress of 80 per cent of the ultimate tensile strength of steel (f_{pu} = 1600 N/mm^2). The cube strength of concrete at transfer is 30 N/mm^2.

(a) Calculate the transmission length.

(b) Compute the bond stress at 1/4 and 1/2 the transmission length from the end.

(c) Calculate the overall average bond stress.

Solution.

$$L_t = \sqrt{\frac{\sqrt{f_{cu}} \times 10^3}{\beta}} = \sqrt{\frac{\sqrt{30} \times 10^3}{0.0235}} = 485 \text{ mm}$$

Bond stress is given by,

$$(\tau_{bp})_x = (\tau_{bp})_{max} \cdot e^{-4\psi x/\phi} = 7.42\, e^{-(4 \times 0.00725 \times x)/\phi}$$

If ϕ = 5 mm,

$$\tau_{dp} = 7.42\, e^{-0.0058x}$$

Bond stress at $L_t/4$ is given by,

$$\tau_{bp} = [7.42 e^{-0.0058 \times 121.25}] = 3.7 \text{ N/mm}^2$$

(at 121.25 mm from end)

Bond stress at $L_t/2$ is given by,

$$\tau_{bp} = [7.42 e^{-0.0058 \times 242.5}] = 1.82 \text{ N/mm}^2$$

(at 242.5 mm from end)

Overall average bond stress is given by,

$$\tau_{\mathrm{bp}}\,(\text{average}) = \left[\frac{19.6 \times 0.8 \times 1600}{\pi \times 5 \times 485}\right] = 3.30\ \mathrm{N/mm^2}.$$

9.4 Transverse Tensile Stresses

Transverse tensile stresses of considerable magnitude develop in the transfer zone due to the concentration of tendons at the ends. These stresses are influenced by jacking and the method of releasing the tendons from the pretensioning beds. Generally, the tensile stresses are found to be maximum at or near the centroidal section of the end faces of the beams. If the tensile stresses exceed the tensile strength of concrete, horizontal cracking occurs. A number of cases of cracks developed in precast pretensioned members are reported by Fountain[12]. It has been found that the method of distributing tendons at the ends has a greater influence on the end-zone cracking.

The problem of end-zone cracking in pretensioned I-beams has been experimentally investigated by Marshall and Mattock[13], and also by Arthur and Ganguli[14]. The former investigations have led to the determination of tensile stresses by the empirical equation of the type,

$$f_{\mathrm{v}} = \left(\frac{KM}{b_{\mathrm{w}} d^2}\right)$$

where f_{v} = transverse tensile stress at the centroid of the end face

M = resulting bending moment between the prestressing force and the internal prestress developed in concrete on the centroidal axis

i_{w} = thickness of web

h = overall depth of the beam

K = constant, having values of 9 and 18 depending upon the slope and distribution of tendons at the ends

Recent investigations, by Marshall[15] and Krishna Murthy[16], involving extensive tests on pretensioned I-beams indicate that the transverse tensile stress distribution in the transfer zones can be computed by an expression of the type,

$$f_{\mathrm{v}} = \frac{10M}{b_{\mathrm{w}} h L_{\mathrm{t}}}(1 - x/L_{\mathrm{t}})e^{-3.5xL_{\mathrm{t}}}$$

where L_{t} = transmission length, to be computed by the expression outlined in Section 9.2

x = distance from the end face

The maximum tensile stress is found to occur at the centroid of the end face when $x = 0$ and the magnitude of the stress is given by,

$$f_{\mathrm{v(max)}} = \left(\frac{10M}{b_{\mathrm{w}} h L_{\mathrm{t}}}\right)$$

9.5 End-Zone Reinforcement

In the transfer zone of pretensioned beams, transverse reinforcements are necessary to prevent the failure of the end zones due to the cracking of concrete as a consequence of large transverse tensile stresses, which often exceed the tensile strength of concrete. The theoretical distribution of tensile stress is shown in Fig. 9.3, which is based on the empirical equation proposed by Krishna Murthy[16]. For purposes of design of end reinforcement, a linear variation of tensile stress over half the transmission length has been assumed to compute the splitting tensile force[17].

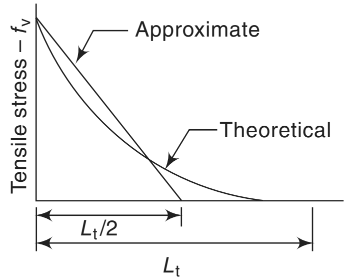

Fig. 9.3 *Theoretical distribution of tensile stress*

If F_{bst} = transverse tensile force, then

$$F_{bst} = \frac{1}{2} f_{v(\max)} \frac{L_t}{2b_w}$$

If A_{av} = area of vertical steel required

f_s = permissible stress in the reinforcement

$$A_{sv} = \frac{F_{bst}}{f_s} = 1/2\left[\frac{f_{v(\max)} L_t}{f_s 2b_w}\right]$$

But $$f_{v(\max)} = \left(\frac{10M}{b_w h L_t}\right)$$

Hence, $$A_{sv} = \left(\frac{2.5M}{f_s h}\right)$$

Reinforcement is provided in the form of closed stirrups enclosing all the tendons. Wherever single-leg stirrups are used, care should be taken to anchor the stirrups to the bottom and top tendons with cross-pieces. The first stirrup should be placed as close to the end face as possible with due regard to the minimum cover requirements. About half of the total reinforcement is preferably located within a length equal to one-third of the transmission length from the end, the rest being distributed in the remaining distance. Proper compaction of concrete in the end zones by vibration is essential to achieve dense concrete associated with high strength.

Example 9.4 A pretensioned beam of 8 m span has a symmetrical I-section. The flanges are 200 mm wide and 60 mm thick. The web thickness is 80 mm and the overall depth of girder is 400 mm. The member is prestressed by 8 wires of 5 mm diameter located on the tension side such that the effective eccentricity is 90 mm. The initial stress in the wires is 1280 N/mm^2 and the cube strength of concrete at transfer is 42 N/mm^2.

(a) Determine the maximum vertical tensile stress developed in the transfer zone.
(b) Design suitable mild steel reinforcement, assuming the permissible stress in steel as 140 N/mm^2.

Solution. The distribution of 5 mm diameter high-tensile wires in the cross-section is shown in Fig. 9.4, along with the longitudinal stress distribution at a distance equal to the transmission length from the end face of the member.

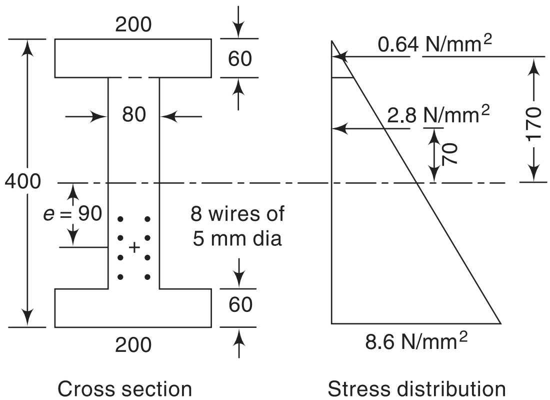

Fig. 9.4 *Distribution of prestress*

$$A_c = 46400 \text{ mm}^2$$
$$I = 847 \times 10^6 \text{ mm}^4$$
$$Z_b = Z_t = Z = (4235 \times 10^3) \text{ mm}^3$$

Total prestressing force, $P = (19.6 \times 8 \times 1280) = 200 \times 10^3 \text{ N} = 200 \text{ kN}$

$$\text{Stress at the bottom fibre} = \left[\frac{P}{A} + \frac{Pe}{Z}\right]$$
$$= \left[\frac{200 \times 10^3}{464 \times 10^2} + \frac{200 \times 10^3 \times 90}{4235 \times 10^3}\right]$$
$$= 8.6 \text{ N/mm}^2 \text{ (compression)}$$

$$\text{Stress at the top fibre} = \left[\frac{P}{A} - \frac{Pe}{Z}\right] = \left[\frac{200 \times 10^3}{464 \times 10^3} - \frac{200 \times 10^3 \times 90}{4235 \times 10^3}\right] = 0$$

Taking into consideration all the forces above the centroidal axis of the section, External moment due to prestressing force = 0

The internal moment due to the distribution of prestress developed is obtained as,

$$M = [(200 \times 60 \times 0.64 \times 170) + (140 \times 80 \times 2.8 \times 70)] = 351 \times 10^4 \text{ N mm}$$

Transmission length,

$$L_t = \sqrt{\frac{\sqrt{f_{cu}} \times 10^3}{0.0235}} \quad \text{for 5 mm-diameter wires}$$

$$L_t = \sqrt{\frac{\sqrt{42} \times 10^3}{0.0235}} = 525 \text{ mm}$$

Maximum vertical tensile stress near the end face

$$= \left(\frac{10M}{b_w h L_t}\right) = \left(\frac{10 \times 351 \times 10^4}{80 \times 400 \times 525}\right) = 2.09 \text{ N/mm}^2$$

Area of vertical reinforcement A_{sv}

$$= \left(\frac{2.5M}{f_s h}\right) = \left(\frac{2.5 \times 351 \times 10^4}{140 \times 400}\right) = 158 \text{ mm}^2$$

Provide three bars of 6 mm-diameter stirrups (two-legged) in the transfer zone.

9.6 Flexural-Bond Stresses

Pretensioned or post-tensioned beams with bonded tendons develop bond stresses between steel and concrete when the sections are subjected to transverse shear forces due to the rate of change of moment along the beam length. In the case of uncracked members, bond stresses are computed by considering the complete section, which is effective. Figure 9.5 shows a beam with bonded tendons subjected to transverse loads,

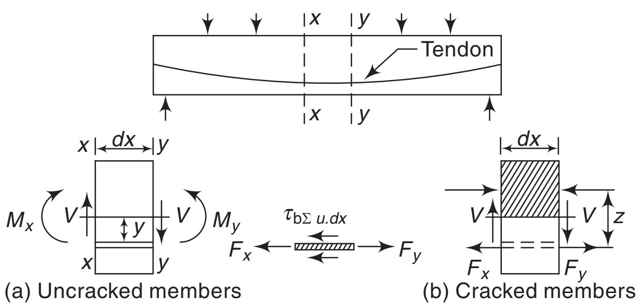

Fig. 9.5 *Flexural-bond stresses*

where τ_b = bond stress between steel and concrete

V = shear force

M_x and M_y = moments at sections xx and yy

Σu = total perimeter of the tendons

y = distance of the tendon from the centroidal axis

I = second moment of area of the section

α_e = modular ratio = (E_s/E_c)

A_s = area of steel

f_x and f_y = bending stress in concrete at the level of steel at sections xx and yy

From Fig. 9.5(a), considering the forces and moments,

$$(M_y - M_x) = Vdx = \left[\left(\frac{f_y I}{y}\right)\times\left(\frac{f_x I}{y}\right)\right]$$

$$\therefore \qquad Vdx = \left(\frac{I}{\alpha_e A_s y}\right)(\alpha_e A_s f_y - \alpha_e A_s f_x) = \frac{I}{\alpha_e A_s y}(F_y - F_x)$$

$$Vdx = \left(\frac{I}{\alpha_e A_s y}\right)(\tau_b\, \Sigma u dx)$$

$$\therefore \qquad \tau_b = \left(\frac{\alpha_e A_s y V}{I\, \Sigma u}\right) \tag{9.1}$$

If round wires are used,

$$\left(\frac{A_s}{\Sigma u}\right) = \Phi/4$$

where Φ = diameter of the wires,

then $$\tau_b = \left(\frac{V y \alpha_e \Phi}{4I}\right) \tag{9.2}$$

In the case of cracked flexural members, bond stresses change suddenly at the cracks due to the abrupt transfer of tension from concrete to steel in the vicinity of the cracks. The bond stresses gradually reduce to a minimum value in between the cracks. The local bond stress can be evaluated in cracked sections by using the conventional linear theory of tracked reinforced concrete sections.

Considering the cracked sections of a beam of length dx as shown in Fig. 9.5(b),

$$Vdx = (F_y - F_x)Z$$

where Z = lever arm between the compressive force in concrete and the tensile steel force

If τ_b = bond stress developed

$$Vdx = (\tau_b\, \Sigma u dx)Z$$

$$\therefore \qquad \tau_b = \left(\frac{V}{z\Sigma u}\right) \tag{9.3}$$

Example 9.5 A post-tensioned prestressed concrete rectangular beam, 240 mm wide and 500 mm depth, is grouted before the application of live loads. The steel consists of three tendons, each made up of 12 numbers of 7 mm-diameter wires encased in a thin metallic hose of 30 mm diameter with an effective cover of 50 mm. The modulus of elasticity of steel and concrete are 210 and 35 kN/mm^2, respectively. The beam spans 10 m and supports two concentrated loads of 250 kN each at the third points. Compute the unit bond stress,

(a) between each wire and grout; and
(b) between the hose and the concrete

Solution.
Maximum shear force in the beam, $V = 250$ kN

Second moment of area, $I = \left(\dfrac{(240 \times 500^3}{12}\right) = (25 \times 10^8)\ \text{mm}^4$

Modular ratio, $\alpha_e = (E_s/E_c) = 6$

$y = 200$ mm

(a) Bond stress between each wire and grout is given by,

$$= \left(\frac{Vy\alpha_e\Phi}{4I}\right) = \left(\frac{250 \times 10^3 \times 200 \times 6 \times 7}{4 \times 25 \times 10^8}\right) = 0.21\ \text{N/mm}^2$$

(b) Bond stress between the hose and the concrete is calculated as,
Area of steel in one hose, $A_s = (12 \times 38.5) = 462\ \text{mm}^2$
Hose diameter = 30 mm
Hose circumference = $(\pi \times 30) = 94$ mm
Bond stress between the hose and the concrete

$$= \left(\frac{V\alpha_e A_s y}{\Sigma u I}\right) = \left(\frac{250 \times 10^3 \times 6 \times 462 \times 200}{94 \times 25 \times 10^8}\right) = 0.59\ \text{N/mm}^2$$

Example 9.6 A prestressed beam of rectangular section, 200 mm wide and 500 mm deep is pretensioned by five high-tensile wires of 7 mm diameter located at an eccentricity of 150 mm. The maximum shear force at quarter span section is 200 kN. If the modular ratio as 6, compute the bond stress developed assuming (a) the section is uncracked (b) the section is cracked.

Solution. Given data:

$V = 200$ kN, $b = 200$ mm, $D = 500$ mm,
$e = 50$ mm, $y = [250 - 100] = 150$ mm
$\Phi = 7$ mm, $\alpha_e = 6$, $I = [bD^3/12] = [(200 \times 500^3)/12] = (21 \times 10^8)\ \text{mm}^4$
$d = 400$ mm $z = [(7/8)400] = 350$ mm, $\Sigma u = (5 \times \pi \times 7) = 109.9$

(a) Section uncracked

Bond stress is, $\tau_b = \left[\dfrac{Vy\alpha_e\Phi}{4I}\right] = \left[\dfrac{200 \times 10^3 \times 150 \times 6 \times 7}{4 \times 21 \times 10^8}\right] = 0.15\ \text{N/mm}^2$

(b) Section cracked

Both stress is $\tau_b = \left[\dfrac{V}{z\Sigma u}\right] = \left[\dfrac{200 \times 10^3}{350 \times 109.9}\right] = 0.15\ \text{N/mm}^2$

9.7 Code Provisions for Bond and Transmission Length

The general provisions in the Indian code (IS: 1343) for the transmission length are expressed in terms of the diameter of the wire, bar or strand, taking into consideration the surface characteristics of the tendons.

In the absence of values based on actual test results, the following values are recommended for the transmission length, provided the concrete is well compacted and its strength at transfer is not less than 35 N/mm^2 and the tendons are released gradually:

1	Plain and indented wires	100 ϕ
2	Crimped wires	65 ϕ
3	Strands	30 ϕ

Note 1: ϕ is the diameter of the tendon.

Note 2: The recommended values of transmission length apply to wires of diameter not exceeding 5 mm and strands of diameter not exceeding 18 mm.

It is recommended that one-half of the transmission length shall overhang the support in simply supported beams and the whole of the transmission length should extend beyond the supports in the case of fixed ends.

The British code (BS EN: 1992–1–1) recommends an empirical equation for the computation of transmission length in the absence of experimental evidence.

The following equation is recommended where the initial prestressing force does not exceed 75 per cent of the characteristic strength of the tendon and where the ends of the units are fully compacted:

$$L_t = \frac{K_t \phi}{\sqrt{f_{ci}}}$$

where f_{ci} = concrete strength at transfer

ϕ = nominal diameter of the tendon

K_t = coefficient for the type of tendon and is selected from the following:

(a) Plain or indented wire (including crimped wire with a small wave height): $K_t = 600$;

(b) Crimped wire with a total wave height of not less than $0.15 = K_t = 400$;

(c) Seven-wire strand or super strand: $K_t = 240$; and

(d) Seven-wire drawn strand: $K_t = 360$.

In the American Concrete Institute code, (ACI 318M–2011), the development length of the strand proposed is based on tests using 5, 7.5 and 12.5 mm-diameter strands. For three- and seven-wire strands, it is stipulated that they should extend a distance beyond the critical section equal to

$$= \left(f_{ps} - \frac{2}{3} f_{se}\right) \frac{d_b}{7}$$

where d_b is the nominal diameter of the strand and f_{ps} and f_{sc} are as defined in Section 7.3.3.

The ACI code recommendations are based on the investigations of Kaar[18] and Hanson[19]. It includes both the length required to develop the effective prestress f_{se} and also the additional length over which the strand must be bonded to the concrete so that the tensile stress f_{ps} may also develop in the strand at the limit state of collapse of the member. In general, the transmission length for plain smooth wires is considerably greater than that for deformed bars or strands due to the absence of a mechanical interlock.

The bond lengths recommended in German specifications[20] are compiled in Table 9.2 for different types of wires.

Table 9.2 *German specifications for bond length*

Type of Wire	*Diameter, mm*	*Bond Length, l_b, mm*
Drawn steel (deformed)	3 to 8	600
Two- or three-wire strand	2 to 3	700
Seven-wire strand	2 to 4	1000
Transversely-ribbed steel	20 to 40-mm^2 area	500

Note: Transmission length = $\sqrt{l_b^2 + s^2}$

where l_b = bond length

s = disturbance length, which is equal to the distance from the wires to the edge or the distance between the wires.

The FIP[21] recommendations regarding the anchorage length to ensure transmission of the prestress to the concrete include the following limits:

(a) For wire tendons (100–140) ϕ

(b) For seven-wire strands (45–90) ϕ

where ϕ is the diameter of the tendons.

References

1. Hoyer, E and E Friedrich, “Beitrag zur frage der Haftspannung in Eisen betonbauteilen”, *Beton and eisen* (Berlin), Vol. 38, No. 6, 1939, pp 107–110.
2. Evans, RH and GW Robinson, “Bond stresses in prestressed concrete from X-ray photographs”, *Proceedings of the Institution of Civil Engineers*, London, March 1955, Part 1, Vol. 4, pp 212–235.
3. Guyon, Y, *Prestressed Concrete*, Contractors Record Ltd., London, 1953.
4. Marshall, WT, and D Krishna Murthy, “Transmission length of prestressing tendons from concrete cube strengths at transfer”, *The Indian Concrete Journal*, Vol. 43, No. 7, July 1969, pp 244–253.
5. Rusch, H, and G Rehm, “Tests for determining the transmission length of prestressing wires”, *Translation No. CJ. 120, Cement and Concrete Association*, London.
6. Marshall, WT, “A theory for end-zone stresses in pretensioned concrete beams,” *Journal of the Prestressed Concrete Institute*, April 1966, Vol. 11, pp 45–51.
7. Janney, R, “Nature of bond in pretensioned prestressed concrete,” *Journal of the American Concrete Institute, Proceedings*, Vol. 50, May 1954, pp 717–736.

8. Bjuggren, U, Strangbeton-Forspand Betong, betongindustrie Strangbeton-fabriken, Stockholm, 1942.
9. Leonhardt, F, *Prestressed Concrete Design and Constructions*, Second edition, Wilhelm Ernet and Sohn, Berlin, 1964, pp 80–83.
10. Ros, MR Empa Bericht Nr. 155. Vorgespannter *Beton*, Zurich, Marz.1946.
11. Marshall, G, "End anchorage and bond stresses in prestressed concrete," *Magazine of Concrete Research*, Vol. 1, No. 3, 1949, pp 123–127.
12. Fountain, RS, "A field inspection of prestressed concrete bridges," *Structural Bureau, Portland Cement Association*, Chicago, lllinois, USA, 1963.
13. Marshall, WT, and AH Mattock, "Control of horizontal cracking in the ends of pretensioned prestressed concrete girders," *Journal of the Prestressed Concrete Institute*, Vol. 7, Oct. 1962, pp 56–74.
14. Arthur, PD, and S Ganguli, "Tests on end zone stresses in pretensioned concrete I beams," *Magazine of Concrete Research*, Vol. 17, June 1965, pp 85–96
15. Marshall, WT, and D Krishna Murthy, "Design of end-zone reinforcement for pretensioned concrete beams," *Proceedings of the Sixth Congress of the Federation Internationale de la Precontrainte*, Prague, June, 1970.
16. Krishna Murthy, D, "A method of determining the tensile stresses in the end zones of pretensioned beams," *The Indian Concrete Journal*, Vol. 45, No. 7, July 1971, pp 286–297.
17. Krishna Murthy, D "'Design of end-zone reinforcement to control horizontal cracking in pretensioned concrete members, at transfer-I," *The Indian Concrete Journal*, Vol. 47, No. 9, Sept. 1973, pp 346–351.
18. Kaar, P and D Magura, "Effort of strand blanketing on performance of pretensioned girders," Journal of the Prestressed Concrete Institute, Vol. 10, No. 6, Dec. 1965, pp 20–34. *Also Portland Cement Association Development Department Bulletin*, D-97.
19. Hanson, SW, and PH Kaar, "Flexural bond tests of pretensioned beams," Journal of the American Concrete Institute, Proceedings, Vol. 55, No. 7, Jan 1959, pp 783–802. *Also Portland Cement Association Development Department Bulletin*, D-28.
20. Leonhardt, F, *Prestressed Concrete, Design and Construction*, Second edition, Wilhelm Ernst and Sohn, Berlin 1964, pp 79–86.
21. FIP *Recommendations: Practical Design of Reinforced and Prestressed Concrete Structures*, Thomas Telford Limited, London, 1984, p. 10.

Review Questions

9.1 Briefly explain the mechanism by which prestressing force is transferred to concrete in pretensioned members.

9.2 Explain with sketches the variation of bond stress, stress in steel and concrete in the transmission zone of pretensioned members.

9.3 What is transmission length? List the various factors influencing transmission length.

9.4 What are flexural bond stresses? How do you compute bond stress between (a) High-tensile wire and grout, and (b) the cable hose and concrete.

9.5 What are the factors influencing the transverse tensile stress in the end zone of pretensioned members?

9.6 Distinguish between the terms (a) adhesion, (b) friction and (c) dilatancy, with respect to the transfer of prestress in pretensioned members.

9.7 How do you calculate the flexural bond stress in uncracked and cracked pretensioned members?

9.8 What is the transmission length recommended in the I.S. code for strands?

9.9 Discuss briefly the IS: 1343 code provisions regarding bond and transmission length.

9.10 Outline the various methods by which bond between concrete and steel tendons can be improved.

Exercises

9.1 A post-tensioned prestressed concrete beam, 300 mm wide and 600 mm deep, is provided with two cables of 50 mm diameter each containing 12 wires of 8 mm diameter. The effective cover to the cables is 100 mm. The modulus of elasticity of steel and concrete are 210 and 35 kN/mm^2, respectively. The beam spans 12 m and supports a uniformly distributed live load of 50 kN/m. If the cables are grouted before the application of live loads, calculate the unit bond stress,
(a) between each wire and grout, and
(b) between the cable hose and concrete.

[Ans: (a) 0.133 N/mm^2 (b) 0.256 N/mm^2]

9.2 A pretensioned beam of rectangular section, 200 mm wide and 450 mm deep, is prestressed by 10 wires of 5 mm diameter located at an effective eccentricity of 150 mm. The maximum shear force at a particular section is 120 kN. If the modular ratio is 6, calculate the flexural bond stress developed assuming,
(a) the section as uncracked,
(b) the section as cracked.

[Ans: (a) 0.088 N/mm^2 (b) 2.18 N/mm^2]

9.3 A pretensioned beam, 160 mm wide and 320 mm deep, is prestressed by four plain wires of 7 mm diameter at an eccentricity of 100 mm. If the cube strength of concrete at transfer is 40 N/mm^2, estimate the transmission length at the ends of the pretensioned units using
(a) IS: 1343–1980 code provisions,
(b) BS: 8110–1985 code recommendations.

[Ans: (a) 700 mm (b) 664 mm]

9.4 A pretensioned beam, 200 mm wide and 500 mm deep, is prestressed by seven-wire 15 mm-diameter strands at an effective eccentricity of 200 mm. The cube strength of concrete at transfer is 35 N/mm^2. Estimate the transmission length for the strands using
(a) Indian
(b) British
(c) American code recommendations

[Ans: (a) 450 mm (b) 609 mm (c) 750 mm]

Objective-type Questions

9.1 Transfer of prestress in pretensioned members is due to
(a) bearing on end face
(b) shear resistance
(c) bond between concrete and steel

9.2 The transmission length at the end of a pretensioned member depends upon
(a) tensile strength of concrete
(b) diameter of the high-tensile wire
(c) ultimate tensile strength of steel

9.3 The bond stress between steel wire and concrete at the end of a pretensioned beam is
(a) maximum at a distance equal to the depth of the beam
(b) maximum at the end face
(c) maximum very near the end face

9.4 At the end face of a pretensioned beam the tensile stress in steel is
(a) maximum
(b) zero
(c) minimum

9.5 The transmission length in a pretensioned beam is inversely proportional to
(a) the diameter of the high-tensile wire
(b) Poisson's ratio of concrete
(c) coefficient of friction between steel and concrete

9.6 The transmission length according to the Indian standard code (IS: 1343 for strands is
(a) 65 φ where φ = diameter of the strand
(b) 30 φ
(c) 100 φ

9.7 Very near the end face of a pretensioned beam, the stresses developed in concrete are
(a) compressive
(b) tensile
(c) shear

9.8 At a distance equal to the transmission length from the end face of a pretensioned beam, the force in the tendon is
(a) zero
(b) 50 per cent of the initial prestressing force
(c) equal to the initial prestressing force

9.9 The bond stress between tendons and the grout is inversely proportional to the
(a) diameter of the tendon
(b) modular ratio
(c) second moment of area

9.10 The transmission length at the ends of a pretensioned beam is the least when the tendons used are
(a) strands
(b) crimped wires
(c) plain wires

Answers to Objective-type Questions

9.1 (c)	9.2 (b)	9.3 (b)	9.4 (b)	9.5 (c)
9.6 (b)	9.7 (b)	9.8 (c)	9.9 (c)	9.10 (a)

10 Anchorage Zone Stresses in Post-tensioned Members

10.1 Introduction

In the anchorage zone or the end block of a post-tensioned prestressed concrete element, the state of stress distribution is complex and three-dimensional in nature. In most post-tensioned members, the prestressing wires are introduced in cable holes or ducts, pre-formed in the members, and then stressed and anchored at the end faces. As a result of this, large forces, concentrated over relatively small areas, are applied on the end blocks. These highly discontinuous forces which are applied at the end, while changing progressively to continuous linear distribution, develop transverse and shear stresses.

According to St. Venant's principle, the stress distribution at a distance far away from the loaded face (normally at a distance equal to or greater than the depth of the beam) can be computed from the simple bending theory. The zone between the end of the beam and the section where only longitudinal stress exists is generally referred to as the anchorage zone or end block.

The transverse stresses developed in the anchorage zone are tensile in nature over a large length and since concrete is weak in tension, adequate reinforcement should be provided to resist this tension. Hence, from the point of view of the designer, it is essential to have a good knowledge of the distribution of stresses in the anchorage zone, so that he/she can provide an adequate amount of steel, properly distributed to sustain the transverse tensile stresses.

10.2 Stress Distribution in End Block

The forces on the end block of a post-tensioned prestressed concrete member are shown in Fig. 10.1(a). A physical concept of the state of stress in the transverse direction, that is, normal to planes parallel with the top and bottom surfaces of the beam, may be obtained by considering these lines of force as individual fibres acting as curved stuts inserted between end force 2 P and the main body of the beam. The curvature of the struts, being convex towards the centre line of the block, induces compressive stresses in zone A. In zone B, the curvature is reversed in direction and the struts tend to deflect outwards, separating from each other and consequently developing transverse tensile stresses. In zone *C*, the struts are straight and parallel so that no transverse stresses are induced; only longitudinal stresses develop in this zone.

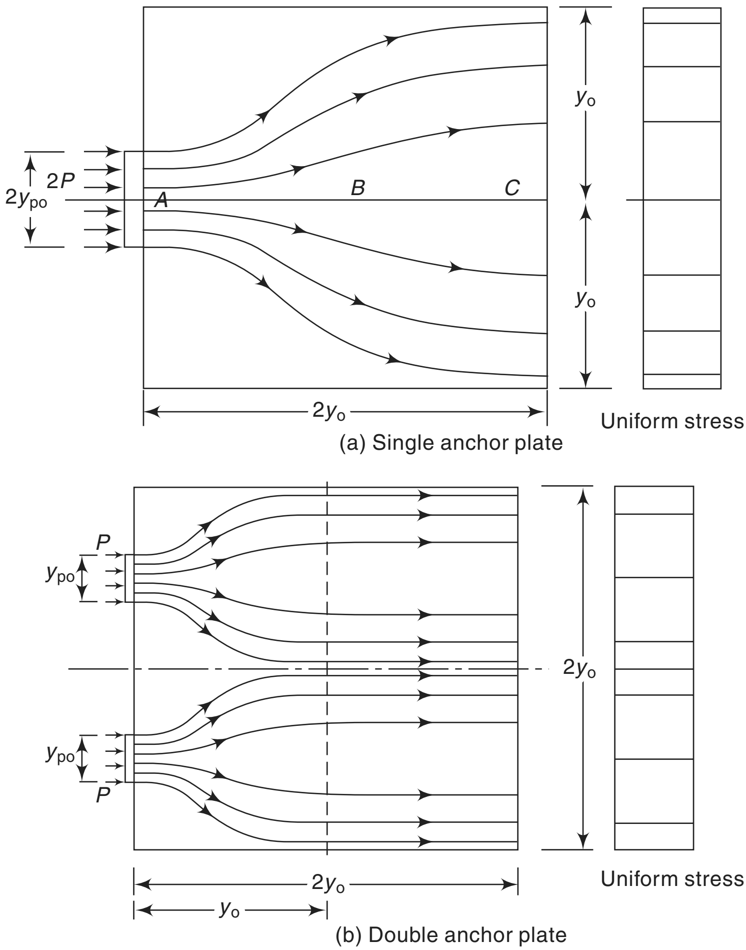

Fig. 10.1 *Transmission of forces in end block*

In Fig. 10.1(b), the same end block is subjected to the same total load applied through two zones symmetrically disposed in the upper and lower halves of the beam. Since the lines of force follow the same pattern with half the radius of curvature, the length of the anchorage zone is halved. The transverse tension developed is also proportionately reduced. In a similar way, the greater the number of points of application of the prestressing force on the end block, the more uniform is the stress distribution.

The idealised stress distribution in an end block with the compressive and tensile stress paths is shown in Fig. 10.2(a). The effect of transverse tensile stress is to develop a zone of bursting tension in a direction perpendicular to the anchorage force, resulting in horizontal cracking as shown in Fig. 10.2(b).

Since concrete is weak in tension, suitable reinforcements are generally provided in the transverse direction to resist the bursting tension.

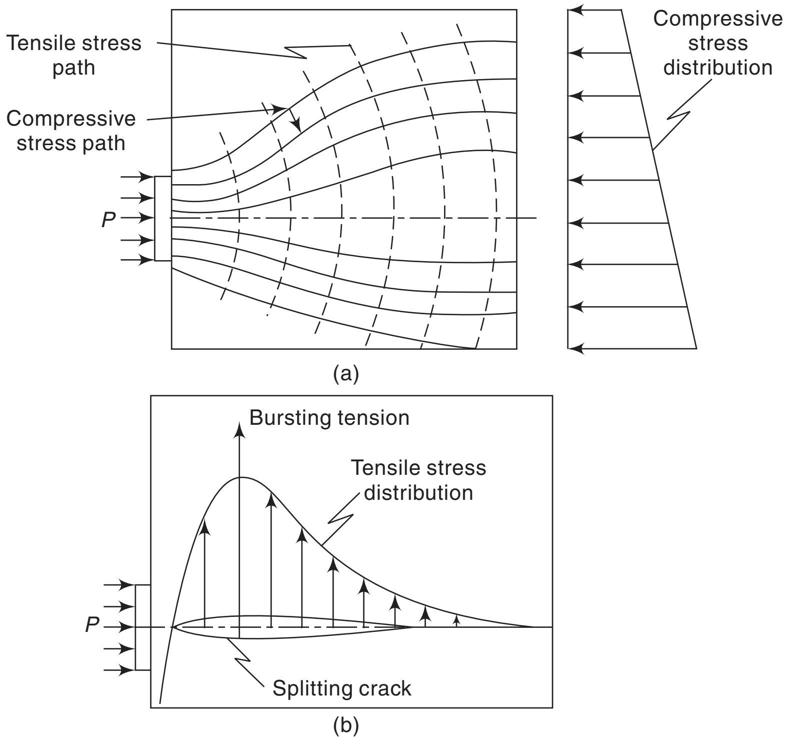

Fig. 10.2 *End blocks of post-tensioned beams (a) Idealised stress paths (b) Bursting tension and spitting cracks*

The distribution of transverse stresses in the anchorage zone subjected to a symmetrically placed prestressing force, which is distributed over a small area for increasing ratio of y_{po}/y_o varying from zero to 0.50, has been investigated by Guyon[1]. The results are shown in Fig. 10.3. The lines of equal transverse tensile stress are termed as isobars. The figure shows the influence of the height of the anchor plate on the distribution of compressive and tensile stresses in the transverse direction. The ratio of transverse tensile stress to the average compressive stress gradually decreases with the increase in the ratio of the depth of anchor plate to that of the end block.

10.3 Investigations on Anchorage Zone Stresses

A number of investigators have studied the stress distribution in the anchorage zone using empirical equations or theoretical solutions based on two or three-dimensional elasticity or experimental techniques. The important investigations were those done by Magnel[2], Guyon[3], Iyengar[4,5], Zielinski and Rowe[6], Yettram and Robbins[7] and Chandrasekhara *et al*[8]. The main aim of

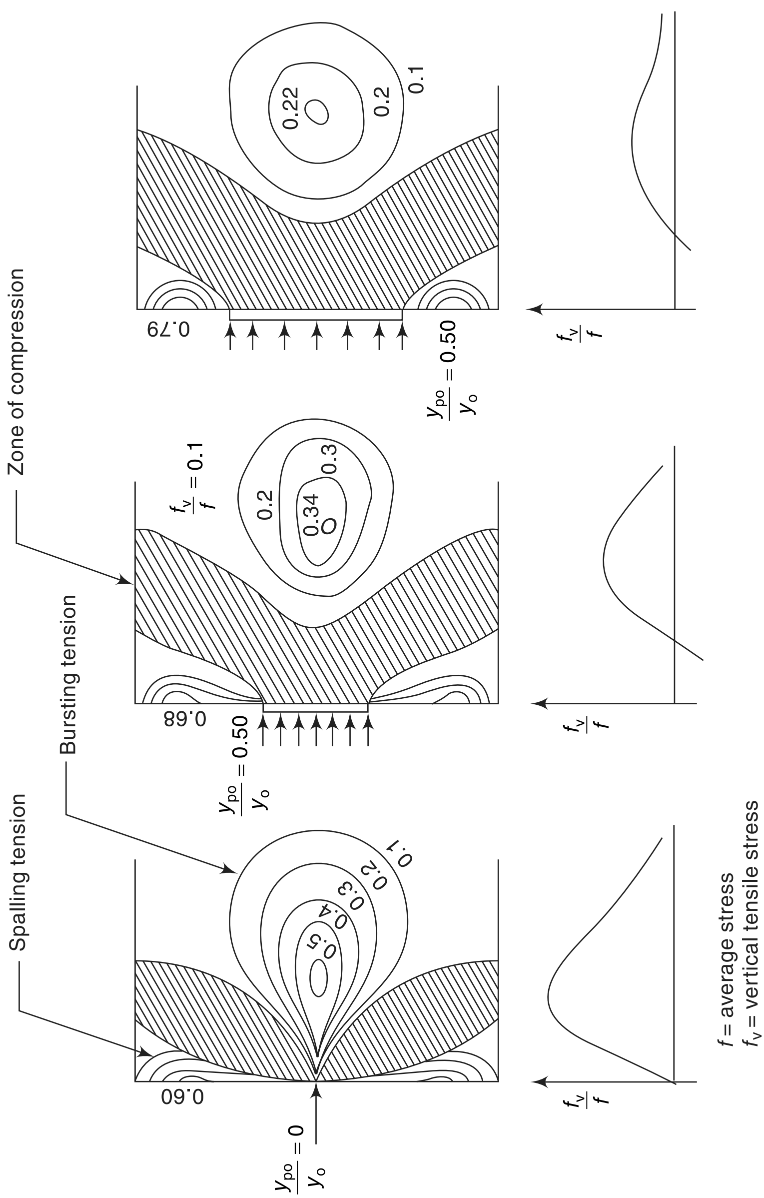

Fig. 10.3 *Isobars of transverse tensile stress*

stress analysis in the anchorage zone is to obtain the transverse tensile stress distribution in the end block from which the total transverse bursting tension could be computed.

A concise description of the methods of Magnel, Guyon, Zielinski and Rowe is presented to highlight the results of theoretical and experimental investigations.

10.3.1 Magnel's Method

In this method, the end block is considered as a deep beam subjected to concentrated loads due to anchorages on one side and to normal and tangential distributed loads from the linear direct stress and shear stress distribution from the other side. The forces acting on the end block and the stresses acting on any point on the horizontal axis parallel to the beam are shown in Fig. 10.4, with the following notations:

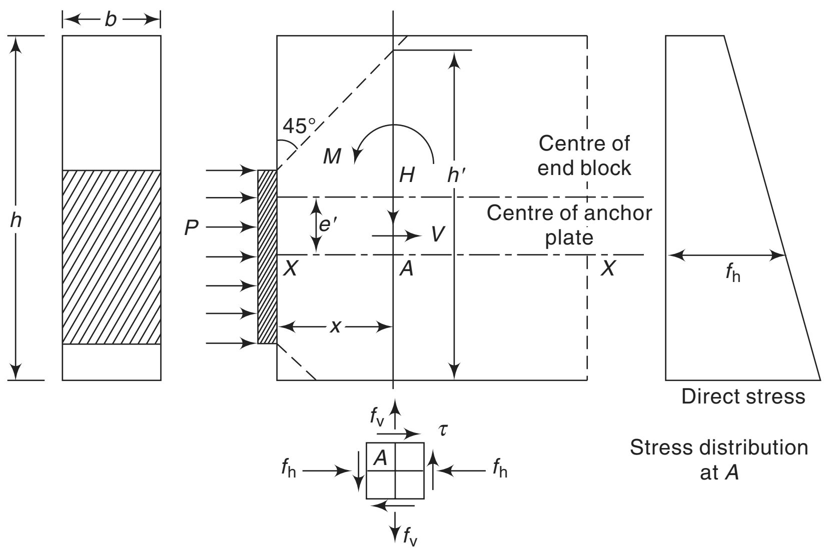

Fig. 10.4 *Forces acting on the end block*

M = bending moment
H = direct force (vertical) (directions shown in the figure are +ve)
V = shear force (horizontal)
f_v = vertical stress
f_h = direct stress (at point A shown in the figure)
τ = shear stress

The stress distribution across the section can be approximated by the following equations:

$$f_v = K_1\left(\frac{M}{bh^2}\right) + K_2\left(\frac{H}{bh}\right)$$

$$\tau = K_3\left(\frac{V}{bh}\right)$$

$$f_h = \frac{P}{bh}\left(1+12\frac{e'^2}{h'^2}\right)$$

Constants K_1, K_2, and K_3 are shown in Table 10.1 for varying distance from the end face of the beam.

Table 10.1 *Coefficients for stresses in end blocks (Magnel)*

Distance from far end, x/h	K_1	K_2	K_3
0	20.00	–2.000	0.000
0.10	9.720	0.000	1.458
0.20	2.560	1.280	2.048
0.30	–1.960	1.960	2.058
0.40	–4.320	2.160	1.728
0.50	–5.000	2.000	1.250
0.60	–4.480	1.600	0.768
0.70	–3.240	1.080	0.378
0.80	–1.760	0.560	0.128
0.90	–0.520	0.160	0.018
1.00	0	0	0

The direct stress f_h is computed by assuming that the concentrated load disperses at 45° and considering the depth of the section intercepted between the dispersion lines at the required point on the horizontal axis.

The principal stresses acting at the point are computed by the general equations:

$$f_{max} \text{ or } f_{min} = \left(\frac{f_v + f_h}{2}\right) \pm \frac{1}{2}\sqrt{(f_h - f_v)^2 + 4\tau^2}$$

$$\tan 2\theta = \left(\frac{2\tau}{f_v - f_h}\right)$$

The bursting tension is computed from the distribution of principal tensile stress on the required axis and suitable reinforcements are designed to take up this tension.

The application of Magnel's method is illustrated with the help of the following two examples:

Example 10.1 The end block of a prestressed concrete beam, rectangular in section, is 100 mm wide and 200 mm deep. The prestressing force of 100 kN is transmitted to concrete by a distribution plate, 100 mm wide and 50 mm deep, concentrically located at the ends. Calculate the position and magnitude of the maximum tensile stress on the horizontal section through the centre and edge of the anchor plate. Compute the bursting tension on these horizontal planes,

Solution. Given data:

$$P = 100 \text{ kN}$$
$$h = 200 \text{ mm}$$
$$b = 100 \text{ mm}$$

Direct stress, $f_h = \left(\dfrac{100 \times 10^3}{200 \times 100}\right) = 5 \text{ N/mm}^2$

Normally, the vertical stress f_v and the principal tensile stress are critical at $x = 0.5\,h$. Referring to Fig. 10.5,

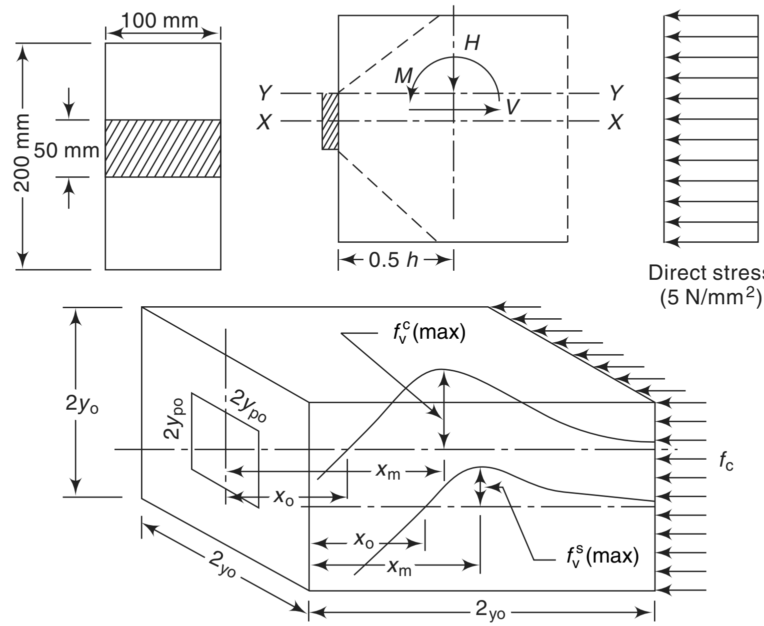

Fig. 10.5 *Forces acting on the end block*

For section XX

At $\dfrac{x}{h} = 0.5$ from Table 10.1

$$K_1 = -5.00$$
$$K_2 = 2.00$$
$$K_3 = 1.25$$

$$M = \left[(5 \times 100 \times 100)\left(\frac{100}{2}\right) - \left(\frac{100 \times 10^3}{2}\right)\left(\frac{50}{4}\right)\right] = 1875 \times 10^3 \text{ N mm}$$

$$V = 0 \text{ and } H = 0$$

$$\therefore \quad f_v = -5\left(\frac{1875 \times 10^3}{100 \times 200^2}\right) = -2.35 \text{ N/mm}^2$$

$$f_h = +5 \text{ N/mm}^2$$

The principal tensile stress (acting at 0.5 h = 100 mm from the end) is given by,

$$f_{\min} = \left(\frac{5-2.35}{2}\right) - \frac{1}{2}\sqrt{(5+2.35)^2 + 0} = -2.35 \text{ N/mm}^2$$

Therefore, the total splitting tension, assuming parabolic distribution of stress as shown in Fig. 10.6, is given by,

$$F_{\text{bst}} = [(2/3 \times 150 \times 2.35)100] = 23500 \text{ N}$$

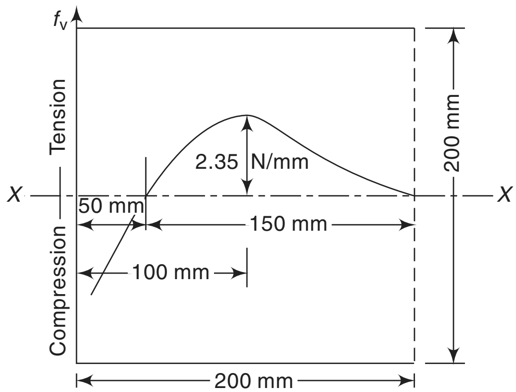

Fig. 10.6 *Distribution of tensile stress*

For section YY (passing through edge of plate)
Stresses at $x = 0.5h = 100$ mm from end

$$M = (100 \times 75 \times 5 \times 75/2) = 14 \times 10^5 \text{ N mm}$$
$$V = -(100 \times 75 \times 5) = -37500 \text{ N (acting towards the end of beam)}$$
$$H = 0$$

$$f_v = -5\left(\frac{14 \times 10^5}{100 \times 200^2}\right) + 0 = -1.75 \text{ N/mm}^2$$

$$\tau = 1.25\left(\frac{-37500}{100 \times 200}\right) = -2.35 \text{ N/mm}^2$$

$$f_h = +5 \text{ N/mm}^2$$

Principal tensile stress

$$= \left(\frac{5-1.75}{2}\right) - \frac{1}{2}\sqrt{(5+1.75)^2 + 4(-2.35)^2} = -2.475 \text{ N/mm}^2$$

Angle of inclination of the plane of principal stress with respect to the vertical plane is,

$$\tan 2\theta = \left(\frac{2\tau}{f_v - f_b}\right) = \left(\frac{-2 \times 2.35}{-1.75 - 5.0}\right) = 0.7$$

$\therefore$ $2\theta = 35°$ and $\theta = 17.5°$

Tensile stress component in the vertical direction

$$= (2.475 \times \sec 17.5°) = 2.6 \text{ N/mm}^2$$

Bursting tension, $F_{\text{bst}} = (2/3 \times 150 \times 2.6)100 = 26000$ N (on axis YY)

Example 10.2 The end block of a prestressed concrete beam, 100 mm wide and 200 mm deep, supports an eccentric prestressing force of 100 kN, the line of action of which coincides with the bottom kern of the section. The depth of the anchor plate is 50 mm. Estimate the magnitude and position of the principle tensile stress on a horizontal plane passing through the centre of the anchorage plate.

Referring to Fig. 10.7,

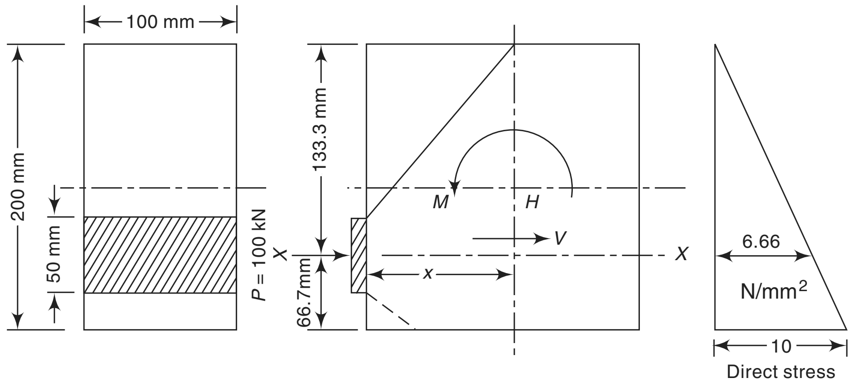

Fig. 10.7 *Forces acting on the end block*

Solution.

Stresses on XX

$$M = \left[\left(\frac{1}{2}\times 6.66\times 133.3\times 100\right)1/3\times 133.3\right]$$

$$-\,[(50\times 10^3)12.5] = 1345\times 10^3 \text{ N mm}$$

$$V = \left[\left(\frac{1}{2}\times 6.66\times 133.3\times 100\right) - (50\times 10^3)\right] = -5612 \text{ N}$$

$$H = 0$$

At $x = 0.5h = 100$ mm from end face

$$f_h = +6.666 \text{ N/mm}^2$$

$$f_v = -5\left[\frac{1345\times 10^3}{100\times 200^2}\right] = -1.66 \text{ N/mm}^2$$

$$\tau = 1.25\left[\frac{-5612}{100\times 200^2}\right] = -0.35 \text{ N/mm}^2$$

Principle tensile stress,

$$f_{min} = \left(\frac{6.66-1.66}{2}\right) - \frac{1}{2}\sqrt{(6.666+1.66)^2 + 4(-0.35)^2} = -1.7 \text{ N/mm}^2$$

Assuming the magnitude of the tensile stress in the vertical direction also as 1.7 N/mm^2, bursting tension

$$F_{bst} = (2/3\times 150\times 1.7)100 = 17000 \text{ N}$$

10.3.2 Guyon's Method

Guyon has developed design tables[9] for the computation of bursting tension in end blocks which are based on his earlier mathematical investigations[3] concerning the distribution of stresses in end blocks subjected to concentrated loads. The concept of symmetrical or equivalent prism for eccentric cables, and the method of partitioning for the analysis of stresses developed due to multiple cables have been introduced by Guyon.

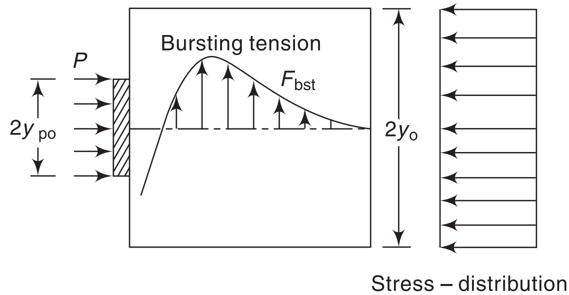

Fig. 10.8 *Evenly distributed force systems (Guyon)*

The distribution of forces at the ends are treated under the categories of *force evenly distributed* and *forces not evenly distributed*.

Forces evenly distributed When the forces are arranged such that the resultant of the stress distribution at a distance equal to the depth of the end block coincides with the line of action of the force as shown in Fig. 10.8, then the forces are considered to be evenly distributed. For eccentric forces and multiple cables, the symmetric prism method may be used. This consists of a prism of concrete of side equal to twice the distance of the prestressing force from the nearest free edge as shown in Fig. 10.9.

The position of zero stress, maximum transverse stress and its magnitude for the forces which are evenly distributed are computed by using the coefficients given in Table 10.2 under the category of distributed axial forces. According to Guyon, the bursting tension is expressed as,

$$F_{bst} = 0.3P[1 - (y_{po}/y_o)^{0.58}]$$

where P = anchorage force

y_{po}/y_o = distribution ratio

where $2y_{po}$ = depth of the anchorage plate

$2y_o$ = depth of the equivalent prism

Forces not evenly distributed When it is not possible to arrange the end forces evenly, Guyon recommends that transverse tensile stresses be investigated along *successive resultants*, such as (a) resultant of all forces, (b) resultant of smaller groups of forces, and (c) lines of action of individual forces.

The line of action of the resultant force is taken as the axis of an *equivalent prism* of length and depth equal to twice the distance of axis from the free

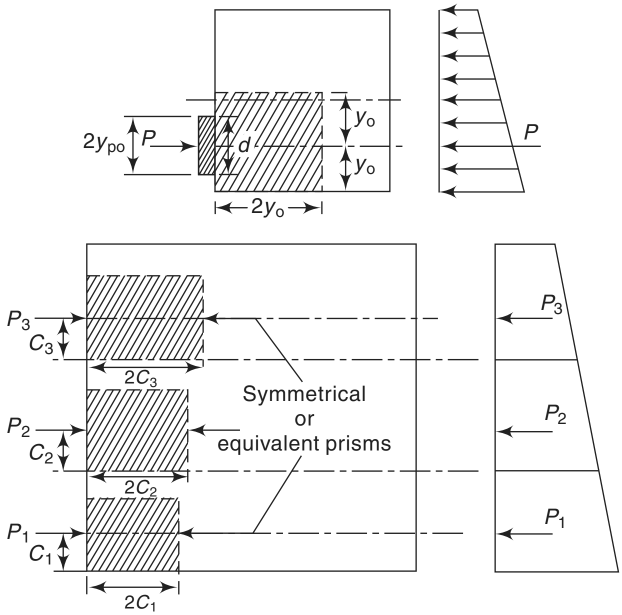

Fig. 10.9 *Evenly distributed force with equivalent prisms*

edge or the adjoining equivalent prism. The transverse stress distribution is computed by using the coefficients given in Table 10.2, under the category of concentrated eccentric force and eccentric shear force. Since the coefficients are applicable for forces at intervals of

Table 10.2 *Vertical stresses along axis at ends of prestressed beams (Guyon) (Ratios of local stress to average stress across whole section) + = compression; – = tension*

(a) Distributed axial force

Distribution Ratio y_{po}/y_o	*Position of Zero Stress* $x/2y_o$	*Position of Maximum Stress* $x/2y_o$	*Ratio of Maximum Tensile Stress to Average Stress*
0.00	0.00	0.17	0.50
0.10	0.09	0.24	0.43
0.20	0.14	0.30	0.36
0.30	0.16	0.36	0.33
0.40	0.18	0.39	0.27
0.50	0.20	0.43	0.23
0.60	0.22	0.44	0.18
0.70	0.23	0.45	0.13
0.80	0.24	0.46	0.09

(b) Concentrated eccentric force

Eccentricity of Force $e/2y_o$	Distance of Stress from end of Beam, $x/2y_o$						
	0	1/12	1/6	1/4	1/3	1/2	3/4
+1/2	–2.187	–0.913	–0.428	–0.014	+0.307	+0.399	+0.192
3/8	–1.222	–0.601	+0.125	+0.192	+0.250	+0.242	+0.122
+1/4	–0.758	–0.025	+0.238	+0.154	+0.062	–0.024	–0.016
+1/8	–0.566	+1.004	+0.074	–0.144	–0.266	–0.262	–0.128
0	0.000	–0.448	–0.500	0.462	–0.423	–0.314	–0.161
–1/8	–0.566	+1.004	+0.074	–0.144	–0.266	–0.262	–0.128
–1/4	–0.758	–0.025	+0.238	+0.154	+0.062	–0.024	–0.016
–3/8	–1.222	–0.601	+0.125	+0.192	+0.250	+0.242	+0.122
–1/2	–2.187	–0.913	–0.428	–0.014	+0.307	+0.399	+0.192

(c) Eccentric shear force

Eccentricity of Force $e/2y_o$	Distance of Stress from end of Beam, $x/2y_o$						
	0	1/12	1/6	1/4	1/3	1/2	3/4
+1/2	—	0	0	0	0	0	0
+3/8	+5.06	+2.96	+0.87	+0.19	–0.05	–0.14	–0.07
+1/4	+4.00	+3.10	+1.52	+0.44	–0.22	–0.20	–0.10
+1/8	+5.66	+2.96	+0.87	+0.19	–0.05	–0.14	–0.07
–0	—	0	0	0	0	0	0
–1/8	–5.66	–2.96	–0.87	–0.19	+0.05	+0.14	+0.07
–1/4	–4.00	–3.10	–1.52	–0.44	+0.22	+0.20	+0.10
–3/8	–5.66	–2.96	–0.87	–0.18	+0.05	+0.14	+0.07
–1/2	—	0	0	0	0	0	0

one-eighth of the prism depth, the end forces have to be replaced by a statically, equivalent system of normal and shear forces acting at these regular intervals as shown in Fig. 10.10.

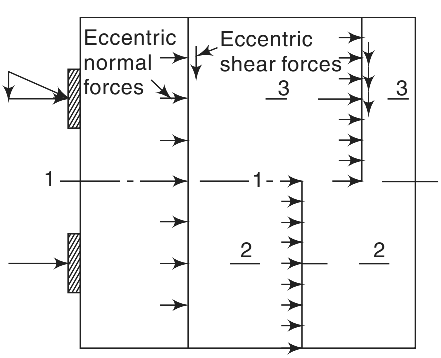

Fig. 10.10 *Distribution of normal and shear forces*

Stress analysis is considerably simplified by the use of influence lines presented by Evans and Bennett[10]. Suitable reinforcements are designed to resist bursting tension over the region where the tensile stress exceeds the permissible tensile strength of concrete as outlined in Sec. 10.3.

The application of Guyon's method is illustrated by the following three numerical examples.

Example 10.3 Using Guyon's method, compute the position and magnitude of maximum tensile stress and bursting tension for the end block with concentric anchor force of 100 kN as detailed in Example 10.1.

Solution. Given data:

$$P = 100 \text{ kN}$$
$$2y_{po} = 50 \text{ mm}$$
$$2y_o = 200 \text{ mm}$$

$\therefore$ Distribution ratio $y_{po}/y_o = 0.25$

From Table 10.2,

Position of zero stress from the end face $= 0.15(2y_o) = 30$ mm

Position of maximum stress $= 0.33(2y_o) = 66$ mm

$$\text{Maximum tensile stress} = 0.345(P/A) = 0.345 = \left(\frac{100 \times 10^3}{200 \times 100}\right) = 1.725 \text{ N/mm}^2$$

$$\text{Bursting tension, } F_{bst} = 0.3P[1 - (y_{po}/y_o)^{0.58}]$$
$$= (0.3 \times 100 \times 10^3)[1 - (0.25)^{0.58}] = 16575 \text{ N}$$

If the yield stress in mild steel = 260 N/mm^2, then

$$\text{Area of steel required} = \left[\frac{16575}{(0.87 \times 260)}\right] = 73 \text{ mm}^2$$

Example 10.4 For the rectangular end block with an eccentric anchor force of 100 kN, as detailed in Example 10.2, compute the maximum tensile stress and the total splitting tension using Guyon's method.

Solution. Given data:

$$P = 100 \text{ kN}$$
$$2y_{po} = 50 \text{ mm}$$

Depth of the symmetric prism $2y_o = 133$ mm

$\therefore$ Distribution ratio $y_{po}/y_o = (50/133) = 0.375$

Position of zero stress $= (0.175)(2y_o) = 23.5$ mm

Position of maximum stress $= (0.382)(2y_o) = 51$ mm

$$\text{Maximum tensile stress} = (0.285P/A) = 0.285 \times \left(\frac{100 \times 10^3}{100 \times 133}\right) = 2.13 \text{ N/mm}^2$$

$\therefore$ Total splitting tension

$$F_{bst} = 0.3\,P[1 - (y_{po}/y_o)^{0.58}]$$
$$= (0.3 \times 100 \times 10^3)[1 - (0.375)^{0.58}] = 13015 \text{ N}$$

However, using the approximate formula for the area of stress diagram, Bursting tension $= (213 \times 110 \times 2.13)\ 100 = 15600$ N.

Example 10.5 An end block of a prestressed concrete girder, 200 mm wide and 320 mm deep, is subjected to two concentrated anchorage forces of 100 and 120 kN as shown in Fig. 10.11. Analyse using

Guyon's method (or vertical tensile stress distribution due to the loads for axes 11 and 22).

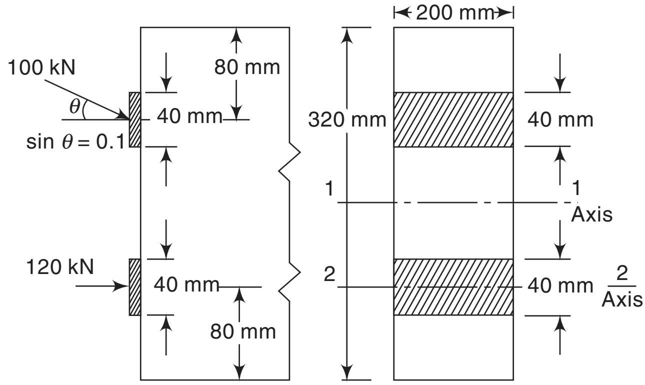

Fig. 10.11 *Forces acting on the end block*

Solution. For axes 11 and 22, the statically equivalent forces acting at one-eighth points of the corresponding equivalent prisms are detailed in Fig. 10.12. The vertical stress distribution over axes 11 and 22 is computed by considering the direct and shear forces, as shown in Table 10.3, by using the coefficients of Table 10.2.

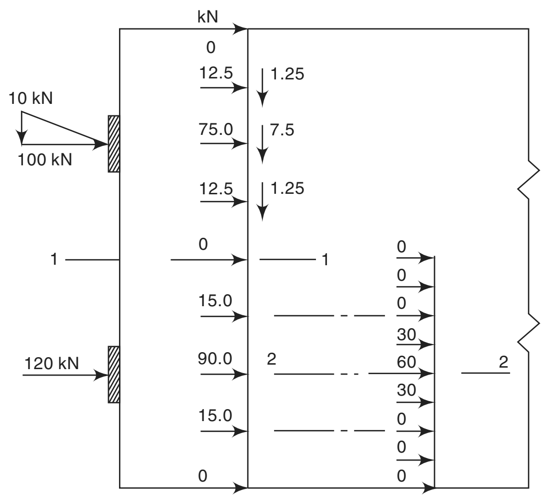

Fig. 10.12 *Statically equivalent force system in end block*

From the stress distribution diagrams, the bursting tension acting over axes 11 and 22 can be computed by approximate formulae or by numerical integration.

For axis 22,

Total splitting tension = (2/3 × 140 × 1.20)200 = 24080 N = 24.08 kN.

Table 10.3 *Transverse stress distribution*

(a) Vertical Stress Along Axis 11

b = 200 mm, $2y_o$ = 320 mm, P = Force (N), $b(2y_o)$ = 64000 mm^2, Average stress = $[P/b(2y_o)]$ – = tension, + = compression

Position *($e/2y_o$)*	*Force P* *(N)*	*Average Stress* $\left(\frac{P}{b2y_o}\right)$N/mm^2	*Distance from end,* $=\frac{x}{2y_o}$						
			0	*1/12*	*1/6*	*1/4*	*1/3*	*1/2*	*3/4*
(i) Direction forces									
+1/2	0	0	—	—	—	—	—	—	—
+3/8	12500	0.195	–0.240	–0.117	+0.024	+0.038	+0.049	+0.049	+0.024
+1/4	75000	1.180	–0.900	–0.029	+0.295	+0.182	+0.070	–0.028	–0.019
+1/8	12500	0.195	–0.110	+0.195	+0.007	–0.028	–0.052	–0.0151	–0.025
0	0	0	—	—	—	—	—	—	—
–1/8	15000	0.235	–0.133	+0.235	+0.017	–0.034	–0.062	–0.061	–0.030
–1/4	90000	1.410	–1.070	–0.035	+0.340	+0.220	+0.087	–0.034	–0.022
–3/8	15000	0.235	–0.290	0.142	+0.029	+0.045	+0.059	+0.057	+0.028
–1/2	0	0	—	—	—	—	—	—	—
(ii) Shear forces									
+3/8	1250	0.020	+0.100	+0.060	+0.017	+0.0038	–0.001	–0.0028	–0.0014
+1/4	7500	0.120	+0.480	+0.370	+0.180	+0.052	–0.026	+0.024	–0.012
+1/8	1250	0.020	+0.144	+0.060	+0.017	+0.0038	–0.001	–0.0028	–0.0014
Total for (i) and (ii)			–2.049	+0.597	+0.926	+0.482	+0.123	–0.098	–0.059
(b) Vertical Stress along Axis 22. Direct Forces									
+1/8	30000	0.94	–0.53	+0.945	+0.069	–0.135	–0.250	–0.245	–0.120
0	60000	1.88	0.0	–0.840	–0.940	–0.840	–0.790	–0.590	–0.300
–1/8	30000	0.94	–0.53	+0.945	+0.069	–0.135	–0.250	–0.245	–0.120
Total			–1.06	+1.05	–0.802	–1.010	–1.290	–1.080	–0.540

10.3.3 Zielinski and Rowe's Method

Experimental investigations on concrete prismatic specimens were conducted by Zielinski and Rowe[6] using the technique of surface-strain measurements. The concrete prisms simulated the end blocks and the parameters investigated include the ratio of loaded to cross-sectional area, the cable duct or hole, type of anchorages, cracking and ultimate loads. The studies revealed that the distribution of transverse stress and ultimate load of the end block is not significantly affected by,

1. The anchorage being either embedded or external,
2. The material of the anchorage, and
3. The method of anchoring the wires.

Empirical relations have been developed by Zielinski and Rowe to compute the maximum transverse tensile stress and the bursting tension[11]: Referring to Fig. 10.13, where an end block is subjected to a concentrated load at the end face, the distribution of transverse stress is found to be maximum at a distance equal to $0.5y_o$.

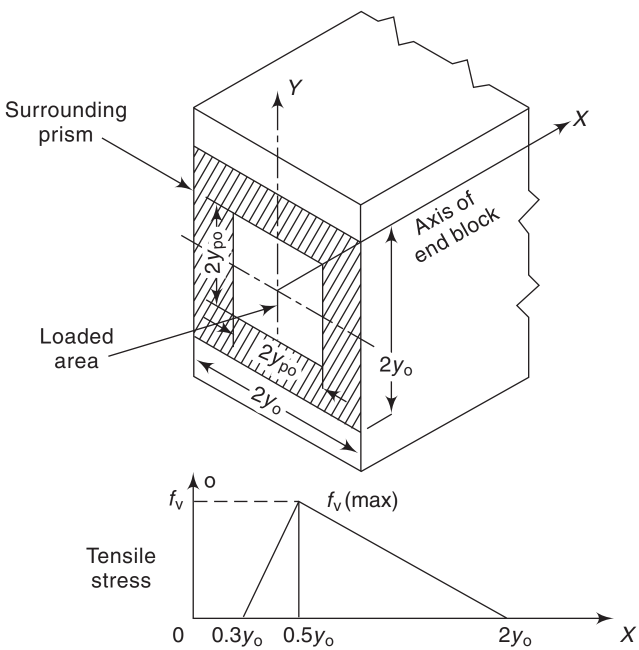

Fig. 10.13 *Tensile stress distribution in end block (Zielinski-Rowe)*

Using the following notations,

$2y_o$ = side of the surrounding prism (similar to the equivalent prism of Guyon's method)

$2y_{po}$ = side of loaded or punching area

y_{po}/y_o = ratio of sides of loaded to bearing area of the prism

f_v = transverse tensile stress

f_c = average compressive stress in the prism

P_k = applied compressive force on the end block (tendon jacking force)
F_{bst} = bursting tension
$f_{v(max)}$ = maximum transverse tensile stress

The recommended equations are,

Tensile stress, $f_{v(max)} = f_c\left[0.98 - 0.825\left(\dfrac{y_{po}}{y_o}\right)\right]$

valid for ratio of (y_{po}/y_o) = 0.3 to 0.7

and Bursting tension, $F_{bst} = P_k\left[0.48 - 0.4\left(\dfrac{y_{po}}{y_o}\right)\right]$

If allowance is made for tension taken by concrete, the corrected value of the bursting tension is given by

$$F_{bst(corrected)} = F_{bst}\left[1 - \left(\frac{f_t}{f_{v\,(max)}}\right)^2\right]$$

where f_t = permissible tensile strength of concrete

The reinforcement required to resist the bursting tension is to be arranged between $0.2y_o$ and $2y_o$ where the intensity of stress is maximum. The application of Zielinski and Rowe's method is illustrated by the following two examples.

Example 10.6 Estimate the position and magnitude of the maximum transverse tensile stress and bursting tension for the end block with a concentric anchor force of 100 kN, as detailed in Example 10.1, using Rowe's method.

Solution. Given data:

$$P_k = 100 \text{ kN}$$
$$2y_{po} = 50 \text{ mm}$$
$$2y_o = 100 \text{ mm}$$

$$\therefore \quad \frac{y_{po}}{y_o} = 0.5$$

$$f_c = \left(\frac{100 \times 10^3}{100 \times 100}\right) = 10 \text{ N/mm}^2$$

$$f_{v(max)} = f_c\,[0.98 - 0.825\,(y_{po}/y_o)]$$
$$= 10[0.98 - 0.825\,(0.5)] = 5.68 \text{ N/mm}^2$$

acting at a distance equal to $(0.5 \times 50) = 25$ mm from the end face. Bursting tension is given by,

$$F_{bst} = (100 \times 10^3)[(0.48 - 0.4 \times 0.5)] = 28000 \text{ N}$$

If the permissible tensile stress in concrete is assumed as 2 N/mm^2, the corrected value of the bursting tension is,

$$F_{bst(corrected)} = 28000\left[1 - \left(\frac{2}{5.68}\right)^2\right] = 24500 \text{ N}$$

Example 10.7 The end block of a prestressed beam, 200 mm wide and 300 mm deep, has two Freyssinet anchorages (100 mm diameter) with their centres at 75 mm from the top and bottom of the beam. The force transmitted by each anchorage being 200 kN, estimate the maximum tensile stress and the bursting tension developed.

Solution.

Anchorage diameter $= 100$ mm

Equivalent side of square $2y_{po} = \sqrt{\dfrac{\pi}{4} \times 100^2} = 89$ mm

Side of the surrounding prism $2y_o = 150$ mm

$\therefore \quad \dfrac{y_{po}}{y_o} = 0.593$

Average compressive stress $f_c = \left(\dfrac{200 \times 10^3}{150 \times 150}\right) = 8.9$ N/mm^2

Tensile stress $f_{v(max)} = 8.9\,[0.98 - 0.825(0.593)] = 4.45$ N/mm^2

Transverse tension $F_{bst} = 200 \times 10^3[0.48 - 0.4(0.593)] = 50000$ N $= 50$ kN.

10.3.4 British Code Provisions

The British code of practice, BS EN: 1992–1–1 provides a table of the design values of the bursting force, which is expressed as a fraction of the axial force applied by a tendon to a square concrete end block. The bursting tension varies with the ratio of loaded to bearing area of the end block and the codified provisions are compiled in Fig. 10.14. The experimental investigations of Zielinski and Rowe

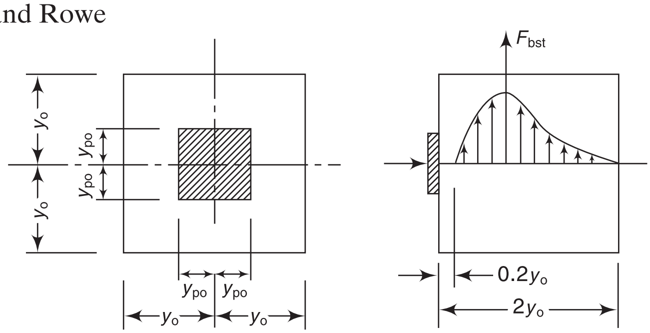

y_{po}/y_0	0.2	0.3	0.4	0.5	0.6	0.7
F_{bst}/P_k	0.23	0.23	0.20	0.17	0.14	0.11

Fig. 10.14 *Design bursting tension in end blocks (British Code BS: 8110–1985)*

form the basis of the British code provisions. The ratio of punching to bearing area, varying from 0.3 to 0.7, covers the range of values generally encountered in the use of various patented commercial anchorages.

In the case of large bridge girders with massive end block supporting multiple anchorages, the end block is divided into a series of symmetrically loaded prisms for the computation of the bursting tension. The design of bursting tension as provided by the British code is significantly higher than that of Yettram Robbin's results but lower than that of Zielinski and Rowe's[6].

10.3.5 Indian Code Provisions

The provisions of the Indian Standard Code IS: 1343 for the computation of the bursting tensile force in the end blocks is based on the work of Zielinski and Rowe and hence are similar to the British code provisions.

The bursting tensile force F_{bst} is obtained from the expression,

$$F_{bst} = P_k \left[0.32 - 0.3 \left(\frac{y_{po}}{y_o} \right) \right]$$

where P_k = tendon jacking force

$\left(\frac{y_{po}}{y_o} \right)$ = distribution ratio

The reinforcement is designed to sustain this bursting tension and it is assumed to act at its design strength of 0.87 f_y. The stress, however, is limited to a value corresponding to a strain of 0.1 per cent when the concrete cover is less than 50 mm. The designed reinforcement is distributed in the zone of 0.2 y_o to $2y_o$ from the loaded face of the end block.

If groups of anchorages are encountered, the end block is divided into a series of symmetrically loaded prisms and each prism is analysed for bursting tensile forces using the recommended expression.

10.4 Comparative Analysis

The distribution of transverse tensile stress in an end block is mainly influenced by the concentration ratio y_{po}/y_o, and a knowledge of the tensile stress distribution is essential for computing the bursting tension and for the design of reinforcements in the end block. A comparative analysis of the salient results of some of the important investigations based on two-dimensional analysis is presented in Table 10 4. The maximum transverse tensile stress is expressed as a fraction of the average compressive stress and the position of zero and maximum stresses are expressed in terms of the depth of the end block.

The large difference in the ratio of maximum to average stress as reported by investigators, such as Magnel[2], Guyon[3], Bleich[12] and Morsch[13], is clearly noticeable in comparison with the exact solution of Iyengar[14]. This difference is attributed to the simplifying approximations made by various investigators for the solution of the two-dimensional elasticity problem. In Table 10.5, the results of transverse tensile stress variation at the centre and surface of the end block, based on the three-dimensional analysis of the various authors, such as Rowe and Zielinski[6], Iyengar and Prabhakara[5], Yettram and Robbins[7], Chandrashekara *et al.*[8] Krishna Raju, *et al*,[14] are compiled.

Table 10.4 *Comparison of transverse tensile stress using two dimensional analysis*

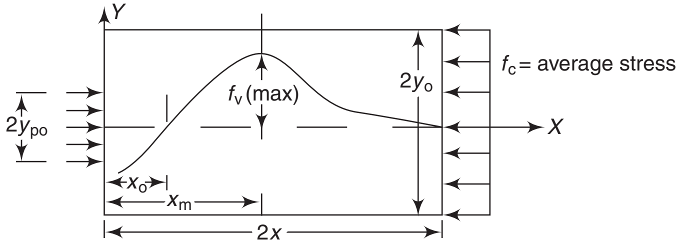

Authors	$\frac{x}{y_o}$	$\frac{y_{po}}{y_o}$	$\frac{x_o}{y_o}$	$\frac{x_m}{y_o}$	$\frac{f_{v\,(max)}}{f_c}$
Morsch	1	0.3 – 0.7	0	1.0	0.26 – 0.16
Magnel	1	0.3 – 0.7	0.5	1.0	0.43 – 0.32
Guyon	1	0.1 – 0.9	0.2 – 0.45	0.5 – 0.9	0.42 – 0.06
Bleich	1	0.1 – 0.9	0.2 – 0.32	0.5 – 0.6	0.59 – 0.07
Iyengar	1	0 – 0.9	0 – 0.25	0.25 – 1.0	0.48 – 0.05

A comparison of the results presented in Tables 10.4 and 10.5 indicates that idealising the end-block problem as two-dimensional, one can lead to erroneous results. The surface transverse stresses obtained from the experimental investigation (Zielinski-Rowe, Chandrasekhara–Iyengar) are significantly greater than those obtained from the theoretical investigations (Iyengar–Prabhakara and Yettram–Robbins). The reasons for the discrepancy between the theoretical and experimental investigations are mainly due to the limitations regarding the idealised assumptions of homogeneity and isotropy for concrete in the theoretical investigations.

In view of the widely varying results and heterogeneous nature of concrete, it is advisable to adopt the worst distribution of transverse tensile stress (as reported by Zielinski-Rowe) for computing the bursting tension and designing the end-block reinforcement. The British code provisions, containing design values of the bursting tension expressed as a fraction of the axial force, is by far the simplest to use in the design office.

10.5 Anchorage Zone Reinforcement

The main reinforcement in the anchorage zone should be designed to withstand the bursting tension, which is determined by the transverse stress distribution on the critical axis, usually coinciding with the line of action of the largest individual force. For plate and embedded (Freyssinet) type of anchorages, the typical arrangement of reinforcement in end blocks is shown in Fig. 10.15. Mats, helics, loops or links are generally provided in perpendicular directions. Tests by Zielinski and Rowe have shown that helical reinforcement is more efficient than mat reinforcement. In view of the short available bond lengths, loops, hooks or right-angle bends are necessary, even with deformed bars.

Table 10.5 *Comparison of some important results: Three-dimensional analysis*

Authors	*Concentration Ratio*	*Centroid*			*Surface*			*Remarks*
	$\frac{y_{po}}{y_o}$	$\frac{x_o}{y_o}$	$\frac{x_m}{y_o}$	$\frac{f^c_{v(max)}}{f_c}$	$\frac{x_o}{y_o}$	$\frac{x_m}{y_o}$	$\frac{f^s_{v(max)}}{f_c}$	
Zielinski and Rowe	0.1 – 0.4	—	—	—	0.18 – 0.2	0.5	0.85 – 0.4	From experiments on concrete prisms ($\mu = 0.15$)
Iyengar and Prabhakara	0.01 – 0.09	0.1 – 0.55	0.2 – 0.95	2.14 – 0.03	0.38	0.85	0.25 – 0.03	Theoretical solution ($\mu = 0.15$)
Yettram and Robbins	0.04 – 0.49	0.2 – 0.6	0.45 – 0.94	0.56 – 0.13	0.15 – 0.35	0.77 – 0.70	0.4 – 0.22	Theoretical (Finite element) ($\mu = 0.125$)
Chandrashekhara, Jacob and Iyengar	0.05 – 0.25	0.30	0.45 – 0.50	0.55 – 0.35	0.12 – 0.15	0.60 – 0.40	0.65–0.6	Photo-elastic investigations ($\mu = 0.45$)
Krishna Raju, Basavarajaiah and Mahadevappa	0.1 – 0.8	—	—	—	—	0.32 – 0.50	0.65 – 0.30	Experiments on concrete prisms ($\mu = 0.15$)

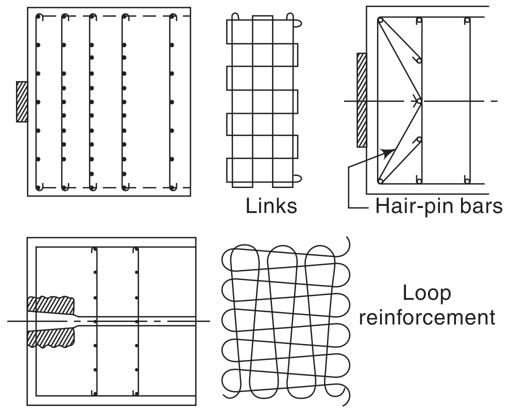

Fig. 10.15 *Arrangement of reinforcement in end blocks*

In cases where spalling or secondary tension develops at the corners, suitable steel in the form of hair-pin bars should be provided to prevent the failure of corner zones. Suitable pockets are generally provided behind the anchorages so that the secondary reinforcements can be bent as shown in Fig. 10.16, and the pocket filled with mortar after prestressing operations. There must always be enough space for the fixing and handling of the hydraulic jack, especially at the soffits of beams when using cap cables, and this should be considered while designing the form work (Fig. 10.17).

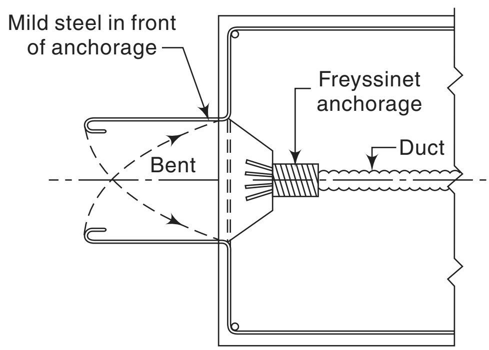

Fig. 10.16 *Pockets behind anchorages*

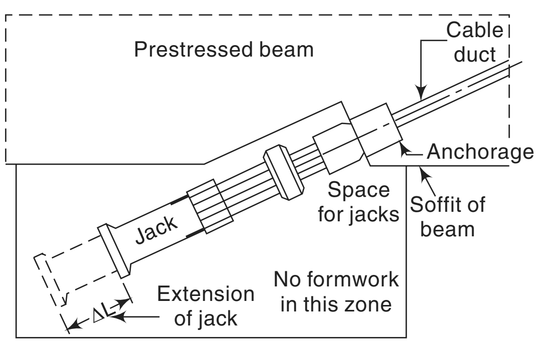

Fig. 10.17 *Provision for jack at soffit or beam*

In the case of end blocks, where bearing plates are positioned close to the edges of block as shown in Fig. 10.18, the steel cage should be arranged so that the bearing plates do not overlap with it. This precaution is necessary to prevent the spalling of concrete at the corners during stressing due to the different elastic modulus of the plane containing the reinforcement.

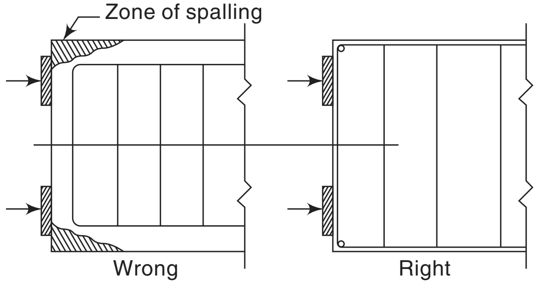

Fig. 10.18 *Arrangement of steel cage in anchorage zone*

According to Morice[15], it is always advisable to provide a little extra reinforcement in doubtful situations, since the cost of the end anchorage steel is a very small proportion of that of the entire structural member.

The designing and detailing of the anchorage zone reinforcement is illustrated by the following three examples.

Example 10.8 The end block of a prestressed concrete girder is 200 mm wide and 300 mm deep. The beam is post-tensioned by two Freyssinet anchorages each of 100 mm diameter with their centres located at 75 mm from the top and bottom of the beam. The force transmitted by each anchorage being 2000 kN. Compute the bursting force and design suitable reinforcements according to the Indian Standard Code IS: 1343 provisions.

Solution.

Anchorage diameter = 100 mm

Equivalent side of the square $= 2y_{po} = \sqrt{\frac{\pi}{4} \times 100^2} = 89$ mm

Side of the surrounding prism $= 2y_o = 150$ mm

Distribution ratio $= \left(\frac{2y_{po}}{2y_o}\right) = \left(\frac{89}{150}\right) = 0.593$

Bursting tensile force $= F_{bst} = P_k\left[0.32 - 0.3\left(\frac{y_{po}}{y_o}\right)\right]$

$$= 2000[0.32 - 0.3(0.593) = 286 \text{ kN}]$$

Using 10 mm-diameter mild steel links with yield stress of 260 N/mm^2

Number of bars required $= \left[\frac{286 \times 1000}{0.87 \times 260 \times 79}\right] = 16$

The reinforcement is arranged in the zone between $0.2y_o$ and y_o. Hence, $0.2y_o = [0.2 \times 75] = 15$ mm and $y_o = 75$ mm. 16 nos. of 10 mm-diameter bars are arranged at a spacing of 40 mm in front of the anchorage both in the longitudinal and transverse directions as shown in Fig. 10.19.

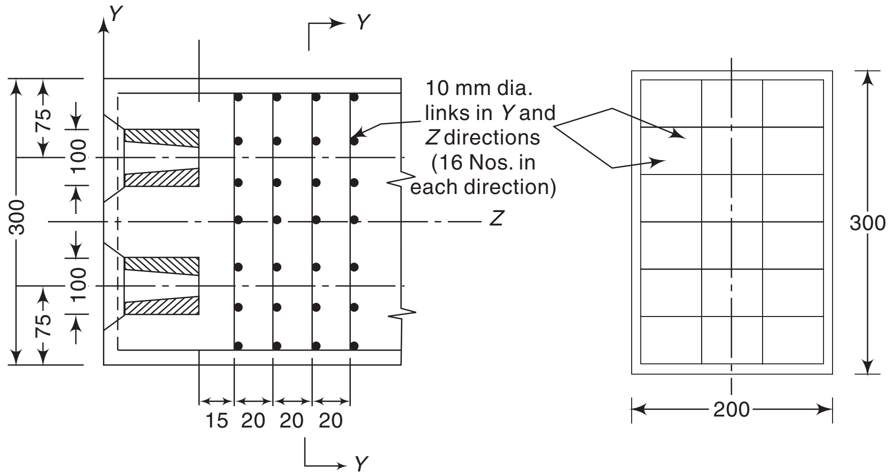

Fig. 10.19 *Arrangement of anchorage zone reinforcement*

Example 10.9 The end block of a post-tensioned prestressed member is 550 mm wide and 550 mm deep. Four cables, each made up of seven wires of 12 mm-diameter strands and carrying a force of 1000 kN, are anchored by plate anchorages, 150 mm by 150 mm, located with their centres at 125 mm from the edges of the end block. The cable duct is of 50 mm diameter. The 28-day cube strength of concrete f_{cu} is 45 N/mm^2. The cube strength of concrete at transfer f_{ci}, is 25 N/mm^2. Permissible bearing stresses behind anchorages should conform with IS: 1343. The characteristic yield stress in mild steel anchorage reinforcement is 260 N/mm^2. Design suitable anchorages for the end block.

Solution.

$$P_k = 1000 \text{ kN}$$
$$2y_{po} = 150 \text{ mm}$$
$$2y_o = 250 \text{ mm}$$
$$y_{po}/y_o = 0.6$$

Area of the cable duct $= \left(\dfrac{\pi \times 50^2}{4}\right) = 2000 \text{ mm}^2$

Net area of the surrounding prism $= [(250)^2 - (2000)] = 60500 \text{ mm}^2$

Average compressive stress $f_c = \left(\dfrac{1000 \times 10^3}{60500}\right) = 16.5 \text{ N mm}^2$

According to IS: 1343, the bearing stress shall not exceed $0.48 f_{ci} \sqrt{\dfrac{A_{br}}{A_{pun}}}$ or 0.8 f_{ci}, whichever is smaller,

where A_{br} = bearing area

A_{pun} = punching area

$A_{br} = 60500 \text{ mm}^2$

$$A_{\text{pun}} = 22500 \text{ mm}^2$$

$$\therefore \quad \frac{A_{\text{br}}}{A_{\text{pun}}} = 2.70$$

Bearing stress limited to $= 0.48 \times 25 \times \sqrt{2.70} = 19.7 \text{ N/mm}^2$ or (0.8×25)
$= 20 \text{ N/mm}^2$

Actual bearing stress $= 16.5 \text{ N/mm}^2$

Using IS: 1343 code specifications,

Bursting tension $\quad F_{\text{bst}} = P_K\left[0.32 - 0.3\left(\frac{y_{\text{po}}}{y_{\text{o}}}\right)\right]$

$$F_{\text{bst}} = 1000\,[0.32 - 0.3(0.6)] = 140 \text{ kN}$$

Using 10 mm diameter HYSD links,

$$\text{No. of bars} = \left[\frac{140 \times 1000}{0.87 \times 260 \times 79}\right] = 8$$

Provide 8 bars of 10 mm diameter.

Example 10.10 The end block of a post-tensioned beam is 80 mm wide and 160 mm deep. A prestressing wire, 7 mm in diameter, stressed to 1200 N/mm^2 has to be anchored against the end block at the centre. The anchorage plate is 50 mm by 50 mm. The wire bears on the plate through a female cone of 20 mm diameter. Given the permissible stress in concrete at transfer, f_{ci}, as 20 N/mm^2 and the permissible shear in steel as 94.5 N/mm^2, determine the thickness of the anchorage plate.

Solution.

Force in wire $= \dfrac{(38.5 \times 1200)}{(1000)} = 46.2 \text{ kN}$

$$2y_{\text{po}} = 50 \text{ mm}$$
$$2y_{\text{o}} = 80 \text{ mm}$$

$$\therefore \quad \left(\frac{y_{\text{po}}}{y_{\text{o}}}\right) = 0.625$$

Average stress, $\quad f_{\text{c}} = \left(\dfrac{46.2 \times 10^3}{80 \times 80}\right) = 7.25 \text{ N/mm}^2$

Permissible bearing pressure $= (0.48 \times 20)\sqrt{\dfrac{80 \times 80}{50 \times 50}} = 15.36 \text{ N/mm}^2$

or $(0.8 \times 20) = 16 \text{ N/mm}^2$, whichever is smaller.

The actual bearing stress is only 7.25 N/mm^2.

Female cone diameter = 20 mm

Punching circumference $= \pi \times 20 = 62.86$ mm

If $\quad t$ = thickness of anchorage plate,

$$(62.86 \times 94.5 \times t) = 46.2 \times 10^3$$

$$\therefore \quad t = 7.8 \text{ mm}$$

Use an anchorage plate of 8 mm thickness.

Example 10.11 The solid end block of a post-tensioned prestressed beam of 25 m span, with three cables, each of 7–15 mm strands, tensioned to 1200 kN is shown in Fig. 10.20. The anchorage plates are square with a side length of 180 mm. Design the end block for bursting forces and sketch the details of reinforcements according to the provisions of the Indian Standard Code IS: 1343–1980.

Solution. The end block has been divided into three equal areas, with one anchorage located approximately at the centroid of each area. The sections of the equivalent prisms corresponding to each anchorage force are shown in Fig. 10.20. The bursting tension may now be calculated for each prism as follows:

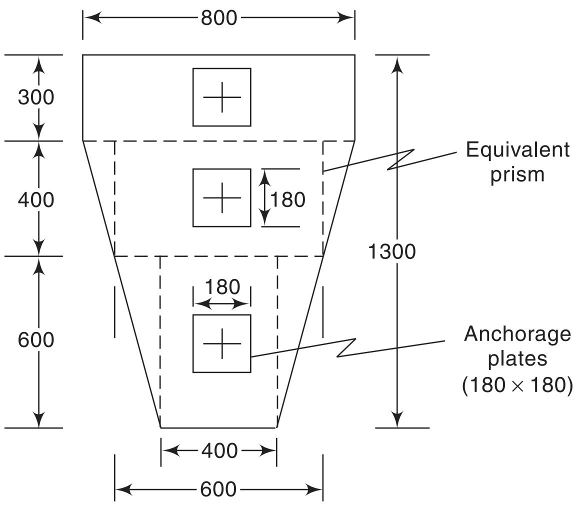

Fig. 10.20 *End block with anchorages*

Bottom anchorage

For vertical bursting force, $\left(\dfrac{y_{po}}{y_o}\right) = \left(\dfrac{180}{600}\right) = 0.3$

$$F_{bst} = P_k\left[0.32 - 0.3\left(\frac{y_{po}}{y_o}\right)\right]$$

$$= 1200[0.32 - 0.3(0.3)] = 276 \text{ kN}$$

Resistance of 5 – 10 mm stirrups (100 mm centres)

$$= (5 \times 2 \times 79 \times 0.87 \times 415) = 285 \text{ kN}$$

For horizontal bursting force, $\left(\dfrac{y_{po}}{y_o}\right) = \left(\dfrac{180}{400}\right) = 0.45$

$$F_{bst} = 1200[0.32 - 0.3(0.45)] = 222 \text{ kN}$$

Resistance of 4 – 10 mm stirrups (100 mm centres)

$$= (4 \times 2 \times 79 \times 0.87 \times 415) = 228 \text{ kN}$$

In the same way, the bursting forces are evaluated for the centre and top anchorage and it is found that the required resistance can be provided by 10 mm stirrups at 100 mm centres. A possible arrangement of the stirrups in the end block is shown in Fig. 10.21. Since the bursting forces do not extend over the whole length of the end block, the spacing of the stirrups is increased from 100 mm to 200 mm at the end remote from the anchorages.

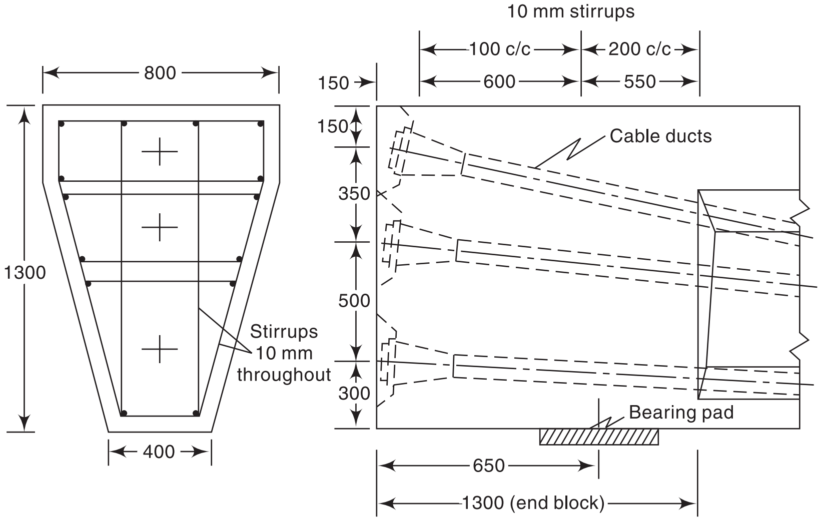

Fig. 10.21 *Details of end block reinforcement*

Example 10.12 The end block of a post-tensioned continuous girder of spans 40 m is 800 mm wide and 2000 mm deep. The Freyssinet anchorages used for the stands has plates of size 340 mm by 340 mm. Each of the three stands carry a force of 4000 kN and the three anchorage plates are spaced at intervals 500 mm along the depth of the end block. Design suitable anchorage reinforcement for the end block using Fe-415 HYSD bars according to IS: 1343 code specifications.

Solution.

$$P_k = 4000 \text{ kN} \qquad f_y = 415 \text{ N/mm}^2$$

$$2y_o = 800 \text{ mm} \qquad 2y_{po} = 340 \text{ mm}$$

$$\text{Ratio } \left[\frac{y_{po}}{y_o}\right] = \left[\frac{340}{800}\right] = 0.425$$

According to the Indian Standard Code (IS: 1343), bursting tension is computed as

$$F_{bst} = P_k\left[0.32 - 0.3\left(\frac{y_{po}}{y_o}\right)\right] = 4000[0.32 - 0.3 \times 0.425] = 770 \text{ kN}$$

Using Fe-415 HYSD bars, the area of steel required is computed as,

$$A_{st} = \left\{\frac{770 \times 10^3}{0.87 \times 415}\right\} = 2132 \text{ mm}^2$$

Provide 16 mm-diameter bars at 150 mm centres in the horizontal plane distributed in the region from $0.2y_o$ to $2y_o$ (80 mm to 800 mm). In the vertical plane, the ratio $f_o(y_{po}/y_o)$ being larger the magnitude of bursting tension is less. However, the same reinforcements are provided in the vertical plane in the form of a mesh to resist bursting tension.

References

1. Guyon, Y, *Prestressed Concrete*, John Wiley & Sons, New York, 1960, pp 127–174.
2. Magnel, G, "Design of the ends of prestressed concrete beams," *Concrete and Constructional Engineering*, Vol. 44, No. 5, 1949, pp 141–148.
3. Guyon, Y, "Contraintes dans les pieces prismatiques soumises a des forces appliquces sur leurs bases, au voisimage deces bases," *Publications of International Association for Bridge and Structural Engineering*, Vol. 11, 1951, pp 165–226.
4. Iyengar, KTS, "Two-dimensional theories of anchorage zone stresses in post-tensioned beams," *Journal of the American Concrete Institute*, *Proceedings*, Vol. 59, No. 10, 1962, pp 1443–1446.
5. Iyengar, KTS, and MK Prabhakara, "Anchor zone stresses in prestressed concrete beams," *Journal of Structural Division*, *Proceedings of American Society of Civil Engineers*, Vol. 97, No. ST3, 1971, pp 807–824.
6. Zielinski, J, and RE Rowe, "An investigation of the stress distribution in the anchorage zone of post-tensioned concrete members," *Research Report No. 9*, Cement and Concrete Association, London, Sept. 1960.
7. Yetiram, AL and K Robbins, "Anchorage zone stresses in axially post-tensioned member of uniform rectangular section," *Magazine of Concrete Research*, London, Vol. 21, No. 67, 1969, pp 103–112.
8. Chandrashekara, K, Jacob Abraham and KTS Iyengar, "Three-dimensional photo elastic analysis of anchorage zone stresses in post-tensioned concrete members," *Final Report*, Dept. of Civil Engineering, Indian Institute of Science, March 1974.
9. Guyon, Y, *Prestressed Concreete*, Contractors Record Ltd, Chapter 6, London, 1953.
10. Evans, RH and EW Bennett, *Prestressed Concrete* (*Theory and Design*), Chapman and Hall, London, 1958, pp 102–104.
11. Rowe, RE, "End block stresses in post-tensioned concrete beams," *Structural Engineer*, London. Vol. 41, No. 2, 1963, pp 54–68.
12. Bleich. F, "Der gerade stab mit rechteekquerschnitt als ebenes problem," *Der Bauingenieur* (Berlin), No. 9, 1923, pp 255–259, and No. 10, 1923, pp 304–307.
13. Mörsch, E, "Uber die berechnung der gelenkquader", *Beton und Eisen*, Berlin, No.12, 1924, pp 156–161.
14. Krishna Raju, N, BS. Basavarajaiah, and P Mahadevappa, "Experimental investigations on anchorage zone stresses," 17*th Congress of Theoretical and Applied Mechanics Society of India*, Ranchi, Dec. 1972.
15. Morice, PB and EH Cooley, *Prestressed Concrete—Theory and Practice*, Pitman, London, 1958, pp 311–313.

Review Questions

10.1 Explain the terms (a) end block, (b) anchorage zone, and (c) bursting tension, with reference to post-tensioned prestressed members.

10.2 Sketch the typical tensile stress distribution in an end block of a post-tensioned beam with a single anchorage.

10.3 Explain with sketches the effect of varying the ratio of depth anchorage to the depth of end block on the distribution of bursting tension.

10.4 What are the various methods generally used for the investigation of anchorage zone stresses?

10.5 Briefly outline the Magnel's method of computing the horizontal and transverse stresses in end blocks subjected to concentrated force from anchorage.

10.6 How do you compute the bursting tension in an end block subjected to evenly distributed forces using Guyon's method?

10.7 Explain Guyon's method of computing bursting tension in the case of end blocks subjected to forces not evenly distributed with multiple anchorages.

10.8 Explain with sketches the concept of equivalent or symmetric prism in end blocks subjected to forces with multiple anchorages.

10.9 Explain the basis of the empirical relations developed by Zelinski and Rowe to compute the transverse tensile stress and bursting tension in end blocks.

10.10 Sketch the typical arrangement of reinforcements in end blocks of post-tensioned prestressed concrete beams with single and multiple anchorages.

Exercises

10.1 The end block of a prestressed concrete beam, rectangular in section is 120 mm wide and 300 mm deep. The prestressing force of 250 kN is transmitted to concrete by a distribution plate, 120 mm wide and 75 mm deep, concentrically located at the ends. Calculate the position and magnitude of the maximum tensile stress on the horizontal section through the centre of the end block using the methods of (a) Magnel, (b) Guyon, and (c) Rowe. Design the reinforcement for the end block for the maximum transverse tension. Yield stress in steel = 260 N/mm^2. **[Ans: (a) 3.3 N/mm^2 (150 mm); (b) 2.415 N/mm^2 (99 mm); (c) 8 N/mm^2 (30 mm); A_s = 252 mm^2]**

10.2 A prestressing force of 250 kN is transmitted through a distribution plate 120 mm wide and 120 mm deep, the centre of which is located at 100 mm from the bottom of an end block having a section 120 mm wide and 300 mm deep. Evaluate the position and magnitude of the maximum tensile stress on a horizontal section passing through the centre of the distribution plate using the methods of (a) Magnel, (b) Guyon, and (c) Rowe. Find the area of steel necessary to resist the largest tensile force resulting from any of these methods. Yield stress in steel = 260 N/mm^2. **[Ans: (a) 1.72 N/mm^2 (150 mm); (b) 1.875 N/mm^2 (88 mm); (c) 5.04 N/mm^2 (50 mm); A_s = 265 mm^2]**

10.3 The end block of a prestressed concrete beam, 200 mm wide and 400 mm deep, has two anchor plates, 200 × 50 mm deep, at 80 mm from the top and 200 × 80 mm deep located 100 mm from the bottom of the beam, transmitting forces of 250 and 300 kN, respectively.

(a) Find the position and magnitude of the maximum tensile stress on a horizontal section passing through the centre of the beam using Guyon's method.

(b) Evaluate the maximum tensile stress on sections passing through the larger and smaller prestressing forces using Guyon's and Rowe's method.

[Ans: (a) 5.515 N/mm²;
(b) 2.09 N/mm² section through larger force 4.9 N/mm²]

10.4 The end block of a prestressed beam, 250 mm wide and 500 mm deep in section, is prestressed by two cables carrying forces of 450 kN each. One of the cables is parabolic, located 125 mm below the centre line at the centre of span (10 m) and anchored at a point 125 mm above the centre line at the ends. The second cable is straight and located 100 mm from the bottom of the beam. The distribution plates for the cables are 100 mm deep and 250 mm wide. Calculate the maximum tensile stress along the axis of the beam using Guyon's method. Also evaluate the maximum tensile stresss on horizontal sections passing through the centre of anchor plates using Guyon's and Rowe's method.

10.5 A Freyssinet anchorage (125 mm diameter), carrying 12 wires of 7 mm diameter stressed to 950 N/mm², is embedded concentrically in the web of an I-section beam at the ends. The thickness of the web is 225 mm. Evaluate the maximum tensile stress and the bursting tensile force in the end block using Rowe's method. Design the reinforcement for the end block.

[Ans: 5 N/mm²; 125 kN; 550 mm²]

10.6 The end block of a prestressed beam 500 mm wide and 1050 mm deep contains six Freyssinet cables, each carrying a force of 266 kN anchored through 100 mm-diameter anchorages, which are spaced 150 mm apart at the end of the beam. Calculate the maximum tensile stress and the bursting tension and design the reinforcement for the end block using Rowe's method. Adopt yield stress in mild-steel reinforcement as 260 N/mm².

[Ans: 11.8 N/mm²; 64.95 kN:A_s = 290 mm²]

10.7 A high-tensile cable comprising 12 strands of 15 mm diameter (12 K15 of PSC Freyssinet system) with an effective force of 2500 kN is anchored concentrically in an end block of a post-tensioned beam. The end block is 400 mm wide by 800 mm deep and the anchor plate is 200 mm wide by 260 mm deep. Design suitable anchorage zone reinforcements using Fe-415 grade HYSD bars using IS: 1343 code provisions.

[Ans: Bursting tension = 425 kN, A_{st} = 1177 mm², 10 mm-diameter bars spaced at 100 mm centres both ways over a length of 400 mm from the end face]

10.8 The end block of a post-tensioned beam is 500 mm wide and 1000 mm deep. Two cables, each comprising 55 numbers of 7 mm diameter high-tensile wires carrying a force of 2800 kN, are anchored using the BBRV system square anchor-plate of side 305 mm. The anchor-plate centres are located symmetrically at 250 mm from the top and bottom edges of the beam. Using Fe-415 grade high-yield bars, design suitable reinforcements in the end block using Indian standard code recommendations.

[Ans: Bursting tension = 384 kN, A_{st} = 1063 mm^2, 10 mm-diameter bars at 150 mm centres both ways over a length of 500 mm]

Objective-type Questions

10.1 In the anchorage zone of a post-tensioned PSC beam, the stress distribution is
(a) uniaxial
(b) biaxial
(c) triaxial

10.2 The anchorage zone in a post-tensioned PSC beam extends over a length of
(a) half the depth of the beam
(b) twice the depth of the beam
(c) depth of the beam

10.3 In the anchorage zone of a post-tensioned beam splitting cracks due to bursting tension develop in the direction of
(a) depth of beam
(b) inclined at 45 degrees to the axis of the beam
(c) horizontal axis of the beam

10.4 The transverse tensile stress in the anchorage zone depends mainly on the
(a) depth of the beam
(b) width of the beam
(c) ratio of anchorage depth to overall depth

10.5 The simplest method of analysis of bursting tension in anchorage zone is due to
(a) Magnel
(b) Guyon
(c) Iyengar

10.6 The concept of equivalent prism for eccentric cables was developed by
(a) Magnel
(b) Rowe and Zeilinski
(c) Guyon

10.7 Experimental investigations on end blocks of concrete prisms were conducted by
(a) Guyon
(b) Rowe and Zeilinski
(c) Magnel

10.8 The bursting tension in the anchorage zone is a function of the ratio of
(a) width to depth of end block
(b) depth of anchorage to width of end block
(c) depth of anchorage to depth of equivalent prism

10.9 According to the Indian standard specifications, the bearing stress at the anchorage zone of post-tensioned prestressed concrete beams is inversely proportional to the
(a) bearing area
(b) punching area
(c) cross-sectional area

10.10 In the case of post-tensioned prestressed concrete members, the zone of spalling is generally at the
(a) centre of the cross-section
(b) in front of the anchorages
(c) at corners of the end face

Answers to Objective-type Questions

10.1 (c)	10.2 (c)	10.3 (c)	10.4 (c)	10.5 (b)
10.6 (b)	10.7 (b)	10.8 (c)	10.9 (b)	10.10 (c)

11 Limit-state Design Criteria for Prestressed Concrete Members

11.1 Introduction

A comprehensive knowledge of the behaviour of structural concrete elements under different types of loading is essential for producing safe, serviceable and economic designs of concrete structures. According to Bennett[1], design is essentially a creative rather than a routine analytical activity in which the structural behaviour is only one of a number of functional, constructional, aesthetic and economic considerations. A successful design should not only satisfy the requirements of safety against total collapse of the structure due to various causes, but also ensure that the serviceability of the structure is not impaired while resisting normal working loads.

Rowe et al.[2] have defined the purpose of design as "the provision of a structure complying with the client's requirements". A structural engineer is often required to assist the client in defining his requirements more precisely. Once the basic requirements have been defined, the structural engineer becomes a member of an integrated team. The primary object of structural design is to obtain a structural solution which can result in the greatest overall economy by providing the maximum assistance in satisfying all the other requirements of the structure.

The limit-state design philosophy recognises the need to provide safe and serviceable structures at an economic price and at the same time presents a clearer idea of the margins of safety actually employed to cover uncertainty and ignorance of the function as well as the performance of structure in actual practice. It is important to note that the limit-state design proposals have been evolved from the provisions of various earlier codes, and the resulting changes in design, being minimal, provide the designer a greater freedom of choice. In addition, the formulation of new design proposals are such that any new research data on loads, variability of materials and workmanship, and methods of analysis can be readily incorporated in the comprehensive limit-state format.

11.2 Inadequacies of the Elastic and Ultimate Load Methods

The permissible or working stress method of design, pioneered by the German professor, Morsch, is also sometimes referred to as the *elastic theory of design*.

In this method, the permissible stresses in concrete and steel are assumed to be a fraction of the specified strength of the individual material and a constant modular ratio is assumed for all loading conditions with the elastic behaviour of concrete and steel.

The inadequacy of the working load design in predicting ultimate loads of a structure was recognised after the First World War. The factor of safety applied to the constituent materials does not present a realistic picture of the degree of safety against the collapse of the composite material, such as reinforced concrete used in the structural component. Over the past two decades, the codes of practise have gradually laid more emphasis on the inelastic behaviour of structural concrete members by introducing the ultimate load or the load factor method of design. The main feature of the ultimate load method of design is the application of varying load factors for different types of loads to arrive at the required ultimate load for which the member is to be designed.

The ultimate load method of design ensures the safety of the structure against the collapse limit state only and as such does not give any information about the behaviour of the structure at service loads and the range between service and collapse loads. A structure designed solely by the ultimate-load method, although having a desirable margin of safety against collapse, may not be serviceable due to excessive deflections and/or development of objectionable cracks at service loads. This type of distress is particularly noticeable in structures designed by ultimate-load methods using high-strength materials.

The ultimate-load design concepts have been extended to the design of continuous beams and frames where it is referred to as *limit-state design*. This involves a redistribution of moments due to the development of plastic hinges and an eventual collapse when the last critical hinge is formed. The ultimate-load analysis of slabs by the yield-line theory[3] also suffers from similar deficiencies in that the deformation characteristics of the slab at service loads cannot be predicted by ultimate-load methods. These discrepancies, inherent in elastic and ultimate-load methods, have naturally paved the way for the development of comprehensive design methods that involve the criteria of safety and serviceability.

11.3 Philosophy of Limit-State Design

In erstwhile USSR as far back as 1930, problems were considered concerning the formulation of a design concept to take into account the variabilities inherent in the materials of construction, design process and building construction. This exercise finally culminated in a new philosophy of design, termed the *limit-state approach*, which was incorporated in the Russian code in 1954. Basically, limit-state design is a method of designing structures based on a statistical concept of safety and the associated statistical probability of failure.

The method of design for a structure must ensure an acceptable probability that the structure, during its life, will not become unfit for its intended use. This acceptable probability should give a satisfactory balance between the initial and maintenance costs during the life of the structure, together with the cost of those insurance premiums that are based on the probability of the structure becoming unfit for its designed purpose. This philosophy was adopted and elaborated by the European Concrete Committee (CEB) to form the basis of the committee's original publication[4] in 1964 and later, in conjunction with the International Federation for Prestressing (FIP), issued a complimentary report[5] dealing with prestressed concrete in 1966. The influence of this work was evident in the American code[6], the British code[7] and the Indian standard codes[8, 9] for structural concrete published between 1970 and 2000.

A comprehensive critical review of the limit-state design concepts embodied in the various codes was presented by the author in his reports for reinforced concrete[10] and prestressed concrete[11]. Further research during the last decade has resulted in the revised versions of the CEB-FIP model code[12] for concrete structures, FIP[13] recommendations, British standard code. BS EN: 1992–1–1[14] and the latest version of the American Concrete Institute building code requirements ACI 318M–2011[15].

11.4 Criteria for Limit States

In general, a satisfactory design must ensure the achievement of an acceptable probability that the specified life of a structure is not curtailed prematurely due to the attainment of an unsatisfactory condition or limit-state, which covers the various forms of failure. There are several limit states at which the structure ceases to function; the most important among them being the limit state of collapse, excessive deflection and cracking. Each of these limit states may be attained due to different types of loading configurations; however, in practice, only one or two of these are of primary significance in design.

Some of the important criteria concerning prestressed concrete for the ultimate limit state are given as follows:

1. Failure of one or more critical sections in flexure, shear, torsion, or due to their combinations.
2. Bursting of prestressed concrete end blocks.
3. Bearing failure at supports, anchorages or under-concentrated imposed loads.
4. Bond and anchorage failure of reinforcement.
5. Failure of connections between precast and cast *in situ* elements.
6. Failure due to elastic instability of members.

The limit state of collapse may also be attained due to fatigue, vibrations, corrosive environment, impact as a consequence of explosions or earthquakes and disintegration due to fire or frost.

The structure may be rendered unfit for its intended purpose due to various serviceability limit states being reached, such as:

1. Excessive deflection or displacement, adversely affecting the finishes and causing discomfort to the users of the structure, and
2. Excessive local damage resulting in cracking or spalling of concrete, which impairs the efficiency or appearance of the structure.

11.5 Design Loads and Strengths

The design loads for various limit states are obtained as products of the characteristic loads and partial safety factors, and are expressed as:

$$F_d = g_f F_k$$

where F_d = appropriate design load
γ_f = partial safety factor for loads
F_k = characteristic load

The characteristic load F_k, which is independent of the limit state considered and is seldom exceeded in service is defined as,

Characteristic load = (mean load + $k \times$ standard deviation)

where k is a factor, so chosen as to ensure that the probability of the characteristic load being exceeded is small. A value of 1.64 for k ensures the probability that the characteristic load is exceeded by only five per cent during the intended life of the structure.

The statistical data required to define the characteristic loads for different types of occupancy is not readily available, since loading statistics are invariably difficult to compile as they need systematic observations and recording of data over a long period of time. In the absence of statistical observations and recording of data on loading, the nominal imposed loads provided in various national codes, such as IS: 875–1987[16], BS: 6399[17], CP3–1972[18] and standards ANSI–A–58.1[19] may be treated as characteristic loads.

The characteristic values of the loads take account of expected variations but do not allow for the following:

1. Possible unusual increases in load beyond those considered in deriving the characteristic load.
2. Inaccurate assessment of effects of loading and unforeseen stress distribution within the structure.
3. Variations in dimensional accuracy achieved in construction.

Partial safety factors, γ_f, are therefore used for each limit state being reached. The values of partial safety factors for loads recommended in the British, Indian and American codes and FIP recommendations are compiled in Tables 11.1 to 11.6.

Table 11.1 *Partial safety factors for loads (γ_f) ultimate limit state (BS EN: 1992-1-1-2004 & Euro Code-2)*

Persistent or Transient Design Situation	*Permanent Actions (G_k)*		*Leading Variable Actions ($Q_{k,1}$)*		*Accompanying Variable Action (Q_{k1})*	
	Unfavorable	*Favorable*	*Unfavorable*	*Favorable*	*Unfavorable*	*Favorable*
(a) For checking the static equilibrium of a building structure	1.10	0.90	1.50	0	1.50	0

(*Contd.*)

Table 11.1 *(Contd.)*

(b) For the design of structural members (excluding geotechnical actions)	1.35	1.50	1.50	0	1.50	0
(c) As an alternative to (a) and (b) to design for both situations with one set of calculations	1.35	1.15	1.50	0	1.50	0

Where, G_k = Characteristic permanent load and Q_k = Characteristic variable load

Table 11.2 *Partial safety factor for loads (γ_f) (IS: 1343-2012)*

Load Combination	*Limit State of Collapse*				*Limit State of Serviceability*			
	DL	*IL*	*WL*	*P*	*DL*	*IL*	*WL*	*P*
(i) $(DL + IL + P)$	1.5	1.5	-	1.0	1.0	1.0	-	1.1 or 0.9^+
(ii) $(DL + WL + P)$	1.5 or 0.9^*	-	1.5	1.0	1.0	-	1.0	1.1 or 0.9^+
(iii) $(DL + IL + WL + P)$	1.2	1.2	1.2	1.0	1.0	0.8	0.8	1.1 or 0.9^+

Notes

1. While considering earthquake effects, substitute *EL* for *WL*.
2. While assessing the long-term effects due to creep, the dead load and that part of the imposed load likely to be permanent may only be considered.
3. While verifying the limit state for stability, with external prestress, where an increase of the value of prestress can be unfavorable, partial factor of 1.3 shall be used.

* This value is to be considered when stability against overturning or stress reversal is critical.

\+ The structure shall be checked both for upper and lower characteristic values shown. The values are for post tensioning with bonded tendons. In case of pretensioning or unbonded tendons, it shall be taken as 1.05 or 0.95 instead of the above value.

Table 11.3 *Partial safety factor for loads (γ_f) (ACI: 318-2011)*

$$U = 1.2\,D + 1.6\,L + 0.5\,(L_r \text{ or } S \text{ or } R)$$
$$U = 1.2\,D + 1.6\,(L_r \text{ or } S \text{ or } R) + (1.0\,L \text{ or } 0.5\,W)$$
$$U = 1.2\,D + 1.0\,W + 1.0\,L + 0.5\,(L_r \text{ or } S \text{ or } R)$$
$$U = 1.2\,D + 1.0\,E + 1.0\,L + 0.2\,S$$
$$U = 0.9\,D + 1.0\,W$$
$$U = 0.9\,D + 1.0\,E$$

(Contd.)

Where

U = Ultimate load
D = Dead load
L = Live load
S = Snow load
R = Rain load or related internal moments and forces
W = Wind load
E = Earthquake loads
L_r = Roof live load

Table 11.4 *Partial safety factor for loads (γ_f) (FIP-1984)*

Type of Loads	*Limit State of Collapse*	*Limit State of Serviceability*
Permanent loads	1.35	1.00
Variable loads	1.50	1.00

FIP recommendations regarding partial safety factors are comprehensive, as they provide for a combination coefficients for basic variable actions as well as for other variable factors depending upon different types of structures, such as dwellings, offices, parking areas and highway bridges.

The design strength of materials are expressed as,

$$f_d = (f_k/\gamma_m)$$

where f_k is the characteristic strength of the material which corresponds to the 28-day cube compressive strength of concrete or the tensile strength of tendons below which the failures are not more than five per cent. In the absence of statistical data, the characteristic strengths of concrete and steel may be taken as the works cube strength and the specified proof or yield strength, respectively, as provided for in the codes.

The partial safety factor (γ_m) for materials has a value which depends upon the importance of the limit state being considered, materials to which it applies, and differences between the strengths of the materials when tested and when incorporated in construction during the service life of the structure. The design strengths of materials for each limit state are obtained by using the values of the partial safety factors compiled in Table 11.5 (a) and (b) as provided for in the various codes. The American Code ACI 318M–2011 provides for reduction factors to be applied to the nominal strength of structural members in flexure, shear, torsion and compression to account for the inaccuracies in construction. The reduced strength of a member is defined as its design strength. The values of reduction factors for various types of structural elements are compiled in Table 11.6.

Table 11.5 (a) *Partial safety factors for materials (γ_m) (IS: 1343-2012)*

Materials	*Partial Safety Factor (γ_m)*
Steel	1.15
Concrete	1.50

Table 11.5 (b) *Partial safety factors for materials (γ_m) (IS: 1343-2012)*

Limit State	*Persistent and Transient*		*Accidental*	
	Concrete	*Reinforcing and Prestressing Steel*	*Concrete*	*Reinforcing and Prestresing Steel*
Strength				
Flexure	1.50	1.15	1.20	1.00
Shear	1.50	1.15	1.20	1.00
Bond	1.50	1.15	1.20	1.00
Serviceability	1.00	1.00	-	-

Table 11.6 *Capacity or strength reduction factors (ACI 318M-11)*

S.No.	*Type Force*	ϕ
1.	Tension controlled sections	0.90
2.	Compression controlled sections	
	(a) Members with spiral reinforcement	0.75
	(b) Other reinforced concrete members	0.65
3.	Shear and torsion	0.75
4.	Bearing on concrete	0.65
5.	Post-tensioned anchorage zones	0.85
6.	Strut and Tie models	0.75
7.	Flexural sections in pretensioned members	0.75
	(a) Free end of member to end of transfer length	0.75 to
	(b) Free end of member to development length	0.9
8.	Structural members resisting earthquakes (shear)	0.60
9.	For joint and diagonally reinforced coupling beams (shear)	0.85
10.	For structural plain concrete (flexure, compression, shear)	0.60

11.6 Strength and Serviceability Limit States

11.6.1 Limit State of Collapse

The basic principles of estimating the ultimate strength of prestressed concrete members in flexure are well established and many of the codes have simplified the provisions based on idealised stress blocks of concrete in compression as presented in Chapter 7. While the Indian and British code methods are limited to under-reinforced sections in flexure based on the effective reinforcement ratio, the American code method provides empirical relations to compute the ultimate flexural strength of under- and over-reinforced sections, as well as of sections with compression reinforcement.

The rigorous strain compatibility method of analysis, which involves the use of idealised stress–strain curves of steel and concrete, can also be used for an accurate assessment of the flexural strength of sections with reinforcements in the tension and compression zones. The current Indian, British and American codes have more or less similar provisions for the computation of the shear strength of prestressed members that fail in web-shear or flexure-shear cracking modes.

11.6.2 Serviceability Limit States

The primary serviceability limit states are those that correspond to excessive deflections and cracking. It is customary in most codes to safeguard against excessive deflections under the serviceability limit state, either indirectly by prescribing minimum span/depth ratio for the member or directly specifying a maximum permissible deflection expressed as a fraction of the span.

The provisions of the British code BS EN: 1992–1–1 and Indian code IS: 1343 with regard to the final deflection, as presented in Section 6.6 are similar. According to the American code ACI: 318M–2011, the permissible deflections vary from a maximum of span/180 to a minimum of span/480, depending on the type of member and the seriousness of damage to the adjoining structural elements.

Short-term deflections of prestressed members of class-1 and 2 types under service load are influenced by the magnitude of the prestressing force and its profile, applied load and self-weight of the member and flexural rigidity of the uncracked concrete section. The effective modulus method, which involves the creep coefficient of concrete outlined in Sections 6.5.1 and 6.5.2 can be used to estimate the long-term deflections.

The estimation of deflections of partially prestressed members, grouped as class 3-type which are cracked under service loads, involves the computation of the flexural rigidity or moment curvature characteristic of cracked prestressed members, as provided for in the various codes and discussed in detail in Chapter 6.

The limit state of cracking is particularly important in the case of partially prestressed members, according to Abeles[20] who has contributed much information about members with limited prestress. According to the various national codes, prestressed concrete structures are grouped into three classes, the requirements for which are as follows:

Class 1 Structures No tensile stresses are permitted under service loads and hence the structure is crack-free at the working load stage. Members are often referred to as fully prestressed, requiring higher quantity of prestressing steel associated with higher cost. Generally, Class 1-type members are preferred for containment structures housing atomic reactors, pressure pipes and in important structures where cracking at service loads is not acceptable.

Class 2 Structures In this type, limited tensile stresses of magnitude not exceeding the modulus of rupture of concrete are permitted under working loads. Members are often referred to as moderately prestressed. Visible cracks are not permitted in this type. Abeles[21] has used such structures in British Railways with very satisfactory results.

Class 3 Structures Tensile stresses of magnitude exceeding both the modulus of rupture of concrete and the visible cracking of limited width are permitted under service loads as compiled in Table 11.7. Members are referred to as partially prestressed. Untensioned reinforcement is generally designed to control crack widths and to meet the load factor requirements against the limit-state of collapse. Class 3-type constitute the most economical of prestressed concrete structures due to limited prestressing forces and high-tensile steel requirements. The estimation of crack width in Class 3-type members is essential for checking the serviceability criterion.

Table 11.7 *Hypothetical flexural tensile stresses for Type 3 members (IS: 1343-2012)*

S. No.	*Type of Tendon*	*Limiting Crack Width (mm)*	*Stress in Concrete for Grade*				
			M-30	*M-35*	*M-40*	*M-45*	*M-50 and above*
1.	Pretensioned	0.1	-	-	4.3	4.4	4.8
		0.3	-	-	5.0	5.4	5.8
2.	Grouted and	0.1	3.2	3.6	4.1	4.4	4.8
	Post-tensioned	0.2	3.8	4.4	5.0	5.4	5.8
3.	Pretensioned						
	Tendons distributed	0.1	-	-	5.3	5.8	6.3
	in tension zone close	0.2	-	-	6.3	6.8	7.3
	to tension face						

Note: When additional reinforcement is distributed within the tension zone and positioned close to the tensioned face of concrete, the hypothetical tensile stresses may be increased by an amount which is proportional to the cross-sectional area of the additional reinforcement expressed as a percentage of the cross-sectional area of the concrete. For 1 per cent of additional reinforcement, the stress may be increased by 4 N/mm^2 for members with pretensioned and grouted post-tensioned tendons and by 3 N/mm^2 for other members. For other percentages of additional reinforcement the stresses may be increased in proportion excepting that the total hypothetic tensile stress shall not exceed 0.25 times the characteristic compressive strength of concrete.

For members of other depths, the stresses given above should be multiplied by the following factors:

Depth (m)	*Factor*
0.2 and less	1.1
0.4	1.0
0.6	0.9
0.8	0.8
1.0 and over	0.7

11.7 Crack Widths in Prestressed Members

Several prominent investigations by Beeby[22], ACI Committee-224[23] and Nawy[24] have indicated that the width of cracks developed in type-3 prestressed members is governed by (i) the average strain at the level at which cracks are considered, (ii) the minimum cover to the tension steel, (iii) the overall depth of the member, and (iv) the neutral axis depth. Several empirical relations have been suggested by the early investigators to estimate the width of cracks involving the various influencing parameters. The recent British and Euro code specifications regarding the estimation of crack widths in structural concrete members consider additional influencing parameters like the variation in the creep coefficient with relative humidity and notional size of the member in addition to the four primary parameters mentioned before. The various methods of determining the crack widths are briefly reviewed as follows:

1. Beeby and Nawy's Method

Based on the investigations by Beeby and Nawy, the Indian Standard Code (IS: 456-2000) recommends the empirical equation given by,

$$\omega_{cr} = \left[\frac{3\,a_{cr}\,\varepsilon_m}{1+2\left(\dfrac{a_{cr-}\ C_{min}}{h-x}\right)}\right] \tag{11.1}$$

Where ω_{cr} = design surface crack width

a_{cr} = distance from the point considered to the surface of the nearest longitudinal bar (refer to Fig. 11.1)

ε_m = average strain at the level where cracking is being considered;

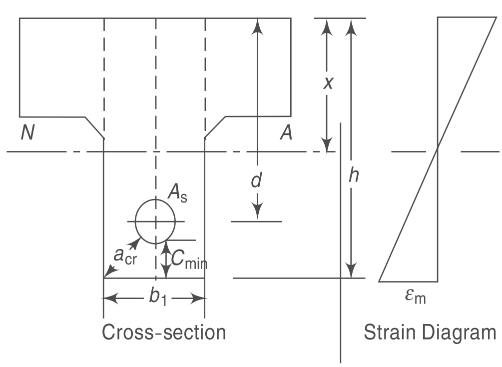

Fig. 11.1 *Cracking in prestressed beams*

This value is calculated by allowing for the stiffening effect of concrete in the tension zone, and obtained from Eq.(11.2).

C_{min} = minimum cover to the tension steel
h = overall depth of the member
x = neutral-axis depth, calculated on the assumption of a cracked section (obtained from Fig. 6.13 (a)).

This value of x is then used to obtain the strain using the equation,

$$\varepsilon_m = \varepsilon_1 \frac{b_t(h-x)(a'-x)}{3E_s A_s(d-x)} \tag{11.2}$$

where ε_1 = strain at the level considered; calculated on the assumption of a cracked section, with the concrete modulus E_c taken as half its value (to allow for creep effects)

b_t = width of the section at the centroid of the tension steel

a' = distance from the compression face to the point at which the crack is being calculated

A_s = area of tension reinforcement

ε_1 is computed by the relation

$$\varepsilon_1 = \left[\frac{M \bullet x_1}{0.5E_c I_c}\right] \tag{11.3}$$

where x_1 = distance measured from the neutral axis to the point at which the strain ε_1 is sought

M = moment at the section

A negative value of ε_m indicates that the section is uncracked.

There are two special cases to be considered.

Case 1 Directly over a bar, the distance a_{cr} is equal to the concrete cover C_{min}. Equation (11.1) then reduces to

$$\omega_{cr} = 3C_{min}\varepsilon_m \tag{11.4}$$

Case 2 When the distance a_{cr} is large, Eq. (11.1) approaches the following limit:

$$\omega_{cr} = 1.5(h-x)\varepsilon_m \tag{11.5}$$

In structural members, ε_m is a maximum at the tension face: if $(h - x)$ is sufficiently small for the crack width at the tension face not to exceed the permissible limit of 0.3 mm, it will not exceed that limit anywhere. This is the reason for smaller crack widths in slabs under service loads, provided the thickness does not exceed about 200 mm. Nawy et al.[25, 26, 27] based on extensive research work, have developed empirical relations to predict the maximum width of cracks and their mean spacing in pretensioned and post-tensioned beams. According to their investigations, the stabilised mean crack spacing, a_{cs}, can be expressed as,

$$a_{cs} = C\left(\frac{A_t}{\Sigma O}\right) \tag{11.6}$$

where A_t = effective concrete area in tension as defined in Fig. 11.2

ΣO = sum of the circumferences of the reinforcing elements

C = an empirical constant, determined from tests, with values of 1.2 for pretensioned and 1.54 for post-tensioned prestressed beams

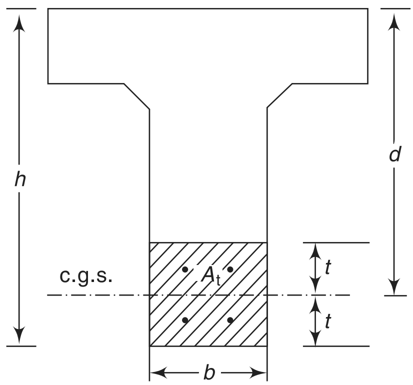

Fig. 11.2

The width of cracks are influenced by the net stress in the tendons, their surface characteristics and the effective concrete area in tension. Based on experimental investigations, the following empirical relations are suggested for the estimation of maximum crack width for design purposes.

(a) Expression for pretensioned beams:

$$\omega_{\max} = 8.33 \times 10^{-3}\left(\frac{A_t}{\Sigma O}\right)(\Delta f_s) \tag{11.7}$$

(b) Expression for post-tensioned beams:

$$\omega_{\max} = 9.66 \times 10^{-3}\left(\frac{A_t}{\Sigma O}\right)(\Delta f_s) \tag{11.8}$$

where $\omega_{\max}$ = maximum crack width at level of reinforcements

A_t = effective concrete area in tension

ΣO = sum of the perimeters of the reinforcing bars

Δf_s = Net increase in stress in the prestressing tendon beyond the decompression load expressed as kN/mm^2

The FIP recommendations of 1984 include a formula for the computation of characteristic crack-width, based on the formula recommended in CEB/FIP[28] model code for concrete structures as follows:

$$\omega_k = S\left[1.5 + \frac{3.5c}{S}\right]\frac{\sigma_s}{E_s}\left[1 - \left(\frac{M_r}{M}\right)^2\right] \tag{11.9}$$

where ω_k = characteristic crack width

S = bar spacing

c = concrete cover to reinforcement

σ_s = steel stress under loads

E_s = modulus of elasticity of reinforcement

M_r = cracking moment

M = moment under loads considered

The British and Indian standard codes on prestressed concrete prescribe maximum limiting crack widths of 0.1 mm for members exposed to aggressive environment and 0.2 mm for all other members.

The permissible crack widths for different types of exposure recommended in FIP–1984 are compiled in Table 11.8. ACI Committee–224 prescribes maximum permissible crack widths for different types of exposure as detailed in Table 11.9.

Table 11.8 *Crack widths for durability requirements (FIP–1984)*

Exposure	*Prestressed Concrete*	*Reinforced Concrete*
Mild	$\omega \leq 0.2$ mm	$\omega \leq 0.4$ mm
Normal	$\omega \leq 0.1$ mm	$\omega \leq 0.2$ mm
Severe	No decompression	$\omega \leq 0.1$ mm

Table 11.9 *Maximum permissible flexural crack widths (ACI Committee–224)*

Exposure Conditions	*Crack Width* (mm)
1. Dry air or protective membrane	0.41
2. Humidity; moist air, soil	0.30
3. De-icing chemicals	0.18
4. Sea water and sea water spray, wetting and drying	0.15
5. Water-retaining structures (excluding non pressure pipes)	0.10

A critical review of the maximum permissible crack widths specified in various countries indicates that the major influencing parameters are the function of the structural element and the environmental conditions to which the structure is liable to be exposed. In general, the maximum permissible crack width varies from a minimum of 0.1 mm for severe exposure conditions to a maximum of 0.2 mm for mild environment.

2. Gergely Lutz Formula

The American[29] and Canadian[30] practise for the estimation of crack width in concrete structural members is based on the investigations of Gergely and Lutz[31]. Comparative investigations undertaken by Ganesan[32] and Srinivas[33] using the large number of experimental test results reported by Clark, Hognestad, Base and others, indicate that the best results of maximum probable crack width is predicted by the Gergeley and Lutz formula expressed as,

$$\omega_{cr} = (11 \times 10^{-6}) \sqrt[3]{d_c \left(\frac{A_e}{n}\right)} \left[\frac{D - x}{d - x}\right] f_{st}$$

Where

d_c = thickness of concrete cover measured from the extreme tension fibre to the centre of the nearest bar

A_e = effective area of concrete in tension surrounding the main tension reinforcement having the same centroid as the tension steel $[2(D - d)b_w]$ as shown in Fig. 11.3

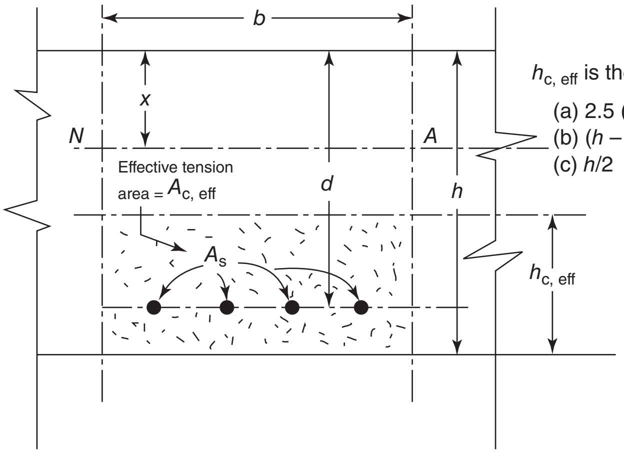

Fig. 11.3 *Effective concrete tension area*

n = number of bars in tension (in case different diameters are used, n shall be taken as the total steel area divided by the area of the largest diameter bar)

f_s = stress at the centroid of the tension steel

3. BS EN: 1992-3-2006 Code Method

However, the British code (BS EN: 1992-3-2006) and Euro code (EC-2) have specified a detailed method for estimation of cracks by considering several influencing parameters in cracked structural concrete members as follows:

The expression for the design crack width is expressed as,

$$w_k = s_{r,\,max}\,(\varepsilon_{sm} - \varepsilon_{cm})$$

Where

w_k = the design crack width

$s_{r,\,max}$ = the maximum crack spacing

ε_{sm} = the mean strain in the reinforcement allowing for the effects of tension stiffening of the concrete, shrinkage, etc.

ε_{cm} = the mean strain in the concrete between cracks

The value of $(\varepsilon_{sm} - \varepsilon_{cm})$ is given by the expression:

$$(\varepsilon_{sm} - \varepsilon_{cm}) = \left[\frac{\sigma_s - k_t\left(\dfrac{f_{ct,eff}}{\rho_{\rho,eff}}\right)(1 + \alpha_e \rho_{\rho,eff})}{E_s}\right] \geq 0.6\left(\frac{\sigma_s}{E_s}\right)$$

Where σ_s = stress in tension reinforcement calculated using the cracked concrete section

k_t = a factor that accounts for the duration of loading (0.6 for short-term load and 0.4 for long-term load)

$\rho_{\rho,\,eff} = (A_s/A_{c,\,eff})$ = effective reinforcement ratio based on an effective concrete tension area as shown in Fig. 11.3

$f_{ct, eff}$ = concrete tensile strength at the time of cracking which depends on the grade of concrete

α_e = modular ratio = $[E_s/E_c]$

The maximum crack spacing $s_{r, max}$ is given by the empirical formula:

$$s_{r,max} = [3.4c + 0.425\ k_1\ k_2\phi/\rho_{\rho, eff}]$$

where ϕ = bar diameter (or average value if bars of different sizes have been used)

c = cover to the reinforcement

k_1 = 0.8 for high bond bars and

k_2 = 0.5 for flexure and 1.0 for direct tension

A_s = area of reinforcement within an effective tension area of concrete $A_{c, eff}$.

The effective tension area is that area of the concrete cross-section which will crack due to the tension developed in flexure. Generally, the effective tension area should be taken as having a depth equal to 2.5 times the distance from the tension face of the concrete to the centroid of the reinforcement, although for slabs, the depth of this effective area should be limited to $(h - x)/3$, where h is the overall depth of concrete section and x is the depth of neutral axis. An overall upper limit of $(h/2)$ also applies.

The revised Indian Standard Code IS: 1343-2012 does not recommend any specific method for estimating the width of cracks, except that it permits cracks of 0.1 and 0.2 mm in type-3 members in which hypothetical tensile stresses listed in Table 11.7 are permitted depending upon the type of prestressing, grade of concrete and the percentage of reinforcement in the tension zone.

Example 11.1 A class 3-type post-tensioned prestressed concrete beam of 10 m span has a cross-section shown in Fig. 11.4. The beam is post-tensioned using three high tensile bars of 40 mm diameter located at an effective depth of 700 mm. The effective prestressing

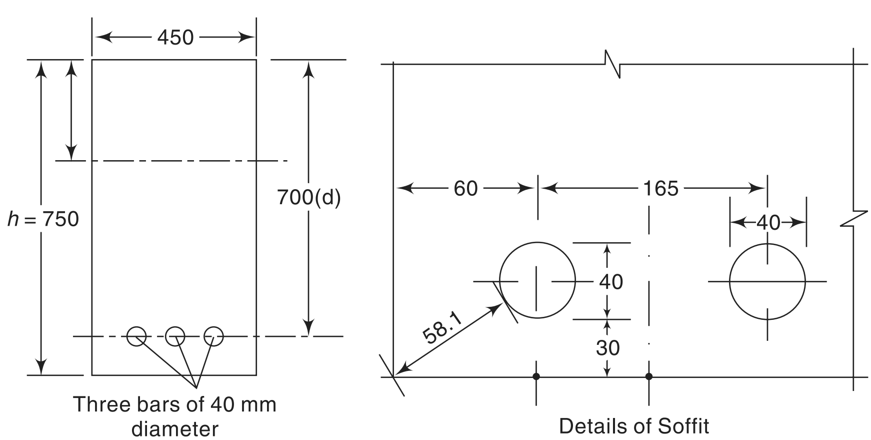

Fig. 11.4 *Post-tensioned prestressed concrete beam*

force in each bar after all losses is 600 kN. Given $f_{ck} = 40$ N/mm^2, $E_c = 28$ kN/mm^2, compute the maximum probable crack width in the tension zone if the service load moment at mid span is 1040 kN.m, using the following methods:

(a) IS: 456-2000 code method
(b) Gergely Lutz formula
(c) FIP-1984 recommendations
(d) BS EN: 1992-3-2006 code method

Solution.

(a) IS: 456-2000 code method

Effective prestressing force = $P = (3 \times 600) = 1800$ kN

Eccentricity = $e = (375 - 50) = 325$ mm

Second moment of area of cross-section = $I = \left(\dfrac{450 \times 750^3}{12}\right) = (1582 \times 10^7)$ mm^4

Section modulus = $Z = \left(\dfrac{I}{y}\right) = \left(\dfrac{(1582 \times 10^7)}{375}\right) = (4218 \times 10^4)$ mm^3

Effective prestress at the bottom fibre of the beam is

$$\sigma_b = \left(\frac{1800 \times 10^3}{450 \times 750}\right) + \left(\frac{1800 \times 10^3 \times 325 \times 375}{(1582 \times 10^7)}\right) = 19.2 \text{ N/mm}^2$$

Hence, the decompression moment is computed as

$$M_o = (\sigma_b \cdot Z) = (19.2 \times 4218 \times 10^4)/10^6 = 810 \text{ kN.m}$$
$$M_d = \text{service load moment} = 1040 \text{ kN.m}$$

Difference of service load moment and decompression moment is

$$M = (M_d - M_o) = (1040 - 810) = 230 \text{ kN.m}$$

Allowing for creep effects, the effective modulus of elasticity of concrete is calculated using the value of creep coefficient ($\phi = 2.2$) given in IS:456, for 7 days age at loading.

$$E_{c,\text{eff}} = \left(\frac{E_c}{1+\phi}\right) = \left(\frac{28}{1+2.2}\right) = 8.75 \text{ kN/mm}^2$$

$$\text{Modular ratio} = \alpha_e = \left(\frac{E_s}{E_{c,\text{eff}}}\right) = \left(\frac{200}{8.75}\right) = 22.8$$

$$\text{Area of tendons} = A_s = 3 \times \pi \times \left(\frac{40^2}{4}\right) = 3769 \text{ mm}^2$$

Overall depth = $h = 750$ mm and effective depth = $d = 700$ mm

The neutral axis depth (x) and the second moment of area of the cracked section (I_{cr}) are obtained from Figs. 6.13 (a) and (b) from the parameter $\left(\dfrac{\alpha_e A_s}{b.d}\right)$

$$\left(\frac{\alpha_e A_s}{b.d}\right) = \left(\frac{22.8 \times 3769}{450 \times 700}\right) = 0.27$$

Reading out the values of the ratios from Fig. 6.13 (a) and (b), we have

$$\left(\frac{x}{d}\right) = 0.50 \quad \therefore x = (0.5 \times 700) = 350 \text{ mm}$$

$$\left(\frac{I_{cr}}{b.d^3}\right) = 0.105 \quad \therefore I_{cr} = (0.105 \times 450 \times 700^3) = (162 \times 10^8) \text{ mm}^4$$

Tensile strain in steel corresponding to the moment M is obtained as

$$\varepsilon_s = \left[\frac{\alpha_e M(d-x)}{E_s I_c}\right] = \left[\frac{22.8(230 \times 10^6)(700-350)}{(200 \times 10^3)(162 \times 10^8)}\right] = 0.00056$$

Tensile strain in concrete at the soffit is

$$\varepsilon_h = \left(\frac{h-x}{d-x}\right)\varepsilon_s = \left(\frac{750-350}{700-350}\right)0.00056 = 0.00063$$

The average strain at the soffit, considering the stiffening effect of the concrete in the tension zone is computed as,

$$\varepsilon_m = \varepsilon_h - \left[\frac{b(h-x)(a'-x)}{3E_s A_s(d-x)}\right]$$

$$= 0.00063 - \left[\frac{450(750-350)(750-350)}{3 \times 200 \times 10^3 \times 3769\,(700-350)}\right] = 0.00054$$

(i) Crack width directly under the bar

$$\omega_{cr} = 3\,C_{min}\varepsilon_m = (3 \times 30 \times 0.00054) = 0.048 \text{ mm}$$

(ii) Crack width at the bottom corner

$$a_{cr} = \sqrt{50^2 + 60^2} = 58.1 \text{ mm}$$

$$\varepsilon_m = 0.00054,\ x = 350 \text{ mm}\ h = 750 \text{ mm}$$

$$\omega_{cr} = \frac{3a_{cr}\varepsilon_m}{1 + 2\left[\dfrac{a_{cr} - C_{min}}{h-x}\right]} = \frac{3(58.1)(0.00054)}{1 + 2\left[\dfrac{58.1-30}{750-350}\right]} = 0.075 \text{ mm}$$

(iii) Crack width at the soffit, mid way between the two bars

$$a_{cr} = \sqrt{82.5^2 + 50^2} = 76.4 \text{ mm}$$

$$\varepsilon_m = 0.00054,\ x = 350 \text{ mm},\ h = 750 \text{ mm}$$

$$\omega_{cr} = \frac{3a_{cr}\varepsilon_m}{1 + 2\left[\dfrac{a_{cr} - C_{min}}{h-x}\right]} = \frac{3(76.4)(0.00054)}{1 + 2\left[\dfrac{76.4-30}{750-350}\right]} = 0.104 \text{ mm}$$

(b) Gergely Lutz formula

$$\omega_{cr} = (11 \times 10^{-6})\sqrt[3]{d_c\left(\frac{A_e}{n}\right)}\left[\frac{D-x}{d-x}\right]f_{st}$$

Substituting the numerical values,

$$d_c = 50 \text{ mm},\ x = 350 \text{ mm},\ D = 750 \text{ mm},\ d = 700 \text{ mm}$$

$$A_e = 2(D - d)b_w = 2(750 - 700) = 4500 \text{ mm}^2$$
$$n = 3$$
$$f_{st} = \left(\frac{\alpha_e M(d - x)}{I_{cr}}\right) = \left(\frac{22.8 \times 230 \times 10^6 (700 - 350)}{(162 \times 10^8)}\right) = 113 \text{ N/mm}^2$$
$$\omega_{cr} = (11 \times 10^{-6}) \sqrt[3]{50\left(\frac{4500}{3}\right)} \left[\frac{750 - 350}{700 - 350}\right] 113$$
$$= 0.059 \text{ mm}$$

(c) FIP-1984 recommendations

$$\omega_k = S\left[1.5 + \frac{3.5c}{S}\right]\left(\frac{\sigma_s}{E_s}\right)\left[1 - \left(\frac{M_r}{M}\right)^2\right]$$

In the present example,

$$S = 165 \text{ mm}$$
$$c = 30 \text{ mm}$$
$$\sigma_s = 0.113 \text{ kN/mm}^2$$
$$E_s = 200 \text{ kN/mm}^2$$
$$M_r = 810 \text{ kN.m}$$
$$M = 1040 \text{ kN.m}$$
$$\omega_k = 165\left[1.5 + \frac{(3.5 \times 30)}{165}\right]\left(\frac{0.113}{200}\right)\left[1 - \left(\frac{810}{1040}\right)^2\right]$$
$$= 0.078 \text{ mm}$$

(d) BS EN: 1992-3-2006 code method

$$\omega_k = s_{r,\max} (\varepsilon_{sm} - \varepsilon_{cm})$$
$$= s_{r,\max}\left[\frac{\sigma_s - k_t\left(\frac{f_{ct,eff}}{\rho_{\rho,eff}}\right)(1 + \alpha_e \rho_{\rho,eff})}{E_s}\right] \geq 0.6\left(\frac{\sigma_s}{E_s}\right)$$

Substituting the relevant values, we have

$$f_{ck} = 40 \text{ N/mm}^2,\ E_s = 200 \text{ kN/mm}^2$$
$$E_c = 5000\sqrt{40} = 31000.6 \text{ N/mm}^2 = 31.6 \text{ kN/mm}^2$$
$$f_{ct,eff} = 0.7\sqrt{f_{ck}} = 0.7\sqrt{40} = 4.4 \text{ N/mm}^2$$
$$k_t = 0.4 \text{ for long-term loading}$$
$$\text{Notional size} = \left(\frac{2A_c}{u}\right) = \left(\frac{2 \times 450 \times 750}{(2 \times 750) + 450}\right) = 346 \text{ mm}$$

Assuming loading at 28 days and relative humidity of 50 per cent, interpolate the value of Creep coefficient = $\phi_o = 2.4$ (using the Table 2.7)

Long-term modulus of elasticity of concrete = $E_{c,eff} = \left[\dfrac{E_c}{1+\phi}\right] = \left[\dfrac{31.6}{1+2.4}\right]$

$= 9.3$

$$\text{Modular ratio} = \alpha_e = \left(\frac{E_s}{E_{c,\,eff}}\right) = \left(\frac{200}{9.3}\right) = 21.5$$

For the cracked section, neutral axis depth = x = 350 mm, d = 700 mm

$A_s = 3769\ \text{mm}^2$ and b = 450 mm

$h_{c,\,eff}$ = Effective depth of tension zone is the least of

(a) 2.5 $(h - d)$ = 2.5 (750 – 700) = 125 mm
(b) $(h - x)/3$ = (750 – 350)/3 = 133.3 mm
(c) $(h/2)$ = (750/2) = 375 mm

$\therefore \quad h_{c,eff} = 125$ mm

$$\rho_{\rho,eff} = \left[\frac{A_s}{b.h_{c,eff}}\right] = \left[\frac{3769}{450 \times 125}\right] = 0.067$$

Cover to reinforcement = c = 30 mm

Diameter of tendon = ϕ = 40 mm

Spacings of tendons = 165 mm

For high bond bars, $k_1 = 0.8$ and $k_2 = 0.5$ for flexure

Maximum final crack spacing is computed using the relation

$$S_{r,\,max} = [3.4\,c + (0.425 \times k_1 \times k_2 \times \phi)/\rho_{\rho,\,eff}]$$
$$= [(3.4 \times 30) + (0 \times 40)/0.067]$$
$$= 203\ \text{mm}$$

σ_s = Net increase in stress in tendons beyond the decompression

$$\sigma_s = \left(\frac{\alpha_e M(d-x)}{I_{cr}}\right) = \left(\frac{21.5 \times 230 \times 10^6\ (700-350)}{(162 \times 10^8)}\right) = 107\ \text{N/mm}^2$$

Substituting the relevant values, the crack width is computed using the equation,

$$\omega_k = s_{r,max}\left[\frac{\sigma_s - k_t\left(\dfrac{f_{ct,eff}}{\rho_{\rho,eff}}\right)(1+\alpha_e\rho_{\rho,eff})}{E_s}\right] \geq 0.6\left(\frac{\sigma_s}{E_s}\right)$$

$$= 203\left[\frac{107 - 0.4\left(\dfrac{4.4}{0.067}\right)(1 + 21.5 \times 0.067)}{(200 \times 10^3)}\right] \geq 0.6\left(\frac{107}{(200 \times 10^3)}\right)$$

$$= \ 0.043\ \text{mm} \geq 0.00032\ \text{mm}$$

Example 11.2 A post-tensioned prestressed concrete beam of T-section, as shown in Fig. 11.5, is prestressed with twelve 11.1 mm diameter seven-ply strands and additionally reinforced with four 20 mm diameter non-prestressed steel bars. The locations of the neutral axis and the centre of gravity of the steel are shown in Fig. 11.5. Assuming $f_c' = 35$ N/mm^2, $E_c = 28$ kN/mm^2, $E_s = 200$ kN/mm^2, estimate the mean stabilised crack spacing and the crack widths at the steel level and at the soffit of the beam for a net increase in stress in the prestressing tendons beyond a decompression of 0.2 kN/mm^2. Check whether the beam satisfies the serviceability criteria for crack control for humidity and moist air condition.

Solution.

Effective concrete area in tension, $A_t = (300 \times 200) = 60000\ \text{m}^2$

$$\Sigma O = (12 \times \pi \times 11.1) + (4 \times \pi \times 20) = 670\ \text{mm}$$

Mean stabilised crack spacing is obtained as,

$$a_{cs} = 1.54\left(\frac{A_t}{\Sigma O}\right) = 1.54\left(\frac{6 \times 10^4}{670}\right) = 138\ \text{mm}$$

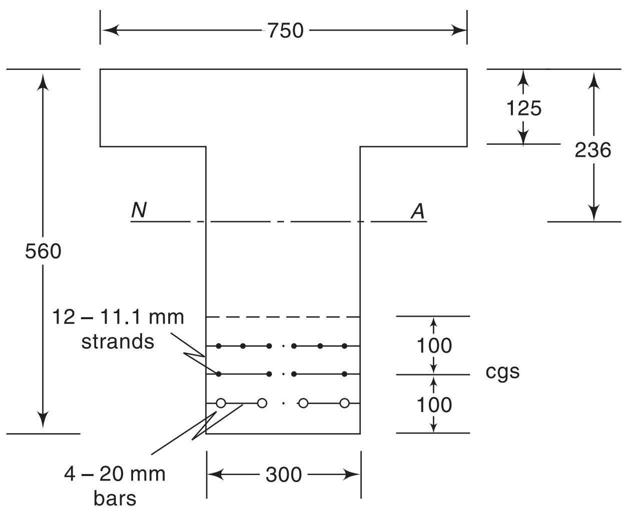

Fig. 11.5

Maximum crack width at the centroidal level of steel is

$$\omega_{max} = 9.66 \times 10^{-3}\left(\frac{A_t}{\Sigma O}\right)\Delta f_s$$

where $\Delta f_s = 0.2\ \text{kN/mm}^2$

$$\omega_{max} = 9.66 \times 10^{-3}\left(\frac{6 \times 10^4}{670}\right)0.2 = 0.173\ \text{mm}$$

Maximum crack width at the tensile face of the beam is

$$\omega'_{\max} = 0.173\left(\frac{560-236}{560-236-100}\right) = 0.25 \text{ mm}$$

Maximum allowable crack width for humidity and moist air exposure conditions is 0.30 mm (Table 11.9). Hence, the beam satisfies the serviceability limit state for limiting crack width.

11.8 Principles of Dimensioning Prestressed Concrete Members

In the design of prestressed concrete members, the minimum required resistance is predetermined for certain limit states, such as collapse, deflection and cracking. For each of these, the design value of the resistance must equal or exceed the sum of the design loads obtained by multiplying the specified characteristic loads by the appropriate partial safety factors. The design strength of the material being known, the problem generally reduces to the determination of suitable dimensions for the member, that is, the cross-sectional details, followed by the design of prestress required and the corresponding eccentricity and area of reinforcement for the section.

The trial and error method of assuming a certain section and checking its resistance using the appropriate design formula is often time consuming since a section satisfying the requirements at the serviceability limits may be deficient at the limit state of collapse. This naturally leads to a repeated modification of the cross-section until it caters to the prescribed requirements at various limit states. A direct method for computing the leading dimensions of a section is often feasible, as in the case of pure flexure, where the necessary effective depth and breadth of the compression face are controlled mainly by the collapse limit state. In the case of flanged members, the width and depth of the compression flange is also fixed on the basis of the collapse limit state, while the thickness of the web is based on ultimate shear or on practical considerations of having curved cables with minimum cover requirements. However, the minimum prestressing force required and the corresponding eccentricity are controlled by the serviceability limit states at which the stresses are not to exceed the permissible values.

The limit state of deflection rarely influences the design of prestressed members (Classes 1 and 2), since the member will be normally uncracked at service loads. In addition, a precamber will be provided by the initial upward deflection due to the prestress.

In the case of members subjected to axial tension, the concrete section and the minimum prestress are mainly controlled by the permissible stresses at service loads and in some cases (walls of tanks) by practical considerations. However, the designed section is checked at the limit states of cracking and collapse and additional reinforcements, if required, are to be designed to ensure the desired load factors against collapse and cracking.

The dimensioning of prestressed members subjected to axial load and bending is generally done by considering the serviceability limit states governed by the allowable stresses in the concrete at the stages of transfer of prestress and working loads. The required cross-sectional dimensions and the prestress may be determined by solving the stress condition equations formulated for the opposite extreme faces of the section or by the aid of design charts[34] for the different cases of members with uniform or non-uniform prestress.

References

1. Bennett, EW, *Structural Concrete Elements*. Chapman and Hall, London, 1973, pp 149–170.
2. Rowe, RE, WB Cranston, and BC Best, "New Concepts in the Design of Structural Concrete," *Structural Engineer*, Vol. 43, 1965, pp 399–403.
3. Johanson, KW, *Yield Line Theory*, Cement and Concrete Association, London, 1964.
4. *CEB Recommendations for International Code of Practice for Reinforced Concrete*, American Concrete Institute and Cement and Concrete Association, London, 1964.
5. FIP–CEB: *Joint Committee Practical Recommendations for the Design and Construction of Prestressed Concrete Structures*, June 1966.
6. ACI: 318–77: *ACI Standard Building Code Requirements for Reinforced Concrete*, American Concrete Institute, Detroit, Michigan, 1977.
7. CP 110 Part 1: 1972: *Code of Practice for the Structural Use of Concrete*. British Standards Institution, London, Nov. 1972.
8. IS: 456–2000, *Indian Standard Code of Practice for Plain and Reinforced Concrete for General Building Construction*, Bureau of Indian Standards, New Delhi, 2000 (Fourth revision).
9. IS: 1343, *Indian Standard Code of Practice for Prestressed Concrete* (Second revision), Bureau of Indian Standards, New Delhi (To be published).
10. Krishna Raju, N, "Limit state design for structural concrete," *Proceedings of the Institution of Engineers* (*India*), Vo1. 51, Jan 1971, pp 138–143.
11. Krishna Raju, N, "Limit state design of prestressed concrete members," Engineering design, *Special Issue on Prestressed Concrete*, *Journal of National Design and Research Forum*, (*Institution of Engineers India*), April 1979, pp 16–21.
12. *CEB/FIP Model Code for Concrete Structures* (MC 78), Committee Euro-International du Beton, Paris, 1978.
13. *FIP Recommendations for Practical Design of Reinforced and Prestressed Concrete Structures*, Thomas Telford, London, 1984.
14. BS EN: 1992–1–1, Euro Code 2 – Design of Concrete Structures, General Rules and Rules for Buildings, British Standards Institution, 2004.
15. ACI 318M–2011, Building Code Requirements for Structural Concrete and Commentary, American Concrete Institute, Farmington Hills, Michigan, 2011.
16. IS: 875–1987, *Indian Standard Code of Practice for Design Loads* (*Other than Earthquake*) *for Buildings and Structures* (second revision), Bureau of Indian Standards, New Delhi, 1989.

17. BS: 6399, *Design Loading for Buildings*, *Part-I*, *Code of Practice for Dead and Imposed Loads*, British Standards Institution, 1972.
18. CP 3, *Code of Basic Data for the Design of Buildings, Chapter V Loading and Part 2, Wind Loads;* British Standards Institution, London, 1972.
19. ANSI A-58.1, *Building Cade Requirements tor Minimum Design Loads in Buildings and Other Structures*, American National Standards Institute.
20. Abeles, PW, "Design of partially prestressed members," *Journal of the American Concrete Institute*, Vo1. 65, 1967, pp 669–672.
21. Abeles, PW, "Partial prestressing in limit state design," *Seminar on Problems of Prestressing*, Indian National Group of the IABSE, Preliminary Publications, Madras, Jan–Feb 1970, pp II43–II65.
22. Beeby, AW, "The prediction and control of flexural cracking in reinforced concrete members," *Proceedings of the ACI Symposium on Cracking, Deflection and Ultimate Load of Concrete Slab Systems*, American Concrete Institute, Detroit, 1971, pp 55–75.
23. ACI Committee 224, *Control of Cracking in Concrete Structures*, American Concrete Institute, Detroit, 1984.
24. Nawy, EG, Structural elements strength, serviceability and ductility, *Handbook of Structural Concrete*, edited by Kong, FK, Evans, RH, Cohen, E and Roll F; Pitman, London and McGraw-Hill, New York, 1983, Chapter 12, pp 12–70 to 12–76.
25. Nawy EG and JG Potyondy, "Flexural cracking behaviour of pretensioned prestressed concrete I- and T-beams," *Journal of the American Concrete Institute* Vol. 65, 1971, pp. 335–360.
26. Nawy, EG and PT Huang, "Crack and deflection control of pretensioned prestressed beams," *Journal of the Prestressed Concrete Institute*, Vol. 22, 1977, pp 30–47.
27. Nawy, EG, and JY Chiang, "Serviceability behaviour of post-tensioned beams," *Journal of the Prestressed Concrete Institute*, Vol. 25 1980 pp 74–95.
28. *CEB/FIP Model Code for Concrete Structures*, English edn, Cement and Concrete Association, London, 1978.
29. ACI 318R-05, Commentary on Building Code requirements for Reinforced Concrete, American Concrete Institute, Detroit, U.S.A, 2005.
30. CSA Standard A 23.3-04, design of Concrete Structures, Canadian Standards Association, Mississauga, Ontario, Canada, 2004.
31. Gergeley, P and Lutz, LA, Maximum Crack Width in Reinforced Concrete Flexural Members, Causes, Mechanism and Control of Cracking in Concrete (SP-20), American Concrete Institute, Detroit, U.S.A, 1968, pp. 87-117.
32. Ganesan, N and Shivananda, KP, Comparison of International Codes for the Prediction of Maximum Width of Cracks in Reinforced Concrete Flexural Members, Indian Concrete Journal, November, 1996, pp.635-641.
33. Srinivas, N and Menon, D, Design Criteria for Crack Control in R.C. liquid Retaining Structures, Need for a Revision of IS: 3370 (Part-II), 1965, Indian Concrete Journal, August 2001, pp. 451-458.
34. Bennett, EW, The Design of Prestressed Members Subjected to Axial Force and Bending, Concrete and Constructional Engineering, London, Vol. 61, August 1966, pp. 267-274.

Review Questions

11.1 Distinguish clearly between (a) working stress or elastic design (b) ultimate load design and (c) limit-state design.

11.2 What are the inadequacies of working stress and ultimate load design methods?

11.3 Explain the terms (a) design load (b) design strength (c) characteristic load (d) characteristic strength and (e) partial safety factors. Express the relation between these terms.

11.4 What are serviceability limit states? Discuss briefly the IS: 1343 code recommendations regarding serviceability limit states.

11.5 How do you classify the various types of prestressed concrete structures? Mention their practical applications.

11.6 What are class 3-type or partially prestressed members? Mention their advantages.

11.7 What are hypothetical tensile stresses? Discuss their use in class 3-type members.

11.8 List the factors influencing the width of cracks in prestressed concrete members.

11.9 Briefly explain a method of estimating the surface crack width of partially prestressed members.

11.10 Briefly discuss the principles of dimensioning prestressed concrete members.

Exercises

11.1 The tie member of a concrete truss with a rectangular section 200 mm by 250 mm, is prestressed by 20 high-tensile wires of 7 mm diameter initially stressed to 950 N/mm^2. The loss ratio is 0.8. The tie is designed to support a working tensile force of 500 kN, without developing any tensile stress in the concrete. The modulus of elasticity of steel is 200 kN/mm^2. Estimate using Nawy's method the width of cracks developed in the tie when it supports a tensile force of 640 kN. **[Ans: 0.302 mm]**

11.2 A prestressed concrete beam of rectangular section 200 mm by 450 mm, is provided with a supplementary reinforcement consisting of four deformed bars of 20 mm diameter at an effective cover of 50 mm from the soffit. If the increase of stress in the untensioned reinforcement from the stage of decompression of concrete to the service load is 100 N/mm^2, estimate the maximum width of cracks developed at the soffit of the beam using the British code (BS: 8110–1985) method. Assume $E_s = 200$ kN/mm^2 and $E_c = 28$ kN/mm^2. **[Ans: 0.062 mm]**

11.3 A prestressed concrete slab of a road bridge deck is 400 mm thick with parallel post-tensioned cables. The supplementary steel consists of 20 mm-diameter bars of grade Fe–415 provided at an effective depth of 36.0 mm. The spacings of the untensioned reinforcement is 200 mm. If the stress in steel under service loads is 230 N/mm^2, the cracking moment and service load moments being 400 and 500 kN m, respectively, estimate the width of crack at soffit of slab using the FIP–1984 recommendations. Assume $E_s = 200$ kN/mn^2. **[Ans: 0.16 mm]**

11.4 A prestressed concrete highway tee beam and slab bridge has the following design parameters:
Overall depth of slab = 200 mm
Effective depth = 165 mm
Reinforcements: 10 mm diameter bars at 125 mm c/c
$f_{ck} = 25$ N/mm^2, $f_y = 415$ N/mm^2
At the service load moment, the stress in steel is 228 N/mm^2
Depth of neutral axis = 41 mm
Modulus of elasticity of steel = 200 kN/mm^2
Using the IS: 456-2000 code method, estimate the width of crack in the slab.

[Ans: 0.13 mm]

11.5 A doubly reinforced concrete beam of width 250 mm and overall depth 400 mm, is reinforced with 3 bars of 28 mm diameter on the tension side at an effective cover of 52 mm and 3 bars of 20 mm diameter on the compression side at an effective cover of 48 mm at the mid span section of the beam. The tensile stress developed in steel under a service load moment was computed as 224 N/mm^2. The neutral axis depth was determined as 146 mm. If the modulus of elasticity of steel is 200 kN/mm^2, estimate the width of crack at the soffit using the IS code method. **[Ans: 0.18 mm]**

Objective-type Questions

11.1 In elastic design of prestressed concrete structures
(a) ultimate loads are considered
(b) factor of safety against collapse is assured
(c) permissible stresses in materials are considered

11.2 In ultimate load design of prestressed concrete structures limit state of
(a) deflection is considered
(b) cracking is considered
(c) collapse is considered

11.3 Limit state design ensures desirable safety factors at the limit state of
(a) collapse and service (b) collapse (c) service

11.4 The partial safety factor for dead and live loads at the limit state of collapse is
(a) 1.2 (b) 1.6 (c) 1.5

11.5 The partial safety factor for combined dead, live and wind loads at the limit state of serviceability is
(a) 1.2 (b) 0.8 (c) 1.0

11.6 The partial safety factor for strength of concrete at limit state of collapse is
(a) 1.15 (b) 1.20 (c) 1.50

11.7 The partial safety factor for strength of steel at limit state of collapse is
(a) 1.50 (b) 1.20 (c) 1.15

11.8 According to IS: 1343 Code in Type-1 prestressed concrete structures
(a) tensile stress of limited magnitude are permitted
(b) limited width of cracks are permitted
(c) tensile stresses are not permitted

11.9 The width of cracks in a prestressed beam is influenced by the parameter
   (a) flexural rigidity
   (b) maximum shear force
   (c) modular ratio

11.10 The maximum probable cracks width is inversely proportional to the
   (a) stress in tendon
   (b) modulus of elasticity of steel
   (c) cover to steel

Answers to Objective-type Questions

11.1 (c)	11.2 (c)	11.3 (a)	11.4 (c)	11.5 (b)
11.6 (c)	11.7 (c)	11.8 (c)	11.9 (c)	11.10 (b)

12 Design of Prestressed Concrete Sections

12.1 Design of Sections for Flexure

12.1.1 Stress Conditions

Minimum section modulus Prestressed sections under the action of flexure should satisfy the limits specified for permissible stresses at the transfer stage of prestress and at service loads. Expressions for the minimum section moduli required, prestressing force and the corresponding eccentricity are developed using the four stress relationships established for the two extreme fibres of the section and considering the two critical combinations of prestress and moments[1]. The general critical combinations considered are as follows:

1. The maximum prestressing force at transfer together with the minimum moments sustained by the section, and
2. The minimum prestressing force after all losses in combination with the maximum design moment for the serviceability limit state.

Referring to Fig. 12.1, the four fundamental conditions for stresses at transfer and service loads are as follows:

At transfer

Top fibres $$\left(f_{\text{sup}} + \frac{M_{\text{g}}}{Z_{\text{t}}}\right) \geq f_{\text{tt}} \quad (12.1)$$

Bottom fibres $$\left(f_{\text{sup}} - \frac{M_{\text{g}}}{Z_{\text{t}}}\right) \leq f_{\text{ct}} \quad (12.2)$$

At working load

Top fibres $$\left(\eta f_{\text{sup}} + \frac{M_{\text{g}}}{Z_{\text{t}}} + \frac{M_{\text{q}}}{Z_{\text{t}}}\right) \leq f_{\text{ew}} \quad (12.3)$$

Bottom fibres $$\left(\eta f_{\text{inf}} - \frac{M_{\text{g}}}{Z_{\text{b}}} - \frac{M_{\text{q}}}{Z_{\text{b}}}\right) \geq f_{\text{tw}} \quad (12.4)$$

From Eqs 12.1 and 12.3, we have

$$\left(\frac{M_{\text{q}} + (1-\eta)M_{\text{g}}}{Z_{\text{t}}}\right) \leq (f_{\text{cw}} - \eta f_{\text{tt}}) \leq f_{\text{tr}}$$

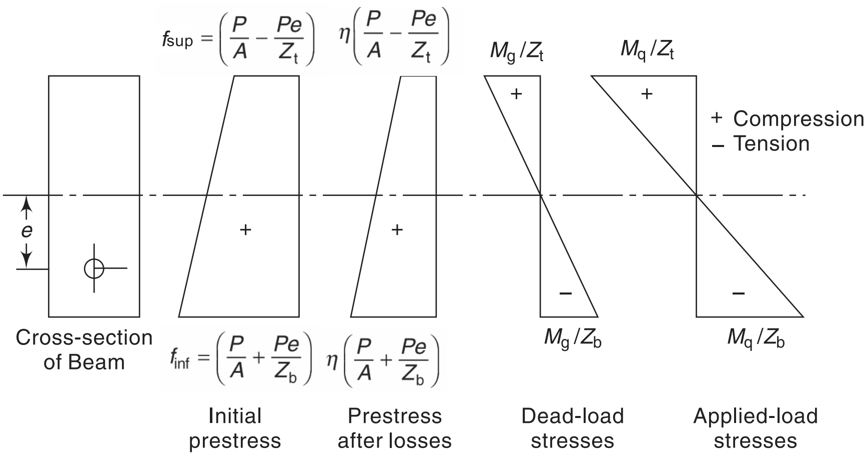

Fig. 12.1 *Stress due to prestress, dead and applied loads*

Similarly from Eqs 12.2 and 12.4, we have

$$\left(\frac{M_q + (1-\eta)M_g}{Z_b}\right) \le (\eta f_{ct} - f_{tw}) \le f_{br}$$

where f_{tr} and f_{br} are the ranges of stress at top and bottom fibres, respectively. Hence, the design formulae for the required section moduli are expressed as

$$Z_t \ge \left[\frac{M_q + (1-\eta)M_g}{f_{tr}}\right] \tag{12.5a}$$

$$Z_b \ge \left[\frac{M_q + (1-\eta)M_g}{f_{br}}\right] \tag{12.6a}$$

In cases where permanent dead loads in addition to the self-weight acts on the member, these equations are modified and used in the form given as follows:

$$Z_t \ge \left[\frac{(M_q + M_g) - \eta M_{min}}{f_{tr}}\right]$$

$$Z_t \ge \left[\frac{M_d - \eta M_{min}}{f_{tr}}\right] \tag{12.5b}$$

$$Z_b \ge \left[\frac{M_d - \eta M_{min}}{f_{br}}\right] \tag{12.6b}$$

The working moment, M_d, includes the effect of self-weight, permanent dead load and live loads, whereas the minimum moment, M_{min}, is due to the self-weight of the member or due to the moments developed during the handling of the element. The values of the allowable stresses in concrete at the extreme fibres of the member are generally specified depending upon the 28-day compressive strength of concrete. The range of compressive and tensile stresses permitted by the Indian, British and American codes has been outlined in Section 2.1.3 and Table 2.2.

The loss ratio, h, generally lies in the range of 0.75 to 0.80 for pretensioned members and between 0.80 to 0.85 for post-tensioned members. The minimum moment, M_{min}, is frequently the self-weight moment of the beam, but a lower value is possible during handling of prestressed members, such as lifting of a precast beam at points other than the supports.

It is important to note that the size of the concrete section is influenced both by the applied or live load moment and the minimum moment. However, in the case of beams with large ratios been applied to minimum moments, the cross-section is highly influenced by the applied moments and the self-weight may be considered to be counteracted by the prestress. When the minimum moment is of comparatively large magnitude, it can no longer be completely counterbalanced by the prestressing force within the cross-section. This situation is generally encountered in large-span post-tensioned girders with considerable self-weight moments.

Prestressing force Generally, the section selected is somewhat greater than the minimum indicated by Eqs 12.5 or 12.6 and consequently the prestress can lie between an upper and lower limits. Any value of the prestress within these limits may be safely used without exceeding the permissible stresses at the extreme fibres. However, the minimum prestressing force required will be obtained by selecting the maximum tensile prestress, indicated by Eq. 12.1 at the top fibre and the minimum compressive prestress, indicated by Eq. 12.4 corresponding to the bottom fibre. Rearranging these equations,

$$f_{sup} \geq \left(f_{tt} - \frac{M_g}{Z_t} \right) \tag{12.7}$$

$$f_{inf} \geq \left[\frac{f_{tw}}{\eta} + \frac{(M_q + M_g)}{\eta Z_b} \right] \tag{12.8}$$

In these equations, Z_t and Z_b correspond to the actual values of the section selected.

Eliminating e from the equations,

$$f_{sup} = \left(\frac{P}{A} - \frac{Pe}{Z_t} \right) \quad \text{and} \quad f_{inf} = \left(\frac{P}{A} + \frac{Pe}{Z_b} \right)$$

We have the expression for the minimum prestressing force as

$$P = \frac{A(f_{inf} Z_b + f_{sup} Z_t)}{(Z_t + Z_b)} \tag{12.9}$$

Similarly, eliminating P from the equations, the corresponding maximum eccentricity is given by

$$e = \frac{Z_t Z_b (f_{inf} - f_{sup})}{A(f_{sup} Z_t + f_{inf} Z_b)} \tag{12.10}$$

where f_{inf} and f_{sup} are to be computed from Eqs 12.7 and 12.8. Alternatively, graphical methods developed by Magnel[2] and Bennett[3] may be used for determining the prestressing force and the corresponding eccentricity.

In Magnel's method, the four stress conditions (Eqs 12.1 to 12.4), combined with prestress equations, yield four linear relationships when plotted on a graph with A/P as the ordinate and e as the abscissa. The possible combinations of the prestressing force and eccentricity are represented by points lying within the quadrilateral formed by the four lines.

In the simple graphical method suggested by Bennett, the stress distribution diagram is obtained by a graphical construction involving the use of the direct stress and radius of gyration. The graphical construction also enables a rapid examination of the range of possible positions and values of the prestressing force.

The computation of the minimum prestressing force and the corresponding maximum eccentricity by Magnel's graphical method and analytical procedure is illustrated by the following examples:

Example 12.1 A post-tensioned prestressed beam of rectangular section 250 mm wide is to be designed for an imposed load of 12 kN/m, uniformly distributed on a span of 12 m. The stress in the concrete must not exceed 17 N/mm² in compression or 1.4 N/mm² in tension at any time and the loss of prestress may be assumed to be 15 per cent. Calculate

(a) the minimum possible depth of the beam
(b) for the section provided, the minimum prestressing force and the corresponding eccentricity
(c) check the results of case (b) by Magnel's graphical method

Solution.

Imposed load, $q = 12$ kN/m, $\eta = 0.85$,
Breadth of section, $b = 250$ mm, $f_{ct} = f_{cw} = 17$ N/mm²
Overall depth of section h mm, $f_{tt} = f_{tw} = -1.4$ N/mm²

Live-load moment, $$M_q = \left(\frac{12 \times 12^2}{8}\right) = 216 \text{ kN m}$$

Dead-load moment, $$M_g = \left[\frac{(bh) \times 24 \times 12^2}{10^6 \times 8}\right] = \frac{432bh}{10^6} \text{ kN m}$$

$$= 432\, bh \text{ N mm}$$

Range of stress at bottom fibre, $$f_{br} = (\eta f_{ct} - f_{tw}) = [0.85 \times 17 - (-1.4)]$$
$$= 15.85 \text{ N/mm}^2$$

(a) Minimum section modulus is given by

$$Z_b = \left[\frac{M_q + (1-\eta)M_g}{f_{br}}\right]$$

$$\therefore \quad \left(\frac{bh^2}{6}\right) = \left[\frac{(216 \times 10^6) + (1 - 0.85)432bh}{15.85}\right]$$

Substituting $\qquad b = 250$ mm and simplifying, $h^2 - 24.5\,h - 325000 = 0$

$\therefore \qquad h = 580$ mm

(b) For the section provided ($b = 250$ mm and $h = 580$ mm)

Area of section, $A = (145 \times 10^3)\ \text{mm}^2$

$$Z_b = Z_t = (14 \times 10^6)\ \text{mm}^3$$

Self-weight moment, $M_g = (625 \times 10^5)$ N mm

$(M_q + M_g) = (2785 \times 10^5)$ N mm

$$f_{sup} = \left(f_{tt} - \frac{M_g}{Z_t}\right) = \left[-1.4 - \frac{625 \times 10^5}{14 \times 10^6}\right] = -5.9\ \text{N/mm}^2$$

$$f_{inf} = \left[\frac{f_{tw}}{\eta} + \frac{(M_q + M_g)}{\eta Z_b}\right] = \left[\frac{-1.4}{0.85} + \frac{2785 \times 10^5}{0.85 \times 14 \times 10^6}\right] = 22\ \text{N/mm}^2$$

Minimum prestressing force is given by

$$P = \left[\frac{A(f_{inf} Z_b + f_{sup} Z_t)}{Z_b + Z_t}\right] = \left[\frac{145 \times 10^3 (22 - 5.9) 14 \times 10^6}{28 \times 10^6}\right]$$

$$= 1170000\ \text{N} = 1170\ \text{kN}$$

Corresponding eccentricity is given by

$$e = \left[\frac{Z_t Z_b (f_{inf} - f_{sup})}{A(f_{sup} Z_t + f_{inf} Z_b)}\right] = \left[\frac{(14 \times 10^6)^2 \times \{22 - (-5.9)\}}{145 \times 10^3 (22 - 5.9) 14 \times 10^6}\right]$$

$$= 167.5\ \text{mm}$$

(c) Magnel's graphical solution. The four fundamental Eqs 12.1 to 12.4 are recast in the following form:

$$\frac{P}{A}\left[1 - \left(\frac{ey}{r^2}\right)\right] + \left(\frac{M_g}{Z_t}\right) \geq f_{tt}$$

$$\frac{P}{A}\left[1 + \left(\frac{ey}{r^2}\right)\right] - \left(\frac{M_g}{Z_t}\right) \leq f_{ct}$$

$$\frac{\eta P}{A}\left[1 - \left(\frac{ey}{r^2}\right)\right] + \frac{(M_g + M_q)}{Z_t} \leq f_{cw}$$

$$\frac{\eta P}{A}\left[1 + \left(\frac{ey}{r^2}\right)\right] - \frac{(M_g + M_q)}{Z_b} \leq f_{tw}$$

where $\qquad r^2 = \left(\frac{I}{A}\right)$ and $y = \left(\frac{h}{2}\right)$

$$I = \left[\frac{(250 \times 580^3)}{12}\right] = (4064 \times 10^6)\ \text{mm}^4$$

$$Z_t = Z_b = Z = (14 \times 10^6)\ \text{mm}^3 \text{ and } y = \left(\frac{580}{2}\right) = 290\ \text{mm}$$

$$A = (250 \times 580) = (145 \times 10^3)\ \text{mm}^2$$

$$\left(\frac{M_g}{Z_t}\right) = \left[\frac{(625 \times 10^5)}{14 \times 10^6}\right] = 4.464$$

$$\left[\frac{(M_g + M_q)}{Z}\right] = \left[\frac{(2785 \times 10^5)}{14 \times 10^6}\right] = 19.892$$

$$r^2 = \left[\frac{(4064 \times 10^6)}{(145 \times 10^3)}\right] = 28 \times 10^3 \text{ mm}^2$$

$$\left(\frac{r^2}{y}\right) = \left[\frac{(28 \times 10^3)}{290}\right] = 96.55 \text{ mm}$$

Substituting the numerical values in the equations, we have

$$\left(\frac{P}{A}\right)(1 - 0.0103\, e) + 4.464 = -1.4$$

$$\left(\frac{P}{A}\right)(1 + 0.0103\, e) - 4.464 = 17$$

$$\left(\frac{0.85P}{A}\right)(1 - 0.0103\, e) + 19.892 = 17$$

$$\left(\frac{0.85P}{A}\right)(1 + 0.0103\, e) - 19.892 = -1.4$$

Rewriting the above linear equations in terms of the parameters (A/P) and e, we have

$$\left(\frac{A}{P}\right) = \left[\left(-\frac{1}{5.864}\right) + \left(\frac{0.0103 e}{5.864}\right)\right] \qquad 12.1(a)$$

$$\left(\frac{A}{P}\right) = \left[\left(\frac{1}{21.464}\right) + \left(\frac{0.0103\, e}{21.464}\right)\right] \qquad 12.2(a)$$

$$\left(\frac{A}{P}\right) = \left[\left(-\frac{0.85}{2.892}\right) + \frac{(0.85 \times 0.0103\, e)}{2.892}\right] \qquad 12.3(a)$$

$$\left(\frac{A}{P}\right) = \left[\left(\frac{0.85}{18.492}\right) + \frac{(0.85 \times 0.0103\, e)}{18.492}\right] \qquad 12.4(a)$$

Equations 12.1(a) to 12.4(a) are graphically represented as shown in Fig. 12.2. The intercepts of (A/P) corresponding to $e = 0$ in the above equations are obtained as (-170×10^{-3}), (45.9×10^{-3}), (-294×10^{-3}) and (46×10^{-3}). The intercepts of e corresponding to zero values of (A/P) are 96.55 and –96.55.

The four equations intersect each other in a quadrilateral, which is shaded, indicating the feasible zone of solutions.

The minimum prestressing force corresponding to the maximum eccentricity as governed by the Eqs 12.1(a) and 12.4(a) are read out from Fig. 12.2 having the value $(A/P) = 124 \times 10^{-3}$, yielding

$$P = \left[\frac{(145 \times 10^3 \times 10^3)}{124}\right] = (1169 \times 10^3) \text{ N} = 1169 \text{ kN}$$

and $\qquad e = 168$ mm

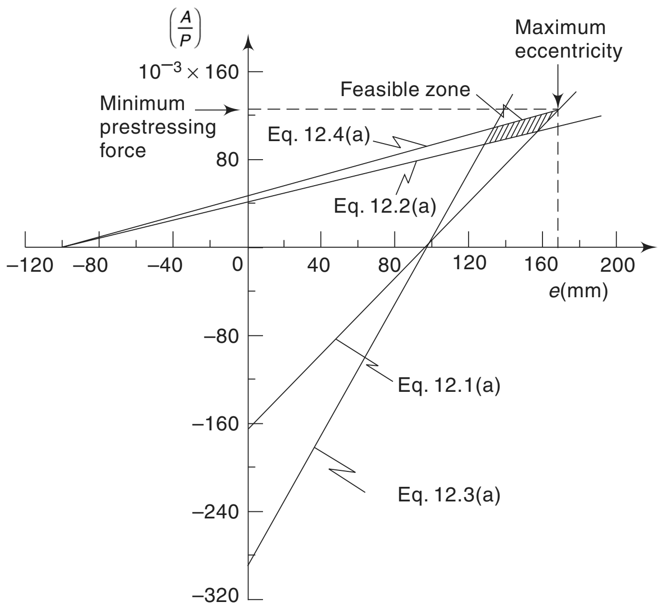

Fig. 12.2 *Magnel's graphical solution for prestressing force and eccentricity*

These values of the prestressing force and the eccentricity are nearly the same as those obtained in case (b).

Example 12.2 A prestressed girder has to be designed to cover a span of 12 m, to support an uniformly distributed live load of 15 kN/m. M-45 Grade concrete is used for casting the girder. The permissible stress in compression may be assumed as 14 N/mm^2 and 1.4 N/mm^2 in tension. Assume 15 per cent losses in prestress during service load conditions. The preliminary section proposed for the girder consists of a symmetrical I-section with flanges 300 mm wide and 150 mm thick. The web is 120 mm wide by 450 mm deep.

(a) Check the adequacy of the section provided to resist the service loads.
(b) Design the minimum prestressing force and the corresponding eccentricity for the section.

Solution.

$$L = 12 \text{ m} \qquad \text{Loss ratio} = \eta = 0.85$$
$$f_{ct} = 14 \text{ N/mm}^2 \qquad f_{tt} = f_{tw} = -1.4 \text{ N/mm}^2$$
$$q = 15 \text{ kN/m} \qquad y = y_t = y_b = 375 \text{ mm}$$

Area of section $= A = [(2 \times 200 \times 150) + (120 \times 450)] = 144000 \text{ mm}^2$

$$\text{Section moment of area} = I = \left[\frac{300 \times 750^3}{12} - \frac{180 \times 450^3}{12}\right] = (918 \times 10^7) \text{ mm}^4$$

$$\text{Section modulus} = Z = Z_t = Z_b = \left[\frac{I}{y}\right] = \left[\frac{(918 \times 10^7)}{375}\right] = (24.48 \times 10^6) \text{ mm}^3$$

$$\text{Self-weight of girder} = g = \left[\frac{144000}{10^6}\right] 24 = 3.456 \text{ kN/m}$$

$$\text{Dead-load moment} = M_g = \left[\frac{gL^2}{8}\right] = \left[\frac{3.456 \times 12^2}{8}\right] = 62.208 \text{ kN m}$$

$$\text{Live-load moment} = M_q = \left[\frac{qL^2}{8}\right] = \left[\frac{15 \times 12^2}{8}\right] = 270 \text{ kN m}$$

$$f_{br} = (\eta f_{ct} - f_{tw}) = [(0.85 \times 14) - (-1.4)] = 13.3 \text{ N/mm}^2$$

(a) Check for adequacy of section

$$Z_b \geq \left[\frac{M_q + (1-\eta)M_g}{f_{br}}\right] = \left[\frac{(270 \times 10^6) + (1 - 0.85)(62.208 \times 10^6)}{13.3}\right]$$

$$= (21 \times 10^6) \text{ mm}^3 > Z_b \text{ provided}$$

Hence, the section provided is adequate to resist the loads safely.

(b) Minimum prestressing force and corresponding eccentricity

$$f_t = \left[f_{tt} - \frac{M_g}{Z_t}\right] = \left[-1.4 - \frac{(62.208 \times 10^6)}{(24.48 \times 10^6)}\right] = -3.94 \text{ N/mm}^2$$

$$f_b = \left[\frac{f_{tw}}{\eta} + \frac{M_g + M_q}{\eta Z_b}\right] = \left[\frac{-1.4}{0.85} + \frac{(62.208 + 270) \times 10^6}{0.85(24.48 \times 10^6)}\right] = 14.36 \text{ N/mm}^2$$

Prestressing force is computed using the relation

$$P = \left[\frac{A(f_t Z_t + f_b Z_b)}{(Z_t + Z_b)}\right] = \left[\frac{144000[(-3.94 + 14.36)24.48 \times 10^6]}{(2 \times 24.48 \times 10^6)}\right]$$

$$= (747.28 \times 10^6)\text{N} = 747.28 \text{ kN}$$

Eccentricity is obtained by the relation

$$e = \left[\frac{Z_t Z_b (f_b - f_t)}{A(f_t Z_t + f_b Z_b)}\right] = \left[\frac{(24.48^2)(10^{12})[14.36 - (-3.94)]}{144000[(-3.94 + 14.36)24.48 \times 10^6]}\right] = 298.5 \text{ mm}$$

Example 12.3 A prestressed beam has a symmetrical I-section in which the depth of each flange is one-fifth of the overall depth and the web is thin enough to be neglected in bending calculations. At the point of maximum bending moment, the prestressing force is located at the centre of the bottom flange and the total loss of prestress is 20 per cent. If there is to be no tensile stress in the concrete at any time, show that the dead load must be at least one-seventh of the live load.

Solution.

Overall depth = h

Breadth of flange = b

Thickness of flange = 0.2 h

Assuming b = 1 unit

$$e = 0.4h$$

$$\eta = 0.8$$

$$I = \left[\frac{1 \times h^3}{12} - \frac{(0.6h)^3}{12}\right] = 0.065h^3$$

$\therefore$ $$Z = 0.13h^2$$

Limiting stress conditions are,

$$\left[\frac{P}{A} - \frac{Pe}{Z} + \frac{M_g}{Z}\right] = 0 \qquad (12.11)$$

$$0.8\left[\frac{P}{A} + \frac{Pe}{Z} - \frac{M_g}{Z} - \frac{M_q}{Z}\right] = 0 \qquad (12.12)$$

Multiplying Eq. 12.11 by 0.8 and dividing,

$$\frac{\left(\frac{1}{A}\right) - \left(\frac{e}{Z}\right)}{\left(\frac{1}{A}\right) + \left(\frac{e}{Z}\right)} = -\left[\frac{(0.8M_g)}{(M_q + M_g)}\right]$$

Simplifying

$$0.57(M_g + M_q) = 0.8M_g(5.57)$$

$$M_g = \left(\frac{1}{7}\right)M_q$$

Example 12.4 A pretensioned beam 80 mm wide and 120 mm deep, is to be designed to support working loads of 4 kN, each concentrated at the third points over a span of 3 m. If the permissible stresses in tension are zero at transfer and 1.4 N/mm^2 under working loads, design the number of 3 mm wires and the corresponding eccentricity required at the mid-span section. Permissible tensile stress in wires is 1400 N/mm^2. The loss of prestress is 20 per cent and the density of concrete is 24 kN/m^3.

Solution.

Self-weight of the beam, $g = (0.08 \times 0.12 \times 24) = 0.23$ kN/m

Section modulus, $Z_b = Z_t = (80 \times 120^2)/6 = 192 \times 10^3$ mm^3

Self-weight moment, $M_g = (0.23 \times 3^2)/8 = 0.26$ kN m

Live-load moment, $M_q = (4 \times 1) = 4$ kN m

Permissible stresses, $f_{tt} = 0$, $f_{tw} = -1.4$ N/mm^2

Required prestress at bottom and top fibres is given by

$$f_{inf} = \left[\frac{f_{tw}}{\eta} + \frac{(M_q + M_g)}{\eta Z_b}\right] = \left[\frac{-1.4}{0.8} + \frac{4.26 \times 10^6}{0.8 \times 192 \times 10^3}\right] = 26.00 \text{ N/mm}^2$$

$$f_{sup} = \left(f_{tt} - \frac{M_g}{Z_t}\right) = \left[0 - \frac{0.26 \times 10^6}{192 \times 10^3}\right] = -1.35 \text{ N/mm}^2$$

Minimum prestressing force P is obtained by the expression,

$$P = \left[\frac{A(f_{inf}Z_b + f_{sup}Z_t)}{Z_b + Z_t}\right] = \left[\frac{9600(26.00 - 1.35)192 \times 10^3}{2 \times 192 \times 10^3}\right]$$

$$= 120785 \text{ N} = 121 \text{ kN}$$

The corresponding eccentricity is given by

$$e = \frac{Z_b Z_t (f_{inf} - f_{sup})}{A(f_{sup} Z_t + f_{inf} Z_b)}$$

If $$Z_b = Z_t$$

$$e = \frac{Z(f_{inf} - f_{sup})}{A(f_{inf} + f_{sup})} = \left[\frac{192 \times 10^3 (27.35)}{9600(24.65)}\right] = 22 \text{ mm}$$

Area of 3 mm wire = 7.05 mm^2

Safe force in each wire = $(7.05 \times 1400) = 9870$ N

$\therefore$ Number of wires $= \dfrac{(121000)}{(9870)} = 12.3 \ \underline{\Omega}\ 13$

12.1.2 Limitation of Prestress in Long Spans

In the case of lightly loaded beams with long spans in which the minimum moment is relatively large, the theoretical value of eccentricity *e*, determined from Eq. 12.10, indicates the position of the prestressing force. This force is either below the soffit of the section or too low for tendons to be accommodated with sufficient cover. In such cases, the theoretical eccentricity is reduced so that the prestressing force lies within the section at the lowest practicable position. Consequently, the magnitude of the prestressing force is to be increased so that the prestress at the bottom is unaltered (Fig. 12.3). There will be a reduction in the negative prestress at top at the transfer stage and an increase in the compressive stress at the top fibre under service loads. In the case of heavy girders associated with very large self-weight moments, the minimum stress developed at transfer for the top fibre will be compressive in nature due to the limitations of the position of the prestressing force.

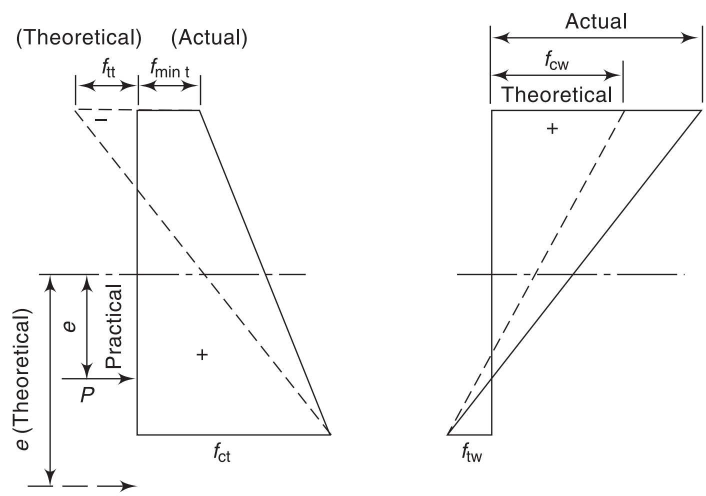

Fig. 12.3 *Limitation of prestress due to large minimum moments*

The minimum stress developed at transfer f_{mint} is computed from equations

$$\left(f_{\text{sup}} + \frac{M_{\min}}{Z_t}\right) \geq f_{\text{mint}}$$

and
$$\left(\eta f_{\text{inf}} - \frac{M_{\min}}{Z_b} - \frac{M_q}{Z_b}\right) \geq f_{\text{tw}}$$

By substituting, $f_{\text{sup}} = \left(\dfrac{P}{A} - \dfrac{Pe}{Z_t}\right)$ and $f_{\text{inf}} = \left(\dfrac{P}{A} + \dfrac{Pe}{Z_b}\right)$

and eliminating P from the resulting equations, we get

$$f_{\text{mint}} = \left[\frac{M_{\min}}{Z_t} + \frac{Z_b(Z_t - Ae)}{\eta Z_t(Z_t + Ae)}\left(\frac{M_d}{Z_b} + f_{\text{tw}}\right)\right] \tag{12.13}$$

The revised section modulus, obtained by using the value of f_{mint} in the range of stress f_{tr} and using the Eq. 12.5, should be checked, and if the chosen section satisfies this criteria, the magnitude of the prestressing force is computed from Eq. 12.9.

Alternatively, the required prestressing force P acting at known eccentricity e, which can develop the required prestress f_{inf} at the bottom fibre, is computed directly by the expression

$$P = \left(\frac{A\, f_{\text{inf}} Z_b}{Z_b + Ae}\right) \tag{12.14}$$

where A and Z_b are the cross-sectional area and the section modulus of the cross-section actually provided.

Example 12.5 An unsymmetrical I-section having the following section properties is used for a bridge girder.

The thickness of top and bottom flanges are 200 and 250 mm, respectively. The width of top and bottom flanges are 750 and 450 mm, respectively. The thickness of web is 150 mm, overall depth is 1000 mm and the area of section is 345000 mm^2. $Z_t = 95 \times 10^6$ mm^3, $Z_b = 75 \times 10^6$ mm^3 and the position of the centroid of the section is 440 mm from the top. If the permissible tensile and compressive stresses at transfer and working loads are not to exceed zero in tension and 15 N/mm^2 in compression, determine the prestressing force required and the corresponding eccentricity to resist self-weight and applied moments of 1012 and 450 kN m, respectively. The loss ratio is 0.85.

Solution. Given data

$f_{tt} = f_{tw} = 0$

$f_{ct} = f_{cw} = 15$ N/mm^2 $\qquad \eta = 0.85$

$M_g = 1012$ kN m $\qquad Z_t = (95 \times 10^6)$ mm^3

$M_q = 450$ kN m $\qquad Z_b = (75 \times 10^6)$ mm^3

$M_d = 1462$ kN m $\qquad A = 345000$ mm^2

$$f_{\text{sup}} = \left(f_{tt} - \frac{M_g}{Z_t}\right) = \left[0 - \frac{1012 \times 10^6}{95 \times 10^6}\right] = -10.6 \text{ N/mm}^2$$

$$f_{\text{inf}} = \left[\frac{f_{\text{tw}}}{\eta} + \frac{M_{\text{g}} + M_{\text{q}}}{\eta Z_b}\right] = \left[0 + \frac{1462 \times 10^2}{0.85 \times 75 \times 10^6}\right]$$

$$= 23 \text{ N/mm}^2$$

$$\therefore \quad \text{Prestressing force, } P = \left[\frac{A(f_{\text{inf}} Z_{\text{b}} + f_{\text{sup}} Z_{\text{t}})}{Z_{\text{t}} + Z_{\text{b}}}\right]$$

$$= \left[\frac{345 \times 10^3 (23 \times 75 - 10.6 \times 95) 10^6}{170 \times 10^6}\right] = 146 \times 10^4 \text{ N}$$

$$\text{Eccentricity, } e = \left[\frac{Z_{\text{t}} Z_{\text{b}} (f_{\text{inf}} - f_{\text{sup}})}{A(f_{\text{sup}} Z_{\text{t}} + f_{\text{inf}} Z_{\text{b}})}\right]$$

$$= \left[\frac{95 \times 75 \times 10^6 (23 + 10.6)}{247.71 \times 10^{12}}\right] = 967 \text{ mm}$$

Maximum possible eccentricity (with suitable cover of 100 mm)

$$= (1000 - 440 - 100) = 460 \text{ mm}$$

Providing the maximum possible eccentricity, $e = 460$ mm, the prestressing force, P, required to develop the prestress, f_{inf}, is obtained as,

$$P = \left(\frac{A\, f_{\text{inf}} Z_{\text{b}}}{Z_{\text{b}} + Ae}\right)$$

$$= \left[\frac{345 \times 10^3 \times 23 \times 75 \times 10^6}{(75 \times 10^6) + (345 \times 10^3 \times 460)}\right] = (2547 \times 10^3) \text{ N} = 2547 \text{ kN}$$

12.1.3 Limiting Zone for the Prestressing Force

The prestress along the length of the beam is generally adjusted by varying the eccentricity of the prestressing force. This practise is generally used in post-tensioned beams by using curved cables. In the case of pretensioned members, the tendons may be deflected by using deviating devices fixed to the mould before casting. After having once determined the magnitude of the prestressing force for the critical section, it is possible to fix up the limiting zone for the force bounded by the upper and lower limits expressed as a function of the minimum and maximum moments, sectional properties, prestressing force and the permissible stresses in concrete at transfer and working loads.

The limiting zone is defined by four equations obtained by combining the stress conditions of Eqs 12.1 to 12.4 and the prestress equations for the top and bottom fibres given by

$$f_{\text{sup}} = \left(\frac{P}{A} - \frac{Pe}{Z_{\text{t}}}\right)$$

$$f_{\text{inf}} = \left(\frac{P}{A} + \frac{Pe}{Z_{\text{b}}}\right)$$

Combining these relations with Eqs 12.1 to 12.4, and noting that $M_g = M_{min}$, the following equations are obtained:

$$e \le \left[\frac{-Z_t f_{tt}}{P} + \frac{Z_t}{A} + \frac{M_{min}}{P}\right] \tag{12.15}$$

$$e \le \left[\frac{Z_b f_{ct}}{P} - \frac{Z_b}{A} + \frac{M_{min}}{P}\right] \tag{12.16}$$

$$e \ge \left[\frac{-Z_t f_{cw}}{\eta P} + \frac{Z_t}{A} + \frac{M_d}{\eta P}\right] \tag{12.17}$$

$$e \ge \left[\frac{Z_b f_{tw}}{\eta P} - \frac{Z_b}{A} + \frac{M_d}{\eta P}\right] \tag{12.18}$$

The curves represented by two of these four equations are given in Fig. 12.4. Positive eccentricities are plotted below the centroid of the section. The permissible tendon zone is controlled by only two of the above four equations, as can be seen from the figure. In the case of prismatic members with a constant prestressing force, the permissible tendon zone is controlled by Eqs 12.16 and 12.17. The use of these equations is illustrated in the following examples.

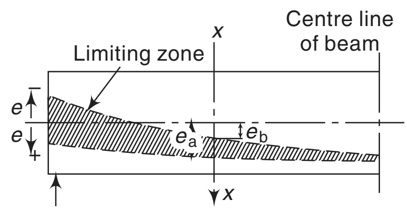

Fig. 12.4 *Limiting zone for prestressing force*

Example 12.6 A prestressed beam has an unsymmetrical I-section with an overall depth of 1840 mm. The top and bottom flange widths are 1800 and 820 mm, respectively. The thickness of the top flange varies from 180 mm at the ends to 430 mm at the junction of the web, which is 180 mm thick. The thickness of the bottom flange varies from 150 mm at the ends to 450 mm at the junction of the web. The beam is designed for a simply supported span of 40 m. The permissible compressive stress at the transfer and working load is limited to 16 N/mm^2, while the tensile stress at the transfer and working load is limited to zero and 1.4 N/mm^2, respectively. The loss ratio is 0.80. Calculate

(a) the permissible uniformly distributed imposed load
(b) the magnitude of the prestressing force if at the mid-span section it is located 130 mm from the soffit
(c) the vertical limits within which the cable must lie at mid-span and support sections

Solution.

Properties of I-section:

$A = 1016500\ \text{mm}^2 \quad y_t = 700\ \text{mm} \quad I = (4442 \times 10^8)\ \text{mm}^4$

$y_b = 1140\ \text{mm} \quad Z_b = (39 \times 10^7)\ \text{mm}^3 \quad Z_t = (63 \times 10^7)\ \text{mm}^3$

$e = (1140 - 130) = 1010\ \text{mm}$

Self-weight, $g = (1.0165 \times 1 \times 24) = 24.4\ \text{kN/m}$

$$M_g = (24.4 \times 40^2)/8 = 4880 \text{ kN m}$$

(a) If M_q = live-load moment, the minimum section modulus required is given by

$$Z_b = \left[\frac{M_q + (1-\eta)M_g}{f_{br}}\right]$$

$$f_{br} = (\eta f_{ct} - f_{tw}) = [(0.8 \times 16) - (-1.4)] = 14.2 \text{ N/mm}^2$$

$\therefore$ $$39 \times 10^7 = \left[\frac{M_q + (1-0.8)4820 \times 10^6}{14.2}\right]$$

Solving $$M_q = (qL^2/8) \times 10^6 = (4574 \times 10^6) \text{ N mm}$$

$\therefore$ $$q = 22.87 \text{ kN/m}$$

(b) The minimum prestressing force is obtained by the limiting stress conditions

$$\frac{P}{A}\left(1 + \frac{ey_b}{i^2}\right) - \frac{M_g}{Z_b} = 16.0$$

$$\frac{P}{A}\left(1 + \frac{ey_b}{i^2}\right) - \left(\frac{M_g + M_q}{Z_b}\right) = -1.4$$

Also $$e = 1010 \text{ m}$$

$$i^2 = (I/A) = 437000 \text{ and } y_b = 1140 \text{ mm}$$

Solving, $$P = 7900 \text{ kN}$$

(c) Substituting the values of the limiting stresses,

$$f_{tt} = 0, f_{tw} = -1.4$$

$$f_{ct} = f_{cw} = 16.0 \text{ N/mm}^2$$

in Eqs 12.16 and 12.17, the limits of the cable are obtained.

At the centre of span

$$e \le \left[\frac{Z_b f_{ct}}{P} - \frac{Z_b}{A} + \frac{M_{min}}{P}\right]$$

$$\le \left[\frac{39 \times 10^7 \times 16}{7900 \times 10^3} - \frac{39 \times 10^7}{1.0165 \times 10^6} + \frac{4880 \times 10^6}{7900 \times 10^3}\right] \le 1024 \text{ mm}$$

and $$e \ge \left[\frac{Z_b f_{tw}}{\eta P} - \frac{Z_b}{A} + \frac{M_d}{\eta P}\right]$$

$$\ge \left[\frac{39 \times 10^7 \times (-1.4)}{0.8 \times 7900 \times 10^3} - \frac{39 \times 10^7}{1.0165 \times 10^6} + \frac{9454 \times 10^6}{0.8 \times 7900 \times 10^3}\right] \ge 1026 \text{ mm}$$

At the support section

$$e \le (790 - 385) \le 405 \text{ mm}$$

and $$e \ge (-86 - 385) \ge -471 \text{ mm}$$

Example 12.7 The cross-sectional area of an unsymmetrical prestressed I-beam designed to carry a central point load on a simply supported span of 15 m is 194000 mm^2. The second moment of area is equal to 197×10^8 mm^4. The overall depth of the section is 900 mm, with the centroid located at 520 mm from the soffit. The maximum permissible stresses are 14 N/mm^2 in compression and zero in tension. The loss ratio is 0.8. Calculate

(a) the breadth of a rectangular section, having the same depth designed for the same loading
(b) the value of the point load
(c) the saving in steel and concrete of the I-section compared to the rectangular section
(d) the maximum eccentricities of the cable at mid-span for the two sections

Solution.

Area of concrete section, $A = 194000$ mm^2

Second moment of area, $I = 197 \times 10^8$ mm^4

$y_b = 520$ mm, $y_t = 380$ mm, $\eta = 0.8$

Permissible stresses,

$$f_{ct} = f_{cw} = 14 \text{ N/mm}^2, f_{tt} = f_{tw} = 0$$

$$Z_b = \left(\frac{197 \times 10^8}{520}\right) = 38 \times 10^6 \text{ mm}^3$$

$$Z_t = \left(\frac{197 \times 10^8}{380}\right) = 52 \times 10^6 \text{ mm}^3$$

(a) If b is the width of the rectangular section,

$$(b \times 900^2)/6 = (38 \times 10^6); \quad \therefore \; b = 280 \text{ mm}$$

Area of rectangular section = $(280 \times 900) = (252 \times 10^3)$ mm^2

Second moment of area = (17×10^9) mm^4

(b) Self-weight, g_i, of the I-section = $(0.194 \times 24) = 4.65$ kN/m

Self-weight moment of the I-section, $M_g = \left[\frac{(4.65 \times 15^2)}{8}\right] = 130$ kN m

If M_q = live-load moment,

$$Z_b = \left[\frac{M_q + (1-\eta)M_g}{f_{br}}\right]$$

$$f_{br} = (\eta f_{ct} - f_{tw}) = (0.8 \times 14) = 11.2 \text{ N/mm}^2$$

$\therefore$ $$38 \times 10^6 = [M_q + (1-0.8)130 \times 10^6]/11.2$$

Solving, $$M_q = \left(\frac{QL}{4}\right) = 400 \text{ kN m}$$

$\therefore$ $$Q = 106.66 \text{ kN}$$

(c) The limiting stress conditions are

$$\frac{P}{A}\left[1 + \frac{ey_b}{i^2}\right] - \left(\frac{M_g y_b}{I}\right) = 14 \qquad (12.19)$$

$$\frac{P}{A}\left[1 - \frac{ey_t}{i^2}\right] + \left(\frac{M_g y_t}{I}\right) = 0 \qquad (12.20)$$

Multiplying Eq. 12.19 by y_t and Eq. 12.20 by y_b and adding

$$\frac{P}{A}(y_b + y_t) = 14 y_t$$

$$\therefore \quad P = \left[\frac{(14 y_t A)}{h}\right], \text{ where } \qquad h = (y_b + y_t)$$

For the I-section $$P = \left(\frac{14 \times 380 \times 194 \times 10^3}{900}\right) = (115 \times 10^4)\text{ N}$$

For the rectangular section

$$P = \left(\frac{14 \times 450 \times 252 \times 10^3}{900}\right) = (175 \times 10^4)\text{ N}$$

(d) Saving in concrete $= \dfrac{(252 - 194)}{252} \times 100 = 23\%$

Saving in steel $= \dfrac{(175 - 115)}{176} \times 100 = 34.3\%$

Self-weight of the rectangular section = $(0.252 \times 24) = 6.05$ kN/m

M_g (rectangular section) = $(6.05 \times 15^2)/8 = 170$ kN m

Section modulus (rectangular section) = $(17 \times 10^9)/450 = 37.8 \times 10^6$ mm^3

Maximum permissible eccentricities of the cable at mid-span section,

(I-section) $$e_{max} = \left[\frac{38 \times 10^6 \times 14}{115 \times 10^4} - \frac{38 \times 10^6}{194 \times 10^3} + \frac{130 \times 10^6}{115 \times 10^4}\right] = 379 \text{ mm}$$

(Rectangular section) $$e_{max} = \left[\frac{37.8 \times 10^6 \times 14}{176 \times 10^4} - \frac{37.8 \times 10^6}{252 \times 10^3} + \frac{170 \times 10^6}{176 \times 10^4}\right]$$

$$= 250 \text{ mm}$$

12.1.4 Design of Sections for the Limit State of Collapse in Flexure

In the design of prestressed concrete members for the limit state of collapse, the distribution of compressive stress in the section at the ultimate failure stage is considered and the effective depth required is estimated by equating the total ultimate moment with the internal resisting couple. A comparative analysis of the various code recommendations indicate that the maximum design value of the moment of resistance of rectangular and flanged sections vary from $0.08 f_{ck}bd^2$ to $0.2 f_{ck}bd^2$, depending upon the recommendations of the stress block parameters.

The maximum ultimate moment of resistance of a rectangular section, according to the Indian standard code IS: 1343, is given by

$$M_{ud} = (0.21 f_{ck}bd^2)$$

The dimensions based on this expression are the minimum values. It is often preferable to use a larger section, because it means saving on the costly prestressing tendons.

In the case of flanged sections, a reasonable proportion of $h_f/d = 0.2$ to 0.25 and $b_w/d = 0.2$ to 0.3, so that the ultimate moment varies from $0.08 f_{ck}bd^2$ to $0.12 f_{ck}bd^2$.

Assuming a suitable value for the breadth of the compression face b, generally of the order of 0.5 h for T-sections and 0.6 to 0.8 h for I-sections, the effective and overall depth of the section is designed by providing suitable cover requirements.

The area of high tensile and untensioned reinforcement required to mobilise the desired flexural strength is computed using the force equilibrium at the limit state of collapse. However, the tensile reinforcement index should not exceed the specified permissible values. The limitation of reinforcement will result in under-reinforced sections, ensuring progressive collapse of members.

Example 12.8 A pretensioned prestressed concrete beam of rectangular section is required to support a design ultimate moment of 100 kN m. Design the section of f_{ck} is 50 N/mm^2 and f_p = 1600 N/mm^2.

If b and d are the breadth and effective depth of the section, respectively, assuming the ratio $(x_u/d) = 0.5$.

Solution.

We have $\quad M_u = 0.36\, f_{ck} b x_u\,(d - 0.42x_u) = 0.14\, f_{ck}\, bd^2$

Assuming $\quad b = 0.5\, d$,

$$d^3 = \left(\frac{M_u}{0.14 \times f_{ck} \times 0.5}\right) = \left(\frac{100 \times 10^6}{0.15 \times 50 \times 0.5}\right)$$

Solving $\quad d = 300$ mm and hence $b = 150$ mm

and $\quad x_u = (0.5 \times 300) = 150$ mm

From Table 7.1, for $(x_u/d) = 0.5$

$$f_{pu} = 0.87\, f_p$$

$$\therefore \quad A_p = \left[\frac{M_u}{0.87 f_p (d - 0.42x_u)}\right] = \left[\frac{100 \times 100^6}{0.87 \times 1600(300 - 0.42 \times 150)}\right] = 300 \text{ mm}^2$$

Adopt a section, 150 mm wide by 350 mm deep, with 300 mm^2 of high-tensile steel located at an effective depth of 300 mm.

Example 12.9 A post-tensioned bonded beam of unsymmetrical I-section is required to support a design ultimate moment of 1200 kN m. Determine the overall depth and thickness of the compression flange required if f_{ck} is 35 N/mm^2 and f_p = 1500 N/mm^2.

Solution.

For flanged sections, $M_{ud} = 0.08\, f_{ck} bd^2$

Assuming $b = 0.5\, d$ and $b_w = 0.25\, b$

$$\therefore \quad d^3 = \left[\frac{(1200 \times 10^6)}{(0.10 \times 35 \times 0.5)}\right]$$

$$\therefore \quad d = 1000 \text{ mm and } b = 500 \text{ mm}$$

Thickness of top flange = $h_f = 0.2\, d = (0.2 \times 1000) = 200$ mm

Thickness of the web = $b_w = 0.25b = (0.25 \times 500) = 125$ mm

Assuming the neutral-axis depth, $x_u = h_f = 200$ mm

$$M_u = 0.87\, f_p A_p (d - 0.42x_u)$$

$$\therefore \; A_p = \left[\frac{M_u}{0.87 f_p (d - 0.42 x_u)}\right] = \left[\frac{1200 \times 10^6}{0.87 \times 1500(1000 - 0.42 \times 200)}\right] = 1003 \text{ mm}^2$$

12.2 Design of Sections for Axial Tension

Due to the presence of precompression, prestressed concrete is ideally suited for the design of members subjected to axial tension. Notable examples of members in which axial tension is the primary force are tie members of trusses, walls of cylindrical tanks, silos and pipes subjected to internal pressure. The design essentially consists of determining the cross-sectional area of the member and the required prestressing force to safely support the axial tensile load conforming to the limit state of serviceability and collapse.

According to the Indian Standard Code IS: 1343[4], no tensile stresses are permitted in Class-1 members. However, in Class-2 members, tensile stresses of up to 3 N/mm^2 are permitted at serviceability limit states. Class-3 type members are not generally recommended for resisting direct tension.

The cross-sectional area of concrete is determined from the stress conditions at transfer and working loads as detailed below.

If N_d = design tensile load
N_{min} = minimum tensile load (generally zero)
f_c = compressive prestress in concrete
f_{ct} = permissible compressive stress in concrete at transfer of prestress
h_{tw} = permissible tensile stress in concrete under working load
η = prestress loss ratio
A = equivalent area of concrete

At the transfer stage

$$\left[f_c - \frac{N_{min}}{A}\right] \le f_{ct} \tag{12.21}$$

At the working load stage

$$\left[\eta f_c - \frac{N_d}{A}\right] \ge f_{tw} \tag{12.22}$$

From the two stress conditions, the area of the section is given by the relation

$$A = \left(\frac{N_d - \eta N_{min}}{\eta f_{ct} - f_{tw}}\right) \tag{12.23}$$

If the minimum load and permissible tensile stresses are zero, the cross-sectional area is obtained from the expression,

$$A = \left(\frac{N_d}{\eta f_{ct}}\right) \tag{12.24}$$

The cross-sectional area determined by the expressions is sometimes not practicable, especially in the case of circular water tanks. In such cases, the thickness required is fixed, based on practical considerations of housing the vertical cables and proper compaction of the concrete in the walls of the tank. The minimum thickness for cast *in situ* walls is 100 mm and for precast walls, 125 mm, according to Nawy[5]. However, in the case of large tanks with walls having vertical cables, a minimum thickness of 150 mm is generally required.

12.2.1 Load Factor—Limit State of Cracking and Collapse

Members subjected to direct tension, such as the walls of liquid-retaining structures, are generally designed to have suitable global load factors against cracking and collapse. According to the Indian standard code IS: 3370 (Part III) 1967[6], the load factors against cracking and collapse should be not less than 1.2 and 2, respectively. The cracking load generally corresponds to the stage where the tensile stress developed in the member reaches a value equal to the tensile strength of concrete. However, the cracking load of a prestressed member assembled from precast blocks is computed on the assumptions that concrete is incapable of resisting any tensile stress.

If N_{cr} = cracking load

f_t = tensile strength of concrete = $0.24\sqrt{f_{ck}}$

then $N_{cr} = A(f_c + f_t)$

$$\text{Load factor against cracking} = \left(\frac{N_{cr}}{N_d}\right)$$

For ordinary tension members, such as ties of trusses, ring beams, and railroad ties, a minimum load factor of 1.5 to 2, depending upon the importance of the tension member in the structure, is recommended by Nawy[5].

At the limit state of collapse, the concrete member is completely cracked at the critical section and the entire axial load is resisted by the tendons. If the area of steel provided in the cross-section based on the serviceability limit state is insufficient to provide the desired load factor against collapse, additional reinforcements are designed and distributed uniformly in the section. These are normally mild or medium-strength steels which are also helpful in reducing shrinkage cracks in members.

The design of prestressed concrete members for axial tension is illustrated by the following examples:

Example 12.10 Design a suitable section for the tie member of a prestressed concrete truss to carry a design tensile force of 600 kN. Assume the permissible compressive stress in concrete at transfer as 15 N/mm² and tension is not allowed under service loads. Loss of prestress is 20 per cent. High-tensile wires of 8 mm diameter with an ultimate tensile strength of 1400 N/mm² with an initial stress of 800 N/mm² are available for use. The direct tensile strength of concrete is 3 N/mm². A load factor of 2 against collapse and 1.25 against cracking is to be ensured in the design.

Solution.

Tensile force = $N_d = 600$ kN

$f_{ct} = 15\ \text{N/mm}^2 \quad f_{tw} = 0 \quad \eta = 0.80$

$$\text{Area of concrete section} = \left[\frac{N_d}{\eta f_{ct}}\right] = \left[\frac{600 \times 10^3}{0.8 \times 15}\right] = 50000\ \text{mm}^2$$

Adopt a section 200 mm by 250 mm (Area = 50000 mm^2)

$$\text{Compressive prestress} = \left[\frac{600 \times 10^3}{0.8 \times 50000}\right] = 15\ \text{N/mm}^2$$

$$\text{Prestressing force required} = P = \left[\frac{15 \times 50000}{1000}\right] = 750\ \text{kN}$$

$$\text{Number of 8 mm wires} = \left[\frac{750 \times 10^3}{50 \times 800}\right]$$

$$= 18.75 \text{ (use 20 wires of 8 mm diameter)}$$

$$\text{Ultimate tensile strength of the tie} = \left[\frac{20 \times 50 \times 0.87 \times 1400}{1000}\right] = 1218\ \text{kN}$$

$$\text{Load factor against collapse} = \left[\frac{1218}{600}\right] = 2.03 > 2$$

$$\text{Cracking load} = \left[\frac{50000(0.8 \times 15 + 3)}{1000}\right] = 750\ \text{kN}$$

$$\therefore \quad \text{Load factor against cracking} = \left(\frac{750}{600}\right) = 1.25$$

Example 12.11 Design the thickness and circumferential reinforcement required for a cylindrical tank wall subjected to a design tensile force of 500 kN/m. f_{ct} = 16 N/mm^2, f_{tw} = –0.8 N/mm^2, direct tensile strength of concrete = 2.5 N/mm^2 and η = 0.85. High-tensile wires of 5 mm diameter (UTS = 1700 N/mm^2) with an initial stress of 1000 N/mm^2 may be used. Desirable load factors against collapse and cracking should not be less than 2 and 1.25, respectively.

Solution.

$$A = \left(\frac{N_d}{\eta f_{ct} - f_{tw}}\right) = \left(\frac{500 \times 10^3}{0.85 \times 16 + 0.8}\right) = 34700\ \text{mm}^2/\text{m}$$

$$\text{Thickness of wall} = \left(\frac{34700}{1000}\right) = 34.7\ \text{mm}$$

Based on practical considerations, a minimum thickness of 100 mm is provided.

$$\text{Prestress required} = \frac{1}{0.85}\left[\left(\frac{500 \times 10^3}{100 \times 100}\right) - 0.8\right] = 5\ \text{N/mm}^2$$

$$\text{Prestressing force} = \left[\frac{(5 \times 100 \times 1000)}{(1000)}\right] = 500\ \text{kN}$$

$$\text{No. of 5 mm wires} = \left(\frac{500 \times 10^3}{19.6 \times 10^3}\right) = 26$$

$$\text{Pitch of wires} = \left(\frac{1000}{26}\right) = 38.5\ \text{mm}$$

$$\text{Ultimate tensile force} = \left[\frac{(26 \times 19.6 \times 0.87 \times 1700)}{(1000)}\right] = 754 \text{ kN}$$

Required ultimate tensile force = $(2 \times 500) = 1000$ kN

$\therefore$ Additional tensile force required = $(1000 - 754) = 264$ kN

$$\text{Area of mild steel reinforcement} = \left[\frac{246 \times 10^3}{0.87 \times 280}\right] = 1010 \text{ mm}^2$$

Provide 6 mm bars on each face at a spacing of 54 mm.

$$\text{Cracking load} = \left[\frac{100 \times 1000(0.85 \times 5 + 2.5)}{(1000)}\right] = 675 \text{ kN}$$

$$\text{Load factor against cracking} = \left(\frac{675}{500}\right) = 1.35$$

12.3 Design of Sections for Compression and Bending

12.3.1 General Features

Prestressing is not beneficial for members under axial compression. However, most compression members, such as long columns and piles, are subjected to bending moments and axial forces due to handling. In some members, such as portal frames and masts, the sections are subjected to compression and bending. Even in axially loaded columns, the external loads are rarely concentric. As a result, the concrete section is subjected to tension at the side farthest from the line of action of the longitudinal load. The cracking that develops can be prevented by prestress in the columns.

The design recommendations of the prestressed Concrete Institute[7] for short and long columns is based on the research reports of Zia and Moriadith[8], Lin and Lakhwara[9], Aroni[10], and various other investigators. The load-moment interaction diagrams are more or less similar to those of the reinforced concrete columns except that precompression exists in prestressed concrete columns. The analysis of prestressed concrete columns is also based on the same assumptions adopted regarding stresses and strains in concrete for reinforced concrete columns.

12.3.2 Load-Moment Interaction Curves for Prestressed Concrete Short Columns

The primary modes of failure observed in short prestressed concrete columns are similar to those of the reinforced concrete columns as outlined under the following four categories:

Compression Failure (Concentric Loading) This type of failure mode develops under concentric loads. The section is considered to have failed when the concrete strain ε_0 reaches a value of 0.002.

Compression Failure (Small Eccentricity) The failure mode develops when the extreme fibre strain ε_{cu} in concrete reaches a value of 0.003, while the strain in the prestressing steel at the far side is below the yield strain. The eccentricity e of the axial load is smaller than the balanced eccentricity e_b.

Balanced Failure (Balanced Eccentricity) Balanced failure develops when there is simultaneous tension yielding of prestressing steel and crushing of concrete. The eccentricity of the axial load is defined as balanced eccentricity e_b.

Initial Tension Failure (Large Eccentricity) In this failure mode, the steel yields prior to the crushing of concrete. The eccentricity e is larger than the balanced eccentricity e_b.

The general load—moment interaction diagram associated with the various load eccentricities controlling the compression, balanced and tension modes of failure is shown in Fig. 12.5 based on the work of Nawy[11].

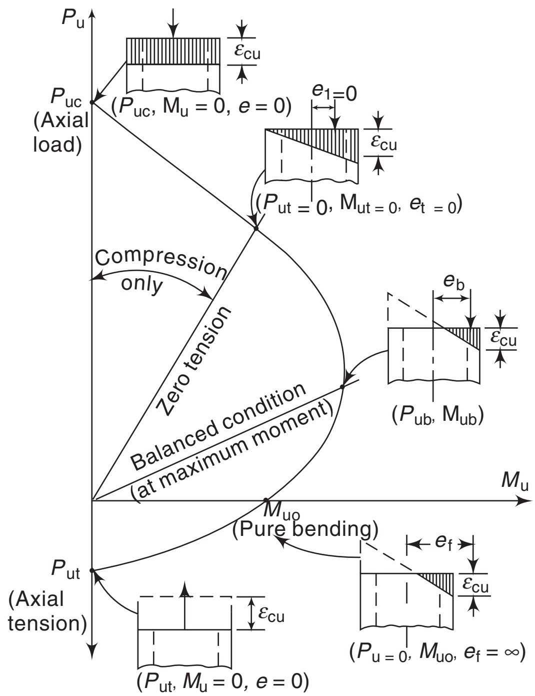

Fig. 12.5 *Load–moment interaction diagrams*

The following notations are used in the development of load-moment interaction curves for prestressed concrete columns with uniform prestress.

P = effective prestress in concrete after all losses
A_{ps} = area of prestressing steel in the tension zone
A'_{ps} = area of prestressing steel in the compression zone
d = effective depth
E_s = modulus of elasticity of prestressing steel
e = eccentricity of the normal load
P_u = ultimate axial load
M_u = ultimate moment
ε_{pe} = effective strain in tendons after all losses
ε_{ce} = strain in concrete due to creep, shrinkage and relaxation losses
f'_c = cylinder compressive strength of concrete
a = equivalent rectangular stress block depth
x = depth of the neutral axis
C = compressive force in concrete

T = tensile force in steel
f_{ps} = tensile stress in steel in the tension zone
f'_{ps} = tensile stress in steel in the compression zone
f_{pe} = effective stress in tendons

Referring to Fig. 12.6,

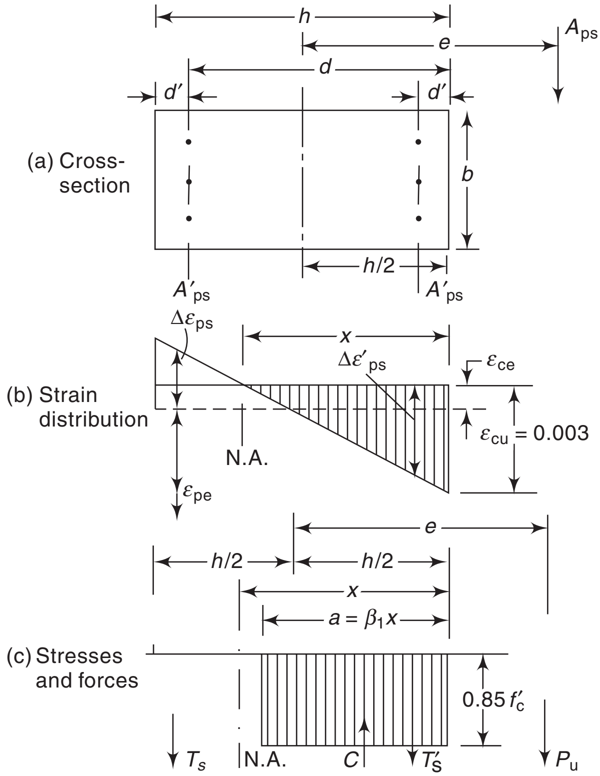

Fig. 12.6 *Stress–strain and forces in typical eccentrically loaded short column*

$$C = 0.85 f'_c ba$$

$$T_s = A_{ps} f_{ps} \qquad T'_s = A'_{ps} f'_{ps}$$

Force equilibrium yields the relations,

$$P_u = C - T_s - T'_s \tag{12.25}$$

$$\varepsilon_{pe} = \left(\frac{f_{pe}}{E_s}\right) = \left[\frac{P}{(A_{ps} + A'_{ps})E_s}\right] \tag{12.26}$$

The change in strain in the prestressing steel in the compression and tension zones, as the compression member passes from the effective prestressing stage to the ultimate load, is expressed as

$$\Delta\varepsilon'_{ps} = \varepsilon_{cu}\left(\frac{x - d'}{x}\right) - \varepsilon_{ce} \tag{12.27}$$

and

$$\Delta\varepsilon_{ps} = \varepsilon_{cu}\left(\frac{d - x}{x}\right) + \varepsilon_{ce} \tag{12.28}$$

$$T_s = A_{ps}f_{ps} = A_{ps}E_s\,(\varepsilon_{pe} + \Delta\varepsilon_{ps})$$

$$= A_{ps}E_s\left[\varepsilon_{pe} + \varepsilon_{cu}\left(\frac{d-x}{x}\right) + \varepsilon_{ce}\right] \tag{12.29}$$

Similarly, $$T'_s = A'_{ps}f'_{ps} = A'_{ps}E_s(\varepsilon_{pe} - \Delta\varepsilon'_{ps})$$

$$= A'_{ps}E_s\left[\varepsilon_{pe} - \varepsilon_{cu}\left(\frac{x-d'}{x}\right) + \varepsilon_{ce}\right] \tag{12.30}$$

Moment equilibrium about the centroid of the section results in the relation,

$$M_u = P_u e = C\left(\frac{h}{2} - \frac{a}{2}\right) - T'_s\left(\frac{h}{2} - d'\right) + T_s\left(d - \frac{h}{2}\right) \tag{12.31}$$

The above series of equations are helpful in constructing load-moment interaction diagrams for any section or in non-dimensional series of load-moment interaction diagrams for various concrete strength levels. The design strength are evaluated as,

Design $P_{ud} = \phi P_u$

Design $M_{ud} = \phi M_u$

where ϕ = strength reduction factor which varies from a minimum of 0.70 to a maximum of 0.90 as shown in Fig. 12.7. The value is influenced by the type of failure mode, compressive strength of concrete and the gross area of concrete section (A_g).

Example 12.12 A prestressed concrete compression member with square cross-section and a side of 350 mm is reinforced with eight 12.7 mm-diameter seven-wire stress relieved strands distributed equally on the opposite faces as shown in Fig. 12.8. The effective prestress after all losses is 1000 N/mm^2. Construct the load—moment interaction diagrams with appropriate strength reduction factors. Consider strands that are fully developed throughout the length of the member. Assume the following data:

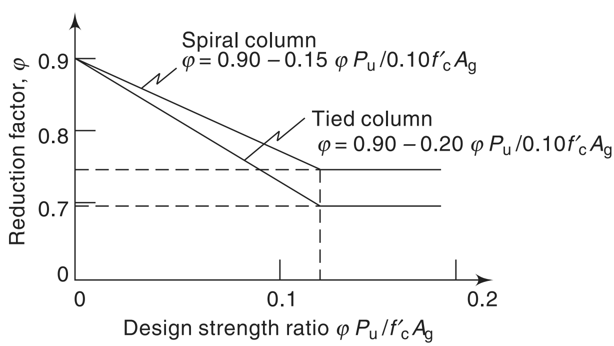

Fig. 12.7 *Variation of reduction factor ϕ*

Solution.

$f_{ps} = 1650$ N/mm^2

$f'_c = 50$ N/mm^2

$$E_{ps} = 200 \text{ kN/mm}^2$$
$$\varepsilon_{cu} = 0.003$$
$$\varepsilon_{ce} = 0.0005$$
$$\varepsilon_{py} = \text{yield strain of strand} = 0.012$$
$$d = \text{effective depth} = 300 \text{ mm}$$
$$b = 350 \text{ mm}$$
$$d' = 50 \text{ mm}$$

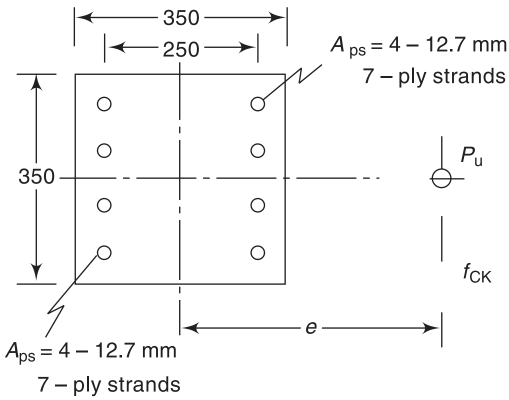

Fig. 12.8 *Cross-section of column*

$$h = 350 \text{ mm} \qquad A_{ps} = (4 \times 98.7) = 395 \text{ mm}^2$$
$$\varepsilon_{pe} = 0.0052 \qquad A'_{ps} = (4 \times 98.7) = 395 \text{ mm}^2$$

Case 1

Axial compression, $M_u = 0$ $x = \infty$

Depth of compressive stress block, $a = 350$ mm

Effective depth = 300 mm

Compressive force = $C = 0.85 f'_c ba$

$$= \left[\frac{(0.85 \times 50 \times 350 \times 350)}{1000}\right] = 5206 \text{ kN}$$

$$T'_s = A'_{ps} E_{ps}\left[\varepsilon_{pe} - \varepsilon_{cu}\left(\frac{x - d'}{x}\right) + \varepsilon_{ce}\right]$$

$$= (395 \times 200)\left[0.0052 - 0.003\left(\frac{\infty - 50}{\infty}\right) + 0.0005\right] = 213 \text{ kN}$$

$$T_s = A_{ps} E_{ps}\left[\varepsilon_{pe} + \varepsilon_{cu}\left(\frac{d - x}{x}\right) + \varepsilon_{ce}\right]$$

$$= (395 \times 200)\left[0.0052 + 0.003\left(\frac{300 - \infty}{\infty}\right) + 0.0005\right] = 213 \text{ kN}$$

$$P_u = C - T'_s - T_s = [5206 - 213 - 213] = 4780 \text{ kN}$$

$$M_u = C\left(\frac{h}{2}-\frac{a}{2}\right) - T_s'\left(\frac{h}{2}-d'\right) + T_s\left(d-\frac{h}{2}\right)$$

$$= 5206\left(\frac{350}{2}-\frac{350}{2}\right) - 213\left(\frac{350}{2}-50\right) + 213\left(300-\frac{350}{2}\right) = 0$$

$$\therefore \quad \text{Eccentricity,} \quad e_1 = \left(\frac{M_u}{P_u}\right) = 0$$

Case 2: Neutral axis outside the section

$$x = 400 \text{ mm}$$

$$a = \beta_1 x = (0.75 \times 400) = 300 \text{ mm}$$

$$C = \left[\frac{(0.85 \times 50 \times 350 \times 300)}{1000}\right] = 4462 \text{ kN}$$

$$T_s' = 395 \times 200 \left[0.0052 - 0.003\left(\frac{400-50}{400}\right) + 0.0005\right] = 245 \text{ kN}$$

$$T_s = 395 \times 200 \left[0.0052 - 0.003\left(\frac{400-300}{400}\right) + 0.0005\right] = 391 \text{ kN}$$

$$P_u = C - T_s' - T_s = (4462 - 245 - 391) = 3826 \text{ kN}$$

$$M_u = 4462\left(\frac{350}{2}-\frac{300}{2}\right) - 245\left(\frac{350}{2}-50\right) + 391\left(300-\frac{350}{2}\right)$$

$$= 129800 \text{ kN mm}$$

$$\therefore \quad e_2 = \left(\frac{M_u}{P_u}\right) = \left(\frac{129800}{3826}\right) = 34 \text{ mm}$$

Case 3: Zero tension at the tension face and x = 350 mm

$$\beta_1 = [0.85 - (f_c' - 30)0.008] = \{0.85 - (50-30)0.008\} = 0.70$$

$$a = \beta_1 x = (0.7 \times 350) = 245 \text{ mm}$$

$$C = \left[\frac{(0.85 \times 50 \times 350 \times 245)}{1000}\right] = 3644 \text{ kN}$$

$$T_s' = 395 \times 200 \left[0.0052 - 0.003\left(\frac{350-50}{350}\right) + 0.0005\right] = 247 \text{ kN}$$

$$T_s = 395 \times 200 \left[0.0052 + 0.003\left(\frac{300-350}{350}\right) + 0.0005\right] = 416 \text{ kN}$$

$$P_u = C - T_s' - T_s$$

$$= (3644 - 247 - 416) = 2981 \text{ kN}$$

$$M_u = 3644\left(\frac{350}{2}-\frac{263}{2}\right) - 247\left(\frac{350}{2}-50\right) + 416\left(300-\frac{350}{2}\right)$$

$$= 179639 \text{ kN mm}$$

$$\therefore \quad e_3 = \left(\frac{M_u}{P_u}\right) = \left(\frac{179639}{2981}\right) = 60.2 \text{ mm}$$

Case 4: Balanced section: P_{ub}, M_{ub}, e_b Assuming the strain in the tensile strands to be equal to the incremental strain $\Delta\varepsilon_{py}$ beyond the service load level, trial value of $\Delta\varepsilon_{py} = 0.0014$. From Fig. 12.6,

$$\frac{x}{(d-x)} = \left(\frac{\varepsilon_{cu}}{\Delta\varepsilon_{py}}\right) = \left(\frac{0.003}{0.0014}\right)$$

$$\therefore \quad x = 205 \text{ mm}$$

$$a = (\beta_1 x) = (0.70 \times 205) = 144 \text{ mm}$$

$$C = \frac{(0.85 \times 50 \times 350 \times 144)}{1000} = 2142 \text{ kN}$$

$$T'_s = 395 \times 200 \left[0.0052 - 0.003\left(\frac{205-50}{205}\right) + 0.0005\right] = 272 \text{ kN}$$

$$T_s = 395 \times 200 \left[0.0052 + 0.003\left(\frac{350-350}{205}\right) + 0.0005\right] = 560 \text{ kN}$$

$$P_{ub} = C - T'_s - T_s$$

$$= (2142 - 272 - 560) = 1310 \text{ kN}$$

$$M_{ub} = 2142\left(\frac{350}{2} - \frac{154}{2}\right) - 272\left(\frac{350}{2} - 50\right) + 560\left(300 - \frac{350}{2}\right)$$

$$= 256626 \text{ kN mm}$$

$$\therefore \quad e_4 = \left(\frac{M_{ub}}{P_{ub}}\right) = \left(\frac{256626}{1310}\right) = 196 \text{ mm}$$

Case 5: Pure bending: $P_u = 0$ Neglecting the effect of compression steel, A'_{ps}, we have

$$a = \left(\frac{A_{ps} f_{ps}}{0.85 f'_c b}\right) = \left(\frac{395 \times 1650}{0.85 \times 50 \times 350}\right) = 43.8 \text{ mm}$$

$$x = \left(\frac{a}{\beta_1}\right) = \left(\frac{43.8}{0.70}\right) = 62.5 \text{ mm}$$

$$M_u = A_{ps} f_{ps} \left(d - \frac{a}{2}\right)$$

$$= 395 \times 1650 \left(300 - \frac{43.8}{2}\right) = 181.2 \times 10^6 \text{ N mm} = 181.2 \text{ kN m}$$

$$\therefore \quad e_5 = \left(\frac{M_u}{P_u}\right) = \frac{181.2}{0} = \infty$$

Figure 12.9 shows the load-moment interaction diagrams.

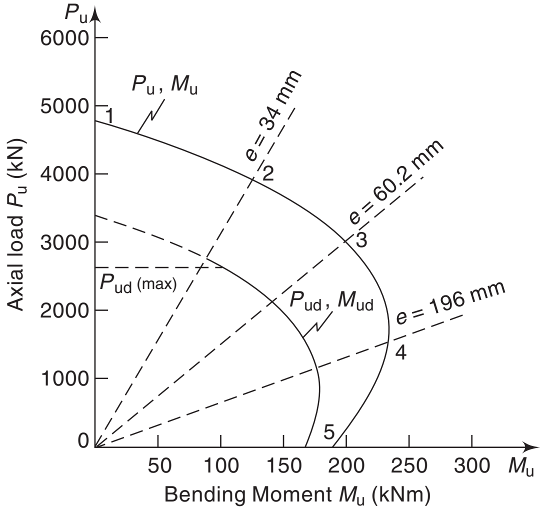

Fig. 12.9 *Load–moment interaction diagram*

The design ultimate load and moments are obtained by applying the appropriate strength reduction factor ϕ shown in Fig. 12.7. According to ACI 318M–2011[12], the maximum design axial load strength for tied prestressed columns should not exceed 0.80 ϕP_u, and for prestressed columns with a helical spiral binding, the value should not exceed 0.85 ϕP_u. Accordingly,

$$P_{ud} = \text{maximum design axial load} = 0.80\ \phi P_u$$
$$= (0.80 \times 0.7 \times 4780) = 2677 \text{ kN}$$

The maximum permissible design load-moment interaction curve is also shown in Fig. 12.9 and the corresponding values of the ordinates of points 1 to 5 are compiled in Table 12.1.

Table 12.1 *Load Moment interaction diagram coordinates*

Point	x (mm)	a (mm)	P_u (kN)	M_u (kN m)	ϕ	P_{ud} (kN)	M_{ud} (kN m)	e (mm)
1	∞	350	4780	0	0.7	3346	0	0
2	400	300	3826	129.8	0.7	2678	90.8	34.0
3	350	245	2981	179.6	0.7	2086	125.7	60.2
4	205	144	1310	256.6	0.7	917	179.6	196
5	62.5	43.8	0	181.2	0.9	0	163.0	∞

The design of reinforced concrete sections subjected to axial load and bending moment, by using interaction charts is well established.

In contrast to the design charts presented by the Prestressed Concrete Institute for the design of prestressed compression members subjected to compression and bending based on ultimate limit state, Bennett[13] proposed design charts with dimensionless parameters expressed in terms of the service loads and moments, and section properties and permissible stresses in concrete expressed as a fraction of the characteristic strength. These charts are useful in dimensioning columns of I-section with non-uniform prestress and allowing desirable tensile stresses in concrete as in Class 3-type members.

12.3.3 Design of Slender (Long) Prestressed Columns

When the slenderness ratio exceeds the limits for short columns, the compression member will buckle and fail due to instability before reaching the limit state of material failure. The ultimate strain in the compression face of concrete at buckling load will be less than 0.003. The load-moment interaction diagram for a slender column is shown in Fig. 12.10. The buckling effect produces an additional moment of $P_{ud}\,\Delta$, which reduces the load carrying capacity of the column from point B to C in the interaction diagram.

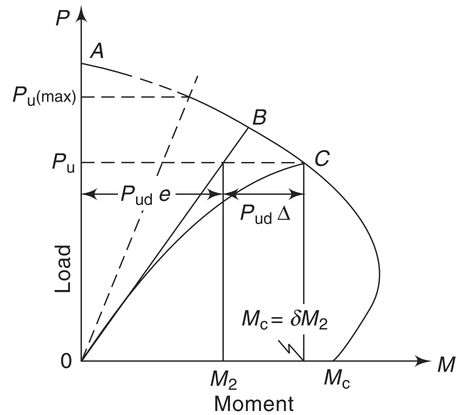

Fig. 12.10 *Load–moment interaction diagram*

The total moment at C is $P_{ud}e + P_{ud}\,\Delta$ and the column can be designed for the larger or magnified moment M_c as a nonslender column. The ratio M_c/M_2 is termed as the magnification factor δ. According to the ACI code, the stability analysis is not required for the following lower limit values of the slenderness ratio which is given by

$$\left(\frac{kL_u}{r}\right) < 34 - 12\left(\frac{M_1}{M_2}\right) \text{ for braced frames} \tag{12.32}$$

$$\left(\frac{kL_u}{r}\right) < 22, \text{ for unbraced frames} \tag{12.33}$$

where L_u = length of the member between the end supports

k = column length factor having the following values depending upon the end conditions:

(a) Both column ends pinned (no lateral motion), $k = 1.0$
(b) Both column ends fixed, $k = 0.5$
(c) One end fixed and other free, $k = 2.0$
(d) Both column ends fixed, lateral motion exists, $k = 1.0$

In a structural frame, the actual end restraint generally lies somewhere between the hinged and fixed conditions. The actual value of k can be determined from the Jackson and Moreland alignment charts[14] for braced and unbraced frames. Alternatively, the following equations suggested in the ACI code commentary are useful in computing the value of k.

Braced Compression Members An upper bound to the effective length factor may be taken as the smaller of the following expressions:

$$k = [0.7 + 0.05(\psi_A + \psi_B)] \leq 1.0 \tag{12.34}$$

and

$$k = (0.85 + 0.05\,\psi_{min}) \leq 1.0 \tag{12.35}$$

where ψ_A and ψ_B are the values of ψ at the two ends of the column and ψ_{min} is the smaller of the two values. ψ is the ratio of the stiffness of all compression members to the stiffness of all flexural members in a plane at one end of the column and defined as,

$$\psi = \frac{\Sigma EI/L_u\,(\text{columns})}{\Sigma EI/L_n\,(\text{beams})} \tag{12.36}$$

where
L_u = unsupported length of the column
L_n = clear span of the beams
r = radius of gyration

Unbraced Compression Member Restrained at Both Ends The effective length may be taken as follows:

For $\psi_m < 2$,
$$k = \left(\frac{20 - \psi_m}{20}\right)\sqrt{1 + \psi_m} \tag{12.37}$$

For $\psi_m \geq 2$,
$$k = 0.9\,\sqrt{1 + \psi_m} \tag{12.38}$$

where ψ_m is the average of the ψ values at the two ends of the compression member.

Unbraced Compression Members Hinged at One End The effective length factor may be taken as follows:

$$k = 2.0 + 0.3\psi \tag{12.39}$$

where ψ is the value at the restrained end.

The radius of gyration, $r = \sqrt{I_g/A_g}$, can be taken as 0.3 h for rectangular sections, where h is the column dimension perpendicular to the axis of bending. For circular sections, r is taken as 0.25 h.

Two methods have been recommended for the design of slender prestressed columns.

Moment magnification method In this method, which is applicable in cases where $(kL_u/r) < 100$, the design of the member is based on a magnified moment expressed as,

$$M_c = \delta M_2 = \delta_b M_{2b} + \delta_s M_{2s} \tag{12.40}$$

where δ_b, and δ_s are magnification factors for gravity loads and lateral loads, such as wind loads, applied to the predominantly gravity load moment M_{2b} and the larger end moment M_{2s}, respectively.

In the case of frames braced with shear walls against side sway, the entire moment acting on the column is considered to be M_{2b} and δ_s is assumed to be zero. Normally, if the lateral deflection of the frame is less than span $L_n/1500$, the frame is considered as a braced frame.

The moment magnification factors δ_b and δ_s are influenced by the slenderness of the member, stiffness of the entire frame, applied moment at the ends and the design cross-section. They are evaluated using the expressions,

$$\delta_b = \left[\frac{C_m}{1 - P_{ud}/\phi P_c}\right] \geq 1 \tag{12.41}$$

and

$$\delta_s = \left[\frac{1}{1 - \Sigma P_{ud}/\phi \Sigma P_c}\right] \geq 1 \tag{12.42}$$

where P_c = Euler buckling load = $\pi^2 EI/(kL_u)^2$

kL_u = effective length (between points of inflection)

ΣP_{ud} ΣP_c = summations for all columns in a storey

L_u = unsupported length of a column

C_m = a factor relating the actual moment diagram to an equivalent uniform moment diagram for braced members subject to end loads only

EI = flexural rigidity of the section

The factor

$$C_m = 0.6 + 0.4\left(\frac{M_1}{M_2}\right) \geq 0.4 \tag{12.43}$$

where $M_1 \leq M_2$ and $(M_1/M_2) > 0$ if no point of inflection exists between the column ends (single curvature). For other conditions, $C_m = 1.0$. When the computed end eccentricities are less than $(15 + 0.03\,h)$ mm, one may use the computed end moment to evaluate M_1/M_2 in Eq. 12.43.

If computation shows that there is essentially no moment at the ends, the ratio of M_1/M_2 should be taken as equal to 1. The estimated value of the flexural rigidity EI must include the effects of cracking and creep under long-term loading. For all members,

$$EI = \left[\frac{(E_c I_g/5) + E_s I_s}{1 + \beta}\right] \tag{12.44}$$

For lightly reinforced members ($\rho \leq 3\%$), this may be simplified to

$$EI = \left(\frac{E_c I_g/2.5}{1 + \beta}\right) \tag{12.45}$$

where

$$\beta = \left(\frac{\text{Factored dead load moment}}{\text{Factored total moment}}\right) \leq 1$$

The salient steps to be followed in the design of slender columns using moment magnification method are as follows:

(a) Check for side sway and compute the magnification factors δ_b and δ_s if there is appreciable side sway. If the side sway is negligible, assume $\delta_s = 0$. Assume a suitable cross-section and calculate the eccentricity using the greater of the end moments and check for the minimum allowable eccentricity given by

$$\left(\frac{M_2}{P_u}\right) \geq (15 + 0.03h) \text{ mm}$$

Adopt the minimum value if the given eccentricity is less than the specified minimum.

(b) Compute ψ_A and ψ_B using Eq. 12.36, and k using Eqs 12.37 to 12.39. Calculate kL_u/r and determine whether the column is short or long. If the column is slender and kL_u/r is less than 100, compute the magnified moment M_c. Then, using the value obtained, calculate the equivalent eccentricity to be used if the column is to be designed as a short column. If kL_u/r is greater than 100, a second-order analysis considering the effect of deflections is required.

(c) The equivalent nonslender column is designed according to the method outlined in Section 12.3.2.

Second-order analysis In the case of slender columns with the parameter kL_u/r exceeding 100, a second-order analysis is required. In this method, the effect of deflection is taken into account and an appropriate reduced tangent modulus for the concrete is used. The design is made with the aid of computers by solving the set of simultaneous equations needed to determine the size of the slender column. In general, the majority of columns in concrete building frames rarely have the slenderness ratio kL_u/r greater than 100 and hence do not necessitate a second-order analysis.

Example 12.13 A square tied prestressed bonded unbraced column in a framed building is subjected to uniaxial bending.

Clear height of the column = 5 m

Factored design external load, $P_{ud} = 1200$ kN

Factored end moments are, $M_1 = 40$ kN m and $M_2 = 100$ kN m

$$f'_c = 40 \text{ N/mm}^2,\ E_c = 36 \text{ kN/mm}^2$$

The ratios of factored dead-load moments to total moments, $\beta = 0.4$. Ratio of stiffness of column to beams at the top (ψ_A) and bottom (ψ_B) of the column being 1 and 2, respectively. Adopting 12.7 mm diameter seven-ply stress-relieved strands with $f_{pu} = 1860$ N/mm^2 conforming to IS: 6006–1983, design the column section and the required number of strands, considering gravity loads only and assuming negligible lateral side sway due to wind.

Solution.

Check for side sway and minimum eccentricity Since the frame has no appreciable side sway, the entire moment M_2 is taken as M_{2b} and magnification factor $\sigma_s = 0$. By trial and adjustment, assume a column section 400 mm by 400 mm with four strands as shown in Fig. 12.11.

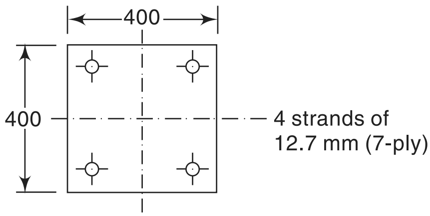

Fig. 12.11 *Cross selection of slender column*

$$\text{Actual eccentricity} = \left(\frac{M_{2b}}{P_{ud}}\right) = \left(\frac{100 \times 10^6}{1200 \times 10^3}\right) = 83.33 \text{ mm}$$

$$\text{Minimum allowable eccentricity} = (15 + 0.03\,h)$$
$$= (15 + 0.03 \times 400) = 27 \text{ mm} < 83.33 \text{ mm.}$$

Hence, adopt M_{2b} = 100 kN m as larger of the moments M_1 and M_2 on the column.

Computation of Euler buckling load For the unbraced compression member restrained at both ends,

$$\psi_m = \left(\frac{\psi_A + \psi_B}{2}\right) = \left(\frac{1+2}{2}\right) = 1.5$$

Since $\psi_m < 2$, the column-length factor is given by

$$k = \left(\frac{20 - \psi_m}{20}\right)\sqrt{1+\psi_m} = \left(\frac{20-1.5}{20}\right)\sqrt{1+1.5} = 1.462$$

$$\text{Slenderness ratio} = \left(\frac{kL_u}{r}\right) = \left(\frac{1.462 \times 5000}{0.3 \times 400}\right) = 60.9$$

Since 60.9 > 22 and < 100, adopt the moment magnification method.

$$I_g = \left(\frac{400^4}{12}\right) = (2133 \times 10^6) \text{ mm}^4$$

$$E_c = 36 \text{ kN/mm}^2$$

The flexural rigidity of the column is computed as

$$EI = \left[\frac{E_c I_g/2.5}{1+\beta}\right] = \left[\frac{(36000 \times 2133 \times 10^6)/2.5}{1+0.4}\right] = (21.9 \times 10^{12}) \text{ N mm}^2$$

$$(kL_u)^2 = (1.462 \times 5000)^2 = 53.43 \times 10^6 \text{ mm}^2$$

$$\text{Euler bucking load, } P_c = \left[\frac{\pi^2 EI}{(kL_u)^2}\right] = \left[\frac{\pi^2 \times 21.9 \times 10^{12}}{(53.43 \times 10^6)}\right]$$
$$= (4050 \times 10^3) \text{ N} = 4050 \text{ kN.}$$

Moment magnification factor For unbraced column, $C_m = 1.0$

Assuming strength reduction factor $\phi = 0.7$

The moment magnification factor is given by

$$\delta_b = \frac{C_m}{\left(1 - \dfrac{P_{ud}}{\phi P_c}\right)} = \frac{1.0}{\left(1 - \dfrac{1200}{0.7 \times 4050}\right)} = 1.73$$

Required ultimate load and moments

Design moment = $M_c = M_{ud} = \delta_b M_{2b} = (1.73 \times 100) = 173$ kN m

Hence, the required ultimate load and moments are obtained as

$$P_u = \left(\frac{P_{ud}}{\phi}\right) = \left(\frac{1200}{0.7}\right) = 1714 \text{ kN}$$

$$M_u = \left(\frac{M_{ud}}{\phi}\right) = \left(\frac{173}{0.7}\right) = 247 \text{ kN m}$$

$$e = \left(\frac{M_u}{P_u}\right) = \left(\frac{247 \times 10^6}{1714 \times 10^3}\right) = 144 \text{ mm}$$

Design of section Referring to the load-moment interaction diagram shown in Fig. 12.12, which is based on the Prestressed Concrete Institute's Design Handbook[7], a square section, 400 mm by 400 mm, with four numbers of 12.7 mm-diameter stress relieved strands will safely resist the required ultimate load and moments.

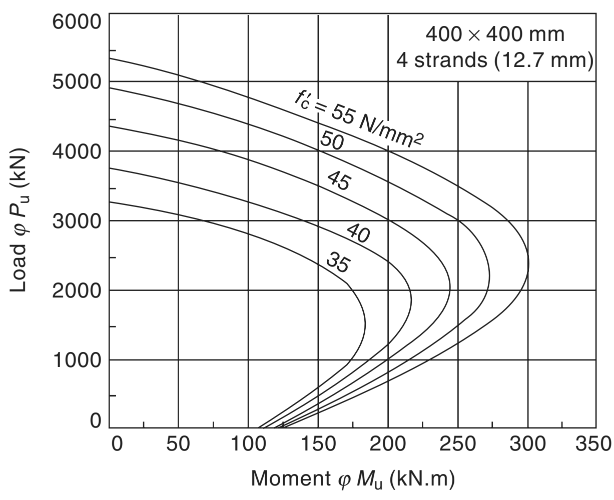

Fig. 12.12 *Load–moment interaction diagram for prestressed concrete column*

12.3.4 Design of Prestressed Concrete Compression Members in Biaxial Bending

The corner columns of framed buildings are subjected to biaxial bending with moments about the x and y axes as shown in Fig. 12.13. In such cases, the neutral axis is inclined at an angle θ to the x-axis. The angle θ depends on the interaction of the moments M_{ux} and M_{uy} and the magnitude of the load P_u.

A rigorous analysis of compression members with biaxial bending is possible using the strain compatibility method. In this method, a trial section with reinforcement is assumed and the equilibrium of force and moments examined for an assumed position of neutral axis. This type of procedure involves a number of trials to arrive at a suitable cross-section to resist the required design moments in the x and y directions.

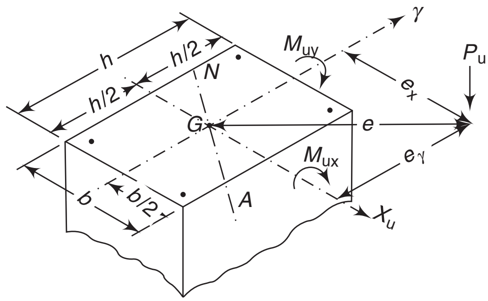

Fig. 12.13 *Biaxial loaded column*

Alternatively, the load contour method of analysis, detailed by Nawy[14] and generally termed *Bresler–Parme contour method,* is ideally suited for the design of biaxially loaded columns.

The design procedure is outlined under the following steps:

1. Given the ultimate moments M_{ux} and M_{uy}, select a suitable rectangular section having a ratio of h/b, approximated to M_{ux}/M_{uy}.
2. Determine the larger of the equivalent required uniaxial moments M_{ux} or M_{uy} by either of the following equations:

(a) For $(M_{uy}/M_{ux}) > \dfrac{b}{h}$

$$M_{uy1} = M_{uy} + M_{ux}\left(\frac{b}{h}\right)\frac{(1-\beta)}{\beta} \tag{12.46}$$

(b) For $(M_{uy}/M_{ux}) \leq b/h$,

$$M_{ux1} = M_{ux} + M_{uy}\left(\frac{h}{b}\right)\frac{(1-\beta)}{\beta} \tag{12.47}$$

where β is an interaction contour factor whose values are shown in Fig. 12.14. Generally, the value of β is assumed to be between 0.5 and 0.7.

The controlling required moment strength M_{ux1} or M_{uy1} for designing the section is the larger of the two values determined by the equations.

3. The assumed cross-section is provided with 1 to 2 per cent area of steel on each of the two faces parallel to the axis of bending of the larger equivalent moment.
4. Verify the ultimate load-carrying capacity P_u of the assumed column section. In the completed design, the same amount of longitudinal steel should be used on all the four faces.
5. Calculate the actual nominal moment capacity M_{uxn} for equivalent uniaxial bending about the x-axis. Its value should be at least equal to the required moment capacity M_{ux1}.
6. Compute the actual nominal moment capacity M_{uyn} for the equivalent uniaxial bending about the y-axis.

7. The moment value M_{uy} corresponding to the ratio M_{ux}/M_{uxn} and the trial value of β is read out from the contour plot shown in Fig. 12.14.
8. If M_{uy} is less than the required value, the procedure is repeated by a second trial until the two values of M_{uy} converge by changing either the section or the values of β.

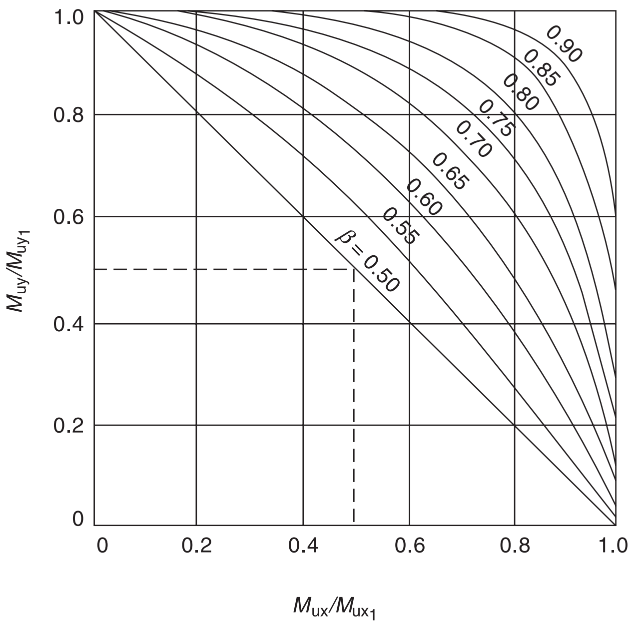

Fig. 12.14 *Contour β-factor for rectangular columns in biaxial bending*

Example 12.14 A square tied prestressed bonded corner column of a multistorey building frame is subjected to an ultimate load P_u = 2142 kN at an equal eccentricity of 70 mm along the *x*-and *y*-axis, respectively. f'_c = 40 N/mm^2. Design a suitable column section and reinforcements for the column subjected to biaxial bending moments.

Solution.

1. Data:

$$P_u = 2142 \text{ kN}$$
$$e_x = e_y = 70 \text{ mm}$$
$$\therefore \quad M_{ux} = P_u e_y = (2142 \times 0.07) = 150 \text{ kN m}$$
$$M_{uy} = P_u e_x = (2142 \times 0.07) = 150 \text{ kN m}$$

Since $(M_{ux}/M_{uy}) = (150/150) = 1$, select a square column section with $(b/h) = 1$.

2. The required equivalent uniaxial moment M_{ux1} and M_{uy1} are computed assuming $\beta = 0.5$

$$M_{ux1} = M_{ux} + M_{uy} = \left(\frac{h}{b}\right)\left(\frac{1-\beta}{\beta}\right) = 150 + 150\,(1)\left(\frac{1-0.5}{0.5}\right) = 300 \text{ kN m}$$

Similarly, M_{uy1} = 300 kN m.

3. Assume a trial cross-section of 400 mm by 400 mm with four 12.7 mm-diameter strands. Using the load-moment interaction diagram shown in Fig. 12.12, the maximum nominal ultimate load corresponding to the maximum nominal ultimate moment for the selected section corresponding to $f'_c = 40$ N/mm^2 is read out.

$$\phi P_u = (0.7 \times 2142) = 1500 \text{ kN}$$

$$\phi M_{uxn} = (0.7 \times 300) = 210 \text{ kN m}$$

$\therefore$ $$M_{uxn} = 300 \text{ kN m}$$

Similarly, $$M_{uyn} = 300 \text{ kN m}$$

$$\text{Ratio of } \left(\frac{M_{ux}}{M_{uxn}}\right) = \left(\frac{150}{300}\right) = 0.5$$

From Fig. 12.14 the value of (M_{uy}/M_{uyn}) corresponding to $(M_{ux}/M_{uxn}) = 0.5$ and the value of $\beta = 0.5$ is obtained as 0.5.

$\therefore$ $$M_{uy} = 0.5\,M_{uyn} = (0.5 \times 300) = 150 \text{ kN m}$$

The selected section can safely resist the biaxial moments.

12.3.5 Practical Design Recommendations

Prestressed concrete compression members should have a minimum average effective prestress of not less than 1.55 N/mm^2. According to ACI 318M–2011, a minimum non-prestressed reinforcement ratio of one per cent should be provided in compression members with an effective prestress of lower than 1.55 N/mm^2. The code also prescribes that the minimum diameter of the ties should not be less than 10 mm and that longitudinal bars spaced more than 150 mm apart should be supported by lateral ties.

Closely spaced spiral reinforcement increases the ultimate load capacity of the column due to confinement of concrete in the core. Spirals are particularly useful in increasing the ductility of the member and hence are preferred in high earthquake zones. The minimum spiral reinforcement ratio is given by

$$\rho_s = 0.45\left(\frac{A_g}{A_c} - 1\right)\left(\frac{f'_c}{f_y}\right) \tag{12.48}$$

where ρ_s = ratio of the volume of helical reinforcement to the volume of the core

A_g = gross area of section = $\left(\dfrac{\pi D^2}{4}\right)$

D = diameter of the column

A_c = core area = $\left(\dfrac{\pi D_c^2}{4}\right)$

D_c = core of the column measured to the outside diameter of the helix

f'_c = cylinder compressive strength of concrete

f_y = yield strength of spiral reinforcement

If S = pitch of spirals
a_s = cross-sectional area of spiral
d_s = diameter of spiral wire
then the pitch of spiral is computed as,

$$S = \frac{4a_s(D_c - d_s)}{D_c^2 \rho_s} \tag{12.49}$$

The pitch of spirals is limited to a range of 25 to 75 mm and the spiral should be well anchored by providing at least 1½ extra turns when splicing rather than welding of spirals is used.

12.4 Design of Prestressed Sections for Shear and Torsion

The effect of shear is to induce tensile stresses on diagonal planes and prestressing is beneficial since it reduces the magnitude of the principal tensile stress in concrete. Curved cables are advantageous in reducing the effective shear and, together with the horizontal compressive prestress, reduce the magnitude of the principal tension. The nature of the shear and principal stresses developed in sections subjected to transverse loads has been discussed in Section 8.1.

The various codes recommend empirical relations to estimate the ultimate shear resistance of the section by considering the flexure shear and web shear cracking modes. The design shear resistance should exceed the ultimate shear due to the transverse loads. If not, suitable transverse reinforcements are designed to resist the balance shear force.

The provisions for the design of shear reinforcements prescribed in the British, American and Indian Standard Codes have been dealt within Section 8.4. In members with thin webs, such as I- and T-sections, nominal shear reinforcements have to be provided to prevent cracking due to variations in temperature.

12.5 Design of Prestressed Members for Bond

Pretensioned or post-tensioned members with bonded tendons develop bond stresses between steel and concrete when the sections are subjected to transverse shear forces due to the rate of change of moment along the length of the beam. In the case of type 1 and 2 members, which are uncracked at service loads, the flexural bond stresses developed are computed by considering the complete section as outlined in Section 9.6.

In type 3 members with partial prestress where cracks of limited width are permitted under service loads, the bond stress in cracked sections is evaluated by using the conventional linear theory of cracked reinforced concrete sections. The Indian Standard Code IS: 1343 provides for the transmission length in terms of diameter and type of tendons.

The recommendations of the British, American, German and FIP regarding the bond and transmission lengths are detailed in Section 9.7. In the case of pretensioned members, the computation of the transmission length at the ends is of practical significance since the support positions are influenced by bond and transmission length.

12.6 Design of Prestressed Members for Bearing

In the case of post-tensioned members, where prestress is transferred to concrete by means of external anchorages, the bearing pressures developed behind the anchorages have to be investigated and suitably controlled to prevent crushing failure of the end-block zone.

According to the Indian Standard Code IS: 1343, the permissible unit-bearing pressure on the concrete after allowing for all losses is limited to

$$0.48 f_{ci} \sqrt{\frac{A_{br}}{A_{pun}}} \quad \text{or} \quad 0.8 f_{ci} \tag{12.50}$$

whichever is smaller. In this expression,

f_{ci} = cube strength of concrete at transfer
A_{br} = bearing area
A_{pun} = punching area

The effective punching area is generally the contact area of the anchoring device and the bearing area is taken as the maximum area of that portion of the member which is geometrically similar and concentric to the effective punching area. The American practise[14] is to limit the bearing stress f_b due to the high-stress concentration under the anchorage bearing plates, both at the initial prestress and after losses. Thus,

At initial prestress, $$f_b = 0.8 f_{ci} \sqrt{\left(\frac{A_{br}}{A_{pun}}\right) - 0.2} \le 1.25 f_{ci} \tag{12.51}$$

After losses at service loads,

$$f_b = 0.6 f_{ci} \sqrt{\left(\frac{A_{br}}{A_{pun}}\right)} \le f_{ci} \tag{12.52}$$

Example 12.15 The end block of a post-tensioned girder is 200 mm wide and 600 mm deep. The girder is prestressed by a concentric cable carrying an effective force of 800 kN. The cable has to be anchored against the end block using an anchor plate at the centre of the girder. If the cube strength of concrete is at transfer is 30 N/mm^2 and the permissible shear stress in steel is 100 N/m^2, design the size and thickness of the steel anchor plate.

Solution.

Effective force in the cable = P = 800 kN

Assuming an anchor plate of size 100 mm by 100 mm,

Bearing area = $A_{br} = (200 \times 200) = 40000 \text{ mm}^2$

Punching area = $A_{pun} = (100 \times 100) = 10000 \text{ mm}^2$

Permissible shear stress in steel = 100 N/mm^2

$$\text{Actual bearing pressure} = f_b = \left[\frac{800 \times 10^3}{40000}\right] = 20 \text{ N/mm}^2$$

Maximum permissible bearing pressure = $0.48\, f_{ci}\sqrt{\dfrac{A_{br}}{A_{pun}}}$ or $0.8\, f_{ci}$ whichever is smaller

$$f_b = 0.48 \times 30 \times \sqrt{\frac{40000}{10000}} \text{ or } (0.8 \times 30) \text{ N/mm}^2 = 28.8 \text{ N/mm}^2 \quad \text{or} \quad 24 \text{ N/mm}^2$$

The actual bearing pressure of 20 N/mm^2 is less than the permissible bearing pressure. Punching circumference of the anchor plate = $(4 \times 100) = 400$ mm

If t = thickness of the steel anchor plate, we have the relation

$$(400 \times 100 \times t) = (800 \times 10^3)$$

$\therefore$ solving $t = 20$ mm

Hence, adopt an anchor plate of size 100 mm by 100 mm with a thickness of 20 mm.

References

1. Evans, RH and Bennett EW, *Prestressed Concrete,* Chapman and Hall, London, 1958, pp 115–118.
2. Magnel, G, *Prestressed Concrete,* Concrete Publications, London, 1948, pp 19–26.
3. Bennett, EW, "A graphical method for the design of prestressed beams", *Concrete and Constructional Engineering,* Vol. 53, November 1959, pp 399–403.
4. IS: 1343-2012 *Indian Standard Code of Practice for Prestressed Concrete*, (Second Revision), B.I.S. New Delhi, 2012, pp. 1–56.
5. Nawy, Edward G, *Prestressed Concrete* (A Fundamental Approach), Prentice-Hall, Englewood Cliffs, New Jersey, 1989, pp 499–509.
6. IS: 3370 (Part III)–1967, *Indian Standard Code of Practice for Concrete Structures for the Storage of Liquids,* Part III, Prestressed Concrete Structures; seventh reprint 1986, Indian Standards Institution, New Delhi, pp 3–11.
7. *Prestressed Concrete Institute (PCI) Design Handbook,* third edition, Prestressed Concrete Institute, Chicago, 1985.
8. Zia, P and FL Moriadith, "Ultimate load capacity of prestressed concrete columns," *Journal of the American Concrete Institute,* Vol. 63, 1986, pp 767–788.

9. Lin, TY and TR Lakhwara, "Ultimate strength of eccentrically loaded partially prestresed columns," *PCI Journal,* Vol. II, 1986, pp 37–49.
10. Aroni, S, "Slender prestressed concrete columns," *Journal of the Structural Division of ASCE.*, Vol. 94, ST4, April 1968, pp 875–904.
11. Nawy, EG, *Reinforced Concrete—A Fundamental Approach,* Englewood Cliffs, Prentice-Hall, New Jersey, 1985.
12. ACI: 318M–2011, *Building Code Requirements for Reinforced Concrete and Commentary,* American Concrete Institute, Farmington Hills, Michigan, 2011.
13. Bennett, EW, "The design of prestressed members subjected to axial force and bending," *Concrete and Constructional Engineering,* Vol. 61, August 1966, pp 267–274.
14. Nawy, EG, *Prestressed Concrete*—A Fundamental Approach, Prentice-Hall, Englewood Cliffs, New Jersey, 1989, pp 478–499 and pp 129–143.

Review Questions

12.1 What are the fundamental conditions for stresses at transfer and service loads in the design of prestressed concrete sections?

12.2 Explain the terms (a) minimum section modulus (b) maximum eccentricity (c) minimum prestressing force and (d) loss ratio.

12.3 Derive an expression for minimum section modulus in terms of dead and live load moments, loss ratio and range of stress.

12.4 Explain the significance of minimum prestressing force, corresponding maximum eccentricity in the design of prestressed concrete sections. Derive expressions for them from first principles.

12.5 Discuss briefly the limitation of prestress in members having long spans with relatively large dead load bending moments. How do you design the prestressing force in such members?

12.6 What are the advantages of prestressing in the design of concrete members subjected to axial tension? What are the load factors generally specified against cracking and collapse in such members?

12.7 What are load-moment interaction diagrams in columns? Explain with sketches the different types encountered in columns subjected to compression and bending.

12.8 Discuss briefly the design of slender prestressed concrete columns.

12.9 Briefly explain the design procedure you would recommend for columns subjected to biaxial bending moments.

12.10 Write a brief note on the design of prestressed concrete members for (a) shear and torsion (b) bond and (c) bearing. Mention the appropriate codal recommendations.

Exercises

12.1 A prestressed concrete beam of rectangular section 90 mm wide and 180 mm deep, is to be designed to support two imposed loads of 3.5 kN, each located at one-third points over a span of 3 m. If there is to be no tensile stress in the concrete at transfer and service loads, calculate the minimum prestressing force and the corresponding eccentricity. $D_c = 24$ kN/m^3. Loss, ratio = 0.8.

[Ans: P = 74.5 kN; e = 35.6 mm]

12.2 A prestressed concrete T-beam is to be designed to support an imposed load of 4.4 kN/m over an effective span of 5 m. The T-beam is made up of a flange 400 mm wide and 40 mm thick. The rib is 100 mm wide and 200 mm deep. The stress in the concrete must not exceed 15 N/mm^2 in compression and zero in tension at any stage. Check for the adequacy of the section provided, and calculate the minimum prestressing force necessary and the corresponding eccentricity. Assume 20 per cent loss of prestress.

[Ans: P = 181 kN: e = 78 mm]

12.3 A post-tensioned beam of span 15 m and overall depth 900 mm has uniform symmetrical cross-section of area 2×10^5 mm^2 and the second moment of area of 212×10^8 mm^4 units. The prestress is provided by a cable tensioned to a force of 1450 kN at transfer. If the beam is to support a uniformly distributed live load of 21 kN/m and the minimum load is that due to the self-weight of the beam, calculate the vertical limits within which the cable must lie along the beam length. The permissible compressive stresses at transfer and working load are 14 and 16.8 N/mm^2, respectively. The tensile stresses at transfer and working load are zero and 1. 75 N/mm^2, respectively. $D_c = 24$ kN/m^3. Loss of prestress = 20 per cent. **[Ans: At mid span: e_a = 312 mm; e_b = 249 mm;**

At support: e_a = 219 mm; e_b = 376 mm]

12.4 A prestressed I-section of minimum overall depth 300 mm is required to have an ultimate flexural strength of 86 kN m. Find (a) suitable minimum dimensions of the top flange, and (b) the total number of 5 mm wires required in the bottom flange. The cube strength of concrete is 60 N/mm^2 and the tensile strength of steel is 1600 N/mm^2. **[Ans: (a) 160 mm; (b) 13 numbers]**

12.5 Design the prestressing force required for the tie member of reinforced concrete truss. The service-load tension in the tie member is 360 kN and the thickness of the member is fixed as 150 mm. The permissible compressive stress in concrete at transfer is 15 N/mm^2 and tension is not permitted under service loads. The loss ratio is 0.8. High-tensile wires of 7 mm diameter, tensioned to a stress of 1000 N/mm^2 and having an $f_{Pu} = 1500$ N/mm^2 are available for use. The tensile strength of concrete is 2.5 N/mm^2. A load factor of 1.7 at the limit state of collapse and 1.2 against cracking is to be provided in the design.

[Ans: Section 150 mm by 200 mm; Prestressing force = 450 kN;

Number of 7 mm wires = 12]

12.6 A prestressed concrete compression member with a square cross-section of 400 mm a side is reinforced with four strands of 12.7 mm diameter at each corner with an effective cover of 50 mm. If $f_{ps} = 1650$ N/mm^2, $f_c = 40$ N/mm^2, f_{pe} = 1000 N/mm^2 and $E_{ps} = 200$ kN/mm^2, construct the load-moment interaction diagram and determine the maximum moment capacity of the section and the corresponding axial load. Assume suitable data regarding the strains in concrete and steel. **[Ans: P_u = 2000 kN, M_u = 220 kN m]**

12.7 A prestressed concrete column, 600 mm by 600 mm in section, is reinforced with eight strands of 12.7 mm diameter which are symmetrically placed at an effective cover of 50 mm. Given the cylinder compressive strength of concrete as 50 N/mm^2. The tensile strength of strands as 1650 N/mm^2, the effective stress in steel after all losses as 1000 N/mm^2, and the ultimate strain in concrete as 0.003, construct the load–moment interaction diagram and compute the following:

(a) The safe load and moment corresponding to the balanced condition, and

(b) The moment corresponding to the pure bending condition.

[Ans: (a) 500 kN and 870 kN m (b) 350 kN m]

12.8 A prestressed concrete beam having a symmetrical I-section is to be designed to support a live load of 15 kN/m over an effective span of 12 m. The I-section is made up of flanges 300 mm wide by 150 mm thick and the web is 120 mm thick and 450 mm deep. The permissible stress in concrete may be assumed as 14 N/mm^2 in compression and 1.4 N/mm^2 in tension. Loss of stress is 15 per cent. Determine the minimum prestressing force and the corresponding eccentricity.

[Ans: Prestressing force = 747 kN and Eccentricity = 299 mm]

Objective-type Questions

12.1 The minimum section modulus of a prestressed concrete section is influenced by

(a) the range of stress at top fibre

(b) the compressive stress at top fibre

(c) range of stress at bottom fibre

12.2 The minimum prestressing force is a function of

(a) range of stress at top fibre

(b) range of stress at bottom fibre

(c) prestress at top and bottom fibre

12.3 In the design of prestressed concrete sections, the number of fundamental stress conditions to be considered are

(a) two (b) four (c) three

12.4 The limiting zone for prestressing force in a PSC beam has a maximum range at

(a) centre of span (b) support section (c) at one-fourth span

12.5 The tie member of a prestressed concrete truss should be designed for

(a) compressive forces

(b) tensile forces

(c) combined tension and bending

12.6 Design of PSC columns subjected to axial loads and moments is simplified by

(a) load-deflection diagrams

(b) load-moment interaction diagrams

(c) stress-strain diagrams

12.7 Prestressed concrete beam sections of long span having dead-load moments larger than live-load moments should be designed by assuming the maximum possible

(a) prestressing force (b) eccentricity (c) compressive stress

12.8 Magnel's graphical solution is helpful in designing minimum prestressing force and the corresponding

(a) minimum eccentricity

(b) maximum eccentricity
(c) feasible eccentricity

12.9 In the case of prestressed sections designed for flexure and torsion, the section has to be designed for
(a) flexure only
(b) shear due to torsion
(c) equivalent bending moment

12.10 The maximum permissible bearing stress in end block zones of post-tensioned prestressed concrete members is inversely proportional to
(a) bearing area
(b) punching area
(c) cube strength of concrete

Answers to Objective-type Questions

12.1 (c)	12.2 (c)	12.3 (b)	12.4 (b)	12.5 (b)
12.6 (b)	12.7 (b)	12.8 (b)	12.9 (c)	12.10 (b)

13 Design of Pretensioned and Post-tensioned Flexural Members

13.1 Dimensioning of Flexural Members

In dimensioning prestressed concrete flexural members, the effective depth and breadth of the section at the compression face are determined solely on the basis of the ultimate flexural strength requirements. If the section is of T- or unsymmetrical I-shape, the general relation between the ultimate moment, cube strength and dimensional parameters of the section for the rectangular stress block assumed in the British code BS EN: 1992–1–1[1] is given by the following expression:

$$M_{ud} = 0.405 f_{cu} b_w \times (d - 0.45x) + 0.45 f_{cu}(b - b_w) h_f (d - 0.5 h_f)$$

Recasting the expression, we have

$$M_{ud} = f_{cu} b d^2 \left[\left(\frac{b_w}{b}\right)\left(\frac{x}{d}\right)\left(0.405 - 0.182\frac{x}{d}\right) + \left(1 - \frac{b_w}{b}\right)\left(\frac{h_f}{d}\right) \times \left(0.45 - 0.225\frac{h_f}{d}\right)\right]$$

If the depth of the stress block is limited to 0.5 d, then

$$M_{ud} = f_{cu} b d^2 \left[0.157\left(\frac{b_w}{b}\right) + \left(1 - \frac{b_w}{b}\right)\left(\frac{h_f}{d}\right)\left(0.45 - 0.225\frac{h_f}{d}\right)\right]$$

This relation is useful in studying the influence of parameters h_f/d and b_w/b on the dimensionless parameter $M_{ud}/f_{cu}bd^2$. A chart showing the relationship between these parameters as suggested by Bennett[2] is shown in Fig. 13.1 and is found to be very useful for the preliminary dimensioning of prestressed sections.

In the case of unsymmetrical I girders, the range of values of h_f/d and b_w/b for economical designs is generally 0.15 to 0.25 and 0.2 to 0.3, respectively. However, the thickness of web, b_w, is designed based on the dual criteria of resisting the ultimate shear and housing the cables with adequate cover.

For the above range of values, the parameter, $M_{ud}/f_{cu}bd^2$, varies from 0.075 to 0.107 for the stress block of the British code. The corresponding values for the stress block proposed in the IS code ranges from 0.09 to 0.13. The breadth of the compression face may be suitably assumed either by considering the number of girders covering a given width of bridge deck of a suitable ratio of $b'd$ being in the range of 0.4 to 0.6.

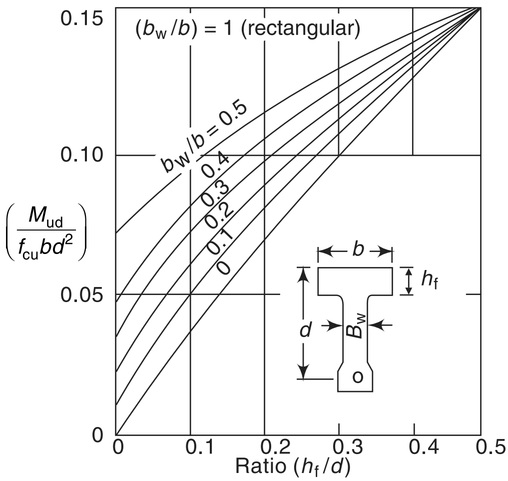

Fig. 13.1 *Chart for preliminary dimensioning of prestressed concrete sections*

The thickness of the web is generally determined on the basis of shear strength considerations discussed in Section 8.3.2. The condition that the principal tensile stress is not to exceed the tensile strength of concrete yields a criterion of the type

$$b_w > \left[\frac{V_u}{\left(\frac{I}{S}\right) f_t \left(1 + \frac{f_{cp}}{f_t}\right)^{1/2}}\right]$$

The value of the shear moment arm I/S varies between 0.67 and 0.85 h for I sections. The ratio, f_{cp}/f_t, generally varies between 2 and 3 for small-span girders with straight tendons. For long-span girders with curved tendons, the ratio, f_{cp}/f_t can be taken between 3 and 4 and the effective shear as 0.8 V_u, since the curved cables contribute to the ultimate shear resistance of the section.

Hence, the following expressions can be used for the preliminary estimation of the web thickness:

1. For small-span girders with straight tendons,

$$b_w = 0.85\left(\frac{V_u}{f_t h}\right) \tag{13.1}$$

2. For long-span girders with curved cables,

$$b_w = 0.60\left(\frac{V_u}{f_t h}\right) \tag{13.2}$$

In the case of small-span prestressed members, thinner webs of about 40 to 60 mm may be used. However, in the case of long span, heavily loaded girders where large, curved cables have to pass through the webs, a minimum thickness of 120 to 150 mm is mandatory to accommodate the cables with adequate cover.

13.2 Estimation of Self-Weight of Beams

To compute the total ultimate moment required for the design of prestressed beams, a knowledge of the self-weight of the beam is often necessary. Generally, the self-weight may be assumed on the basis of previous experience. The use of design chart containing dimensions of beams for various spans and applied loads as recommended by Magnel[3] is very useful in this regard. However, Bennett[2] recently proposed a simple formula for estimating the self-weight of the girder by considering several influencing parameters.

The relation between the self-weight (minimum load) and the ultimate load is given by the expression,

$$\left(\frac{w_{\text{min}}}{w_{\text{ud}}}\right) = \left[\frac{KD_{\text{c}}g\beta(L/h)L}{f_{\text{cu}}\,(d/h)^2}\right] \tag{13.3}$$

where w_{min} = self-weight or minimum load
L = effective span of the beam
w_{ud} = ultimate design load
D_{c} = density of the concrete member
g = acceleration due to gravity
β = moment coefficient (e.g., 0,125 for simply supported beam)
h = overall depth of girder
K = numerical constant

Typical maximum values of the ratio, L/h, are 25 for simply supported beams, 35 for fixed beams and 15 for cantilevers. The ratio, d/h, usually lies between 0.85 and 0.95 and where there is uncertainty, the lower value should be used.

The value of the numerical constant K is between 6 and 7.5 for rectangular sections and I-section girders of short spans, while it takes a value between 4 and 5 for flanged T- or I-section girders of long spans.

The ultimate design load includes the self-weight enhanced by partial factor of safety γ_{f1} and the live load enhanced by γ_{f2}. Hence, the following relation:

$$w_{\text{ud}} = (\gamma_1 q + \gamma_{f2} w_{\text{min}})$$

Rearranging,

$$w_{\text{ud}} = \left[\frac{\gamma_{f1} q}{1 - \gamma_{f2}(w_{\text{min}}/w_{\text{ud}})}\right] \tag{13.4}$$

The ratio of $(w_{\text{min}}/w_{\text{ud}})$ obtained from Eq. 13.3 is used in Eq. 13.4 to estimate the design ultimate load. The partial factors of safety to be used for dead and live loads at the limit state of collapse are outlined in Section 11.5.

13.3 Design of Pretensioned Beams

Example 13.1 Design a pretensioned roof purlin to suit the following data:

Effective span = 6 m

Applied load = 5 kN/m

Load factors

For dead load = 1.4

For live load = 1.6

Concrete cube strength, $f_{cu} = 50\ \text{N/mm}^2$
Cube strength at transfer, $f_{ci} = 30\ \text{N/mm}^2$
Tensile strength of concrete, $f_t = 1.7\ \text{N/mm}^2$
Modulus of elasticity of concrete, $E_c = 34\ \text{kN/mm}^2$
Loss ratio, $\eta = 0.8$

Permissible stresses

At transfer: Compressive stress, $f_{ct} = 15\ \text{N/mm}^2$

Tensile stress, $f_{tt} = -1\ \text{N/mm}^2$

At working load: Compressive stress, $f_{cw} = 17\ \text{N/mm}^2$

Tensile stress, $f_{tw} = 0$

7 mm high-tensile steel wires having an ultimate tensile strength, $f_{pu} = 1600\ \text{N/mm}^2$ are available for use.

Solution.

Design Calculations

1. Ultimate moments and shears

Using Eq. 13.3,

$$\left(\frac{w_{min}}{w_{ud}}\right) = \left[\frac{7.5 \times 2400 \times 9.81 \times 0.125 \times 25 \times 6}{50 \times 10^6 \times 0.85^2}\right] = 0.094$$

$$w_{ud} = \left[\frac{(1.6 \times 5)}{1 - 1.4(0.094)}\right] = 9.25\ \text{kN/m}$$

$$\therefore \quad w_{min} = (0.094)(9.25) = 0.86\ \text{kN/m}$$

$$M_u = (0.125 \times 9.25 \times 6^2) = 42\ \text{kN m}$$

$$V_u = (0.5 \times 9.25 \times 6) = 27.75\ \text{kN}$$

$$M_g = (0.125 \times 0.86 \times 6^2) = 3.86\ \text{kN m}$$

$$M_q = (0.125 \times 5 \times 6^2) = 22.50\ \text{kN m}$$

2. Cross-sectional dimensions

For flanged sections, referring to Fig. 13.1,

$$M_u = 0.10\, f_{cu} b d^2 \text{ and if } b = 0.5\, d$$

$$\therefore \quad d = \left(\frac{42 \times 10^6 \times 2}{0.10 \times 50}\right)^{1/3} = 270\ \text{mm}$$

$$\frac{d}{h} = 0.85$$

$$\therefore \quad h = 315\ \text{mm}$$

Adopt effective depth, $d = 275$ mm
and overall depth, $h = 320$ mm
Width of flange = 160 mm
Thickness of flange = $(0.2 \times 275) = 55$ mm
Since sloping flanges are used, increase the flange thickness by 20 per cent:
$\therefore$ Average thickness of flange = 70 mm

$$\text{Approximate thickness of web} = \left(\frac{0.85\,V_u}{f_t h}\right) = \left(\frac{0.85 \times 27.75 \times 10^3}{1.7 \times 320}\right) = 43 \text{ mm}$$

Adopt thickness of web = 50 mm
The symmetrical I-section is shown in Fig. 13.2. The properties of the section are,

$$\text{Area,} \quad A = 31400 \text{ mm}^2$$
$$I = 3700 \times 10^5 \text{ mm}^4$$
$$Z_{inf} = Z_{sup} = Z = (230 \times 10^4) \text{ mm}^3$$

Self-weight, g = 0.76 kN/m, which is less than the assumed value of 0.86 kN/m.

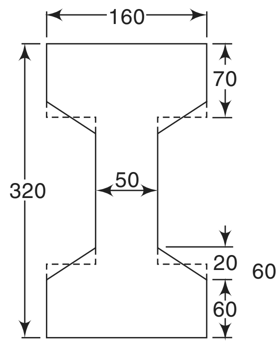

Fig. 13.2 *Symmetrical I-section*

3. Minimum section modulus

$$\text{Range of stress,} \quad f_{br} = (\eta f_{ct} - f_{cw}) = (0.8 \times 15 - 0) = 12 \text{ N/mm}^2$$

$$f_{tr} = (f_{cw} - \eta f_u) = [17 - 0.8 \times (-1)] = 17.8 \text{ N/mm}^2$$

Minimum section modulus is given by

$$Z_b \geq \left[\frac{M_q + (1-\eta)M_g}{f_{br}}\right] \geq \left[\frac{(22.50 \times 10^6) + (1 - 0.8)3.86 \times 10^6}{12}\right]$$
$$\geq (182 \times 10^4) \text{ mm}^3$$

The I-section selected satisfies the requirements regarding the self-weight moment and section modulus.

4. Prestressing force and eccentricity

$$P = \left[\frac{A(f_{inf}Z_b + f_{sup}Z_t)}{Z_t + Z_b}\right]$$

$$f_{inf} = \left[\left(\frac{f_{tw}}{\eta}\right) + \frac{(M_q + M_g)}{\eta Z_b}\right] = \left[(0) + \frac{(26.36 \times 10^6)}{(0.8 \times 230 \times 10^4)}\right] = 14.3 \text{ N/mm}^2$$

$$f_{sup} = \left(f_u - \frac{M_g}{Z_t}\right) = \left[-1 - \frac{(3.86 \times 10^6)}{(230 \times 10^4)}\right] = -2.68 \text{ N/mm}^2$$

$$\therefore \quad P = \left[\frac{31400 \times 230 \times 10^4 (14.3 - 2.68)}{2 \times 230 \times 10^4}\right] = 182000 \text{ N} = 182 \text{ kN}$$

The number of 7 mm wires initially stressed to 1200 N/mm^2 is given by

$$= [(182000)/(38.5 \times 1200)] = 3.95$$

Four high-tensile wires of 7 mm are sufficient.

$$\text{Eccentricity, } e = \left[\frac{Z_t Z_b (f_{inf} - f_{sup})}{A(f_{sup} Z_t + f_{inf} Z_b)}\right] = \left[\frac{230 \times 10^4 (14.3 + 2.68)}{31400(14.3 - 2.68)}\right] = 105 \text{ mm}$$

5. Check for ultimate flexural strength

$$A_{ps} = (38.5 \times 4) = 154 \text{ mm}^2$$

$$f_{pu} = 1600 \text{ N/mm}^2 \qquad f_{cu} = 50 \text{ N/mm}^2$$

$$b = 160 \text{ mm} \qquad d = 265 \text{ mm}$$

$$\left(\frac{A_{ps} f_{pu}}{b d f_{cu}}\right) = \left(\frac{154 \times 1600}{160 \times 265 \times 50}\right) = 0.116$$

From Table 7.3, assuming $\left(\dfrac{f_{pe}}{f_{pu}}\right) = 0.5$,

the corresponding values of $\left(\dfrac{f_{pb}}{0.87 f_{pu}}\right) = 0.99$

$\therefore \quad f_{pb} = (0.99 \times 0.87 \times 1600) = 1378 \text{ N/mm}^2$

and $\quad \left(\dfrac{x}{d}\right) = 0.24$

$$x = (0.24 \times 265) = 63.6 \text{ mm}$$

$$\therefore \quad M_u = f_{pb} A_{ps} (d - 0.45\,x) = [1378 \times 154\,(265 - 0.45 \times 63.6)]$$

$$= (50 \times 10^6) \text{ N mm} = 50 \text{ kN m}$$

Separate untensioned reinforcement is not required, as the actual flexural strength exceeds the design ultimate moment of 42 kN m.

6. Check for ultimate shear strength

(a) *Section at support (uncracked in flexure)*

Ultimate shear, $V_u = 27.75$ kN

Effective prestress at centroid,

$$f_{cp} = \left(\frac{\eta P}{A}\right) = \left(\frac{0.8 \times 182000}{31400}\right) = 4.65 \text{ N/mm}^2$$

$$V_{cw} = 0.67\, b\, h\, (f_t^2 + 0.8 f_{cp} f_t)^{1/2}$$

$$= \left[0.67 \times 50 \times 320 \frac{(1.7^2 + 0.8 \times 4.65 \times 1.7)^{1/2}}{10^3}\right] = 33.2 \text{ kN}$$

$\therefore \quad V_{cw} > V_u.$

Hence, it is safe against shear failure.

(b) *Section cracked in flexure with maximum shear*

At any section distant x from end support,

$$f_{cp} = \left[\frac{0.8 \times 182 \times 10^3}{31400} + \frac{0.8 \times 182 \times 10^3 \times 105}{230 \times 10^4}\right] = 11.30 \text{ N/mm}^2$$

$$M_o = \left(\frac{0.8 f_{ep} I}{y_b}\right) = \left(\frac{0.8 \times 11.3 \times 3700 \times 10^5}{160 \times 10^6}\right) = 21 \text{ kN m}$$

$$\left(\frac{M_o}{M_{max}}\right) = \left(\frac{21}{42}\right) = 0.5$$

From Fig. 13.3, the position of the critical section is obtained as

$$\frac{x}{L} = 0.26$$

Hence, $x = (0.26 \times 6) = 1.56$ m from the left support

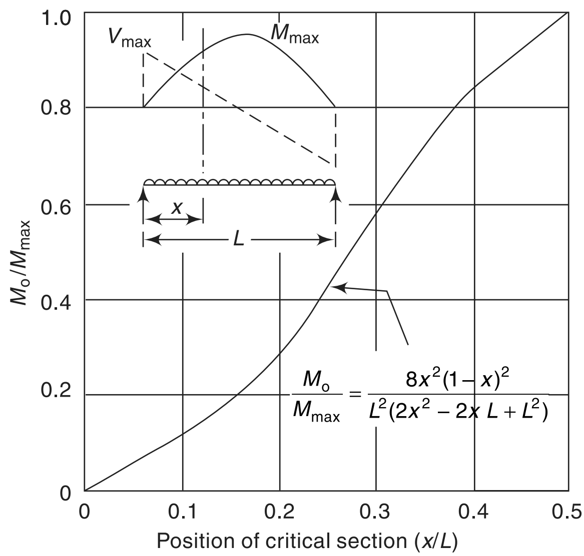

Fig. 13.3 *Position of critical shear section in a prestressed beam (Bate and Bennet)*

At this section

$$M = 0.5 \times 9.25 \times 1.56(6 - 1.56) = 32 \text{ kN m}$$

$$V = V_{max}\left[1 - 2\left(\frac{x}{L}\right)\right]$$

$$= 27.75\ (1 - 2 \times 1.56/6) = 13.4 \text{ kN}$$

$$f_{pe} = (0.8 \times 1200) = 960 \text{ N/mm}^2 \ngtr 0.6 f_{pu}$$

$$= \left(\frac{100 A_{ps}}{b_w d}\right) = \left(\frac{100 \times 154}{50 \times 265}\right)\ 1.17\%$$

From Table 8.1, the ultimate average shear resistance of concrete,

$$\tau_c = 0.70 \text{ N/mm}^2$$

$$\therefore \quad V_{cf} = \left[\left(1 - 0.55\frac{f_{pe}}{f_{pu}}\right)\tau_c b_w d + M_o\left(\frac{V}{M}\right)\right]$$

$$= \left[\frac{(1-0.55\times 960/1600)0.7\times 50\times 265+21\times(13.4/32)}{1000}\right] = 15.0 \text{ kN}$$

Since $V < 0.5\, V_{cf}$, the minimum shear reinforcement must be provided. Thus,

$$\frac{A_{sv}}{S_v} = \left(\frac{0.4 b_w}{0.87 f_{yv}}\right) = \left(\frac{0.4\times 50}{0.87\times 260}\right) = 0.09 \text{ mm}^2/\text{mm}$$

Provide 5 mm mild steel links at a spacing of 160 mm as shown in Fig. 13.4.

7. Check for limit state of deflection

The deflection due to the prestressing force

$$= \left(\frac{PeL^2}{8E_c I}\right)$$

$$= \left\{\frac{182\times 10^3\times 105\times 6^2\times 1000^2}{8\times 34\times 10^3\times 3700\times 10^5}\right\}$$

$= 6.8$ mm (upward)

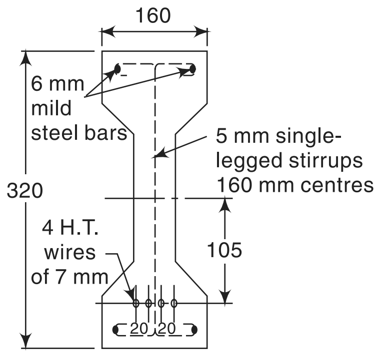

Fig. 13.4 *Arrangement of reinforcement in purlin*

Deflection due to self-weight,

$$g = \left(\frac{5\, g\, L^4}{384\, E_c I}\right)$$

$$= \left[\frac{5\times 0.76\times 6^4\times 1000^4}{384\times 34\times 10^3\times 3700\times 10^5}\right] = 1.02 \text{ mm}$$

Deflection due to live load, q

$$= \left(\frac{5\, q\, L^4}{384\, E_c I}\right) = \left[\frac{5\times 5\times 6^4\times 1000^4}{384\times 34\times 10^3\times 3700\times 10^5}\right] = 6.7 \text{ mm}$$

The effective or long-term modulus of elasticity is expressed as

$$E_{ce} = \left(\frac{E_c}{1+\phi}\right)$$

Where ϕ is the creep coefficient which depends upon the relative humidity, notional size of member and age at loading as given in Table 2.7.

Assuming that the sides and soffit are exposed to the atmosphere, the notional size is computed as

$$\left(\frac{2A_c}{u}\right) = \left(\frac{2\times 31400}{(2\times 320)+160}\right) = 78.5 \text{ mm}$$

In the present case, assuming a relative humidity of 50 per cent and age at loading as 28 days, interpolate the value of long-term creep coefficient from Table 2.7 as $\phi = 2.8$.

$\therefore \qquad E_c = (1+\phi)\, E_{ce} = 3.8\, E_{ce}$

Using long-term modulus for dead loads and short-term modulus for live loads, the resultant deflection is estimated to be

$$a_{max} = [(3.8 \times 1.02) + 6.7 - (0.8 \times 6.8)] = 5.13 \text{ mm}$$

The deflection is well within the maximum permissible limit of (span/250) = 24 mm.

13.4 Design of Post-tensioned Beams

Example 13.2 Design a post-tensioned roof girder to suit the following data:

Effective span = 30 m Live load = 9 kN/m
Dead load (excluding self-weight) = 2 kN/m
Load factors

For dead load = 1.4

For live load = 1.6

Cube strength of concrete, $f_{cu} = 50$ N/mm^2
Cube strength at transfer, $f_{ci} = 35$ N/mm^2
Tensile strength of concrete, $f_t = 1.7$ N/mm^2
Modulus of elasticity of concrete, $E_c = 34$ kN/mm^2
Loss ratio, $\eta = 0.85$
8 mm diameter high-tensile wires having a characteristic tensile strength f_{pu} = 1500 N/mm^2 are available for use. The modulus of elasticity of high tensile wires is 200 kN/mm^2. Design the beam as a class 1 structure according to British code provisions.

Solution.

Design Calculations

1. Ultimate Moments and Shears

Using Eq. 13.3,

$$\left(\frac{w_{min}}{w_{ud}}\right) = \left[\frac{5 \times 2400 \times 9.81 \times 0.125 \times 25 \times 30}{50 \times 10^6 \times 0.85^2}\right] = 0.31$$

Ultimate load, excluding the factored self-weight.

$$= [(1.4 \times 2) + (1.6 \times 9)] = 17.2 \text{ kN/m}$$

$$w_{ud} = \left[\frac{17.2}{(1 - 1.4 \times 0.31)}\right] = 30 \text{ kN/m}$$

$$w_{min} = (0.31 \times 30) = 9.3 \text{ kN/m}$$

Ultimate moment, $M_u = (0.125 \times 30 \times 30^2) = 3400$ kN m
Ultimate shear, $V_u = (0.5 \times 30 \times 30) = 450$ kN

2. Cross-sectional Dimensions

From the preliminary chart (refer to Fig. 13.1) for ratios $(h_f/d) = 0.23$ and $(b_w/b) = 0.25$ and assuming $b = 0.5\, d$,

$$M_u = (0.10\, f_{cu} b d^2)$$

$$\therefore \qquad d = \left(\frac{3400 \times 10^6}{0.10 \times 50 \times 0.5}\right)^{1/3} = 1130 \text{ mm}$$

$$\therefore \qquad h = \left(\frac{1130}{0.85}\right) = 1300$$

$$b = 600 \text{ mm } h_f = (0.2 \times 1130) = 250 \text{ mm}$$

Adopt an effective depth, $d = 1150$ mm

$$\text{Thickness of web} = b_w = \left(\frac{0.6\,V_u}{f_t h}\right) = \left(\frac{0.6 \times 450 \times 10^3}{1.7 \times 1300}\right) = 120 \text{ mm}$$

Since cables of diameter 50 mm have to pass through the web, the minimum thickness of web from practical considerations (with a clear cover of 50 mm) = $(50 + 2 \times 50) = 150$ mm.

The dimensions of the bottom flange should be such as to accommodate the cables as well as the anchorages at the ends of the members with suitable minimum cover requirements. The cross-section of the beam is shown in Fig. 13.5.

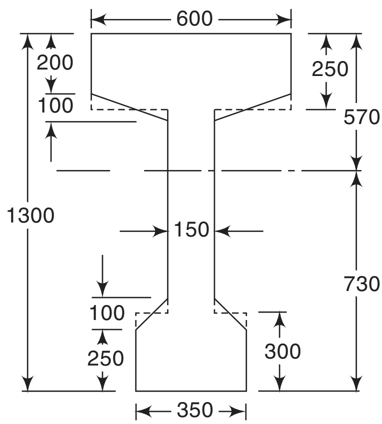

Fig. 13.5 *Cross-section of post-tensioned beam*

3. Properties of Section

Cross-sectional area, $A = 367{,}500$ mm^2
Distance of centroid from the top = 570 mm
Second moment of area, $I = (72490 \times 10^6)$ mm^4
Section modulus

$$Z_t = (127 \times 10^6) \text{ mm}^3$$

$$Z_b = (99 \times 10^6) \text{ mm}^3$$

4. Design Moments and Shear Forces

Actual self-weight of the girder = $(0.3675 \times 24) = 8.8$ kN/m
Minimum moment, $M_{min} = (0.125 \times 8.8 \times 30^2) = 990$ kN m
Design working load = $(2 + 8.8 + 9) = 19.8$ kN/m
Working moment, $M_d = (0.125 \times 19.8 \times 30^2) = 2230$ kN m

5. Permissible Stresses and Range of Stress

For $f_{cu} = 50$ N/mm^2 and $f_{ci} = 35$ N/mm^2, according to BS EN: 1992–1–1 recommendations,

$$f_{ct} = 0.5\, f_{ci} = 17.5 \text{ N/mm}^2$$

for class 1 structure, $f_{tt} = f_{tw} = 0$

$\therefore$ $f_{br} = (\eta f_{ct} - f_{tw}) = (0.85 \times 17.5) = 15$ N/mm^2

and $f_{cw} = 0.33 f_{cu} = (0.33 \times 50) = 16.5$ N/mm^2

$\therefore$ $f_{tr} = (f_{cw} - \eta f_{tt}) = 16.5$ N/mm^2

6. Check for Minimum Section Modulus

$$Z_b \geq \left[\frac{(M_d - \eta M_{min})}{f_{br}}\right] \geq \left[\frac{(2230 \times 10^6 - 0.85 \times 990 \times 10^6)}{15}\right] \geq (93 \times 10^6) \text{ mm}^3$$

Since $f_{tr} > f_{br}$, the section modulus, Z_t, will be less than this value. The section modulus of the designed unsymmetrical section exceeds the minimum value.

7. Check for Eccentricity and Prestressing Force

$$f_{sup} = \left(f_{tt} - \frac{M_{min}}{Z_t}\right) = \left[0 - \frac{(990 \times 10^6)}{(127 \times 10^6)}\right] = -7.8 \text{ N/mm}^2$$

$$f_{int} = \left(\frac{f_{tw}}{\eta}\right) + \left(\frac{M_d}{\eta Z_b}\right) = \left[0 + \frac{(2230 \times 10^6)}{(0.85 \times 99 \times 10^6)}\right] = 26.5 \text{ N/mm}^2$$

From Eq. 12.10,

$$e = \left[\frac{Z_t Z_b (f_{inf} - f_{sup})}{A(f_{inf} Z_b + f_{sup} Z_t)}\right] = \left[\frac{127 \times 99 \times 10^{12}(26.5 + 7.8)}{367500 \times 10^6 (26.5 \times 99 - 7.8 \times 127)}\right] = 730 \text{ mm}$$

The theoretical value of the eccentricity determined as above is impracticable since it falls at the bottom edge of the section. Hence, by providing suitable cover provisions for cables, the maximum possible eccentricity,

$$e = (1300 - 570 - 150) = 580 \text{ mm}$$

The prestressing force corresponding to this eccentricity is obtained from Eq. 12.14 as

$$P = \left[\frac{A f_{inf} Z_b}{Z_b + Ae}\right] = \left[\frac{(367500 \times 26.5 \times 99 \times 10^6)}{(99 \times 10^6) + (367500 \times 580)}\right]$$

$$= (3200 \times 10^3) \text{ N} = 3200 \text{ kN}$$

Using Freyssinet cables, 12 – 8 mm diameter and stressed to 1100 N/mm^2,

$$\text{Force in each cable} = \left[\frac{(12 \times 50 \times 1100)}{(1000)}\right]$$

$$= 660 \text{ kN}$$

$$\therefore \quad \text{Number of cables} = \left(\frac{3200}{660}\right) = 5$$

The cables are arranged at the central span section as detailed in Fig. 13.6.

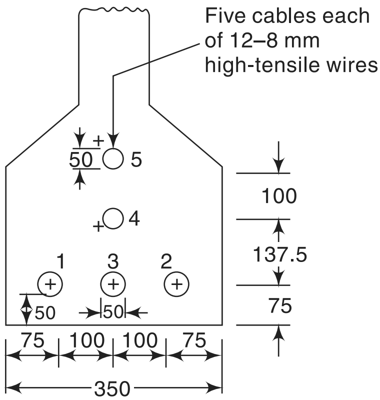

Fig. 13.6 *Arrangement of cables*

8. Permissible Tendon Zone

The permissible tendon zone at the centre of the span and the support section is computed using Eqs 12.16 and 12.18.

$$e \le \left[\left(\frac{Z_b f_{ct}}{P}\right) - \left(\frac{Z_b}{A}\right) + \left(\frac{M_{min}}{P}\right)\right]$$

$$\le \left[\left(\frac{99 \times 10^6 \times 17.5}{3200 \times 10^3}\right) - \left(\frac{99 \times 10^6}{367500}\right) + \left(\frac{990 \times 10^6}{3200 \times 10^3}\right)\right] \le 582 \text{ mm}$$

$$e \ge \left[\left(\frac{Z_b f_{tw}}{\eta P}\right) - \left(\frac{Z_b}{A}\right) + \left(\frac{M_d}{\eta P}\right)\right]$$

$$\ge \left[0 - \left(\frac{99 \times 10^6}{367500}\right) + \left(\frac{2230 \times 10^6}{0.85 \times 3200 \times 10^3}\right)\right] \ge 550 \text{ mm}$$

Similarly, at the support section,

$$-272 \text{ mm} \le e \le 272 \text{ mm}$$

The prestressing force should lie within the above prescribed limits. The cables are curved following a parabolic shape towards the support section. The profile of the resultant prestressing force along the span is shown in Fig. 13.7.

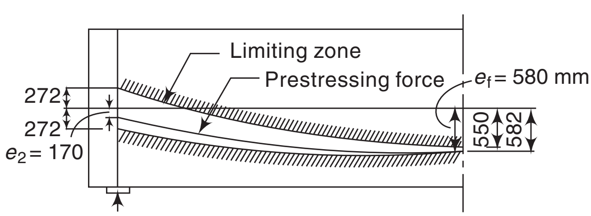

Fig. 13.7 *Limiting zone and prestressing force*

9. Check for Ultimate Flexural Strength

At the centre-of-span section,

$$A_{ps} = 3000 \text{ mm}^2 \qquad d = 1150 \text{ mm}$$
$$f_{cu} = 50 \text{ N/mm}^2 \qquad b_w = 150 \text{ mm}$$
$$f_{pu} = 1500 \text{ N/mm}^2 \qquad b = 600 \text{ mm}$$
$$h_t = 250 \text{ mm}$$

Design ultimate moment $M_{ud} = 3400$ kN m

According to BS EN: 1992–1–1

$$A_{ps} = (A_{pw} + A_{pf})$$

$$A_{pf} = 045 f_{cu}(b - b_w)\left(\frac{h_f}{f_{pu}}\right) = \left[(0.45 \times 50)(600 - 150)\left(\frac{250}{1500}\right)\right] = 1680 \text{ mm}^2$$

$$A_{pw} = (3000 - 1680) = 1320 \text{ mm}^2$$

$$\text{Ratio} = \left(\frac{f_{pu} A_{pw}}{f_{cu} b_w d}\right) = \left(\frac{1500 \times 1320}{50 \times 150 \times 1150}\right) = 0.23$$

From Tables 7.3, assuming $(f_{pe}/f_{pu}) = 0.5$, we get $\left(\dfrac{f_{pb}}{0.87 f_{pu}}\right) = 0.875$

$$\therefore \quad f_{pb} = (0.87 \times 1500 \times 0.875) = 1142 \text{ N/mm}^2$$

$$\left(\frac{x}{d}\right) = 0.44 \quad \text{or} \quad x = (0.44 \times 1150) = 506 \text{ mm}$$

$$\begin{aligned}
\therefore \quad M_{ud} &= f_{pb} A_{pw}(d - 0.45x) + 0.45 f_{cu}(b - b_w) h_f (d - 0.5 h_f) \\
&= [(1142 \times 1320)\,(1150 - 0.45 \times 506) \\
&\qquad + (0.45 \times 50)\,(600 - 150)\,250\,(1150 - 0.5 \times 250)] \\
&= (3935 \times 10^6) \text{ N mm} = 3935 \text{ kN m} > 3400 \text{ kN m}
\end{aligned}$$

The moment capacity is adequate. Hence, supplementary reinforcement is not necessary. However, longitudinal reinforcement of not less than 0.2 per cent of the cross-sectional area is to be provided to safeguard against shrinkage cracking. 16 mm diameter mild steel or deformed bars provided as shown in Fig. 13.8.

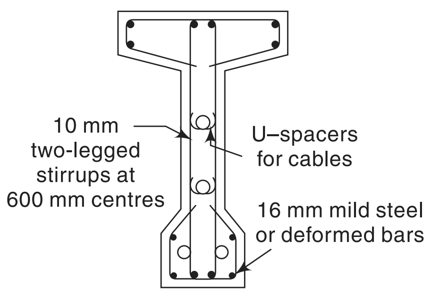

Fig. 13.8 *Arrangement of longitudinal and web reinforcements*

10. Check for Shear Strength

(a) *Section at support (uncracked in flexure)*

Required ultimate shear, $V_u = 450$ kN

$$f_{cp} = \left(\eta \frac{P}{A}\right) = \left[\frac{(0.85 \times 3200 \times 10^3)}{(367500)}\right] = 7.4 \text{ N/mm}^2$$

$$\text{Slope of cable,} \quad \theta = \left(4\frac{e}{L}\right) = \left[\frac{(4 \times 410)}{(30 \times 1000)}\right] = 0.0547$$

$$V_{cw} = [0.67\, bh\, (f_t^2 + 0.8 f_{cp} f_t)^{(1/2)} + \eta P \sin\theta]$$

$$= \left[0.67 \times 150 \times 1300 \frac{(1.7^2 + 0.8 \times 7.4 \times 1.7)^{1/2}}{(1000)} + (0.85 \times 3200 \times 0.0547)\right] = 617 \text{ kN}$$

This is greater than V_u. Hence, the support section is safe against shear failure.

(b) *Span section cracked in flexure* ($M = M_o$)

$$f_{ep} = \left(\frac{0.85 \times 3200 \times 10^3}{367500}\right) + \left(\frac{0.85 \times 3200 \times 10^3 \times 580}{99 \times 10^6}\right) = 23.4 \text{ N/mm}^2$$

$$M_o = (0.8 f_{ep} Z_b) = \left[0.8 \times 23.4 \times \left(\frac{99 \times 10^6}{1000}\right)\right] = 1850 \text{ kN m}$$

$$\therefore \quad \left(\frac{M_o}{M_{max}}\right) = 0.545$$

From Fig. 13.3 the position of the critical section,

$$\left(\frac{x}{L}\right) = 0.275$$

$$\therefore \quad x = (0.275 \times 30) = 8.25 \text{ m}$$

At this section,

$$M = 0.5 \times 30 \times 8.25(30 - 8.25) = 2680 \text{ kN m}$$

$$V = 450\left(1 - 2 \times \frac{8.25}{30}\right) = 203 \text{ kN}$$

$$f_{pe} = (0.85 \times 1100) = 935 \text{ N/mm}^2 (\geq 0.6 f_{pu} = 900 \text{ N/mm}^2)$$

$$\left(\frac{100 A_{ps}}{b_w \cdot d}\right) = \left(\frac{100 \times 3000}{150 \times 1150}\right) = 1.74 \text{ per cent}$$

From Table 8.2, the ultimate average shear resistance of concrete,

$$\tau_c = 0.90 \text{ N/mm}^2$$

$$\therefore \quad V_{cf} = \left[\left(1 - 0.55 \frac{f_{pe}}{f_{pu}}\right)\tau_c b_w d + M_o\left(\frac{V}{M}\right)\right]$$

$$= \left[\left(1 - 0.55 \times \frac{900}{1500}\right) 0.9 \times 150 \times \frac{1150}{(1000)} + \frac{(1850 \times 203)}{2680}\right] = 246 \text{ kN}$$

Since the actual shear (203 kN) is less than the shear resistance of the section, only minimum reinforcements are provided in the web, given by

$$\frac{A_{sv}}{S_v} = \frac{0.4\, b_w}{0.87 f_{yv}} = \left[\frac{0.4 \times 150}{0.87 \times 260}\right] = 0.265 \text{ mm}^2/\text{mm}$$

The maximum spacing of the stirrup is limited to 0.75 d_t or 4 b_w.
Allowing for 30 mm cover, $d_t = 1270$ mm

$\therefore$ Spacing must not exceed $(0.75 \times 1270) = 950$ mm or $(4 \times 150) = 600$ mm

Using 10 mm two-legged stirrups ($A_{sv} = 158$ mm^2)

$$S_v = 158/0.265 = 600 \text{ mm}$$

The arrangement of stirrups and spacers for tendons is shown in Fig. 13.8.

11. Check for Deflection at Serviceability Limit

Eccentricity of prestressing force at centre of span, $e_1 = 580$ mm
At support section, $e_2 = 170$ mm

$$a_p = \left[\frac{PL^2}{48\,E_c I}\;(5e_1 + e_2)\right]$$

$$= \left[\left(\frac{3200 \times 10^3 \times 30^2 \times 10^6}{48 \times 34 \times 10^3 \times 72490 \times 10^6}\right)(5 \times 580 + 170)\right] = 74.7 \text{ mm (upward)}$$

$$a_g = \left(\frac{5\,g\,L^4}{384 E_c I}\right)\left[\frac{5 \times 10.8 \times (30 \times 1000)^4}{384 \times 34 \times 10^3 \times 72490 \times 10^6}\right] = 46 \text{ mm}$$

$$a_q = \left[\frac{5\,q\,L^4}{384\,E_c I}\right] = \left[\frac{5 \times 9 \times (30 \times 1000)^4}{384 \times 34 \times 10^3 \times 72490 \times 10^6}\right] = 38.5 \text{ mm}$$

Assuming that the sides and soffit are exposed to the atmosphere, the notional size is computed as

$$\left(\frac{2A_c}{u}\right) = \left(\frac{2 \times 367500}{(2 \times 1300) + 350}\right) = 249 \text{ mm}$$

In the present case, assuming a relative humidity of 80 per cent and age at loading as 28 days, interpolate the value of long-term creep coefficient from Table 2.7 as $\phi = 1.7$.

$$\therefore \qquad E_c = (1 + \phi)\, E_{ce} = 2.7\, E_{ce}$$

$\therefore$ Resultant maximum long-term deflection is computed as

$$a_{max} = [(2.7 \times 46) + 38.5 - (0.85 \times 74.7)] = 99 \text{ mm}$$

which is less than the permissible code limit of (span/250) = (30000/250) = 120 mm.

12. Anchorage Zone Reinforcement

The equivalent prisms on which the anchorage forces are considered to be effective are detailed in Fig. 13.9.
For cables 1 and 2,

$$2y_{po} = 150 \text{ mm and } 2y_o = 200 \text{ mm}$$

$$\therefore \quad \left(\frac{y_{po}}{y_o}\right) = (75/100) = 0.75$$

For cables 3, 4 and 5,

$$2y_{po} = 150 \text{ mm and } 2y_o = 300 \text{ mm}$$

$$\therefore \quad \left(\frac{y_{po}}{y_o}\right) = (75/100) = 0.50$$

Initial jacking force in each cable = 640 kN

Considering cables forces 1 and 2 together, from Fig. 10.14

$$\text{Bursting tension, } F_{bst} = (0.17 \times 2 \times 640) = 140 \text{ kN}$$

For each of the cables 3, 4 and 5,

$$\text{Bursting tension, } F_{bst} = (0.17 \times 640) = 109 \text{ kN}$$

Using mild-steel links and considering the larger bursting tension,

$$A_{st} = \left(\frac{140 \times 10^3}{0.87 \times 260}\right) = 620 \text{ mm}^2$$

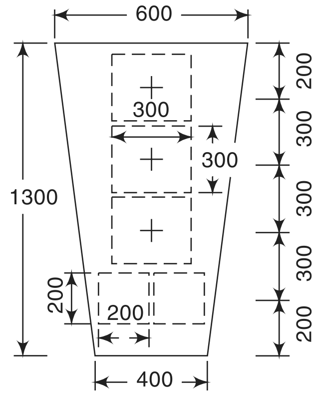

Fig. 13.9 *Arrangement of anchorage forces and equivalent prisms*

A possible arrangement of reinforcement, using 12 mm-diameter links in the vertical and horizontal directions, is shown in Fig. 13.10.

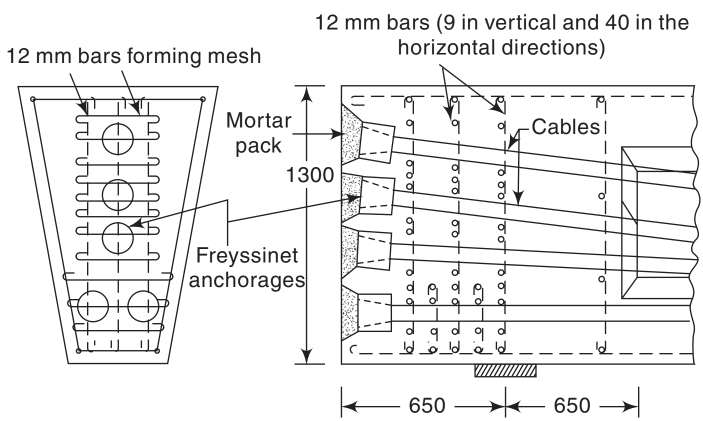

Fig. 13.10 *Arrangement of reinforcement in anchorage blocks*

13.5 Design of Partially Prestressed Members

13.5.1 Advantages of Limited Prestressing

In partially prestressed members, limited tensile stresses are permitted in concrete under service loads with controls on the maximum width of cracks and depending upon the type of prestressing and environmental conditions.

The use of partial prestressing was first proposed by Emperger in 1939 and further progress in this field was mainly due to the sustained work of Abeles[4] Birkenmeier[5], Goschy[6] and others. The West German Code DIN 4227 had provided for partial prestressing even before the CEB–FIP[7] provisions were introduced in 1970.

The main point in favour of partial or limited prestressing is that untensioned reinforcement is required in the cross-section of a prestressed member for various reasons, such as to resist the differential shrinkage, temperature effects and handling stresses. Hence, this reinforcement can cater for the serviceability requirements, such as control of cracking and, partially, for the ultimate limit state of collapse which can result in considerable reductions in the costlier high-tensile steel. The saving in prestressing steel contributes to an overall saving in the cost of the structure. Thurlimann[8] reported that the saving in prestressing steel is to the extent of 30 per cent if partial prestressing is used in accordance with the Swiss code SIA 162–1968[9]. Optimum design studies by Ramaswamy and Raman[10] have substantiated the fact that considerable savings in the high-tensile steel occurs in partially prestressed structural elements.

Fully prestressed members are prone to excessive upward deflections, especially in bridge structures where dead loads form a major portion of the total service loads, and these deflections may increase with time due to the effect of creep. It is also well established that fully prestressed members, due to their higher rigidity, have a lower energy absorption capacity in comparison with partially prestressed members, which exhibit a ductile behaviour. Even Freyssinet [11], who advocated full prestressing in the early days, later observed that in a road bridge where the chance of an unfavourable load being applied twice in the life of the structure is one in ten thousand, there is no disadvantage in allowing tensile stress of about 5 N/mm^2 in a concrete where the strains are appropriately guided. High-tensile steel and mild steel have been used as untensioned reinforcement. The present practice is to use high yield strength deformed bars which are considerably cheaper than prestressing steel and at the same time have higher yield strength and better crack control characteristics by virtue of their surface configuration as compared to mild steel bars with plain surface.

13.5.2 Computation of Width of Cracks

The CEB–FIP model code[12], along with the Indian Code IS: 1343[13], the American Code ACI: 318M–2011[14], and the Australian Code AS: 1481–1974[15], recognise partially prestressed members in which tensile stresses are permitted under service loads with limitations on the permissible width of cracks (refer to Section 11.6).

The method of calculating the crack width is of considerable importance in checking the limit state of cracking at service loads. It is well established that the width of crack, primarily depending upon the stress in the reinforcement, is also influenced by the cover and the type of reinforcement. Several empirical relations have been developed to estimate the width of cracks, but it is considered that a calculation based on the stress in the reinforcement, obtained by the conventional theory of cracked reinforced concrete section, is inherently more accurate than a computation based on the fictitious tensile stress in an uncracked section[16–21].

The cracked section analysis of a partially prestressed flanged section with tensioned high-tensile steel and untensioned reinforcement is carried out under the following assumptions:

1. The strain distribution across the section is linear.
2. The tensile strength of the concrete below the neutral axis is neglected.

The stresses and strains developed and the forces acting on a cracked prestressed concrete section which is subjected to a moment M in excess of the cracking moment M_{cr} is shown in Fig. 13.11. Just prior to the application of the moment, the tensile strain in the prestressing steel is ε_{pe} and the compressive strain in concrete at the tendon level is ε_{ce}. These strains can be evaluated from the prestressing force acting at this stage.

$$\varepsilon_{pe} = \left(\frac{P}{A_p E_p}\right) \tag{13.5}$$

$$\varepsilon_{ce} = \frac{P}{E_c}\left[\frac{e^2}{I_c} + \frac{1}{A_c}\right] \tag{13.6}$$

where P = effective prestressing force
e = eccentricity of tendons
A_c = cross-sectional area of the concrete section
I_c = second moment of area of the concrete section

Upon application of the moment, the concrete compressive strain in the bottom fibre reduces to zero and then becomes tensile. With M acting, the tensile strain in the reinforcing steel is ε_s and the strain in the concrete at the level of the tendon has changed from a compression of ε_{oc} to a tension of ε_{cp}. The strain distribution in the section is assumed to be linear and hence defined by the neutral-axis depth d_n and top fibre strain ε_o.

The strain in the reinforcing steel at a depth d_s is

$$\varepsilon_s = \varepsilon_o \frac{(d_s - d_n)}{d_n} \tag{13.7}$$

The tensile strain in the concrete at the level of the prestressing steel is

$$\varepsilon_{cp} = \varepsilon_o \frac{(d_p - d_n)}{d_n} \tag{13.8}$$

The prestressing steel undergoes a strain of $(\varepsilon_{ce} + \varepsilon_{cp})$ during the application of M, so that the total tensile strain in the tendon is

$$\varepsilon_p = \varepsilon_{pe} + \varepsilon_{ce} + \varepsilon_o \frac{(d_p - d_n)}{d_n} \tag{13.9}$$

The tensile force in the prestressing and reinforcing steel are, respectively,

$$T_p = A_p E_p \varepsilon_p \tag{13.10}$$

$$T_s = A_s E_s \varepsilon_s \tag{13.11}$$

In the concrete compressive zone, the resultant compressive force is

$$C = 0.5\ \varepsilon_o\ E_c b d_n \tag{13.12}$$

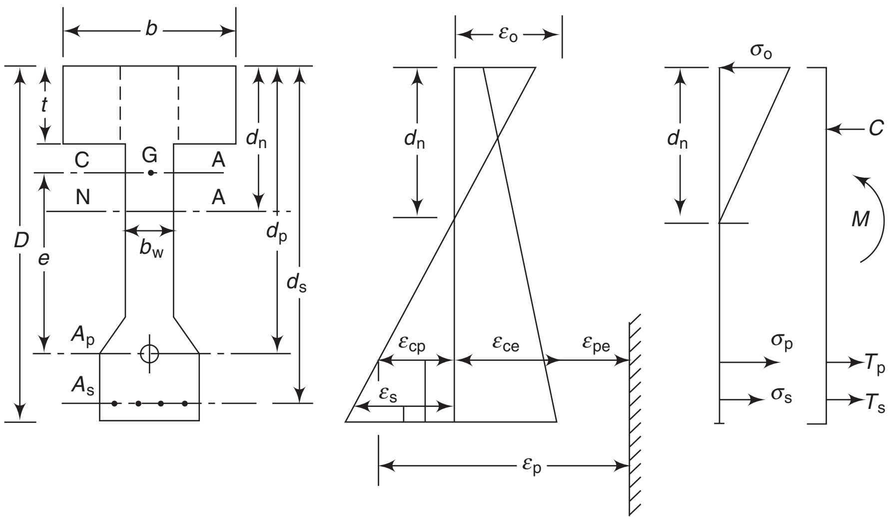

Fig. 13.11 *Cracked section analysis*

Equation 13.12 is valid provided the neutral axis is in the flange, $d_n < t$. The force C then acts at a depth

$$d_z = \frac{1}{3} d_n \tag{13.13}$$

If the neutral axis is in the web of a T-section, the force C has to be reduced by an amount C_n given by

$$C_n = 0.5\ \varepsilon_o E_c\ (b - b_w)\ \frac{(d_n - t)^2}{d_n} \tag{13.14}$$

which can be regarded as a negative force acting at a depth

$$d_{zn} = t + \frac{1}{3}(d_n - t)\ \ (d_n - t) \tag{13.15}$$

Equations 13.5 to 13.15 allow the internal forces and hence M, to be calculated from the strain distribution in the section, i.e., from ε_o and d_n. Usually in a cracked section analysis, M is known and the strain and stresses have to be determined by trial and error. It is convenient to start with a trial value of d_n and find the corresponding value of ε_o. At all stages of loading, the longitudinal force equilibrium must be satisfied.

$$(C - C_n) = (T_p + T_s) \tag{13.16}$$

By substituting expressions already derived for the various forces, an equation relating ε_o to d_n derived by Warner[22] is useful for computations and is expressed as follows;

$$\varepsilon_o = \left\{ \frac{A_p E_p(\varepsilon_{ce} + \varepsilon_{pe})}{\frac{1}{2}E_c\left[b_w d_n + (b - b_w)t\left(1 + \frac{d_n - t}{d_n}\right)\right] - \left[A_s E_s\left(\frac{d - d_n}{d_n}\right) + A_p E_p\left(\frac{d_p - d_n}{d_n}\right)\right]} \right\} \quad (13.17)$$

This equation allows ε_o to be determined for any chosen value of d_n in the range $D > d_n > t$. For rectangular sections, b_w must be replaced by b. If the neutral axis is in the flange ($d_n < t$), Eq. 13.17 can be used provided the term in the denominator containing $(b - b_w)$ is set to zero and b_w is set to b. It is important to note that the present analysis assumes a linear elastic behaviour and that inelastic behaviour in either concrete or steel may develop as the neutral axis rises into the flange.

After evaluating the trial value of d_n, the internal forces can be evaluated and the moment corresponding to d_n can be obtained.

$$M = (T_p d_p + T_s d_s + C_n d_{zn} - C d_z) \quad (13.18)$$

Usually, the computations are made for two appropriate d_n values of $0.5D$ and $0.35D$. The resulting values of M will usually bracket the working moment, which can then be found by interpolation. The entire sequence of calculations is sufficiently small to be programmed on a modern calculator.

According to the European concrete committee, the width of a crack is related to the stress in the reinforcement. In the case of partially prestressed beams, the FIP, BS EN: 1992–1–1 and IS: 1343 codes limit the width of cracks under service loads to 0.1 mm in an aggressive environment and to 0.2 mm in normal situations. Alternatively, the British and Indian codes provide for the limitation of crack width by computation of hypothetical flexural tensile stresses as detailed in Table 11.7. Investigations by Parameswaran et al.[23] have indicated that the hypothetical tensile stress method is suitable for predicting with reasonable accuracy, the maximum width of cracks in class-3 type members.

The use of approximate and rigorous methods of estimation of the width of cracks in Class 3 type (partially prestressed) members are illustrated by the following examples:

Example 13.3 Design a partially prestressed post-tensioned beam (Class 3-type) to suit the following data:

Effective span = 30 m
Live load = 9 kN/m
Dead load (excluding self-weight) = 2 kN/m
Load factors = 1.4 for dead load and 1.6 for live load

28-day cube compressive strength, $f_{cu} = 50$ N/mm^2
Strength of concrete at transfer, $f_{ci} = 35$ N/mm^2
Loss ratio, $\eta = 0.85$
Tensile strength of concrete = 1.7 N/mm^2
Permissible tensile stress under service loads = 6 N/mm^2
Maximum width of crack under service loads not to exceed 0.1 mm. 8 mm diameter high-tensile wires having an ultimate tensile strength of 1500 N/mm^2 are available for use.

Solution. The design of a fully prestressed post-tensioned beam for the same span and service loads is presented in Section 13.4. The design calculations for a partially prestressed beam are similar with regard to

1. ultimate moments and shear forces
2. cross-sectional dimensions
3. properties of section
4. design moments and shear forces

The permissible stresses in concrete at the stage of transfer and service loads are as follows:

$$f_{ct} = (0.5 \times 35) = 17.5 \text{ N/mm}^2$$

$$f_{cw} = (0.33 \times 50) = 16.5 \text{ N/mm}^2$$

$$f_{tt} = f_{tw} = -6 \text{ N/mm}^2$$

$$f_{\text{inf}} = \left(\frac{f_{tw}}{\eta}\right) + \left(\frac{M_d}{\eta Z_b}\right)$$

$$= \left[\left(-\frac{6}{0.85}\right) + \frac{(2230 \times 10^6)}{(0.85 \times 99 \times 10^6)}\right] = 19.5 \text{ N/mm}^2$$

Maximum permissible eccentricity, $e = 580$ mm

$$\therefore \qquad P = \left[\frac{A f_{\text{inf}} z_b}{Z_b + Ae}\right] = \left[\frac{367500 \times 19.5 \times 99 \times 10^6}{(99 \times 10^6) + (367500 \times 580)}\right]$$

$$= (2400 \times 10^3) \text{ N} = 2400 \text{ kN}$$

The magnitude of the prestressing force is 75 per cent of that required for the fully prestressed beam. Hence, four Freyssinet cables containing 12 wires of 8 mm diameter stressed to 1000 N/mm^2, each providing a force of 600 kN, are provided.

Force developed in tendons at the limit state of collapse

$$= \frac{(2400 \times 0.87 \times 1500)}{1000} = 2950 \text{ kN}$$

Assuming the concrete compression to be located at the centre of flange thickness,

$$M_u = \left[\frac{2950(1150 - 125)}{1000}\right] = 3050 \text{ kN m}$$

But the ultimate moment required, M_{ud} = 3400 kN m
Hence, balance moment = (3400 – 3050) = 350 kN m

If A_{us} = area of untensioned reinforcement made up of deformed bars (f_y = 420 N/mm^2), which are provided at the soffit at a cover of 30 mm, then

$$A_{us}(0.87f_y)\,(1300 - 125 - 30) = 350 \times 10^6$$

$$\therefore \quad A_{us} = 830 \text{ N/mm}^2$$

Five 20 mm diameter high yield bars are sufficient for providing the required area as well as for limiting the width of cracks.

$$A_{su} = 1570 \text{ mm}^2$$

Percentage of untensioned reinforcement $= \dfrac{(100 \times 1570)}{(350 \times 300)} = 1.49$

Check for Stresses

$$P = 2400 \text{ kN} \qquad A = (0.3675 \times 10^6) \text{ mm}^2$$

$$\frac{P}{A} = 6.6 \text{ N/mm}^2 \qquad e = 580 \text{ mm}$$

$$\frac{Pe}{Z_b} = 14.1 \text{ N/mm}^2 \qquad Z_b = (99 \times 10^6) \text{ mm}^3$$

$$\frac{Pe}{Z_t} = 11.0 \text{ N/mm}^2 \qquad \eta = 0.85$$

$$\frac{M_{min}}{Z_t} = 7.8 \text{ N/mm}^2 \qquad \frac{M_d}{Z_t} = 17.8 \text{ N/mm}^2$$

$$\frac{M_{min}}{Z_b} = 10 \text{ N/mm}^2 \qquad \frac{M_d}{Z_b} = 22.5 \text{ N/mm}^2$$

Stage	*Prestress*	*Stresses due to Loads*		*Resultant Stresses*
		M_{min}	M_d	(N/mm^2)
At transfer	Top (6.6 – 11) = –4.4	7.8	—	+3.4
	Bottom (6.6 + 14.1) = 20.7	–10.0	—	+10.7
At service	Top (0.85) × (–4.4) = –3.8	—	17.8	+14.0
loads	Bottom (0.5 × 20.7) = 17.5	—	–22.5	–5.0

The stresses are within the permissible limits.

Check for Width of Cracks According to the Indian Standard Code (IS: 1343-2012), the maximum permissible hypothetical tensile stress for a crack width of 0.1 mm in post-tensioned grouted beams of M-50 grade concrete is 4.8 N/mm^2. For every one per cent additional untensioned reinforcement in the tension zone, the permissible tensile stress can be increased by 4 N/mm^2. Using five bars of 20 mm diameter at an effective cover of 40 mm, the crack width will be less than 0.1 mm. In the present case, the tensile stress at the soffit is only 5 N/mm^2 without any additional reinforcement in comparison with the permissible tensile stress of 6 N/mm^2 given in the data. Hence, the beam satisfies the limit state of serviceability of cracking according to the Indian Standard Code.

Example 13.4 The cross-section of a class-3 type post-tensioned T-girder, designed to resist a service load moment of 1560 kN m is shown in Fig. 13.12. The beam is prestressed by a cable containing 19 strands of 12.7 mm diameter stressed to 1133 N/mm^2. The supplementary reinforcements comprise six bars of 24 mm diameter. Using the rigorous method of cracked section analysis, estimate the width of cracks developed in the beam under the working moment. Adopt M-50 Grade concrete and Fe-415 HYSD bars.

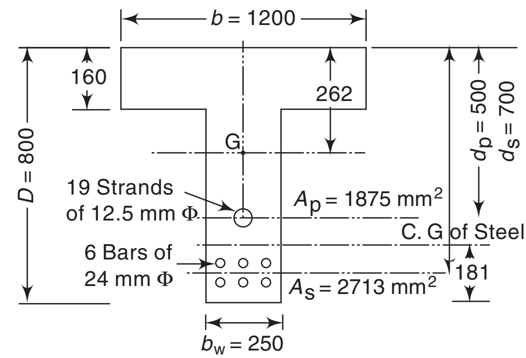

Fig. 13.12 *Cross-section of partially prestressed T-girder*

Solution.

Properties of Section

$$A_c = (160 \times 1200) + (250 \times 640) = 352000 \text{ mm}^2$$

$$A_s = \left(6 \times 3.14 \times \frac{24^2}{4}\right) = 2713 \text{ mm}^2$$

$$A_p = (19 \times 98.7) = 1875 \text{ mm}^2$$

$$I_c = (1983 \times 10^7) \text{ mm}^4$$

$$E_s = E_p = 200 \text{ kN/mm}^2 \quad E_c = 31.6 \text{ kN/mm}^2$$

Effective stress in tendons = 1133 N/mm^2

Prestressing force, $P = (1875 \times 1133) = 2124 \times 10^3$ N

Eccentricity, $e = 238$ mm

Strains in Tendons and Concrete

$$\varepsilon_{pe} = \left(\frac{\sigma_p}{E_p}\right) = \left(\frac{1133}{200 \times 10^3}\right) = 0.0057$$

$$\varepsilon_{ce} = \frac{P}{E_c} = \left[\frac{e^2}{I_c} + \frac{1}{A_c}\right] = \left(\frac{2124 \times 10^3}{31.6 \times 10^3}\right)\left[\left(\frac{238^2}{1983 \times 10^7}\right) + \left(\frac{1}{352000}\right)\right] = 0.00032$$

Cracking Moment Compressive prestress at soffit,

$$\sigma_b = \left[\left(\frac{2124 \times 10^3}{352 \times 10^3}\right) + \left(\frac{2124 \times 10^3 \times 238 \times 538}{1983 \times 10^7}\right)\right] = 19.7 \text{ N/mm}^2$$

Modulus of rupture of concrete, $f_r = 0.7\sqrt{f_{ck}} = 0.7\sqrt{50} = 4.95 \text{ N/mm}^2$

$$M_{cr} = \left\{[19.7 + 4.95]\frac{[1983 \times 10^7]}{538}\right\} = (902 \times 10^6) \text{ N mm} = 902 \text{ kN m}$$

Computation of ε_o for Trial d_n

Assuming a trial $d_n = 250$ mm and $\varepsilon_{ce} = 0.00032$

$\varepsilon_{pe} = 0.0057$ $\quad b = 1200$ mm $\quad t = 160$ mm

$b_w = 250$ mm $\quad d_p = 500$ mm $\quad d_s = 700$ mm

$A_p = 1875 \text{ mm}^2$ $\quad A_s = 2713 \text{ mm}^2$ $\quad E_c = 31.6 \text{ kN/mm}^2$

$E_p = 200 \text{ kN/mm}^2$

Using Eq. (13.17),

$$\varepsilon_o = \left\{\frac{A_p E_p(\varepsilon_{ce} + \varepsilon_{pe})}{\frac{1}{2}E_c\left[b_w d_n + (b - b_w)t\left(1 + \frac{d_n - t}{d_n}\right)\right] - \left[A_s E_s\left(\frac{d - d_n}{d_n}\right) + A_p E_p\left(\frac{d_p - d_n}{d_n}\right)\right]}\right\}$$

$$\varepsilon_o = \left\{\frac{(1875 \times 200 \times 10^3)(0.00032 + 0.0057)}{\left(\frac{1}{2} \times 31.6 \times 10^3\right)\left[(250 \times 250) + (1200 - 250)160\left(1 + \frac{250 - 160}{250}\right)\right] - \left[(2713 \times 200 \times 10^3)\left(\frac{700 - 250}{250}\right) + (1875 \times 200 \times 10^3)\left(\frac{500 - 250}{250}\right)\right]}\right\}$$

$$= 0.00076$$

Forces and Moment

$$d_n = 250 \text{ mm}$$
$$\varepsilon_o = 0.00076$$
$$\varepsilon_{pe} = 0.0057$$
$$\varepsilon_{ce} = 0.00032$$

$$\varepsilon_s = \varepsilon_o \frac{(d_s - d_n)}{d_n} = \left[0.00076\frac{(700 - 250)}{250}\right] = 0.001368$$

$$\varepsilon_p = \left[\varepsilon_{pe} + \varepsilon_{ce} + \varepsilon_o \frac{(d_p - d_n)}{d_n}\right]$$

$$= \left[0.0057 + 0.00032 + 0.00076 \frac{(500 - 250)}{250}\right] = 0.00678$$

$$T_s = A_s E_s \varepsilon_s = (2713 \times 200 \times 10^3 \times 0.001368) = 742276 \text{ N} = 742.27 \text{ kN}$$

$$T_p = A_p E_p \varepsilon_p = (1875 \times 200 \times 10^3 \times 0.00678) = 2542500 \text{ N} = 2542.5 \text{ kN}$$

$$C = 0.5\, \varepsilon_o E_c b d_n = (0.5 \times 0.00076 \times 31.6 \times 10^3 \times 1200 \times 250)$$

$$= 3602400 \text{ N} = 3602.4 \text{ kN}$$

$$C_n = 0.5 \varepsilon_o E_c (b - b_w) \frac{(d_n - t)}{d_n}$$

$$= \left[0.5 \times 0.00076 \times 31.6 \times 10^3 \times 950 \frac{(250 - 160)^2}{250}\right]$$

$$= 369606 \text{ N} = 369.6 \text{ kN}$$

$$d_{zn} = \left[t + \frac{1}{3}(d_n - t)\right] = \left[160 + \frac{1}{3}(250 - 160)\right] = 190 \text{ mm}$$

$$d_z = \frac{1}{3} d_n = \left(\frac{1}{3} \times 250\right) = 83.33 \text{ mm}$$

$$M = T_p d_p + T_s d_s + C_n d_{zn} - C d_z$$
$$= [(2542.5 \times 0.5) + (742.27 \times 0.7) + (369.6 \times 0.19) - (3602.4 \times 0.0833)]$$
$$= 1561 \text{ kNm.}$$

Since the computed value of the moment M is nearly equal to the service load moment of 1560 kN m, the assumed value of $d_n = 250$ is correct. If not, a new trial value of d_n is assumed and the computation procedure is repeated until the moment values are nearly equal.

Computation of Crack Width using Different Methods

(1) British Code Method (BS EN: 1992-3-2006) The British code method, outlined in Section 11.7, considers the tension stiffening effect of concrete in the tension zone. It is used to estimate the width of cracks in this example.

$$\omega_k = s_{r,max} (\varepsilon_{sm} - \varepsilon_{cm})$$

$$= s_{r,max} \left[\frac{\sigma_s - k_t \left(\dfrac{f_{ct,eff}}{\rho_{\rho,eff}}\right)(1 + \alpha_e \rho_{\rho,eff})}{E_s}\right]$$

$$(\varepsilon_{sm} - \varepsilon_{cm}) = \left[\frac{\sigma_s - k_t \left(\dfrac{f_{ct,eff}}{\rho_{\rho,eff}}\right)(1 + \alpha_e \rho_{\rho,eff})}{E_s}\right] \geq 0.6 \left(\frac{\sigma_s}{E_s}\right)$$

Substituting the relevant values in this example, we have

$f_{ck} = 50$ N/mm^2, $E_s = 200$ kN/mm^2, $I_{cr} = (1983 \times 10^7)$ mm^4

$y_t = 262$ mm and $y_b = 538$ mm, $Z_b = (1983 \times 10^7)/538 = (36.8 \times 10^6)$ mm^3

$$E_c = 5000\sqrt{50} = 35000 \text{ N/mm}^2 = 35 \text{ kN/mm}^2$$

$$\alpha_e = [E_s/E_c] = [200/35] = 5.7$$

$$f_{ct,eff} = 0.7\sqrt{f_{ck}} = 0.7\sqrt{50} = 4.9 \text{ N/mm}^2$$

Neutral axis depth determined by trial and error method

$= d_n = x = 250$ mm

$k_t = 0.4$ for long-term loading

$h_{c,eff}$ = Effective depth of the concrete in tension zone which is the least of the following three distances:

1. 2.5 times the distance from the tension face of concrete to the centroid of the reinforcement (2.5 times the effective cover)
2. $[(h - x)/3]$ where h = overall depth of beam and x = neutral axis depth
3. $[h/2]$

For the cracked section, neutral axis depth $= x = 250$ mm, $d = 700$ mm

1. $h_{c,eff} = 2.5(100)$ mm $= 250$ mm
2. $[(800 - 250)/3] = 183.3$ mm
3. $\left(\dfrac{800}{2}\right) = 400$ mm

The least effective depth of concrete in tension area $= h_{c,eff} = 183.3$ mm

$A_s = 2713$ mm^2 and $b_w = 250$ mm

$$\rho_{\rho,eff} = \left[\frac{A_s}{b \cdot h_{c,eff}}\right] = \left[\frac{2713}{250 \times 183.3}\right] = 0.059$$

Effective cover to reinforcement $= c = 100$ mm

Minimum cover to untensioned reinforcement $= c_{min} = 38$ mm

Diameter of tendon $= \phi = 24$ mm, for high bond bars, $k_1 = 0.8$ and for flexure, $k_2 = 0.5$

Maximum final crack spacing is computed using the relation

$$\begin{aligned} S_{r,max} &= [3.4 c_{min} + (0.425 \times k_1 \times k_2 \times \phi)/\rho_{\rho,eff}] \\ &= [(3.4 \times 38) + (0.425 \times 0.8 \times 0.5 \times 24)/0.059] \\ &= 198 \text{ mm} \end{aligned}$$

σ_s = Net increase in stress in tendons beyond the decompression

$= 107$ N/mm^2

Substituting the relevant values, the crack width is computed using the equation for ω_k,

Moment required to create a tensile stress equal to the cracking tensile stress of concrete at the soffit is computed as

$$M_{cr} = (f_b\, Z_b) = [4.9 \times (36.8 \times 10^2)]/10^6 = 180 \text{ kN.m}$$

$$\text{Stress in steel} = \sigma_s = \left[\frac{M_{cr}}{\left(d - \frac{x}{3}\right)A_{st}}\right]$$

$$= \left[\frac{180 \times 10^6}{\left(700 - \frac{250}{3}\right)2713}\right] = 107 \text{ N/mm}^2$$

$$(\varepsilon_{sm} - \varepsilon_{cm}) = \left[\frac{107 - 0.4\left(\frac{4.9}{0.059}\right)(1 + 5.7 \times 0.059)}{200 \times 10^3}\right] \geq 0.6\left(\frac{107}{200 \times 10^3}\right)$$

$$= 0.00031 \geq 0.0003$$

$$\omega_k = s_{r,max}\,(\varepsilon_{sm} - \varepsilon_{cm})$$

$$= (198 \times 0.00031)$$

$$= 0.061 \text{ mm}$$

(2) Indian Standard Code (IS: 456-2000) The Indian Standard Code method is based on the earlier British code (BS: 8110-1985).

In this method, the design surface crack width is computed using the relation,

$$w_{cr} = \left\{\frac{3a_{cr} \times \varepsilon_m}{1 + \left[\frac{2(a_{cr} - c_{min})}{h - x}\right]}\right\}$$

Where

a_{cr} = distance from the point considered to the surface of the nearest longitudinal bar

c_{min} = minimum cover to the longitudinal bar

ε_m = average steel strain at the level considered

h = overall depth of member

x = depth of neutral axis

Substituting the numerical values, we have, for the point on the soffit of beam between the reinforcing bars = s = 60 mm and minimum cover = 38 mm

Where s = spacing between the bars = 60 mm

$$a_{\text{cr}} = \sqrt{(0.5s)^2 + c_{\text{min}}{}^2} = \sqrt{30^2 + 38^2} = 48.4 \text{ mm}$$

$$\varepsilon_{\text{m}} = \varepsilon_1 - \left[\frac{b_w(h-x)(a'-x)}{3E_s A_s(d-x)}\right]$$

and $\varepsilon_1 = \dfrac{f_s}{E_s}\left[\dfrac{h-x}{d-x}\right]$ also $f_{\text{s}} = 107$ N/mm^2 and $E_{\text{s}} = 200$ kN/mm^2

$h = 800$ mm, $d = 700$ mm, $A_{\text{s}} = 2713$ mm^2,

$x = 250$ mm and $a' = 800$ mm

$$\varepsilon_1 = \frac{f_s}{E_s}\left[\frac{h-x}{d-x}\right] = \left(\frac{107}{200 \times 100^3}\right)\left[\frac{800-250}{700-250}\right] = 0.00065$$

$$\varepsilon_{\text{m}} = \varepsilon_1 - \left[\frac{b_w(h-x)(a'-x)}{3E_s A_s(d-x)}\right]$$

$$= 0.00065 - \left[\frac{250(800-250)(800-250)}{3(200 \times 100^3)2713(700-250)}\right]$$

$$= 0.00055$$

$$w_{\text{cr}} = \left\{\frac{3a_{\text{cr}} \times \varepsilon_{\text{m}}}{1 + \left[\dfrac{2(a_{\text{cr}} - c_{\text{min}})}{h-x}\right]}\right\} = \left\{\frac{3 \times 48.4 \times 0.00055}{1 + 2\left[\dfrac{(48.4-38)}{800-250}\right]}\right\}$$

$$= 0.077 \text{ mm}$$

(3) Gergely-Lutz Formula (American Practice) Crack width at the soffit of the beam located between the bars is expressed as

$$\omega_{\text{cr}} = (11 \times 10^{-6})\sqrt[3]{d_{\text{c}}\left(\frac{A_{\text{e}}}{n}\right)}\left[\frac{D-x}{d-x}\right]f_{\text{st}}$$

Substituting the numerical values in the formula

d_{c} = effective cover

= distance from centre of steel bars to the soffit of the beam

= (38 + 12) = 50 mm

$A_{\text{e}} = (b_{\text{w}} \times 2d_{\text{c}}) = (250 \times 2 \times 50) = 25000$ mm^2

n = number of bars in the tension zone = 6

$(D - x) = (800 - 250) = 550$ mm

$(d - x) = (700 - 250) = 450$ mm

f_{st} = Stress in the centroid of the tension steel = 107 N/mm^2

$$\omega_{cr} = (11 \times 10^{-6}) \sqrt[3]{50\left(\frac{25000}{6}\right)} \left[\frac{550}{450}\right] 107$$
$$= 0.085 \text{ mm}$$

A comparative analysis indicates that the British code results in the least values of crack widths in comparison with the Indian code and the Gergely-Lutz method, since the British code method includes all the influencing parameters including the tension stiffening effect of concrete. Consequently, the crack widths predicted are the least in comparison with the other methods.

References

1. BS EN: 1992–1–1 Euro Code–2, Design of Concrete Structures, General Rules and Rules for Buildings, British Standards Institution, 2004.
2. Bennett, E W, *Structural Concrete Elements*, Chapman and Hall Ltd., London, 1973, pp 173–177.
3. Magnel, G, *Prestressed Concrete*, Concrete Publications Ltd., London, 1950.
4. Abeles, P W, "Fully and partially prestressed concrete," *Journal of the ACI*, Vo1.16, No. 3, January1945, pp 181–214.
5. Birkenmeier M, "Design of partially prestressed structures in accordance with the (1966) standards of the Swiss Association of Engineers and Architects," *Annls Inst. Tech. Batim*, Vol. 21(241) 1968, pp 57–64.
6. Goschy, B, "Partially stressed reinforced concrete," *Melyepitestud*, *Szle*, Vol. 14, No. 2, 1964, pp 81–83.
7. CEB-FIP, Joint Committee, *International Recommendations for the Design and Construction of Concrete Structures*, Cement and Concrete Association, London, June 1970.
8. Thurlimann, B and R Calfisch, "Teilweitse vorgespannter beton," *Dentscher Benton Tag*, *1969*.
9. "Norm fur die berchnung von konstructionen aus beton, stahlbeton and spann beton," *Schweizerischer Ingeltieurund Architekten Verein* SIA Technische Norm 162, Zurich, 1968.
10. Ramaswamy, G S and N V Raman, "Optimum design of prestressed concrete sections for minimum cost by non-linear programming," *Sixth FIP Congress*, Prague, June 1970.
11. Freyssinet, E, "Birth of prestressing," Speech on the occasion of his jubilee as an engineer, translated by AJ Harris, from the French original in Travaux, Cement and Concrete Association, London, July–August 1954.
12. CEB-FIP Committee, *Model Code for Concrete Structures*, Comite Euro-International du Beton, (English translation), Paris, 1978.
13. IS: 1343–2012, *Indian Standard Code of Practice for Prestressed Concrete* (second revision), Indian Standards Institution, New Delhi, 2012, pp. 1-56.
14. ACI 318M–2011, *Building Code Requirements for Structural Concrete and Commentary*, American Concrete Institute, Farmington Hills, Michigan, 2011.
15. AS: 1481–1974, Standards Association of Australia, *Prestressed Concrete Code*, Sydney, 1974.

16. Bennett, E W, and C S Chandrashekhar, “Calculation of the width of cracks in class 3 prestressed beams,” *Proceedings of the Institution of Civil Engineers*, London, Vol. 49, July 1971, pp 333–346.
17. Beeby, AW, and H P J Taylor, “Cracking in partially prestressed members,” *Preliminary Publications*, *6th FIP Congress*, Prague, 1970.
18. Krishna Raju, N, “Flexural behaviour of pretensioned concrete beams with limited prestress,” *Building Science*, UK, Vol. 8, 1973, pp 179–185.
19. Krishna Raju, N et al., “Limit state behaviour of pretensioned I-beams with limited prestress,” *Indian Concrete Journal*, Vol. 49, No. 7, July 1975, pp 213–218.
20. Krishna Raju, N et al., “Stresses in tensioned and untensioned reinforcement of concrete beams with limited prestress,” 18th *Congress of Theoretical and Applied Mechanics Society of India*, Madras, December, 1973, pp 1–10.
21. Desayi, P, “A method for determining the spacing and width of cracks in partially prestressed concrete beams,” *Proceedings of Institution of Civil Engineers* (London), Part 2, 1975, Vol. 59, pp 411–428.
22. Warner, R F, Prestressed concrete and partially prestressed concrete, *Handbook of Structural Concrete*, edited by Kong, FK, Evans, RH, Roll, F and Cohen, E, Arnold Heinemann Publishers (India), Pitman Books Ltd, 1983, pp 19–1 to 19–52.
23. Parameswaran, V S, and Annamalai, G, “Flexural behaviour of class-3 type beams,” *Indian Concrete Journal*, Vol. 49, No. 7, July 1975, pp 206–212.

Review Questions

13.1 Briefly outline the basic principles underlying the dimensioning of flexural members. How do you select the preliminary dimensions of prestressed concrete sections?

13.2 Explain the theoretical basis of selecting the preliminary dimensions for the thickness of web in prestressed beams with short and long spans.

13.3 What are the various checks you would apply while designing pretensioned flexural members?

13.4 What are the factors influencing the width of cracks in prestressed members?

13.5 Explain the terms (a) hypothetical tensile stress, and (b) effective depth of concrete in tension.

13.6 How do you select the preliminary dimensions of post-tensioned beams having an unsymmetrical I-section?

13.7 How do you check a designed unsymmetrical I-section prestressed girder for flexural and shear strength?

13.8 Sketch a typical I-section prestressed concrete girder showing the position of cables, longitudinal and transverse reinforcements at the centre of span and support sections. Show the profile of the cables along the span.

13.9 Sketch a typical end block of a long span girder with several cables showing the arrangement of anchorage zone reinforcement.

13.10 What are the advantages of partial or limited prestressing? How do you compute the width of cracks at critical sections in partially prestressed concrete beams?

Exercises

13.1 Design a pre-tensioned symmetrical I beam for an effective span of 7 m to support a superimposed load of 6 kN/m. The beam is to be precast in a factory and is to be designed for handling at any point along its length during transport and erection. Load factors against failure by bending or hear:

For dead load = 1.5

For live load = 2.5

Permissible stresses:

At transfer,

Compressive stress = 14 N/mm^2

Tensile stress = 1.4 N/mm^2

At working load,

Compressive stress = 16 N/mm^2

Tensile stress = 1.4 N/mm^2

The specified 28-day cube strength of concrete is 50 N/mm^2. The prestressing force is to be provided by 5 mm diameter high-tensile wires having an ultimate tensile strength of 1600 N/mm^2. The loss ratio is 0.8. Design the beam and sketch the cross-section showing the arrangement of wires. Check the safety of the beam for the limit states of cracking, deflection and collapse.

**[Ans: b = 190 mm, h = 380 mm, d = 325 mm, b_w = 40 mm,
h_f = 70 mm, A = 36200 mm^2, Z = 3670000 mm^3,
P = 198 kN, e = 135 mm;
Number of 5 mm diameter wires = 8;
Untensioned reinforcement = three bars of 16 mm diameter]**

13.2 A straight, precast pretensioned beam of I-section is to be designed to support a uniformly distributed imposed load of 8 kN/m in addition to the self-weight of the member the effective span of the simply supported beam is to be 9 m. Using concrete of grade M-45 with permissible compressive stress in concrete at transfer and working loads as 15 N/mm^2, and 5 mm diameter high-tensile steel wires of UTS = 1600 N/mm^2, which are initially stressed to 1200 N/mm^2, design the cross-sections of the girder as a class-1 member without allowing any tension under working loads. Assume the loss of prestress due to elastic deformation, creep, shrinkage and other factors as 20 per cent. Sketch the cross-section of the girder at the centre of span showing the arrangement of wires. Load factors of 1.5 for dead load and 2.5 for live load may be assumed.

**[Ans: b = 260 mm, h = 520 mm, b_w = 50 mm.
h_f = 100 mm, A = 68000 mm^2, Z = 9510000 mm^3,
P = 376 kN; e = 184 mm;
Number of 5 mm diameter high-tensile wires = 16;
Four mild steel bars of 12 mm diameter]**

13.3 A post-tensioned, prestressed concrete girder having a span of 40 m between bearings is required for an aircraft hangar. The live load on the girder is 5 kN/m. The specified 28-day cube strength is 50 N/mm^2. The cube strength of concrete at transfer is 30 N/mm^2. Permissible stresses should conform to the provisions of IS: 1343. The prestress is to be provided by seven-wire 15 mm strand cables, each tensioned to 1200 kN, housed in cable ducts of 64 mm. Ultimate tensile strength of each cable = 1750 kN. Loss ratio = 0.80.

The design has to comply with the various limit states of deflection, cracking and collapse. Design the following particulars:

(a) the cross-section of the girder,

(b) cable profile, and

(c) end block.

[Ans: b = 700 mm, h = 1500 mm, d = 1300 mm, $b_w = h_f$ = 200 mm, Bottom flange width and depth = 350 mm and 300 mm, respectively; P = 4500 kN; e = 680 mm; No. of cables = 5]

13.4 A post-tensioned prestressed concrete beam for the roof of an industrial structure has a simply supported span of 25 m. The beam has to support a dead load of 2 kN/m, together with an imposed load of 15 kN/m in addition to the self-weight. The grade of concrete specified is M-40. The compressive strength of concrete at transfer is 35 N/mm^2. The loss ratio is 0.80. The 64 mm cables containing 7–15 mm strands with an ultimate load capacity of 1750 kN are available. Using IS: 1343 provisions, design the cross-section of the girder to comply with various limit states. Sketch the details of cables in the cross-section and the profile of cables along the depth and length of the beam. Also, design the anchorage zone reinforcement.

[Ans: b = 700 mm, h = 1500 mm, b_w = 150 mm, d = 1250 mm, Bottom flange = 350 mm wide × 250 mm deep; P = 2750 kN; e = 630 mm; 2 cables; Untensioned reinforcement = 10 mild steel bars of 25 mm diameter]

13.5 A post-tensioned prestresseed concrete girder of a bridge deck spanning over 24 m has the following cross-sectional details at the centre of the span: width and thickness of the top flange = 2000 mm and 200 mm, respectively, overall depth of the girder = 1400 mm.

Thickness of the web = 200 mm width and depth of bottom flange = 500 and 400 mm, respectively. The service load design moment is 3700 kN m and the minimum moment is 1930 kN m. If the compressive stress at transfer and the tensile stress under working loads in concrete are 15 N/mm^2 and zero, respectively, check the adequacy of the section and design the prestressing force located at an eccentricity of 700 mm. Assume a loss ratio of 0.85.

[Ans: Prestressing force = 4540 kN]

13.6 A class-3 type partially prestressed T-girder designed to support a live load of 8 kN/m over an effective span of 20 m is made up of a top flange, 1000 mm wide by 120 mm thick, with a rib 300 mm wide. The overall depth of the girder is 720 mm. The tensioned steel consists of nine strands of 12.5 mm diameter with a tensile strength of 1750 N/mm^2, located at 585 mm from the top. The untensioned steel is of seven cold worked deformed bars, of 25 mm diameter with f_y = 425 N/mm^2, located 80 mm from the soffit of the girder. The effective prestressing force in the tendons is 830 kN. Estimate the width of the cracks developed under service loads and check the crack width using the hypothetical tensile stresses provided for in the British and Indian codes.

[Ans: w_{max} = 0.223 mm]

13.7 The mid-span section of slab of a prestressed concrete tee beam bridge is 200 mm thick and reinforced with 10 mm diameter spaced at 125 mm intervals at an effective cover of 35 mm. The section is subjected to a maximum moment of 22 kN.m per metre width under service loads. If M-25 grade concrete and Fe-415 HYSD bars are used, estimate the width of cracks developed using (a) the Indian Standard Code, and (b) Gergely-Lutz formula.

[Ans: (a) 0.126 mm; (b) 0.217 mm]

13.8 A doubly reinforced concrete beam of a bridge superstructure is 250 mm wide and 400 mm overall deep and reinforced with three bars of 28 mm diameter on the tension at an effective depth of 348 mm, and three bars of 20 mm on the compression side at an effective cover of 48 mm. The maximum service load moment at the section under service loads is 124 kN.m. If M-25 grade concrete and Fe-415 HYSD bars are used, calculate the maximum probable width of cracks developed in the beam using (a) IS: 456-2000, and (b) Gergely-Lutz formula.

[Ans: (a) 0.182 mm; (b) 0.237 mm]

Objective-type Questions

13.1 In the case of unsymmetrical I-girders, the desirable ratio of breadth of flange to effective depth should be in the range of
(a) 0.2 to 0.4 (b) 0.4 to 0.6 (c) 0.6 to 1.0

13.2 The thickness of web in PSC girders is determined from the considerations of
(a) flexural strength
(b) compressive strength
(c) tensile strength

13.3 In designing PSC flexural members, the breadth of compression flange is determined on the basis of
(a) ultimate shear strength
(b) ultimate flexural strength
(c) ultimate tensile strength

13.4 The dimensions of the tension flange of long span PSC girder is influenced by
(a) ultimate flexural strength
(b) ultimate shear strength
(c) considerations of housing cables

13.5 The clear cover to cables in a PSC post-tensioned girder should be not less than
(a) 25 mm (b) 50 mm (c) 100 mm

13.6 Excessive upward deflections are likely in the case of members designed as
(a) partially prestressed
(b) moderately prestressed
(c) fully prestressed

13.7 The minimum thickness of web of a long span PSCI-section girder should be not less than
(a) 100 mm (b) 150 mm (c) 300 mm

13.8 Failure of PSC beams due to fracture of steel is prevented by using steel of
(a) 0.35 per cent (b) 0.15 per cent (c) 0.2 per cent

13.9 According to the Indian Standard Code (IS: 1343-2012), the hypothetical tensile stress (N/mm^2) permitted for type-3 members for a limiting crack width of 0.1 mm using M-40 grade concrete is
(a) 4.8 (b) 4.4 (c) 4.1

13.10 The method which considers the maximum number of influencing parameters in the determination of crack widths at serviceability limit states in structural concrete members is
(a) IS: 456 code
(b) BS EN: 1992 code
(c) Gergely-Lutz formula

Answers to Objective-type Questions

13.1 (b)	13.2 (c)	13.3 (b)	13.4 (c)	13.5 (b)
13.6 (c)	13.7 (b)	13.8 (c)	13.9 (c)	13.10 (b)

14 Composite Construction of Prestressed and *in situ* Concrete

14.1 Composite Structural Members

In a composite construction, precast prestressed members are used in conjunction with the concrete cast *in situ*, so that the members behave as monolithic unit under service loads. Generally, the high-strength prestressed units are used in the tension zone while the concrete, which is cast *in situ* of relatively lower compressive strength, is used in the compression zone of the composite members. The composite action between the two components is achieved by roughening the surface of the prestressed unit on to which the concrete is cast *in situ*, thus giving a better frictional resistance, or by stirrups protruding from the prestressed unit into the added concrete, or by castellations on the surface of the prestressed unit adjoining the concrete which is cast *in situ*.

The phenomenon of differential shrinkage between the concrete cast *in situ* and the prestressed units also contributes to the monolithic action of the composite member. Composite construction was first tried for a motor-way bridge in 1940 and detailed calculations were presented by Morsch in 1943.

The advantages in using precast prestressed units in association with the *in situ* concrete are:

1. Appreciable saving in the cost of steel in a composite member compared with a reinforced or prestressed concrete member.
2. Sizes of precast prestressed units can be reduced due to the effect of composite action.
3. Low ratio of size of the precast unit to that of the whole composite member.
4. In many cases, precast prestressed units serve as supports and dispense with the form work for placement of *in situ* concrete.
5. Composite members are ideally suited for constructing bridge decks without the disruption of normal traffic.
6. Efficient utilisation of material in a composite section in which the low- and medium-strength concrete of *in situ* construction resists compressive forces while the high-strength prestressed units resist the tensile forces.
7. The precast prestressed units which require skilled labour and workmanship can be cast in a factory or casting yard and conveyed to the site of construction.

8. Combination of lightweight concrete for the cast *in situ* slab results in reduced dead loads, leading to economy in the overall costs.

14.2 Types of Composite Construction

The most common type of composite construction consists of a number of precast prestressed inverted T-beams, placed side by side and connected by a continuous top slab of *in situ* concrete[1]. This type of construction is widely used in the construction of bridge decks. Transverse prestressing is also used to develop monolithic action in the lateral direction. The dead weight of the deck can be considerably reduced by using voids or lightweight longitudinal cores in the space between the precast prestressed units. For large-span composite bridge decks of spans exceeding 30 m, the commonly used precast prestressed concrete units consist of I, unsymmetrical T or box sections[2]. The concrete cast *in situ* forms the deck slab, interconnecting the precast units. Typical cross-sections of bridge decks with different types of precast units are compiled in Fig. 14.1(a).

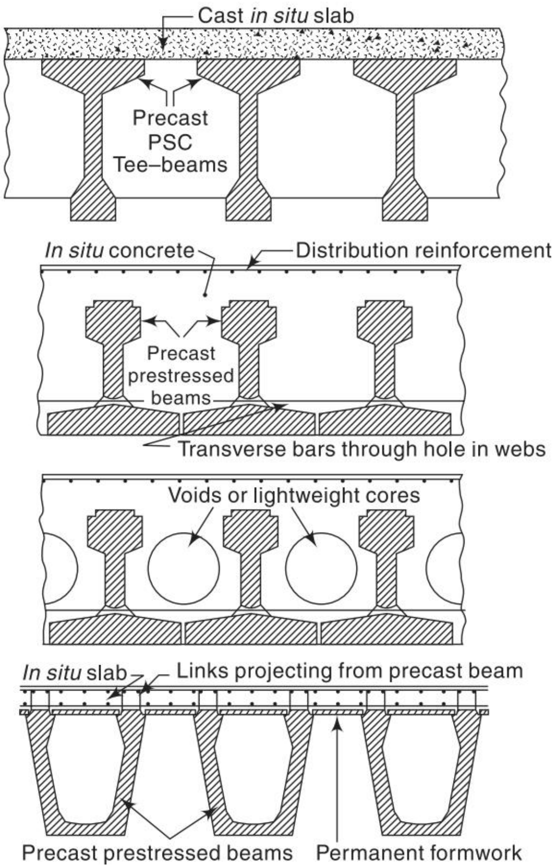

Fig. 14.1(a) *Composite bridge decks with precast prestressed elements*

The precast prestressed I- and T-beams have been standardised by the Cement and Concrete Association[3] for use in the construction of bridge decks of span varying from 7 to 36 m. Standard I and T units are extensively used as highway bridge beams in USA[4].

Typical cross-sectional details and the sectional properties of the standard inverted T-beams developed by the Ministry of Transport and Cement Concrete Association, London, is shown in Fig. 14.1(b) and Table 14.1.

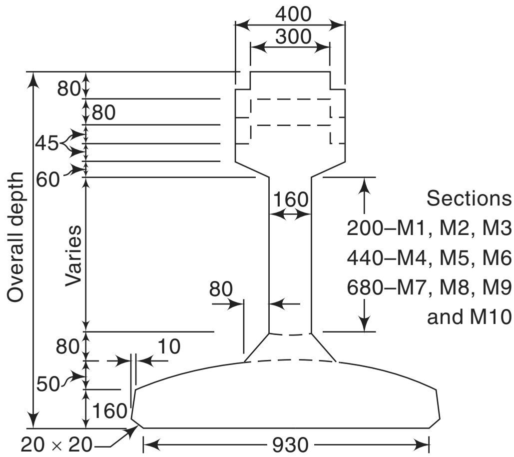

Fig. 14.1(b) *Cross-section of standard C and CA beams*

Table 14.1 *Section properties of MOT/C and CA standards beams*

Number	*Overall depth* (mm)	*Area* (mm^2)	*Height of Centroid Above Bottom Fibre* (mm)	*Section Moduli* ($mm^3 \times 10^6$)		*Dead Load* (kN/m)
				Top Fibre	*Bottom Fibre*	
M1	640	284,650	220	24.72	47.17	6.71
M2	720	316,650	265	35.64	61.04	7.46
M3	800	348,650	310	46.96	74.31	8.21
M4	880	323,050	302	43.41	85.95	7.61
M5	960	355,050	357	59.39	100.33	8.37
M6	1040	387,050	409	75.39	116.23	9.12
M7	1200	393,450	454	66.46	123.16	8.52
M8	1200	393,450	454	87.39	143.57	9.27
M9	1280	425,450	512	108.09	161.96	10.02
M10	1360	457,450	568	128.65	179.36	10.78

The use of prestressed concrete tie beam in a reinforced concrete truss considerably reduces the cross-sectional dimensions of the bottom chord member, which is subjected to high degree of tension in the case of large span trusses. Reinforced and prestressed concrete trusses are generally used for spans ranging from 18 to 36 m and this form of construction is ideally suited for industrial structures[5].

The dead-load stress developed in the precast prestressed units can be minimised by propping them while casting the concrete *in situ*. This method of construction is termed as *propped construction*. If the precast units are not propped while placing the *in situ* concrete, stresses are developed in the unit due to the self-weight of the member and the dead weight of the *in situ* concrete. This method of construction is referred to as *unpropped construction*.

14.3 Analysis of Stresses

The stresses developed in the prestressed and cast *in situ* concrete are computed using the simple bending equations until the stage of cracking. If the precast prestressed unit is unpropped during the placing of *in situ* concrete, the stresses that develop in the precast unit are sum of stresses due to the self-weight of the member, the prestressing force acting at a given eccentricity and that due to the self-weight of the *in situ* cast concrete. After the *in situ* concrete has hardened, the whole section is assumed to be monolithic and the stresses that develop due to subsequent live loads are computed using the properties of the composite section.

However, if the precast unit is propped during the placing of *in situ* concrete, the stresses developed due to the self-weight of the *in situ* concrete are computed using the section modulus of the composite section. In all cases the live-load stresses are based on the composite section. The typical stress distribution at various stages of loading in propped and unpropped constructions is shown in Fig. 14.2.

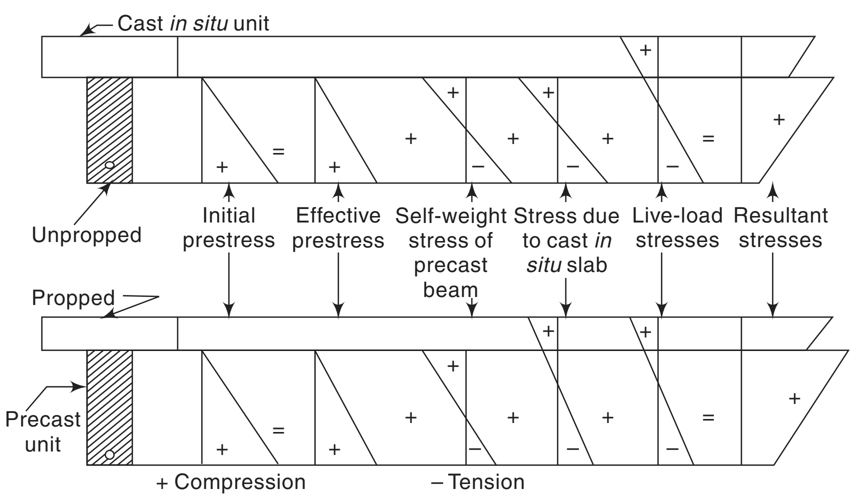

Fig. 14.2 *Stress distribution in unpropped and propped composite construction*

In most composite constructions which involve precast prestressed units and *in situ* cast concrete the latter is invariably of low- or medium-strength concrete while the former are generally made of high-strength concrete of grade exceeding M-35. Consequently, the modulus of elasticity of the two parts will be different. For computing live-load stresses, the effect of different moduli between the cast *in situ* and precast units is considered by using the modular ratio of precast to *in situ* concrete for calculating the area, centroid, second moment of area and second modulus of the equivalent composite section.

In most practical instances; the modulus of elasticity of *in situ* concrete of grade M-20 will be about 25 kN/mm^2, while the modulus of concrete in precast prestressed units could vary from 28 to 36 kN/mm^2 for concrete grades of M-30 to M-60. Hence, the modular ratio varies in the range of 1.1 to 1.5. However, this value could be larger if lightweight concrete with a modulus in the range of 5 to 12 kN/mm^2 is used in conjunction with precast units made of normal-weight aggregates.

The computation of stresses developed at the various stages in precast pretensioned and *in situ* cast concrete is illustrated by the following examples.

Example 14.1 A precast pretensioned beam of rectangular section has a breadth of 100 mm and a depth of 200 mm. The beam with an effective span of 5 m, is prestressed by tendons with their centroids coinciding with the bottom kern. The initial force in the tendons is 150 kN. The loss of prestress may be assumed to be 15 per cent. The beam is incorporated in a composite T-beam by casting a top flange of breadth 400 mm and thickness 40 mm. If the composite beam supports a live load of 8 kN/m^2, calculate the resultant stresses developed in the precast and *in situ* cast concrete assuming the pretensioned beam as (a) unpropped and (b) propped during the casting of the slab. Assume the same modulus of elasticity for concrete in precast beam and *in situ* cast slab.

Solution.

Section properties of the pretensioned beam

$$A = (100 \times 200) = 20000 \text{ mm}^2$$

$$Z = \left[\frac{(100 \times 200^2)}{6}\right] = (667 \times 10^3) \text{ mm}^3$$

Initial prestressing force, $P = 150$ kN

Stresses due to prestressing force $= \left(\dfrac{2P}{A}\right)$

$$= \left[\frac{(2 \times 150 \times 10^3)}{(20000)}\right] = 15 \text{ N/mm}^2$$ at the bottom and zero at the top fibre, respectively.

Effective prestress after losses $= (0.85 \times 15) = 12.8$ N/mm^2

Self-weight of the precast beam $= (0.1 \times 0.2 \times 24 \times 10^3) = 480$ N/m

Self-weight moment = $(0.125 \times 480 \times 5^2) = 1500$ Nm

Stresses at top and bottom fibre = $\left[\dfrac{(1500000)}{(667 \times 10^3)}\right] = \pm 2.25$ N/mm^2

Self-weight of *in situ* cast slab = $(0.04 \times 0.4 \times 24 \times 10^3) = 384$ Nm
Moment due to slab weight = $(0.125 \times 384 \times 5^2) = 1200$ Nm

Stresses due to slab weight in the precast section = $\left[\dfrac{(1200000)}{(667 \times 10^3)}\right] = \pm 1.8$ N/mm^2

Section properties of the composite section

Distance of the centroid from the top fibre = 87 mm

Second moment of area, $I = (1948 \times 10^5)$ mm^4

Second moduli, $Z_t = (225 \times 10^4)$ mm^3

$Z_b = (128 \times 10^4)$ mm^3

Live load on the composite section = $(0.4 \times 1 \times 8000) = 3200$ N/m
Maximum live-load moment = $(0.125 \times 3200 \times 5^2) = 10000$ Nm
Live load stresses in the composite section

$$\text{At top} = \left(\frac{10^7}{225} \times 10^4\right) = 4.45 \text{ N/mm}^2 \text{ (compression)}$$

$$\text{At bottom} = \left(\frac{10^7}{128} \times 10^4\right) = 7.85 \text{ N/mm}^2 \text{ (tension)}$$

If the pretensioned beam is propped, the self-weight of the slab acts on the composite section.
Moment due to slab weight = 1200 Nm
Stresses due to this moment in the composite section

$$\text{At top} = \left(\frac{1200000}{225 \times 10^4}\right) = 0.53 \text{ N/mm}^2 \text{ (compression)}$$

$$\text{At bottom} = \left(\frac{1200000}{128 \times 10^4}\right) = 0.94 \text{ N/mm}^2 \text{ (tension)}$$

The distribution of stresses for the various stages of loading for the propped and unpropped construction is shown in Fig. 14.3.

Example 14.2 Compute the resultant stresses developed in the precast pretensioned beam and cast *in situ* slab for the unpropped case if the modulus of elasticity of concrete in slab and beam are different. Assume E_c (prestressed beam) = 35 kN/mm^2.

Solution.

Ratio of modulus of elasticity = $\left(\dfrac{35}{28}\right) = 1.25$

Properties of equivalent composite section

Area of *in situ* slab = $(400 \times 40) = 16000 \text{ mm}^2$
Area of prestressed beam = $(200 \times 100) = 20000 \text{ mm}^2$

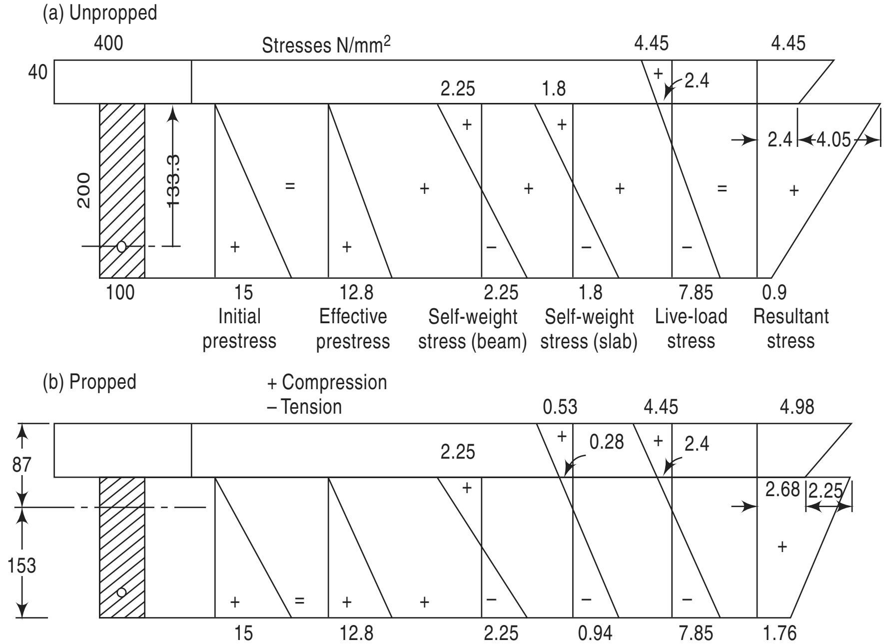

Fig. 14.3 *Stresses in precast pretensioned beam and cast in situ slab*

The centroid of the equivalent composite section is determined by taking moments about an axis passing through the soffit of the beam.

If y = distance of the centroid from the soffit,

$$(16 + 1.25 \times 20)\, 10^3 \times y = (16 \times 10^3 \times 220) + (1.25 \times 20 \times 10^3 \times 100)$$

$$\therefore \qquad y = 146 \text{ mm}$$

Second moment of area of the equivalent composite section is given by,

$$I_e = \left[\left(\frac{400 \times 40^3}{12} + 16 \times 10^3 \times 74^2\right) + 1.25\left(\frac{100 \times 200^3}{12} + 20 \times 10^3 \times 46^2\right)\right]$$

$$= (226 \times 10^6) \text{ mm}^4.$$

Live-Load Moment = 10^7 N mm

Stresses developed in cast in situ slab

$$\text{At the top of slab} = \frac{(10^7 \times 94)}{(226 \times 10^6)} = +4.15 \text{ N/mm}^2$$

$$\text{At the bottom of slab} = \frac{(10^7 \times 54)}{(226 \times 10^6)} = +2.2 \text{ N/mm}^2$$

Stresses developed in the pretensioned beam

$$\text{At top} = \left[\frac{(10^7 \times 54)}{(226 \times 10^6)}\right] \times 1.25 = +2.75 \text{ N/mm}^2$$

$$\text{At bottom} = \left[\frac{(10^7 \times 146)}{(226 \times 10^6)}\right] \times 1.25 = -8.1 \text{ N/mm}^2$$

The resultant stresses developed in the precast beam and *in situ* cast slab are shown in Fig. 14.4. The effect of using concrete with different moduli of elasticity in beam and slab results in an increase in the compressive stress at the top fibre of the beam with a corresponding decrease in the compressive stresses developed in the *in situ* cast slab.

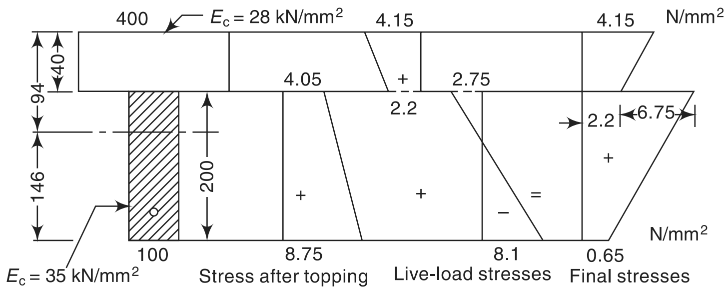

Fig. 14.4 *Stress distribution*

14.4 Differential Shrinkage

In composite members using precast prestressed units *in situ* cast concrete, a considerable proportion of the total shrinkage will have already taken place in the precast prestressed beam before the casting and hardening of the *in situ* concrete. Due to the high water/cement ratios used in the *in situ* concrete, there will be considerable shrinkage of this part in the composite section. Consequently, the differential shrinkage between the precast and *in situ* cast units results in stresses in both. The magnitude of differential shrinkage is influenced by the composition of concrete and the environmental conditions to which the composite member is exposed. In the absence of exact data, a general value of 100 micro strains is provided for in the British code BS: 8110[6] for computing shrinkage stresses.

A reasonable estimation of stresses developed due to differential shrinkage may be made using the following assumptions:

1. The shrinkage is uniform over the *in situ* part of the section, and
2. Effect of creep and increase in modulus of elasticity with age and the component of shrinkage, which is common to both the units is negligible.

The method of computing the stresses is illustrated in Fig. 14.5, in which the *in situ* cast slab is first allowed to undergo the full amount of differential shrinkage ε_{cs}. Tensile forces of intensity N_{sh} are then applied to each end acting at the centroid of the cast *in situ* slab so that the slab is restored to the length of the precast element. Consequently, the uniform tensile stress induced in the *in situ* concrete is $\varepsilon_{cs} E_c$ and the magnitude of the tensile force is computed as $N_{sh} = \varepsilon_{cs} E_c A_i$, where A_i = area of the *in situ* concrete section

E_c = modulus of elasticity of the *in situ* concrete

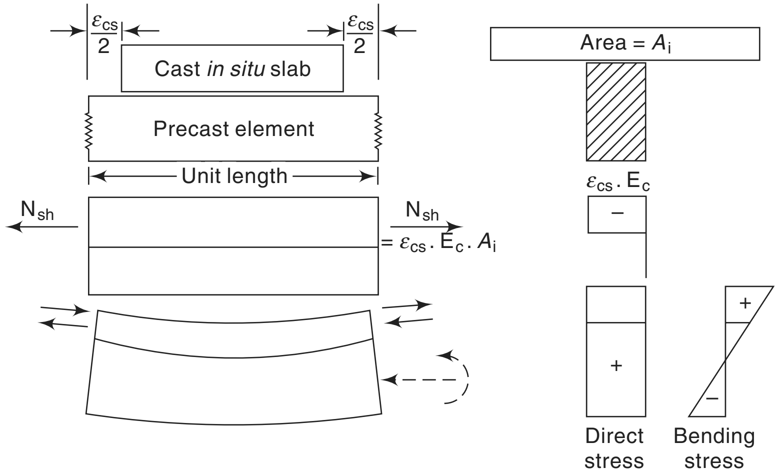

Fig. 14.5 *Stresses due to differential shrinkage*

The composite member is in a state of internal equilibrium without any external forces acting on it. Hence, the tensile force must be balanced by the application of a compressive force of equal magnitude along the same line. The compressive force applied at the centroid of the cast *in situ* slab is equivalent to a direct compressive force acting at the centroid of the composite section together with a bending moment which will induce direct and bending stresses in the composite section. These stresses are superposed on the existing tensile stresses in the cast *in situ* slab to compute the final stresses.

Example 14.3 A composite T-beam is made up of a pretensioned rib 100 mm wide and 200 mm deep, and a cast *in situ* slab 400 mm wide and 40 mm thick having a modulus of elasticity of 28 kN/mm^2. If the differential shrinkage is 100×10^{-6} units, determine the shrinkage stresses developed in the precast and cast *in situ* units.

Solution.

Differential shrinkage, $\varepsilon_{cs} = 100 \times 10^{-6}$

Area of *in situ* concrete, $A_i = (400 \times 40) = 16000$ mm^2

Uniform tensile stress induced in the cast *in situ* slab = $\varepsilon_{cs} E_c$

$$= (100 \times 10^{-6})(28 \times 10^3) = 2.8 \text{ N/mm}^2$$

Force, $N_{sh} = \varepsilon_{cs} E_c A_i = [(100 \times 10^{-6})\ (28 \times 10^3)\ (16 \times 10^3)] = (44.8 \times 10^3)$N

The centroid of the composite section is located 87 mm from the top fibre. Eccentricity of the compressive force, N_{sh}, from the centroid of the composite section = (87 – 20) = 67 mm

$\therefore$ Moment = $(44.8 \times 10^3) \times 67 = 3 \times 10^6$ N mm

Second moment of area of the composite section = (1948×10^5) mm^4

Section moduli for the various fibres:

Top fibre, $Z_t = (225 \times 10^4)\ \text{mm}^3$

Bottom fibre, $Z_b = (128 \times 10^4)\ \text{mm}^3$

Junction, $Z_j = (414 \times 10^4)\ \text{mm}^3$

$$\text{Direct compressive stress} = \left[\frac{(44.8 \times 10^3)}{(36 \times 10^3)}\right] = 1.24\ \text{N/mm}^2$$

Bending stress:

$$\text{Top fibre} = \frac{(3 \times 10^6)}{(225 \times 10^4)} = 1.33\ \text{N/mm}^2$$

$$\text{Bottom fibre} = \frac{(3 \times 10^6)}{(128 \times 10^4)} = 2.34\ \text{N/mm}^2$$

$$\text{Junction} = \frac{(3 \times 10^6)}{(414 \times 10^4)} = 0.72\ \text{N/mm}^2$$

Differential shrinkage stresses:

(a) In precast pretensioned beam (+ compression – tension)
At the top of beam = (1.24 + 0.72) = 1.96 N/mm²
At the bottom of beam = (1.24 – 2.34) = –1.10 N/mm²

(b) In *in situ* cast slab,
At the top of slab = (1.24 + 1.33 – 2.8) = –0.23 N/mm²
At the bottom of slab (junction) = (1.24 + 0.72 – 2.8) = –0.84 N/mm²

The resultant shrinkage stress distribution is shown in Fig. 14.6.

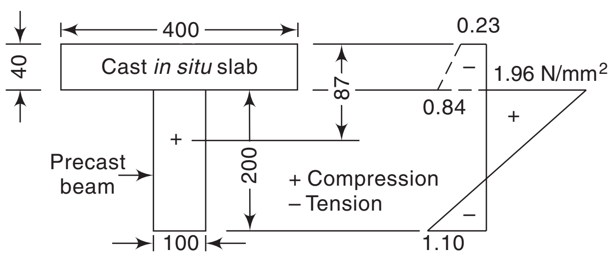

Fig. 14.6 *Stresses due to differential shrinkage*

Example 14.4 A composite beam of rectangular section is made up of a pretensioned inverted T-beam having a slab thickness and width of 150 and 1000 mm, respectively. The rib size is 150 mm by 850 mm. The cast *in situ* concrete has a thickness and width of 1000 mm with a modulus of elasticity of 30 kN/mm². If the differential shrinkage is 100×10^{-6} units, estimate the shrinkage stresses developed in the precast and cast *in situ* units.

Solution.

Differential shrinkage, $\varepsilon_{cs} = 100 \times 10^{-6}$

Referring to Fig. 14.7,

Area of *in situ* concrete, $A_i = 872500\ \text{mm}^2$

Area of the composite section, $A_c = 1150 \times 10^3\ \text{mm}^2$

Uniform tensile stress induced in the cast *in situ* slab

$$= \varepsilon_c E_{cs} = [(100 \times 10^{-6})(30 \times 10^3)] = 3.0 \text{ N/mm}^2$$

Force, $N_{sh} = \varepsilon_c E_c A_i = [(100 \times 10^{-6})(30 \times 10^3)(872500)] = 2617500 \text{ N}$

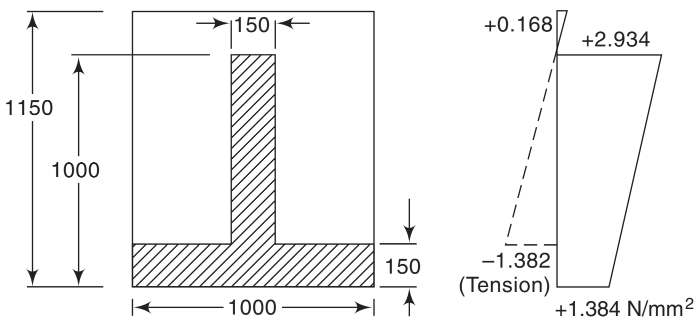

Fig. 14.7 *Differential shrinkage stresses*

The centroid of the composite section is located 575 mm from the top fibre. Eccentricity of the compressive force, N_{sh}, from the centroid of the composite section = (575 – 500) = 75 mm

$\therefore$ Moment = $(2617500) \times 75 = (196.3 \times 10^6)$ N mm

Second moment of area of the composite section = (126739×10^6) mm^4

Section moduli for the various fibres

Pretensioned beam: Top fibre = (298×10^6) mm^3

Bottom fibre = (220×10^6) mm^3

In situ slab: Top fibre = (220×10^6) mm^3

Bottom fibre = (298×10^6) mm^3

Direct compressive stress in the composite section

$$= \left(\frac{2617500}{1150 \times 10^3}\right) = 2.276 \text{ N/mm}^2$$

Bending stress

$$\text{Top fibre} = \left[\frac{(196.3 \times 10^6)}{(220 \times 10^6)}\right] = 0.892 \text{ N/mm}^2$$

$$\text{Bottom fibre} = \left[\frac{(196.3 \times 10^6)}{(220 \times 10^6)}\right] = 0.892 \text{ N/mm}^2$$

$$\text{Junction} = \left[\frac{(196.3 \times 10^6)}{(298 \times 10^6)}\right] = 0.658 \text{ N/mm}^2$$

Differential shrinkage stresses

(a) In the precast pretensioned beam (compression +ve),
At the top of beam = (2.276 + 0.658) = 2.934 N/mm^2
At the bottom of beam = (2.276 – 0.892) = 1.384 N/mm^2

(b) In *in situ* cast slab

At the top of slab = (2.276 + 0.892 – 3.00) = 0.168 N/mm^2

At the bottom of slab = (2.276 – 0.658 – 3.00) = –1.382 N/mm^2

The resultant shrinkage stress distribution is shown in Fig. 14.7.

14.5 Deflection of Composite Members

In the case of composite members, deflections are computed by taking into account the different stages of loading as well as the differences in the modulus of elasticity of concrete in the precast prestressed unit and the *in situ* cast element. The initial deflection due to the prestress, self-weight of the beam and the weight of the *in situ* cast concrete, if the beam is not propped, is computed on the basis of the section and the modulus of elasticity of the precast unit. The live-load deflection is always estimated using composite section properties. If the precast beam is propped during construction, the deflection due to the dead weight of *in situ* concrete is also computed on the basis of the composite section.

When the modulus of elasticity of the precast and *in situ* cast concretes are different, the flexural rigidity is worked out by computing the equivalent second moment of area of the composite section using the modular ratio as outlined in Example 14.2. The deflection computed under service loads should not exceed the limiting values prescribed in the codes as discussed in Section 11.6. The method of estimating deflections in composite members is illustrated in the following examples:

Example 14.5 A composite T-girder of span 5 m is made up of a pretensioned rib, 100 mm wide and 200 mm deep, with an, *in situ* cast slab, 400 mm wide and 40 mm thick. The rib is prestressed by a straight cable having an eccentricity of 33.33 mm and carrying an initial force of 150 kN. The loss of prestress may be assumed to be 15 per cent. Check the composite T-beam for the limit state of deflection if it supports an imposed load of 3.2 kN/m for (a) unpropped construction and (b) propped construction. Assume a modulus of elasticity of 35 kN/mm^2 for both precast and *in situ* cast elements.

Solution.

Self-weight of precast beam = 0.48 N/mm

Self-weight of *in situ* cast slab = 0.384 N/mm

Imposed load on composite section = 3.2 N/mm

I for precast section = (667×10^5) mm^4

I for composite section = (1948×10^5) mm^4

Modulus of elasticity, $E = (35 \times 10^3)$ N/mm^2

$$\text{Deflection due to prestress} = \left(\frac{PeL^2}{8EI}\right) = \left[\frac{150 \times 10^3 \times 33.33 \times 5000^2}{8 \times 35 \times 10^3 \times 667 \times 10^5}\right]$$

$$= 6.7 \text{ mm (upward)}$$

Effective deflection after losses = (0.85 × 6.7) = 5.7 mm
Deflection due to self-weight of precast beam

$$\left(\frac{5gL^4}{384EI}\right) = \left[\frac{5 \times 0.48 \times 5000^4}{384 \times 35 \times 10^3 \times 667 \times 10^5}\right] = 1.7 \text{ mm}$$

Deflection of precast beam due to self-weight of cast *in situ* slab

$$= \left[\frac{(1.7 \times 0.384)}{(0.48)}\right] = 1.34 \text{ mm}$$

Deflection of composite beam due to live load

$$= \left[\frac{5 \times 3.2 \times 5000^4}{384 \times 35 \times 10^3 \times 1948 \times 10^5}\right] = 3.83 \text{ mm}$$

Deflection of composite beam due to self-weight of cast *in situ* slab

$$= \left(\frac{5 \times 0.384 \times 5000^4}{384 \times 35 \times 10^3 \times 1948 \times 10^5}\right) = 0.47 \text{ mm}$$

(a) Unpropped construction:
Resultant deflection under service loads = (–5.7 + 1.7 + 1.34 + 3.83) = 1.17 mm

(b) Propped construction:
Resultant deflection under service loads = (–5.7 + 1.7 + 0.47 + 3.83) = 0.30 mm

According to IS: 1343, the maximum permissible deflection under service loads is limited to a value of (span/250) = (5000/250) = 20 mm.

However, this value includes the long-term effects of creep and shrinkage. If the creep coefficient is assumed to be 3.0, final resultant deflections for unpropped and propped constructions are 3.51 and 0.9 mm, respectively, which are well within the permissible limits specified in the code.

Example 14.6 Estimate the deflections under service loads for the composite T-beam of Example 14.5, if the modulus of elasticity of concrete in the precast beam and *in situ* cast slab are 35 and 28 kN/mm^2, respectively.

Solution.

Ratio of modulus of elasticity, α_e = (35/28) = 1.25
The second moment of area of the equivalent composite section is computed as in Example 14.2.

$$I_e = (226 \times 10^6) \text{ mm}^4$$
$$E = (28 \times 10^3) \text{ N/mm}^2$$

Deflection due to live load only on composite section

$$= \left[\frac{5 \times 3.2 \times 5000^4}{384 \times 28 \times 10^3 \times 226 \times 10^6}\right] = 4.12 \text{ mm}$$

Deflection due to self-weight of cast *in situ* slab on composite section

$$= \left(\frac{4.12}{3.2} \times 0.384\right) = 0.49 \text{ mm}$$

(a) Unpropped construction:

Resultant deflection under service loads = (–5.7 + 1.7 + 1.34 + 4.12)
= 1.46 mm

(b) Propped construction:

Resultant deflection under service loads = (–5.7 + 1.7 + 0.49 + 4.12)
= 0.61 mm

14.6 Stresses at Serviceability Limit State

The maximum permissible stresses in the precast prestressed concrete and the *in situ* cast concrete are mainly governed by the compressive strength of concrete in the respective elements. In general, the permissible stresses in a precast prestressed concrete are governed by the normal rules used for prestressed concrete as detailed in Table 2.1. However, certain exceptions are made regarding high stresses developed at the interface of the precast and *in situ* cast elements. The British code BS: 8110 provides for a higher value of compressive stress, equal to 0.5 f_{cu}, which is 50 per cent higher than the normally allowable value in prestressed elements.

The higher value of compressive stress is permissible only in composite sections with the stipulation that the failure of the section is due to excessive elongation of steel. This requirement is to safeguard against the explosive compressive failure of the concrete at the limit state of collapse.

The permissible flexural tensile stress in the *in situ* concrete at the contact surface with the prestressed element, as prescribed in the British code BS EN: 1992–1–1 varies from 3.2 to 5.0 N/mm^2 corresponding to various grades of concrete shown in the following table.

These stresses may be increased by up to 50 per cent, provided that the allowable tensile stress for the prestressed unit is reduced by the same amount. The higher values of flexural tensile stresses are permitted since it has been proved by experiments that the development of cracking, which is visible, is prevented by the uncracked prestressed concrete which is bonded to the *in situ* concrete.

Grade of in situ concrete	*Allowable flexural tensile stress,* N/mm^2
25	3.2
30	3.6
40	4.4
50	5.0

14.7 Flexural Strength of Composite Sections

The ultimate strength of composite prestressed sections in flexure is governed by the same principles used for ordinary prestressed sections discussed in Chapter 7. In the case of composite sections, the percentage of tensioned reinforcement is less than that in most simple beams, so that the section is invariably under-reinforced. The compression zone generally consists entirely of *in situ* concrete of lower compressive strength, and the value of the cube strength of concrete to be used in flexural strength equations will obviously be that of *in situ* cast concrete. However, if the compression zone contains a part of the precast element, the average compressive strength computed by considering the cross-sectional areas of *in situ* and precast concrete is used in the computations of compressive force. The following examples illustrate the method of estimating the ultimate flexural strength of composite sections.

Example 14.7 The cross-section of a composite beam is of T-section having a pretensioned rib, 80 mm wide and 240 mm deep, and an *in situ* cast slab, 350 mm wide and 80 mm thick. The pretensioned beam is reinforced with eight wires of 5 mm diameter with an ultimate tensile strength of 1600 N/mm^2, located 60 mm from the soffit of the beam. The compressive strength of concrete in the *in situ* cast and precast elements is 20 and 40 N/mm^2, respectively. If adequate reinforcements are provided to prevent shear failure at the interface, estimate the flexural strength of the composite section.

Solution.

$$A_p = (20 \times 8) = 160 \text{ mm}^2 \qquad f_{ck} = 20 \text{ N/mm}^2$$

$$f_p = 1600 \text{ N/mm}^2 \qquad b = 350 \text{ mm} \qquad d = 240 \text{ mm}$$

The effective reinforcement ratio is given by

$$\left(\frac{f_p A_p}{f_{ck} b d}\right) = \left(\frac{1600 \times 160}{20 \times 350 \times 240}\right) = 0.152$$

Referring to Table 7.1,

$$\left(\frac{f_{pu}}{0.87 f_p}\right) = 1.0$$

$$\therefore \qquad f_{pu} = (0.87 \times 1600) = 1392 \text{ N/mm}^2$$

$$\left(\frac{x_u}{d}\right) = 0.326$$

$$\therefore \qquad x_u = (0.326 \times 240) = 78 \text{ mm}$$

Since $x_u = 78$ mm is less than the thickness of the flange (80 mm), the stress block is entirely within the *in situ* concrete. Hence, the flexural strength of the composite section is obtained as

$$M_u = f_{pu} A_p (d - 0.42\, x_u) = \left[1392 \times 160 \,\frac{(240 - 0.42 \times 78)}{10^6}\right] = 46.15 \text{ kN m}$$

Example 14.8 A composite beam of rectangular section is made up of a precast prestressed inverted T-beam having a rib, 100 mm by 780 mm, and a slab, 400 mm wide and 200 mm thick. The *in situ* cast concrete has a thickness of 800 mm and a width of 400 mm. The precast T-beam is reinforced with high-tensile wires (f_{pu} = 1600 N/mm^2) having an area of

800 mm^2 and located 100 mm from the soffit of the beam. If the cube strength of concrete in the *in situ* cast slab and prestressed beam is 20 and 40 N/mm^2, respectively, estimate the flexural strength of the composite section.

Solution. The compression zone of the composite beam comprises the precast and the *in situ* cast elements of which the former is about 25 per cent and the latter 75 per cent. Hence, the average compressive strength of concrete in the stress block is given by

$$f_{ck} = [(40 \times 0.25) + (20 \times 0.75)] = 25 \text{ N/mm}^2$$

$$f_p = 1600 \text{ N/mm}^2 \qquad d = 900 \text{ mm}$$

$$A_p = 800 \text{ mm}^2 \qquad b = 400 \text{ mm}$$

The effective reinforcement ratio is given by

$$\left(\frac{A_p f_p}{bd\, f_{ck}}\right) = \left(\frac{800 \times 1600}{400 \times 900 \times 25}\right) 0.142$$

From Table 7.1,

$$\left(\frac{f_{pu}}{0.87 f_p}\right) = 1.00$$

$\therefore$ $$f_{pu} = (0.87 \times 1600) = 1392 \text{ N/mm}^2$$

and $$\left(\frac{x_u}{d}\right) = 0.29$$

or $$x_u = (0.29 \times 900) = 261 \text{ mm}$$

$\therefore$ $$M_u = f_{pu} A_p (d - 0.42 x_u)$$

$$= \left[\frac{1392 \times 800(900 - 0.42 \times 261)}{10^6}\right] = 880 \text{ kN m}$$

14.8 Shear Strength of Composite Sections

The support sections of composite members where web shear cracks are likely to develop should be checked under service loads for safety against cracking in shear. As outlined in Section 8.1, the principal tension developed in the webs of precast elements in the composite section is computed using the values of the shear and bending stresses in the section. If the principal tensile stress exceeds the design tensile strength of concrete, suitable reinforcements are to be designed according to the elastic design principles.

The ultimate shear strength of composite sections with web-shear or flexure-shear cracks is computed using the empirical expressions suggested in the British, American and Indian standard codes presented in Section 8.2. If the shear at the section under design ultimate loads exceeds the shear strength, suitable shear reinforcements are designed according to the design code provisions outlined in Section 8.3. The composite action of the integral unit is mainly dependent upon an effective shear connection at the contact surface between the precast and *in situ* cast elements.

Effective bonding between the two parts of a composite beam may be developed by providing castellations in the precast unit or by roughening the contact surface of the precast unit before placing the *in situ* concrete, or by projecting reinforcements from the precast unit which serve as shear connectors[7]. In the design of shear connection, it is generally assumed that the natural bond at the interface contributes a part of the required shear resistance, depending upon the strength of the *in situ* cast concrete and the roughness of the precast element. Any extra shear resistance over and above this should be provided by shear connectors.

Horizontal shear is generally governed by the ultimate limit state. The British code (BS EN: 1992–1–1) identifies three types of surfaces in the design provisions for the maximum permissible design ultimate horizontal shear stress at the interface.

The horizontal shear force, at the interface of the precast and *in situ* components, due to the design ultimate loads is the total compression from that part of the compression zone above the interface, calculated from the ultimate bending moment. The average horizontal design shear stress is computed by dividing the horizontal shear force by the area, which is obtained as the product of the contact width of the bear and its length between the point of zero moment. The average design shear stress is then distributed in proportion to the vertical design shear force diagram to obtain the horizontal shear stress at any point along the length of the members. The design shear stress should not exceed the values compiled in Table 14.2 for different types of surfaces.

Table 14.2 *Design ultimate horizontal shear stress at interface (BS EN: 1992–1–1)*

Precast Unit	*Surface Type*	*Grade of in situ Concrete* (N/mm^2)		
		25	*30*	*40 and over*
Without links	As cast or as extruded	0.4	0.55	0.65
	Brushed, screeded or rough tamped	0.6	0.65	0.75
	Washed to remove laitance or treated with retarder and cleaned	0.7	0.75	0.80
With nominal links projecting into *in situ* concrete	As cast or as extruded	1.2	1.8	2.0
	Brushed, screeded or rough tamped	1.8	2.0	2.2
	Washed to remove laitance or treated with retarder and cleaned	2.1	2.2	2.5

When links are provided, their cross-sectional area should be at least 0.15 per cent of the contact area. The spacing of links in T-beam ribs with composite flanges should exceed neither four times the minimum thickness of the *in situ* concrete nor 600 mm. In addition, the links should be adequately anchored on both sides of the interface.

When the horizontal shear stress exceeds the values given in Table 14.2, links are designed to resist the total horizontal shear force. The amount of steel required A_h (mm^2/m) is obtained from the equation,

$$A_h = \left(\frac{1000\, b\tau_h}{0.87 f_y}\right)$$

where τ_h = horizontal shear stress
b = contact width
f_y = characteristic strength of reinforcement

According to the American code ACI 318M–2011[8], the horizontal shear stress at the interface for the ultimate limit state is computed using the expression

$$\tau_h = \left(\frac{V_u}{\phi b d}\right)$$

where τ_h = ultimate horizontal shear stress
V_u = ultimate shear force
b = contact width of precast section
d = effective depth measured from the extreme compression fibre to the centroid of the prestressing reinforcement.

The permissible values of the horizontal shear stress for different types of contact surfaces is specified as:

1. 0.6 N/mm^2, when ties are not provided and the contact surface of the precast element is free of laitance and intentionally roughened to an amplitude of 5 mm.
2. 0.6 N/mm^2, when minimum vertical ties, according to Section 8.3.3, are provided and the contact surface is not roughened.
3. 2.5 N/mm^2, when minimum vertical ties are provided and the contact surface is roughened to an amplitude of 5 mm.
4. When shear stress exceeds 2.5 N/mm^2, then shear friction reinforcement is to be designed and the required area of reinforcements is given by

$$A_{vf} = \left(\frac{V_u}{\phi f_y \mu}\right)$$

where f_y = characteristic tensile strength of tie reinforcement
ϕ = capacity reduction factor having a value of 0.85 for shear computations
μ = coefficient of friction having the following values:

(a)	Concrete placed monolithically	1.4 λ
(b)	Concrete placed against hardened concrete with surface intentionally roughened	1.0 λ
(c)	Concrete placed against hardened concrete not intentionally roughened	0.6 λ

(d) Concrete anchored to rolled structural steel by headed studs or by reinforcing bars — $0.7\,\lambda$

where λ = 1.0 for normal density concrete
= 0.85 for "sand low density" concrete
= 0.75 for "all low density" concrete

The ties consisting of single bars, multiple-leg-stirrups or vertical legs of welded-wire fabric should have a spacing not exceeding four times the least dimension of the supported element, nor 600 mm, whichever is less.

The Indian Standard Code IS: 1343 does not make any specific recommendations regarding the shear stresses in composite sections. However, the general recommendations regarding shear and principal tensile stresses which are detailed in Section 8.1 can as well be used for composite sections.

Example 14.9 A precast pretensioned rib 100 mm wide and 200 mm deep, is to be connected to an M-25 Grade cast *in situ* concrete slab 400 mm wide and 40 mm thick. Estimate the ultimate shearing force which will cause separation of the two elements for the following two cases conforming to BS EN: 1992–1–1 code specifications:

(a) If the surface is rough tamped and without links to withstand a horizontal shear stress of 0.6 N/mm^2, and
(b) With nominal links and the contact surfaces are as cast to withstand a horizontal shear stress of 1.2 N/mm^2.

Assume the moduli of elasticity of precast and cast *in situ* concrete are equal.

Solution.

Area of cast *in situ* slab = $A = (400 \times 40) = 16000$ mm^2
Width of precast rib = b = 100 mm
Centroid of the composite T-section located at 87 mm from top
Second moment of area of composite section = $I = (1948 \times 10^5)$ mm^4
Distance of centroid of cast *in situ* slab from centroid of composite section
$y = (87 - 20) = 67$ mm

Case (a)

If V_u = ultimate shearing force
τ = Shear stress = 0.6 N/mm^2

$$\tau = \left[\frac{V_u A y}{I b}\right]$$

$$V_u = \left[\frac{\tau I b}{A y}\right] = \left[\frac{(0.6 \times 1948 \times 10^5 \times 100)}{(16000 \times 67)}\right] = 10902 \text{ N} = 10.902 \text{ kN}$$

Case (b) When nominal links are used, the design ultimate shear stress, τ = 1.2 N/mm^2. Ultimate shear resistance is expressed as

$$V_u = \left[\frac{\tau I b}{A y}\right] = \frac{(1.2 \times 1948 \times 10^5 \times 100)}{(16000 \times 67)} = 21804 \text{ N} = 21.804 \text{ kN}$$

Example 14.10 A composite bridge deck is made up of a pretensioned rectangular beam having a width of 300 mm and depth of 600 mm. The cast *in situ* slab is 500 mm wide and 150 mm thick. The ultimate shear force at the support section is 392 kN. (a) Estimate the horizontal shear stress at the junction of precast and *in situ* slab, (b) Neglecting the shear resistance between the surfaces, design suitable vertical reinforcements to resist the shear force at support section using Fe-415 HYSD bars.

Solution.

Design ultimate shear force = $V_u = 392$ kN

Area of cast *in situ* slab = $A = (500 \times 150) = 75000$ mm^2

Centroid of composite section is located at 340 mm from the top fibre

Second moment of area of composite section = $I = (12985 \times 10^4)$ mm^4

Fe-415 Grade HYSD bars for link reinforcement.

First moment of area of cast *in situ* slab about the centroid is calculated as,

$$Ay = [(500 \times 150)]\,[(340 - 75)] = (19.875 \times 10^6)\text{ mm}^3$$

(a) Shear stress at the junction = $\tau = \left[\dfrac{V_u Ay}{Ib}\right] = \left[\dfrac{392 \times 10^3 \times 19.875 \times 10^6}{12985 \times 10^6 \times 300}\right]$

$$= 2\text{ N/mm}^2$$

(b) Effective depth of the composite section = $d = (750 - 50) = 700$ mm

Using 10 mm diameter Fe-415 HYSD bars two-legged vertical links, spacing is computed as

$$S_v = \left[\frac{A_{sv}\,0.87\,f_y\,d}{V_u}\right] = \left[\frac{2 \times 79 \times 0.87 \times 415 \times 700}{392 \times 10^3}\right] = 101\text{ mm}$$

Adopt 10 mm diameter vertical links at a spacing of 100 mm near the supports.

Example 14.11 A composite beam, 5 m span is of T-section and consists of a precast prestressed concrete rectangular beam, 100 mm wide and 240 mm deep. The cast *in situ* slab is 400 mm wide and 60 mm thick. The prestressed beam contains high-tensile steel of area 180 mm^2 located 50 mm from the soffit. The grade of concrete in the prestressed beam and cast *in situ* slab is M-40 and M-25, respectively. $f_{pu} = 1600$ N/mm^2 and the ratio of effective to ultimate tensile stress in tendons is 0.5. Design suitable reinforcements for resisting horizontal shear between the prestressed beam and cast *in situ* slab using the provisions of

(a) British code

(b) American code

Solution. Given data:

f_{cu} (*in situ* concrete) = 25 N/mm^2

f_{cu} (prestressed concrete) = 40 N/mm^2

$A_{ps} = 180$ mm^2

$f_{pu} = 1600$ N/mm^2

Effective depth, $d = 250$ mm

The ultimate moment capacity of the composite section is first computed.

$$\left(\frac{f_{pu}A_{ps}}{f_{ck}bd}\right) = \left(\frac{1600 \times 180}{25 \times 400 \times 250}\right) = 0.115$$

From Table 7.3,

$$\left(\frac{f_{pb}}{0.87 f_{pu}}\right) = 0.99$$

$\therefore \qquad f_{pb} = (0.87 \times 1600 \times 0.99) = 1378 \text{ N/mm}^2$

and $\qquad \left(\frac{x}{d}\right) = 0.26$

$$x = (0.26 \times 250) = 65 \text{ mm}$$

Depth of the rectangular stress block $= 0.9\,x = (0.9 \times 65) = 58.5$ mm

$\therefore \qquad M_u = 1378 \times 180\,(250 - 0.45 \times 65) = 55 \times 10^6 \text{ N/mm} = 55 \text{ kN m}$

The compressive force above the interface

$$C = (0.45 f_{cu} b\, 0.9x) = (0.45 \times 25 \times 400 \times 0.9 \times 65) = 263 \times 10^3 \text{ N} = 263 \text{ kN}$$

The average horizontal shear stress between support and centre of span sections is

$$\tau = \left(\frac{263 \times 10^3}{100 \times 2500}\right) = 1.052 \text{ N/mm}^2$$

Since $\qquad M_u = 55$ kN m

If $\qquad w_u =$ ultimate uniformly distributed load,

$$0.125\, w_u L^2 = 55$$

$\therefore \qquad w_u = 17.6$ kN/m

$\therefore$ Shear force at support, $V_u = 0.5\, w_u L$

$$(0.5 \times 17.6 \times 5) = 44 \text{ kN}$$

$\therefore \qquad \tau_h = \left(\frac{V_u}{bd}\right) = \frac{(44 \times 10^3)}{(100 \times 250)} = 1.76 \text{ N/mm}^2$

Case (a) According to the British code, the average design shear stress is distributed in proportion to the vertical design shear force diagram to obtain the horizontal shear stress at any point.

Since the shear force is maximum at the support section and zero at the centre of span, the design shear stress at support is twice the average design of shear stress and is given by

$$\tau_h = (2 \times 1.052) = 2.10 \text{ N/mm}^2$$

Since this value of shear stress at interface exceeds the permissible value for the rough tamped surface with nominal links according to Table 14.2, shear reinforcements are designed using the expression

$$A_h = \left(\frac{1000\, b\tau_h}{0.87 f_y}\right)$$

Using Fe-415 grade steel and 8 mm-diameter two-legged links,

$$A_h = \left(\frac{1000 \times 100 \times 2.10}{0.87 \times 415}\right) = 582 \text{ mm}^2/\text{m}$$

Spacing of links, $$S = \left[\frac{(1000 \times 100)}{(582)}\right] = 170 \text{ mm}$$

Case (b) According to the American Code,

$$\tau_h = \left(\frac{V_u}{\phi bd}\right) = \left(\frac{44 \times 10^3}{0.85 \times 100 \times 250}\right) = 2.07 \text{ N/mm}^2$$

Since the shear stress does not exceed 2.5 N/mm^2, the contact surface should be roughened to an amplitude of 5 mm and minimum vertical ties, computed from the following equations, provided using two-legged links of 6 mm diameter, Fe-250 grade steel.

$$S = \left(\frac{A_v 3 f_y}{\phi_w}\right) = \left(\frac{2 \times 28 \times 3 \times 250}{100}\right) = 420 \text{ mm}$$

Also, $$S = \left(\frac{A_v 80 f_y d}{A_{ps} f_{pu}}\right)\sqrt{\frac{b_w}{d}} = \left[\left(\frac{2 \times 28 \times 80 \times 250 \times 250}{180 \times 1600}\right)\sqrt{\frac{100}{250}}\right] = 612 \text{ mm}$$

However, the maximum spacing is limited to four times the thickness of *in situ* slab, i.e., $(4 \times 60) = 240$ mm.

Hence, adopt 6 mm-diameter, two-legged links at a spacing of 240 mm centres.

14.9 Design of Composite Sections

The dimensioning of composite sections involves determining the required size of the composite section using a standard precast prestressed beam of known section properties in order to support the required design service loads. Alternatively, it may become necessary to determine the section modulus of the precast prestressed section for a composite slab of given depth. In either case, formulae relating the section moduli of the precast prestressed and composite section, loading on the member, permissible stresses in the concrete and loss ratio, may be developed by considering various stages of loading as detailed in Section 12.1.1.

The critical stress condition generally occurs at the soffit of the precast prestressed element under minimum and maximum moments. Hence, at the stage of transfer, when the minimum moment (self-weight of precast beam) is acting on the precast prestressed beam, the stress condition is,

$$\left(f_{inf} - \frac{M_{min}}{Z_b}\right) \le f_{ct} \tag{14.1}$$

If Z'_b = section modulus of the bottom fibre of the composite section

M = moment acting on the precast part of a composite section during construction

M' = moment acting on the composite section which is generally due to imposed loads

η = loss ratio

We then have the stress condition at the soffit of the composite section,

$$\left(\eta f_{\text{inf}} - \frac{M}{Z_b} - \frac{M'}{Z'_b}\right) \geq f_{\text{tw}} \tag{14.2}$$

By eliminating the prestress, f_{inf}, from Eqs 14.1 and 14.2, the required section modulus of the composite section is given by

$$Z'_b \geq \left[\frac{Z_b M'}{Z_b(\eta f_{\text{ct}} - f_{\text{tw}}) - (M - \eta M_{\min})}\right] \tag{14.3}$$

The prestress required at the bottom and top fibres of the precast prestressed beam is computed using the following equations:

$$f_{\text{inf}} \geq \left[\frac{f_{\text{tw}}}{\eta} + \frac{M}{\eta Z_b} + \frac{M'}{\eta Z'_b}\right] \tag{14.4}$$

$$f_{\text{sup}} \geq \left[f_{\text{tt}} - \frac{M_{\min}}{Z_t}\right] \tag{14.5}$$

The prestressing force and the corresponding eccentricity are directly obtained by Eqs 12.9 and 12.10.

If it is required to determine the section modulus of the precast prestressed section in a composite slab of given depth, Eq. 14.3 is arranged in an alternative form of the type,

$$Z_b \geq \left[\frac{Z'_b(M - \eta M_{\min})}{Z'_b(\eta f_{\text{ct}} - f_{\text{tw}}) - M'}\right] \tag{14.6}$$

The required prestress is calculated using Eqs 14.4 and 14.5 and the stresses developed in the *in situ* and prestressed components are checked under working loads.

The practical use of the design equations developed above is demonstrated in the design of composite sections in the following examples:

Example 14.12 Design a composite slab for the bridge deck using a standard inverted T-section. The top flange is 250 mm wide and 100 mm thick. The bottom flange is 500 mm wide and 250 mm thick. The web thickness is 100 mm and the overall depth of the inverted T-section is 655 mm. The bridge deck has to support a characteristic imposed load of 50 kN/m^2 over an effective span of 12 m. Grade-40 concrete is specified for the precast pretensioned T-with a compressive strength at transfer of 36 N/mm^2. Concrete of grade-30 is used for the *in situ* part. Determine the minimum prestress necessary and check for safety under serviceability limit state.

Solution.

Section properties:

Area of pretensioned T = 180500 mm^2

Position of centroid = 220 mm from the soffit

Second moment of area, $I = 81.1 \times 10^8$ mm^4
Section modulus, $Z_t = 18.7 \times 10^6$ mm^3
Section modulus, $Z_b = 37 \times 10^6$ mm^3

Using straight, parallel pretensioned tendons with a loss ratio of $\eta = 0.8$, the minimum moment for propped construction $M_{min} = 0$.

The overall depth of the composite slab is estimated as (655 + 95) = 750 mm

Load due to self-weight of the precast beam and the *in situ* concrete is given by,

$$g = 0.75 \times 0.5 \times 24 = 9 \text{ kN/m}$$

Corresponding moment, $M = (0.125 \times 9 \times 12^2) = 162$ kN m

Live-load moment, $M' = (0.125 \times 0.5 \times 50 \times 12^2) = 450$ kN m

Permissible compressive stress in concrete at transfer according to the code is $0.5 f_{ci} = (0.5 \times 36) = 18$ N/mm^2

Permissible tensile stress in concrete under service loads, $f_{tw} = -1$ N/mm^2. The minimum section modulus required for the composite section is given by

$$Z'_b \geq \left[\frac{37 \times 10^6 \times 450 \times 10^6}{37 \times 10^6 (0.8 \times 18 + 1) - 10^6 (162 - 0)}\right] \geq 41 \times 10^6 \text{ mm}^3$$

If h = total depth of composite slab

$$\left(\frac{bh^2}{6}\right) = (41 \times 10^6) \qquad \text{where } b = 500 \text{ mm}$$

$\therefore$ h = 705 mm

The total depth of 750 mm is adequate.

$$Z'_b = \left[\frac{500 \times 750^2}{6}\right] = (46.87 \times 10^6) \text{ mm}^3$$

The minimum prestress required is obtained as,

$$f_{inf} = \left[-\frac{1}{0.8} + \frac{162 \times 10^6}{0.8 \times 37 \times 10^6} + \frac{450 \times 10^6}{0.8 \times 46.87 \times 10^6}\right] = 16.2 \text{ N/mm}^2$$

$$f_{sup} = (-1 - 0) = -1 \text{ N/mm}^2$$

The minimum prestressing force P is computed as,

$$P = \left[\frac{A(f_{inf} Z_b + f_{sup} Z_t)}{(Z_t + Z_b)}\right] = \left[\frac{180500 \times 10^6 (16.2 \times 37 - 1 \times 18.7)}{(55.7 \times 10^6 \times 10^3)}\right] = 1881 \text{ kN}$$

The eccentricity of the prestressing force is,

$$e = \left[\frac{Z_t Z_b (f_{inf} - f_{sup})}{A\,(f_{inf} Z_b + f_{sup} Z_t)}\right] = \left[\frac{18.7 \times 37 \times 10^{12} (16.2 + 1)}{180500 \times 10^6 (16.2 \times 37 - 1 \times 8.7)}\right] = 113 \text{ mm}$$

A suitable system of tendons is arranged with straight parallel wires distributed in the bottom and top flanges so as to achieve the required eccentricity.

The stresses due to prestress and the loads developed in the precast and *in situ* cast concrete are shown in Fig. 14.8.

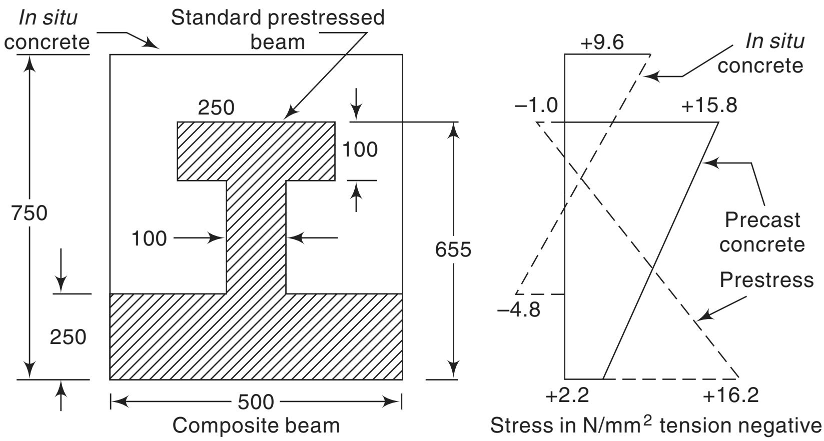

Fig. 14.8 *Design of composite deck slab using a standard prestressed beam*

Example 14.13 Design a precast prestressed inverted T-section to be used in a composite slab of total depth 600 mm and width 300 mm. The composite slab is required to support an imposed load of 16 kN/m^2 over a span of 14 m. The compressive stress in concrete at transfer and the tensile stress under working loads may be assumed to be 20 and 1 N/mm^2, respectively. The loss ratio is 0.85. Determine the prestressing force required for the section.

Solution. Load due to self-weight of the precast beam and *in situ* concrete,

$$g = (0.3 \times 0.6 \times 24) = 4.32 \text{ kN/m}$$

Corresponding moment, $M = (0.125 \times 4.32 \times 14^2) = 105$ kN m

moment due to live loads, $M' = (0.125 \times 0.3 \times 1 \times 16 \times 14^2) = 118$ kN m

Section modulus, $Z'_b = \left[\dfrac{(300 \times 600^2)}{6}\right] = 18 \times 10^6 \text{ mm}^3$

The required section modulus of the precast prestressed inverted *T* is given by

$$Z_b \geq \left[\frac{18 \times 10^6 (105 \times 10^6 - 0)}{18 \times 10^6 (0.85 \times 20 + 1) - 118 \times 10^6}\right] \geq 9.2 \times 10^6 \text{ mm}^3$$

An inverted *T* with the following dimensions and section properties will provide the required section modulus.

Thickness and width of the top flange = 100 mm and 150 mm, respectively

Thickness and width of the bottom flange = 100 mm and 300 mm, respectively

Thickness of the web = 60 mm

Overall depth of the T-section = 500 mm

$$A = (63 \times 10^3) \text{ mm}^2$$

$$Z_b = (9.5 \times 10^6) \text{ mm}^3$$

$$Z_t = (6 \times 10^6) \text{ mm}^3$$

The minimum prestressing force required is estimated by using the design expression:

$$P = \left[\frac{63 \times 10^3 \times 10^6(19.54 \times 9.5 - 1 \times 6)}{15.5 \times 10^6 \times 10^3}\right] = 730 \text{ kN}$$

The corresponding eccentricity,

$$e = \left[\frac{9.5 \times 6 \times 10^{12}(19.54 + 1)}{63 \times 10^3 \times 10^6(19.62 \times 9.5 - 1 \times 6)}\right] = 102 \text{ mm}$$

The required number of high-tensile wires may be suitably arranged in the bottom and top flanges to provide the required eccentricity, and the stresses are checked as in the previous example. Standard bridge beams for spans of 7 to 36 m developed by Somerville and Tiller[9], and the detailing of the Cement and Concrete Association standard inverted T-beams and of composite slabs as presented by Green[10] are useful in the design of composite sections.

References

1. Gweritte, TJ and KW, Mautner, "Recent developments of prestressed concrete construction with resulting economy in the use of steel," *Structural Engineer*, July 1940.
2. Sarkar, S *et al.*, *Handbook for Prestressed Concrete Bridge Design*, S.E.R.C. Publications, Roorkee, 1967.
3. Manton, BH and CB, Wilson, *MOT/C and CA Standard Bridge Beams*, Publication No. 32.012, Cement and Concrete Association, London, 1970.
4. Anderson, AR, "How beam design affects prestressed concrete bridge costs," *Engineering New Record*, Vol. 159, Oct. 1957, pp 326–328.
5. Graduck, II, *Prestressed Concrete*, Oxford and IBH Publishing Co., Delhi, 1967, pp 87–96.
6. BSEN: 1992–1–1, Euro Code-2–Design of Concrete Structures, General Rules and Rules for Buildings, British Standards Institution, 2004.
7. Bate, SCC and EW Bennett, *Design of Prestressed Concrete*, Surrey University Press in Association with International Textbook Company Limited, London, 1976, pp 95–100.
8. ACI: 318M–2011, *Building Code Requirements for Structural Concrete*, American Concrete Institute, Farmington Hills, Michigan, 2011.
9. Somerville, G and RM Tiller, *Standard Bridge Beams for Spans From 7 m to 36 m*, Cement and Concrete Association Publication, 32. 005, London, 1970.
10. Green, JK, *Detailing for Standard Prestressed Concrete Bridge Beams*, Cement and Concrete Association Publication 46.018, London, 1973.

Review Questions

14.1 What are the advantages of using composite construction with prestressed and *in situ* concrete in structural members?

14.2 Sketch some typical cross-sections of composite bridge decks with precast prestressed elements.

14.3 Distinguish between propped and unpropped construction methods in composite construction using stress diagrams at various stages of construction.

14.4 What is differential shrinkage? Explain its importance in composite construction.

14.5 Explain with sketches, the stresses developed due to differential shrinkage in structural elements comprising precast prestressed and cast *in situ* concrete elements.

14.6 How do you compute the shrinkage and resultant stresses in composite members?

14.7 Briefly outline the method of estimating the deflection of composite members in cases of (a) unpropped construction and (b) propped construction.

14.8 Briefly outline the method of computing the ultimate flexural and shear strength of composite sections.

14.9 Specify the various steps involved in the design of composite sections.

14.10 Briefly explain the factors affecting the shear strength of composite sections.

Exercises

14.1 A rectangular pretensioned concrete beam has a breadth of 100 mm and depth of 230 mm, and the prestress after all losses have occurred is 12 N/mm^2 at the soffit and zero at the top. The beam is incorporated in a composite T-beam by casting a top flange of breadth 300 mm and depth 50 mm.

Calculate the maximum uniformly distributed live load that can be supported on a simply supported span of 4.5 m, without any tensile stresses occurring, if

(a) the slab is externally supported while casting, and

(b) the pretensioned beam supports the weight of the slab while casting.

[Ans: (a) 21.6 kN/m^2; (b) 20.5 kN/m^2]

14.2 A composite bridge deck of span 12 m is made up of a precast prestressed symmetrical I-section and an *in situ* cast slab. The precast I-beams are spaced at 750 mm centres and the top slab of the *in situ* concrete is 120 mm thick. The cross-sectional details of the precast I-beams are as follows:

Thickness of top and bottom flanges = 110 mm
Width of top and bottom flanges = 200 mm
Thickness of web = 75 mm
Depth of precast I-beam = 500 mm
Self-weight of precast concrete = 24 kN/m^3
Self-weight of cast *in situ* concrete = 23.5 kN/m^3
The prestressed beam is unpropped during the placing of *in situ* concrete.
The form work load is estimated to be 0.2 kN/m of the span.

If the compressive prestress in the beams is 15 N/mm^2 at the bottom and zero at the top, calculate the maximum stresses developed in the precast and *in situ* cast concrete under an imposed load of 5 kN/m^2, assuming,

(a) the modular ratio of cast *in situ* to precast concrete to be 1.0; and

(b) the modular ratio of cast *in situ* to precast concrete to be 0.8.

[Ans: ***in situ* cast concrete**	**Precast concrete**
(a) +2.3 N/mm^2 (at top)	**+10.2 N/mm^2 (junction)**
(b) +2.1 N/mm^2 (at top)	**+10.5 N/mm^2 (junction)**

14.3 The mid-span section of a composite T-beam comprises a pretensioned beam, 300 mm wide and 900 mm deep, and an *in situ* cast slab, 900 mm wide and 150 mm deep. The effective prestressing force located 200 mm from the soffit of the beam is 2180 kN. The moment due to the weight of the precast section is 273 kN m at mid-span. After this is erected in place, the top slab is cast producing a moment of 136.5 kN m at mid-span.

After the slab concrete is hardened, the composite section is to carry a maximum live-load moment of 750 kN m. Compute the resultant final stresses at,

(a) the top of slab; and

(b) the top and bottom of the precast section.

Also estimate the ultimate moment capacity of the composite cross-section using Indian standard code provisions:

Area of steel = 2340 mm^2

Cube strength of slab concrete = 35 N/mm^2

Tensile strength of steel = 1680 N/mm^2

[Ans: (a) 7.35 N/mm^2; (b) 9.57 N/mm^2 at top and 0.63 N/mm^2 at bottom (all stresses compressive); Ultimate moment = 3180 kN m]

14.4 The deck of a prestressed concrete bridge with an overall depth of 300 mm is made up of an inverted T-section, with *in situ* concrete laid over it. The precast prestressed T-section has the following dimensions and properties:

Width and depth of slab = 300 and 80 mm

Width and depth of stem = 70 and 160 mm

Height of centroid from soffit = 80 mm

Second moment of area = 1472×10^5 mm^4

Prestress at bottom = 11 N/mm^2 (compression)

Prestress at top = 1 N/mm^2 (tension)

Modulus of elasticity of concrete = 35 kN/mm^2

The bridge has a span of 6 m and the precast beams are required to support the weight of the web concrete infill without any propping. When the infill, which may be assumed to have a modulus of elasticity of 28 kN/m^2, has hardened, a uniformly distributed live load of 13 kN/m^2 is applied.

Calculate the resultant final stresses at

(a) the top and bottom of the precast beams, and

(b) the highest and lowest points in the concrete infill.

[Ans: (a) top: 12.4 N/mm^2; bottom: 1.3 N/mm^2 (compression); (b) top: 3.65 N/mm^2 (compression); bottom: 1.54 N/mm^2 (tension)]

14.5 A composite T-section girder consists of a pretensioned rectangular beam, 120 mm wide and 240 mm deep, with an *in situ* cast slab, 360 mm wide and 60 mm deep, laid over the beam. The pretensioned beam contains eight wires of 5 mm diameter, located 30 mm from the soffit. The tensile strength of the high-tensile steel is 1600 N/mm^2 and the cube strength of concrete in the top slab is 20 N/mm^2.

(a) Estimate the flexural strength of the composite section.
(b) Calculate the ultimate shear which will cause separation of the two parts of the girder if,
   (i) The surface contact is roughened to withstand a shear stress of 1 N/mm^2, and
   (ii) 10 mm mild steel stirrups (two-legged) are placed at 100 mm centres. Ultimate shear stress across the stirrups = 190 N/mm^2.

[Ans: (a) 62 kN m; (b) (i) 26.3 kN (ii) 59.3 kN]

14.6 A composite bridge deck is made up of an *in situ* cast slab 120 mm thick and symmetrical I-sections of precast pre-tensioned beams having flange width and thickness of 200 mm and 110 mm, respectively. Thickness of web = 75 mm. Overall depth of I-section = 500 mm. Spacings, of I-beams = 750 mm centres. The modulus of elasticity of *in situ* slab concrete is 30 kN/mm^2. Estimate the stresses developed in the composite member due to a differential shrinkage of 100×10^{-6} between the precast and cast *in situ* elements.

**[Ans: Beam bottom = 0.96 N/mm^2 (tension), top = 2.18 N/mm^2 (compression)
Slab-bottom = 0.82 N/mm^2, top = 0.07 N/mm^2 (tension)]**

14.7 Design the required depth of a composite deck slab of a bridge using the standard inverted T-beam M_1 of C and C.A. (refer to 14.9) to support an imposed load of 15 kN/m^2 on an effective span of 15 m. Determine the minimum prestressing force required and the corresponding eccentricity. Assume grade 40 concrete in the precast beam with a compressive strength at transfer of 35 N/mm^2. The compressive strength of concrete in the *in situ* cast slab is 30 N/mm^2. f_{ct} = 17.5 N/mm^2, f_{tw} = –2.9 N/mm^2.

**[Ans: Depth of slab = 740 mm; Prestressing force = 2750 kN;
Eccentricity = 112 mm]**

14.8 A composite tee beam is made up of a pretensioned rib 300 mm thick and 1000 mm deep and a cast *in situ* slab of 200 mm thickness and 1500 mm width. The modulus of elasticity of cast *in situ* slab is 28 kN/mm^2. If the differential shrinkage is 0.0001 units, estimate the shrinkage stresses developed in precast and cast *in situ* units.

**[Ans: (a) Precast pretensioned beam
At top: 2.03 N/mm^2 (Compression) and
At bottom: –0.84 N/mm^2 (Tension)
(b) Cast in situ slab
At top: 0.28 N/mm^2 (Compression) and At bottom:
–0.77 N/mm^2 (Tension)]**

Objective-type Questions

14.1 In composite construction, prestressed elements are used advantageously in the
(a) compression zone (b) shear zone (c) tension zone

14.2 The composite action between the precast prestressed and cast *in situ* elements is achieved by rendering the surface of the prestressed unit
(a) smooth (b) roughened (c) with dowels

14.3 Composite construction using PSC and cast *in situ* concrete is adopted in
(a) water tanks (b) pipes (c) bridges

14.4 Differential shrinkage between precast pretensioned unit and cast *in situ* members generally induces at the soffit of precast unit
(a) compressive stress (b) tensile stress (c) shear stress

14.5 For computing the deflections of composite beams due to live load, the second moment of area to be used should be based on that of
(a) cast *in situ* unit (b) precast unit (c) composite section

14.6 Flexural strength computations of composite beams is generally done by using the compressive strength of concrete in
(a) precast prestressed unit
(b) cast *in situ* unit
(c) composite member

14.7 In composite construction, the dead loads can be reduced by using cast *in situ* concrete made up of
(a) normal aggregates
(b) lightweight aggregates
(c) crushed granite aggregates

14.8 Composite construction is economical since the ratio of size of precast unit to that of the whole composite member is
(a) increased (b) reduced (c) constant

14.9 The design ultimate shear resistance of a composite member is directly proportional to the
(a) cross-sectional area of cast *in situ* slab
(b) second moment of area of composite section
(c) distance of centroid of cast *in situ* slab from centroid of composite section

14.10 In composite members with precast beam connected to a cast *in situ* slab, the stresses due to differential shrinkage induces
(a) direct stress
(b) bending stress
(c) direct and bending stress

Answers to Objective-type Questions

14.1 (c)	14.2 (b)	14.3 (c)	14.4 (b)	14.5 (c)
14.6 (b)	14.7 (b)	14.8 (b)	14.9 (b)	14.10 (c)

15 Statically Indeterminate Structures

15.1 Advantages of Continuous Members

Continuity in prestressed concrete construction is advantageous in many respects. In statically indeterminate prestressed concrete structures, the following benefits are noteworthy:

1. The bending moments are more evenly distributed between the centre of span and the supports of members.
2. Reduction in the size of members results in lighter structures.
3. The ultimate load carrying capacity is higher than in a statically determinate structure due to the phenomenon of redistribution of moments.
4. Continuity of the members in framed structures leads to increased stability.
5. Continuous girders are formed by segmental construction using precast units connected by prestressed cables.
6. In continuous post-tensioned girders, the curved cables can be suitably positioned to resist the span and support moments.
7. A reduction in the number of anchorages in a continuous prestressed beam in comparison with a series of simply-supported beams. Only one pair of post-tensioning anchorages and a single stressing operation can serve several members.
8. In continuous prestressed structures, the deflections are comparatively small as compared to simply supported spans.

15.2 Effect of Prestressing Indeterminate Structures

When an indeterminate structure is prestressed, redundant reactions will develop due to the redundancies exercising a restraint at the supports. While a statically determinate structure is free to deform when prestressed, a continuous structure cannot deform freely. However, the deflections should conform to the law of consistent deformation. The redundant reactions, which develop as a consequence of prestressing an indeterminate structure, result in secondary moments. The formation of redundant reactions and secondary moments are examined with reference to a two-span continuous beam, prestressed by a straight cable located at a uniform eccentricity throughout the span as shown in Fig. 15.1(a).

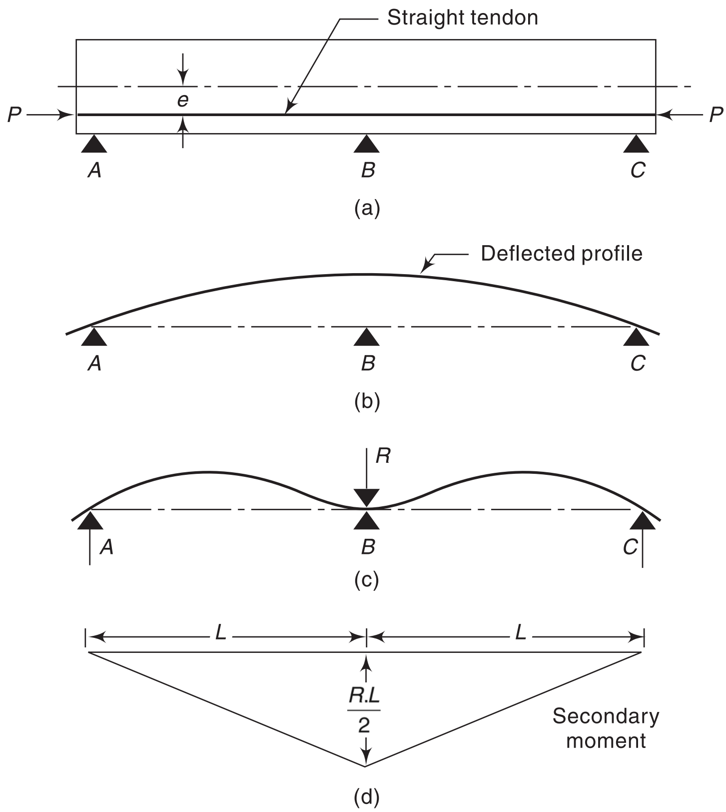

Fig. 15.1 *Redundant reactions and secondary moments in a continuous PSC beam*

Under the action of the prestressing force, P, the beam will deflect as shown in Fig. 15.1(b), if it is not restrained at the central support B. A redundant reaction R, as shown in Fig. 15.1(c), develops at the central support if the beam is restrained at B, so that deflections are not possible at this support. As a consequence of this redundant reaction acting downwards, secondary moments, as shown in Fig. 15.l(d), develop in the continuous beam ABC.

The various disadvantages encountered in continuous prestressed concrete members are as follows:

1. Loss of prestress due to friction is appreciable in long cables with reversed curves and considerable curvature.
2. Secondary stresses due to prestressing, creep, shrinkage and temperature, and settlements of supports may induce very high stresses unless they are controlled or provided for in the design.
3. Cables positioned to cater for secondary moments are not generally suitable to provide the required ultimate moment under a given system of loads.
4. The computation of collapse or ultimate load is influenced by the degree of redistribution of moments in the continuous structure.

The problem of excessive frictional losses can be tackled by reducing the curvature of the cables housed in members of variable depth and also by temporarily overstressing the tendons from both ends. Stresses due to secondary moments can be eliminated by selecting suitable tendon profiles which do not induce secondary moments. It is also possible to provide for secondary stresses in the design. If under-reinforced sections are used, the redistribution of moments will be more or less complete, resulting in higher collapse loads. These loads could be estimated by using the well-established plastic theory as applied to structural steel members.

15.3 Methods of Achieving Continuity

Continuity in prestressed concrete construction is achieved by using curved or straight cables which are continuous over several spans as shown in Figs 15.2(a) and (b). It is also possible to develop continuity between two precast beams by using cap cables as shown in Fig. 15.2(c). Alternatively, short, straight tendons may be used over the supports to develop continuity between two precast prestressed beams as shown in Fig. 15.2(d).

Based on the method of construction, continuous beams may be clasified as 'fully continuous beams' in which tendons are generally continuous from one end to the other, and 'partially continuous' where each span is first precast as a simple beam and the elements are assembled to form a continuous member by using cap cables or short tendons over the supports.

Regarding their suitability for applying them in a given situation, several methods of developing continuity in prestressed concrete construction have been critically examined by Lin[1] and Visvesvaraya *et al.*[2] They have also outlined the types of tendons to be used for continuous prestressed structures.

15.4 Definitions of Common Terms

The terms commonly used in the study of continuous prestressed concrete members are defined as follows:

Primary moment The primary moment is the apparent bending moment at a section in a statically indeterminate structure due to the actual eccentricity of the tendons from the centroidal axis. Referring to Fig. 15.3, the primary moment at every cross-section of the two-span continuous beam is $-Pe$, as it is a hogging moment.

Secondary moment (parasitic bending moment) Secondary moments are additional moments induced at a section of a statically indeterminate structure due to the redundant reactions developed as a consequence of prestressing the structure. The variation of secondary moment in a two-span continuous beam prestressed by a straight eccentric tendon is shown in Fig. 15.3.

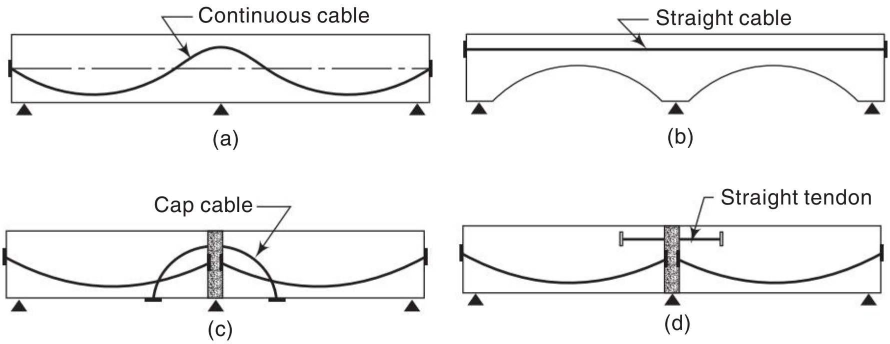

Fig. 15.2 *Cable layouts for continuous beams*

Resultant moment The resultant moment at a section of an indeterminate prestressed structure is the sum of the primary and secondary moments.

$$\text{RM} = (\text{PM} + \text{SM})$$

Pressure or thrust line The pressure line is the locus of the resultant compression at different sections of the structural member. The shift of the pressure line from the centroidal axis is obtained as the ratio of the resultant moment and the prestressing force at the section. The resultant thrust line for a two-span continuous beam is shown in Fig. 15.3.

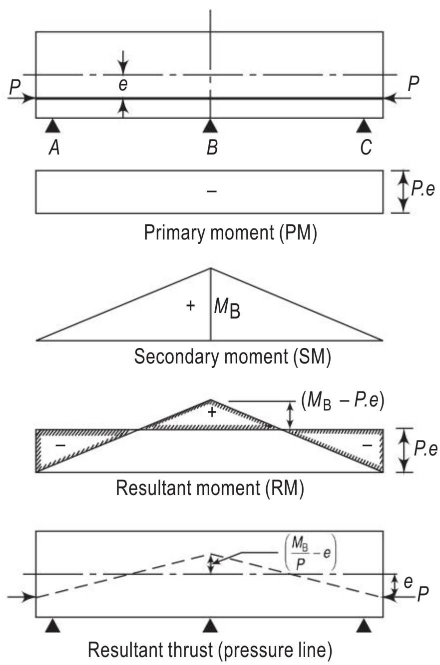

Fig. 15.3 *Pressure line in a continuous prestressed beam*

Line of prestress (CGS line) The locus of the centroid of the prestressing force along the structure is the line of prestress or centre of gravity of the steel line.

Concordant cable or tendon profile A tendon profile in which the eccentricity is proportional at all cross-sections to the bending moment caused by any loading on a rigidly supported statically indeterminate structure is a concordant profile.

Stressing a tendon laid to such a profile does not induce any redundant reactions and hence the secondary moments are zero.

According to Guyon[3], tendons in statically indeterminate structures, placed to coincide with the pressure or thrust line, do not induce secondary bending moments in the structure.

The resultant thrust line in a two-span continuous beam, prestressed by a parabolic cable with zero eccentricity at all the supports is shown in Fig. 15.4. If the tendon profile is made to coincide with the resultant thrust line, the redundant reactions are completely eliminated and the cable profile may be considered as concordant.

Transformation profile A transformation profile is any tendon profile consisting of straight lines between the rigid supports and having zero eccentricity at simple end supports. A tendon following such a profile will produce support reactions and uniform longitudinal compression but no bending moments.

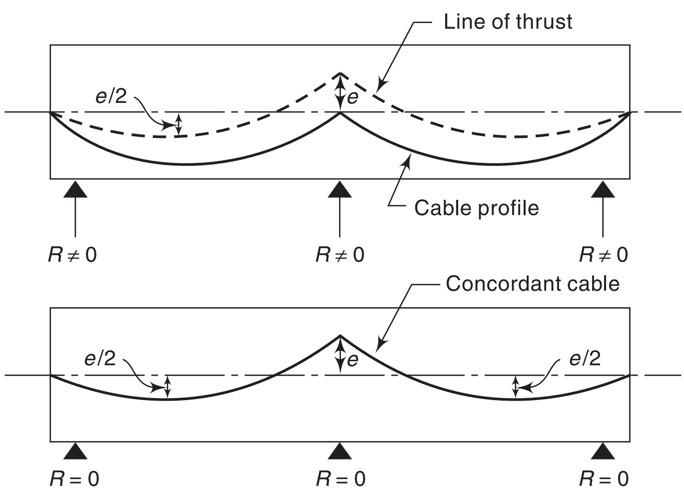

Fig. 15.4 *Line of thrust and concordant cable profile*

15.5 Methods of Analysis of Secondary Moments

In addition to the basic assumptions, such as the elastic behaviour of materials and linear strain distribution across the section, the following assumptions are generally made for the analysis of secondary moments in continuous prestressed concrete members:

1. The effect of change in the length of members due to the prestressing force and external loading is negligible.
2. The cable friction is considered to be negligible so that the prestressing force is constant at all points of the cable.

There are several methods for analysing statically indeterminate prestressed structures to compute the secondary moments that develop from prestressing the structure.

The most commonly used methods are based on the principles of

(a) Three moment theorem
(b) Consistent deformation
(c) Tendon reaction

The methods specified in (b) and (c) are also generally referred to as the flexibility influence coefficients method and the method of equivalent loads, respectively. The merits and demerits of these methods and their suitability for given cases are outlined with the help of examples.

15.5.1 Theorem of Three Moments

The classical method of linear structural analysis, such as the three or four moment theorem, can be conveniently used to analyse the secondary moments developed in a continuous prestressed concrete structure. In this method, the free bending moment diagram to be considered is that due to the primary moment represented by the tendon profile, with the longitudinal axis of the member as the horizontal axis. The method can also handle members of variable cross-section along the length of the structure. Referring to Fig. 15.5 and considering the sagging moments as positive, the general form of the three moment equation takes the form,

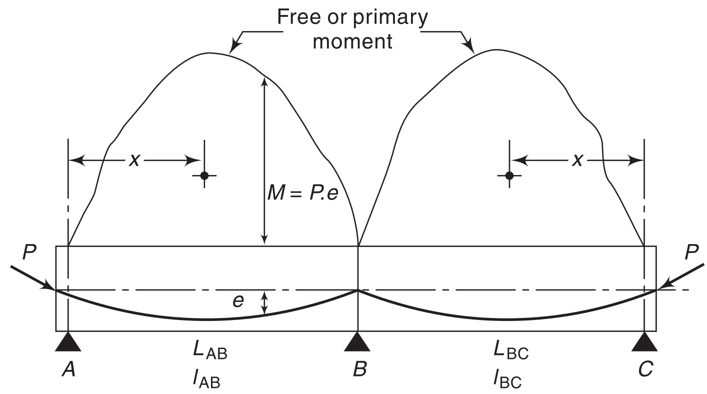

Fig. 15.5 *Analysis of secondary moments by the theorem of three moments*

$$\left[\frac{L_{AB}}{I_{AB}}M_{AB}+\frac{L_{AB}}{I_{AB}}2M_{AB}+\frac{L_{BC}}{I_{BC}}2M_{BC}+\frac{L_{CB}}{I_{BC}}M_{CB}\right]$$

$$=\left[\frac{6}{L_{AB}I_{AB}}\int_0^{L_{AB}} Mx\,dx-\frac{6}{L_{BC}I_{BC}}\int_0^{L_{BC}} Mx\,dx\right]$$

where M_{AB}, M_{BA}, M_{BC} and M_{CB} are the secondary moments developed as a consequence of prestressing the structure. M is the free bending moment (primary moment) at a distance x from the end supports. However,

$$\int Mxdx = \int Pexdx = P\int exdx$$

$= P$ [moment of the area between the cable profile and the centroidal axis about the support]

Substituting the terms,

$$K=\left[-\frac{6P}{L^2}\int exdx\right]$$

and

stiffness ratio, $$k=\left[\left(\frac{I_{AB}}{L_{AB}}\right)\Big/\left(\frac{I_{BC}}{L_{BC}}\right)\right]$$

The simplified form of the three moment equation is given by,

$$(M_{AB}+2M_{BA}+2kM_{BC}+kM_{CB})=(K_{BA}+kK_{BC})$$

Depending upon the degree of indeterminacy of the structure, a suitable number of equations are formulated and then solved to evaluate the secondary moments. The resultant moment at any section is computed as the sum of primary and secondary moments.

Example 15.1 A continuous prestressed concrete beam ABC ($AB = BC = 10$ m) has a uniform rectangular cross-section with a width of 100 mm and depth of 300 mm. The cable carrying an effective prestressing force of 360 kN is parallel to the axis of the beam and located at 100 mm from the soffit.

(a) Determine the secondary and resultant moment at the central support B.
(b) If the beam supports an imposed load of 1.5 kN/m, calculate the resultant stresses at top and bottom of the beam at B. Assume density of concrete as 24 kN/m^3.
(c) Locate the resultant line of thrust through beam AB.

Solution. Applying the three moment theorem to the continuous beam ABC shown in Fig. 15.6,

$$(M_{AB}+2M_{BA}+2kM_{BC}+kM_{CB})=(K_{BA}+kK_{BC})$$

Since the ends A and C are simply supported,

$$M_{AB}=M_{CB}=0$$

Also $k = 1$ and $M_{BA} = M_{BC} = M_B$

$$K_{BA}=K_{BC}=\left(-\frac{6P}{L^2}\int exdx\right)=\left\{-\frac{6\times 360}{10\times 10}[-(0.05)\times 10\times 5]\right\}=54\,\text{kN m}$$

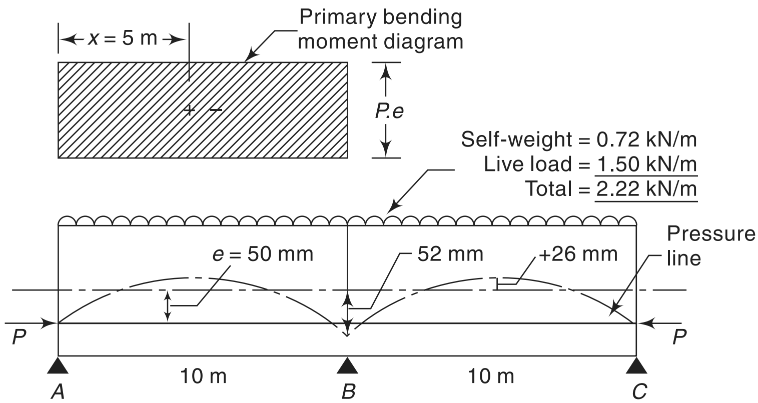

Fig. 15.6 *Two-span continuous prestressed concrete beam*

$\therefore \qquad 4M_B = (2 \times 54) = 108$ kN m

SM at B is $\quad M_B = 27$ kN m

Resultant moment at B due to prestress = (PM + SM)

$$= [(-360 \times 0.05) + 27)] = 9 \text{ kN m}$$

$$w_d = (1.50 + 0.72) = 2.22 \text{ kN m}$$

$$\text{Moment at } B \text{ due to loads} = -\left(\frac{w_d L^2}{8}\right) = -\left(\frac{2.22 \times 10^2}{8}\right) = 27.75 \text{ kN m}$$

$\therefore$ Total resultant moment at $B = (9 - 27.75) = -18.75$ kN m

Stresses at the central support section B are

$$\text{Top fibre stress} = \left[\frac{360 \times 10^3}{100 \times 300} - \frac{18.75 \times 10^6}{1.5 \times 10^6}\right] = -0.5 \text{ N/mm}^2 \text{ (tension)}$$

$$\text{Bottom fibre stress} = \left[\frac{360 \times 10^3}{100 \times 300} + \frac{18.75 \times 10^6}{1.5 \times 10^4}\right] = +24.5 \text{ N/mm}^2 \text{ (compression)}$$

Pressure line position

At $A = -5$ cm

$$\text{At } B = \left(\frac{M}{P}\right) = \left(\frac{-18.75 \times 1000}{360}\right) = -52 \text{ mm}$$

Resultant moment at centre of span

$$= \left[\frac{-Pe}{4} + \frac{w_d L^2}{16}\right] = \left[\frac{-360 \times 0.05}{4} + \frac{2.2 \times 10^2}{16}\right] = +9.25 \text{ kN m}$$

Shift of pressure line from the centroidal axis at mid-span points

$$= \left(+\frac{9.25 \times 1000}{360}\right) = +26 \text{ mm}$$

The pressure line location is shown in Fig. 15.6.

Example 15.2 A prestressed beam having a rectangular cross-section with a width of 120 mm and a depth of 300 mm is continuous over two spans, $AB = BC = 8$ m. The cable with zero eccentricity at the ends and an eccentricity of 50 mm towards the top fibres of the beam over the central support, carries an effective force of 500 kN.

(a) Calculate the secondary moment developed at B.

(b) If the beam supports concentrated loads of 20 kN each at mid-points of span, evaluate the resultant stresses at the central support section B.

(c) Locate also the position of the pressure line at section.

Solution.

$$P = 500 \text{ kN} \qquad Z_t = Z_b = 18 \times 10^5 \text{ mm}^3 \qquad Q = 20 \text{ kN}$$

$$e = 50 \text{ mm} \qquad A = 36 \times 10^3 \text{ mm}^2 \qquad g = 0.86 \text{ kN/m and}$$

$$L = 8 \text{ m}$$

$$M_A = M_C = 0$$

$$K_{AB} = K_{BC} = \left[-\frac{6P}{L^2}\int exdx\right] = -\frac{6P}{L^2}\left[\frac{1}{2}Le\frac{2}{3}L\right] = -2Pe$$

Applying the three moment equation for spans AB and BC,

$$4M_B = (-2Pe - 2Pe) = -4Pe$$

$$\text{SM at } B = M_B = -Pe$$

$$\text{RM at } B = (PM - SM) = (+Pe - Pe) = 0$$

Moment at B due to self-weight and imposed loads is given by,

$$M_B = \left[-\frac{gL^2}{8} - \frac{3QL}{16}\right] = \left[-\frac{0.86 \times 8^2}{8} - \frac{3 \times 20 \times 8}{16}\right] = -36.88 \text{ kN m}$$

Stresses at section B:

$$\text{At top} = \left[\frac{500 \times 10^3}{36 \times 10^3} - \frac{36.88 \times 10^6}{18 \times 10^5}\right] = -6.6 \text{ N/mm}^2 \text{ (tension)}$$

$$\text{At bottom} = \left[\frac{500 \times 10^3}{36 \times 10^3} + \frac{36.88 \times 10^6}{18 \times 10^5}\right] = +34.4 \text{ N/mm}^2 \text{ (compression)}$$

Position of pressure line from the centroidal axis

$$\text{At } B = \left(\frac{M_B}{P}\right) = \left(\frac{-36.88 \times 1000}{500}\right) = -73.5 \text{ mm}$$

(below centroidal axis)

Example 15.3 Two simply supported beams, $AB = BC = 10$ m, of rectangular cross-section, each post-tensioned by means of two parabolic cables ($P = 300$ kN each) with eccentricities of zero at the supports and 150 mm at mid-span, are converted into a continuous beam by tensioning a parabolic cap cable carrying a force of 300 kN. The ends of the cap cable are located at 3 m from the central support. The cable centre is 50 mm from the top of the beam over the central support B. The beam is 200 mm wide and 600 mm deep.

(a) Calculate the secondary moment induced at B.

(b) Locate the resultant line of thrust through the beam AB.

(c) Evaluate the resultant prestress along the top and bottom of the beam.

Solution. The position of the cables in two simply supported beams and the primary bending moment diagram due to the cap cable are shown in Fig. 15.7.

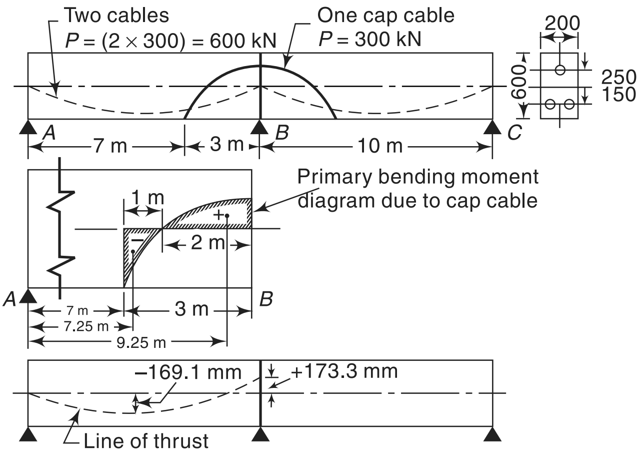

Fig. 15.7 *Continuous beam with cap cable*

Applying the theorem of three moments to spans AB and BC,

$M_A = M_C = 0$, since they are simple end supports.

$$K_{BA} = K_{BC} = \left(-\frac{6P}{L^2}\int exdx\right)$$

$$= \left\{-\frac{6\times300}{10\times10}[-(0.25\times1\times0.3\times7.25)+(0.67\times2\times0.25\times9.25)]\right\}$$

$$= -46 \text{ kN m}$$

$\therefore\ 4M_B = (-2\times46) = -92$

$\therefore$ Secondary moment at B, $M_B = \left(-\dfrac{92}{4}\right) = -23$ kN m

Resultant moment at B = (SM + PM) = (–23 + 75) = +52 kN m

Resultant moment at A = 0

Resultant moment at the centre of span $AB = \left\{\left(-\dfrac{23}{2}\right) - (600\times0.15)\right\}$
$= -101.5$ kN m

Position of line of thrust from the centroidal axis, at A = 0

At centre of $AB = \left(-\dfrac{101.5}{600}\times1000\right) = -169.1$ mm

At $B = \left(+\dfrac{52}{300}\times1000\right) = +173.3$ mm

$A = (200\times600) = (12\times10^4)$ mm^2

$Z_b = Z_t = (12\times10^6)$ mm^3

Resultant stresses, at $A = \left(\dfrac{600\times10^3}{12\times10^4}\right) = 5$ N/mm^2

At mid-span of $AB = \left[\dfrac{600\times10^3}{12\times10^4}\pm\dfrac{101.5\times10^6}{12\times10^6}\right] = (5.0\pm8.5)$

Stress at top = –3.5 N/mm^2 (tension)
Stress at bottom = +13.5 N/mm^2 (compression)

$$\text{At } B = \left[\frac{900 \times 10^3}{12 \times 10^4} \pm \frac{52 \times 10^6}{12 \times 10^6}\right] = 7.5 \pm 4.4$$

Stress at top = +11.9 N/mm^2 (compression)
Stress at bottom = –3.1 N/mm^2 (tension)

If the continuous beam supports the self-weight and imposed loads, the stresses developed due to these effects are superposed on the computed stresses.

15.5.2 Method of Consistent Deformation (Flexibility Influence Coefficients)

The most commonly used methods for the analysis of structures with a high degree of statical indeterminacy are the stiffness (displacement) and force (compatibility) methods. The latter method, based on the principle of consistent deformation, is suitable for computing secondary moments in statically indeterminate prestressed concrete structures.

The flexibility method[4] involves the formation of simultaneous equations in terms of the unknown reaction components, flexibility coefficients and displacements at any point due to the external load on the structure. Accordingly, if R_1, R_2, R_3, …, R_n are the unknown reaction components (forces, moments) at the points 1, 2, 3, … *n*.

f_{ij} = flexibility influence coefficient which gives the displacement developed at the point *i*, due to a unit reaction at the point *j*,

and u_i = displacement at the point *i* due to external load on the structure, the compatibility equations can be written as:

$$f_{11}R_1 + f_{12}R_2 + \dots f_{1n}R_n + u_1 = 0$$
$$f_{21}R_1 + f_{22}R_2 + \dots f_{2n}R_n + u_2 = 0$$
$$\dots \quad \dots \quad \dots \quad \dots$$
$$f_{n1}R_1 + f_{n2}R_2 + \dots f_{nn}R_n + u_n = 0$$

Using the matrix formation, these equations can be expressed in the compact form,

$$FR = -u$$

where F is the flexibility matrix of the structure. The large set of simultaneous equations are easily solved by using a computer.

The flexibility influence coefficients for the formation of the flexibility matrix are obtained using the following integrals:

$$f_{ij} = \int \frac{m_i m_j}{EI} ds$$

$$u_i = \int \frac{m_o m_i}{EI} ds$$

where m_i = moment due to a unit reaction at the point i

m_j = moment due to a unit reaction at the point j

m_o = moment due to the external load on the structure

ds = element of length of a member

EI = flexural rigidity of the section

Some of the commonly used product integrals for computing flexibility influence coefficients are shown in Fig. 15.8.

m_i \ m_i	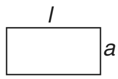	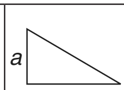	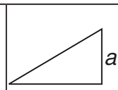	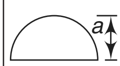	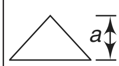	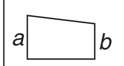
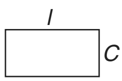	lac	$\frac{1}{2}lac$	$\frac{1}{2}lac$	$\frac{2}{3}lac$	$\frac{1}{2}lac$	$\frac{1}{2}l(a+b)c$
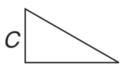	$\frac{1}{2}lac$	$\frac{1}{3}lac$	$\frac{1}{6}lac$	$\frac{1}{3}lac$	$\frac{1}{4}lac$	$\frac{1}{6}l(2a+b)c$
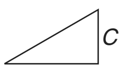	$\frac{1}{2}lac$	$\frac{1}{6}lac$	$\frac{1}{3}lac$	$\frac{1}{3}lac$	$\frac{1}{4}lac$	$\frac{1}{6}l(a+2b)c$
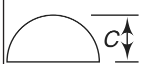	$\frac{2}{3}lac$	$\frac{1}{3}lac$	$\frac{1}{3}lac$	$\frac{8}{15}lac$	$\frac{5}{12}lac$	$\frac{1}{3}l(a+b)c$
	$\frac{1}{2}lac$	$\frac{1}{4}lac$	$\frac{1}{4}lac$	$\frac{5}{12}lac$	$\frac{1}{3}lac$	$\frac{1}{4}l(a+b)c$
	$\frac{1}{2}la(c+d)$	$\frac{1}{6}la(2c+d)$	$\frac{1}{6}la(c+2d)$	$\frac{1}{3}la(c+d)$	$\frac{1}{4}la(c+d)$	$\frac{1}{6}l\{a(2c+d)$ $+b(2d+c)\}$

Fig. 15.8 *Product integrals for flexibility influence coefficients*

For computing secondary moments developed due to prestressing an indeterminate concrete structure, the term m_o corresponds to the primary moment induced along the length of the member due to eccentricity of the tendons. The integral of this moment is equal to the product of the prestressing force and the area intercepted between the tendon profile and the axis of the member. The moments induced by unit reactions designated as m_i are generally linear and the product integral $m_o\,m_i$ for each span can be computed using Fig. 15.8. The use of this general method is illustrated with the following examples.

Example 15.4 A continuous prestressed concrete beam ABC ($AB = BC = 10$ m) having a rectangular section with a width of 200 mm and depth of 400 mm is prestressed by a parabolic cable carrying an effective force of 100 kN. The cable is concentric at supports A, B and C and has an eccentricity of 100 mm towards the soffit of the beam at the centre of span sections. Calculate the secondary and resultant moments developed in the beam due to prestressing at B.

Solution. Referring to Fig. 15.9, the primary moment diagram, m_o, due to the eccentricity of the cable and the moment induced due to a unit reaction at B are used for computing the flexibility influence coefficients.

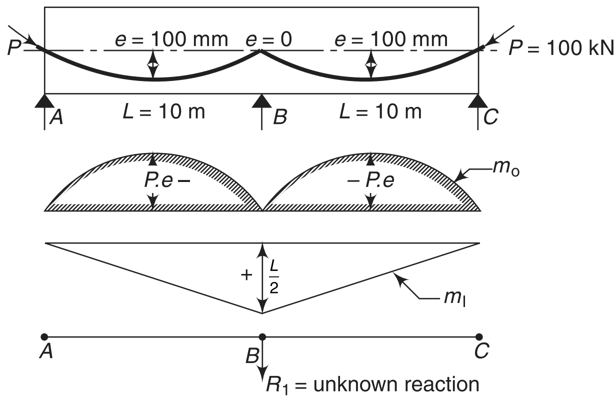

Fig. 15.9 *Redundant reaction analysis by flexibility influence coefficients*

Using the expressions for product integrals shown in Fig. 15.8,

$$u_1 = \int \frac{(m_o m_i ds)}{EI} = \left(\frac{1}{3}\right) Lac, \quad \text{for the triangular and parabolic diagrams}$$

$$= 2\frac{\left[\frac{1}{3} \times L(-Pe) \times \frac{L}{2}\right]}{EI} = -\left(\frac{PeL^2}{3EI}\right)$$

$$f_{11} = \int \frac{(m_i M_j ds)}{EI}, \text{ since } i = j = 1 = \left(\frac{1}{3}\right) Lac, \quad \text{for triangular diagrams}$$

$$= \left\{2\left[\frac{1}{3} \times L \times \frac{L}{2} \times \frac{L}{2}\right] \Big/ EI\right\} = +\left(\frac{L^3}{6EI}\right)$$

Hence, the compatibility equation is

$$f_{11}R_1 + u_1 = 0$$

where R_1 = reaction induced at B

$$\left\{\left(\frac{L^3}{6EI}\right) R_1 - \frac{PeL^2}{3EI}\right\} = 0$$

$$\therefore \qquad R_1 = \left(\frac{2Pe}{L}\right)$$

Secondary moment developed at $B = \left(R_1 \times \frac{2L}{4}\right)$

$$= \left(\frac{2Pe}{L} \times \frac{2L}{4}\right) = Pe = (100 \times 0.1) = 10 \text{ kN m}$$

RM at B = (PM + SM) = (0 + 10) = 10 kN m.

Example 15.5 A prestressed concrete portal frame *ABCD* fixed at *A* and *D* has columns $AB = CD = 5$ m and transom $BC = 10$ m. The members have a cross-section 100 mm wide and 300 mm deep throughout. The columns are prestressed by a straight cable with an eccentricity of 50 mm towards the outside of frame at *B* and *C*. Transform *BC* is prestressed by a parabolic cable having an eccentricity of 50 mm above the centroid at *B* and *C* and 100 mm below the centroid at the centre of *BC*. The prestressing force in all the cables = 200 kN. Calculate the secondary moments developed at *A* and *B*.

Solution. The portal frame being symmetrical, half the frame is analysed by introducing two redundant reactions R_1 and R_2 at the mid-span section of transom *BC*. Figure 15.10 shows the moment m_o developed due to the prestressing and the moments m_1 and m_2 induced by applying unit reactions R_1 and R_2. The flexibility coefficients are evaluated by using the product integrals given in Fig. 15.8.

$$u_1 = \int \frac{(m_o m_i ds)}{EI} = \frac{200}{EI}\left[\left(\frac{1}{6} \times 5 \times 5 \times 0.1\right) - \left(\frac{1}{2} \times 5 \times 0.05\right)\right] = \left(-\frac{42}{EI}\right)$$

$$u_2 = \int \frac{(m_o m_2 ds)}{EI} = \frac{200}{EI}\left[\left(\frac{1}{2} \times 5 \times 1 \times 0.1 - 5 \times 0.05 \times 1\right)\right]$$

$$\left[+(5 \times 0.05 \times 1) - \frac{2}{3} \times 5 \times 0.15 \times 1\right] = \left(\frac{-50}{EI}\right)$$

$$f_{11} = \int \frac{(m_1 m_1 ds)}{EI} = \frac{1}{EI}\left(\frac{1}{3} \times 5 \times 5 \times 5\right) = \left(\frac{41.66}{IE}\right)$$

$$f_{12} = f_{21} = \int \frac{(m_1 m_2 ds)}{EI} = \frac{1}{EI}\left(\frac{1}{2} \times 5 \times 5 \times 1\right) = \left(\frac{12.5}{EI}\right)$$

$$f_{22} = \int \frac{(m_2 m_2 ds)}{EI} = \frac{1}{EI}[(5 \times 1 \times 1) + (5 \times 1 \times 1)] = \left(\frac{10}{EI}\right)$$

Since *EI* is constant throughout the frame, the compatibility equations are expressed as,

$$f_{11}R_1 + f_{12}R_2 + u_1 = 0$$

$$f_{21}R_1 + f_{22}R_2 + u_2 = 0$$

Substituting the values of the influence coefficients,

$$41.66R_1 + 12.5R_2 - 42 = 0$$

$$12.50R_1 + 10.0R_2 - 50 = 0$$

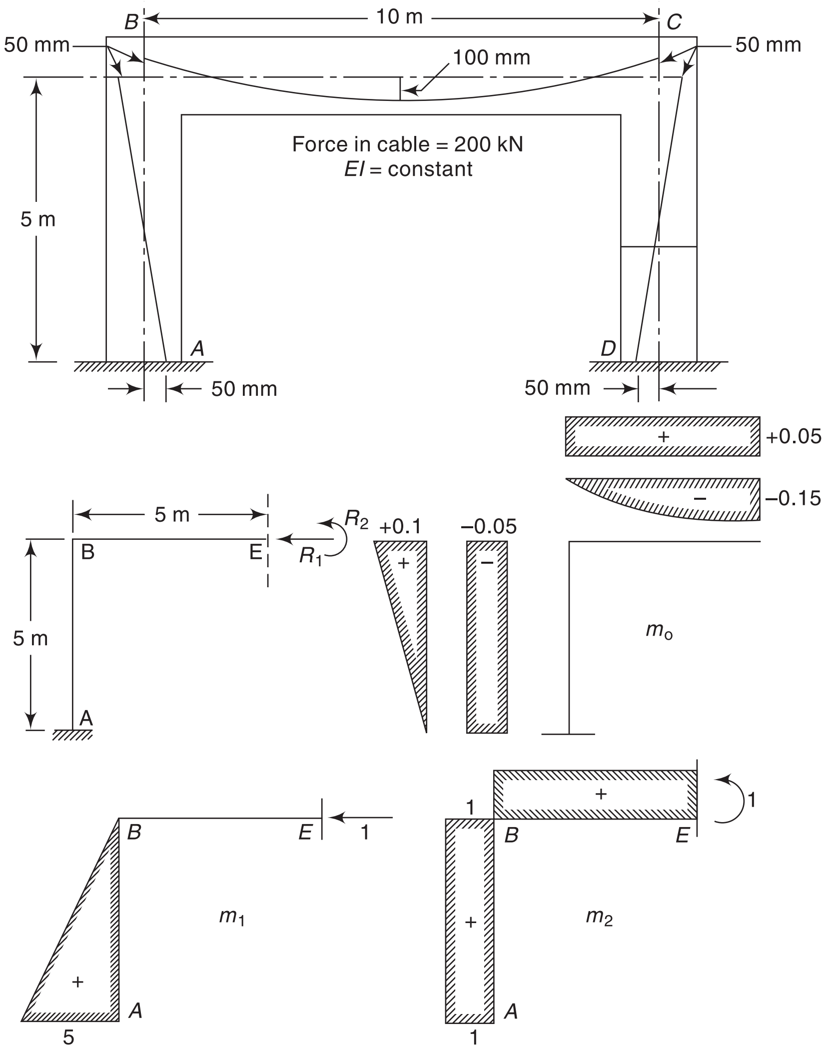

Fig. 15.10 *Computation of secondary moment in a portal frame by flexibility influence coefficients*

Solving,

$$R_1 = -0.8 \text{ kN}$$

$$R_2 = +60 \text{ kN m}$$

The secondary moments at A and B are given by,

$$M_A = (6 - 0.8 \times 5) = 2 \text{ kN m}$$

$$M_B = 6 \text{ kN m}$$

The resultant moments are obtained as the sum of primary and secondary moments at each of the sections.

15.5.3 Tendon Reaction or the Method of Equivalent Loads

The tendon reaction method, suggested by Guyon, for analysing statically indeterminate prestressed structures is based on the principle of replacing the tendon by an equivalent system of loads acting on the concrete member which correspond to the reactions exerted by the tendon on concrete. The continuous structure with the equivalent load system is analysed by any of the classical procedures, such as the stiffness or the force methods for the moments and forces developed in the system.

It is important to note that the analysis of the indeterminate structure supporting the equivalent loads directly yields the resultant moments. Consequently, the secondary moments, if required, are obtained as the difference of the resultant and primary moments at every cross-section of the structure. If the continuous structure supports external loads, these can be combined with the equivalent loads representing the effect of the tendon reactions on concrete and the resulting moments can be computed by the moment distribution method. The shift in the pressure of thrust line can be obtained as the ratio of the resultant moment to the prestressing force at any desired section of the indeterminate structure.

The system of equivalent loads representing the reaction of the tendons on concrete depends upon the magnitude of the prestressing force and the cable profile. Figure 15.11 shows a continuous beam prestressed by a cable with different profiles along the length of the beam and the corresponding equivalent load system. In general, the following tendon reactions are associated with the different shapes of cable profiles:

1. Straight portion of cable	No reaction
2. Sharp angles in cable	Concentrated load
3. Curved cables	Uniformly distributed load
4. End anchorages	Axial thrust with a fixing moment

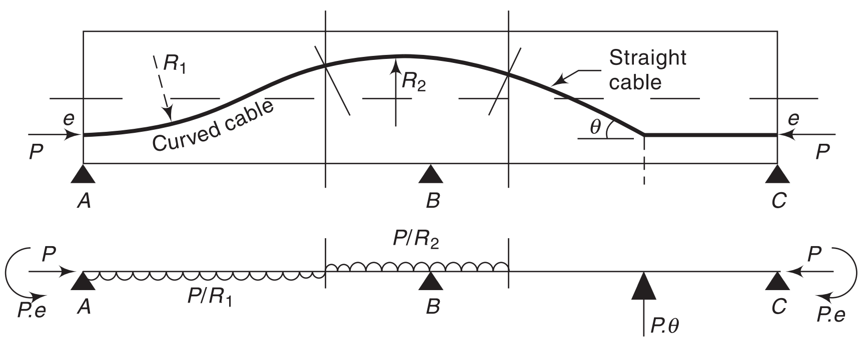

Fig. 15.11 *Tendon profile and equivalent load system*

In the case of curved cables, if the radius of curvature of the curve is R and the prestressing force in the cable is P, the equivalent uniformly distributed load is given by P/R. If the cable is parabolic, the equivalent u.d.1. is estimated as $w_e = 8\,Pe/L^2$, where e is the eccentricity of the cable at the centre of span of length L.

In the case of cables with sharp deviations of angles of magnitude θ, the equivalent concentrated load is $P\theta$ as shown in Fig. 15.11.

The tendon reaction method is used to analyse the statically indeterminate prestressed concrete structures as outlined in the following examples.

Example 15.6 A continuous concrete beam ABC ($AB = BC = 8$ m) has a uniform rectangular cross-section 100 mm wide and 300 mm deep. A cable carrying an effective prestressing force of 500 kN is parallel to the axis of the beam and located at a constant eccentricity of 50 mm towards the soffit. The continuous beam supports, in addition to the self-weight, concentrated loads of 20 kN at the centre of each span. Determine the resultant moment developed at centre support B and locate the position of the pressure line at this section.

Solution. The tendon reaction due to a straight cable at an eccentricity e is equivalent to an axial thrust of intensity P and a moment at the end support equivalent to Pe. The fixed end moments due to self-weight g and concentrated load Q at the centre of each span are computed as $gL^2/12$ and $QL/8$.

The resultant moment at the centre support B is obtained by the moment distribution procedure as follows:

A		B			C
Tendon reaction					
$-Pe$	$\rightarrow$	$-\frac{Pe}{2}$	$+\frac{Pe}{2}$	$\leftarrow$	$+Pe$
Fixed end moments					
$-\left(\frac{gL^2}{12}+\frac{QL}{8}\right)$		$+\left(\frac{gL^2}{12}+\frac{QL}{8}\right)$	$-\left(\frac{gL^2}{12}+\frac{QL}{8}\right)$		$+\left(\frac{gL^2}{12}+\frac{QL}{8}\right)$
$+\left(\frac{gL^2}{12}+\frac{QL}{8}\right)$	$\rightarrow$	$+\left(\frac{gL^2}{24}+\frac{QL}{16}\right)$	$-\left(\frac{gL^2}{24}+\frac{QL}{16}\right)$	$\leftarrow$	$-\left(\frac{gL^2}{12}+\frac{QL}{8}\right)$
Resultant moments					
$-Pe$		$\left(-\frac{Pe}{2}+\frac{gL^2}{8}+\frac{3QL}{16}\right)$	$\left(\frac{Pe}{2}-\frac{gL^2}{8}-\frac{3QL}{16}\right)$		$+Pe$

In this example,

$$g = (0.1 \times 0.3 \times 24) = 0.72 \text{ kN m} \qquad Q = 20 \text{ kN}$$

$$P = 500 \text{ kN} \qquad e = 0.05 \text{ m}$$

$$L = 8 \text{ m} \qquad Pe = 25 \text{ kN m}$$

$$\left(\frac{gL^2}{8}\right) = 5.76 \text{ kN m} \qquad \left(\frac{3QL}{16}\right) = 30 \text{ kN m}$$

Hence,
Resultant moment at $B = (5.76 + 30 - 12.5) = 23.26$ kN m (hogging moment)

Shift of pressure line above the centroidal axis at the support section $B = \left(\dfrac{M}{P}\right) = (23.26 \times 1000)/(500) = 46.52$ mm.

Example 15.7 A continuous beam ABC ($AB = BC = 10$ m) is prestressed by a parabolic cable carrying an effective force of 200 kN. The cable profile is shown in Fig. 15.12. The beam supports dead and live loads of 0.24 and 2.36 kN/m, respectively. Calculate the resultant moments developed in the beam and locate the pressure line.

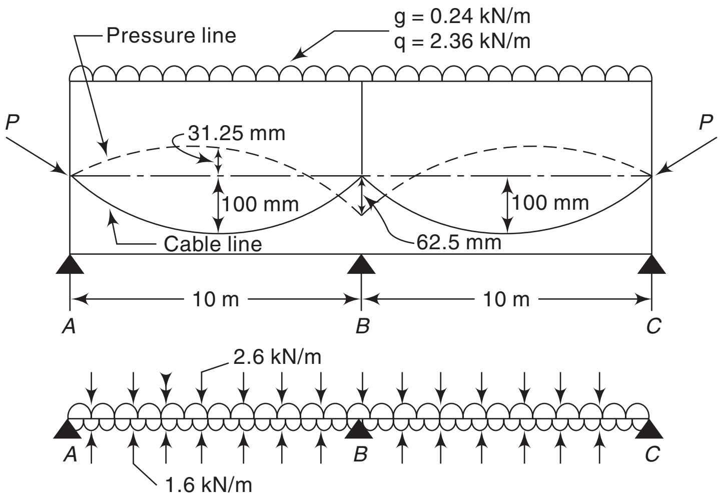

Fig. 15.12 *Continuous beam with equivalent load systems*

Solution. The continuous beam with external loads and the equivalent load system is shown in Fig. 15.12.

Total external load = $(g + q) = (0.24 + 2.36) = 2.6$ kN/m
Equivalent uniformly distributed load due to tendon reaction

$$= \left(\frac{8Pe}{L^2}\right) = \left[\frac{(8 \times 200 \times 0.10)}{(10 \times 10)}\right] = 1.6 \text{ kN/m (acting upwards)}$$

Resultant load on beam, $w_r = (2.6 - 1.6) = 1.0$ kN/m

The fixed end moments due to this loading = $\left(\dfrac{w_r L^2}{12}\right)$

The resultant moments after moment distribution are obtained as,

$$M_A = 0,\ M_B = \left(\frac{w_r L^2}{8}\right) \text{ and } M_C = 0$$

Resultant moment at $B = \left(\dfrac{w_r L^2}{8}\right) = \left(\dfrac{1 \times 10^2}{8}\right) = 12.5$ kN m (hogging)

$$\text{Resultant moment at centre of span} = \left(\frac{w_r L^2}{8}\right) - \left(\frac{w_r L^2}{16}\right) = \left(\frac{w_r L^2}{16}\right)$$

$$= 6.25 \text{ kN m (sagging)}$$

Location of pressure line

Shift of pressure line from the centroidal axis,

At $A = 0$

At centre of span = $(6.25 \times 1000)/200 = 31.25$ mm (above centroidal axis)

At $B = (12.5 \times 1000)/(200) = 62.50$ mm (below centroidal axis)

The position of the thrust or pressure line is shown in Fig. 15.12.

15.6 Concordant Cable Profile

Prestressing a statically indeterminate structure generally results in secondary moments due to the redundant reactions developed at the intermediate supports. However, it is possible to arrange the cable profile in a way that the structure does not deform at the supports or at other points of restraint. In such a case, redundant reactions and secondary moments are not induced by prestressing the cables. Tendon profiles which do not induce secondary moments are referred to as concordant profiles.

Depending upon the degree of indeterminacy of the structure, concordant tendon profiles satisfy a set of geometrical conditions, derived from Mohr's moment area theorems. Thus for a two-span continuous beam ABC with a degree of indeterminacy of one, the condition of concordant profile is given by,

$$\left[\frac{A_1 x_1}{(EI)_1}\right] + \left[\frac{A_2 x_2}{(EI)_2}\right] = 0$$

where A_1 and A_2 are the free bending moment (primary moment) diagrams representing the area between the cable profile and the longitudinal axis of the beam in the adjacent spans (refer to Fig. 15.5), x_1 and x_2 represent the distances of the centroid of the moment diagrams from the exterior supports, and $(EI)_1$ and $(EI)_2$, are the flexural rigidities of spans AB and BC. A two-hinged portal and a fixed rectangular portal frame with symmetrical arrangements of cables being statically indeterminate to the second degree should satisfy two equations for concordancy. Correspondingly, a fixed rectangular portal prestressed by an unsymmetrical system of tendons with a degree of indeterminacy of three has to satisfy three equations of concordancy.

Example 15.8 A continuous concrete beam ABC ($AB = BC$) has a uniform cross-section throughout its length. The beam is prestressed by a straight cable carrying an effective force P. The cable has an eccentricity e towards the soffit at end supports A and C and $e/2$ towards the top fibre at the central support B. Show that the cable is concordant.

Solution. Referring to Fig. 15.13, the geometrical condition of concordancy is expressed as,

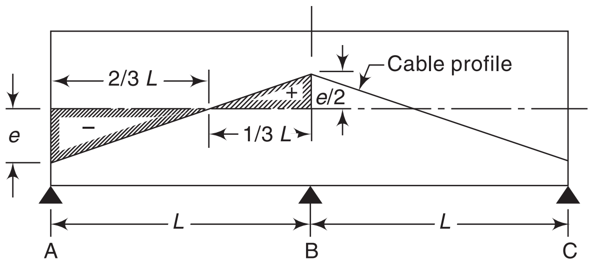

Fig. 15.13 *Concordant cable profile*

$$[A_1x_1 + A_2x_2] = 0$$

Since EI is constant for spans AB and BC,

$$A_1x_1 = P\int_0^{AB}(exdx) = P\left[-\left(\frac{1}{2}\times\frac{2L}{3}\times e\times\frac{1}{3}\times\frac{2L}{3}\right)\right]\left[+\left(\frac{1}{2}\times\frac{L}{3}\times\frac{e}{2}\times\frac{8}{9}\times L\right)\right] = 0$$

$$A_2x_2 = 0$$

Hence the given cable profile is concordant.

Example 15.9 A two-span continuous beam $ABC(AB = BC = 10$ m) is of rectangular section, 200 mm wide by 500 mm deep. The beam is prestressed by a parabolic cable, concentric at end supports and having an eccentricity of 100 mm towards the soffit of the beam at centre of spans and 200 mm towards the top at mid-support. The effective force in the cable is 500 kN.

(a) Show that the cable is concordant
(b) Locate the pressure line in the beam when it supports a live load of 5.6 kN/m in addition to its self-weight.

Solution.

Cross-section of beam (rectangular): $b = 200$ mm and $D = 500$ mm
Eccentricity of cable: At end supports: $e = 0$
At mid-support: $e = 200$ mm towards top fibre
At centre of spans: $e = 100$ mm towards the soffit
Prestressing force $= P = 500$ kN, Span: $AB = BC = L = 10$ m
By joining a line between the cables at end support and centre of span, the effective eccentricity at centre of span is obtained as $e = (100 + 100) = 200$ mm.

Using the tendon reaction method, the equivalent uniformly distributed load acting upwards is given by

$$w_e = \left[\frac{8Pe}{L^2}\right] = \left[\frac{8\times 500\times 0.2}{10^2}\right] = 8 \text{ kN/m}$$

Dead weight of the beam $= g = (0.2\times 0.5\times 24) = 2.4$ kN/m
Live load on the beam $= q$ ...... $= 5.6$ kN/m
Total load on the beam $= (g + q)$ ...... $= 8.0$ kN/m (acting downwards)
Considering the two-span continuous beam carrying an imposed load of 8 kN/m due to prestressing force, the resultant moment at mid support B is calculated as,

RM at $B = 0.125\, w_e L^2 = (0.125 \times 8 \times 10^2) = 100$ kN m

Primary moment PM at $B = P.e = (500 \times 0.2) = 100$ kN m

Hence, secondary moment at B is = [RM – PM] = [100 – 100] = 0

Hence, the cable is concordant.
The total downward load due to dead weight and live load are counterbalanced by the upward load developed due to the prestressing force. Hence, bending stresses are zero along the beam.
However, direct stress due to prestressing force computed as,

$$\text{Direct stress} = \left(\frac{P}{A}\right) = \left(\frac{(500 \times 10^3)}{(200 \times 500)}\right) = 5 \text{ N/mm}^2$$

Pressure line coincides with centroidal axis.

15.7 Guyon's Theorem

In statically indeterminate prestressed concrete structures, it is possible to make simple modifications to a predetermined tendon profile without altering the pressure line in the members. This is an important property of continuous prestressed beams, first enunciated by Guyon as follows: "In a continuous prestressed beam, if the tendon profile is displaced vertically at any of the intermediate supports by any amount, but without altering its intrinsic shape between the supports, the resultant line of thrust is unchanged."

The operation of displacing the cable at intermediate supports while holding the positions of the end anchorages constant without changing the intrinsic shape (that is, curvature and bends) is also referred to as *linear transformation* of the cable. Guyon's theorem can easily be proved by considering a continuous structure prestressed by a straight cable as shown in Fig. 15.3. If the prestressing force in the cable is P, the resultant moment at the central support section B is $Pe/2$ and the shift of the pressure line is $e/2$ above the centroidal axis. These computations are simplified by using the tendon reaction method. If the cable is linearly transformed by displacing it vertically at the central support so that the eccentricity is zero at this section, the resultant moment has the same value of $Pe/2$ and the shift in the pressure line is the same as in the previous case. However, it is important to note that as a result of linear transformation of the tendons, additional reactions are induced while there is no change in the resultant moment distribution.

Guyon's theorem of linear transformation of cables is of considerable practical significance in the design of concordant cable profiles in continuous prestressed concrete structures.

Example 15.10 A prestressed concrete continuous beam of two equal spans AB = BC = 10 m is prestressed by a continuous cable having a parabolic profile between the supports. The eccentricity of the cable is zero at all three supports and 100 mm towards the soffit at centres of spans. The beam is of rectangular section, 100 mm wide and 300 mm deep. The effective force in the cable is 100 kN. Determine the resultant thrust line in the beam. Show that there is no change in the thrust line if the cable is linearly transformed with a vertical shift of 100 mm towards the top of beam at interior support B.

Solution. Referring to Fig. 15.14, the equivalent uniformly distributed load on the beam when the cable is concentric at the three supports A, B and C is given by,

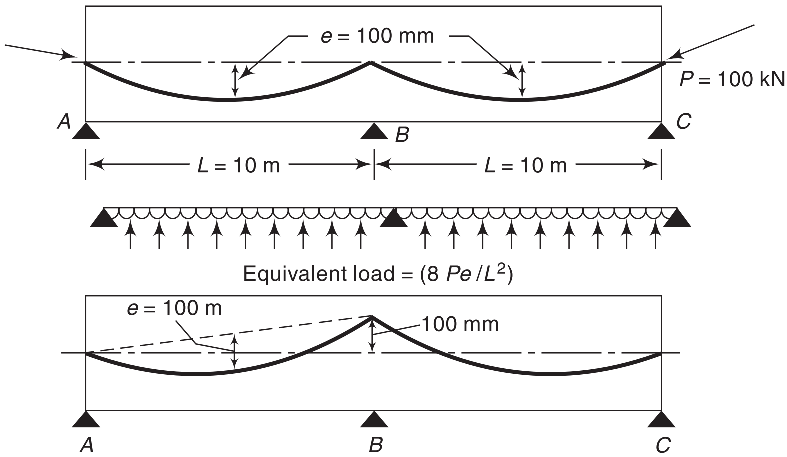

Fig. 15.14 *Linear transformation of parabolic cable profile*

$$w_e = \left(\frac{8Pe}{L^2}\right) = \left(\frac{8 \times 100 \times 0.1}{10 \times 10}\right) = 0.8 \text{ kN/m}$$

Resultant moment at $B = (0.125\, w_e L^2) = (0.125 \times 0.8 \times 10^2) = 10$ kN m

Shift of thrust line at $B = \left(\dfrac{M}{P}\right) = \left(\dfrac{10 \times 1000}{100}\right) = 100$ mm

(from centroidal axis)

If the cable is linearly transformed with a vertical shift of 100 mm towards the top fibres at support B, the equivalent load is unchanged since the eccentricity e measured from the line joining the cable centres at A and B to the bottom of the cable at the mid-span still remains unchanged at 100 mm, as shown in Fig. 15.14. Hence, there is no change in the resultant moment and position of thrust line at B.

15.8 Effect of Axial Deformation and Tertiary Moments

In the case of prestressed structures comprising unidirectional members, such as continuous beams, the axial contraction due to the effect of prestressing does not significantly influence the force and moment in the continuous structure. However, in structures like portal frames with members in different directions, prestressing of transform results in an axial contraction, which in turn introduces tertiary moments in the frame due to the lateral displacement of the junction of the transform and column members. According to Bennet[5], the main effects to be considered are:

1. Reduction in the magnitude of prestressing force in a particular member due to the restraint of the adjacent members.
2. The development of tertiary moments due to the bending deformation of the indeterminate structure due to axial contraction under the action of the prestressing force.

Consider a portal frame $ABCD$, fixed at A and D. The effect of prestressing transform BC on the tertiary moments developed in the frame is influenced by the geometrical properties of the individual members and the magnitude of the prestressing force. The prestressing force of magnitude P applied to transom BC is distributed as P_{BA} applied transversely to leg BA, component P_{BC} being the force experienced by transform BC.

In Fig. 15.15, it can easily be seen that for compatibility, the lateral deflection Δ of end B of column AB should be equal to the axial contraction of one half of transform BC. This leads to the condition,

$$\left(\frac{P_{BA}L_{BA}^3}{3EI_{BA}}\right) = \Delta = \left(\frac{P_{BC}L_{BC}}{2EA_{BC}}\right)$$

Hence,
$$\left(\frac{P_{BA}}{P_{BC}}\right) = \left(\frac{1.5L_{BC}I_{BA}}{L_{BA}^3 A_{BC}}\right)$$

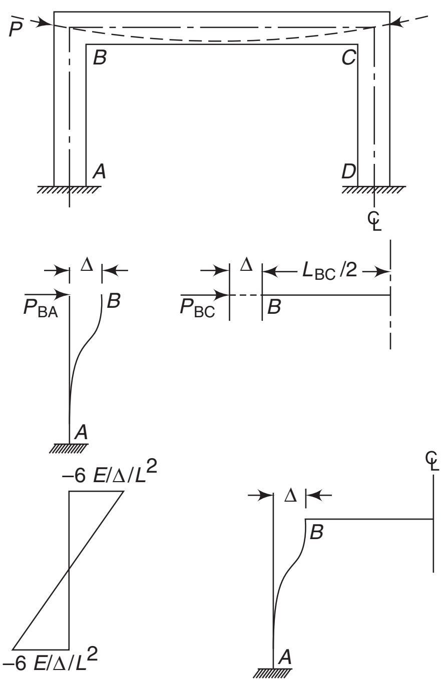

Fig. 15.15 *Effect or axial shortening on prestressing force and moments*

For the practical range of sections and prestressing forces, this ratio being negligibly small, the whole of the prestressing force may be assumed to be resisted by transom BC. However, point B moves horizontally by an amount Δ due to the action of the prestressing force P, which results in anticlockwise moments of magnitude $6EI_{BA}\Delta/L^2_{BA}$ developing at B and A.

The resulting tertiary moments due to these fixed-end moments at joints A and B can be evaluated by the moment distribution procedure as illustrated in the following example.

Example 15.11 Estimate the tertiary moments developed in the portal frame $ABCD$ of Example 15.5, if the transom is prestressed by a cable carrying an effective force of 200 kN. Assume the modulus of elasticity of concrete in the members as 34 kN/mm^2. $AB = CD = 5$ m and $BC = 10$ m. All members are of constant section which is 100 mm wide and 300 mm deep. Find also the ratio of the prestressing force shared by the column and transom.

Solution.

$$A_{BC} = (100 \times 300) = 30{,}000 \text{ mm}^2$$

$$I_{AB} = \left(100\frac{(300)^3}{12}\right) = (225 \times 10^6) \text{ mm}^4$$

If P_{AB} and P_{BC} are the forces resisted by the column and transform respectively, then

$$\left(\frac{P_{AB}}{P_{BC}}\right) = \left[\frac{1.5L_{BC}I_{BA}}{L^3_{BA}A_{BC}}\right] = \left[\frac{1.5 \times 10{,}000 \times 225 \times 10^6}{500^3 \times 30{,}000}\right] = 0.0009$$

This ratio being negligibly small, for all practical purposes, the entire prestressing force of 200 kN may be assumed to be resisted by transform BC.

If Δ = Lateral deflection of end B of leg AB, which is also equal to the axial contraction of one half of transom BC,

$$\Delta = \left[\frac{P_{BC}L_{BC}}{2EA_{BC}}\right] = \left[\frac{200 \times 10{,}000}{2 \times 34 \times 30{,}000}\right] = 0.98 \text{ mm}$$

The fixed end moments developed at A and B due to this deflection are given by,

$$M_{FAB} = M_{FBA} = \left[\frac{-6EI_{AB}}{L^2_{AB}}\right] = \left[\frac{-6 \times 34 \times 225 \times 10^6 \times 0.98}{5000^2 \times 1000}\right]$$

$$0 = -1.8 \text{ kN m}$$

These fixed end moments have to be distributed using the moment distribution method.

$$\text{Stiffness ratio} = \left[\frac{I_{BC}}{L_{BC}} \times \frac{L_{AB}}{I_{AB}}\right] = \left[\frac{225 \times 10^6}{10{,}000} \times \frac{5000}{225 \times 10^6}\right] = 0.5 : 1$$

The stiffness of BC is halved, reducing this ratio to 0.25 : 1 to enable the moment distribution to be carried out in one-half of the symmetrical frame.

Distribution factors at joint B are given by,

$$d_{BA} = \frac{1.00}{(1+0.25)} = 0.8$$

$$d_{BC} = \frac{0.25}{(1+0.25)} = 0.2$$

The moment distribution is performed to estimate the tertiary moments developed as given below.

A		B		C
		0.8	0.2	
–1.80		–1.80		
+0.72	←	+1.44	+0.36	
–1.08		–0.36	+0.36	

The tertiary moment is +0.36 kN m (sagging) in transom *BC* and varies linearly in *AB* from –1.08 kN m (hogging) at *A* to +0.36 kN m (sagging) at *B*.

Comparing with the magnitude of secondary and primary moments (refer to Example 15.5), tertiary moments are, respectively, 54 per cent of the secondary moment and 11 per cent of the primary moment at *A*. The corresponding values at *B* being 6 per cent and 3.6 per cent, respectively.

15.9 Ultimate Load Analysis of Continuous Prestressed Members

15.9.1 Limit State of Collapse

The ultimate load carrying capacity of a statically determinate prestressed concrete structure is mainly controlled by the flexural strength of a critical section in the member. In contrast to this, the ultimate load carrying capacity of an indeterminate prestressed concrete structure depends upon the flexural strength of several critical sections and their rotation capacity. However, a highly conservative estimate of the ultimate resistance of the structure is obtained by assuming the collapse to occur when the moment, calculated by the linear elastic theory, first reaches a value equal to the flexural strength at any section. In majority of the cases, the actual ultimate load exceeds the theoretical ultimate load computed on the basis of the linear elastic theory, mainly because of the phenomenon of redistribution of moments.

It is a well-established fact that prestressed concrete members exhibit non-linear moment-curvature relationships, in the post-cracking stage indicating decreased flexural rigidity with increasing moments approaching failure. Due to the large deformations at the critical sections in a statically indeterminate structure, a concentration of curvature builds up over a few clearly defined short lengths of the member, such as the interior supports and mid-span points of a continuous beam. These plastic zones are idealised as hinges at which a rotation is considered to take place.

The ultimate load carrying capacity of the indeterminate structure depends on the degree of redistribution of moments, which, in turn, is influenced by the rotation capacity of the hinging regions. The ductility of the reinforced concrete sections depends upon the properties of concrete and steel and the percentage of reinforcement and its disposition in the section. The upper limit of the ultimate strength of the structure, corresponding to full (100 per cent) redistribution of moment, is characterised by the formation of hinges at critical sections attaining the flexural strength. The final collapse is by transforming the structure, or part of the structure, into a mechanism. If partial redistribution takes place due to the constraints imposed by limited hinge rotations, the ultimate strength of the structure lies in between the upper limit outlined above and the lower limit corresponding to the computations based on the linear elastic theory. Figure 15.16 illustrates the limits of moment redistribution and the mechanism of failure in a uniformly loaded continuous beam of three spans.

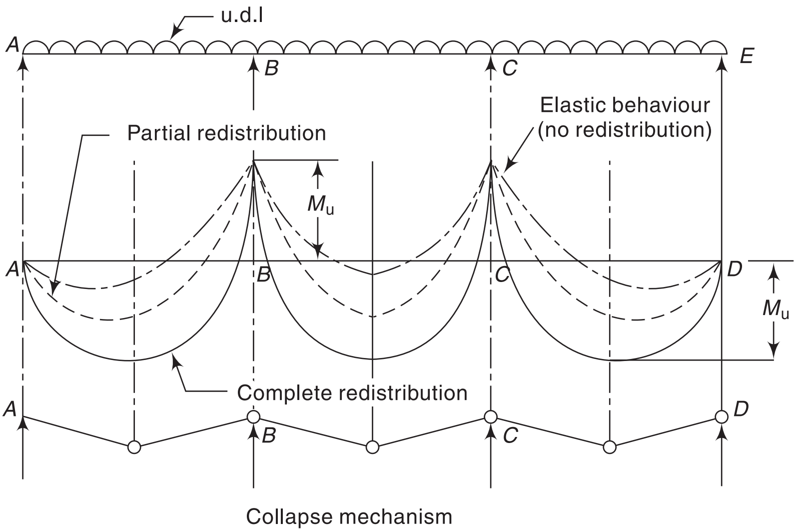

Fig. 15.16 *Redistribution of moments in a three-span continuous beam*

15.9.2 Computation of Ultimate Loads

The upper bound to the ultimate load carrying capacity of a continuous prestressed concrete structure can be obtained by using the well-known principles of limit analysis, developed for steel structures by Baker[6] and his team at Cambridge in UK and by Prager[7] in USA. Investigations by Ernst[8] and Cranston[9] have shown that in the case of well-designed structural concrete members with under-reinforced sections, there will be ample rotation capacity, permitting the development of the hinges at the critical sections, thus leading to the formation of a collapse mechanism. The ultimate load-carrying capacity of some of the continuous prestressed structures is examined here, based on the assumption of elastic distribution and complete redistribution of moments.

Referring to Fig. 15.17, where a two-span continuous beam supports a uniformly distributed load, the ultimate load is computed using the following notations:

M_{u1} = ultimate flexural strength of the support section

M_{u2} = ultimate flexural strength of the centre-of-span section

M_g = self-weight moment

g = uniformly distributed dead load

q_u = ultimate live load

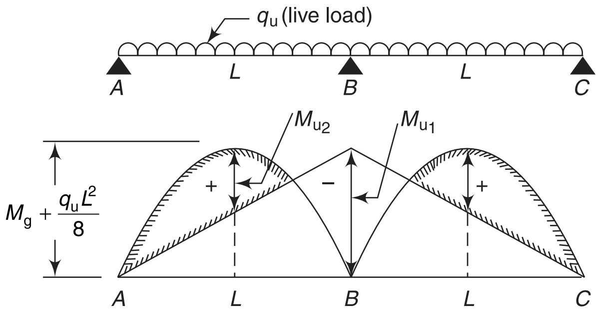

Fig. 15.17 *Two-span continuous beam with uniformly distributed load*

Referring to the moment diagram at the limit state of collapse, we have

$$\left[M_g + \frac{q_u L^2}{8}\right] = \left[M_{u2} + \frac{1}{2}M_{u1}\right]$$

$$\left[\frac{gL^2}{8} + \frac{q_u L^2}{8}\right] = \left[M_{u2} + \frac{1}{2}M_{u1}\right]$$

$$\therefore \qquad q_u = \frac{8}{L^2}\left(M_{u2} + \frac{1}{2}M_{u1}\right) - g$$

If $\qquad M_{u1} = M_{u2} = M_u$

$$q_u = [(12M_u/L^2) - g] \tag{15.1}$$

Assuming elastic distribution of moments,

$$M_{u1} = \left[\frac{(g + q_u)L^2}{8}\right]$$

$$\therefore \qquad q_u = [(8/L^2)M_{u1} - g] \tag{15.2}$$

Comparing Eqs 15.1 and 15.2, it can be seen that if complete redistribution takes place, the ultimate load supported is 1.5 times the ultimate load based on the elastic distribution of moments. Similarly, for a two-span continuous beam supporting concentrated loads at the centre of span as shown in Fig. 15.18,

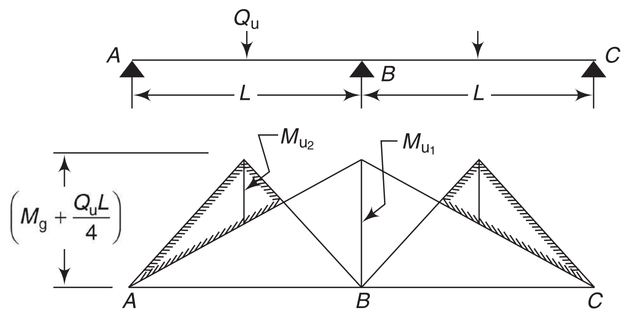

Fig. 15.18 *Two-span continuous beam with concentrated loads*

the ultimate live load at the limit state of collapse, assuming complete redistribution, is given by

$$Q_u = \frac{A}{L}\left(M_{u2} + \frac{1}{2}M_{u1} - M_g\right)$$

Example 15.12 A continuous beam *ABCD* ($AB = BC = CD = 10$ m) supports a uniformly distributed live load of q kN/m. The beam has a rectangular section with a width of 300 mm and overall depth 600 mm throughout. It is prestressed by a concordant cable located 100 mm from the soffit at mid-span points and from the top of the beam at supports B and C. The cross-sectional area of the cable is 600 mm^2. The ultimate strength of the cable and concrete is 1600 N/mm^2 and 40 N/mm^2, respectively. If the density of concrete is 24 kN/m^3, estimate the magnitude of the live load supported by the beam at the limit state of collapse, assuming

(a) elastic distribution of moments, and
(b) full redistribution of moments.

Solution.

Self-weight of beam, $g = (0.3 \times 0.6 \times 24) = 4.32$ kN/m

The flexural strength of span and support sections are computed using the following section properties and details:

$$A_p = 600 \text{ mm}^2 \qquad f_p = 1600 \text{ N/mm}^2$$
$$d = 500 \text{ mm} \qquad f_{ck} = 40 \text{ N/mm}^2$$
$$b = 300 \text{ mm}$$

Effective reinforcement ratio $= \left(\dfrac{A_p f_p}{b d f_{ck}}\right) = \left(\dfrac{600 \times 1600}{300 \times 500 \times 40}\right) = 0.16$

From Table 7.1, for the ratio $\left(\dfrac{f_{pu}}{0.87 f_p}\right) = 1.0$

$\therefore \qquad f_{pu} = (0.87 \times 1600) = 1392$ N/mm^2

and $\qquad \left(\dfrac{x_u}{d}\right) = 0.35$

or $\quad x_u = (0.35 \times 500)$

$x_u = 175$ mm

$$\therefore \quad M_u = f_{pu}A_p\,(d - 0.42\,x_u) = (1392 \times 600)\left[\frac{(500 - 0.42 \times 175)}{10^6}\right] = 356 \text{ kN m}$$

(a) Assuming elastic distribution of moments, if q_u = ultimate live load, then

$$M_u = 0.125\,(g + q_u)\,L^2$$

or $\quad 356 = 0.125\,(4.32 + q_u)\,100$

$\therefore \quad q_u = 24.16$ kN/m

(b) Assuming full redistribution of moments,

if q_u = ultimate live load and $M_{u1} = M_{u2} = M_u$, then

$$\left(q_u \frac{L^2}{8} + g\frac{L^2}{8}\right) = (M_{u2} + 0.5\,M_{u1}) = 1.5\,M_u$$

$$\therefore \quad q_u = \left(12\frac{M_u}{L^2} - g\right) = \left(\frac{(12 \times 356)}{100}\right) - 4.32 = 38.4 \text{ kN/m}$$

Example 15.13 A continuous beam of two equal spans of 30 m each has a rectangular section 500 mm wide and 1000 mm deep throughout the spans. The beam is prestressed by a concordant cable having high tensile strands of cross-sectional area 3000 mm^2, 100 mm from the top of the beam at mid-support section. If the beam supports uniformly distributed service load of 8 kN/m throughout the span lengths, estimate the load factor against failure assuming. f_{pu} = 1700 N/mm^2, f_{ck} = 50 N/mm^2 and density of concrete as 24 kN/m^3, for the two cases,

(a) Elastic distribution of moments and

(b) Complete redistribution of moments

Solution. Continuous beam of two equal spans of 30 m each

Cross-section of the beam: b = 500 mm and D = 1000 mm

Effective depth = d = 900 mm with cover of 100 mm

A_p = 3000 mm^2, f_p = 1700 mm^2, f_{ck} = 50 N/mm^2

Dead weight of the beam = $g = (0.5 \times 1 \times 24) = 12$ kN/m

Live load on the beam = q = 8 kN/m

Span length = L = 30 mm

Referring to Table 4.1, compute the effective reinforcement ratio given by

$$\left[\frac{f_p\,A_p}{f_{ck}\,b\,d}\right] = \left[\frac{1700 \times 3000}{50 \times 500 \times 900}\right] = 0.22$$

Interpolating from the table, we have the ratio,

$$\left[\frac{f_{pu}}{0.87\,f_p}\right] = 0.93 \text{ and } \left(\frac{x_u}{d}\right) = 0.44$$

$$\therefore \quad M_u = f_{pu}A_p(d - 0.42x_u) = (0.93 \times 0.87 \times 1700)[900 - (0.42 \times 0.44 \times 900)]$$

$$= (3027 \times 10^6) \text{ N mm} = 3027 \text{ kN m}$$

(a) Assuming elastic distribution of moments

$$M_u = 0.125\,(g + q_u)L^2$$
$$3027 = 0.125(12 + q_u) \times 30^2$$

Solving $\quad q_u = 14.9$ kN/m $\quad \therefore \quad$ Load factor $= \left[\dfrac{14.9}{6}\right] = 2.48$

(b) Assuming complete redistribution of moments

$$q_u = \left[\frac{12\,M_u}{L^2} - g\right] = \left[\frac{(12 \times 3027)}{30^2} - 12\right] = 28.36 \text{ kN/m}$$

Load factor against collapse $= \left(\dfrac{28.36}{8}\right) = 3.54$

15.9.3 Code Provisions for Moment Redistribution

Experimental investigations by Lin[10] and Macchi[11] indicated that the redistribution of moments may not always be complete. The difficulty in assessing the degree of redistribution is due to the use of theoretical values of the flexural strength of critical sections which exhibits a certain degree of scatter in the test values. A rigorous analysis of statically indeterminate prestressed structures at the limit state of collapse, involving detailed computations of hinge rotation, has been attempted in the report of the Institution of Civil Engineers[12] and by Bennett and Cooke[13].

Most present-day codes permit a limited amount of redistribution of moments when checking a structure at the limit state of collapse and thus overcome the lengthy computations involved in the rigorous method, which is not suitable for the design office. According to the Indian Standard Code IS: 1343, the redistribution of moments is permitted under the following conditions:

(a) Equilibrium between the internal forces and the external loads is maintained for appropriate load combinations.

(b) The ultimate moment of resistance provided at any section of a member is not less than 80 per cent of the moment at that section obtained from an elastic maximum moment diagram covering all appropriate combinations of loads.

(c) The elastic moment at any section in a member due to a particular combination of loads shall not be reduced by more than 20 per cent of the numerically largest moment covering all appropriate combination of loads.

(d) At sections where the moment capacity after redistribution is less than that from the elastic maximum moment diagram, the following relationship shall be satisfied:

$$\left[\left(\frac{x_u}{d}\right) + \left(\frac{\delta_M}{100}\right)\right] \le 0.5$$

where x_u = depth of the neutral axis
d = effective depth
δ_M = percentage reduction in moment

(e) In multistorey framed structures involving lateral stability, the reduction in moment allowed is restricted to 20 per cent for structures up to four storeys and 10 per cent for structures over four storeys.

The British code of practise BS EN: 1992–1-1[14] permits the redistribution of peak moments up to a maximum of 30 per cent. The code formally defines the moment redistribution ratio β_b as

$$\beta_b = \left(\frac{\text{moment at a section after redistribution}}{\text{moment at the section before redistribution}}\right) \leq 1$$

The neutral axis depth x should be checked to ensure the condition that

$$\left(\frac{x}{d}\right) \leq (\beta_b - 0.4) \text{ or } 0.6, \text{ whichever is less}$$

The percentage of moment redistribution allowed in design by the American code ACI: 318M–2011[15] depends upon the percentage of tensioned and untensioned reinforcement in the section. In sections where minimum area of bonded reinforcement up to 0.4 per cent is provided, the negative moments calculated by the elastic theory for any assumed loading arrangement may be increased or decreased by not more than

$$20\left[1 - \frac{\omega_p + \dfrac{d}{d_p}(\omega - \omega')}{0.36\beta_1}\right] \text{per cent}$$

where ω, ω', ω_p, d, d_p and β_1 are defined in Section 7.3.3. Redistribution of negative moment is permitted only when the section at which moment is reduced is so designed that

$$\omega_p, \left[\omega_p + \left(\frac{d}{d_p}\right)(\omega - \omega')\right] \qquad \text{or} \qquad [\omega_{pw} + (d/d_p)(\omega_w - \omega'_w)]$$

whichever is applicable, is not greater than 0.24 β_1. The choice of 0.24 β_1 as the largest tension reinforcement index ensures the adequate rotation capacity of the sections. However, the maximum permissible magnitude of redistribution is about 20 per cent, which is comparable to the values provided in the Indian and British codes.

15.10 Determination of Concordant Tendon Profile

In the design of continuous prestressed concrete members, it is often necessary to determine a cable profile lying within the limiting zone of thrust and also satisfying the conditions of concordancy. A general method based on the principle of virtual work is outlined for determining the concordant cable profile.

The deflection at any point in a beam due to the loading is expressed as,

$$a = \int \frac{Mmdx}{EI}$$

where M = primary moment (moment due to the actual eccentricity of the tendon at any cross-section)

m = moment due to unit load applied at the point where deflection is required

EI = flexural rigidity of the beam

Using finite differences, the deflection a can be expressed as,

$$a = \sum \frac{KMm}{E}$$

where $K = \left(\frac{dx}{I}\right)$ that is, a summation constant

In a prestressed beam, the primary moment is given by $M = Pe$, where P is the prestressing force located at an eccentricity e.
Hence,

$$a = \sum \frac{PemK}{E}$$

Since P and E are constant along the length of the beam,

$$a = \left(\frac{P}{E}\right) \Sigma Kme$$

For a concordant cable profile, $a = 0$.
Consequently, to obtain concordancy, the eccentricity of the cable along the length of the beam is arranged to satisfy the conditions, $\Sigma Kme = 0$. The method for determining a concordant profile is illustrated by the following example.

Example 15.14 A post-tensioned prestressed concrete propped-cantilever AC is 9 m long, fixed at C and propped at A. The cantilever beam has been designed to carry its own weight and a live load of 500 kN applied at B, distant 3 m from the fixed end. The beam is of uniform rectangular cross-section, 40 cm deep. The permissible limits of the tendon zone measured (positive downwards) from the centre line of the beam have been found to be as given below.

Distance from A, (m)	0	1.5	3.0	4.5	6.0	7.5	9.0
Upper limit, (cm)	–8.4	–4.5	–1.75	+ 0.25	+ 1.5	–8.5	–12.0
Lower limit, (cm)	+8.4	+10.0	+10.5	+10.0	+9.1	+7.8	–12.0

(a) Determine a concordant tendon profile for this beam and show it on an elevation of the beam to a suitable scale.

(b) Assuming that the tendon eccentricity must not exceed 100 mm, apply a linear transformation to reduce to a minimum the slope of tendon at C and draw an elevation of the transformed profile. What is the effect of this transformation on the support reaction at A if the horizontal component of the prestressing force is 520 kN?

Solution. The span of the propped cantilever is divided into six equal parts and the limiting zone of thrust is shown in Fig. 15.19. The computation of the trial values of Kme is outlined in Table 15.1. Simpson's rule can be used for evaluating the summation constant and the eccentricity of the cable is adjusted so that $\Sigma Kme = 0$ within a few trials. The concordant tendon profile is plotted using the values of the final eccentricity of the cable at various sections.

If the tendon eccentricity is not to exceed 100 mm, applying linear transformation, if y is the vertical downward shift of the cable at fixed support C, and considering point 6 (section at B), the following condition is obtained:

$$50 + \left(\frac{2}{3}\right)y = 100$$

$$\therefore \qquad y = 75 \text{ mm}$$

The linearly transformed profile is also shown in Fig. 15.19. It is important to note that the slopes of the transformed profile are comparatively lesser than those of the original profile.

If the horizontal component of the prestressing force is 520 kN, the increase of reaction at A is given by,

$$R_A = \left(\frac{Pe}{L}\right) = \left(\frac{520 \times 0.075}{9}\right) = 4.35 \text{ kN}$$

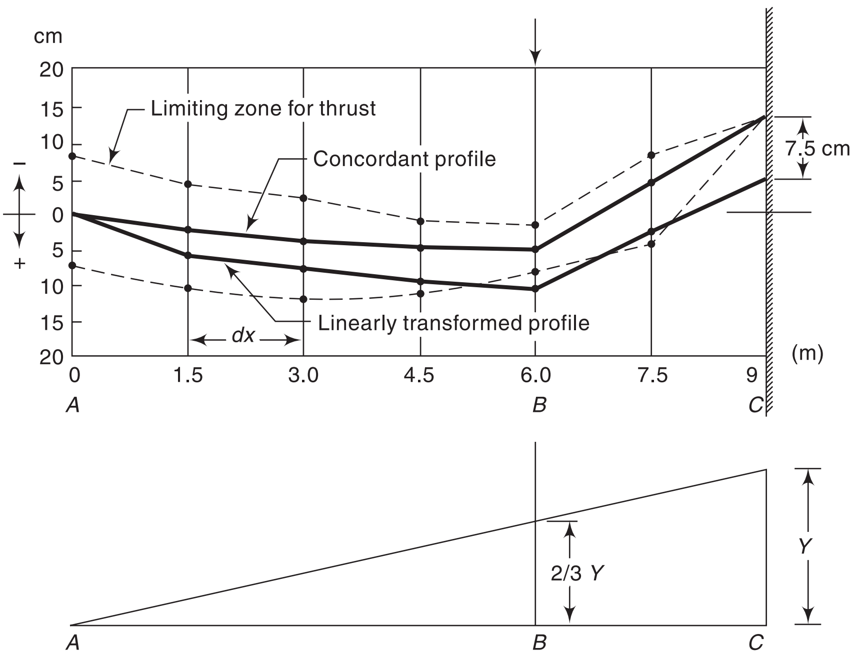

Fig. 15.19 *Concordant and linearly transformed profile*

Table 15.1 *Determination of concordant profile*

Position of point, (m)	I	*Simpson's rule coefficient,* q	$\frac{dx}{3}$ (m)	$K = \frac{qdx}{3I}$	*Unit moment diagram* (m)	Km	*First trial* e_1 (cm)	Kme_1	*Second trial* e_2 (cm)	Kme_2	*Third trial* e_3 (cm)	Kme_3
0	1	1	0.5	0.5	0	0	0	0	0	0	0	0
1.5	1	4	0.5	2.0	1	2	+4.5	+9.0	+3.0	+6.0	+3.0	+6.0
3.0	1	2	0.5	1.0	2	2	+4.8	+9.6	+4.0	+8.0	+4.0	+8.0
4.5	1	4	0.5	2.0	3	6	+5.1	+30.6	+4.2	+25.2	+4.5	+27.0
6.0	1	2	0.5	1.0	4	4	+5.0	+20.0	+4.25	+17.0	+5.0	+20.0
7.5	1	4	0.5	2.0	5	10	+0.0	0.0	–2.5	–25.0	–2.5	–25.0
9.0	1	1	0.5	0.5	6	3	+12.0	–36.0	–12.0	–36.0	–12.0	–36.0
							$\Sigma Kme_1 = +33.2$		$\Sigma Kme_2 = -5.0$		$\Sigma Kme_3 = 0$	

15.11 Design of Continuous Prestressed Concrete Beams

The design of statically indeterminate prestressed concrete structures involves the computations of maximum and minimum moments at various cross-sections of the members so as to obtain the range of moments which generally determines the cross-sectional dimensions of the member. The various steps involved in the design of continuous prestressed structures are summarised as follows:

1. Calculate the maximum positive and negative moments due to the live and dead load moments at various sections of the member and hence compute the range of moment, which is obtained as the difference of the maximum and minimum moments at a cross-section.

$$M_r = (M_{max} - M_{min})$$

2. The overall cross-sectional dimensions are fixed using the permissible compressive stress in concrete, f_c, by the equation,

$$Z = \left(\frac{bh^2}{6}\right) = \left(\frac{M_r}{f_c}\right)$$

Assuming a suitable value of $b = 0.4 - 0.5\,h$, the overall depth h is obtained.

3. The minimum prestressing force required is estimated by the expression,

$$P = \left[M_r \Big/ \left(\frac{h}{3}\right)\right]$$

4. The limiting zone for thrust is obtained by plotting (M_{max}/P) and (M_{min}/P) at each section measured from the upper and lower kern, respectively.
5. The profile of a cable lying within the limiting zone and suitable for a concordant profile is determined.
6. The stresses developed at transfer and working loads are checked at important sections.
7. The cable profile, if necessary, may be linearly transformed to reduce the slopes at supports with due regard to cover requirements.

The use of this design procedure is illustrated in the following example of a two-span continuous beam:

Example 15.15 Design a continuous prestressed beam of two spans ($AB = BC = 12$ m) to support a uniformly distributed live load of 10 kN/m. Tensile stresses are not permitted in concrete and the compressive stress in concrete is not to exceed 13 N/mm^2. Sketch the details of the cable profile and check for stresses developed at the support and span sections.

Solution.

1. *Maximum positive and negative moments under different combinations of live load*

The various load combinations to be considered to determine the maximum and minimum moments at various points along the span are shown in Fig. 15.20.

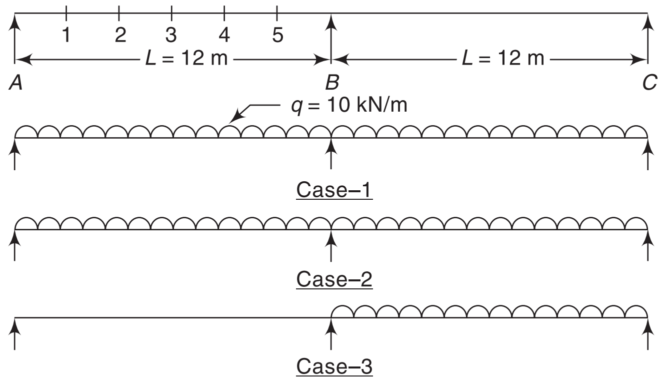

Fig. 15.20 *Loading patterns for maximum positive and negative moments*

The maximum range of live load moment at support section B,

$$M_{qr} = 0.125qL^2 = (0.125 \times 10 \times 12^2) = 180 \text{ kN m}$$

Assuming the width of the rectangular section to be used b = 250 mm, the overall depth is obtained as,

$$Z = \left[\frac{250 \times h^2}{6}\right] = \left[\frac{M_{qr}}{f_c}\right] = \left[\frac{180 \times 10^6}{13}\right]$$

$$\therefore \qquad h = \sqrt{\frac{6 \times 180 \times 10^6}{13 \times 250}} = 570 \text{ mm}$$

A rectangular section 250 mm wide and 600 mm deep is adopted.
Self-weight of beam = $(0.25 \times 0.60 \times 24) = 3.6$ kN/m

The maximum and minimum moments developed due to the loading patterns at various points from A to B are compiled in Table 15.2.

The moments at each of the points are expressed as $M = kw_d L^2$, where k is the moment coefficient whose values are shown within brackets in the table and can be obtained from Reynold's design handbook[16]. Using the values of the maximum positive (M_{Lp}) and negative (M_{Lg}) live-load and dead-load moments, the minimum prestressing force required is given by,

$$P = \left[\frac{M_{max} - M_{min}}{h/3}\right] = \left[\frac{180 \times 10^3}{600/3}\right] = 900 \text{ kN}$$

Table 15.2 *Computation of maximum positive and negative moments*

$g = 3.5$ kN/m $\qquad L = 12$ m

$q = 10$ kN/m $\qquad M = kw_d L^2$

Location	*Loading Pattern*			*Maximum Moments due to Live Load,* kN/m		*Dead-load Moments* M_g
	Case 1	*Case 2*	*Case 3*	M_{Lp}	M_{Ln}	kN m
A	(0)	(0)	(0)			
	0	0	0	0	0	0
1	(0.048)	(0.059)	–(0.010)	85.0	–14.4	25.0
	69.0	85.0	14.4			
2	(0.070)	(0.091)	–(0.021)	130.0	–30.2	36.0
	101.0	130.0	30.2			
3	(0.062)	(0.093)	–(0.036)	135.0	–45.0	32.0
	90.5	135.0	45.0			
4	(0.033)	(0.070)	–(0.042)	101.0	–60.5	17.4
	47.5	101.0	60.5			
5	–(0.036)	(0.017)	–(0.052)	24.5	–75.0	–18.8
	52.0	24.5	75.0			
B	–(0.125)	–(0.063)	–(0.063)	0	–180.0	–65.0
	180.0	90.5	90.0			

2. *Limiting zone for thrust*

Using the values of the maximum positive and negative live- and dead-load moments at each of the points from A to B, the minimum (M_1) and maximum (M_2) moments, the range of moments, and the position of the limits of the thrust zone are determined as shown in Table 15.3.

3. *Determination of concordant profile*

Using the trial and error procedure outlined in Section 15.10, a suitable profile lying within the limiting zone and satisfying the requirements of concordancy is determined using the procedure outlined in Table 15.4. The concordant profile of trial 2 is shown in Fig. 15.21.

4. *Check for stresses at sections* 3 *and B*

Section 3

$P = 9000$ kN $\qquad \left(\dfrac{P}{A}\right) = 6$ N/mm^2,

$Z = (15 \times 10^6)$ mm^3 $\qquad \left(\dfrac{Pe}{Z}\right) = 5.16$ N/mm^2,

$A = (15 \times 10^4)$ mm^2, $\qquad e = 86$ mm

$M_{max} = 167$ kN m $\quad$ and $\quad M_{min} = -13$ kN m

Table 15.3 *Determination of limiting zone for thrust line*

Location point	M_{Lp} (kN m)	M_{Ln} (kN m)	M_g (kN m)	Maximum Moment $M_2 = M_{Lp} + M_g$ (kN m)	Minimum Moment $M_1 = M_{Ln} + M_g$ (kN m)	Range of Moment $M_2 - M_1$ (kN m)	(M_2/P) from Upper Kern (mm)	(M_1/P) from Lower Kern (mm)	Eccentricity $e_2 = (M_2/P) - 100$, (mm)	Eccentricity $e_1 = (M_1/P) + 100$ (mm)
A	0	0	0	0	0	0	0	0	–100.0	+100.0
1	85.0	–14.4	25.0	110.0	10.6	99.4	122.0	11.8	22.0	111.8
2	130.0	–30.2	36.0	166.0	5.8	160.2	184.0	6.4	84.0	106.4
3	135.0	–45.0	32.0	167.0	–13.0	180.2	186.0	–14.0	86.0	86.0
4	101.0	–60.5	17.4	118.4	–43.1	161.5	132.0	–48.0	32.0	52.0
5	24.5	–75.0	–18.8	5.7	–93.8	99.5	6.30	–104.0	–93.7	–4.0
B	0	–180.0	–65.0	–65.0	–245.0	180.0	–72.0	–72.0	–172.0	–172.0

Table 15.4 *Determination of concordant profile*

Point	I	Simpson's rule coefficient q	$\frac{d_x}{3}$	$K = \frac{qdx}{3I}$	Unit moment diagram, m	Km	First trial e_1, (cm)	Kme_1	Second trial e_2, (cm)	Kme_2
A	1	1	2/3	0.667	0	0	0	0	0	0
1	1	4	2/3	2.667	0.167	0.440	+6.0	+2.64	+6.7	+2.97
2	1	2	2/3	1.333	0.333	0.440	+9.0	+3.96	+9.7	+4.30
3	1	4	2/3	2.667	0.500	1.333	+8.6	+10.66	+8.6	+11.50
4	1	2	2/3	1.333	0.667	0.880	+4.0	+3.52	+4.0	+3.52
5	1	4	2/3	2.667	0.833	2.230	–5.0	–11.15	–4.8	–10.70
B	1	1	2/3	0.667	1.000	0.667	+17.2	–17.2	–17.2	–11.50
							$\Sigma Kme_1 = -1.87$			$\Sigma Kme_2 = +0.09$

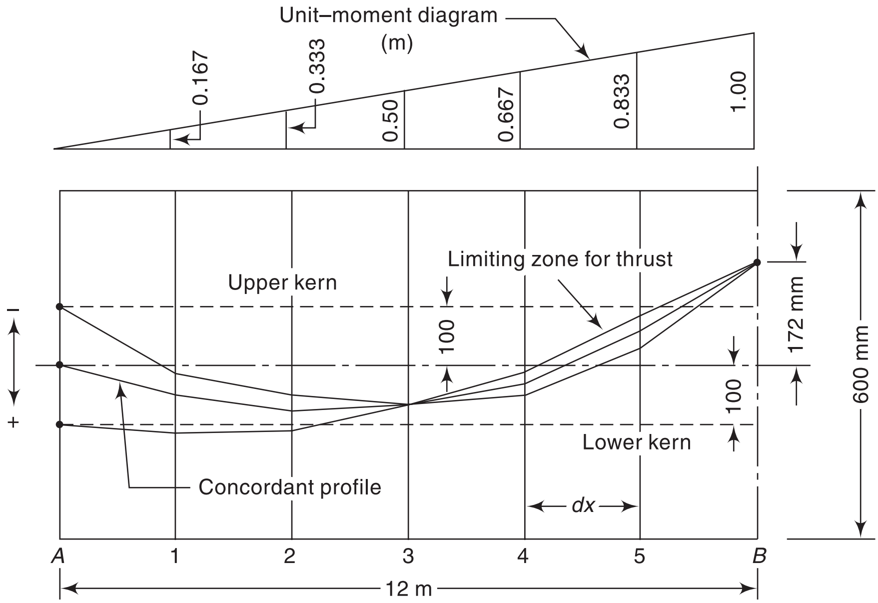

Fig. 15.21 *Limiting zone for thrust and concordant profile*

Stresses in N/mm^2		*+Compression*		*–Tension*	
Fibre	*Prestress*	*Max. load stress*	*Min. load stress*	*Max. stress*	*Min. stress*
Top	6 – 5.16 = 0.84	$\left(\frac{167\times10^6}{15\times10^6}\right)$ = 11.2	$\left(\frac{-13\times10^6}{15\times10^6}\right)$ = –0.87	12.04	–0.03
Bottom	6 + 5.16 = 11.16	–11.2	+0.87	–0.04	12.03

Section B

$$P = 900 \text{ kN} \qquad P/A = 6 \text{ N/mm}^3$$
$$Z = (15\times10^6)\text{ mm}^3 \qquad Pe/Z = 10.32 \text{ N/mm}^2$$
$$A = (15\times10^4)\text{ mm}^2 \qquad e = 172 \text{ mm}$$
$$M_{max} = -65 \text{ kN m} \quad \text{and} \quad M_{min} = -245 \text{ kN m}$$

Fibre	*Prestress*	*Max. load stress*	*Min. load stress*	*Max. stress*	*Min. stress* (N/mm^2)
Top	6 + 10.32 = 16.32	$\left(\frac{-65\times10^6}{15\times10^6}\right)$ = –4.35	$\left(\frac{245\times10^6}{15\times10^6}\right)$ = –16.32	11.97	0
Bottom	6 – 10.32 = –4.32	+4.45	+16.32	0.03	12.0

15.12 Design of Prestressed Portal Frames

In the design of unidirectional members, like continuous beams, the axial contraction due to the effect of prestressing is generally neglected as it has very little influence on the force and moments in the structure. But in the case of two-dimensional structures, such as portal frames and bents, the axial contraction of the members significantly influences the primary and secondary moments in the structure. This aspect has been closely examined in Section 15.8 and Example 15.11, where it is observed that tertiary moments developed at the fixed support of a portal frame due to the prestressing of the transom are approximately 54 and 11 per cent of the secondary and primary moments, respectively. Hence, the effect of axial shortening is also considered in the design of portal frames.

The data available for purpose of design is the overall shape of the structure and the loading conditions. The computations of maximum and minimum live-load bending moments require a knowledge of the stiffness of the members of the frame. The moments and thrusts are determined by assuming a suitable stiffness ratio by the normal methods of structural analysis[17]. The section of each member is determined such that it is capable of withstanding the maximum variation of moments at the section.

The direct force developed in the members is made up of three parts: the thrust due to prestress N_p, thrust developed due to the dead load N_g and that due to the live load N_1 for maximum moment condition M_1 and N_2 for minimum moment condition M_2. It is important to note that the critical moment conditions at different sections may be due to the combination of different loading conditions[18]. Hence, if N_A = total thrust in a member under maximum moment condition $M_1 + M_g$ and N_B = total thrust in a member under minimum moment condition, then

$$N_A = N_p + N_g + N_1 \tag{15.3}$$

$$N_B = N_p + N_g + N_2 \tag{15.4}$$

Assuming that the resultant thrust N_A and N_B, pass through the kern points for the maximum and minimum moment conditions, resulting in zero tension and maximum compressive stress at the extreme fibres of the section as shown in Fig. 15.22 and representing M_L for the maximum moment variation, $M_1 - M_2$ the following relation is obtained:

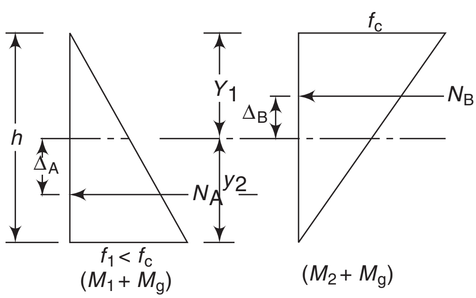

Fig. 15.22 *Stress distribution under maximum and minimum moment conditions*

$$M_L = N_A\Delta_A + N_B\Delta_B \tag{15.5}$$

where Δ_A and $-\Delta_B$ are the core limits I/Ay_1 and $-I/Ay_2$, respectively.

Substituting the values of N_A and N_B from Eqs 15.3 and 15.4 in Eq. 15.5, and assuming a rectangular section of overall depth h, we have

$$M_L = \left[(N_p + N_g)\frac{h}{3} + (N_1 + N_2)\frac{h}{6}\right] \tag{15.6}$$

But $$N_B = \frac{1}{2}f_c A = (N_p + N_g + N_2) \tag{15.7}$$

If $$A = bh$$

then $$N_p + N_g = \left[\frac{1}{2}f_c A - N_2\right] \tag{15.8}$$

Hence, $$M_L = \left[\frac{1}{6}f_c bh^2 + \frac{1}{6}(N_1 - N_2)h\right] \tag{15.9}$$

Similarly, if $$N_2 > N_1$$

then $$M_L = \left[\frac{1}{6}f_c bh^2 + \frac{1}{6}(N_2 - N_1)h\right] \tag{15.10}$$

The second terms being always negative, the section required will generally be larger than that for beams required to support the same moment variation. Since b and h are the only unknowns in the above expressions, by choosing a suitable width, the depth of the section can be determined. The dead-load moments, M_g and thrust N_g, may now be calculated by the normal methods, and by using Eq. 15.8, the required prestressing force can be estimated.

The limiting zone can now be determined easily by plotting the ratios $M_1 + M_g/N_p$ and $M_2 + M_g/N_p$ in each member on lines at a distance of N/N_p times the core distances from the line of centroids, using the appropriate value of N for the two moment conditions. The plotting lines in rectangular sections correspond to the values, $(h/6)$ (N_A/N_p) and $(-h/6)$ (N_B/N_P), respectively. The typical bending moments developed in a portal frame with pinned ends under dead and concentrated live load at centre of span, together with the limiting zones, are shown in Fig. 15.23. Having determined the limiting zone, it is necessary to locate a concordant cable profile lying within the limiting zone. The cable profile, if required, may be linearly transformed to suit practical requirements.

The procedure detailed above is applied to the design of a portal frame hinged at the supports.

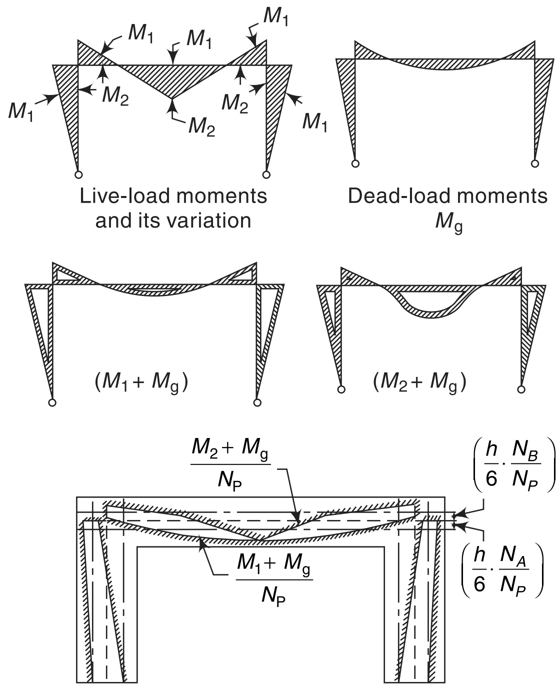

Fig. 15.23 *Bending moments and limiting zones*

Example 15.16 A two-pinned portal frame, 9 m high with a span of 15 m, is to be designed to support a uniformly distributed live load of 14.6 kN/m on the transom. The permissible stresses are not to exceed 14 N/mm^2 in compression with zero tension. Design the frame and sketch the details of the concordant profile in the legs and transom.

Solution. The moments and force in the frame are analysed by moment distribution or column analogy method by assuming a suitable stiffness ratio between the leg and transom members. In this case, assuming the transom and legs of the same cross-section, the moments and thrusts analysed are as follows:

Live-load moments and thrusts

Moments at knee = –240 kN m (hogging)

Transom mid-span moments = +185 kN m (sagging)

Vertical reaction in legs = 111.25 kN

Horizontal thrust = 26.17 kN

The dimensions of the critical sections are estimated by using Eqs 15.9 and 15.10.

For the transom, $M_L = 185$ kN m, and

$$N_1 - N_2 = -26.17 \text{ kN}$$

Assuming a breadth of 300 mm for the rectangular section from Eq. 15.9, the following is obtained,

$$(185 \times 10^6) = \left(\frac{1}{6} \times 14 \times 300(h)^2\right) + \left(\frac{1}{6}(-26.17 \times 10^3)h\right)$$

Hence, $h = 525$ mm

Similarly for the legs,

$$M_L = 240 \text{ kN m}$$

and $N_2 - N_1 = -111.25$ kN

Hence, $$(240 \times 10^6) = \left(\frac{1}{6} \times 14 \times 300h^2\right) - \left(\frac{1}{6} \times 111.25 \times 10^3 \times h\right)$$

$\therefore$ $h = 600$ mm

However, a uniform section of 300 × 600 mm is adopted for the legs and transom.

Dead load = (0.3 × 0.6 × 2.4) = 0.432 kN/m

The bending moment and thrusts developed in the members due to dead load are obtained as,

Knee moment = –72 kN m

Transom mid-span moment = 55.25 kN m

Vertical reaction in legs = 33.37 kN

Horizontal thrust = 3.38 kN

The prestressing force required in the transom and legs is obtained from Eqs 15.3 and 15.4 as,

$$N_P = \left[\frac{1}{2} f_c bh - N_g - N_1\right]$$

or $$N_P = \left[\frac{1}{2} f_c bh - N_g - N_2\right]$$

For the transom, $$N_P = \left[\frac{1}{2} \times \frac{14}{1000} \times 300 \times 600 - 3.38 - 26.17\right] = 1230 \text{ kN}$$

For the legs, $$N_P = \left[\frac{1}{2} \times \frac{14}{1000} \times 300 \times 600 - 33.37 - 111.25\right] = 1145 \text{ kN}$$

Determination of the cable zone

The permissible core limits are evaluated for each of the members under various load conditions. The core limits for a beam of rectangular section is $\pm h/6$, but, due to the presence of applied loading thrusts, they have to be modified by multiplying them by the factor N/N_P. The factor N/N_P for the various members is computed as follows:

(a) Transom (under dead load only),

$$\left(\frac{N}{N_p}\right) = \left(\frac{1230 + 3.38}{1230}\right) = 1.002$$

(b) Transom (under live load + dead load),

$$\left(\frac{N}{N_p}\right) = \left[\frac{(1230 + 3.38 + 26.17)}{1230}\right] = 1.022$$

(c) Top of legs (dead load only),

$$\left(\frac{N}{N_p}\right) = \left(\frac{1145 + 33.47}{1145}\right) = 1.03$$

(d) Top of legs (under live load + dead load),

$$\left(\frac{N}{N_p}\right) = \left(\frac{1145 + 33.47 + 111.25}{1145}\right) = 1.10$$

The value of the ratio N/N_P indicates that the effect of axial thrusts is negligible in all the cases except (d).

The limiting zone can be obtained as the limiting bending moment diagrams plotted to a scale of I/N_P on the corresponding core limits as follows:

1. *Leg foot zone limits*

   Since there are no moments due to the loads at the hinged supports and

   $$\left(\frac{h}{6}\right) = \left(\frac{600}{6}\right) = 100 \text{ mm}$$

   the distances measured from the centroidal axis are as follows:

   (a) Upper limits (towards outside of frame) = –100 × 1.03 = –103 mm

   (b) Lower limit (towards inside of frame) = 100 × 1.10 = 110 mm

2. *Leg top zone limits*

   (a) Upper (outer) limit,

   $$\left(\frac{M_2 + M_g}{N_p} - \frac{h}{6}\frac{N}{N_p}\right) = \left(-\frac{72 \times 10^3}{1145}\right) - (100 \times 1.03) = -165 \text{ mm}$$

   (b) Lower (inner) limit,

   $$\left(\frac{M_1 + M_g}{N_p} + \frac{h}{6}\frac{N}{N_p}\right) = \left(-\frac{312 \times 10^3}{1145}\right) + (100 \times 1.10) = -162 \text{ mm}$$

3. *Transom mid-span zone limits*

   (a) Upper limit,

   $$\left(\frac{M_2 + M_g}{N_p}\right) - \left(\frac{h}{6}\frac{N}{N_p}\right) = \left(\frac{240.25 \times 10^3}{1230}\right) - (100 \times 1.022) = 94 \text{ mm}$$

   (b) Lower limit,

   $$\left(\frac{M_1 + M_g}{N_p}\right) + \left(\frac{h}{6}\frac{N}{N_p}\right) = \left(\frac{55.25 \times 10^3}{1230}\right) + (100 \times 1.022) = 145 \text{ mm}$$

4. *Transom end zone limits*

   (a) Upper limit,

   $$\frac{M_2 + M_g}{N_p} - \left(\frac{h}{6}\frac{N}{N_p}\right) = -\frac{72 \times 10^3}{1230} - (100 \times 1.022) = -158 \text{ mm}$$

   (b) Lower limit,

   $$\left(\frac{M_1 + M_g}{N_p}\right) + \left(\frac{h}{6}\frac{N}{N_p}\right) = \left(-\frac{312 \times 10^3}{1230}\right) + (100 \times 1.022) = -151 \text{ mm}$$

The limiting zone with the limits marked for the critical sections in the transom and legs is shown in Fig. 15.24.

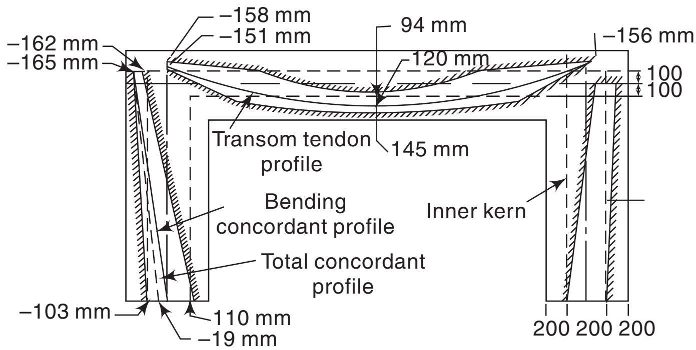

Fig. 15.24 *Limiting zone and concordant profiles in two-pinned portal frame*

Determination of bending concordant profile

A suitable cable profile lying within the cable zone can be determined by considering the moments developed for the two cases of loading. The eccentricity of the cable can be estimated by the expression,

$$e = -\left(\frac{M_g}{P}\right) + \left(\frac{M_1 + M_2}{2P}\right)$$

The eccentricity required for the prestressing force at the transom ends is given by,

$$e = -\left(\frac{72 \times 10^3}{1230}\right) - \left(\frac{240 \times 10^3}{2 \times 1230}\right) = -156 \text{ mm}$$

At transom mid-span,

$$e = \left(\frac{55.25 \times 10^3}{1230}\right) + \left(\frac{185 \times 10^3}{2 \times 1230}\right) = 120 \text{ mm}$$

Eccentricity at the leg top is given by,

$$e = -\left(\frac{72 \times 10^3}{1145}\right) - \left(\frac{240 \times 10^3}{2 \times 1145}\right) = -165 \text{ mm}$$

The cable profile following these values of eccentricity is straight in the leg portions and parabolic in the transom portion. To ensure total concordance, the additional eccentricity required to provide for the feet separation equivalent to the transom shortening under prestress must be determined. Assuming that only leg bending takes place, the additional eccentricity e_1 in transom is zero and additional eccentricity e_2 at the feet of legs is given by[18],

$$e_2 = \left(\frac{3N_{p1} I_2 L}{N_{p2} A_1 h^2}\right)$$

where N_{p1} and N_{p2} are the prestressing force in the transom and legs, respectively,

A_1 = cross-sectional area of transom
I_2 = second moment of area of leg
L = length of transom, and
h = height of leg

$$e_2 = \left[-3 \times \frac{1230}{1145} \times \frac{(1/12)(300)(600)^3}{(300) \times (600)} \times \frac{15 \times 10^3}{(9000)^2} \right] = -19 \text{ mm}$$

The bending and totally concordant profiles are shown in Fig. 15.24.

References

1. Lin, TY, *Prestressed Concrete Structures,* John Wiley and Sons, Inc. 1960, pp 288–292.
2. Visvesvaraya, HC and N Raghavendra, "Continuity in prestressed concrete construction," *Seminar on Problems of prestressing,* Madras, 1970, pp 1–91–94.
3. Guyon, Y, *Prestressed Concrete,* Vols. 1 and 2, Contractors Record Ltd., London, 1953.
4. Morice, PB, and EH, Cooley, *Prestressed Concrete Theory and Practice,* Sir Isaac Pitman and Sons Ltd., London, 1958; pp 105–110.
5. Bate, SCC and EW Bennett, *Design of Prestressed Concrete,* Surrey University Press, London, 1976, pp 130–132.
6. Baker, JF, MR Horne, and J Heyman, *The Steel Skeleton.* Vo1. 2. Cambridge University Press, London, 1956.
7. Prager, W and PG Hodge, *Theory of Perfectly Plastic Solids,* John Wiley and Sons, Inc., New York, 1951.
8. Ernst, GC, "Moment and shear redistribution in two-span continuous reinforced concrete beams," *Proceedings of the American Concrete Institute*, Vol. 55, Nov. 1958, pp 573–589.
9. Cranston, WB, "Tests on reinforced concrete portal frames," *Cement and Concrete Association Technical Report No.* TRA/392, London, 1965.
10. Lin, TY, "Strength of continuous prestressed concrete beams under static and repeated loads," *Journal of the American Concrete Institute, Proceedings,* Vol. 26, 1955, pp 1037–1059.
11. Macchi, G, "Etude experimentale de poutres continues pre contraintes dans la domaine plastique et al., a rapture (Experimental study of continuous prestressed concrete beams in the plastic range at failure)," *Federation, Internatianale Precontrainte, 2nd Congress,* Amsterdam, 1955.
12. Institution of Civil Engineers, "'Ultimate load design of concrete structures," *Research Committee Report, Proceedings of the Institution of Civil Engineers,* Vol. 21, Feb. 1962, pp 400–431.
13. Bennett, EW, N Cooke, and LP Naughton, "Deformation of continuous prestressed concrete beams and its effect on the ultimate load," *Proceedings of the Institution of Civil Engineers,* London, Vol. 37, May, 1967, pp. 57–74, Disc 38, Dec. 1967, pp 769–774.
14. BS EN: 1992–1–1, Euro code-2, Design of Concrete Structures, General Rules and Rules for Buildings, British Standards Institution, 2004.
15. ACI: 318M–2011, *Building Code Requirements for Structural Concrete and Commentary,* American Concrete Institute, Farmington Hills, Michigan, 2011.
16. Reynolds, CE, *Reinforced Concrete Designer's Handbook,* Concrete Publications Ltd., London, pp 219–225.

17. Marshall, WT and HM Nelson, *Structures,* Pitman, London, 1970, pp 1–442.
18. Morice, PB and Cooley, EH, *Prestressed Concrete Theory and Practice,* Sir Isaac Pitman and Sons Ltd, London, 1958, pp 85–96.

Review Questions

15.1 What are the advantages of continuous members in prestressed concrete structures?

15.2 Explain the terms (a) primary moment, (b) secondary moment, (c) resultant moment, and (d) redundant reaction, with respect to continuous prestressed concrete beams.

15.3 Explain with sketches the various methods of achieving continuity in prestressed concrete members.

15.4 What are cap cables? Where are they used?

15.5 Explain the terms (a) line of thrust, and (b) concordant cable, in prestressed concrete continuous structures.

15.6 List the commonly used method to analyse secondary moments in prestressed concrete continuous members.

15.7 Explain with sketches the tendon reaction or the method of equivalent loads for analysing the statically indeterminate prestressed concrete structures.

15.8 State Guyon's theorem of linear transformation of cables and its practical application.

15.9 What are concordant cables? Sketch a typical concordant cable profile in a two-span continuous prestressed concrete beam.

15.10 Briefly explain the various steps involved in the design of continuous prestressed concrete beams and portal frames.

Exercises

15.1 A two-span continuous prestressed concrete beam ABC ($AB = BC = 15$ m) has a uniform cross-section with a width of 250 mm and depth of 600 mm. A cable carrying an effective prestressing force of 500 kN is parallel to the axis of the beam and located at an eccentricity of 200 mm.

(a) Determine the secondary and resultant moment developed at the mid-support section B.

(b) If the beam supports an imposed load of 2.4 kN/m, calculate the resultant stresses developed at the top and bottom of the beam at B. Also locate the resultant line of thrust through the beam AB.

[Ans: (a) Secondary moment at B = +150 kN m;
Resultant moment at B = +50 kN m
(b) Stress at top = –4.58 N/mm^2 (tension);
Stress at soffit = +11.22 N/mm^2 (compression)]

15.2 A two-span continuous beam ABC ($AB = BC = 10$ m) is of rectangular section, 200 mm wide and 500 mm deep. The beam is prestressed by a parabolic cable, concentric at end supports and having an eccentricity of 100 mm towards the soffit of the beam at centre of spans and 200 mm towards the top of beam at mid support *B*. The effective force in the cable is 500 kN.

(a) Show that the cable is concordant.

(b) Locate the pressure line in the beam when, in addition to its self-weight, it supports an imposed load of 5.6 kN/m.

[Ans: (a) SM at *B* = 0; (b) Pressure line coincides with the centroidal axis]

15.3 A continuous concrete beam *ABC* (*AB* = *BC* = 10 m) has a uniform rectangular cross-section, 100 mm wide and 300 mm deep. A cable carrying an effective prestressing force of 360 kN varies linearly with an eccentricity of 50 mm towards the soffit at the end supports to 50 mm towards the top of beam at mid-support *B*.

(a) Determine the resultant moment at *B* due to prestressing only.

(b) If the eccentricity of the cable at *B* is +25 mm, show that the cable is concordant. **[Ans: (a) RM at *B* = +9 kN m]**

15.4 A three-span continuous prestressed concrete prismatic beam of depth 2 m is prestressed by a design prestressing force of 3300 kN. The spans are *AB* = *CD* = 30 m and *BC* = 40 m. The eccentricities of the prestressing force at different locations along the beam are given in the following table:

x, measured from A	0	15	30	50	70	85	100
Eccentricity *e*, mm	0	–260	+450	–410	+450	–260	0

Note: – below the centroid, + above the centroid

(a) If the cable profile is parabolic between the supports, evaluate the equivalent load and hence compute the moments produced at supports of mid-span points, due to prestressing.

(b) Also locate the position of the pressure line.

(c) Suggest a suitable concordant profile.

[Ans: (a) Equivalent load = 14.2 kN/m; Moments at *B* and *C* = +1800 kN m; Moments at mid-points of *AB* = –700 kN m; BC = –1050 kN m; (b) Position of pressure line at *B* and *C* = + 545 mm: At centre of mid-span = –317 mm: At centre of end-span = –212 mm; (c) Same as pressure line]

15.5 A two-span continuous concrete beam *ABC* (*AB* = *BC* = 12 m) has a rectangular section, 300 mm wide and 800 mm deep. The beam is prestressed by a cable carrying an effective force of 700 kN. The cable has a linear profile in the span *AB* and parabolic profile in span *BC*. The eccentricities of the cable are +50 mm at *A*, –100 mm at a distance of 7 m from A and +200 mm at support *B* and –200 mm at mid span of *BC* (–below and + above centroidal axis).

(a) Evaluate the resultant moment developed at *B* due to the prestressing force.

(b) Sketch the line of thrust in the beam if it supports, a uniformly distributed load of 5 kN/m which includes the self-weight of the beam.

(c) Find the resultant stress distribution at the mid-support section for condition (b). **[Ans: (a) RM at *B* = + 170 kN m**
(b) Pressure Line: at *A* = +50 mm, at 7 m from *A* = –24.4 mm at *B* = +115.4 mm, at centre of *BC* = –113.7 mm
(c) stress at top = 5.44 N/mm^2 and stress at bottom = 0.39 N/mm^2 (compression)]

15.6 A prestressed portal frame *ABCD* fixed at *A* and *D* has the following section properties:

Member	*Length* (m)	*Sectional Area* (cm^2)	*Second Moment of Area* (cm^4)	*Section Modulus* (cm^3)
AB and *CD*	4.5	190	16,000	1280
BC	6.0	190	24,000	1600

The columns *AB* and *CD* are prestressed by a straight cable (effective force in cable = 160 kN) with an eccentricity of 50 mm towards the inside of frame at *A* and *D* and 50 mm towards the outside of frame at *B* and *C*. The horizontal member BC is prestressed by a cable (effective force = 140 kN) with a parabolic profile having an eccentricity of 50 mm above the centroid at *B* and *C* and 100 mm below the centroid at the centre of *BC*. The overall depth of *AB* and *CD* is 250 mm and that of *BC* is 300 mm.

(a) Calculate the secondary moments developed at *A* and *B*.

(b) Find the displacement of the line of thrust in the members *AB* and *BC*.

[Ans: (a) M_A = + 3.2 kN m; M_B = 1.6 kN m:
(b) 20 mm at A
10 mm at top of column
11.4 mm in member BC]

15.7 A prestressed two-hinged portal frame has column *AB* = *CD* = 4.8 m and transom BC = 9 m. The members have a cross-section, 125 mm wide and 300 mm deep throughout. The columns are prestressed by a straight cable with an eccentricity of 75 mm towards the outside off-frame at *B* and *C* with zero eccentricity at the hinges *A* and *D*. The transom is prestressed by a straight cable having an eccentricity of 100 mm below centroid at the centre of *BC* and 75 mm above the centroid at *B* and *C*.

If all the cables are tensioned in a force of 225 kN (neglecting self-weight), calculate

(a) the secondary moment developed at *B*,

(b) the resultant stress distribution at *B* and centre of *BC*, and

(c) the displacement of the line of thrust at *B* and centre of *BC*.

[Ans: (a) –3.82 kN m: (b) At *B*, stress = 13 N/mm^2 (compression) outside face and 1 N/mm^2 (tension) inside face:
At centre of *BC*, 8 N/mm^2 (tension) outside face and 20 N/mm^2 (compression) inside face;
(c) Line of prestress displaced 17 mm inward at *B* and centre of *BC*]

15.8 A continuous beam *ABC* (*AB* = *BC* = 20 m) has a rectangular section, 400 mm wide and 600 mm deep, throughout the two spans and is prestressed by a concordant cable having a cross-sectional area of 1700 mm^2 located 60 mm from the top of the beam at *B*. If the beam supports a uniformly distributed superimposed service load of 4.24 kN/m throughout the spans, estimate the load factor against failure assuming,

(a) elastic distribution of moments; and

(b) complete redistribution of moments.

Adopt f_p = 1600 N/mm^2 and f_{ck} = 40 N/mm^2, D_c = 24 kN/m^3

[Ans: (a) 2.44 (b) 3.66]

15.9 Design a prestressed concrete beam continuous over two equal spans of 9 m to support live loads of 30 kN each at the centre of span. The loads may be applied independently or jointly. Permissible stress being zero in tension and 15 N/mm^2 in compression. Loss ratio = 0.85. Determine a concordant profile and show it on an elevation of the beam. Allowing for a minimum cover of 100 mm, sketch a suitable transformed profile to reduce the slope of the tendons at the central support to a minimum. Check for the limit states of serviceability and collapse. **[Ans: Rectangular section 200 mm wide and 400 mm deep; Prestressing force = 510 kN]**

15.10 Design a two-pinned portal frame 7.5 m high with a span of 12 m to support a uniformly distributed live load of 15 kN/m on the transom with stress limits of 14 N/mm compression and zero tension. Assume that the transom and legs have the same section.

[Ans: Section of leg and transom: 300 mm wide and 450 mm deep Prestressing force for: Transom = 960 kN, Legs = 870 kN]

Objective-type Questions

15.1 Continuity in prestressed concrete structures results in
(a) an increase in the size of members
(b) reduction in the size of members
(c) neither increase nor decrease in the size of members

15.2 In comparison with simply supported structures, continuous prestressed concrete structures exhibit
(a) no change in the ultimate strength
(b) lower ultimate strength
(c) higher ultimate strength

15.3 In comparison with simply supported beams, in continuous prestressed concrete prestressed concrete beams the deflections
(a) lower
(b) higher
(c) more or less similar

15.4 Prestressing a continuous concrete beam results in
(a) primary moments
(b) secondary moments
(c) tertiary moments

15.5 When compared with simply supported beams, prestressed concrete continuous beams require
(a) lesser number of anchorages
(b) increased number of anchorages
(c) the same number

15.6 In prestressed concrete beams, prestressing results in secondary moments due to
(a) static reactions
(b) redundant reactions
(c) deformations

15.7 Stressing concordant cables in continuous structures results in
(a) primary reactions
(b) zero redundant reactions
(c) axial thrust

15.8 Tendon reaction method of analysing prestressed concrete continuous members involves the principles of
(a) redundant reactions
(b) secondary moments
(c) equivalent load system

15.9 The ultimate load carrying capacity of a continuous beam depends on the
(a) type of loads on the beam
(b) number spans
(c) degree of redistribution of moments

15.10 The design of a prestressed concrete continuous beam involves the computation of
(a) maximum moments
(b) range of moments
(c) minimum moments

Answers to Objective-type Questions

15.1 (b)	15.2 (c)	15.3 (a)	15.4 (b)	15.5 (a)
15.6 (b)	15.7 (b)	15.8 (c)	15.9 (c)	15.10 (b)

16 Prestressed Concrete Pipes and Tanks

16.1 Circular Prestressing

Liquid retaining structures, such as circular pipes, tanks and pressure vessels are admirably suited for circular prestressing. The circumferential hoop compression induced in concrete by prestressing counterbalances the hoop tension developed due to the internal fluid pressure. A reinforced concrete pressure pipe requires a large amount of reinforcement to ensure low-tensile stresses resulting in a crack-free structure. However, circular prestressing eliminates cracks and provides for an economical use of materials. In addition, prestressing safeguards against shrinkage cracks in liquid retaining structures.

In circular prestressing, the member may be prestressed by overlapping tendons within the ducts so as to minimise frictional losses as shown in Fig. 16.1(a). An alternative method is to wrap the high-tensile wires under tension around precast cylindrical members as shown in Fig. 16.1(b). This method was developed much earlier than linear prestressing and has been in use for a considerable period of time for the production of pressure pipes[1]. The tension in the wire is produced by pulling it through a die [Fig. 16.l(c)], which reduces its section, consequently developing the required amount of tensile stress in the steel. The wrapped wires are generally protected against corrosion by a coating of cement mortar. Recent developments reported by Doanides[2], include the use of picovex mortar which consists of a proprietary epoxy resin formulation containing coal tar used as the binder of a sand filled mortar.

In Czechoslovakia, helical prestressing has been used in which the wire feeding device is moved longitudinally as the pipe is rotated. This operation induces triaxial stresses in the material.

In erstwhile USSR, self-stressing cement techniques have been successfully used for producing small diameter pipes. A preformed spiral of high-strength steel is placed in the forms, the concrete made by using expanding cement is placed and consolidated, and the completed unit is cured under carefully controlled conditions to achieve the correct degree of expansion after the set.

It is important to note that calcium chloride must never be used as an accelerating admixture in prestressed concrete since a number of failures of prestressed concrete pipes and tanks have been recorded due to the phenomenon of chloride corrosion.

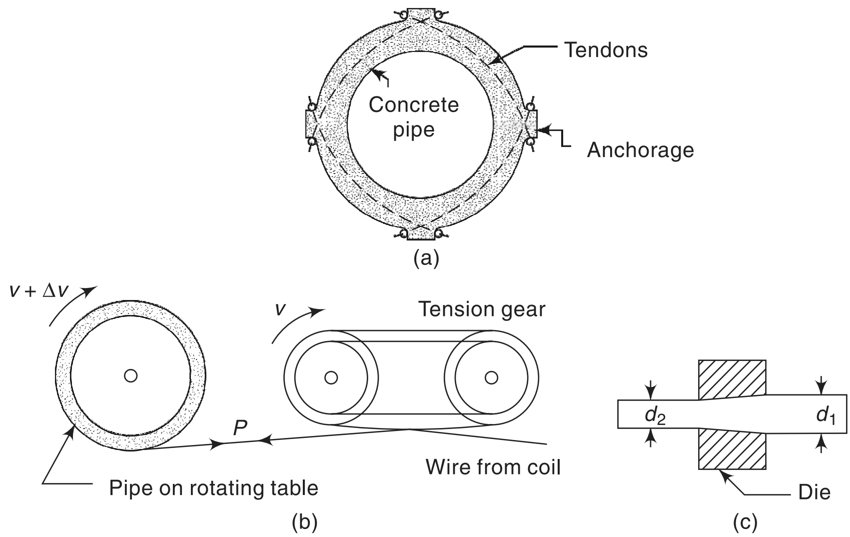

Fig. 16.1 *Circular prestressing of pipes*

It is well-established that prestressed concrete pipes are ideally suited for a pressure range of 0.5 to 2 N/mm[2, 3]. For this pressure range, while cast iron and steel pipes are not economical, reinforced concrete pipes are not practicable due to their limited cracking strength. The technique of prestressing pipes was first introduced in 1930 and ever since, numerous pipelines have been installed throughout the world. Over the last five decades, several new techniques have been developed for manufacturing prestressed concrete pressure pipes by various proprietary organisations which have patented their systems. Prestressed pipes have been extensively used recently in the water supply scheme of Greater Madras to convey water from Veeranam Lake to the city. Each of the prestressed concrete pipes was 6 m long with an internal diameter of 1.676 m and a maximum working pressure of about eight atmospheres.

16.2 Types of Prestressed Concrete Pipes

According to Ooykaas[4], prestressed concrete pipes may be classified depending upon the method of manufacture under the following groups:

Monolyte construction The method developed by Freyssinet[5] as early as in 1930 is based on the principle that a mix of fresh concrete subjected to triaxial pressure behaves in some respects like a solid body. If steel is embedded in such a mass of concrete, which is deformed while the pressure is maintained, the steel also experiences the deformation of the surrounding concrete. The manufacturing process consists of pouring concrete under high frequency vibration in a vertically placed steel mould consisting of an inner and outer shell. The outer shell, consisting of longitudinal sections held together by spring assembles, permits the mould to expand while the inner steel mould is covered with an expansible rubber membrane.

Steam curing is adopted for accelerated curing of concrete and the main advantage of this method is that stressing and production are achieved in a single cycle.

Two-stage construction The method of manufacturing a non-cylinder pipe (without the steel cylinder) was developed by Lewiston Pipe Corporation around 1930[6]. In the first stage, the concrete is cast over a tensioned longitudinal reinforcement. In the second stage, the concrete pipes after curing are circumferentially stressed by means of a spiral wire wound under tension and protected by a coat of mortar. The main function of the longitudinal prestress is to prevent cracking in concrete during circumferential winding and cracking due to the bending stresses developed during the handling and installation of pipes. The longitudinal section of a noncylinder pipe with socket and spigot joints is shown in Fig. 16.2. These prestressed pipes, which were produced by the Vacuum Concrete (Overseas) Co. Inc. in collaboration with an Indian firm, are to be used for the Veeranam scheme to convey water to Madras.

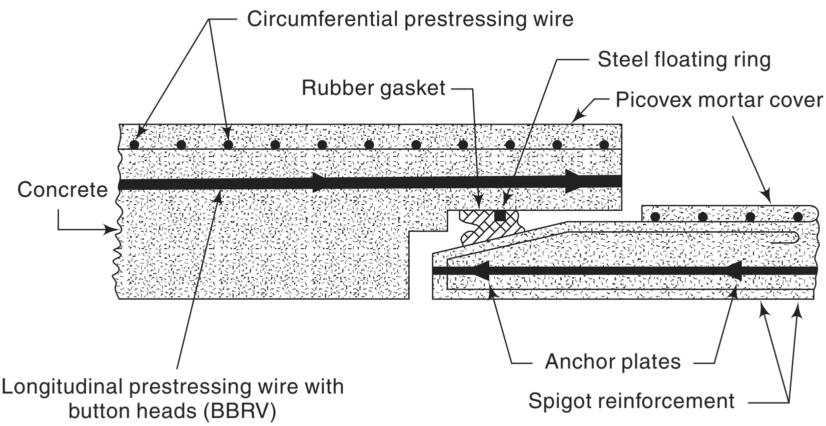

Fig. 16.2 *Typical longitudinal section of non-cylinder prestressed concrete pipe*

In the case of cylinder pipes developed by the Lock Joint Company, USA, in 1942, a welded cylinder of 16 gauge steel is lined with concrete on the inside, and the steel pipe wrapped with a helix of highly stressed wire. Tubular fasteners are used for the splices and for end-fixing of the wire, and the pipe is finished with a coating of rich mortar. These pipes, generally referred to as 'prestressed concrete lined cylinder pipes' are suitable up to 1.2 m diameter. A second type of cylinder pipe was developed in 1950, in which the steel cylinder with joint rings is embedded in the concrete core so that the circumferential wire winding is in contact with concrete instead of contact being with the steel cylinder. The protective coating is either cement concrete or mortar. Since the core thickness can be varied to resist higher stresses, these pipes, generally referred to as 'prestressed concrete embedded cylinder pipes', are suitable for diameters up to 3.6 m. Figures 16.3 and 16.4 show the sectional details of the two types of cylinder pipes.

The technique of double winding and double coating is employed wherever high pressures are involved with larger diameter of pipes.

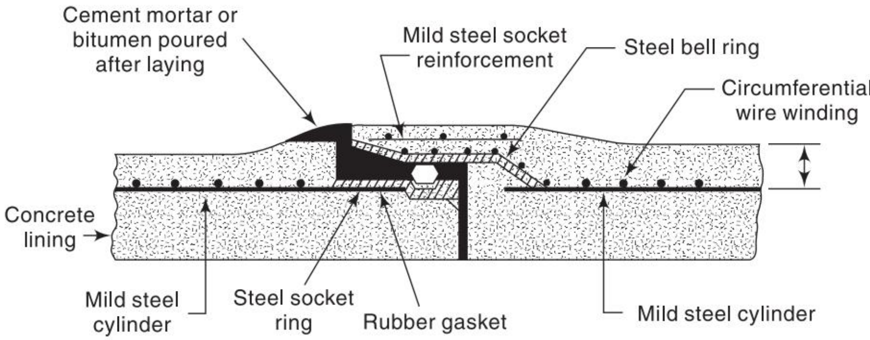

Fig. 16.3 *Typical longitudinal section of prestressed concrete lined cylinder pipe*

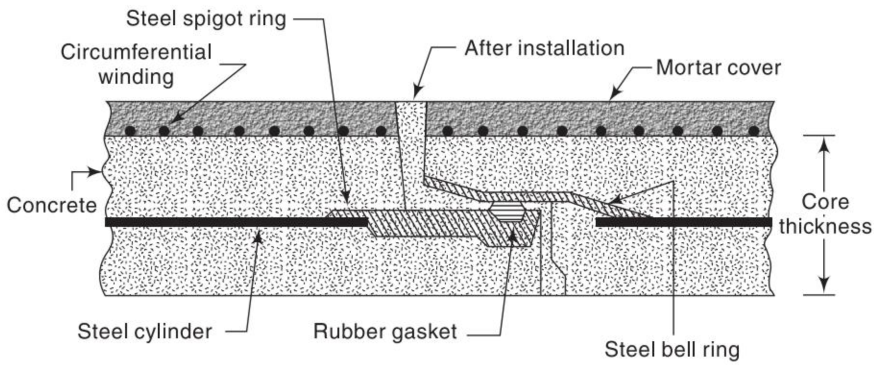

Fig. 16.4 *Typical longitudinal section of prestressed concrete embedded cylinder pipe*

16.3 Design of Prestressed Concrete Pipes

16.3.1 Criteria of Design

The design of prestressed concrete pipes should cover the various stages in which critical conditions of stresses are likely to develop, in the order of their occurrence, during the process of manufacture, handling, erection and under service, with due regard to the critical combinations of loading conditions.

According to the Indian standard code IS: 784,[7] the design of prestressed concrete pipes should cover the following five stages:

1. Circumferential prestressing, winding with or without longitudinal prestressing.
2. Handling stresses with or without longitudinal prestressing.

3. Condition in which a pipe is supported by saddles at extreme points with full water load but zero hydrostatic pressure.
4. Full working pressure conforming to the limit state of serviceability.
5. The first crack stage corresponding to the limit state of local damage.

In addition, it is also necessary to examine the stage of bursting or failure of pipes corresponding to the limit state of collapse, mainly to ensure a desirable load factor against collapse.

16.3.2 Design of Non-cylinder Pipes

Circumferential Wire Winding The design principles outlined in Section 12.2.1 for members subjected to axial tension, is used for determining the minimum thickness of concrete required and the pitch of circumferential wire winding on the pipe.

If N_d = hoop tension developed under working pressure
t = thickness of concrete pipe
D = diameter of the pipe
W_w = hydrostatic pressure
f_{ct} = permissible compressive stress in concrete at transfer
$f_{min,w}$ = permissible stress in concrete under working pressure

Then considering the equilibrium of the pipe shown in Fig. 16.5, we have

$$\left(\frac{W_w D}{2t}\right) < (\eta f_{ct} - f_{min.w}) \quad \therefore \quad t > \left[\frac{W_w D/2}{\eta f_{ct} - f_{min.w}}\right] > \left[\frac{N_d}{\eta f_{ct} - f_{min.w}}\right] \tag{16.1}$$

In the case of liquid retaining structures, to ensure water tightness, the value of $f_{min,w}$ is either zero or a minimum compressive stress of 20 per cent of the ultimate compressive strength of concrete as provided for in IS: 784, which is on the conservative side. However, limited tensile stresses are permitted in Class-2 members according to the British code as outlined in Table 2.1.

The American Water Works Association standard, AWWA C 331–64[8], permits a tensile stress of the order of $0.3\sqrt{f_{cy}}$ N/mm^2 under the serviceability limit state.

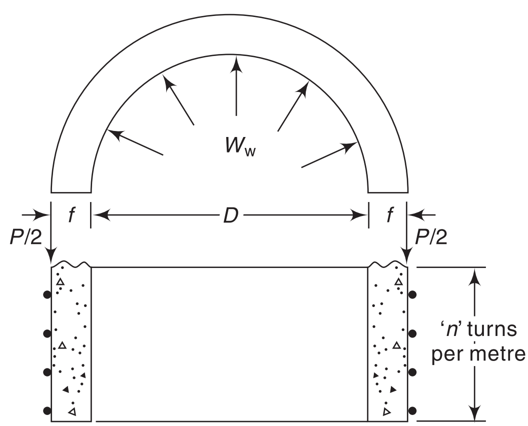

Fig. 16.5 *Circumferential winding in prestressed pipes*

If the wan thickness provided is greater than the minimum value t, the actual stress in concrete can be reduced and hence the amount of reinforcement is also correspondingly reduced.

If f_c = actual compressive stress in concrete

then
$$f_c = \left[\frac{N_d}{\eta t} + \frac{f_{min.w}}{\eta}\right] \tag{16.2}$$

At transfer, the prestressing force P per metre length of the pipe is given by,
$$P = (1000 \times 2t \times f_c)$$
where t is in mm and f_c is in N/mm^2.

If A_s = cross-sectional area of wire/m length of pipe
f_s = stress in wire at transfer
n = number of turns of circumferential wire winding/m length of pipe
d = diameter of wire

then
$$A_s = \left(\frac{2\pi d^2 n}{4}\right) = \left(\frac{2000tf_c}{f_s}\right)$$

Since
$$A_s f_s = P$$
$$\left(\frac{2\pi d^2 n}{4}\right) f_s = 2000\, tf_c$$

$\therefore$
$$n = \left(\frac{4000tf_c}{\pi d^2 f_s}\right) \tag{16.3}$$

Losses of Prestress Due to the elastic deformation of concrete during circumferential wire winding, there is a loss of prestress which depends upon the modular ratio α_e and the reinforcement ratio ρ.

If f_{si} = initial stress in steel
f_{se} = effective stress in steel after winding for compatibility of strains

then
$$\left(\frac{f_{si} - f_{se}}{E_s}\right) = \left(\frac{f_c}{E_c}\right) = \left(\frac{A_s f_{se}}{2000t}\right)\left(\frac{1}{E_c}\right)$$

If
$$\left(\frac{A_s}{2000t}\right) = \rho = \left(\frac{f_c}{f_s}\right) \text{ and } \left(\frac{E_s}{E_c}\right) = \alpha_e$$

then
$$f_{si} = (1 + \alpha_e \rho) f_{se} \tag{16.4}$$

For prestressed concrete pipes, the percentage reinforcement varies between 0.5 and 1 per cent and the modular ratio between 5 and 6. Hence, the loss due to elastic deformation is about 3 to 6 per cent of the initial stress.

In addition to the elastic deformation loss, various other losses of stress due to steel relaxation, creep and shrinkage of concrete should also be considered to arrive at an overall estimate of the losses of prestress.

Example 16.1 A prestressed concrete pipe is to be designed to withstand a fluid pressure of 1.6 N/mm^2. The diameter of the pipe is 1200 mm and shell thickness is 100 mm. The maximum compressive stress in concrete at transfer is 16 N/mm^2. A residual compression of 1 N/mm^2 is expected to be maintained at service loads. Loss ratio is 0.8, high-tensile wires of 5 mm diameter initially stressed to 1 kN/mm^2 are available for use. Determine:

(a) The number of turns of wire per metre length

(b) The pitch of wire winding

Solution.

Diameter of concrete pipe = D = 1200 mm
Fluid pressure = N_d = 1.6 N/mm^2
Thickness of concrete shell = t = 100 mm
Diameter of high-tensile wires = d = 5 mm
Initial stress in wires = f_s = 1000 N/mm^2
Compressive stress in concrete at transfer = f_{ct} = 16 N/mm^2
Residual compressive at service loads = $f_{\text{min, w}}$ = 1 N/mm^2
Loss ratio = η = 0.8

The required thickness of the concrete pipe is evaluated using the relation,

$$t > \left[\frac{N_d}{(\eta f_{ct} - f_{\text{min,w}})}\right] > \left[\frac{1.6(0.5 \times 1200)}{(0.8 \times 14) - 1}\right] > 94.1 \text{ mm}$$

Thickness provided = 100 mm. Hence, the compressive stress in concrete is given by,

$$f_c = \left[\frac{W_w D}{2\eta t} + \frac{f_{\text{min}\cdot\text{w}}}{\eta}\right] = \left[\frac{1.6 \times 1200}{2 \times 0.8 \times 100} + \frac{1}{0.8}\right] = 13.25 \text{ N/mm}^2$$

Number of turns HT wire winding is given by the relation,

$$n = \left[\frac{4000(t + \alpha_e t_s) f_c}{\pi d^2 f_s}\right] = \left[\frac{(4000 \times 100 \times 13.25)}{(\pi \times 5^2 \times 1000)}\right] = 68 \text{ turns/metre}$$

$$\text{Pitch of wire winding} = \left[\frac{1000}{68}\right] = 14.7 \text{ mm.}$$

Example 16.2 A non-cylinder prestressed concrete pipe of 1.6 m diameter with a core thickness of 100 mm is required to withstand a working pressure of 1 N/mm^2. Determine the pitch of a 5 mm diameter wire winding if the high-tensile initial stress in the wire is limited to 1000 N/mm^2. The permissible maximum and minimum stresses in concrete are 12 N/mm^2 (compression) and zero (tension). The loss ratio is 0.8. If the direct tensile strength of concrete is 2 N/mm^2, estimate the load factor against cracking.

Solution.
Minimum thickness of pipe required,

$$t > \left[\frac{1.0(1600/2)}{0.8\times 12 - 0}\right] > 84\,\text{mm}$$

Thickness provided = 100 mm

$$\therefore \qquad f_c = \left[\frac{1\times 1600}{2\times 0.8\times 100}\right] = 10\ \text{N/mm}^2$$

$$\text{No. of wires/m, } n = \left[\frac{4000\times 100\times 10}{\pi 5^2 \times 1000}\right] = 51\ \text{turns/m}$$

$$\text{Pitch of winding} = \left(\frac{1000}{51}\right) = 19.6\ \text{mm}$$

$$\text{Hoop tension due to fluid to pressure} = \left(\frac{1\times 1600}{2\times 100}\right) = 8\ \text{N/mm}^2$$

Hoop compression due to prestress = 10 N/mm^2
$\therefore$ Resultant compressive stress in concrete = (10 – 8) = 2 N/min^2
Tensile strength of concrete = 2 N/mm^2
Additional fluid pressure required to develop a tensile stress of 4 N/mm^2 in concrete is given by,

$$= \left(\frac{2\times 100\times 4}{1600}\right) = 0.5\ \text{N/mm}^2$$

$\therefore$ Cracking fluid pressure = (1 + 0.5) = 1.5 N/mm^2
Working pressure = 1 N/mm^2
Load factor against cracking = (1.5/1) = 1.5.

Longitudinal Stresses due to Winding When the concrete pipe is progressively wound using tensioned wires, the hoop compression reduces the diameter of the pipe and induces longitudinal bending stresses along the length of the pipe. To prevent the failure of the pipe due to circumferential cracking as a consequence of the longitudinal tensile stresses during wire winding, the pipes are generally prestressed in the longitudinal direction using high-tensile wires. The longitudinal precompression also helps to resist the flexural tensile stresses developed due to external loads and non-uniform settlement of soil below the pipe bedding.

According to Doanides[2], the longitudinal bending stresses during winding are transient, reaching a maximum value of 0.355 f_v near the ends of the pipe and more or less a constant value of 0.283 f_v at the middle region of the pipe length, where f_v is the average hoop compressive stress due to circumferential wire winding,

$$f_v = \frac{pR}{t} = \frac{PR}{R_o x t}$$

where p = external pressure due to wire wrapping
R = internal radius
R_o = external radius
t = thickness of pipe shell
x = pitch of wire winding
P = prestressing force per wire

For practical reasons, wire wrapping generally starts at a certain distance from the very end of the spigot and gradually covers the whole length of the pipe. Due to the partial loading, a transient stress of 0.60 f_v and a permanent stress of 0.355 f_v develops at the spigot end of the pipe. The suggested criteria for the design of longitudinal prestressing is that the permissible tensile strength, without any additional reinforcement (taking into account the induced longitudinal compression), should not exceed a value of $0.8\sqrt{f_{ci}}$ for transient stress and $0.5\sqrt{f_{ci}}$ for permanent stress, where f_{ci} is the compressive strength of concrete at the stage of wire winding. If the tensile stress exceeds these limits, an additional longitudinal reinforcement cage must be provided at the spigot end to prevent extensive cracking for the transient loading. Ooykaas[9] numerically examined the stresses developed when a short length at the end of the pipe is left unwound for the case of 1500 mm-diameter pipe with a thickness of 72.5 mm. Based on analytical studies, Curtis and Cowan[10] proposed an approximate formula for the design of the longitudinal prestressing force given by,

$$P_L = (0.275\,T + t f_{\text{min, w}})$$

where P_L = longitudinal prestressing force per unit of circumference
T = tangential prestressing force per unit length
t = thickness of the pipe
$f_{\text{min, w}}$ = minimum permissible stress in concrete (tensile stresses being negative)

The Australian standard[11] provides for a minimum effective longitudinal prestress of one-third of the circumferential prestress less 2.4 N/mm^2. However, the prestress should be not less than 0.7 N/mm^2 and the maximum tensile stress developed, when the pipe filled with water acting longitudinally as a beam in the event of an earth failure, is limited to a value of 2.4 N/mm^2.

According to IS: 784[7], the longitudinal steel should be designed so that the pipe, acting as a hollow circular beam, supports, without cracking, three times its own weight together with the weight of the full volume of water in the pipe when it is supported by knife edges at its external ends. Since prestressed concrete pipes have a length to diameter ratio that seldom exceeds 6, the longitudinal stresses caused by external loads due to non-uniform settlements or load conditions during transportation and installation are usually too small to significantly influence the main design parameters. The design of longitudinal prestressing is illustrated by the following example.

Example 16.3 A non-cylinder prestressed concrete pipe of internal diameter 1000 mm and thickness of concrete shell 75 mm is required to convey water at a working pressure of 1.5 N/mm^2. The length of each pipe is 6 m. The maximum direct compressive stresses in concrete are 15 and 2 N/mm^2. The loss ratio is 0.8.

(a) Design the circumferential wire winding using 5 mm-diameter wires stressed to 1000 N/mm^2.

(b) Design the longitudinal prestressing using 7 mm wires tensioned to 10.00 N/mm^2. The maximum permissible tensile stress under the critical transient loading (wire wrapping at spigot end) should not exceed $0.8\sqrt{f_{ci}}$, where f_{ci} is the cube strength of concrete at transfer = 40 N/mm^2.

(c) Check for safety against longitudinal stresses that develop, considering the pipe as a hollow circular beam as per IS: 784 provisions.

Solution. Given data:

D = 1000 mm $\quad f_{ct}$ = 15 N/mm^2 $\quad W_w$ = 1.5 N/mm^2

$f_{min,\,w}$ = 2 N/mm^2 $\quad t$ = 75 mm $\quad f_s$ = 1000 N/mm^2 $\quad L$ = 6 m

(a) Circumferential wire winding

Compressive stress in concrete,

$$f_c = \left[\frac{N_d}{\eta t} + \frac{f_{min.w}}{\eta}\right] = \left[\frac{1.5(1000/2)}{0.8 \times 75} + \frac{2}{0.8}\right] = 15 \text{ N/mm}^2$$

Number of turns, $$n = \left(\frac{4000tf_c}{\pi d^2 f_s}\right) = \left(\frac{4000 \times 75 \times 15}{\pi \times 5^2 \times 1000}\right) = 57 \text{ turns/m}$$

Pitch of winding = $\left(\dfrac{1000}{57}\right)$ = 17.5 mm.

(b) Longitudinal prestressing

Critical transient stress at spigot end = 0.6 × hoop stress = 0.6 × 15 = 9 N/mm^2

Maximum permissible tensile stress $= 0.8\sqrt{f_{ci}} = 0.8\sqrt{40} = 5$ N/mm^2

Hence, the tensile stress of 9 – 5 = 4 N/mm^2 should be counterbalanced by longitudinal prestressing. Cross-sectional area of the pipe

$$= (\pi \times 1.075 \times 0.075)\text{ m}^2$$

If P is the longitudinal prestressing force required, then

$$P = \left[\frac{\pi \times 1.075 \times 0.075 \times 10^6 \times 4}{10^3}\right] \text{kN} = 1013 \text{ kN}$$

Using 7 mm wires stressed to 1000 N/mm^2,

Force in each wire = 38.5 kN

∴ Number of wires = $\left(\dfrac{1013}{38.5}\right)$ = 27 *(c) Check for flexural stresses as per IS: 784*

Considering the pipe as a beam of hollow circular section over a span of 6 m,
Three times self-weight = $(3\pi \times 1.075 \times 0.075 \times 24) = 18.30$ kN/m
Weight of water = $(\pi \times 1^2 \times 10)/4 = 7.90$ kN/m

Total udl on pipe = 26.20 kN/m

$$\text{Maximum bending moment} = \left(\frac{26.2 \times 6^2}{8}\right) = 118 \text{ kN m}$$

$$\text{Second moment of area, } I = \left[\frac{\pi(1.15^4 - 1^4)}{64}\right] = 0.0365 \text{ m}^4$$

$$\text{Flexural tensile stress} = \left[\frac{118 \times 10^6 \times 575}{0.0365 \times 10^{12}}\right] = 1.88 \text{ N/mm}^2 \text{ (tension)}$$

Longitudinal prestress = 4 N/mm^2
∴ Resultant stress in concrete = (4 – 1.88) = 2.12 N/mm^2 (compression)
The resultant stress being compressive, the pipe is safe against cracking.

16.3.3 Design of Cylinder Pipes

The design principles of cylinder pipes are similar to those of the non-cylinder pipes, except that the required thickness of concrete is computed by considering the equivalent area of the light gauge steel pipe embedded in the concrete.
If

$$t_s = \text{thickness of steel pipe}$$

$$\alpha_e = \text{modular ratio} = \left(\frac{E_s}{E_c}\right)$$

The thickness of concrete pipe required is given by,

$$t = \left[\frac{N_d}{\eta f_{ct} - f_{min.w}} - \alpha_e t_s\right] \tag{16.5}$$

The prestress required in the concrete at transfer is

$$f_c = \left[\frac{N_d}{\eta(t + \alpha_e t_s)} + \frac{f_{min.w}}{\eta}\right] \tag{16.6}$$

The number of turns of circumferential wire winding per metre length of pipe is

$$n = \left[\frac{4000(t + \alpha_e t_s) f_c}{\pi d^2 f_s}\right] \tag{16.7}$$

The failure of non-cylinder pipes is due to the excessive cracking of concrete, resulting in the decrease of internal fluid pressure. The mechanism of failure is one of progressive collapse due to excessive leakage without any sudden fracture of steel. However, in the case of cylinder pipes, there are possibilities of the pipe bursting due to the yielding of the steel cylinder accompanied by the excessive elongation or fracture of the circumferential wire winding.

The bursting fluid pressure is estimated by the expression,

$$P_u = \left[\frac{f_{pu}A_s + f_y A_{cs}}{D}\right]$$

Since $\quad A_{ps} = \left(\dfrac{\pi d^2}{2} n\right) = 1.57\ d^2 n\ \text{mm}^2/\text{m} = 0.00157\ d^2 n\ \text{mm}^2/\text{mm}$

and $\quad A_{cs} = 2t_s$

$$\therefore \quad p_u = \left[\frac{0.00157 d^2 n f_{pu} + 2t_s f_y}{D}\right]$$

where $\quad p_u$ = bursting pressure, N/mm^2

d = diameter of wire winding, mm

n = number of turns per metre length of pipe

f_{pu} = tensile strength of wire winding, N/mm^2

f_y = yield stress of steel cylinder, N/mm^2

t_s = thickness of steel cylinder, mm

D = diameter of steel cylinder, mm

Example 16.4 A prestressed concrete cylinder pipe is to be designed using a steel cylinder of 1200 mm internal diameter and thickness 1.5 mm. The service internal hydrostatic pressure in the pipe is 0.8 N/mm^2. 4 mm diameter high-tensile wires initially tensioned to a stress of 1 kN/mm^2 are available for circumferential winding. The yield stress of mild steel cylinder is 280 N/mm^2. The maximum permissible compressive stress in concrete at transfer is 15 N/mm^2 and no tensile stress is permitted under service load conditions. Determine the thickness of the concrete lining and the number of turns of circumferential wire winding and the factor of safety against bursting. Assume modular ratio as 6 and loss ratio as 0.8.

Solution.

Hydrostatic pressure inside the pipe = N_d = 0.8 N/m^2

Internal diameter of steel cylinder pipe = D = 1200 mm

Thickness of steel pipe = t_s = 1.5 mm

Yield stress of mild steel pipe = f_y = 280 N/mm^2

Permissible compressive stress in concrete at transfer = f_{ct} = 14 N/mm^2

Permissible tensile stress in concrete = $f_{min.w}$ = 0

Diameter of HT wire winding = 4 mm

Initial stress in wires = f_s = 1000 N/mm^2

Modular ratio = α_e = 6 and Loss ratio = η = 0.8

Ultimate tensile strength of wire = f_{pu} = 1600 N/mm^2

The required thickness of the concrete pipe is evaluated using the relation,

$$t > \left[\frac{N_{\mathrm{d}}}{(\eta f_{\mathrm{ct}} - f_{\mathrm{min.w}})} - \alpha_{\mathrm{e}} t_{\mathrm{s}}\right] > \left[\frac{0.8(0.5 \times 1200)}{(0.8 \times 14) - 0} - (6 \times 15)\right] > 33.85\,\mathrm{mm}$$

Use 34 mm thick concrete lining. Hence, $f_{\mathrm{c}} = 14\ \mathrm{N/mm^2}$
Number of turns HT wire winding is given by the relation,

$$n = \left[\frac{4000(t - \alpha_{\mathrm{e}} t_{\mathrm{s}}) f_{\mathrm{c}}}{\pi d^2 f_{\mathrm{s}}}\right] = \left[\frac{4000(34 + 6 \times 1.5)14}{(\pi \times 4^2 \times 1000)}\right] = 48\ \text{turns/metre}$$

Bursting pressure is estimated by the equation

$$P_{\mathrm{u}} = \left[\frac{0.00157\, d^2 n f_{\mathrm{pu}} + 2 t_{\mathrm{s}} f_{\mathrm{y}}}{D}\right] = \left[\frac{(0.00157 \times 4^2 \times 48 \times 1600) + (2 \times 1.5 \times 280)}{1000}\right]$$

$$= 2.769\ \mathrm{N/mm^2}$$

$$\text{Factor of safety against bursting} = \left[\frac{\text{bursting pressure}}{\text{working pressure}}\right] = \left[\frac{2.769}{0.8}\right] = 3.46.$$

16.4 General Features of Prestressed Concrete Tanks

16.4.1 Applications

Prestressed concrete tanks have been widely used for the storage of fluids, such as water, oil, gas, sewage, granular materials like cement, process and liquids chemicals, slurries and, more recently, cryogens[12]. Water storage tanks of large capacity are invariably made of prestressed concrete. Recent applications include special forms of prestressed concrete tanks, which are triaxially prestressed and serve as containment vessels and biological shields for nuclear reactors.

Prestressed concrete tanks are generally cylindrical with diameters up to 100 m and liquid depths up to 36 m, and capacities of about 50 million litres. Tanks have been built for storing liquid oxygen at –230°C with capacities up to one million litres[13]. Prestressed concrete, although watertight, is not gastight where vapours under pressure are to be stored. In such cases, a thin membrane liner of steel provides rigidity and increases the steel tensile capacity of the prestressed concrete. The metal liner concept has proved so successful that it is being increasingly used in America, even for large water tanks. In the case of sanitary structures like sludge digestion tanks, spherical shapes are preferred and, for practical reasons, the tank is made up of a top and bottom conical shell connected by a circular cylindrical intermediate portion[14].

An ingenious method of casting spherical shells at the centre with conical shapes towards the top and bottom was first adopted by Finsterwalder[15] for the large sludge digestion tanks at the sewage treatment works in Berlin and Frankfurt, using a formwork consisting of sectorial units which can be rotated about the central axis and the tank prestressed, sectorwise, with coupled tendons and splices. The most impressive example of a prestressed conical shell is the 58 m high tower at Orebro in Sweden which comprises a conical shell, with an external diameter of 46 m, supported on a tail tower. The tank with a water storage capacity of 9000 m^3 is prestressed by 206 Freyssinet cables each made up of 12 wires of 7 mm diameter[16].

16.4.2 Shapes of Prestressed Concrete Tanks

Cylindrical tanks are by far the most commonly used types from structural and constructional considerations. Some of the largest prestressed concrete tanks constructed are circular in shape. A cylindrical shape is well suited for circumferential wire wrapping, which constitutes the major prestressing operation in tanks. Square or rectangular tanks, spanning either vertically or horizontally, are required for industrial use. Square tanks are advantageous for storage in congested urban and industrial sites where land space is a major constraint.

Multi-celled tanks have been constructed using interlocking polygons and circular shapes, especially for the storage of cement in silo construction. The hexagonal units are prestressed together to achieve monolithic action by transverse and/or vertical tendons. Prestressed concrete tanks of hyperboloidal shape were first constructed in France[17]. The main advantage of this shape is the considerable reduction in the thickness of concrete shell and the use of the same set of straight wires to produce circumferential and vertical prestress. Doubly curved shells have also been used to take advantage of the efficiency of the shell action of the concrete, combined with the prestressing at the edges. Some of the shapes of prestressed concrete tanks outlined above are compiled in Fig. 16.6.

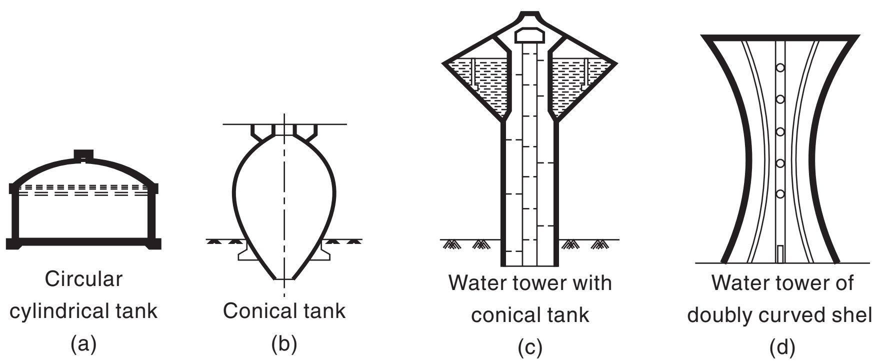

Fig. 16.6 *Shapes of prestressed concrete tanks*

16.4.3 Economic Dimensional Proportions of Circular Tanks

A majority of the prestressed concrete tanks built all over the world are of circular shape. With experience, it has been found that the cost of the circular cylindrical prestressed concrete tank is influenced by the ratio of diameter to height. Table 16.1 and Fig. 16.7 show the economical dimensions of the various structural components of circular tanks for capacities varying from 378 to 37800 m^3. These provisions are based on the experience of the Preload Engineering Company, New York, which has constructed a large number of tanks in USA[18] The economic proportion of diameter to height of circular cylindrical tanks was found to be 4 : 1.

Table 16.1 *Economic dimensional proportions for water tanks (Preload Engineering Co., New York) (Refer to Fig. 16.7 for abbreviations)*

Capacity, m^3	*Dimensions*, m								
	A	*B*	*C*	*D*	*E*	*F*	*G*	*H*	*J*
378	12.50	3.15	1.56	0.12	0.12	0.05	0.05	0.20	0.15
945	16.90	4.30	2.11	0.12	0.12	0.05	0.05	0.22	0.15
1890	21.35	5.35	2.67	0.12	0.12	0.05	0.05	0.30	0.17
2835	24.40	6.10	3.05	0.12	0.15	0.05	0.05	0.36	0.19
3780	26.95	6.70	3.36	0.12	0.18	0.05	0.05	0.38	0.22
5670	30.80	7.80	3.86	0.12	0.23	0.05	0.05	0.43	0.25
7570	33.85	8.55	4.23	0.12	0.24	0.05	0.06	0.48	0.27
9450	36.40	9.15	4.55	0.22	0.26	0.05	0.06	0.51	0.30
18900	46.00	11.45	5.75	0.22	0.44	0.05	0.10	0.69	0.38
37800	57.90	14.50	7.24	0.22	0.74	0.05	0.11	0.89	0.49
Economic proportion in USA $B : A = 1 : 4$									

The dimensions of wall thickness given in the table refers to the conditions that the walls of the tank are not continuous with the base slab, but they are free to slide, being supported on a neoprene pad. The tank roof is usually of dome-type, with prestressed ring beams at the junction of the dome and tank walls. However, for very large (about 50,000 m^3) capacity of tanks having diameters of up to 90 m, it is preferable to construct a mushroon-type roof, supported either on a number of internal supports or on beams.

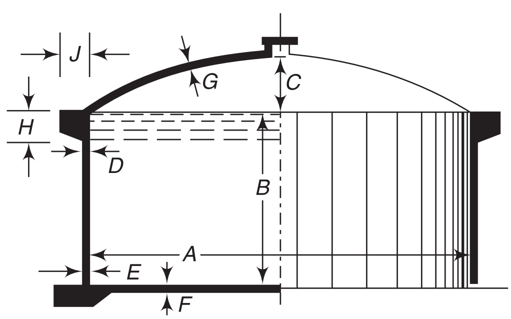

Fig. 16.7 *Economical dimensional proportions*

16.4.4 Tank Floors

The base slab forming the floor or the tank is generally made of reinforced concrete constructed on a flat bituminous surfacing or on a thin concrete binding with the interposition of a sliding layer such as oil paper, so that the slab can move over the compacted soil bed. The slab should be sufficiently flexible so that it can adapt itself to the local deformations of the precompacted subsoil. The reinforcements in the slab should be well distributed to control the cracking of the slab due to shrinkage and temperature changes.

In the case of large tanks, the base slab is subdivided by joints which are sealed by water stops as shown in Fig. 16.8. The floor slabs are cast in panels and, according to the British standard BS 8007[19], the maximum length of side of such panels should not exceed 7.5 m for reinforced slabs and 6 m for nominal slabs. Nominal slabs may be formed out of 50 to 80 mm thick gunite reinforced with 0.5 per cent of steel distributed in each of the principal directions. The shotcreting technique has been widely used for the construction of base slabs by the Preload Engineering Company in America.

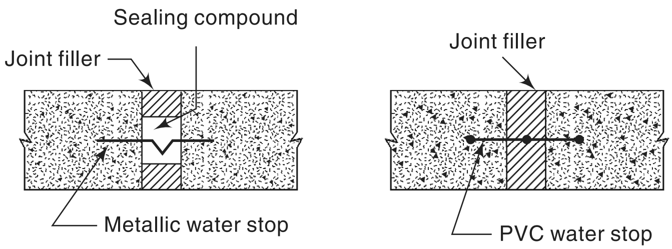

Fig. 16.8 *Typical construction joints in tank floor slabs*

The Indian standard code IS : 3370[20] stipulates that floor slabs of tanks resting on the ground should be provided with a nominal reinforcement of not less than 0.15 per cent and the floor slabs should be cast in panels of area not more than 4.5 m^2 with contraction or expansion joints. These slabs are to be cast over a layer of concrete not less than 75 mm thick with a sliding layer of bitumen paper provided to prevent the bond between the screed and the floor slab.

The problems associated with the cracking of floor slabs when they are left empty and allowed to dry out over long periods can be overcome by uniform prestressing. According to Leonhardt[21], circumferential prestressing will obviate the risk of cracking in cases where tank slabs of more than 20 m diameter are constructed as jointless structures.

16.4.5 Junctions of Tank Wall and Base Slab

The joint between the walls of the tank and floor slab may be any one of the following three types:

1. Fixed base
2. Hinged base
3. Sliding base

The ring tension and bending moments developed in the walls of the tank are mainly influenced by the type of connection between the walls and the base slab. The junction between the tank wall and footing is the most vulnerable location as far as leakage is concerned and hence in the case of tanks storing penetrating liquids, it is necessary to form the wall and footing in monolithic construction as shown in Fig. 16.9. This type of connection is generally well suited for shallow tanks with diameters up to 30 m, where the fixing moment developed at the wall base does not result in excessively high stresses and congestion of reinforcement.

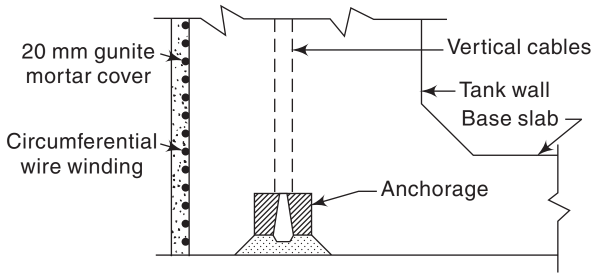

Fig. 16.9 *Tank wall with fixed base*

The hinged base is not generally adopted for prestressed concrete. An excellent example of resilient connection between the base and the wall can be found in the tanks designed by Buyer[22]. In this type, the tank wall is supported over an annular bearing resting on the footing from which the base slab is isolated by a joint containing a compressible filling. This arrangement facilitates the junction between the wall and the base slab to rotate about the annular bearing. Alternatively, the hinged joint can also be formed by circumferential wire wrapping to the bottom portion of the wall and then packing the groove with cement mortar as shown in Fig. 16.10.

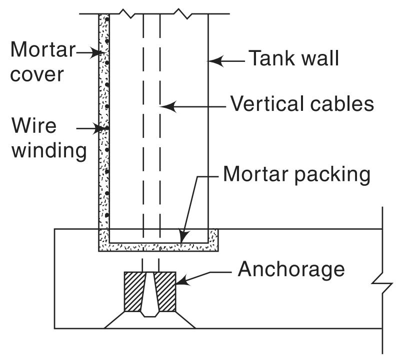

Fig. 16.10 *Tank wall with hinged base*

In the case of large tanks and especially for those which have to store hot liquids, a movable or sliding joint is the ideal solution to minimise or completely eliminate the moments at the base of the wall. A sliding joint is made by interposing rubber or neoprene pads at the junction of the wall and the base. The Preload Engineering Company has developed this type of sliding base in which a vertical water stop is inserted between two rubber strips as shown in Fig. 16.11. In the present state of art, single neoprene pads have also been used. The main function of these pads is to allow for free horizontal movement of the wall relative to the base by shear deformation of the rubber joint, which does not exceed a critical value of 30 degrees. The horizontal shear force developed for producing this deformation is influenced by the thickness of the pad and the shore hardness of the material. The various methods of forming the joints between the tank walls and the base slab have been reported by Ager[23].

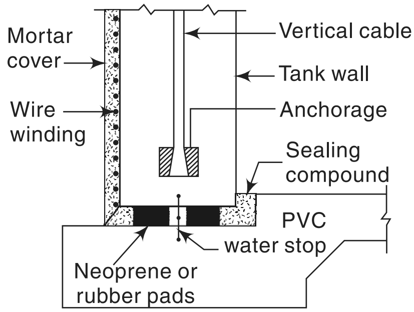

Fig. 16.11 *Tank wall with sliding base*

16.4.6 Circumferential Wire Winding Methods

The most common method of wire wrapping for circular tanks consists of a traction machine, referred to as 'merry go round' and developed by the Preload Engineering Company. The machine is suspended from a trolley which runs along the top of the tank walls. The high-tensile wire is drawn through a die while it is wound on the tank to achieve the designed tension in the wire. As a precaution, the wires are anchored by clips in the wall at regular intervals to ensure that, in the event of wire fracture, the winding does not get detached. Joining of wires is generally done by spring loaded torpedo splices. With improvements over the years, the winding speed is about 4.5 m/s.

The BBRV tank winding machine developed by Vogt is a substantially lighter and simpler version with winding speed of 1 m/s. In this type, the prestressing wire is unwound from a pulley, whose circumference is smaller than that of the drive wheel by an amount corresponding to the extension of the wire required to obtain the desired prestress. The propelling wheels pressing against the tank wall are driven by a torsionally rigid drive rod as shown in Fig. 16.12.

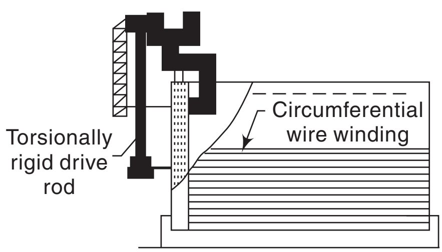

Fig. 16.12 *Wire winding machine for circular cylindrical tanks*

Circumferential prestressing is also possible by an ingenious method, developed by Baur[24], which involves the 'barrel hoop principle'. In this method, the successive turns of wire wound round the tank walls having an inward batter are knocked downwards to achieve the desired extension and force in the wire.

Circumferential prestressing is also possible by the use of embedded tendons enclosed in sheaths which are prestressed and anchored against pilaster-like vertical ribs on the outside face of tank walls. It is preferable to limit the curved lengths of the cable by providing jacking points spaced at every one-third of the circumference of the tank wall, mainly to overcome the considerable friction losses.

In the case of rectangular tanks, either cast *in situ* or precast and assembled, it is more advantageous to use tendons embedded in cable sheaths. This method is invariably adopted for triaxial prestressing of the concrete containment vessels of nuclear reactors.

16.5 Analysis of Prestressed Concrete Tanks

The bending moments and ring tension, developed in circular water tanks due to the hydrostatic pressure, depend upon factors, such as the type of fixity between the tank wall and the base slab, the diameter of the tank, the thickness of the wall and the elastic constants of the material forming the walls. The analysis is generally based on Timoshenko's general theory of cylindrical shells[25], with the assumption that the thickness of the tank wall is small in relation to the diameter.

The vertical bending moment, M_w, and the ring tension, N_d, developed at a distance x from the base of the tank (Fig. 16.13) are expressed as:

$$N_d = \frac{Et}{D\beta^3 K}\ e^{-\beta x}\{M_o\beta(\cos\beta x - \sin\beta x) + N_o \cos\beta x)$$

$$M_w = \frac{1}{\beta}\ e^{-\beta x}\{M_o\beta(\cos\beta x + \sin\beta x) + N_o \sin\beta x)$$

where D = diameter of the tank

t = thickness of the tank wall

$$\beta = \sqrt[4]{\frac{12(1 - v_c^2)}{D^2 t^2}}$$

$$K = \left[\frac{Et^3}{12(1 - v_c^2)}\right]$$

v_c = Poisson's ratio

M_o and N_o are the moment and shear acting at the base of the tank, with their values depending upon the pressure distribution and the conditions of fixity at the base. A diagrammatic representation of the variation of bending moments and ring tension in the walls of tanks for different types of bases is shown in

Fig. 16.14. Maximum bending moments develop in the case of tanks with a fixed base while the ring tension is maximum for the free-base condition. In the case of tanks with walls resting on rubber or neoprene pads, a comparatively smaller magnitude of bending moments is generated due to the radial frictional force developed at the base junction. According to Crom[26], the base shear can be estimated for a maximum coefficient of friction μ of 0.5, which is not likely to be exceeded.

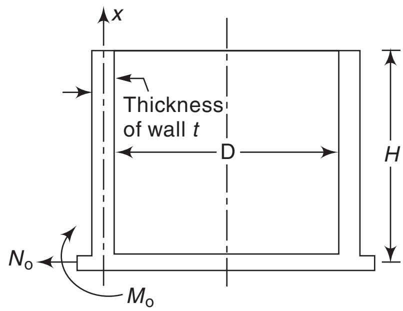

Fig. 16.13 *Analysis of circular cylindrical tank*

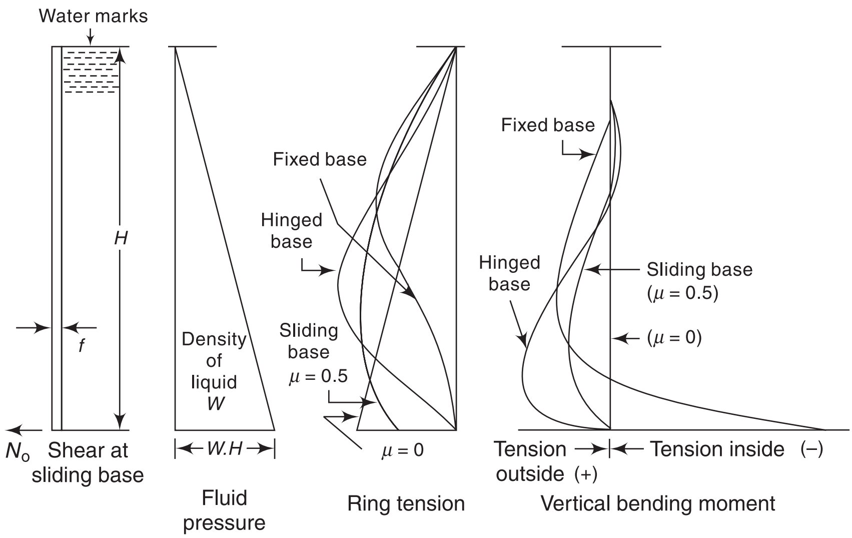

Fig. 16.14 *Ring tension and bending moments in cylinder tank walls*

The maximum bending moment developed in the tank wall due to a base shear N_o has a value of $0.247\,N_0\sqrt{Rt}$, where R is the internal radius and t the thickness of the tank wall. The maximum moment occurs at approximately one-fifth the height of the wall under pressure, measured from the base.

The coefficients compiled in Tables 16.2 to 16.5, which are recommended in IS : 3370[27], are immensely useful in the design office for computing bending moments and ring tension developed in circular tanks with different types of base connections. The Indian Standard Code also contains tables of moment and shear coefficients for the design of rectangular tanks with walls fixed or hinged at the bottom and free or hinged at the top.

Table 16.2 *Moments in cylindrical walls—Fixed base free at top (IS: 3370 Part IV)*
Moment M_w = (Coefficient) × (wH^3) kN m/m Positive sign indicates tension at the outside face

$\frac{H^2}{Dt}$	Coefficients at point									
	0.1H	*0.2H*	*0.3H*	*0.4H*	*0.5H*	*0.6H*	*0.7H*	*0.8H*	*0.9H*	*1.0H*
0.4	+.0005	+.0014	+.0021	+.0007	–.0042	–.0150	–.0302	–.0529	–.0816	–.1205
0.8	+.0011	+.0037	+.0063	+.0080	+.0070	+.0023	–.0068	–.0224	–.0465	–.0795
1.2	+.0012	+.0042	+.0077	+.0103	+.0112	+.0090	+.0022	–.0108	–.0311	–.0602
1.6	+.0011	+.0041	+.0075	+.0107	+.0121	+.0111	+.0058	–.0051	–.0232	–.0505
2.0	+.0010	+.0035	+.0068	+.0099	+.0120	+.0115	+.0075	–.0021	–.0185	–.0436
3.0	+.0006	+.0024	+.0047	+.0071	+.0090	+.0097	+.0077	+.0012	–.0119	–.0333
4.0	+.0003	+.0015	+.0028	+.0047	+.0066	+.0077	+.0069	+.0023	–.0080	–.0268
5.0	+.0002	+.0008	+.0016	+.0029	+.0046	+.0059	+.0059	+.0028	–.0058	–.0222
6.0	+.0001	+.0003	+.0008	+.0019	+.0032	+.0046	+.0051	+.0029	–.0041	–.0187
8.0	.0000	+.0001	+.0002	+.0008	+.0016	+.0028	+.0038	+.0029	–.0022	–.0146
10.0	.0000	.0000	+.0001	+.0004	+.0007	+.0019	+.0029	+.0028	–.0012	–.0122
12.0	.0000	–.0001	+.0001	+.0002	+.0003	+.0013	+.0023	+.0026	–.0005	–.0104
14.0	.0000	.0000	.0000	.0000	.0001	+.0008	+.0019	+.0023	+.0001	–.0090
16.0	.0000	.0000	–.0001	–.0002	–.0001	+.0004	+.0013	+.0019	+.0001	–.0079

	Coefficients at point				
	.80H	*.85H*	*.90H*	*.95H*	*1.00H*
20.0	+.0015	+.0014	+.0005	–.0018	–.0063
24.0	+.0012	+.0012	+.0007	–.0013	–.0053
32.0	+.0007	+.0003	+.0007	–.0008	–.0040
40.0	+.0002	+.0005	+.0005	–.0005	–.0032
48.0	.0000	+.0001	+.0005	–.0003	–.0026
56.0	.0000	.0000	+.0004	–.0001	–.0023

Table 16.3 *Ring tension cylindrical walls—Fixed base free at top (IS: 3370-Part IV)*
Ring tension N_d = (Coefficient × wHR kN/m)

$\frac{H^2}{Dt}$	Coefficients at point									
	0.1H	0.2H	0.3H	0.4H	0.5H	0.6H	0.7H	0.8H	0.9H	1.0H
0.4	+0.149	+0.134	+0.120	+0.101	+0.082	+0.066	+0.049	+0.029	+0.014	+0.004
0.8	+0.263	+0.239	+0.215	+0.190	+0.160	+0.130'	+0.096	+0.063	+0.034	+0.010
1.2	+0.283	+0.271	+0.254	+0.234	+0.209	+0.180	+0.142	+0.099	+0.054	+0.016
1.6	+0.265	+0.268	+0.268	+0.266	+0.250	+0.226	+0.185	+0.134	+0.075	+0.023
2.0	+0.234	+0.251	+0.273	+0.285	+0.285	+0.274	+0.232	+0.172	+0.104	+0.031
3.0	+0.134	+0.203	+0.267	+0.322	+0.357	+0.362	+0.330	+0.262	+0.157	+0.052
4.0	+0.067	+0.164	+0.256	+0.339	+0.403	+0.429	+0.409	+0.334	+0.210	+0.073
5.0	+0.025	+0.137	+0.245	+0.346	+0.428	+0.477	+0.469	+0.398	+0.259	+0.092
6.0	+0.018	+0.119	+0.234	+0.344	+0.441	+0.504	+0.514	+0.447	+0.301	+0.112
8.0	–0.011	+0.104	+0.218	+0.335	+0.443	+0.534	+0.575	+0.530	+0.381	+0.151
10.0	–0.011	+0.098	+0.208	+0.323	+0.437	+0.542	+0.608	+0.589	+0.440	+0.179
12.0	–0.005	+0.097	+0.202	+0.312	+0.429	+0.543	+0.628	+0.633	+0.494	+0.211
14.0	–0.002	+0.098	+0.200	+0.306	+0.420	+0.539	+0.639	+0.666	+0.541	+0.241
16.0	–0.000	+0.099	+0.199	+0.304	+0.412	+0.531	+0.641	+0.687	+0.582	+0.265

	Coefficients at point				
	.75H	.80H	.85H	.90H	.95H
20.0	+0.716	+0.654	+0.520	+0.325	+0.115
24.0	+0.746	+0.702	+0.577	+0.372	+0.137
32.0	+0.782	+0.768	+0.663	+0.459	+0.182
40.0	+0.800	+0.805	+0.731	+0.530	+0.217
48.0	+0.791	+0.828	+0.785	+0.593	+0.254
56.0	+0.763	+0.838	+0.824	+0.536	+0.285

Table 16.4 *Moments in cylindrical walls—Hinged base free at top (IS: 3370-Part IV)*
Moment M_w = (Coefficient × wH^3) kN m/m Positive sign indicates tension at the outside

$\frac{H^2}{Dt}$	*Coefficients at point*									
	0.1H	*0.2H*	*0.3H*	*0.4H*	*0.5H*	*0.6H*	*0.7H*	*0.8H*	*0.9H*	*1.0H*
0.4	+.0020	+.0072	+.0151	+.0230	+.0301	+.0348	+.0357	+.0312	+.0197	0
0.8	+.0019	+.0064	+.0133	+.0207	+.0271	+.0319	+.0329	+.0292	+.0187	0
1.2	+.0016	+.0058	+.0111	+.0177	+.0237	+.0280	+.0296	+.0263	+.0171	0
1.6	+.0012	+.0044	+.0091	+.0145	+.0195	+.0236	+.0255	+.0232	+.0155	0
2.0	+.0006	+.0033	+.0073	+.0114	+.0158	+.0199	+.0219	+.0205	+.0145	0
3.0	+.0004	+.0018	+.0040	+.0063	+.0092	+.0127	+.0152	+.0153	+.0111	0
4.0	+.0001	+.0007	+.0016	+.0033	+.0057	+.0083	+.0109	+.0118	+.0092	0
5.0	.0000	+.0001	+.0006	+.0016	+.0034	+.0057	+.0080	+.0094	+.0078	0
6.0	.0000	.0000	+.0002	.0000	+.0019	+.0039	+.0062	+.0078	+.0068	0
8.0	.0000	.0001	–.0002	.0000	+.0007	+.0020	+.0038	+.0057	+.0054	0
10.0	.0000	.0000	–.0002	–.0001	+.0002	+.0011	+.0025	+.0043	+.0045	0
12.0	.0000	.0000	–.0001	.0002	.0000	+.0005	+.0017	+.0032	+.0039	0
14.0	.0000	.0000	.0000	–.0001	.0001	.0000	+.0012	+.0026	+.0033	0
16.0	.0000	.0000	.0000	–.0001	–.0002	–.0004	+.0008	+.0022	+.0029	0

	Coefficients at point				
	.75H	*.80H*	*.85H*	*.90H*	*.95H*
20.0	+.0008	+.0014	+.0020	+.0024	+.0020
24.0	+.0005	+.0010	+.0015	+.0020	+.0017
32.0	.0000	+.0005	+.0009	+.0014	+.0013
40.0	.0000	+.0003	+.0006	+.0011	+.0011
48.0	.0000	+.0001	+.0004	+.0008	+.0010
56.0	.0000	.0000	+.0003	+.0007	+.0008

Table 16.5 *Ring tension in cylinder walls—Hinged base free at top (IS: 3370-Part IV)*
Ring tension N_d = (Coefficient) × (wHR) kN/m Positive sign indicates tension

$\frac{H^2}{Dt}$	Coefficients at point									
	0.0H	*0.1H*	*0.2H*	*0.3H*	*0.4H*	*0.5H*	*0.6H*	*0.7H*	*0.8H*	*0.9H*
0.4	+0.474	+0.440	+0.395	+0.352	+0.305	+0.264	+0.215	+0.165	+0.111	+0.057
0.8	+0.423	+0.402	+0.381	+0.358	+0.330	+0.297	+0.249	+0.202	+0.145	+0.076
1.2	+0.350	+0.355	+0.361	+0.362	+0.358	+0.343	+0.309	+0.256	+0.186	+0.098
1.6	+0.271	+0.303	+0.341	+0.369	+0.385	+0.385	+0.362	+0.314	+0.233	+0.124
2.0	+0.205	+0.260	+0.321	+0.373	+0.411	+0.434	+0.419	+0.369	+0.280	+0.151
3.0	+0.074	+0.179	+0.281	+0.375	+0.449	+0.506	+0.519	+0.479	+0.375	+0.210
4.0	+0.017	+0.137	+0.253	+0.367	+0.469	+0.545	+0.579	+0.553	+0.447	+0.256
5.0	–0.008	+0.114	+0.235	+0.356	+0.469	+0.562	+0.617	+0.606	+0.503	+0.294
6.0	–0.011	+0.103	+0.223	+0.343	+0.463	+0.566	+0.639	+0.643	+0.547	+0.327
8.0	–0.015	+0.096	+0.208	+0.324	+0.443	+0.564	+0.661	+0.697	+0.621	+0.386
10.0	–0.008	+0.095	+0.200	+0.311	+0.428	+0.552	+0.666	+0.730	+0.678	+0.433
12.0	–0.002	+0.097	+0.197	+0.302	+0.417	+0.541	+0.664	+0.750	+0.720	+0.477
14.0	0.000	+0.098	+0.197	+0.299	+0.408	+0.531	+0.659	+0.761	+0.752	+0.513
16.0	+0.002	+0.100	+0.198	+0.299	+0.403	+0.521	+0.650	+0.764	+0.776	+0.543

	Coefficients at point				
	.75H	*.80H*	*.85H*	*.90H*	*.95H*
20.0	+0.812	+0.817	+0.755	+0.603	+0.344
24.0	+0.816	+0.839	+0.793	+0.647	+0.377
32.0	+0.814	+0.861	+0.847	+0.721	+0.436
40.0	+0.802	+0.866	+0.880	+0.778	+0.483
48.0	+0.791	+0.854	+0.900	+0.820	+0.527
56.0	+0.781	+0.859	+0.911	+0.852	+0.563

16.6 Design of Prestressed Concrete Tanks

16.6.1 Criteria of Design

The design of tank walls to resist the hoop tension and moments developed are based on the considerations of desirable load factors against cracking and collapse. According to the Indian Standard Code IS: 3370–Part III, it is desirable to have at least a minimum load factor of 1.2 against cracking and 2 against ultimate collapse. In contrast to these values, the British standard BS: 8007 for liquid retaining structures prescribes a minimum load factor against cracking and collapse of 1.25 and 2.50, respectively. In addition, it is prescribed that the principal compressive stress in concrete should not exceed one-third of the characteristic cube strength and when the tank is full, there should be a residual compressive stress of at least 0.7 N/mm^2. When the tank is empty, the allowable tensile stress at any point is limited to 1 N/mm^2.

The ring prestressing is designed in all cases to counteract the maximum hoop tension developed, based on the assumption that the wall foot is free to slide without frictional resistance. Vertical prestressing will be necessary to cater for the moments developed in the walls, depending upon the restraint or the shear developed at the base, as well as to resist the longitudinal moments induced when the tank is in the partially wound stage. For this condition, the IS code provides that the maximum flexural stress in the tank walls should be assumed to be numerically equal to 0.3 times the hoop compression.

For estimation of resistance to cracking, the code provides values of direct and bending tensile strength of concrete covering the grades from M-35 to M-65. However, these values can be estimated by the empirical relations given by,

$$\text{Direct tensile strength, } f_t = 0.267\sqrt{f_{\text{cu}}} \text{ N/mm}^2$$

$$\text{Flexural tensile strength, } f_{\text{cr}} = 2f_t$$

16.6.2 Design Procedure for Circular Tanks

The procedure to be followed and the salient design equations for the computations of the minimum wall thickness, circumferential prestress, spacing of wires and vertical prestress required are as follows:

1. Estimate the maximum ring tension, N_{d}, and bending moment, M_{w}, in the walls of the tank using the IS code (Tables 16.2 to 16.5).
2. Minimum wall thickness $= \left[\dfrac{N_{\text{d}}}{\eta f_{\text{ct}} - f_{\text{min.w}}}\right]$

   The thickness of the wall provided should be such that a minimum cover of 35 mm is available to the vertical prestressing cables. In practise, the walls are seldom less than 120 mm thick to ensure proper compaction of concrete.
3. The circumferential prestress required is given by,

$$f_c = \left[\frac{N_d}{\eta t} + \frac{f_{min.w}}{\eta}\right] \text{N/mm}^2$$

4. The spacing of wires required at any section is obtained by considerations of the hoop tension due to fluid pressure and hoop compression due to the circumferential wire winding, as follows:

If A_s = cross-sectional area of wire winding, mm^2
w_t = average radial pressure of wires at transfer at a given section, N/mm^2
D = diameter of the tank, mm
s = spacing of wires at the given section, mm
f_s = stress in wires at transfer, N/mm^2
t = thickness of the tank wall, mm
f_c = compressive stress in concrete, N/mm^2

∴ Hoop compression due to prestressing = $\left(\frac{w_t D}{2}\right)$

Equating $$\left(\frac{w_t D}{2}\right) = \left(\frac{f_s A_s}{s}\right)$$

∴ $$w_t = \left(\frac{2 f_s A_s}{sD}\right) \tag{16.8}$$

If N_d = hoop tension due to hydrostatic working pressure, w_w
N_t = hoop compression due to radial pressure of wires, w_t

then $$N_t = N_d\left(\frac{w_t}{w_w}\right) \tag{16.9}$$

also $$N_t = t f_c$$

From Eqs 16.9 and 16.10, the spacing of the wire winding

$$s = \left[\frac{2N_d}{w_w} \times \frac{f_s A_s}{f_c D t}\right] \text{mm} \tag{16.10}$$

5. The vertical prestress required to resist the bending moments in the wall due to the circumferential wire winding and hydrostatic pressure as a consequence of end restraint is computed as follows:

If M_t = vertical moment due to the prestress at transfer,
and M_w = vertical moment due to hydrostatic pressure

then $$M_t = M_w\left(\frac{w_t}{w_w}\right)$$

The compressive prestress required in concrete is expressed as,

$$f_c = \left[\frac{f_{min.w}}{\eta} + \frac{M_w}{\eta Z}\right]$$

where Z is the section modulus of a unit length of wall about an axis in the tangential direction and passing through the centroid.

When the tank is empty, the prestress required

$$f_c = \left[\frac{f_{min.w}}{\eta} + \frac{M_t}{Z}\right] \tag{16.11}$$

The vertical prestressing force required is given by,

$$P = f_c A_c$$

where, A_c is the cross-sectional area of concrete per unit length along the circumference.

According to the Indian Standard Code, the vertical prestressing force is to be designed for 30 per cent of the hoop compression.

The walls of the tank should be suitably reinforced, since circumferential wire winding is generally performed prior to the vertical prestressing of walls. If there is a likelihood of large temperature variations as a result of storing hot liquids, a detailed analysis of temperature stresses developed will be necessary on the lines suggested by Worsch[28] and Born[29].

The design of prestressed concrete tanks with different types of base connections is presented in the following examples:

Example 16.5 A cylindrical prestressed concrete water tank of internal diameter 30 m is required to store water over a depth of 7.5 m. The permissible compressive stress in concrete at transfer is 13 N/mm^2 and the minimum compressive stress under working pressure is 1 N/mm^2. The loss ratio is 0.75. Wires of 5 mm diameter with an initial stress of 1000 N/mm^2 are available for circumferential winding and Freyssinet cables made up of 12 wires of 8 mm diameter stressed to 1200 N/mm^2 are to be used for vertical prestressing. Design the tank walls assuming the base as fixed. The cube strength of concrete is 40 N/mm^2.

Solution. For the required depth of storage of 7.5 m and diameter 30 m, an average wall thickness of 150 mm is tentatively assumed based on Table 16.1,

$$D = 30 \text{ m}, H = 7.5 \text{ m and } t = 150 \text{ mm}, \eta = 0.75$$

$$\left(\frac{H^2}{Dt}\right) = \left(\frac{7.5^2}{30 \times 0.15}\right) = 12.5$$

$$w_w = wH = (10 \times 7.5) \text{ kN/m}^2 = 0.075 \text{ N/mm}^2$$

Referring to Tables 16.2 and 16.3, the maximum ring tension and moments in tank walls for the fixed base condition are:

$$N_d = (0.64 \times 10 \times 7.5 \times 15) = 720 \text{ kN/m} = 720 \text{ N/mm}$$

$$M_w = (0.01 \times 10 \times 7.5^3) = 42.5 \text{ kN m/m} = 42500 \text{ N mm/mm}$$

Minimum wall thickness

$$t = \left[\frac{N_d}{\eta f_{ct} - f_{min.w}}\right] = \left[\frac{720}{(0.75 \times 13) - (1)}\right] = 82.3 \text{ mm}$$

Net thickness available (allowing for vertical cables of diameter 30 mm) is

$$(150 - 30) = 120 \text{ mm}$$

Required circumferential prestress is,

$$f_c = \left[\frac{N_d}{\eta t} + \frac{f_{min.w}}{\eta}\right]$$

$$\therefore \qquad f_c = \left[\frac{720}{0.75 \times 120} + \frac{1}{0.75}\right] = 9.4 \text{ N/mm}^2$$

Spacings of circumferential wire winding at base is,

$$s = \left[\frac{2N_d}{w_w}\frac{f_s A_s}{f_c D t}\right] = \left[\frac{2 \times 720}{0.075} \times \frac{1000 \times 20}{9.4 \times 30 \times 10^3 \times 120}\right] = 11.4 \text{ mm}$$

$\therefore$ Number of wires/metre = 87

Ring tension N_d at 0.1 H(0.75 m) from top is

$$N_d = (0.097 \times 10 \times 7.5 \times 15) = 109 \text{ kN/m} = 109 \text{ N/mm}$$

$$f_c = \left[\frac{109}{0.75 \times 120} + \frac{1}{0.75}\right] = 2.5 \text{ N/mm}^2$$

$$s = \left[\frac{2 \times 109}{0.075} \times \frac{1000 \times 20}{2.5 \times 30 \times 10^3 \times 120}\right] = 64 \text{ mm}$$

Number of wires/metre at the top of tank = 16

Maximum radial pressure due to prestress is,

$$w_t = \left(\frac{2 f_s A_s}{sD}\right) = \left(\frac{2 \times 1000 \times 20}{11.4 \times 30 \times 10^3}\right) = 0.117 \text{ N/mm}^2$$

Maximum vertical moment due to prestress is,

$$M_t = M_w\left(\frac{w_t}{w_w}\right) = 42500\left(\frac{0.117}{0.075}\right) = 67{,}000 \text{ N mm/mm} = (67 \times 10^6) \text{ N mm/m}$$

Considering one metre length of tank along the circumference, the section modulus is

$$Z = \left(\frac{1000 \times 150^2}{6}\right) = (375 \times 10^4) \text{ mm}^3$$

$\therefore$ Vertical prestress required is

$$f_c = \left[\frac{f_{min.w}}{\eta} + \frac{M_t}{Z}\right] = \left[\frac{1}{0.75} + \frac{67 \times 10^6}{375 \times 10^4}\right] = 19.2 \text{ N/mm}^2$$

Since this stress exceeds the permissible value of $f_{ct} = 13$ N/mm^2, the thickness of the tank wall at base is increased to 200 mm. Thus,

$$Z = \left(\frac{1000 \times 200^2}{6}\right) = (666 \times 10^4) \text{ mm}^3$$

$$f_c = \left[\frac{1}{0.75} + \frac{67 \times 10^6}{666 \times 10^4}\right] = 12 \text{ N/mm}^2$$

Vertical prestressing force $= f_c A = \left[\dfrac{(12 \times 1000 \times 200)}{(1000)}\right] = 2400$ kN

Using 8 mm diameter (12 nos.) Freyssinet cables

$$\text{Force/cable} = \left[\frac{(50 \times 12 \times 1200)}{(1000)}\right] = 720 \text{ kN}$$

$$\therefore \quad \text{Spacings of vertical cables} = \left[\frac{1000 \times 720}{2400}\right] = 300 \text{ mm}$$

The approximate vertical prestress required to counteract winding stresses as per IS code is

$$= 0.3\, f_c = (0.3 \times 9.4) = 2.82 \text{ N/mm}^2$$

$$\therefore \quad \text{Vertical prestressing force required} = \left[\frac{(2.82 \times 1000 \times 200)}{(1000)}\right] = 564 \text{ kN}$$

$$\text{Ultimate tensile force in wires at base of tank} = \left[\frac{(87 \times 20 \times 1500)}{(1000)}\right] = 2610 \text{ kN}$$

$$\therefore \quad \text{Load factor against collapse} = \left(\frac{2610}{720}\right) = 3.6$$

$$\text{Direct tensile strength of concrete} = 0.267\sqrt{40} = 1.7 \text{ N/mm}^2$$

$$\text{Cracking load} = \left[(1000 \times 200)\frac{(0.75 \times 9.4 + 1.7)}{(1000)}\right] = 1760 \text{ kN}$$

$$\therefore \quad \text{Factor of safety against cracking} = \left(\frac{1760}{720}\right) = 2.45$$

Nominal reinforcements of 0.2 per cent of the cross-sectional area are to be provided in the circumferential and longitudinal directions. This requirement will be fulfilled by providing 8 mm diameter mild steel bars at 300 mm spacing on both faces at a cover of 20 mm.

Example 16.6 Design the circular cylindrical tank of Example 16.5, assuming the base connections to be hinged, with the other data remaining the same. From Tables 16.4 and 16.5 (tanks with hinged base), the maximum ring tension and moments are obtained for the tank parameter, $(H^2/Dt) = 12.5$.

Solution.

$$N_d = (0.75 \times 10 \times 7.5 \times 15) = 840 \text{ kN/m} = 840 \text{ N/mm}$$

$$M_w = (0.0039 \times 10 \times 7.5^3) = 16.5 \text{ kN m/m} = 16500 \text{ N mm/mm}$$

$$\text{Thickness of wall,} \quad t = \left[\frac{840}{(0.75 \times 13) - (1)}\right] = 96 \text{ mm}$$

Thickness adopted for practical reasons of housing vertical cables of 30 mm diameter = 150 mm

Net thickness available = (150 – 30) = 120 mm

$$\text{Circumferential prestress, } f_c = \left[\frac{840}{0.75 \times 120} + \frac{1}{0.75}\right] = 10.75 \text{ N/mm}^2$$

Spacing of 5 mm wires, $s = \left[\dfrac{2 \times 840}{0.075} \times \dfrac{1000 \times 20}{10.75 \times 30 \times 10^3 \times 120}\right] = 11.6$ mm

Number of wires/metre = 86

Similarly, the nuniber of wires/metre required towards the top of the tank = 16

Radial pressure due to prestress is

$$w_t = \left(\frac{2 \times 1000 \times 20}{11.6 \times 30 \times 10^3}\right) = 0.115 \text{ N/mm}^2$$

Maximum vertical moment due to prestress is

$$M_t = 16500\left(\frac{0.115}{0.075}\right) = 25400 \text{ N mm/mm} = 25.4 \times 10^6 \text{ N mm/m}$$

Considering one metre length, the section modulus,

$$Z = (375 \times 10^4) \text{ mm}^3$$

Vertical prestress required is

$$f_c = \left[\frac{1}{0.75} + \frac{25.4 \times 10^6}{375 \times 10^4}\right] = 8.2 \text{ N/mm}^2$$

Vertical prestressing force = $(8.2 \times 1000 \times 150)/(1000) = 1230$ kN

Spacing of Freyssinet cables containing 12 wires of 8 mm diameter

$$= \left[\frac{1000 \times 720}{1230}\right] = 585 \text{ mm}$$

The minimum values of load factor against collapse of 2 and against cracking of 1.2 are easily available to satisfy the IS code requirements of strength and serviceability.

Example 16.7 A prestressed concrete circular cylindrical tank is required to store 24500 million litres of water. The permissible compressive stress in concrete at transfer should not exceed 13 N/mm^2 and the minimum compressive stress under working pressure should not be less than 1 N/mm^2. The loss ratio is 0.75. High-tensile steel wires of 7 mm diameter with an initial stress of 1000 N/mm^2, are available for winding round the tank. Freyssinet cables of 12 wires of 8 mm diameter which are stressed to 1200 N/mm^2, are available for vertical prestressing. The cube strength of concrete is 40 N/mm^2. Design the tank walls supported on elastomeric pads. Assume the coefficient of friction as 0.5.

Volume of tank = 24500×10^6 litres

Assuming the diameter of tank as 50 m, height of storage = 12.5 m

Solution. From Table 16.1, the thickness of the tank wall at the base is taken as 400 mm which gradually reduces to 200 mm towards the top of tank.

Hydrostatic pressure, $W_w = wH = (10 \times 12.5) = 125$ kN/m^2 = 0.125 N/mm^2

Maximum ring tension, $N_d = (10 \times 12.5 \times 25) = 3125$ kN/m

Self-weight of the wall = $(12.5 \times 0.3 \times 1 \times 24) = 90$ kN/m

Frictional force at base, $N_o = (0.5 \times 90) = 45$ kN/m

Minimum wall thickness at base = $\left[\dfrac{3125}{(0.75\times 13)-(1)}\right] = 360$ mm

Net thickness available (allowing for vertical cables of diameter 40 mm) is (400 – 40) = 360 mm

Circumferential prestress,

$$f_c = \left[\frac{3125}{0.75\times 360}+\frac{1}{0.75}\right] = 13\ \text{N/mm}^2$$

Spacing of circumferential wire winding is

$$s = \left[\frac{2\times 3125}{0.125}\times\frac{1000\times 38.5}{13\times 50\times 10^3\times 360}\right] = 8.3\ \text{mm}$$

Number of wires/metre = 120

Ring tension at 0.75 m from top = $(10\times 0.75\times 25) = 188$ kN/m

Thickness at top = 200 mm

Net thickness = (200 – 40) = 160 mm

$$f_c = \left[\frac{188}{0.75\times 160}+\frac{1}{0.75}\right] = 2.91\ \text{N/mm}^2$$

$$s = \left[\frac{2\times 188}{0.125}\times\frac{1000\times 38.5}{2.91\times 50\times 10^3\times 160}\right] = 50\ \text{mm}$$

Number of wires at top/metre = 20

Maximum radial pressure due to prestress at transfer,

$$w_t = \left[\frac{2\times 1000\times 38.5}{8.3\times 50\times 10^3}\right] = 0.186\ \text{N/mm}^2$$

Maximum vertical moment due to working pressure,

$$M_w = 0.247\,N_o\sqrt{Rt} = (0.247\times 45\sqrt{25\times 0.4}) = 35.5\ \text{kN mm/m}$$
$$= 35500\ \text{N mm/m}$$

Maximum vertical moment due to prestress is,

$$M_t = 35500\left(\frac{0.186}{0.125}\right) = 53000\ \text{N mm/m} = 53\times 10^6\ \text{N mm/m}$$

Considering one metre length of tank along the circumference, the section modulus is,

$$Z = \left[\frac{1000\times 400^2}{6}\right] = 26.6\times 10^6\ \text{mm}^3$$

The vertical prestress required,

$$f_c = \left[\frac{1}{0.75}+\frac{53\times 10^6}{26.6\times 10^6}\right] = 3.33\ \text{N/mm}^2$$

As per the IS code, the minimum vertical prestress required to counteract the winding stresses is,

$$= (0.3\times 13) = 3.9\ \text{N/mm}^2$$

$\therefore$ Vertical prestressing force = $\left[\dfrac{(3.9\times 1000\times 400)}{(1000)}\right] = 1560$ kN

$$\text{Spacings of vertical cables} = \left[\frac{1000 \times 720}{1560}\right] = 460 \text{ mm}$$

Ultimate tensile force in wires at base of tank

$$= \left[\frac{(120 \times 38.5 \times 1500)}{(1000)}\right] = 6900 \text{ kN}$$

$$\text{Load factor against collapse} = \left(\frac{6900}{3125}\right) = 2.2$$

$$\text{Cracking load} = \left[(1000 \times 400)\frac{(0.75 \times 13 + 1.7)}{(1000)}\right] = 4580 \text{ kN}$$

$$\text{Factor of safety against cracking} = \left(\frac{4580}{3125}\right) = 1.47$$

Nominal reinforcements of 0.2 per cent of the cross-section in the circumferential and vertical direction are well distributed on each face.

References

1. Abeles, PW, *An Introduction to Prestressed Concrete,* Vol. II, Concrete Publications Ltd, London, 1966, pp 516–521.
2. Doanides, PJ, "Some notes on the prestressed concrete pipes of the Veeranam aquaduct for the water supply of Madras," *International Symposium on Prestressed Concrete Pipes, Poles, Pressure Vessels and Sleepers, Proceedings,* Vol. 2, Madras, 1972, pp p/3–1 to p/3–40.
3. Joshi, N G, "Prestressed concrete pipes-state of art," *International Symposium on Prestressed Concrete Pipes, Poles, Pressure Vessels and Sleepers, Proceedings,* Vol. 1, Madras, 1972, pp p/0–1 to p/0–29.
4. Ooykaas, GAP, "Prestressed concrete pipes," *Journal of the Institution of Water Engineers,* Vol. 6, 1952, pp 85–109.
5. Freyssinet, E, "Prestressed concrete, principles and applications," *Journal of the Institution of Civil Engineers,* London, Vol. 33, 1950, pp 331–380.
6. Hendrickson, JG, "Prestressed concrete pipe," *Proceedings of the 1st US Conference on Prestressed Concrete,* Massachusetts, 1951.
7. IS: 784–1959, *Indian Standard Specification for Prestressed Concrete Pipes,* Indian Standards Institution, New Delhi, 1959, pp 1–6.
8. C–30/64, AWWA, *Specification for Prestressed Concrete Pressure Pipe, Steel Cylinder Type for Water and Other Liquids,* American Waterworks Association, 1964.
9. Ooykaas, GAP, "Discontinuity in prestressed concrete pipes," *Magazine of Concrete Research,* Vol. 3, March 1952, pp 131–138.
10. Curtis, A R and H J Cowan, "Design of longitudinal cables in circumferentially wound prestressed tanks," *Magazine of Concrete Research,* Vol. 5, March 1954, pp 123–126.
11. A 124–1962, *Australian Standard for Concrete Pressure Pipes,* Australian Water Resources Council Technical Paper No. 9, Canberra, 1975, pp 105–110.
12. Gerwick, Jr Ben C, *Construction of Prestressed Concrete Structure,* Wiley Inter Science, 1971, pp 303–309.

13. Evans, RH and EW Bennett, *Prestressed Concrete Theory and Design,* Chapman and Hall, London, 1962, pp 240–243.
14. Kummer, A and Salz, A "Statik und Konstruction des Zylindrisehen Fanlbehalters der Klaranlage CelIe," *Beton-u Stahlbetonbau,* 54, H-6, 1959 pp 147–152.
15. Kruse, R, "Die Stahlbetonarbeiten fur das Klarwerk Ruhleben," *Beton,* 11, H. 6, 1961, pp 385–394.
16. Erikson, KM, "Chateaud eau a orebro (suede)," *Constructions,* 13 (1958), Mais pp 145–148.
17. Laponche, R and J Arnoult, "Reservoir hyperbolique a paroi mince en beton precontraint," (Thin-walled hyperbolic tank in prestressed concrete), *Travaux,* Vol. 32, 1948, pp 210–212.
18. Preload Engineering Company Inc. "Design of preload tanks," *Bulletin T-19,* New York.
19. BS: 8007–1987, Code of Practice for Design of Concrete Structures for retaining aqueous liquids, British Standards Institution, 1987.
20. IS: 3370–Part III, *Indian Standard Code of Practice for Concrete Structures for the Storage of Liquids Part III-Prestressed Concrete* (Third reprint), Indian Standards Institution, Sept. 1975, pp 5–11.
21. Leonhardt, F, *Prestressed Concrete Design and Construction,* Second Edition, Wilhelm Ernst und Sohn, Berlin, 1964, pp 531–548.
22. Buyer, K, "Zur Berechnurg der Vorspannung geschlossener Kreiszlinderschalen im Stahlbeton Behalterbau," *Beton-u Stahlbetonbau,* Vol. 52, 1957, pp 104–111.
23. Ager, JWA, "Design and construction of liquid retaining structures in prestressed concrete," *Reinforced Concrete Review,* Vol. 2, 1952, pp 509–554.
24. Baur, W, "Vorgespannte Wasserbehalter nach dem Fariefenprinzip," *Beton-u, Stahlbetonbau* 49, Heft 1, 1954, pp 14–15.
25. Timoshenko, S and Woinowsky Krieger, S, *Theory of Plates and Shells,* McGraw-Hill, New York 1959.
26. Crom, JM, "Design of prestressed tanks," *Transactions of the American Society of Civil Engineers,* 117, 1952, pp 89–118.
27. IS: 3370–Part IV, *Indian Standard Code of Practice for Concrete Structures for the Storage of Liquids, Part IV–Design Tables* (Third reprint), Indian Standards Institution, May 1974, pp.14–49.
28. Worsch, G, "Der Kreiszylindrische Behalter mit teilweiserheiber Fullng In," *Beton-kalender* 47, Bd. 2, 1958, pp 31–33.
29. Born, J, "Zur Frage der Wandstarke von Faulturmen," *Wasser u. Boden,* 13, H. 9, 1961, pp 320–323.

Review Questions

16.1 Distinguish with sketches the difference between cylinder and non-cylinder types of prestressed concrete pipes.

16.2 List the various stages to be considered in the design of prestressed concrete pipes.

16.3 What is the effect of circumferential wire winding on longitudinal stresses? How do you compute these stresses and design longitudinal prestressing in circular pipes?

16.4 Briefly outline the salient design features of cylinder and non-cylinder pipes.

16.5 Explain with sketches the different shapes of prestressed concrete water tanks mentioning their advantages.

16.6 What are the different types of joints used between the walls and floor slab of prestressed concrete tanks?

16.7 Explain with sketches the distribution of ring tension and bending moment in circular tanks with fixed, sliding and hinged base.

16.8 What minimum load factors are provided against cracking and ultimate collapse for circular water tanks in the relevant Indian codes?

16.9 What is bursting pressure? How do you calculate the factor of safety against bursting in cylinder pipes?

16.10 Explain the necessity of using vertical cables in tank walls.

Exercises

16.1 Design a non-cylinder prestressed concrete pipe of internal diameter 500 mm to withstand a working pressure of 1 N/mm^2. High-tensile wires of 2 mm diameter stressed to 1200 N/mm^2 at transfer are available for use. Permissible maximum and minimum stresses in concrete at transfer and working loads are 13.5 and 0.8 N/mm^2 (compression), respectively. Loss ratio = 0.8, E_s = 210 kN/mm^2 and E_c = 35 kN/mm^2. Calculate, (a) the minimum thickness of concrete for the pipe, (b) number of turns of wire per metre length of the pipe, (c) the test pressure required to produce a tensile stress of 0.7 N/mm^2 in the concrete when applied immediately after tensioning, and (d) the winding stress in the steel.

[Ans: (a) 25 mm; (b) 90 turns; (c) 1.42 N/mm^2; (d) 1281 N/mm^2]

16.2 A prestressed concrete cylinder pipe is formed by lining a steel cylinder of diameter 750 mm and thickness 2.5 mm with a layer of spun concrete 38 mm thick. If the pipe is required to withstand a hydraulic pressure of 0.85 N/mm^2 without developing any tensile stress in concrete, calculate

(a) the required pitch of 4 mm wires, wound round the cylinder at a tensile stress of 980 N/mm^2,

(b) the test pressure to produce a tensile stress of 1.4 N/mm^2 in the concrete immediately after winding, and

(c) the approximate bursting pressure.

Modular ratio = 6
Tensile strength of wire = 1680 N/mm^2
Yield stress of cylinder = 280 N/mm^2
Loss ratio = 0.85 **[Ans: (a) 32.5 mm; (b) 1.2 N/mm^2; (c) 3.6 N/mm^2]**

16.3 A prestressed concrete pipe of 1.2 m diameter and a core thickness of 75 mm is required to withstand a service pressure intensity of 1.2 N/mm^2. Estimate the pitch of a 5 mm diameter high tensile wire winding if the initial stress is limited to 1000 N/mm^2. Permissible stresses in concrete are 12.5 N/mm^2 in compression and zero in tension. The loss ratio is 0.8. If the direct tensile strength of concrete is 2.5 N/mm^2, estimate the load factor against cracking.

[Ans: Pitch = 21.8 mm, LF = 1.26]

16.4 Design a cylindrical prestressed concrete water tank to suit the following data: Capacity of the tank = 3.5 × 10^6 litres. Ratio of diameter to height = 4, Maximum compressive stress in concrete at transfer not to exceed

14 N/mm^2 (compression). Minimum compressive stress under working load to be 1 N/mm^2. The prestress is to be provided by circumferential winding of 5 mm wires and by vertical cables of 12 wires of 7 mm diameter. The stress in wires at transfer = 1000 N/mm^2. Loss ratio = 0.75. Design the walls of the tank and the details of the circumferential wire winding and vertical cables for the following joint conditions at the base: (a) hinged, (b) fixed, and (c) sliding base (assume coefficient of friction as 0.5).

16.5 Design a prestressed concrete non-cylinder pipe of internal diameter 500 mm to withstand a working pressure of 1 N/mm^2. The permissible maximum and minimum compressive stresses in concrete are 14 N/mm^2 and 0.7 N/mm^2, respectively. Loss ratio is 0.8. High-tensile wires of 3 mm diameter stressed to 1000 N/mm^2 are available for use. Modulus of elasticity of steel and concrete are 250 kN/mm^2 and 35 kN/mm^2, respectively. Calculate
(a) the minimum thickness of the concrete pipe
(b) number of turns of wire winding per metre length of pipe
(c) test pressure required to produce a tensile stress of 0.7 N/mm^2 in concrete
(d) winding stress in steel wire

[Ans: (a) 25 mm (b) 48 turns (c) 1.47 N/mm^2 (d) 1084 N/mm^2]

16.6 A prestressed concrete pipe is to be designed to withstand a fluid pressure of 1.6 N/mm^2. The diameter of the pipe is 1200 mm and shell thickness is 100 mm. The maximum compressive stress in concrete at transfer is 16 N/mm^2. A residual compression of 2 N/mm^2 is expected to be maintained at service load. Loss ratio is 0.8. High-tensile wires of 5 mm diameter stressed to 1000 N/mm^2 are available for use. Determine
(a) the number of turns of wire per metre length
(b) the pitch of wire winding **[Ans: (a) 74 (b) 13.5 mm]**

16.7 A cylindrical prestressed concrete water tank of internal diameter 28 m to store water to a depth of 8 m is to be designed using M-40 Grade concrete. The thickness of tank walls is 150 mm and 5 mm diameter high-tensile wires are available for use. The permissible compressive stress in concrete at transfer is limited to 12 N/mm^2. During service, a residual compressive stress of 1 N/mm^2 is desired in concrete. The initial stress in high-tensile wires is 1000 N/mm^2. The loss of prestress is estimated to be 20 per cent. Assuming the base slab and tank walls are monolithically cast, determine the number of turns of circumferential wire winding per metre height of the tank at base.

[Ans: Number of turns at base = 87 turns/m]

Objective-type Questions

16.1 Circular prestressing is ideally suited for concrete pipes and tanks because
(a) part of the section is stressed
(b) full section is stressed
(c) the section has variable stresses

16.2 Circular prestressing of concrete tanks induces
(a) hoop tension
(b) hoop compression
(c) flexural compression

16.3 Non-cylinder prestressed concrete pipes
(a) are not cylindrical
(b) have a steel cylinder encased in concrete
(c) are cylindrical with concrete shell

16.4 Prestressed concrete cylinder pipes
(a) do not have a steel pipe
(b) have a steel cylinder embedded in concrete
(c) are not cylindrical

16.5 In prestressed concrete pipes circumferential wire winding induces
(a) hoop tension
(b) longitudinal bending stresses
(c) axial compression

16.6 Failure of non-cylinder pipes is due to
(a) bursting
(b) compression of concrete
(c) excessive cracking of concrete

16.7 The economical proportion of diameter to height of circular cylindrical prestressed concrete tanks is
(a) 1:4 (b) 4:1 (c) 2:1

16.8 The walls of a prestressed concrete tank with a sliding base filled with water develops
(a) bending moments
(b) moments and ring tension
(c) only ring tension

16.9 The serviceability limit state of cracking in prestressed concrete tanks is easily satisfied because they are designed as
(a) type-3 members (b) type-1 members (c) type-2 members

16.10 Prestressed concrete tanks with walls fixed at base develop at the base section
(a) ring tension
(b) combined bending and tension
(c) vertical bending Moment

Answers to Objective-type Questions

16.1 (b)	16.2 (b)	16.3 (c)	16.4 (b)	16.5 (c)
16.6 (c)	16.7 (b)	16.8 (c)	16.9 (b)	16.10 (c)

17 Prestressed Concrete Slabs and Grid Floors

17.1 Types of Prestressed Concrete Floor Slabs

Prestressed concrete slab systems are ideally suited for floor and roof construction of industrial buildings where the live loads to be supported are of a higher order and the uninterrupted floor space is desirable, for which reason longer spans between the supporting elements are required.

Solid prestressed slabs 660 mm thick have been used for constructing bridge decks in the USA[1] for spans of 18 m, the slab being prestressed by parabolic post-tensioned cables along the span and straight cables in the transverse direction. Solid precast prestressed plank units 63 mm deep, used in conjunction with *in situ* cast concrete-topping and with an overall depth of slab varying from 100 to 175 mm are suitable for the span range of 3 to 8 m to support superimposed loads varying from 4.0 to 12.5 kN/m^2. Table 17.1 shows the spans and the permissible superimposed loads on solid slabs as recommended by the Concrete Development Company[2].

Table 17.1 *Prestressed concrete floor units*

Solid prestressed plank units 63 mm deep									
Section Details		*Total Superimposed Load,* (kN/m^2)							
Total Slab Depth, (mm)	*In situ Topping Depth,* (mm)	*3.0*	*4.0*	*5.0*	*6.0*	*7.50*	*8.75*	*10.0*	*12.50*
100	38				4.25	3.85	3.65	3.45	3.15
114	50				4.75	4.35	4.05	3.80	3.45
125	63				5.15	4.70	4.40	4.15	3.80
138	76			5.85	5.50	5.00	4.75	4.45	4.10
152	88			6.20	5.80	5.30	5.00	4.75	4.35
165	100		7.00	6.55	6.10	5.60	5.30	5.00	4.55
178	114		7.30	6.75	6.40	.5.85	5.60	5.25	4.85

Note: Spans to the left of the step-line are limited by deflection.

Precast prestressed hollow core slabs, with or without topping are important structural elements in industrialised and large panel building construction[3]. The slabs, produced on long casting beds using the pretensioning system and cut to shorter specified span lengths, are mainly used in one-way floors which are freely supported by transverse walls or beams.

Precast pretensioned cored slabs with different types of cavities are widely used as floor panels of civic and industrial buildings in erstwhile USSR. Graduck[4] reports that these panels are produced in multiples of 2000 mm nominal width and lengths from 3.6 to 6.4 m. Some of the typical slab elements used are shown in Fig. 17.1. Hollow panels of oval cavity-type are more economical for larger spans since they contain the least volume of concrete as compared to round cavity panels. Prestressed concrete ribbons have been used as reinforcements for hollow-cored slabs. These consist of tensioned wires or strands embedded in high grade concrete of star of rectangular cross-sections with dimensions of 40 to 80 mm. Experimental investigations by the author[5] indicate that the inclusion of pretensioned elements in the tension zone of concrete flexural members result in an apparent increase in the loads, causing visible cracking in the *in situ* concrete.

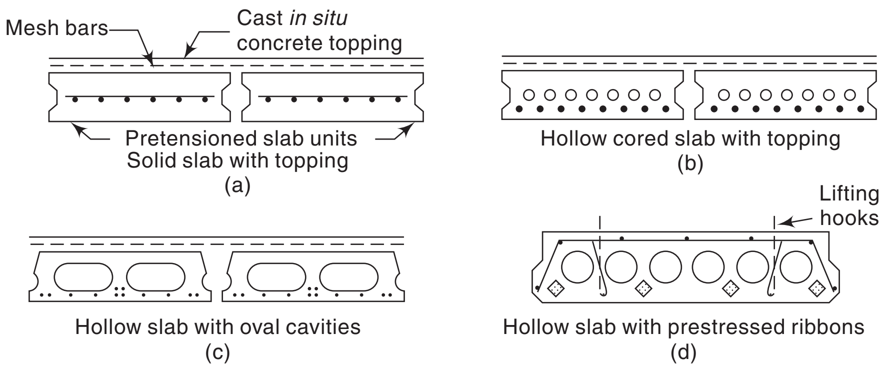

Fig. 17.1 *Cross-section of prestressed concrete floor panels*

Large size roof panels which have ribs in the perpendicular direction are used for spans up to 12 m. Details of a typical ribbed roof panel of size 3 m by 12 m, commonly used in erstwhile USSR, are shown in Fig. 17.2. Prestressed single- and double-T slab panels have been widely used for industrial structures in the USA, owing to their distinct advantage of speed of construction. The monolithic units combining the beam and the slab may be used for spans varying from 6 to 25 m. Typical cross-sections of the single- and double-T slabs and channels are shown in Fig. 17.3. In USA, where long spans are often pre-

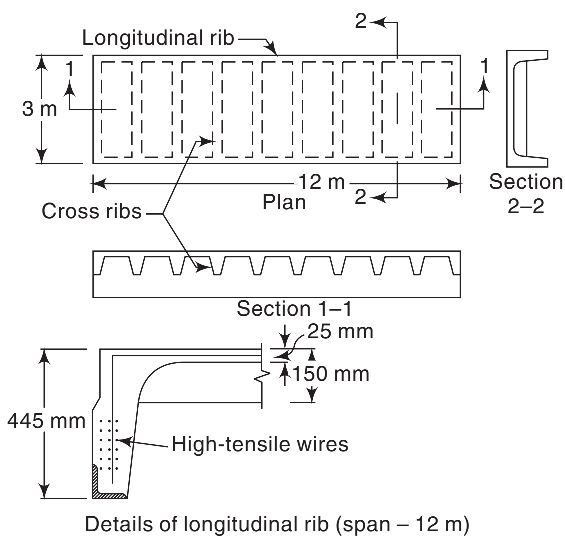

Fig. 17.2 *Prestressed concrete roof panel*

ferred, the double-T unit has found wide acceptance for use in food processing plants, warehouses and automobile industries where service loads are in excess of 5 N/m^2. In addition, the double- and single-T units can also be used as wall units.

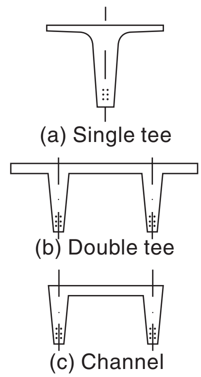

Fig. 17.3 *Typical precast prestressed units for floor systems*

Lift slab construction[6] has been widely used in USA during the last two decades. Flat slabs, as shown in Fig. 17.4, are cast and prestressed at ground level and then lifted into position by hydraulic jacks mounted on the top of columns. The prestressing of the two-way continuous slab reduces the thickness, controls the deflection and eliminates cracks in the slab. Lin[7] reported that the solid prestressed lift slabs are generally most economical for spans ranging from 6 to 10 m.

Prestressed concrete is admirably suited for forming coffered or grid floors with two-way ribs in concrete which are post-tensioned. Prestressed concrete grid floors are more slender, readily amenable to artistic treatment and have smaller deflections under service loads due to the combined effect of the

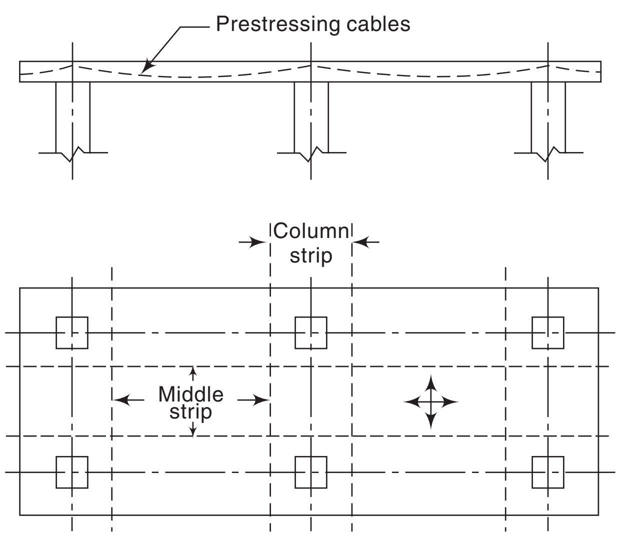

Fig. 17.4 *Continuous prestressed flat slab*

prestress in the principal directions. Salient features of a typical prestressed concrete grid floor are shown in Fig. 17.5. Recent investigations by Dowrick and Narasimhan[8] have shown that prestressed coffered slabs are comparatively cheaper than reinforced concrete grids for flooring schemes of commercial and industrial buildings.

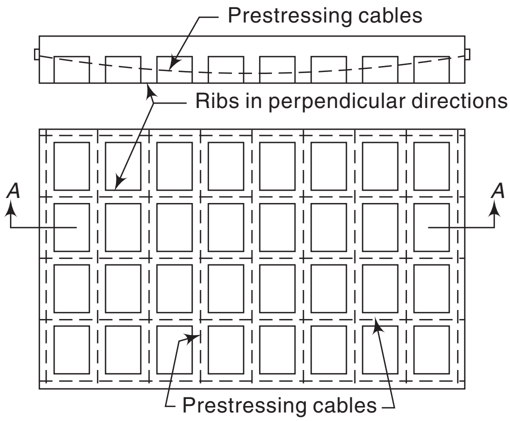

Fig. 17.5 *Prestressed concrete grid floor*

17.2 Design of Prestressed Concrete One-Way Slabs

The design of prestressed concrete one-way slabs spanning between parallel supports is based on the principles of designing members for flexure as outlined in Section 12.1. One-way slabs may be supported across the entire width of the slab by beams, piers or abutments or bearing walls, which are positioned perpendicular to the longitudinal axis of the span, or the supports may be at an angle to the span directions. One-way slabs may be continuous over one or several supports.

Simple or continuous slabs are analysed for design moments by considering a unit width of the slab. The prestressing force and the eccentricity of the cable required at prominent sections to resist the dead and live load moments are determined and the spacing of the cables or wires is fixed based on the availability of the type of tendons. In the case of slabs subjected to heavy concentrated loads, transverse reinforcements in the form of mild steel or deformed bars or prestressed cables will be required to resist transverse moments. An approximate estimate of these moments may be made by using the data of Westergaard[9] or Kawai[10] or Kist and Bouma[11]. Concentric tendons are generally preferred for transverse prestressing of one-way slabs to prevent objectionable deflections in the transverse direction. The slabs designed should conform to the requirements of serviceability and strength. The serviceability requirements include limiting deflections and cracking under working loads, as prescribed in the codes.

Example 17.1 A highway bridge deck slab spanning 10 m is to be designed as a one way prestressed concrete slab with parallel post-tensioned cables carrying an effective force of 620 kN. The deck slab is required to support a uniformly distributed live load of 25 kN/m^2. The permissible stresses in concrete should not exceed 15 N/mm^2 in compression and no tension is permitted at any stage. Design the spacing of the cables and their position at mid-span section. Assume loss of prestress as 20 per cent.

Solution.

Span of the deck slab = 10 m

Distributed working live load = 25 kN/m^2

Force in the cable = 620 kN

Permissible compressive stress in concrete = f_{ct} = 15 N/mm^2

Permissible tensile stress in concrete = $f_{min.w}$ = 0

Loss ratio = η = 0.85

The live- and dead-load moments are computed considering one metre width of the slab.

$$M_g = \left[\frac{25\times 10^2}{8}\right] = 312.5\,\text{kN.m}$$

Let h = overall depth of the slab

b = width of the slab

$$\therefore \quad M_g = \left[\left(\frac{bh}{10^6}\right)\times 24\times\left(\frac{10^2}{8}\right)\right] = \left[\frac{300\,bh}{10^6}\right]\text{kN m} = 300\,bh\ \text{N mm}$$

Range of stress at bottom fibre = $f_{br} = [\eta f_{ct} - f_{min.w}] = [(0.85\times 15) - 0] = 12$ N/mm^2

Hence, the minimum section modulus is given by the expression,

$$Z_b > \left[\frac{bh^2}{6}\right] > \left[\frac{M_q + (1-\eta)M_g}{f_{br}}\right]$$

$$\therefore \quad \left[\frac{1000\times h^2}{6}\right] > \left[\frac{(312.5\times 10^6) + (1-0.8)300\times 1000\times h}{12}\right]$$

or $\quad h^2 - 30h + 156250 = 0$

Solving $\quad h = 410$ mm

$\therefore \quad A = (1000\times 410) = (41\times 10^4)$ mm^2

$$Z_b = Z_t = \left[\frac{1000\times 410^2}{6}\right] = (28\times 10^6)\ \text{mm}^3$$

and $\quad M_g = (300\,bh) = (300\times 1000\times 410) = (123\times 10^6)$ N mm

$$f_t = \left[0 - \left(\frac{123\times 10^6}{0.8\times 28\times 10^6}\right)\right] = 4.4\ \text{N/mm}^2$$

$$f_b = \left[0 + \frac{(312.5+123)10^6}{0.8\times 28\times 10^6}\right] = 19.4\ \text{N/mm}^2$$

The minimum prestressing force required is computed as,

$$P = \frac{A}{2}(f_b + f_t) = \frac{(41\times 10^4)}{2}(19.4 - 4.4)$$

$$= (3075\times 10^3)\text{N} = 3075\ \text{kN}$$

The eccentricity is calculated as,

$$e = \left[\frac{Z(f_b - f_t)}{A(f_b + f_t)}\right] = \left[\frac{28 \times 10^4 (19.4 + 4.4)}{41.4 \times 10^4 (19.4 - 4.4)}\right] = 109 \text{ mm}$$

$$\text{Spacing of the cables} = \left[\frac{(1000 \times 620)}{3075}\right] = 201 \text{ mm}$$

Adopt a spacing of 200 mm centres for the cables in the span direction.

17.3 Design of Prestressed Concrete Two-Way Slabs

The design of a two-way slab supported on all four sides involves the computation of bending moments in the principal directions of the slab. The slabs may be supported on masonry walls or beams and mayor may not be continuous over the supports. Transverse loads are resisted by the development of two-way slab action, resulting in moments in the longer and shorter span directions. The magnitude and nature of moments developed in two-way slabs depend mainly upon the type of load, ratio of the sides of slab, and the degree of restraint at the supports.

The moments developed in a two-way slab may be determined by the elastic analysis, such as those of Westergaard and Pigeaud or, alternatively, by the ultimate load methods, such as Johansen's yield line method[12], or Hillerborg's strip method[13]. The bending moment coefficients, shown in Table 17.2, are provided for by the British standard BS EN: 1992–1–1 for the design of two-way slabs, simply supported on all four sides without any adequate provision to resist torsion and the lifting of corners.

Table 17.2 *Bending moment coefficients for slabs spanning in two-directions at right angles, simply supported on four sides (British Standard BS EN: 1992–1–1)*

L_y/L_x	1.0	1.1	1.2	1.3	1.4	1.5	1.75	2.0
α_x	0.062	0.074	0.084	0.093	0.099	0.104	0.113	0.118
α_y	0.062	0.061	0.059	0.055	0.051	0.046	0.037	0.029

Bending moment coefficients, compiled in Table 17.3, are useful for the design of restrained slabs supported on four sides with provision for torsion at corners as provided in the British as well as Indian Standard Codes[14]. These coefficients are based on the modified distributions of elastic bending moments proposed by Westergaard. Moment coefficients based on the yield line theory and compiled in Table 17.4, and on strip methods suggested by the author[15,16,17] are strictly applicable for the limit state of collapse only. It is also significant to note that coefficients predicted by the simple yield line theory using an orthotropic layout of reinforcement are found to be identical with those derived by the strip method. The moment coefficients derived from the ultimate load methods are generally lower in magnitude than those evaluated from elastic theories thus naturally resulting in savings in reinforcement. However, slabs designed by the ultimate load method should be checked for excessive deflections and/or crack widths under service loads according to the principles of limit-state design[18].

In the case of two-way slabs which are fully prestressed (class 1), the serviceability criterion to be satisfied is generally the constraint imposed on upward deflections under prestress and self-weight, so that tensile stresses are completely eliminated under service loads. The question of limiting cracks within permissible limits arises only in slabs which are designed as partially prestressed systems.

Deflections of slabs which are not cracked under service loads can be estimated by using the deflection coefficients of Timoshenko[19]. The shear coefficients are useful for computing the shear forces developed at the supports.

In prestressed slabs, due to the load balancing effect, the shear forces and stresses developed being negligibly small, shear reinforcements are generally not required. Limited experimental investigations[20, 21] on slabs designed by the strip method indicate that the designs are safe with respect to the limit states of serviceability and strength, with actual load factors against collapse exceeding the theoretical values.

Example 17.2 Design a post-tensioned prestressed concrete two-way slab, 6 m by 9 m, with discontinuous edges, to support an imposed load of 3 kN/m^2. Cables of four wires of 5 mm diameter carrying an effective force of 100 kN are available for use. Design the spacings of cables in the two directions and check for the safety of the slab against collapse and excessive deflection at service loads. Assume $f_{ck} = 40$ N/mm^2, $f_p = 1600$ N/mm^2 and $E_c = 38$ kN/mm^2.

Solution.

$$L_x = 6 \text{ m, and } L_y = 9 \text{ m}$$

Ratio of L_y/L_x $= 1.5$

Thickness of slab $= \left(\dfrac{\text{span}}{50}\right) = (6000/50) = 120$ mm

Self-weight of slab $= (0.12 \times 24 \times 1) = 2.88$ kN/m^2

Live load on slab $= 3.00$ kN/m^2

Finishes, etc. $= 0.12$ kN/m^2

Total service load $= 6.00$ kN/m^2

Total ultimate design load, $W_{ud} = (1.4 \times 3.00) + (1.6 \times 3.00) = 9.00$ kN/m^2

Referring to Table 17.3, working moments in the middle strips are given by,

$$M_{sx} = (0.089 \times 6.0 \times 6^2) = 19.3 \text{ kN m/m}$$
$$M_y = (0.056 \times 6.0 \times 6^2) = 12.1 \text{ kN m/m}$$

Table 17.3 *Bending moment coefficients for rectangular panels supported on four sides with provision for torsion at corners (IS: 456)*

S. No.	*Type of Panel and Moments Considered*		*B.M Coefficient α_x for Short Span*								*B.M Coefficient a_y for Long Span (for all values of L_y/L_x)*
			Values of L_y/L_x								
			1.0	*1.1*	*1.2*	*1.3*	*1.4*	*1.5*	*1.75*	*2.0 (or more)*	
1.	Interior	X	0.032	0.037	0.043	0.047	0.051	0.053	0.060	0.065	0.032
	panels	Y	0.024	0.028	0.032	0.036	0.039	0.041	0.045	0.049	0.024
2.	One short edge	X	0.037	0.043	0.048	0.051	0.055	0.057	0.064	0.068	0.037
	discontinuous	Y	0.028	0.032	0.036	0.039	0.041	0.044	0.048	0.052	0.028
3.	One long edge	X	0.037	0.044	0.052	0.057	0.063	0.067	0.077	0.085	0.037
	discontinuous	Y	0.028	0.033	0.039	0.044	0.047	0.051	0.059	0.065	0.028
4.	Two adjacent edges	X	0.047	0.053	0.060	0.065	0.071	0.075	0.084	0.091	0.042
	discontinuous	Y	0.035	0.040	0.045	0.049	0.053	0.056	0.069	0.069	0.035
5.	Two short edges	X	0.045	0.049	0.052	0.056	0.059	0.060	0.065	0.069	—
	discontinuous	Y	0.035	0.037	0.040	0.043	0.044	0.045	0.049	0.052	0.035
6.	Two long edges	X	—	—	—	—	—	—	—	—	0.045
	discontinuous	Y	0.035	0.043	0.051	0.057	0.063	0.068	0.080	0.088	0.035
7.	Three edges	X	0.057	0.064	0.071	0.076	0.080	0.084	0.091	0.097	—
	discontinuous	Y	0.043	0.048	0.053	0.057	0.060	0.064	0.069	0.073	0.043
8.	Three edges	X	—	—	—	—	—	—	—	—	0.057
	discontinuous	Y	0.043	0.051	0.059	0.065	0.071	0.076	0.087	0.096	0.043
9.	Four edges	X	—	—	—	—	—	—	—	—	—
	discontinuous	Y	0.056	0.064	0.072	0.079	0.085	0.089	0.100	0.107	0.056

X—Negative moment at continuous edge Y—Positive moment at mid-span

Table 17.4 *Bending moment coefficients for the design of rectangular slabs by the yield line theory*

S. No.	Type of Panel and Moments Considered		B.M Coefficient α_x for Short Span								
			Values of L_y/L_x								B.M Coefficient a_y for Long Span (for all values of L_y/L_x)
			1.0	1.1	1.2	1.3	1.4	1.5	1.75	2.0 (or more)	
1.	Interior panels	X	0.025	0.028	0.031	0.035	0.039	0.043	0.045	0.050	0.025
		Y	0.017	0.019	0.021	0.024	0.026	0.028	0.030	0.033	0.017
2.	One edge discontinuous	X	0.030	0.033	0.037	0.040	0.043	0.047	0.051	0.054	0.030
		Y	0.020	0.022	0.025	0.027	0.029	0.031	0.034	0.036	0.020
3.	Two adjacent edges discontinuous	X	0.032	0.036	0.040	0.045	0.048	0.051	0.057	0.063	0.032
		Y	0.021	0.024	0.027	0.030	0.032	0.034	0.038	0.042	0.021
4.	Two short edges discontinuous	X	0.036	0.040	0.043	0.047	0.050	0.053	0.055	0.058	—
		Y	0.024	0.026	0.029	0.031	0.033	0.035	0.037	0.039	0.024
5.	Two long edges discontinuous	X	—	—	—	—	—	—	—	—	0.048
		Y	0.032	0.034	0.037	0.040	0.045	0.050	0.057	0.065	0.032
6. (a)	Three edges discontinuous (one long edge continuous)	X	0.039	0.044	0.048	0.053	0.056	0.060	0.063	0.068	—
		Y	0.026	0.029	0.032	0.035	0.037	0.039	0.042	0.045	0.026
6. (b)	Three edges discontinuous (one short edges continuous)	X	—	—	—	—	—	—	—	—	0.055
		Y	0.037	0.041	0.045	0.049	0.051	0.054	0.064	0.074	0.037
7.	Four edges discontinuous	X	—	—	—	—	—	—	—	—	—
		Y	0.042	0.048	0.054	0.060	0.064	0.068	0.076	0.083	0.042

X—Negative moment at continuous edge Y—Positive moment at mid-span

Total moment in the middle strip (x direction)

$$= (19.3 \times 0.75 \times 9) = 130 \text{ kN m}$$

Using a minimum cover of 30 mm for the tendons at the centre of slab, the distance between the top kern and the centroid of cable

$$= (120 - 20 - 40) = 50 \text{ mm}$$

If $\quad P$ = total prestressing force required in the x direction,

$$(P \times 50) = (130 \times 10^6)$$

$\therefore \quad P = (26 \times 10^5) \text{ N} = 2600 \text{ kN}$

Force in each cable = 100 kN

$\therefore$ Number of cables in x direction (middle strip) = 26

$$\text{Spacing of cables} = \left[\frac{0.75 \times 9 \times 1000}{26}\right] = 260 \text{ mm}$$

Adopt a spacing of 250 mm (four cables per metre).

Total moment in the middle strip (y direction)

$$= (12.1 \times 0.75 \times 6) = 55 \text{ kN m}$$

Providing a cover of 40 mm to cables in y direction,

Distance between cable and top kern = 120 – 40 – 40 = 40 mm

$$\therefore \quad \text{Prestressing force required} = \left[\frac{(55 \times 10^6)}{40 \times 10^3}\right] = 1380 \text{ kN}$$

$\therefore$ Number of cables in y direction (middle strip) = 1380/100 = 14

$$\text{Spacing of cables} = \left[\frac{0.75 \times 6 \times 1000}{14}\right] = 320 \text{ mm}$$

The cable profile is parabolic with maximum eccentricity at the centre and concentric at the supports.

Check for limit state of collapse

Ultimate moment (x direction) = $0.089 \times 9.00 \times 6^2 = 29$ kN m/m

$$A_p = (4 \times 4 \times 20) = 320 \text{ mm}^2$$

$$\left(\frac{A_p f_p}{b d f_{ck}}\right) = \left(\frac{320 \times 1600}{1000 \times 90 \times 40}\right) = 0.142$$

Referring to Table 7.1

$$\left(\frac{f_{pu}}{0.87 f_p}\right) = 1.0$$

$\therefore \quad f_{pu} = (0.87 \times 1600) = 1392 \text{ N/mm}^2$

and $\quad \left(\frac{x_u}{d}\right) = 0.29$

or $\quad x_u = (0.29 \times 90) = 26.1 \text{ mm}$

$\therefore \quad M_u = f_p A_p (d - 0.42 x_u)$

$$= 1392 \times 320 \left(\frac{90 - 0.42 \times 26.1}{10^6}\right) = 35.2 \text{ kN m}$$

The ultimate moment capacity of the slab is higher than the minimum value required. A similar check may be made in the y direction also.

Check for deflection under service loads

The tendons following a parabolic profile in x and y directions induce uniformly distributed loads acting upwards, which are given by,

$$\text{Equivalent load } (x \text{ direction}) = \left(\frac{8Pe}{L_x^2}\right) = \left(\frac{8 \times 400 \times 0.03}{36}\right) = 2.66 \text{ kN/m}$$

$$\text{Equivalent load } (y \text{ direction}) = \left(\frac{8Pe}{L_y^2}\right) = \left(\frac{8 \times 320 \times 0.02}{81}\right) = 0.64 \text{ kN/m}$$

$\therefore$ Unbalanced service load = (6.00 – 2.66 – 0.64)

$$= 2.70 \text{ kN/m}^2 = 0.0027 \text{ N/mm}^2$$

Using deflection coefficients recommended by Timoshenko, for an aspect ratio of $L_y/L_x = 1.5$, the deflection is given by

$$a_{max} = \alpha\left(\frac{qL_x^4}{D}\right)$$

where α = coefficient = 0.00772

q = u.d.l = 0.0027 N/mm^2

$$D = \text{flexural rigidity} = \left[\frac{Eh^3}{12(1-v_c^2)}\right] = \left[\frac{38000 \times 120^3}{12(1-0.15^2)}\right] = 5.62 \times 10^9$$

$$\therefore \quad a_{max} = 0.00772\left(\frac{0.0027 \times 600^4}{5.62 \times 10^9}\right) = 4.85 \text{ mm}$$

$$\text{Maximum permissible long-term deflection} = \left(\frac{6000}{250}\right) = 24 \text{ mm}$$

Check for stresses

Unbalanced load = 2.7 kN/m^2

Moment due to this load (x direction) = $(0.089 \times 2.7 \times 6^2) = 8.7$ kN m

$$\text{Stresses developed} = \left[\frac{8.7 \times 10^6}{(1000 \times 120^2)/6}\right] = 3.33 \text{ N/mm}^2$$

(Compression at top and tension at soffit of slab)

Direct stress due to prestressing force

$$= \left[\frac{400 \times 1000}{1000 \times 120}\right] = 3.66 \text{ N/mm}^2 \text{ (compression)}$$

$\therefore$ Maximum compressive stress in concrete at the top of slab

$$= (3.66 + 3.33) = 7.00 \text{ N/mm}^2$$

which is less than the permissible stress of 13 N/mm^2.

The maximum shear stress under ultimate loads is

$$\left[\frac{0.424 \times 9.00 \times 6000}{(1000 \times 90)}\right] = 0.26 \text{ N/mm}^2$$

which is negligibly small and hence no shear reinforcements are necessary.

17.4 Design of Prestressed Concrete Simple Flat Slabs

A simple prestressed flat slab is generally supported by a network of columns without beams and prestressed in two perpendicular directions. The design of a typical simple flat slab, shown in Fig. 17.6, involves the analysis of moments in the two principal directions so that cables may be arranged to resist these moments. The slab is analysed as a one-way slab and the total number of cables required to resist the moments in each of the two principal directions is determined.

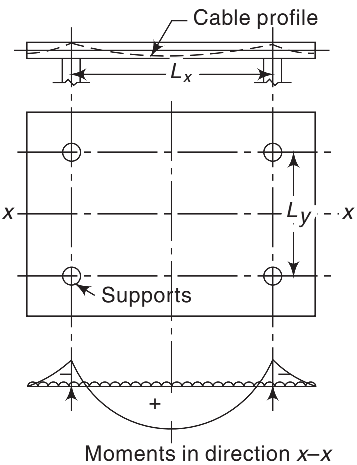

Fig. 17.6 *Prestressed concrete simple flat slab*

The column strips being stiffer than the middle strips, a greater percentage of the tendons are housed in the column strips. The proportioning of the tendons between the column and middle strips may be based on the provisions of codes, such as IS: 456 and BS EN: 1992–1–1, where column strips share a higher proportion of the total moment. Since it is not generally possible to vary the spacing of cables for positive and negative moments in either the column or the middle strips, the total number of cables required in any direction is apportioned in the ratio of 65 and 35 per cent between the column and middle strips. The design of a typical simple flat slab is illustrated by the following example.

Example 17.3 A simple flat slab 12 m by 9 m is supported by four columns so placed as to form a symmetrical rectangular grid, 7 m by 6 m. The cantilevers formed are 2.5 and 1.5 m in the long and short directions of the slab. The live load on the slab is 1 kN/m^2. Prestressing cables consisting of four wires of 5 mm carrying an effective force of 100 kN are available for use. Design the number of cables required and arrange them suitably in the two principal directions.

Solution.

Thickness of slab $= \left(\dfrac{\text{span}}{40}\right) = \left(\dfrac{6000}{40}\right) = 150$ mm

Self-weight of slab $= (0.15 \times 1 \times 1 \times 24) = 3.6$ kN/m^2

Live load on slab $= 1.0$

Finishes, etc. $= 0.4$

5.0 kN/m^2

Total load on four columns $= (5 \times 12 \times 9) = 540$ kN
Reaction on each column $= 135$ kN
The slab is analysed for +ve and –ve moments in the long span (x direction) and short span (y direction)
Moments in the direction of long span:
Positive moment (centre of slab), $M_{xp} = [(270 \times 3.5) - (270 \times 3)]$

$= 135$ kN m

Negative moment (supports), $M_{xn} = (2.5 \times 9 \times 5) \times 1.25 = 141$ kN m

The prestressing force required is designed to resist the maximum moment of 141 kN m in the x direction.

The cables are provided at a distance of 30 mm from the edge of the slab at critical sections. The cable profile is parabolic along the span so that the eccentricity is proportional to the moment at the section as shown in Fig. 17.6. Total prestressing force required in the x direction is given by,

$$P = \left(141 \times \frac{10^3}{70}\right) = 2020 \text{ kN}$$

$\therefore$ Number of cables in the x direction $= \left(\dfrac{2020}{100}\right) = 21$

In the x direction, the widths of column and middle strips are each 3 m. Similarly, in the short span (y direction), the maximum moment occurs at the centre of slab and equals $[(270 \times 3) - (270 \times 2.25)] = 203$ kN m.

$\therefore$ Number of cables in the y direction $= \left(\dfrac{203 \times 10^3}{70 \times 100}\right) = 30$

The column and middle strips are 7 m and 5 m width in the y direction. The total number of cables in each direction are distributed, so that 65 per cent are in column strip and 35 per cent are in middle strip.

The number of cables and their spacing in the x and y directions are obtained as given in the table shown as follows.

Direction	*Column strip*		*Middle strip*	
	No. of cables	*Spacing,* mm	*No. of cables*	*Spacing,* mm
x	14	430	7	430
y	20	350	10	500

17.5 Design of Prestressed Concrete Continuous Flat Slab Floors

The design principles of continuous flat slab floors are similar to those of two-way reinforced concrete slabs. A strip of slab of unit width, continuous over supports, is analysed as a continuous beam. Prestressing of continuous slab results in secondary moments. If the cable profile is concordant, secondary moments can be eliminated. The maximum span up to which prestressed lift slabs are economical depends upon the type of slab. According to Libby[22], solid slabs have a practical limitation of about 10 m while waffle or coffered slabs may be economical up to 16 m.

The profile of the cables in the two principal directions should be so arranged that they do not conflict each other. The number of cables required to resist moments is suitably divided between the column and middle strips as in the case of flat slabs. Since 1955 a number of continuous flat slabs have been built in the USA, in which unbonded tendons have been used. It is generally recognised that bonded tendons are to be preferred both from the point of view of ultimate strength requirements and easy maintenance under adverse exposure conditions.

The design of a continuous flat slab floor involves the computation of maximum and minimum moments for various load combinations and the determination of suitable cable profiles so that the resulting stresses in concrete are within the safe allowable limits as per codes. The problems concerning excessive camber should be overcome by suitably selecting the cable profiles. Shear stresses at the junction of the column and slab should be carefully controlled by proper design and detailing of the critical shear zones.

Example 17.4 Design a continuous prestressed flat slab floor of overall size 16 m by 16 m. The columns are spaced at 7.5 m intervals in the perpendicular direction. The floor slab has to support a superimposed load of 3 kN/m^2. Freyssinet cables, consisting of 12 wires of 5 mm diameter stressed to 1000 N/mm^2, are available for use. Determine the number of cables required and their spacing in each direction.

$$\text{Thickness of slab} = \left(\frac{\text{span}}{40}\right) = (7.5 \times 1000)/(40) = 200 \text{ mm}$$

$$\text{Self-weight of slab} = (0.20 \times 1 \times 1 \times 24) = 4.8 \text{ kN/m}^2$$

$$\text{Live load on slab} = 3.0 \text{ kN/m}^2$$

A unit width of slab is considered in the principal directions and the maximum and minimum moments at support and span sections are analysed for different combinations of live loads. The envelopes of maximum and minimum moments developed for dead and live loads are shown in Fig. 17.7. The design moments evaluated by using coefficients provided in the Reynolds reinforced concrete designer's handbook[23] are obtained as:

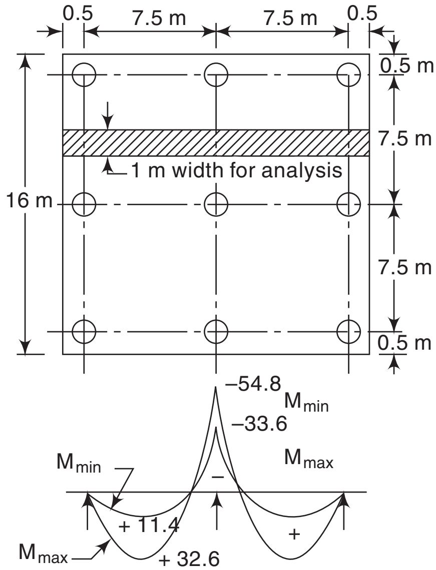

Fig. 17.7 *Envelope of maximum and minimum moments in continuous flat slab*

(a) *Moments due to dead, load,* M_g

Span moment = $kgL^2 = (0.062 \times 4.8 \times 7.5^2) = 16.80$ kN m

Mid-support moment = $(-0.125 \times 4.8 \times 7.5^2) = -33.60$ kN m

(b) *Moments due to live load (positive and negative)*

Span moments:

Positive, $M_{Lp} = (0.093 \times 3.0 \times 7.5^2) = 15.80$ kN m

Negative, $M_{Ln} = (-0.032 \times 3.0 \times 7.5^2) = -5.40$ kN m

Mid-support moments,

Negative, $M_{Ln} = (-0.125 \times 3.0 \times 7.5^2) = 21.20$ kN m

The maximum and minimum moments at support and span are:

(*a*) *At centre span*

$M_{max} = (M_{Lp} + M_g) = (15.80 + 16.80) = 32.60$ kN m

$M_{min} = (M_{Ln} + M_g) = (-5.40 + 16.80) = 11.40$ kN m

$\therefore$ Range of moment = $(M_{max} - M_{min}) = 21.20$ kN m

(*b*) *At mid-support*

$M_{max} = (M_{Lp} + M_g) = (0 - 33.60) = -33.60$ kN m

$M_{min} = (M_{Ln} + M_g) = (-21.20 - 33.60) = -54.80$ kN m

Range of moment = $M_{max} - M_{min} = 21.20$ kN m

Prestressing force

The absolute maximum moment occurs at the mid-support section. Using a minimum cover of 30 mm to the cable, if no tensile stresses are permitted in the section, the distance between the cable and the bottom kern is obtained as,

$(70 + 33.3) = 103.3$ mm

If P = prestressing force

$(P \times 103.3) = (54.80 \times 10^3)$

$\therefore \quad P = 530 \text{ kN}$

The permissible tendon zone along the span, obtained in a manner similar to that outlined in Section 15.11, is shown in Table 17.5 and Fig. 17.8. A concordant cable profile lying within the limiting zone of thrust does not induce any secondary moments and at the same time the stresses in concrete do not exceed the permissible limits. The selected parabolic profile of the concordant cable with eccentricities of +35 mm and –70 mm at centre of span and mid-support section is shown in Fig. 17.8.

Table 17.5 *Permissible tendon zone in continuous prestressed flat slabs*

Location	(M_{max}/P)	(M_{min}/P)	$(e_2 = M_{max}/P - 33.3)$ mm	$(e_1 = M_{min}/P + 33.3)$ mm
Centre of span	+63.30	+21.50	+30.00	+54.80
Mid-support	–63.50	–103.30	–96.80	–70.00

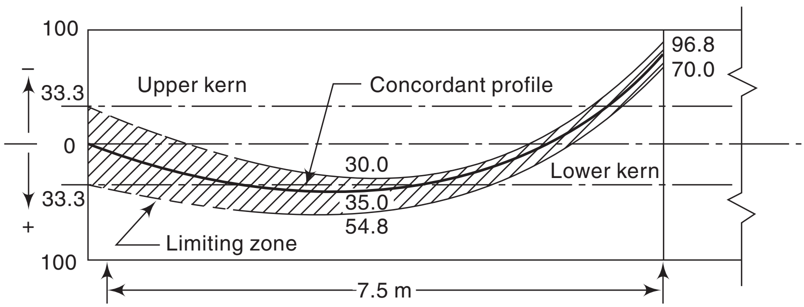

Fig. 17.8 *Permissible tendon zone and concordant cable profile*

Check for stresses

Considering 1 m width of slab,

$$A = (1000 \times 200) = (2 \times 10^5) \text{ mm}^2$$

$$Z = \left(\frac{1000 \times 200^2}{6}\right) = (6666 \times 10^3) \text{ mm}^3$$

$$P = 530 \text{ kN}$$

At centre of span section,

$$e = 35 \text{ mm}$$

$$M_{max} = +32.60 \text{ kN m}$$

$$M_{min} = +11.40 \text{ kN m}$$

$$\left(\frac{P}{A}\right) = \left(\frac{530 \times 10^3}{2 \times 10^5}\right) = 2.65 \text{ N/mm}^2$$

$$\left(\frac{Pe}{Z}\right) = \left(\frac{530 \times 10^3 \times 35}{6666 \times 10^3}\right) = 2.80 \text{ N/mm}^2$$

At mid-support section,

$$e = 70 \text{ mm}$$
$$M_{max} = -33.60 \text{ kN m}$$
$$M_{min} = -54.80 \text{ kN m}$$
$$\left(\frac{P}{A}\right) = \left(\frac{530 \times 10^3}{2 \times 10^5}\right) = 2.65 \text{ N/mm}^2$$
$$\left(\frac{Pe}{Z}\right) = \left(\frac{530 \times 10^3 \times 70}{6666 \times 10^3}\right) = 5.60 \text{ N/mm}^2$$

The maximum and minimum stresses developed are compiled in Table 17.6.

The stresses developed in concrete under maximum and minimum moments are within the safe permissible limits.

Table 17.6 *Stresses developed in continuous flat slab (Value of stress in N/mm^2, +compression, –tension)*

Location		*Prestress*	*Due to M_{max}*	*Due to M_{min}*	*Maximum Stress*	*Minimum Stress*
Centre of span	Top	–0.15	+4.9	+1.7	+4.75	+1.55
	Bottom	+5.45	–4.9	–1.7	+0.55	+3.75
Mid-support	Top	+8.25	–5.05	–8.25	+3.20	+0.0
	Bottom	–2.95	+5.05	+8.25	+2.15	+5.3

Number of cables

Using 12 wires of 5 mm diameter stressed to 1000 N/mm^2, the force in each cable $= \left[\frac{(20 \times 12 \times 1000)}{1000}\right] = 240$ kN

Total prestressing force required for a width of 16 m $= (530 \times 16)$

$= 8480$ kN

Number of cables = (8480/240) = 36

Using 65 per cent of cable in column strip and 35 per cent in the middle strip, the number of cables are obtained as,

$$\text{Column strip} = \left[\frac{65}{100} \times 36\right] = 24$$

$$\text{Middle strip} = \left[\frac{35}{100} \times 36\right] = 14$$

The spacings of cables in the respective strips are,

Column strip = (8.5 × 1000)/24 = 355 mm

Middle strip = (7.5 × 1000)/12 = 625 mm

17.6 Analysis and Design of Prestressed Concrete Grid Floors

A prestressed concrete grid floor consisting of ribs at close intervals in two mutually perpendicular directions and connected by slab in between the ribs can be considered as an orthotropic plate freely supported on four sides.

Timoshenko's[19] analysis may be used to evaluate the moments and shears in the grid which depend upon the deflection surface.

The vertical deflection a at any point of the grid shown in Fig. 17.9 is expressed as,

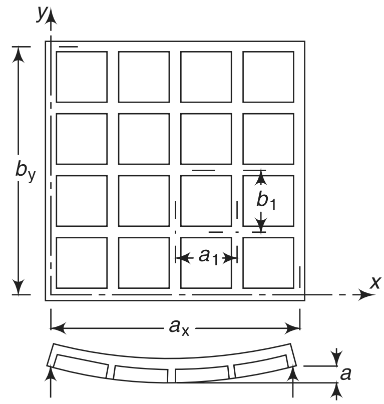

Fig. 17.9 *Deflection characteristics of grid floors*

$$a = \frac{16 w_d}{\pi^6}\left[\frac{\sin\left(\frac{\pi x}{a_x}\right)\sin\left(\frac{\pi y}{b_y}\right)}{\left(\frac{D_x}{a_x^4}\right)+\left(\frac{C_x + C_y}{a_x^2 b_y^2}\right)+\left(\frac{D_y}{b_y^4}\right)}\right]$$

where w_d = total uniformly distributed load per unit area, a_x, b_y = length of plate in x and y directions, D_x, D_y, C_x and C_y are the flexural and torsional rigidities per unit length of plate along x and y direction, respectively.

If a_1 and b_1 are the spacings of the ribs in x and y directions, then

$$D_x = \left(\frac{EI_1}{b_1}\right) \qquad C_x = \left(\frac{C_1}{b_1}\right)$$

$$D_y = \left(\frac{EI_2}{a_1}\right) \qquad C_y = \left(\frac{C_2}{a_1}\right)$$

where EI_1, EI_2, C_1 and C_2 are the flexural and torsional rigidities of the effective section in x and y directions.

The moments and shears are computed using the following expression:

$$M_x = -D_x\left(\frac{\partial^2 a}{\partial x^2}\right) \qquad M_y = -D_y\left(\frac{\partial^2 a}{\partial y^2}\right)$$

$$T_{xy} = -\frac{C_1}{b_1}\left(\frac{\partial^2 a}{\partial x \partial y}\right) \rightarrow T_{yx} = -\frac{C_2}{a_1}\left(\frac{\partial^2 a}{\partial x \partial y}\right)$$

$$Q_x = -\frac{\partial}{\partial x}\left[D_x\left(\frac{\partial^2 a}{\partial x^2}\right)+\frac{C_2}{a_1}\left(\frac{\partial^2 a}{\partial x \partial y}\right)\right]$$

$$Q_y = -\frac{\partial}{\partial y}\left[D_y\left(\frac{\partial^2 a}{\partial y^2}\right) + \frac{C_1}{b_1}\left(\frac{\partial^2 a}{\partial x \partial y}\right)\right]$$

Maximum bending moments occur at centre of span while maximum torsional moments are generated at the corners of the grid and maximum shear forces develop at mid-points of longer side supports. The minimum prestressing force and eccentricity required at centre of span along the mutually perpendicular directions are determined; care being taken to see that the cable profiles in x and y directions do not interfere with each other. The shear stresses developed due to torsional moments and shear should be checked at the critical sections. Due to the parabolic profile of the cables, which are concentric at the supports, the shear due to loads is counterbalanced to a considerable extent by the vertical component of the prestressing force. The author has reported[24] the design of a prestressed concrete grid floor using the above design principles.

Example 17.5 Design a prestressed concrete grid floor to cover a rectangular panel of an office floor, 12 m by 7 m. The superimposed load may be taken as 3 kN/m^2. M-40 grade concrete and Freyssinet cables of 18–5 mm and 12–7 mm are available for use. Design the grid and sketch the details of profiles of the cable in the ribs.

Solution. The arrangement of ribs in the principal directions and the cross-sectional details of the ribs with their effective flange widths are shown in Fig. 17.10. The ribs are spaced at intervals of 1.5 m in the y direction and 1.75 m in the x direction so that $a_1 = 1.75$ m and $b_1 = 1.5$ m. The second moment of area of the T-section in x and y directions may be computed by using Reynold's tables[23].

Area of the section $A = 157200 \text{ mm}^2$

$$I = K b_w h^3$$

where K = constant depending upon the ratio of the thickness of the slab to the overall depth h_f/h and the ratio of the width of rib to the effective flange width b_w/b. Hence,

$$I_1 = I_2 = (0.170 \times 200 \times 300^3) = (92 \times 10^7) \text{ mm}^4$$

$$Z_t = \left[\frac{(92 \times 10^7)}{85}\right] = (1.08 \times 10^7) \text{ mm}^3$$

$$Z_b = \left[\frac{(92 \times 10^7)}{217}\right] = (0.425 \times 10^7) \text{ mm}^3$$

Flexural rigidity per unit length of the plate is given by,

$$D_x = \left(\frac{EI_1}{b_1}\right) = \left[\frac{(92 \times 10^7 \times E)}{(1.5 \times 10^3)}\right] = (61 \times 10^4)\, E$$

$$D_y = \left(\frac{EI_2}{a_1}\right) = \left[\frac{(92 \times 10^7 \times E)}{(1.75 \times 10^3)}\right] = (53 \times 10^4)\, E$$

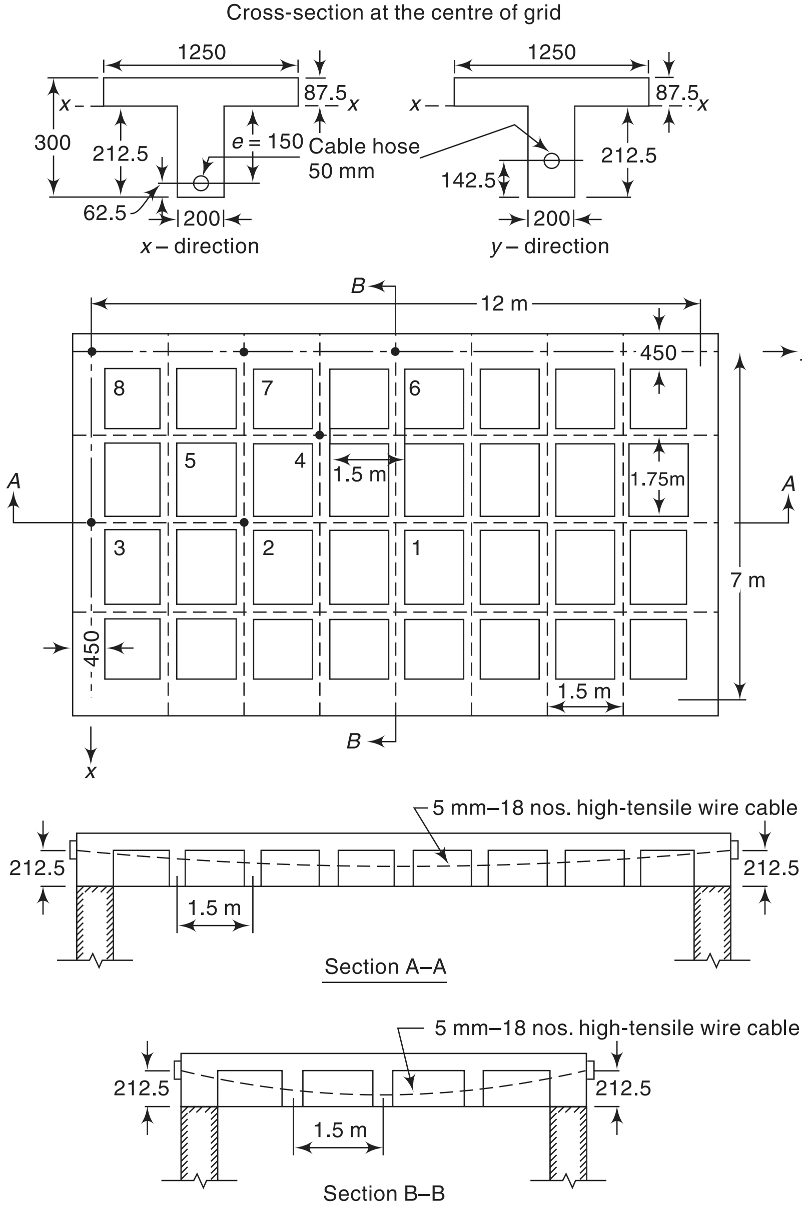

Fig. 17.10 *Prestressed concrete grid floor*

Torsional rigidity of the effective section is computed by using the coefficients recommended by Timoshenko[25].

$$C_1 = C_2 = K_1 G (b_w)^3 h$$

$$= \left[0.196 \frac{E}{2(1+0.15)}(200)^3(300)\right] = (2.04 \times 10^8)\ E$$

$$C_x + C_y = \left[\frac{C_1}{b_1} + \frac{C_2}{a_1}\right]$$

$$= (2.04 \times 10^8)\ E\left[\left(\frac{1}{1.5 \times 10^3}\right) + \left(\frac{1}{1.75 \times 10^3}\right)\right]$$

$$= (2.55 \times 10^5)\ E$$

Computation of loads

Ribs in x direction = $(7 \times 0.2 \times 0.21 \times 7 \times 24)$ = 49.5 kN
Ribs in y direction = $(3 \times 0.2 \times 0.21 \times 12 \times 24)$ = 36.5 kN
Slab (90 mm thick) = $(7 \times 12 \times 0.09 \times 24)$ = 182.0 kN
Floor finishes, etc. = 27.0 kN
Total load = 295 kN
Dead load per m² = $\left[\frac{295}{(12 \times 7)}\right]$ = 3.5 kN/m²
Live load = 3.0 kN/m²
Total design load, w_d = 6.5 kN/m²

Using the flexural and torsional rigidities and the design load, the maximum vertical deflection at the centre of span as computed using the deflection equation is given by,

$$a = 10 \text{ mm}$$

The bending and torsional moments and shears developed at the salient points of the grid are compiled in Table 17.7.

Central rib in x direction

Total bending moment to be resisted by the effective section at the center of the grid in x direction is given by,

$$M_x = (39 \times 1.5) = 58.5 \text{ kN m}$$

Table 17.7 *Moments and shears per metre width (grid floor)*

Point	x	y	M_x	M_y	T_{xy}	T_{yx}	V_x	V_y
	m	m	kN m	kN m	kN m	kN m	kN	kN
1	3.5	6.0	39.0	15.1	0	0	0	0
2	3.5	3.0	28.0	10.5	0	0	0	4.30
3	3.5	0	0	0	0	0	0	6.10
4	1.75	4.5	25.5	9.9	1.86	1.25	13.00	1.65
5	1.75	1.5	12.2	4.1	4.52	3.00	5.35	3.95
6	0	6.0	0	0	0	0	19.60	0
7	0	3.0	0	0	–4.90	3.25	14.00	0
8	0	0	0	0	–6.90	4.60	0	0

Dead-load moment, $M_g = (0.54 \times 58.5) = 31.5$ kN m

Live-load moment, $M_g = (0.46 \times 58.5) = 27.0$ kN m

The minimum section modulus Z_b required to safely resist the dead- and live-load moments is expressed as,

$$Z_b \geq \left[\frac{M_q + (1-\eta)M_g}{f_{br}}\right]$$

Assuming a loss ratio, $\eta = 0.85$, $f_{ct} = 15\ \text{N/mm}^2$, and $f_{tw} = 0$, we have

$$f_{br} = (\eta f_{ct} - f_{cw}) = (0.85 \times 15) = 12.75\ \text{N/mm}^2$$

$$Z_b \geq \left[\frac{(27 + 0.15 \times 31.5)10^6}{12.75}\right] \geq 2.5 \times 10^6\ \text{mm}^3$$

which is less than the value of $Z_b = 4.25 \times 10^6\ \text{mm}^3$ provided by the section. The minimum prestressing force required is obtained from the expression

$$P = \left[\frac{A(f_{inf}\, Z_b + f_{sup}\, Z_t)}{Z_t + Z_b}\right]$$

where $$f_{inf} = \left[\frac{M_q + M_g}{\eta Z_b}\right] = \left[\frac{58.5 \times 10^6}{0.85 \times 4.25 \times 10^6}\right] = 16.3\ \text{N/mm}^2$$

and $$f_{sup} = -\left(\frac{M_g}{Z_t}\right) = -\left(\frac{31.5 \times 10^6}{10.8 \times 10^6}\right) = -2.9\ \text{N/mm}^2$$

$$P = \left[\frac{157200 \times (16.3 \times 4.25 - 2.9 \times 10.8)10^6}{15.05 \times 10^6}\right] = 0.395 \times 10^6\ \text{N} = 395\ \text{kN}$$

Using Freyssinet cables of (18 – 5) mm diameter stressed to 1100 N/mm^2,

$$\text{Force in each cable} = \left[\frac{(18 \times 20 \times 1100)}{1000}\right] = 396\ \text{kN}$$

One cable is provided in central rib at an eccentricity *e* given by,

$$e = \left[\frac{Z_t\, Z_b(f_{inf} - f_{sup})}{A(f_{inf}\, Z_b + f_{sup} Z_t)}\right] = \left[\frac{10.8 \times 4.25 \times 10^{12}(16.3 + 2.9)}{5.95 \times 10^{12}}\right] = 150\ \text{mm}$$

Central rib in y direction

$$M_y = (15.1 \times 1.75) = 26.3\ \text{kN m}$$
$$M_g = (0.54 \times 26.3) = 14.2\ \text{kN m}$$
$$M_q = (0.46 \times 26.3) = 12.1\ \text{kN m}$$

$$f_{inf} = \left(\frac{26.3 \times 10^6}{0.85 \times 4.25 \times 10^6}\right) = 7.3\ \text{N/mm}^2$$

$$f_{sup} = \left(\frac{14.2 \times 10^6}{10.8 \times 10^6}\right) = -1.32\ \text{N/mm}^2$$

$$P = \frac{157200(7.3 \times 4.25 - 1.32 \times 10.8)10^6}{15.05 \times 10^6}$$
$$= (0.175 \times 10^6)\ \text{N} = 175\ \text{kN}$$

The corresponding eccentricity is obtained as,

$$e = \left(\frac{10.8 \times 4.25 \times 10^{12}(7.3 + 1.32)}{2.65 \times 10^{12}}\right) = 150 \text{ mm}$$

This eccentricity is not practicable as it obstructs the cables in the x direction. Hence, the maximum possible eccentricity is obtained as,

$$e = (150 - 20 - 40 - 20) = 70 \text{ mm}$$

The modified prestressing force located at this reduced eccentricity is given by,

$$P = \left[\frac{A\, f_{\text{inf}}\, Z_{\text{b}}}{Z_{\text{b}} + Ae}\right] = \left[\frac{157200 \times 7.3 \times 4.25 \times 10^6}{(4.25 \times 10^6) + (1.572 \times 7 \times 10^6)}\right] = 320 \times 10^3 \text{ N} = 320 \text{ kN}$$

Check for torsional resistance and shear

The ultimate torque T at the corner (point 8) is given by

$$T = (1.5 \times 6.9 \times 0.75) = 7.76 \text{ kN m}$$

Torsional shear stress,
$$\tau_{\text{t}} = \frac{2T}{h_{\text{min}}^2 [h_{\text{max}} - h_{\text{min}}/3]}$$
$$= \frac{2 \times 7.76 \times 10^6}{200^2 [300 - (200/3)]} = 1.65 \text{ N/mm}^2$$

Since τ_{t} exceeds the value of $\tau_{\text{t,min}} = 0.40$ N/mm^2 (From Table 8.4), torsion reinforcements are designed as specified in Section 8.5.1. The ultimate maximum shear at point 6 is

$$V_{\text{u}} = (1.5 \times 19.6 \times 1.5) = 44.1 \text{ kN}$$

$$f_{\text{cp}} = \frac{(175 \times 10^3)}{(300 \times 200)} = 2.91 \text{ N/mm}^2$$

$$f_{\text{t}} = 0.24\sqrt{f_{\text{ck}}} = 0.24\sqrt{40} = 1.51 \text{ N/mm}^2$$

$$V_{\text{cw}} = 0.67 b_{\text{w}} h \sqrt{f_{\text{t}}^2 + 0.8 f_{\text{cp}} f_{\text{t}}}$$

$$= \left[\frac{0.67 \times 200 \times 300\sqrt{1.51^2 + 0.8 \times 2.91 \times 1.51}}{10^3}\right] = 96.48 \text{ kN}$$

Since $V_{\text{cw}} > V_{\text{u}}$, minimum transverse reinforcements are provided as detailed in Section 8.3.2.

References

1. Lin, TY, *Design of Prestressed Concrete Structures*, John Wiley and Sons Inc., First edition, 1960, pp 324–330.
2. Bell, BJ, *Practical Prestressed Concrete Design*, Pitman, London, 1964, pp 344–345.
3. Lewicki, B, "Industrialized construction with large concrete panels," *CEB Bulletin No*. 77, Paris, April, 1971, pp 91–117.

4. Graduck, II, *Prestressed Concrete*, Oxford and IBH Publishing Co., New Delhi, 1967, pp 104–106.
5. Krishna Raju, N et al., “Limit state behaviour of concrete beams with precast pretensioned elements in the tension zone,” *Journal of the Institution of Engineers* (*India*), Vol. 57, Pt. C 1-5 March 1977, pp 261–266.
6. Perimutter, J H, “Types and uses of precast prestressed members,” *Proceedings of the Western Conferences on Prestressed Concrete Buildings*, Los Angeles, California, Edited by Lin and Kelly, Gordon and Breach, Science Publishers, New York, 1962, pp 105–119.
7. Lin, T Y and E X, Rice, Economics of prestressed concrete buildings,” *Indian Construction News*, Vol. 8, No. 5, 1959, pp 126–127.
8. Dowrick, D J and N Narasimhan, “Prestressed vs reinforced concrete flat slabs,” *Concrete*, 12, No. 9, Sept. 1978, pp 16–19.
9. Westergaard, Computation of stresses in bridge slabs due to wheel loads, *Public Roads*, March, 1930.
10. Kawai, T, “Influence surface for moments in slabs continuous on overflexible cross beams,” *Publications of International Association for Bridge and Structural Engineering*, 16, 1957, pp 117–138.
11. Kist, H J, and A L Bouma, “An experimental investigation of slabs subjected to concentrated loads,” *Publications of International Association for Bridge and Structural Engineering*, 14, 1954, pp 85–110.
12. Johanson, K W, *Yield Line Theory*, Cement and Concrete Association, London, 1962.
13. Hillerborg, A, “A plastic theory for the design of reinforced concrete slabs,” *Proceedings of 6th Congress of International Association for Bridge and Structural Engineering*, Stockholm, 1960, p.17.
14. IS: 456 *Indian Standard Code of Practice for Plain and Reinforced Concrete Appendix* C, (Fourth Revision), Bureau of Indian Standards 2000.
15. Krishna Raju, N, “Design of rectangular reinforced concrete slabs supported on all the sides with a short discontinuous edge,” *Building Science*, Vol. 5, 1970, pp 181–185.
16. Krishna Raju, N, “Optimized strip method for the design of freely supported slabs,” *Indian Concrete Journal*, Vol. 45, No. 9, Sept. 1971, pp 390–393.
17. Krishna Raju, N, “Moment coefficients for the design of rectangular slabs with short discontinuous edges,” *Indian Concrete Journal*, Vol. 46, No.11, 1972, pp 466–468.
18. Krishna Raju, N, “Limit state design of two-way reinforced concrete slabs,” *Journal of the Institution of Engineers India*, Vol. 54, CI-I, Sept. 1973, pp 18–22.
19. Timoshenko, S, and S Woinowsky-Krieger, *Theory of Plates and Shells*, 2nd edn., McGraw-Hill, New York, 1959, pp 105–179.
20. Armer, G S T, “Ultimate load tests of slabs designed by the strip method,” *Building Research Station*, London, CP 83/68, 1968.
21. Satish Rao, I, *Strength and Serviceability of Reinforced Concrete Slabs*, M. Tech. Thesis, Karnataka Regional Engineering College, University of Mysore, 1978, pp 1–94.
22. Libby, R J, *Prestressed Concrete*, *Design and Construction*, Ronald Press Company, New York, 1961, pp 266–281.

23. Reynolds, C E, *Reinforced Concrete Designer's Handbook*. Fifth edn, Concrete Publications, London, 1957, pp 211–216.
24. Krishna Raju, N, "The design of prestressed concrete grid floors," *The Indian Concrete Journal*, Vol. 39, No. 1, Jan. 1965, pp 33–35.
25. Timoshenko; S P and J N Goodier, *Theory of Elasticity*, 3rd edn, McGraw-Hill Kogakusha Ltd, 1970.

Review Questions

17.1 Explain briefly the advantages of using prestressed concrete floor slabs mentioning their common applications.

17.2 Sketch the typical cross-sections of prestressed concrete floor panels generally employed in building and bridge construction.

17.3 What type of precast prestressed concrete sections do you recommend for covering large spans? Sketch the typical cross-sections of single tee, double tee and channel units.

17.4 What are the salient design features of prestressed concrete one-way and two-way slab panels?

17.5 What are the advantages of prestressing flat slab floor panels? Sketch the cross-section of a simple flat slab showing the typical cable profile.

17.6 Briefly outline the salient design features of continuous prestressed concrete flat slab floors.

17.7 What are grid or coffered floors? What is the advantage of prestressing such floors? Sketch a typical grid floor showing the cables in the principal directions.

17.8 How do you compute the flexural and torsional rigidities of a prestressed concrete grid floor with beams of different sizes spanning the long and short span directions?

17.9 Discuss briefly the various parameters influencing the central deflection of a simply supported grid floor.

17.10 What are the sections in a grid floor where the torsional moments are maximum under service loads? How do you design these sections?

Exercises

17.1 The floor slab of an industrial structure spanning over 8 m is to be designed as a one-way prestressed concrete slab with parallel post-tensioned cables. The slab is required to support a live load of 10 kN/m^2 with the compressive and tensile stress in concrete at any stage not exceeding 14 and zero N/mm^2, respectively. Design a suitable thickness for the slab and estimate the maximum horizontal spacing of the Freyssinet cables (12 of 5 mm diameter initially stressed to 1200 N/mm^2) and their position at midspan section. The loss ratio is 0.8.

[Ans: Thickness of slab = 220 mm; Spacing of cables = 187 mm]

17.2 Design a post-tensioned prestressed concrete two-way slab, 6 m by 8 m in size, to support a live load of 3 kN/m^2. If cables of four wires of 5 mm diameter stressed to 1000 N/mm^2 are available for use, determine the number of cables in the two principal directions. The stresses in concrete not to exceed 15 N/mm^2 in compression and tensile stresses are not permitted under service loads. The loss ratio is 0.8. Check for the limit states of serviceability and collapse.

[Ans: Thickness of slab = 160 mm; Number of cables = 33 (short span) and 14 (long span)]

17.3 A simple flat slab, 10 m by 8 m in overall size, is supported by four columns which are so placed as to form a symmetrical rectangular grid of 8 m by 6 m with cantilevers of 1 m on all sides. The imposed load on the slab is 1.5 kN/m^2. Prestressing cables consisting of four wires of 4 mm diameter, and stressed to 1000 N/mm^2 are available for use. Design the number of cables required and indicate their arrangement in the two principal directions.

[Ans: Thickness of slab = 150 mm; Number of cables = 103 (1ong span) and 70 (short span)]

17.4 A prestressed concrete continuous flat slab of overall size 16 m by 13 m is supported by nine columns arranged in three rows. The columns are spaced 7.5 and 6 m in the direction of long and short edges, respectively, with a cantilever of 0.5 m all around. The 20 cm thick slab, continuous over two bays in transverse directions, supports a live load of 3 kN/m^2. Assuming the tensile stresses in the slab to be zero under full live load and the minimum cover to the centre of the cable to be 30 mm, determine the magnitude of the prestressing force in the direction of the long span. Using cables of 12 wires of 5 mm, stressed to 1000 N/mm^2 diameter, estimate the number of cables required for the long span direction and arrange them suitably in the column and middle strips.

[Ans: Prestressing force = 530 kN; No. of cables = 29]

17.5 A prestressed concrete waffle slab (grid floor) for a panel of 15 m by 12 m has the ribs arranged at 1.5 m centres in both directions. Design the grid floor assuming it as an orthotropic plate freely supported on four sides, and using the following data:

Live load on floor = 3 kN/m^2
Thickness of slab = 40 mm
Overall depth of floor = 400 mm
Width of ribs = 200 mm
Loss ratio = 0.85

permissible compressive stress in concrete at transfer and service load = 15 N/mm^2. Tensile stresses are not permitted at transfer and working loads.

Sketch the arrangement of cables for the central ribs in the transverse directions.

[Ans: Short span, *P* = 710 kN, *e* = 170 mm, 18 – 7 mm cables
Long span, *P* = 645 kN, *e* = 100 mm, 18 – 7 mm cables]

17.6 A composite floor slab using precast prestressed plank units, 63 mm deep, in conjunction with *in situ* cast concrete is required to support a superimposed load of 8.75 kN/m^2 over an effective span of 5 m. Design the required thickness of the composite slab using the prestressed plank and cast *in situ* concrete and the required prestressing force in the precast units. Assume M-20 grade for *in situ* and M-42 for precast pretensioned units. Permissible stresses should conform to the provisions of the Indian standard code.

[Ans: Thickness of Composite slab = 172 mm
Prestressing Force = 317 kN/m
Eccentricity = 10.5 mm]

17.7 Design a prestressed concrete slab 5 m by 20 m to support a live load of 9 kN/m^2. The slab is simply supported on four sides. 7 mm diameter high-tensile wires. Initially stressed to 1000 N/mm^2 are available for use. Permissible stress in concrete. At transfer and working loads are 15 N/mm^2 in compression and zero in tension. Adopt 20 per cent loss of prestress.

[Ans: Adopt 120 mm thick slab; 7 mm diameter high-tensile wires at 45 mm spacing in the direction of short span at an effective depth of 90 mm]

Objective-type Questions

17.1 Prestressed concrete slab systems are ideally suited for the construction of floor and roof system of industrial buildings to support
(a) light loads
(b) heavy loads over long spans
(c) heavy loads over short spans

17.2 Solid prestressed concrete slabs 600 mm thick have been used in bridge decks for spans up to
(a) 6 m (b) 18 m (c) 12 m

17.3 Solid prestressed concrete slabs with overall depth in the range of 100 to 175 mm have been used for floors to support superimposed varying from
(a) 2 to 4 kN/m^2 (b) 4 to 8 kN/m^2 (c) 4 to 12.5 kN/m^2

17.4 Precast pretensioned cored slab units have been widely used in Russia as floor panels in the span range of
(a) 2 to 4 m (b) 3 to 5 m (c) 3 to 6.4 m

17.5 Large size prestressed concrete roof panels with ribs in the perpendicular direction can be used for spans up to
(a) 4 m (b) 12 m (c) 8 m

17.6 Single and double tee prestressed concrete monolithic units have been used for spans varying from
(a) 4 to 10 m (b) 5 to 15 m (c) 6 to 25 m

17.7 In comparison with continuous reinforced concrete slabs to support heavier loads, prestressing results in
(a) thicker slabs
(b) thinner slabs
(c) no change in thickness

17.8 Prestressed concrete grid floors are more economical and viable in comparison with reinforced concrete grid floors for spans in the range of
(a) 4 to 6 m (b) 6 to 10 m (c) 12 to 15 m

17.9 Maximum bending moment in a grid floor under service load develops at the section located at the
 (a) centre along the short span
 (b) corners
 (c) centre along the long span

17.10 Maximum torsional moments in a grid floor under working loads develop at the
 (a) quarter span along the longer edge beams
 (b) centre of span
 (c) corners of the grid floor

Answers to Objective-type Questions

17.1 (a)	17.2 (c)	17.3 (c)	17.4 (c)	17.5 (b)
17.6 (c)	17.7 (b)	17.8 (c)	17.9 (a)	17.10 (c)

18 Prestressed Concrete Shell and Folded Plate Structures

18.1 Advantages of Prestressing Long-Span Shell Structures

Concrete shell roofs have been widely used to cover large floor spaces of industrial structures. They are generally preferred to other structural forms, as they use a minimum amount of materials yielding maximum structural advantage, the cross-section being optimally used to resist the forces. Reinforced concrete shells are ideally suited to cover floor spaces over medium to long range spans of up to 30 m. In the case of longer spans, the tension developed in the edge beams of cylindrical shells is very high and results in congestion of reinforcement and improper compaction of concrete in these zones. Longer spans exceeding 30 m necessitate the lapping or welding of reinforcement. In addition, the structure may be rendered unfit for its intended use at the serviceability limit states due to excessive deflections and objectionable cracking.

Most of these problems are eliminated by prestressing the edge beams of long-span shell structures. In addition, it gives the following advantages:

1. The parabolic profile of the cables in the edge beam counteracts the deflection due to the dead and live loads, so that the resulting deflection is well within the safe permissible limits.
2. Prestressing the shell considerably reduces the quantity of reinforcement in the structure, as demonstrated by Kirkland and Goldstein[1].
3. Investigations by Marshall[2] have shown that prestressing considerably reduces transverse moments.
4. The development of cracking due to high-tensile stresses at the soffits of edge beams can be completely eliminated by eccentric prestressing. In addition, precompression in concrete inhibits the formation of temperature and shrinkage cracks.
5. The compressive state of stress in the shell membrane results in watertight construction.
6. According to Haas[3], prestressing has a favourable influence in providing adequate safety against the limit state of collapse by inelastic buckling.

The earliest examples of prestressed shells include those constructed at Meerut, India, in 1941[4], over spans of 36 m, with a chord width of 10.5 m, the thickness of the shell being 63 mm. The prestressed shell roof of the aircraft hangar at Karachi was built in 1942 over spans[5] of 40 m. As these shells gave satisfactory performance and were also economical, prestressing in shells began to find extensive application in France, UK, Germany and other countries.

18.2 Methods of Prestressing Shell Structures

In general, concrete shells have thin cross-sections, which preclude the use of large diameter cables. The tendons consisting of 5 to 8 mm diameter wires accommodated in narrow sheaths are conveniently used in post-tensioning the lower parts of the shell membrane as shown in Fig. 18.1.

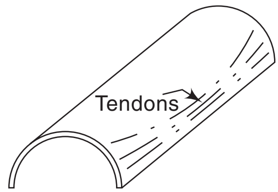

Fig. 18.1 *Arrangement of tendons in large barrel vaults*

To overcome the problem of correctly positioning the curved cables along space curves in the junction of the shell and edge beam, it is the general practise to impart prestress by post-tensioning the curved cables that are housed entirely in the deep edge beams. Figure 18.2 shows the method of arranging curved cables in the edge beams of circular cylindrical shells. The edge beams being invariably deep, it is convenient to arrange the cables one over the other so that maximum eccentricity is available at the centre of span.

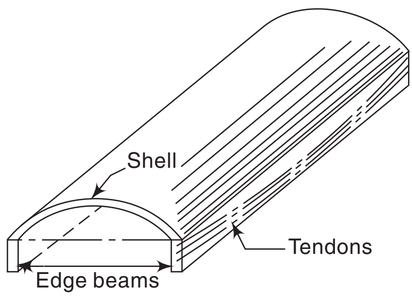

Fig. 18.2 *Arrangement of tendons in edge beams of long shells*

An excellent example of the application of pretensioning in shells is the pretensioned hyperboloid, which is a doubly ruled surface facilitating the use of straight tendons. The arrangement of high-tensile wires in a typical pretensioned hyperboloidal shell roof element is shown in Fig. 18.3.

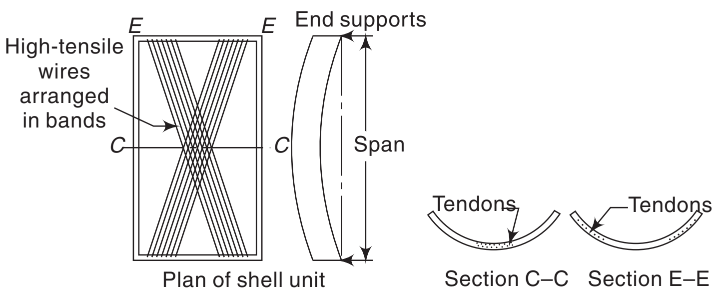

Fig. 18.3 *Arrangement of high-tensile wires in pretensioned hyperboloid*

18.3 Design of Prestressed Concrete Shell Structures

18.3.1 Circular Cylindrical Shell with Prestressed Edge Beams

The general bending theory of thin curved shells is governed by a differential equation of eighth order involving the main shell parameters and deformations. Solutions based on simplifying approximations have been developed by several investigators and a comparative analysis of various analytical approximations is reported by Mc Namee[6]. It is pertinent to note that an exact mathematical solution of the eighth order differential equation would, by itself be no more than an approximate solution due to the inelastic properties of concrete. However, in the case of prestressed shells in which tensile stresses are completely eliminated, the assumptions of elastic behaviour are more relevant than in reinforced concrete shells.

The Donnel-Karman-Jenkins theory[7], considered to be the simplest of the rigorous theories, is applicable for both long and short shells. The ASCE method[8] associated with the design tables is immensely useful in the analysis and design of cylindrical shells with any ratio of width to length. The Schorer–Tottenham[9] formulation is by far the simplest among the various theories, and sufficiently accurate for purposes of design in the range of medium to long shells.

The analysis of circular cylindrical shells with prestressed edge beams is more or less similar to that of reinforced concrete shells. However, the effect of prestressing is to be considered in formulating the boundary conditions at the junction of the shell and the edge beam. In addition to the normal boundary conditions such as zero horizontal displacement and rotation of the shell edge, which are also applicable for reinforced concrete shells, the following additional compatibility conditions have to be satisfied in the case of prestressed shells[10].

1. Compatibility of the vertical deflections of the shell edge and the edge beam at the junction, and
2. Compatibility of the longitudinal displacement of the shell edge and the edge beam at the junction.

The rigorous methods generally involve lengthy computations to estimate the redundant reactions between the shell and the edge beam. In the case of long shells, with span/radius ratio exceeding 3, the beam theory developed by Lundgren[11] can be conveniently used for the preliminary analysis of prestressed shells without the loss of much accuracy[12]. In this method, the shell is considered as a beam of curved cross-section and the flexural and shear stresses are computed using the well-known beam formulas.

If P = prestressing force required in the edge beams located at an eccentricity e, and $f_{\inf}$ = flexural tensile stress developed at the soffit of edge beams as computed from the beam analysis, the condition of zero stress under service loads at the soffit of edge beams results in the expression.

$$f_{\text{inf}} = \left[\frac{P}{A} + \frac{Pey_b}{I}\right]$$

where I = second moment of area of the shell and beam about the neutral axis

A = area of cross-section of shell and beam

y_b = distance of the soffit of edge beam from the neutral axis

The maximum possible eccentricity based on considerations of sufficient cover and housing of cables is generally provided at the centre of span, and the eccentricity is reduced towards the end supports by using parabolic profile to the cables. It is observed that the magnitude of prestressing force resulting from the concept of load balancing is close to the optimum. This is very much desirable in view of the high unit costs of prestressed concrete construction.

The nominal reinforcement provided in the shell should conform to the minimum requirements provided for in various national codes. Most codes specify that the spacing of reinforcement should not exceed five times the thickness of the slab and the minimum reinforcement in the tensile zone to be not less than 0.35 per cent.

The use of beam theory for the design of prestressed shells with edge beams is outlined in the following example.

Example 18.1 Design a circular cylindrical shell with prestressed edge beams to cover an area of 10 m by 50 m, and to support an imposed load of 1 kN/m^2. Estimate the number of cables consisting of 12 wires of 7 mm diameter required in the edge beams.

Solution. The dimensions of the shell with edge beams are first assumed and the analysis is made by using beam theory. The salient dimensions assumed as shown in Fig. 18.4(a) are as follows:

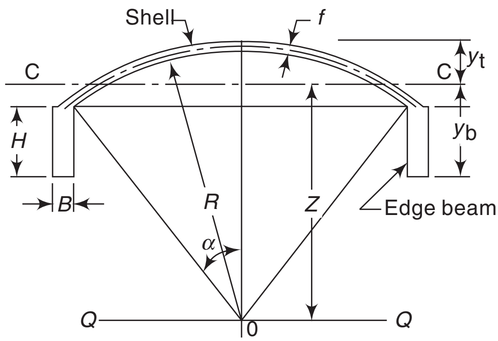

(a) Cross-section of shell with edge beam

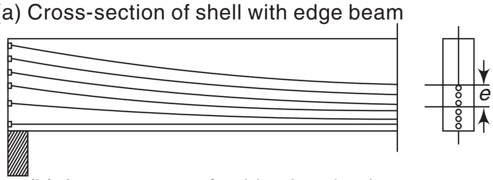

(b) Arrangement of cables in edge beam

Fig. 18.4 *Long shell with prestressed edge beams*

Semi-central angle, α	$= 40° = 0.6981$ radians
Span of shell, L	$= 50$ m
Chord width	$= 10$ m
Radius of shell, R	$= 8$ m
Thickness of shell, t	$= 0.075$ m
Width of edge beam, B	$= 0.18$ m
Depth of edge beam, H	$= 2.20$ m
Rise of shell	$= R(1 - \cos\alpha) = 1.872$ m

The position of the centroidal axis is determined by taking moments of the areas about the axis Q–Q passing through the centre of the arch. Thus,

$$Z = \left[\frac{tR^2 \sin\alpha + \left(R\cos\alpha - \dfrac{H}{2}\right)HB}{Rt\alpha + HB}\right]$$

$$= \left[\frac{(0.075 \times 8^2 \times 0.6428) + (8 \times 0.7660 - 1.1)2.2 \times 0.18}{(8 \times 0.075 \times 0.6981) + (2.2 \times 0.18)}\right] = 6.2 \text{ m}$$

$y_b = 2.272$ m, $\quad y_t = 1.8375$ m

Second moment of area of the shell about the Q–Q axis is given by,

$$I_{SQ} = tR^3\left(\alpha + \frac{1}{2}\sin 2\alpha\right) = 0.075 \times 8^3\left(0.6981 + \frac{1}{2} \times 0.9848\right) = 46 \text{ m}^4$$

Second moment of area of beams about the Q–Q axis is,

$$I_{BQ} = 2\left(\frac{BH^3}{12}\right) + 2BH\left(R\cos\alpha - \frac{H}{2}\right)^2$$

$$= \left(\frac{2 \times 0.18 \times 2.2^3}{12}\right) + \{2 \times 0.18 \times 2.2(8 \times 0.7660 - 1.1)^2\} = 20.321 \text{ m}^4$$

Cross-sectional area of the shell and edge beams is,

$$A = 2(Rt\alpha + HB) = [2(8 \times 0.075 \times 0.6981 + 2.2 \times 0.18)] = 1.628 \text{ m}^2$$

The second moment of area of the shell and edge beams about the centroidal axis C–C is given by,

$$I_C = (I_{SQ} + I_{BQ} - AZ^2) = (46 + 20.321 - 1.628 \times 6.2^2) = 3.74 \text{ m}^4$$

Calculation of loads on the shell

Self-weight $= (1 \times 1 \times 0.075 \times 24) = 1.8$

Live load $= \underline{1.0}$

2.8 kN/m^2 of surface area

Load on shell per metre of span $= (2.8 \times 8 \times 2 \times 0.6981) = 31.3$ kN/m
Self-weight of edge beams $= 2\ (2.2 \times 0.18 \times 24) = 19$ kN/m
Live load on the top of edge of beam $= (2 \times 0.18 \times 1) = 0.36$ kN/m
Total load, $w_d = (31.3 + 19.0 + 0.36) = 50.66$ kN/m

$$\text{Maximum moment, } M = \left[w_d \frac{L^2}{8}\right] = \left[\frac{(50.66 \times 50^2)}{8}\right] = 15831 \text{ kNm}$$

Bending stresses in shell and edge beam

(a) At the top of shell $= \left[\dfrac{(15831 \times 10^6)1837.5}{3.74 \times 10^{12}}\right] = 7.70\ \text{N/mm}^2$ (compression)

(b) At the bottom of shell or top of edge beam

$$= \left[\frac{(15831 \times 10^6)72}{3.74 \times 10^{12}}\right] = 0.30\ \text{N/mm}^2\ \text{(tension)}$$

(c) At the soffit of edge beam

$$= \left[\frac{(15831 \times 10^6)2272}{3.74 \times 10^{12}}\right] = 9.6\ \text{N/mm}^2\ \text{(tension)}$$

Estimation of prestressing force

Locating the centroid of the prestressing force at a distance of 400 mm from the soffit of the edge beams, the available eccentricity is given by,

$$e = (2272 - 400) = 1872\ \text{mm}$$

If the fibre stress at the soffit of the beam is zero under service loads, then

$$\left[\frac{P}{A} + \frac{Pey_b}{I}\right] = 9.6$$

$$P\left[\frac{1}{1.628 \times 10^6} + \frac{1872 \times 2272}{3.74 \times 10^{12}}\right] = 9.6$$

Solving $P = (5500 \times 10^3)\ \text{N} = 5500\ \text{kN}$

Prestressing force required at the centre of span for each beam

$$= \left(\frac{5500}{2}\right) = 2750\ \text{kN}$$

Using Freyssinet cables, 12–7 mm stressed to 1000 N/mm^2,

Force in each cable = 460 kN

Number of cables $= \left(\dfrac{2750}{460}\right) = 6$

The eccentricity of the prestressing force is gradually decreased towards the end supports by using parabolic cable profiles as shown in Fig. 18.4(b).

Check for stresses at crown

Stress at crown due to prestressing force

$$= \left(\frac{5500 \times 10^3}{1.628 \times 10^6}\right) - \left(\frac{5500 \times 10^3 \times 1872 \times 1837.5}{3.74 \times 10^{12}}\right) = -1.7\ \text{N/mm}^2\ \text{(tension)}$$

Stress at crown due to dead and live loads = 7.7 N/mm^2 (compression)

Resultant stress at crown = (7.7 – 1.7) = 6.0 N/mm^2 (compression).

18.3.2 Pretensioned Hyperboloid Shells

Hyperbolic paraboloid shells, grouped under the category of doubly curved anticlastic shells, were first successfully used as roofing units by Silberkuhl[13] in Germany. Parts of one-sheet hyperboloid units, with a geometric form closely following a circular curve in the length (span) direction and hyperbolic curve in the direction of width, are well suited for mass production since they are ruled surfaces. The units are suitable for pretensioning as the high-tensile wires can be easily arranged to follow the straight line generators of the shell units[14]. The pretensioning wires intersect in the middle region of the roof units and hence are very favourably located with a large eccentricity to resist the longitudinal bending moments in the shell, which functions more or less as a beam.

Precast pretensioned hyperbolic paraboloid shell units, 25 m long and with a shell thickness of 60 mm, have been used for a storage building at Essen, Germany. Le Corbusier adopted this elegant form of construction for the roof of the legislative assembly hall at Chandigarh, India. The individual shell units can easily be connected at the ridge by a cast *in situ* mortar joint as shown in Fig. 18.5(a), and the units being doubly curved, rain-water is easily drained along the direction of the length.

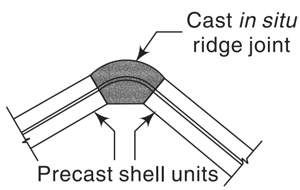

(a) Ridge joint in pretensioned hyperboloid roofs

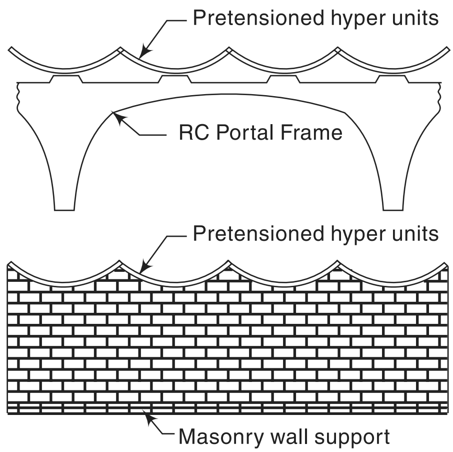

(b) Method of supporting hyperboloidal shells

Fig. 18.5 *Precast pretensioned hyper shell roofs*

The support for the shells are normally made up of portal frames, or reinforced concrete beams or masonry walls, with seating saddles formed to receive the shells as shown in Fig. 18.5(b).

The span to chord width ratio of the hyperboloidal shell unit being large, with values in the range of 5–10, the structural behaviour of the shell under a system of transverse loads is more akin to that of a beam with a curved cross-section. Computing the geometrical properties of the shell is simplified if the hyperbolic curve is replaced by a parabola having the same chord width and overall depth, as reported by Ramaswamy and Sayeed[15]. However, recent comparative studies by Naik *et al.*,[16] have shown that the geometrical properties of shell units with hyperbolic, parabolic or circular cross-sections are not significantly different as shown in Fig. 18.6 and Table 18.1. Hence, the design prestressing force will not be significantly different if the cross-section is approximated to any of the three curves, provided the chord width, thickness and central depth are the same for the different cross-sectional shapes.

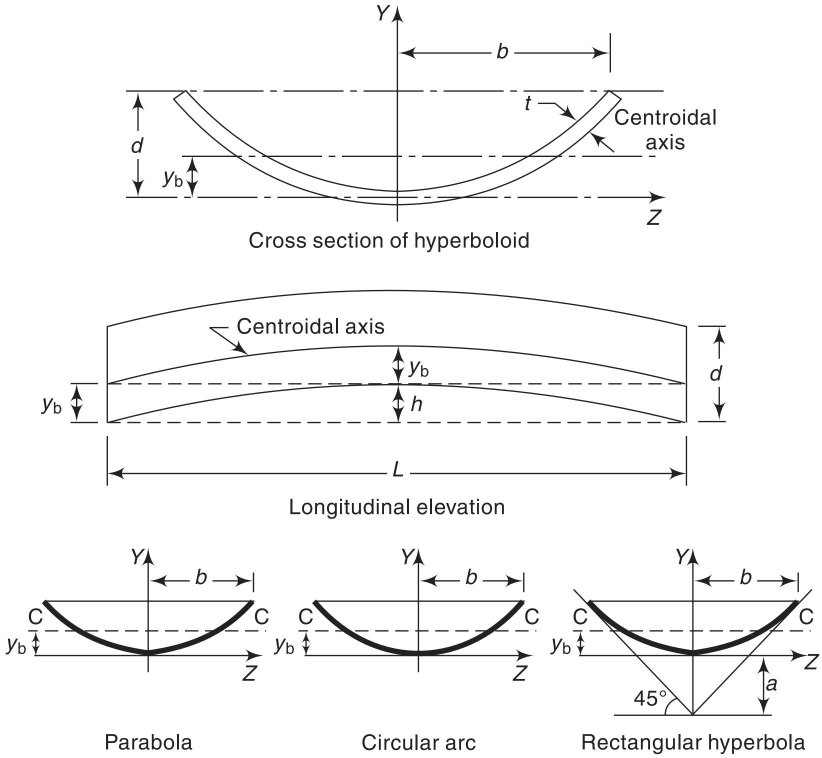

Fig. 18.6 *Types of cross-section of pretensioned shell unit*

Table 18.1 *Geometrical properties of shell units*

Type of Section	*Parabola*	*Circular Arc*	*Rectangular Hyperbola* $(y^2 - z^2) = a^2$, $a = 3/4\ b$
Length of unit for $z = b$	2.2942 b	2.3172 b	2.277 b
Distance of centroidal axis from bottom of section, y_b	0.1831 b	0.1712 b	0.1958 b
Second moment of area, I_c	0.0536 b^3t	0.0512 b^3t	0.0555 b^3t

Thickness of shell = t; width of shell unit = 2 b

The design of the chord width and the span is mainly influenced by the crane capacity available at site. Table 18.2 shows the salient features of the hyperboloidal shells designed by considering the cross-section to follow a parabolic profile for spans varying from 15 m to 30 m. The typical details of the design of a 15 m span hyperboloidal shell are presented in the following example.

Table 18.2 *Salient features of pretensioned shell roof elements for different spans*

Description	*Span,* m			
	15	*20*	*25*	*30*
Length of unit L, m	16	21	26	31
Semi-width of element b, m	1.05	1.20	1.60	2.10
Thickness of unit, t, mm	60	80	100	100
Weight of single unit, kN	55.5	111	229	358
Cross-sectional area, cm^2	1445	2200	3670	4818
Centroidal distance, y_b mm	192.3	219.7	293.0	384.6
Second moment of area, cm^4	372570	741519	2197097	4967600
Eccentricity at mid span, mm	162.3	179.7	253.0	344.6
Initial prestressing force, kN	602	1321	2390	3375
Area of high tensile steel, mm^2	392	862	1811	2616

Example 18.2 Design a pretensioned hyperboloid shell roof element for a warehouse using the following data:

Clear span = 15 m
Length of warehouse = 30 m
Loading as per IS: 875–1964
Materials: Concrete M-50 grade and high-tensile steel wire conforming to IS: 1785
Permissible stresses:
Cube strength, $f_{cu} = 50$ N/mm^2
Cube strength at transfer, $f_{ct} = 35$ N/mm^2
At transfer $f_{ct} = 16$ N/mm^2 (compression)
At working loads

$f_{cw} = 18$ N/mm^2 (compression)
$f_{tt} = f_{tw} = 0$

Initial stress in 5 mm diameter high-tensile wires = 1200 N/mm^2
Loss ratio = 0.8
Modulus of rupture of concrete = 5.0 N/mm^2
Tensile strength of concrete = 1.7 N/mm^2
Available crane capacity at site = 60 kN

Solution.

Design

Clear span of the shell unit = 15 m
Overall length of the unit = 16 m
Semi-width of the element, $b = 1.05$ m
Thickness of the shell, $t = 0.06$ m
Assuming the cross-section of shell to correspond to a parabolic curve, weight of shell unit = $(2.2942 \times 16 \times 1.05 \times 0.06 \times 24) = 55.5$ kN
The self-weight of each unit is less than the available crane capacity of 60 kN.
Width of the shell unit = 2.10 m
Area of concrete, $A_c = (2.2942 \times 1050 \times 60) = 144500$ mm^2

Centroidal distance from the soffit, $y_b = (0.1831 \times 1050) = 192.3$ mm
Distance of the top fibre from the centroidal axis, $y_t = 332.7$ mm
Second moment of area of section about the neutral axis (see Table 18.1)

$$I_c = (0.0536 \times b^3 \times t) = [0.0536 \times (1050)^3 \times 60] = (37257 \times 10^5)\ \text{mm}^4$$

Section modulus,

$$Z_b = (0.2928 \times b^2 \times t) = [0.2928 \times (1050)^2 \times 60] = (19372 \times 10^3)\ \text{mm}^3$$

$$Z_t = (0.1693 \times b^2 \times t) = [0.1693 \times (1050)^2 \times 60] = 11199 \times 10^3)\ \text{mm}^3$$

Loads and moments

Self-weight of the unit = $(0.1445 \times 24) = 3.5$ kN/m
Live load on the roof = 0.75 kN/m^2
Total live load = $(0.75 \times 2.10) = 1.6$ kN/m
∴ Total design load = 5.1 kN/m
Maximum bending moment at mid-span

$$M_d = [(5.1 \times 8.0 \times 7.5) - (0.5 \times 5.1 \times 8^2)] = 142.8\ \text{kN m}$$

Dead-load moment, $M_g = [(3.5 \times 8.0 \times 7.5) - (0.5 \times 3.5 \times 8^2)] = 98$ kN m
Eccentricity, e, at mid-span is given by,

$$e = y_b - (\text{cover + diameter of the high-tensile wire}).$$

$$= 192.3 - (25 + 5) = 162.3\ \text{mm}$$

Effective prestressing force is expressed as,

$$P_e = \left[\frac{M_d}{(Z_b/A_c) + e}\right] = \left[\frac{142.8 \times 10^6}{\left(\dfrac{19372 \times 10^3}{144500}\right) + 162.3}\right] = 481840\ \text{N}$$

∴ Initial prestressing force,

$$P_t = (1.25 \times 481840 = 602300)\ \text{N}$$

The number of 5 mm diameter high-tensile wires (stressed to 1200 N/mm^2) required

$$= \left[\frac{602300}{20 \times 1200}\right] = 26\ \text{wires}$$

The wires are arranged in two layers at the centre span spread over two bands towards the supports as shown in Fig. 18.7.

The radius of curvature of the shell in the longitudinal direction is,

$$R = \left(\frac{L^2}{8e}\right) = \left(\frac{16^2}{8 \times 0.1623}\right) = 197\ \text{m}$$

The wires are arranged to be concentric over the end supports.

The compressive stresses developed at the top and bottom fibres of the shell at mid-span and end sections are obtained as,

Stage of Loading	*Section*	*Compressive Stress,* N/mm^2	
		Top Fibre	*Bottom Fibre*
At transfer	Mid-span	4.19	4.16
	End section	4.17	4.24
Under service loads	Mid-span	9.10	0.0
	End section	3.23	3.39

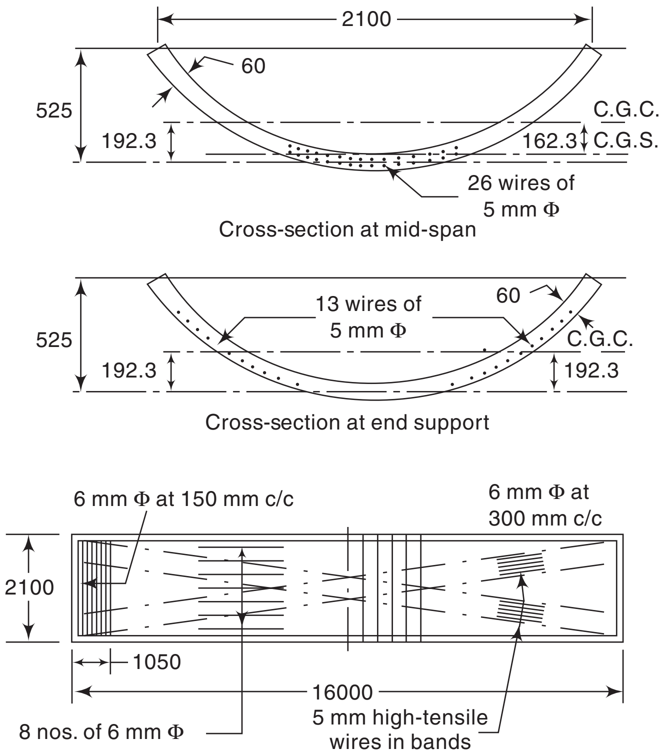

Fig. 18.7 *Reinforcement details in pretensioned hyperboloid unit*

Check for limit state of collapse in flexure

$$A_p = 520 \text{ mm}^2, \qquad d = 495 \text{ mm}, \qquad b = 120 \text{ mm}$$

Thus, $$\left(\frac{A_p f_p}{bd\, f_{ck}}\right) = \left(\frac{520 \times 1600}{120 \times 495 \times 50}\right) = 0.28$$

From Table 7.1 for pretensioned members,

$$\frac{f'_{pu}}{0.87 f_p} = 1.0$$

and $$\frac{x_u}{d} = 0.60$$

$\therefore$ $$f_{pu} = (0.87 \times 1600) = 1392 \text{ N/mm}^2$$

or $$x_u = (0.60 \times 495) = 297 \text{ mm}$$

$\therefore$ $$M_u = f_{pu} A_p (d - 0.42 x_u)$$

$$= [1392 \times 520(495 - 0.42 \times 297)/10^6] = 268 \text{ kN m}$$

$$\therefore \text{ Load factor against collapse} = \left(\frac{268}{142.8}\right) = 1.876$$

Check for ultimate shear strength at support

$$f_{ck} = 50 \text{ N/mm}^2, \quad f_t = 0.24\sqrt{f_{ck}} = 0.24\sqrt{50} = 169 \text{ N/mm}^2$$

$$f_{cp} = \left(\frac{P}{A}\right) = \left(\frac{602300}{144500}\right) = 4.17 \text{ N/mm}^2$$

Shear strength of the support section is

$$V_{cw} = \left[0.67 b_w h \sqrt{f_t^2 + 0.8 f_{cp} f_t}\right]$$

$$= \left\{\frac{[0.67 \times 120 \times 525\sqrt{1.69^2 + 0.8 \times 4.17 \times 1.69}]}{10^3}\right\}$$

$$= 123 \text{ kN}$$

Ultimate shear $\quad V_u = (1.5 \times 5.1 \times 0.5 \times 16) = 61.2 \text{ kN}$

$$\therefore \text{ Load factor against collapse} = \left(\frac{123}{61.2}\right) = 2.0$$

Nominal reinforcements of 6 mm-diameter bars are provided at 300 mm centres in both the longitudinal and transverse directions. The details of reinforcements are shown in Fig. 18.7.

18.4 Design of Prestressed Concrete Folded Plate Structures

Folded or hipped plates are widely used for roofs of industrial structures, coal bunkers and cooling towers. The simplicity of the form used for casting folded plates makes them competitive shell construction for covering large floor spaces. The plates have a triangular or trapezoidal zig-zag cross-sectional shape and prestressing is generally done by curved cables or straight tendons lying within the plate in the longitudinal direction to counteract the beam action. A notable example of the use of folded plates with curved cables are in the covering of the roof of the town hall of Marl in Westphalia, Germany[17], over spans of 60 m. In this case, the folded plates, 20 cm thick and 3 m deep were cast *in situ* with the cables located in the plates and at their junction. Abeles[18] has reported the use of curved and straight cables in a cast *in situ* hipped plate, 12.5 m wide and 35 m long, for the roof of a church in California.

The simple structural configuration of the folded plate is well suited for pretensioning and prefabrication. The pretensioning technique is adapted with advantage in some of the systems of prefabricated folded-roof constructions developed over the last two decades. In the leap system[18], a continuous hinge is formed along the adjoining edge, with the folds precast and pretensioned together in the prestressing bed and connected by transverse reinforcement. In the Costain system[19] developed in Britain, each plate is prestressed on the casting bed and the plates are connected by a valley junction. V- or W-shaped units are connected by an *in situ* cast ridge joint. The different types of folded plate roofs using V, W and butterfly V units are shown in Fig. 18.8. The cross-sectional details of a typical V unit for a 20 m span and a butterfly V unit for 25 m span are shown in Fig. 18.9.

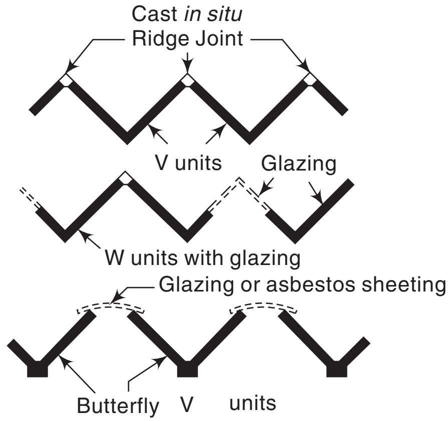

Fig. 18.8 *Types of folded plate roofs (Costain system)*

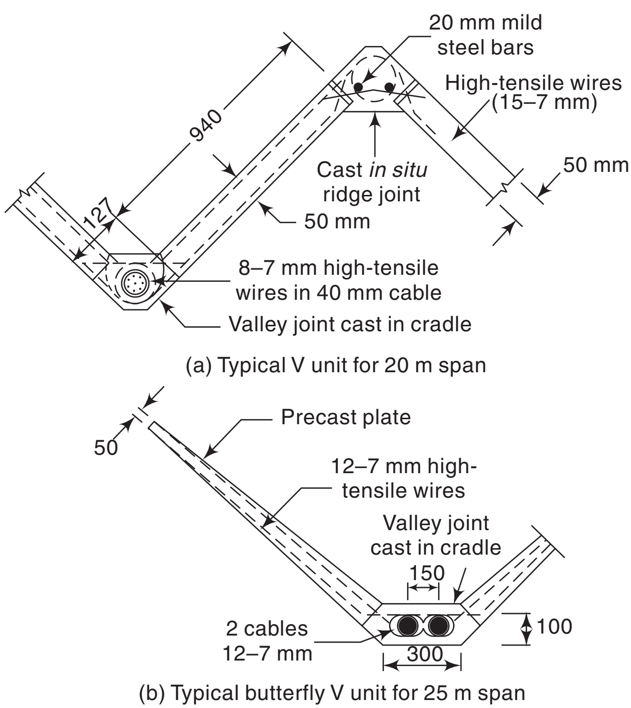

Fig. 18.9 *Cross-section of prestressed folded plate roofs*

Folded plates resist the system of transverse loads by plate and slab action. The loads acting normal to each plate cause transverse bending between the junctions of the plates which can be considered as imaginary supports of a continuous slab. This transverse bending is termed as *slab action*. The transverse moments developed in the plates can be determined by a continuous beam analysis, assuming the supports are at the junctions of the plates. The plates being supported at their ends on traverses bend under the action of loads in their own plane as shown in Fig. 18.10. The longitudinal bending of the plates in their own plane is termed as *plate action*. Several methods have been developed over the years for the analysis of folded plates. The prominent among them being the procedures developed by Gaafar[20], Simpson[21] and Whitney which are suitable for folded plates of all proportions. The iteration method[22, 23] is a simplified version and is suitable for the analysis of certain types, such as V-shaped folded plates, where early convergence is possible. All these methods consider the effect of relative joint displacements. The suitability of the various methods are presented in a report prepared by the ASCE task committee on folded plate construction[24].

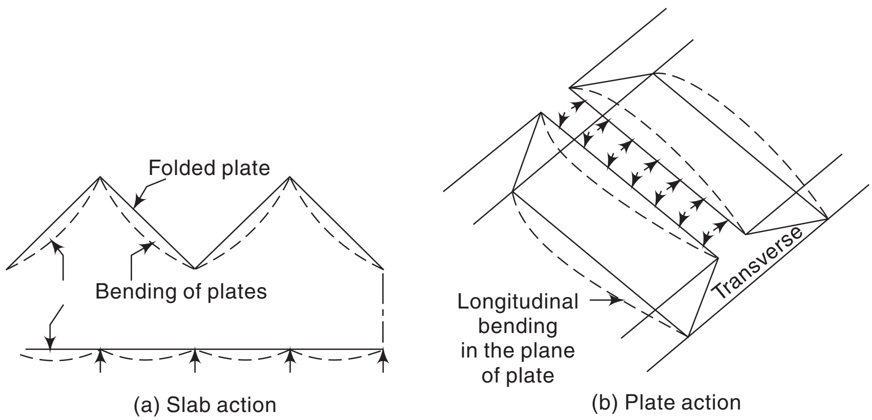

Fig. 18.10 *Deformational characteristics of folded plates*

In the case of folded plates, prestressing is resorted to only when the spans are longer, with the span/depth ratios exceeding four. In the case of long folded plates, the beam action is predominant and hence the analysis of stresses in the plate is generally done without the loss of much accuracy by using the beam approximation. The prestressing force and the eccentricity required are computed by using the condition that, under service loads, the tensile stresses developed in the plate are counter-balanced by the compressive stresses due to prestressing so that the resultant stresses are zero at the soffit of the centre-of-span section.

The folded plate is also analysed for transverse moments by considering the plate as a continuous slab with imaginary supports at the junctions. The transverse reinforcements are designed to resist these moments. According to IS: 2210[25] nominal reinforcements consisting of 10 mm bars are to be provided in the compression zones at 200 mm centres. The maximum spacing of reinforcements in any direction is limited to five times the thickness of the member and the minimum reinforcement in the section should conform to the provisions in various national codes. The design of a precast pretensioned folded plate for a span of 30 m is outlined in the following example.

Example 18.3 Design a pretensioned folded plate roof for the loading bay of a biscuit factory measuring 30 m by 90 m. The live load on the roof may be taken as 1 kN/m^2. 8 mm-diameter high-tensile wires are available for use. The ultimate tensile strength of the wires is 1500 N/mm^2. M-45 grade concrete may be used for the casting of folded plates. The tensile strength of concrete is 1.6 N/mm^2. V-shaped folded plates, 100 mm thick with a depth of 1/15 span, are proposed over a span of 30 m. The typical cross-section of the folded plate unit is shown in Fig. 18.11(a).

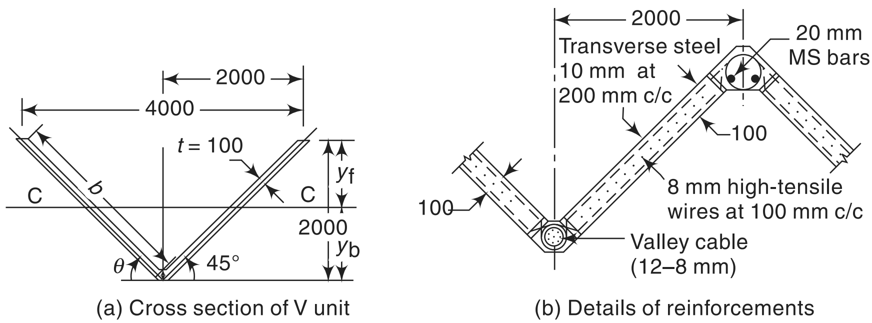

Fig. 18.11 *Cross-section of folded plate unit for 30 m span*

Solution.

Span = 30 m

Thickness of the plate, t = 100 mm

Depth of the V-plate unit = (1/15) × 30 = 2 m

Angle of inclination of the plate unit = θ = 45 degrees

Width of the plate, $b = 2\sqrt{2}$ m

Sectional properties of the V-unit

Cross-sectional area, $A = (2 \times 2\sqrt{2} \times 0.1) = 0.568\ \text{m}^2$

$$\text{Second moment of area}, I_c = \left[\frac{4t \sin^2\theta \left(\frac{b}{2}\right)^3}{3}\right] = \left[\frac{4 \times 0.1 \times 0.5(\sqrt{2})^3}{3}\right] = 0.190\ \text{m}^4$$

The distance of extremes fibres from the centroidal axis is

$$y_t = y_b = 1\ \text{m}$$

$\therefore$ Section modulus, $Z_b = Z_t = (I_c/y_b) = 0.190\ \text{m}^3$

Loads

Self-weight $(24 \times 0.1 \times 2 \times 2\sqrt{2}) = 13.80$ kN/m

Live load = $(1 \times 2 \times 2\sqrt{2}) = 5.65$

Finishes, etc. = 0.55

Total load, w_d = 20.00 kN/m

$$\text{Maximum moment, } M = \frac{(20 \times 30^2)}{8} = 2250 \text{ kN m}$$

$$\text{Longitudinal bending stress at soffit, } \left(\frac{M}{Z_b}\right) = \left(\frac{2250 \times 10^6}{0.190 \times 10^9}\right) = 12.8 \text{ N/mm}^2$$

If the centre of gravity of the high-tensile wires is kept at the bottom kern point, then eccentricity,

$$e = \left(\frac{I}{Ay_t}\right) = \left(\frac{0.190 \times 10^{12}}{0.568 \times 10^6 \times 10^3}\right) = 333.3 \text{ mm}$$

If P = effective prestressing force required to impart a compressive stress, f_{inf} at the soffit, it can be expressed as,

$$P = \left[\frac{f_{inf} A Z_b}{Z_b + Ae}\right] = \left[\frac{12.8 \times 0.568 \times 10^6 \times 0.190 \times 10^9}{(0.190 \times 10^9) + (0.568 \times 10^6 \times 333.3)}\right]$$

$$= (0.360 \times 10^7) \text{ N} = 3600 \text{ kN}$$

Using 8 mm diameter high-tensile wires stressed to 1200 N/mm^2,

$$\text{Number of wires} = \left(\frac{3600}{60}\right) = 60$$

Providing one cable of 12–8 mm at the valley junction, the remaining 48 wires are distributed between the two plates.

∴ Number of wires in each plate = 24

If e = eccentricity of the group of wires in the plane of the plate, then

$$[(48 \times e) + (12 \times 1420)] = 60 \times 473$$

$$\therefore \quad e = 174 \text{ mm}$$

$$\text{Spacing of wires in each plate} = \left[\frac{2(1420 - 174)}{24}\right] = 103 \text{ mm}$$

Provide 24 wires at a spacing of 100 mm in the plane of the plate.

Transverse reinforcements

The folded plate is analysed for slab action by considering it as a continuous slab over imaginary supports at the junctions of the plates. Transverse load on the continuous slab = 5 kN/m

Maximum moment occurs in the end plate which cantilevers over a 2 m span. Thus,

$$M_{max} = \left(\frac{w_d L^2}{2}\right) = \left[\frac{(5 \times 2^2)}{2}\right] = 10 \text{ kN m/m}$$

10 mm diameter mid-steel bars are provided at a spacing of 100 mm centres for the end plates. The transverse moments being less in the interior plates, the spacing may be increased to 200 mm.

Check for limit state of collapse in flexure

$$\left(\frac{A_p f_p}{b d f_{ck}}\right) = \left(\frac{3000 \times 1600}{284 \times 1333 \times 45}\right) = 0.28$$

From Table 7.1, $(f_{pu}/0.87f_p) = 1.0$

$$\therefore \quad f_{pu} = (0.87 \times 1600) = 1392 \text{ N/mm}^2$$

and $$\left(\frac{x_u}{d}\right) = 0.6$$

or $$x_u = (0.6 \times 1333) = 800 \text{ mm}$$

$$\therefore \quad M_u = f_{pu} Ap(d - 0.42x_u)$$

$$= \frac{[1392 \times 3000(1333 - 0.42 \times 800)]}{10^6} = 4163 \text{ kN m}$$

$\therefore$ Load factor against collapse = (4163/2250) = 1.85

Check for limit state of collapse in shear

$$f_{ck} = 45 \text{ N/mm}^2, \quad f_t = 0.24\sqrt{f_{ck}} = 0.24\sqrt{45} = 1.6 \text{ N/mm}^2$$

$$f_{cp} = \left[\frac{(3600 \times 10^3)}{(0.568 \times 10^6)}\right] = 6.33 \text{ N/mm}^2$$

Shear strength of support section is

$$V_{cw} = \left[0.67 b_w h \sqrt{f_t^2 + 0.8 f_{cp} f_t}\right]$$

$$= \left\{\frac{[0.67 \times 284 \times 2000\sqrt{1.6^2 + 0.8 \times 6.33 \times 1.6}]}{10^6}\right\}$$

$$= 1240 \text{ kN}$$

Ultimate shear, $V_u = (1.5 \times 20 \times 0.5 \times 30) = 450$ kN

$\therefore$ Load factor against collapse = (1240/450) = 2.75

Nominal shear reinforcements of 0.1 per cent of the cross-sectional area of the plate in plan is provided, which also serve to resist the transverse moments. The arrangement of longitudinal and transverse reinforcements are shown in Fig. 18.11(b).

18.5 Design of Domes with Prestressed Ring Beams

18.5.1 General Features

Concrete domes are generally preferred for covering circular tanks and for roofs of large-span circular structures, such as sports arenas and churches, where an uninterrupted floor space is desirable. A prestressed concrete hemispherical dome of 40 m diameter has been used for the roof of the atomic reactor at Kota, Rajasthan, India[26]. The spherical domes are supported by a ring beam at the base, which can be conveniently prestressed by winding tensioned wires or by cables to counteract the hoop tension developed in the ring beam. The main disadvantage of the reinforcement becoming congested in large diameter reinforced concrete ring beams is overcome by prestressing the ring beams. In addition, there are significant savings in cost, when compared with other equivalent roofs of conventional design.

The thickness of the reinforced concrete spherical dome is generally not less than 1/500 of the diameter, with values of 5–10 cm for domes in the range of 25–50 m respectively. The reinforcement in the dome is made up of a wire mesh and the concrete is placed in concentric rings over a preformed framework or the dome can be formed by gunniting using microconcrete.

The peripheral ring beam is prestressed by circumferential wire winding, similar to that of tank walls, or by cables housed in the ring beams with anchorage points at 90° spacing, opposed and phased at 45°.[27] In the case of cables, due provision should be made for the loss of prestress due to friction, which may be about 10 to 15 per cent due to the large curvature of the cables. When the dome and the tank wall are one integral unit, the tank walls are thickened towards the top, to provide sufficient cross-section for the ring beam, and prestressed by a multilayer wire winding as shown in Fig. 18.12(a). The continuity between the dome and the tank walls introduces in the latter bending moments which can be obviated by introducing an annular hinge in conjunction with a rubber joint at the base of the ring beam as shown in Fig. 18.12(b).

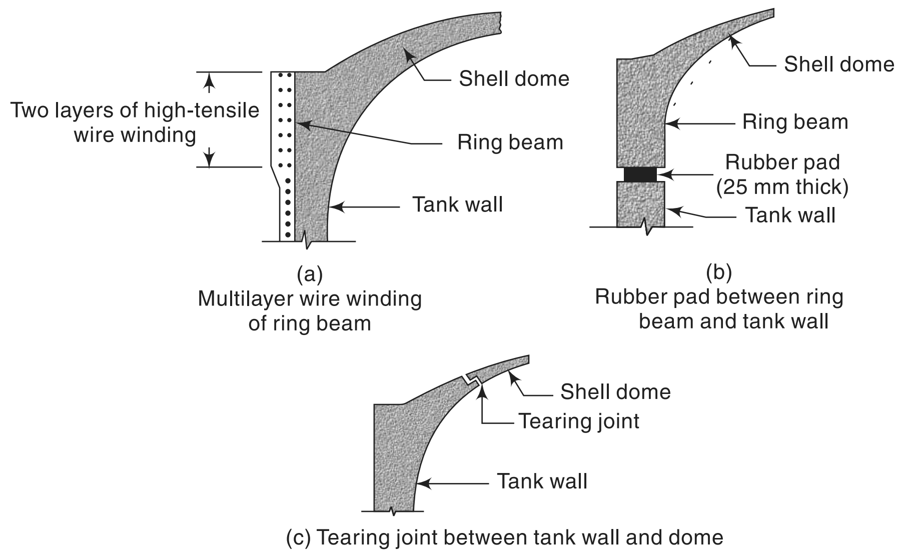

Fig. 18.12 *Ring beam, shell dome and tank wall connections*

In the case of fuel tanks, it is necessary to provide a tearing joint, as shown in Fig. 18.12(c), to minimise damage to the tank walls under explosion. According to Leonhardt, the joint should be designed to open out at an internal pressure of 5 kN/m^2.

The economic dimensional proportions of the dome and the ring beam for tank diameters varying from 12.5 m to 57.9 m, recommended by the Preload Engineers, New York, is compiled in Table 16.1. The size of the ring beam gradually increases from 150 mm × 200 mm to 490 mm × 890 mm for the range of diameters mentioned above.

18.5.2 Design Aspects of Prestressed Domes

The stresses developed in a thin shell dome are analysed by the membrane theory of shells. The dome is characterised by three geometrical parameters, as shown in Fig. 18.13 which are designated as,

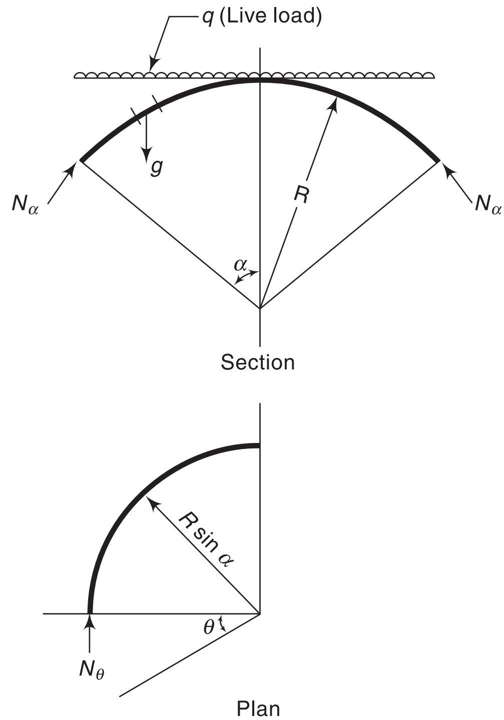

Fig. 18.13 *Membrane forces in a spherical shell*

R = radius of the dome

α = angle between the normal and the vertical axis

θ = horizontal angle

The membrane forces at any point on the dome comprises the meridional, N_α, and circumferential, N_θ, forces which are constant for all values of θ, with any particular value of α. The force components can be estimated by the following expressions:

$$N_\alpha = \left[\frac{gR}{(1+\cos\alpha)}\right]$$

$$N_\alpha = \left(\frac{qR}{2}\right)$$

where g is the dead weight of the shell per unit area of the surface and q is the imposed load per unit area in the plan.

$$N_\theta = gR\left(\cos\alpha - \frac{1}{1+\cos\alpha}\right)$$

$$N_\theta = \left[\frac{qR}{2}\cos 2\alpha\right]$$

Spherical shells are generally designed with a rise of one-eighth of the base diameter, which corresponds to a value of $\alpha = 28°\ 4'$. These shells being shallow, the dead and live loads may be assumed to be evenly distributed over the surface area. The circumferential forces are compressive for values of α less than 45°, while the meridional forces are compressive for all values of α.

Shallow domes transfer large magnitudes of thrusts to the wall supports. Therefore, ring beams are provided at the base of the domes.

The hoop tension in the ring beam is given by,

$$N = \left(\frac{W}{2\pi}\right)\cot\alpha \tag{18.1}$$

where W is the total load on the dome and is expressed as,

$$W = 2R^2\, w_d\,(1 - \cos\alpha)$$

where w_d = total load (DL + LL) per unit area of surface

α = semicentral angle.

If

P_e = effective prestressing force required to counteract the hoop tension N

η = loss ratio

f_{ct} = permissible compressive stress in concrete at transfer

A_c = area of concrete in the ring beam

then

$$A_c = \left(\frac{N}{\eta f_{ct}}\right) \tag{18.2}$$

An approximate estimate of the required prestressing force and the sectional area of the ring beam may be made by using Eqs 18.1 and 18.2. Edge disturbances will develop due to the continuity between the dome and the ring beam. The redundant moments and forces developed at the junction of the dome and the ring beam are solved by formulating the compatibility conditions at the edges[28]. Approximate formulae, based on the analysis by Timoshenko[29], are useful in computing the effect of moments and thrusts acting at the circumference of the shell, on the forces and moments developed in the shell dome. The resultant stresses in the dome are obtained as the algebraic sum of the membrane stresses and the effect of redundant moments and forces. An analysis of a prestressed dome of 30 m diameter and a rise of 3.75 m[(28)] indicates that the membrane stresses are considerably modified at the junction of the shell and the ring beam and at angles greater than 10°. The membrane stresses are not significantly influenced by the edge disturbances.

Example 18.4 A spherical dome is to be designed to cover a circular tank of 36 m diameter. The rise of dome is one-eighth of the diameter. The thickness of the dome is 1/500 of the diameter and the live load on dome is 1.5 kN/m^2. Design the dome and a suitable prestressed ring girder for the dome given the permissible compressive stress in the concrete as 14 N/mm^2. The loss ratio is 0.8. Use 7 mm diameter high-tensile wires initially stressed to 100 N/mm^2 to provide the necessary prestress.

Solution. Given data:

Diameter of the dome = 36 m

Rise of dome = [(1/8)36] = 4.5 m

Thickness of dome = $[(1/500)](36 \times 10^3) = 72$ mm

Adopt thickness = t = 75 mm

If R = Radius of the shell dome.

$[R - 4.5]^2 + 18^2 = R^2$ Solving, $R = 38.25$ m

$$\begin{aligned}
\text{Semicentral angle} &= \alpha = 28°4' \\
\cos\alpha &= 0.8823 \text{ and } \cot\alpha = 1.88 \\
\text{Self-weight} &= (0.075 \times 24) = 1.8 \text{ kN/m}^2 \\
\text{Live load on dome} &= 1.5 \text{ kN/m}^2 \\
\text{Total load on dome } w_d &= 3.3 \text{ kN/m}^2
\end{aligned}$$

Meridional thrust is computed by the relation,

$$N_d = \left[\frac{w_d R}{1+\cos\alpha}\right] = \left[\frac{3.3 \times 38.25}{1+0.8823}\right] = 67 \text{ kN/m}$$

$$\text{Maximum meridional compressive stress} = \left[\frac{67 \times 1000}{1000 \times 75}\right] = 0.893 \text{ N/mm}^2$$

Nominal reinforcement of 0.25 per cent of the concrete section is provided in the meridional and circumferential directions

$$\begin{aligned}
\text{Total load on the dome} = W &= 2\pi R^2 w_d(1 - \cos\alpha) \\
&= [2\pi \times 38.25^2 \times 3.3(1 - 0.8823)] = 3570 \text{ kN}
\end{aligned}$$

$$\text{Hoop tension in ring beam} = N = \left(\frac{W}{2\pi}\right)\cot\alpha = \left(\frac{3570}{2\pi}\right) \times 1.88 = 1068 \text{ kN}$$

Initial prestressing force = P = [(1068/0.8)] = 1424 kN

$$\text{Cross-sectional area of ring beam is given by } A_c = \left[\frac{1068 \times 10^3}{0.8 \times 14}\right] = 95357 \text{ mm}^2$$

Providing a ring beam 250 mm wide by 400 mm deep (A_c = 100000 mm^2)

$$\text{Number of 7 mm diameter high-tensile wires} = \left[\frac{1424 \times 10^3}{38.4 \times 1000}\right] = 37 \text{ wires}$$

References

1. Kirkland, CW and A Goldstein. "The design and construction of large span prestressed concrete shell roof," *The Structural Engineer*, London, Vol. 29, April 1951, pp 107–127.
2. Marshall, WT, "The elimination of moments in shell roofs by prestressing," *Proceedings of the Institution of Civil Engineers*, Vol. 3, Part III, April 1954, pp 276–282.
3. Haas, AM, "Prestressed shells and precast units," A-19, *Proceedings of the World Conference on Prestressed Concrete*, San Francisco, July, 1957.
4. "Important shell Structures in India," Central Building Research Institute Symposium on Shell Structures, *Indian Concrete Journal*, Vol. 33, Dec. 1959, pp 469–471.
5. Sexton, CG, "Prestressed reinforced concrete hangar at the civil airport of Karachi," *Journal of the Institution of Civil Engineers*, Vol. 29, Dec. 1947, pp 109–130.
6. Mcnamee, "Existing methods for the analysis of concrete shell roofs," *Proceedings of the Symposium on Concrete Shell Roof Construction*, Cement and Concrete Association, London, 1954, pp 45–50.
7. Jenkins, RS, "Theory and design of cylindrical shell structures," *The O.N. Arup Group of Consulting Engineers*, Bulletin, 1, London, 1947.
8. Design of cylindrical concrete shell roofs, *Manual of Engineering Practice*, No. 31, American Society of Civil Engineers, 1952.
9. Tottenham, H, "Simplified method of design for cylindrical shell roofs," *The Structural Engineer*, London, Vol. 32, June 1954, pp 161–180.
10. Dabrowski, R, "Analysis of prestressed cylindrical shell roofs," *Journal of the Structural Division, Proceedings of the American Society of Civil Engineers*, ST 5, October 1963.
11. Lundgren, H, "Cylindrical shells," Vol. 1. Cylindrical roofs, *The Institution of Danish Civil Engineers*. The Danish Technical Press, Copenhagen, 1949 (Third Printing, January, 1960).
12. Ramaswamy, GS, *Design and Construction of Concrete Shell Roofs*, McGraw-Hill, Inc., 1968, pp 187–199.
13. Haeusler, E, "Precast prestressed hyperboloids of revolution," *I.AS.S. Bulletin* No. 6, A-7, Madrid, 1959,
14. Tedesko, A, "Shell at Denver-hyperboloic paraboloidal structure of wide span," *Journal of the American Concrete Institute*, Vol. 57, No. 4, October 1960, pp 403–412.
15. Ramaswamy, GS and NR, Sayeed, "Simplified analysis of pretensioned hyperboloid roofing units," *Bulletin of the International Association for Shell and Spatial Structures*, Vol. 55, Madrid.
16. Naik, LS, G, Venkatachala, NL, Manjunath, and MH Nanjundaswamy, "Design of precast pretensioned hyperboloid roof elements for a warehouse" B.Tech. Dissertation, University of Mysore, Karnataka Regional Engineering College, 1978, pp 17–35.
17. Leonhardt, F, *Prestressed Concrete Design and Construction*, Wilhelm Ernst and Sohn, Berlin, Second Edition, 1964, pp 590–591.

18. Abeles, PW, "The development of prestressed concrete in the United States," *Civil Engineering and Public Works Review*, Vol. 49, Part 3, 1959, pp 387–390.
19. Adler, F, "Precast plate units for roof construction," Paper No. 6641, *Proceedings of the Institution of Civil Engineers*, London, November 1962, pp 321–326.
20. Gaafar, I, "Hipped plate analysis considering joint displacements," Paper 2696, *Transactions of the American Society of Civil Engineers*, Vol. 119, 1954, pp 743–784.
21. Simpson, H, "Design of folded plate roofs," *Journal of the Structural Division, Proceedings of the American Society of Civil Engineers*, Vol. 84, Jan. 1958.
22. Brielmaier, A A, "Prismatic folded plates," *Journal of the American Concrete Institute*, Vol. 59, March 1962, pp 407–410.
23. Rao, G S, "Analysis of folded plate roofs by iteration," *Indian Concrete Journal*, Vol. 36, No. 10, October 1962, pp 365–370.
24. Phase I—Report on folded plate construction, report of the Task Committee on folded plate construction, *Journal of the Structural Division, Proceedings of the American Society of Civil Engineers*, Vol. 60, ST 6, December 1963, pp 365–370.
25. IS: 2210–1962. *Indian Standard Criteria for the Design of Reinforced Concrete Shell Structures and Folded Plates*, Indian Standards Institution, New Delhi, 1963, pp 21–22.
26. Recent prestressed concrete construction in India, *Report of the Prestressed Concrete Group of the Institution of Engineers* (India), Sixth F.I.P. Congress, Praha, June, 1970, pp 4–10.
27. Bell, B, *Practical Prestressed Concrete*, Theory and Design, Pitman, London, 1964, pp 256–281.
28. Bennett, E W, *Prestressed Concrete Theory and Design*, Chapman and Hall, London, 1958, pp 257–265.
29. Timoshenko, S, *Theory of Plates and Shells*, McGraw-Hill, New York, 1940.

Review Questions

18.1 Briefly outline the advantages of prestressing long-span shell structures.

18.2 Sketch the typical distribution of prestressing tendons in large panel vaults and circular cylindrical shells with edge beams.

18.3 Explain the design procedure of computing the required prestressing force in edge beams of long-span circular shells.

18.4 What are the advantages of prestressing hyperboloid shells? Sketch a typical cross-section of a pretensioned hyperboloid unit showing the arrangement of high-tensile wires in cross-section and plan.

18.5 Bring out the advantages of prestressing long span folded plates. Sketch the typical cross-section of folded plates showing the distribution of tendons in the section.

18.6 What is the necessity of prestressing the ring beams of domes covering large areas? Sketch a typical ring beam of a concrete dome covering the circular water tank, showing the distribution of high-tensile tendons.

18.7 Explain with reasons the advantages of using prestressed ring beams at the base of large capacity dome silos of diameter exceeding 100 m. What is the disadvantage of using reinforced concrete ring beams?

18.8 Sketch a typical folded plate roof structure used for long spans showing the details of the location of the cables and reinforcements.

18.9 Distinguish between slab action and plate action with reference to the forces developed in folded plate structures.

18.10 Sketch a typical V-shaped folded plate used for a long span showing the location of the prestressing cables in the cross-section.

Exercises

18.1 A concrete cylindrical shell roof covering an area of 10 m by 30 m is to be designed with prestressed edge beams. Using the beam approximation, prepare a preliminary design for the edge beams using the following data:

Radius of the shell = 7.5 m
Thickness of the shell = 75 mm
Semi-central angle = 40°
Width of the edge beam = 150 mm
Depth of the edge beam = 1500 mm
Imposed load on the shell = 1 kN/m^2

The centroid of the cables (12 wires of 7 mm diameter stressed to 1000 N/mm^2) is located at a distance of 300 mm from the soffit of the beam. Calculate the prestressing force necessary in each beam for zero stress at the soffit under:

(a) dead load + half live load; and
(b) dead load + live load.
(c) Also find the number of cables required in each beam for case (a).

[Ans: (a) 890 kN; (b) 102 kN; (c) 2 cables]

18.2 A pretensioned hyperboloidal shell is required to cover the roof of a bus depot 30 m by 60 m. The loading should conform to IS: 875. M-50 grade concrete and high-tensile wires conforming to IS: 1785 are available for use. Design the shell units and check for load factors against collapse in flexure and shear. Also check for stresses under serviceability limit state.

[Ans: Size of unit = 4.2 m wide and 31 m long; Thickness of shell = 100 mm; Prestressing force = 3375 kN]

18.3 Design a V-shaped pretensioned folded plate roof to cover an industrial warehouse measuring 20 m by 50 m. Loading is as per IS: 875. M-45 grade concrete and 5 mm high-tensile wires are available for use. Check for stresses under working loads and for load factors required as per IS: 1343 in flexure. Sketch the details of wires in the plates and the valley junction cable in the cross-section of the pretensioned units.

[Ans: Width of plate = 1.9 m; Thickness = 100 mm; Prestressing force = 1450 kN, 32 wires of 5 mm in each plate and 12–5 mm cable at the valley junction]

18.4 A spherical dome is to be designed to cover a circular tank of 36 m diameter. The rise of the dome is one-eighth of the diameter, the thickness of the dome is 1/500 diameter and the live load on the dome is 1.5 kN/m^2. Design a suitable prestressed ring girder for the dome given the permissible compressive stress in the concrete as 14 N/mm^2. The loss ratio is 0.8. Use 7 mm diameter high-tensile wires, initially stressed to 1000 N/mm^2, to provide the necessary prestress.

[Ans: Ring beam 200 mm by 470 mm; No. of 7 mm wires = 28]

18.5 A trapezoidal shaped folded plate is to be designed to cover an area of 32 m by 30 m. The span length of the folded plate is 32 m. the superimposed load is 0.75 kN/m^2.

The trapezoidal units have the following dimensions:
Width of top horizontal plate = 2000 mm
Width of bottom horizontal plate = 1000 mm
Centre-to-centre distance between the valleys = 7000 mm
Slope of the inclined plates = 45 degree
Height of the folded plate = 2000 mm
Thickness of top and bottom plates = 100 mm
Thickness of inclined plates = 80 mm

Adopt M-35 Grade concrete and 7 mm diameter high-tensile wires initially stressed to 1050 N/mm^2 are available for use.

Design the number of wires in the folded plates.

[Ans: 40 wires of 7 mm diameter in the valley plate and 41 wires distributed in the inclined plates]

Objective-type Questions

18.1 Prestressed concrete shell and folded plate structures are ideally suited for
(a) domestic buildings (b) aircraft hangars (c) office buildings

18.2 Longitudinal prestressing of barrel vault shells results in
(a) increase of longitudinal moments
(b) increase of transverse moments
(c) reduction of transverse moments

18.3 Prestressed concrete shell structures are economical for industrial buildings spanning
(a) 15 to 20 m (b) 30 m and more (c) 10 to 15 m

18.4 Parabolic profile of cables in the edge beams of long shell structures
(a) increases the longitudinal deflections
(b) counteracts the deflection due to dead and live loads
(c) increases transverse deflections

18.5 Prestressing of shells results in
(a) decrease of factor of safety against collapse
(b) increase of cracking
(c) increase of factor of safety against cracking and collapse

18.6 Hyperboloid shells facilitate the use of
(a) curved tendons (b) sloping tendons (c) straight tendons

18.7 Long-span folded plate structures are generally prestressed using cables located in
(a) ridge joints (b) sloping plates (c) valley joints

18.8 Hyperboloid shells are doubly curved having
   (a) parabolic curve in the longitudinal direction and circular curve in the transverse direction
   (b) hyperbolic curve in the longitudinal direction and circular curve in the transverse direction
   (c) circular curve in the longitudinal direction and hyperbolic curve in the transverse direction

18.9 The prestressing cables in a long span V-shaped folded plate roof is generally located at the
   (a) top junction of plates
   (b) centre of the inclined plates
   (c) valley junction of plates

18.10 The form work required to cast hyperbolic paraboloid shell units is possible by using
   (a) singly curved surfaces
   (b) doubly curved surfaces
   (c) straight line surfaces

Answers to Objective-type Questions

18.1 (b)	18.2 (c)	18.3 (b)	18.4 (b)	18.5 (c)
18.6 (c)	18.7 (c)	18.8 (c)	18.9 (c)	18.10 (c)

19 Prestressed Concrete Poles, Piles, Sleepers, Pressure Vessels and Pavements

19.1 Prestressed Concrete Poles

19.1.1 General Features

During the last two decades, prestressed concrete poles have been gradually replacing the traditional poles made of wood, or steel or reinforced concrete. The earliest prestressed concrete poles were designed and constructed in 1933 by Freyssinet[1] for a railway signalling equipment in France and for the desert environment in Algeria where blowing sand destroyed both wood and steel poles.

Prestressed concrete poles are currently mass produced and are widely used in most countries for railway power and signal lines, lighting poles, antenna masts, telephone transmission, low and high voltage electric power transmission and substation towers.

The main advantages of prestressed concrete poles are:

1. Resistance to corrosion in humid and temperate climates and to erosion in desert areas.
2. Freeze-thaw resistance in cold regions.
3. Easy handling due to less weight than other poles.
4. Fire resistant, particularly to grass and bush fires near the ground line.
5. Easily installed in drilled holes in ground with or without concrete fill.
6. Lighter because of reduced cross-section when compared with reinforced concrete poles.
7. Clean and neat in appearance and requiring negligible maintenance for a number of years, thus ideally suited for urban installations.
8. Have increased crack resistance, rigidity and can resist dynamic loads better than reinforced concrete poles.

These advantages have resulted in the rapid development and use of different types of prestressed poles in various countries, such as UK, USA, France, Germany, Italy, Japan, Norway, Poland, Spain, Switzerland, India, erstwhile Czechoslovakia and USSR. In Japan, the Nippon Concrete Industries produce more than 54,000 of spun prestressed concrete poles every month, while France uses more than 400,000 concrete poles every year. In erstwhile USSR, poles have been used for the transmission of power up to 330 kV[2]. In India, the use of prestressed concrete poles has so far been confined to lighting columns and for the transmission of power of up to 11 kV.

In view of the crash programme of rural electrification in India, it is estimated that there will be a demand for two million poles annually, which will further increase due to the electrification of new railway lines during the next decade[3].

In India, prestressed concrete poles are generally manufactured by the long-line method. Spinning of poles of tubular section is favoured in countries like, France, Germany, Japan, erstwhile Czechoslovakia and USSR[4].

19.1.2 Shapes of Prestressed Concrete Poles

The maximum moment of resistance in a pole is generally required at the base and, consequently, the maximum cross-sectional area is required at the base section. Poles are generally tapered with a hollow core to reduce the weight, which also helps in providing a race way for electric wires. Typical cross-sections of transmission line poles widely employed in different countries are shown in Fig. 19.1. For small lengths of up to 12 m, the square or rectangular sections are preferable as they are easily manufactured and occupy less space in transportation. Vierendeel poles are also preferred for small lengths due to economy in the use of materials. However, they have a larger exposed surface with thin elements and are susceptible to corrosion, I-sections of 10 m lengths have been widely used in the British railways while V-sections have been employed in South African railways[5].

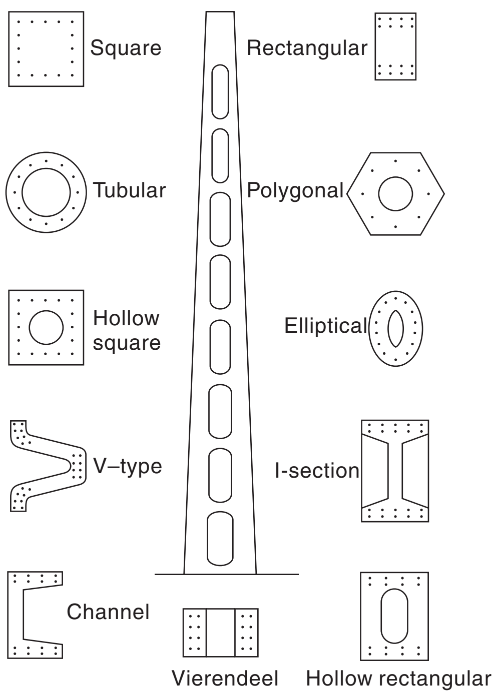

Fig. 19.1 *Cross-sections of prestressed concrete poles*

Tubular sections are idealy suited for longer poles. BBRV-type prestressed concrete poles are manufactured in standard lengths of 9, 12, 15, and 18 m and up to a maximum diameter of 750 mm using the spinning process.

19.1.3 Design Considerations

Prestressed concrete poles for power transmission lines are generally designed as members with uniform prestress since they are subjected to bending moments of equal magnitude in opposite directions. The poles are generally designed for the following critical load conditions:

1. Bending due to wind load on the cable and on the exposed face.
2. Combined bending and torsion due to eccentric snapping of wires.
3. Maximum torsion due to skew snapping of wires.
4. Bending due to failure of all the wires on one side of the pole.
5. Handing and erection stresses.

The load factors required for strength and serviceability are prescribed in the codes of various countries. The Indian Standard Code IS: 1678–1960[6] provides for a load factor of 2.5 for transverse bending strength. German and erstwhile Czechoslovakian standards prescribe a load factor of 1.75 and 2.0, respectively, against the limit state of collapse. The flexural strength of the pole in the direction of the cable line should be not less than one quarter of the strength in the transverse direction. Smaller load factors ranging from 1.1 to 1.5 are prescribed for failure due to combined bending and torsion as a result of snapping of wires. Under over-load conditions, progressive failure of the pole is ensured by designing the critical section as under-reinforced, which gives ample warning before failure. The use of mild- or high-strength deformed bars, in addition to the high-tensile wires, would impart sufficient ductility to the member.

In the case of tapered poles with a reduced cross-section towards the top, the effective prestressing force should be reduced in proportion to the cross-section by the techniques of debonding or by dead ending or looping some of the tendons at mid-height. According to Gerwick[7], a constant cross-section proves to be a better solution in many cases since the top must be as strong as the base for resisting torsion, with the added advantage of the effective use of prestressing and easier connections.

19.1.4 Partially Prestressed Pretensioned Poles

Uniformly prestressed members designed for equal flexure in opposite directions, without permitting tensile stresses under working loads, require a larger cross-section and prestressing force. Prestressed poles designed as fully prestressed, corresponding to Class 1 structures of FIP–CEB classification[8], generally possess very high load factors against the limit state of collapse. This is due to the small range of stress permissible in the extreme fibres of members subjected to equal bending in opposite directions.

Class 2 partially prestressed poles, in which limited tensile stresses of the order of the modulus of rupture are permitted, may develop microcracks at working loads, but are free from visible cracks. In Class 3 structures, tensile stresses in excess of the modulus of rupture are permitted, resulting in visible cracks under service loads. Both Class 2 and Class 3 partially prestressed poles result in considerable savings in steel and concrete. This is demonstrated in the following example in which a partially pretensioned pole of 10 m height is designed for wind loads prevailing in the west coast of India[9].

Example 19.1 A partially prestressed pretensioned mast is to be designed to suit the following data:

Spacing of poles = 100 m
Free-standing height of the pole above the ground = 10 m

The pole is to carry twin-conductor high-voltage lines (60 cm apart) on a cross tree at 9 m above-ground level.
Conductor size: effective over all diameter = 10 mm
Tension in each conductor = 5 kN
Poles are to be located in Mangalore;
Wind pressure for this zone (IS: 875–1964) = 10 N/mm^2
28-day cube strength of concrete = 50 N/mm^2
Modulus of elasticity of concrete = 40.5 kN/mm^2
Modulus of rupture of concrete = 5 N/mm^2
High-tensile wires of 5 mm diameter available.
Ultimate tensile strength = 1600 N/mm^2
Loss ratio = 0.7
Permissible stress in concrete under service loads:
Compressive stress in concrete, f_{cw} = 18 N/mm^2
Tensile stress in concrete, f_{tw} = 5 N/mm^2

Solution.

(a) Design of section The wind load acting on conductors and pole (assuming the width of pole to be 150 mm) is calculated by using the basic maximum wind-pressure prescribed in IS: 875. The wind forces acting on the pole in the transverse direction are shown in Fig. 19.2.
Maximum working moment at ground level, M_d = 25.5 kN m
If the permissible compressive and tensile stresses, f_{cw} and f_{tw}, are both reached under service loads, the section modulus is given by the expression,[10]

$$Z_t = Z_b > \left[\frac{2M_d}{f_{cw} - f_{tw}}\right]$$

Hence, the section modulus required is

$$Z_t = Z_b > \left[\frac{2 \times 25.5 \times 10^6}{18 - (-5)}\right] > 223 \times 10^4 \text{ mm}^3$$

$$\text{Overall depth, } h = \sqrt{\frac{6 \times 223 \times 10^4}{150}} = 300 \text{ mm}$$

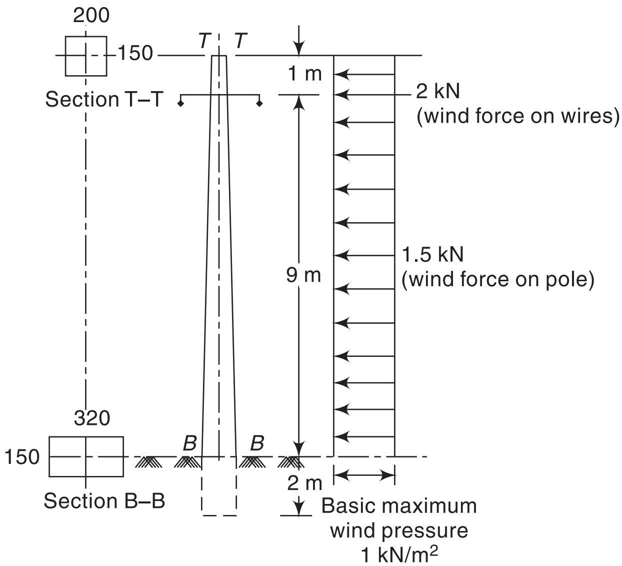

Fig. 19.2 *Forces acting on mast*

A pole with a cross-section of 150 mm by 320 mm is adopted for the base section. Since the pole is subjected to equal bending in opposite directions, the member should be designed for uniform prestress.

$$\text{Prestress in member} = \left[\frac{f_{\text{tw}}}{\eta} + \frac{M_{\text{w}}}{\eta Z}\right] = \left[\frac{-5}{0.7} + \frac{25.5 \times 10^6}{0.7 \times 25 \times 10^5}\right] = 7.5 \text{ N/mm}^2$$

$$\text{Initial prestressing force} = \left[\frac{(7.5 \times 150 \times 320)}{1000}\right] = 360 \text{ kN}$$

Permissible force in 5 mm wire = $(19.6 \times 0.8 \times 1600/1000) = 25$ kN

$$\text{Number of wires required} = \left(\frac{360}{25}\right) = 14.5$$

16 wires are provided at the base section, arranged as shown in Fig. 19.3.

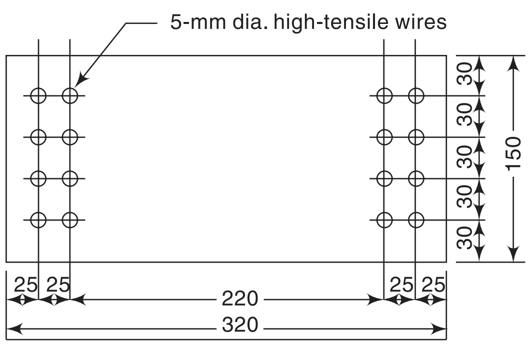

Fig. 19.3 *Arrangement of wires at base section*

(b) Check for limit state of collapse The ultimate strength of cross-sections is calculated according to the recommendations of IS: 1343.

$$\left(\frac{A_p f_p}{b d f_{ck}}\right) = \left(\frac{156.8 \times 1600}{150 \times 282.5 \times 50}\right) = 0.118$$

From Table 7.1, $(f_{pu}/0.87 f_p) = 1.0$

$$\therefore \quad f_{pu} = 1392 \text{ N/mm}^2$$

and $(x_u/d) = 0.24$

$$(x_u) = (0.24 \times 282.5) = 67.8 \text{ mm}$$

$$\therefore \quad M_u = \left\{\frac{[1392 \times 156.8(282.5 - 0.42 \times 67.8)]}{10^6}\right\} = 55 \text{ kN m}$$

$$\therefore \quad \text{Load factor against collapse} = \left(\frac{55}{25.5}\right) = 2.16$$

For the longitudinal direction (along the direction of wire),

$$\left(\frac{A_p f_p}{b_d f_{ck}}\right) = \left(\frac{156.8 \times 1600}{320 \times 105 \times 50}\right) = 0.15$$

From Table 7.1, $f_{pu} = 1392 \text{ N/mm}^2$

and $x_u = (0.326 \times 105) = 34$ mm

$$\therefore \quad M_u = \left\{\frac{[1392 \times 156.8(105 - 0.42 \times 34)]}{10^6}\right\} = 19.8 \text{ kN m}$$

Minimum strength required in this direction = 0.25 × transverse strength

= (0.25 × 55) = 13.75 kN m

The section designed satisfies the requirement for the limit state of collapse.

(c) Check for limit state of cracking

Working moment = 25.5 kN m

Tensile stress at the extreme fibre of concrete at working moment = 5 N/mm^2.

Maximum crack width is computed by the expression suggested by Beeby and Taylor[11] as,

$$w_{max} = \left[K f_{tw} \frac{(h - d_n)}{E_c}\right]$$

$$= \left[(1.75 \times 5)\frac{(320 - 160)}{40.5 \times 10^3}\right] = 0.035 \text{ mm}$$

The maximum crack width is less than the permissible value of 0.1 mm as provided for in the codes for aggressive environment.

(d) Check for limit state of deflection The cross-sectional dimensions of the pole are reduced from 150 × 320 mm at ground level to 150 × 200 mm at the top. The maximum deflection at the head of the mast was computed based on the variable cross-section of the pole under working loads.

Maximum deflection = 39 mm

The computed maximum deflection is marginally higher than the permissible value of span/250 as prescribed in IS: 456. However, the maximum wind loads adopted act very rarely and only for a short duration, and in the case of transmission poles, the deflection is not considered to be critical and hence it is not a controlling factor in design.

(e) Check for torsion due to skew snapping of wires Skew snapping of wires will induce torsion in the pole. The maximum ultimate torsional moment is computed as,

$$T = (1.5 \times 5000 \times 600) = 4.5 \times 10^6 \text{ N mm}$$

The section of the pole at the top (150 mm by 200 mm) will be checked for torsional stresses.

Torsional shear stress, $$\tau_t = \frac{2T}{h_{min}^2\left[h_{max} - \left(\frac{h_{min}}{3}\right)\right]}$$

or $$\tau_t = \left\{\frac{2 \times 4.5 \times 10^6}{150^2\left[200 - \left(\frac{150}{3}\right)\right]}\right\} = 2.66 \text{ N/mm}^2$$

Referring to Table 8.4, τ_t is less than the maximum value of τ_{tu}, $= 5$ N/mm^2 and greater than $\tau_{t,\,min} = 0.4$ N/mm^2.

Hence, longitudinal and transverse reinforcements are to be designed according to the procedure outlined in Section 8.5.1.

Using 12 mm diameter two-legged links, the spacing is given by,

$$s = \left(\frac{A_{sv} 0.8 x_1 y_1 0.87 f_{yv}}{T}\right)$$

$$= \left(\frac{2 \times 113 \times 0.8 \times 110 \times 160 \times 0.87 \times 415}{2 \times 4.5 \times 10^6}\right) = 127 \text{ mm}$$

The cross-sectional area of longitudinal reinforcement is given by,

$$A_s = \left(\frac{A_{sv}}{s}\right)\left(\frac{f_{yv}}{f_y}\right)(x_1 + y_1)$$

$$= \left(\frac{2 \times 113 \times 415}{127 \times 415}\right)(110 + 160) = 488 \text{ mm}^2$$

Four longitudinal bars of 12 mm diameter are provided as corner bars, along with two-legged links at 125 mm centres.

Failure of wires on the side of the pole will induce severe bending in the direction of the lines. It has been suggested by Bell[12] that the pole need not be designed for this extreme condition as it is far in excess of normal requirement and would prove prohibitive in cost.

(f) Debonding of wires The number of wires required, section properties and stresses at different sections of the pole are compiled in Table 19.1. To

Table 19.1 *Resultant stresses in pretensioned pole*

Height from Ground Level, m	*Size of Section,* mm	*Area of Section,* $mm^2 \times 10^3$	*Section Modulus, Z,* $mm^3 \times 10^4$	*Working Moment,* M_d kN m	*Stress due to Moment* M_d/Z, N/mm^2	*Number of Wires Required*	*Number of Wire Debonded*	*Number of Wires Active*	*Prestress after Losses,* N/mm^2	*Final Stresses* N/mm^2
0	150 × 320	48	250	25.5	±10.2	16	0	16	+5.2	+15.4
										–5.0
2	150 × 296	44	220	18.8	±8.5	9	4	12	+4.8	+13.3
										–3.7
4	150 × 272	41	186	12.7	±6.8	5	8	8	+3.4	+10.2
										–3.4
6	150 × 248	37	154	7.2	+4.7	0	12	4	+1.9	+6.6
										–2.8
8	150 × 224	33.5	125	2.3	±1.8	0	12	4	+2.1	+3.9
										+0.3
10	150 × 200	30	100	0	0	0	12	4	+2.4	+2.4

reduce the prestress towards the head of the mast, prestressed wires may be debonded in stages as shown in Table 19.1. For debonding the wires, polyvinyl chloride tubing, having a wall thickness of 1 mm, may be used to the required length before the concrete is placed. Due considerations should be given to the required transmission length of wires before fixing the length of debonding.

(g) Comparison with fully prestressed Class 1 poles Table 19.2 shows the quantities of materials required for fully and partially prestressed poles. Considerable saving in both steel and concrete is evident if partially prestressed poles are adopted in place of fully prestressed design.

Table 19.2 *Material requirements for fully and partially prestressed poles*

Type of Pole	*Size of Section at*		*Number of 5 mm High-tensile Wires Required*	*Quantity of Concrete Per pole*,* m^3	*Quantity of High-tensile Steel Per pole,* kg
	Base, mm	*Top,* mm			
Fully pre-stressed pole (class 1)	150 × 380	150 × 200	24	0.549	45
Partially pre-stressed pole, (class 2)	150 × 320	150 × 200	16	0.486	30

*Length of pole embedded in the ground is assumed as 2 m.
Overall length of pole = 12 m

19.2 Prestressed Concrete Piles

19.2.1 Advantages of Prestressed Concrete Piles

During the last two decades, prestressed concrete piling has been extensively used as a versatile substructure component for marine structures and multistoreyed buildings throughout the world. The main advantages, according to Gerwick[13], of prestressed concrete piles over traditional reinforced concrete and steel piles are:

1. High load and moment carrying capacity.
2. Standardisation in design for mass production.
3. Excellent durabillity under adverse environmental conditions.
4. Crack-free characteristics under handling and driving.
5. Resistance to tensile loads due to uplift.
6. Combined load moment capacity.
7. Good resistance to hand-driving loads and penetration into hard strata.
8. Piles can be lengthened by splicing.
9. Ease of handling, transporting and driving.
10. Overall economy in production and installation.
11. Adaptability to both developed and developing countries in tropical, subarctic and desert regions.

12. Use of solid and hollow cross-sectional configurations to suit design requirements.
13. Ease of connections with pile caps to form pier, trestle and jetty bents to support bridge or wharf decks.
14. Effective use of fender piling to resist the kinetic energy of ship impact.
15. Particularly advantageous for deep foundations to carry heavy loads in weak soils.

Prestressed concrete piles have been widely used in marine structures for fender piles, sheet piles and soldier piles mainly due to their excellent durability under both freeze thaw and salt spray attack.

Prestressed concrete piles have been used as friction piles in sands, silts and clays and as bearing piles on rocky strata, and in sizes as small as 250 mm diameter with lengths up to 36 m. Larger diameters of up to 4 m is used in Oester Schelde bridge in Netherlands. Piles of considerable length of up to 80 m cast and driven in one piece were used for the off-shore platform in the gulf of Maracaibo, Venezuela.

According to Shu-T'ien Li[14], the full potential of prestressed concrete as a composite material in piling would be attained only through optimum analysis, optimum prestress and optimum design, in view of the world demand for piles exceeding 80 million metres per year.

19.2.2 Types and Cross-sectional Shapes of Prestressed Concrete Piles

Depending upon the functional behaviour and the locations used, prestressed concrete piles are classed under eight different categories for the purposes of design:

1. Bearing piles
2. Sheet piles
3. Combined hearing and sheet piles
4. Pier trestle and jelly bent piles (pile bents)
5. High tower and stack piles (subject to uplift)
6. Caisson piles
7. Anchor piles
8. Fender piles

The different cross-sectional shapes of piles used and their merits are compiled in Table 19.3[13].

19.2.3 Design Considerations

The primary considerations in the design of prestressed concrete piles are the stresses developed during handling and driving, which are temporary in nature, and the stresses developed due to permanent loads (dead and live loads),

Table 19.3 *Cross-sectional shapes for prestressed concrete piles*

S. No.	*Cross-sectional Shape of Pile*	*Merits and Demerits*
1.	Triangular	High ratio of skin-friction perimeter to cross-sectional area; low manufacturing cost but low bending resistance.
2.	Square	Good ratio of skin-friction perimeter to cross-sectional area; low manufacturing cost; good bending resistance on major axes.
3.	Pentagon or octagon	Approximately equal bending strength on all axes; good penetrating ability; good column stability; prone to surface defects during casting due to large number of faces and edges.
4.	Circular	Equal bending strength on all axes with absence of corners; good aesthetics and high durability; minimum wave and current loads; good column stability, manufacturing costs generally higher, surface defects are unavoidable.
5.	Rectangular with or without semi-circular ends	Greater bending strength about the shorter axis; minimum surface to wave and current forces; difficulty of orientation.
6.	I and star	High bending resistance; high manufacturing costs; difficulty of orientation.

repetitive loads (live loads) and transient loads, such as wind, earthquake, etc. The permissible stresses in concrete and steel for different conditions of loading as provided by the PCI committee on prestressed concrete piling[15] are compiled in Table 19.4.

Handling Stresses and Impact Allowance The flexural stresses developed under different handling conditions, such as lifting from casting beds, storage and transportation, should be investigated. The stress analysis is generally based on the weight of the pile plus a 50 per cent allowance for impact with tensile stresses limited to $0.5\,(f_{cy})^{1/2}$.

Driving Stresses The dynamic stresses developed during pile driving are complex functions of pile and soil properties and are influenced by driving resistance, hammer weight and stroke, cushioning materials and other parameters. The driving stresses are alternately compression and tension, reaching values of about 7–28 N/mm^2 (compressive) and 10 N/mm^2 (tensile) and even higher under certain conditions. Tensile stresses are likely to develop in piles, which are longer than 12 m, under soft driving conditions at the tip. In the case of shorter piles, tensile driving stresses rarely develop and the minimum effective prestress values, as provided by various authorities throughout the world to resist driving stresses, range from 2.8 to 8.4 N/mm^2.

Service Load Stresses The stresses that develop in the pile due to primary service loads like axial compression or tension, either independently or in combination with moments, should conform to the safe permissible values shown in Table 19.4. The safe permissible axial load on a prestressed pile is given by,

Table 19.4 *Permissible stresses in concrete and steel (Prestressed piles)*

Concrete Stresses		
1.	Uniform axial compression for foundation piles fully embedded in soils providing lateral support	$0.33\, f_{cy} - 0.27\, f_{cp}$ where f_{cp} = effective compressive prestress
2.	Uniform axial tension: Permanent and repetitive Transient	0 $0.5(f_{cy})^{1/2}$
3.	Compression due to bending: Normal Marine work and bridges	 $0.45\, f_{cy}$ $0.40\, f_{cy}$
4.	Tension due to bending: Permanent and repetitive Transient	 $0.34\, (f_{cy})^{1/2}$ or zero in corrosive environment $0.5(f_{cy})^{1/2}$
5.	For combined loading, concrete stresses should be checked in interaction: $\left(\dfrac{f_a}{F_a} + \dfrac{f_b}{F_b}\right) \le 1$	where F_a = allowable direct stress F_b = allowable compressive stress in bending
6.	Effective prestress (recommended values): For piles 12 – 52 m For piles shorter than 12 m	 4.9 – 8.4 N/mm^2 2.8 – 4.9 N/mm^2
Steel Stresses		
1.	Temporary stresses: Due to temporary jacking force, but not greater than the maximum value recommended by the manufacturer of steel; Pretensioning tendons immediately after transfer or post-tensioning tendons immediately after anchoring; Tension due to transient loads	 $0.8 f_{pu}$ $0.70 f_{pu}$ Concrete governs
2.	Effective prestress	$0.6 f_{pu}$ or $0.80 f_{py}$ (whichever is smaller)
3.	Unstressed prestressing steel	$0.5\, f_{py}$(max. 210 N/mm^2)

$$N = A_c(0.33\,f_{cy} - 0.27\,f_{cp})$$

where f_{cp} = effective prestress after all losses

f_{cy} = cylinder compressive strength

A_c = area of concrete

The design of piles subjected to axial load and moment is simplified by the use of load moment interaction diagrams prepared by the Prestressed Concrete Institute[16]. The interaction diagrams have been prepared for the ultimate load capacity of common pile sizes and cross-sectional shapes (square, octagonal and round) for concrete strengths of 35, 42, 49 and 56 N/mm^2 and for effective prestress levels of 4.9 and 8.4 N/mm^2. A typical interaction diagram involving parameters, such as the ultimate axial load, moment and slenderness ratio of 350 mm solid octagonal pile is shown in Fig. 19.4. The allowable service loads and section properties of various shapes and sizes of piles are compiled in Table 19.5. The data is useful for the design of piles of specific shapes for concentric service loads.

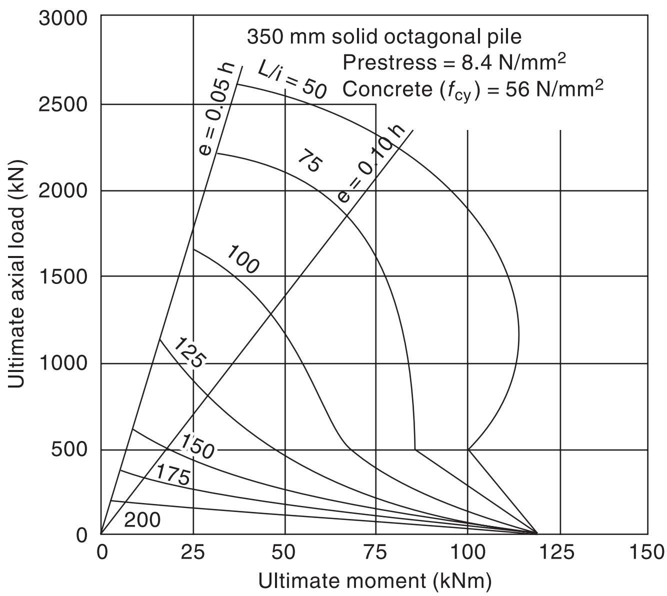

Fig. 19.4 *Load–moment characteristics of prestressed piles*

19.2.4 Pile Reinforcements

The rebound tensile stresses are resisted by the effective prestress together with the tensile strength of concrete. Hence, the steel tendon area at yield should have an equal or greater force than the prestress plus concrete tensile strength to prevent failure due to low-cycle fatigue. Based on theory and experience, Gerwick[13] recommends a minimum tendon area of not less than 0.5 per cent of the concrete section, while the AASHO-PCI standards prescribe the minimum reinforcing steel to be 1–1.5 per cent of the gross concrete section.

Table 19.5 *Section properties and allowable service loads of prestressed concrete piles*

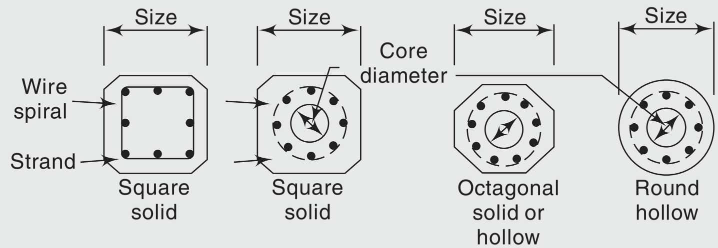

Size mm	*Core Dia,* mm	*Area,* $mm^2 \times 10^3$	*Weight,* kN/m	*Moment of Inertia,* $mm^4 \times 10^6$	*Section Modulus,* $mm^3 \times 10^6$	*Radius of Gyration,* mm	*Perimeter,* mm	*Allowable Concrete Service Load,* kN — *Cylinder Strength,* f_{cy} N/mm^2: 35	42	49	56
(1)	*(2)*	*(3)*	*(4)*	*(5)*	*(6)*	*(7)*	*(8)*	*(9)*	*(10)*	*(11)*	*(12)*
					Square piles						
250	Solid	62.5	1.50	325	2.60	72	1000	652	790	950	1100
300	Solid	90.0	2.16	675	4.50	87	1200	940	1160	1360	1580
350	Solid	122.5	2.95	1250	7.15	101	1400	1280	1570	1870	2150
400	Solid	160.0	3.85	2130	10.60	118	1600	1680	2050	2440	2830
450	Solid	202.5	4.87	3400	15.20	132	1800	2130	2600	3090	3560
500	Solid	250.0	6.00	5200	20.70	146	2000	2630	3200	3800	4400
500	275	174.5	4.20	4950	19.80	161	2000	2000	2440	2900	3340
600	Solid	360.0	8.65	10800	36.00	174	2400	3760	4600	5480	6300
600	300	270.0	6.50	10400	34.70	190	2400	3030	3700	4400	5080

(*Contd.*)

Table 19.5 (*Contd.*)

Octagonal Piles											
600	350	237.5	5.70	10100	33.60	196	2400	2760	3390	4000	4630
600	375	220.0	5.30	9800	32.70	199	2400	2610	3200	3800	4380
250	Solid	52.0	1.25	216	1.73	65	830	535	660	770	900
300	Solid	74.8	1.69	433	2.87	77	1000	770	948	1110	1290
350	Solid	102.0	2.45	822	4.70	90	1160	1050	1290	1520	1760
400	Solid	133.0	3.20	1400	7.00	103	1330	1370	1690	1980	2300
450	Solid	168.0	4.05	2230	9.90	116	1500	1730	2130	2500	2900
500	Solid	207.0	4.98	3420	13.70	129	1660	2140	2630	3100	3580
500	275	135.0	3.25	3130	12.50	146	1660	1390	1710	2000	2320
550	Solid	253.0	6.08	5020	18.30	141	2000	2600	3200	3750	4350
550	325	156.0	3.75	4480	16.30	164	2000	1610	1980	2320	2680
600	Solid	300.0	7.20	7100	23.60	154	2000	3100	3800	4450	5180
600	375	165.0	3.95	6120	20.40	181	2000	1700	2090	2450	2840
Round Piles											
900	650	303.0	7.28	23400	52.0	280	2830	3130	3830	4500	5220
1200	950	420.0	10.10	61800	102.5	382	3780	4320	5300	6250	7250
1350	1100	480.0	11.50	91000	135.0	435	4250	4950	6080	7150	8300

The tendons are distributed in a circular pattern with circular spiral ties in the case of round, hexagon and octagonal piles. Both circular and square patterns have been used with square piles. Since there is no significant difference in the behaviour of square piles with square or circular pattern of reinforcement, the latter is predominant in current practise in view of the savings and increased efficiency of circular spiral and ease of manufacture.

Spiral binding is provided throughout the length of the pile and at a closer pitch towards the head and tip of the pile to counteract the bursting forces developed during driving conditions. Based on observed data, the Concrete Society of UK recommends a minimum of 0.6 per cent spiral over a length equal to three times the least dimension of the pile for the end zones. According to Gerwick, the amount of spiral reinforcement should be about one per cent at the head and tip for a length of 300 mm and 0.6 per cent for the next 600 mm which reduces to 0.3 per cent (solid piles) and 0.4 per cent (hollow core piles) in the body of the pile. The typical details of reinforcements in a pile according to AASHOPCI standards are shown in Fig. 19.5.

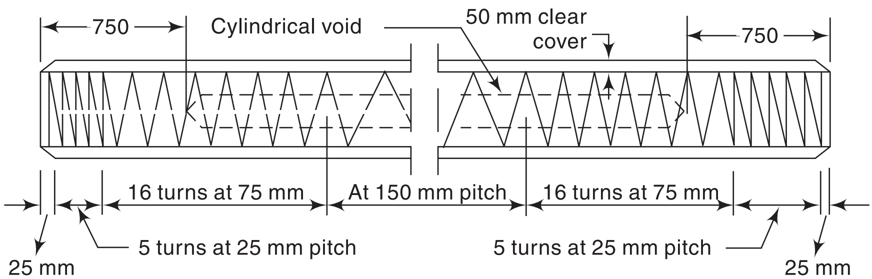

Fig. 19.5 *Typical details of pile reinforcement (AASHO–PCI standards)*

19.2.5 Pile Shoes

Pile shoes are required for driving through extremely soft materials like buried timbers and rocky strata. However, for driving prestressed concrete piles into sands, silts, clays and soft shales, pile shoes are unnecessary. Pile shoes are formed by thick steel plates or stubs welded to the reinforcing bar anchors and firmly embedded into the pile tip as shown in Fig. 19.6. The shape of the tip may be varied to suit driving conditions. Field experience indicates that a square tip with chamfered corners is

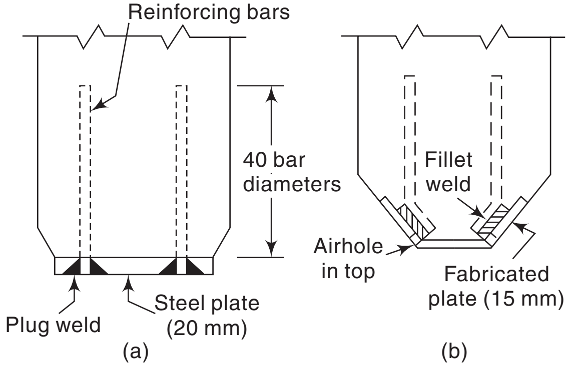

Fig. 19.6 *Types of pile shoes*

preferable to a pointed or wedge shaped tip since the latter causes the pile to deflect and develops high bending stresses which result in the failure of the shoe and pile.

The design of a prestressed concrete pile to resist axial loads independently or associated with bending using the design tables and interaction diagrams is illustrated by the following examples.

Example 19.2 The ground floor columns of an industrial shed are to be supported on prestressed piles of 10 m length. Each pile is subjected to an axial load of 2500 kN. The specified cylinder compressive strength of concrete is 35 N/mm^2. The permissible effective prestress is not to exceed 4.9 N/mm^2. Design a suitable pile of (a) square section, and (b) octagonal section. Also design the number of strands (7–12.5 mm) required for the piles if the ultimate tensile strength of the strand is 165 kN.

Solution.

$$N = A_c(0.33 f_{cy} - 0.27 f_{cp})$$

Assuming the effective prestress, $f_{cp} = 4.9$ N/mm^2,

$$(2500 \times 10^3) = A_c(0.33 \times 35 - 0.27 \times 4.9)$$

$$\therefore \quad A_c = (245 \times 10^3)\ \text{mm}^2$$

Referring to Table 19.5, a solid square pile of 500 mm size and a solid octagonal pile of 550 mm can be adopted.

$$\text{Prestressing force} = \left[\frac{4.9 \times 245 \times 10^3}{1000}\right] = 1200\ \text{kN}$$

Effective force in each strand (7–12.5 mm) under service load

$$= (0.6 \times 165) = 99\ \text{kN}$$

$$\therefore \quad \text{Number of strands} = \left(\frac{1200}{99}\right) = 12$$

Example 19.3 A multistoreyed building is to be supported on prestressed concrete pile foundations. The piles have an effective height of 5 m and they have to support a total axial service load of 1100 kN together with a moment of 37.5 kN m. Design a suitable pile to support these loads, assuming a uniform load factor of 2 against collapse. The pile is to be designed to be lifted at any point along its length for installation.

Solution.

Service loads: $N = 1100$ kN

$M = 37.5$ kN m

Ultimate loads: $N_u = 2\,(1100) = 2200$ kN

$M_u = 2(37.5) = 75$ kN m

Referring to the interaction diagram (Fig. 19.4); select the 350 mm solid octagonal pile.

From Table 19.5, section properties of the piles are:

$$A = (1.02 \times 10^5)\ \text{mm}^2 \qquad w_d = 2.45\ \text{kN/m}$$
$$Z = (4.70 \times 10^6)\ \text{mm}^3 \qquad i = 90\ \text{mm}$$

$\therefore$ Slenderness ratio, $\left(\dfrac{L}{i}\right) = 5 \times \left(\dfrac{1000}{90}\right) = 55.5$

Eccentricity, $e = \left(\dfrac{M_u}{N_u}\right) = \left(\dfrac{75 \times 1000}{2200}\right) = 34\ \text{mm}$

$\therefore$ Ratio $\left(\dfrac{e}{h}\right) = \left(\dfrac{34}{350}\right) = 0.097$

The ultimate moment and load capacity of the 350 mm solid octagonal pile for $M_u = 75$ kN m and $\left(\dfrac{L}{i}\right) = 55.5$, from Fig. 19.4 is,

Axial load, $P_u = 2250$ kN
Effective prestress = 8.4 N/mm^2

$\therefore$ Initial prestressing force $= \left(\dfrac{8.4 \times 1.02 \times 10^5}{0.85 \times 10^3}\right) = 1030$ kN

Use eight strands (7–12.5 mm wire) initially stressed to 1120 N/mm^2.

Handling stresses

Self-weight of pile	= 2.45 kN/m
Impact allowance (50%)	= 1.23 kN/m
	w_d = 3.68 kN/m

Maximum moment in the pile when lifted at centre is given by,

$$M = \left[(3.68)\frac{(2.5^2)}{2}\right] = 11.5\ \text{kN m}$$

Tensile bending stress $= \left[\dfrac{(11.5 \times 10^6)}{(4.70 \times 10^6)}\right] = 2.45$ N/mm^2

Resultant stress = 8.4 – 2.45 = 5.95 N/mm^2 (compression).
Hence, the pile is safe against handling stresses.

19.2.6 Sheet Piles

Prestressed concrete sheet piles are ideally suited for the construction of water-front bulk heads, cut-off walls, groins, wave baffles and retaining walls to support soil and hydrostatic pressure in embankments or in excavations. Since prestressed concrete piles resist tensile stresses under driving and bending stresses under service loads, they are preferred to timber and steel for marine structures, such as soldier beams, back stays and transverse struts. The high-strength concrete used in sheet piles with proper compaction, provides excellent resistance to corrosion and other destructive effects of the aggressive marine environment.

Typical cross-sections of sheet piles which have found extensive application in harbour structures as reported by Gerwick[13] are shown in Fig. 19.7. In the design of prestressed concrete sheet piles, the stresses developed during handling, storage, hauling, driving and service load stresses due to soil and hydrostatic pressure have to be considered in their critical combinations. According to Shu-T'ien Li[17], the guiding principles for the selection of optimum prestress required are as follows:

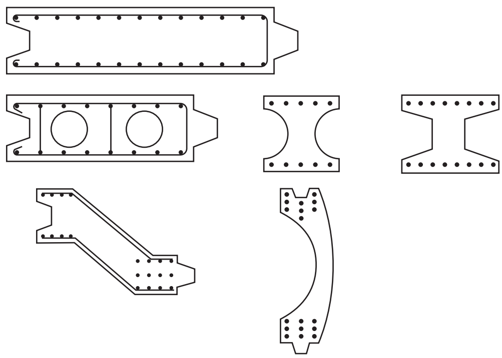

Fig. 19.7 *Typical cross-sections of prestressed concrete sheet plies*

1. Under driving conditions, the maximum amplitude of the compressive wave, together with the prestress, should not exceed the permissible compressive stress in concrete.
2. Larger eccentricity resulting in excessive camber is harmful during driving, while limited eccentricity for prestress with slight camber on the final compression side is beneficial in resisting service load stresses.
3. The prestress, together with the allowable tensile stress, should counteract the maximum amplitude of the tensile stress wave during recoil.
4. Under service loads, the prestress, in conjunction with the allowable tensile stress in concrete, should counteract the bending tensile stresses developed due to the lateral pressure either over supports or in the spans.

In the design of sheet piles, tensile stresses of up to 50 per cent of the modulus of rupture are commonly permitted. However, cracking is not permitted under serviceability limit state, especially at the salt water splash zone. The minimum prestress required is about 5 N/mm^2 for piles installed by vibration or driving. In the case of piles installed by jetting, a greater eccentricity of prestress is permissible.

19.3 Prestressed Concrete Sleepers

19.3.1 Early Development and Use of Sleepers

Prestressed concrete sleepers were first introduced in France around 1940[18] and later developed and used by the British and German federal railways after the Second World War. The large-scale experimental investigations and field observations conducted during the period between 1949 and 1953 with three million sleepers on the track, confirmed the advantages of the concrete sleeper as a new structural member of the permanent way[19]. During the last 20 years, concrete sleepers have been increasingly used by the world railway system in high speed and heavy traffic density tracks. To date, there are more than 100 million prestressed concrete sleepers of the monoblock type in service. Considerable progress has been made in the past few decades in the design and production of sleepers and rail fastenings. Each country has adopted particular types of sleepers depending upon the cost of materials and labour, national track requirements and availability of indigenous know-how.

The state of art reports and the excellent surveys by Kunze[20], Ager[21] and Sambamoorthi *et al.*[22], clearly indicate the rapid progress achieved in the design, manufacture and testing of prestressed concrete sleepers in various countries. The Indian railways has embarked on a track modernisation programme with the introduction of long welded rails, concrete sleepers and elastic fastenings. It is estimated that by 2001 the annual demand in India for prestressed concrete sleepers will exceed five million.

19.3.2 Types of Prestressed Sleepers

The developments in sleeper design, extending over the last three decades, has resulted in the adoption of different types. The prominent types which have been adopted by the railways of the various countries are:

1. Two-block sleepers connected by a pipe filled with concrete and containing high-tensile bars for compressing the concrete in the blocks. The Swedish SJ-101 tie shown in Fig. 19.8(a) belongs to this category.
2. Longitudinal sleepers located continuously under the rails and connected by flexible tie bars for gauge retention are shown in Fig. 19.8(b).
3. Beam-type single-piece prestressed concrete sleepers, which are quite similar to the conventional wooden-type sleepers in shape, length and supporting area. The British F-23, French VW, German B-70, Japanese 3 Ta and the Indian RDSO-T/2495 are some of the prominent sleepers in the beam type which are shown in Fig. 19.8(c). In contrast to the two-block type, the beam-type sleepers are flexurally stiff over their entire length, and have the additional advantage of providing greater measure of rigidity to the track if the rails are tightly fastened to the sleepers, preventing rotation at the seatings and buckling of the rails. Solid heavy prestressed sleepers have thus made possible the adoption of long welded rails, resulting in smooth running and increased safety of the vehicles and the permanent way.

19.3.3 Design Considerations of Sleepers

The principal function of the rail road tie is to distribute the wheel loads carried by the rails to the ballast. Although the sleeper is a simple determinate structural element, it is not possible to precisely evaluate the loads, to which a concrete sleeper is subjected to during its service life, due to the various uncertainties and complexities inherent in the variables involved, together with the inadequate knowledge of the dynamics of the track structure.

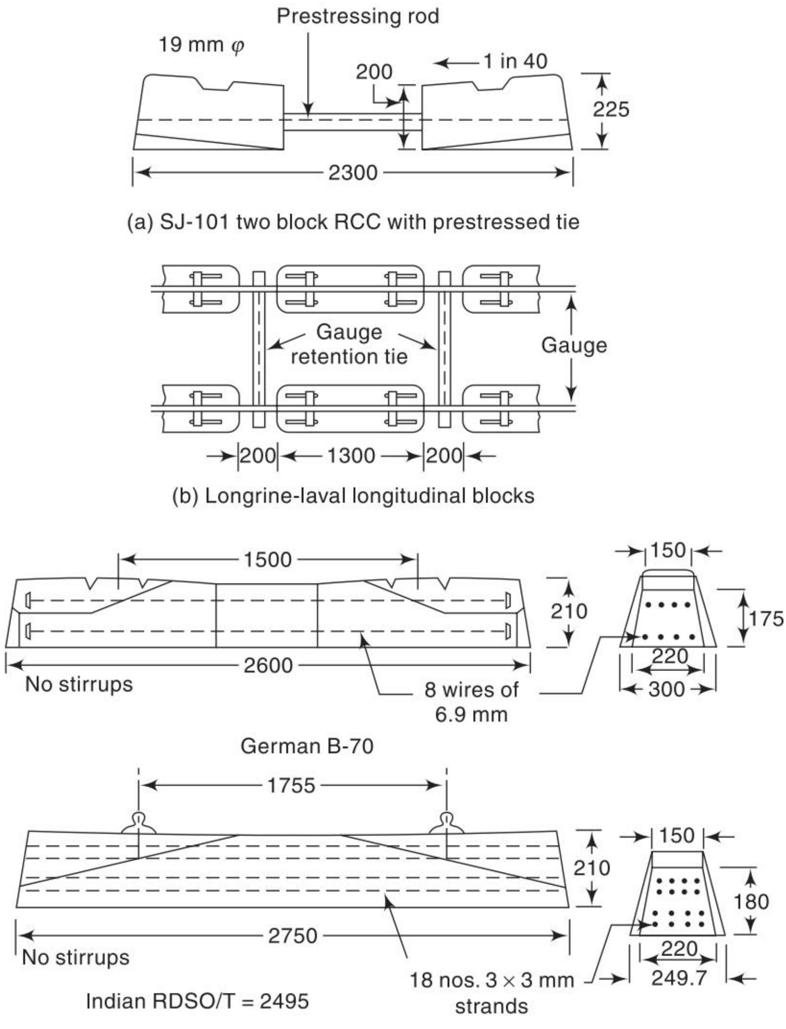

Fig. 19.8 *Different types of prestressed concrete sleepers*

The various factors influencing the design of sleepers are:

1. The static and dynamic loads imposed on rail seats depend upon the type of track (straight or curved), its construction and standard of maintenance, the axle loads and their spacing, the running characteristics, speed and standard of maintenance of vehicles.
2. The ballast reaction on the sleeper, which is influenced by the shape of the sleeper, its flexibility and spacing, the unit weight of the rail, the standard of maintenance of the track and the characteristics of the ballast.

The loading standards and the associated hypothetical ballast pressure distribution have been evolved by various national railway organisations, based on the laboratory and field investigations. The static loads are increased to account for the dynamic effects. The loading criteria and the different conditions of loading adopted by the German, British and Indian railways are shown in Figs 19.9, 19.10 and 19.11, respectively.

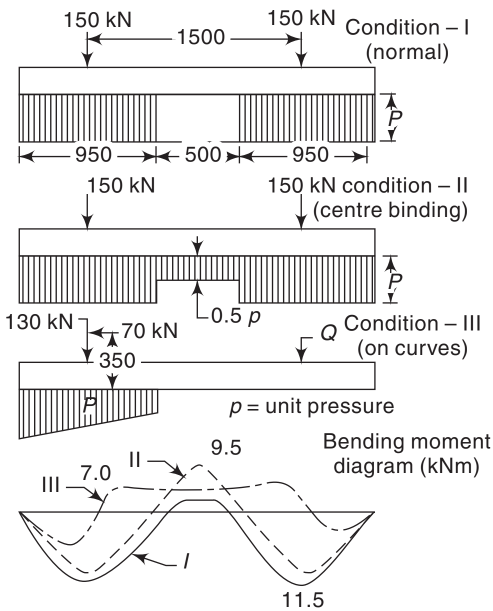

Fig. 19.9 *German B-58 sleeper (Loading and bending moment diagrams)*

The design loads provided for the Indian RDSO-sleeper are more or less similar to those of the German B-58. The loads were adopted based on field observations on the following lines.

Static and Dynamic Loads A static wheel load of 110 kN at the rail head with the heaviest locomotive was found to cause a vertical sleeper reaction of 60 kN on a straight track at the rail seat. On curved tracks, the maximum horizontal wheel load was observed to be 120 kN acting at the rail head. Considering the distribution of this load among several sleepers, it was estimated that 60 per cent of the horizontal reaction (70 kN) is to be resisted by each sleeper. Due to lateral forces in curved tracks, the magnitude of the vertical force is increased on the outer rails and reduced on the inner rails. The force Q shown in Figs 19.9 and 19.11 is a passive rail pressure exerted by the rail to balance the overturning of the sleeper. To allow for dynamic effects, the German and Indian railways have adopted a design load of 150 kN at each rail seat based on the static load of 60 kN which is amplified by a dynamic factor of 150 per cent under different conditions of loading.

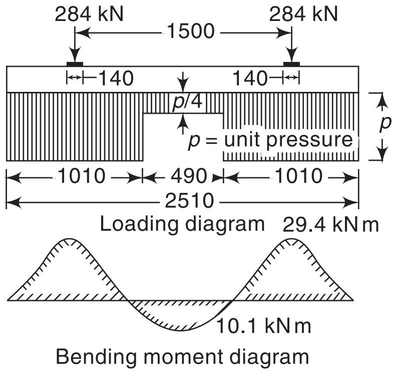

Fig. 19.10 *British F-23 sleeper (Loading and bending moment diagrams)*

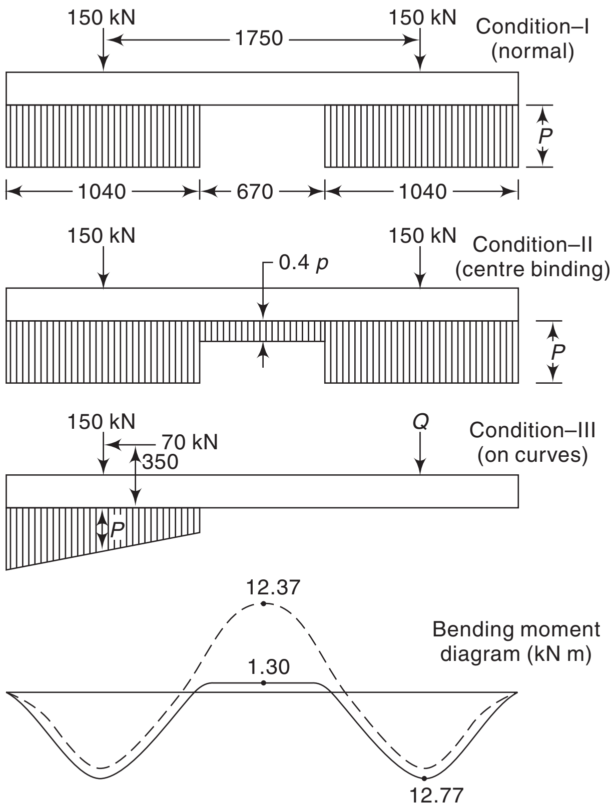

Fig. 19.11 *Indian PCS-2A sleeper (Loading and bending moment diagrams)*

Ballast Reaction The hypothetical distribution of ballast reactions assumed for purposes of design is such that the bending moments computed on the basis of the assumed pressure distribution should more or less conform to the bending moments actually developed at the critical sections, such as the rail seat and centre of sleeper, based on extensive field observations. In addition, the pressure on the ballast should not exceed the permissible allowable pressure on the formation.

The centre binding coefficient, α, defined as the ratio of the intensity of pressure at the centre to that under the rail seat depends upon the maintenance standards, climatic conditions and the length of the sleeper. The values of the coefficient, α, assumed by the various railways are compiled in Table 19.6. The higher values of the coefficient are usually associated with adverse climatic conditions. The ballast is well packed under the rail seats, while the central portion of the sleeper is kept loose to avoid centre binding. But the packing gradually works loose under service over a period of time and the reaction starts building up towards the centre of the sleeper. It is reported by Sikka and Singh[23] that the moment at the centre of the sleeper shoots up by more than tenfold, if the centre binding coefficient increases from zero to 0.5.

Table 19.6 *Values of centre binding coefficient*

Country	*Centre binding coefficient, α*	*Conditions*
Germany	0.50	Frost heaving
Britain	0.25 to 0.50	Depending upon the category of line and maintenance standards; higher value for lower category lines
India	0.40	Broad gauge; no frost heaving
Pakistan	0.40	Broad gauge; no frost heaving

Field observations by the German railways indicate that for sleepers designed for a bending resistance higher than 10 kN m at the centre, the percentage of failures due to cracking of concrete is of the order of one per cent. Hence, the Indian sleeper for broad gauge is designed for a moment capacity exceeding 10 kN m at the centre to safeguard against adverse formations due to the black cotton soil.

19.3.4 Comparison of Various Designs

The salient design features of sleepers of some of the prominent railway systems are compiled in Table 19.7. While most European countries (except erstwhile USSR) have adopted a gauge length of 1.435 m. Indian railways have adopted a broad gauge of 1.676 m, necessitating the use of a longer sleeper. It is interesting to note that the axle loads of the various railways are almost similar in magnitude but the design and resistance moments adopted differ considerably. In the case of the British sleeper F-23, higher vertical rail seat loads and design moments are due to their wider sleeper spacing of 76 cm compared to 63 cm for the German, French and Indian sleepers. It is relevant to note that despite the widely varying design features, European sleepers have been reported to have given satisfactory performance over long periods of service in the track.

Table 19.7 *Comparison of design features of various sleepers*

S. No.	Sleeper designation	German B-58	British F-23	French VW	Indian RDS O/T-2495 Alt-1
1	2	3	4	5	6
1.	Distance between c/c of rails, mm	1500	1500	1500	1755
2.	Design BM, kN m, due to external loads at				
	(1) rail seat	11.50	20.4	—	12.77
	(2) centre	9.50	±10.1	—	–12.37
3.	Safe moments of resistance, kN m, of sleeper at				
	(1) rail seat (bottom)	12.20	30.7	10.4	15.50
	(2) centre (top)	–12.10	–12.1	–6.0	–12.40
4.	Length of sleeper, m	2.40	2.51	2.30	2.75
5.	Residual prestressing force, kN	270	404	300	350
6.	Details of tendons	8/6.9 mm wires	26/5 mm wires	20/5 mm wires	18/3 mm strands
7.	Quantity of high-tensile steel, kg	5.4	10.5	7.0	8.4
8.	Weight of sleeper, kg	235	286	150	282
9.	Concrete strength at 28 days, N/mm^2	60 (20 cm cube)	50 (15 cm cube)	50 (15 cm cube)	52.5
10.	Concrete strength at transfer, N/mm^2	50	28	35	42
11.	Transverse reinforcement	Nil	Nil	Helix	Nil
12.	Cement content, kg/m^3	390	390	350	500
13.	Method of prestressing	<···············Pretensioning···············>			
14.	Method of manufacture	Individual moulds	Long line	Long line	Long line

Indian railways have introduced mono-block prestressed concrete sleepers in the major routes during 1973–74, after detailed investigations by the Research Designs and Standards Organisation[24] and the Structural Engineering Research Centre, Madras[25], regarding the design, development, production and testing of sleepers suited to the Indian conditions. A recent report by Aravindan[26] indicates the satisfactory performance of Indian sleepers in service over a period of time. Prestressed concrete sleepers were found to be not only a favourable choice but also a technical necessity for high-speed and heavy-density tracks from the point of maintainability of track geometry and riding comfort requirements.

The approach of the German federal railways, which is one of the largest users of sleepers, to date, is to evolve optimum designs by successive improvements of earlier marginal designs based on the feedback information from field observations. Recent types include B-70 and B-75, which are longer, heavier and stronger than the B-58 design and suitable for high speed tracks. Similarly, the American rail roads have increased the strength requirement of the sleeper at the rail seat and at the centre in their successive revisions of prestressed concrete sleeper specifications.

19.3.5 Tests for Acceptance of Sleepers

The draft Indian railway standard specifications have laid down acceptance criteria by specifying the minimum cracking and ultimate loads of sleepers. According to this standard, the cracking load should be not less than 18.5. 6.0 and 5.25 *t* for sections at the rail seat bottom, top and bottom of the centre of span, respectively. A minimum failure load of 37.14 *t* has been prescribed for the rail seat bottom section. For testing of sleepers under dynamic loads, the Indian railways has tentatively stipulated a load range of 5–20 *t* and a frequency of 500 cycles per minute for two million cycles applied at the rail seat, the sleeper being supported on a span of 560 mm below the rail seat. The resulting crack after removal of the load should not exceed 0.05 mm in width.

Previous investigations on the fatigue characteristics of plain concrete[27], reinforced concrete[28] and prestressed concrete[29,30] members have indicated that so long as pulsating loads do not exceed 50 per cent of the static ultimate strength of the member in compression or flexure, fatigue failures are rare and the fatigue strength of the member has been extrapolated to exceed 10 million cycles.

The axle loads and train speeds have been gradually increasing over the last few years and it is quite likely that speeds of about 200 km/h could be a common feature for the rolling stock in the next 20–30 years. Some of the advanced countries are already experimenting to develop a new form of permanent way consisting of continuous concrete slab with longitudinal and transverse prestressing without ballast, known as ballastless track, to cater to the needs of the high-speed and high-density traffic of the twenty-first century.

19.4 Prestressed Concrete Pressure Vessels

19.4.1 Introduction

It is estimated that in the coming years, the worldwide annual demand for all forms of energy will increase tremendously and numerous electrical power plants will be required to fulfil this stupendous energy requirement. The demand is all the more acute in developing and under-developed nations and, in view of the limited fossil fuel reserves, the only viable alternative is nuclear power. According to a survey published by the International Atomic Energy Agency in 2000, it is expected that there will be a tremendous increase in the operating reactors in the world by the end of the present century.

The rapid development in the field of nuclear power plants has been made possible by the use of prestressed concrete for the construction of the main vessel, which serves the dual functions of being a pressure container for the reactor coolant and a biological shield, replacing the costly steel pressure vessel. In the present-day reactors, concrete is invariably used as a radiation-shielding material against high-energy X-rays, gamma rays and neutrons because it combines the radiation absorption properties with good mechanical characteristics, is durable and can be moulded to any desirable shape. According to Cockcroft[31], the advent of the prestressed concrete pressure vessel reduces the probability of a catastrophic release of fission products by orders of magnitude. It is also possible, by a suitable arrangement of the boilers and ducts within the pressure vessel to remove the need for large external components capable of direct release of fission products to the atmosphere in the event of fracture.

For developing countries like India, the utilisation of prestressed concrete in nuclear structures is economically more appealing. This is because in the construction of such structures, semi-skilled labour and locally available materials could be used to a greater extent, obviating the costly purchase and transportation of large and heavy steel vessels fabricated abroad. Based on the satisfactory performance of prestressed concrete pressure vessels for advanced gas-cooled reactors, the nuclear power plants in UK are being located much closer to the population centres. The Hartlepool and the Heysham power stations are located at a distance of only 5.5 and 1.6 km from the respective town centres.

19.4.2 Advantages of Prestressed Concrete Pressure Vessels

The use of prestressed concrete biological shields for reactor and containment vessels offers many advantages. The salient benefits as reported by Kulka and Whal[32] are briefly summarised as follows:

1. Reduced possibility of sudden-bursting failures triggered by local cracking, due to the high redundancy of the tendon concrete system. Progressive mode of collapse is ensured so that ample time is available for taking precautionary measures against core melting.
2. High degree of strength reliability, since at the time of initial tensioning, each tendon is proof tested in tension and concrete in compression.
3. The unbonded tendon system provides for periodic surveillance so that retensioning or replacement of damaged tendons is possible during the service life of the reactor.

4. The concrete in the vessel walls being under triaxial compression, higher load factors are available against cracking and failure of the material.
5. Ability to adequately anchor high-pressure piping directly to the concrete through penetration sleeves.
6. Experimental investigations[33] indicate that stress concentrations in concrete due to circular holes do not significantly influence the static and fatigue strength of concrete.
7. Excellent radiation absorption characteristics of high-strength and high-density concrete.
8. Durability and resistance of concrete to moderate temperatures.
9. Feasibility of constructing bigger vessels to withstand higher pressures in the larger plants of the future.

19.4.3 Essential Features

Prestressed Concrete Reactor Vessels (PCRV) The main components of a prestressed concrete reactor vessel of the advanced gas-cooled reactor type (AGR) consists of a reactor core containing stainless steel-clad fuel elements with carbon dioxide as the coolant at working pressures of 3.5–4.2 N/mm^2. The present practice is to use an integral reactor design with the entire gas circuit, including boilers, stand pipes and air blowers located within a single pressure vessel. Generally, the shape of the PCRV is determined by the manner in which the boiler units are located with respect to the reactor core. Cylindrical and spherical shapes have been used for the Oldbury and Wylfa[34] pressure vessels constructed in UK. The typical features of the Oldbury pressure vessel are shown in Fig. 19.12. To make the PCRV leak-tight, a metal liner is provided on the inside of the wall. The maximum temperature on the inside faces of the walls and temperature gradient across the walls of a PCRV are reduced by providing a thermal shield and a cooling system behind the liner. A typical PCRV has a number of penetrations (500 or more), such as refuelling and control rod penetrations and access penetrations.

There has been a rapid development in the technology of PCRVs ever since the first of them was built at Marcoule, France, in 1956. At present, there are more than 25 PCRVs, most of them being located in France and UK. A review of the design and construction of these vessels[35] indicates that PCRVs have been used only for gas-cooled reactors, ranging from CO_2-cooled graphite-moderated to high-temperature helium-cooled versions. The trend is to adopt integrated designs in which the pressure vessel houses the reactor core and the primary steam supply system. The BBRV and Freyssinet system of prestressing are generally preferred and the maximum temperature and temperature gradient permitted are still limited to conservative values which are not detrimental to concrete components.

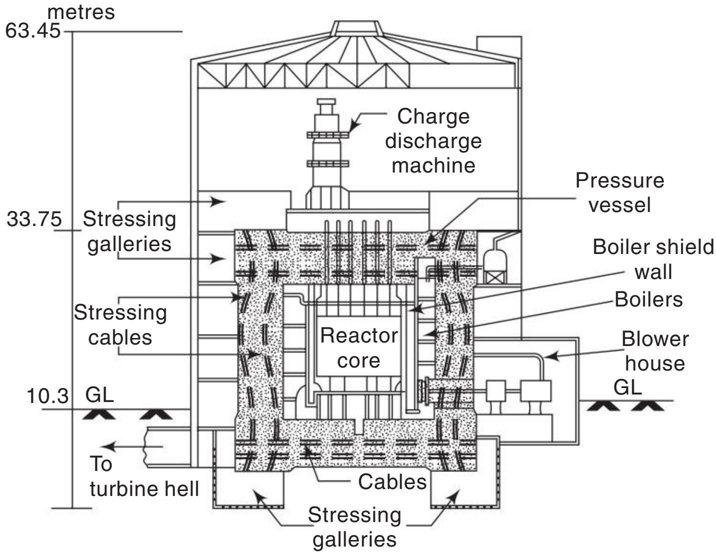

Fig. 19.12 *Transverse elevation of Oldbury pressure vessel*

A major innovation in the layout of reactor components and in prestressing the concrete vessels is incorporated in the two-unit AGR station at Hartlepool, UK, where boilers are housed in vertical cavities passing through the full height of the vessel. This ingenious layout is different from that of the preceding AGR units like Oldbury and Wylfa, in which the boilers are grouped around the reactor core within the same vessel cavity and protected from the core by a shield wall consisting of calcium hydroxide in steel tubes. In the podded boiler concept, the need for special shielding for the boilers is eliminated and the absence of horizontal penetrations in the vessel wall permits the use of slip from construction and circumferential wire winding for prestressing the cylindrical vessel, resulting in considerable economy coupled with speedy construction. The cross-section and plan of the Hartlepool AGR with pod boilers is shown in Fig. 19.13.

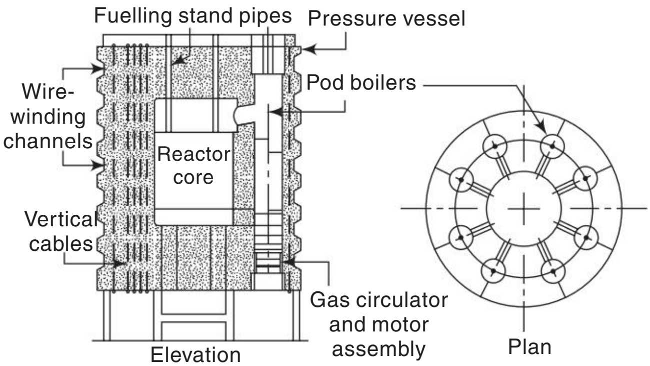

Fig. 19.13 *Hartlepool prestressed concrete pressure vessel*

Prestressed Concrete Containment Vessels (PCCV) Prestressed concrete containment vessels have been extensively used for light watercooled reactors in which the working pressures are of a lower order than gas-cooled reactors. Containment vessels were first developed and used in France and later widely used in USA and India. A PCCV is a secondary containment and the final barrier between nuclear fission products and the environment. In the case of pressurised water reactors, which are (PWR) widely used in USA, the containment generally consists of a cylindrical concrete vessel capped with a shallow dome supported on a flat foundation slab as shown in Fig. 19.14. A liner is generally provided at the inside face of the vessel to make the PCCV leak-tight.

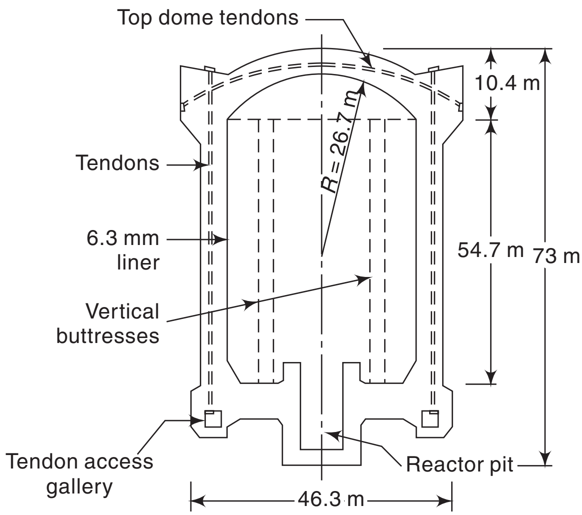

Fig. 19.14 *Elevation of a typical containment vessel*

A steel plate 6–10 mm thick is used as a liner in commercial power plants of USA, while nonmetallic coatings like vinyl/epoxy paints are used in France and Canada. In the case of the Kalpakkam atomic power station located in Tamil Nadu, India, shielding is provided by a double containment system with an inner cylinder of 600 mm thick prestressed concrete surrounded by an outer wall of rubble masonry 711 mm thick. The two walls are separated by an annular air space 1 m wide by 33.5 m above ground level with a provision for venting the gases in the annular space through the stack in a controlled manner.

19.4.4 Analysis and Design

Reactor Vessels The nuclear concrete pressure vessel is an integral part of a complex plant and hence its design is developed in parallel with and profoundly influenced by the remainder of the reactor plant. Both elastic and ultimate load analyses are used to examine the stresses, strains and movements of the vessel structure under serviceability states and the overall factor of safety against collapse. The various loads to be considered in the design include dead loads, live loads, internal pressure, prestress loads, pipe loads and the various reactions. Creep, shrinkage and temperature deformations are important design considerations in the long-term behaviour of the vessel with an effective life period, which may be in excess of 30 years.

According to Rockenhauser[36], a PCRV is analysed for loads at the following stages of construction and operation:

1. During construction
2. Non-pressurised vessel after prestressing
3. Non-pressurised vessel after initial heating
4. Pressurised vessel after initial heating
5. Pressurised vessel at the start of operations
6. Pressurised vessel at the end of design life
7. Non-pressurised vessel at the end of design life

The detailed elastic analysis calls for a method which will account for three-dimensional stresses. Several computer programmes have been developed by Zienkiewicz[37], Otter[38], Gross[39], and others for the analysis of a reactor vessel idealised as an axisymmetric thick walled structure. The programmes are based on finite difference methods of the finite element technique or the dynamic relaxation approach. Generally, the programmes analyse the structure for prestress, pressure, temperature and dead loads. Computer programmes have also been developed by Rashid and Rockenhauser[40], idealising the vessels as an asymmetric assemblage of three-dimensional elements such as tetrahedra.

In the ultimate load analysis, several failure mechanisms and associated ultimate loads are examined, thus satisfying conditions of equilibrium between the loads and the resisting capacity of the structure. The lower bound solution represents very nearly the actual ultimate load of the vessel. Several possible modes of collapse, such as failure of walls and failure of end caps, have been examined by Finigan[41].

The design philosophy generally applicable for a PCRV is:

1. The structure must have an elastic response for all possible combinations of design loads and under test pressure, the stresses developed in the materials being restricted to the values in the relevant codes of practise.
2. The vessel must have a gradual mode of failure under pressure overloads with large deformations before ultimate failure.
3. The pressure at ultimate failure state must be at least 2.5 times the design pressure.

A comparative analysis of the salient design features of the major PCRVs in UK and USA is shown in Table 19.8.

Containment Vessels Prestressed concrete containment vessels are analysed and designed for the maximum credible accident pressure and temperature in conjunction with the wind, earthquake and other environmental forces[42]. According to Halligan[43], a PCCV is generally analysed for the following load combinations:

Table 19.8 *Typical details of prestressed concrete reactor vessels (UK and USA)*

Characteristics	*Units*	*Oldbury*	*Wylfa*	*Dungeness-B*	*Hartlepool*	*Fort St. Vrain*
Power output	MW	300	590	600	622	330
Shape	—	Cylindrical	Spherical	Cylindrical	Cylindrical	Cylindrical
Factor of safety	—	3.00	2.65	2.5 (barrel) 3.0 (caps)		
Design pressure	N/mm^2	2.64	2.95	3.36	4.53	4.85
Mean temperature gradient	°C	30	15	20	—	—
Concrete temperature	°C	55	—	55	60	65
Internal diameter	m	23.50	29.30	20.0	13.12	9.47
Wall thickness	m	4.57	3.40	3.8	—	2.25
Cap thickness	m	6.72	3.60	6.2	5.60	4.73
No. of penetrations less than 0.6 m diameter	—	514	463	505	—	—
No. of penetrations greater than 0.6 m diameter	—	8	8	38	—	—
Liner thickness	mm	12.5	20	12.5	—	—
Total load on foundation pads	t	65000	80000	40000	—	—
Prestressing steel	t	2544	2292	2120	—	—
Reinforcement	t	2800	2438	1220	—	670
Total number of tendons	—	4294	1338	966	—	—
Prestressing system	—	Freyssinet-12/15 mm strand	Freyssinet-36/15 mm strands	BBRV-163/7 mm wires	CCL-wire winding 28 strands of 18 mm dia	BBRV (modified 170/6.3 mm wires
Jack force/tendon	kN	2050	6000	7340	7920	6000
Ultimate strength of tendons	kN	2730	8200	9750	—	—
Concrete						
Aggregate type	—	Lime stone	Lime stone	Flint		
A/C ratio	—	5.1	4.9	4.6	—	—
W/C ratio	—	0.47	0.45	0.43	—	—
Minimum 28-day cube strength	N/mm^2	42.0	37.80	42.0	—	—

1. Transfer of prestress
2. Over-load test condition
3. Sustained prestress and normal live and dead loads
4. Design accident condition
5. Earthquake, wind and other environmental forces

In the case of PCCV, the ratio of the wall thickness to the overall dimensions is much smaller than in the case of reactor vessels, hence the vessel can be analysed by the thin-shell theory without sacrificing much accuracy in the results. Rigorous analysis will be required at the haunch portion between the dome and the cylinder and around the openings in the walls of the vessel.

The two basic criteria for the design of containments are:

1. When a metal liner is provided, its safety should be ensured under all loading conditions. The criterion used in liner design is such as to limit the maximum membrane strain under any load combination to 0.005 and the maximum combined membrane and flexural strain to 0.01.
2. The structure is designed to have a low-strain elastic response such that its behaviour is predictable under all design loadings. Typical details of such prestressed concrete containment vessels are shown in Table 19.9.

Table 19.9 *Typical details of prestressed concrete containment vessels*

Name of Plant	*Type of Reactor*	*Power Output,* MW	*Dimensions,* m		*Con-crete,* m^3	*Design Pressure* N/mm^2	*Prestress-ing Steel,* *t*
			Inside Diameter	*Height*			
Palisades (USA)	PWR	785	35.4	58	13000	0.387	1067
Turkey point No. 3 (USA)	PWR	728	35.4	52	11900	0.415	908
Point beach No. 1 (USA)	PWR	474	32	44.8	10300	0.422	812
Oconee No. 1 (USA)	PWR	822	35.4	64.1	14400	0.415	1168
EL-4 at Brennilis (France)	HWGCR	70	46.0	55.6	9600	0.16	500
Kalpakkam (India)	PHWR	200	39.7	52.8	—	0.115	350

PWR — Pressurised light-water moderated and cooled reactor

HWGCR — Heavy water moderated, gas-cooled reactor

PHWR — Pressurised heavy water moderated and cooled reactor

Since the performance requirements of reactor and containment vessels are more stringent than those for ordinary structures, the existing design practices and codes for reinforced and prestressed concrete structures are inadequate. The provisions of ACI 349[44] and ASME code[45] are useful in design of concrete pressure vessels.

19.4.5 Prestressing Tendons for Pressure Vessels

The prestressing systems which are widely used for pressure vessels are:
1. Freyssinet
2. BBRV (button head)
3. SEEE, strand system
4. CCL system

It is reported that prestressing materials, labour and equipment account for 60–70 per cent of the cost of a prestressed concrete pressure vessel,[46] and hence the importance of the choice of the prestressing system. In typical prestressed concrete pressure vessels, the circumferential prestressing forces required are about 60–1000 MN/m for the cylindrical walls of the vessel. Various design considerations, such as the crossing of the longitudinal and circumferential tendons and, openings in the vessel and anchorage zones, call for a reduction in the number of tendons, thus entailing prestressing forces of about 4000–8000 kN per tendon. The latest developments include the 10 MN Freyssinet tendons made up of 61/15 mm strand and the BBRV tendons consisting of 121, 163, or 187 wires of 7 mm diameter with ultimate loads of 7.7, 10.2 and 12 MN, respectively. The use of circumferential wire winding in place of independent curved tendons results in considerable economy due to the reduction in the number of anchorages. In the Hartlepool vessel, circumferential wire winding has been adopted resulting in considerable advantages.

Generally, the prestressing tendons are not grouted in the case of pressure vessels, and protection against corrosion is ensured by filling the ducts with a petroleum-based jelly. The unbonded tendons facilitate pretensioning operations whenever required and the force in the tendons can be checked periodically.

19.5 Prestressed Concrete Pavements

19.5.1 General Features

The provision of joints at close intervals in a concrete pavement to permit expansion or contraction is detrimental from the considerations of strength and riding quality. The stresses in a slab resting on an elastic medium under the action of a concentrated load increases as the load approaches the free edge and is a maximum when the load is at the corner zones. Hence, smaller slab sizes in a long roadway result in a large number of high-stress zones, such as corners and edges. Due to the differential vertical movement between adjacent slabs, the riding quality of the road deteriorates as the number of joints increase within a given stretch of the road.

The advantages of prestressing the pavements were realised as early as in 1939, when it was used in America to prevent the formation of shrinkage and temperature cracks during the early life of the concrete[47]. Longitudinal prestressing can effectively eliminate the formation of cracks in slabs. In addition, expansion joints and weak edge zones are entirely eliminated by the introduction of moderate precompression in the concrete slabs. The introduction of the jet aircraft has necessitated the use of jointless runways, as the sealing compounds used as joint fillers cannot withstand the high temperatures of the exhaust gases of the jet engine.

Realising the immense advantages of prestressing the pavements, Freyssinet[48] used it for prestressing part of the runways at Orly airport as early as in 1947. Since then, prestressed roads and airport runways have been constructed in a number of countries in the world.

Prestressed concrete offers the advantages of a smoother surface, a water-tight covering for the subgrade, a longer life and a significant reduction in the construction joints in air-field runways and taxiways. Many major airports, such as Schiphol (Amsterdam), Laguardia (New York), Algiers and Kuwait, have been constructed utilising prestressed concrete.

19.5.2 Methods of Prestressing Pavements

Longitudinal prestressing of the slabs is achieved either by external prestressing against rigid abutments or by internal prestressing by means of tensioned bars or cables. The method of external prestressing by using flat jacks against fixed abutments at the ends of the slab has the following disadvantages:

1. Difficulty of providing unyielding abutments; yielding of abutments reduces the prestress in the slab.
2. The compressive stress in the slab gradually decreases with time due to the shrinkage and creep of concrete.
3. The system of external prestressing is applicable only to straight cables lying wholly in one plane. If applied to curved slabs, instability of the system develops due to the buckling effect.

The method of internal prestressing by different arrangement of cables and anchorages lying within the slab is ideally suited for long runways. Typical layouts of cables and anchorages used in the internal prestressing system is shown in Fig. 19.15. The simplest and the most commonly used arrangement of longitudinal and transverse cables used for prestressing a two-lane road slab is shown in Fig. 19.15(a). The transverse prestress eliminates the need for using dowel bars across the longitudinal joint.

By using oblique cables as shown in Fig. 19.15(b), longitudinal and transverse prestress is produced in the slab. The ratio of longitudinal to transverse prestress depends on the angle of inclination of cables and can be varied to suit the length/width ratio of the pavement. This system was used by Freyssinet for experimental road slabs and was also adopted for the first experimental prestressed road in UK.[49] The oblique cable system requires a large number of anchorages in the case of long runways. Alternatively, the slabs can be prestressed by two anchorage yokes positioned at the centre of the slab as shown in Fig. 19.15(c). The wires are fanned out at the ends of the slabs to form an anchorage by bond. At the ends of the slab, prestress is available in both directions, while in the other portions of the slab, transverse bending has to be resisted by steel reinforcement or by transverse system of cables.

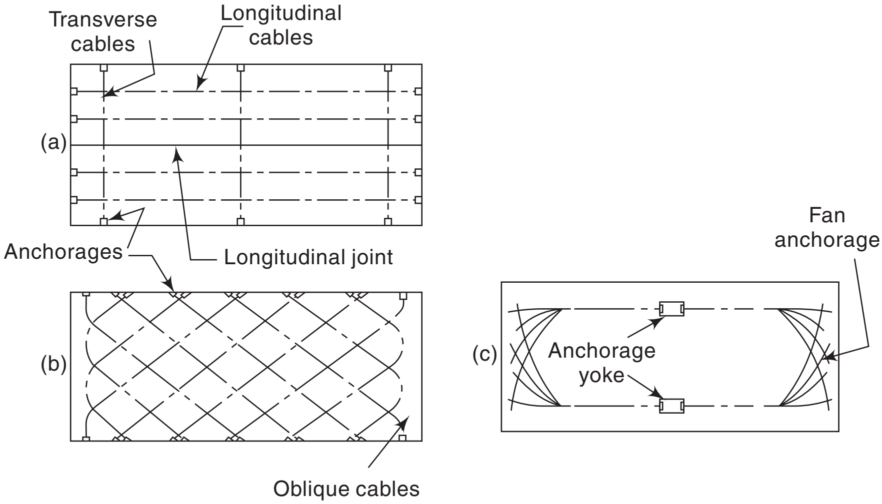

Fig. 19.15 *Internal prestressing methods for pavements*

19.5.3 Design of Prestress in Pavements

The precompression required in a concrete pavement is significantly influenced by the friction between the subgrade and the pavement. The prestress in the slab gradually decreases towards the centre from the edges due to the friction as shown in Fig. 19.16.

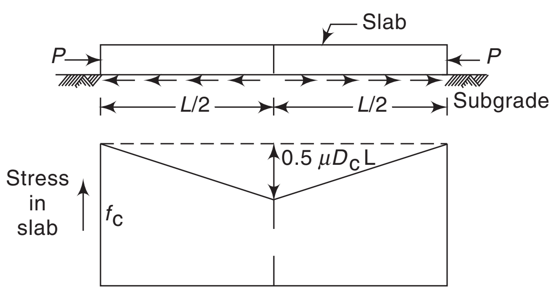

Fig. 19.16 *Loss of prestress in slab due to friction of subgrade*

If f_c = compressive prestress in concrete at the ends of slab
μ = coefficient of friction between subgrade and pavement
D_c = density of pavement
L = length of pavement

The minimum prestress available at the centre of slab = $f_c - 0.5\ \mu\ D_c L$. Tests have indicated that the coefficient of friction varies between 1.0 and

1.5. The high values are due to edge friction and other additional restraints. For slabs laid on a thin bed of sand, Weil[50] recommends a value of $\mu = 1.0$. However, if the sand surface is covered with a paper or polyethylene sheeting, the coefficient of friction is further reduced to 0.6. If the subgrade is levelled by a cement mortar base coated with a layer of tallow or paraffin or overlaid with two layers of paper coated with a sliding compound, the coefficient of friction is further reduced to 0.25–0.5. The recommended thickness of prestressed concrete slabs is 150–200 mm for roads and 160–240 mm for runways[51].

Stress computations in a slab, 120 m long, laid on a subgrade having a modulus of 80 N/cm^3 and a friction coefficient of 0.6 indicate tensile stresses of about 5–6 N/mm^2 under a 100 kN wheel load with a ground pressure of 0.7 N/mm^2.[52] These high-tensile stresses develop at the bottom of the slab. Leonhardt recommends the use of limited prestressing in runway slabs so that tensile stresses of 2–3 N/mm^2 is permitted in concrete, which corresponds to about half the tensile strength of the material. Accordingly, a longitudinal prestress of 2–3 N/mm^2 is recommended, which completely eliminates tensile stresses at the top of the slab[53].

Investigations on stresses developed in highway slabs in Germany and USA due to temperature and shrinkage have indicated that bending stresses due to temperature are about 3–3.5 N/mm^2, depending upon the climate and thickness of the slab, while the effects due to shrinkage are negligibly small.

In the case of slabs with oblique cables, with an arrangement as shown in Fig. 19.17, the longitudinal and transverse prestress are expressed as components of the forces in the oblique cable system in the direction of the length and width of the slab. Hence, if

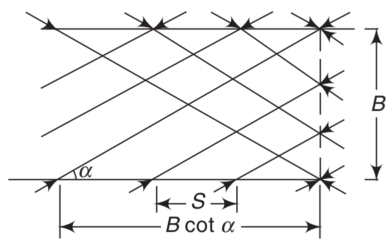

Fig. 19.17 *Oblique cable system for pavements*

B = width of slab
t = thickness of slab
s = spacing of cables
P = prestressing force in each cable
L = length of slab
α = obliquity of the cables

the minimum longitudinal and transverse prestress at the centre of slab, allowing for losses due to friction, is expressed as:

$$\text{Minimum longitudinal prestress, } f_{cL} = \left[\frac{2P \cot\alpha \cos\alpha}{ts}\right] - (0.5\,\mu D_c L)$$

$$\text{Minimum transverse prestress, } f_{cT} = \left[\frac{2P \sin\alpha}{ts}\right] - (0.5\,\mu D_c B)$$

If the cables have to be arranged at an angle α and a spacing s, ensuring a specified minimum longitudinal and transverse prestress, they can be computed using the following equations:

$$\tan \alpha = \sqrt{\frac{2f_{cT} + \mu D_c B}{2f_{cL} + \mu D_c L}} \qquad S = \left[\frac{4P \sin \alpha}{t(2f_{cT} + \mu D_c B)}\right]$$

In the case of motorways, the transverse prestress is eliminated if the slab is provided with longitudinal joints spaced at intervals of 3.75 m, with the slab thickness not less than 200 mm. However, the slab has to be lightly reinforced in the transverse direction. In the case of multilane highways and airfield runways which have widths that exceed 60 m without longitudinal joints, transverse prestress is essential. Tests carried out in USA[54] indicate that the transverse prestress of 70 per cent of the longitudinal prestress would result in the slabs performing satisfactorily. However, the minimum value of transverse prestress should be not less than 1.2 N/mm^2.

The design of prestressed runways is illustrated in the following examples:

Example 19.4 Design a suitable longitudinal and transverse prestressing system for a two-lane highway, 7.5 m wide and 100 m long. The thickness of the slab is 150 mm. The coefficient of friction between the slab and subgrade is estimated to be 1.5. Freyssinet cables of 12–5 mm are available for use at site. A minimum longitudinal prestress of 2 N/mm^2 should be ensured.

Solution. The longitudinal prestress required at the ends of the slabs after allowing for loss due to friction is given by,

$$f_c = (2 + 0.5\mu\, D_c L) = \left\{(2) + \left[\frac{(0.5 \times 1.5 \times 24 \times 10^3 \times 100)}{10^6}\right]\right\} = 3.80 \text{ N/mm}^2$$

$$\text{Total prestressing force, } P = \left[\frac{(3.8 \times 7.5 \times 1000 \times 150)}{1000}\right] = 4300 \text{ kN}$$

$$\text{Force in each cable} = \left[\frac{20 \times 1200 \times 12}{1000}\right] = 288 \text{ kN}$$

$$\text{Spacing of longitudinal cables} = \left[\frac{7.5 \times 1000 \times 288}{4300}\right] = 500 \text{ mm}$$

$$\text{Transverse prestress} = (0.7 \times 3.80) = 2.66 \text{ N/mm}^2$$

$$\therefore \quad \text{Force/m} = \left[\frac{2.66 \times 1000 \times 150}{1000}\right] = 399 \text{ kN/m}$$

$$\therefore \quad \text{Spacing of transverse cables} = \left[\frac{(288 \times 1000)}{399}\right] = 720 \text{ mm}$$

Example 19.5 Design an oblique cable system for an airport runway, 150 m long and 20 m wide, using Freyssinet cables of 12–5 mm diameter. The coefficient of friction between the pavement and the subgrade may be taken as 1.0. Determine the obliquity and spacing of cables. The thickness of pavement is 200 mm and the minimum longitudinal and transverse prestress should be not less than 2 and 1.5 N/mm^2, respectively.

Solution. Given

$$t = 200 \text{ mm} \qquad B = 20 \text{ m}$$
$$f_{cL} = 2 \text{ N/mm}^2 \qquad L = 150 \text{ m}$$
$$f_{cT} = 1.5 \text{ N/mm}^2 \qquad \mu = 1.0$$

$$\therefore \quad \tan\alpha = \sqrt{\frac{2f_{cT} + \mu D_c B}{2f_{cL} + \mu D_c L}}$$

$$\mu D_c B = (1.0 \times 24 \times 10^3 \times 20)/10^6 = 0.48 \text{ N/mm}^2$$
$$\mu D_c L = (1.0 \times 24 \times 10^3 \times 150)/10^6 = 3.60 \text{ N/mm}^2$$

$$\therefore \quad \tan\alpha = \sqrt{\frac{(2\times 1.5) + 0.48}{(2\times 2) + 3.60}} = 0.68$$

$$\therefore \quad \alpha = 34°13'$$

Spacing of cables, $$s = \left[\frac{4P\sin\alpha}{t(2f_{cT} + \mu D_c B)}\right]$$

Force in each cable, $$P = \left[\frac{(20\times 1200\times 12)}{1000}\right] = 288 \text{ kN}$$

Spacing $$s = \left[\frac{4\times 288\times 10^3\times 0.5622}{200(2\times 1.5 + 0.48)}\right] = 930 \text{ mm}$$

References

1. Bennett, E W, *Prestressed Concrete Theory and Design*, Chapman and Hall, London, 1962, pp 185–187.
2. Dimitriev, S A, "Prestressed concrete poles," *Proceedings of the Symposium on Mass Produced Prestressed Concrete Elements*, Madrid, June 1968, pp 59–80.
3. Venkateswara Rao, A, "Application of AVRO system for the manufacture of poles", *Proceedings of the International Symposium on Prestressed Concrete Pipes*, *Poles*, *Pressure Vessels and Sleepers*, Madras 1972, paper PL/7, pp 1–8.
4. Zacharia George *et al*., "Prestressed concrete poles state of art," *Proceedings of the International Symposium on Prestressed Concrete Pipes*, *Poles*, *Pressure Vessels and Sleepers*, Madras 1972, PL/0, pp 1–35.
5. Macerata, S, "Prestressed concrete conductor mast in South Africa", *Concrete and Constructional Engineering*, 45, 1950, pp 13–19.
6. IS: 1678–1998 (Reaffirmed 2003), *Specification for Prestressed Concrete Pole for Overhead Power Traction and Telecommunication Lines*, BIS, New Delhi-1998, pp 1–6.
7. Gerwick, B C, *Construction of Prestressed Concrete Structures*, Wiley Inter Science, New York, 1971, pp 343–348.
8. *Practical Recommendations for the Design and Construction of Prestressed Concrete Structures*, FIP-CEB Committee report, June 1966, Cement and Concrete Association, London, pp 1–81.
9. Krishna Raju, N and L N Ramamurthy, "Limit state design of pretensioned partially prestressed concrete poles," *Proceedings of the International*

Symposium on Prestressed Concrete Pipes, Poles, Pressure Vessels and Sleepers, Madras 1972, Paper PL/6, pp 1–15,

10. Abeles, PW, *An Introduction to Prestressed Concrete*, II, Concrete Publications Limited, London, 1966, pp 462–464.
11. Beeby, AW and HPJ Taylor, *Cracking in Partially Prestressed Members*, Sixth FIP Congress, Prague, June 1970, pp 1–12.
12. Bell, BJ, *Practical Prestressed Concrete Design*, Pitman, London, 1964, pp 85–90.
13. Gerwick, BC, *Construction of Prestressed Concrete Structures*, Wiley Inter Science, New York, 1971, pp 167–208.
14. Shu-T'ien LI and Tony Chen-Yeh LIU, "Prestressed concrete piling—Contemporary design practice and recommendations," *Journal of the American Concrete Institute, Proceedings*, 67, No. 3, March 1970, pp 201–220.
15. "Recommended practice for design, manufacture and installation of prestressed concrete piling developed by PCI committee on prestressed concrete piling," *Journal of the Prestressed Concrete Institute*, 22, March/April 1977, pp 20–49.
16. *Design of Prestressed Concrete Piles*, Prestressed Concrete Institute Chicago, Illinois, 1977.
17. Shu-T'ien LI, "Functional optimum prestress for different classes of prestress concrete piling," *Seminar on Problems of Prestressing, Preliminary Publication*. Indian National Group of IABSE, Madras 1970, pp 1–1 to 1–22.
18. Freyssinet, E, "Une revolution dans I'rart de batir les constructions pre contraintes", *Travaux* 25, Nr. 101. Nov. 1941, pp 335–359.
19. Werner Bruckner, W and AG, Thost., "Some notes on the design, manufacture and use of Thosti BBRV prestressed concrete sleepers," *Proceedings of the International Symposium on Prestressed Concrete Pipes, Poles, Pressure Vessels and Sleepers*, Madras 1972, Paper.
20. Kunze Walter, E, "Survey of European concrete cross ties," *Proceedings of the Structural Division of ASCE*, 88, April 1962, pp 111–135.
21. Ager, JWA, "General report on prestressed concrete railway sleepers, mass produced prestressed precast elements," *Proceedings of the Symposium held at the Institute Eduardo Torroja de la Construction. del Cemento*, Madrid 3 and 4 June 1968, FIP June 1968, pp 81–91.
22. Sambamoorthi, RM *et al.*, "Prestressed concrete sleepers state of art," *Proceedings of the International Symposium on Prestressed Concrete Pipes, Poles, Pressure Vessels and Sleepers*, Vol. 1, Madras 1972, pp SL/0–23.
23. Sikka, NK and SP Singh, "Some aspects of design of mono-block prestressed concrete sleepers," *Proceedings of the International Symposium on Prestressed Concrete Pipes, Poles, Pressure Vessels and Sleepers*, Vol. 1, Madras 1972, pp SL/2–24.
24. *Draft lndian Railway Standard Specifications for BG Prestressed Concrete Sleepers* (Pretensioned type), Research Design and Standards Organisation, Ministry of Railways, Lucknow, July 1975.
25. "Investigation on prestressed concrete mono-block sleepers," *Project Report of SERC*, Madras, Sept. 1975.
26. Aravindan, N, "Mono-block prestressed concrete sleepers on Indian railways, a performance review", *All-India Seminar on Prestressed Concrete Structures, Proceedings*, Vol. 1, Madurai, 1979, pp 239–254.

27. Krishna Raju, N, “Prediction of fatigue life of plain concrete in compression”, *Building Science*, London, 4, 1969, pp 99–102.
28. Hajnal Konyi, K, “Comparative tests on beams reinforced with plain round and tentor bars under repeated loading,” *Symposium on Bond and Crack Formation in Reinforced Concrete*, *RILEM Bulletin*, Vol. 1, Stockholm, June 1957.
29. Ekberg, CE Jr, RE Walther and RG Slutter, “Fatigue resistance of prestressed concrete in bending,” *American Society of Civil Engineers*, *Journal of Structural Division*, Paper 1304, Vol. 83, No. ST-4,1957.
30. Venuti, WJ, “A statistical approach to the analysis of fatigue failure of prestressed concrete beams,” *Journal of the American Concrete Institute*, *Proceedings*, Vol, 62, No. 11, Nov. 1965, pp 1375–1394.
31. Cockcroft, J, “Opening remarks–Conference on prestressed concrete pressure vessels”, *Institution of Civil Engineers*, London, 1968, pp 1–2.
32. Kulka Felix and W Wahl Howard, “American practices in the design of prestressed concrete containment structures,” *Journal of the Prestressed Concrete Institute*, June 1968.
33. Krishna Raju, N, “Effect of stress concentrations on the static and fatigue strength of concrete in compression,” *Journal of Materials and Structures*, RILEM, Paris, 3(14) March/April, 1970, pp 85–89.
34. Hay, JD, “The construction of prestressed concrete pressure vessels in Britain,” *13th Annual Convention of the Prestressed Concrete Institute*, *Montreal*, Concrete Society, London, Oct. 1967, pp 1–12.
35. Tan Chen, P, “A review of the technology of prestressed concrete reactor pressure vessels,” *Nuclear Safety*, 11(1), Jan/Feb. 1970.
36. Rockenhauser, W, “Structural design criteria for primary containment structures (prestressed concrete reactor vessels),” *Nuclear Engineering and Design*, 9(4), April 1969.
37. Zienkiewicz, OC, DRJ Owen, and DV Phillips, “Finite element method in analysis of reinforced and prestressed concrete structures,” *Preprints of the First International Conference on Structural Mechanics in Reactor Technology*, *Berlin*, Sept. 1971, Paper M5/l.
38. Otter, JRH, “Computations for prestressed concrete reactor pressure vessels using dynamic relaxation,” *Nuclear Structural Engineering*, 1, Jan. 1965, pp 61–75.
39. Gross, H, “Thermo-visco-elastic axisymmetric stress analysis by finite element and finite difference computer techniques,” *Preprints of the First International Conference on Structural Mechanics in Reactor Technology*, Berlin, Sept. 1971, Paper M5/5.
40. Rashid, YR and W Rockenhauser, “Pressure vessels analysis by finite element techniques,” *Proceedings of the Conference on Prestressed Concrete Pressure Vessels*, London, March 1967, pp 375–383.
41. Finifan, ACGI, “Ultimate analysis of the Dungeness B Vessel,” *Proceedings of the Conference on Prestressed Concrete Pressure Vessels*, London, March 1967, pp 323–328.
42. Appa Rao, TVS, MS Rao, and S Arthanari, “Prestressed concrete pressure vessels-state of the art,” *Proceedings of the International Symposium on Prestressed Concrete Pipes*, *Poles*, *Pressure Vessels and Sleepers*, 1, Madras 1972, Paper PR/0, pp 1–29.

43. Halligan, D W, "Structural design criteria for secondary containment structures," *Nuclear Engineering and Design*, *8(4)*, Nov/Dec 1968.
44. Report of the ACI-Code Committee 349, "Criteria for reinforced concrete nuclear power containment structures," *Journal of the American Concrete Institute*, *Proceedings*, 69(1), Jan. 1972, pp 2–10.
45. Asme, *Boiler and Pressure Vessels Code*, Section IV, *Nuclear Power Plant Components*, *Division 2*, *Concrete Reactor Vessel and Containments*, Asme, May 1971, (Draft).
46. Burrow, RED, "Prestressing tendon systems," *Proceedings of the Conference on Prestressed Concrete Pressure Vessels*, London, March 1967, pp 251–257.
47. Russe, FW, "A stress cured concrete pavement," *Engineering News Record*, 123, Nov. 1939, pp 632.
48. Netter, L, and E Becker, "Piste en beton precontraint (prestressed concrete runway)", *Travaux*, 32, 1948, pp 147–154 and 179–186.
49. Mcintosh, A J W and J Mercer, "Construction of a prestressed road at Crawly New Town," *Proceedings of the Institution of Civil Engineers*, Part II, 1, 1952, pp 220–234.
50. Well, G, Der Verschiebewiderstand Von Beton fahrbahnplatten, *Beton Stropen Jahrbuch Fachverband Zement*, Köln, 1960, pp 183–206.
51. Leonhardt, Fritz, *Prestressed Concrete Design and Construction*, Wilhelm Ernst and Sohn, Berlin 1964, pp 554–567.
52. Rose, E A, Spannbeton in Strassenbau, *Beton Strassen Jahrbuch*, *Fachverband Zement*, Köln, 1960, pp 41–96.
53. Stott, J P, *"Prestressed concrete roads," Proceedings of the Institution of Civil Engineers*, Part II, Vol. 4, 1955, pp 491–538.
54. Renz, C F and P L Melville, "Experience with prestressed concrete air field pavements in the United States," *Journal of Prestressed Concrete Institute* 6(1), March 1961, pp 75–92.

Review Questions

19.1 What are the advantages of prestressed concrete poles?

19.2 Explain with sketches the different types of cross-sections generally used for poles.

19.3 List the various design criteria to be considered while designing poles for power transmission lines.

19.4 What are the advantages of partially prestressed pretensioned poles?

19.5 Sketch the typical details of reinforcements generally adopted in prestressed concrete piles.

19.6 Explain with sketches, the typical cross-sections of prestressed concrete sheet piles.

19.7 What are the different types of prestressed concrete sleepers? Mention their design considerations.

19.8 What are the advantages of prestressed concrete pressure vessels?

19.9 What are the prestressing systems generally used for pressure vessels? Explain with practical examples.

19.10 What are the advantages of prestressed concrete pavements? Briefly outline the design features of prestressed concrete pavements.

Objective-type Questions

19.1 Prestressed concrete electric poles are generally prestressed with
(a) eccentric prestress (b) axial prestress (c) transverse prestress

19.2 Prestressed concrete poles are mass produced using
(a) separate forms for each unit
(b) long line method of pretensioning
(c) post-tensioning each unit

19.3 The ideal cross-section for a prestressed concrete pole to resist various types of lateral forces is
(a) square (b) rectangular (c) circular

19.4 In the design of PSC electric poles, combined bending and torsion develops due to
(a) wind load
(b) skew snapping of wires
(c) eccentric snapping of wires

19.5 Most widely used cross-section of a prestressed concrete pole is
(a) square (b) octagon (c) circle

19.6 Prestressed concrete sleepers should be designed to resist
(a) static loads
(b) static and dynamic loads
(c) dynamic loads

19.7 The Indian PSC sleeper for broad gauge is designed for a moment capacity exceeding
(a) 5 kN m (b) 10 kN m (c) 8 kN m

19.8 Unbonded tendons used for prestressing of nuclear reactor containment vessels result in
(a) higher load factor against collapse
(b) prevent leakage
(c) periodic surveillance and retensioning

19.9 In the case of embankments to retain soils, it is preferable to adopt
(a) bearing piles
(b) sheet piles
(c) anchor piles

19.10 The primary advantage of prestressing the airport pavements is to
(a) increase the bearing strength
(b) resist dynamic loads
(c) prevent shrinkage and temperature cracks

Answers to Objective-type Questions

19.1 (b)	19.2 (b)	19.3 (b)	19.4 (b)	19.5 (a)
19.6 (b)	19.7 (b)	19.8 (c)	19.9 (b)	19.10 (c)

20 Introduction to Optimum Design of Prestressed Concrete Structures

20.1 Principles of Optimisation

According to Gallaghar and Zienkiewicz[1], the primary objective of structural optimisation is to determine the most suitable combination of design variables resulting in satisfactory performance of the structure subject to the behavioural and geometric constraints imposed, with the goal of optimality being defined by the objective function for specified loading or environmental conditions. The basic features of the structural optimisation problem are:

1. Design variables
2. Objective function
3. Constraints

Basically, the process of optimum design of prestressed concrete structures is treated as a mathematical programming problem in which the total cost or quantity of material is minimised, subject to certain functional constraints, such as the limitation of stresses, deflections and crack widths at serviceability limit states and strength requirements at the limit state of collapse.

Solution to optimisation problems involve lengthy and tedious computations. The advent of high-speed electronic computers revived the interest in optimisation techniques after the pioneering work of Dantzig[2], who developed the simplex algorithm for the solution of linear programming problems.

20.2 Methods of Optimisation

The first approach is the *theory of layout*, in which uniaxial members are arranged to yield a minimum volume structure for specific loads and materials based on the theorems of Maxwell wand and later developed by Cox[3]. The second approach developed in 1950 before the advent of computers in 1940 was termed as *the simultaneous mode of failure approach* in which each component of the structure reaches its limit of strength as the structure reaches the limit state of collapse. This approach has limited applicability to practical design as reported by Shanley[4].

The third major approach of structural optimisation is based on the concept of the *criterion of optimality* developed by Prager[5] and Taylor[6] using the principles of structural mechanics. Using this approach and finite element techniques, large scale computer programmes have been developed by Venkayya[7] to solve transmission tower problems yielding minimum weight design.

The fourth major development is the *Mathematical Programming Formulations*, first applied to structural optimisation problems by Livesley[8] and Pearson[9].

The structural optimisation problem is generally expressed in the mathematical form, involving the design variables, objective function and constraints as,

minimise $Z = F(x)$ subject to $G_j(x) \leq 0 \qquad j = 1, 2, \ldots, m,$

where x is the design variable, represented by the column vector of dimensions n. Each design is represented by x is a point in hyper-space defined by the design variables.

$F(x)$ = the objective or merit function
$G_j(x)$ = constraints
m = number of constraints

Design variables The design variables are generally grouped as,

(a) Dimensional variables represented by the member sizes, such as the thickness of a plate, cross-sectional area of a member and second moment of area of a flexural member.
(b) Configuration or geometric variables, represented by the co-ordinates of element joints.
(c) Variables involving the mechanical or physical properties of the material, such as strength, modulus of elasticity, density, etc.

In most of the structural optimisation problems, the geometry and material properties are pre-assigned and selection of sizes forms the main problem.

Constraints A constraint is a limitation imposed directly on a variable in order that a design is acceptable. They are expressed as equality/inequality form under the following groups:

(a) Side constraints are specified limitations (minimum/maximum) which are of explicit form.
(b) Behaviour constraints are imposed on the structural response such as deflections, expressed by formulae presented in design specifications.

Objective function In a structural design problem, there should be a well-defined criterion such as performance or cost of the structure which is judged as a design variable. This index is generally referred to as objective cost or merit function comprising cost of steel or concrete.

20.3 Optimisation Techniques

The process of optimisation begins with an acceptable design point in a mathematical programming method followed by selection of a new point so as to minimise the objective function. In linear/non-linear programming, there are several well-established techniques for selecting a new point and to proceed towards the optimum point.

20.3.1 Linear Programming

In a linear programming problem, the objective function and constraints are linear functions of the design variables and the solution is based on the elementary properties of systems of linear equations. In the mathematical formulation of the linear programming problem, properties of systems proportionality, additivity, divisibility and deterministic features are utilised. Linear programming problems are conveniently solved by the revised simplex method[10].

20.3.2 Non-linear Programming

In non-linear programming problems, the objective function and/or constraints are non-linear functions of the design variables. Some of the prominent techniques to sole such problems are:

1. Method of feasible directions
2. Sequential unconstrained minimisation technique (SUMT)
3. Sequential linear programming
4. Dynamic programming

The two well-known procedures based on the philosophy of the method of feasible directions are Rosen's gradient projection algorithm[11] and Zoutendijk's procedure[12]. In the sequential unconstrained minimisation technique, the constrained minimisation problem is converted into an unconstrained one by introducing an interior or exterior penalty function. The simplified method suggested by Fiacco and McCormick[13] is useful in solving structural design problems.

In sequential linear programming, the non-linear objective function and constraints are linearised in the vicinity of the starting point by using the move limit method of Pope and the improved method suggested by Ramakrishnan and Bhavikatti[14] for optimisation problems.

Dynamic programming developed by Bellman[15] in the early 1950's is basically a mathematical approach for multistage decision problems. This technique has been used for optimising the shape of pin jointed structures like transmission towers by Palmer and Sheppard[16].

20.4 Application to Prestressed Concrete Structures

In the design of prestressed concrete structural elements, the objective or merit function is generally the total cost of the member per unit length comprising the individual costs of concrete, high-tensile steel and supplementary reinforcement. In a typical flexural member, the objective function can be expressed as,

$$F(x) = [C_c A + C_s A_s + C_p A_p] \tag{20.1}$$

where $F(x)$ = cost of the member per unit length

C_c C_s and C_p = unit costs of concrete, supplementary and high-tensile steel, respectively.

A, A_s and A_p = areas of concrete, supplementary and high-tensile steel, respectively.

The constraints imposed in the design of a prestressed concrete flexural member are generally the following:

1. Stresses developed at the top and bottom fibres of the critical section at the stage of transfer of prestress and under service loads. These conditions yield four inequalities, expressed as (Refer to Eqs 12.1 to 12.4).

$$\left[\frac{P}{A} - \frac{Pe}{Z_t} + \frac{M_g}{Z_t}\right] \geq f_{tt} \tag{20.2}$$

$$\left[\frac{P}{A} + \frac{Pe}{Z_b} + \frac{M_g}{Z_b}\right] \leq f_{ct} \tag{20.3}$$

$$\left[\frac{P}{A} - \frac{Pe}{Z_t} + \frac{M_g + M_q}{Z_t}\right] \leq f_{cw} \tag{20.4}$$

$$\left[\frac{P}{A} + \frac{Pe}{Z_b} + \frac{M_g + M_q}{Z_b}\right] \geq f_{tw} \tag{20.5}$$

2. Code requirements for the limit state of collapse to ensure desirable load factors against flexural failure which can be written as,

$$M_u \geq [\gamma_{f_1} M_g + \gamma_{f_2} M_q] \tag{20.6}$$

3. Deflection constraint at the limit state of serviceability which takes the form,

$$a \leq a_p \tag{20.7}$$

where a and a_p are the actual and permissible deflection, which is usually a small fraction of the span.

4. Limitation on the minimum and maximum ratios of reinforcement in the section is expressed in the form,

$$\rho_{min} \leq \rho \leq \rho_{max} \tag{20.8}$$

where ρ is the ratio of reinforcement provided, ρ_{min} is the minimum ratio required to prevent failure by fracture of steel in tension and ρ_{max} is the maximum permissible ratio to ensure failure of the section by yielding of steel.

In the design of fully prestressed (class 1) members, all the constraints as given in Eqs 20.2 to 20.8 are valid. However, in the case of partially prestressed members where cracks of limited width are permissible under working loads, an additional constraint to impose the limitations on the width of the crack is required. This can be expressed as,

$$w \leq w_p \tag{20.9}$$

where w is the actual crack width and w_p is the permissible crack width. Additional constraints are imposed on the geometrical dimensions of the cross-section, such as the minimum thickness of the web and bottom flange, based on practical requirements of housing the cables with due regard to cover requirements. The constraints being nonlinear, the optimal solution is obtained by nonlinear programming techniques discussed in Section 20.3.2.

According to Ramaswamy and Raman[17], the complete definition of the optimum design of prestressed beams involves 27, 26, and 40, constraints for class 1, 2 and 3 type beams, respectively. Further, they have reported a saving of 60 per cent in high-tensile steel in Class 3-type beam, compared to a fully prestressed class 1 type beam. Several optimisation studies have been conducted on prestressed concrete structures during the last decade. Notable among them being the computer programmes developed by Freyermuth[18] at the Portland cement Association. Also, comparative studies have been carried out by Sarkar *et al.*,[19] for prestressed concrete bridge decks conforming to the Indian Roads Congress Bridge Loading Standards.

Future studies in this field should include cost estimates of alternative schemes, formwork design, probabilistic design considering the variability of load applications and material properties. Reliability of prestressed concrete structural systems like beams and frames has been examined by Ranganathan[20]. Application of geometric programming to structural optimisation problems has been attempted by Templeman[21] in which the emphasis is on the optimal distribution of the total cost among the various terms in the objective function instead of on the values of the variables.

Structural optimisation, together with the efficient management of labour, materials and the use of new construction techniques, development and use of indigenous and new materials like high performance and nano concretes, would result in considerable economy in the overall costs of prestressed concrete structural systems.

References

1. Gallaghar, R H and O C Zienkiewicz, *Optimum Structural Design, Theory and Applications*, John Wiley and Sons, 1973, pp. 7–17.
2. Dantzig, G B, *Linear Programming and Extensions*, Princeton University Press, Princeton, New Jersey, 1963.

3. Cox, H, *The Design of Structures of Least Weight*, Pergamon Press, Oxford, 1965.
4. Shanley, F, *Weight Strength Analysis of Aircraft Structures*, Dover, New York, 1960.
5. Prager, W and P Marcel, *Optimality Criteria in Structural Design*, Affdltr, May 1971 pp 70 – 166.
6. Taylor, J, "Optimal Design of Structural Systems, An Energy Formulation," *AIAA Journal*, Vol. 7, 1969, pp. 1404–1406.
7. Venkayya, VB, "Design of Optimum Structural Elements", *Computers and Structures*, Vol. 1, No. ½, 1971, pp. 265–309.
8. Livesley, RK, "The Automatic Design of Structural Frames", *Quarterly Journal of Mechanics and Applied Mathematics*, Vol. 9, 1956, p. 257.
9. Pearson, C, "Structural Design by high speed computing machines", *Proceedings of ASCE Conference on Electronic Computation*, Kansas City, Missouri, 1958.
10. Kunzi, HP, HG Tzchach and CA Sehnder, *Numerical Methods of Mathematical Optimisation*, Academic Press, New York, 1968.
11. Rosen, JB, "The gradient projection method for non-linear programming", *Journal of the Society for Industrial and Applied mathematics, Part I, Linear Constraints*, Vol. 8, No.1, 1960, pp. 181–217. Part II, *Nonlinear Constraints*, Vol. 9, No. 4, 1961, pp. 514–532.
12. Zoutendijk, G, *Methods of Feasible Directions*, Elsevier Publishing Company, Amsterdam, 1960.
13. Fiacco, AV and GP, McCormick, *Nonlinear Programming Sequential Unconstrained Minimisation Techniques*, John Wiley, New York, 1968.
14. Ramakrishnan, CV and SS Bhavikatti, "Improvements in the Move Limit method of sequential linear programming", *Annual Convention of Computer Society of India*, Poona, January 1977.
15. Bellman, RE, *Dynamic Programming*, Princeton University Press, Princeton, New Jersey, 1957.
16. Palmer, AC and DJ Sheppard, "Optimizing the shape of pin jointed structures", *Proceedings of the Institution of Civil Engineers*, London, Vol. 47, 1970, pp. 363–376.
17. Ramaswamy, GS and NV Raman, "Optimum Design of Prestressed Concrete Sections for minimum cost by nonlinear programming", *FIP, VI Congress, Prague*, June 1970, pp. 1–7.
18. Freyermuth, Cl, "Computer programme for analysis and design of simple span precast prestressed high way or railway bridges." *Publication SRO33, IOE*, Portland Cement Association, Skokie, Illinois, 1968.
19. Sarkar S et al., *Hand Book of Prestressed Concrete Bridges*, Structural Engineering Research Centre, Roorkee, 1969, pp. 226–233.
20. Ranganathan, R, "Reliability of Systems and Prestressed Concrete Structures", *All India Seminar on Prestressed Concrete Structures, Proceedings*, *Madurai*, Vol. 1, March 1979, pp. 33–39.
21. Templeman, AB, "Structural design for minimum cost using the method of geometric programming," *Proceedings of the Institution of Civil Engineers*, London, Vol. 46, 1970, pp. 459–472.

Review Questions

20.1 What are the basic principles of optimisation?
20.2 Briefly outline the various methods of optimisation.
20.3 Explain the terms (a) design variables (b) constraints (c) objective function, with respect to mathematical programming formulations.
20.4 What are optimisation techniques? Briefly explain the techniques of linear and non-linear programming.
20.5 Discuss briefly the application of optimisation techniques in the analysis and design of prestressed concrete structures.

Objective-type Questions

20.1 Optimum design of prestressed concrete structures involves the determination of
(a) most economical cost of the structure
(b) factors affecting the durability of the structure
(c) combination of design variables to achieve satisfactory performance of the structure
20.2 Basic features of the structural optimisation problem are
(a) cost of materials of construction
(b) design variables, objective functions and the constraints
(c) cost of repairs and maintenance
20.3 Design variables generally comprise
(a) member sizes (b) method of design (c) limitation of strength
20.4 Constraints imposed are generally
(a) physical property of material
(b) member sizes
(c) stresses developed at extreme fibres
20.5 The objective function in the design of prestressed concrete beams is
(a) cost of steel and concrete
(b) method of design
(c) minimum or maximum strength
20.6 Linear programming problems can be solved by
(a) moment distribution method
(b) simplex method
(c) slope deflection method
20.7 Non-linear programming problems are generally solved by
(a) simplex algorithm
(b) consistent deformation method
(c) method of feasible directions
20.8 In the design of prestressed concrete structural elements, the objective function is generally
(a) the material properties
(b) the total cost of the member
(c) the method of analysis

20.9 In the optimum design of prestressed concrete poles, significant economy in the use of materials is possible by using
 (a) Type-1 structures
 (b) Type-2 structures
 (c) Type-3 structures

20.10 In the design of large span structural concrete trusses, optimum design should aim at adopting prestressing for
 (a) compression members
 (b) tension members
 (c) diagonal members

Answers to Objective-type Questions

20.1 (c)	20.2 (b)	20.3 (a)	20.4 (c)	20.5 (a)
20.6 (b)	20.7 (c)	20.8 (b)	20.9 (c)	20.10 (b)

21 Prestressed Concrete Bridges

21.1 General Aspects

Prestressed concrete is ideally suited for the construction of medium- and long-span bridges. Ever since the development of prestressed concrete by Freyssinet in the early 1930s, the material has found extensive application in the construction of long-span bridges, gradually replacing steel which needs costly maintenance due to the inherent disadvantages of corrosion under aggressive atmospheric conditions.

Solid slabs are used for the span range of 10 to 20 m, while T-beam slab decks are suitable for spans in the range of 20 to 40 m. Single or multicell box girders are preferred for larger spans of the order of 30 to 70 m. Prestressed concrete is ideally suited for long-span continuous bridges in which precast box girders of variable depth are used for spans exceeding 50 m. Prestressed concrete has been widely used throughout the world for simply-supported, continuous, balanced cantilever, suspension, hammer-head and bridle-chord-type bridges in the span range of 20 to 500 m.[1, 2, 3]

21.2 Advantages of Prestressed Concrete Bridges

Prestressed concrete which is made up of high-strength concrete and high-tensile steel has distinct advantages in bridge construction. The salient benefits accruing from the use of prestressed concrete in bridges are outlined as follows:

1. High-strength concrete and high-tensile steel, besides being economical, make for slender sections, which are aesthetically superior.
2. Prestressed concrete bridges can be designed as Class 1-type structures without any tensile stresses under service loads, thus resulting in a crack-free structure.
3. In comparison with steel bridges, prestressed concrete bridges require very little maintenance.
4. Prestressed concrete is ideally suited for composite bridge construction in which precast prestressed girders support the cast *in situ* slab deck. This type of construction is very popular since it involves minimum disruption of traffic.
5. Post-tensioned prestressed concrete finds extensive applications in long-span continuous girder bridges of variable cross-section. Not only does

it make for sleek structures, but it also effects considerable saving in the overall cost of construction.

6. In recent years, partially prestressed concrete (type-3 structure) has been preferred for bridge construction, because it offers considerable economy in the use of costly high-tensile steel in the girder.

21.3 Pretensioned Prestressed Concrete Bridge Decks

Pretensioned prestressed concrete bridge decks generally comprise of precast pretensioned units used in conjunction with cast *in situ* concrete, resulting in composite bridge decks which are ideally suited for small and medium spans in the range of 20 to 30 m. In general, pretensioned girders are provided with straight tendons. The use of seven-wire strands has been found to be advantageous in comparison with plain or indented wires. In USA[4], deflected strands are employed in larger girders.

In UK, the precast prestressed I- and inverted T-beams have been standardised by the Cement and Concrete Association[5] for use in the construction of bridge decks of spans varying from 7 to 36 m. Standard I- and T-units are widely employed in highway bridge beams in USA[6]. Recently, in UK, Y-beams, have been developed to replace the M-beams which were introduced in 1960. The design and development of the Y-beams, which are superior to M-beams, are ideally suited for medium spans of 15 to 30 m.

The typical cross-section of the standard inverted Y-beams developed by the research group in UK[7, 8, 9] is shown in Fig. 21.1 and the section properties of the Y-beam are compiled in Table 21.1. The salient features of composite bridge decks with precast pretensioned standard beams are shown in Fig. 21.2.

Table 21.1 *Section properties of standard Y-beams (UK)*

Section	*Depth* (mm)	*Area* (mm^2)	*Height of Centroid above Soffit* y_b (mm)	*Section Modulus*		*Approximate Self-weight* (kN/m)
				Top Fibre Z_t ($mm^3 \times 10^6$)	*Bottom Fibre* Z_b ($mm^3 \times 10^6$)	
Y-1	700	309202	255.24	24.85	43.40	7.42
Y-2	800	339882	298.68	35.02	58.78	8.14
Y-3	900	373444	347.12	47.88	76.27	8.95
Y-4	1000	409890	399.71	63.53	95.41	9.82
Y-5	1100	449220	455.72	82.06	116.02	10.78
Y-6	1200	491433	514.50	103.58	138.00	11.78
Y-7	1300	536530	575.54	128.15	161.31	12.86
Y-8	1400	584708	638.54	155.98	186.01	14.02

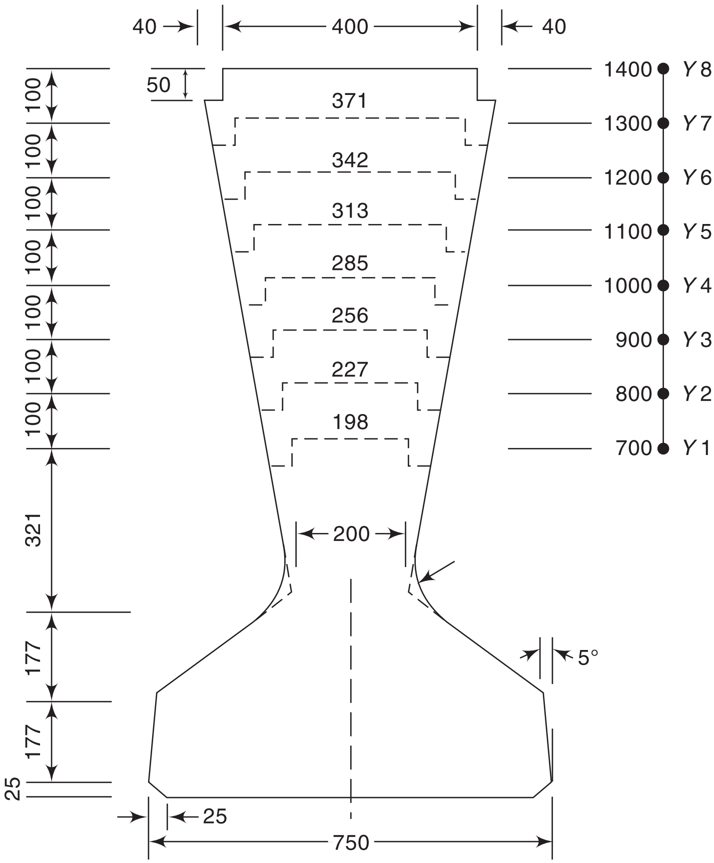

Fig. 21.1 *Cross-section of standard Y-beams (UK)*

21.4 Post-tensioned Prestressed Concrete Bridge Decks

Post-tensioned bridge decks are generally adopted for longer spans exceeding 20 m. Bridge decks with precast post-tensioned girders of either T-type or box-type, in conjunction with a cast *in situ* slab are commonly adopted for spans exceeding 30 m. Post-tensioning facilitates the use of curved cables, which improve the shear resistance of the girders[10].

Post-tensioning is ideally suited for prestressing long-span girders at the site of construction, without the need for costly factory-type installations like pretensioning beds. Segmental construction is ideally suited for post-tensioning work. In this method, a number of segments can be combined by prestressing,

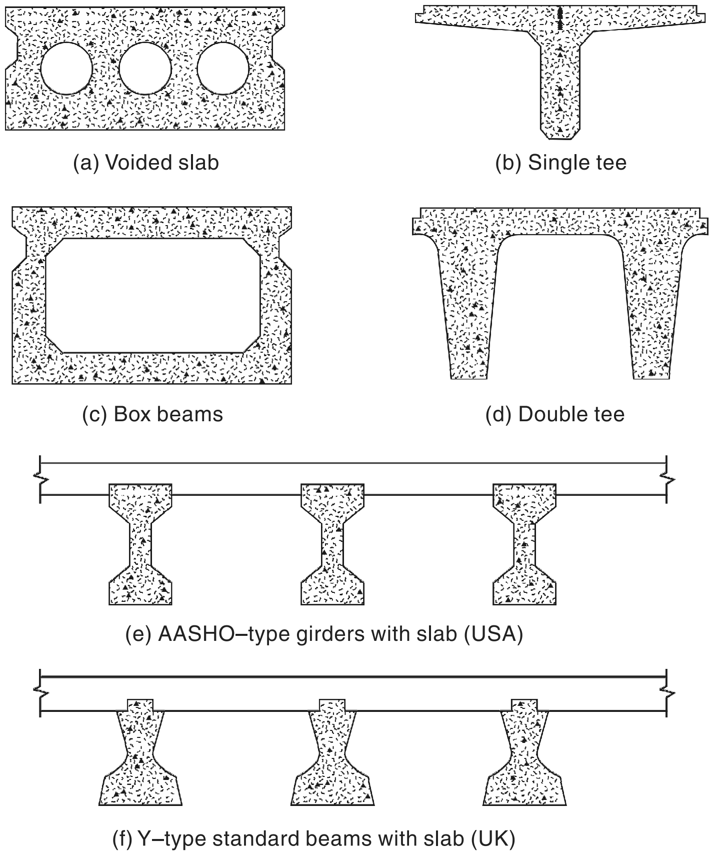

Fig. 21.2 *Typical cross-sections of pretensioned prestressed concrete bridge decks*

resulting in an integrated structure. In India, a large number of long-span bridges have been constructed using the cantilever method of construction[11]. Some of the notable examples being the Barak bridge at Silchar built in 1960 with a main span of 130 m and the Lubha bridge in Assam with a span of 130 m between the bearings. Long-span continuous prestressed concrete bridges are invariably built of multicelled box girder segments of variable depth using the post-tensioning system. Typical cross-sections of post-tensioned prestressed concrete bridge decks are shown in Fig. 21.3. The salient features of the cantilever construction method using cast *in situ* segments and precast concrete elements are shown in Figs 21.4(a), (b) and (c).

21.5 Design of Post-tensioned Prestressed Concrete Slab Bridge Deck

Design a post-tensioned prestressed concrete slab bridge deck for a national highway crossing to suit the following data:

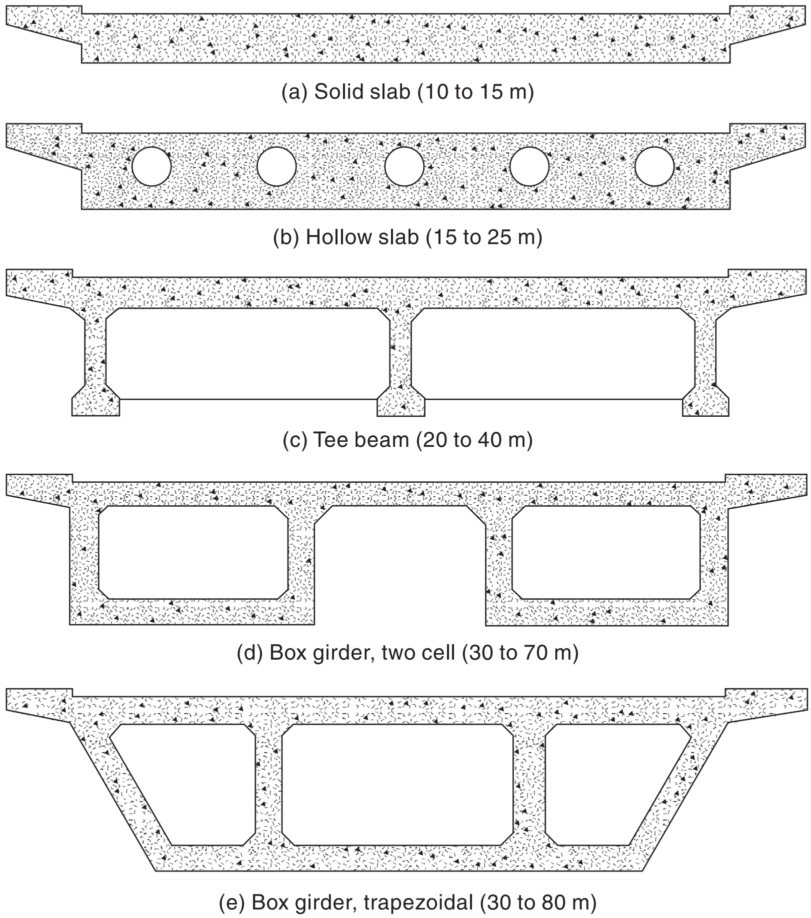

Fig. 21.3 *Typical cross-section of post-tensioned prestressed concrete bridge decks*

Data

Clear span	10 m
Width of bearing	400 mm
Clear width of roadway	7.5 m
Footpath	1 m on either side
Kerbs	600 mm wide
Thickness of wearing coat	80 mm
Live load	IRC Class AA tracked vehicle
Type of structure	Class 1 type

Materials: M-40 grade concrete and 7 mm diameter high-tensile wires with an ultimate tensile strength of 1500 N/mm^2 housed in cables with 12 wires and anchored by Freyssinst anchorages of 150 mm diameter.

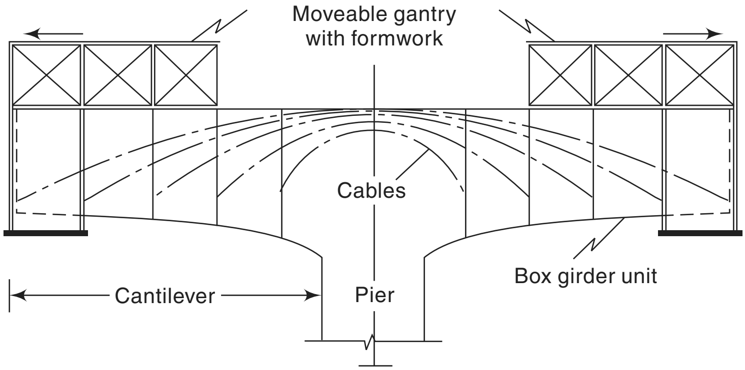

(a) Using cast *in situ* segments

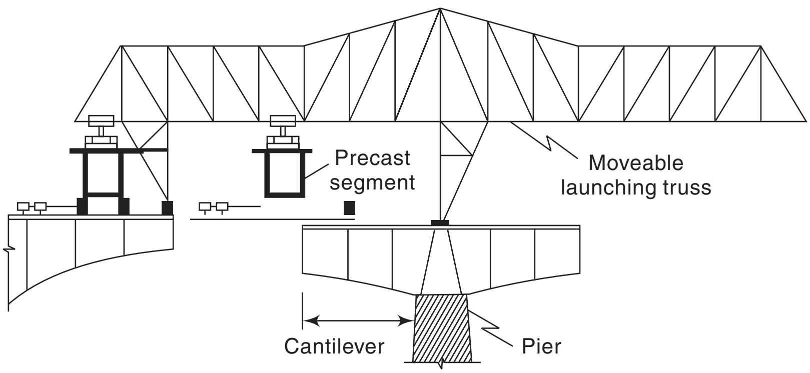

(b) Using precast girder segments

(c)

Fig. 21.4 *Cantilever method of construction of prestressed concrete bridges*

For supplementary reinforcement, adopt Fe-415 grade HYSD bars.
Compressive strength at transfer, $f_{ci} = 35\ \text{N/mm}^2$
Loss ratio = 0.8

The design should conform to the recommendations of the codes IRC: 6 – 2014[12], IRC: 112 – 2011[13], and IS: 1343 – 2012[14].

Permissible stresses The permissible compressive stresses in concrete at transfer and working loads, as recommended in IRC–18 are as follows:

$$f_{ct} = 15 \text{ N/mm}^2 < 0.45\, f_{ci} = (0.45 \times 35) = 15.75 \text{ N/mm}^2$$

Loss ratio, $\eta = 0.80$

$$f_{cw} = 12 \text{ N/mm}^2 < 0.33\, f_{ck} = (0.33 \times 40) = 13.2 \text{ N/mm}^2$$

$$f_{tt} = f_{tw} = 0$$

Depth of slab and effective span Assuming the thickness of the slab at 50 mm per metre of span for highway bridge decks, the overall thickness of the slab = (10 × 50) = 500 mm
Width of bearing = 400 mm
Effective span = 10.4 m
The cross-section of the deck slab is shown in Fig. 21.5.

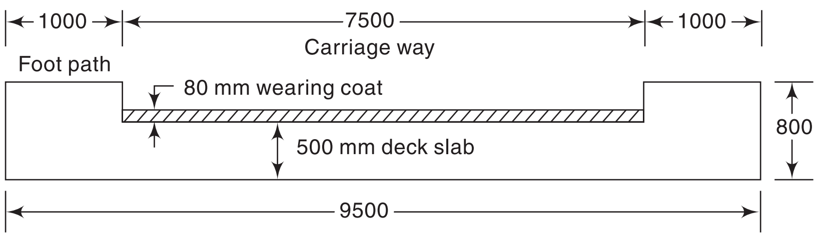

Fig. 21.5 *Cross-section of deck slab*

Dead-load bending moments Dead weight of slab = (0.5 × 24) = 12 kN/m^2
Dead weight of WC = (0.08 × 22) = 1.76 kN/m^2
Total dead load = 14.00 kN/m^2
Dead-load bending moment (M_g) = (14 × 10.4^2)/8 = 190 kN m

Live load bending moments Generally, the bending moment due to live load will be maximum for IRC class *AA* tracked vehicle. Impact factor for the class *AA* tracked vehicle is 25 per cent for the 5 m span, which decreases linearly to 10 per cent for the 9 m span.
∴ Impact factor = 10 per cent for a span of 10.4 m
The tracked vehicle is placed symmetrically on the span.
Effective length of load = [3.6 + 2 (0.5 + 0.08)] = 4.76 m
Effective width of the slab perpendicular to the span is expressed as,

$$b_e = kx\left(1 - \frac{x}{L}\right) + b_w$$

Referring to Fig. 21.6,

$$x = 5.2 \text{ m}, \quad L = 10.4 \text{ m}, \quad B = 9.5 \text{ m}$$

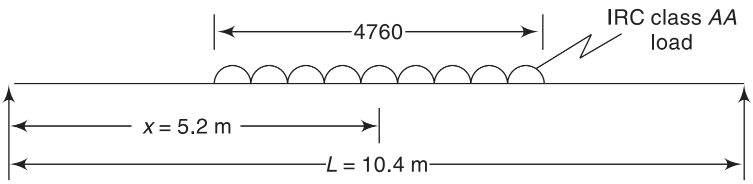

Fig. 21.6 *Position of load for maximum bending moment*

$$\therefore \qquad \left(\frac{B}{L}\right) = \left(\frac{9.5}{10.4}\right) = 0.913$$

and $\qquad b_w = (0.85 + 2 \times 0.08) = 1.01$ m

From Table 21.2 for $\left(\frac{B}{L}\right) = 0.913$,

and simply supported slabs, $k = 2.37$

Table 21.2 *Values of constant k (IRC: 112–2011)*

$\left(\frac{B}{L}\right)$	*Values of k*		$\left(\frac{B}{L}\right)$	*Values of k*	
	For Simply Supported Slabs	*For Continuous Slabs*		*For Simply Supported Slabs*	*For Continuous Slabs*
0.1	0.40	0.40	1.1	2.60	2.28
0.2	0.80	0.80	1.2	2.64	2.36
0.3	1.16	1.16	1.3	2.72	2.40
0.4	1.48	1.44	1.4	2.80	2.48
0.5	1.72	1.68	1.5	2.84	2.48
0.6	1.96	1.84	1.6	2.88	2.52
0.7	2.12	1.96	1.7	2.92	2.56
0.8	2.24	2.08	1.8	2.96	2.60
0.9	2.36	2.16	1.9	3.00	2.60
1.0	2.48	2.24	2.0 and above	3.00	2.60

$$\therefore \qquad b_e = 2.37 \times 5.2\left(1 - \frac{5.2}{10.4}\right) + 1.01 = 7.172 \text{ m}$$

The tracked vehicle is placed close to the kerb with the required minimum clearance as shown in Fig. 21.7.
Net effective width of dispersion = 8.261 m
Total load of two tracks with impact = $(700 \times 1.10) = 770$ kN

$$\text{Average intensity of load} = \left[\frac{770}{(4.76 \times 8.261)}\right] = 19.58 \text{ kN/m}^2$$

Maximum bending moment due to live load is given by

$$M_q = [(19.58 \times 4.76)\ 0.5 \times 5.2] - [(19.58 \times 4.76)\ 0.5 \times 0.25 \times 4.76] = 187 \text{ kN m}$$

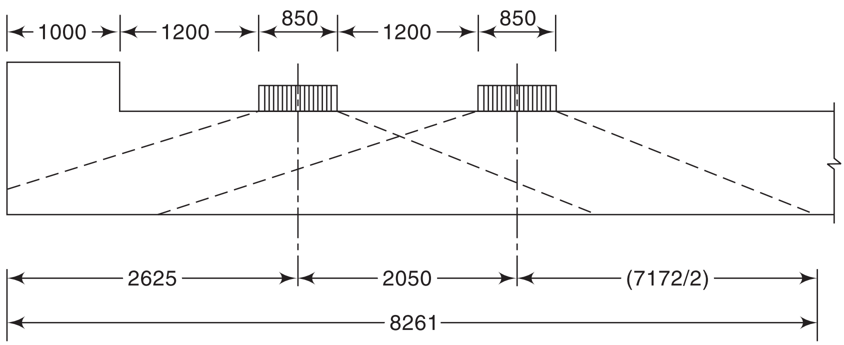

Fig. 21.7 *Effective width of dispersion for IRC class AA tracked vehicle*

Shear due to Class AA tracked vehicle For maximum shear force at the support section, the IRC class *AA* tracked vehicle is arranged as shown in Fig. 21.8.

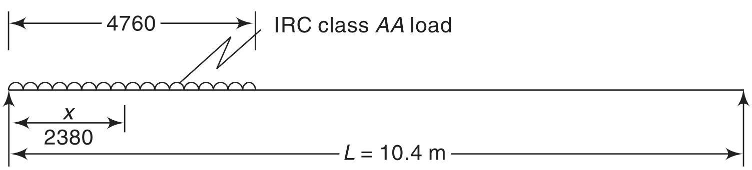

Fig. 21.8 *Position of load for maximum shear*

Effective width of dispersion is given by

$$b_e = kx\left(1 - \frac{x}{L}\right) + b_w$$

where $x = 2.38$ m, $L = 10.4$ m, $B = 9.5$ m, $b_w = 1.01$ m

$$\left(\frac{B}{L}\right) = \left(\frac{9.5}{10.4}\right) = 0.913$$

$\therefore$ From Table 21.2, for $\left(\dfrac{B}{L}\right) = 0.913$, the value of $k = 2.37$.

$$\therefore \qquad b_e = \left[2.37 \times 2.38\left(1 - \frac{2.38}{10.4}\right) + 1.01\right] = 5.364 \text{ m}$$

Referring to Fig. 21.7,

Width of dispersion for two tracks

$$= \left[2625 + 2050 + \left(\frac{5364}{2}\right)\right] = 7357 \text{ mm}$$

$$\therefore \quad \text{Intensity of load} = \left[\frac{770}{(4.76 \times 7.357)}\right] = 22 \text{ kN/m}^2$$

$$\therefore \quad \text{Shear force, } V_A = \frac{(22 \times 4.76 \times 8.02)}{10.4} = 80.75 \text{ kN}$$

$$\text{Dead-load shear} = (0.5 \times 14 \times 10.4) = 72.8 \text{ kN}$$

$$\therefore \quad \text{Total design shear} = (80.75 + 72.80) = 153.55 \text{ kN}$$

Check for minimum section modulus

Dead-load moment, M_g = 190 kN m

Live-load moment, M_q = 187 kN m

Section modulus $\quad Z_t = Z_b = Z = \left(\dfrac{1000 \times 500^2}{6}\right) = 41.66 \times 10^6 \text{ mm}^3$

The permissible stress in concrete at transfer, (f_{ct}), is obtained from IRC–18.

$$f_{ct} = 15.0 \text{ N/mm}^2, f_{cw} = 12.0 \text{ N/mm}^2, f_{tw} = 0$$

Loss ratio, $\eta = 0.8$

$$\begin{aligned} f_{br} &= (\eta f_{ct} - f_{tw}) = (0.8 \times 15 - 0) \\ &= 12.0 \text{ N/mm}^2 \end{aligned}$$

The minimum section modulus is given by,

$$\begin{aligned} Z_b &\geq \left[\frac{M_q + (1-\eta)M_g}{f_{br}}\right] \\ &\geq \left[\frac{187 \times 10^6 + (1-0.8)190 \times 10^6}{12}\right] \\ &\geq 18.75 \times 10^6 \text{ mm}^3 < 41.66 \times 10^6 \text{ mm}^3 \text{ provided} \end{aligned}$$

Hence, the section selected is adequate to resist the service loads without exceeding the permissible stresses.

Minimum prestressing force The minimum prestressing force required is computed using the relation,

$$P = \left[\frac{A(f_{inf} Z_b + f_{sup} Z_t)}{Z_b + Z_t}\right]$$

where $\quad f_{sup} = \left(f_{tt} - \dfrac{M_g}{Z_t}\right) = \left(0 - \dfrac{190 \times 10^6}{41.66 \times 10^6}\right) = -4.56 \text{ N/mm}^2$

and $\quad f_{inf} = \left(\dfrac{f_{tw}}{\eta} + \dfrac{M_g + M_g}{\eta Z_b}\right) = \left(0 + \dfrac{(187 + 190) \times 10^6}{0.8 \times 41.66 \times 10^6}\right)$

$$= 11.31 \text{ N/mm}^2$$

$$\therefore \qquad P = \left[\frac{1000 \times 500 \times 41.66 \times 10^6 (11.31 - 4.56)}{2 \times 41.66 \times 10^6}\right]$$
$$= 1687.5 \times 10^3 \text{ N}$$
$$= 1687.5 \text{ kN}$$

Using Freyssinet cables containing 12 wires of 7 mm diameter which are stressed to 1200 N/mm^2,

$$\text{Force in each cable} = \left[\frac{(12 \times 38.5 \times 1200)}{1000}\right] = 554 \text{ kN}$$

$$\therefore \text{ Spacing of cables} = \left(\frac{1000 \times 554}{1687.5}\right) = 328 \text{ mm}$$

Eccentricity of cables The eccentricity of the cables at the centre of span is obtained from the relation

$$e = \left[\frac{Z_t Z_b (f_{inf} - f_{sup})}{A(f_{sup} Z_t + f_{inf} Z_b)}\right]$$
$$= \left[\frac{(41.66)^2 \times 10^{12} (11.31 + 4.56)}{1000 \times 500 \times 41.66 \times 10^6 (-4.56 + 11.31)}\right]$$
$$= 195 \text{ mm}$$

The cables are arranged in a parabolic profile with a maximum eccentricity of 195 mm at the centre of span which reduces to zero (concentric) at supports.

Check for stresses at service loads

$$P = 1687.5 \text{ kN}, e = 195 \text{ mm}$$
$$A = (1000 \times 500) = 5 \times 10^5 \text{ mm}^2$$
$$Z_t = Z_b = Z = 41.66 \times 10^6 \text{ mm}^3$$
$$M_g = 190 \text{ kN m} \qquad M_q = 187 \text{ kN m}$$
$$\left(\frac{P}{A}\right) = \left(\frac{1687.5 \times 10^3}{5 \times 10^5}\right) = 3.375 \text{ N/mm}^2$$
$$\left(\frac{P_e}{Z}\right) = \left(\frac{1687.5 \times 10^3 \times 195}{41.66 \times 10^6}\right) = 7.89 \text{ N/mm}^2$$
$$\left(\frac{M_g}{Z}\right) = \left(\frac{190 \times 10^6}{41.66 \times 10^6}\right) = 4.56 \text{ N/mm}^2$$
$$\left(\frac{M_q}{Z}\right) = \left(\frac{187 \times 10^6}{41.66 \times 10^6}\right) = 4.48 \text{ N/mm}^2$$

Stresses at transfer

At top of slab $= (3.375 - 7.89 + 4.56) = 0.045$ N/mm^2

At bottom of slab $= (3.375 + 7.89 - 4.56) = 6.705$ N/mm^2

Stresses at working loads

At top of slab $= [0.8\,(3.375 - 7.89) + 4.56 + 4.48] = 5.428\ \text{N/mm}^2$

At bottom of slab $= [0.8\,(3.375 + 7.89) - 4.56 - 4.48] = -\,0.028\ \text{N/mm}^2$

The actual stresses developed are within the permissible limits.

Check for Ultimate Flexural Strength

The moment of resistance of rectangular slab section of 1 m width is evaluated by using the expression specified in IS: 1343-2012 code as,

$$M_u = f_{pb}\,A_{ps}\,(d - 0.42\,x_u)$$

Where f_{pb} = tensile stress in the tendons at failure
f_{pe} = effective prestress in tendons
A_{ps} = area of prestressing tendons in the tension zone
d = effective depth to the centroid of the steel area
x_u = neutral axis depth

For pretensioned and post-tensioned members with effective bond, the values of f_{pb} and x_u are interpolated using the values given in Table 7.1. The values of the various parameters are computed as,

$$A_{ps} = [(12 \times 38.5 \times 1000)/328] = 1408\ \text{mm}^2$$
$$d = 445\ \text{mm}$$
$$f_{pu} = 1500\ \text{N/mm}^2$$
$$f_{ck} = 40\ \text{N/mm}^2$$
$$b = 1000\ \text{mm}$$

Compute the ratio $\left(\dfrac{A_{ps} f_{pu}}{b.d.f_{ck}}\right) = \left(\dfrac{1408 \times 1500}{1000 \times 445 \times 40}\right) = 0.118$

Refer Table 7.1 and interpolate the values of the ratios $\left(\dfrac{f_{pb}}{0.87\,f_{pu}}\right)$ and (x_u/d) as, $\left(\dfrac{f_{pb}}{0.87\,f_{pu}}\right) = 1.0$ and $(x_u/d) = 0.267$

Hence, $f_{pb} = (1.0 \times 0.87 \times 1500) = 1305\ \text{N/mm}^2$

and, $x_u = (0.267 \times 445) = 118.8\ \text{mm}$

$\therefore$
$$M_u = f_{pb}\,A_{ps}\,(d - 0.42\,x_u)$$
$$= [(1305 \times 1408)\,(445 - 0.42 \times 1188)]$$
$$= (727.8 \times 10^6)\ \text{N.mm} = 727.8\ \text{kN.m}$$

According to IRC: 6-2014, the required moment of resistance is given by

$$M_u = [(1.35\,M_g + 1.5\,M_q)]$$
$$= [(1.35 \times 190) + (1.5 \times 187)]$$
$$= 537\ \text{kN.m} < 727.8\ \text{kN.m}$$

Hence, the ultimate moment capacity of the designed section is greater than the required ultimate moment.

Check for Ultimate Shear Strength

Required ultimate shear force $= [(1.35\ V_g + 1.5\ V_q)]$
$= [(1.35 \times 72.8) + (1.5 \times 87.72)]$
$= 130$ kN

The design shear resistance of the support section is calculated by using the equation specified in IRC: 112-2011 clause 10.3 as,

$$V_{\mathrm{Rd.c}} = \left(\frac{I \cdot b_w}{s}\right)\sqrt{(f_{ctd})^2 \mp k_1 \sigma_{cp} f_{ctd}} + \eta P \sin\theta$$

Where I = second moment of area of gross cross-section
S = first moment of area between centroidal axis and compression fiber about centroidal axis
f_{ctd} = design value of concrete tensile strength = (f_{ct}/γ_m)
K_1 = constant depending upon transmission length and has a value of 1 for post-tensioned beams
σ_{cp} = mean compressive stress at centroidal axis = $(\eta P/A_c)$
η = loss ratio
P = prestressing force
θ = slope of the cable at support section

Computing the numerical values of the various parameters, we have

$$I = \left(\frac{bD^3}{12}\right) = \left(\frac{1000 \times 500^3}{12}\right) = (10.4 \times 10^9)\ \mathrm{mm}^4$$

$$S = \left(\frac{1000 \times 250 \times 250}{2}\right) = (31.25 \times 10^6)\ \mathrm{mm}^3$$

$f_{ctd} = (f_{ct}/\gamma_m) = (3/1.5) = 2$ since $f_{ct} = 3\mathrm{N/mm}^2$ for $f_{ck} = 40\ \mathrm{N/mm}^2$
$\sigma_{cp} = (\eta P/A_c) = [(0.8 \times 1687.5 \times 10^3)/(1000 \times 500)] = 2.7\ \mathrm{N/mm}^2$
$\theta = (4e/L) = [(4 \times 195)/(10.4 \times 1000)] = 0.075$

$$\therefore \quad V_{\mathrm{Rd.c}} = \left(\frac{I \cdot b_w}{s}\right)\sqrt{(f_{ctd})^2 \mp k_1 \sigma_{cp} f_{ctd}} + \eta P \sin\theta$$

$$= \left(\frac{(10.4 \times 10^9)1000}{31.25 \times 10^6}\right)\sqrt{(2)^2 \mp 1 \times 2.7 \times 2}$$

$$+ (0.8 \times 1687.5 \times 10^3 \times 0.075)\ \mathrm{N}$$

$$= (493.69 \times 10^3)\ \mathrm{N}$$

$$= 493.69\ \mathrm{kN} > 130\ \mathrm{kN}$$

The shear resistance of the support section is greater than the required ultimate shear force.

Supplementary Reinforcement

According to clause 16.5.1 of IRC: 112-2011, the minimum longitudinal reinforcement should be not less than that given by the relation,

$$A_{\mathrm{s.min}} = 0.26\ (f_{ctm}/f_{yk})\ b_t\ d \text{ but not less than } 0.0013\ b_t\ d$$

Where b_t = mean width of the tension zone

$$A_{s.min} = [0.26\ (3/415)\ (1000 \times 450)] \text{ but not less than } (0.0013 \times 1000 \times 450)$$
$$= 846 \text{ mm}^2/\text{m or } 585 \text{ mm}^2/\text{m}$$

Provide 10 mm diameter Fe-415 HYSD bars at a spacing of 200 mm both at top and bottom faces of the slab in the longitudinal and transverse directions.

Check for Serviceability Limit States

(a) Limit state of deflection At service loads, deflections due to prestressing force, dead load and live load is computed as follows:

$$\text{Dead load} = g = 14 \text{ kN/m} = 0.014 \text{ kN/mm}$$

Live load spread over a length of 4.76 m is assumed as a concentrated load at centre of span is computed as,

$$Q = (4.76 \times 19.58) = 93.2 \text{ kN}$$

Effective prestressing force after losses = $\eta P = (0.8 \times 1687.5) = 1350$ kN

$$E_c = 33 \text{ KN/mm}^2$$
$$I = (10.4 \times 10^9) \text{ mm}^4$$

Upward deflection due to prestressing force:

$$a_P = \left(\frac{5\,PeL^2}{48\,E_C I}\right) = \left(\frac{5 \times 1350 \times 195 \times 10400^2}{48 \times 33 \times (10.4 \times 10^9)}\right) = 8.69 \text{ mm (upwards)}$$

Downward deflection due to dead weight:

$$a_g = \left(\frac{5gL^4}{384\,E_c I}\right) = \left(\frac{5 \times 0.014 \times 10400^4}{384 \times 33 \times (10.4 \times 10^9)}\right) = 6.2 \text{ mm (downwards)}$$

Downward deflection due to live load:

$$a_Q = \left(\frac{QL^3}{48\,E_c I}\right) = \left(\frac{93.2 \times 10400^3}{48 \times 33 \times (10.4 \times 10^9)}\right) = 6.36 \text{ mm (downwards)}$$

Maximum deflection due to prestress + self weight + live loads

$$a_r = (a_p + a_g + a_Q) = (-8.69 + 6.2 + 6.36) = 5.67 \text{ mm}$$

Long-term deflection considering the effect of creep is limited to (span/250). Notional size of cross-section = $(2A_c/u) = [(2 \times 1000 \times 500)/2000] = 500$ mm.

From Table 2.7, interpolate the final creep coefficient for the given notional size of 500 mm at relative humidity of 50 per cent and age at loading of 28 days as $\phi = 2.50$.

Effective modulus of elasticity of concrete

$$= E_{c,eff} = \left[\frac{E_c}{1+\phi}\right] = \left[\frac{E_c}{1+2.5}\right] = \left[\frac{E_c}{3.5}\right]$$

Maximum long-term deflection = $(3.5 \times 5.67) = 19.84$ mm < $(10400/250) = 41.6$ mm

Maximum permissible deflection due to live loads only $\leq \left(\dfrac{span}{800}\right) = \left(\dfrac{10400}{800}\right)$ = 13 mm > 6.36 mm

(b) Limit state of cracking The deck slab has been designed as a Class-1 type structure without any tensile stresses at service loads. Hence, the serviceability limit state of cracking is automatically satisfied.

Hence, the slab is safe regarding the serviceability limit state of deflection and cracking according to the specifications of IRC: 112-2011.

Design of End Block Reinforcement

At the support section, concentric cables carrying a force of 554 kN are spaced at intervals of 328 mm. The end block has to be designed for bursting tension due to the anchorage force.

The bursting tensile force is computed using the Table 21.3 as recommended in IRC: 112-2011.

Table 21.3 *Design bursting tensile force in end blocks (Table 13.1 of IRC: 112-2011)*

(Y_{po}/Y_o)	0.3	0.4	0.5	0.6	0.7
(F_{bst}/P_k)	0.26	0.23	0.19	0.16	0.12

In the present design problem,

$$P_k = 554 \text{ kN}$$
$$2Y_{po} = 150 \text{ mm}$$
$$2Y_o = 328 \text{ mm}$$
$$\text{Ratio } (Y_{po}/Y_o) = (150/328) = 0.457$$

Interpolating the value of (F_{bst}/P_k) for $(Y_{po}/Y_o) = 0.457$ from Table 21.3,

$$(F_{bst}/P_k) = 0.185$$
$$\therefore \quad F_{bst} = (0.185 \times 554) = 103 \text{ kN}$$

Using 10 mm diameter Fe-415 HYSD bars as end block reinforcement,

$$\text{Area of steel required} = \left(\frac{103 \times 10^3}{0.87 \times 415}\right) = 285 \text{ mm}^2$$

Provide 10 mm diameter bars at 100 mm centers in the vertical and horizontal directions as a mesh in front of the anchorages at 100 and 200 mm, respectively.

Reinforcement Details in the Deck Slab

The reinforcement details in the cross-section and longitudinal section of the deck slab are shown in Figs 21.9 and 21.10.

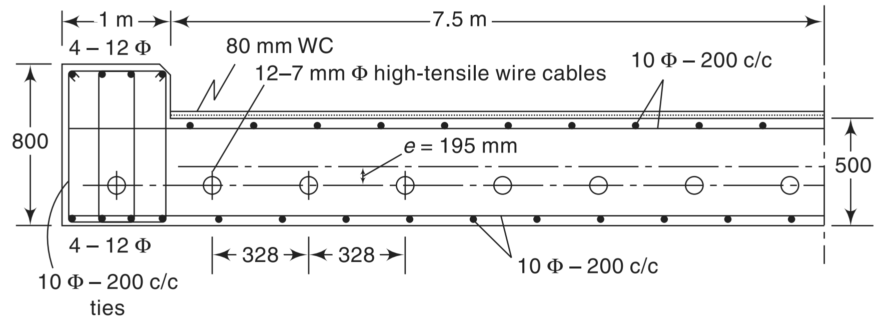

Fig. 21.9 *Cross-section of deck slab at centre of span*

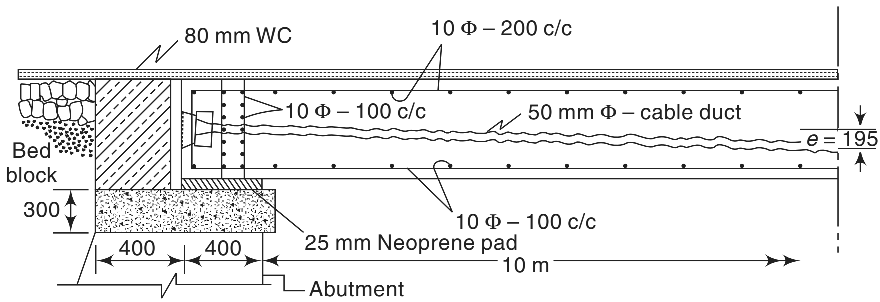

Fig. 21.10 *Longitudinal section of deck slab*

21.6 Design of Post-tensioned Prestressed Concrete T-Beam Slab Bridge Deck

Design a post-tensioned prestressed concrete T-beam slab bridge-deck for a national highway crossing to suit the following data:

Data

Effective span = 30 m

Width of road = 7.5 m

Kerbs = 600 mm on each side

Footpath = 1.5 m wide on each side

Thickness of wearing coat = 80 mm

Live load = IRC class AA tracked vehicle

For the deck slab, adopt M-20 grade concrete

For prestressed concrete girders, adopt M-50 grade concrete with cube strength at transfer as 40 N/mm^2

Loss ratio = 0.85

Spacings of cross girders = 5 m

Adopt Fe-415 grade HYSD bars. Seven-ply HT strands of 15.2 mm diameter conforming to IS: 6006–1983 are available for use.
Design the girder as class 1 type structure.
Permissible stress in concrete at transfer = 18 N/mm^2
Permissible stress in concrete at service loads = 16 N/mm^2
The design should conform to the specifications of the codes IRC: 6-2014, IRC: 112-2011 and IS: 1343-2012.

Stresses in Concrete and Steel

For M-20 grade concrete and Fe-415 HYSD bars adopt the following parameters.

$$f_{ck} = 20 \text{ N/mm}^2 \text{ and } f_y = 415 \text{ N/mm}^2$$
$$M_u = 0.138\, f_{ck}\, bd^2$$

For M-50 grade concrete and high tensile steel cables

$$f_{ck} = 50 \text{ N/mm}^2$$
$$f_{ct} = 18 \text{ N/mm}^2$$
$$f_{cw} = 16 \text{ N/mm}^2$$
$$E_c = 35 \text{ kN/mm}^2$$

Freyssinet system H.T cables of Type 7K-15 (7 strands of 15.2 mm diameter) in 65 mm cable ducts conforming to IS: 6006-1983.[15]

Cross-section of deck Four main girders are provided at intervals of 2.5 m.
Thickness of deck slab = 250 mm
Wearing coat = 80 mm
Kerbs 600 mm wide by 300 mm deep are provided.
The cross-section of the deck is shown in Fig. 21.11.

The main girders are precast and the slab connecting the girders is cast *in situ*.
Spacing of cross girders = 5 m
Spacing of main girders = 2.5 m

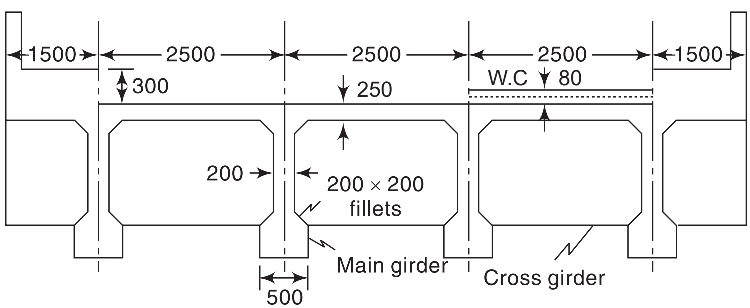

Fig. 21.11 *Cross-section of bridge deck*

Design of the interior slab panel

(a) Bending moments

Dead weight of slab = $(1 \times 1 \times 0.25 \times 24)$	=	6.00 kN/m^2
Dead weight of WC = (0.08×22)	=	1.76
Total dead load		7.76 kN/m^2

Live load is IRC class *AA* tracked vehicle. One wheel is placed at the centre of panel as shown in Fig. 21.12.

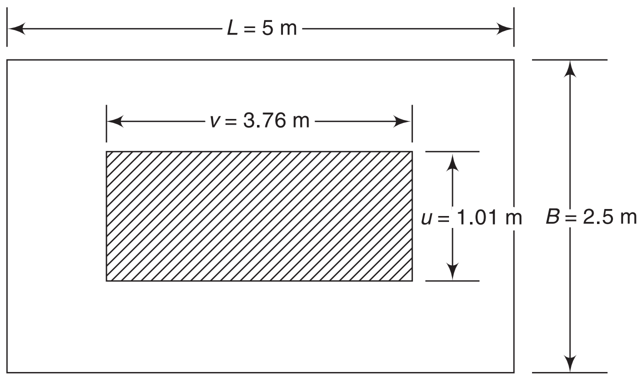

Fig. 21.12 *Position of IRC class AA wheel load for maximum bending moment*

$$u = (0.85 + 2 \times 0.08) = 1.01 \text{ m}$$
$$v = (3.60 + 2 \times 0.08) = 3.76 \text{ m}$$
$$\left(\frac{u}{B}\right) = \left(\frac{1.01}{2.5}\right) = 0.404$$
$$\left(\frac{v}{L}\right) = \left(\frac{3.76}{5.0}\right) = 0.752$$
$$K = \left(\frac{B}{L}\right) = \left(\frac{2.5}{5.0}\right) = 5.0$$

Referring to Pigeaud's curves (Fig. 21.13),

$$m_1 = 0.098 \quad \text{and} \quad m_2 = 0.02$$
$$\therefore \qquad M_B = W(m_1 + 0.15\, m_2) = 350(0.098 + 0.15 \times 0.02) = 35.35 \text{ kN m}$$

As the slab is continuous, design BM = 0.8 M_B. Design bending moment including the impact and continuity factor is given by,

M_B (short span) $= (1.25 \times 0.8 \times 35.35) = 35.35$ kN m

Similarly, $M_L = W(m_2 + 0.15\, m_1)$

$= 350(0.02 + 0.15 \times 0.098) = 12.14$ kN m

M_L (long span) $= (1.25 \times 0.8 \times 12.14) = 12.14$ kN m

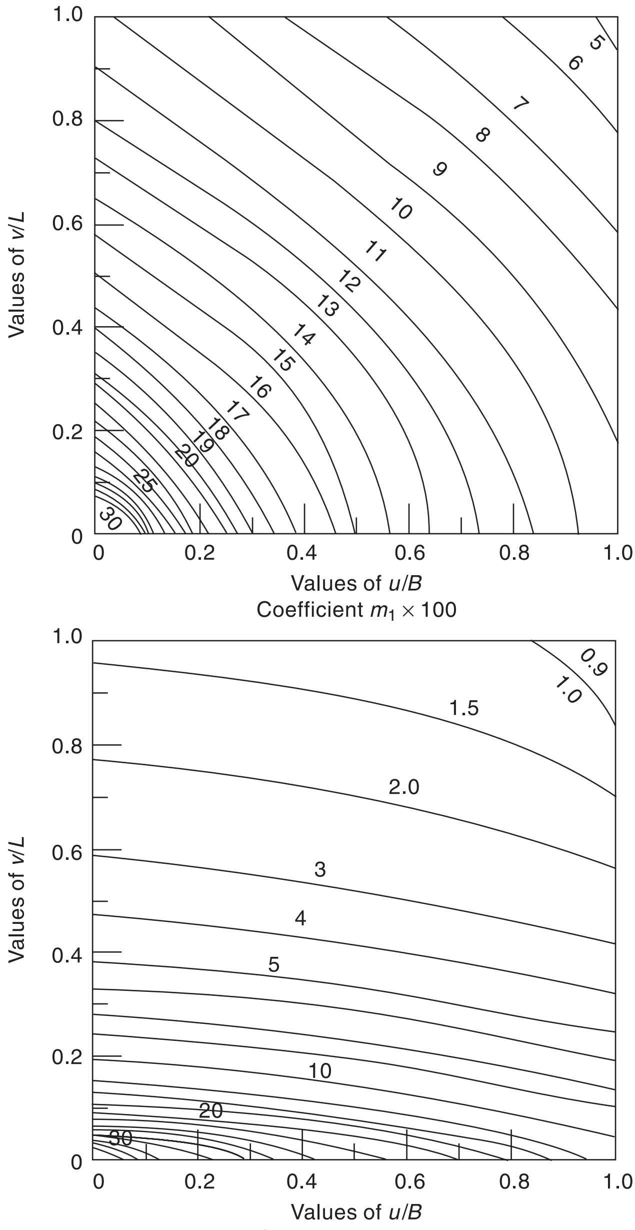

Fig. 21.13 *Moment coefficients m_1 and m_2 for $K = 0.5$ (Pigeaud's curves)*

(b) Shear forces

Dispersion in the direction of span

$$= [0.85 + 2\,(0.08 + 0.25)] = 1.51 \text{ m}$$

For maximum shear, load is kept such that the whole dispersion is in the span. The load is kept at (1.51/2) = 0.755 m from the edge of the beam as shown in Fig. 21.14.

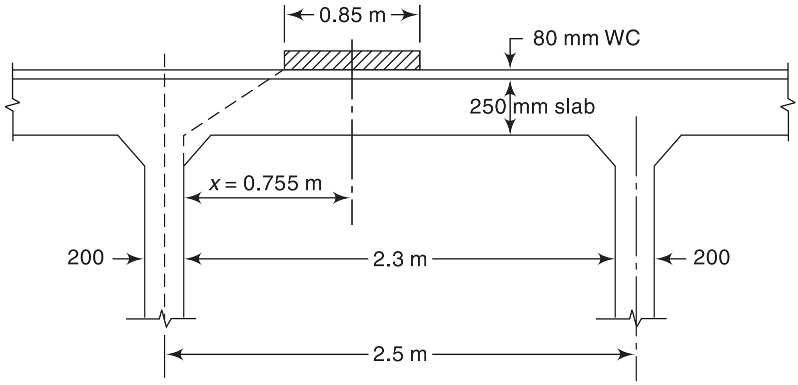

Fig. 21.14 *Position of wheel loads for max shear*

Effective width of the slab $= kx[1 - (x/L)] + b_w$

Breadth of the cross girder = 200 mm

Clear length of panel = (5 – 0.2) = 4.8 m

$$\therefore \quad \left(\frac{B}{L}\right) = (4.8/2.3) = 2.08$$

From Table 21.1, k for the continuous slab is obtained as 2.60.

Effective width of the slab $= 2.6 \times 0.755\,[1 - (0.755/2.3)] + 3.6 + (2 \times 0.08)$

$= 5.079$ m

Load per metre width = (350/5.079) = 70 kN

Shear force/metre width = 70 (2.3 – 0.755)/2.3 = 47 kN

Shear force with impact $= (1.25 \times 47) = 58.75$ kN

(c) Dead-load bending moments and shear forces

$$\text{Dead load} = 7.76 \text{ kN/m}^2$$

$$\text{Total load on panel} = (5 \times 2.5 \times 7.76) = 97 \text{ kN}$$

$$(u/B) = 1 \text{ and } (v/L) = 1$$

as the panel is loaded with a uniformly distributed load.

$$k = \left(\frac{B}{L}\right) = \left(\frac{2.5}{5}\right) = 0.5 \quad \text{and} \quad \left(\frac{1}{k}\right) = 2.0$$

From Pigeaud's curves (refer to Fig. 21.15),

$$m_1 = 0.047, \qquad m_2 = 0.01$$

$$M_B = 97\,(0.047 + 0.15 \times 0.01) = 4.70 \text{ kN m}$$

$$M_L = 97\,(0.01 + 0.15 \times 0.047) = 1.65 \text{ kN m}$$

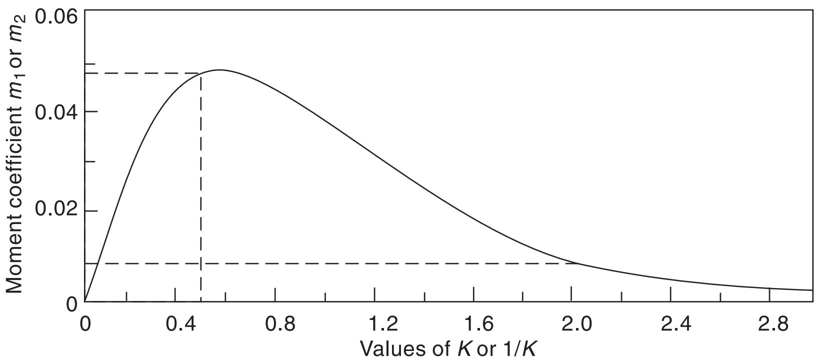

Fig. 21.15 *Moment coefficients for slabs completely loaded with uniformly distributed load, coefficient is m_1 for k and m_2 for 1/k*

Design BM, including the continuity factor,

$$M_B = (0.8 \times 4.7) = 3.76 \text{ kN m}$$

$$M_L = (0.8 \times 1.65) = 1.32 \text{ kN m}$$

Dead-load shear force = $(0.5 \times 7.76 \times 2.3) = 8.924$ kN

Design Service Load Moments and Shear Forces

Short span moment = $M_B = (35.35 + 3.76) = 39.11$ kN.m

Long span moment = $M_L = (12.14 + 1.32) = 13.46$ kN.m

Shear Force = $V = (V_g + V_L) = (8.92 + 58.75) = 67.67$ kN

Design ultimate load moments and shear forces are computed by applying appropriate load factors to the service load moments.

Total design short span ultimate moment (M_{Bu})

$$= [1.35\, M_d + 1.5\, M_L]$$
$$= [(1.35 \times 3.76) + (1.5 \times 35.35)]$$
$$= 58.1 \text{ kN.m/m}$$

Total design long span ultimate moment (M_{Lu})

$$= [(1.35 \times 1.32) + (1.5 \times 12.14)]$$
$$= 20 \text{ kN.m/m}$$

Total design ultimate shear force

$$= V_u = [(1.35 \times 8.92) + (1.5 \times 58.75)] = 90.26 \text{ kN}$$

Design of Deck Slab and Reinforcements

Effective depth of slab required = $d = \sqrt{\dfrac{M_u}{0.138 f_{ck}.b}} = \sqrt{\dfrac{58.1 \times 10^6}{0.138 \times 20 \times 1000}}$

$$= 145 \text{ mm}$$

Adopt effective depth, $d = 200$ mm and overall depth of 250 mm.

Using 12 mm diameter bars,

Effective depth provided = 200 mm

$$\left(\frac{M_u}{b.d^2}\right) = \left(\frac{58.1 \times 10^6}{1000 \times 200^2}\right) = 1.45, \text{ using M-25 grade concrete and Fe-415 HYSD bars}$$

Read out the percentage of reinforcement required from Table 2 of SP: 16 Design Aids.

$$p_t = 0.443 = \left(\frac{100 A_{st}}{b.d}\right)$$

Solving,

$$A_{st} = \left(\frac{0.443 \times 1000 \times 200}{100}\right) = 886 \text{ mm}^2$$

For short span, provide 12 mm diameter bars at 120 mm centers (A_{st} provided = 942 mm^2); for long span, provide 10 mm diameter bars at 150 mm centers.

Check for Ultimate Flexural Strength

$$\begin{aligned} M_u &= (0.87 \times 415 \times 942 \times 200)\left[1 - \frac{942 \times 415}{1000 \times 200 \times 20}\right] \\ &= (61.42 \times 10^6) \text{ N.mm} \\ &= 61.42 \text{ kN.m} > 58.1 \text{ kN.m (hence, safe)} \end{aligned}$$

Check for Ultimate Shear Strength

The ultimate shear strength of the reinforced concrete deck slab is checked by using the equation specified in IRC: 112-2011, Clause 10.3.

$$V_{Rd.c} = [0.12K\,(80\,\rho_1 f_{ck})^{0.33}] b_w.d$$

where

$$K = 1 + \sqrt{\frac{200}{d}} \le 2.00 = \left[1 + \sqrt{\frac{200}{200}}\right] = 2.00$$

and

$$\rho_1 = \left(\frac{A_{sl}}{b_w.d}\right) \le 0.02$$

$$= \left(\frac{942}{1000 \times 200}\right) = 0.0047$$

$$\begin{aligned} V_{Rd.c} &= [0.12 \times 2.00(80 \times 0.0047 \times 20)^{0.33}](1000 \times 200) \text{ N} \\ &= (96 \times 1000) \text{ N} \\ &= 96 \text{ kN} > 90.26 \text{ kN (hence, safe)} \end{aligned}$$

Design of longitudinal girders

(a) Reaction factors Using Courbon's theory, the IRC class *AA* loads are arranged for maximum eccentricity as shown in Fig. 21.16.

Reaction factor of outer girder *A* is

$$R_A = \frac{2W_1}{4}\left[1 + \frac{4I \times 3.75 \times 1.1}{(2I \times 3.75^2) + (2I \times 1.25^2)}\right] = 0.764\, W_1$$

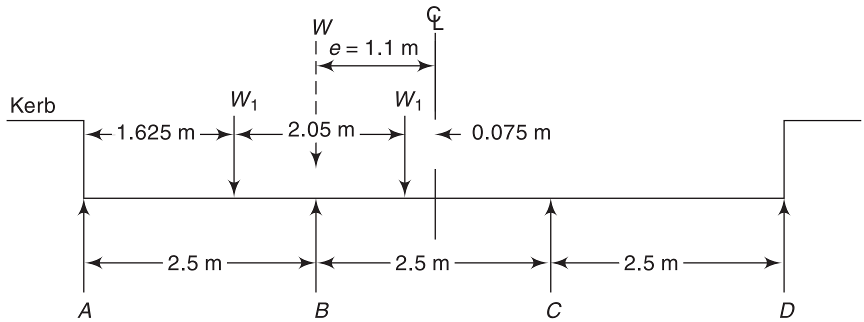

Fig. 21.16 *Transverse disposition of IRC class AA tracked vehicle*

Reaction factor for inner girder B is

$$R_B = \frac{2W_1}{4}\left[1 + \frac{4I \times 1.25 \times 1.1}{(2I \times 3.75^2) + (2I \times 1.25^2)}\right] = 0.588\ W_1$$

If $\quad W$ = axle load = 700 kN

$W_1 = 0.5\ W$

$\therefore \quad R_A = (0.764 \times 0.5\ \text{W}) = 0.382\ \text{W}$

$R_B = (0.588 \times 0.5\ \text{W}) = 0.294\ \text{W}$

(b) Dead load from slab per girder The dead load of the deck slab is calculated with reference to Fig. 21.17.

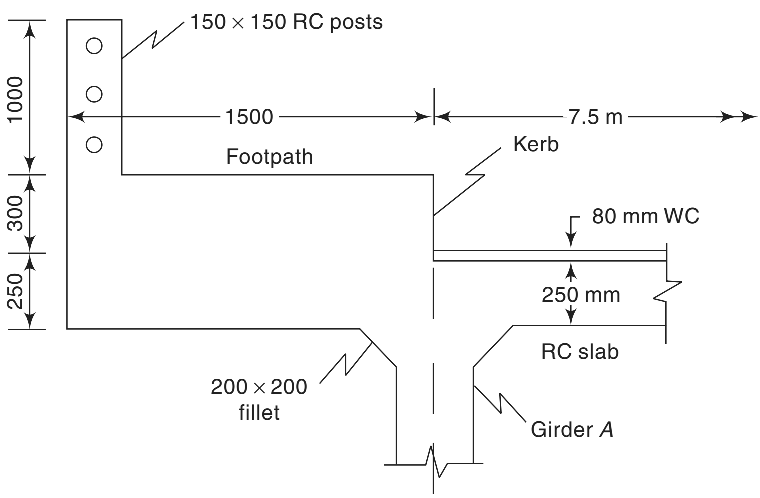

Fig. 21.17 *Details of footpath, kerb, parapet and keck slab*

Weight of

(i) Parapet railing	0.92 kN/m
(ii) Footpath and kerb = $(0.3 \times 1.5 \times 24)$	10.08
(iii) Deck slab = $(0.25 \times 1.5 \times 24)$	9.00
	20.00 kN/m

Total dead load of the deck = [(2 × 20) + (7.76 × 7.5)] = 98.2 kN/m. It is assumed that the deck load is shared equally by all the four girders.

$$\left(\frac{\text{Dead load}}{\text{Girder}}\right) = \left(\frac{98.2}{4}\right) = 24.55 \text{ kN/m}$$

(c) Dead load of the main girder The overall depth of the girder is assumed to be 1800 mm at the rate of 60 mm for every metre of span.

Span of the girder = 30 m

Overall depth = (60 × 30) = 1800 mm

The bottom flange is selected so that four to six cables are easily accommodated in the flange. The section of the main girder selected is shown in Fig. 21.18.

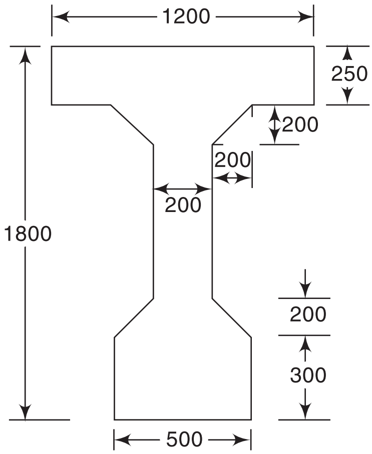

Fig. 21.18 *Cross-section of prestressed concrete girder*

Dead weight of the rib = (1.15 × 0.2 × 24) = 5.52 kN/m

Dead weight of the bottom flange = (0.5 × 0.4 × 24) = 4.80

10.32 kN/m

Weight of the cross girder = (0.2 × 1.25 × 24) = 6 kN/m

(d) Dead-load moments and shears in the main girder

Reaction from deck slab on each girder = 24.55 kN/m

Weight of the cross girder = 6 kN/m

Reaction on the main girder = (6 × 2.5) = 15 kN/m

Self-weight of the main girder = 10.32 kN/m

Total dead load on the girder = (24.55 + 10.32) = 34.87 kN/m

The maximum dead-load bending moment and shear force is computed using the loads shown in Fig. 21.19. Thus,

$$M_{\max} = [(0.125 \times 34.87 \times 30^2) + (0.25 \times 15 \times 30) + (15 \times 10) + (15 \times 5)] = 4261 \text{ kN m}$$

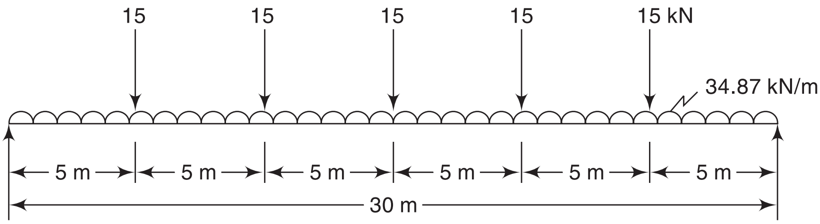

Fig. 21.19 *Dead load on main girder*

Dead-load shear at support,

$$V_{max} = [(0.5 \times 34.87 \times 30) + (0.5 \times 75)] = 561 \text{ kN}$$

(e) Live-load bending moments in the girder

Span of the girder = 30 m

Impact factor (class AA) = 10%

The live load is placed centrally on the span as shown in Fig. 21.20. Bending moment at the centre of span = 0.5(6.6 + 7.5) 700 = 4935 kN/m

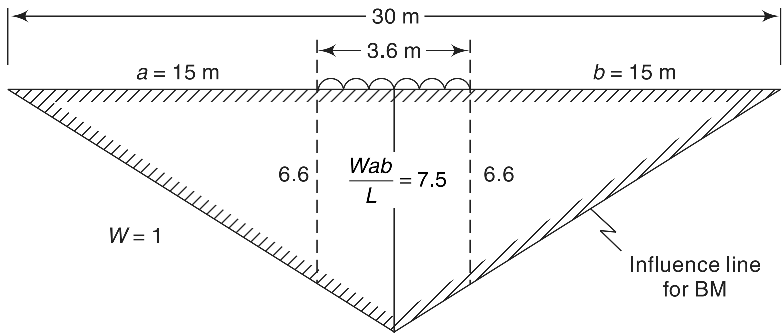

Fig. 21.20 *Influence line for bending moment in girder*

BM, including the impact and reaction factors, for the outer girder is,

Live-load BM = (4935 × 1.1 × 0.382) = 2074 kN m

For inner girder, BM = (4935 × 1.1 × 0.294) = 1596 kN m

(f) Live-load shear forces in girders For estimating the maximum live load shear in the girders, the IRC class AA loads are placed as shown in Fig. 21.21.

Reaction of W_2 on girder $B = \left[\dfrac{(350 \times 0.45)}{2.5}\right] = 63$ kN

Reaction of W_2 on girder $A = (350 \times 2.05)/2.5 = 287$ kN

Total load on girder $B = (350 + 63) = 413$ kN

Maximum reaction in girder $B = \left[\dfrac{(413 \times 28.2)}{30}\right] = 388$ kN

Maximum reaction in girder $A = \left[\dfrac{(287 \times 28.2)}{30}\right] = 270$ kN

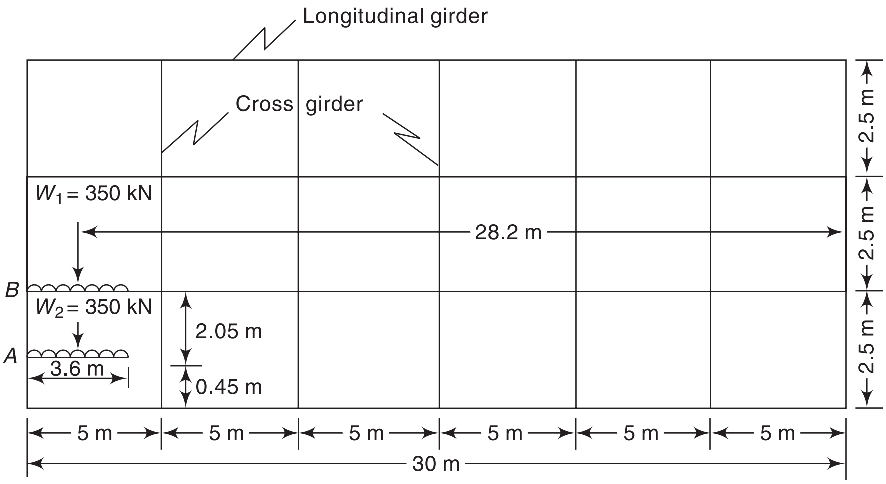

Fig. 21.21 *Position of IRC class AA loads for maximum shear*

Maximum live-load shear with impact factor in the inner girder

$$= (388 \times 1.1) = 427 \text{ kN}$$

Outer girder $= (270 \times 1.1) = 297$ kN

(g) Design bending moments and shear forces The design moments and shear forces are compiled in Table 21.4.

Table 21.4 *Abstract of design moments and shear forces in main girders*

Bending Moment	*DLBM*	*LLBM*	*Total BM*	*Units*
Outer girder	4261	2074	6335	kN m
Inner girder	4261	1596	5857	kN m
Shear Force	*DLSF*	*LLSF*	*Total SF*	*Units*
Outer girder	561	297	858	kN
Inner girder	561	427	988	kN

(h) Properties of main girder section The main girder section is as shown in Fig. 21.22 for computational purposes. The properties of the section are:

$$A = (73 \times 10^4) \text{ mm}^2$$

$$y_t = 750 \text{ mm} \quad y_b = 1050 \text{ mm} \quad I = (2924 \times 10^8) \text{ mm}^4$$

$$Z_t = \left(\frac{I}{Y_t}\right) = \left[\frac{(2924 \times 10^8)}{750}\right] = (3.89 \times 10^8) \text{ mm}^3$$

$$Z_b = \left(\frac{I}{Y_b}\right) = \left[\frac{(2924 \times 10^8)}{1050}\right] = 2.78 \times 10^8 \text{ mm}^3$$

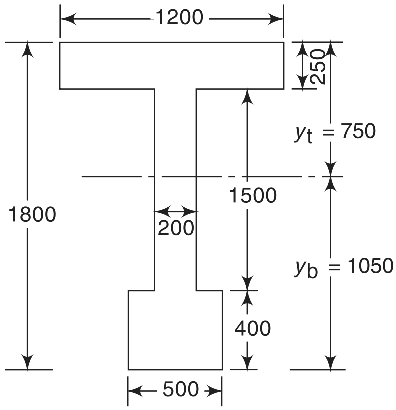

Fig. 21.22 *Cross-section of main girder*

(i) Check for minimum section modulus

$f_{ck} = 50\ \text{N/mm}^2$ $\quad\quad \eta = 0.85$

$f_{ct} = 18\ \text{N/mm}^2$ $\quad\quad M_g = 4261\ \text{kN m}$

$f_{ci} = 40\ \text{N/mm}^2$ $\quad\quad M_q = 2074\ \text{kN m}$

$f_{tt} = f_{tw} = 0$ $\quad\quad M_d = (M_g + M_q) = 6335\ \text{kN m}$

$f_{cw} = 16\ \text{N/mm}^2$

$f_{br} = (\eta f_{ct} - f_{tw}) = (0.85 \times 18 - 0) = 15.3\ \text{N/mm}^2$

$f_{tr} = (f_{cw} - \eta f_{tt}) = 16\ \text{N/mm}^2$

$$f_{inf} = \left(\frac{f_{tw}}{\eta}\right) + \left(\frac{M_d}{\eta Z_b}\right)$$

$$= \left[0 + \frac{(6335 \times 10^6)}{(0.85 \times 2.78 \times 10^8)}\right] = 26.80\ \text{N/mm}^2$$

$$Z_b = \left[\frac{M_q + (1-\eta)M_g}{f_{br}}\right]$$

$$= \left[\frac{(2074 \times 10^6) + (1 - 0.85)4261 \times 10^6}{15.3}\right]$$

$$= (1.77 \times 10^8)\ \text{mm}^3 < (2.78 \times 10^8)\ \text{mm}^3$$

Hence, the section provided is adequate.

(j) Prestressing force

Allowing for two rows of cables, cover required = 200 mm

Maximum possible eccentricity, $e = (1050 - 200) = 850$ mm

Prestressing force is obtained as,

$$P = \frac{(Af_{\text{inf}}Z_b)}{(Z_b + Ae)}$$

$$= \left[\frac{(0.73 \times 10^6 \times 26.80 \times 2.78 \times 10^8)}{(2.78 \times 10^8) + (0.73 \times 10^6 \times 850)}\right]$$

$$= (6053 \times 10^3)\ \text{N} = 6053\ \text{kN}$$

Using the Freyssinet system, anchorage type 7K–15 (seven strands of 15.2 mm diameter) in 65 mm cables ducts, (IS: 6006–1983) (Appendix-3),

Force in each cable = $(7 \times 0.8 \times 260.7) = 1459$ kN

$$\therefore \text{Number of cables} = \left(\frac{6053}{1459}\right) = 5$$

Area of each strand = 140 mm^2
Area of seven strands in each cable = $(7 \times 140) = 980$ mm^2
Area of strands in five cables $A_p = (5 \times 980) = 4900$ mm^2
The cables are arranged at the centre of span section as shown in Fig. 21.23.

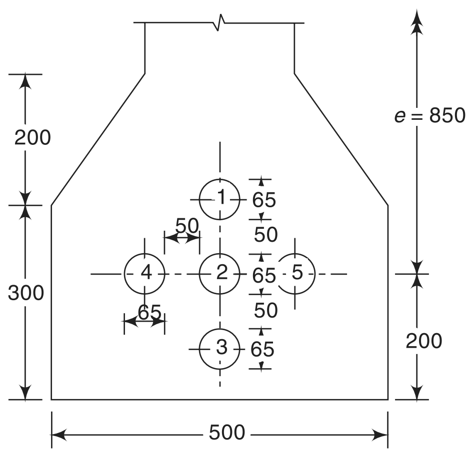

Fig. 21.23 *Arrangement of cable at centre-of-span section*

(k) Permissible tendon zone

At the support section,

$$e \leq \left[\left(\frac{Z_b f_{ct}}{P}\right) - \left(\frac{Z_b}{A}\right)\right]$$

$$\leq \left[\frac{(2.78 \times 10^8 \times 18)}{(6053 \times 10^3)} - \frac{(2.78 \times 10^8)}{(0.73 \times 10^6)}\right] \leq 445\ \text{mm}$$

and $$e \geq \left[\left(\frac{Z_b f_{tw}}{\eta P}\right) - \left(\frac{Z_b}{A}\right)\right]$$

$$\geq \left[0 - \frac{(2.78 \times 10^8)}{(0.73 \times 10^6)}\right] \geq -380 \text{ mm}$$

The five cables are arranged to follow a parabolic profile, with the resultant force having an eccentricity of 180 mm towards the soffit at the support section. The position of cables at the support section is shown in Fig. 21.24.

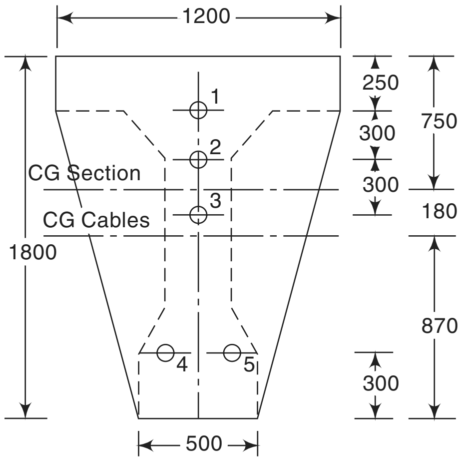

Fig. 21.24 *Arrangement of cables at support section*

Check for stresses For the centre of span section, we have

$P = 6053$ kN $\qquad Z_t = 3.89 \times 10^8$ mm^3

$e = 850$ mm $\qquad \eta = 0.85$

$A = 0.73 \times 10^6$ mm^2 $\qquad M_g = 4261$ kN m

$Z_b = 2.78 \times 10^8$ mm^3 $\qquad M_q = 2074$ kN m

$$\left(\frac{P}{A}\right) = \frac{(6053 \times 10^3)}{(0.73 \times 10^6)} = 8.29 \text{ N/mm}^2$$

$$\left(\frac{Pe}{Z_t}\right) = \frac{(6053 \times 10^3 \times 850)}{(3.89 \times 10^8)} = 13.22 \text{ N/mm}^2$$

$$\left(\frac{Pe}{Z_b}\right) = \frac{(6053 \times 10^3 \times 850)}{(2.78 \times 10^8)} = 18.50 \text{ N/mm}^2$$

$$\left(\frac{M_g}{Z_t}\right) = \frac{(4261 \times 10^6)}{(3.89 \times 10^8)} = 10.95 \text{ N/mm}^2$$

$$\left(\frac{M_g}{Z_b}\right) = \frac{(4261 \times 10^6)}{(2.78 \times 10^8)} = 15.32 \text{ N/mm}^2$$

$$\left(\frac{M_q}{Z_t}\right) = \frac{(2074 \times 10^6)}{(3.89 \times 10^8)} = 5.33 \text{ N/mm}^2$$

$$\left(\frac{M_q}{Z_b}\right) = \frac{(2074 \times 10^6)}{(2.78 \times 10^8)} = 7.46 \text{ N/mm}^2$$

At the transfer stage

$$\sigma_t = \left[\left(\frac{P}{A}\right) - \left(\frac{Pe}{Z_t}\right) + \left(\frac{M_g}{Z_t}\right)\right]$$

$$= (8.29 - 13.22 + 10.95) = 6.02 \text{ N/mm}^2$$

$$\sigma_b = \left[\left(\frac{P}{A}\right) + \left(\frac{Pe}{Z_b}\right) - \left(\frac{M_g}{Z_b}\right)\right]$$

$$= [8.29 + 18.50 - 15.32] = 11.47 \text{ N/mm}^2$$

At the working load stage

$$\sigma_t = \left[\eta\left(\frac{P}{A}\right) - \eta\left(\frac{Pe}{Z_t}\right) + \left(\frac{M_g}{Z_t}\right) + \left(\frac{M_q}{Z_t}\right)\right]$$

$$= [0.85(8.29 - 13.22) + 10.95 + 5.33] = 12.09 \text{ N/mm}^2 \text{ (compression)}$$

$$\sigma_b = \left[\eta\left(\frac{P}{A}\right) + \eta\left(\frac{Pe}{Z_b}\right) - \left(\frac{M_g}{Z_b}\right) - \left(\frac{M_q}{Z_b}\right)\right]$$

$$= [0.85(8.29 + 18.50) - 15.32 - 7.46] = -0.01 \text{ N/mm}^2 \text{ (Tension)}$$

All the stresses at the top and bottom fibres at transfer and service loads are well within the safe permissible limits.

Check for ultimate flexural strength

For the centre-of-span section,

$$A_p = (5 \times 7 \times 140) = 4900 \text{ mm}^2$$
$$b = 1200 \text{ mm}$$
$$d = 1600 \text{ mm}$$
$$b_w = 200 \text{ mm}$$
$$f_{ck} = 50 \text{ N/mm}^2$$
$$f_p = 1862 \text{ N/mm}^2$$
$$D_f = 250 \text{ mm}$$

According to the specifications of IRC: 6-2014, the design ultimate moments and shear forces in the girder are calculated by applying the partial safety factors for dead and live loads as follows:

The required design ultimate bending moment in the outer girder is evaluated as,

$$M_u = [1.35\ M_d + 1.5\ M_L\ ]$$
$$= [(1.35 \times 4261) + (1.5 \times 2074)$$
$$= 8864 \text{ kN.m}$$

According to IS: 1343–2012, the ultimate flexural strength of the centre-of-span section is computed as follows:

$$A_p = (A_{pw} + A_{pf})$$

$$A_{pf} = 0.45 f_{ck}(b - b_w)\left(\frac{D_f}{f_p}\right)$$

$$= (0.45 \times 50)\ (1200 - 200)\left(\frac{250}{1862}\right) = 3021 \text{ mm}^2$$

$\therefore$ $$A_{pw} = (4900 - 3021) = 1879 \text{ mm}^2$$

$$\text{Ratio} = \left(\frac{A_{pw} f_p}{b_w d f_{ck}}\right) = \left(\frac{1879 \times 1862}{200 \times 1600 \times 50}\right) = 0.218$$

From Table 7.1, for the post-tensioned beams with effective bond, we have

$$\left(\frac{f_{pb}}{0.87 f_{pk}}\right) = 0.93$$

$\therefore$ $$f_{pb} = (0.93 \times 0.87 \times 1862) = 1506 \text{ N/mm}^2$$

and $$\left(\frac{x_u}{d}\right) = 0.43$$

or $$x_u = (0.43 \times 1600) = 688 \text{ mm}$$

$\therefore$ $$M_u = [f_{pb} A_{pw}(d - 0.42\ x_u) + 0.45 f_{ck}(b - b_w) D_f (d - 0.5 D_f)]$$
$$= [1506 \times 1879\ (1600 - 0.42 \times 688)$$
$$+ 0.45 \times 50 \times 1000 \times 250\ (1600 - 0.5 \times 250)]$$
$$= 12006 \times 10^6 \text{ N mm} = 12006 \text{ kN m}$$

$$M_u = 12006 \text{ kN.m} > 8864 \text{ kN.m (hence, safe)}$$

Check for Ultimate Shear Strength

$$\text{Ultimate shear force} = V_u = [(1.35\ V_g + 1.5\ V_q)]$$
$$= [(1.35 \times 561) + (1.5 \times 4.27)]$$
$$= 1398 \text{ kN}$$

The design shear resistance of the support section is calculated by using the equation specified in IRC: 112-2011 clause 10.3 as,

$$V_{Rd.c} = \left(\frac{I.b_w}{s}\right)\sqrt{(f_{ctd})^2 \mp k_1 \sigma_{cp} f_{ctd}} + \eta P \sin\theta$$

Computing the numerical values of the various parameters, we have

$$I = \left(\frac{b_w D^3}{12}\right) = \left(\frac{200 \times 1800^3}{12}\right) = (972 \times 10^8)\text{mm}^4$$

$$S = \left(\frac{200 \times 750 \times 750}{2}\right) = (56.2 \times 10^6)\ \text{mm}^3$$

$f_{ctd} = (f_{ct}/\gamma_m) = (3.5/1.5) = 2.33$ since $f_{ct} = 3.5$ N/mm^2 for $f_{ck} = 50$ N/mm^2

$\sigma_{cp}\ (\eta P/A_c) = [(0.85 \times 6053 \times 10^3)/(73 \times 10^4)] = 7.04$ N/mm^2

$\theta = (4e/L) = [(4 \times 670)/(30 \times 1000)] = 0.089$

$$V_{Rd.c} = \left(\frac{I.b_w}{s}\right)\sqrt{\left(f_{ctd}\right)^2 \mp k_1\sigma_{cp}f_{ctd}} + \eta P \sin\theta$$

$$= \left(\frac{(972 \times 10^8)200}{56.2 \times 10^6}\right)\sqrt{(2.33)^2 \mp 1 \times 7.04 \times 2.33}$$

$$+ (0.8 \times 6053 \times 10^3 \times 0.089)\ \text{N}$$

$$= (2021 \times 10^3)\ \text{N}$$

$$= 2021\ \text{kN} > 1398\ \text{kN}$$

Provide nominal stirrups of 10 mm diameter 2 – legged stirrups of Fe-415 HYSD bars at a maximum spacing of 300 mm throughout the span according to the specifications of IRC: 112-2011.

Supplementary Reinforcements

According to Clause 16.5.1.1 of IRC: 112-2011, minimum longitudinal reinforcements of not less than 0.13 per cent of gross cross-sectional area are to be provided to safeguard against shrinkage cracking.

$$A_{SL} = \{0.0013 \times 0.73 \times 10^6) = 949\ \text{mm}^2$$

20 mm diameter bars are provided in the compression flange as shown in Fig. 21.25.

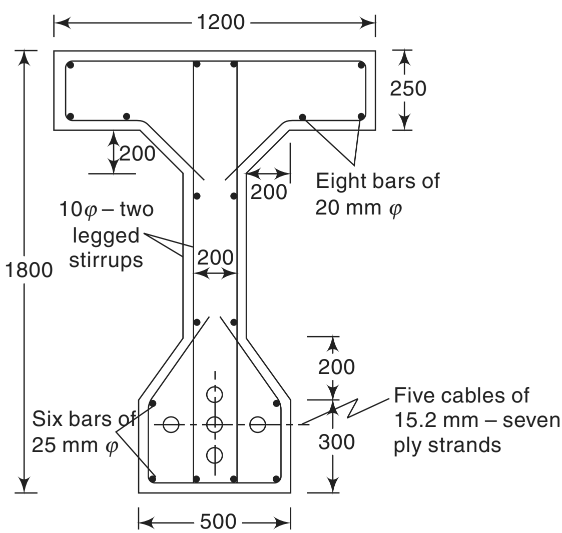

Fig. 21.25 *Reinforcement details at centre-of-span section*

Design of End Block

Solid end blocks are provided at end supports over a length of 1.5 m. Typical equivalent prisms on which the anchorage forces are considered to be effective are detailed in Fig. 21.26.

In the horizontal plane, we have the data,

$$P_K = 1459 \text{ kN}, 2Y_{po} = 225 \text{ mm} \quad \text{and} \quad 2Y_o = 900 \text{ mm}$$

Hence, the ratio $(Y_{po}/Y_o) = (112.5/450) = 0.25$

Interpolating from Table 21.3, the bursting tension is computed as,

$$F_{bst} = (0.26 \times 1459) = 380 \text{ kN}$$

Area of steel required to resist this tension is obtained as,

$$A_s = [(380 \times 10^3)/(0.87 \times 415)] = 1052 \text{ mm}^2$$

Provide 10 mm diameter bars at 100 mm centres in the horizontal direction. In the vertical plane, the ratio of (Y_{po}/Y_o) being higher, the magnitude of bursting tension is smaller. However, the same reinforcements are provided in the form of a mesh both in the horizontal and vertical directions as shown in Fig. 21.26.

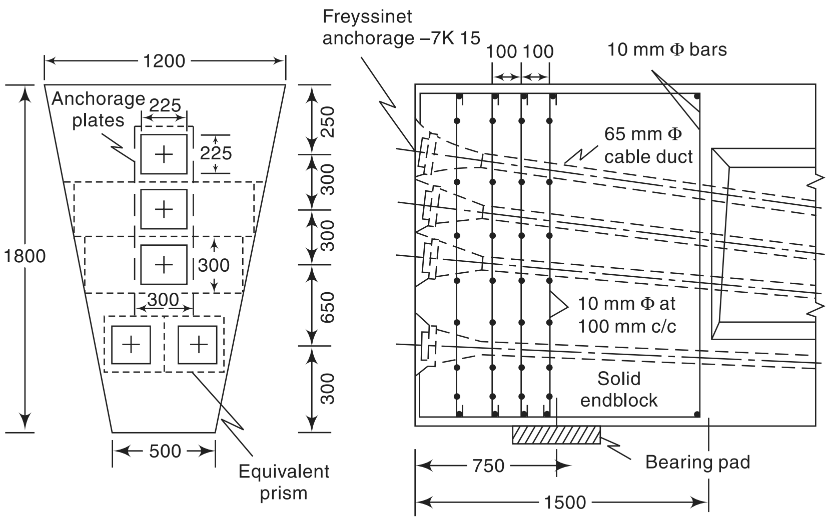

Fig. 21.26 *Equivalent prisms and anchorage zone reinforcement*

Cross Girders

Cross girders of width 200 mm and depth 1250 mm are provided at intervals of 5 m along the span of the main girders. Nominal reinforcements of 0.15 per cent of the cross-section, consisting of 12 mm diameter bars spaced two at top, two at mid-depth and two at bottom are provided in the cross girders. Nominal stirrups made up of 10 mm diameter two legged links are provided at 200 mm centres. Two straight H.T cables each consisting of 12 high tensile wires of

7 mm diameter are positioned at mid third points along the depth of the cross girders.

21.7 Design of Post-tensioned Prestressed Concrete Continuous Two-Span Beam and Slab Bridge Deck

Design a post-tensioned prestressed concrete continuous beam and slab bridge deck for a national highway crossing using the following data:

Data

Width of carriage way = 7.5 m
Two continuous spans of 40 m each
Kerbs: 600 mm wide on each side
Wearing coat thickness = 80 mm
Live load: IRC Class AA tracked vehicle
For prestressed concrete girders, adopt M-60 grade concrete with compressive strength of concrete at transfer as 40 N/mm^2.
For cast-in-situ deck slab, adopt M-20 grade concrete.
Spacings of cross girders = 5 m
Spacing of main girders = 2.5 m
Loss ratio = 0.8
High tensile strands of 15.2 mm diameter conforming to IS: 6006-1983 and Fe-415 HYSD bars are available for use.
Design the bridge deck as Class-1 type structure conforming to the codes IS: 6-2014, IRC: 112-2011 and IS: 1343-2012.

Maximum permissible stresses in concrete and steel

According to the given data, we have for M-60 grade concrete.
Compressive strength of concrete = f_{ck} = 60 N/mm^2
Adopt permissible stress in concrete at transfer = f_{ct} = 20 N/mm^2
Permissible tensile stress (Class–1 type structure) = $f_{tt} = f_{tw} = 0$
Ultimate tensile strength of 12 wires of 7 mm diameter high tensile cables = f_p = 1500 N/mm^2
Maximum permissible stress in the H.T cable = 1200 N/mm^2
Modulus of elasticity of concrete = E_c = 37 kN/mm^2
For M-20 grade concrete and Fe-415 HYSD bars adopt the following parameters.
f_{ck} = 20 N/mm^2 and f_y = 415 N/mm^2
$M_u = 0.138\, f_{ck}\, b\, d^2$

Cross-section of deck

Four main girders are provided at intervals of 2.5 m
Thickness of deck slab = 250 mm
Wearing coat = 80 mm

Kerbs, 600 mm wide by 300 mm deep, are provided at each end
Spacing of cross girders = 5 m
The overall depth of the main girders is assumed at 50 mm per metre of span
$\therefore$ Overall depth of girder = $(50 \times 40) = 2000$ mm
Thickness of top and bottom flanges = 400 mm
Thickness of web = 200 mm
The section properties of the main girder are as follows:
Cross-sectional area, $A = 0.88\ \text{m}^2$
Second moment of area, $I = 0.447\ \text{m}^4$

$$y_b = y_t = 1\ \text{m}$$

Section modulus = $Z_t = Z_b = Z = 0.447\ \text{m}^3$

The main girders are precast and the deck slab is cast *in situ*. The cross-sections of the bridge deck and the girders are shown in Figs 21.27 and 21.28, respectively.

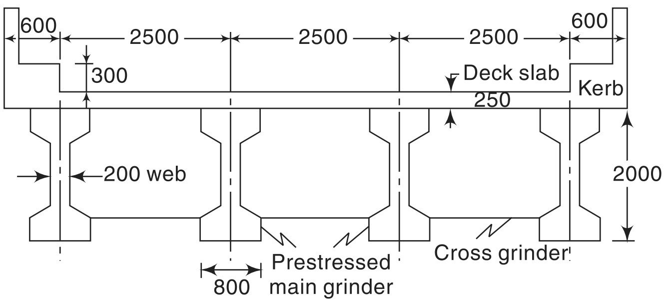

Fig. 21.27 *Cross-section of bridge deck*

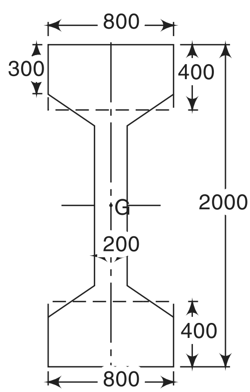

Fig. 21.28 *Cross-section of main girder*

Design of interior slab panel The slab panel, 2.5 m by 5 m, is supported on all the four sides.
The design is similar to that presented in Example 21.6.

Design of continuous longitudinal girders

(a) Reaction factors The spacing of the girders being the same as in Example 21.6, the reaction factor for the outer girder, $R_A = 0.382$ W.

(b) Loads acting on the main girder

Self-weight of slab = (0.25×25) $= 6.25$ kN/m^2

Weight of WC = (0.08×22) $= 1.76$

Total load 8.00 kN/m^2

Load from slab and WC = $(8 \times 2.5) = 20$ kN/m

Self-weight of the main girder = $(0.88 \times 25) = 22$ kN/m

Weight of cross girders assumed to act as uniformly distributed load = 5 kN/m

$\therefore$ Total dead load on the main girder, $g = 47$ kN/m

(c) Dead-load moments and shear forces

Dead-load moment at the mid-support section,

$$M_{gB} = 0.125\, gL^2 = (0.125 \times 47 \times 40^2) = 9400 \text{ kN m}$$

Dead-load moment at the mid-span section,

$$M_{gD} = 0.071\, gL^2 = (0.071 \times 47 \times 40^2) = 5340 \text{ kN m}$$

Dead-load shear is maximum near the mid-support section and is computed as follows:

$$V_g = 0.62\, gL = (0.62 \times 47 \times 40) = 1166 \text{ kN}$$

Referring to the influence line for bending moments at the mid-span section *D* shown in Fig. 21.29, the maximum live-load moment at the mid-span is computed as,

$$M_D = \left(\frac{7.3 + 8.12}{2}\right) 700 = 5397 \text{ kN m}$$

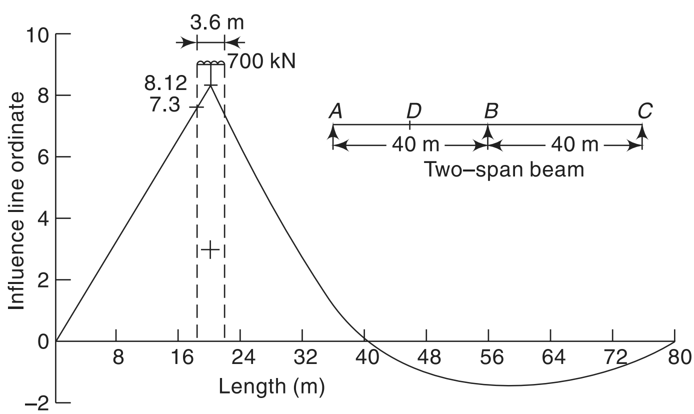

Fig. 21.29 *Influence line for bending moment at mid-span D*

Similarly, from Fig. 21.30, using the influence line for bending moment at the mid support, the live-load bending moment at support *B* is computed as,

$$M_B = (3.76 \times 700) = 2632 \text{ kN m}$$

The live-load bending moments, including the reaction factor and impact factors for the exterior girder are,

$$M_{qD} = (5397 \times 1.1 \times 0.382) = 2268 \text{ kN m}$$
$$M_{qB} = (2632 \times 1.1 \times 0.382) = 1106 \text{ kN m}$$

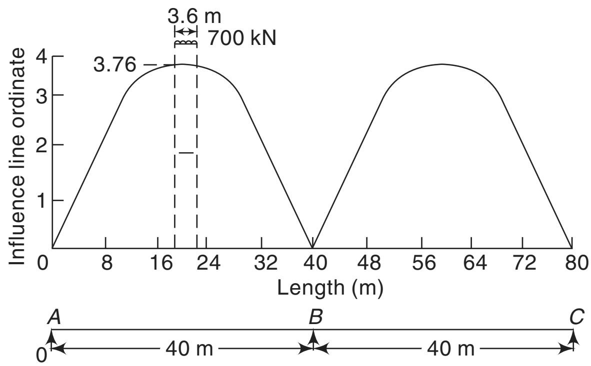

Fig. 21.30 *Influence line for bending moment at mid-support B*

(d) Live-load shear forces in girder The maximum live-load shear develops in the interior girders when the IRC class AA loads are placed near the mid-support as shown in Fig. 21.31.

$$\text{Reaction of } W_2 \text{ on girder } B = \left[\frac{(350 \times 0.45)}{2.5}\right] = 63 \text{ kN}$$

$$\text{Reaction of } W_2 \text{ on girder } A = \left[\frac{(350 \times 2.05)}{2.5}\right] = 287 \text{ kN}$$

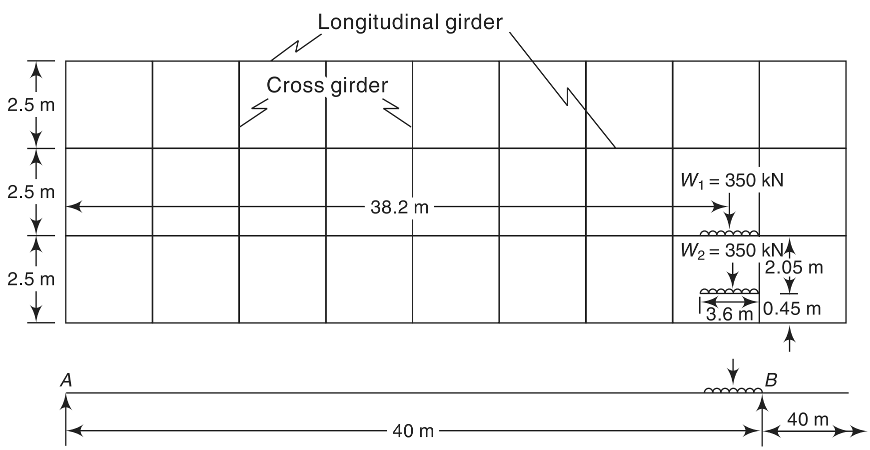

Fig. 21.31 *Position of IRC class AA loads for maximum shear*

$\therefore$ Total load on girder $B = (350 + 63) = 413$ kN

$$\text{Maximum reaction in girder } B = \left[\frac{(413 \times 38.2)}{40}\right] = 394 \text{ kN}$$

Maximum live-load shear with impact factor in the inner girder

$$= (394 \times 1.1) = 434 \text{ kN}$$

(e) Design bending moments and shear forces The design bending moments and shear forces at service loads and ultimate loads as stipulated IRC: 6-2014 are compiled in Table 21.5.

Table 21.5 *Service load and ultimate load moments and shear forces in longitudinal girders*

(a) Bending Moments (Outer Girder)

Section	*Dead Load B.M (M_g)*	*Live Load B.M (M_q)*	*Service Load B.M ($M_g + M_q$)*	*Ultimate Load B.M (1.35 M_g + 1.5 M_q)*	*Units*
Mid span at (D)	5340	2268	7608	10611	kN.m
Mid support at (B)	9400	1106	10506	14349	kN.m

(b) Shear Forces (Inner Girder)

Section	*Dead Load S.F (V_g)*	*Live Load S.F (V_q)*	*Service Load S.F ($V_g + V_q$)*	*Ultimate Load S.F (1.35 V_g + 1.5 V_q)*	*Units*
Middle support section	1116	434	1550	2158	kN

(f) Check for minimum section modulus At the mid-support section B,

$$M_g = 9400 \text{ kN m}$$

$$M_q = 1106 \text{ kN m}$$

$$M_d = (M_g + M_q) = 10506 \text{ kN m}$$

$$f_{br} = (\eta f_{ct} - f_{tw}) = (0.8 \times 20 - 0) = 16 \text{ N/mm}^2$$

$$f_{inf} = \left[\left(\frac{f_{tw}}{\eta}\right) + \left(\frac{M_g}{\eta z_b}\right)\right]$$

$$= \left[0 + \frac{(10506 \times 10^6)}{(0.8 \times 0.447 \times 10^9)}\right] = 29.37 \text{ N/mm}^2$$

$$Z_b \geq \left[\frac{M_q + (1-\eta)M_g}{f_{br}}\right]$$

$$\geq \left[\frac{(1106 \times 10^6) + (1 - 0.8)9400 \times 10^6}{16}\right]$$

$$\geq (0.186 \times 10^9) \text{ mm}^3 < (0.447 \times 10^9) \text{ mm}^3$$

Hence, the section provided is adequate.

(g) Prestressing force For the two continuous spans AB and BC, a concordant cable profile is selected such that the secondary moments are zero. The cable profile selected is shown in Fig. 21.32. The maximum possible eccentricity at the mid-support section B is determined by providing suitable cover to house the cables. Assuming a cover of 250 mm,

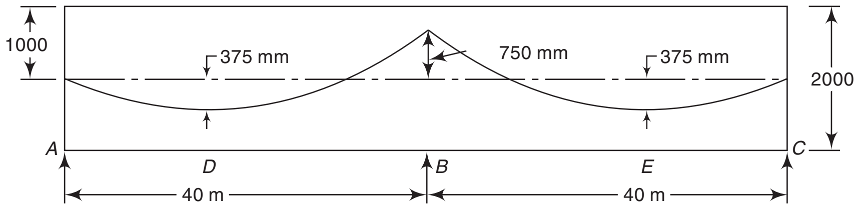

Fig. 21.32 *Concordant cable profile*

Maximum possible eccentricity, $e = (1000 - 250) = 750$ mm
Prestressing force is obtained from the relation,

$$P = \left[\frac{(Af_{\text{inf}}Z_b)}{(Z_b + Ae)}\right]$$

$$= \left[\frac{(0.88 \times 10^6 \times 29.37 \times 0.447 \times 10^9)}{(0.447 \times 10^9) + (0.88 \times 10^6 \times 750)}\right] = 10434000 \text{ N} = 10434 \text{ kN}$$

Using the Freyssinet system, anchorage-type 19K-15 (19 strands of 15.2 mm diameter) in 95 mm cable ducts (Table A.3.3 of Appendix-3),
Force in each cable = $(19 \times 0.8 \times 260.7) = 3962$ kN
Provide three cables carrying an initial prestressing force

$$P = (3 \times 4000) = 12000 \text{ kN}$$

Area of each strand of 15.2 mm diameter = 140 mm^2
Area of 19 strands in each cable = $(19 \times 140) = 2660$ mm^2
Total area in the three cables = $A_p = (3 \times 2660) = 7980$ mm^2

The cables are arranged in a parabolic concordant profile so that their centroid has an eccentricity of 750 mm towards the top fibre at the mid-support section B and an eccentricity of 375 mm towards the soffit at the mid-span section D. The centroid of the cables is concentric at the end supports A and C. The selected cable profile is shown in Fig. 21.33.

(h) Check for stresses

(a) Centre-at-span section

$$P = 12000 \text{ kN} \qquad \eta = 0.80$$
$$e = 375 \text{ mm} \qquad M_g = 5340 \text{ kN m}$$
$$A = 0.88 \times 10^6 \text{ mm}^2 \qquad M_q = 2268 \text{ kN m}$$
$$Z = 0.447 \times 10^9 \text{ mm}^3$$

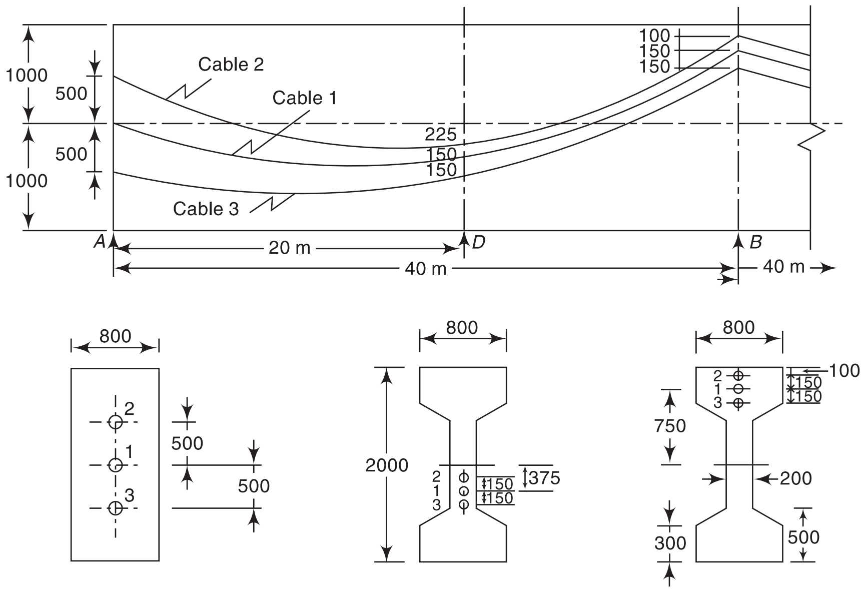

Fig. 21.33 *Cable layout in main girder*

$$\left(\frac{P}{A}\right) = \left[\frac{(12000 \times 10^3)}{(0.88 \times 10^6)}\right] = 13.63 \text{ N/mm}^2$$

$$\left(\frac{Pe}{Z}\right) = \left[\frac{(12000 \times 10^3 \times 375)}{(0.447 \times 10^6)}\right] = 10.06 \text{ N/mm}^2$$

$$\left(\frac{M_g}{Z}\right) = \left[\frac{(5340 \times 10^6)}{(0.447 \times 10^9)}\right] = 11.94 \text{ N/mm}^2$$

$$\left(\frac{M_q}{Z}\right) = \frac{(2268 \times 10^6)}{(0.447 \times 10^9)} = 5.07 \text{ N/mm}^2$$

At the stage of transfer

$$\sigma_t = \left[\left(\frac{P}{A}\right) - \left(\frac{Pe}{Z}\right) + \left(\frac{M_g}{Z}\right)\right]$$

$$= [13.63 - 10.06 + 11.94] = 15.51 \text{ N/mm}^2$$

$$\sigma_b = \left[\left(\frac{P}{A}\right) + \left(\frac{Pe}{Z}\right) - \left(\frac{M_g}{Z}\right)\right]$$

$$= [13.63 + 10.06 - 11.94] = 11.75 \text{ N/mm}^2$$

At the service load state

$$\sigma_t = \left[\eta\left(\frac{P}{A}\right) - \eta\left(\frac{Pe}{Z}\right) + \left(\frac{M_g}{Z}\right) + \left(\frac{M_q}{Z}\right)\right]$$

$$= [0.8(13.63 - 10.06) + 11.94 + 5.07]$$

$$= 19.86 \text{ N/mm}^2 < 20 \text{ N/mm}^2$$

$$\sigma_b = \left[\eta\left(\frac{P}{A}\right) + \eta\left(\frac{Pe}{Z}\right) - \left(\frac{M_g}{Z}\right) - \left(\frac{M_q}{Z}\right)\right]$$

$$= [0.8(13.63 + 10.06) - 11.94 - 5.07] = 1.94 \text{ N/mm}^2$$

(b) Mid-support section

$P = 12000$ kN $\qquad \eta = 0.80$

$e = 750$ mm $\qquad M_g = 9400$ kN m

$A = (0.88 \times 10^6)$ mm^2 $\qquad M_q = 1106$ kN m

$Z = (0.447 \times 10^9)$ mm^3

$$\left(\frac{P}{A}\right) = 13.63 \text{ N/mm}^2$$

$$\left(\frac{Pe}{Z}\right) = \frac{(12000 \times 10^3 \times 750)}{(0.447 \times 10^9)} = 20.13 \text{ N/mm}^2$$

$$\left(\frac{M_g}{Z}\right) = \frac{(9400 \times 10^6)}{(0.447 \times 10^9)} = 21.02 \text{ N/mm}^2$$

$$\left(\frac{M_q}{Z}\right) = \frac{(1106 \times 10^6)}{(0.447 \times 10^9)} = 2.47 \text{ N/mm}^2$$

At the stage of transfer

$$\sigma_t = [13.63 + 20.13 - 21.02] = 12.74 \text{ N/mm}^2$$

$$\sigma_b = [13.63 - 20.13 + 21.02] = 14.52 \text{ N/mm}^2$$

At the service load stage

$$\sigma_t = [0.8(13.63 + 20.13) - 21.02 - 2.47] = 3.52 \text{ N/mm}^2$$

$$\sigma_b = [0.8(13.63 - 20.13) + 21.02 + 2.47] = 18.29 \text{ N/mm}^2$$

The stresses in general are within the maximum permissible limit of 20 N/mm^2.

(i) Check for Ultimate Flexural Strength

(a) Centre of span section

The ultimate flexural strength of the Tee-section girder is computed using the specifications of IS: 1343-2012.

$A_p = 7980$ mm^2 $\qquad D_f = 200$ mm $\qquad f_p = 1862$ N/mm^2

$b = 800$ mm $\qquad d = 1375$ mm $\qquad M_u$ (Required) $= 10611$ kN.m

$b_w = 200$ mm $\qquad f_{ck} = 60$ N/mm^2

$A_p = (A_{pw} + A_{pf})$

$$A_{pf} = 0.45\, f_{ck}\,(b - b_w)\left(\frac{D_f}{f_p}\right) = \left[0.45 \times 60\,(800 - 200)\left(\frac{200}{1862}\right)\right] = 1740 \text{ mm}^2$$

$$A_{pw} = (7980 - 1740) = 6240 \text{ mm}^2$$

$$\text{Ratio}\left[\frac{A_{pw} f_p}{b_w d f_{ck}}\right] = \left[\frac{6240 \times 1862}{200 \times 1375 \times 60}\right] = 0.70$$

From Table-11 of IS: 1343, interpolate the values of the ratio ($f_{pb}/0.87f_{pu}$) and (x_u/d) corresponding to the above ratio of 0.70.

$$\left(\frac{f_{pb}}{0.87\, f_{pu}}\right) = 0.75 \text{ and } (x_u/d) = 0.653$$

$$\begin{aligned}
f_{pb} &= (0.75 \times 0.87 \times 1862) = 1214.9 \text{ N/mm}^2\\
x_u &= (0.653 \times 1375) = 897.8 \text{ mm}\\
\therefore \quad M_u &= \{f_{pb} A_{pw}(d - 0.42\, x_u) + 0.45\, f_{ck}(b - b_w)\, D_f(d - 0.5\, D_f)\}\\
&= \{1214.9 \times 4500\,(1375 - 0.42 \times 897.8\}\\
&\quad + \{0.45 \times 60(800 - 200)\, 400(1375 - 0.5 \times 400)\}\\
&= (13070 \times 10^6) \text{ N.mm}\\
&= 13070 \text{ kN.m} > 10611 \text{ kN.m (hence, safe)}
\end{aligned}$$

(b) Mid support section

All the parameters are the same except the effective depth, $d = 1750$ mm and M_u (required) = 14349 kN.m

$$\text{Ratio}\left[\frac{A_{pw} f_p}{b_w d f_{ck}}\right] = \left[\frac{4500 \times 1862}{200 \times 1750 \times 60}\right] = 0.40$$

From Table 11 of IS: 1343, interpolate the values of the ratio (f_{pb} / $0.87f_{pu}$) and (x_u/d) corresponding to the above ratio of 0.40.

$$\left(\frac{f_{pb}}{0.87\, f_{pu}}\right) = 0.75 \text{ and } (x_u/d) = 0.653$$

$$\begin{aligned}
f_{pb} &= (0.75 \times 0.87 \times 1862) = 1214.9 \text{ N/mm}^2\\
x_u &= (0.653 \times 1750) = 1142.75 \text{ mm}\\
\therefore \quad M_u &= \{f_{pb} A_{pw}(d - 0.42\, x_u) + 0.45\, f_{ck}(b - b_w)\, D_f(d - 0.5\, D_f)\}\\
&= \{1214.9 \times 4500\,(1750 - 0.42 \times 1142.75\}\\
&\quad + \{0.45 \times 60(800 - 200)\, 400(1750 - 0.5 \times 400)\}\\
&= (16987 \times 10^6) \text{ N.mm}\\
&= 16987 \text{ kN.m} > 14349 \text{ kN.m (hence, safe)}
\end{aligned}$$

Hence, the mid span and support sections satisfy the code specifications for the limit state of ultimate strength.

(j) Check for Ultimate Shear Strength The mid support section is checked for the ultimate shear strength.

Shear strength required = 2158 kN

The design shear resistance of the support section is calculated by using the equation specified in IRC: 112-2011 clause 10.3 as,

$$V_{\text{Rd.c}} = \left(\frac{I.b_{\text{w}}}{s}\right)\sqrt{(f_{\text{ctd}})^2 \mp k_1\sigma_{\text{cp}}f_{\text{ctd}}} + \eta P \sin\theta$$

Computing the numerical values of the various parameters, we have

$$I = \left(\frac{b_{\text{w}}D^3}{12}\right) = \left(\frac{200 \times 2000^3}{12}\right) = (1333 \times 10^8)\ \text{mm}^4$$

$$S = \left(\frac{200 \times 1000 \times 1000}{2}\right) = (100 \times 10^6)\ \text{mm}^3$$

$f_{\text{ctd}} = (f_{\text{ct}}/\gamma_{\text{m}}) = (4.0/1.5) = 2.66$ since $f_{\text{ct}} = 4.0\ \text{N/mm}^2$
for $f_{\text{ck}} = 60\ \text{N/mm}^2$
$\sigma_{\text{cp}} = (\eta P/A_{\text{c}}) = [(0.8 \times 12000 \times 10^3)/(88 \times 10^4)] = 10.9\ \text{N/mm}^2$
$\theta = (4e/L) = [(4 \times 750)/(40 \times 1000)\} = 0.075$

$$\therefore \quad V_{\text{Rd.c}} = \left(\frac{I.b_{\text{w}}}{s}\right)\sqrt{\left(f_{\text{ctd}}\right)^2 \mp k_1\sigma_{\text{cp}}f_{\text{ctd}}} + \eta P \sin\theta$$

$$= \left(\frac{(1333 \times 10^8)200}{100 \times 10^6}\right)\sqrt{(2.66)^2 \mp 1 \times 10.9 \times 2.33}$$

$$+ (0.8 \times 12000 \times 10^3 \times 0.089)\ \text{N}$$

$$= (2371 \times 10^3)\ \text{N}$$

$$= 2371\ \text{kN} > 2158\ \text{kN}$$

Nominal shear reinforcements of 10 mm diameter two legged stirrups are designed using the ralation

$$S_{\text{v}} = \left(\frac{0.87 f_{\text{y}} A_{\text{sv}}}{0.4b}\right) = \left(\frac{0.87 \times 415 \times 2 \times 79}{0.4 \times 200}\right) = 713\ \text{mm}$$

The stirrups are provided at a maximum spacing of 300 mm throughout the span as per IRC: 112-2011 specifications.

(k) Supplementary Reinforcements According to Clause 16.5.1.1 of IRC: 112-2011, minimum longitudinal reinforcements of not less than 0.13 per cent of gross cross-sectional area are to be provided to safeguard against shrinkage cracking.

$$A_{\text{SL}} = \{0.0013 \times 88 \times 10^4) = 1144\ \text{mm}^2$$

The details of reinforcements and cables provided at mid span and support sections are shown in Fig. 21.34.

(l) Design of end block Solid end blocks, 800 mm by 2000 mm, are provided for length of 2 m from each of the two end-faces of the girders. The equivalent prisms on which the anchorage forces are considered to be effective are shown in Fig. 21.35(a).

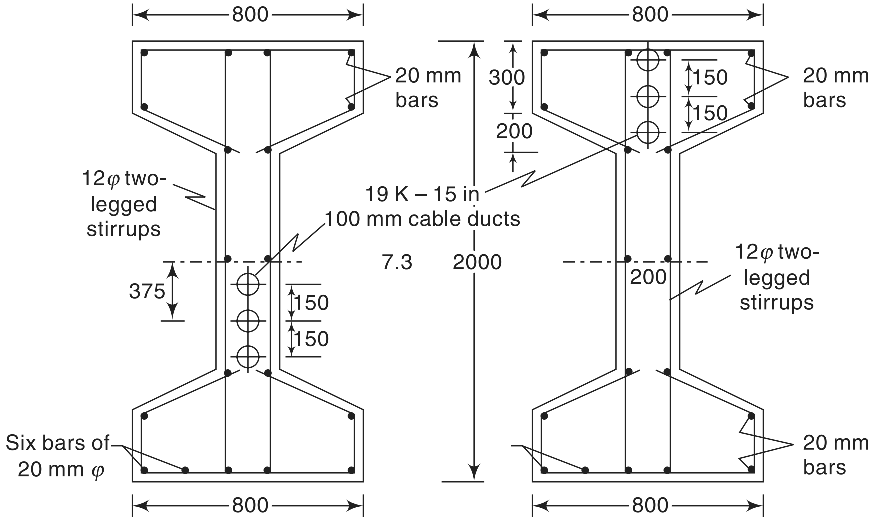

Fig. 21.34 *Reinforcement details at mid-span and mid-support sections*

In the horizontal plane, we have the data,

$$P_K = 4000 \text{ kN}, 2Y_{po} = 340 \text{ mm} \quad \text{and} \quad 2Y_o = 800 \text{ mm}$$

Hence, the ratio $(Y_{po}/Y_o) = (340/800) = 0.425$
Interpolating from Table 21.3, the bursting tension is computed as,

$$F_{bst} = (0.22 \times 4000) = 880 \text{ kN}$$

Area of steel required to resist this tension is obtained as,

$$A_s = [(880 \times 10^3)/(0.87 \times 415)] = 2437 \text{ mm}^2$$

Provide 16 mm diameter bars at 150 mm centres in the horizontal plane distributed in the region $0.2Y_o$ to $2Y_o$ (80 to 800 mm) as shown in Fig. 21.35. In the vertical plane, the ratio of (Y_{po}/Y_o) being larger, the magnitude of bursting tension is less. However, the same reinforcements are provided in the vertical plane in the form of a mesh to resist bursting tension.

(m) Cross girders Cross girders of width 200 mm and depth 1600 mm are provided with nominal reinforcements of 0.13 per cent of the cross-section comprising 12 mm diameters spaced two at the top and bottom and two each at distances of 700 mm from the top and bottom of the girders, respectively. Nominal stirrups of 10 mm diameter, two-legged links are also provided at 200 mm centres. Two cables, consisting of 12 numbers of 7 mm high-tensile wires, are positioned at mid-third points along the depth, with a nominal prestress to provide lateral stiffness to the bridge deck system.

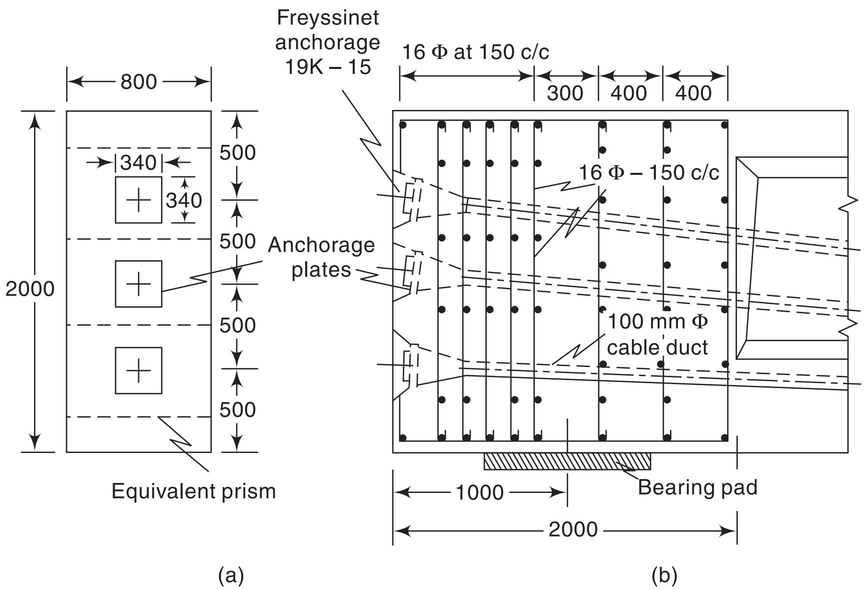

Fig. 21.35 *Anchorage zone reinforcement in end block*

21.8 Design of Post-tensioned Prestressed Concrete Continuous Two-Span Cellular Box Girder Bridge Deck

A cellular multicelled prestressed concrete box girder deck is to be designed for a national highway crossing. The proposed bridge deck is made up of two continuous spans each of 50 m. The road width is 7.5 m with foot paths 1.25 m on each side. The box girder is proposed to have four cells 2 m wide and 2 m deep, and should support IRC Class AA tracked vehicle loading. Design the cellular bridge deck adopting M-60 grade concrete, Fe-415 HYSD bars and high-tensile steel strands of 15.2 mm diameter conforming to the relevant Indian standards.

Data

Two continuous spans of 50 m each ($L = 50$ m)
Cross-section: Multicelled box girder with cell dimensions of 2 m wide by 2 m deep
Road width = 7.5 m with foot paths: 1.25 m wide on either side of road way
Wearing coat = 80 mm, Thickness of web = 300 mm to house 27K-15 Freyssinet anchorages
(27 strands of 15.2 mm diameter in 110 mm diameter cables)
(Refer to Appendix-3, Table A.3.3 for details of Freyssinet Anchorages)

Thickness of top and bottom slabs = 300 mm
Concrete grade: M-60 and Loss ratio = 0.80
Type of tendons: High-tensile strands of 15.2 mm diameter conforming to IRC: 6006–2000
Type of supplementary reinforcements: Fe-415 HYSD bars
Design the bridge deck conforming to the relevant IRC and IS Codes.

Maximum Permissible Stresses in Concrete and Steel

According to the given data, we have for M-60 grade concrete

Compressive strength of concrete = f_{ck} = 60 N/mm^2

Adopt permissible stress in concrete at transfer = f_{ct} = 20 N/mm^2

Permissible tensile stress (Class 1 type structure) = $f_{tt} = f_{tw} = 0$

Modulus of elasticity of concrete = E_c = 37 kN/mm^2

Loss ratio = 0.8

High tensile strands of 15.2 mm diameter conforming to IS: 6006-1983 and Fe-415 HYSD bars are available for use.

Type of supplementary reinforcement = Fe-415 HYSD bars having f_y = 415 N/mm^2

Cross-section of Box Girder

Overall depth of the box girder = $\left(\frac{span}{25}\right) = \left(\frac{50}{25}\right)$ = 2 m

Width of roadway = 7.5 m

Width of foot paths = (2 × 1.25) = 2.5 m

Total width of box girder at road level = (7.5 + 2.5) = 10 m

Spacing between webs = 2 m

4 celled box girder is used

Thickness of web is based on the diameter of the cable used

Thickness of web = (diameter of the cable duct for housing 27-K strands of Freyssinet system + cover to cable and web reinforcements)
= (150 + 150) = 300 mm

At end supports where anchorages are located, web thickness increased to 600 mm

Thickness of bottom and top flanges = 300 mm

The two span multi-celled box girder spans and cross-section of the deck and web girder are shown in Figs 21.36 (a), (b) and (c).

Section properties of the symmetrical web girder, shown in Fig. 21.36 (c), are as follows:

Cross-sectional area = A = 1.62 m^2

Second moment of area of cross-section = I = 0.94 m^4

Distance of the extreme fibre from centroid = $y = y_t = y_b$ = 1 m

Section modulus = $Z = Z_t = Z_b = (I/y)$ = 0.94 m^3

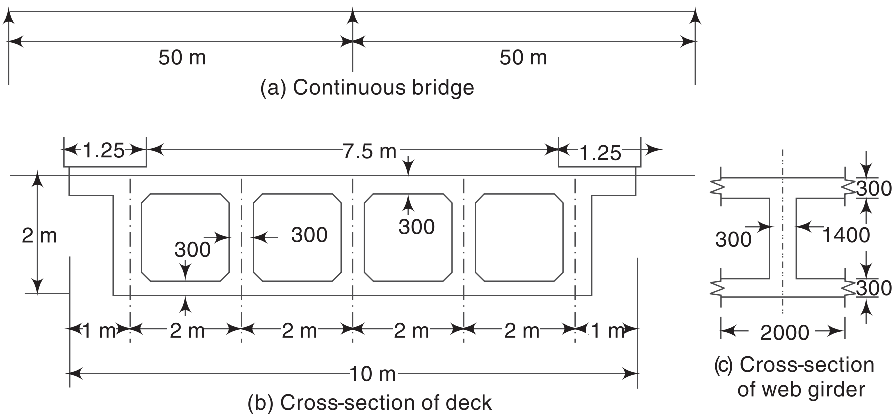

Fig. 21.36 *Two-span box girder bridge deck*

Design of Slab Panel

(a) Dead load bending moments

Dead weight of slab = $(1 \times 1 \times 0.3 \times 24) = 7.20$ kN/m^2
Dead weight of W.C = (0.08×22)…… = 1.76
Total Dead load = g…… $\cong 9.00$ kN/m^2
Referring to the bending moment coefficients compiled in Appendix-6 and Fig. 21.37.

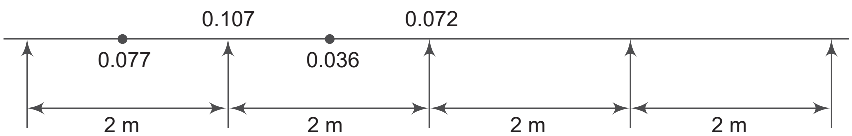

Fig. 21.37 *Dead load bending moment coefficients in four span continuous slab*

Maximum negative bending moment due to dead load at supports

$= (0.107 \times gL)$

$= (0.107 \times 9 \times 2) = 1.93$ kN·m/m

Maximum positive bending moment at centre of span

$= (0.077 \times gL)$

$= (0.077 \times 9 \times 2) = 1.38$ kN·m/m

Maximum shear force = $(0.60 \times gL) = (0.60 \times 9 \times 2) = 10.8$ kN

(b) Live load bending moments The slab panel is continuous over webs in the transverse direction and free in the longitudinal direction. The slab spanning in the transverse direction is designed for IRC Class AA tracked loading using the procedure specified in IRC: 112–2011. When IRC Class AA tracked vehicle traverses on the deck, maximum bending moment in the transverse direction of the slab will develop when one tracked wheel occupies the centre of slab as shown in Fig. 21.38.

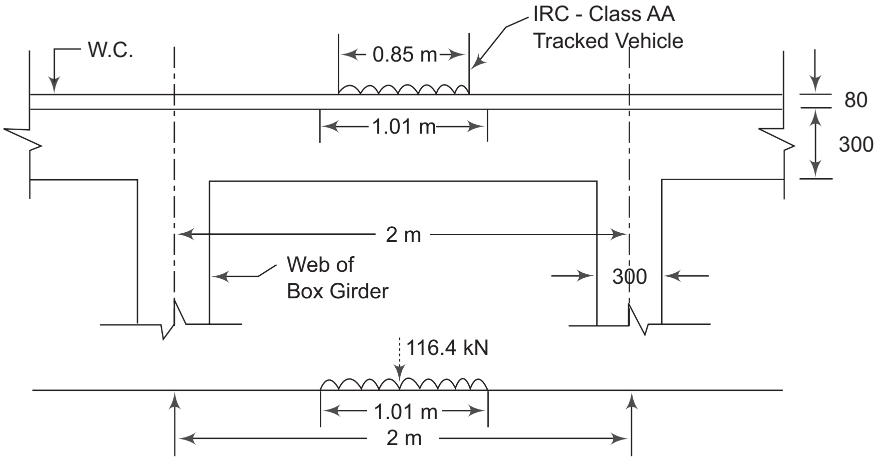

Fig. 21.38 *Position of IRC Class AA load for maximum B.M. in slab*

The effective width of dispersion of the wheel through the wearing coat is computed as,

$$u = [0.85 + (2 \times 0.08)] = 1.01 \text{ m}$$
$$v = [3.60 + (2 \times 0.080)] = 3.76 \text{ m}$$

Average intensity of wheel load with impact factor

$$= \left[\frac{1.25 \times 350}{3.76 \times 1.01}\right] = 115.20 \text{ kN/m}^2$$

Concentrated load acting at the centre of span in the transverse direction is computed as,

$$Q = (115.20 \times 101) = 116.4 \text{ kN}$$

Referring to the bending moment and shear force coefficients compiled in Fig. 21.39.

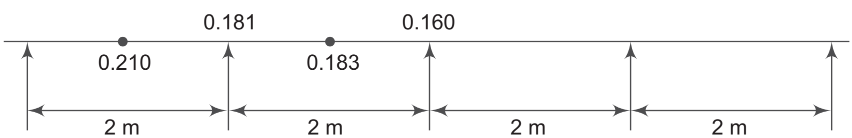

Fig. 21.39 *Live load bending moment and shear force coefficients in four span continuous slab*

Maximum positive B.M at middle of end span = $[0.210\ QL]$

$$= [0.210 \times 116.4 \times 2] = 48.9 \text{ kN·m}$$

Maximum negative B.M at penultimate support = $[0.181\ QL]$

$$= [0.181 \times 116.4 \times 2] = 48.13 \text{ kN·m}$$

Maximum shear force = $[0.60\ Q] = [0.60 \times 116.4] = 69.8$ kN

(c) Design ultimate bending moments and shear forces The design ultimate bending moments are obtained by applying the appropriate safety factors to the service load bending moments and shear force as follows:

$$\text{Total positive bending moment} = M_{up} = [1.35\, M_d + 1.5\, M_L] = [(1.35 \times 1.38) + (1.5 \times 48.9)] = 74.2 \text{ kN.m}$$

$$\text{Total negative bending moment} = M_{un} = [1.35\, M_d + 1.5\, M_L] = [(1.35 \times 1.93) + (1.5 \times 42.13)] = 65.8 \text{ kN.m}$$

$$\text{Total maximum shear force} = [1.35\, V_g + 1.5\, V_q] = [(1.35 \times 10.8) + (1.5 \times 69.8)] = 119.3 \text{ kN}$$

(d) Design of deck slab and reinforcements

$$\text{Effective depth of slab required} = d = \sqrt{\frac{M_u}{0.138\, f_{ck} b}} = \sqrt{\frac{74.2 \times 10^6}{0.138 \times 60 \times 1000}} = 94.7 \text{ mm}$$

Overall depth adopted = 300 mm

Adopt effective depth, $d = 250$ mm and overall depth of 300 mm

The area of tension reinforcement required to resist the moment is calculated by the equation,

$$M_u = 0.87\, f_y A_{st} d \left[1 - \frac{A_{st} f_y}{b.d.f_{ck}}\right]$$

$$(74.2 \times 10^6) = (0.87 \times 415 \times A_{st} \times 250)\left[1 - \frac{A_{st} \times 415}{1000 \times 250 \times 60}\right]$$

Solving, $A_{st} = 2074 \text{ mm}^2$

Provide 20 mm diameter bars at 150 mm centres ($A_{st} = 2094 \text{ mm}^2$) as main reinforcements and 12 mm diameter bars at 150 mm centres as distribution reinforcements.

(e) Check for ultimate shear strength The ultimate shear strength of the reinforced concrete deck slab is checked by using the equation,

$$V_{Rd.c} = [0.12\, K\, (80\, \rho_1 f_{ck})^{0.33}]\, b_w.d$$

where $$K = 1 + \sqrt{\frac{200}{d}} \le 2.00 = \left[1 + \sqrt{\frac{200}{250}}\right] = 1.89$$

and $$\rho_1 = \left(\frac{A_{st}}{b_w.d}\right) \le 0.02$$

$$= \left(\frac{2094}{1000 \times 250}\right) = 0.008$$

$$V_{\text{Rd.c}} = [0.12 \times 1.89\,(80 \times 0.008 \times 60)^{0.33}]\,(1000 \times 250)\text{ N}$$
$$= (191.6 \times 1000)\text{ N}$$
$$= 191.6\text{ kN} > 119.3\text{ kN (hence, safe)}$$

Design of Web Girder

(a) Dead-load bending moments and shear forces The continuous box girder is treated as an assemblage of I-sections with web serving the function of a main girder and flanges of symmetrical size as shown in Fig. 21.36(c).

Self-weight of flanges = $(2 \times 0.3 \times 24)$ = 14.40 kN/m^2
Self-weight of WC … = $(1 \times 1 \times 22)$ = 1.76
Total load … = 16.16
Self-weight of web = $(1.4 \times 0.3 \times 24)$= 10.08

Total load on each I-girder = g = [(2 × 16.16) + 10.08] = 43 kN/m

The dead-load bending moment coefficients for a two-span continuous beam is shown in Fig. 21.40. The dead-load bending moments at mid-support and mid-span sections are computed as,

$$M_{gB} = 0.125\,gL^2 = (0.125 \times 43 \times 50^2) = 13438\text{ kN}\cdot\text{m}$$
$$M_{gD} = 0.071\,gL^2 = (0.071 \times 43 \times 50^2) = 7633\text{ kN}\cdot\text{m}$$

Dead-load shear is maximum near the mid-support section and is computed as,

$$V_g = 0.62\,gL = (0.62 \times 43 \times 50) = 1333\text{ kN}$$

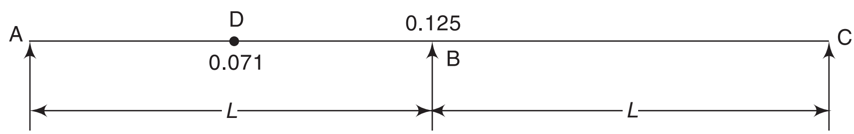

Fig. 21.40 *Dead-load bending moment coefficients*

(b) Live-load bending moments in continuous web girder Maximum live-load reaction occurs in the web girder when the transverse disposition of the IRC Class AA tracked vehicle load is arranged to have the maximum eccentricity with respect to the centre of the bridge deck as shown in Fig. 21.41.

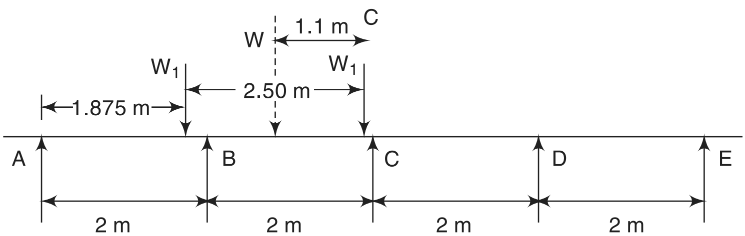

Fig. 21.41 *Position of IRC class AA live loads for maximum reaction in girder*

Maximum reaction due to live loads in girder B is computed as,

$$R_B = \left[\frac{W \times 1.1}{2}\right] = 0.55\ \text{W} = (0.55 \times 700) = 385\ \text{kN}.$$

Hence, the concentrated load = Q = 385 kN

This load acting over a length of 3.6 m in the longitudinal direction is positioned at the centre of span of the two span continuous beam as shown in Fig. 21.42 to compute the maximum positive and negative moments.

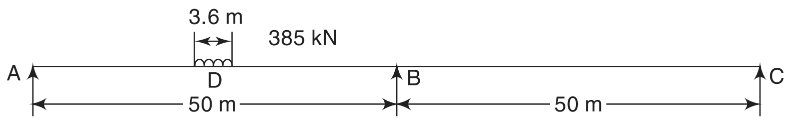

Fig. 21.42 *Position of live loads for maximum moments in two span continuous beam*

The live-load bending moment coefficients for maximum positive and negative moments in a two-span continuous beam are shown in Fig. 21.43.

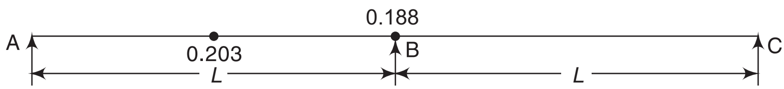

Fig. 21.43 *Live load bending moment coefficients for a two-span continuous girder*

Maximum positive live-load bending moment with impact factor at centre of span is computed as,

$$\begin{aligned} M_{max}(\text{positive}) &= (\text{IF})(0.203\ QL) \\ &= (1.10)\ (0.203 \times 385 \times 50) \\ &= 4298\ \text{kN} \cdot \text{m} \end{aligned}$$

Maximum negative live-load bending moment with impact factor at mid-support is computed as,

$$\begin{aligned} M_{max}(\text{negative}) &= (\text{IF})(0.0938\ QL) \\ &= (1.1)(0.188 \times 385 \times 50) \\ &= 3981\ \text{kN} \cdot \text{m} \end{aligned}$$

(c) Live-load shear force in girder The maximum live-load shear force develops in the interior webs when the IRC Class AA loads are placed near the mid support as shown in Fig. 21.44.

Reaction of load W on interior girder = $\left(\dfrac{350 \times 48.2}{50}\right)$ = 338 kN

Maximum live-load shear force with impact = (338 × 1.1) = 372 kN

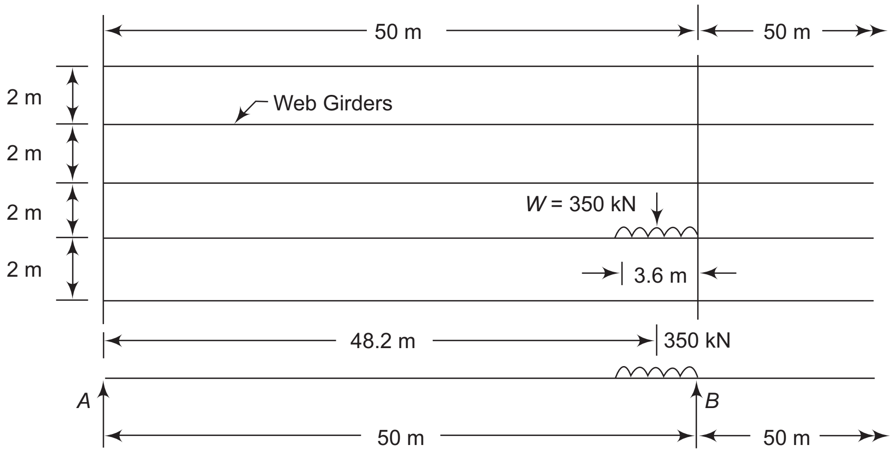

Fig. 21.44 *Position of IRC class AA loads for maximum shear force in web girder*

(d) Design bending moments and shear forces The design bending moments and shear forces at service and ultimate loads are compiled in Table 21.6.

Table 21.6 *Service load and ultimate load moments and shear forces in web girders*

(a) Bending Moments (Outer Web Girder)					
Section	*Dead Load BM* (M_g)	*Live Load B.M* (M_q)	*Service Load B.M* ($M_g + M_q$)	*Ultimate Load B.M* ($1.35 M_g + 1.5 M_q$)	*Units*
Mid-span at (D)	7633	4298	11931	16751	kN·m
Mid-support at (B)	13438	3981	17419	24113	kN·m
(b) Shear Forces (Inner Girder)					
	Dead Load S.F (V_g)	*Live Load S.F* (V_q)	*Service Load S.F* ($V_g + V_q$)	*Ultimate Load S.F* ($1.35\ V_g + 1.5\ V_q$)	*Units*
Middle support section	1333	372	1705	2357	kN

(e) Check for minimum section modulus at service loads At the mid support section B, the dead and live load moments are listed as:

$$M_{gB} = 13438 \text{ kN}\cdot\text{m}$$

$$M_{QB} = 1986 \text{ kN}\cdot\text{m}$$

$$M_{dB} = [M_{gB} + M_{QB}] = [13438 + 3981] = 17419 \text{ kN}\cdot\text{m}$$

$$f_{br} = [\eta f_{ct} - f_{tw}] = [(0.8 \times 20) - 0] = 16 \text{ N/mm}^2$$

$$f_{inf} = \left[\frac{f_{tw}}{\eta} + \frac{M_g}{\eta Z_b}\right] = \left[0 + \frac{13438 \times 10^6}{0.8 \times 0.94 \times 10^9}\right] = 17.86 \text{ N/mm}^2$$

$$Z_b \geq \left[\frac{M_q + (1-\eta)M_g}{f_{br}}\right] \geq \left[\frac{(3981 \times 10^6) + (1 - 0.8)13438 \times 10^6}{16}\right]$$

$$\geq (0.416 \times 10^9) \text{ mm}^3 < (0.94 \times 10^9) \text{ mm}^3 \text{ (section provided).}$$

Hence, section provided is adequate.

(f) Prestressing force For the two continuous spans AB and BC, a concordant cable profile is selected such that the secondary moments are zero. The cable profile selected with eccentricity at mid-support twice that at mid-spans is shown in Fig. 21.45.

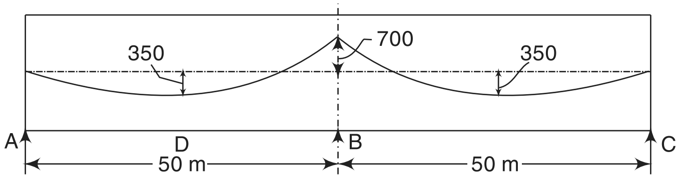

Fig. 21.45 *Concordant cable profile*

Providing an effective cover = 300 mm
Maximum possible eccentricity at support = e = (1000 – 300) = 700 mm
Prestressing force is computed from the relation,

$$P = \left[\frac{Af_b Z_b}{Z_b + Ae}\right] = \left[\frac{(1.62 \times 10^6)(17.86)(0.94 \times 10^6)}{(0.94 \times 10^6) + (1.62 \times 10^6 \times 700)}\right]$$

$$= 13109932 \text{ N} = 13110 \text{ kN}$$

Using Freyssinet system with anchorage type 27K-15 (27 strands of 15.2 mm diameter) in 110 mm-diameter cable ducts (Refer to Appendix-3 of Reference-3)
Force in each cable = $(27 \times 0.8 \times 265)$ = 5724 kN
Provide three cables carrying an initial prestressing force of

$$P = (3 \times 5000) = 15000 \text{ kN}$$

Area of each strand of 15.2 mm-diameter tendon = 140 mm^2
Area of 27 strands in each cable = (27×140) = 3780 mm^2
Total area in three cables = A_p = (3×3780) = 11340 mm^2

The cables are arranged in a parabolic concordant profile so that the centroid of the group of cables has an eccentricity of 700 mm towards the top fibre at mid-support section B and an eccentricity of 350 mm towards the soffit at mid-span section D. The centroid of the cables is concentric at the end supports A and C. The selected cable profile is shown in Fig. 21.46.

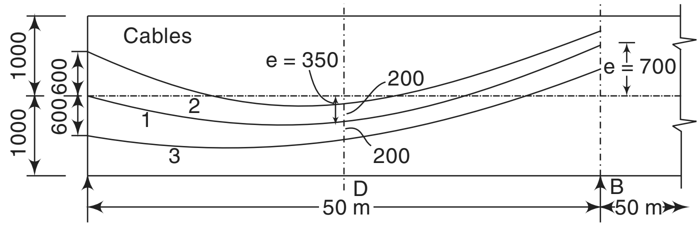

Fig. 21.46 *Profiles of individual cables in span*

(g) Check for stresses at service loads

(i) Centre of span section

$$P = 15000 \text{ kN} \qquad \eta = 0.80$$
$$e = 350 \text{ mm} \qquad M_g = 7633 \text{ kN}\cdot\text{m}$$
$$A = (1.62 \times 10^6) \text{ mm}^2 \qquad M_q = 4298 \text{ kN}\cdot\text{m}$$
$$Z = (0.94 \times 10^9) \text{ mm}^3$$

$$\left(\frac{P}{A}\right) = \left[\frac{15000 \times 10^3}{1.62 \times 10^6}\right] = 9.25 \text{ N/mm}^2$$

$$\left(\frac{Pe}{Z}\right) = \left[\frac{15000 \times 10^3 \times 350}{0.94 \times 10^9}\right] = 5.58 \text{ N/mm}^2$$

$$\left(\frac{M_g}{Z}\right) = \left[\frac{7633 \times 10^6}{0.94 \times 10^9}\right] = 8.12 \text{ N/mm}^2$$

$$\left(\frac{M_q}{Z}\right) = \left[\frac{4298 \times 10^6}{0.94 \times 10^9}\right] = 8.12 \text{ N/mm}^2$$

At transfer stage, the stresses at extreme fibres are computed as,

$$\sigma_1 = \left[\frac{P}{A} - \frac{Pe}{Z} + \frac{M_g}{Z}\right] = [9.25 - 5.58 + 8.12] = 11.79 \text{ N/mm}^2$$

$$\sigma_b = \left[\frac{P}{A} - \frac{Pe}{Z} + \frac{M_g}{Z}\right] = [9.25 + 5.58 - 8.12] = 6.71 \text{ N/mm}^2$$

At service load stage, the stresses at extreme fibres are computed as,

$$\sigma_1 = \left[\frac{\eta P}{A} - \frac{\eta Pe}{Z} + \frac{M_g}{Z} + \frac{M_q}{Z}\right]$$
$$= [0.8\,(9.25 - 5.58) + 8.12 + 4.57]$$
$$= 15.62 \text{ N/mm}^2 < 20 \text{ N/mm}^2$$

$$\sigma_b = \left[\frac{\eta P}{A} - \frac{\eta Pe}{Z} - \frac{M_g}{Z} - \frac{M_q}{Z}\right]$$
$$= [0.8\,(9.25 + 5.58) - 8.12 - 4.57]$$
$$= -0.8 \text{ N/mm}^2 \text{ (Negligible tension)}$$

(ii) Mid-support section

$P = 15000$ kN $\eta = 0.80$

$e = 700$ mm $M_g = 13438$ kN·m

$A = (1.62 \times 10^6)$ mm^2 $M_q = 3981$ kN·m

$Z = (0.94 \times 10^9)$ mm^3

$$\left(\frac{P}{A}\right) = \left[\frac{15000 \times 10^3}{1.62 \times 10^6}\right] = 9.25 \text{ N/mm}^2$$

$$\left(\frac{Pe}{Z}\right) = \left[\frac{15000 \times 10^3 \times 700}{0.94 \times 10^9}\right] = 11.16 \text{ N/mm}^2$$

$$\left(\frac{M_g}{Z}\right) = \left[\frac{13438 \times 10^6}{0.94 \times 10^9}\right] = 14.29 \text{ N/mm}^2$$

$$\left(\frac{M_q}{Z}\right) = \left[\frac{3981 \times 10^6}{0.94 \times 10^9}\right] = 4.23 \text{ N/mm}^2$$

At transfer stage, the stresses at extreme fibres are computed as,

$$\sigma_t = [9.25 + 11.16 - 14.29] = 5.12 \text{ N/mm}^2$$
$$\sigma_b = [9.25 - 11.16 + 14.29] = 12.38 \text{ N/mm}^2$$

At service load stage, the stresses at extreme fibres are computed as,

$$\sigma_t = [0.8\,(9.25 + 11.16) - 14.29 - 4.23] = -2.19 \text{ N/mm}^2$$
$$\sigma_b = [0.8\,(9.25 - 11.16) + 14.29 + 4.23] = 16.89 \text{ N/mm}^2$$

All the stresses are well within the maximum permissible limits of 20 N/mm^2 and no tensile stresses develop at transfer load stage.

(h) Check for ultimate flexural strength

(i) Centre of span section

$A_p = 11340$ mm^2 $D_f = 300$ mm $f_p = 1862$ N/mm^2

$b = 2000$ mm $d = 1350$ mm m_u (required) $= 16751$ kN·m

$b_w = 300$ mm $f_{ck} = 60$ N/mm^2

$A_p = (A_{pw} + A_{pf})$

$$A_{pf} = 0.45\, f_{ck}\,(b - b_w)\left(\frac{D_f}{f_P}\right)$$

$$= \left[0.45 \times 60\,(2000 - 300)\left(\frac{300}{1862}\right)\right] = 7395 \text{ mm}^2$$

$$A_{pw} = (11340 - 7395) = 3945 \text{ mm}^2$$

$$\text{Ratio}\left[\frac{A_{pw} f_p}{b_w d f_{ck}}\right] = \left[\frac{3945 \times 1862}{300 \times 1350 \times 60}\right] = 0.30$$

From Table 11 of IS: 1343, interpolate the values of the ratio ($f_{pb}/0.87f_{pu}$) and (x_u/d) corresponding to the above ratio of 0.30

$$\left(\frac{f_{pb}}{0.87\,f_{pu}}\right) = 0.85 \text{ and } (x_u/d) = 0.558$$

$$f_{pb} = (0.85 \times 0.87 \times 1862) = 1377 \text{ N/mm}^2$$

$$x_u = (0.558 \times 1375) = 787.25 \text{ mm}$$

$$\therefore \quad M_u = [f_{pb}A_{pw}(d - 0.42\,x_u) + 0.45\,f_{ck}(b - b_w)\,D_f(d - 0.5\,D_f)]$$

$$= [1377 \times 3945\,(1375 - 0.42 \times 787.25)]$$

$$+ [0.45 \times 60\,(2000 - 300)\,300(1375 - 0.5 \times 300)]$$

$$= (22541 \times 10^6) \text{ N.mm}$$

$$= 22541 \text{ kN.m} > 16751 \text{ kN.m (hence, safe)}$$

(ii) Mid-support section

$A_p = 11340$ mm^2 $\quad D_f = 300$ mm $\quad f_p = 1862$ N/mm^2

$b = 2000$ mm $\quad d = 1700$ mm $\quad M_u$ (required) $= 24113$ kN.m

$b_w = 300$ mm $\quad f_{ck} = 60$ N/mm^2

$$A_{pf} = \left[0.45\,f_{ck}\,(b - b_w)\left(\frac{D_f}{f_p}\right)\right]$$

$$= \left[0.45 \times 60\,(2000 - 300)\left(\frac{300}{1862}\right)\right] = 7395 \text{ mm}^2$$

$$A_{pw} = (11340 - 7395) = 3945 \text{ mm}^2$$

$$\text{Ratio}\left[\frac{A_{pw}f_p}{b_w d f_{ck}}\right] = \left[\frac{3945 \times 1862}{300 \times 1700 \times 60}\right] = 0.24$$

From Table 11 of IS: 1343, interpolate the values of the ratio ($f_{pb}/0.87f_{pu}$) and (x_u/d) corresponding to the above ratio of 0.24.

$$\left(\frac{f_{pb}}{0.87\,f_{pu}}\right) = 0.91 \text{ and } (x_u/d) = 0.472$$

$$f_{pb} = (0.91 \times 0.87 \times 1862) = 1474 \text{ N/mm}^2$$

$$x_u = (0.472 \times 1700) = 802.4 \text{ mm}$$

$$\therefore \quad M_u = \{f_{pb}A_{pw}(d - 0.42\,x_u) + 0.45\,f_{ck}\,(b - b_w)D_f(d - 0.5\,D_f)\}$$

$$= [1474 \times 3945\,(1700 - 0.42 \times 802.4)$$

$$+ \{0.45 \times 60\,(2000 - 300)\,300(1700 - 0.5 \times 300)\}$$

$$= (29269 \times 10^6) \text{ N.mm}$$

$$= 29269 \text{ kN.m} > 24113 \text{ kN.m (hence, safe)}$$

The ultimate flexural strength of centre of span and mid support sections are greater than the required design ultimate moment. Hence, the design satisfies the limit state of collapse as specified in IRC: 112–2011.

(i) Check for ultimate shear strength The mid support section is checked for the ultimate shear strength.

Shear strength required = 2357 kN

The design shear resistance of the support section is calculated by using the equation specified in IRC: 112–2011 clause 10.3 as,

$$V_{\text{Rd.c}} = \left(\frac{I.b_w}{s}\right)\sqrt{(f_{\text{ctd}})^2 \mp k_1\sigma_{\text{cp}} f_{\text{ctd}}} + \eta P \sin\theta$$

Computing the numerical values of the various parameters, we have

$$I = \left(\frac{b_w D^3}{12}\right) = \left(\frac{300 \times 2000^3}{12}\right) = (2000 \times 10^8)\ \text{mm}^4$$

$$S = \left(\frac{300 \times 1000 \times 1000}{2}\right) = (150 \times 10^6)\ \text{mm}^3$$

$$f_{\text{ctd}} = (f_{\text{ct}}/\gamma_m) = (4.0/1.5) = 2.66 \text{ since } f_{\text{ct}} = 4.0 \text{ N/mm}^2 \text{ for } f_{\text{ck}} = 60 \text{ N/mm}^2$$

$$\sigma_{\text{cp}} = (\eta P/A_c) = [(0.8 \times 15000 \times 10^3)/(1.62 \times 10^6)] = 7.4 \text{ N/mm}^2$$

$$\theta = (4e/L) = [(4 \times 700)/(50 \times 1000)] = 0.056$$

$$\therefore \quad V_{\text{RD.c}} = \left(\frac{I.b_w}{s}\right)\sqrt{(f_{\text{ctd}})^2 \mp k_1\sigma_{\text{cp}} f_{\text{ctd}}} + \eta P \sin\theta$$

$$= \left(\frac{(2000 \times 10^8)300}{150 \times 10^6}\right)\sqrt{(2.66)^2 \mp 1 \times 7.4 \times 2.66}$$

$$+ (0.8 \times 15000 \times 10^3 \times 0.056)\ \text{N}$$

$$= (2740 \times 10^3)\ \text{N}$$

$$= 2740 \text{ kN} < 2357 \text{ kN}$$

Nominal shear reinforcements of 10 mm diameter two legged stirrups are designed using the relation,

$$S_v = \left(\frac{0.87\, f_y A_{sv}}{0.4b}\right) = \left(\frac{0.87 \times 415 \times 2 \times 79}{0.4 \times 300}\right) = 475 \text{ mm}$$

The stirrups are provided at a maximum spacing of 300 mm throughout the span as per IRC: 112–2011 specifications.

(j) Supplementary reinforcements According to Clause 16.51 of IRC: 112–2011, minimum longitudinal reinforcements of not less than 0.13 per cent of gross cross-sectional area are to be provided to safeguard against shrinkage cracking.

$$A_{\text{SL}} = (0.0013 \times 1.62 \times 10^6) = 2106 \text{ mm}^2$$

12 mm diameter bars are distributed in the cross-section as shown in top and bottom flanges and web of the girder as show in Fig. 21.47

(k) Design of end blocks The width of webs are increased to 600 mm near the end supports to house the anchorages. Typical equivalent prisms on which the anchorage forces are considered to be effective are detailed in Fig. 21.48.

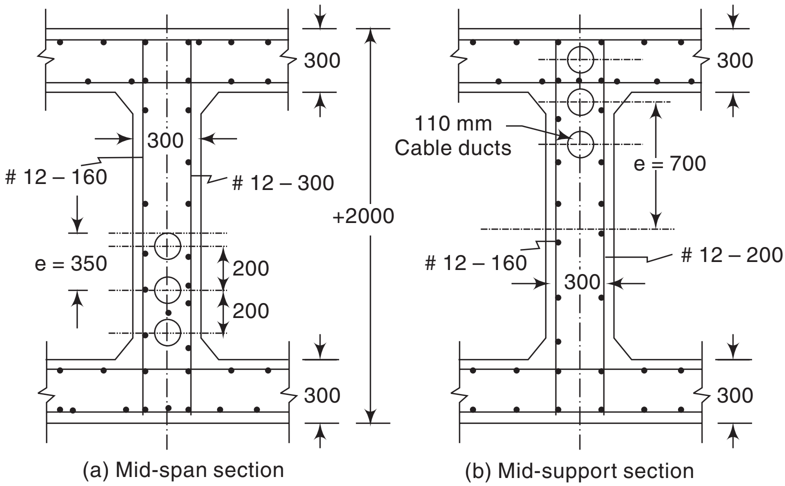

Fig. 21.47 *Details of reinforcements and cables at mid span and support sections*

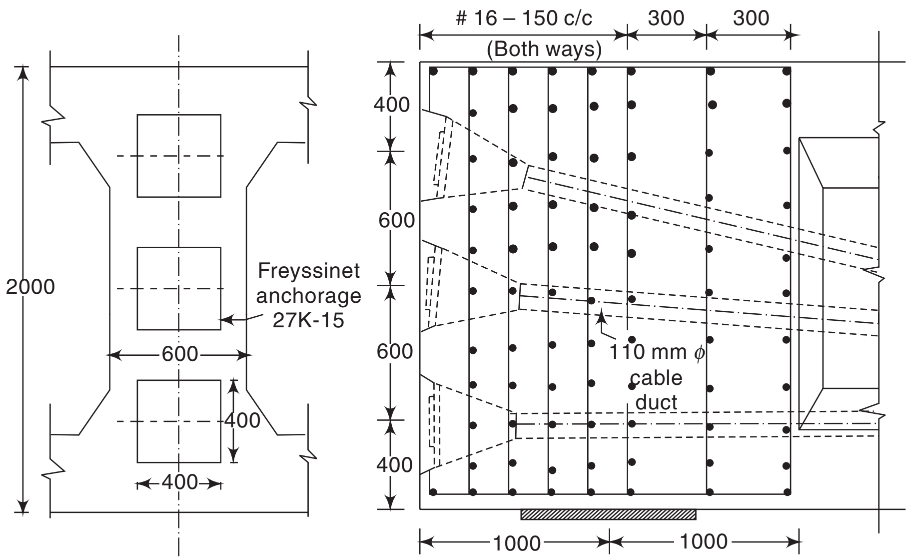

Fig. 21.48 *Anchorage zone reinforcements in end block*

In the horizontal plane, we have the data,

$$P_K = 5000 \text{ kN}, \qquad 2Y_{po} = 400 \text{ mm and } 2Y_o = 600 \text{ mm}$$

Hence, the ratio $(Y_{po}/Y_o) = (200/300) = 0.66$

Interpolating from Table 21.3, the bursting tension is computed as,

$$F_{bst} = (0.14 \times 5000) = 700 \text{ kN}$$

Area of steel required to resist this tension is obtained as,

$$A_s = [(700 \times 10^3)/(0.87 \times 415)] = 1938 \text{ mm}^2$$

Provide 16 mm diameter bars at 150 mm centres in the horizontal direction. In the vertical plane, the ratio of (Y_{po}/Y_o) being higher, the magnitude of bursting tension is smaller. However, the same reinforcements are provided in the form of a mesh both in the horizontal and vertical directions as shown in Fig. 21.48.

References

1. Subba Rao, TN, Long Span Prestressed Concrete Bridges in India, *Seminar on Problems of Prestressing, Indian National Group of the IABSE, Preliminary Publication*, Madras, Jan/Feb 1970 pp 1–130.
2. Jhonson Victor, D, *Essentials of Bridges Engineering*, 2nd edn, Oxford and IBH Publishing Co, New Delhi, 1978, pp 159–205.
3. Krishna Raju N, *Design of Bridges*, (Fourth Edition) Oxford and IBH Publishing Co, New Delhi, 2009, pp 200–264.
4. Libby, JR, *Modern Prestressed Concrete*, 3rd edn, Van Nostrand Reinhold Company, USA, 1986, pp 485–536.
5. Manton, BH and CB Wilson, "MOT/C and CA, Standard bridge beams," *Publication No. 32.012, Cement and Concrete Association, London* 1970.
6. Anderson, AR, "How beam design affects prestressed concrete bridge costs," *Engineering News Record*, Vol. 159, Oct. 1957, pp 326–328.
7. Taylor, HPJ, LA Clark, CC Banks, "The Y-beam: a replacement for the M-beam and slab bridge decks," *Journal of the Institution of Structural Engineers*, London, Vol. 68, No. 23, December 1990, pp 459–465.
8. Regan, PE, "Behaviour of precast, prestressed Y-beams in shear, in torsion and in negative bending," *Journal of the Institution of Structural Engineers*, London, Vol. 68, No. 23, December 1990, pp 466–473.
9. Hambly, EC and BA Nicholson, "Prestressed beam integral bridges," *Journal of the Institution of Structural Engineers*. London, Vo1. 68, No. 23, December 1990, pp 474–481.
10 Bate, SCC and EW, Bennett, *Design of Prestressed Concrete*, Surrey University Press in association with the International Textbook Company Ltd, London, 1976, pp 70–85.
11. Finster Walder, U, Free cantilever construction of prestressed concrete and mushroom shaped bridges, *First International Symposium on Concrete Bridge Design, A.C.I, Special Publication, SP-23*, American Concrete Institute, Detroit, 1969, pp 467–494.
12. IRC: 6–2014, *Standard Specifications and Code of Practice for Road Bridges, Section II, Loads and Stresses*, Indian Roads Congress, New Delhi, 2000, pp 1–84.
13. IRC: 112–2011, Codes of Practice for Concrete Road Bridges, I.R.C., New Delhi, 2011, pp. 1–280.
14. IS: 1343–2012, Indian Standard Code of Practice for Prestressed Concrete (2nd Revision) B.I.S, New Delhi, 2012, pp. 1–55.
15. IS: 6006–1983, Indian Standard Code Specification for Uncoated Stress Relived Strand for Prestressed Concrete (1st Revision), Indian Standards Institutions, New Delhi, 1st Reprint, Oct. 1989.

Review Questions

21.1 List the various advantages of prestressed concrete bridges.

21.2 Explain with sketches the typical pretensioned and post-tensioned bridge decks commonly used in the construction of bridges.

21.3 Briefly explain the cantilever method of constructing prestressed concrete bridges with sketches.

21.4 Explain the various steps involved in the design of short span prestressed concrete solid slab decks for national highways to support IRC loads.

21.5 Sketch a typical cross-section of a tee beam and slab bridge deck comprising longitudinal and cross girders for a two-lane highway showing the various structural components.

21.6 Explain the method of designing a slab deck integral with longitudinal and cross girders using Pigeaud's method to support live loads due to IRC class AA tracked vehicle.

21.7 Outline a method of determining the distribution of live loads between the longitudinal girders of a tee beam and slab bridge deck supporting IRC loads. How do you determine the maximum live load design moments in the girders.

21.8 A typical tee beam and slab bridge deck 7.5 m wide and spanning 16 m has 3 longitudinal girders spaced at 2.5 m intervals. The cross girders are spaced at 4 m intervals. Determine the reaction factors for the longitudinal girders using Courbon's method and evaluate the maximum live-load bending moment and shear force in the main and cross girders when an IRC Class AA tracked vehicle moves over the bridge deck.

21.9 Sketch the typical longitudinal and cross-sections of tee beam and slab bridge deck showing the position of cables at centre of span and at supports. Also sketch the details of reinforcements generally used in the anchorage zone of the main girder.

Exercises

21.1 A prestressed concrete slab, 400 mm thick with parallel post-tensioned cables, is provided for a road bridge of effective span 8 m. The live-load analysis indicates an equivalent live load of 40 kN/mm^2. The force at transfer in each of the cables is 400 kN. If the compressive stress permissible in concrete at transfer is 16 N/mm^2, design the slab as Class 1-type member and determine the spacing of the cables and their eccentricity at mid-span. Assume a loss ratio of 0.8.

[Ans: Spacing of cables = 125 mm, Eccentricity of cable = 95 mm]

21.2 A box girder of a prestressed concrete bridge of span 40 m has overall dimensions of width 1200 mm and depth 1800 mm. The uniform thickness of the walls is 200 mm. The live-load analysis indicates a maximum live-load moment of 2000 kN m. The compressive strength of concrete at transfer is 16 N/mm^2. The loss ratio is 0.8. Cables consisting of 12 high-tensile wires of 8 mm diameter initially stressed to 1000 N/mm^2 are available for use. Design the box girder as Class 1-type structure and determine the number of cables required at the centre-of-span section and their position from the centroidal axis.

[Ans: Prestressing force = 7090 kN, Number of cables = 12, Eccentricity = 800 mm]

21.3 Design a post-tensioned prestressed concrete T-beam and slab bridge-deck to suit the following data:

Effective span = 24 m, width of carriage-way = 7.5 m

Kerbs 600 mm wide on either side of road. Spacing of the main and cross girders are 2 and 4 m, respectively. Loading is IRC class AA. Adopt M-45 grade concrete and high-tensile steel strands conforming to IS: 6006 and supplementary reinforcement comprising Fe-415 grade bars. Permissible stress, as specified in IRC: 112–2011, η (Loss Ratio) is 0.85.

[Ans: Thickness of slab = 200 mm, bottom flange = 500 mm wide by 400 mm deep, overall depth of girder = 1400 mm, thickness of web = 200 mm, Freyssinet cables (7 ply – 15.2 mm strands), four nos at an eccentricity of 705 mm at the centre of span]

21.4 A post-tensioned prestressed concrete slab deck has to be designed for a national high way crossing. Design the deck slab using the following data:

Clear span = 10 m

Width of bearing = 400 mm

Clear width of road way = 15 m

Thickness of wearing coat = 80 mm

Live load: IRC Class AA tracked vehicle

Type of structure: Class 1 type

Materials: M-40 Grade Concrete and Cables containing 12 high-tensile wires of 7 mm diameter initially stressed to 1200 N/mm^2 and Fe-415 HYSD bars

Compressive strength of concrete at transfer = 35 N/mm^2

Percentage loss of prestress = 20 per cent

Design the deck slab and determine the spacing of cables.

[Ans: Thickness of slab = 500 mm and spacing of cables = 300 mm]

21.5 An unsymmetrical I-section post-tensioned prestressed concrete girder is to be designed for a bridge deck. The girder has the following dimensions:

Top Flange: 1200 mm wide and thickness varying from 100 mm at the edges to 240 mm at the junction of web

Bottom Flange: 1000 mm wide and thickness varying from 260 mm at edges to 360 mm at the junction of the web

Overall depth of girder = 1800 mm

Thickness of web = 225 mm

The girder is subjected to a dead-load bending moment of 5300 kN m and a live-load bending moment of 3000 kN m. Check the adequacy of the section provided to resist the design bending moments and design the number of cables required assuming the force in each cable as 1400 kN and the eccentricity as 1050 mm.

[Ans: Section Modulus (Provided) = 4.01 × 10^8 mm^3, Section Modulus (Required) = 2.47 × 10^8 mm^3 Number of cables = 5]

21.6 A prestressed concrete multicell continuous box girder bridge deck is proposed for a National Highway Crossing of a river 120 m wide. Design the bridge deck continuous, over two spans of 60 m each to suit the following data:

Road width = 15 m
Foot paths: 1 m on either side
Wearing coat = 100 mm
Type of loading: IRC Class AA tracked vehicle
Grade of Concrete: M-60
High-tensile steel: Strands conforming to IS: 6006
Anchorages; Freyssinet K type anchorages
Spplementary steel: Fe-415 Grade HYSD bars
Size of box cells: 2 m by 2 m cellular box girder
The design should conform to the Indian standard codes IRC-6–2014 and IRC: 112–2011
Sketch the details of reinforcements at critical sections of the multicell girder and at the anchorage zone.

Objective-type Questions

21.1 Long span continuous girder bridges of variable cross-section are built using
(a) pretensioned construction
(b) post-tensioned construction
(c) cast *in situ* post-tensioned construction

21.2 Use of prestressed concrete in construction results in
(a) large size members
(b) heavy construction
(c) slender structures

21.3 For bridge decks of short span ranging from 15 to 25 m, it is economical to use
(a) reinforced concrete tee beam and slab
(b) steel girder and cast *in situ* slab
(c) prestressed concrete cored slab

21.4 Medium-span bridge decks in the range of 20 to 40 m are generally built using
(a) composite deck using steel girder and RC slab
(b) prestressed concrete tee beam and slab
(c) reinforced concrete tee beam and slab

21.5 For long-span continuous bridge decks in the span range of 30 to 80 m, it is economical to use
(a) prestressed concrete box girders
(b) reinforced concrete box girders
(c) steel plate girder with reinforced concrete slab

21.6 In the design of prestressed concrete solid slab bridge decks covering 10 m span, the bending moment is maximum for
(a) IRC Class A loads
(b) IRC Class AA tracked vehicle loads
(c) IRC Class AA wheeled vehicle loads

21.7 Bending moments in slabs supported on all the sides and carrying concentrated wheel loads is determined using
(a) Rankine-Groshoff theory
(b) Pigeaud's curves
(c) Influence coefficients

21.8 The minimum thickness of the web of a prestressed I-section girder of a bridge to accommodate a cable of 50 mm diameter should be not less than
(a) 100 mm (b) 200 mm (c) 400 mm

21.9 In Tee-beam and slab type bridge deck, the maximum moments due to IRC wheel loads develop in the
(a) interior girders (b) middle girder (c) exterior girder

21.10 According to the IRC: 112-2011, specifications regarding the serviceability limit state of deflection, the maximum deflection of the deck under vehicular live loads is limited to a value of
(a) span/250 (b) span/1000 (c) span/800

Answers to Objective-type Questions

21.1 (b)	21.2 (c)	21.3 (c)	21.4 (b)	21.5 (a)
21.6 (b)	21.7 (b)	21.8 (b)	21.9 (c)	21.10 (c)

22 Prestressed Concrete Trusses

22.1 General Features

Reinforced concrete trusses were first used for covering large span workshop floors in Russia during the middle of 19th century. In comparison with solid panel structures like grids, flat slabs and shells, trusses are skeletal structures and offer several advantages over the traditional types of reinforced concrete roofing solutions. Roof systems used for industrial structures in the coastal regions are normally subjected to adverse environmental conditions. In such situations, reinforced concrete truss systems are preferred to steel trusses due to their superior durability characteristics. Many countries in Europe[1,2] and especially U.S.S.R, have developed and extensively used the reinforced concrete trussed roofs of different configuration to suit the spans varying from 10 – 30 m. The most favourable configuration of the top chord is obtained in the bow string type truss having top chord members of varying slopes from the centre of span and towards the supports. Various types of truss configurations used for spans in the range of 18 – 30 m are shown in Fig. 22.1.

22.2 Dimensions of Trusses

The height of reinforced concrete truss at mid-span is in the range of 1/7 to 1/9 of its span length. The span of the trusses generally lies in the range of 18–30 m. The width of the various compression and tension members is kept constant at 200–350 mm depending upon the span of the truss. The depth of top boom members which are in compression generally is in the range of 200–300 mm. The bottom tie member should be of sufficient size to house the pretensioned wires or post-tensioned cables. The depth is around 200 mm for spans of 15 m increasing to 300 mm for spans of 30 m. The depths of diagonal web members which are in compression and tension generally vary in the narrow range of 100–150 mm.

The use of concrete trusses with modular coordination for spans of 6, 9, 12, 15, 18, 24, 30 and 36 m and with a base module of 3 m is most common for industrial buildings of East European countries such as Russia[3], Poland, Slovakia and Germany. Branko Zezelji[4] has reported the construction of reinforced concrete trusses with prestressed tie members for spans up to 60 m in erstwhile Yugoslavia.

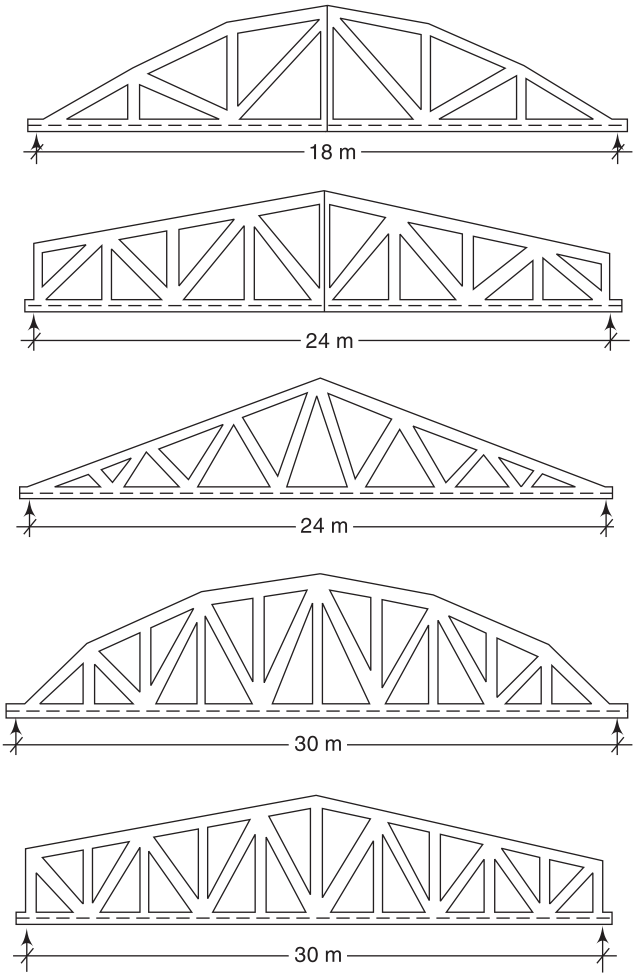

Fig. 22.1 *Typical configurations of precast reinforced concrete trusses with prestressed tie*

22.3 Material Requirements

Concrete used in trusses is normally of grade ranging from M-35 to M-60 which can be considered as high-strength concrete. The reinforcements consist of mild steel or HYSD bars together with high-tensile steel wires or cables used in the tie member. The material requirement per truss varies with the span and spacing of trusses. Table 22.1 shows the requirements of materials for precast reinforced concrete trusses designed to support roof loads of 3.5–5.3 kN/m^2 according to Murashev[1].

Table 22.1 *Material requirements for precast roof trusses*

Type of Truss	*Weight of Truss* (kN)	*Grade of Concrete* (N/mm^2)	*Material Requirement per Truss*	
			Steel (kg)	*Concrete* (m^3)
1. Truss spacing = 6 m				
Prestressed bow string truss with cable reinforcement span				
(a) 18 m	4.3–4.8	30	338–433	1.72–1.9
(b) 24 m	8.8–10	30–40	621–689	3.50–4.0
(c) 30 m	15.2–17.0	30–40	1041–1219	6.08–6.8
Polygonal built-up from blocks with prestressed bottom chord having wire cable				
(a) 18 m	6.58	40	514–529	2.63
(b) 24 m	9.60	40	744–765	3.85
(c) 30 m	13.20	40	1135–1186	5.28
2. Truss spacing = 12 m				
Prestressed bow string of linear element with wire reinforcement				
(a) 18 m	7.7–9.1	30–40	491–759	3.06–3.63
(b) 24 m	14.9–17.4	30–50	1018–1367	5.95–6.96
(c) 30 m	25.5–29.8	30–50	1422–2213	10.20–11.90
Prestressed bow string with bar reinforcement				
(a) 18 m	7.6–9.1	30–40	563–962	3.06–3.63
(b) 24 m	14.9–17.4	30–50	1238–1822	5.95–6.96
(c) 30 m	25.5–29.8	30–50	1778–2981	10.20–11.90

The material requirements vary with the span and grade of concrete. The quantity of concrete per truss varies from a minimum of 1.9 m^3 for lower span of 18 m to 11.9 m^3 for higher span of 30 m. The corresponding value of steel in kg varies from 433 to 2981. The weight of truss also increases proportionately from a minimum of 4.8 to 29.8 kN.

22.4 Constructional Features

The chords and struts of trusses are designed to have the same width for convenience in fabricating in a horizontal position. If precast roof slabs are used for roof covering, the upper chord panels are made equal to house two or three precast slabs or roofing sheets which are usually about 2 to 3 m. The lower tension chord is prestressed with the use of bunched high strength wires or cables house in preformed ducts. For spans in the range of 18 to 24 m, the trusses are made in one piece but when spans run from 24 to 30 m, they are made in two pieces with the joint in mid span.

Polygonal trusses with inclined top chords are generally made of 6 m blocks, half trusses with 3 m panels. Due to higher tensions developed in the diagonal members of large span trusses, prestressing them becomes inevitable. In general, polygonal trusses are less economical than the bow type with regard to material and labour costs. At the ends of trusses near the supports, 10 to 12 mm thick steel bearing plates are anchored and embedded while casting and these serve as bearing pads for fixing of trusses to the columns.

22.5 Analysis of Forces in Truss Members

The analysis of force components in reinforced concrete trusses subjected to external loads is more or less similar to the procedure adopted for steel trusses. It is well-established that the assumption of hinged joints holds good for concrete trusses also. The rigidity of the joints does not significantly affect the forces developed in the members of the truss. Consequently, the analysis is generally carried out on the assumption of hinged joints.

The trusses are analysed for dead, wind and snow loads applied to the joints of the top chord as specified in the Indian Standard Codes[5,6]. The loads due to the suspended mechanical handling is applied at the panel joints of the bottom chord. When loads are applied to the chords of a truss between the panel points, the bending moments developed are determined by assuming the chord as a continuous beam with spans equal to the distance between the joints. In the design of trusses, the forces developed during fabrication and erection should also be analysed along with that of the initial stresses developed due to prestressing of the bottom chord member.

The bottom chord members of the trusses are generally subjected to tension and in the case of larger span ranges, the large magnitude of tension developed is generally resisted by concentric prestressing of the tie member using a high tensile cable. The reader may refer to separate monographs by Rowe[7] and Bate[8] for limit state design and the Indian Standard Code IS: 3201[9] for design of precast trusses.

If Δ = contraction of the bottom chord due to precompression
P = prestressing force
A = cross-sectional area of bottom chord
L = length of the bottom chord
E_c = modulus of elasticity of concrete

Then we have the relation,

$$\Delta = \left(\frac{PL}{AE_c}\right)$$

The displacements at the ends of truss members in a direction perpendicular to their longitudinal axis caused by the elastic contraction Δ, is determined with the aid of Williot Mohr diagram.

If δ = Displacement at the ends of members
M = Bending moment developed in the members

Then the moments in the members are obtained by the relation,

$$M = \left(\frac{6EI\delta}{L^2}\right)$$

In the case of large span trusses with larger magnitudes of prestressing force in the bottom chord, the secondary moments developed in the various members due to contraction of the bottom chord should be investigated and considered in the design of the members.

22.6 Design Example

A reinforced concrete truss is to be designed for a workshop floor to suit the following data:

Effective span of the truss between the bearings = 25 m
Spacings of trusses = 5 m
Central rise of truss = 4.13 m

The fink type truss shown in Fig. 22.2 supports reinforced concrete purlins at intervals of 1.35 m and the roof is covered by coated metallic sheets. The bottom chord member is to be prestressed. The analysis of force components of the truss due to dead, live and wind loads are compiled in Table 22.2.

Design suitable reinforcements in the truss members. Adopt M-35 grade concrete and Fe-415 grade HYSD bars as reinforcements. Freyssinet system high tensile cables comprising 12 wires of 7 mm diameter are available for prestressing the tie member. The design should conform to the specifications of the Indian Standard Codes, IS: 3201[9], IS: 1343-2012[10] and SP: 16-1980[11]. Sketch the details of reinforcements in the members of the truss.

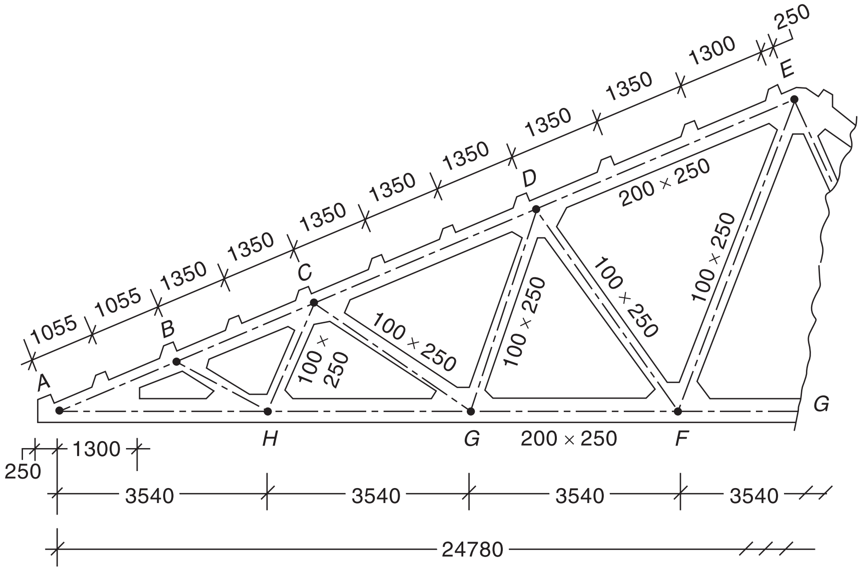

Fig. 22.2 *Precast reinforced concrete truss with prestressed tie*

Table 22.2 *Forces in truss members*

Member	*Cross-sectional Dimensions (mm × mm)*	*Direct Force*		*Bending Moment (kN.m)*
		Compression (kN)	*Tension (kN)*	
AB	200 × 250	395	—	4.3
BC	200 × 250	364	—	12.0
CD	200 × 250	297	—	16.0
DE	200 × 250	236	—	16.0
BH	100 × 250	36	—	—
CG	100 × 250	62	—	—
DF	100 × 250	72	—	—
AH	200 × 250	—	377	4.0
HG	200 × 250	—	335	—
GF	200 × 250	—	268	—
FG	200 × 250	—	225	—
CH	100 × 250	—	18	—
DG	100 × 250	—	35	—
EF	100 × 250	—	59	—

1. Design of Compression Members

(a) Member AB

$$P_u = (1.5 \times 395) = 592.5 \text{ kN} \qquad b = 250 \text{ mm}$$

$$M_u = (1.5 \times 4.3) = 6.45 \text{ kN.m} \qquad D = 200 \text{ mm}$$

$$L = 2.11 \text{ m} \qquad f_{ck} = 35 \text{ N/mm}^2$$

$$f_y = 415 \text{ N/mm}^2$$

$$\text{Effective length} = L_e = (0.65 \times 2.11) = 1.37 \text{ m}$$

$$\left(\frac{L_e}{D}\right) = \left(\frac{1.37}{0.2}\right) = 6.85 < 12$$

$$\left[\frac{P_u}{f_{ck} \cdot b \cdot D}\right] = \left[\frac{592.5 \times 10^3}{35 \times 250 \times 200}\right] = 0.338$$

$$\left[\frac{M_u}{f_{ck} \cdot b \cdot D^2}\right] = \left[\frac{6.45 \times 10^6}{35 \times 250 \times 200^2}\right] = 0.023$$

Adopting cover of 40 mm, $\left(\frac{d'}{D}\right) = \left(\frac{40}{200}\right) = 0.20$

Referring to Chart-34 of SP: 16[11] (Fig. 22.3), read out the ratio $\left(\frac{p}{f_{ck}}\right) = 0.$

Hence, provide minimum reinforcement of 0.8 per cent of the cross-section

$$A_s = \left(\frac{0.8 \times 250 \times 200}{100}\right) = 400 \text{ mm}^2$$

Provide 4 bars of 12 mm diameter ($A_s = 452$ mm^2) and 6 mm diameter ties at 120 mm centres.

(b) Member BC

$$\text{Length, } L = 2.70 \text{ m}$$

$$\text{Effective length} = L_e = (0.65 \times 2.70) = 1.755 \text{ m}$$

$$\text{Ultimate load} = P_u = (1.5 \times 364) = 546 \text{ kN}$$

$$\text{Ultimate moment} = M_u = (1.5 \times 12) = 18.0 \text{ kN.m}$$

$$\left(\frac{L_e}{D}\right) = \left(\frac{1.755}{0.2}\right) = 8.77 < 12$$

$$\left[\frac{P_u}{f_{ck} \cdot b \cdot D}\right] = \left[\frac{546 \times 10^3}{35 \times 250 \times 200}\right] = 0.312$$

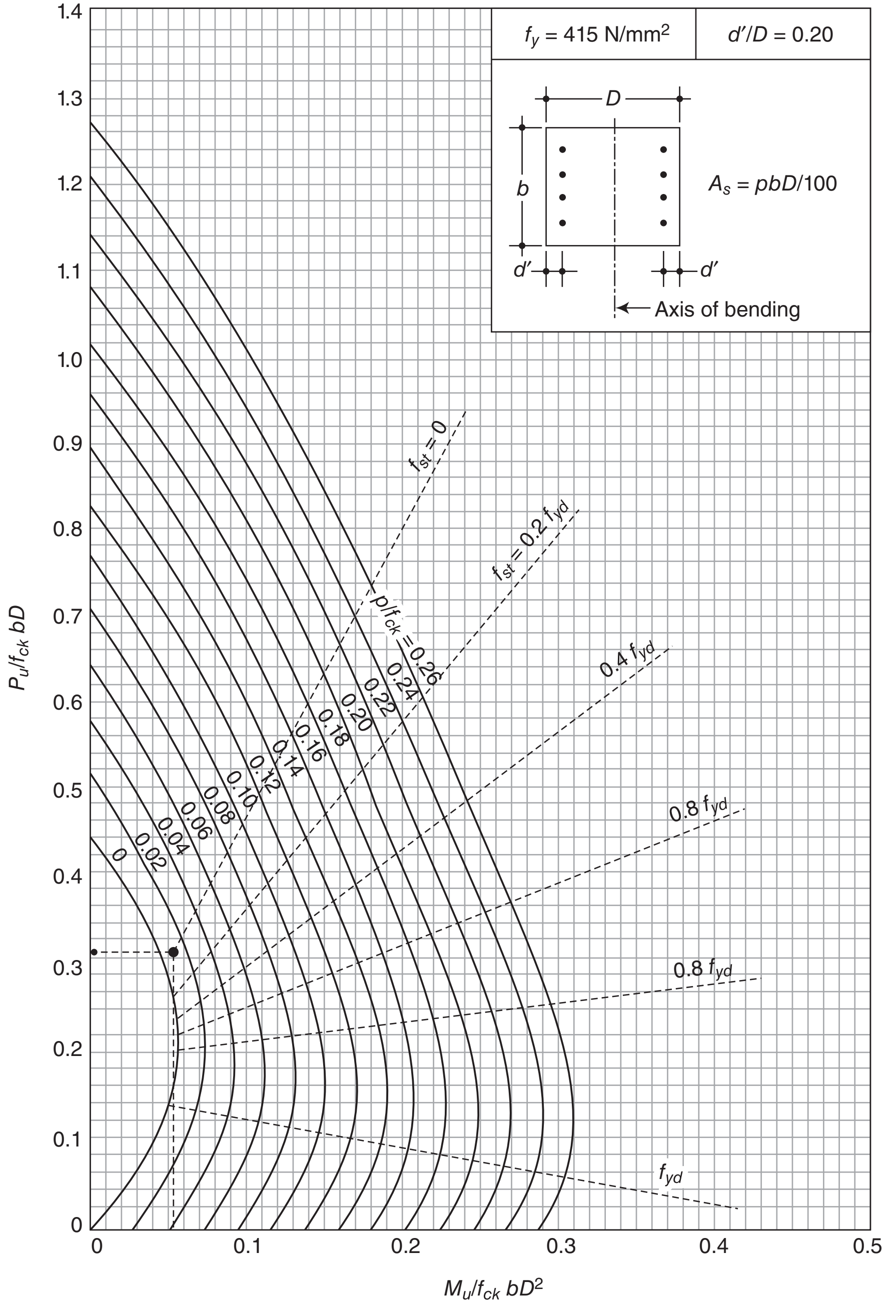

Fig. 22.3 *Compression with bending-rectangular section reinforcement distributed equally on two sides (SP:16 Chart-34)*

$$\left[\frac{M_u}{f_{ck} \cdot b \cdot D^2}\right] = \left[\frac{18 \times 10^6}{35 \times 250 \times 200^2}\right] = 0.051$$

Referring to Chart 34 of SP:16 (Fig. 22.3),

$$\left(\frac{p}{f_{ck}}\right) = 0.01 \quad \therefore \quad p = (35 \times 0.01) = 0.35$$

$$A_s = \left(\frac{0.35 \times 250 \times 200}{100}\right) = 175 \text{ mm}^2 < A_{s,\min}$$

Provided minimum reinforcement of 0.8 per cent of cross-section,

$$A_s = \left(\frac{0.8 \times 250 \times 200}{100}\right) = 400 \text{ mm}^2$$

Provide 4 bars of 12 mm diameter ($A_s = 452$ mm^2) and 6 mm diameter ties at 120 mm centres.

(c) Member CD

$$\text{Length, } L = 4.05 \text{ m}$$

$$\text{Effective length} = L_e = (0.65 \times 4.05) = 2.632 \text{ m}$$

$$\text{Ultimate load} = P_u = (1.5 \times 297) = 445.5 \text{ kN}$$

$$\text{Ultimate moment} = M_u = (1.5 \times 16) = 24.0 \text{ kN.m}$$

$$\left(\frac{L_e}{D}\right) = \left(\frac{2.632}{0.2}\right) = 13.16 > 12$$

Hence, the member is to be designed as a long column and slenderness effects have to be considered in the design.

The additional moments to be considered in design are computed as,

$$M_{ux} = \left(\frac{P_u.D}{2000}\right)\left(\frac{L_e}{D}\right)^2 = \left(\frac{445.5 \times 0.2}{2000}\right)13.16^2 = 7.71 \text{ kN.m}$$

$\therefore$ Total moment $= M_u = (24 + 7.71) = 31.71$ kN.m and $P_u = 445.5$ kN

$$\left[\frac{P_u}{f_{ck} \cdot b \cdot D}\right] = \left[\frac{445.5 \times 10^3}{35 \times 250 \times 200}\right] = 0.254$$

$$\left[\frac{M_u}{f_{ck} \cdot b \cdot D^2}\right] = \left[\frac{31.71 \times 10^6}{35 \times 250 \times 200^2}\right] = 0.09$$

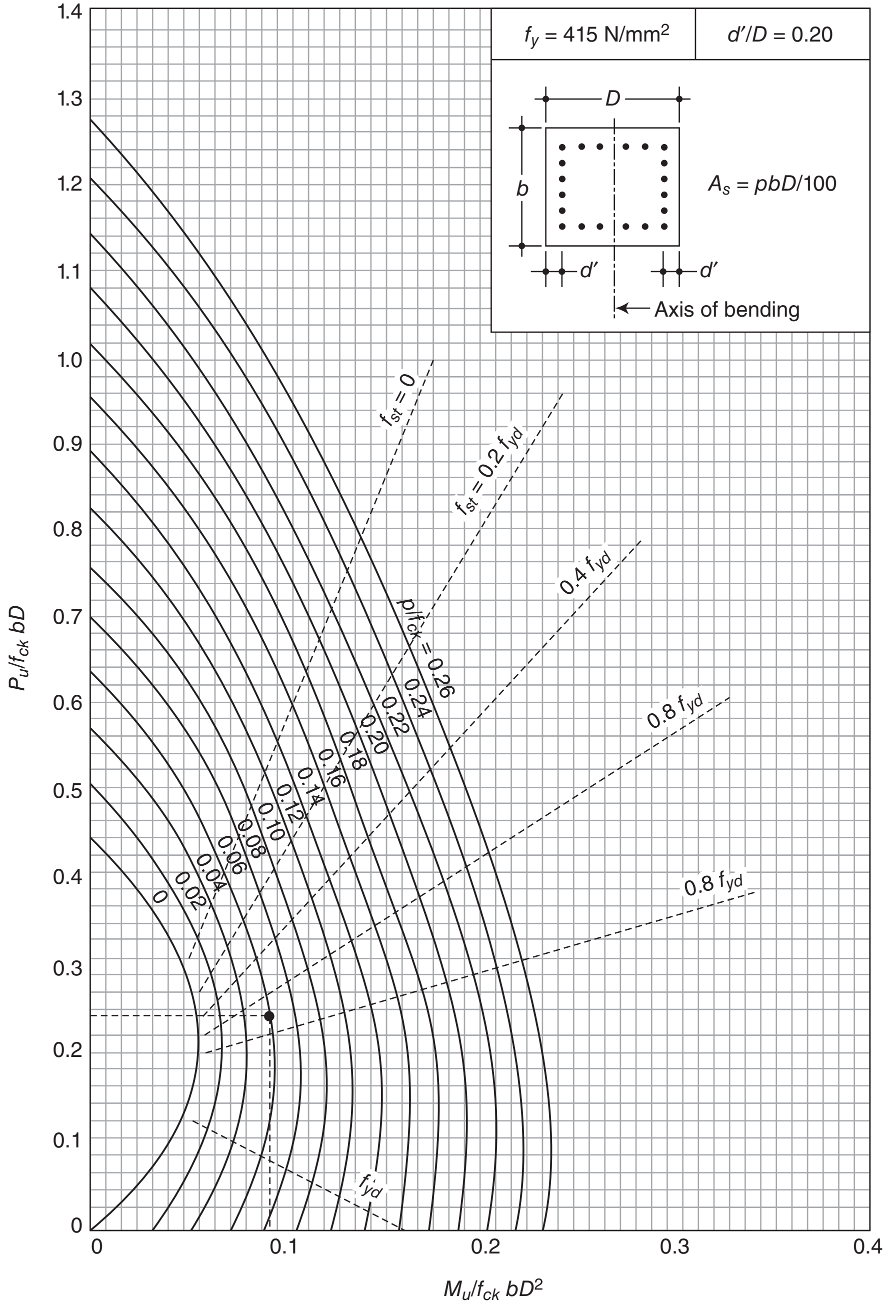

Fig. 22.4 *Compression with bending-rectangular section reinforcement distributed equally on four sides (SP:16 Chart-46)*

Referring to Chart-46 of SP: 16[2] (Fig. 22.4),

$$\left(\frac{p}{f_{ck}}\right) = 0.06 \qquad \therefore \quad p = (35 \times 0.06) = 2.10$$

$$A_s = \left(\frac{2.10 \times 250 \times 200}{100}\right) = 1050 \text{ mm}^2$$

Provide 4 bars of 16 mm and 4 bars of 10 mm diameter ($A_s = 1120$ mm^2) and 6 mm diameter ties at 120 mm centres.

(d) Member DE

$$\text{Length, } L = 4.00 \text{ m}$$

$$\text{Effective length} = L_e = (0.65 \times 4.00) = 2.6 \text{ m}$$

$$\text{Ultimate load} = P_u = (1.5 \times 236) = 354 \text{ kN}$$

$$\text{Ultimate moment} = M_u = (1.5 \times 16) = 24.0 \text{ kN.m}$$

$$\left(\frac{L_e}{D}\right) = \left(\frac{2.6}{0.2}\right) = 13 > 12$$

Hence, the member is to be designed as a long column and slenderness effects have to be considered in the design.

The additional moments to be considered in design are computed as,

$$M_{ux} = \left(\frac{P_u \cdot D}{2000}\right)\left(\frac{L_e}{D}\right)^2 = \left(\frac{354 \times 0.2}{2000}\right)13^2 = 5.98 \text{ kN.m}$$

$\therefore$ Total moment $= M_u = (24 + 5.98) = 29.98$ kN.m and $P_u = 445.5$ kN

$$\left[\frac{P_u}{f_{ck} \cdot b \cdot D}\right] = \left[\frac{354 \times 10^3}{35 \times 250 \times 200}\right] = 0.202$$

$$\left[\frac{M_u}{f_{ck} \cdot b \cdot D^2}\right] = \left[\frac{29.98 \times 10^6}{35 \times 250 \times 200^2}\right] = 0.085$$

Referring to Chart-46 of SP: 16 (Fig. 22.4),

$$\left(\frac{p}{f_{ck}}\right) = 0.055 \qquad \therefore \quad p = (35 \times 0.055) = 1.925$$

$$A_s = \left(\frac{1.925 \times 250 \times 200}{100}\right) = 963 \text{ mm}^2$$

Provide 4 bars of 16 mm and 4 bars of 10 mm diameter ($A_s = 1120$ mm^2) and 6 mm diameter ties at 120 mm centres.

(e) Member DF

$$P_u = (1.5 \times 72) = 108 \text{ kN}$$

Section adopted is (100 × 250) mm

$$\left(\frac{L_e}{D}\right) = \left(\frac{0.65 \times 4.1}{0.1}\right) = 26.65 > 12$$

Additional moments to be considered are,

$$M_{\text{ux}} = \left(\frac{P_u.D}{2000}\right)\left(\frac{L_e}{D}\right)^2 = \left(\frac{108 \times 0.1}{2000}\right)26.65^2 = 3.83 \text{ kN.m}$$

Since the forces and moments are of small magnitude, provide minimum reinforcements of 0.8 per cent of the cross-section.

$$As = \left(\frac{0.8 \times 100 \times 250}{100}\right) = 200 \text{ mm}^2$$

Provide 2 bars of 12 mm diameter ($A_s = 226 \text{ mm}^2$) with 6 mm ties at 120 mm centres.

2. Design of Tension Members

(a) Member AH

The tie member is designed as class 1-type structure without any cracks at working loads.

Precompression is provided by a prestreeing cable in the tie member.

Tensile force in the member = $N_d = 377$ kN

Bending moment = $M = 4.0$ kN.m

Permissible compressive stress in concrete of M-35 grade at transfer = σ_{ct} = 15 N/mm^2.

Permissible tensile stress at working loads = $\sigma_{tw} = 0$ and loss ratio = $\eta = 0.8$.

∴ Area of concrete section required

$$= \left(\frac{N_d}{\eta\sigma_{ct}}\right) = \left(\frac{377 \times 10^3}{0.8 \times 15}\right) = 31{,}333 \text{ mm}^2$$

Section adopted is (200 × 250) = 50,000 mm^2

$$\therefore \text{ Compressive prestress} = \left(\frac{377 \times 10^3}{0.8 \times 50000}\right) = 9.43 \text{ N/mm}^2$$

$$\text{Prestressing force} = P = \left(\frac{9.43 \times 50000}{1000}\right) = 471.5 \text{ kN}$$

Using 7 mm diameter high tensile wires initially stressed to 1100 N/mm^2 and having an ultimate tensile strength of 1500 N/mm^2, the number of wires required is given by,

$$n = \left(\frac{471.5 \times 10^3}{38.5 \times 1100}\right) = 11.13$$

Use one Freyssinet cable containing 12 wires of 7 mm diameter with suitable end anchorages.

$$\text{Ultimate tensile strength of tie} = \left[\frac{12 \times 38.5 \times 0.87 \times 1500}{1000}\right] = 603 \text{ kN}$$

$$\text{Load factor against collapse} = \left(\frac{603}{377}\right) = 1.6 > 1.5$$

Assuming direct tensile strength of concrete as 4 N/mm^2,

$$\text{Cracking load} = \left[\frac{50000(0.8 \times 9.43) + 4.0}{1000}\right] = 577.2 \text{ kN}$$

$$\therefore \text{ Load factor against cracking} = \left(\frac{577.2}{377}\right) = 1.53 > 1.25$$

Provide 4 bars of 12 mm and 4 bars of 10 mm diameter as untensioned reinforcement with 6 mm diameter ties at 200 mm centres.

The tie member AH can also be designed as a reinforced member without prestressing in which more reinforcements are required to resist tension with bending moment.

$$P_\text{u} = (1.5 \times 377) = 565.5 \text{ kN}$$

$$M_\text{u} = (1.5 \times 4) = 6.0 \text{ kN.m}$$

$$\left[\frac{P_u}{f_{ck} \cdot b \cdot D}\right] = \left[\frac{565.5 \times 10^3}{35 \times 250 \times 200}\right] = 0.323$$

$$\left[\frac{M_u}{f_{ck} \cdot b \cdot D^2}\right] = \left[\frac{6 \times 10^6}{35 \times 250 \times 200^2}\right] = 0.017$$

Referring to Chart-80 of SP: 16 (Fig. 22.5),

$$\left(\frac{p}{f_{ck}}\right) = 0.10 \qquad \therefore \quad p = (35 \times 0.10) = 3.5$$

$$A_s = \left(\frac{3.5 \times 250 \times 200}{100}\right) = 1750 \text{ mm}^2$$

Provide 8 bars of 18 mm diameter distributed equally on all sides (A_st provided = 2035 mm^2) with 10 mm stirrups at 120 mm centres.

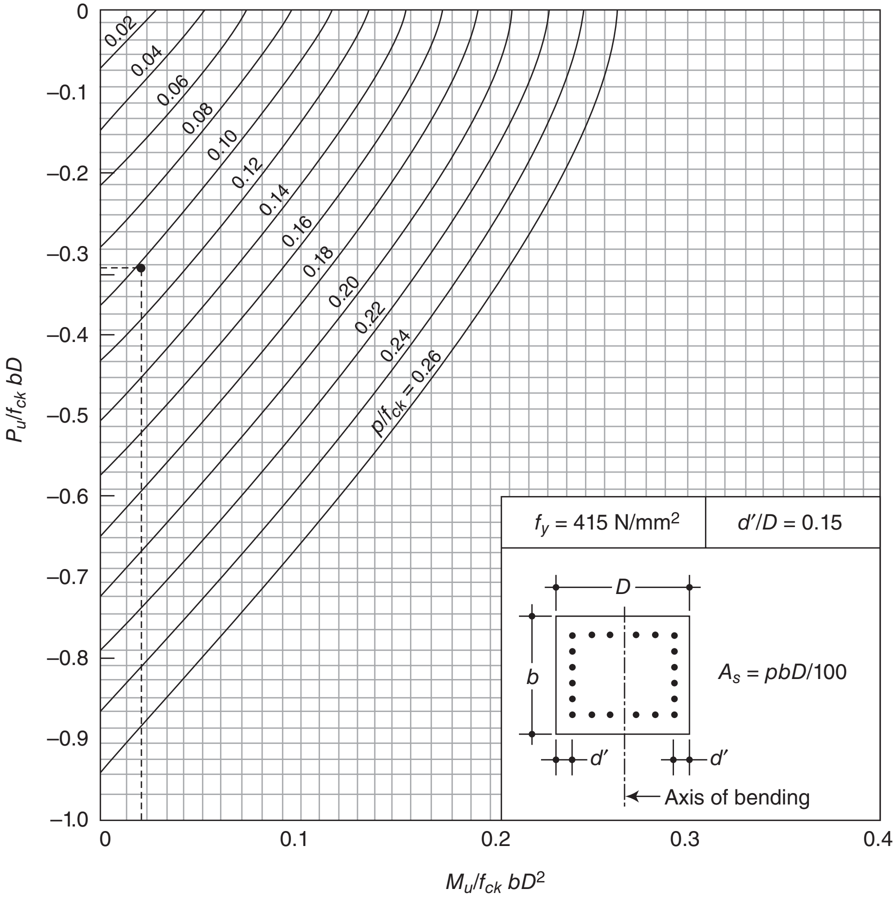

Fig. 22.5 *Tension with bending-rectangular section reinforcement distributed equally on four sides (SP:16 – Chart 80)*

Member EF

Adopting a section of size 100 by 250 mm, maximum design tensile force $= N_d = 59$ kN

$$\therefore \text{ Area of steel} = A_s = \left(\frac{59 \times 10^3}{230}\right) = 257 \text{ mm}^2$$

$$\text{Modular ratio of M-35 grade concrete is} = m = \left(\frac{280}{3 \times 11.5}\right) = 8.1$$

Using 2 bars of 16 mm diameter ($A_s = 404$ mm^2),

$$\text{Tensile stress} = \left[\frac{N_d}{A_c + (m-1)A_s}\right] = \left[\frac{59 \times 10^3}{(250 \times 100) + (8.1 - 1)\,404}\right]$$

$$= 2.11\ \text{N/mm}^2 < 4\ \text{N/mm}^2$$

Provide single legged ties of 6 mm diameter at 200 mm centres.
Typical reinforcement details are shown in Fig. 22.6.

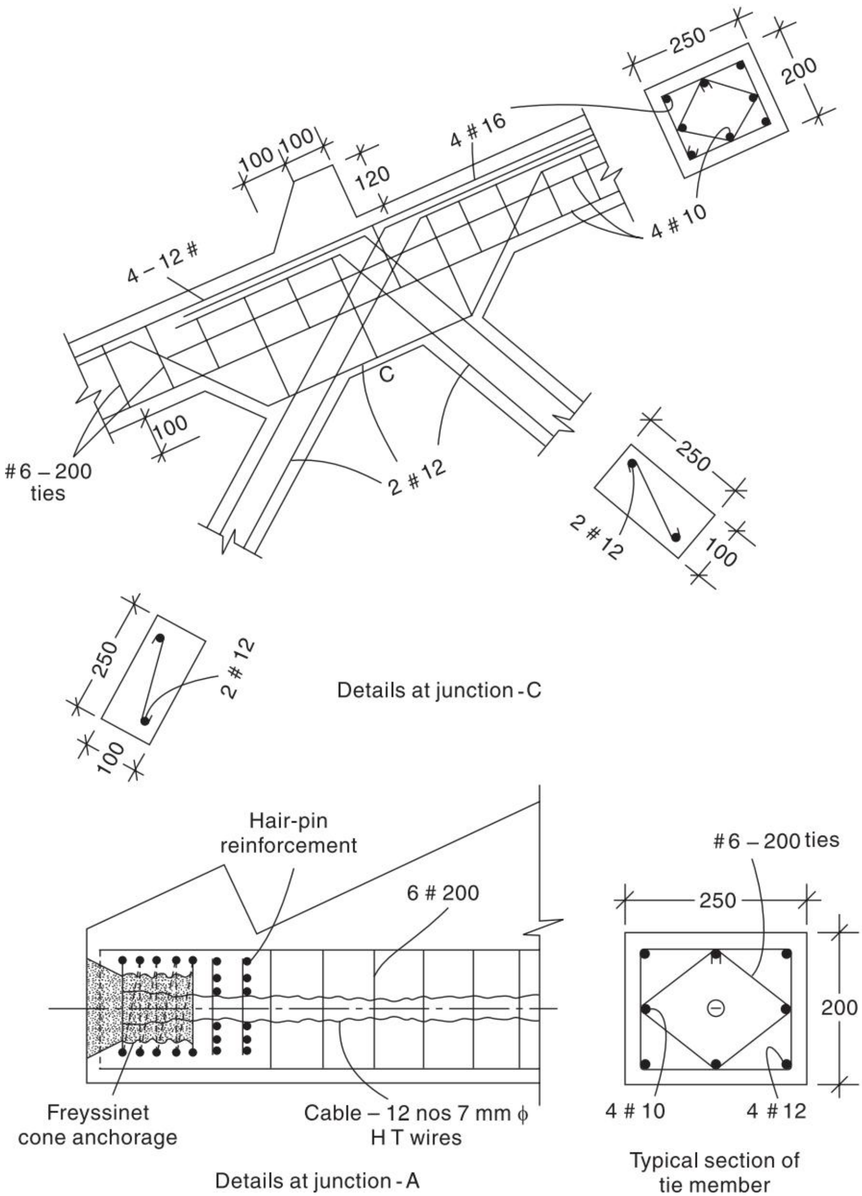

Fig. 22.6 *Reinforcement details in truss*

References

1. Murashev, V, Sigalov, E, Baikov, V., Design of Reinforced Concrete Structures, Mir Publishers, Moscow, 1968.
2. Sigalov, E, Strongin, S., Reinforced Concrete, Foreign Languages Publishing House, Moscow, 1962.
3. Dunham, C.W., Advanced Reinforced Concrete, McGraw-Hill Book Co., New York, 1964.
4. Graduck, H., Prestressed Concrete, Oxford & I.B.H, New Delhi,1968.
5. IS: 875–1987, (Parts 1 to 5) Code of Practice for Design Loads, Bureau of Indian Standards, New Delhi, 1989.
6. Reynolds, C and Steedman, J., Reinforced Concrete Designers Hand Book, Eighth Edition, Cement and Concrete Association, London, 1976.
7. Rowe, R.E., Cranston, W.B., and Best, B.C., New Concepts in the Design of Concrete, Structural Engineer, Vol. 43, 1965, pp. 339-403.
8. Bate, S.C.C., Why Limit State Design, Concrete, March 1968, pp. 103-108.
9. IS: 3201-1965, *Indian Standard Specification: Criteria for Design and Construction of Precast Concrete Trusses*, Bureau of Indian Standards, New Delhi, 1965.
10. IS: 1343-2012, Indian Standard for Prestressed Concrete (Second revision), B.I.S. New Delhi, 2012, pp.1-56,
11. SP: 16 -1980, Design Aids for Reinforced Concrete to IS: 456, Bureau of Indian Standards, New Delhi, 1980.

Review Questions

22.1 In what situations would you recommend the use of reinforced concrete trusses for the roofing system of structures? Mention their advantages.

22.2 Explain with sketches the different types of truss configurations used for various spans in the range of 10 to 30 m.

22.3 Explain briefly the constructional features of reinforced concrete trusses indicating the material requirements.

22.4 Outline the reasons for prestressing the bottom boom tie member of the concrete truss.

22.5 Sketch a typical tie member of a reinforced concrete truss with a prestressed tie member showing the details of high tensile wires and the end anchorages.

22.6 Write a brief note on the nature of forces developed in the various members of concrete trusses subjected to dead, live and wind loads.

22.7 What grade of concrete is generally used in the construction of reinforced concrete trusses? Explain with reasons the necessity for using higher grade concretes.

22.8 What are the forces to be considered in the design of a typical compression member of a reinforced concrete truss?

22.9 What are the simplifying assumptions made in the analysis of reinforced concrete trusses? How do you justify these assumptions?

22.10 What happens if the tie member is not prestressed? Is it advantageous to design the bottom boom tie as a reinforced member?

Exercises

1. A reinforced concrete truss of polygonal parallel chord type is proposed for the roof system of an industrial structure for a span of 24 m, comprising 8 bays of 3 m each. The truss height is 2.5 m. Spacings of trusses = 6 m. The roof is covered by precast ribbed slabs of size 3 m by 6 m each weighing 24 kN. Live load on roof is 1.5 kN/m^2. The top and bottom boom members are 250 mm wide by 250 mm deep, while the diagonal and vertical members are of cross-section 250 mm by 150 mm. Analyse the frame for dead and live loads only and design the typical members of the truss using M-40 grade concrete and FE-415 HYSD bars. Also, design the bottom tie as a prestressed member using Freyssinet cables comprising 12 wires of 7 or 8 mm diameter with an ultimate strength of 1500 N/mm^2.
2. The compression and tension members of an 18 m span reinforced concrete truss are subjected to the forces shown in the table given as follows:

Member	*Cross-sectional Dimensions (mm × mm)*	*Length of Member (m)*	*Forces (kN)*	*Moment (kN.m)*
AB	200 × 240	1.8	300 (compression)	3.5
BC	200 × 240	3.6	240 (compression)	12.0
AH	200 × 240	3.0	320 (tension)	—

Using M-40 grade concrete and Fe-415 HYSD bars, design suitable reinforcements in the members. Also, design the tie AH as a prestressed member using suitable number of 7 mm diameter high tensile wires initially stressed to 1000 N/mm^2. Sketch the details of reinforcements in the cross-section of the members.

3. The top chord member of a reinforced concrete truss is subjected to a compressive force of 240 kN together with a bending moment of 3.0 kN.m. The bottom chord tie member is subjected to a tensile force of 220 kN. The members have a breadth of 200 mm and a depth of 180 mm. The length of compression member is 1.6 m while that of the tie is 2.5 m. Using M-35 grade concrete and Fe-415 HYSD bars, design the reinforcements in the members. Also, design the tension member with the required magnitude of prestress using high tensile wire of 7 mm diameter having an ultimate tensile strength of 1500 N/mm^2 and initially stressed to 1000 N/mm^2.

4. A fink type reinforced concrete truss is to be designed for warehouse to suit the following data:

Effective span of the truss = 18 m

Type of truss = fink type

Roof cladding = Asbestos sheets supported on precast pretensioned purlins
Spacings of trusses = 6 m
Wind pressure = 1.5 kN/m^2
Central rise = one fourth span
Grade of concrete = M-40
Reinforcements = Fe-415 HYSD bars and high tensile wires of 7 mm diameter with an ultimate tensile strength of 1500 N/mm^2.
Design the reinforcements in the typical compression and tie members.

Objective-type Questions

22.1 Reinforced concrete trusses are preferred in structures located in
(a) arid zones
(b) hilly areas
(c) coastal areas with aggressive environmental conditions

22.2 Reinforced concrete trusses were first developed and widely used for structural roofs in
(a) Australia
(b) Europe
(c) America

22.3 The diagonal members of a reinforced concrete truss are generally subjected to
(a) bending
(b) torsion
(c) compression or tension

22.4 The bottom boom members of concrete trusses are primarily subjected to
(a) compression
(b) tension
(c) flexure

22.5 The type of reinforcements used for large span reinforced concrete trusses is
(a) mild steel
(b) high tensile steel
(c) HYSD bars

22.6 The critical forces in the various members of the concrete truss is analysed for
(a) dead load
(b) live load
(c) dead load + live load + wind load

22.7 The diagonal members of a reinforced concrete truss are generally
(a) prestressed
(b) reinforced and prestressed
(c) reinforced

22.8 The tie member of a reinforced concrete truss is generally designed as
(a) axially prestressed
(b) transversely prestressed
(c) eccentrically prestressed

22.9 In the design of top boom members of a concrete truss loaded between the joints, the forces to be considered in design are
(a) axial forces
(b) eccentric forces
(c) axial force and bending moment

22.10 Reinforced concrete trusses are preferably
(a) cast at site in the vertical position
(b) cast at site in the horizontal position
(c) cast at site over the supporting columns

Answers to Objective-type Questions

22.1 (c)	22.2 (b)	22.3 (c)	22.4 (b)	22.5 (b)
22.6 (c)	22.7 (c)	22.8 (a)	22.9 (c)	22.10 (b)

23 Planning and Economical Aspects of Prestressed Concrete Structures

23.1 Introduction

Planning, analysis and design are the logical steps to be followed before beginning the construction of any prestressed concrete structure. From ancient times, construction of a structure has always been one of the most fascinating challenges to man's ingenuity. Architectural capabilities constitute the essence of the conceptual and aesthetic aspects of structures. The domain of construction activity involves several known and unknown features such as management of materials and labour, mobilisation of suitable cost-effective techniques, treacherous foundation problems, adverse weather conditions, planning and scheduling of the construction process to a time bound frame, constant interaction with the design engineer, architect, site engineer, construction workers and the ability to take sound and daring decisions at times of crisis.

According to Raina[1], "Engineering is not just solving theoretical problems, nor is it a matter of blind adherence to graphs, design charts and formulas. It is more meaningful to have an approximate solution to an exact problem rather than an exact solution to an approximate problem. Practical engineers must be more conceptual than mere perceptual, more creative than mere analytical and more visual than mere mathematical. Construction engineers should have wide experience involving several types of structures rather than isolated narrow specialisation. Expertise and original skills are attained from relentless understanding and practise rather than mere theoretical knowledge. Good and sound judgment are attained from wide practical experience and often experience comes from bad judgment."

23.2 Structural Forms for High Rise Structures

In the case of large floor and roof coverings using prestressed concrete as material, there are several types of structural forms for adoption. Some of them are as follows:

1. Tee beam and slab floors
2. Continuous beam and slab floors

3. Coffered or grid floors
4. Flat slab floors
5. Folded plate roofs
6. Shell-type roofs
7. Spherical domes
8. Trussed and framed roofs
9. Composite construction using prestressed and reinforced concrete

23.3 Structural Forms for Bridges

For medium and long spans, prestressed concrete is ideally suited for the super structure of bridges. The structural forms generally used for bridges are listed as follows.

1. Solid slabs (10–15 m)
2. Voided or hollow slabs (15–25 m)
3. Rigid frame bridges (15–30 m)
4. Tee beam and slab (20–40 m)
5. Two-cell box girders (30–70 m)
6. Multicell box girders (40–80 m)
7. Balanced cantilever-type bridges (20–30 m)
8. Continuous girders of variable depth (30–40 m)
9. Cable-stayed bridges (100–500 m)

Prestressed concrete has more or less replaced reinforced concrete as the most suitable material for bridge construction due to its inherent advantages of high strength coupled with durability, energy absorption under dynamic loads, ability to resist repetitive loads, freedom from cracks, easy mould ability to desired shape, economy and ease of maintenance.

23.4 Structural Forms for Aircraft Hangars

Over the last few decades, increased airway traffic has necessitated the development and use of large aircraft like Boeing-747 and Airbus-320. The servicing of these aircraft requires large aircraft hangars with unrestricted space for easy movement of aircraft. The structural forms generally used for aircraft hangars are compiled as follows:

1. *Prestressed concrete barrel shells* (Refer to Chapter 18 for design details) with longitudinal beams of spans in the range of 40–60 m. The shells and the edge beams are supported by transverse prestressed edge beams having a span range of 50–60 m.
2. *Prestressed concrete folded plates* (Refer to Chapter 18 for design details) of spans in the range of 50–90 m with prestressing cables housed in the valley portions and the folded plates built into prestressed transverse deep edge beams of spans 40–50 m, supported on reinforced concrete columns.

3. *Twin cantilever folded plate roofs* with a central service complex. The continuous folded plate roof is stayed by prestressed concrete ties. This type of planning provides an unrestricted clear space of 60–90 m on either side of the central service complex. The cantilever folded plate roof complex requires significantly lower quantities of materials like concrete and prestressing cables due to the unique feature of the structural form.

23.5 Structural Forms for Irrigation and Waterway Works

Reinforced concrete is ideally suited and widely adopted for the construction of large gravity dams like Bhakra dam, Hirakud and Rihand dams. Canals, aqueducts and syphons are generally required for transportation of water for irrigation purposes over long distances. The structural forms widely used for water transportation are as follows:

1. Prestressed concrete box sections with longitudinal deep girders and cross girders with slab between the girders.
2. Concrete tubular aqueducts prestressed both longitudinally and transversely with diameters in the range of 3–5 m and spans varying from 30–50 m. This structural form serves the dual purpose of water transportation in the tubular duct and the top portion is used for the road way.
3. Prestressed concrete circular sections with loop cables for transverse prestressing to resist water pressure as in the case of syphons.

23.6 Structural Forms for Energy Structures

Reinforced and prestressed concrete are widely used for energy structures like dams, surge shafts in hydroelectric power stations. The use of prestressed concrete biological shields for nuclear reactor and containment vessels offers several advantages. Prestressed concrete pressure vessels can be triaxially prestressed resulting in higher load factors against limit states of service and ultimate failure. The structural form normally used comprises a cylindrical concrete vessel capped with a shallow dome. Cylindrical and spherical shapes have been used for the Oldbury and Wylfa pressure vessels[2].

In the case of Kalpakkam nuclear power station[3], located in Tamil Nadu, India, shielding is provided by a double containment system with an inner cylinder of 600 mm thick prestressed concrete surrounded by an outer wall of rubble masonry 711 mm thick. The two walls are separated by an annular air space 1 m wide. In general, prestressed concrete reactor and containment vessels are cylindrical in shape facilitating slip form method of construction and circumferential prestressing, resulting in considerable economy coupled with speedy construction.

23.7 Concepts of Planning with Practical Examples

23.7.1 General Aspects

Planning of any structure like a building, bridge, marine structure, or storage structure requires a comprehensive knowledge of the various parameters like site conditions, availability of skilled labour and materials, transportation facilities, seismic nature of the terrain, subsoil water conditions, choice of material like steel, reinforced or prestressed concrete, weather and durability considerations, client requirements and the funds earmarked for the structure. It is important to note that there is no single form of design which would be most economical in a given situation. To arrive at an economical design, several alternatives using different materials and structural configurations should be examined and a comparative analysis is made which will lead to an optimal design.

Developing countries like India lack to some extent the economic and social infrastructure which is always important in the process of planning. Many of the public sector projects in India are planned according to the whims and fancies of the ruling politicians and bureaucrats without a careful evaluation of the local needs of the population and ground realities. According to Raina[4], "Correct technology for the environment prevailing at a particular time in the particular part of the world under question can be considered as the appropriate technology". In general, appropriate technology must necessarily involve the prevailing local infrastructure, like raw materials, man power, plant and machinery, power and financial resources. An excellent example of appropriate technology can be found in the low-cost suspension bridges built by Girish Bharadwaj[5] in South India.

23.7.2 Prestressed Concrete Aircraft Hangars

Prestressed concrete with superior durability characteristics and reduced maintenance costs is ideally suited for aircraft hangars requiring large column free spaces. An excellent example being the Indian Airlines Airbus hangar in Mumbai with a covered roof comprising prestressed concrete folded plates cantilevering on opposite sides from the main service complex. A typical cross-section of the hangar is shown in Fig. 23.1. The cantilevers have a span of 62.3 m on either side of the 27.4 m wide central service complex. The continuous folded plates of 7.62 m module with webs inclined at 45 degrees are stayed by prestressed concrete ties. The hangar provides a clear uninterrupted space of 91.4 m with an average height of 13 m so that two airbus aircrafts can easily be parked in the hangar. The airbus hangar was designed by STUP consulting engineers for the Indian Airlines Corporation.

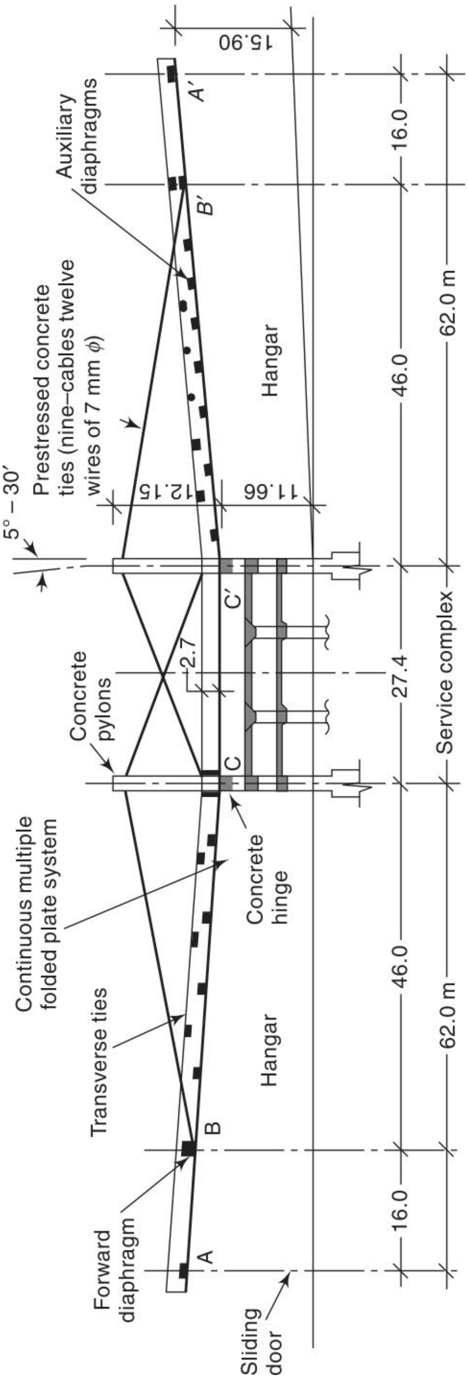

Fig. 23.1 *Longitudinal section of the Indian Airlines hangar, Mumbai*

The Boeing hangar at Santacruz Airport, Mumbai, is another notable example of prestressed concrete structure covering an uninterrupted column free area of 101 m by 45.73 m. The roof consists of 10 barrel shells of 45.73 m span with 12.2 m chord width supported on longitudinal prestressed edge beams. The frontal beams of depth 6.1 m are also prestressed with a span of 48.8 m over clear door openings with their soffit 15.2 m above the floor. The aircraft hangar planned, designed and constructed by Gammon India Limited, is shown in Fig. 23.2.

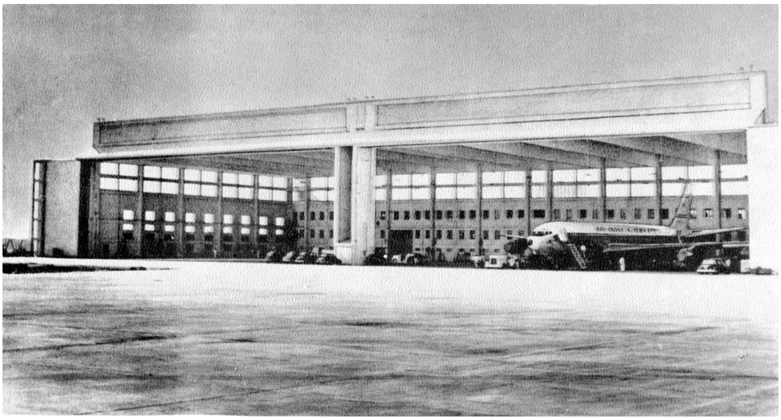

Fig. 23.2 *Boeing hangar at Santacruz Airport, Mumbai*

23.7.3 Prestressed Concrete Aqueducts

An excellent example of the application of prestressed concrete in aqueducts is the Gomati Aqueduct having 12 equal spans of 31.8 m. The structure is designed as a rigid box section of 12.8 m by 6.7 m carrying a discharge of 357 cumecs. The depth of two main prestressed girders is 9.9 m, weighing as much as 550 per girder per span. Gomati Aqueduct is the biggest and the longest aqueduct in India constructed by Hindustan Construction Company Ltd. Mumbai, for the UP state irrigation department. The top of the aqueduct serves as a roadway.

The Bhima Aqueduct, shown in Fig. 23.3, is an excellent example of planning hydraulic and highway elements in a single structure. The aqueduct is 947 m long with spans of 41.5 m with a truncated circular cross-section of 4.8 m diameter with a pipe thickness of 200 m. A flat slab 3.75 m wide at the top serves as a roadway.

23.7.4 Prestressed Concrete Syphons

The Kunu Syphon, planned and designed by STUP Consultants[6], is located on the main canal of the Chambal irrigation system in India. The prestressed concrete syphon, shown in Fig. 23.4, has an internal diameter of 6.1 m with a wall thickness varying from 279 mm to 482 mm near the anchorage zones. The siphon is 1798.8 m long and is subjected to a maximum pressure due to a head of 25.9 m of water. When it crosses the Kunu River of length 274.4 m, it functions as an aqueduct.

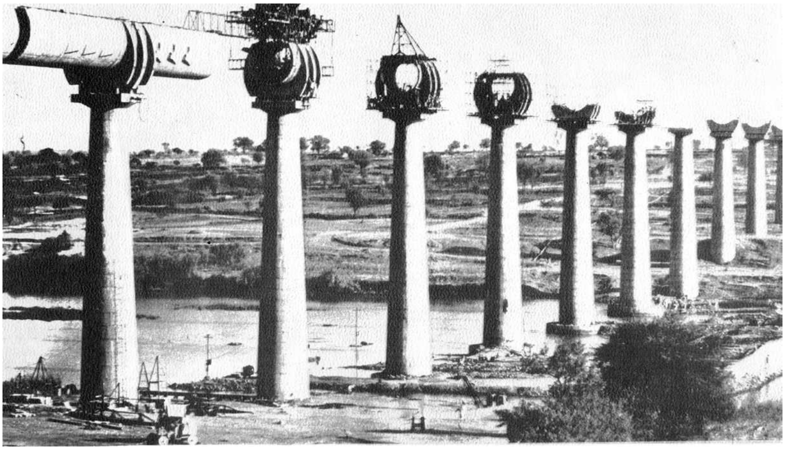

Fig. 23.3 *Bhima aqueduct near Sholapur, Maharashtra*

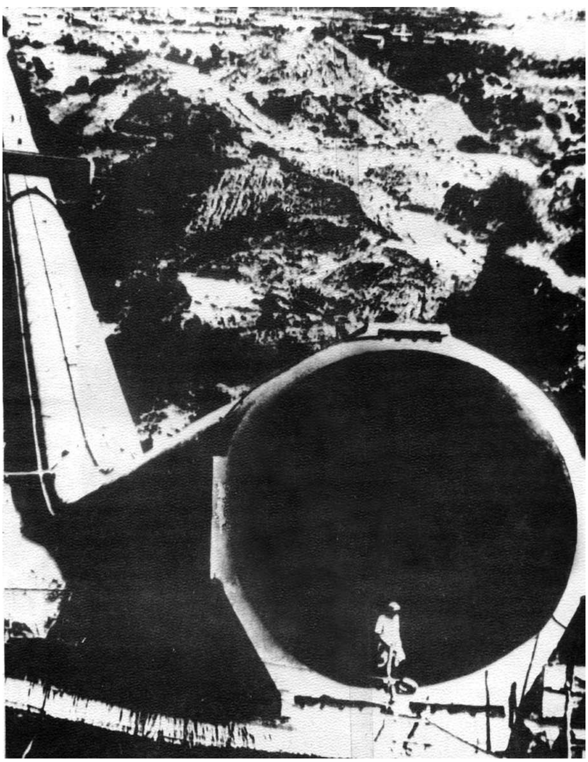

Fig. 23.4 *Kunu syphon*

23.7.5 Prestressed Concrete Nuclear Power Structures

The application of prestressed concrete in nuclear containment structures is well established in Indian atomic reactors. In the latter part of the 20th century, India has planned and built several atomic power stations at Tarapur, Rajasthan, Kalpakkam, Narora, Kakrapur and Kaiga, spread over several states in India[6]. Figures 23.5 to 23.7 show the dimensional details of the Rajasthan, Kalapakkam and Narora reactor containment structures with

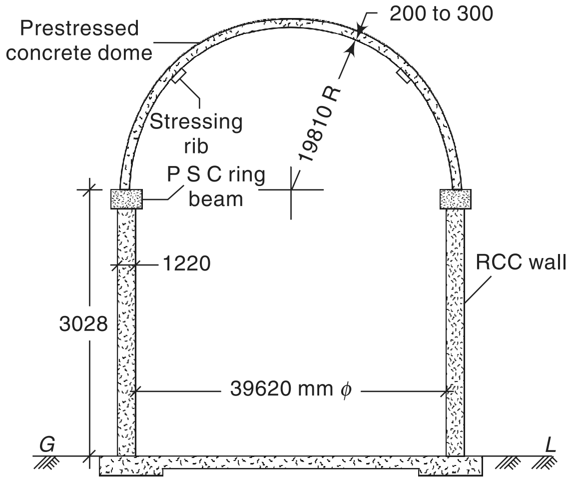

Fig. 23.5 *Rajasthan atomic power reactor vessel at Kota*

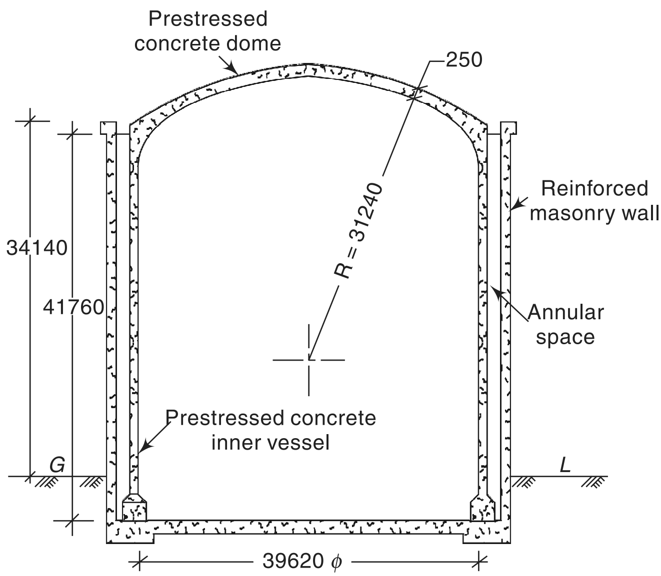

Fig. 23.6 *Madras atomic power reactor vessel with Outer Masonry Wall at Kalpakkam*

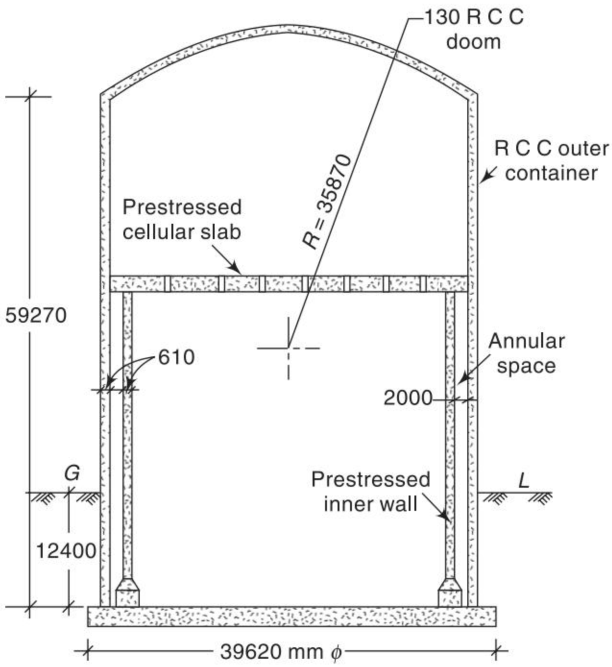

Fig. 23.7 *Narora atomic power reactor vessel with outer container*

domes of prestressed or reinforced concrete. The salient design parameters of various atomic power plants are compiled in Table 23.1. The Kalpakkam and Narora reactors have an inner cylindrical wall of prestressed concrete and an outer reinforced concrete wall with an annular space between them serving as a double barrier against radiation leakage.

Table 23.1 *Salient design parameters of atomic power plants of Indian reactor vessels*

	Parameter	*Rajasthan Atomic Power Plant*	*Madras Atomic Power Plant*	*Narora Atomic Power Plant*
1.	Design pressure (N/mm^2)	0.042	0.116	0.125
2.	Test pressure (N/mm^2)	0.053	0.091	0.144
3.	Peak temperature (°C) (Accident condition)	71	96	120
4.	Maximum allowable leakage rate (Per cent of contained volume/hour at design)	0.1	0.02	* Lp: 0.1 Ls: 0.1
5.	Testing requirements	(i) Pre-operational pressure at test pressure and leakage rate test at design pressure. (ii) Periodic leakage rate tests at less than design pressure		
6.	Means of prestress	Dousing	Suppression pool	Suppression pool

* Lp – Primary containment leakage rate
Ls – Secondary containment leakage rate

23.7.6 Prestressed Concrete Silos

Prestressed concrete silos are generally preferred in place of reinforced concrete silos for the storage of fertilisers, cement and other products mainly due to their superior strength, durability and economy in the overall costs. Figure 23.8 shows the precast prestressed concrete silo at Nangal built by M/s. Gammon India Ltd. for the Fertilizer Corporation of India. The parabolic shaped thin concrete shell segments are precast and combined by cast *in situ* joints and prestressed by cables in the longitudinal and transverse directions at modular intervals to achieve integrity of joints resulting in large uninterrupted space inside the shell. The thickness of concrete in the shell is in the range of 50 to 75 mm. The Nangal silo has a width of 32 m and 312 m length with the height of the crown 20 m from the floor. Typical examples of such silos can be found in Mangalore Fertilizers and Chemicals Ltd. factory located near the Mangalore harbour at Panambur.

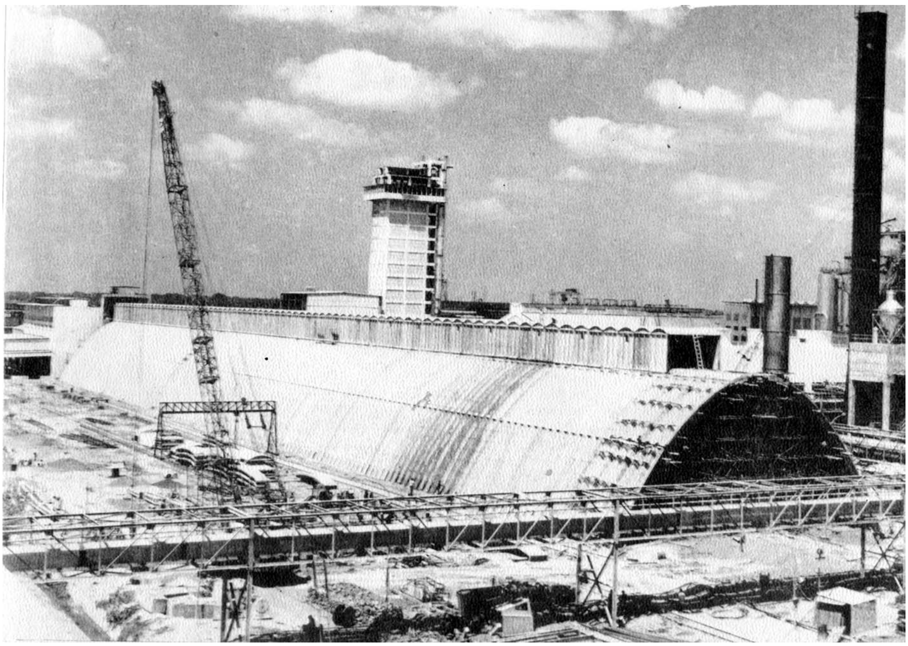

Fig. 23.8 *Precast prestressed concrete silo at Nangal*

23.7.7 Prestressed Concrete Domes and Water Tanks

Most of the atomic reactor containment structures of circular shape having diameters in the range of 40 m are covered by prestressed concrete domes with ring beams. Economical dimensions of prestressed concrete circular water tanks with a capacity in the range of 400 to 40000 m^3 are compiled in Table 16.1. Typical example of ball-shaped prestressed concrete reservoir having a capacity of four million litres is shown in Fig. 23.9. The ball tank was planned and built by STUP Consultants and Gammon India Ltd. for the department of atomic energy. The diameter of the tank is around 10 m and the circular walls are prestressed both in the circumferential and meridional directions. Figure 23.10 shows another notable example of prestressed overhead water tank at Haza Al Ain, United Arab Emirates, designed by STUP Consultants. The special feature of this tank is that the structural elements were precast at ground level and lifted to the top by using Dywidag high tensile bars with suitable couplers.

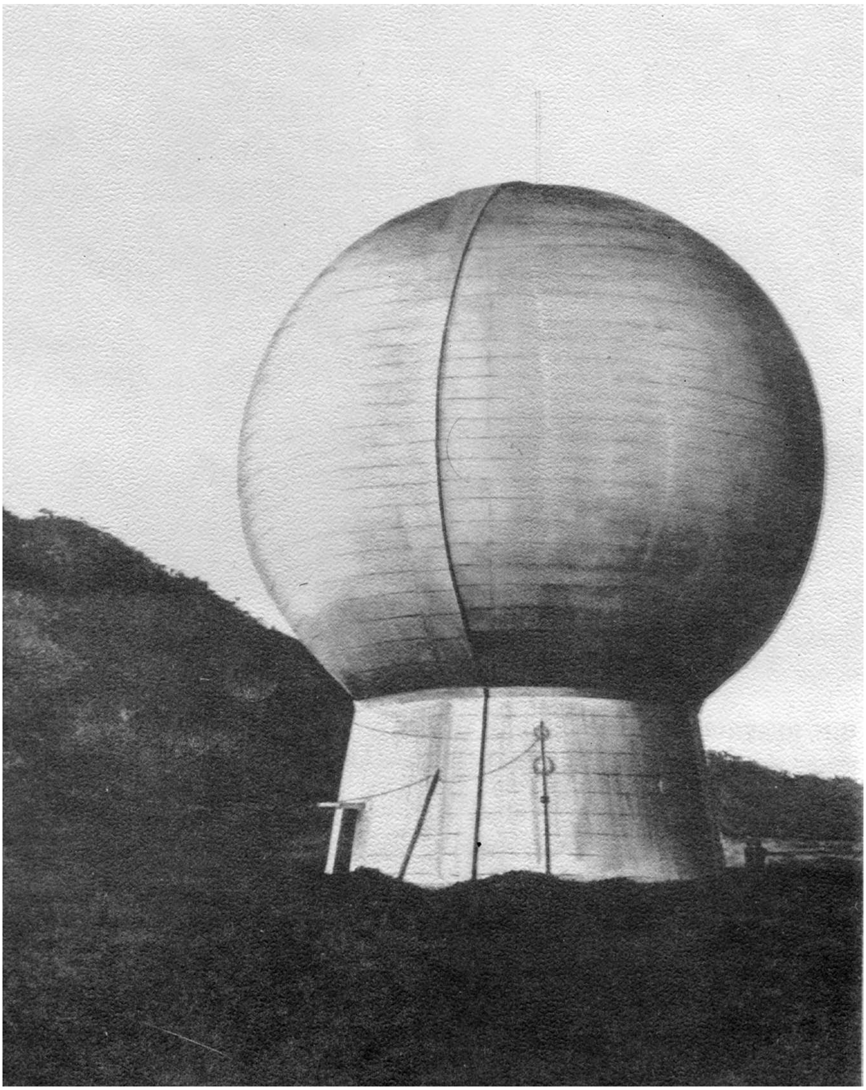

Fig. 23.9 *Prestressed concrete ball tank, Trombay, Maharashtra*

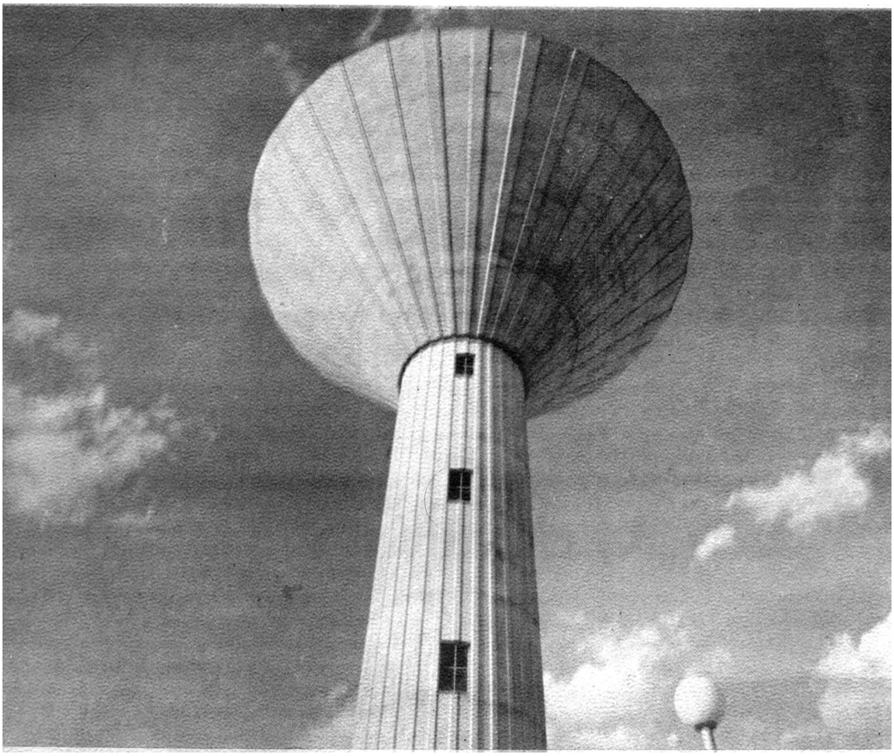

Fig. 23.10 *Prestressed concrete overhead reservoir at Haza Al Ain, UAE*

23.7.8 Prestressed Concrete Bridges

The design aspect of several types of prestressed concrete bridge decks is presented in great detail in Chapter 21. The planning and economical aspects are important aspects to be considered in selecting the type of bridge deck. In general, the quantities of concrete and steel expressed per unit area of deck can be considered as indicative of economic use of materials, although these factors are not the only ones which govern the overall cost of the bridge. The various primary factors influencing the total cost of a bridge are:

1. The length of individual spans
2. The type of cross-section of deck
3. The number of longitudinal girders
4. The width of bridge deck
5. The depth and type of foundations
6. The cost of formwork
7. The cost of materials and labour
8. The type of construction such as cast *in situ* or precast
9. The methods of erection of precast elements

Based on extensive practical experience, Raina[4] compiled the approximate quantities of concrete and steel required for unit area of deck with different types of bridge configuration for a specified type of loading and design criteria as shown in Fig. 23.11. The data helps to select the type of bridge with economical use of materials from alternatives like simply supported, continuous, portals and bow string girder bridge types in the span range of 35 to 140 m.

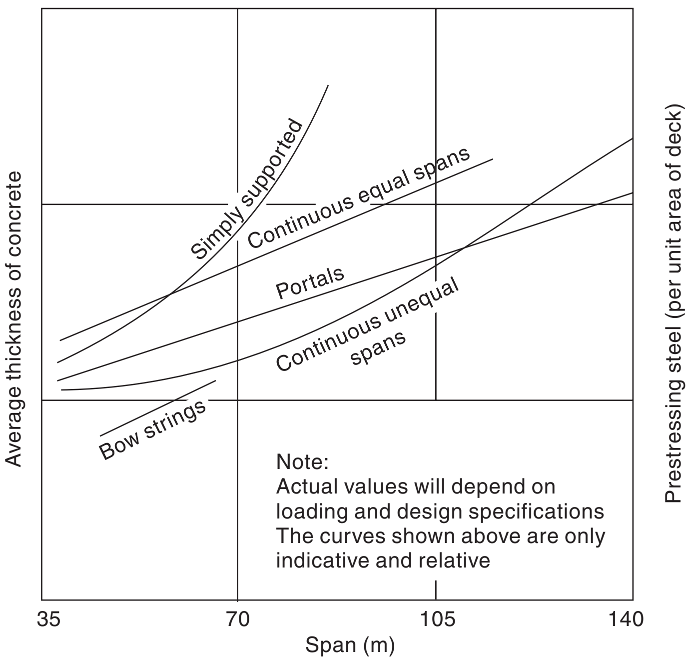

Fig. 23.11 *Approximate quantities of concrete and steel in various types of bridge decks*

The typical cross-sections of various types of prestressed concrete bridge deck configurations are shown in Fig. 23.12. Precast pretensioned or post-tensioned voided slabs are economical for spans of 10 to 25 m with span/depth ratios of 25 to 30. Precast Tee, I and box girders with cast *in situ* slabs are suitable for spans up to 50 m. Raina[4] graphically compared the variation in the quantities of concrete, prestress and reinforcement with the depth of bridge deck for different types of structural configurations in Fig. 23.13. As early as in 1969, Sarkar *et al.*[7] reported the variation of the cost of bridge deck in relation to span and the number of longitudinal girders in a tee girder bridge deck, based on a rigorous computational analysis. Figure 23.14 shows that the cost increased with increasing number of girders for spans in the range of 15 to 35 m.

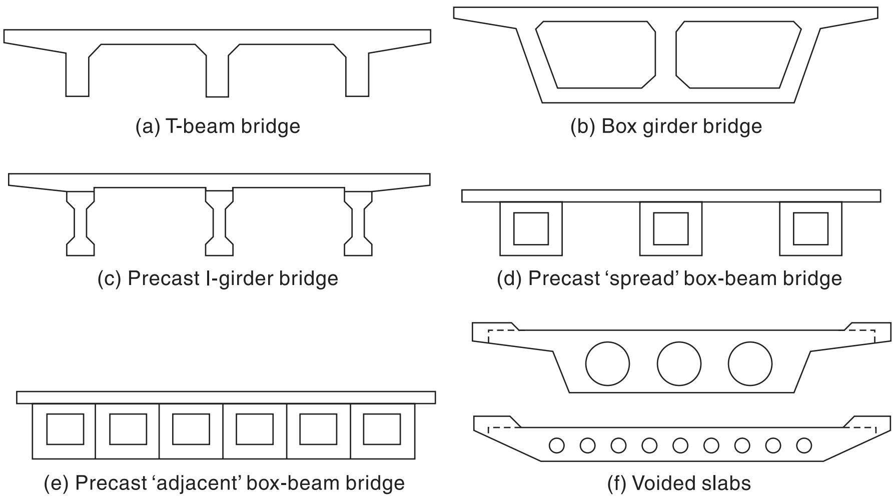

Fig. 23.12 *Typical cross-sections of prestressed concrete bridge decks*

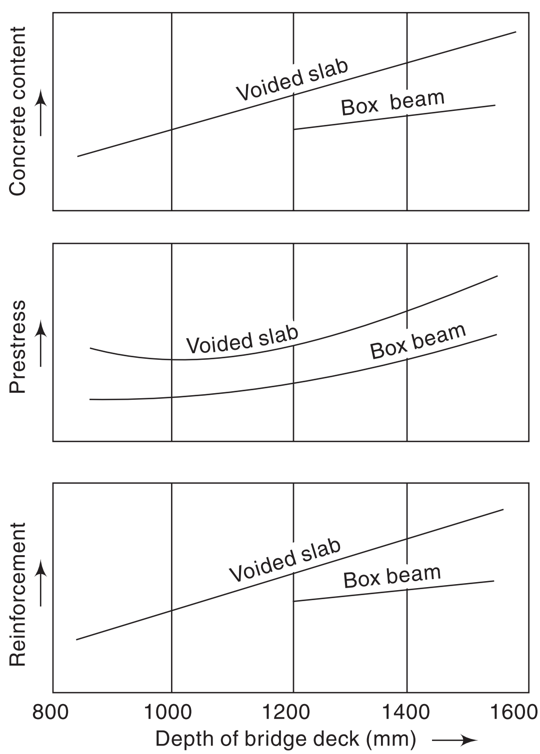

Fig. 23.13 *Variation of concrete content, prestress and reinforcement with depth of bridge deck*

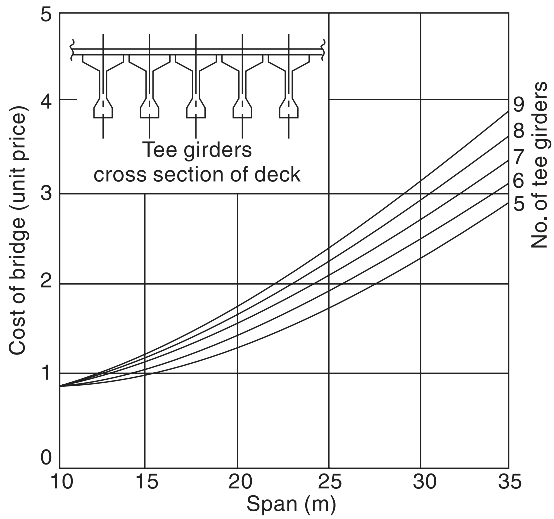

Fig. 23.14 *Variation of cost of bridge with span and number of tee-girders*

During the last three decades, cable-stayed bridges have been found to be economical for long spans. Prof. Leonhardt[8] designed the first cable bridge across the river Rhine in Dusseldorf in 1952. Thereafter, hundreds of cable-stayed bridges have been built in different countries with spans in the range of 100 to 1000 m. A comprehensive list of world's prominent cable-stayed bridges built in various countries and their salient features are compiled in Table 23.2.

Table 23.2 *World's prominent cable-stayed bridges*

S. No.	*Name of the Bridge*	*Material of Deck*	*Span* (m)	*Height of Tower* (m)	*Year*
1.	Rafael Urdaneta (Venezuela)	Concrete	235	68	1962
2.	Dnepr Bridge (USSR)	Concrete	144	30	1963
3.	Knie (Germany)	Steel	320	114	1969
4.	Duisburg (Germany)	Steel	350	50	1970
5.	Wadikuf (Libya)	Concrete	282	50	1972
6.	Mesapatomia (Argentina)	Concrete	340	97	1972
7.	Westgate (Australia)	Steel	336	46	1974
8.	Kholbrand (Germany)	Steel	325	98	1974
9.	Saint-Nazaire (France)	Steel	404	67	1975
10.	Brazo-Largo (Argentina)	Steel	330	48	1976
11.	Zarate (Argentina)	Steel	330	67	1976
12.	Brotonne (France)	Concrete	320	65	1976
13.	Luling (USA)	Steel	376	75	1980
14.	Dames Point (USA)	Concrete	396	92	1995

(*Contd.*)

Table 23.2 *(Contd.)*

	Indian Cable-stayed Bridges				
1.	Haridwar (Uttarakhand)	Concrete	130	20	1990
2.	Jogighopa (Assam)	Concrete	286	50	1995
3.	Akkar (Sikkim)	Concrete	154	56	1995
4.	Vidyasagar Sethu (Kolkata)	Concrete and Steel	452	100	1995
5.	Vivekananda Tollway bridge (Kolkata)	Concrete and Steel	110	40	2008
	Longest and Highest Cable-stayed Bridges				
1.	Messina Straits (Italy)	Steel	1800	-	1982
2.	Normandie Bridge (France)	Concrete and Steel	624	-	1996
3.	Millau Bridge (France)	Concrete and Steel	400	300	2004
4.	Sutong Bridge (China)	Concrete and Steel	1088	-	2008

Figure 23.15 shows the Akkar Bridge in Sikkim, with a central tower supporting the concrete deck by 34 cables, each containing 37 high-tensile wires of 7 mm diameter, covering a span of 154 m with cross girders at 3 m intervals. Cable-stayed bridges are preferred to conventional suspension bridges for long spans mainly due to the reduction in bending moments in the stiffening girder resulting in smaller section of the girders leading to considerable economy in overall costs.

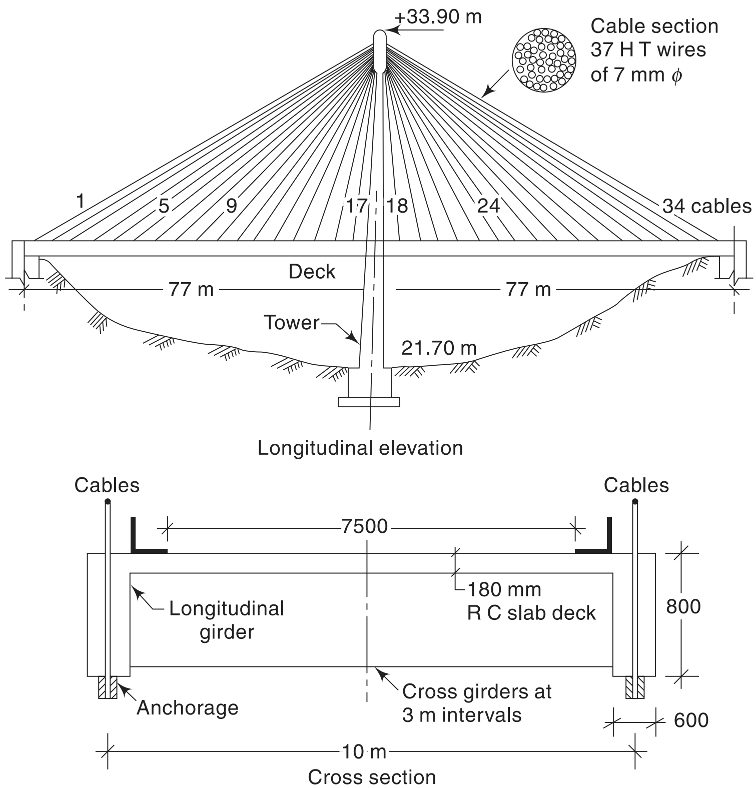

Fig. 23.15 *Akkar bridge at Sikkim*

Detailed economic analysis by Fritz Leonhardt[9] indicates that cable-stayed bridges are structurally efficient and cost effective for low, medium and long spans, varying from 40 to 1800 m. Highway bridges can be built of prestressed concrete with spans up to 700 m and rail road bridges up to a span of 400 m. Figure 23.16 shows the comparison of steel required for suspension and cable-stayed bridges in the span range of 500 to 1800 m. For a bridge of 1800 m main span and 38 m width, a suspension bridge requires 46,000 tonnes of steel whereas a cable-stayed bridge needs only 19,200 tonnes, indicating more than 50 per cent savings in the quantity of steel required in the cable-stayed bridge.

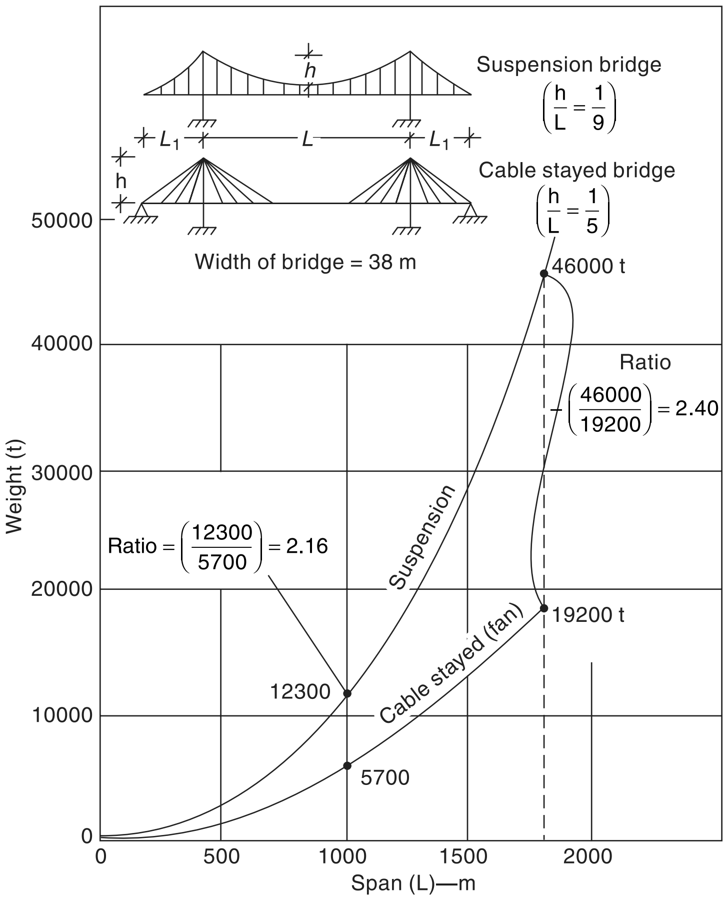

Fig. 23.16 *Comparison of quantity of cable steel for suspension and cable-stayed bridges*

The second Hooghly Bridge (Vidyasagar Sethu) at Kolkota, shown in Fig. 23.17, is an excellent example of a cable-stayed bridge comprising of a main span of 457.2 m and two side spans of 182.8 m each. The deck is made up of a concrete slab 230 mm thick, two outer steel I-girders 28.10 m apart and a central I-girder. The deck is suspended by cable-stays comprising of parallel wire cables of BBR-HIAM type with their own anchorage system. The bridge provides for two three-lane carriage ways 12.3 m each and 2.5 m footpaths. The cable-stayed bridge costing 600 million rupees was found to be cost effective in comparison with other types.

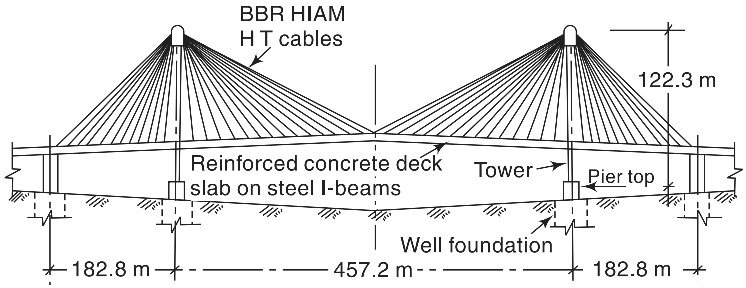

Fig. 23.17 *Vidyasagar Sethu cable-stayed bridge*

A comprehensive list of prominent cable-stayed bridges built in several countries around the world is compiled in Table 23.2. The reader may refer to a separate monograph[10] by the author for more examples of prestressed concrete bridges.

23.7.9 Prestressed Concrete Buildings

Prestressed concrete is ideally suited for office, industrial and commercial buildings where large column free open spaces are required. Precast pretensioned cored slabs having circular or elliptical cavities have been widely used in Russia for floor panels of multistorey buildings. Prestressed concrete grid or coffered floors are found to be comparatively cheaper to cover large areas as floor and roof panels according to the investigations by Dowrick and Narasimhan[10].

Haeusler[11] reported the use of precast prestressed hyperboloid's of revolution to cover large floor areas as early as in 1959 due to its inherent advantage of precasting the structural elements. The reader may refer to Table 18.2 which presents the salient economic features of pretensioned hyperboloid units suitable for spans in the range of 15 to 30 m. Pretensioned hyperboloid units have proved to be the most economical type for covering large spaces due to the least consumption of materials coupled with ease of casting.

Prestressed concrete folded plate roof units outlined in Section 18.4 have been widely used for industrial structures like aircraft hangars, automobile factories mainly due to their low cost per unit area in comparison with the traditional structural forms. Prestressed hollow inverted pyramidal units have been used as a transfer girder system by Nori *et al.*[12] to support the four storey complex housing the administration building for Engineering Construction Corporation Ltd. at Manapakkam in Chennai.

An excellent example of application of precast prestressed units can be seen in the planning, design, construction and economical aspects of an industrial building for the Larsen and Tubro Ltd. factory in Bangalore as reported by Patel *et al.*[13] The factory measuring 60 m by 160 m in plan comprises of 20 m by 20 m column grid with a clear height of 10 m. Except for the substructure and columns, the building is entirely constructed using precast structural components of five different types. Figure 23.18 shows the longitudinal and cross-section through the building.

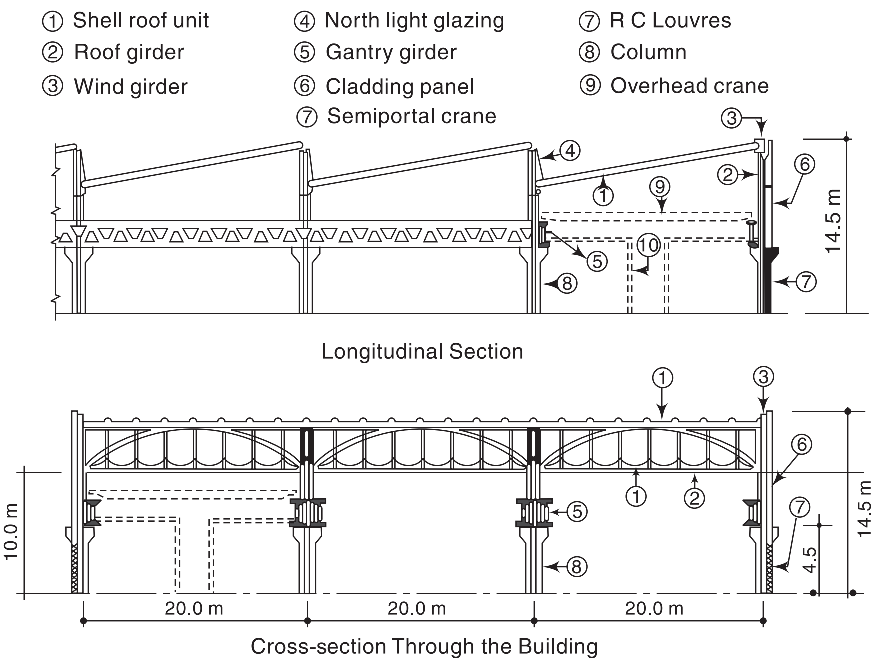

Fig. 23.18 *Longitudinal and cross-section through the building*

The principal roof elements are:

1. Precast prestressed hypar shell units 20 m long by 2.5 m wide.
2. Bow string arched unit with prestressed tie supporting hypar shells over a span of 20 m.
3. Precast prestressed gantry girder resting on cast *in situ* columns.

Figure 23.19 shows the details of precast bow string roof girder. A comparative economic analysis of different types of roof units comprising (a) hypar shells, (b) post-tensioned single tee units, and (c) partially prestressed double tee units, is shown in Table 23.3. Based on the analysis, the hypar shells were found to be the most economical with the least quantity of material consumption per unit plan area and were selected for the roof covering.

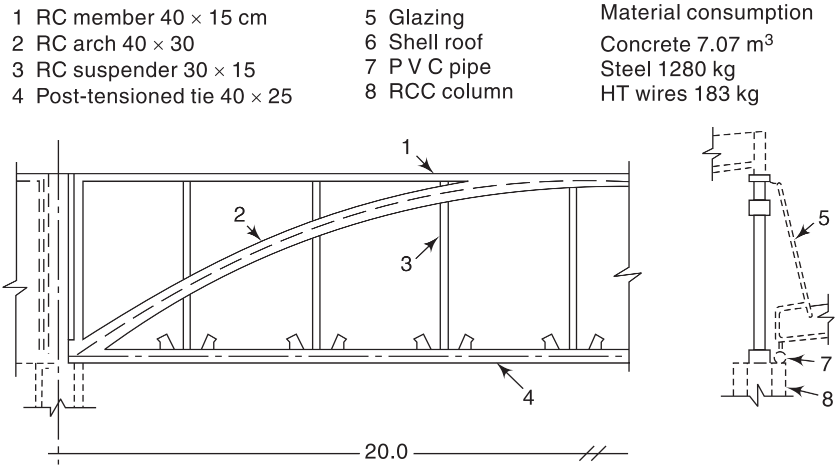

Fig. 23.19 *Precast prestressed bow girder with post-tensioned tie*

Table 23.3 *Quantities of materials required per m² of plan area*

S. No.	*Type of Roof Unit*	*Span* (m)	*Concrete* (m^3)	*Mild Steel* (kg)	*High-tensile Steel Wires* (kg)
1.	Hyper shell unit as executed, including diaphragm and lugs	20	7.56	6.32	3.86
2.	Single-tee (Post-tensioned)	20	12.40	6.00	5.50
3.	Partially prestressed double tee units	16.5	8.10	6.70	4.24

Another notable example of innovative application of prestressed concrete in building can be seen in the construction of 11 storied cast *in situ* structure having eight upper storeys resting on reinforced concrete arched girders with prestressed concrete ties spanning 18 m as shown in Fig. 23.20. This arrangement is ideally suited for large column free space for conference halls, auditoriums, sports stadiums and industrial structures. The reader may refer to the published literature[14] for further information.

23.7.10 Prestressed Concrete Flyovers

Prestressed concrete flyovers are widely used for road crossings in major cities throughout the world. During the last decade, number of flyovers has been constructed in major cities like New Delhi, Mumbai, Kolkota, Chennai, Hyderabad and Bangalore. The basic structural form adopted for the superstructure of recent flyovers constructed in Chennai[15] comprises of continuous spans of precast prestressed concrete I-girders topped by cast *in situ* reinforced concrete deck slab with single columns resting on pile foundations as shown in Fig. 23.21. The present trend is to adopt central single columns to minimise the obstruction to traffic at ground level.

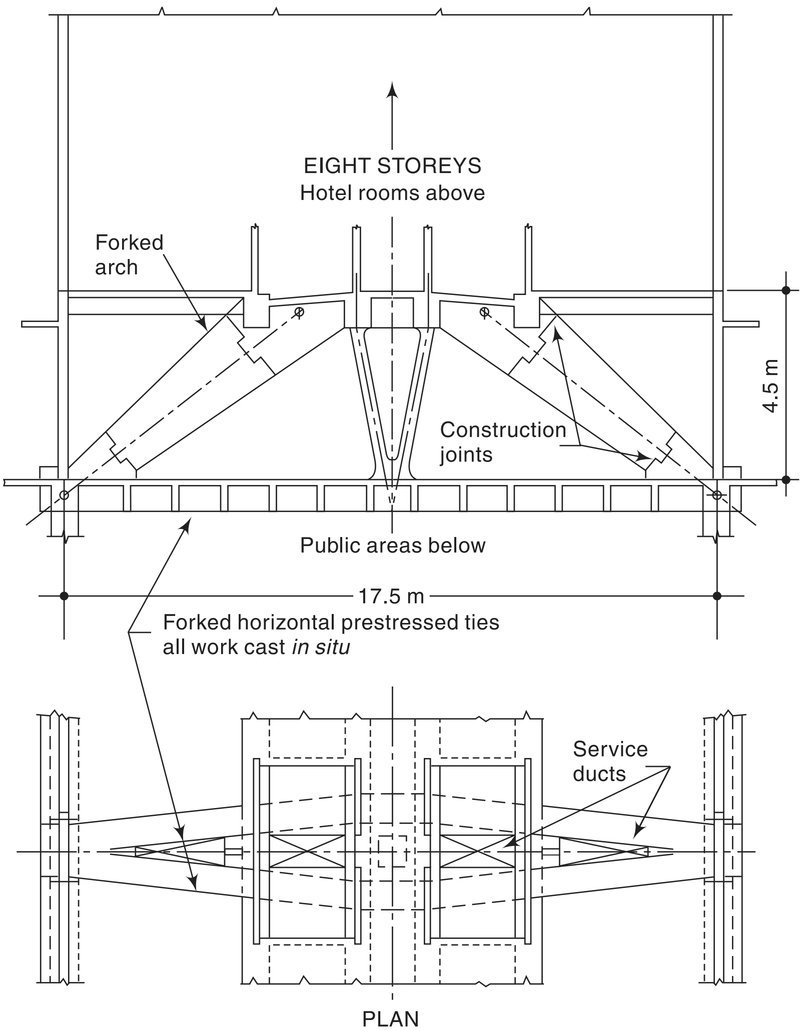

Fig. 23.20 *Prestressed concrete forked horizontal ties supporting eight storeys of an hotel in Chennai*

The cross-sectional details of the Sirsi Circle flyover in Bangalore[16] are shown in Fig. 23.22. The superstructure consists of a precast post-tensioned concrete continuous box girder with curved bottom spanning over eight spans each of about 36 m. The overall depth of the girder over the piers is limited to 2.3 m. The bridge deck is of segmental construction using M-40 grade concrete using precast segments 2.9 m long. The box girder segmental units were precast adopting the long line match casting technique of producing one full span of 12 segments at a time. The segments were erected using a specially developed gantry crane system. At supports, the box girder is supported over two POT-PTFE bearings. The single central pier has circular cross-section of

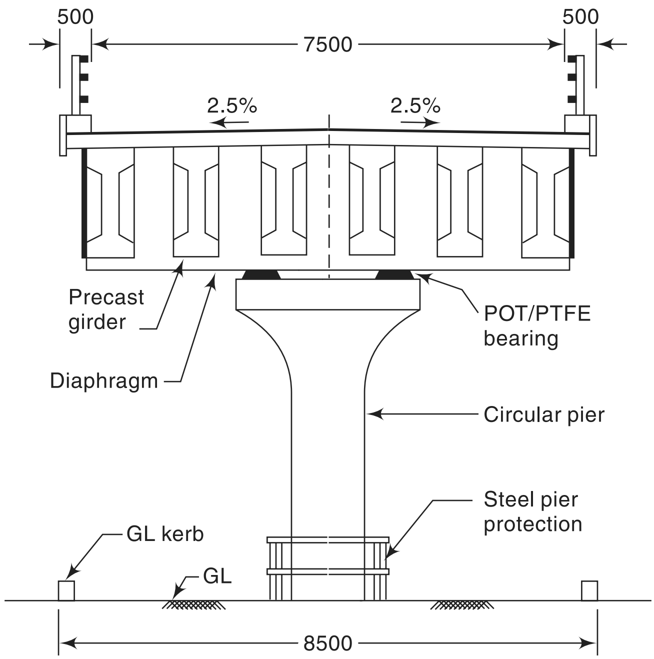

Fig. 23.21 *Prestressed concrete flyover in Chennai*

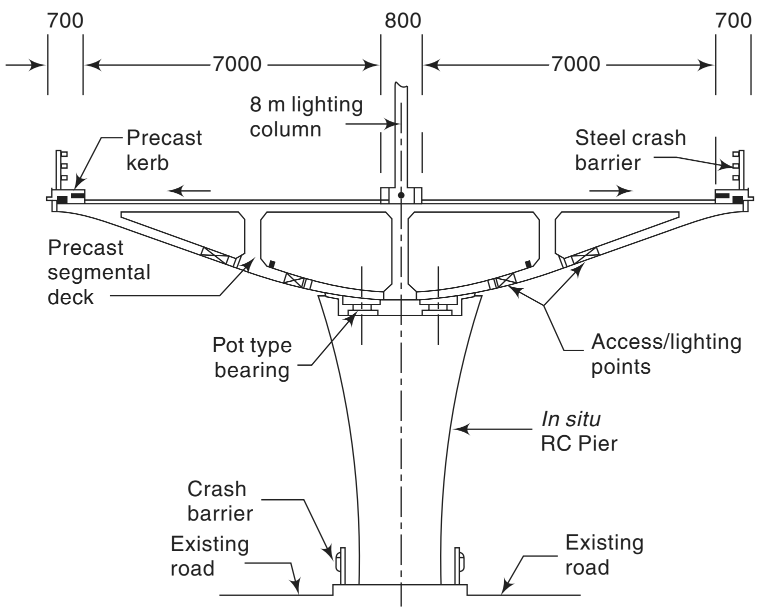

Fig. 23.22 *Prestressed concrete flyover in Bangalore*

2 m diameter at the bottom with an elliptical cross-section at the top. The pier rests on a pile cap connecting four piles of 1000 mm diameter made up of M-30 grade concrete. Bangalore, christened as the information technology capital of India, is witnessing the construction of several types of flyovers to facilitate smooth flow of ever increasing traffic. The reader may refer to Raina[4] for the analysis and design aspects of flyovers.

References

1. Raina, VK, *Concrete Bridge Practice, Analysis, Design and Economics*, Tata McGraw Hill Publishing Co., New Delhi, 1991, pp.viii.
2. Hay, JD, The Construction of Prestressed Concrete Pressure Vessels in Britain, *13th Annual Convention of the Prestressed Concrete Institute, Montreal*, Concrete Society, London, Oct.1967, pp.1–12
3. Tandon, MC, Alimchandani, CR, and Venkataramani, S, “Energy Structures,” Concrete Structures of India, *Compiled by Maharashtra India Chapter of American Concrete Institute’s Fall Convention at New York, 1984*, First Reprint, January 1985, pp.105–118.
4. Raina, VK, *Concrete Bridge Practice, Analysis, Design and Economics*, Tata McGraw Hill Publishing Co. Ltd, New Delhi, 1991, pp.604–607.
5. Bhanutez, N, The Bridges built by GIRISH Bharadwaj that Saves Lives, *The Week Magazine*, March 28, 2004, pp.16–17.
6. Tandon, MC, Alimchandani, CR, and Venkataramani, S, “Achievements in Structural Concrete Perceived through Some Outstanding Structures in Prestressed Concrete,” Concrete Structures of India, *Compiled by Maharashtra India Chapter of American Concrete. Institute’s Fall Convention at New York, 1984*, pp.63–72.
7. Sarkar, S *et al.*, *Hand Book for Prestressed Concrete Bridges,* Structural Engineering Research Centre, Roorke, U.P, 1969, p. 223.
8. Leonhardt F, New Trends in Design and Construction of Long Span Bridges and viaducts (Skew, flat slabs, torsion box), *Preliminary Publication of Eighth Congress of International Association for Bridge and Structural Engineering* (IABSE), New York, 1968.
9. Leonhardt F, and Zellener, W Cablle Stayed Bridges, *IABSE Surveys -13/80, IABSE Periodical*, 2/1980, May, 1980.
10. Krishna Raju, N, *Design of Prestressed Concrete Bridges*, CBS Publishers, New Delhi, Second Edition, 2018.
11. Haeusler, E, Precast Prestressed Hyperboloids of Revolution, *IASS Bulletin* No.6, A-7, Madrid, 1959.
12. Nori, V *et al.*, Prestressed Inverted Pyramids Support Four Storey Office Building, *The Indian Concrete Journal*, Vol. 57, No. 10, October 1983, pp. 253–256.
13. Shirish, B Patel and Vasudev, V NORI, Planning, Design and Construction and Economics of a Precast Industrial Building at Bangalore, *The Indian Concrete Journal*, Vol. 52, No. 11, 1978, pp. 283–292.
14. Recent Prestressed Concrete Construction in India, Report of the Prestressed Concrete Group of the Institution of Engineers (India), *Sixth F.I.P Congress*, Praha, June 1970, pp. 4–10.

15. Raghavan, N and Reddy, RB, Planning and designing Urban Flyovers—Chennai experience, *Proceedings of The Conference on Road Infrastructure Management, Bangalore, 2000*, pp. 330–338.
16. Naidu, MP and Sankaralingam, C, Precast Segmental Construction of Sirsi Flyover–Bangalore, *Souvenir, IRC Diamond Jubilee Session, Highways Department Tamil Nadu, January 2000*, pp. 97–108.

Review Questions

23.1 Briefly outline the economical aspects of prestressed concrete structures with practical examples.

23.2 What are the typical prestressed concrete structural forms generally adopted for high-rise buildings and bridge structures?

23.3 Briefly outline the prestressed concrete structural forms suitable for aircraft hangars, irrigation, waterway and energy structures.

23.4 What are the salient factors to be considered while planning of prestressed concrete structures for different requirements and functions? Outline the basic concepts of planning?

23.5 Explain with sketches and practical examples the application of prestressed concrete in the construction of aircraft hangars, aqueducts, siphons and trusses.

23.6 What are the advantages of using prestressed concrete in nuclear power structures? Enumerate with practical examples.

23.7 What are the advantages of using prestressed concrete in storage structures like silos and water tanks? Explain citing relevant examples.

23.8 Explain the application of prestressed concrete in large domes and long-span bridges citing examples.

23.9 What is the specific advantage of using cable-stayed bridges in preference to suspension bridges to cover large spans?

23.10 Mention the various types of structural forms adopted in the construction of prestressed concrete bridge structures.

Objective-type Questions

23.1 Structural form ideally suited for high-rise offices, residential floors and roofs is
- (a) coffered slab
- (b) tee beam and slab
- (c) composite construction

23.2 Most economical and aesthetic structural form preferred for modern bridge construction suitable for long spans of 500 m is
- (a) balanced cantilever decks
- (b) continuous girder decks
- (c) cable-stayed decks

23.3 For construction of aircraft hangars in coastal areas, the ideal structural form is
(a) steel trussed structure
(b) prestressed concrete folded plates
(c) reinforced concrete barrel shells

23.4 The material ideally suited for the construction of large capacity aqueduct is
(a) reinforced concrete
(b) steel
(c) prestressed concrete

23.5 For roofs of industrial warehouses located in coastal areas, the type of roof generally selected is
(a) steel trusses
(b) prestressed concrete trusses
(c) reinforced concrete shells

23.6 The material ideally suited for containment vessels of nuclear power structures is
(a) steel
(b) reinforced concrete
(c) prestressed concrete

23.7 For storage of chemical fertilisers of large capacity, the ideal type of structure is made up of
(a) steel trusses
(b) reinforced concrete shells
(c) prestressed concrete silos

23.8 The roof of nuclear pressure vessels is generally covered by
(a) reinforced concrete domes
(b) prestressed concrete domes
(c) steel domes

23.9 The most economical type of bridges selected to cover very long span bay structures is
(a) multi-celled box girders
(b) cable-stayed bridges
(c) suspension bridges

23.10 For large span urban flyovers, the most preferred type of prestressed concrete deck is generally
(a) tee beam and slab deck
(b) trussed girders
(c) multi-celled box girders

Answers to Objective-type Questions

23.1 (b)	23.2 (c)	23.3 (b)	23.4 (c)	23.5 (b)
23.6 (c)	23.7 (c)	23.8 (b)	23.9 (b)	23.10 (c)

24 Construction of Prestressed Concrete Structures

24.1 Construction Management

Construction of any structure forms only a small part of the whole gamut of construction management. The modern approach in construction management involves several diverse functionaries like, designers, estimators, constructors, supervisors, accountants, financial managers, corporate secretaries, tax planners working under professional managers.

According to Raina[1], construction management functions comprise of the following central activities:

1. Tendering and winning the contract for a given work
2. Contract negotiations
3. Developing liaison with clients
4. Mobilising financial resources for the work
5. Maintaining proper accounts
6. Work planning
7. Work supervision
8. Project progress control and monitoring
9. Maintenance of good labour relations
10. Engineering and completion of work

Critical Path Method (CPM) and Project Evaluation and Review Techniques (PERT) are widely used in the management of project work. With the advent of computers, data processing, preparation of working drawings, work scheduling, materials management, controlling the various activities of the project and updating the various tasks have become more simpler and they can be efficiently handled with less paper work.

24.2 Construction Materials

Before starting the construction of any prestressed concrete structure, it is essential to consider the minimum requirements for material and workmanship which will result in a structure that will perform satisfactorily in various limit states [2]. The design assumptions and contract documents should be based on these construction considerations. High-strength concrete and high-tensile steel are the two basic materials for the construction of prestressed concrete structures. A brief review of the developments in the field of concrete and steel over the last few decades will help the construction engineer to select the materials most suitable for the construction of the structure with strength and durability at minimum cost.

High-strength concrete The production, properties and codal requirements of high-strength concrete have been outlined in great detail in Section 2.1. Phenomenal research developments in the field of concrete have resulted in significant increase in the grade of concrete from M-40 in 1960 to M-120 in 2011.

Although the minimum grade specified in the Indian Standard Code IS: 1343 for post-tensioned concrete is M-30 and for pretensioned concrete is M-40, most of the concretes used in the present-day construction have strengths above M-60 due to superior quality of Indian cements and improvements in workmanship both at site and the precasting yard or factory.

Good quality concrete of desired properties can easily be produced by proper selection of materials and codified methods of design with proper control over water/cement and aggregate/cement ratios, method of mixing and vibrating the wet concrete in the structural formwork followed by appropriate curing over period of time. Recent advances in concrete technology include the development of rheodynamic concrete, high performance concrete, nano concrete and ultra high-strength concrete eminently suitable for use in prestressed concrete structures.

Rheodynamic concrete, generally referred to as Self Compacting Concrete (SCC), is able to flow under its own weight and completely fill the formwork, even in the presence of dense reinforcements without the need for any vibration whilst maintaining homogeneity and resulting in concrete of high early strength and durability. Degussa-MBT Construction Chemicals (India)[3] have developed revolutionary type of admixtures using nano polymers which can be used to bring together functional groups aimed at targeted performances in concrete. Based on nano science, they have developed a range of nano polymers with the following applications:

(a) Zero energy system A system of polymers with longer side chains and shorter main chains to facilitate high early strengths in concrete without steam curing and with specific applications in precast reinforced and prestressed concrete unit manufacturing industry.

(b) Glenium sky A custom made nano polymer facilitating long haul concrete mix stability with development of high early strength coupled with high durability of hardened concrete suitable for prestressed concrete flyovers.

(c) Rheo fit A nano polymer range which meets the wider expectations as aesthetics, economics, durability and performance of manufactured concrete products. The application of nano technology in the production of nano polymers has revolutionised the concrete industry. Self-compacting concrete is commonly used in Europe, Japan, North America, Dubai, Singapore and Taiwan. In India, this technique has gained popularity with some of the major projects such as Delhi Metro Rail Corporation, Nuclear Power Corporation and Indian Space Research Organisation.

The reader may refer to a separate monograph[4] by the author for up-to-date information dealing with different types of concrete and their mix design.

High-tensile steel Prestressing reinforcement should be of high-strength steel wire, high-strength seven-wire strand or high-strength alloy bars. The mechanical properties of various types of high-strength steels are outlined in Section 2.2. The prestressing steel, sheathing and anchorages should be stored at site in such a way as to provide them with adequate corrosion protection. After stressing the steel in the sheath, it should be provided with permanent protection as soon as possible preferably within one week. While providing protection by pressure grouting of cement, care should be taken that the neighbouring cables are penetrated by grout.

The various types of prestressing tendons used in the construction of nuclear containment vessels have been outlined with practical examples in Section 19.4.5. Generally, the prestressing tendons are not grouted in the case of nuclear pressure vessels and protection against corrosion is ensured by filling the ducts with petroleum-based jelly. The unbonded tendons facilitate retensioning operations whenever required and the force in the tendons can be checked at periodical intervals.

24.3 Construction and Expansion Joints

Construction joints should be planned in advance, preferably located at points of minimum shear and should be nearly perpendicular to the principal lines of stress. Keys should be made by embedding water soaked bevelled timbers in soft concrete and should be removed after the concrete has set. When the work is resumed, the surface of the concrete previously placed should be thoroughly cleaned of dirt, scum, laitance, loosely projecting aggregates and other soft materials using stiff wire brushes. Construction joints are generally either vertical or horizontal. In roadway slabs, construction joints shall be formed vertical and in true alignment. Shear keys in construction joints should be constructed as shown in working site plans. In the case of box girder webs, these shear keys are normally shown on the plans to the full width.

An expansion joint implicitly also refers to a contraction joint and hence it is more rational to designate it as a movement joint. These joints become necessary due to the following reasons:

1. Thermal expansion and contraction of the superstructure and in certain cases even the substructure
2. Shrinkage of concrete
3. Creep or inelastic deformation of concrete

4. Elastic shortening under prestress
5. Displacements of the structure under load or any other action.

The design of the joint should allow free translation, deflection and rotation of the structure at the edges without damage or inconvenience to the traffic. The expansion joint should be strong enough to withstand the knocking of the wheels of vehicles passing over the bridge deck. The present trend is to adopt elastomeric (Neoprene) compression seals for expansion joints in bridge decks. The typical detail of an expansion joint using compression seal is shown in Fig. 24.1. These are made of polychloroprene, known as Neoprene. The open cell compression seal is dependent upon its ability to maintain pressure on the joint side walls with varying degree of stress. The reader may refer to the monograph by Raina[1] for detailed descriptions of different types of elastomeric joint seals and their physical properties.

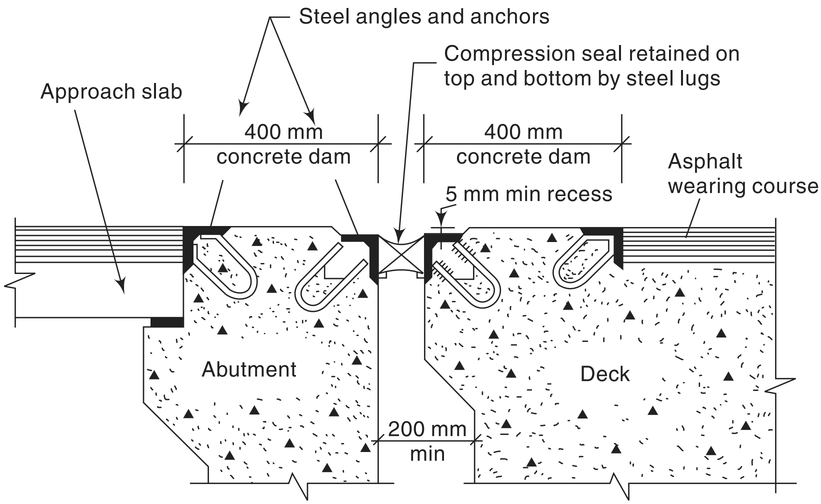

Fig. 24.1 *Typical detail of expansion joint*

24.4 Construction Techniques

24.4.1 General Aspects

Rapid developments in the construction techniques of prestressed concrete structures over the last several decades have resulted in several novel methods of construction keeping in pace with the advances in materials of construction. Prestressed concrete being ideally suited for large spans, is much less used for substructures than for super structures. Although, Freyssinet invented the most exciting building material "*Prestressed Concrete*" in 1928, the big boom in its application came only after the Second World War. Prestressed concrete dominated the bridge construction during the post-war period. Out of the 500 bridges built in war torn Germany during 1949–53, 70 per cent of them were built using prestressed concrete.

Construction techniques rapidly developed in Europe, America, Japan and even in India during 1960–1970, resulting in beam bridges reaching spans up to 160 m. Morandi's bridge across the lake of Maricabo was under construction with spans of 235 m with the help of stay cables. In 1970, the longest span of beams reached 230 m in Japan and for cable-stayed concrete bridges, spans up to 300 m were successfully implemented.

Ulrich Finisterwalder[5] of Germany revolutionised the construction of prestressed concrete bridges by developing the technique of cantilever construction. This novel technique eliminates the use of false work and the double cantilever box beam structure is built from piers without the use of formwork to support the beams on the span. The span range for economical application of box beam bridges built by cantilever construction technique is believed to lie normally in the range of 50 to 200 m. However, Hamana bridge[6] in Japan has pushed this upper limit further with a span of 240 m and Urado bay bridge in Japan has a span of 270 m, constructed using cantilever construction technique.

24.4.2 Cantilever Construction

Most of the long span bridges are built using prestressed concrete and those built by the cantilever method developed by Finisterwalder, demonstrate the latest refinements of this construction technique. This method eliminates the use of expensive formwork and scaffolding especially for bridges in deep valleys and rivers with large depth of water.

Basically, there are two major methods of cantilever construction classified as follows:

1. Cast *in situ* construction
2. Construction using precast segments

Cast in situ Construction In this method, the bridge is cast *in situ* with sections 3 to 6 m long, cantilevering symmetrically on both sides of the pier. The formwork for cast *in situ* construction is supported by steel framework attached to the completed part of the bridge and the formwork moves from one completed section to the next part.

The sequential operations in this method are as follows:

(a) Fabrication of steel truss and shuttering to suit the length of the cantilever beam.
(b) Placing of reinforcement and duct tubes to house the high-tensile cables.
(c) Concreting using the designed strength of concrete mix.
(d) Curing the concrete until it develops the desired compressive strength.
(e) Threading the high-tensile cables in the ducts followed by stressing process using jacks and anchoring and grouting of the cables.
(f) Releasing the formwork and moving on to the next section.

Since the prestress can be applied only after the concrete develops the desired strength (approximately two-thirds the 28-day cube strength) after one week, normal construction time is one section per week, but this time can be reduced by using steam curing. Figure 24.2 shows the cast *in situ* cantilever method of construction used for Boussens Bridge over the Garonne River in France having spans of 49 to 96 m. The supporting formwork to facilitate the concreting of the cantilever portion of the bridge abuts the previously constructed section. The typical cross-section comprises of box girder of constant or variable depth with cables running in the ribs and flanges. A notable example of cast *in situ* cantilever construction of the Bassein Creek Bridge built by Gammon India Company at Bombay is shown in Fig. 24.3.

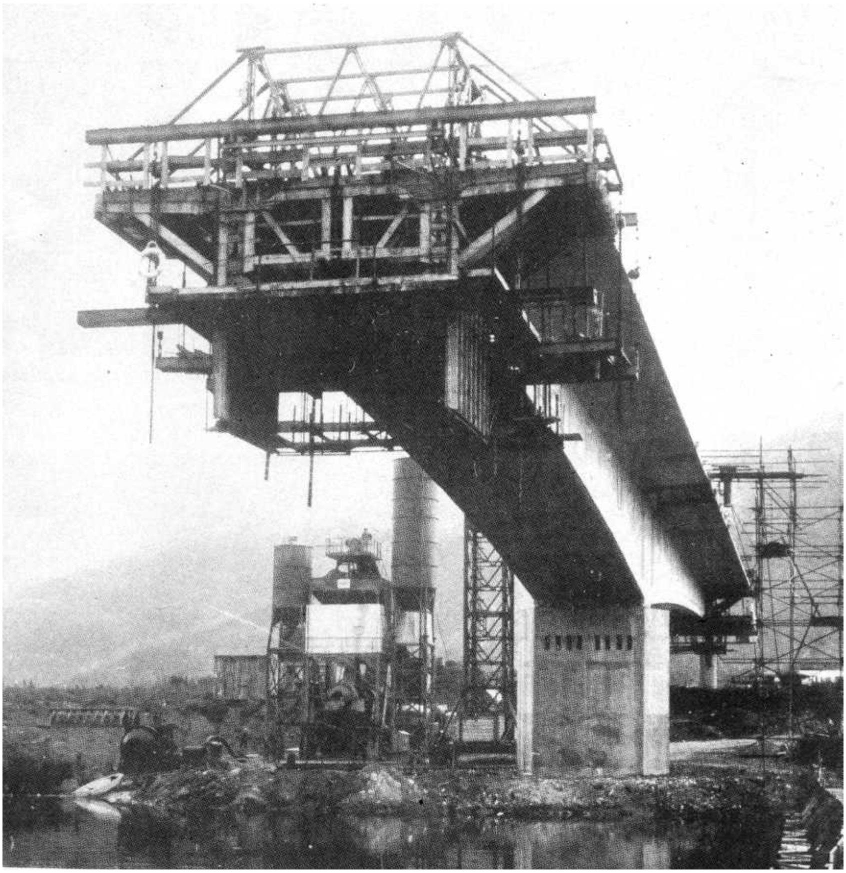

Fig. 24.2 *Cast in situ cantilever construction of Boussens Bridge in France*

Construction Using Precast Segments In this type of construction, the bridge segments comprising of structural elements (mainly segmental single or multicell box girders) are cast in a casting yard using special forms and they are transported to the work site. The precast segments are placed in position by means of a mobile launching girder or when access under the bridge is possible, with barges or trucks by means of a crane or a mobile hoist located at the extremity of the cantilevers.

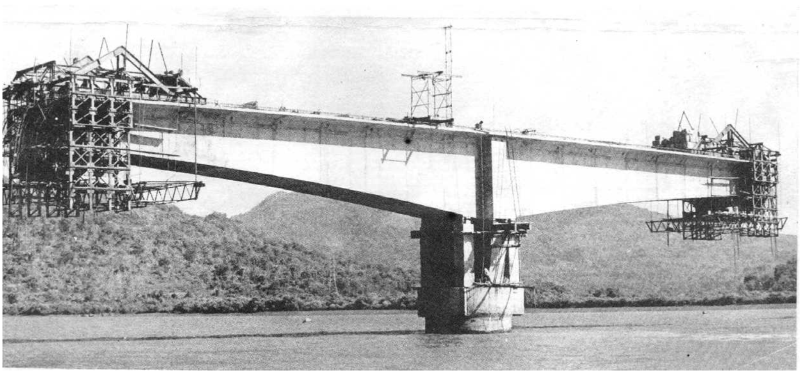

Fig. 24.3 *Cast in situ construction of segmental box sections of Bassein Creek Bridge*

The main advantage of using precast segmental units is that they can be cast on ground near the work site well in advance with better quality of units than those cast *in situ*. In the cast *in situ* method, at least a week's time is required to move the formwork to the next incremental length. In the precast segmental system, the units can be brought to site and lifted by cranes to join them to the previous units by using temporary stressed cables system. The rate of construction will be faster in the precast method than in the cast *in situ* method.

Figure 24.4 shows the bridge between the Oleren Island and the continent in France built by the precast segmental cantilever system of construction.

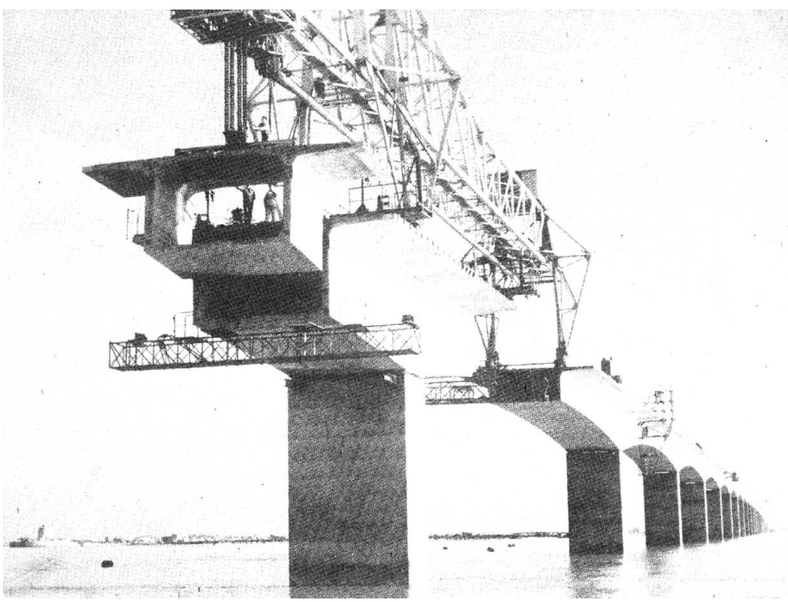

Fig. 24.4 *Precast segmental cantilever construction of bridge between Oleren island and the Continent (France)*

This bridge is made up of 26 main spans of 79 m each built by using single cell precast box girders. The method of casting cellular units in a casting yard is shown in Fig. 24.5. The units are provided with preformed ducts to house the prestressing cables. Figure 24.6 shows the precast multibox cellular units stacked for storage at the casting yard. The transportation of the precast segments by tractor trailer is shown in Fig. 24.7.

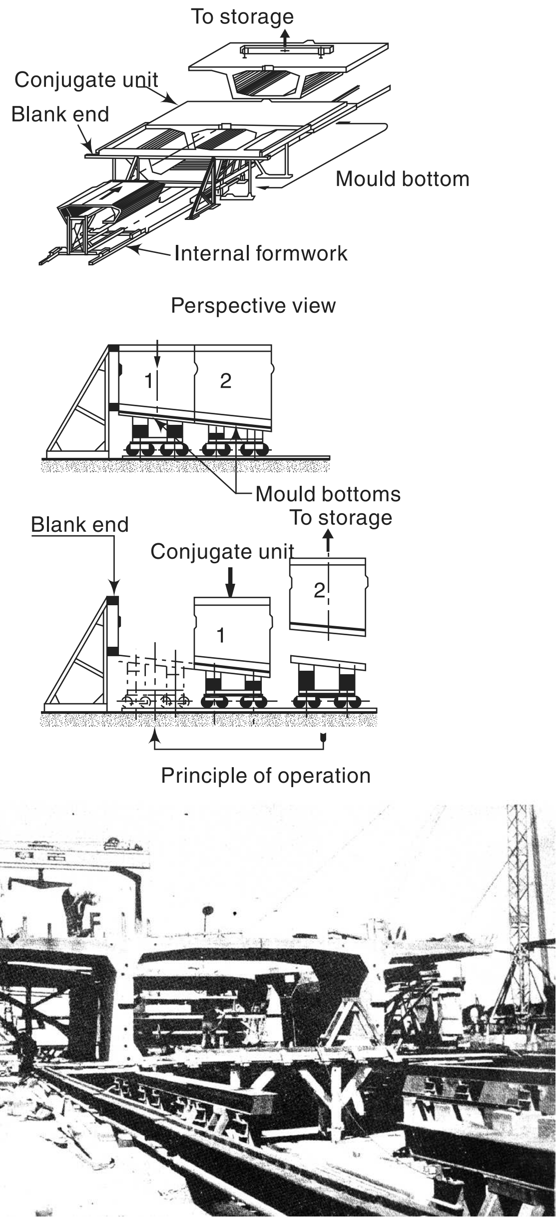

Fig. 24.5 *Precasting scheme of cellular box girders*

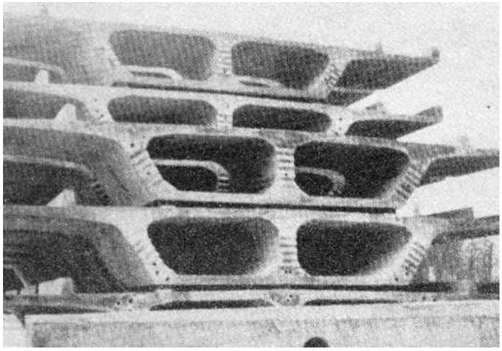

Fig. 24.6 *Storage of precast cellular box units*

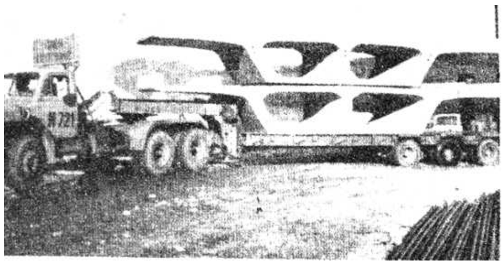

Fig. 24.7 *Transportation of precast cellular box units*

A novel method of positioning the precast single cell box girder segments was used in the construction of Castejon Bridge in Spain. Figure 24.8 shows the transportation of the segment by ropeway and a winch travelling between the steel towers positioned over the piers. In the case of large spans, several launching girders supported on three piers are used to lift the precast elements to the desired location. An excellent example of this type of erection can be seen in Fig. 24.9, where piers are separated by 80 m spans for the bridge between Rio and Niteroi across the Guanabara Bay in Brazil. The schematic diagram shows the precast elements towed to the work site by barges and lifted to join them to the cantilevers on either side of the pier.

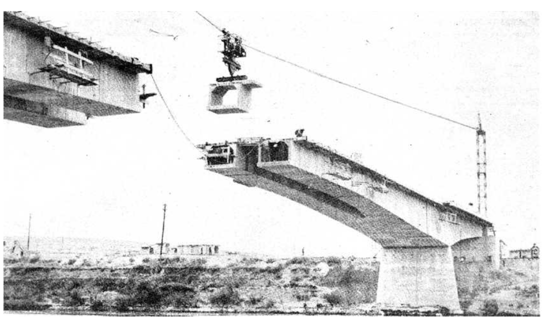

Fig. 24.8 *Erection of precast units using cableway for Castejon Bridge in Spain*

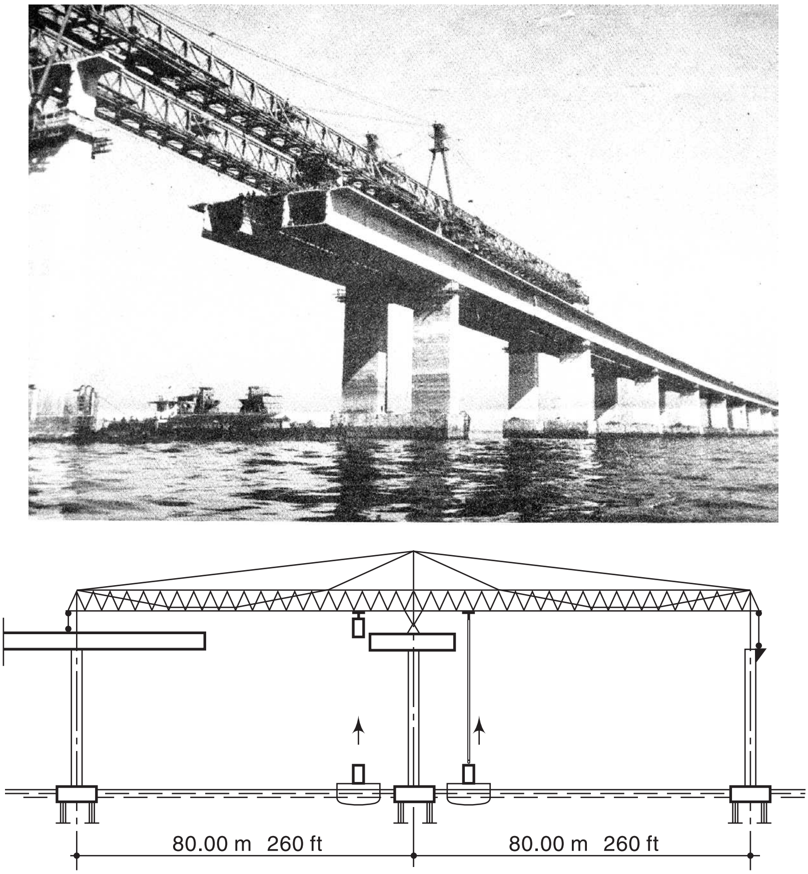

Fig. 24.9 *Canilever construction of bridge between Rio and Niteroi across Gunabara Bay in Brazil*

24.4.3 Choice of Spans and the Method of Construction

The selection of either cast *in situ* or precast segmental construction is governed by the size of the bridge, span lengths, precasting facilities available at site and the equipment available for transportation of heavy precast girders along with suitable cranes and mechanical equipment. The cantilever method has been successfully used in the span range of 50 to 200 m. For small spans of less than 50 m and for elevated roads or flyovers where scaffolding beneath the structure must be avoided, precast segmental construction is preferred. At present for spans over 70 m, prestressed concrete single or multicell box girders compete successfully with steel construction.

According to Raina[6], for average conditions of profile, piers and foundations, the most economical span range is from 70 to 110 m for cantilever construction. In this span range, variable depth girders are often used, whereas constant depth elements are preferred for smaller spans. For very large spans exceeding 110 m, cast *in situ* method of construction is adopted since the precast segments are too heavy and the equipment for transportation and erection is prohibitively costly. Generally, the choice between cast *in situ* and precast segmental construction is influenced mainly by the surface area of the bridge, precasting plant, erection facilities and construction time limitations. Hence, for precast construction, a minimum approximate area of 5000 m^2 is recommended based on experience. Using standardised equipment such as floating or truck cranes and adopting smaller modular segments for short span, precast segmental construction has been used successfully for city flyovers and viaducts.

24.4.4 Prestressing Cables

In cantilever construction technique, the following salient points are important regarding the prestressing system:

1. After erection of each modular section, cables should be threaded into the ducts.
2. Cable forces should be such that cable congestion at the top of the cross-section near the piers is avoided, overcoming the possibility of excess stress concentration near the anchorages.
3. The voids in the duct around the cable must be large enough for proper grouting.
4. The commonly used cables comprise 12 wires of 13 mm strand cable and 12 wires of 8 mm diameter cable (Freyssinet system) and other similar cables of BBRV systems.

24.4.5 Epoxy Bonding of Precast Segmental Box Girders

Precast segments are joined at site using epoxy resins. Pressure should be exerted on the joint by means of post-tensioning the high-tensile cables. The pressure should be as uniform as possible with a minimum of 0.25 N/mm^2 at any point. The thickness of the epoxy joint is normally about 1 to 1.5 mm. Epoxy bonding agents comprising resin and hardener should be mixed until it is of uniform colour using a mechanical mixer operating at not more than 600 rpm.

Epoxy bonding agents should be insensitive to damp conditions during application and after curing. It should exhibit high bonding strength to cured concrete, resistant to water and should exhibit low creep characteristics. It should have a tensile strength greater than that of concrete. The epoxy bonding agent should function as a lubricant during the joining of the precast elements, serve as a filler to accurately match the mating surfaces of the segments being joined and as a durable, watertight bond at the joint.

24.4.6 Innovative Construction Techniques

The reconstruction of highways in Germany after the Second World War necessitated the development of innovative techniques for the construction of long span bridges. Engineers like Dischinger, Finisterwalder, and Birkenmaier[7] pioneered the development and use of cable-stayed bridges. Further, Leonhardt[8] contributed immensely for the innovative construction techniques resulting in wide spread use of cable-stayed bridges throughout the world during the latter half of the 20th century. Podolony and Muller[9] also contributed to the design and construction techniques of prestressed concrete segmental bridges. In the case of prestressed concrete bridges, the method of construction significantly affects the nature of stresses developed in the superstructure and hence suitable precautions have to be taken during the construction procedure. Some of the prominent construction techniques generally used for the construction of prestressed concrete bridges outlined elsewhere[10] are listed as follows:

The Staging Method This method of construction technique is adopted when low clearance is required below the deck and supporting formwork does not interfere with the traffic. This method facilitates rapid construction by maintaining correct geometry of the structure with relatively low cost. This method has been used in the construction of the Rhine river bridge at Maxau, Japan.

In long viaduct structures, a segmental span by span (stage by stage) construction is advantageous. The moveable formwork may be supported from the ground. The traveller consists of a steel super structure which is moved from the completed portion of the structure to the next span to facilitate the casting or supporting of the precast units. A typical span by span assembly of precast segments using the staging method is shown in Fig. 24.10.

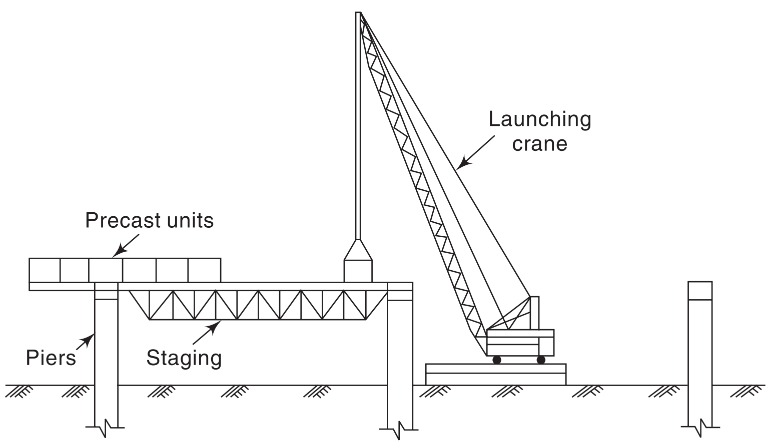

Fig. 24.10 *Staging method of span by span assembly of precast segments*

Incremental Launching or Push out Technique This technique was first developed by Dr. Fritz Leonhardt and Willi Baur and implemented on the Rio Caroni bridge in Venezuela built in 1962. Segments of the bridge superstructure are cast at site in lengths of 10 to 30 m in stationary forms located behind the abutments. Each unit is cast directly against the previous unit. After the concrete attains the desired strength, the new unit is joined to the previous unit by post-tensioning. The assembly of units is pushed forward in a step-wise manner to permit casting of the succeeding segments. Figure 24.11 shows the incremental launching sequence of the push out technique in building the bridge.

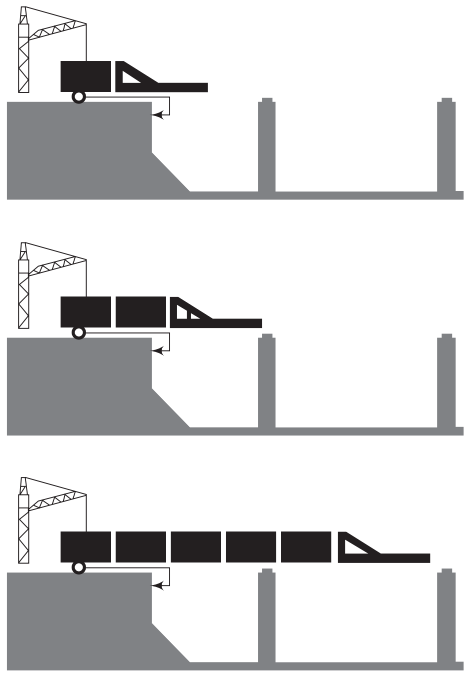

Fig. 24.11 *Incremental launching technique*

Normally, a work cycle of one week is required for casting and launching the segment. To allow the superstructure to move forward, special low friction sliding bearings are provided at the top of various piers with proper lateral guides. The main problem is to ensure the safety of stresses in the superstructure under its own self-weight during all stages of launching at various critical sections. According to Raina[1], this construction technique has been applied to the spans up to 60 m without the use of temporary false-work bents. Also, spans up to 100 m have been built using temporary supporting bents. The main girders must have a constant depth generally varying from 1/12 to 1/16th of the longest span.

Progressive Placement Construction Method In this method, the construction starts at one end of the structure and proceeds continuously to the other end. In contrast to the balanced cantilevered construction in which the superstructure proceeds on both sides of the pier, in the progressive placement technique, the precast segments are placed from one end of the structure to the other in successive cantilevers on the same side of the various piers. At present, this method has been found to be practicable and economical in the span range of 30 to 90 m.

The main feature of this method comprises a moveable temporary stay arrangement to limit the cantilever stresses during construction to a reasonable level. The precast segmental units are transported over the completed portion of the deck to the tip of the cantilever span under construction, where they are positioned by a swivel crane that moves over the deck. The segments are held in position by temporary stay cables passing through a tower located over the preceding pier. This construction method has been used for the Linn cove viaduct in North Carolina, USA.

Cantilever Construction Method The cantilever method of erection is the latest and the most economical and popular method for the construction of long span precast or cast *in situ* segmental bridges. This method is also ideally suited for the construction of cable-stayed bridge decks. The erection proceeds from either side of the pylon or tower in the form of two free cantilevers which balance each other. The units may also be supported by the stay cables depending upon their spacing and size of precast segmental units. The main advantage of the cantilever technique of construction is that the traffic below the bridge is not hindered during erection.

The newly planned Second Vivekananda tollway bridge just north of Kolkota is an excellent example of an extradosed bridge, a hybrid structure combining elements of cable-stayed post-tensioned prestressed concrete box girders. The nine span extradosed bridge stretching across Hooghly river in India is Asia's first multispan extradosed bridge and one of only three extradosed bridges in Asia outside Japan, according to Egemen Ayna, principal engineer of the International Bridge Technologies (IBT) who is the design consultant for the bridge project.

The bridge with a total length of 880 m comprises of seven spans of 110 m and two of 55 m length. The bridge deck comprising of post-tensioned prestressed concrete box girders is supported by a single central suspension system instead of two planes of cable stays. Eight cables composed of 63 to 73 strands each of 15 mm diameter extend from both sides of the 2 m wide pylons as shown in Fig. 24.12. The pylons of height 14 m are supported on Caisson foundations having a diameter of 11 m and sunk to a depth of 45 m below the river bed. The concrete wall thickness of the Caisson is 2 m.

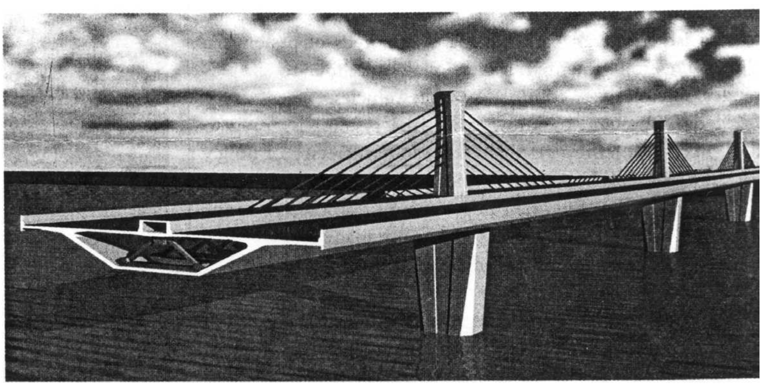

Fig. 24.12 *Second Vivekananda extradosed PSC bridge across Hooghly river near Kolkata*

According to Ayna[11], a typical box girder bridge would have had a depth of 6 m. However, the Second Vivekananda Bridge lowers that profile by approximately 2.5 m. Also, the bridge with a constant depth profile is a departure from the variable depth seen in other extradosed bridges. At present, the bridge project is under construction by the well-known construction company, M/s. Larsen and Toubro Ltd.

During the last decade, construction techniques developed have shown major progress towards simplification and reduction of erection equipment. The construction procedure must, however, be well planned using sequential computations for the alignment, forces, exact lengths and angles considering temperature and creep influences which depend on seasonal, climatic and daily environmental conditions. The collective experience and knowledge gained through research and practise during the last fifty years will help in evolving innovative applications and methods in the construction of prestressed concrete structures.

References

1. Raina, VK, *Concrete Bridge Practice, Construction, Maintenance and Rehabilitation*, Tata McGraw-Hill Publishing Co. Ltd, New Delhi, 1988, pp. 381–396
2. Krishna Raju, N, Limit State Design of Prestressed Concrete Members, Engineering Design, Special Issue on Prestressed Concrete, *Journal of National Design and research Forum*, Institution of Engineers (India), April 1979, pp.16–21.
3. Degussa Construction Chemicals (India) Pvt Ltd, Product Promotional Pamphlet-C-68, MIDC, Thane, Belapur Road, Yurbhe, Nava Mumbai, July 2006.
4. Krishna Raju, N, Design of Concrete Mixes (Fifth Edition), C.B.S. Publishers and Distributors, New Delhi, 2012.
5. Finisterwalder U, Modern Designs for Prestressed Concrete Bridges, *Concrete and Constructional Engineering.*
6. Raina, VK, *Concrete Bridge Practice, Analysis, Design and Economics*, Tata McGraw-Hill Publishing Co, Ltd., New Delhi, 1991.
7. Birkenmaier, M, Recent Developments and Trends in Design and Construction of Cable Stayed Bridges, *Proceedings of the 9th Congress, FIP*, Stockholm, June, 1982.
8. Fritz Leonhardt, "Cable Stayed Bridges with Prestressed Concrete", *Prestressed Concrete Institute Journal*, September/October-1987 (Special report), pp. 52–79.
9. PodolonyW, Jr and Muller, J, *Construction and Design of Prestressed Concrete Segmental bridges*, John Wiley and Sons, New York, 1982.
10. Krishna Raju, N, *Design of Bridges* (Fourth Edition), Oxford and IBH Publishers, New Delhi, 2009, pp. 530–540.
11. Jessica Binns, Extradosed Bridge Distinguishes Tollway Project in India, *Civil Engineering*, Vol. 75, No. 2, February 2005, p. 20.

Review Questions

24.1 What are the prominent activities involved in construction management?

24.2 What are the controlling factors in the production of high-strength concrete mixes required for prestressed concrete?

24.3 Explain the importance of batching and mixing of various ingredients in the production of high-strength concrete.

24.4 What precautions would you take while placing concrete in the forms?

24.5 Explain the techniques of compacting concrete by vibrators to achieve concrete of uniform density.

24.6 What are construction and expansion joints? Explain with sketches their locations and function.

24.7 What precautions would you take in assembling high-tensile wires, strands and cables with special reference to sheathing and anchorages.

24.8 Explain briefly the following two methods of cantilever construction:
(a) Cast *in situ* construction
(b) Construction with precast segments

24.9 Enumerate the various factors to be considered in the choice of spans and the method of construction of prestressed concrete bridges.

24.10 Explain with practical examples the following innovative construction techniques of prestressed concrete bridges:
(a) The staging method
(b) Incremental launching or push out technique
(c) Progressive placement construction method

Objective-type Questions

24.1 Modern construction management functions can be planned effectively by
(a) work planning and supervision
(b) maintaining good labour relations
(c) CPM and PERT techniques

24.2 Durability of concrete is ensured by using the minimum cement content of
(a) 400–450 kg/m^3 (b) 200–250 kg/m^3 (c) 300–360 kg/m^3

24.3 Workability of high-strength concrete with low W/C ratio is improved by using
(a) set retarding admixtures
(b) super plasticisers
(c) air entraining admixtures

24.4 In massive structures, fresh concrete is generally placed in horizontal layers of thickness not more than
(a) 100 mm (b) 500 mm (c) 300 mm

24.5 In the case of concreting deep girders, it is preferable that concrete is deposited
(a) first at centre of span and working towards ends

(b) evenly in horizontal layers for the full length
(c) from one end and working towards the other end

24.6 Prestressed concrete members should be compacted by mechanical vibrators having frequencies in the range of
(a) 1500 to 2000 cpm
(b) 2000 to 3000 cpm
(c) 3200 to 3600 cpm

24.7 In the construction of long concrete structures the construction joint should be located at points of
(a) maximum bending moment
(b) maximum shear force
(c) minimum shear force

24.8 For expansion joints in bridge decks, the modern trend is to adopt
(a) steel expansion joints
(b) poured sealants and joint fillers
(c) elastomeric compression seals

24.9 The cantilever method of construction is ideally suited for bridges in the span range of
(a) 20 to 50 m
(b) 50 to 200 m
(c) 500 to 1000 m

24.10 The thickness of epoxy joints used to bind the precast elements in a prestressed concrete bridge using the cantilever construction method is normally in the range of
(a) 0.5 to 1 mm
(b) 2 to 3 mm
(c) 1.0 to 1.5 mm

Answers to Objective-type Questions

24.1 (c)	24.2 (c)	24.3 (b)	24.4 (c)	24.5 (b)
24.6 (c)	24.7 (b)	24.8 (c)	24.9 (b)	24.10 (c)

25 Maintenance and Rehabilitation of Prestressed Concrete Structures

25.1 Introduction

The fundamental objective of maintenance management of prestressed concrete structures is to preserve the structure in such a way that it will function satisfactorily at the various limit states[1,2,3] immediately after construction and also over the period covering the life span of the structure. Good maintenance practise requires periodical surveillance, identification of local damage, deterioration and loss of durability of the structure due to environmental and other load effects. In such cases, local repairs are needed. In prestressed concrete structures, the primary problem encountered is the damage caused to the anchorages and unbonded tendons due to rusting under exposure to humid weather conditions.

The present-day American, British and the Indian Standard Code[4] for prestressed concrete permits the use of type 3 or partially prestressed members in which tensile stresses of limited magnitude are permitted giving rise to local cracks in concrete of width up to 0.2 mm under normal service loads. These cracks may provide access of water under severe exposure conditions to the prestressing tendons resulting in rusting which leads to explosive failure of the structure due to the sudden breaking of the tendons as a result of reduced cross-section.

25.2 General Aspects of Maintenance and Rehabilitation

The overall objective of the maintenance of prestressed concrete structures is to identify the need for structural integrity, periodical surveillance, repairs, rehabilitation and replacement depending upon the local conditions. The maintenance management system must also provide guidelines and methodologies to enable local engineers to reach rational, cost-effective decisions regarding maintenance and rehabilitation of distressed structures.

According to Gokhale and Rohra[5], periodical inspections, repairs and rehabilitation constitute the primary aspect of good and effective maintenance. This aspect is assuming more and more importance due to the rapid increase in the number of prestressed concrete structures built during the last few decades of the 20th century as a result of easy availability of good quality cements, steel, epoxy compounds and various other building materials along with innovative methods of construction of complex structures.

It is a well-established fact that the total number of prestressed concrete structures already built is much more in comparison with the structures under construction, but the amount of energy and the resources spent on preventive maintenance and/or rehabilitation of structures is negligible in comparison with that spent on new structures.

Prestressed concrete is widely adopted for the construction of bridges and this category of structures needs periodical supervision, maintenance and rehabilitation. Many of the bridges built in 1950s are likely to show signs of distress. Rehabilitation of structures may be required due to several reasons. Some common causes are constructional deficiency, environmental effects, deficiency in design, overloading of structures, either due to unanticipated loading or due to accidents, and user made changes in the structures during the service life of the structure.

The problem of rehabilitation of each structure is unique for the particular structure. Hence, the use of common techniques for rehabilitation of various structures is limited.

As far as maintenance is concerned, several new cementatious materials and epoxy resins and compounds have been developed during the last decades which are highly effective in protecting the basic structure from the destructive effects of severe exposure conditions in the environment. It is important that maintenance and rehabilitation engineers must study the basic designs, history of construction, changes in loading on the structure, environmental changes, etc. After careful analysis of all these factors, the engineer will be able to work out a strategy for a long lasting rehabilitation measure for the distressed structure.

25.3 Maintenance Methodology

Maintaining prestressed concrete structures of various types in a fit and serviceable condition is the primary function of a maintenance engineer. Investment towards effective periodical maintenance forms only a fraction of the cost to be incurred due to major repairs to rehabilitate the structure. Hence, it is always advisable to establish a programmed preventive maintenance system to detect any signs of distress in the initial stages itself through inspection procedures and appropriate repairs.

During the last two decades, structural engineers and builders of major structures have recognised the importance of proper maintenance as a prerequisite to ensure safety and serviceability of the structure during its lifetime. Recent developments in the field of instrumentation have resulted in various types of instruments which could monitor the strength of *in situ* concrete, cracking in concrete, and rusting in reinforcements. Also, methods have been codified to evaluate the *in situ* strength of slabs to sustain the designed loads by actual loading of the slab panel and monitoring the deflections developed at the soffit of the slab. Structural concrete slab panels and beams exhibiting distress can be repaired by external bonding of steel plates to the soffit by using epoxy adhesives. Hollows, honey combs and cavities in concrete can be repaired by the process of guniting and shotcreting applied pneumatically with impact force.

25.4 Inspection of Structures

All types of remedial and preventive maintenance or minor repair work, including replacement of components, should be planned at periodical intervals without inconveniencing the users of the structure. Original completion reports must be filed and these should form the basis for detailed periodic inspections. The data collected should be scientifically evaluated from time to time to assess the needs for remedial measures. In the case of prestressed concrete bridge structures, three categories of bridge inspection are necessary to collect the performance data of bridges according to Raina[6].

Routine inspection Under this category, general inspections are carried out quickly and frequently by highway maintenance engineers having reasonably practical knowledge of highway structures, though not necessarily experts in design, detailing and constructional aspects or experts in special problems of bridge inspection. This type of inspection is required to identify fairly obvious deficiencies which could lead to accidents or major future repairs or maintenance problems. Such routine inspections should be done at intervals of one or two months.

Detailed inspection This type of inspection can be further divided as general and major, depending upon the frequency and extent of inspection, respectively.

(a) General inspection is normally made annually; it should cover all the structural elements and is mainly a visual inspection supplemented by standard instrumental aids, invariably followed by a written report.

(b) Major inspection is generally more intensive involving detailed examination of all structural elements, even requiring setting up of special access facilities (like soffits of long span beams and articulation locations, bearing, etc.) where required. Depending upon the importance of the structure, this type of inspection is spaced between two and three years or may be at smaller intervals for sensitive structures which are exposed to aggressive environments (e.g., structures in coastal zones, marine structures, nuclear power structures, etc.).

Special inspection Special inspections are resorted to under extraordinary situations such as earthquakes, high intensity/abnormal loadings, floods, etc. These inspections should be exhaustive including structural testing (e.g., using instruments like ultrasonic pulse velocity apparatus to detect microcracks and excessive deflections using dial gauges, etc.) and computations using structural analysis. For this type of inspection, experienced bridge engineers should be involved in the investigation team.

The timing of this type of inspection should be such that the most critical evaluation of the performance of the structure is obtained. For example, structural elements such as foundations, bridge piers and protective works are inspected before, during and after the floods. Bearings and joints should be inspected during temperature extremes while cracks at the soffits of prestressed concrete girders should be inspected under severe loading conditions. The inspection team should be led by a qualified and experienced bridge engineer who is familiar with the design and constructional features of the structure to be inspected, so that the observations are properly and accurately assessed resulting in a meaningful technical report, containing details of distress/deficiency and recommendations for appropriate repairs of the inspected structure.

25.5 Inspection Instrumentation

Prestressed concrete structures showing visible signs of distress in the form of surface cracks, spalling of concrete should be subjected to special inspection using instruments to assess the extent of damage to the structure. Modern testing equipment which could be of use to the specialised inspection team are listed as follows:

1 Rebound hammer (Schmidt hammer) for *in situ* evaluation of compressive strength or grade of concrete.
2. Ultrasonic pulse velocity apparatus for detection of cracks in concrete.
3. Snooper crawler and adjustable ladders.
4. Magnetic detector for measuring thickness of concrete cover and for locating reinforcement bars.
5. Mechanical extensometer, transparent templates and microscope for reading of crack widths on the surface of the concrete.
6. Hydraulic jacks, pressure transducers or load cells for measurement of forces, etc.
7. Electronic strain gauges for measurement of strains in concrete and steel.
8. Vibration measuring equipment.
9. Electrical resistance meter (for rust pockets).

These instruments are very useful to evaluate the strength of *in situ* concrete and the distress caused due to the development of microcracks in concrete. The author[7] has used these instruments extensively for evaluating the strength of prestressed concrete lattice girders in Ramkumar Mills at Rajajinagar, Bangalore. Rebound hammer has been used by the author[8] for testing the integrity of reinforced concrete beams, columns and slabs at Darus Salam hostel complex located in Bangalore and also for testing the roof slab of explosion bunker[9] at M/s. Astra Indian detonators Ltd., Bangalore.

A wide variety of electronic equipment is presently available in the market of many countries for monitoring and inspection of distress in different types of structures. Ultrasonic meters are used to determine the degree of deterioration, distress and/or material imperfections that are relevant to the structural integrity of the structure to be inspected. Pachometer is used to locate the steel reinforcements and measures the sizes of the bars embedded in concrete to an accuracy of 3 mm.

In the case of bridges greater than 10.7 m in height and in those bridges which cannot be inspected from beneath due to rugged terrain or watery situations, a mechanical contraption widely known as Barin's snooper vehicle is ideally suited for inspection work. The snooper is mounted on a heavy duty truck with a swivelling platform and the underside of the bridge deck can be inspected by using the hydraulically operated platform. Typical schematic diagram of a snooper system is shown in Fig. 25.1. Setting up of the snooper system truck on the road is shown in Fig. 25.2 and this will help to examine the distress developed in the soffit of the deck slab, main girder and cross girders.

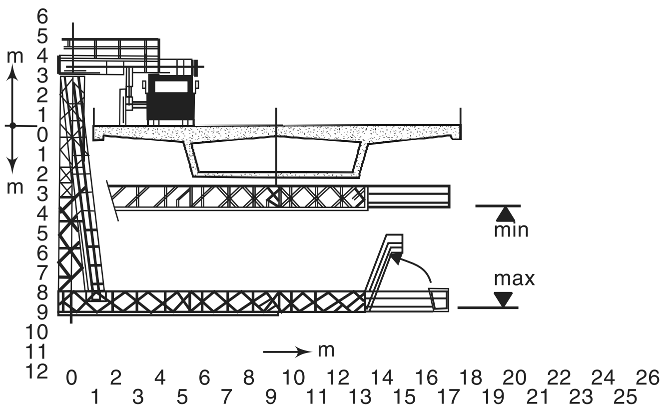

Fig. 25.1 *Barin's snooper system for inspection of bridges*

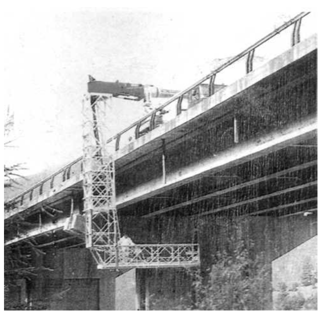

Fig. 25.2 *Snooper platform to inspect the soffit of bridge beck*

25.6 Cracks in Prestressed Concrete Members Remedy and Repairs

In prestressed concrete members, cracks may develop due to a variety of reasons. Concrete can crack in its plastic phase, when it is still not set, due to plastic shrinkage and settlement. Concrete during its hardening phase (during the first three to four weeks after setting) is likely to develop cracks due to constraint to early thermal movement and/or drying shrinkage or due to differential settlement of supports. In its hardened state, concrete can crack due to overload, faulty construction, inadequate detailing, sulphate attack on cement concrete, alkali-aggregate reaction and long-term drying shrinkage.

Typical examples of intrinsic cracks in a hypothetical concrete structure, essentially showing their type and location are shown in Fig. 25.3. Table 25.1 compiles the various types of cracks, their common location of occurrence, causes of cracking, time of appearance and remedial measures to be read in conjunction with Fig. 25.3, as reported by Raina[10]. In the case of prestressed concrete I-section girders with thin webs, cracks may develop due to shrinkage, temperature and loads in the web of girders. These can be prevented by suitable detailing of web reinforcement to resist the shear force. Horizontal reinforcements uniformly distributed over the depth of the web prevent the shrinkage cracks while vertical reinforcements resist the diagonal tension cracks. Figure 25.4 shows the typical method of remedial measure used in thin webs of I-girders to resist web shear, temperature and shrinkage cracks.

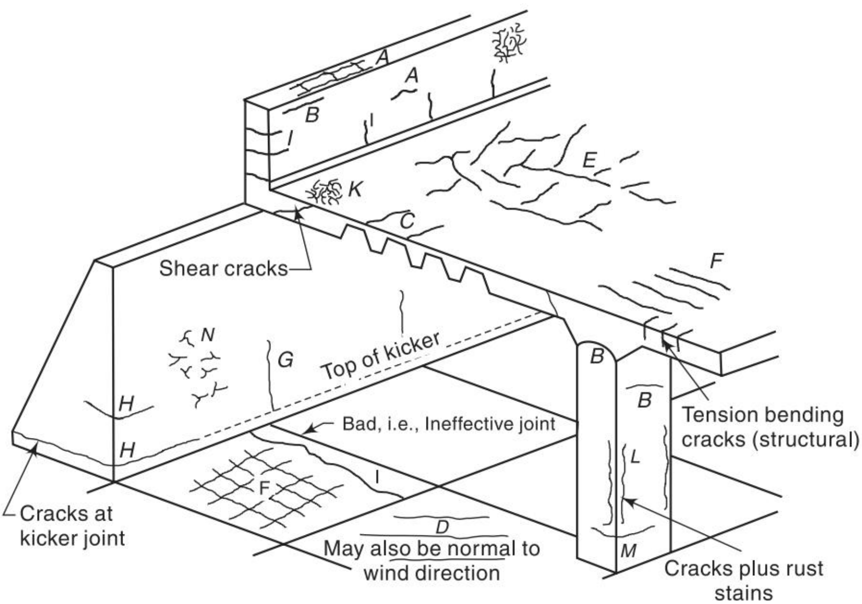

Fig. 25.3 *Typical examples of intrinsic cracks in a hypothetical concrete structure (Refer to Table 25.1 for details of A, B, C, etc.)*

Table 25.1 *Types of cracks in concrete structures, causes, location and remedy (Ref. 10 and Fig. 25.3)*

Types of Intrinsic Cracks (not Caused by Loading)	*Letter Legend (see Fig. 25.3)*	*Sub division*	*Most Common Location of Occurrence*	*Primary Cause (excluding restraint)*	*Secondary Causes/ Factors*	*Remedy Assuming (Basic Redesign is Impossible)*	*Time of Appearance*
Plastic settlement cracks	A	Over the reinforcement	Deep sections	Excess bleeding	Rapid early drying conditions	Reduce bleeding do air entrainment or revibrate mildly	Ten minutes to three hours
	B	arching	Top of columns trough and				
	C	Change of depth	waffle slabs				
Plastic shrinkage cracks	D	Diagonal (may be normal to wind direction)	Roads and slabs Reinforced concrete slabs	Rapid early drying	Low rate of bleeding and fast surface	Improve early curing and	Thirty minutes to six hours
	E	Random	Reinforced	Ditto plus steel near surface			
	F	Over reinforcement (even mesh type)	concrete slabs				
Early thermal contraction cracks	G	External restraint	Thick walls	Excess heat generation	Rapid cooling/ curing by relatively cold water	Reduce heat and/or insulate	One day to two or three weeks
	H	Internal restraint	Thick slabs	Excess temperature gradients			

(*Contd.*)

Table 25.1 *(Contd.)*

Long-term drying shrinkage cracks	I		Thin slabs and walls	Absence of movements joints, or inefficient joint	Excess shrinkage and inefficient curing	Reduce water content and improve curing	Several weeks or months
Crazing cracks (occur only on surface)	J K	Against form work Floated concrete	Fair faced concrete slabs	Impermeable form work over trowelling	Rich mixes poor curing	Improve curing and finishing	One to seven days sometimes much later
Cracks due to corrosion of reinforcement (expansive reaction can lead to spalling of contraction)	L (and rust stains)	Natural and slow, or fast if excessive calcium chloride present	Columns and beams precast concrete	Lack of cover and dampness Excess calcium chloride and dampness	Poor quality concrete	—	More than about two years
Cracks due to alkali-aggregate reaction (expansive reaction)	N	(May show gel type or dried resin type deposit in crack)	(Damp locations)	Reactive silicates and carbonates in aggregates acting on alkali in cement	—	—	More than five years

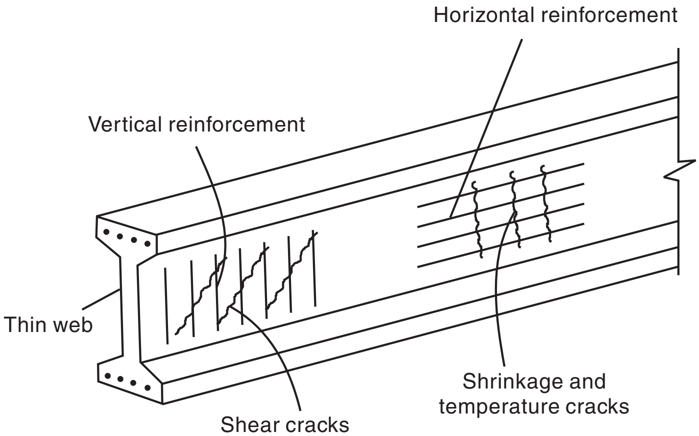

Fig. 25.4 *Detailing of reinforcements for shrinkage and shear cracks in pretensioned T-beams with thin webs*

When there are instances of multiple dormant random cracking in the soffit of deck slab and the side face of longitudinal and cross girders, epoxy resin injection or grouting and sealing techniques may be successfully adopted. In the epoxy injection method, cracks as narrow as 0.05 mm can be sealed. This method has been successfully used in repair of cracks in buildings, bridges, dams and other structures. Figure 25.5(a) shows the epoxy resin sealing of cracks in deck slab and girders while Fig. 25.5(b) shows the epoxy sealing of cracks in the soffit of slab, main beam and diaphragm of a bridge deck.

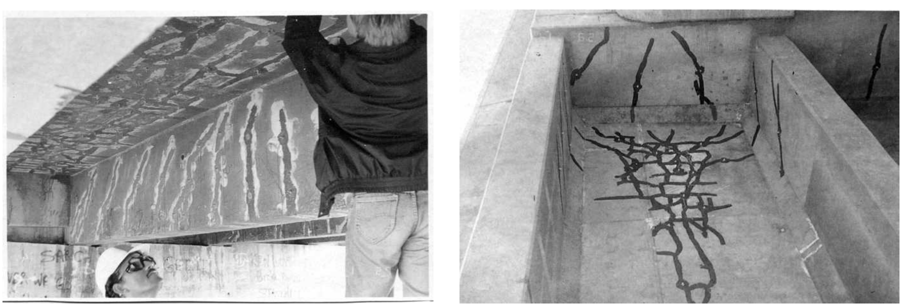

(a) (b)

Fig. 25.5 *Epoxy sealing of cracks in deck slab, main girder and diaphragm in bridge deck*

In the case of dormant cracks wider than about 1 mm, it is more economical to use the grouting and sealing technique. This method involves enlarging the crack along its exposed face (recessing) and then the crack is cleaned and grouted. The surface is then sealed with a suitable joint sealant. Various other techniques widely used for repair of dormant or dead cracks include dry packing, polymer impregnation[11] overlays and surface treatments and autogenous healing.

The type of sealant is selected based on the amount of movement and the limitations imposed by the size of the recess which can be cut together with the type of crack, i.e., either vertical or horizontal. The following three types of sealants are generally used depending upon their suitability in a given situation.

1. Mastics are asphalts with a low melting point with added fillers or fibres. They are recommended where the total movement will not exceed 15 per cent of the width of the groove. The groove should be cut so that it has a depth to width ratio of 2:1. Mastics are the cheapest of the sealants but their use should be restricted to vertical situations or those not exposed to traffic.

2. Thermoplastics comprising asphalts, pitches and coal tar become liquid or semi-viscous when heated. The pouring temperature is usually above 100° C. The groove depth to width ratio should be 1:1 and the total design movement is of the order of 25 per cent of the groove width. These materials soften less than mastics but they may extrude under high ambient temperatures and they may be degraded by ultraviolet light, losing elasticity after a few years of exposure to direct sunlight.

3. Elastomers include a wide range of materials such as polysulphides, epoxy polysulphides, polyurethane, silicones and acrylics. These materials are advantageous since they can be used without heating. They have excellent adhesion to concrete and are not susceptible to softening within the normal range of ambient temperatures. Normally, elastomers exhibit a higher degree of elongation of as much as 100 per cent extension but in practice, this should be limited to 50 per cent (i.e., ±25 per cent). The groove depth to width ratio should be 1:2. The material should be prevented from adhering to the bottom so that the crack remains free as a live crack.

25.7 Repairs and Rehabilitation of Structures

25.7.1 Classification of Damage

The rehabilitation of a distressed prestressed concrete structure involves strengthening of the damaged portion and this process is influenced by the degree of damage suffered by the structure.

Minor Damage Minor damage requires superficial patching by using epoxy grout or guniting using shotcrete. The damaged and delaminated concrete is removed by hand tools and the surface is cleaned before the application of epoxy grout. All cracks should be sealed by the epoxy pressure injection applied from the soffit and rising to the top, along the cracks against gravity.

Moderate Damage Moderate damage involves extensive spalling and cracking of concrete. Epoxy grout or microconcrete is generally applicable as in minor repairs. However, it is recommended that welded wire fabrics be attached to drilled dowels placed at about 500 mm spacing or to the existing reinforcement in the damaged area. If the prestressing strands or reinforcements are exposed, sufficient care must be taken so as not to damage the steel during the cleaning operation. The exposed strands should be coated with epoxy resin bonding compound or slurry cement grout before patching.

Severe Damage Severely damaged prestressed concrete girders require a detailed structural analysis and a design check based on the conditions of the damage and the best engineering assumptions and judgement. A comprehensive review of the calculations and detailed examination of the damage will help in selecting a cost-effective and appropriate-restoration technique for the damaged structure. If the loss of prestress is excessive resulting in tensile cracks, preloading method should be seriously considered in making concrete repairs in order to restore the equivalent full or partial prestress effect, as per original designs. The repair procedure may also include epoxy resin pressure injection, shotcreting and additional welded fabric with drilled anchors and guniting.

25.7.2 Repair and Rehabilitation of Damaged Concrete

Repair and rehabilitation of damaged or spalled concrete is done by removing the unsound or loose concrete by providing temporary supports to the girder to relieve dead load stresses. In the case of prestressed concrete bridge decks, special stress check up is essential before starting the repair works. Figure 25.6 shows the typical details of repairs to the spalled concrete of bridge deck girders. Expansion bolts or grout rebars are drilled into the sound concrete from the soffit and wire mesh is placed to the sides and welded to the existing bars. Gunite or shotcrete is applied as shown in Fig. 25.6.

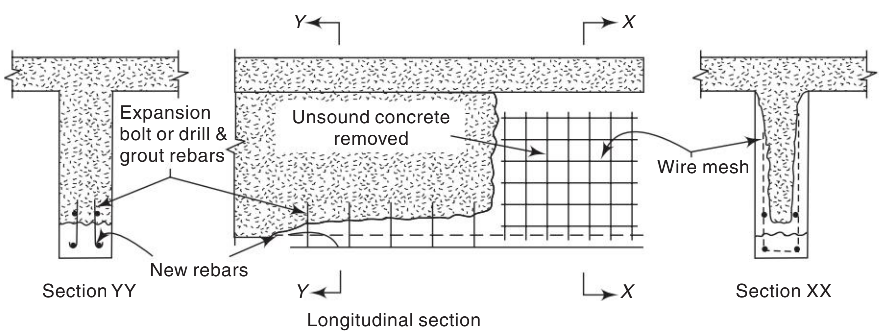

Fig. 25.6 *Repair—Rehabilitation of damaged/spalled concrete*

In many cases of heavily loaded girders, shear distress is observed near the supports in the form of diagonal tension cracks. Shear cracks may arise due to improper detailing or compaction of concrete near the support zone. In such cases, holes are drilled diagonally and rebars are placed and grouted to arrest the shear cracks as shown in Fig. 25.7. Repairs against shear distress can also be done by jacketing stirrups as shown in Fig. 25.8. In this method, the deck slab concrete is carefully removed to permit positive anchoring of additional vertical stirrups placed around the existing beam. After priming the exposed surfaces, epoxy mortaring or shotcreting or guniting is done providing a new concrete jacket over the old girder.

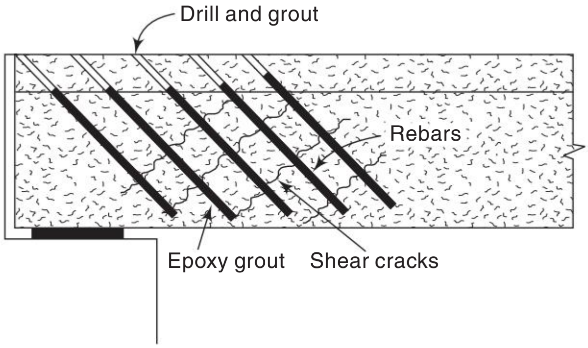

Fig. 25.7 *Repair of shear cracks by stitching rods and epoxy grouting*

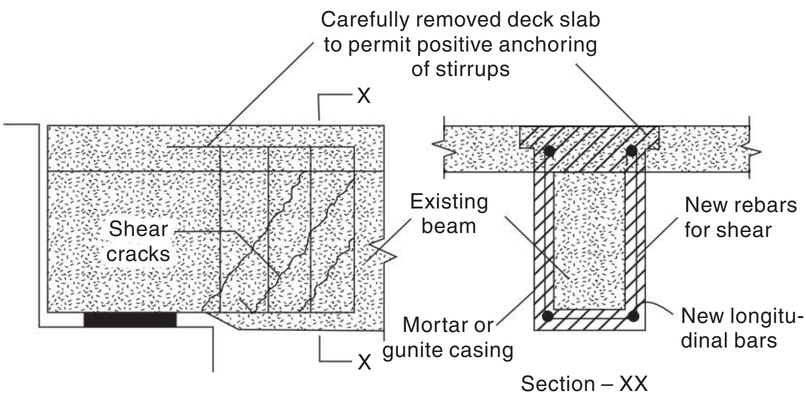

Fig. 25.8 *Repairs against shear distress by jacketing stirrups*

Bridge girders located in zones of very severe exposure conditions are likely to suffer extensive spalling of concrete exposing the reinforcements. In such cases, the unsound or loose concrete around the girder is removed and repairing against the loss of concrete section is done by jacketing the girder using a steel form as shown in Fig. 25.9. The gap between the girder and the steel box is filled by epoxy concrete grout.

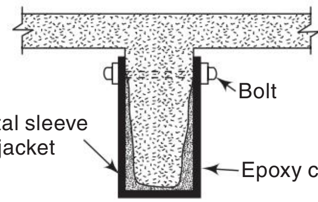

Fig. 25.9 *Repair of girder by metal sleeve jacket*

Crack propagation in the concrete girders can be arrested by using the principle of *post-tensioning*. Figure 25.10 shows this technique in which tensile cracks in the girders are arrested by inducing compression using tension ties fixed to the guide angles which in turn are fixed to the sides of the girder at locations of tensile cracks. The rods or wires are tensioned by tightening the end nuts or by turning of turn buckles in the rods against the anchoring devices. It is necessary to check the stresses to guard against any possible adverse effects.

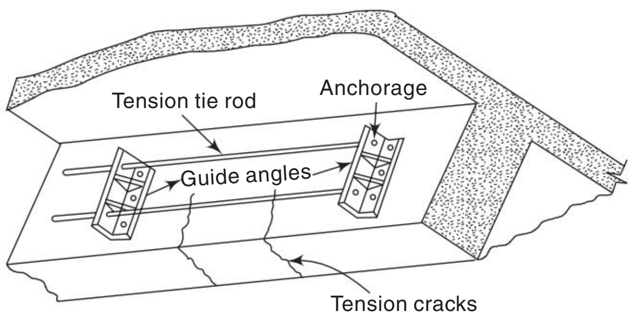

Fig. 25.10 *Crack arrest by post-tensioning principle*

25.8 Repair of Girders Damaged by Collision

Pretensioned prestressed concrete members may get damaged during transportation or due to collision. In such cases, the damaged portion can be repaired and rehabilitated provided the damage is only local and not extensive so as to rule out the use of the structural element.

Figure 25.11 shows the method of repairing the bottom flange of a pretensioned girder partially damaged at the sides so that the high-tensile wires or strands are not exposed. The damaged portion is cleaned and dowel bars are introduced into the drilled holes to a depth of not less than 75 mm and then covered using mortar or nonshrink grout as shown in Fig. 25.11(a). If the damage extends over a larger depth covering the sloping sides, a steel wire mesh is embedded and repaired by applying mortar or non-shrink grout as shown in Fig. 25.11(b).

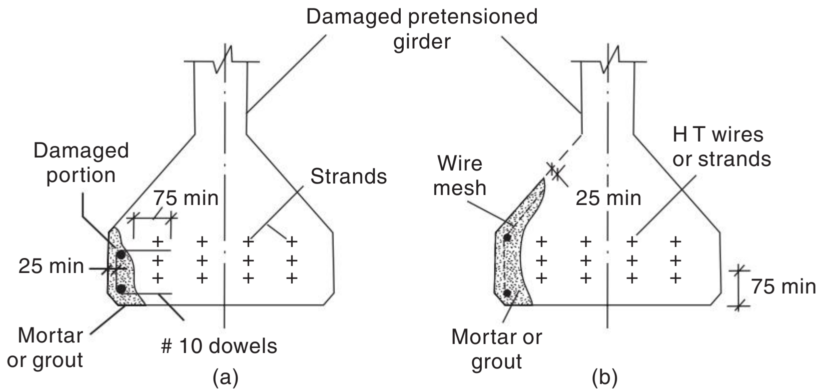

Fig. 25.11 *Repair to pretensioned girders damaged by collision*

In some cases, the damage is more severe and deeper so that the high-tensile wires and strands are exposed. In such cases, the damaged portion is repaired by using links and dowels along with wire mesh tied to the reinforcements. The entire damaged part is repaired using mortar or non-shrink grout as shown in Figs 25.12(a) and (b).

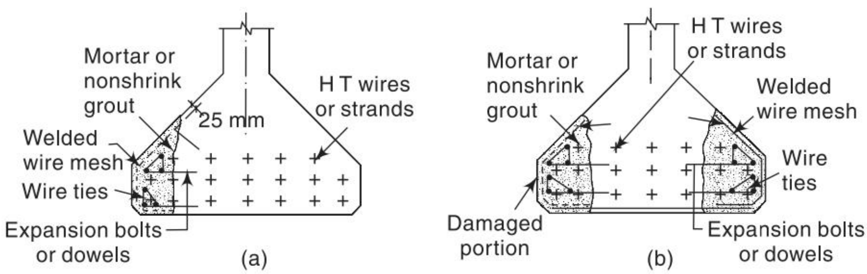

Fig. 25.12 *Repair to damaged pretensioned girders*

25.9 Restoration of Strength of Prestressed Concrete Girders

Due to various reasons such as corrosion of reinforcements due to extreme exposure conditions, especially when unbonded tendons are used, the high-tensile strands may get damaged resulting in loss of prestress in the girder. This type of situation is common for structures located in the coastal zones where humidity and temperature are high. The damaged strands can be effectively spliced or strengthened by external forces[10]. The following strengthening methods can be conveniently used to restore the strength of damaged prestressed concrete girders.

Method-1 In the case of damaged prestressed concrete I-girders, post-tensioning rods (one on either side of the web) in conjunction with jacking (concrete) corbels located outside the damaged areas can be used to restore the strength of the prestressed girder. To start with, the calculated preload is applied and the damaged concrete is repaired. After the repaired concrete has gained the desired strength, the preload is removed. Figure 25.13 shows the method of locating the high-strength rods on the roughened sloping bottom flange of the girder. After constructing the jacking corbels, final post-tensioning of the rods is done as per the design strength requirements. Suitable spiral and link reinforcements should be used in the jacking corbels to strengthen the concrete.

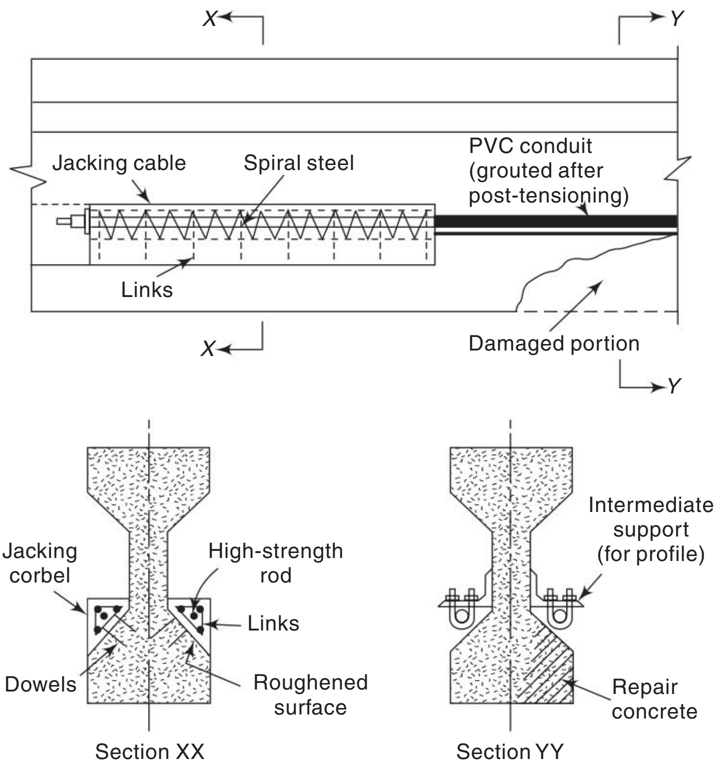

Fig. 25.13 *Restoration of girder by post-tensioning*

Method-2 In this method, the damaged concrete is first repaired by applying the required preload and the concrete corbels are constructed with the required conventional steel reinforcement. Figure 25.14 shows the method of adding external reinforced concrete to restore the strength of the damaged girder. 16 mm-diameter steel dowels are used to anchor the corbels to the bottom flange. In this method, repair and restoration is done by adding external reinforced concrete.

Method-3 In this method, preload is applied prior to the repair of the damaged concrete and removed after the completion of repairs. A metal sleeve jacket is installed (as shown in Fig. 25.15) around and beyond the damaged area (up to a minimum of 1 m). The gap between the metal sleeve and girder is filled with epoxy grout by pressure injection.

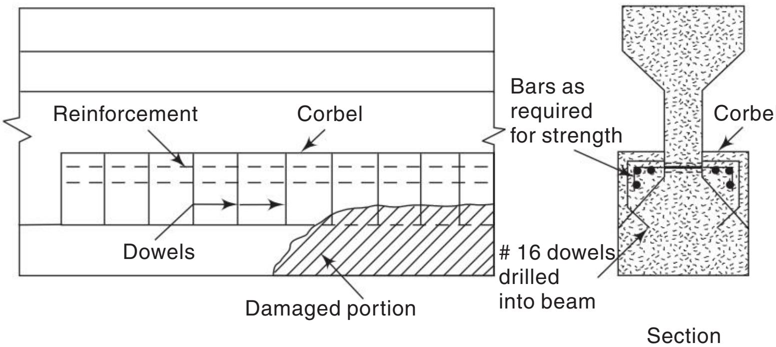

Fig. 25.14 *Restoration by adding external reinforced concrete*

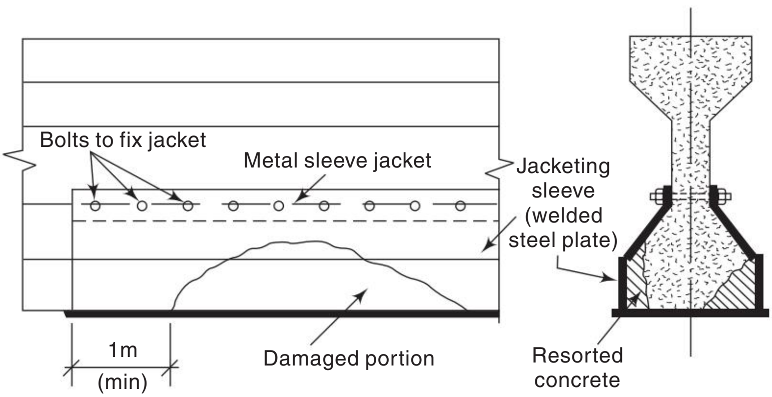

Fig. 25.15 *Restoration by addition of metal sleeve jacket*

25.10 Strengthening Concrete Structures by Externally Bonded Steel Plates

In many cases, it becomes necessary to increase the load bearing capacity of an existing reinforced or prestressed concrete girder due to various reasons. According to Raina[10], two fundamental methods of strengthening/repair are possible with epoxy resin adhesives which are:

1. The depth of the structural element is increased by adding a new layer of concrete on top of an existing cross-section and bonding the old and new elements with modern epoxy resin adhesives.
2. The total reinforcement in the cross-section is increased by epoxy bonding of thin steel plates on the tension face of the beam to increase the flexural and shear strength.

The range of application of this strengthening technique is ideally suited for the following situations:

1. Restoration of structures by rectifying constructional deficiencies that impair the safety of the structure as a result of faulty dimensioning, corrosion of reinforcements, insufficient reinforcements, overloading, etc.
2. Strengthening of an existing structural element by increasing its load bearing capacity.
3. Altering the load supporting structural system by changing spans by shifting or removing of supports, conversion of continuous beam to single span beam and vice versa, etc.

The first reported attempts to strengthen concrete flexural elements by externally bonded steel plates were attempted in France around 1964–65. Practical applications date back to 1966–67 in France and South Africa followed by Japan and Russia. In Switzerland, this method has been extensively used in both buildings and bridges for the last three decades. Experiments conducted at Transport and Road research laboratory in UK by Irwin[12] and MacDonald[13] have conclusively proved the efficacy of strengthening concrete beams by externally bonded steel plates. Experiments conducted by Krishna Raju and Nadgir[14] have shown that reinforced concrete beams, when epoxy bonded with steel plates on the tension face, exhibited significant increase of up to 30 per cent in the ultimate flexural strength in comparison with non-plated beams.

Generally, any grade of structural steel is suitable for bonded reinforcing plates. Plate gauges below 3 mm are not suitable because sand blasting can deform them. Steel plates between 6 and 16 mm thick were used in some strengthening works in Switzerland and England. Pretreatment of the concrete surface is generally carried out by sand blasting, shot blasting, grinding or roughening with pneumatic needle gun or granulating hammer. The grain structure of the concrete must be exposed before the steel plates are fixed. The adhesive joint is generally between 1 and 3 mm thick. Tests have shown that the tensile shear strength of the adhesive is initially proportional to the square root of the thickness. However, the tensile shear strength reaches a maximum and then starts decreasing as the adhesive thickness is further increased. Hence, thinner layers prove stronger and have greater resistance than thicker ones. The method of improving the strength of concrete structural elements by epoxy bonding of steel plates has been successfully used to increase the shear strength of beams.

25.11 Case Studies of Repairs and Rehabilitation of Concrete Structures

Ever since the development and wide spread use of prestressed concrete gained momentum after the Second World War, innumerable number of buildings and bridges have been built in various countries using prestressed concrete for long spans. Many of these structures built during the early period are showing signs of distress after decades of service. Rapid developments in the field of cement technology and chemical adhesives have paved the way for effective repair and rehabilitation of various types of concrete structural elements. A brief survey of the various structures repaired, strengthened and rehabilitated is compiled in the following paragraphs.

Swanley Bridges in UK[15] These highway bridges form part of the M-25 and M-20 motorway intersection. The superstructure is made up of a continuous slab supported on inclined piers. Shortly after the bridge was opened for traffic, cracks were observed on the soffit of deck slab at the end sections. A design review indicated that the reinforcements at the cracked locations were inadequate. Hence, the missing reinforcement was introduced in the form of bonded steel plates 6 mm thick, 250 mm wide and 3 to 6 m long plates bonded in three layers in each strip. Each strip of reinforcement was 12 m long and 15 strips were distributed over the entire width of the bridge. On top of the slab, above the pier, as many as four steel plates were bonded together over a length of 12 m. All together 449 plates were epoxy bonded within a period of 20 days including pretreatment of concrete and plates. Somerard[15] reported in detail the rehabilitation and testing of the repaired structure under dynamic loading.

Gizener Bridge, Muotta Valley, Switzerland[10] The concrete deck slab and girders of this bridge built in the year 1911 and located in Switzerland had to be strengthened to withstand planned future loading. The damaged parts of the bridge deck slab was repaired using epoxy resin mortar. A new cross beam was introduced at the centre of span. 15 mm thick steel plates were bonded to the soffit of the main girders and 10 mm thick plates to the cross girders. The plates were 200 and 150 mm wide, respectively. The efficacy of the repair and rehabilitation was confirmed by load tests conducted by the Federal Material Testing Institute.

Obra Singrauli Bridge No. 93[5] The superstructure of Obra Singrauli Bridge, located on Eastern Railway in India comprises of four numbers of 18.3 m spans and one number of 24.4 m span. Decking is made up of two prestressed concrete girders stressed with Freyssinet system of post-tensioning. After 15 years of service, the prestressed girders developed large number of cracks at the junction of girder and deck slab on both internal and external faces. Also longitudinal cracks were observed in the bottom flange of the girders and vertical cracks at the junction of diaphragms and main girders. Some of the cracks were as large as 3 mm.

Investigations revealed that vertical stirrup reinforcement and the shear connectors at the junction of top flange of the girder and deck slab were insufficient. The bridge being on a railway line was subjected to vibrations. The repeated vibrations in vertical direction might have contributed to the development of longitudinal cracks. Some of the cracks were also attributed to the corrosion of steel. The bridge deck was strengthened by pumping low viscosity epoxy resin to seal the various cracks developed in the deck.

After the sealing of cracks, the longitudinal girders were prestressed vertically at 1.2 m intervals using 12.5 mm strands with anchorages provided at the top of the deck in conjunction with an I-section beam and a steel saddle at the soffit as shown in Fig. 25.16.

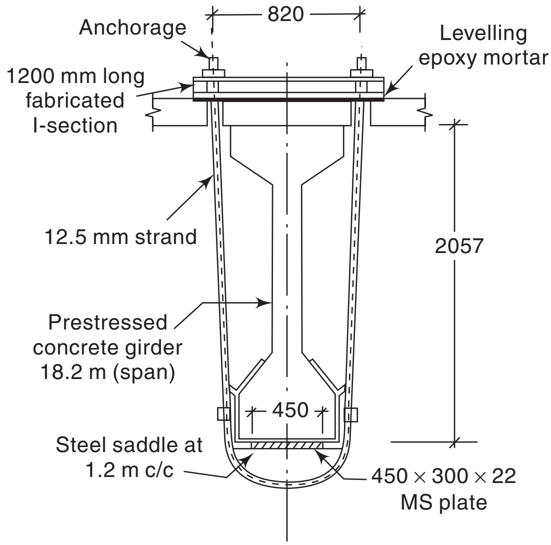

Fig. 25.16 *Restoration of PSC girder (Obra Singrauli bridge No. 93)*

Tests conducted on post-rehabilitated deck showed decreased strains in the central portion of the girders indicating improvement in stiffness of the deck system.

Quinton Bridges in UK[15] The project involving four bridges on the M-5 motorway at the Quinton interchange west of Birmingham comprises of a superstructure with spans of 16.5, 27 and 16.5 m. The deck is made up of voided slabs 90–105 cm thick. Routine inspection indicated cracks in the soffit of end and central sections. Review of design calculations indicated deficient tensile reinforcements at certain locations of the deck slab. The following two rehabilitation methods were examined:

(a) Installation of prestressing elements
(b) External reinforcement with bonded on steel plates

A comparative analysis indicated the bonded reinforcement to be more effective in spite of the fact that the technology was new in the year 1975. Accordingly, the end sections were strengthened with steel plates 6 mm thick. A double layer of 6 mm thick plates was employed at the middle of central span. Along the sides of the central span, where distress was more, three layers of 12 mm thick steel plates measuring about 3 m long and 250 mm wide were fastened to the soffits of the slab with screw plugs spaced at intervals of 450 or 900 mm. The soffit of the deck slab was pretreated to remove the unevenness and shoulders before the steel plates were bonded using epoxy resin. Subsequent tests indicated that the reinforced bridge slabs were flexurally stiffer indicating lesser deflections after the rehabilitation work.

Katepura Bridge, Maharashtra[5] The superstructure of Katepura Bridge in Maharashtra state comprises simply supported prestressed concrete girders with RCC deck slab. The bridge has four spans of 37.8 m. The girders were cast in place over temporary staging and side shifted to position after necessary post-tensioning of the girders. Each girder has 16 cables and the cables were stressed in two stages. During the construction period, when the stage prestressing was being carried out for a girder, it cracked with a sound. The cracks appeared near the end-block as shown in Fig. 25.17. Detailed investigations revealed that the concrete in the end-block portion of the girder was not homogeneous.

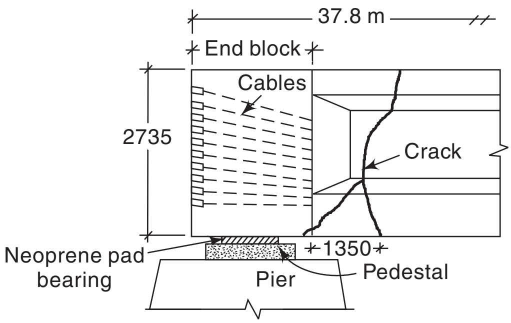

Fig. 25.17 *Restoration of end block of prestressed concrete girder—Katepura bridge (Maharashtra)*

Restoration of the end block of the girder was done by completely dismantling the concrete in the end block after destressing of the cables. New reinforcement was welded with the existing reinforcement of the girder. New concrete with vertical joint was provided with extra care. After the concrete attained the desired strength, prestressing was carried out in stages. The girder was load tested and found to be satisfactory at serviceability limit states.

Chambal Bridge[5] Chambal Bridge is on a state highway connecting Uttar Pradesh and Madhya Pradesh, built across river Chambal near Etawah in Uttar Pradesh. The bridge is 592 m long with a bridge deck comprising single cell reinforced concrete box girder of 11.1 m length projecting on either side of the pier. The suspended span comprises of two prestressed concrete girders with reinforced concrete deck slab of span 40.6 m. Cast steel rocker and roller bearings have been provided at articulations for supporting the suspended span. Soon after the bridge was constructed and opened to traffic in 1975, it developed distress due to improper placing of roller bearings. It was observed that the suspended span between two intermediate piers shifted towards downstream side at roller end by about 20 mm. Subsequently, heavy loads were transported over the bridge by the Department of Atomic Energy. The deviation towards the downstream gradually increased with the passage of time to about 110 mm.

Investigations revealed that the bearings were not at right angles to the axis of the bridge and the level of downstream side bearing was lower by 35 mm as compared to the elevation of upstream bearing. Hence, due to transverse inclination of the bearings towards downstream, the span had a tendency to move in the transverse direction.

The basic scheme of rehabilitation provided an access from the decking to the roller end articulation to inspect and replace the bearings. A steel inspection cum working platform was suspended from the bridge deck near the roller end articulation. Lifting and rotating the suspended span was done by placing a heavy steel truss over hammer head and roller end articulation. The trusses were tied to the hammer head at one end and to the prestressed concrete girder at the other end using steel suspenders. Freyssi flat jacks and PTFE/stainless steel sliding arrangements were introduced under the trusses near articulation on hammer head. The span was lifted by operating the flat jacks. The old roller bearings were replaced with new ones which were properly aligned and levelled with epoxy mortar. The traffic over the bridge was diverted only for three days during the course of the rehabilitation work which was carried out by Uttar Pradesh State Bridge Corporation.

References

1. Rowe, RE, Cranston, WB, and BEST, BC, "New Concepts in the Design of Structural Concrete," *Structural Engineer*, Vol. 43, 1965, pp. 399–403.
2. FIB-CEB *Joint Committee Practical Recommendations for the Design and Construction of Prestressed Concrete Structures*, June 1966.
3. Krishna Raju, N, "Limit State Design for Structural Concrete," *Proceedings of the Institution of Engineers (India)*, Vol. 51, Jan. 1971, pp. 138–143.
4. IS: 1343–2012, *Indian Standard Code of Practice for Prestressed Concrete* (Second Revision) BIS, New Delhi, 2012, pp. 1–54.
5. Gokhale, PS and Rohra, MR, *Restoration of Distressed Concrete Structures—Case Studies, Concrete Structures of India*, Compiled by Maharashtra India Chapter of American Concrete Institute and presented at ACI's Fall Convention at New York, 1984, First Report, Jan. 1985, pp. 149–167.
6. Raina, VK, *Concrete Bridge Practice, Construction, Maintenance and Rehabilitation*, Tata McGraw-Hill Publishing Co., New Delhi, 1988, pp. 287–326.
7. Krishna Raju, N, *Report of Rebound Hammer and Ultrasonic Pulse Velocity Tests on Prestressed Concrete Lattice Girders in Ramkumar Mills*, Rajajinagar, Bangalore, Civil Engineering department, MS Ramaiah Institute of Technology, Bangalore, Oct. 1992, pp. 1–13.

8. Krishna Raju, N, *Technical Report on Rebound (Schmidt) Hammer Tests on RCC beams, Columns and Slabs in Darus Salam Hostel and Office Complex at Site No. 332*, Queens Road, Bangalore, Civil Engineering Department, M.S Ramaiah Institute of Technology, Bangalore, 1986, pp. 1–20.
9. Krishna Raju, N, *Technical Report on Ultra Sonic Pulse Velocity Tests on Roof Slab of Explosion Bunker, M/S Astra Indian detonators Limited*, Bangalore, Civil Engineering department, MS Ramaiah Institute of Technology, Bangalore, 1986, pp. 1–15.
10. Raina, V K, *Concrete Bridges, Inspection, Repair, Strengthening, Testing, Load Capacity Evaluation*, Tata McGraw-Hill Publishing Co, New Delhi, 1994, pp. 10–63.
11. Krishna Raju, N, *Design of Concrete Mixes*, Fourth Edition, CBS Publishers and Distributors, New Delhi, 2002, pp. 210–215.
12. Irwin, CAK, "The Strengthening of Concrete Beams by Bonded Steel Plates, Transport and Research Laboratory," Department of Environment, *Supplementary Report-160 UC*, Crawthorne, Berkshire, UK, 1975.
13. MacDonald, MD, "The Flexural Behaviour of Concrete Beams with Bonded External Reinforcement, Transport and Research Laboratory," Department of Environment, *Supplementary Report-415*, Crowthorne, Berkshire, UK, 1978.
14. Krishna Raju, N and Nadgir, NS, "Limit State Behaviour of Reinforced Concrete Beams Strengthened by Epoxy Bonded Steel Plates," *Indian Concrete Journal*, Vol. 65, No. 3, March 1991, pp. 124–129.
15. Sommerard, T, Swanley's Steel Plate Patch-UP, *New Civil Engineer*, London, 1977, No. 247, 16 June, 1977, pp. 18/19.
16. Irwin, C A K, "The Strengthening of Concrete Beams by Bonded Steel Plates, Transport and Road Research Laboratory," Department of Environment, *Supplementary Report* 160 UC, Crowthorne, Berkshire, UK, 1975.

Review Questions

25.1 Briefly outline the salient aspects of maintenance and rehabilitation of prestressed concrete structures.

25.2 What is the necessity of inspection of structures? Explain the terms (a) routine inspection, (b) detailed inspection, and (c) special inspection with respect to maintenance of prestressed concrete structures.

25.3 What is inspection instrumentation? List the various modern testing equipment used for investigating the damage and distress in prestressed concrete structures.

25.4 Explain different types of cracks developed in prestressed concrete structural elements and their remedial measures.

25.5 Explain the method of sealing cracks using epoxy resins.

25.6 How do you classify the damage and distress in prestressed concrete structural elements?

25.7 Explain with sketches the method of repair and rehabilitation of damaged concrete due to flexure and shear cracks.

25.8 Explain with sketches the method of repairing prestressed concrete girders damaged by collision.

25.9 How do you restore the strength of prestressed concrete girders damaged due to corrosion of high-tensile tendons? Explain the remedial measures adopted with sketches.

25.10 Explain with sketches the method of strengthening prestressed concrete girders by externally bonded steel plates using epoxy resins.

Objective-type Questions

25.1 Proper maintenance of prestressed concrete structures is important to ensure
(a) the strength of structure under designed loads
(b) against excessive deflection
(c) safety and serviceability during its lifetime

25.2 Routine inspection of prestressed concrete bridge structures is normally undertaken at intervals of
(a) 6 to 9 months
(b) 1 to 2 months
(c) 9 to 12 months

25.3 General inspection of prestressed concrete bridge decks involving all structural elements is made at intervals of
(a) one month
(b) one year
(c) two years

25.4 Inspection instrumentation generally used for detection of cracks in concrete is
(a) rebound hammer
(b) magnetic detector
(c) ultrasonic pulse velocity apparatus

25.5 To locate the steel reinforcements and to measure the sizes of steel bars embedded in concrete, the instrument used is
(a) mechnical extensometer
(b) electronic strain gauge
(c) Pachometer

25.6 Shrinkage cracks developed at the soffits of bridge deck slabs is repaired using
(a) guniting
(b) epoxy resins
(c) surface coating with rich mortar

25.7 Repairs of cracks in concrete beams by jacketing stirrups is necessary when there is
(a) flexural distress
(b) bond failure
(c) shear distress

25.8 Prestressed I-girders severely damaged due to corrosion of reinforcements is restored by
   (a) epoxy grouting
   (b) guniting
   (c) using post-tensioning rods with jacking corbels located outside the damaged zone.

25.9 Cracks due to alkali-aggregate reaction are likely to occur in prestressed concrete girders located in
   (a) dry zones
   (b) coastal areas
   (c) hilly areas

25.10 The flexural strength of existing prestressed concrete girders can be strengthened by
   (a) grouting techniques
   (b) external cables
   (c) externally bonded steel plates

Answers to Objective-type Questions

25.1 (c)	25.2 (b)	25.3 (a)	25.4 (c)	25.5 (c)
25.6 (b)	25.7 (c)	25.8 (c)	25.9 (b)	25.10 (c)

26 Prestressed High-Performance Concrete

26.1 Introduction

In recent years, the terminology **High-Performance Concrete** is being increasingly used in the reinforced and prestressed concrete industry in journals and articles. In general, high performance concrete refers to concrete with a characteristic compressive strength in the range of 60 to 120 N/mm^2. At the turn of the 20th century, concrete compressive strength was in the range of 10 to 20 N/mm^2. However by 1960, it was in the range of 25 to 40 N/mm^2. Deterioration, long-term poor performance and inadequate resistance to aggressive environment, coupled with greater demands for more sophisticated architectural form, led to the accelerated research into the microstructure of cements and concretes and more elaborate codes and standards. At present, high performance concrete is invariably preferred for precast and cast *in situ* prestressed concrete structures due to the superior properties of the material in comparison with the traditional and ordinary high-strength concrete.

The American Concrete Institute (ACI)[1,2] defines high performance concrete as concrete meeting special combinations of performance and uniformity requirements that cannot always be achieved routinely when using conventional constituents and normal mixing, placing and curing practises. A commentary to the definition states that a high performance concrete is one in which certain characteristics are developed for a particular application and environment. Examples of characteristics that may be considered critical for an application are grouped as:

1. Ease of placement and easy compaction without segregation and mouldability
2. High early strength, superior characteristic strength and mechanical properties
3. Low permeability and increased density
4. Low heat of hydration and higher toughness, wear and fatigue resistance
5. Volume stability and durability

26.2 Mix Ingredients for High Performance Concrete

In addition to the basic ingredients such as cement, aggregates, admixtures and water, the most commonly used supplementary cementatious materials used for producing high performance concrete are:

Silica fume Silica fume is a waste by-product in the production of silicon and its alloys. It is available in different forms, of which the most commonly used is in the densified form. In developed countries, it is already available blended with cement for ready use. Although it is possible to make high-strength concrete without using silica fume, it is easier to make high-performance, high-strength concrete in the strength range of 60 to 100 N/mm^2 using silica fume.

Fly ash Fly ash has been used extensively in concrete for a number of years. However, the properties of fly ash vary significantly depending upon the source when compared to silica fume. Most fly ashes will result in strengths not exceeding 70 N/mm^2. For higher strengths, silica fume must be used in conjunction with fly ash. For the production of high-strength concrete, fly ash is used at a dosage of about 15 per cent of cement content.

Ground granulated blast furnace slag Slags are generally suitable for producing high-strength concrete at a dosage rate between 15 to 30 per cent of cement content. However, for the production of very high-strength concrete exceeding 100 N/mm^2, it is necessary to use the slag in conjunction with silica fume. Most commonly, the mix design methods are empirical in nature based mostly on several trial mixtures to decide the final mix proportions to suit the specification requirements like strength, durability and long-term performance.

26.3 High Performance Concrete Mix Proportions and Properties

Most of the high performance concrete mix proportioning methods are semi-analytical and usually provide aggregate proportioning and calculation of W/C ratio based on compressive strength followed by trial mixes to finalise the desired mix proportions[3]. Many investigators have used the ACI method as the basis for selecting the basic proportions followed by trial mixtures using silica fume, fly ash and super plasticisers. Based on exhaustive experimental investigations, Sobolev and Soboleva[4] have developed an empirical method of design of high performance concrete mixes. Table 26.1 contains the basic mix proportioning data which is useful for selecting the ingredients required for HPC concrete of desired 28-day compressive strength along with the required cement and silica fume content, super plasticiser dosage, water content and quantities of coarse and fine aggregates required per unit volume of concrete.

Table 26.1 *Design table for high performance concrete mix proportions*

Silica Fume Content (%)	*SF 5*	*SF 10*	*SF 15*	*SF 20*
Concrete Mix Proportions (kg/m^3)				
Cement	426	449	468	478
Silica fume	22	50	83	120
Total binder	448	499	550	598
Super plasticiser	2.2	5.0	8.3	12.0
Water	153	142	132	121
Coarse aggregate	1169	1155	1136	1119
Fine aggregate	630	622	612	603
Concrete Mix Parameters				
Silica fume (%)	5	10	15	20
W/C ratio	0.342	0.284	0.239	0.203
Cement paste volume (m^3)	0.298	0.307	0.318	0.327
[FA/(Total aggregate)]	0.35	0.35	0.35	0.35
Properties of Fresh Concrete				
Slump (mm)	100	100	100	100
Density of concrete (kg/m^3)	2402	2422	2438	2453
Air content (%)	2.5	2.5	2.5	2.5
Properties of Hardened Concrete (Compressive Strength–N/mm^2*)*				
1 day	16.8	24.1	34.4	45.1
3 days	28.6	42.2	63.0	84.9
7 days	50.1	67.2	84.8	102.5
28 days	60.0	80.0	100.0	120.0
Cost of Concrete per m^3				
US (Dollars)	46	54	63	73

26.4 Advantages of Using High Performance Concrete in Prestressed Concrete Structures

After an exhaustive study of the production, properties and uses of high performance concrete, Sai Prasad and Kamalesh Jha[5] summarised the various advantages of using high performance concrete in structural concrete elements as follows:

1. Reduction in sectional dimensions of the structural member with reduction in self-weight.
2. Reduction in formwork and foundation costs.
3. Savings in real estate costs in high-rise constructions located in congested areas.

4. Reduction in the number of supports and the supporting foundations due to longer spans.
5. Higher resistance to freezing and thawing and chemical attack with improved durability.
6. Reduced maintenance and repair costs associated with lower depreciation costs.
7. Reduction in the thickness of floor slabs and supporting beam sections.
8. HPC structures experience low creep and shrinkage and reduced permeability.

26.5 Prestressed High Performance Concrete Structures

High performance concrete is rapidly emerging as the basic structural material of the 21st century for innumerable number of applications such as pavements, high-rise structures, large building complexes, storage structures, towers, trusses, marine structures, aircraft hangars, silos, highway structures, rehabilitation projects, bridge deck overlays, railway bridges, prestressed concrete tanks, pipes piles and sleepers, nuclear power stations, grid floors, folded plate and shell roofs for industrial structures. A brief review of several important applications of high performance concrete reported by a working group of European Concrete Committee/International Federation for Prestressed Concrete (CEB–FIP) and other sources is presented in the following paragraphs.

High-strength–High performance concrete pavements High-performance–High-strength concrete pavements have been used in Norway because of the need to provide increased wear resistance to steel studded tyres as reported by Gjorv *et al*[6]. Highways E-6 and E-18 were paved with high-strength concrete having a thickness of 180 mm with concrete volumes of the order of 22,000 m^3. The concrete used had a characteristic compressive strength of 85 to 90 N/mm^2. The fresh concrete had a slump of 20 to 60 mm. After four years of service, the wearing resistance of the pavements was found to be satisfactory except for some longitudinal cracks which developed close to the joints which was attributed to fatigue.

Typical bridge structures The benefits of using high-strength–high-performance concrete for bridges are well known to bridge engineers. Based on an extensive survey of published literature, Zia[7] *et al.* and other researchers concluded that the use of high-strength–high-performance concrete would enable the standard prestressed concrete girders to span longer distances with slender cross-sections and support heavier live-loads and have better durability under aggressive environmental conditions. In an earlier report of the National Research Council, Zia[8] claims that the use of high-strength–high-performance concrete for bridges has received much wider and earlier acceptance in Europe and Japan than in US and lists several bridges built in those countries in the chronological order from 1968 to 1990 as shown in Table 26.2.

Table 26.2 *Data of prestressed concrete bridges built in Europe, USA and Japan using high-strength–high-performance concrete*

S. No.	*Name of Bridge*	*Location*	*Year*	*Maximum Span* (m)	*Max. Design Concrete Strength* (N/mm^2)
1.	Nitta Highway Bridge	Japan	1968	30	59
2.	Kaminoshima Highway Bridge	Japan	1970	86	59
3.	Second Ayaragigawa Bridge	Japan	1973	50	60
4.	Iwahana Bridge	Japan	1973	45	89
5.	Ootanable Railway Bridge	Japan	1973	24	79
6.	Fukamitsu Highway Bridge	Japan	1974	26	69
7.	Akkagawa Railway Bridge	Japan	1976	46	79
8.	Kylesku Bridge	Scotland	–	79	53
9.	Deutzer bridge+	Germany	1978	185	69
10.	Tower Road Bridge	Washington	1981	49	62
11.	East Huntington Bridge	W.Virginia	1984	274	55
12.	Annacis Bridge	Vancouver	–	–	55
13.	Sylans Viaduct	France	1986	–	60
14.	Re Island Bridge	France	1987	–	60
15.	Braker Lane Bridge	Texas	1987	26	66
16.	Pont du Joigny	France	1988	46	60
17.	Pont du Pertuiset	France	1988	88	110
18.	Arc sur la Rance	France	1989	-	60
19.	Giske Bridge	Norway	1989	52	55
20.	Sandhomoya+	Norway	1989	154	55
	+ Lightweight Concrete				

(a) Bridges in Japan Japan National Railways built three high-strength concrete bridges in 1973 which are of historical importance. Japan National Railways built three high-strength concrete bridges in 1973 which are of historical importance. The high-strength–high-performance concrete was adopted to minimise the dead-loads and deflections under total design service rolling loads of the rail coaches. Additional advantage accrued by using high-strength concrete was significant reduction in maintenance costs and these first generation of high-strength concrete bridges have performed according to all the expectations without any major repairs and disruption of traffic. The second Ayaragigawa bridge was the first high-strength–high-performance concrete bridge built using post-tensioned bulb T-beams. The bridge with a 60^o skew and the design concrete strength of 60 N/mm^2 was chosen to reduce the self-weight of T-girders to less than 150 t for lifting.

Iwahana Railway bridge was the first medium span prestressed concrete trussed bridge in Japan made with high-strength concrete with a compressive strength 89 N/mm^2. The 45 m single span Warren truss bridge was selected to satisfy the clearance beneath the bridge and to reduce deflections. The truss elements were prefabricated and joined at site using concrete in preference to steel to overcome the problem of noise and vibrations and to reduce the maintenance costs under adverse environmental conditions.

The Akkagawa Railway Bridge spanning 305 m was built using prestressed concrete Warren trusses of 45 m maximum span lengths. The compressive strength of concrete at site was 96 N/mm^2. After casting, the members were steam cured at 65^{o}C for 12 hours and then were autoclave cured at 180^{o}C, 10 atmospheres pressure, for an additional period of 20 hours. The different part were assembled into 45 m span units and lifted into position. The joints were cast *in situ* with high-strength concrete.

(b) Bridges in France High-strength self-compacting concrete (flowable concrete) with characteristic compressive strength of 80 N/mm^2 at 28 days was adopted for the construction of Pertuiset cable-stayed bridge over Loire river in France. The concrete was designed to have slump of more than 200 mm to facilitate easy deposition of concrete in the towers. A water/cement ratio of 0.33 with suitable super plasticisers was adopted for casting the deck slab of 180 mm thickness and the pylons supporting the cables at the top.

High performance and High-strength concrete of characteristic strength 97 N/mm^2 was used in the construction of Elom Bridge spanning 400 m. High-strength was achieved for concrete used in this cable-stayed bridge by using silica fume to attain structural efficiency and durability. For the same reason, high-strength concrete of 60 N/mm^2 was chosen for the Normandie bridge, which was also a cable-stayed bridge with a long span of 624 m, constructed during 1990–95.

(c) Bridges in Norway The majority of all concrete highway structures built in Norway since 1989 have followed a general requirement of using a water/binder ratio of less than 0.40 combined with the use of silica fume mainly to improve the chloride resistance due to deicing agents and marine environment. According to a CEB-FIP report of 1994, the annual consumption of such concrete ranged from 150,000 to 200,000 m^3. Sandhomoya Bridge was built in 1989 using Light Weight High-Strength Concrete (LWHSC) of 56 N/mm^2. The three-span cantilever bridge with a central span of 154 m derives its advantage of reduced weight and increased strength due to the use of light weight high-strength concrete.

Strongsundet Bridge built using four 65 m long precast girders in 1990 was post-tensioned. High-strength concrete of 75 N/mm^2 with a water/cement ratio of 0.35 was used. The Stovset Bridge built in 1992–93 is a prestressed concrete cantilever bridge was cast using lightweight high-strength concrete (LWHSC) of 74 N/mm^2. The bridge covering a central span of 220 m had the advantages of reduced self-weight and increased strength due to adoption of LWHSC.

(d) Bridges in Canada Portneuf Bridge constructed in Quebec in 1992, uses precast post-tensioned girders of 24.8 m span. The average concrete strength was 75 N/mm^2 with a water/cement ratio of 0.29 and an air content of 5 to 7.5 per cent. By using high-strength concrete, smaller loss of prestress and consequently larger permissible stresses and smaller cross-section were achieved. The service life of the structure improved with enhanced durability.

(e) Bridges in United States of America The application of high-strength–high-performance concrete in the United Sates was more centred towards high-rise buildings in the early period than in bridges. During the last 30 years, prestressed concrete has been the choice for long-span girder bridges like the Lin Cove Viaduct of 180 m span built in 1976. The Dames Point Bridge of 396 m span and the Sunshine Sky Way Bridge of 365 m span are excellent examples of prestressed concrete cable-stayed bridges built in USA towards the end of 20th century. The trend is clear that more bridges will be built with higher and higher concrete strength and superior properties in the foreseeable future as the industry becomes more familiar with advances in concrete technology.

Standardised pretensioned girders were first used in USA for the construction of the Brake Lane Bridge over I-35 in Austin. Type-C girders, each 26 m long and spaced at 2.6 m were designed for a specified compressive strength of 66 N/mm^2 but the field strength achieved was of the order of 92 N/mm^2 at 28 days and 51 N/mm^2 in 17 hours necessary for the release of high-tensile wires from the pretensioning bed.

The advantages of using high-strength concrete in the construction of highway bridges was investigated by actual testing of the pretensioned tee girder under fatigue or repetitive loads by Roller *et al.*[9] Four full-size 1370 mm deep pretensioned bulb tee girders were cast with 68 N/mm^2 concrete. The girders with a span length of 21.3 m, contained the same number and configuration of longitudinal prestressing strands and same amount of web steel. The girders tested in flexure and shear satisfied the design and specification requirements.

26.6 Typical Examples of High-Performance Concrete Mixes Used in Major Structures

Two Union Square Building, Seattle, Washington (USA) A good example of the use of high-performance and high-strength concrete in the range of 138 N/mm^2 at 56 days is the two Union Square Building located in Seattle, Washington. The high-strength concrete had a modulus of elasticity of 53.8 kN/mm^2. The details of design and actual mix proportions of high-strength– high-performance concretes are compiled in Table 26.3.

The Burj Khalifa, Dubai, UAE (World's Tallest Building) The world's tallest building soaring up to a height of 828 m and designed by Skidmore Owings and Merrill was built using high performance concrete taking advantage of the latest advances in materials technology and construction techniques. The columns and walls of the building were cast tusing concrete with a 28 day characteristic strength of 60 to 80 N/mm^2. The tower raft supported on

194 bored cast in place piles of 1.5 m diameter was cast using self-compacting concrete of M-60 Grade made of cement, fly ash and aggregates with a water/cement ratio of 0.34.

Table 26.3 *Typical mix details of high-performance and high-strength concrete*

Mix Details	*Cement Content* (kg)	*Silica Fume Content* (litres)	*Fine Aggregate* (kg)	*Coarse Aggregate* (kg)	*Water* (kg)	*Super Plasticizer (WR Grace)* *Dartard-40* (kg)	*Mighty-150* (kg)
Actual (1)	433	45.2	528	848	98	0.507	4.45
Actual (2)	433	45.2	528	858	98	0.507	7.45
Design Mix	430	32 kg+	498	818	95	1.42	(up to 11)

Note: The first and second row of values represent actual mix proportions
The third row indicates design mix proportions
+ Weight of solid silica fume only. Water contained as part of the emulsion must be subtracted from the total water allowed.

26.7 Ultra High-Performance Concrete and its Structural Applications

Introduction Ultra High Performance Concrete (UHPC) was first developed by Brunauer *et al.*[10] around 1973. Ultra high performance concrete (UHPC) is also referred to as Reactive Powder Concrete[11]. The UHPC generally refers to concrete with a characteristic compressive strength exceeding 120 N/mm^2 and possibly attaining 200 N/mm^2.

RPC is a high-strength, ductile material formulated by combining various ingredients like, Portland cement, silica fume, quartz flour, fine silica sand, high range water reducer, steel or organic fibres and water. The concrete made with all these materials is capable of providing compressive strengths of up to 200 N/mm^2 and flexural strength of up to 50 N/mm^2.

The ingredients of ultra high-strength concrete are usually supplied in a three component premix comprising:

(a) Reactive powder (Portland cement, silica fume, quartz flour and fine silica and
(b) Superplasticisers (High range water reducers)
(c) Steel or organic fibres like polypropylene fibres

Water is added before mixing the ingredients to achieve the desired workability before depositing in the structural formwork. The fibres impart ductile behaviour to the high-strength performance concrete with the capacity to deform and support flexural and tensile loads even after initial cracking. The use of this material for construction is simplified by the elimination of reinforcing steel bars and the material can be virtually self-placed or dry cast to the desired shape.

The superior durability characteristics are due to as combination of fine powders selected for their grain size not exceeding 600 μm and chemical reactivity. The unique combination of these various ingredients results in maximum compactness of the resulting concrete with a small disconnected pore structure.

Mix Ingredients for UHPC The following materials are required for the preparation of ultra high performance concrete:

(a) Portland cement
(b) Silica fume
(c) Coarse aggregate
(d) Fine aggregate
(e) Steel or polypropylene fibres
(f) Super plasticisers
(g) Water

The recommended percentages of ingredients according to Ductal Lafarge Company[12] who have specialised in the commercial production of ultra high-performance and high-strength concrete are compiled in Table 26.4.

Table 26.4 *Recommended percentages of ultra high-performance concrete ingredients*

S. No.	*Mix Ingredient*	*Percentage by Weight*
1.	Portland cement	10 to 15
2.	Coarse aggregate (gravel or crushed rock)	35 to 45 –
3.	Fine aggregete (sand)	24 to 48
4.	Silica fume	4 to 5% by weight of CA
5.	Super plasticiser	3 to 5% by weight of cement
6.	Polypropylene fibres	Equal to the amount of silica fume
7.	Water	8 to 10% of overall volume of the mix

Structural Properties

(a) Strength

Compressive strength: 120 to 200 N/mm^2
Flexural strength: 15 to 25 N/mm^2
Modulus of elasticity: 45 to 50 kN/mm^2

(b) Durability

Freeze/Thaw resistance (after 300 cycles): 100%
Oxygen permeability: $< 10^{-20}$ m^2
Carbonation depth: < 0.5 mm
Abrasion (Relative volume loss index): 1

Applications of UHPC

(a) Foot bridge and railway station platform structures Ultrahigh performance concrete has been used for a number of innovative solutions including projects such as transportation structures, acoustic sound panels, seal walls, bridge anchor plates and beams for power plant cooling towers. In Seoul, Korea, a famous pedestrian bridge named as the "Footbridge of Peace" has a 130 m span arch constructed entirely with a proprietary product of UHPC. It is considered as a structural and architectural wonder. The arch bridge has no middle supports and has a platform thickness of just 45 mm.

Perry and Zakariasen[13] reported the first use of UHPC for the construction of a train station canopy. The Shawnessy Light Rail Transit (LRT) station constructed during 2003–2004, forming a part of the southern expansion to Calgary's LRT system, is considered as the first structure to use UHPC. The station platform roof is made up of 24 thin shelled canopies 5.1 m by 6 m having thickness of just 20 mm, supported on single columns.

UHPC technology has a unique combination of superior technical characteristics including ductility, strength, and durability while providing highly mouldable products with a high quality of surface finish. The design strength of the concrete used in the canopies was 130 N/mm^2. In addition to the canopies, the other components include struts, columns, beams and gutters. The total volume of concrete used for the station totalled 80 m^3.

(b) Precast prestressed concrete bridge structures Structural performance of precast prestressed concrete bridge girders built with high performance and ultra high performance concrete has been reported by Almansour and Lounis[14].

A comparative analysis of the bridge decks comprising HPC and UHPC girders supporting the deck slab was made to demonstrate the economical advantage of using the UHPC in place of HPC. The bridge deck with a total lane width of 12.5 m and a span length of 45 m was designed according to the Canadian Highway Bridge Design Code requirements with no cracking criterion at the serviceability limit state. The design of superstructure was achieved through an iterative procedure. The required number of girders, cross-sectional dimensions and area of prestressing steel were optimised to achieve minimum weight of the superstructure.

The following two types of bridge decks were designed to comply with all the serviceability and ultimate limit states prescribed in Canadian Highway Bridge design code[15].

(i) A typical cast *in situ* concrete deck slab on precast/prestressed HPC girders, and
(ii) A typical cast *in situ* concrete deck slab on precast/prestressed UHPC girders.

The slab thickness in both cases was of the order of 175 mm corresponding to the minimum thickness specified in the Canadian Highway Bridge Design Code. The precast prestressed girders were selected from the available sections specified by the Canadian Prestressed Concrete Institute[16]. Table 26.5 compiles the details of deck, girders, concrete grade and type of high-tensile steel used in the bridge decks for both types of concrete.

Table 26.5 *Structural details of HPC and UHPC bridge decks*

S. No.		*High Performance Concrete (HPC)*	*Ultra High Performance Concrete (UHPC)*
1.	Width of bridge deck	12.45 m	12.45 m
2.	Thickness of slab	175 mm	175 mm
3.	No. of girders	5	4
4.	Depth of girders (mm)	900 mm and 1200 mm	900 mm, 1200 mm and 1600 mm
5.	Girder spacing	2.5 m	3.333 m
6.	Grade of concrete		
	(a) Slab	30 N/mm^2	30 N/mm^2
	(b) Girders	40 N/mm^2	175 N/mm^2
7.	Type of prestressing	Low relaxation seven ply strands of nominal diameter 12.7 mm and Steel nominal area of 98.7 mm^2 with a tensile strength of 1860 N/mm^2 for both HPC and UHPC bridge decks	

The cross-section of the bridge deck with HPC and UHPC concrete adopting five and four girders, respectively, and having the same width is shown in Fig. 26.1.

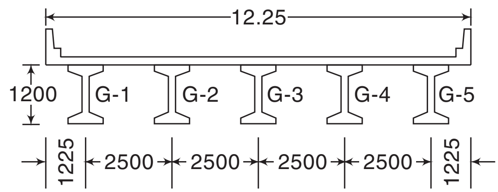

(a) High-performance concrete bridge deck

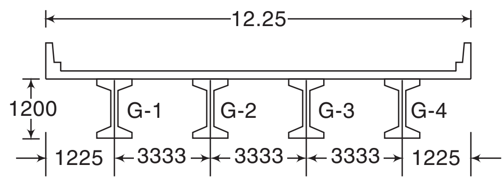

(b) Ultra high-performance concrete bridge deck

Fig. 26.1 *Prestressed concrete bridge deck using HPC and UHPC*

A comparative analysis of the material consumption in HPC and UHPC bridge decks clearly indicated the economical advantages of using UHPC in place of HPC as follows:

1. UHPC bridge decks enabled a considerable reduction in the concrete volume of up to 49 per cent for girder depths of 1200 mm and 65 per cent for girder depths of 900 mm.

2. The weight of the girders per unit area of the bridge was reported as 0.481 tons/m^2 for HPC bridges and 0.196 tons/m^2 for UHPC bridges adopting 900 mm girders and 0.288 tons/m^2 adopting 1200 mm girders.
3. The total weight per unit area of the superstructure, including the deck slab was observed to be 0.901 tons/m^2 for HPC and 0.616 tons/m^2 for UHPC decks adopting 900 mm girders. Consequently, UHPC results in 32 per cent reduction in the total weight of the superstructure and 59.3 per cent reduction in the weight of girders.
4. The prestressing steel area required for decks using 900 mm girders was 39 per cent higher than that used for 1600 mm girders and only 14 per cent higher when 1200 mm girders were used.

References

1. Russel Henry, G, What is High Performance Concrete? *Journal of Concrete Products*, January, 1999.
2. ACI Committee 211, *Guidelines for selecting proportions for high-strength concrete with Portland cement and fly ash* (ACI 211-4R), American Concrete Institute, Detroit, 1993.
3. Dewar, JD, A Concrete Laboratory in a Computer—Case Studies of Simulation of Laboratory Trial Mixes, *ERMCO-95*, *Proceedings of the XIth European Ready Mixed Concrete Congress*, Istanbul, 1995, pp. 185–193.
4. Sobolev, KG and Soboleva, SV, High Performance Concrete Mix Proportioning, *Special Publication, SP: 179-26*, American Concrete Institute, Detroit, Michigan, USA.
5. Saiprasad, PV and Kamalesh Jha, *High Performance Concrete*, A Project work undertaken for Course No. 624 at IRICE, Pune, India, 2009.
6. Gjorv, OE, Baerland, T, and Ronning, HR, Abrasion Resistance of High-strength Concrete Pavements, *Concrete International Design and Construction*, Vol. 12, No. 1, 1990, pp. 45–48.
7. Zia, P, Schemmel, JJ and Tallman, TE, *Structural Applications of High Strength Concrete, Final Report*, Center for Transportation Engineering Studies, Department of Civil Engineering, North Carolina State University, NC, June 1989, 330 pp.
8. Zia, P, Leming, ML and Ahamad, SH, *High-performance Concrete; A State* of the *Art Report*, Strategic Highway Research Program, National Research Council.
9. Roller, JJ, and Martin, BT, Russel, HG, and Bruce, Jr RN, Performance of Prestressed High-strength Concrete Bridge Girders, *PCI Journal*, Vol. 38, No. 3, 1993, pp. 34–45.
10. Brunauer, S, Yudenfreund, I, Odler and J Skalny, Hardened Portland Cement Paste of Low Porosity, VI Mechanism of the Hydration Processes, *Cement and Concrete Research*, Vol. 3, 1973, pp. 129–147.
11. Perry, VH, "What is Reactive Powder Concrete?", *High-performance Concrete Bridge Reviews*, No. 16, July–August 2001.

12. Lafarge North America, Technical Characteristics; UHPC with organic fibers. *National Building Code of Canada*, 1995.
13. Perry, VH, Zakariasan, D, First use of High performance concrete for innovative train station canopies, *Concrete Technology- Today*, August 2004, pp. 1–8.
14. Almansour, H and Lounis, Z, Structural Performance of Precast Prestressed Bridge Girders Built with Ultra High Performance Concrete, *Second International Symposium on Ultra High Performance Concrete,* Kassel, Germany, March 2008, pp. 822–830.
15. Canadian Standards Association (CAN/CSA:S-606), *Canadian Highway Bridge Code (CHBDC–06)*, 2006.
16. Canadian Prestressed Concrete Institute (CPCI), *Design Manual, Precast and Prestressed Concrete*, III Edition, 1996.

Review Questions

26.1 Briefly outline the characteristic features of high-performance prestressed concrete.

26.2 What are the basic mix ingredients of high-performance prestressed concrete?

26.3 List the advantages of high-performance concrete used in precast structural units.

26.4 Distinguish between high-strength and high-performance prestressed concrete.

26.5 Outline the applications of high-performance concrete in prestressed structures.

26.6 Write a brief note on the practical applications of high-performance concrete in prestressed concrete bridge structures.

26.7 Distinguish between high-performance and ultra high-performance concrete.

26.8 List the basic ingredients of ultra high-performance concrete used in precast prestressed structural elements.

26.9 Write a brief note on the strength characteristics of ultra high-performance concrete.

26.10 What are the specific applications of ultra high-performance concrete with reference to prestressed concrete structures?

Objective-type Questions

26.1 The workability of high-performance concrete used in prestressed concrete structures is

(a) the same as that of ordinary concrete
(b) superior to that of ordinary concrete
(c) less than that of ordinary concrete

26.2 The void content in high performance concrete in comparison with ordinary concrete is

(a) more (b) same (c) less

26.3 In aggressive environmental conditions, the prestressed concrete structure should be constructed using
(a) high-strength concrete
(b) high-performance concrete
(c) ordinary concrete

26.4 In prestressed concrete structures, there will be better deflection and crack control by using
(a) ordinary concrete
(b) high-performance concrete
(c) high-strength concrete

26.5 In comparison with high-strength concrete, the flow characteristics of high-performance concrete is
(a) higher
(b) lower
(c) same

26.6 Prestressed high-performance concrete structures experience
(a) low creep and shrinkage
(b) same creep and shrinkage
(c) higher creep and shrinkage

26.7 In the construction of prestressed concrete water tanks, high-performance concrete is preferred due to
(a) reduced permeability
(b) similar permeability
(c) increased permeability

26.8 The compressive strength of prestressed concrete girders made of ultra high-performance concrete will be in the range of
(a) 40 to 60 N/mm^2
(b) 100 to 200 N/mm^2
(c) 60 to 80 N/mm^2

26.9 Ultra high-performance concrete is preferred in the construction of prestressed concrete bridge girders mainly for
(a) the reduction in depth
(b) the increase in depth
(c) increase in number of girders

26.10 Permeability of high performance concrete is lower than that of normal concrete due to
(a) reduced porosity
(b) higher modulus of elasticity
(c) high wear resistance

Answers to Objective-type Questions

26.1 (b)	26.2 (c)	26.3 (b)	26.4 (b)	26.5 (a)
26.6 (a)	26.7 (a)	26.8 (b)	26.9 (a)	26.10 (a)

27 Prestressed Nano Concrete

27.1 Introduction

Nano technology dealing with the production and application of physical, chemical and biological systems at scales ranging from a few nanometres to submicron dimensions has found its way into the domain of concrete technology. Nano technology was first introduced in the famous lecture of Nobel laureate Richard P Feynman[1], **"There's plenty of Room at the Bottom",** delivered in 1959 at the California Institute of Technology. The terminology popularly referred to as nano technology itself was coined by Prof. Nario Tan-guchi in 1974. The predictions of Feynman to a large extent have been realised today as we celebrated the Golden Jubilee of nano technology on December 29, 2009. Nano technology is expected to produce goods and services worth 2.6 trillion dollars in the year 2014 globally. A total of 400,000 research papers and 10,000 patents have already come out in this area. Annual research publications worldwide were nearly 60,000 in the year 2009. Nano technology has extensive applications in plain, reinforced and prestressed concrete structures due to the overall improvement of the various intrinsic properties of concrete like flow ability, durability and strength in flexure, compression, tension and torsion.

According to Konstantin Sobolev[2], nano technology has changed and will continue to change our vision, expectations and abilities to control the material world. Significant achievements in this domain comprise the ability to observe the structure of material ingredients at their atomic level and measure the strength and hardness of micro and nanoscopic phases of composite materials. Among new nano-engineered polymers are highly efficient super plasticisers for concrete and high-strength fibres with exceptional energy absorbing capacity. Nano particles like silicon dioxide were found to be effective additives to polymers and also to improve the self-compacting capacity, workability and strength of concrete which is of paramount importance in the prestressed concrete industry.

Construction industry uses large quantities of Portland cement for infrastructure development throughout the world. Better understanding of the extremely complex structure of cement-based materials at the nano level will apparently result in a new generation of concretes with improved strength and durability. The new types of concretes should not only be sustainable, but also be cost and energy effective and at the same time meet the demands of the modern society. Nano binders or nano-engineered cement-based materials with nano sized cementatious components or other nano sized particles form the next groundbreaking research domain. At present, developed countries like USA, Japan, Germany, USSR and France are spending billions of dollars per year on nano technology research funding for the creation of new materials, devices and systems at molecular, nano and microlevel[3].

Nano technology of concrete is set on a path to revolutionise the construction industry by changing the structural properties of concrete to better suit the requirements of structural components. Already, several innovative nano products are available in the market which are of immense value in the construction industry dealing with prestressed concrete structural elements. The rapid development of the field of materials science on the nano scale has opened up a new window of understanding into traditional construction materials like cement and concrete. Nano cements and concretes with their associated benefits like overall cost savings and energy consumption coupled with increase in strength and durability play a significant role in the future of prestressed concrete construction industry.

27.2 Nano Cements

Nano cements are particularly suitable as coatings and repair materials. TX Active™ is a quality label developed by Heideberg cement and Italicementi which shows the durability and photo catalytic functionality of the finished product. This is a self-cleaning cement due to its special formula which is efficient in destroying atmospheric pollutants. In Milan, a commercial building's 3000 m^2 surface coated with this cement is functioning satisfactorily.

Iglesia Dives (Church) in Misericordia is a well-known building where TX Active cement has been used. In addition to its self-cleaning property, TX Active cement plays a role in reducing pollution. This product has also been used in the construction of two white concrete gateway elements in the 1-35W bridge over the Mississippi River in Minneapolis (USA).

EMACO™ nano cement product from BASF is a concrete repair material with exceptional properties such as improved bond strength, density and impermeability, reduced shrinkage and cracking tendency coupled with improved tensile strength. It also provides improved compatibility with concrete. This product has found application in the renovation of office buildings in Brussels, in the waste water plant in France and in the renovation of a bridge structure and cooling towers in Spain.

Chronolia™, developed by Lafarge Company, is a quick setting cement used in ready mix concrete made possible by nano technology and the understanding of crystalline growth. Agilia™, developed by Lafarge, is considered as the world's first self-compacting and self-levelling concrete. It generated 2.4 per cent of sales volumes and 12 per cent of Lafarge concrete business in 2006. One million cubic metres of Agilia concrete was sold in the year 2006.

Ductal™, also developed by Lafarge, is one of the first commercial concretes exhibiting high mechanical strength, durability and self-healing properties.

27.3 Nano Technology of Concrete

Portland cement is the most widely used material in the construction industry with an estimated production surpassing six billion cubic metres per year[4]. The prominent advantages of this material are availability of raw materials for production throughout the world, low cost, ease of construction, setting at room temperature and desirable properties. In addition to these advantages, modern day concrete made with cement and aggregates has an excellent performance record of over 180 years. In general, Portland cement is typically used as cementing material with fine and coarse aggregates to create products that are a few mm to several metres thick. The average size of Portland cement particle is in the range of 50 microns. In some applications requiring thinner and stronger products with faster setting time, microcement with a maximum particle size of about 5 microns has been used. By reducing the particle size by an order of magnitude, it is possible to obtain Nano-Portland cement.

For decades, major development in the performance of concrete was achieved with applications of superfine particles of fly ash or silica fume. Nano technology has made it possible to introduce nano silica to improve the properties of concrete. At the micro level, there is a good analogy between reinforced concrete and fibre reinforced composites. According to Balaguru[5], the lessons learnt from fibre reinforced concrete can also be effectively used for composites made using short discrete fibres, both at micro and nano levels. For example, the use of fibre reinforced concrete containing 0.5 per cent steel fibres is well-established in the construction industry to make thin and strong structural elements. The same advantages can be obtained by using 0.5 per cent carbon nano tubes in high performance composites exhibiting superior mechanical and electrical properties.

The differences in the particle size distribution and specific area of ingredients in conventional, high-strength/high performance and nano engineered concretes are graphically illustrated in Fig. 27.1. The figure clearly indicates the particle size (nm) and specific surface (m^2/kg) of coarse and fine aggregate, Portland cement and fly ash, silica fume and nano silica.

In the present state-of-the-art, one can claim that concrete utilises nano technology because it contains nano particles as ingredients including nano water particles and nano air voids. By using nano technology, we should be able to control the amount and distribution of the nano ingredients inside the final product to achieve the desired properties. The scalar distribution of the various ingredients of concrete is shown in Fig. 27.2. It is essential to create proper chemical and mechanical tools to control nano scale pores and the placement of calcium-silicate hydration products to produce concrete which can be termed as a product of nano technology.

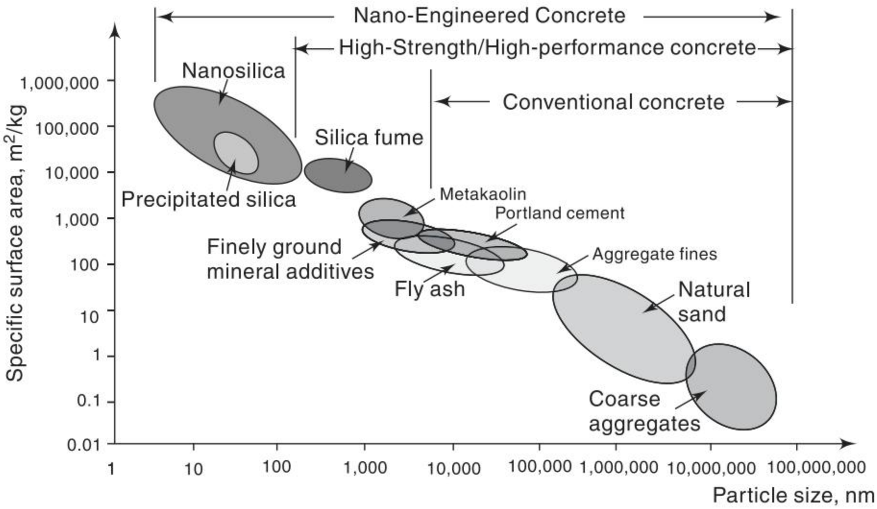

Fig. 27.1 *Particle size and specific surface area of different types of concrete materials*

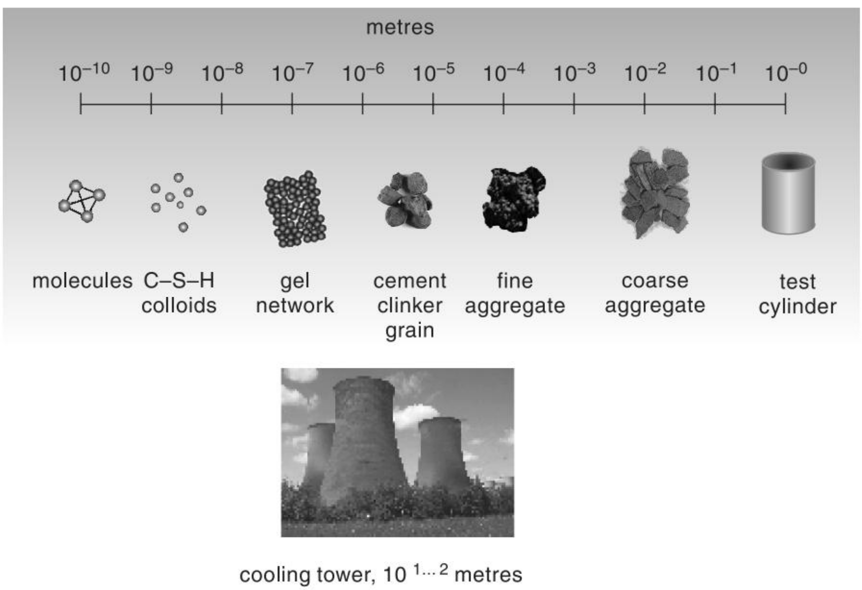

Fig. 27.2 *Scales of various constituents of concrete and a typical application*

27.4 Nano Concrete Production and Properties

Gaia concrete Gaia Nano Silica is the first nano additive for concrete developed by Rouzbeh Shahsavari, a doctoral student from MIT School of Engineering. This product has opened doors for the development of different types of nano additives replacing the micro silica largely used to produce silica fume concrete during the last decades of the 20^{th} century.

The technology was extended by Ulmen SA in association with Ferrada *et al.*[6] of Cognoscible Technologies to commercially produce Gaia nano silica for use at ready mixed concrete facilities certified by Environmental Management Systems (ISO 14001). Roclano Technologies has obtained the rights for marketing in Spain and Portugal. This product is available in liquid form which facilitates the uniform distribution of nano silica particles in concrete.

According to Ferrada *et al.*, the concrete mixtures with Gaia exhibit perfect workability without segregation or bleeding. Gaia combines the effects of water reduction coupled with increase in slump. This makes the design of self-compacting concrete an extremely easy task. The development of strength in plain and Gaia nano concrete is illustrated in Fig. 27.3.

The application of Gaia at a dosage of 1.3 per cent (by weight of dry cement) results almost two-fold increase in the compressive strength at seven and 28 days. The early strength of concrete with Gaia is 68.2 N/mm^2 which is nearly three times that of the control concrete. The 28-day compressive strength of concrete made with Gaia demonstrates a classical dependence on water/cement ratio as shown in Fig. 27.4. The experimental data clearly demonstrated the positive action of nano particles on the microstructure and properties of cement-based materials.

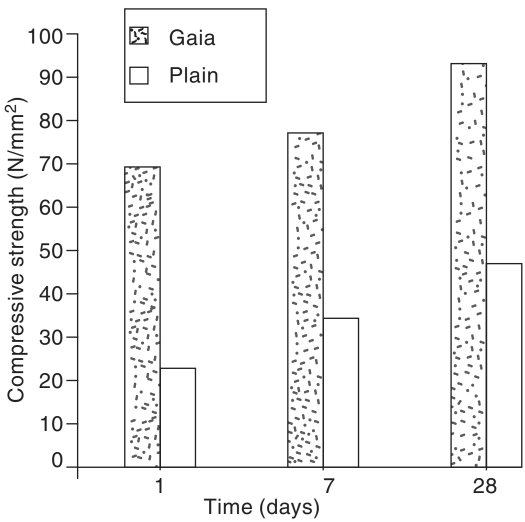

Fig. 27.3 *Compressive strength of plain and Gaia nano concrete*

Cuore nano concrete Micro silica has been one of the world's most widely used additives in concrete for over 80 years. Its properties allow high compressive strength, durability and impermeability and they have been part of many important concrete structures. Its main disadvantage being its relatively high cost and contamination which adversely affects the environment

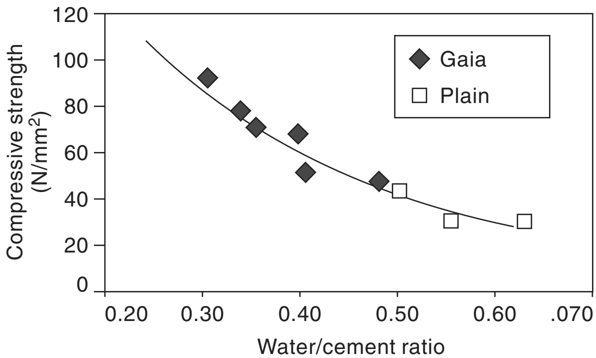

Fig. 27.4 *Relation between W/C ratio and compressive strength of plain and Gaia nano concrete*

and the health of the construction workers. Micro silica as a powder is one-thousandth fold thinner than cigarette smoke. Hence, operators must take special precautions to avoid inhaling micro silica to prevent silicosis, a deadly disease of the lungs. In the middle of 2003, a product which could replace micro silica was developed having better characteristics incurring a lower cost and also fulfilling environmental regulations of ISO-14001. Using tools of physics, chemistry and recent nano technology, a revolutionary product Cuore Nano Silica was developed which had superior advantages in comparison with micro silica. A litre bottle of nano silica was equivalent to a barrel full of micro silica, extra cement and super plasticising admixtures.

The Cuore nano silica product was tested in concrete used for over a year in the world's largest subterranean copper mines to prove its long-term characteristics. Cuore concrete takes care of the environment and also the operator's health. The new product surpassed the expectations of its design and gave concrete not only the high initial and final strength but also increased plasticity of the wet concrete and impermeability to the hardened concrete with cost and cement savings of up to 40 per cent. Also, it lowered the levels of environmental contamination.

The nano particles of silica turn into nano particles of cement (nano cement) in the chemical reaction that takes place in the concoction of concrete. The advent of Cuore nano silica concrete in the market has revolutionised the concept of concrete products and their applications in the construction industry[7]. The salient properties of concrete with Cuore nano silica (Civil Engineering Portal) are as follows:

- Cuore concrete is 88 per cent more efficient than micro silica added to concrete and super plasticisers.
- It exhibits high compressive strength (H-70).
- The product cost is drastically lower than using traditional production method or formulas.
- The concrete has an air content of 0 to 1 per cent.
- The nano silica concrete has a plasticity comparable to that of polycorbilate technology. Hence, the use of super plasticising additive is not necessary.

- High workability with reduced water/cement ratio (For Example, 0.2).
- Easy homogenisation of concrete and the reduction of mixing time allow the concrete plants to increase the production.

Cuore nano silica complies with environmental and health regulations prescribed in ISO-14001. It also protects operators from the danger of being contaminated with silicosis and does not spoil the environment. After successfully passing all the tests, the material is used commercially in different parts of the world. The following immediate benefits in using the Cuore nano silica concrete to the user have been identified as reported by Pascal Maes[8].

1. Concrete with good workability, compressive and tensile strengths.
2. Cessation of superplasticisers utilisation.
3. Cessation of silicosis disease risk to operators.
4. High impermeability and reduction in cement content using Cuore nano silica.
5. Compressive strengths of 70 to 100 N/mm^2 have been reported at 28 days.

Nano concrete using silica fume, fly ash and nano silica Collepardi *et al.*[9] investigated the properties of high performance nano concretes made by using optimum proportions of silica fume, fly ash and nano silica to manufacture concrete structural elements suitable for production in precast industry involving steam curing. Among the pozzolanic materials, silica fume appears to be the best performing siliceous product for high performance concretes (HPC). Its behaviour is related to the high content (>90%) of amorphous silica in the form spherical grains in the range of 0.01 to 1 μm. However, silica fume is not available in large amounts and it is also the most expensive mineral additive costing about 0.25 to 0.50 Euros/kg in Europe. Nano silica produced synthetically in the form of water emulsion of ultra fine particles in the colloidal state having particles of size 1 to 50 nm by Skarp and Sarkar[10] is available in the European market at a price of 0.45 to 0.90 Euros/kg of water emulsion.

Two different types of concretes with properties such as flowing and self-compacting were produced with different combinations of the basic pozzolanic ingredients together with cement, aggregates and superplasticiser as compiled in Tables 27.1 and 27.2, respectively. The mixes designated as SF and FA contained only silica fume and fly ash, respectively, while the mixes TC1 and TC2 contained all the three pozzolanic ingredients. A constant water/cement ratio of 0.44 was maintained in all the concrete mixes. The nano silica (UFACS) used was in the form of aqueous emulsion having 25 per cent dry content. The slump observed in flowing concretes varied from 230 to 270 mm while that in self-compacting concretes, it varied between 730 and 740 mm.

The results indicate that the strength development of silica fume concrete is better than the fly ash concrete in both flowing and self-compacting mixes regardless of the curing temperature. However, the difference in the strength development between the silica fume mix (SF) and the ternary combination (TC1 and TC2) appears to be significant only for concretes cured at 20°C,

Table 27.1 *Flowing nano concrete mixes*

Mix No.	*Cement Content* (kg/m^3)	*Silica Fume* (kg/m^3)	*Fly Ash* (kg/m^3)	*Nano Silica* (kg/m^3)	*Aggregate* (kg/m^3)	*Water* (kg/m^3)	*Super Plasticiser* (Per cent)	*28 day Comp. Strength* (N/mm^2)	*90 day Comp. Strength* (N/mm^2)
SF	396	59	0	0	1800	174	0.87	65	78
FA	396	0	59	0	1800	175	0.61	55	66
TC1	393	21	29	7.8	1790	173	0.60	52	68
TC2	395	15	40	5.1	1800	174	0.55	50	66

Table 27.2 *Self-compacting nano concrete (SCNC) mixes*

Mix No.	*Cement Content* (kg/m^3)	*Silica Fume* (kg/m^3)	*Fly Ash* (kg/m^3)	*Nano Silica* (kg/m^3)	*Aggregate* (kg/m^3)	*Water* (kg/m^3)	*Super Plasticiser* (Per cent)	*28 day Comp. Strength* (N/mm^2)	*90 day Comp. Strength* (N/mm^2)
SF	423	60	0	0	1775	186	1.30	66	78
FA	424	0	61	0	1780	186	1.20	55	65
TC1	425	21	30	7.4	1785	187	1.18	58	67
TC2	425	15	40	4.9	1780	187	1.10	57	70

especially at longer ages. In the case of steam cured concrete, no differences were observed in both types of mixes.

Based on these investigations, the authors have concluded that use of nano silica will reduce the quantity of costlier silica fume in concrete mixes. The results of this work also indicate that for steam cured high performance concrete (HPC), which is normally used in precast industry, the combined use of silica fume, fly ash and nano silica will be economical without loss of compressive strength at longer ages.

27.5 Prestressed Nano Concrete Bridge Structures

Nano concrete mix used in bridge decks Nano concrete is under use for highway bridge structural deck slabs and girders in European countries and Japan from the last decade of the 20th century. The Federal Highway Administration of USA (FHWA) commissioned a comprehensive research programme in 2001 in association with MIT to develop prestressed nano concrete structural elements for use in the US Highway transportation system which heavily depends upon concrete and steel. The research programme has developed modular precast/prestressed nano concrete elements like grid slabs, I and double tee shaped (π) girders for extensive use in highway bridges. Around 85 per cent of the old bridges in USA have a span range of 20 to 35 m and the FHA has planned to use the newly developed precast prestressed nano concrete elements having increased strength and enhanced durability in the construction of the superstructure decks of bridges. Graybeal[11] reported the details of the nano concrete mix used in the precast prestressed girders and their structural behaviour under loads. The nano concrete mix ingredients are compiled in Table 27.3.

Table 27.3 *Nano concrete mix ingredients*

S. No.	*Mix Ingredient*	*Quantity* (kg/m^3)	*Per cent (by weight)*
1.	Portland cement (15 μm)	712	28.5
2.	Fine sand (150–600 μm)	1020	40.8
3.	Silica Fume (1 μm)	231	9.3
4.	Ground Quartz (10 μm)	211	8.4
5.	Super Plasticiser	30.7	1.2
6.	Accelerator	30.0	1.2
7.	Steel Fibres (0.2 mm)	156	6.2
8.	Water	109	4.4

Bridge decks in USA The first UHPC concrete bridge in USA was built by FHWA at the Turner Fairbank Highway research centre in Mclean, Virginia in 2004. The bridge deck with a single lane of 4.9 m and spanning over 21 m is made up of a double tee or Pi-girder, developed by Massachusetts Institute of

Technology, is shown in Fig. 27.5. The precast prestressed concrete girder is made by using a proprietary nano concrete mix named Ductal™, developed by Lafarge. The girder is designed to support the AASHTO loadings for US highway bridges covering spans in the range of 20 to 35 m which is roughly 85 per cent of the US bridge inventory. The girders achieve a maximum span/depth (*L*/*H*) ratio of 35 and an overall weight reduction of approximately 30 per cent compared to the traditional standard normal concrete girders. The Pi-girder is also used for a three span bridge in the Buchanan County (US) with the centre span cast using UHPC concrete.

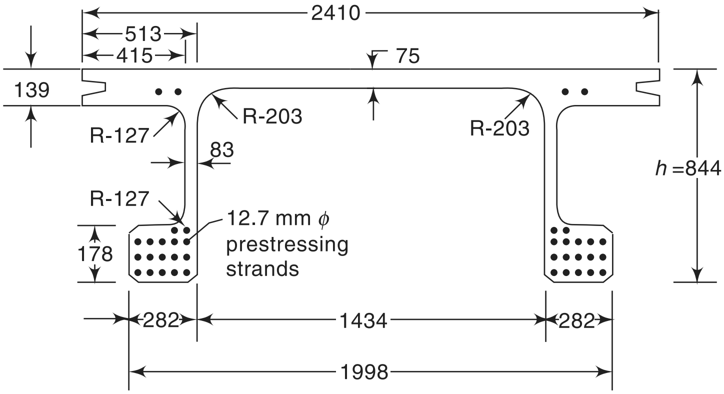

Fig. 27.5 *Cross-section of double tee or Pi-girder*

The ductal concrete mix formulation comprising of cement, granular materials, nano silica and low water/cement/ratio, results in dense concrete with low porosity, ultra high compressive and flexural strength coupled with high durability. The girders were pretensioned using 12.7 mm low relaxation prestressing strands with an ultimate tensile stress of 1860 N/mm^2. No supplementary reinforcements were provided in the girders and the high-strength nano concrete had to resist the secondary tensile forces due to shear, temperature and shrinkage.

The Mars Hill Bridge in Wapello County, Iowa (USA), was built in 2006 using modified UHPC -I- girders, shown in Fig. 27.6. The girders with a length of 33 m and an overall depth of 1.067 m were precast using nano concrete. The girders were pretensioned using 24 nos of 12.7 mm low relaxation prestressing strands. No supplementary reinforcements were provided in the girders and the high-strength fibre reinforced nano concrete had to carry all the secondary tensile forces due to shear, temperature and shrinkage and the bridge is under use from 2006.

In most of the highway bridge decks, the I and double tee-shaped prestressed girders are spaced at intervals of 2.4 to 3 m and the space between the girders is covered by cast *in situ* or precast concrete slabs. Garcia *et al.*[12] reported the structural behaviour of two-way ribbed bridge deck slabs developed by the Federal Highway Administration research programme. The two-way precast prestressed concrete grid is made up of ribs, 76 mm wide and 204 mm overall

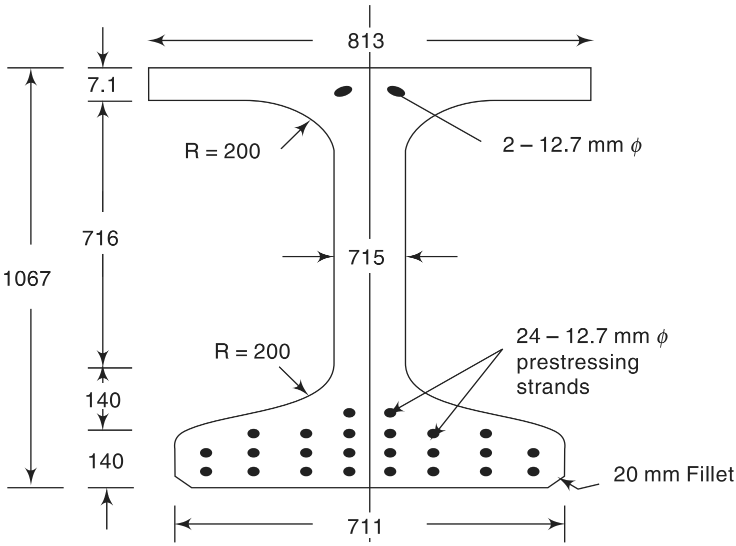

Fig. 27.6 *Modified UHPC I-girder*

deep, spaced at intervals of 610 mm connected by a 64 mm thick slab using UHPC concrete. The two-way grid slab with overall dimensions of 11.6 m wide by 2.4 m in the direction of traffic is used as the deck slab supported on precast prestressed I-girders forming the superstructure of the bridge. Figure 27.7 (a), (b) and (c) shows the cross-section of the rib, bridge deck with I-girders and the plan, respectively. Composite action between girders and deck is assured

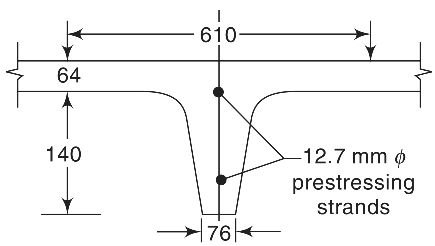

Fig. 27.7 (a) *Rib section*

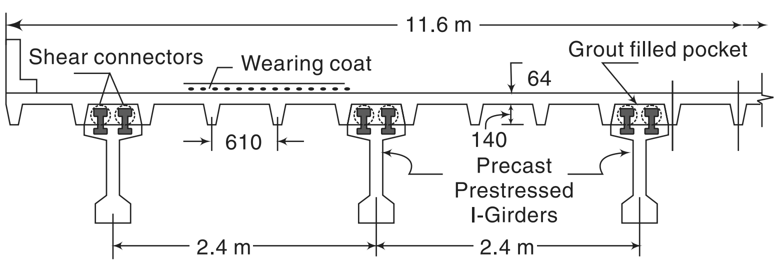

Fig. 27.7 (b) *Two-way ribbed deck panel supported on I-girders*

(*Contd.*)

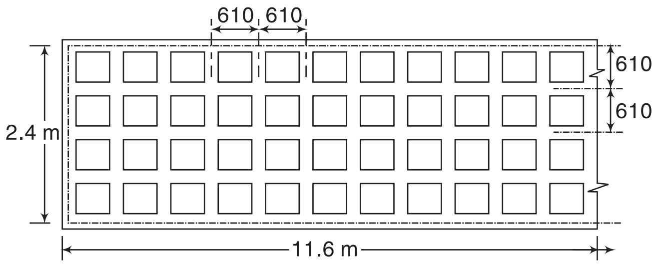

Fig. 27.7 (c) *Plan of two-way ribbed deck panel*

by shear connectors extending from girder into pockets created between webs of deck panel. The pockets are filled with grout to facilitate composite action.

Bridge decks in East Asian countries During the last decade, nano concrete is being increasingly adopted for foot and highway bridges, airport runways, environmental protective panels and for architectural applications in Australia, Japan and Korea.

(a) Shepherds Creek Road Bridge (Australia) The superstructure of the Shepherds Creek Road Bridge in New South Wales, Australia, comprises of 16 precast pretensioned nano concrete I-beams of 600 mm overall depth and 330 mm flange width and a web thickness of 100 mm. The beams spanning over 15 m are spaced at 1.3 m centres and connected by a cast *in situ* reinforced concrete deck slab 170 mm thick. The concrete slab was cast on 25 mm thick permanent precast Reactive Powder Concrete (RPC) formwork panels spaced between the I-beams. The beams are prestressed using 15.2 mm strands with 6 nos in the top flange and 14 nos. in the bottom flange.

(b) Papatoetoe Pedestrian Bridge (Australia) The Papatoetoe Pedestrian Bridge with a total length of 175 m was built using two precast pi-shaped ductal concrete segments with majority of spans being 20 m. The deck slab and webs are 50 mm thick and the high compressive strength of nano concrete has eliminated the use of normal reinforcements. The webs are provided with circular cavities to reduce the weight of the structure. The longitudinal elevation and cross-section of the main girders are shown in Fig. 27.8.

(c) Torisaki River Bridge (Hokkaido) for Highway Traffic (Japan) The Torisaki River Bridge comprises a corrugated steel web girder erected over a maximum span of 54.5 m and a launching nose length of 45 m. The lower chords of the girder are made up of UHPC. The composite girder of the highway bridge built in 2006 has a road width of 11.3 m. After completion of the launching, the nose portion is transformed to the permanent girder. A list of UHPC Bridges constructed in Japan during the last decade is compiled in Table 27.4.

Fig. 27.8 *Papatoetoe Pedestrian Bridge (Australia)*

Table 27.4 *List of UHPC bridge applications in Japan*

S. No.	*Name (Location)*	*Type*	*Span* (m)	*Width* (m)	*Year*	*Remarks*
1.	Akakura (Yamagata)	Foot Bridge	35	3.5	2004	Box Girder
2.	Tahara (Aichi)	Foot Bridge	12	2.6	2004	Box Girder
3.	Horikashi (Fukuoka)	Highway	16	8.5	2005	Composite-I Girder
4.	Keiouno (Tokyo)	Foot bridge	11	2.0	2005	Box Girder
5.	Torisaki (Hokkaido)	Highway	54	11.3	2006	Launching Nose
6.	Toyota (Aichi)	Foot Bridge	28	4.5	2007	Box Girder
7.	Sanken-ike (Fukuoka)	Foot bridge	Two of 40	3.5	2007	Box Girder

(d) Haneda Airport Paving Slabs (Japan) The expansion of the Haneda Airport Runway-D into the sea bay will utilise the world's largest single project application of UHPC (ductal) in the world to date. The construction work started in July 2007 and Taiheiyo cement (under licence from Lafarge) is responsible for the production of UHPC for precasting the concrete slabs. This unique project is an excellent example of how weight savings and durability result in an overall economical solution for an airport runway project. Approximately 7000 UHPC precast, pretensioned slabs of overall size 7.8 m by 3.6 m were used providing a runway area of 200,000 m^2. The ribbed and pretensioned slabs utilised 24000 m^3 of UHPC in the project. Table 27.5 shows the advantages of using the UHPC slabs instead of the normal prestressed concrete slabs.

Table 27.5 *Salient features of UHPC and normal PSC slabs*

S. No.	*Details of Slab*	*Normal PSC Slab*	*UHPC Slab*
1.	Weight of each slab	221 kN (100%)	97 kN (44%)
2.	Average dead load including Fillers	7.84 kN/mm^2	3.83 kN/mm^2
3.	Average slab depth	320 mm	136

The ribbed and pretensioned slabs using high-strength strands were designed for an ultimate wheel load of 320 kN. However, the prototype tests showed the ultimate load carrying capacity of the slab as 600 kN/wheel. The cost reduction in the steel jacketed supporting structure resulted in significant overall savings due to the use of lighter UHPC slabs for the airport runway.

(e) Sunyado Foot Bridge, Seoul (South Korea) Sunyado (Peace) Foot Bridge in Seoul, South Korea, is the longest existing foot bridge in the world, constructed using Reactive Powder (Nano) Concrete with a single span of 120 m. The foot bridge comprises six precast, post-tensioned segments of pi-shaped cross-section. The top deck slab is 30 mm thick and 4.3 m wide. The two webs are 160 mm thick with an overall depth of 1300 mm connected by transverse ribs spaced at 1.225 m. The longitudinal girders are prestressed by three tendons comprising 12.7 mm diameter sheathed and greased mono strands. The transverse ribs are prestressed by a single 12.7 mm diameter strand. The six arch-shaped segments were post-tensioned to form the arched foot bridge spanning over 120 m. The arch is supported at each end on RCC foundations 9 m deep resisting the horizontal thrust of the arch. Figure 27.9 shows the longitudinal elevation of the longest arch shaped foot bridge.

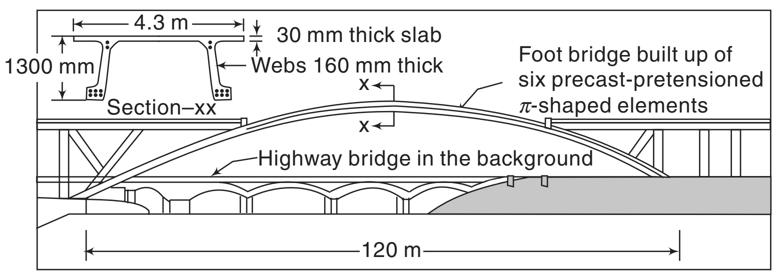

Fig. 27.9 *Sunyado foot bridge (South Korea)*

(f) Gyeomjae Bridge (South Korea) The Gyeomjae Bridge has been designed to serve the dual purpose of vehicular and pedestrian traffic adopting Ultra High Performance Concrete (Dctal). The bridge comprises a double box girder cross-section serving as a highway with hanging pedestrian walkways attached to the sides of the box girder as shown in Fig. 27.10.

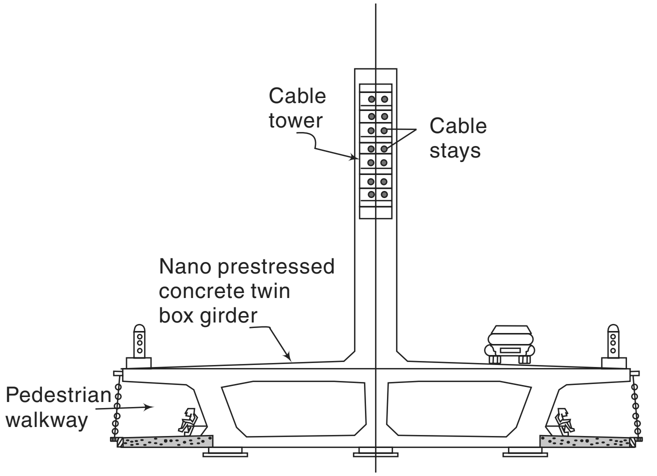

Fig. 27.10 *Gyeomjae cable-stayed bridge (South Korea)*

The walkway consists of thin plank type segments, post-tensioned through a longitudinal rib to form modules which are lifted into place as a single unit. The planks are further ribbed transversely to provide torsional rigidity and bending strength.

The UHPC modules are suspended from the main concrete box girder using hanger bars and a steel pin joint on the inside. Each UHPC pedestrian walk- way module with a width of 4 m and 6 m length weighs only 4.5 t. The whole bridge is supported by cable stays passing over a central tower with cables on either side supporting the double box girder with cantilever walkways.

The practical applications of nano concrete in prestressed concrete structures described above, clearly establishes the economical, aesthetic and environmental advantages of using nano concrete in prestressed concrete constructions in developing countries like India.

References

1. Feynman, R, There is Plenty of Room at the Bottom (Reprint from speech delivered at the Annual meeting of the West of the American Physical Society), *Engineering Science Journal*, Vol. 23, 1960, pp. 22–36.
2. Sobolov, K and Gutierrez, MF, How Nano Technology Can Change the Concrete World, *American Ceramic Society Bulletin*, Vol. 84, No.10, October 2005, pp. 14–18.
3. Collepardi, M *et al.*, Combination of Silica Fume, Fly Ash and Amorphous Nano-Silica in Super Plasticized High Performance Concretes, *Proceedings of the First International Conference on Innovative Materials and Technologies for Construction and Rehabilitation*, Lecce, Italy, 2004, pp. 459–468.
4. Balaguru, P and Shah, SP, *Fibre Reinforced Cement Composites*, McGraw-Hill Publications, New York, 1992, 530 pp.
5. Balaguru, P and Chan, P, High-strength Composites for Repair, Rehabilitation and Strengthening of Concrete, *Indian Concrete Institute Journal*, No. 3, 2003, pp. 7–18.

6. Ferrada MG, M Escobar, W Dominguez, RV Ferrada and PI Avalos, "U-Silice ISO-14001: Silice A favor del medio Ambiente"; in *XIV Jornadas Chilenas del Harmigon*, Valdivia, Chile, 2003.
7. Collepardi M, Ogoumah-Olagot, Skarp U and Troli, R, Influence of Amorphous Colloidal Silica on the Properties of Self-Compacting Concretes, *Proceedings of the International Conference: Challenges in Concrete Construction— Innovations and Developments in Concrete Materials and Construction*, Dundee, UK, 2002, pp. 473–83.
8. Pascal Maes, Cuore Nano Silica Concrete—*A Report published in Civil Engineering Portal, 2009.*
9. Collepardi M, Collepardi S, Skarp U and Troli, Optimization of Silica Fume, Fly Ash and Amorphous Nano-Silica in Super Plasticized High Performance Concretes, *Proceedings of 8th CANMET/ ACI International Conference on Fly Ash, Silica Fume, Slag and Natural Pozzolans in Concrete, SP-221*, Las Vegas, 2004, pp. 495–506.
10. Skarp, U and Sarkar, SL, Enhanced Properties of Concrete Containing Colloidal Silica, *Concrete Producer*, December 2000, pp. 1–4.
11. Graybeal, B, Structural Behavior of UHPC—I Girder, *US Federal Highway Authority Report No. FHWA-HRT-06-115, Mclean, Virginia*, USA August 2006.
12. Garcia, H, Greybeal, B, Analysis of Ultra High Performance Concrete Two-way Ribbed Bridge Deck Slab, *National Technical Information Service Report No. PB 2007–112112*, August 2007, Springfield, Virginia, USA.

Review Questions

27.1 What are the basic ingredients used in the production of nano concrete?
27.2 Briefly outline the necessity and development of nano concrete with particular emphasis on the development of compressive strength.
27.3 Distinguish between high-performance concrete and nano concrete.
27.4 What are the salient properties of nano concrete?
27.5 What are the structural advantages of using nano concrete in prestressed structures?
27.6 Outline briefly the range of compressive strength achieved in nano concrete.
27.7 List the type of prestressed concrete structures for which nano concrete is ideally suited.
27.8 Explain briefly the use of nano concrete in the construction of prestressed concrete bridge structures and its advantages.
27.9 Distinguish between nano silica and silica fume and their use in nano concrete.
27.10 List the advantages of using nano concrete in bridge decks.

Objective-type Questions

27.1 The development of nano concrete is based on the research investigations in the field of
(a) cement technology
(b) nano technology
(c) concrete technology

27.2 Normal concrete and nano concrete differ in their structural properties mainly due to
- (a) cement content
- (b) type of mixing
- (c) types of basic ingredients

27.3 The rate of development of strength in nano concrete in comparison with normal concrete is
- (a) of the same order
- (b) significantly higher
- (c) low

27.4 Nano concrete is ideally suited for prestressed concrete structures mainly due to
- (a) high flowability
- (b) high compressive strength
- (c) high modulus of elasticity

27.5 Prestressed structural elements made of nano concrete in comparison with normal concrete generally possess
- (a) smaller cross-sectional dimensions
- (b) more or less the same size
- (c) larger cross-sectional dimensions

27.6 For longer span prestressed concrete girder bridges, use of nano concrete results in the reduction of
- (a) cost of construction
- (b) depth of girders
- (c) maintenance costs

27.7 The thickness of slabs of highway bridge decks can be significantly reduced by using
- (a) high-performance concrete
- (b) high-strength concrete
- (c) nano concrete

27.8 The high-strength of nano concrete is attributed mainly to the use of
- (a) micro aggregates
- (b) nano silica
- (c) high grade cement

27.9 For prestressed concrete water retaining structures, use of nano concrete is ideally desirable due to its property of
- (a) high-strength
- (b) high wear resistance
- (c) reduced permeability

27.10 Among various types of concretes, creep and shrinkage are comparatively less in the case of
- (a) normal concrete
- (b) high-strength concrete
- (c) nano concrete

Answers to Objective-type Questions

27.1 (b)	27.2 (c)	27.3 (b)	27.4 (b)	27.5 (a)
27.6 (b)	27.7 (c)	27.8 (b)	29.9 (c)	27.10 (c)

28 Precast Prestressed Concrete Structures

28.1 Introduction

A report by the World Business Council[1] for Sustainable Development indicates that concrete is the most widely used material on earth next only to water. At present, nearly three tons of concrete is produced for every person on this earth, indicating its universal adaptability in the construction industry. Precast concrete was first used by the city engineer, John Alexander Brodie[2], in the year 1905, for the construction of precast paneled buildings in Liverpool, England. Later, this idea was adopted all over the world, particularly in Eastern Europe.

Precast prestressed concrete systems combine with structural and architectural components to create long lasting buildings and structures such as high rise office complexes, landmark bridges, parking structures, stadiums, industrial structures, huge domes of sports complexes, electrification and marine structures. Precast prestressed concrete components are cast at manufacturing sites or factories ensuring rigorous quality control and dimensional specifications and they can be transported to the job site for erection. Precast structures have high durability and strength as well as thermal mass while contributing to increased energy efficiency.

Precast systems use locally available materials and can incorporate recycled supplementary cementatious materials, like fly ash and slag cement, contributing to "Green Buildings". Precast structural elements qualify for a high number of points towards certification under Green Building rating system monitored by the Building Council Leadership in Energy and Environmental Design (LEEDS)[3]. The prominent benefits of prestressed precast elements are variety, flexibility, utility and durability. Tight quality control results in cost efficient mix designs, resulting in smaller structural members and longer spans.

In countries where labour costs are high, precasting technology has developed and flourished extensively. After the World War-II, manpower shortage has forced the Western and European countries to establish massive factories producing standard modular precast units required for building, transportation, electrical transmission, marine applications, off-shore oil drilling platforms, tower structures, and shell and folded plate structures to cover large column free areas. Total precasting has become the buzz word in recent years and the practise is common in many metro areas, especially in residential applications. By combining different precast elements to produce a complete structure, concrete's benefits are maximised. Precast systems can adopt innovation and aesthetics, incorporating a variety of colors and textures to suit the client's requirements.

28.2 Applications of Precast Prestressed Concrete

The development and widespread use of precast prestressed concrete structural elements has revolutionised the building industry with optimum utilisation of the basic material and at the same time, resulting in improved quality control coupled with extensive structural applications.

The extensive research and ingenuity by various investigators[4,5] supported by several companies have resulted in developing precast prestressed concrete products ideally suited for buildings, bridges, railways, power transmission towers, aircraft hangers, liquid storing structures and many other multifarious applications.

The most widely used precast prestressed concrete structural elements are listed as follows:

1. Solid and hollow cored slabs
2. Single and double tee girders
3. Bridge deck systems
4. Electrical transmission lines poles
5. Piles for deep foundations
6. Sleepers for railways
7. Roof trusses
8. Shell and folded plate elements
9. Pipes
10. Drilling platforms

28.3 Precast Prestressed Concrete Slab, Beam and Tee Girders

Precast prestressed concrete slabs are widely used in all types of commercial, residential and industrial buildings, where repetitive use of standard components manufactured in a factory can be fully utilised. The significant benefits of the units include fire resistance, sound control, durability, and rapid construction with attractive exterior treatments.

28.3.1 Solid Slabs

Solid slabs are commonly manufactured in typical widths varying from 1.2 to 3.6 m, with thickness of slab varying from 100 to 300 mm, for spans in the range of 3 to 10 m. Figure 28.1 shows the percentage savings of material in a precast prestressed slab in comparison with a reinforced concrete slab supporting a live load of 4 kN/m^2 over a span of 8 m. In addition, the prestressed slab is superior in many respects than the conventional R.C. slab due to the manufacturing process in a factory.

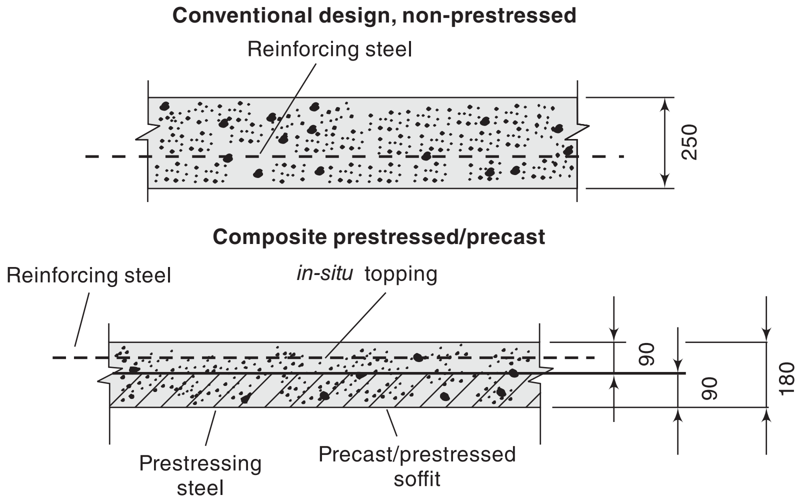

Material	Conventional design, non-prestressed	Prestressed/ precast	Material savings
Concrete	0.25 m^3/m^2	0.18 m^3/m^2	28%
Reinforcing steel	18.30 kg/m^2	6.20 kg/m^2	45%
Prestressing steel	—	3.85 kg/m^2	45%

(Live Load = 4 kN/m^2 and Span = 8 m)

Fig. 28.1 *Comparative analysis of precast prestressed and R.C. slab*

Typical solid precast prestressed slabs ready for installation in roofs and floor construction are shown in Fig. 28.2.

28.3.2 Hollow Cored Slabs

Precast prestressed cored slabs, shown in Fig. 28.3(a), are suitable for spans in the range of 10 to 15 m. The cored slabs have standard widths of 0.6 to 3.6 m with thickness varying from 150 to 300 mm. The span/depth ratios of these cored slabs being 30 to 40 for floors and 40 to 50 for roofs. The method of floor/roof construction using cored slabs is shown in Fig. 28.3(b).

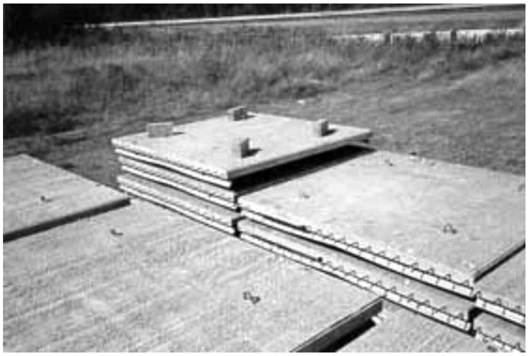

Fig. 28.2 *Solid precast prestressed concrete slabs for roofs and floors*

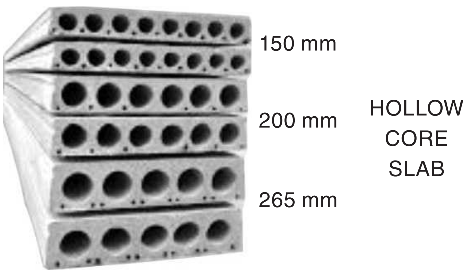

(a) Cored slabs

(b) Floor construction using cored slabs

Fig. 28.3 *Precast prestressed cored slabs in floor construction*

28.3.3 Tee Girders

Precast prestressed single and double tee girders are in use for floor/roof construction since 1950.

Double tee precast units are widely used in multi-storey housing projects and parking structures. Prestressed Concrete Institute[6] has standardised the designs of double tee girders of varying width, overall depth and spans. The standard double tee girders are manufactured by several companies with varying width of slab from 3.6 to 6.6 m, overall depth 460 to 915 mm with stem width tapering from 150 mm at the top to 100 mm at the soffit. For parking structures, double tee girder lengths of about 18 m are ideally suited to maintain open clear distances for drive aisles plus two sets of parking stalls.

Design live loads for double tee girders used in parking structures are normally 2 kN/m^2 or a concentrated wheel load of 14 kN applied over an area of 114 by 114 mm. Prestressing strands typically range in size from 9.5 to

15 mm diameter. Double tee precast/prestressed concrete units are ideal for floor and roof systems requiring long, uninterrupted spans and extra heavy load carrying capabilities resulting in lighter weight structures. The remarkable strength of a double tee is the result of a design and manufacturing system that uses the best attributes of steel and concrete. Typical building uses for double tees include parking decks, water/wastewater treatment plants, food processing plants, heavy industrial buildings, warehouses, indoor pools and gymnasiums. Typical double tee girder units are shown in Fig. 28.4.

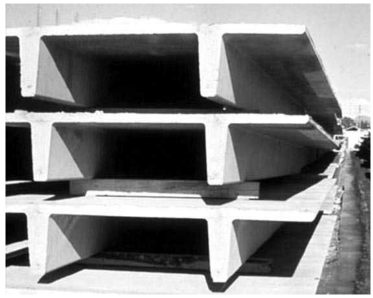

Fig. 28.4 *Typical precast prestressed double tee-floor/roofing units*

Double tees with C-grid carbon fiber mesh replacing conventional steel mesh flange reinforcing eliminates degradation from spalling, cracking and deterioration associated with rust in the corrosion zone. In addition, pretopped carbon cast cover reduces the weight of the unit up to 12 per cent, reducing overall costs. ACI: 362[7] specifies sealants for all precast tees except when using carbon fiber reinforcement replacing steel. Conventional double tee and carbon cast mega tee manufactured by High Precast Parking Systems[8] of Denver, USA, is shown in Fig. 28.5.

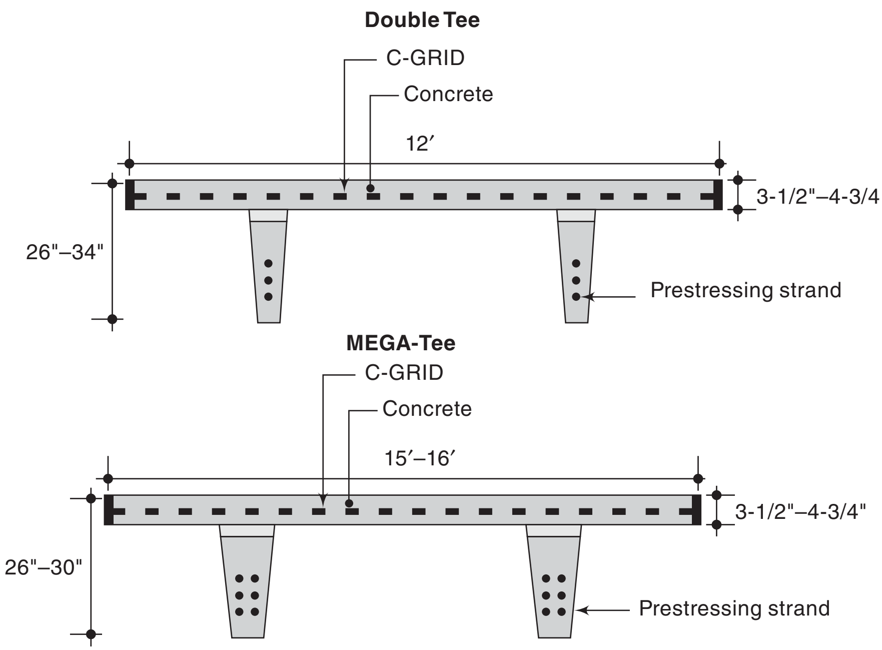

Fig. 28.5 *Conventional double tee and C-grid carbon cast Mega size double tee*

Precast double tee girders are widely used for floor and roof construction in the USA. The use of a typical double tee girder for roof construction is shown in Fig. 28.6.

Fig. 28.6 *Precast prestressed double tee in roof construction*

28.4 Precast Prestressed Concrete Bridge Deck Systems

Precast prestressed concrete is ideally suited for bridge construction where standard modular structural units are used resulting in quality control of materials and dimensions of the members with the added advantage of durability and strength coupled with faster construction. Most of the developed and developing countries resort to precast prestressed modular units for the construction of bridges in the national highway network. Depending upon the span, type of highway and loading standards, several types of precast prestressed concrete structural units manufactured by various commercial organisations are available for use in the construction of the bridge decks.

28.4.1 Precast Pretensioned Bridge Decks

Precast pretensioned solid slab decks are ideally suited for small spans in the range of 5 to 10 m. Figure 28.7 shows the precast slab units ready for dispatch to the work site. The thickness of the slabs vary from 200 to 400 mm depending upon the span and type of highway loading. The span/depth ratio varies from 25 to 30. Pretensioned single tee and double tee girders are preferred for longer span bridge decks. In the UK, the precast and pretensioned I and Y-beams[9] have been standardised by the Cement and Concrete Association[10] for bridge decks of spans varying from 7 to 36 m. Standard I and tee-units are widely used in highway bridge construction in the USA[11].

California Highways Department[12] has standardised precast pretensioned girders of different types for use in bridge construction. The bulb type tee girder, shown in Fig. 28.8, is widely used for spans in the range of 20 to 50 m, while the California wide flange girder, shown in Fig. 28.9, is suitable for larger spans up to 60 m.

Fig. 28.7 *Solid precast prestressed concrete slabs for highway decks*

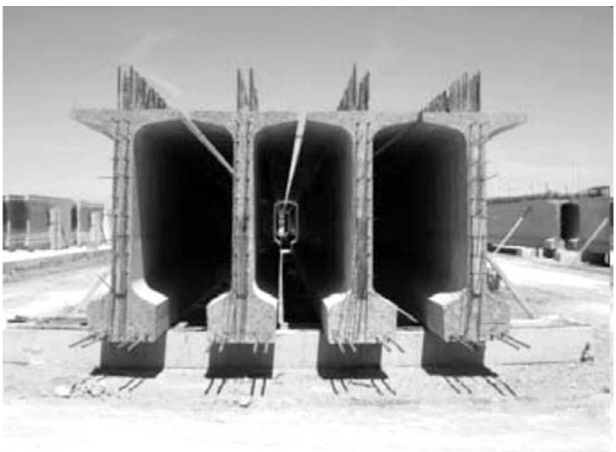

Fig. 28.8 *Pretensioned bulb tee girder*

Fig. 28.9 *Pretensioned wide flange girder*

28.4.2 Precast Post-tensioned Bridge Decks

For medium spans, post-tensioned bridge decks with tee-beams and cast *in situ* slab are commonly used. For longer spans, precast cellular box girders are generally preferred due to its superior resistance to flexural, shear and torsional effects under loads. The modular segmental precast box girders[13] are lifted by cranes and positioned to form the bridge deck before post-tensioning as shown in Fig. 28.10.

Fig. 28.10 *Erection of precast cellular box girders before post-tensioning the bridge deck*

Post-tensioning facilitates the use of curved cables which improve the shear resistance of the girders. Post-tensioning is ideally suited for simply supported or continuous long span bridge construction, avoiding the need for costly factory type installations like pretension beds. Most of the long span bridges in national highway crossings and the flyovers in metropolitan cities are invariably constructed using precast hollow box type segmental construction.

Compared to I and tee girders, box girders have a number of key advantages. Box girders offer better resistance to torsion, which is particularly of benefit if the bridge deck is curved in plane. Box girders can be erected using the method of incremental launching or cantilever method of construction and they offer superior lateral stability to the bridge deck under eccentric loads. In post-tensioned continuous girders, the high tensile cable profile can be arranged to suit the moments developed at the support and mid-span sections. Due to these advantages, they are preferred for urban flyovers in most of the cities in India. A typical curved box girder bridge deck is shown in Fig. 28.11. The reader may refer to Chapter 24 for the staging, incremental launching, progressive placement and cantilever construction methods[14] used for segmental box girder decks of bridges.

Fig. 28.11 *Post-tensioned prestressed concrete curved box girder bridge under construction*

28.5 Precast Prestressed Concrete Trusses

Prestressed concrete trusses[15] are widely used for industrial structures like workshops and automobile assembling plants during the last several decades mainly due to economic factors and durability considerations. The tie member of the truss being in tension is generally prestressed.

The reader may refer to Chapter 22 for details regarding the type of trusses and the design aspects of various members to support, dead, live and wind loads. Figures 28.12 and 28.13 show the typical long span prestressed concrete trusses used for roof construction.

Fig. 28.12 *Warren type precast prestressed concrete roof girder*

Fig. 28.13 *N-type precast prestressed concrete roof truss*

28.6 Precast Prestressed Concrete Shell and Folded Plate Structures

28.6.1 Precast Pretensioned Hyperboloid Shell Roof Elements

Precast pretensioned hyperboloid shells grouped under the category of doubly curved anticlastic shells, first developed by Silberkhul[16] in Germany, have been used in many countries for covering the roofs of large assembly halls in several countries. Le Corbusier used this type shell for the roof of the legislative assembly hall at Chandigarh, India. Pretensioned hyperbolic shell units 25 m long with a shell thickness of 60 mm have been used for a storage building at Essen, Germany. The span to chord width ratio of this type of shells is generally in the range of 5 to 10.

Pretensioned precast HP shells of 20 m span length and 2.5 m wide have been used at Larsen Toubro's Porclain hydraulic excavator factory at Bangalore[17]. The precast pretensioned HP shell units each weighing 9.4 tons have a thickness of 50 mm at the bottom, gradually varying to 100 mm at the edges. The units were prestressed using 32 number of 7 mm diameter high tensile wires arranged to follow the shell profile between the ends. In addition, a welded mesh was used as non prestressed reinforcement tied to the high tensile wires and the shell was cast using high strength concrete using a concrete mould. Each shell unit consumed 3.75 m^3 of high strength concrete, 273 kg of HYSD bars and 201 kg of high tensile wires. Figure 28.14 shows the precast shell elements supported on precast prestressed bow string arched units between columns at 20 m intervals.

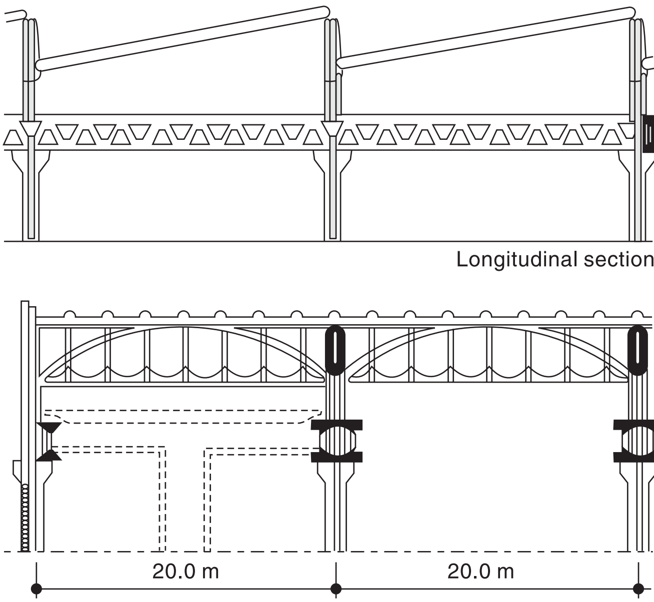

Fig. 28.14 *Precast pretensioned hyperboloid shell roof*

28.6.2 Precast Pretensioned Folded Plate Roof Elements

Folded or hipped plates are generally used for industrial structures due to the simplicity of their form and structural behaviour in resisting external loads by slab and plate action[18]. The thin concrete plates can be pretensioned on a long line pretensioning bed and later cut to the required lengths to suit the span of the roof. (For detailed analysis and design of folded plates, the reader may refer Chapter 18). Figures 28.15 and 28.16 show the erection of folded plate roof[19] and wall panels, respectively, for an industrial structure at Buffalo Industrial Park in San Pedro, Honduras, Central America. The 75 mm thick, 1730 mm wide folded plate units were pretensioned using 6.4 mm-7 wire strands. The folded plate roof covering an area of 30 m by 69 m was divided into two bays with folded plates supported over a central row of columns spaced at 15 m intervals.

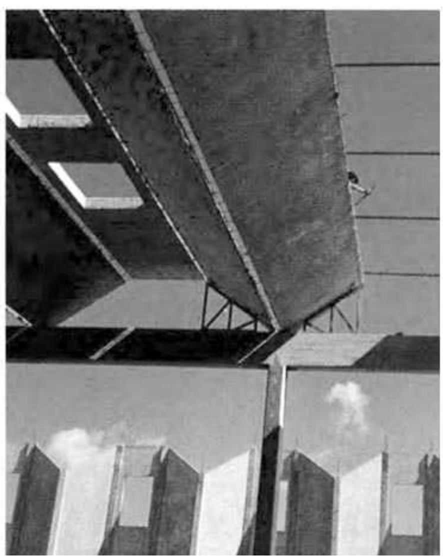

Fig. 28.15 *Folded plate roof construction*

Fig. 28.16 *Folded plate wall panel*

The elliptical dome forming the roof of Kanteerava indoor sports stadium[20] in Bangalore, India, covers an area of 120 m by 90 m. The roof was built using 120 precast folded plates of average width 2 m having a thickness of 40 mm with interconnected ribs. The lower end of the dome is supported on 24 equally spaced anchored columns. Figure 28.17 shows the outside view of the Kanteerava stadium.

Fig. 28.17 *Kanteerava stadium with precast folded plate roof*

28.7 Precast Prestressed Concrete Poles

Precast prestressed concrete poles[21,22] are mass produced for use for supporting electrical power transmission lines, antenna masts and substation towers. The prestressed concrete poles can be manufactured in a long line pretensioning bed in a factory ensuring the specification requirements of the national codes[23]. The main advantages of these poles are resistance to corrosion, fire and high degree of durability under extreme environmental conditions. The reader may refer to Chapter 19 for various types of precast prestressed poles and their design principles.

Precast prestressed concrete poles of different shapes and sizes to suit the industrial needs have been used in the developed and developing countries for the last several decades. Large size spun precast prestressed concrete poles are manufactured by Rocla Pty Ltd. Australia[24], to suit the requirements of high voltage electric power transmission lines. The company has specialised in the designing and manufacturing of prestressed concrete poles conforming to the Australian standards AS: 1170.2-2002, AS/NZ: 4676-2000 and the international quality assurance standard ISO: 9001. Figure 28.18 shows a typical mega size precast prestressed concrete pole used for high voltage power transmission.

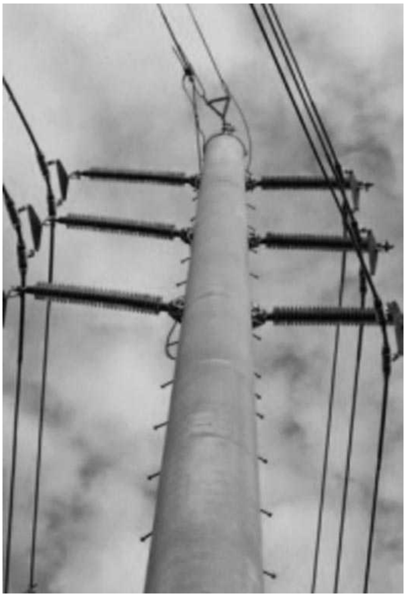

Fig. 28.18 *Precast prestressed concrete power transmission pole*

28.8 Precast Prestressed Concrete Sleepers

Precast prestressed concrete sleepers were first introduced in France, and further developed and used in England, Germany and the USA after the Second World War. At present, the precast concrete sleepers have completely replaced the wooden and steel sleepers and extensively adopted for supporting the railway tract in most of the countries in the world. The state-of-the-art reports and the excellent surveys by Ager[25] and Sambamoorthi[26] clearly indicate the rapid progress achieved in the design, manufacture and testing of precast prestressed concrete sleepers in various countries.

The Indian Hume Pipe Company introduced prestressed monoblock sleepers for Indian Railways in 1970, adopting the long line system for mass production of sleepers. More than five million sleepers made by the company are currently in use in the prestigious routes of Indian Railways. PCM-Rail One Group of Germany, producing precast prestressed sleepers to suit the specifications of several countries, has manufacturing facilities in Germany, South Korea, Romania, Hungary, Spain, Turkey, USA and India. The reader may refer to Chapter 19 for different types of sleepers and their design principles. Figure 28.19 shows the precast prestressed concrete sleepers ready for dispatch. Figure 28.20 shows the use of these PSC sleepers for the construction of railway track.

Fig. 28.19 *Precast prestressed concrete mono block sleepers*

Fig. 28.20 *PSC sleepers suporting the railway track*

28.9 Precast Prestressed Concrete Piles

Precast prestressed concrete piles are vital elements in the foundations of buildings, bridges and marine structures throughout the world. They vary in size from 250 mm square piles used in building foundations to 1676 mm diameter cylindrical piles used in marine structures and bridges. In locations where the bearing capacity of the soil is low and heavy loads have to be transmitted to the foundation, prestressed concrete piling is the ideal solution. Heavy marine structures often rely on prestressed concrete piling driven through deep water for their support. Prestressed concrete piling can be designed to safely support these heavy loads as well as lateral loads caused by wind, waves and earthquakes. In marine environments, these piles can resist corrosion caused by salt water and by thousands of cycles of wetting and drying without any deterioration.

Precast prestressed concrete piles, usually square, octagonal or circular in shape with varying sizes to suit the clients requirements, are manufactured in factories. The AASHO-PCI standards[27] prescribe the minimum reinforcing steel to be 1 to 1.5 per cent of the gross concrete section. PSC sheet piles are ideally suited for the construction of water front bulk heads, cut-off walls, groins, wave baffles and retaining walls to support soil and hydrostatic pressure in embankments or in excavations. Figures 28.21, 28.22 and 28.23 show the casting of piles in a pretensioning bed, stacking of the piles in a storeyard and use of these piles in a marine structure, respectively. The reader may refer to Chapter 19 for design details of different types of piles.

Fig. 28.21 *Precasting of piles in a pretensioning bed*

Fig. 28.22 *Storing of finished piles*

Fig. 28.23 *Construction of marine structure using precast piles*

28.10 Precast Prestressed Concrete Pipes

Precast prestressed concrete pipes[28] are genarally preferred in the construction of water mains with internal hydrosatic pressure. The technique of prestressing pipes was introduced in 1930 and ever since, numerous pipelines have been installed throughout the world. Various proprietary organisations have patented their systems of manufacturing prestressed concrete pipes. Basically, pestressed concrete pipes are manufactured in two types identified as: (a) non cylinder PSC pipes, and (b) cylinder PSC pipes. In non cylinder pipes, the precast concrete pipe is prestressed by circumferential high tensile wire winding, whereas in cylinder pipes, a thin steel cylinder is also used along with precast concrete before the hoop wire winding. Consequently, the thickness of concrete is reduced and higher internal pressures can be allowed in the cylinder PSC pipes.

The Indian Hume Pipe company (IHP), started in 1957, manufactures precast non cylinder prestressed concrete pipes of different sizes by centrifugal spinning process. The pipes are produced with diameters in the range from 300 to 2000 mm and lengths up to 5 m to withstand pressures from 0.5 to 2 N/mm^2 conforming to the specifications of the Indian Standard Code IS: 784-2001[29]. Figures 28.24 and 28.25 show the installation and the socket-spigot joint of typical non cylinder prestressed concrete pipes.

Fig. 28.24 *Installation of typical precast non cylinder prestressed concrete pipe*

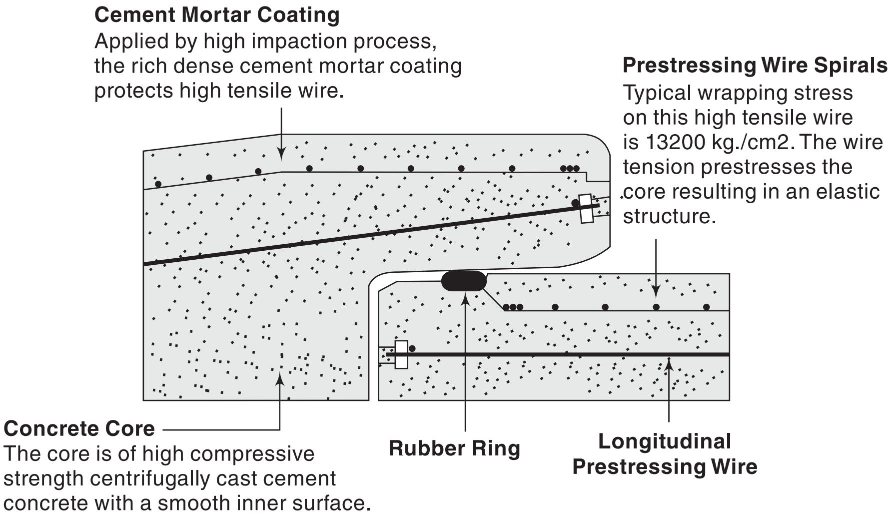

Fig. 28.25 *Typical socket and spigot joint in non cylinder prestressed concrete pipe*

Precast prestressed concrete cylinder pipes are manufactured in diameters varying from 1 to 8 m and in lengths of 5 to 8 m. This type can withstand higher magnitudes of hydrostatic pressure in water mains and also earth pressures due to heavy embankments when used as pipe culverts. This type of pipes are widely used as inverted siphons, sub aqueous sea water cooling lines for nuclear power stations and water mains. Figure 28.26 shows the installation of a typical mega size prestressed concrete cylinder pipe manufactured by Ameron International Company. The reader may refer to Chapter 16 for specific design details of different types of prestressed concrete pipes.

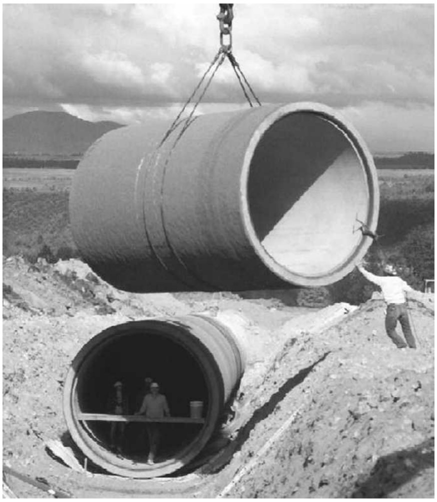

Fig. 28.26 *Installation of Prestressed Concrete Cylinder Pipe (PCCP)*

28.11 Precast Prestressed Concrete Drilling Platforms

Precast prestressed concrete structural elements are incresingly adopted for the construction of oil and gas exploration platforms in the high seas for the last two decades. The main advantage of using the massive precast elements is their superior durabilty characteristics to withstand the icy waters of the arctic region without any deterioration. The massive precast blocks are assembled together by prestressing to form the drilling platform. The concrete platform is designed to withstand the destructive action of sulphate waters and the pressure due to floating ice blocks. The concrete island drilling system (CIDS)[30] has replaced the building of gravel islands, which cost approximately 100 million dollars and is not reuseable.

The CIDS platform costs only 75 million dollars and can be reused at a different location. At present, these types of drilling platforms are being used for the last 20 years to explore numerous locations along the North Alaskan coastline in the Beaufort Sea without showing any deterioration in the hull. These platforms do not leave any footprints on the seabed. Due to these advantages, the CIDS platforms are currently being used along the east coast of Russia. A typical CIDS platform is shown in Fig. 28.27.

Fig. 28.27 *Precast prestressed concrete drilling platform*

References

1. Subramanian. N., Design of Reinforced Concrete Structures, Oxford University Press, New Delhi, 2013, pp. 1-857.
2. Port Cities – Mersey Gateway. Org, Wikipedia Reports.
3. Portland Cement Association Notes on ACI: 318 Building Code Requirements for Structural Concrete with Design Applications, EB-705.
4. Raina. V.K., Concrete Bridge Practice, Construction, Maintenance and Rehabilitation, Tata McGraw Hill Publishing Co. Ltd, New Delhi, 1988, pp. 381-396.
5. Gerwick. B.C., Construction of Prestressed Concrete Structures, Wiley Inter Science, New York, 1971, pp. 303-309.
6. Precast Prestressed Concrete in Buildings and Structures, Portland Cement Association Notes on ACI: 318-05, 2017.
7. ACI: 362- IR-12, Guide for the Design and Construction of Durable Concrete Parking Structures.
8. High Precast Parking Systems - High Concrete Group-Precast Prestressed Concrete Structural Units for Car Parks. Denver, USA.
9. Taylor. H.P.J, L.A. Clark, C.C. Banks, The Y-beam: A replacement for the M-beam and slab bridge decks, Journal of the Institution of Structural Engineers, London, Vol. 68, No. 23, December 1990, pp. 459-465.
10. Manton. B.H. and C.B. Wilson, MOT/C and CA, Standard Bridge Beams, Publication No. 32.012, Cement and Concrete Association, London, 1970.
11. Anderson, A.R., How Beam Design Affects Prestressed Concrete Bridge Costs, Engineering News Record, Vol. 159, October 1957, pp. 326-328.
12. Pretensioned Prestressed Concrete Girders, California Department of Transportation Publication, Sacremento, February 2015, pp. 8/1 to 8/112.
13. W. J. Rohlder, Segmental Bridge Technology Established and Evolving – Report of Bridge Engineering Program, Department of Civil, Structural and Environmental Engineering, University at Buffalo, State University of New York.
14. Podolony. W. Jr and Muller, J., Construction and Design of Prestressed Concrete Segmental Bridges, John Wiley & Sons, New York, 1982.
15. Peter Samir & George Morcous, Precast Prestressed Concrete Truss Girder for Roof Applications, Journal of Structures, Vol. 2014, Hindawai Publishing Corporation, University of Nebraska, Lincoln, Omaha, USA, 2014, pp. 1-13.
16. Haeusler. E., Precast Prestressed Hyperboloid of Revolution, I.A.S.S. Bulletin, No.6, A-7, Madrid, Spain, 1959.
17. Ramakrishna. A., Indian Examples of Large Span Building Structures, IABSE Reports, Zurich, 1994, pp. 101-112,
18. Simpson. H., Design of Folded Plate Roofs, Journal of the Structural Division, Proceedings of the American Society of Civil Engineers, Vol. 84, January 1958.
19. Li Zhenqiang, Precast Prestressed Concrete Folded Plate Industrial Building System, Journal of the Prestressed Concrete, March-April 1992, pp. 30-43.
20. R. Sundaram, Built Constructions – Sustainability in Construction, Shell Structures, Kanteerava Indoor Stadium, Report, Dec/Jan 2016.

21. Dimitriev. S.A., Prestressed Concrete Poles, Proceedings of the Symposium on Mass Produced Prestressed Concrete Elements, Madrid, June 1968, pp. 59 – 80.
22. Zacharia George et al., Prestressed Concrete Poles: State of the Art, Proceedings of the International Symposium on Prestressed Concrete Pipes, Poles, Pressure Vessels and Sleepers, Madras 1972, PL/0, pp. 1-35.
23. IS: 1678-1998 (Reaffirmed 2003), Specification for Prestressed Concrete Poles for Overhead Power Traction and Telecommunication Lines, Bureau of Indian Standards, New Delhi, 1998, pp. 1-6.
24. Rocla Pty Ltd, Duraspun Power Poles, Company Reports, Melbourne & Sydney, Australia.
25. Ager. J.W.A., General Report on Prestressed Concrete Railway Sleepers, Mass Produced Prestressed Precast Elements, Proceedings of the Symposium held at the Institute Eduardo Torroja de la Construction del Cemento, Madrid, 3rd and 4th June 1968, FIP June 1968, pp. 81-91.
26. Sambamoorthi, R.M. et al., Prestressed Concrete Sleepers: State of the Art, Proceedings of International Symposium on Prestressed Concrete Pipes, Poles, Pressure Vessels and Sleepers, Vol. 1, Madras 1972, pp. SL/0-23.
27. Recommendations for Design, Manufacture and Installation of Prestressed Concrete Piling developed by PCi Committee on Prestressed Concrete Piling, Journal of the Prestressed Concrete Institute, March/April 1977, pp. 20-49.
28. Ooykaas. G.A.P., Prestressed Concrete Pipes, Journal of the Institution of Water Engineers, Vol. 6, 1952, pp. 85 – 100.
29. IS: 784-2001, Indian Standard Specification for Prestressed Concrete Pipes (Second Revision), Bureau of Indian Standards, New Delhi, 2001. pp. 1-28.
30. Precast Prestressed Concrete Structures, Civil-on line-Reports, 2010, pp. 1-10.

Review Questions

28.1 Briefly explain the advantages of precast prestressed concrete structural elements in the construction industry.

28.2 Distinguish between precast solid slabs and hollow cored slabs. What is the span range for which they are used in building industry?

28.3 Explain the use of double tee girders in the construction of parking structures. What is a C-grid carbon cast mega tee girder and what are its advantages?

28.4 Explain with sketches the different types of bridge girder decks used for national highway crossings and urban flyovers.

28.5 What are the advantages of using precast prestressed concrete trusses for factory roofs? Sketch a typical warren girder type truss for a factory roof indicating the truss member to be prestressed to resist the forces due to superimposed loads.

28.6 What are the advantages of using the hyperbolic paraboloid shell roof for covering large floor spaces? Sketch a typical pretensioned hyperboloid shell element suitable for a long span roof.

28.7 Mention the advantages of using precast prestressed folded plate elements for covering the roof of an industrial structure with sketches.

28.8 Briefly explain the advantages of precast pretensioned concrete poles in power transmission and sleepers in railway traction. Sketch the different types of cross-sections used in the poles and sleepers.

28.9 Write a brief note on precast prestressed concrete pipes and piles mentioning their applications in the construction industry.

28.10 What are specific advantages of using precast prestressed drilling platforms? Where do you use such platforms for oil and gas exploration?

Objective-type Questions

28.1 Precast prestressed concrete slabs in comparison with non prestressed slabs result in savings of concrete up to a percentage of
(a) 10
(b) 60
(c) 45

28.2 Precast prestressed hollow cored slabs can be used for spans in the range of
(a) 10 to 15 m
(b) 6 to 10 m
(c) 20 to 30 m

28.3 The standard flange width of mega precast double tee girders manufactured by several companies vary in the range of
(a) 1.5 to 3.5 m
(b) 3.6 to 6.6 m
(c) 4.5 to 8.5 m

28.4 The ideal type of precast concrete element suited for the construction of long span curved bridge decks is
(a) double tee girder
(b) pretensioned bulb tee girder
(c) cellular box girder

28.5 In the case of precast concrete trusses used for long spans, the member to be prestressed is
(a) diagonal member
(b) bottom tie member
(c) vertical member

28.6 In the case of a precast pretensioned hyperboloid structural element, the prestressing tendons are
(a) straight
(b) curved
(c) parabolic

28.7 The most economical type of precast prestressed roof suitable for a long span factory is
(a) hollow cored slabs
(b) tee beam and slab
(c) folded plates

28.8 The ideal cross-section preferred for a precast prestressed power transmission pole of length in the range of 25 to 30 m is
(a) octagonal
(b) hollow circular
(c) rectangular

28.9 The minimum percentage of reinforcement in a precast prestressed concrete pile specified in the AASHO-PCI standard is
(a) 0.5 to 1
(b) 1.5 to 2.5
(c) 1 to 1.5

28.10 In precast prestressed concrete pipes, the circumferential wire winding is essential to resist
(a) flexural tension
(b) shear forces
(c) hoop tension

Answers to Objective-type Questions

28.1 (c)	28.2 (a)	28.3 (b)	28.4 (c)	28.5 (b)
28.6 (a)	28.7 (c)	28.8 (b)	28.9 (b)	28.10 (c)

29 Prominent Prestressed Concrete Structures in the World

29.1 General Aspects

The first extensive use of prestressed concrete was mainly due to its widespread application in the domain of bridge construction in Germany[1] during the post war years of 1949–53, when more than 300 bridges were built. The second half of 20th century witnessed a phenomenal explosion in the research, development and extensive use of prestressed concrete[2] in the construction industry of most of the developed and developing countries in the world. The rapid development of precast concrete technology has paved the way for the production of a variety of prestressed concrete structural elements widely used in housing, marine, railway, storage, nuclear, electrical transmission and transportation structures[3].

Steel as a construction material dominated the construction industry in the 18th and 19th centuries due to its intrinsic strength to resist different types of loads. However, steel being costly and amenable for rusting and deterioration under adverse environmental conditions, reinforced and prestressed concrete have replaced steel as a major construction material during the last several decades. The innovative application of prestressed concrete in several types of prominent outstanding structures[3] in the world is presented in the following sections.

29.2 World's Longest Span Prestressed Concrete Bridges

Prestressed concrete is ideally suited for the production of precast elements of superior quality and precision paving the way for use in long span bridges. Rapid developments in construction techniques like cantilever[4], staging and extruded elements[5], have been widely employed in the construction of long span bridges. Table 29.1 lists the top ten longest prestressed concrete bridges around the world with China leading with the maximum number of long span bridges.

The Shibpano Bridge with a span of 330 m located at Chongquing, China, is presently the world's longest span prestressed concrete bridge, and was completed in 2006. At present, China is leading the world with five longest span prestressed concrete bridges, closely followed by Norway with four bridges having spans in the range of 200 to 300 m.

Table 29.1 *List of longest span prestressed concrete bridges in the world*

S. No.	*Bridge*	*Span (m)*	*Location*	*Country*	*Year*	*Notes*
1	Shibanpo	330	Chongqing	China	2006	
2	Stolmasundet	301	Austevoll	Norway	1998	
3	Raftsundet	298	Lofoten	Norway	1998	
4	Sundoy	298	Leirfjord	Norway	2003	
5	Beipanjiang Shuipan	290	Guizhou	China	2013	
6	Sandsfjord	290	Rogaland	Norway	2015	
7	Humen-2	270	Guangdong	China	1997	
8	Sutong-2	268	Suzhou-Nantong	China	2009	
9	Honghe	265	Yuanjiang	China	2003	
10	Gateway-1	260	Brisbane	Australia	1986	

29.3 World's Largest Prestressed Concrete Domes

The Belgrade Fair Hall[6] located in Belgrade, Serbia, is credited to have the world's largest prestressed concrete dome built during the middle of the 20th century. It spans 109 m with a maximum ceiling height of 30.78 m, covering a total area of 21,280 m^2. It includes an arena, ground floor, and three galleries which all serve as exhibition spaces, and it also houses office space in a basement level. Architects Branco Zezelj and Milorad Pantovic used prestressed concrete to overcome the tension resulting from the flexural loads. The process effectively balances out the bending loads, allowing for larger concrete beams and spans. Figure 29.1 shows the plan and elevation showing the ring beam and curved girders.

29.4 World's Largest Prestressed Concrete Tanks

Large prestressed concrete tanks have been used in various countries for the storage of liquids like liquid petroleum gas (LNG) and water. World's largest LNG tanks have been constructed by the Korea Gas Company (KOGAS)[7] and the largest water tanks are located in Syracuse (NY). The technical details of these tanks are presented in next paragraphs.

29.4.1 LNG Storage Tanks

In 2005, KOGAS developed the largest above-ground full containment LNG storage tank in the world, which has a gross capacity of 200,000 m^3. The technical details of the prestressed concrete tank are as follows:

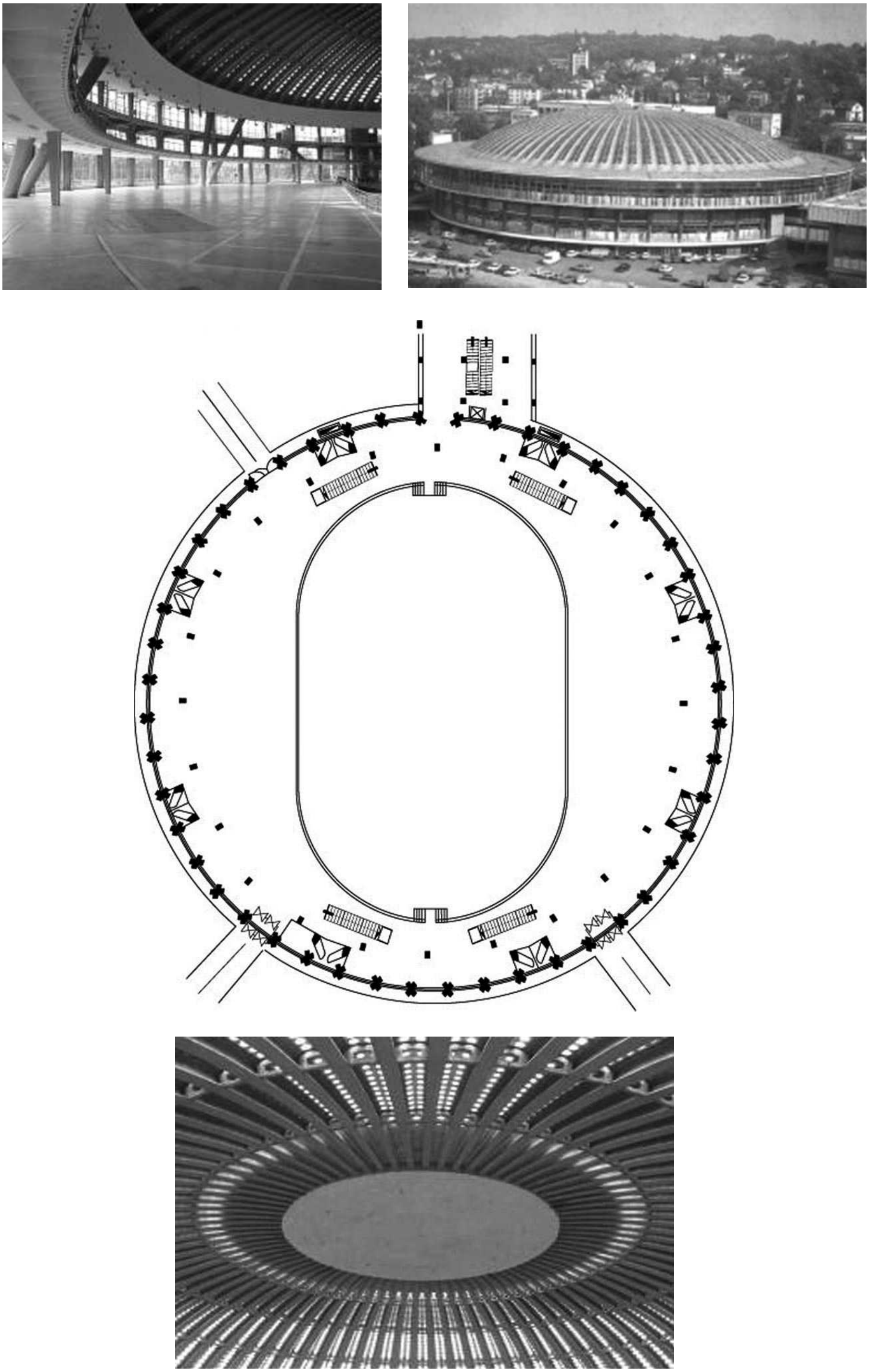

Fig. 29.1 *Belgrade fair hall with the largest prestressed concrete dome*

Capacity of the circular tank = 200 000 m^3

Diameter at bottom of the tank = 91 m

Thickness of bottom slab = 1.8 to 2.1 m

Height of outer concrete cylindrical wall = 40 m

Thickness of prestressed concrete wall

= 1400 mm at base tapering to 750 mm towards the top ring beam.

The tank is parallel sided from the height of 7.5 m to the roof ring beam.

The concrete ring beam at top of wall, 3.2 m high and 1.5 m thick made of prestressed concrete, completes the wall. The function of the ring beam is to restrain the tensile forces which result from the dome structure.

The bottom slab is supported on 1277 steel pipe piles forming the deep foundation. An inner tank made of nickel steel with a diameter of 84 m and height 37.6 m is provided to prevent leakage of LNG gas. The outer tank is composed of reinforced concrete and prestressed concrete. Figure 29.2 shows the largest prestressed concrete LNG storage tank.

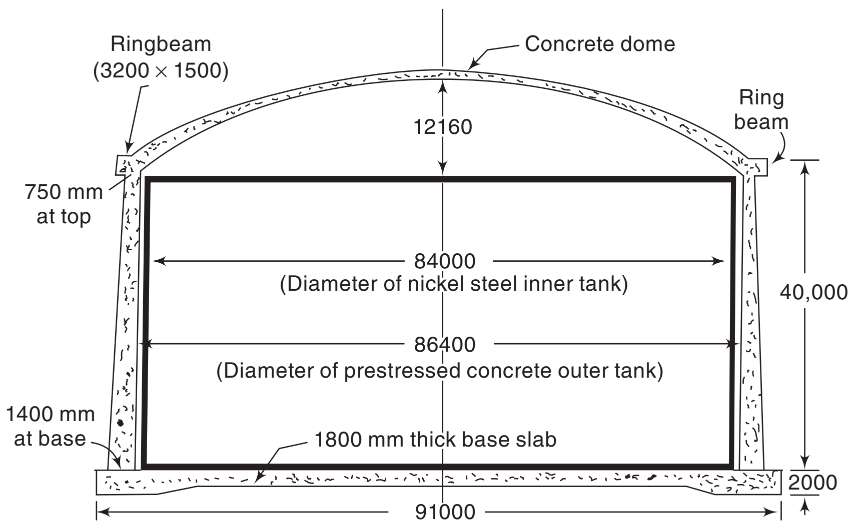

Fig. 29.2 *Prestressed concrete LNG tank of 200,000 m^3 storage capacity*

29.4.2 Water Tanks

Largest prestressed concrete tanks used for storage of large quantities of fluids are generally circular in shape, since the cylindrical shape is well suited for circumferential high tensile wire winding which induces hoop compression counteracting the hoop tension developed in the walls of the tank. DN Tank corporation[8] with its offices located in Dallas (Texas), Sandiego (California) and Boston Massachusetts, has specialised in constructing large capacity prestressed concrete tanks using cast-in-situ and precast wall panels.

The company has recently reported the construction of two large prestressed concrete tanks at the Westcott Reservoir, Syracuse (NY). The twin 32 million gallons (121 mega litres) capacity tanks constructed at a cost of 40 million dollars have added 64 million gallons of storage to cater the water requirements of the city. The tanks having a diameter of 114 m and 13 m tall are considered to be the largest prestressed concrete tanks east of the rocky mountains and among the largest in the world as shown in Fig. 29.3.

Fig. 29.3 *Twin 32 MG water tanks at the Westcott Reservoir, Syracuse, NY*

The company has also reported the construction of 20 million gallons (76 mega litres) capacity circular cylindrical tank as shown in Fig. 29.4. The tank is located in Utah Valley and has a diameter of 72 m and a height of 18 m with a spherical dome roof. The figure shows the operation of circumferential wire winding in progress from the bottom of the tank using a wire winding machine. The walls of the tank are vertically post-tensioned by high tensile cables to resist the moments developed in the walls.

Fig. 29.4 *Utah valley 20 MG Prestressed Concrete Water Tank*

29.5 World's Longest Prestressed Concrete Beams

According to Sharon. J. Rehana's report[9], the longest prestressed concrete beams ever manufactured were successfully installed in the Netherlands. These huge box beams— 68 m long and weighing 218 metric tons, form the main span of the new bridge in Zuidhorn, Netherlands. Long beams are finding increased use in bridges and viaducts. They obviate the need for intermediate supports, resulting in shorter construction periods and allow road traffic and ship more room to flow smoothly.

The construction of the bridge involved rerouting the N355, which separates Noordhorn and Zuidhorn. Congestion caused by the existing lifting bridge over the Van Starkenborgh Canal will be a thing of the past, and the canal will be passable for larger container ships.

The new fixed bridge forms a high and long link over the Van Starkenborgh Canal and is part of the new provincial road. The structure with three spans and four traffic lanes will allow passage of shipping cargo 10 m high and 55 m wide. To construct the large main span, manufacturer Haitsma Beton, produced the longest and heaviest prefabricated concrete beams that the company has ever supplied. The launching of the mega prestressed beams is shown in Fig. 29.5.

Fig. 29.5 *Launching of mega span (68 m) precast prestressed concrete beams*

The second longest span prestressed concrete beam of nearly 182 ft (55 m) has been used for a 60-degree skew bridge on major Oregan highway over rail road tracks in the USA[10]. The precast tee beams having top and bottom flange widths of 5 ft (1.5 m) and 2.5 ft (0.75 m), respectively, and length 182 ft weighed around 90 tons. The beams were prestressed using 56 wires of 15 mm diameter high tensile strands. Figure 29.6 shows the beam being transported to the bridge site for erection.

Fig. 29.6 *55 m long precast prestressed concrete beam used in skew bridge on major Oregan highway*

29.6 World's Largest Prestressed Concrete Pipes

World's largest prestressed concrete pipes were installed in 1970 as part of the aqueduct system delivering 1950 million gallons (7380 mega litres) of Colerado River water per day, to Maricopa, Pinal, and Pima Counties, in Central and Southern Arizona. The Central Arizona Project (CAP) operates and maintains three (3) 21-foot diameter (6.4 m) prestressed concrete non-cylinder pipes (PCP) as part of the aqueduct system. Jim Geisbush[11] reports a case study of the rehabilitation of the largest prestressed concrete pipes in the Central Arizona project.

The case study describes the inspections, assessment, monitoring, and subsequent repair using post-tensioned tendons of the Centennial Wash Siphon. This paper further discusses the ongoing efforts of monitoring, assessing, repairing, and maintenance practises for the largest prestressed concrete pipes in the world. A brief history of the siphons includes manufacturing of the 6.4 m diameter prestressed concrete pipes, installation of the pipelines, and early investigations and repairs. The focus of this paper is on the assessment and monitoring since the last repairs in 2006, specifically newer technologies that have emerged to assist CAP in monitoring and making decisions in the repair methods and locations. Relevant points include a discussion on the excavation of the pipes requiring repair, the repair work (post-tension tendons), and maintenance practises.

The second largest prestressed concrete pipe is located on the main canal of the Chambal irrigation system in India. The prestressed concrete pipe, shown in Fig. 29.7, has an internal diameter of 6.1 m with a wall thickness varying from 279 mm to 482 mm near the anchorage zones. The pipes used in the Kunu siphon system are designed by STUP[12] consultants of Mumbai.

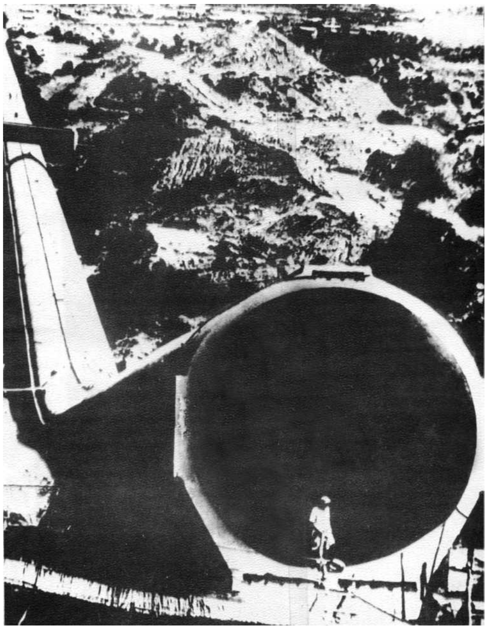

Fig. 29.7 *Kunu Siphon*

29.7 World's Longest Prestressed Concrete Poles

Rocla Pty Limited of Australia[13] manufactures large size spun precast prestressed concrete poles to suit the requirements of high voltage electric power transmission. The company has specialised in the designing and manufacturing of prestressed concrete poles conforming to the Australian standards AS: 1170.2-2002, AS/NZ: 4676-2000 and the international quality assurance standard ISO: 9001.

Economical Rocla Duraspun prestressed concrete poles are produced in lengths in the range of 15.5 m to 38 m. The largest and longest poles of 38 m length have the tip and base diameters varying in the range of 360-540 mm to 930-1110 mm, respectively. These long poles have a mass in the range of 14130 to 22540 kg. Figure 29.8 shows a typical spun prestressed concrete pole used for high voltage electric transmission power lines.

Larger poles are produced in suitable lengths of up to a maximum length of 24 m and assembled by bolted connections at site to suit the local requirements as shown in Fig. 29.9.

The company has the potential to supply poles of length up to 50 m which can withstand tip loads of up to 300 kN.

Fig. 29.8 *Typical mega size spun precast prestressed concrete power pole*

Fig. 29.9 *Assembling of individual prestressed concrete pole units by bolted connections to increase the length of pole*

29.8 World's Longest Span Prestressed Concrete Trussed Girders

World's longest span prestressed concrete trusses have been used for the roof of a coal storage facility in Sharjah (UAE), as reported by Peter Samy[14]. The precast prestressed trusses spanning over 50 m were designed by an American firm, e.construct, USA, LLC. The trusses were precast in two lengths of 25 m each and post-tensioned by high tensile cables housed in the flanges of the trussed girder.

The technical details of the truss are compiled as follows:

Span of the truss = 50 m

Depth of truss = 1.5 m

Span/depth ratio = 33

Length of each panel made up of diagonal and vertical members = 2 m

Total weight of the truss = 40 tons

The cross-section of the truss for the central portion of 32 m, I-section with equal flanges are connected by vertical and diagonal members. The truss is of solid rectangular section towards the supports to facilitate the housing of curved cables towards the supports. Post-tensioning cables include two cables housed in the tension flange each containing 13 high tensile strands of 15.2 mm diameter.

The cables are eccentric and housed in the tension flange at the centre of span and concentric at the supports. The diagonal and vertical members in tension and compression, respectively, are of reinforced concrete. The trusses were used at 10 m intervals for the coal storage facility shed.

Figures 29.10 to 29.12 illustrate the positioning of the trussed girder, details of post-tensioning cables along the span and the various structural elements like the flanges, vertical and diagonal members of the trussed girder.

Fig. 29.10 *50 m span post-tensioned prestressed concrete trussed girder used for the roof of a coal storage facility at Sharjah (UAE)*

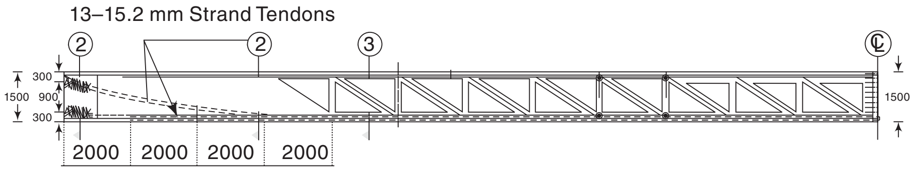

Fig. 29.11 *Post-tensioning cables in prestressed concrete trussed girder*

Fig. 29.12 *Precast prestressed concrete girder with flanges, vertical and diagonal members*

29.9 World's Largest Prestressed Concrete Shell Roofs

29.9.1 Barrel Shells

Prestressed concrete shell roofs are generally preferred to cover large column free spaces suitable for industrial structures like airport hangars, garages and factory sheds. Kirkland and Goldstein[15] reported the design and construction of prestressed concrete barrel shells of large spans. The prestressed concrete shell structure was designed to cover a large floor area of 90 m by 45 m required for the garage of the transportation department of the city of Bournemouth.

The prestressed concrete shell roof structure comprising of nine barrel vaults each of 10 m width and having a span of 45 m constitutes the longest span barrel vault shells used in this category of large span shell construction. Figure 29.13 shows the garage covered by barrel shells with the deep edge beams spanning over 45 m.

Fig. 29.13 *Long span prestressed concrete barrel shell roof with edge beams*

29.9.2 Hyperbolic Paraboloid Shells

Precast prestressed hyperboloid shells elements, 25 m long having a shell thickness of 60 mm, have been used for a storage building at Essen, Germany[16]. Le Corbusier adopted this elegant form of construction for the roof of the legislative assembly hall at Chandigarh, India. HP shells of 20 m span length and 2.5 m wide have been used at Larsen Toubro's Porclain hydraulic excavator factory, Bangalore[17]. The precast pretensioned HP shell units each weighing 9 tons have a thickness of 50 mm at the bottom gradually varying to 100 mm at the edges. The units were prestressed using 32 nos of 7 mm diameter high tensile wires arranged in a criss-cross profile between the ends forming the shell profile. In addition, a welded mesh was used as non prestressed reinforcement tied to the high tensile wires and the shell was cast using high strength concrete. The shell elements spanned between precast prestressed bow string arched units spanning between columns at 20 m intervals. The longitudinal and cross-section of the building is shown in Fig. 29.14.

29.10 World's Longest Span Prestressed Concrete Folded Plates

A typical example of a large span precast prestressed concrete folded plate of span lengths, 30 m used for the roof structure of Asthana Mandapam building complex at Tirupati, has been reported by A. Ramakrishna[18]. The exclusive feature of this building complex is a column free area of 1700 m^2 achieved by a unique roofing system using precast prestressed units comprising of nine folded plate elements each 30 m long and 6.3 m wide, weighing 60 t. The

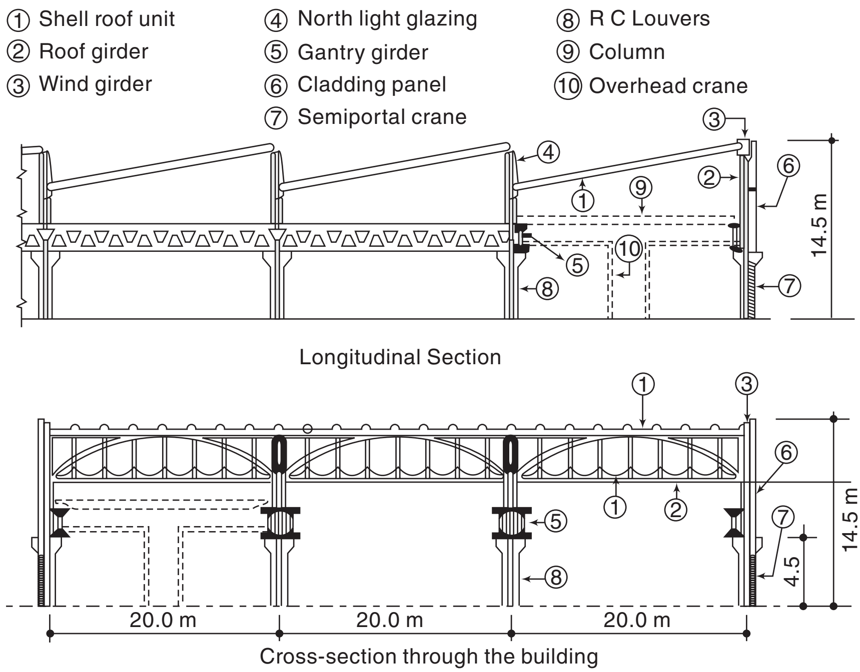

Fig. 29.14 *Longitudinal and cross-section through building with precast hypar shell roof elements supported on bow string truss*

elements were cast on ground in a timber mould and then lifted and placed 10 m above the floor using a sophisticated erection scheme.

Prestressing of the folded plate was done by using two post-tensioned cables, one of 21 m length comprising of six 12.7 mm high tensile strands and another of 30 m length consisting of six similar strands each carrying a force of 15 t. The special feature of the folded plate being the diamond patterned ribs at the bottom of the V-shaped folded plates exhibiting a pleasing view of the ceiling from the ground. The slab of the folded plate unit is only 40 mm thick resulting in considerable economy in the unit cost per area of the roofing system. Figure 29.15 shows the lifting of the folded plates during erection of the roofing system.

29.11 World's Largest Prestressed Concrete Silos

The Seward Silos[19] constructed for the firm Reliant Energy in 2003–04 comprises of three interconnected ash silos which are part of the Seward Re Powering Project in Seward, Pennsylvania. Three 57 m tall interconnected prestressed concrete silos were constructed for the 208 MW power plant. T.E Zebberson company constructed the silos of which, two silos were of 25 m diameter for storing fly ash and the third one of 20 m diameter for storing bed ash.

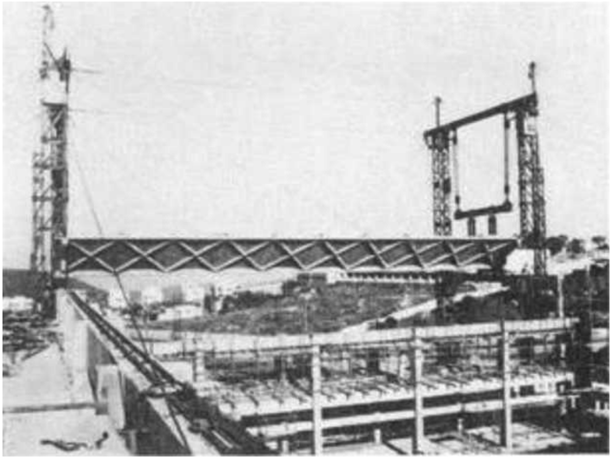

Fig. 29.15 *Erection of 30 m span precast prestressed concrete folded plate*

The silos were built using slip form method and are believed to be the first interconnected silos in the world built using post-tensioning with high tensile strands as the primary circumferential reinforcement. 366 horizontal tendons each comprising of 12-15.2 mm strands were used for post-tensioning the silo walls in conjunction with VSL ES6-12 anchorage system. The post tensioning operation and grouting of the ducts were completed successfully with cold weather grouting made possible through a variety of sophisticated grouting techniques. Figure 29.16 shows the circumferential post-tensioning of the silo walls using the high tensile tendons at the pilasters located at 45 degree intervals. Figure 29.17 shows the casting of the silos using the slip form method.

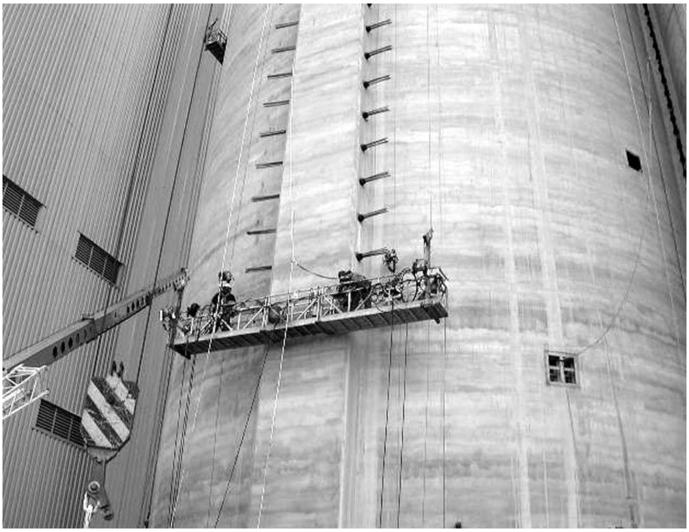

Fig. 29.16 *Post-tensioning of largest prestressed concrete silo*

Fig. 29.17 *Slip form casting of post-tensioned prestressed concrete silos*

29.12 World's Longest Prestressed Concrete Sleepers

At present, Indian railways adopt the largest gauge (Broad Gauge) for railway transportation network with a gauge length of 1755 mm between the centre lines of rails. Consequently, the sleepers used for the railway track have the longest length among the other types used in the world. The Indian Railways Designs and Standards Organization (RDSO)[20] has developed research investigations and tests the RDSO-T/2495, prestressed concrete sleepers to suit the demands of the Indian railways. The mono block pretensioned prestressed concrete sleeper is now used as the standard sleeper for the broad gauge tracks throughout India.

Figure 29.18 shows the technical details of the RDSO-T/2495 sleeper having an overall length of 2750 mm. The sleeper with a trapezoidal cross-section is pretensioned using 18/3 mm high tensile strands. In comparison with other sleepers like the German B-58, British F-23 and French VW, the Indian RDSO-T/2495 has the longest gauge length of 1755 mm, longest overall length of 2750 mm and the heaviest overall weight of 282 kg. Prestressed concrete sleepers are not only a favorable choice but also a technical necessity for high speed and high density traffic of the Indian railways from the point of maintainability of track geometry and riding comfort requirements.

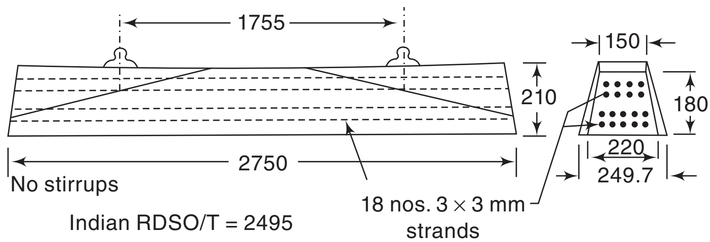

Fig. 29.18 *Indian RDSO-T/2495 pretensioned prestressed concrete sleeper*

References

1. Guyon, Y., Prestressed Concrete, Vol. 1, (4th Edition) C.R. Books Ltd, London, 1960.
2. Leonhardt, F., Prestressed Concrete, Design and Construction, Wilhelm Ernst & Sohn, Berlin, 1964.
3. Raina, V.K., Concrete Bridge Practice, Construction, Maintenance and Rehabilitation, Tata McGraw-Hill Publishing Co, Ltd, New Delhi, 1988.
4. Podolony. W, and Muller. J, Construction and Design of Prestressed Concrete Segmental Bridges, John Wiley & Sons, New York, 1982.
5. Jessica Binns, Extradosed Bridge Distinguishes Toll Way Project in India, Civil Engineering, Vol. 75, No. 2, February 2005, p. 20.
6. Belgrade Fair Hall, Wikipedia, Encyclopedia, Report on Large Domes.
7. Development of the World's Largest Above the Ground Full Containment LNG Storage Tanks, 23rd World Gas Conference, Amsterdam, 2006.
8. Twin Water Tanks of 32 mgd Capacity at the West Cott Reservoir, Syracuse, N.Y. Report from D.N Tank Corporation, New York.
9. Sharan, J. Rehana, World's Longest Concrete Beams Installed, Report of Construction News, Hanley Wood's Commercial Construction Group, Netherlands.
10. Donald P. Merwin, Record Length Precast Beams Ensure Project meets Deadline, Report of 182 ft long precast prestressed concrete beam used for a skew bridge on Major Oregan Highway Over Rail Road Tracks, Aspire, Winter, 2007, pp. 36-37.
11. Jim Geisbush, Repairing the World's Largest Prestressed Concrete Pipe; A Case Study of the Central Arizona Projects Centennial Wash Siphon, ASCE Conference Proceedings, Baltimore, Maryland, USA, 2015.
12. Tandon, M.C., Alimchandani, C.R. and Venkataramani, S., Achievements in Structural Concrete Perceived Through Some Outstanding Structures in Prestressed Concrete, Concrete Structures of India, Compiled by Maharashtra India Chapter of American Concrete Institute's Fall Convention at New York, 1984, pp. 63-72.
13. Rocla Pty Ltd, Duraspun Power Poles, Melbourne & Sydney, Australia.
14. Peter Samy Samir, M.S., Precast Prestressed Concrete Trusses for Roof Applications, University of Nebraska, U.S.A., May 2013, pp. 10-15 and Report

on Precast Prestressed Concrete Trusses for the Roof of Coal Storage Facility at Sharjah (UAE), e.construct, USA.

15. Kirkland, G.W, and Goldstein, A., The Design and Construction of a Large Span Prestressed Concrete Shell Roof, Structural Engineer, London, Vol. 29, No. 4, 1951.
16. Haeusler, E, Precast Prestressed Hyperboloids of Revolution, I.A.S.S. Bulletin, No. 6, A-7 Madrid, 1959.
17. Ramakrishna, A, Indian Examples of Innovation in Concrete Construction & Methods, International Symposium on Innovative World of Concrete (ICI-IWC: 93), Proceedings Vol. 1, August, 1993, Bangalore, India.
18. Ramakrishna, A, Some Indian Examples of Large Span Building Structures, IABSE Reports, Zurich, 1994, pp. 101-112.
19. Interconnected Silos Built with Post-tensioning, Technical Report-VSL Structural Technologies, Pennsylvania.
20. Indian Railway Standard Specifications for Pretensioned Prestressed Concrete Sleepers, Government of India, Ministry of Railways, Serial No. T-39-85, Fourth revision, New Delhi, May 2011.

30 Prospective Progress in Prestressed Concrete

30.1 Introduction

Prestressed concrete has witnessed phenomenal innovations and developments during the last six decades with its impressive footprint in the construction industry. Precasting technology has opened up new vistas for the development and use of a variety of high quality prestressed concrete structural elements, manufactured in a factory, to cater to the ever increasing demands of the building and transportation industry. In 1936, at a special meeting of the British Institution of Structural Engineers in London, the French bridge engineer, Eugene Freyssinet[1], explained the development of a brand new material named as "Prestressed Concrete".

The start of World War II in 1939 delayed further development of prestressed concrete. Also, the technology of producing high-strength concrete and high-strength steel had not sufficiently developed. By 1945, most of Europe's infrastructure, especially its bridges, had been destroyed and needed to be replaced. There was a severe shortage of steel then and hence, prestressed concrete became the preferred material of construction. During this period, working stress design was the sole basis developed for reinforced concrete and the same was used for the design of poles, pipes, bridges and harbour works. Most of these applications occurred in France and other French-speaking countries. Both American and European codes of practise treat prestressed concrete as an integral part of what is now called structural concrete, while the Indian codes are expected to introduce this concept in their next revision.

Gustav Magnel[2], a Belgian professor of engineering, was also considered as an authority of prestressed concrete. He visited North America and Canada in 1950 and inspired, through his lectures and courses, engineers like Lin and Zollman, to become pioneers in the development of prestressed concrete. Magnel built the Walnut Lane Bridge in Philidelphia. In 1950, considered as the first major prestressed concrete bridge in the USA. In India, Coleroon bridge, the first using prestressed concrete, was built during this period using the Freyssinet system.

After six decades of uninterrupted progress, the new material christened as "prestressed concrete" has established itself as the most economical and durable material, capable of resisting different types of forces like tension, flexure, compression, shear, torsion and their combinations with its widespread applications in buildings, bridges, railways, marine, nuclear, electrical transmission, stadiums and airport hangars. Prospective developments in the technology of materials, design procedures, innovative methods of construction should serve as the roadmap for future progress in prestressed concrete industry.

30.2 Developments in Concrete Technology

30.2.1 High Strength Concrete

The progress of prestressed concrete is closely associated with the development of technology to produce high strength concrete from 1950 onwords. At that time, concrete of compressive strength above 40 MPa was designated as high-strength concrete. Several methods were standardised by the British Code[3], ACI Committee 211[4] and Indian Standard Code[5], for producing concrete with characteristic compressive strength in the range of 40 to 60 MPa. Later Collins[6] and Parrott[7] developed methods to achieve compressive strength exceeding 100 MPa. During the last three decades, high performance concrete is generally specified for prestressed concrete structures due to enhanced performance characteristics.

30.2.2 High Performance and Ultra High Performance Concrete (HPC and UHPC)

High performance concrete is generally made with carefully selected high quality ingredients and optimised mix designs. According to ACI Report[8], HPC is defined as “a concrete meeting specified combinations of performance and uniformity requirements that cannot always be achieved routinely by using only conventional materials and normal mixing, placing and curing practises. The requirements may involve enhancement of characteristics such as easy placement, compaction without segregation, long-term mechanical properties, early age strength, permeability, density, heat of hydration, toughness, volume stability, and long service life in severe environments”.

Typically, such concretes will have low water/cement ratios in the range of 0.22 to 0.40. Super plasticisers are usually used to improve workability. Research investigations by Tadros et al.[9] at the University of Nebraska, Michigan, and Georgia Institute of Technology, have reported the production of ultra high performance concrete having strength in the range of 124 to 138 N/mm^2 using non proprietary ingredients and local aggregates rather than silica powder used as an aggregate in proprietary mixes. This process considerably reduces the production cost of UHPC. The reader may refer to Chapter 26 for detailed information regarding the production, structural properties and applications of high performance and ultra high performance concretes in the construction industry.

30.2.3 Silica Fume Concrete

Several investigations over the last four decades by Loland & Gjorv[10], Mehta[11], and Malhotra[12] have conclusively proved the advantage of using silica fume to improve the properties of concrete made with Portland cements. Normally, silica fume constituting 5 to 10 per cent of the weight of cement per unit volume is used in the concrete mixes resulting in significant increase in compressive strength of the concrete. Standard specifications have been evolved by Norway (Norwegian Standard-3474) and Canada (CAN 3-A.123.6), who are the pioneers in the field of Silica Fume concrete.

Notable example of the use of silica fume concrete includes the High Rise Building in Montreal, Canada, for the production of very high compressive strength concrete of around 90 N/mm^2 at 28 days in 1984. Silica fume concrete was also used for the rehabilitation of KInzua Dam in Pennsylvania, by the US army corps of engineers in 1983 to produce concrete of cylinder compressive strength of 100 N/mm^2. The reader may refer to a separate monograph[13] by the author for an in depth treatment of the production, properties of Silica Fume concrete.

30.2.4 Nano Concrete

Nano concrete, based on the principle of nano technology was first introduced by the Nobel laureate, Richard Feynman[14], in 1960. It served as the catalyst for developing nano engineered materials like nano cements and nano additives for significantly improving the workability and strength of concrete.

According to Konstantin Sobolev[15], nano technology of concrete is set on a path to revolutionize the construction industry by changing the structural properties of concrete like strength and durability to better suit the requirements of structural components. Nano cements like TX Active, EMACO, Chronolia, Agilia, and Ductal developed by several companies, have been used as additives to concrete resulting in considerable savings in dead loads and overall cost of the structures. The reader may refer to Chapter 27 (which deals with the applications of nano concrete in prestressed concrete structures) for more details regarding the use of nano concrete in buildings and bridges.

30.3 Prospective Research on Superior Concretes

Research efforts during the last 50 years have resulted in significant increase in the compressive strength of concrete by 400 per cent from 40 MPa in 1960 to over 160 MPa in 2010. Most of the new investigations are on nano sized and nano structured materials. Investigations conducted on nano systems at the Polytechnic Institute[16] indicate that research is progressing on the use of nano silica, nano titanium oxide, nano alumina and nano ferrous oxide in small percentages to produce nano concrete.

30.3.1 Research Studies on the Use of Nano-Silicon Dioxide

Experimental investigations have shown that nano-SiO_2 is more effective in enhancing the strength than silica fume. Addition of only 10 per cent of nano-SiO_2 with dispersing agents increased the 28 day compressive strength of cement mortar by as much as 26 per cent compared to only 10 per cent increase with the addition of silica fume. The degree of dispersion of nano-SiO_2 in the cement paste plays an important role on the strength. Nano-SiO_2 not only behaves as a filler to improve the micro structure but also as an activator to promote pozzolanic reactions to improve the strength.

Further comprehensive research investigations are needed to establish and quantify the various advantages of using nano silica additives in concrete.

30.3.2 Research Investigations on the Use of Nano-Titanium Oxide

Exploratory investigations on the use of nano titanium oxide in concrete has been found to be very effective in self cleaning of the concrete and provides the additional benefit of helping to clean the environment. Primary investigations have shown that Nano-TiO_2 containing concrete acts by triggering a photocatalytic degradation of pollutants such as nitric oxide, carbon monoxide, chlorophenols and aldehydes from vehicular emissions. Detailed research investigations on a large scale at reputed laboratories are required to conclusively establish the beneficial effects of using nano titanium oxide in concrete.

30.4 Developments in Nano Engineered Steels for Structural Applications

The potential benefits of nano technology in the modern engineering industry has inspired a number of leading R&D institutions and manufacturing companies to pursue research in the area of nano structured steels[17]. The focus of the ongoing efforts has been largely manipulation of microstructures at the nano-scale through innovative processing techniques and adoption of novel alloying strategies. This is being aided by employing advanced characterisation methods like high resolution transmission electron microscopy (HRTEM), atom probe tomography (APT), etc., and computational design of materials.

Steel is synonymous with strength. There are two ways of achieving ultra high strength in steels. The first one is to reduce the size of a crystal to such an extent that it is devoid of any defects, which could achieve tensile strengths exceeding 13 GPa in steel whiskers. The second alternative is to introduce a very large density of defects in a metal sample that acts as an obstacle to the motion of dislocations. This has been illustrated by drawing high carbon pearlitic steel wire, which is subjected to intense plastic deformation, thereby, introducing dense dislocation substructure. The carbon steel wire is a remarkable example of nanostructured steel produced on a mass scale.

The high carbon steel wire is an important engineering material used in prestressed concrete, automobile tires, galvanized wires for suspension bridges and power cable wires. In fact, the suspension cables of the world's largest suspension bridge, Akashi Strait Bridge built in Japan in 1998, were made of pearlitic steel wires of 1800 MPa strength. To inhibit softening during hot-dip galvanizing, high-Si and high Si-Cr steel wires have also been developed for high-strength galvanized suspension-bridge wires. Similarly, the pearlitic wire for automobile tyre cords exhibits strengths of about 4000 MPa.

During the last three decades, several steel manufacturing companies like The Nano Steel company, USA, The Questek Innovation, USA, Sandvik Materials Technology, Sweden, JFE, Kawasaki and Nippon Steel Corporations of Japan, are producing high strength steels to suit the needs of different industries. The nano engineered steels and concrete have opened up new vistas for the design and construction of slender and stronger prestressed concrete structures.

30.5 Application of Nano Concrete and Steel in Prestressed Concrete

During the last decade, nano concrete in different forms has been used in countries like USA, South Korea, Australia and Japan, for prestressed concrete buildings and bridge structures. The reader may refer to Chapter 27 for specific details of structures where nano concrete was used. However, examples of structures built using nano concrete in conjunction with nano steel with higher strength than the conventional steels are limited. Research investigations are needed to develop design procedures to exploit the high strengths of both nano concrete and steel.

Prestressed concrete structures built using high strength nano steel and concrete results in slender structures. The national codes of most of the developed countries including India follow the limit state design for structural concrete members in which both the ultimate strength and serviceability criteria like deflection and cracking have to be satisfied. Slender prestressed concrete structures may satisfy the specified ultimate strength but their deflection and cracking under service loads should be examined by comprehensive research investigations. Based on the experimental investigations, the codes can formulate the methods of computing the ultimate strength, deflections and cracking for prestressed concrete structural elements using high strength nano steel and concrete.

References

1. Freyssinet. E., A Revolution in the Technique of the Utilization of Concrete, Structural Engineer, London, 1936, 14(5), 242.

2. George D. Nasser, Maher Tadros, Adam Sevenker and David Nasser, The Legacy of Future of An American Icon; The Precast Prestressed Concrete Double Tee, Journal of the Prestressed Concrete Institute, July/August 2015, pp. 49 – 68.
3. BS EN: 206-1/BS 8500-1:2006, Specifications for Concrete, British Euro Standards, 2006.
4. ACI Committee 211, recommended Practice for Selecting Proportions for No Slump Concrete (ACI: 211.3-75)(Revised in 1975 and Reapproved in 1992).
5. IS: 10262-1982, Indian Standard Recommended Guidelines for Concrete Mix Design. Bureau of Indian Standards, New Delhi, 1980, pp.1-21.
6. Collins. A.R., The Principle of Making High Strength Concrete – Report of Eleven Lectures on Prestressed Concrete given at the Building Exhibition, Cement and Concrete Association, London, November 1949.
7. Parrott. L.L., The Production and Properties of High Strength Concrete, Concrete, Vol. 3, No.11, November 1969, pp. 443-448.
8. ACI: 363R-10-2010, State of the Art Report on High Strength Concrete, American Concrete Institute, Farmington Hills, USA, 2010, p. 65.
9. Tadras Maher. K and George Morcous, Application of Ultra High Performance Concrete to Bridge Girders, Special Report – P1(08) P 310, Lincoln, NE, Nebraska Department of Roads, 2009.
10. Loland, K.E. and Gjorv. O. Silica Fume in Concrete, Research Institute for Cement and Concrete at the Norwegian Institute of Technology, Trondheim, Norway, June 1981, 8 Reports.
11. Mehta, P.K. and Gjorv. O.E., Properties of Portland Cement and Concrete Containing Fly Ash and Condensed Silica Fume. Cement and Concrete Research*,* Vol. 12, No. 5, pp. 587–595.
12. Malhotra, V.M. and Garette, C.G. Silica Fume Concrete: Properties, Application and Limitations. Proceedings of Annual Meeting of Institute of Concrete Technology. Fulmer Grange, Slough, England, June 1982, pp. 1–23.
13. Krishna Raju. N., Design of Concrete Mixes (Fifth Edition), C.B.S. Publishers, New Delhi, 2014, pp. 282-295.
14. Feynman, R. There is plenty of room at the bottom (Reprint from speech delivered at the annual meeting of the West of the American Physical Society). Engineering Science Journal*,* Vol. 23, 1960, pp. 22–36.
15. Sobolov, K. and Gutierrez, M.F. How nanotechnology can change the concrete world, American Ceramic Society Bulletin, Vol. 84, No.10, October 2005, pp. 14–18.
16. Sergiu Calin, Roxana Gintu and Gabriela Dascalu. Summary of Test and Studies done abroad on the Nano Concrete Systems. The Bulletin of the Polytechnic Institute. 2009, Google search reports on nano concrete (Seminars only.com) Published on Jan. 10, 2017.
17. Toshimi Tarui, Jun Takahashi, Hitoshi Tashiro, Nacki Maruyama, Seiki Nishida, “Microstructure Control and Strengthening of High-carbon Steel Wires”, Nippon Steel, Technical Report No. 91, (2005) 56-61.

Appendix 1

Properties of Prestressing Steels

Table A.1.1 *Prestressing wires (IS: 1785–Part-1—1983)*

Nominal Diameter (mm)	*Area* (A_p) (mm^2)	*Weight* (kg/m)	*Ultimate Tensile Strength* f_p (N/mm^2)	$0.8\, f_p\, A_p$ (kN)	f_pA_p (kN)
2.50	4.9	0.037	2010	7.87	9.84
3.00	7.0	0.053	1865	10.44	13.05
4.00	12.5	0.095	1715	17.15	21.43
5.00	20.0	0.150	1570	25.12	31.40
7.00	38.5	0.292	1470	45.27	56.59
8.00	50.0	0.390	1375	55.00	68.75

Table A.1.2 *Prestressing bars (IS: 2090—1983)*

Nominal Diameter (mm)	*Area* (A_p) (mm^2)	*Weight* (kg/m)	*Ultimate Tensile Strength* (f_p) (N/mm^2)	$0.8\, f_p\, A_p$ (kN)	f_pA_p (kN)
10	79	0.62	980	61.93	77.42
12	113	0.89	980	88.59	110.74
16	201	1.58	980	157.58	196.98
20	314	2.47	980	246.17	307.72
22	380	2.98	980	297.92	372.40
25	491	3.85	980	384.94	481.18
28	616	4.83	980	482.94	603.68
32	804	6.31	980	630.33	787.92

Table A.1.3 *Prestressing strands (IS: 6006— 1983) (Seven-wire Strand)*

Nominal Diameter (mm)	*Area* (A_p) (mm^2)	*Weight* (kg/m)	*Ultimate Tensile Strength* (f_p) (N/mm^2)	$0.8 f_p A_p$ (kN)	$f_p A_p$ (kN)
6.3	23.2	0.182	1723	31.97	39.97
7.9	37.4	0.294	1723	51.55	64.40
9.5	51.6	0.405	1723	71.12	88.90
11.1	69.7	0.548	1723	96.07	120.09
12.7	92.9	0.730	1723	128.05	160.06
15.2	139.4	1.094	1723	192.14	240.18
9.5	54.8	0.432	1862	81.63	102.03
11.1	74.2	0.582	1862	110.52	138.16
12.7	98.7	0.775	1862	147.02	183.77
15.2	140.0	1.102	1862	208.54	260.68

Appendix

2 Constants for Beam Sections

Table A.2.1 *Constants for T-sections*

Section	$\frac{b_w}{h}$	$\frac{D_f}{h}$	A	Y_b	Y_t	I	r^2	k_t	k_b
1	0.1	0.1	0.19 bh	0.714 h	0.286 h	0.0179 bh^3	0.0945 h^2	0.132 h	0.333 h
2	0.1	0.2	0.28	0.756	0.244	0.0192	0.0688	0.0910	0.282
3	0.1	0.3	0.37	0.755	0.245	0.0193	0.0520	0.0689	0.212
4	0.1	0.4	0.46	0.735	0.265	0.0202	0.0439	0.0597	0.165
5	0.2	0.1	0.28	0.629	0.371	0.0283	0.1010	0.1610	0.272
6	0.2	0.2	0.36	0.678	0.322	0.0315	0.0875	0.1290	0.272
7	0.2	0.3	0.44	0.691	0.309	0.0319	0.0725	0.1050	0.234
8	0.2	0.4	0.52	0.684	0.316	0.0316	0.0616	0.0900	0.195
9	0.3	0.1	0.37	0.585	0.415	0.0365	0.0985	0.1690	0.237
10	0.3	0.2	0.44	0.626	0.374	0.0408	0.0928	0.1480	0.248
11	0.3	0.3	0.51	0.645	0.355	0.0417	0.0819	0.1270	0.231
12	0.3	0.4	0.58	0.645	0.355	0.0417	0.0720	0.1120	0.203
13	0.4	0.1	0.46	0.559	0.441	0.0440	0.0954	0.1710	0.216
14	0.4	0.2	0.52	0.592	0.408	0.0486	0.0935	0.1580	0.229
15	0.4	0.3	0.58	0.609	0.391	0.0499	0.0860	0.1410	0.220
16	0.4	0.4	0.64	0.612	0.388	0.0502	0.0785	0.1280	0.205
17	1.0	1.0	1.00	0.500	0.500	0.0833	0.0833	0.1670	0.167

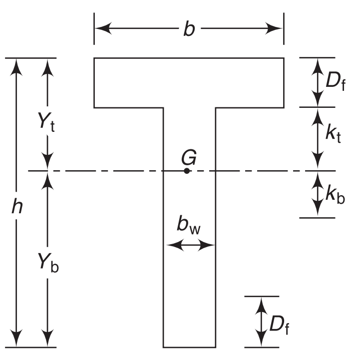

Table A.2.2 *Constants for unsymmetrical I-sections (Ratio of bottom to top flange width = 0.3)*

Section	$\frac{b_w}{b}$	$\frac{D_f}{h}$	A	Y_b	Y_t	I	r^2	k_t	k_b
1	0.1	0.1	0.21 bh	0.650 h	0.350 h	0.0260 bh^3	0.1236 h^2	0.190 h	0.354 h
2	0.1	0.2	0.32	0.675	0.325	0.0345	0.1080	0.160	0.332
3	0.1	0.3	0.43	0.672	0.328	0.0387	0.0900	0.184	0.274
4	0.2	0.1	0.29	0.610	0.390	0.0316	0.1090	0.179	0.280
5	0.2	0.2	0.38	0.647	0.353	0.0378	0.0994	0.153	0.282
6	0.2	0.3	0.47	0.655	0.345	0.0402	0.0856	0.131	0.248

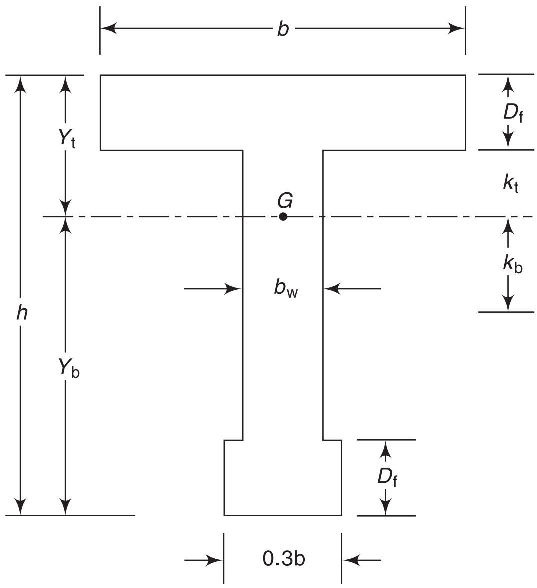

Table A.2.3 *Constants for unsymmetrical I-sections (Ratio of bottom to top flange width = 0.5)*

Section	$\frac{b_w}{b}$	$\frac{D_f}{h}$	A	Y_b	Y_t	I	r^2	k_t	k_b
1	0.1	0.1	0.23 bh	0.597 h	0.403 h	0.0326 bh^3	0.1420 h^2	0.238 h	0.352 h
2	0.1	0.2	0.36	0.611	0.389	0.0464	0.1288	0.210	0.331
3	0.1	0.3	0.49	0.606	0.394	0.0535	0.1090	0.180	0.274
4	0.2	0.1	0.31	0.572	0.428	0.0373	0.1204	0.210	0.282
5	0.2	0.2	0.42	0.595	0.405	0.0488	0.1160	0.195	0.286
6	0.2	0.3	0.53	0.599	0.401	0.0540	0.1020	0.170	0.254
7	0.3	0.1	0.39	0.557	0.430	0.0443	0.1103	0.198	0.250
8	0.3	0.2	0.48	0.582	0.418	0.0510	0.1065	0.183	0.255
9	0.3	0.3	0.57	0.592	0.408	0.0553	0.0970	0.164	0.238

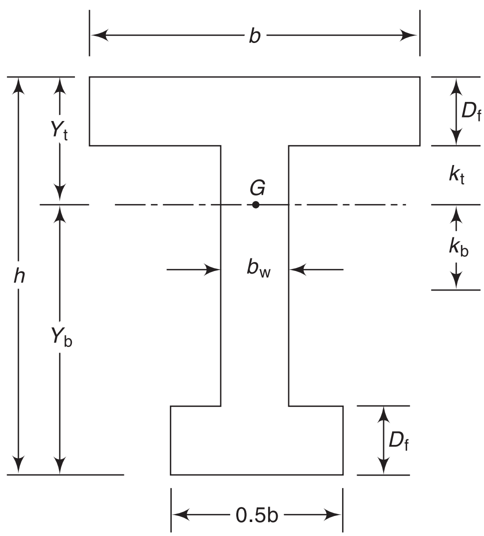

Table A.2.4 *Constants for unsymmetrical I-sections (Ratio of bottom to top flange width = 0.7)*

Section	$\frac{b_w}{b}$	$\frac{D_f}{h}$	A	Y_b	Y_t	I	r^2	k_t	k_b
1	0.1	0.1	0.25 bh	0.554 h	0.446 h	0.0381 bh^3	0.1525 h^2	0.276 h	0.342 h
2	0.1	0.2	0.40	0.560	0.440	0.0560	0.1391	0.248	0.316
3	0.1	0.3	0.55	0.557	0.443	0.0651	0.1182	0.212	0.267
4	0.2	0.1	0.33	0.540	0.460	0.0425	0.1290	0.239	0.280
5	0.2	0.2	0.46	0.552	0.448	0.0578	0.1250	0.228	0.281
6	0.2	0.3	0.59	0.553	0.447	0.0657	0.1113	0.202	0.249
7	0.3	0.1	0.41	0.534	0.466	0.0467	0.1140	0.214	0.244
8	0.3	0.2	0.52	0.546	0.454	0.0598	0.1150	0.210	0.254
9	0.3	0.3	0.63	0.550	0.450	0.0663	0.1051	0.191	0.234

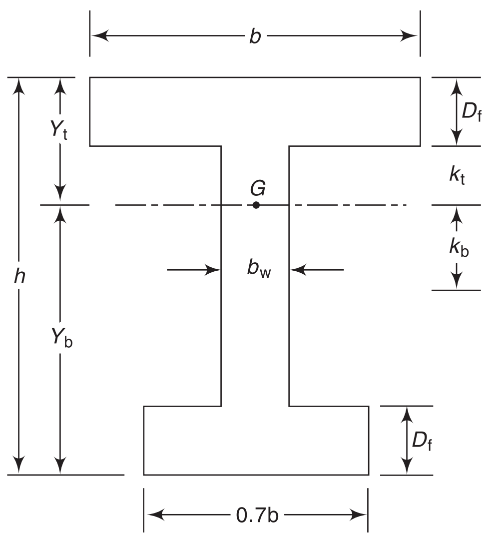

Table A.2.5 *Constants for unsymmetrical I-sections (Ratio of top to bottom flange width = 0.3)*

Section	$\frac{b_w}{b}$	$\frac{D_f}{h}$	A	Y_b	Y_t	I	r^2	k_t	k_b
1	0.1	0.1	0.21 bh	0.350 h	0.650 h	0.0260 bh^3	0.1236 h^2	0.354 h	0.190 h
2	0.1	0.2	0.32	0.325	0.675	0.0345	0.1080	0.332	0.160
3	0.1	0.3	0.43	0.328	0.672	0.0387	0.0900	0.274	0.134
4	0.2	0.1	0.29	0.390	0.610	0.0316	0.1090	0.280	0.179
5	0.2	0.2	0.38	0.353	0.647	0.0378	0.0994	0.282	0.153
6	0.2	0.3	0.47	0.345	0.655	0.0402	0.0856	0.248	0.131

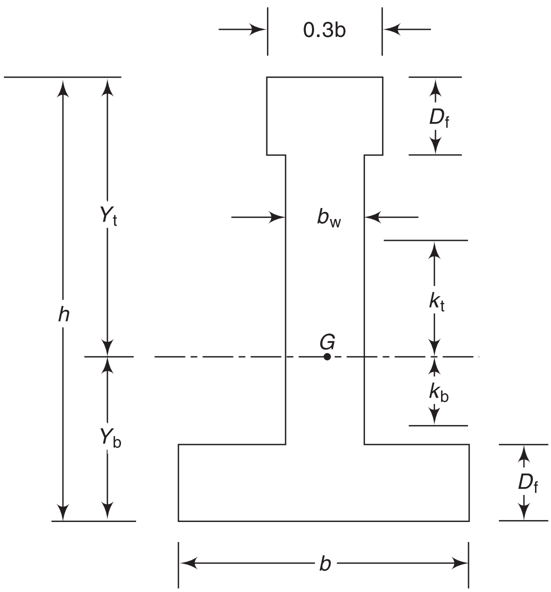

Table A.2.6 *Constants for symmetrical I and box sections*

Section	$\frac{b_w}{b}$	$\frac{D_f}{h}$	A	Y_b	Y_t	I	r^2	k_t	k_b
1	0.1	0.1	0.28 bh	0.500 h	0.500 h	0.0449 bh^3	0.160 h^2	0.320 h	0.320 h
2	0.1	0.2	0.46	0.500	0.500	0.0671	0.146	0.292	0.292
3	0.1	0.3	0.64	0.500	0.500	0.0785	0.123	0.246	0.246
4	0.2	0.1	0.36	0.500	0.500	0.0492	0.137	0.274	0.274
5	0.2	0.2	0.52	0.500	0.500	0.0689	0.132	0.264	0.264
6	0.2	0.3	0.68	0.500	0.500	0.0791	0.117	0.234	0.234
7	0.3	0.1	0.44	0.500	0.500	0.0535	0.121	0.243	0.243
8	0.3	0.2	0.58	0.500	0.500	0.0707	0.122	0.244	0.244
9	0.3	0.3	0.72	0.500	0.500	0.0796	0.111	0.222	0.222
10	0.4	0.1	0.52	0.500	0.500	0.0577	0.111	0.222	0.222
11	0.4	0.2	0.64	0.500	0.500	0.0725	0.113	0.226	0.226
12	0.4	0.3	0.76	0.500	0.500	0.0801	0.105	0.211	0.211

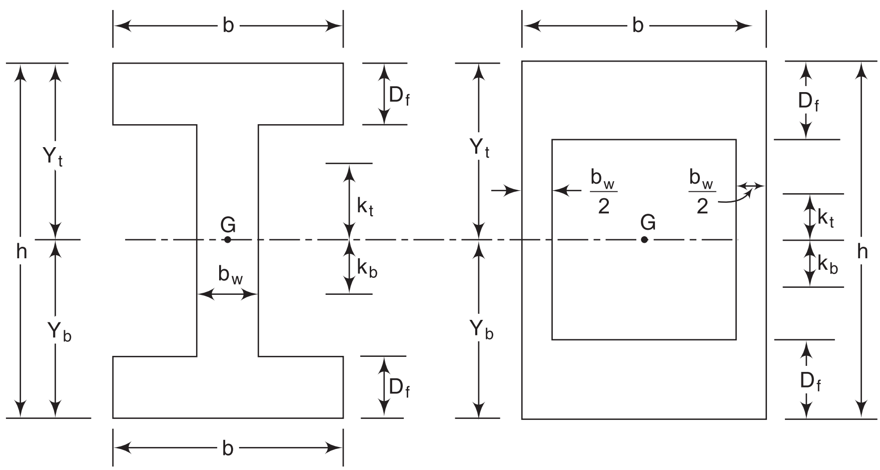

Appendix 3 Post-tensioning Systems

Table A.3.1 *Freyssi anchorage cones*

Freyssinet Prestressed Concrete Co. Ltd. Mumbai

	Tendon Reference *Number of wires*	*12 φ 5* *12*	*12 φ 5 E × T* *12*	*12 φ 7* *12*	*12 φ 7 E × T* *12*	*12 φ 8* *12*	*6T13* *6 (12.7 mm) seven-ply strands*
	Dimensions of male and female cones (mm)						
(a)	Outer diameter, φ_c	96	120	120	150	150	150
(b)	Height of female cone, h	100	100	120	125	125	125
(c)	Nominal outside diameter of connection sleeve, φ_e	32	32	38	38	51	51
	Diameter of grout hole, φ_g	8	—	11	—	11	10
	Height of male cone, b	74	—	95	—	108	110

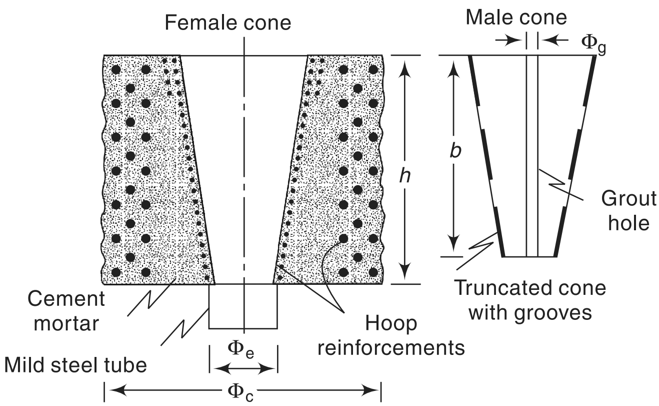

Table A.3.2 *Standard freyssinet prestressing cables*

Tendon System	*Units*	*12 φ 5*	*12 φ 7*	*12 φ 8*	*24 φ 7*	*24 φ 8*	*6T13*	*12T13*
Nominal diameter of wire/strand	mm	5	7	8	7	8	13	13
Nominal UTS of cable	N/mm^2	1600	1500	1400	1500	1400	1800	1800
Number wires/ strand per cable	no	12	12	12	24	24	6	12
Nominal steel area of cable	mm^2	235	462	603	922	1206	557	1115
Nominal ultimate breaking force of cable	kN	376	691	844	1382	1688	1002	2004
Maximum allowable prestressing force	kN	300	553	675	1105	1350	801	1603
Maximum allowable initial stress	N/mm^2	1280	1200	1120	1200	1120	1440	1440
Approximate weight per unit length of cable	kg/m	1.8	3.6	4.7	7.2	9.4	4.5	9.0

Table A.3.3 *PSC freyssinet system (Anchorage details of K-range system)*

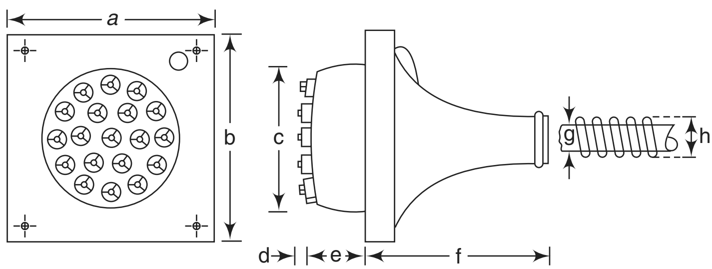

Tendon Reference		*4 K 15*	*7 K 15*	*12 K 15*	*19 K 15*	*27 K 15*	*37 K 15*
No. of 15 mm strands	n	4	7	12	19	27	37
Anchorage block and sheathing dimensions (mm)	a	130	170	200	250	300	420
	b	170	225	260	340	400	495
	c	115	140	160	220	260	320
	d	10	10	10	10	10	10
	e	50	60	60	65	80	95
	f	100	155	175	412	450	480
	g	55	65	75	95	110	130
	h	61	71	81	101	118	140
Characteristic strength of each strand = 265 kN							

Table A.3.4 *CCL system (Wire spiral anchorage details)*

Tendon	*Ultimate Prestressing Force* (kN)	*Type*	*Anchorage Flange Size*	*Length*	*Dia*	*A*	*B*	*C*	*D* (mm)	*E*	*F*	*G*	*H*	*J*	*K*
12 ϕ7	715	S 4	124 × 121	165	42	70	65	65	65	130	100	150	100	150	175
8 ϕ7	475	S 3	140 × 76	178	39	65	60	65	65	130	90	100	120	165	75
4 ϕ7 2 ϕ7	237 118	S 2	70 × 70	83	25	50	45	60	60	115	85	95	85	95	75

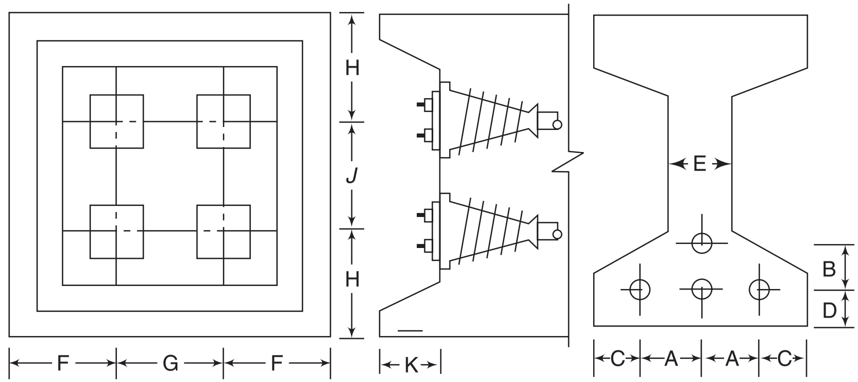

Table A.3.5 *BBRV system (A-type stressing anchorage details)*

Tendon Reference		*A24*	*A34*	*A42*	*A55*	*A61*	*A73*	*A85*	*A97*	*A109*
No. of 7 mm wires	n	24	34	42	55	61	73	85	97	109
Characteristic strength	kN	1542	2185	2699	3535	3920	4692	5463	6234	7005
Jacking Force 70%	kN	1080	1530	1890	2474	2744	3284	3824	4364	4904
Jacking Force 75%	kN	1157	1639	2024	2651	2940	3519	4097	4676	5254
Jacking Force 80%	kN	1234	1748	2159	2828	3136	3753	4370	4987	5604
Bearing plate:										
Side length	A	205	240	270	305	325	355	380	410	430
Thickness	B	25	30	35	40	45	55	60	65	75
Trumpet O/D	C	58	68	73	83	88	93	103	108	113
Anchor Head:										
Thread Diameter	D	110	124	139	158	158	172	185	202	202
Standard Length	E	44	50	56	64	64	69	74	81	81
Chocks	F	117	131	147	168	168	182	196	214	214
Sheathing I/D	G	50	60	65	75	80	85	95	100	105
Sheathing O/D	H	58	68	73	83	88	93	103	108	113

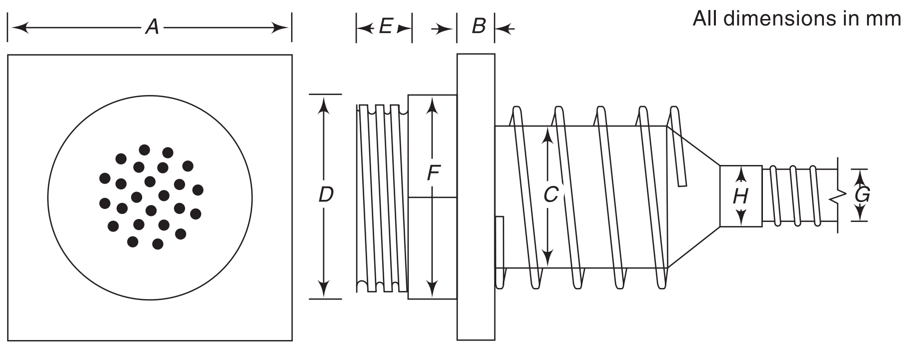

Table A.3.6 *Dywidag single bar anchorage tendon characteristics*

Nominal Diameter	mm	15.87	15.87	25.4	25.4	31.75	31.75	34.92
Actual Diameter	mm	15.0	16.0	26.5	26.5	32.0	32.0	36.0
Ultimate Strength	N/mm^2	1082	1585	1034	1103	1034	11103	1034
Area	mm^2	180.6	200.0	548.4	548.4	806.5	806	1019.4
Ultimate Load (P_u)	kN	193.5	313.5	567.1	604.9	834.0	889.6	1054.1
0.8 P_u	kN	154.8	250.8	453.6	483.9	667.2	711.6	843.2

Anchorage Details						
Bar Diameter	mm	15.87	15.87 S	25.4	31.75	34.92
		76 × 76 × 19	101 × 101 × 25	127 × 140 × 32	152 × 178 × 38	178 × 190 × 44
Solid Anchor Plate	mm					
		51 × 127 × 25	76 × 127 × 25	101 × 165 × 32	127 × 203 × 38	127 × 241 × 44
Nut extension	mm	25.4	41.3	47.6	63.5	69.8
Bar protrusion	mm	50.8	76.2	63.5	76.2	88.9
Pocket Former						
Height	mm	111.1	111.1	177.8	203.2	220.3
Maximum OD	mm	79.3	79.3	130.1	165.1	165.1

(*Contd.*)

Table A.3.6 (*Contd.*)

Coupling Details						
Length	mm	88.9	134.7	134.7	171.4	219.0
Diameter OD	mm	28.5	31.7	50.8	60.3	67.9
Sheathing						
Bar sheathing: OD	mm	25.4	25.4	38.1	44.4	50.8
ID	mm	19.0	19.0	31.7	38.1	44.4
Coupling Sheathing	mm	44.4	44.4	69.8	82.5	95.2
Outer Cover						
Inner Diameter	mm	34.9	34.9	60.3	73.0	85.7

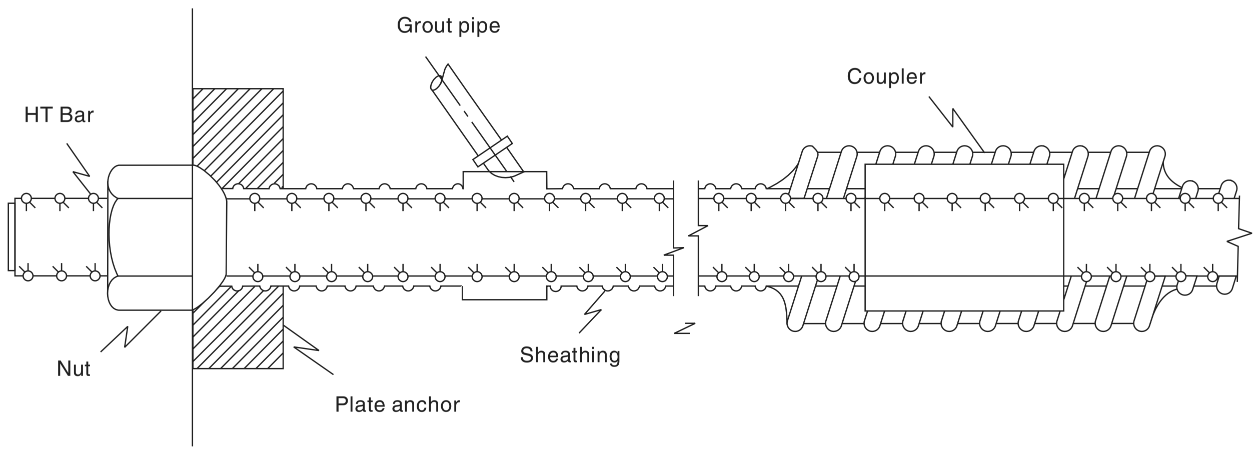

Appendix

4

Grouting of Post-tensioned Ducts

The main objective of grouting the ducts in post-tensioned concrete members are,

(i) to prevent corrosion of the tendons,
(ii) to ensure efficient transfer of stress between the tendons and the concrete member,
(iii) to improve the serviceability and strength characteristics of the concrete member.

The salient recommendations of the Indian (IS: 1343) and British standard codes are as follows:

Formation of ducts The ducts are formed from flexible galvanised corrugated steel tubes with an inside diameter at least 6 mm larger than the tendon diameter. Vents are provided at crests in the duct profile and at intervals not greater than 15 m. Anchorage vents are also provided and it should be possible to close all the vents.

Composition of grout The grout is prepared by using Portland cement and water. Fine sand passing 150 micron IS sieve may be added for grouting ducts of size exceeding 150 mm diameter. The quantity of the sand or filler should not exceed 30 per cent of the mass of cement. Plasticising agents, viscosity modifying agents and gas generating admixtures may be used to improve the fluidity of the grout. The chloride content in the grout from all sources should not exceed 0.1 per cent by mass of the cement.

The Water/Cement ratio of the grout should be as low as possible, consistent with workability. This ratio should not normally exceed 0.45. The comparison strength of 100 mm cubes of the grout tested at 28 days should be not less than 27 N/mm^2.

Batching and mixing of grout The materials of grout should be batched by mass. For a neat cement grout the optimum water/cement ratio will probably be about 0.40 and with a suitable admixture, a water/cement ratio of 0.35 may be adequate.

The grout should be mixed in a mixer capable of producing a homogeneous colloidal grout and after mixing, keeping the grout in slow continuous agitation until it is ready to be pumped into the tendon ducts. The minimum mixing time is generally between one and two minutes.

Mixing should not normally be continued for more than four minutes. Where admixtures are used, the manufacturers recommendation should be followed. All the piping, pumping and mixing equipment should be thoroughly washed with clean water after each series of operations.

Grouting procedure The mixing of the grout is done by adding water to the mixer first followed by cement. The injection procedure should ensure that ducts are completely filled. Ducts should be grouted at a continuous and steady rate of 6 m/min to 12 m/min for horizontal ducts and 2 to 3 m/min for vertical ducts at a pressure not exceeding 2 N/mm^2.

Grouting should continue until the fluidity or density of the grout flowing from the free ends and the vent openings is the same as that of the injected grout. The vents should be closed successively as the filling of the ducts continues and after closing the last vent. The grout pressure should be gradually increased from a minimum of 0.3 N/mm^2 to a full injection pressure of 0.5 N/mm^2 which shall be maintained for at least one minute before closing the injection pipe. Grout not used within 30 minutes of mixing should be rejected.

Vertical and inclined ducts should be grouted from the lowest point, the maximum length grouted in one operation being 50 m. Vents and all other openings should be sealed after grouting to prevent the ingress of moisture, de-icing materials and other corrosive agents.

The effectiveness of grouting can be checked by using nondestructive testing techniques like gamma radiography.

Appendix

5

Torsion Constant for Rectangular Sections

Ratio (*b/h*)	*Value of Constant* α
1.0	0.208
2.2	0.219
5.5	0.231
2.0	0.246
5.5	0.258
3.0	0.267
4.0	0.282
5.0	0.291
10.0	0.312
∞	0.333

Appendix 6

Bending Moment and Shear Force Coefficients for Continuous Beams

		All beams freely supported at end supports	
		All spans loaded	*Incidental load*
Max. bending moment coefficient	*Uniformly distributed load*	0.125 ↑ 0.071 ↑ 0.071 ↑ 0.100 0.100 ↑ 0.080 ↑ 0.025 ↑ 0.080 ↑ 0.107 0.072 0.107 ↑ 0.077 ↑ 0.036 ↑ 0.036 ↑ 0.077 ↑ 0.105 0.080 0.080 0.105 ↑ 0.078 ↑ 0.003 ↑ 0.046 ↑ 0.033 ↑ 0.078 ↑	0.125 ↑ 0.096 ↑ 0.096 ↑ 0.117 0.117 ↑ 0.101 ↑ 0.075 ↑ 0.101 ↑ 0.121 0.107 0.121 ↑ 0.099 ↑ 0.081 ↑ 0.081 ↑ 0.009 ↑ 0.120 0.111 0.111 0.120 ↑ 0.100 ↑ 0.080 ↑ 0.086 ↑ 0.080 ↑ 0.100↑
	Central point load	0.188 ↑ 0.156 ↑ 0.156 ↑ 0.150 0.150 ↑ 0.175 ↑ 0.100 ↑ 0.175 ↑ 0.161 0.107 0.161 ↑ 0.169 ↑ 0.116 ↑ 0.116 ↑ 0.169 ↑ 0.158 0.119 0.119 0.158 ↑ 0.171 ↑ 0.110 ↑ 0.130 ↑ 0.110 ↑ 0.171 ↑	0.188 ↑ 0.203 ↑ 0.203 ↑ 0.175 0.175 ↑ 0.213 ↑ 0.175 ↑ 0.213 ↑ 0.181 0.160 0.181 ↑ 0.210 ↑ 0.183 ↑ 0.183 ↑ 0.210 ↑ 0.179 0.167 0.167 0.179 ↑ 0.211 ↑ 0.181 ↑ 0.191 ↑ 0.181 ↑ 0.211 ↑
	Leads at 1/3 point	0.167 ↑ 0.111 ↑ 0.111 ↑ 0.133 0.133 ↑ 0.123 ↑ 0.034 ↑ 0.123 ↑ 0.143 0.095 0.143 ↑ 0.119 ↑ 0.056 ↑ 0.056 ↑ 0.119 ↑ 0.141 0.106 0.105 0.141 ↑ ↑ ↑ ↑ ↑ ↑	0.167 ↑ 0.139 ↑ 0.139 ↑ 0.157 0.157 ↑ 0.145 ↑ 0.100 ↑ 0.145 ↑ 0.160 0.144 0.160 ↑ 0.143 ↑ 0.111 ↑ 0.111 ↑ 0.143 ↑ 0.159 0.148 0.148 0.159 ↑ ↑ ↑ ↑ ↑ ↑

(*Contd.*)

Max. forces (shear)	*Uniformly distributed*	0.38 0.62 ↑ 0.62 ↑ 0.38 ↑ 0.40 0.50 0.60 ↑ 0.60 ↑ 0.50 ↑ 0.40 ↑ 0.39 0.54 0.46 0.61 ↑ 0.61 ↑ 0.46 ↑ 0.54 ↑ 0.39 ↑ 0.40 0.53 0.50 0.47 0.60 ↑ 0.60 ↑ 0.47 ↑ 0.50 ↑ 0.53 ↑ 0.40 ↑	0.44 0.62 ↑ 0.62 ↑ 0.44 ↑ 0.45 0.58 0.62 ↑ 0.62 ↑ 0.58 ↑ 0.45 ↑ 0.45 0.60 0.57 0.62 ↑ 0.52 ↑ 0.57 ↑ 0.60 ↑ 0.45 ↑ 0.45 0.60 0.59 0.58 0.62 ↑ 0.62 ↑ 0.58 ↑ 0.59 ↑ 0.60 ↑ 0.45 ↑

BM coefficients: Multiply by (span × total load on span) coefficients above the line are for negative BM at supports those under the line are for positive mid-span BM

Shear coefficients: multiply by (total load span)

Author Index

Subject Index

W

Z